

Neural Plasticity

# Acupuncture Therapies and Neuroplasticity 2020

Lead Guest Editor: Jing-Wen Yang

Guest Editors: Zhen Zheng, Lu Wang, and Yongjun Chen



---

**Acupuncture Therapies and Neuroplasticity  
2020**



Neural Plasticity

---

## **Acupuncture Therapies and Neuroplasticity 2020**

Lead Guest Editor: Jing-Wen Yang

Guest Editors: Zhen Zheng, Lu Wang, and Yongjun  
Chen



---

Copyright © 2021 Hindawi Limited. All rights reserved.

This is a special issue published in "Neural Plasticity" All articles are open access articles distributed under the Creative Commons Attribution License, which permits unrestricted use, distribution, and reproduction in any medium, provided the original work is properly cited.

# Chief Editor

Michel Baudry, USA

## Associate Editors

Nicoletta Berardi , Italy  
Malgorzata Kossut, Poland




## Academic Editors

Victor Anggono , Australia  
Sergio Bagnato , Italy  
Michel Baudry, USA  
Michael S. Beattie , USA  
Davide Bottari , Italy  
Kalina Burnat , Poland  
Gaston Calfa , Argentina  
Martin Cammarota, Brazil  
Carlo Cavaliere , Italy  
Jiu Chen , China  
Michele D'Angelo, Italy  
Gabriela Delevati Colpo , USA  
Michele Fornaro , USA  
Francesca Foti , Italy  
Zygmunt Galdzicki, USA  
Preston E. Garraghty , USA  
Paolo Girlanda, Italy  
Massimo Grilli , Italy  
Anthony J. Hannan , Australia  
Grzegorz Hess , Poland  
Jacopo Lamanna, Italy  
Volker Mall, Germany  
Stuart C. Mangel , USA  
Diano Marrone , Canada  
Aage R. Møller, USA  
Xavier Navarro , Spain  
Fernando Peña-Ortega , Mexico  
Maurizio Popoli, Italy  
Mojgan Rastegar , Canada  
Alessandro Sale , Italy  
Marco Sandrini , United Kingdom  
Gabriele Sansevero , Italy  
Menahem Segal , Israel  
Jerry Silver, USA  
Josef Syka , Czech Republic  
Yasuo Terao, Japan  
Tara Walker , Australia  
Long-Jun Wu , USA  
J. Michael Wyss , USA

Lin Xu , China






# Contents

## **Distinctive Alterations of Functional Connectivity Strength between Vascular and Amnesic Mild Cognitive Impairment**

Hui Li , Shuai Gao, Xiuqin Jia, Tao Jiang , and Kuncheng Li 


Research Article (8 pages), Article ID 8812490, Volume 2021 (2021)

## **Effect of Acupuncture Stimulation of Hegu (LI4) and Taichong (LR3) on the Resting-State Networks in Alzheimer's Disease: Beyond the Default Mode Network**

Shaozhen Ji , Hao Zhang , Wen Qin, Ming Liu, Weimin Zheng, Ying Han, Haiqing Song, Kuncheng Li , Jie Lu , and Zhiqun Wang 




Research Article (9 pages), Article ID 8876873, Volume 2021 (2021)

## **The Role of Neuroglial Crosstalk and Synaptic Plasticity-Mediated Central Sensitization in Acupuncture Analgesia**

Zhongxi Lyu, Yongming Guo , Yanan Gong , Wen Fan , Baomin Dou, Ningcen Li, Shenjun Wang, Yuan Xu, Yangyang Liu , Bo Chen , Yi Guo , Zhifang Xu , and Xiaowei Lin 



Review Article (18 pages), Article ID 8881557, Volume 2021 (2021)

## **The Role of Acupuncture Improving Cognitive Deficits due to Alzheimer's Disease or Vascular Diseases through Regulating Neuroplasticity**

Shaozhen Ji , Jiayu Duan, Xiaobing Hou, Li Zhou, Weilan Qin, Huanmin Niu, Shuyun Luo, Yunling Zhang, Piu Chan , and Xianglan Jin 




Review Article (16 pages), Article ID 8868447, Volume 2021 (2021)

## **Electroacupuncture Ameliorates Neuroinflammation-Mediated Cognitive Deficits through Inhibition of NLRP3 in Presenilin1/2 Conditional Double Knockout Mice**

Kun Li, Guoqi Shi, Yang Zhao, Yiwen Chen, Jie Gao, Lin Yao, Jiaying Zhao, Hongzhu Li, Ying Xu , and Yongjun Chen 


Research Article (15 pages), Article ID 8814616, Volume 2021 (2021)

## **Transcutaneous Electrical Acupoint Stimulation in Early Life Changes Synaptic Plasticity and Improves Symptoms in a Valproic Acid-Induced Rat Model of Autism**

Xiaoxi Wang , Rui Ding, Yayue Song, Juan Wang, Chen Zhang, Songping Han, Jisheng Han , and Rong Zhang 






Research Article (14 pages), Article ID 8832694, Volume 2020 (2020)

## **The Instant Effects of Continuous Transcutaneous Auricular Vagus Nerve Stimulation at Acupoints on the Functional Connectivity of Amygdala in Migraine without Aura: A Preliminary Study**

Wenting Luo , Yue Zhang , Zhaoxian Yan , Xian Liu , Xiaoyan Hou , Weicui Chen , Yongsong Ye , Hui Li , and Bo Liu 



Research Article (13 pages), Article ID 8870589, Volume 2020 (2020)

## **The Effectiveness and Safety of Manual Acupuncture Therapy in Patients with Poststroke Cognitive Impairment: A Meta-analysis**




Wei Liu , Chang Rao , Yuzheng Du , Lili Zhang , and Jipeng Yang 

Review Article (15 pages), Article ID 8890521, Volume 2020 (2020)



**Acupuncture for Adults with Diarrhea-Predominant Irritable Bowel Syndrome or Functional Diarrhea: A Systematic Review and Meta-Analysis**

Jianbo Guo, Xiaoxiao Xing, Jiani Wu, Hui Zhang, Yongen Yun, Zongshi Qin , and Qingyong He   
Review Article (16 pages), Article ID 8892184, Volume 2020 (2020)







**EA Improves the Motor Function in Rats with Spinal Cord Injury by Inhibiting Signal Transduction of Semaphorin3A and Upregulating of the Peripheral Nerve Networks**

Rong Hu , Haipeng Xu, Yaheng Jiang, Yi Chen, Kelin He, Lei Wu, XiaoMei Shao , and Ruijie Ma   
Research Article (15 pages), Article ID 8859672, Volume 2020 (2020)




**Early Electroacupuncture Extends the rtPA Time Window to 6 h in a Male Rat Model of Embolic Stroke via the ERK1/2-MMP9 Pathway**

Xin-chang Zhang , Ya-hui Gu, Wen-tao Xu, Yang-yang Song, Ao Zhang, Zhi-hui Zhang, Si-yuan Jiang, Si-qi Chang, and Guang-xia Ni   
Research Article (15 pages), Article ID 8851089, Volume 2020 (2020)



**The Electric Shock during Acupuncture: A Normal Needling Sensation or a Warning Sign**

Yongsong Guo , Ke Zhu , Jing Guo , Yongbing Kuang , Zhihui Zhao , and Weihong Li   
Review Article (7 pages), Article ID 8834573, Volume 2020 (2020)


**Effects of Transcutaneous Auricular Vagus Nerve Stimulation on Peripheral and Central Tumor Necrosis Factor Alpha in Rats with Depression-Chronic Somatic Pain Comorbidity**

Xiao Guo , Yuanyuan Zhao, Feng Huang, Shaoyuan Li, Man Luo, Yu Wang, Jinling Zhang, Liang Li, Yue Zhang, Yue Jiao, Bin Zhao, Junying Wang, Hong Meng, Zhangjin Zhang , and Peijing Rong   
Research Article (10 pages), Article ID 8885729, Volume 2020 (2020)





**Effect of Electroacupuncture on Pain Perception and Pain-Related Affection: Dissociation or Interaction Based on the Anterior Cingulate Cortex and S1**

Yan Shi, Shujing Yao, Zui Shen, Lijiao She, Yingling Xu, Boyi Liu, Yi Liang, Yongliang Jiang, Jing Sun, Yuanyuan Wu, Junying Du, Yilin Zhu, Zemin Wu, Jianqiao Fang , and Xiaomei Shao   
Research Article (10 pages), Article ID 8865096, Volume 2020 (2020)

**Electroacupuncture Pretreatment Elicits Tolerance to Cerebral Ischemia/Reperfusion through Inhibition of the GluN2B/m-Calpain/p38 MAPK Proapoptotic Pathway**





Bao-yu Zhang, Guan-ran Wang, Wen-hua Ning, Jian Liu, Sha Yang, Yan Shen, Yang Wang, Meng-xiong Zhao, and Li Li   
Research Article (14 pages), Article ID 8840675, Volume 2020 (2020)

**Electroacupuncture Involved in Motor Cortex and Hypoglossal Neural Control to Improve Voluntary Swallowing of Poststroke Dysphagia Mice**

Shuai Cui, Shuqi Yao, Chunxiao Wu , Lulu Yao, Peidong Huang, Yongjun Chen , Chunzhi Tang , and Nenggui Xu   
Research Article (18 pages), Article ID 8857543, Volume 2020 (2020)

## Contents




### **Effects and Mechanisms of Acupuncture Combined with Mesenchymal Stem Cell Transplantation on Neural Recovery after Spinal Cord Injury: Progress and Prospects**

Huiling Tang, Yi Guo , Yadan Zhao, Songtao Wang, Jiaqi Wang, Wei Li, Siru Qin, Yinan Gong, Wen Fan, Zelin Chen, Yongming Guo , Zhifang Xu , and Yuxin Fang   
Review Article (13 pages), Article ID 8890655, Volume 2020 (2020)

### **Applications of Acupuncture Therapy in Modulating the Plasticity of Neurodegenerative Disease and Depression: Do MicroRNA and Neurotrophin BDNF Shed Light on the Underlying Mechanism?**

Xia Li, Jun Zhao, Zhigang Li , Li Zhang , and Zejun Huo   
Review Article (17 pages), Article ID 8850653, Volume 2020 (2020)

### **EA Ameliorated Depressive Behaviors in CUMS Rats and Was Related to Its Suppressing Autophagy in the Hippocampus**

Zhinan Zhang , Xiaowen Cai, Zengyu Yao, Feng Wen, Zhiyi Fu, Jiping Zhang, Zheng Zhong, Yong Huang , and Shanshan Qu   
Research Article (9 pages), Article ID 8860968, Volume 2020 (2020)


### **Electroacupuncture on Trigeminal Nerve-Innervated Acupoints Ameliorates Poststroke Cognitive Impairment in Rats with Middle Cerebral Artery Occlusion: Involvement of Neuroprotection and Synaptic Plasticity**

Yu Zheng, Zongshi Qin, Bun Tsoi, Jiangang Shen, and Zhang-Jin Zhang   
Research Article (13 pages), Article ID 8818328, Volume 2020 (2020)


### **Microglia TREM2: A Potential Role in the Mechanism of Action of Electroacupuncture in an Alzheimer's Disease Animal Model**

Yujie Li, Jing Jiang , Qisheng Tang , Huiling Tian , Shun Wang, Zidong Wang, Hao Liu, Jiayi Yang, and Jingyu Ren  
Research Article (8 pages), Article ID 8867547, Volume 2020 (2020)


### **Disease Stage-Associated Alterations in Learning and Memory through the Electroacupuncture Modulation of the Cortical Microglial M1/M2 Polarization in Mice with Alzheimer's Disease**

Long Li, Le Li, Jiayong Zhang, Sheng Huang, Weilin Liu, Zhifu Wang, Shengxiang Liang, Jing Tao, and Lidian Chen   
Research Article (14 pages), Article ID 8836173, Volume 2020 (2020)

### **Machine Learning in Neuroimaging: A New Approach to Understand Acupuncture for Neuroplasticity**

Tao Yin, Peihong Ma, Zilei Tian, Kunnan Xie, Zhaoxuan He, Ruirui Sun, and Fang Zeng   
Review Article (14 pages), Article ID 8871712, Volume 2020 (2020)

### **Acupuncture Modulates Disrupted Whole-Brain Network after Ischemic Stroke: Evidence Based on Graph Theory Analysis**




Xiao Han , He Jin, Kuangshi Li , Yanzhe Ning, Lan Jiang, Pei Chen, Hongwei Liu, Yong Zhang , Hua Zhang, Zhongjian Tan, Fangyuan Cui, Yi Ren, Lijun Bai , and Yihuai Zou   
Research Article (10 pages), Article ID 8838498, Volume 2020 (2020)





---




**Electroacupuncture-Induced Plasticity between Different Representations in Human Motor Cortex**

Weiqin Peng , Tiange Yang, Jiawei Yuan , Jianpeng Huang, and Jianhua Liu 

Research Article (8 pages), Article ID 8856868, Volume 2020 (2020)

## Research Article

# Distinctive Alterations of Functional Connectivity Strength between Vascular and Amnesic Mild Cognitive Impairment

Hui Li <sup>1</sup>, Shuai Gao,<sup>1</sup> Xiuqin Jia,<sup>1</sup> Tao Jiang <sup>1</sup> and Kuncheng Li <sup>2,3</sup>

<sup>1</sup>Department of Radiology, Beijing Chaoyang Hospital, Capital Medical University, Beijing 100020, China

<sup>2</sup>Department of Radiology, Xuanwu Hospital, Capital Medical University, Beijing 10053, China

<sup>3</sup>Beijing Key Lab of MRI and Brain Informatics, Beijing 10053, China

Correspondence should be addressed to Tao Jiang; [jiangt8166@hotmail.com](mailto:jiangt8166@hotmail.com) and Kuncheng Li; [cjr.likuncheng@vip.163.com](mailto:cjr.likuncheng@vip.163.com)

Received 27 May 2020; Revised 2 November 2020; Accepted 30 April 2021; Published 20 May 2021

Academic Editor: Clive.R. Bramham

Copyright © 2021 Hui Li et al. This is an open access article distributed under the Creative Commons Attribution License, which permits unrestricted use, distribution, and reproduction in any medium, provided the original work is properly cited.

Widespread structural and functional alterations have been reported in the two highly prevalent mild cognitive impairment (MCI) subtypes, amnesic MCI (aMCI) and vascular MCI (VaMCI). However, the changing pattern in functional connectivity strength (FCS) remains largely unclear. The aim of the present study is to detect the differences of FCS and to further explore the detailed resting-state functional connectivity (FC) alterations among VaMCI subjects, aMCI subjects, and healthy controls (HC). Twenty-six aMCI subjects, 31 VaMCI participants, and 36 HC participants underwent cognitive assessments and resting-state functional MRI scans. At first, one-way ANCOVA and *post hoc* analysis indicated significant decreased FCS in the left middle temporal gyrus (MTG) in aMCI and VaMCI groups compared to HC, especially in the VaMCI group. Then, we selected the left MTG as a seed to further explore the detailed resting-state FC alterations among the three groups, and the results indicated that FC between the left MTG and some frontal brain regions were significantly decreased mainly in VaMCI. Finally, partial correlation analysis revealed that the FC values between the left MTG and left inferior frontal gyrus were positively correlated with the cognitive performance episodic memory and negatively related to the living status. The present study demonstrated that different FCS alterations existed in aMCI and VaMCI. These findings may provide a novel insight into the understanding of pathophysiological mechanisms underlying different MCI subtypes.

## 1. Introduction

Mild cognitive impairment (MCI), associated with deficits in multiple cognitive domains without notable affection on daily activities, is regarded as a risk state for dementia [1]. The two highly prevalent subtypes, amnesic MCI (aMCI) and vascular MCI (VaMCI), are considered the prodromal stage of Alzheimer's disease (AD) and vascular dementia (VD), respectively [2, 3]. It has been a notion that VaMCI subjects exhibit significant impairment in executive function and semantic memory while aMCI subjects show predominant deficits in episodic memory [4].

Magnetic resonance imaging (MRI) is an important imaging method for pathophysiological mechanism investigation and differential diagnosis of MCI subtypes. Wide-

spread structural abnormalities and functional alterations have been reported in both VaMCI and aMCI groups [5–8]. Gray matter atrophies are mainly distributed in frontal and temporal brain regions, posteromedial cortices, and several subcortical brain sites, especially the medial temporal lobe, including the hippocampus and entorhinal cortex [9]. Using diffusion MRI scanning, microstructural deteriorations within the corpus callosum, capsule, periventricular white matter, cingulum, and occipitofrontal fasciculi have been reported [10–12]. Yu et al. reported significant differences in the relationship between fractional anisotropy (FA) and the Auditory Verbal Learning Test (AVLT) between the VaMCI and aMCI groups [13]. Functional connectivity (FC) changes are predominantly found in the default mode network and the medial temporal lobe [5, 6, 14]. Both

decreased and increased brain activities related to the severity of cognitive decline have been demonstrated. Graph theory-based network analyses also reveal significant dysregulation of the topological organization of functional brain networks [15].

Recently, based on the graph theory, the human brain is considered a complex, interconnected network with a set of nodes linked by connections to support efficient information processing and integration [16]. Converging evidences in both structural [17] and functional network analyses [18] have demonstrated that some specific nodes with a large number of connections (or large degree) [19] play critical roles in fast information integration and communication with minimal energy cost [20]. Previous studies have investigated the changing pattern of functional network centrality by calculating functional connectivity strength (FCS) in some diseases such as social anxiety disorder and provide a novel insight into the understanding of underlying pathophysiological mechanisms [21]. Although previous studies have demonstrated altered FC in different MCI subtypes, the changing pattern in FCS remains unclear.

In the present study, we detected the differences in FCS among VaMCI subjects, aMCI subjects, and healthy control (HC) participants. Then, seed-based connectivity analysis were performed to further explore the detailed resting-state FC alterations, using the clusters showing significant differences in FCS as the seeds. We assumed that these MCI subtypes would show distinct FCS and FC changes within their signature large-scale networks as compared to HC. Further, we would explore how these changes relate to neuropsychological deficits in VaMCI and aMCI.

## 2. Materials and Methods

**2.1. Participants.** The study was conducted under a research protocol approved by the Ethics Committee of Beijing Xuanwu Hospital. Written informed consent was obtained from all participants prior to the study.

Twenty-six aMCI subjects, 31 VaMCI subjects, and 36 HC participants were recruited from Xuanwu Hospital in Beijing between 2017 and 2019. We followed the methods of Li et al. [22]. All participants underwent detailed medical history collection, physical examination, and neuropsychological evaluation by experienced neurologists that have been trained to unify the evaluation criteria. Neuropsychological assessments included Clinical Dementia Rating (CDR), Mini Mental State Examination (MMSE), Montreal Cognitive Assessment (MoCA), and activities of daily living (ADL).

The diagnosis of aMCI followed the criteria stipulated in 2011 by the National Institute on Aging and the Alzheimer's Association [3]. Other two conditions were satisfied as follows: (a) CDR score of 0.5 and a score of at least 0.5 on the memory domain [23] and (b) medial temporal lobe or hippocampal atrophy on MRI [24, 25].

The criteria used for the selection for the HC were as follows: (a) no complaints of cognitive changes, (b) no current or previous diagnosis of any neurological or psychiatric disorders, (c) no neurological deficiencies in physical examina-

tions, (d) no abnormal neurological findings on brain MRI, and (e) CDR score of 0.

The inclusion criteria for the VaMCI were based on the *Diagnostic and Statistical Manual of Mental Disorders* (DSM), fourth edition, for VaMCI [26] including the following: (a) complaint of cognitive impairment, at least at one cognitive domain; (b) objective evidence for cognitive decline; (c) the clinical characteristics being consistent with the vascular etiology; (d) history of cerebrovascular disease, physical examination, and/or neuroimaging evidence for cerebrovascular disease; (c) exclusion of other possible diseases; and (d) ability to maintain independence in daily activities.

Participants were excluded if they had a history of psychiatric disorder and neurological conditions affecting cognition, such as head injury, depression, alcohol use disorder, epilepsy, and Parkinson's disease. Additional exclusion criteria included major medical illness, severe visual or hearing loss, and contraindications for MRI.

**2.2. Magnetic Resonance Imaging Procedures.** The subjects were scanned using a specific 3-Tesla GE scanner (General Electric, MRI750W, America). All participants were asked to remain still, stay awake, and keep their eyes closed. Head motion and scanner noise were reduced using foam padding and earplugs. All subjects underwent clinical standardized axial T2, axial fluid-attenuated inversion recovery (FLAIR), sagittal T1, and resting-state functional MRI (fMRI) scans using an echo-planar imaging (EPI) sequence. The following parameters were used for fMRI images for aMCI and HC participants: repetition time (TR) = 2000 ms, echo time (TE) = 30 ms, flip angle (FA) = 90°, field of view (FOV) = 256 × 256 mm<sup>2</sup>, data matrix = 64 × 64, 36 axial slices, slice thickness/gap = 3/1 mm, and number of repetitions = 180. Meanwhile, the following parameters were used for fMRI images for VaMCI subjects: TR = 2000 ms, TE = 30 ms, FA = 90°, FOV = 220 × 220 mm<sup>2</sup>, slice thickness/gap = 3.6/0.4 mm, 36 axial slices, data matrix = 64 × 64, and number of repetitions = 185. Parameters for axial T2 were as follows: TR = 4581 ms, TE = 82 ms, FOV = 220 × 220 mm<sup>2</sup>, slice thickness/gap = 5.5/1.0 mm, data matrix = 416 × 416, and 20 axial slices. Parameters for sagittal T1 were as follows: TR = 1750 ms, TE = 24 ms, FOV = 240 × 216 mm<sup>2</sup>, slice thickness/gap = 5.5/1.0 mm, data matrix = 288 × 224, and 20 axial slices. Parameters for axial FLAIR were as follows: TR = 7000 ms, TE = 120 ms, FOV = 220 × 220 mm<sup>2</sup>, slice thickness/gap = 5.5/1.0 mm, data matrix = 416 × 416, and 20 axial slices.

**2.3. MRI Data Preprocessing.** Functional image data were preprocessed using the Data Processing Assistant for Resting-State fMRI (DPARSF) software package v4.5 [27] and Statistical Parametric Mapping 12 based on MATLAB 2013a. The first 5 images of each fMRI dataset were discarded to reduce the initial fluctuation of MRI signals in aMCI and HC, while the first 10 images of each fMRI dataset were discarded in VaMCI. The numbers of remaining images were all the same (175 images) in the three groups. Briefly, the fMRI time series were first corrected for within-scan acquisition

time differences between slices and realigned to correct for head motion. The participants with head movement exceeding 2.0 mm of translation or 2.0° of rotation in any direction were excluded. In addition, one-way analysis of variance showed that there was no significant difference in the values of the mean framewise displacement (FD) among the three groups. All the realigned images were spatially normalized to the Montreal Neurological Institute EPI template, and each voxel was resampled to  $3 \times 3 \times 3 \text{ mm}^3$ . To avoid introducing artificial local spatial correlations, the images were not smoothed [28]. Denoising steps included linear detrending and regression of the six motion parameters and their first-order derivatives and regression of white matter and cerebrospinal fluid (CSF) [29]. Then, the time series were temporally band-pass filtered (0.01–0.08 Hz) to reduce the effects of high-frequency physiological noises.

**2.4. Network Analysis.** For each voxel, the time series was extracted and Pearson's correlation coefficients between the time series of the voxel and all other voxels' time series were calculated within a gray matter mask ( $N$  voxels = 58,108). Then, the correlation coefficients greater than 0.2 were averaged over the gray matter mask, and a 3D FCS map for each subject was obtained [30]. Finally, the FCS map was converted to  $z$  scores and smoothed with a 6 mm full width at half-maximum Gaussian kernel.

### 3. Statistical Analyses

**3.1. Demographic and Neuropsychological Variables.** For gender assessment,  $\chi^2$  tests were used. The age, education level, and cognitive performance differences among the three groups were estimated by one-way analysis of variance. These analyses were implemented in SPSS 21.

**3.2. Group Differences in Functional Connectivity Strength.** One-sample  $t$ -tests were performed to identify the patterns of FCS within each group [21], and the significant threshold was set at voxel-level  $p < 0.05$  corrected for multiple comparisons using the family-wise error rate (FWE). To find the altered FCS regions, one-way analysis of covariance (ANCOVA) was then performed to compare the FCS maps among the three groups, with age, gender, and education as covariates. The significant threshold was set at cluster-level  $p < 0.05$ , FWE corrected. The FCS values of the regions showing significant group difference were extracted for *post hoc* pairwise comparisons and partial correlations. *Post hoc* pairwise comparisons were conducted by independent-sample  $t$ -tests to compute the differences between any two groups using SPSS 21.

**3.3. Seed-Based Resting-State Functional Connectivity Analysis.** Seed-based connectivity analysis were performed to further explore the detailed resting-state FC alterations, using the clusters showing significant differences in FCS as the seeds. One-way ANCOVA was performed on the FC maps for each identified seed. The significant threshold was set at voxel-level  $p < 0.05$ , FWE corrected, with age, gender, and years of education as covariates. The FC values of the

regions showing significant group differences were extracted for *post hoc* pairwise comparisons and partial correlations.

**3.4. Relationships between Regional Connectivity Measures and Cognitive Performance.** Partial correlation analysis was performed to explore the relationship between the connectivity measurements (i.e., FCS and seed-based FC) and clinical variables in VaMCI and aMCI separately, with age, gender, and years of education as covariates. Statistical significance was set at  $p < 0.05$ .

## 4. Results

**4.1. Demographics and Clinical Characteristics of the Participants.** The demographic and clinical data are shown in Table 1. Significant differences were found in cognitive assessments among the three groups while age, gender, and education years were matched well. Both MCI subtype groups showed lower scores in MMSE ( $p < 0.001$ ) and MoCA ( $p < 0.001$ ) and higher CDR scores ( $p < 0.001$ ), indicating significant general cognitive decline as compared to HC. Meanwhile, both MCI subtype groups showed higher ADL scores ( $p < 0.001$ ). In addition, the aMCI group showed lower cognitive assessment scores and higher ADL scores than VaMCI.

**4.2. Within-Group FCS Analyses.** The results derived from one-sample  $t$ -tests for the three groups are separately shown in Figures S1–S3. Functional nodes with a large number of connections were found mainly in the temporal and parietal brain regions, as well as several occipital and frontal cortices.

**4.3. Between-Group FCS Analyses.** One-way ANCOVA indicated significant FCS difference in the left middle temporal gyrus (MTG) among the three groups (Table 2, Figure 1).

*Post hoc* analysis revealed that (1) as compared to HC, subjects with aMCI showed significant decreased FCS in the left MTG; (2) as compared to HC, subjects with VaMCI showed significant decreased FCS in the left MTG; and (3) as compared to aMCI, subjects with VaMCI showed significant decreased FCS in the left MTG (Figure 1).

**4.4. Alterations in Seed-Based Resting-State Functional Connectivity.** For further detailed analysis regarding the left MTG FC pattern, the subsequent seed-based FC analysis revealed that the left MTG network in HC was composed of the medial frontal, temporal cortical, and parietal sites. However, the frontal sites were excluded in both aMCI and VaMCI (Figures S4–S6). One-way ANCOVA indicated significant FC differences between the left MTG and the right orbital frontal gyrus (OFG), the left inferior frontal gyrus (IFG), and the right IFG among the three groups. *Post hoc* analysis revealed that significant FC disruptions in the right OFG and the left IFG were found only in VaMCI, while significant reduced FC in the right IFG were found in both aMCI and VaMCI with more serious disruption in the VaMCI group (Table 2, Figure 2).

TABLE 1: Clinical characteristics of subjects with aMCI and VaMCI and HC.

Characteristics	HC ( $n = 36$ )	VaMCI ( $n = 31$ )	aMCI ( $n = 26$ )	Group $p$
Age (years)	64.22 $\pm$ 6.97	64.93 $\pm$ 10.11	66.04 $\pm$ 7.92	0.62
Gender, M/F	17/19	18/13	8/18	0.11
Education (years)	10.72 $\pm$ 5.41	9.00 $\pm$ 2.00	10.77 $\pm$ 4.65	0.08
CDR	0	0.5	0.5	<0.001
MMSR	28.13 $\pm$ 2.77	26.32 $\pm$ 2.05	23.73 $\pm$ 3.85	<0.001
MoCA	25.22 $\pm$ 2.89	23.32 $\pm$ 1.32	19.81 $\pm$ 4.71	<0.001
ADL	20.00 $\pm$ 0.00	20.87 $\pm$ 1.43	22.84 $\pm$ 2.78	<0.001

Values represent means  $\pm$  SD;  $p$  values were derived from the one-way NOVA test comparing the three groups, except for “gender” where the  $p$  value was obtained using the  $\chi^2$  test. MMSE: Mini Mental State Examination; MoCA: Montreal Cognitive Assessment; ADL: activities of daily living; VaMCI: vascular mild cognitive impairment; aMCI: amnesic mild cognitive impairment; HC: healthy control.

TABLE 2: FCS differences and left MTG FC differences among subjects with aMCI and VaMCI and HC.

Brain regions	Cluster size	MNI			$F$ -score
		$x$	$y$	$z$	
FCS					
Lt. MTG	189	-60	-3	-21	9.823
FC					
Rt. OFG	26	33	48	-3	20.8862
Rt. IFG	50	57	33	6	27.3006
Lt. IFG	98	-45	18	18	27.7231

Lt.: left; Rt.: right; FC: functional connectivity; MTG: middle temporal gyrus; OFG: orbital frontal gyrus; IFG: inferior frontal gyrus; VaMCI: vascular mild cognitive impairment; aMCI: amnesic mild cognitive impairment; HC: healthy control; MNI: Montreal Neurological Institute.

**4.5. Correlations between Cognitive Performances and Connectivity Measures.** Partial correlation analysis revealed that the FC values between the left MTG and left IFG were positively correlated with the cognitive performance episodic memory measured by MoCA scores ( $r = 0.41$ ,  $p = 0.03$ , Figure 3(a)) and negatively correlated with ADL scores ( $r = -0.44$ ,  $p = 0.02$ , Figure 3(b)) in the VaMCI group.

## 5. Discussion

Based on resting-state fMRI and graph theory approaches, the present study reported decreased FCS in the left MTG in both VaMCI subjects and aMCI subjects, especially in the VaMCI group. Furthermore, more frontal regions showed disrupted resting-state FC to left MTG in the VaMCI group than in the aMCI group. These aberrant brain connectivities may be the neurobiological mechanism underlying the cognitive deficits.

Based on the computational analysis of anatomic connectivity, Sporns et al. formally defined the cortex nodes that have disproportionately numerous connections as hubs [31]. Network analysis studies using postmortem tracing techniques in nonhuman primates [32], vivo tract-tracing [33], and fMRI in humans [34] further confirmed the existence of hubs. An accurate reference map of prominent cortical hubs consisting of posterior cingulate, lateral temporal,

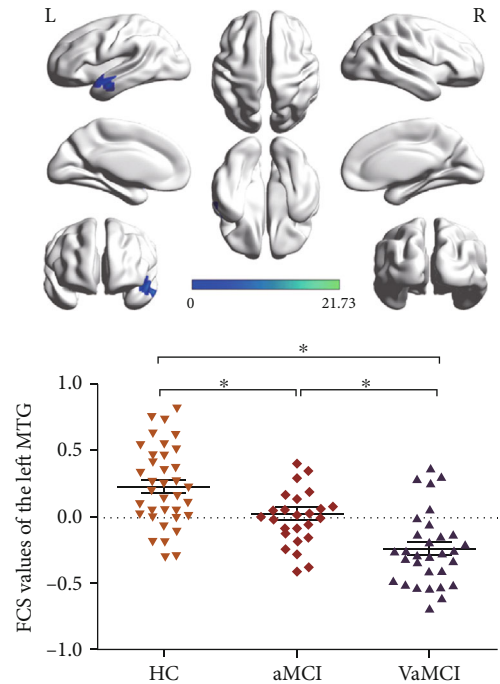


FIGURE 1: The result of one-way ANCOVA and *post hoc* analysis indicated significant decreased FCS in the left MTG among the VaMCI, aMCI, and HC. \* means  $p < 0.05$  in the two-sample  $t$ -test using SPSS21. L: left; R: right; MTG: middle temporal gyrus; FCS: functional connectivity strength; VaMCI: vascular mild cognitive impairment; aMCI: amnesic mild cognitive impairment; HC: healthy control.

lateral parietal, and medial/lateral prefrontal cortices had been obtained, and the left MTG is one of the peak locations of the largest 10 hubs [35].

MTG plays an important role in verbal short-term memory [36] and global cognitive function [37]. Previous studies have shown that MTG is one of the most vulnerable brain regions affected by cognition impairment-related pathological changes. In voxel-based morphometric study, significant gray matter volume reductions in MTG have been reported in both patients with aMCI and VaMCI [38–40]. As for the whole-brain function network, an altered FC pattern and FC density in MTG have been reported by fMRI [5, 41, 42].



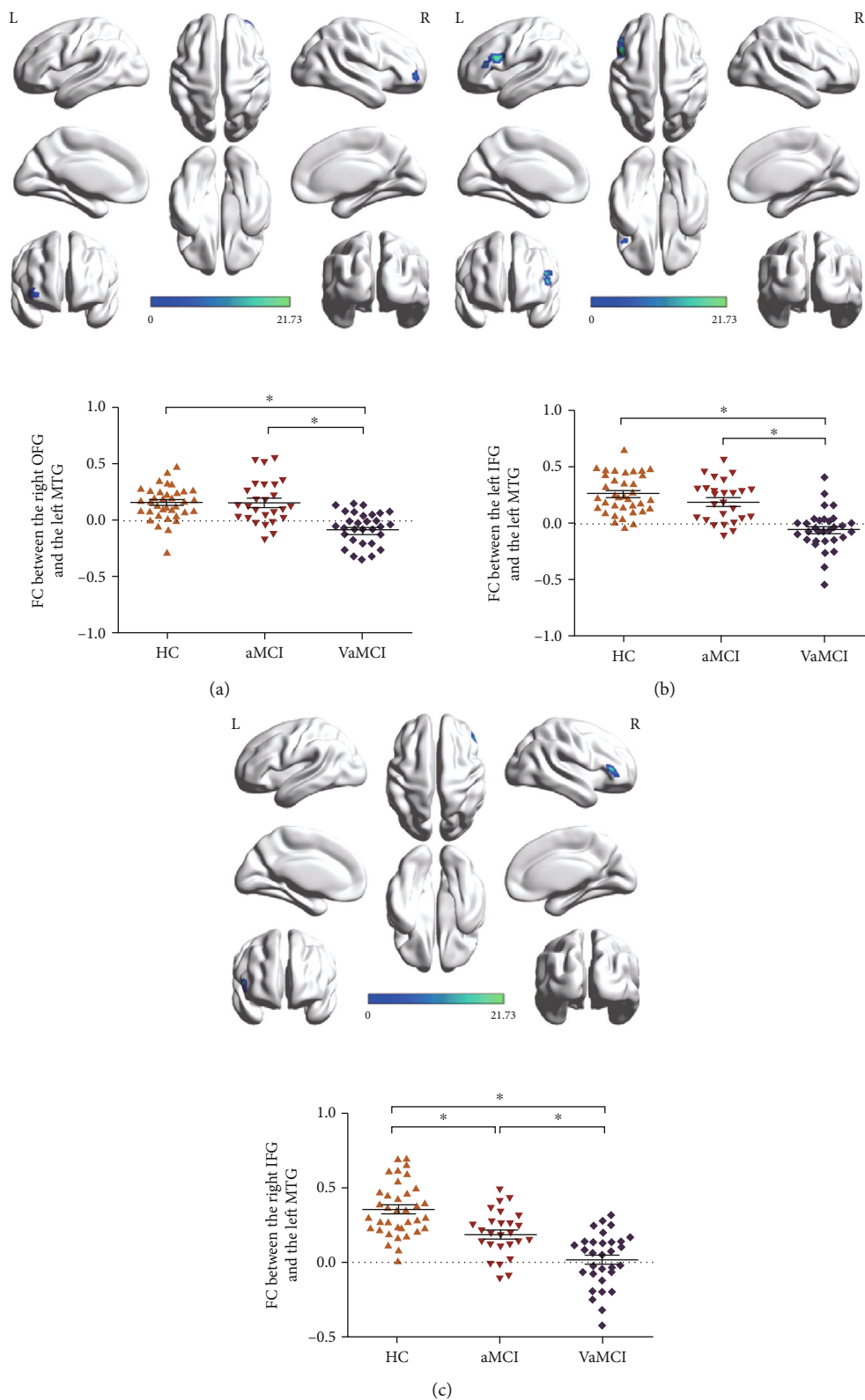


FIGURE 2: The results of one-way ANCOVA and *post hoc* analysis indicated significant decreased FC between the left MTG and the right OFG (a), the left IFG (b), and the right IFG (c) among the three groups. \* means  $p < 0.05$  in the two-sample  $t$ -test using SPSS21. L: left; R: right; FC: functional connectivity; MTG: middle temporal gyrus; OFG: orbital frontal gyrus; IFG: inferior frontal gyrus; VaMCI: vascular mild cognitive impairment; aMCI: amnesic mild cognitive impairment; HC: healthy control.



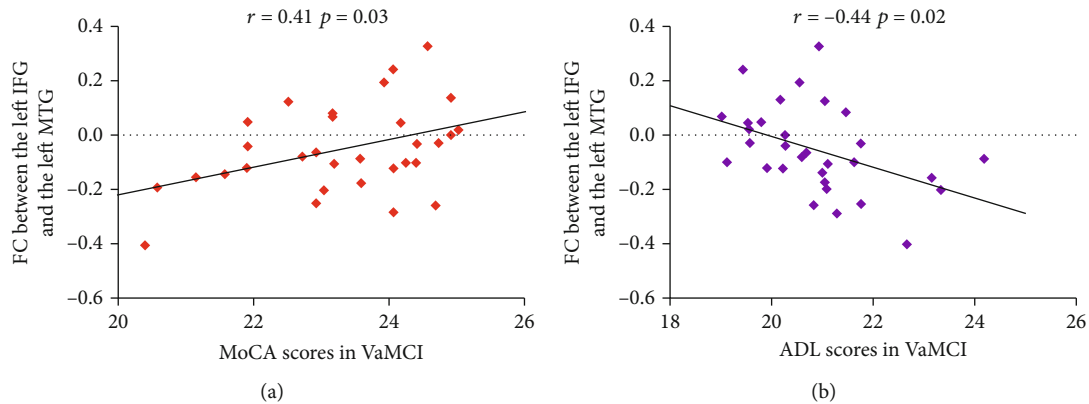


FIGURE 3: (a) The FC values between the left MTG and left IFG were positively correlated with the cognitive performance episodic memory measured by MoCA scores. (b) The FC values between the left MTG and left IFG were negatively correlated with ADL scores. FC: functional connectivity; MTG: middle temporal gyrus; IFG: inferior frontal gyrus; MoCA: Montreal Cognitive Assessment; ADL: activities of daily living; VaMCI: vascular mild cognitive impairment.

In addition, significantly decreased amplitude of low-frequency fluctuation (ALFF) in the left MTG had been reported in VaMCI [43]. In the present study, the left MTG was found to exhibit decreased FCS in the aMCI and VaMCI groups. Furthermore, compared with aMCI, the VaMCI group showed more serious FCS reduction in MTG. These results suggested that, as a critical network node with rich connections, the MTG was preferentially targeted in cognition impairment-related diseases, especially in the VaMCI group.

Subsequently, we made the left MTG-based whole-brain FC maps for further analysis. Notably, reduced FC between the left MTG and some frontal brain regions, including the right OFG and bilateral IFG, were mainly reported in the VaMCI group. Previous studies indicated that the small vessel disease-related cognitive impairments, including the deterioration of psychomotor speed, executive control, and global cognitive function, may be related to disruption and disconnection of the frontal-subcortical pathways [44]. Both IFG and OFG were associated with the executive function [45, 46]. This is consistent with the notion that the dorsolateral prefrontal circuit is involved mainly in executive function [47, 48]. Using fMRI, decreased ALFF and FC in the frontal lobe have been repeatedly reported in VaMCI [49–52]. In addition, orbitofrontal syndromes, such as disinhibition and decreased social behavior, are more frequent in VaMCI than in aMCI. In the present study, disrupted FC between the frontal lobe and MTG was found in the MCI group, especially the VaMCI group. Furthermore, FC values between the left MTG and left IFG were associated with cognitive and living status, each reflected by the MoCA and ADL scores in VaMCI patients, which may be related to the executive dysfunction.

Several limitations need to be considered for this study. First, the sample size of the study was relatively small, and studies with a larger sample will be needed to replicate the current findings. Second, there were some subtle differences between the two MRI sequences. Unified MRI sequence parameters should be used in the future study.

In conclusion, the present study demonstrated for the first time that the MCI was associated with disrupted functional brain networks and significantly decreased FCS in the MTG. Furthermore, disrupted FC between the frontal lobe and MTG was found in the VaMCI group, which may be related to the executive dysfunction. These findings may open a novel way to better understand the pathophysiological mechanisms of MCI.

### Data Availability

The datasets analyzed during the current study are not publicly available due to the unfinished study of the whole project but are available from the corresponding author on reasonable request.

### Conflicts of Interest

The authors declare that they have no conflicts of interest.

### Authors' Contributions

Hui Li and Shuai Gao carried out data collection and wrote the manuscript. Xiuqin Jia carried out data analysis. Tao Jiang and Kuncheng Li contributed to the conceptualization and design of the study and revised the manuscript. Hui Li and Shuai Gao contributed equally to this work.

### Acknowledgments

This work was supported partly by grants from the National Natural Science Foundation of China (62076169) and Beijing Municipal Science and Technology Commission (Z171100000117001).

### Supplementary Materials

The attached file of supplementary materials presents the results derived from one-sample *t*-tests of within-group analysis for the three groups. Figures S1–S3 show the functional nodes with a large number of connections in HC, aMCI,

and VaMCI, separately. Figures S4–S6 show the whole-brain FC of the left MTG in HC, aMCI, and VaMCI, separately. (*Supplementary Materials*)






## References

- [1] S. Gauthier, B. Reisberg, M. Zaudig et al., “Mild cognitive impairment,” *Lancet*, vol. 367, no. 9518, pp. 1262–1270, 2006.
- [2] P. Sachdev, R. Kalaria, J. O’Brien et al., “Diagnostic criteria for vascular cognitive disorders: a VASCOG statement,” *Alzheimer Disease and Associated Disorders*, vol. 28, no. 3, pp. 206–218, 2014.
- [3] M. S. Albert, S. T. Dekosky, D. Dickson et al., “The diagnosis of mild cognitive impairment due to Alzheimer’s disease: recommendations from the National Institute on Aging–Alzheimer’s Association workgroups on diagnostic guidelines for Alzheimer’s disease,” *Alzheimers & Dementia*, vol. 7, no. 3, pp. 270–279, 2011.
- [4] N. L. Graham, T. Emery, and J. R. Hodges, “Distinctive cognitive profiles in Alzheimer’s disease and subcortical vascular dementia,” *Journal of Neurology, Neurosurgery, and Psychiatry*, vol. 75, no. 1, pp. 61–71, 2004.
- [5] L. Yi, J. Wang, L. Jia et al., “Structural and functional changes in subcortical vascular mild cognitive impairment: a combined voxel-based morphometry and resting-state fMRI study,” *PLoS One*, vol. 7, no. 9, 2012.
- [6] Y. W. Sun, L. D. Qin, Y. Zhou et al., “Abnormal functional connectivity in patients with vascular cognitive impairment, no dementia: a resting-state functional magnetic resonance imaging study,” *Behavioural Brain Research*, vol. 223, no. 2, pp. 388–394, 2011.
- [7] D. Y. Lee, E. Fletcher, O. Martinez et al., “Vascular and degenerative processes differentially affect regional interhemispheric connections in normal aging, mild cognitive impairment, and Alzheimer disease,” *Stroke*, vol. 41, no. 8, pp. 1791–1797, 2010.
- [8] X. Li, D. Li, Q. Li et al., “Hippocampal subfield volumetry in patients with subcortical vascular mild cognitive impairment,” *Scientific Reports*, vol. 6, no. 1, 2016.
- [9] M. Pihlajamaki, A. M. Jauhiainen, and H. Soininen, “Structural and functional MRI in mild cognitive impairment,” *Current Alzheimer Research*, vol. 6, no. 2, pp. 179–185, 2009.
- [10] J. M. Papma, M. de Groot, I. de Koning et al., “Cerebral small vessel disease affects white matter microstructure in mild cognitive impairment,” *Human Brain Mapping*, vol. 35, no. 6, pp. 2836–2851, 2014.
- [11] B. Bosch, E. M. Arenaza-Urquijo, L. Rami et al., “Multiple DTI index analysis in normal aging, amnesic MCI and AD. Relationship with neuropsychological performance,” *Neurobiology of Aging*, vol. 33, no. 1, pp. 61–74, 2012.
- [12] D. Medina, L. Detolledo-Morrell, F. Urresta et al., “White matter changes in mild cognitive impairment and AD: a diffusion tensor imaging study,” *Neurobiology of Aging*, vol. 27, no. 5, pp. 663–672, 2006.
- [13] Y. Yu, X. Liang, H. Yu et al., “How does white matter microstructure differ between the vascular and amnesic mild cognitive impairment?,” *Oncotarget*, vol. 8, no. 1, pp. 42–50, 2017.
- [14] A. Lin, A. R. Laird, P. T. Fox, and J. H. Gao, “Multimodal MRI neuroimaging biomarkers for cognitive normal adults, amnesic mild cognitive impairment, and Alzheimer’s disease,” *Neurology Research International*, vol. 2012, Article ID 907409, 17 pages, 2012.
- [15] L. Y. Yi, X. Liang, D. M. Liu et al., “Disrupted topological organization of resting-state functional brain network in subcortical vascular mild cognitive impairment,” *CNS Neuroscience & Therapeutics*, vol. 21, no. 10, pp. 846–854, 2015.
- [16] E. Bullmore and O. Sporns, “Complex brain networks: graph theoretical analysis of structural and functional systems,” *Nature Reviews Neuroscience*, vol. 10, no. 3, pp. 186–198, 2009.
- [17] Y. He and A. Evans, “Graph theoretical modeling of brain connectivity,” *Current Opinion in Neurology*, vol. 23, no. 4, pp. 341–350, 2010.
- [18] Y. He, J. Wang, L. Wang et al., “Uncovering intrinsic modular organization of spontaneous brain activity in humans,” *PLoS One*, vol. 4, no. 4, 2009.
- [19] S. Achard, R. Salvador, B. Whitcher, J. Suckling, and E. Bullmore, “A resilient, low-frequency, small-world human brain functional network with highly connected association cortical hubs,” *Journal of Neuroscience*, vol. 26, no. 1, pp. 63–72, 2006.
- [20] D. S. Bassett and E. T. Bullmore, “Small-world brain networks revisited,” *The Neuroscientist*, vol. 23, no. 5, pp. 499–516, 2017.
- [21] F. Liu, C. Zhu, Y. Wang et al., “Disrupted cortical hubs in functional brain networks in social anxiety disorder,” *Clinical Neurophysiology*, vol. 126, no. 9, pp. 1711–1716, 2015.
- [22] H. Li, X. Jia, Z. Qi et al., “Disrupted functional connectivity of cornu ammonis subregions in amnesic mild cognitive impairment: a longitudinal resting-state fMRI study,” *Frontiers in Human Neuroscience*, vol. 12, 2018.
- [23] R. C. Petersen, J. C. Stevens, M. Ganguli, E. G. Tangalos, J. L. Cummings, and S. T. DeKosky, “Practice parameter: early detection of dementia: mild cognitive impairment (an evidence-based review). Report of the Quality Standards Subcommittee of the American Academy of Neurology,” *Neurology*, vol. 56, no. 9, pp. 1133–1142, 2001.
- [24] P. Scheltens, L. J. Launer, F. Barkhof, H. C. Weinstein, and W. A. Gool, “Visual assessment of medial temporal lobe atrophy on magnetic resonance imaging: interobserver reliability,” *Journal of Neurology*, vol. 242, no. 9, pp. 557–560, 1995.
- [25] M. J. de Leon, J. Golomb, A. E. George et al., “The radiologic prediction of Alzheimer disease: the atrophic hippocampal formation,” *AJNR. American Journal of Neuroradiology*, vol. 14, no. 4, pp. 897–906, 1993.
- [26] American Psychiatric Association, *Diagnostic and Statistical Manual of Mental Disorders*, American Psychiatric Association, Arlington, 5th edition, 2013.
- [27] Y. Chao-Gan and Z. Yu-Feng, “DPARSF: a MATLAB toolbox for “pipeline” data analysis of resting-state fMRI,” *Frontiers in Systems Neuroscience*, vol. 4, no. 13, 2010.
- [28] F. Liu, B. Xie, Y. Wang et al., “Characterization of post-traumatic stress disorder using resting-state fMRI with a multi-level parametric classification approach,” *Brain Topography*, vol. 28, no. 2, pp. 221–237, 2015.
- [29] Y. Behzadi, K. Restom, J. Liau, and T. T. Liu, “A component based noise correction method (CompCor) for BOLD and perfusion based fMRI,” *NeuroImage*, vol. 37, no. 1, pp. 90–101, 2007.
- [30] L. Wang, Z. Dai, H. Peng et al., “Overlapping and segregated resting-state functional connectivity in patients with major depressive disorder with and without childhood neglect,” *Human Brain Mapping*, vol. 35, no. 4, pp. 1154–1166, 2014.

- [31] O. Sporns, C. J. Honey, and R. Kotter, "Identification and classification of hubs in brain networks," *PLoS One*, vol. 2, no. 10, 2007.
- [32] O. Sporns, D. R. Chialvo, M. Kaiser, and C. C. Hilgetag, "Organization, development and function of complex brain networks," *Trends in Cognitive Sciences*, vol. 8, no. 9, pp. 418–425, 2004.
- [33] P. Hagmann, L. Cammoun, X. Gigandet et al., "Mapping the structural core of human cerebral cortex," *PLoS Biology*, vol. 6, no. 7, 2008.
- [34] S. Gupta, J. C. Rajapakse, and R. E. Welsch, "Ambivert degree identifies crucial brain functional hubs and improves detection of Alzheimer's Disease and Autism Spectrum Disorder," *NeuroImage: Clinical*, vol. 25, article 102186, 2020.
- [35] R. L. Buckner, J. Sepulcre, T. Talukdar et al., "Cortical hubs revealed by intrinsic functional connectivity: mapping, assessment of stability, and relation to Alzheimer's disease," *Journal of Neuroscience*, vol. 29, no. 6, pp. 1860–1873, 2009.
- [36] T. Raettig and S. A. Kotz, "Auditory processing of different types of pseudo-words: an event-related fMRI study," *NeuroImage*, vol. 39, no. 3, pp. 1420–1428, 2008.
- [37] B. R. Reed, J. L. Eberling, D. Mungas, M. Weiner, J. H. Kramer, and W. J. Jagust, "Effects of white matter lesions and lacunes on cortical function," *Archives of Neurology*, vol. 61, no. 10, pp. 1545–1550, 2004.
- [38] M. Grau-Olivares, D. Bartrés-Faz, A. Arboix et al., "Mild cognitive impairment after lacunar infarction: voxel-based morphometry and neuropsychological assessment," *Cerebrovascular Diseases*, vol. 23, no. 5-6, pp. 353–361, 2007.
- [39] G. T. Stebbins, D. L. Nyenhuis, C. Wang et al., "Gray matter atrophy in patients with ischemic stroke with cognitive impairment," *Stroke*, vol. 39, no. 3, pp. 785–793, 2008.
- [40] K. Li, W. Chan, R. S. Doody, J. Quinn, and S. Luo, "Prediction of conversion to Alzheimer's disease with longitudinal measures and time-to-event data," *Journal of Alzheimers Disease*, vol. 58, no. 2, pp. 361–371, 2017.
- [41] C. Xue, B. Yuan, Y. Yue et al., "Distinct Disruptive Patterns of Default Mode Subnetwork Connectivity Across the Spectrum of Preclinical Alzheimer's Disease," *Frontiers in Aging Neuroscience*, vol. 11, p. 307, 2019.
- [42] M. Li, G. Zheng, Y. Zheng et al., "Alterations in resting-state functional connectivity of the default mode network in amnesic mild cognitive impairment: an fMRI study," *BMC Medical Imaging*, vol. 17, no. 1, p. 48, 2017.
- [43] C. Li, J. Yang, X. Yin et al., "Abnormal intrinsic brain activity patterns in leukoaraiosis with and without cognitive impairment," *Behavioural Brain Research*, vol. 292, pp. 409–413, 2015.
- [44] J. A. Pettersen, G. Sathiyamoorthy, F. Q. Gao et al., "Microbleed topography, leukoaraiosis, and cognition in probable Alzheimer disease from the Sunnybrook Dementia Study," *Archives of Neurology*, vol. 65, no. 6, pp. 790–795, 2008.
- [45] L. Garcia-Alvarez, J. J. Gomar, A. Sousa, M. P. Garcia-Portilla, and T. E. Goldberg, "Breadth and depth of working memory and executive function compromises in mild cognitive impairment and their relationships to frontal lobe morphometry and functional competence," *Alzheimer's & Dementia: Diagnosis, Assessment & Disease Monitoring*, vol. 11, no. 1, pp. 170–179, 2019.
- [46] E. de Guise, A. Y. Alturki, M. Lague-Beauvais et al., "Olfactory and executive dysfunctions following orbito-basal lesions in traumatic brain injury," *Brain Injury*, vol. 29, no. 6, pp. 730–738, 2015.
- [47] J. M. Unterrainer and A. M. Owen, "Planning and problem solving: from neuropsychology to functional neuroimaging," *Journal of Physiology-Paris*, vol. 99, no. 4-6, pp. 308–317, 2006.
- [48] R. M. Bonelli and J. L. Cummings, "Frontal-subcortical circuitry and behavior," *Dialogues in Clinical Neuroscience*, vol. 9, no. 2, pp. 141–151, 2007.
- [49] Y. Zhuang, Y. Shi, J. Zhang et al., "Neurologic Factors in Patients with Vascular Mild Cognitive Impairment Based on fMRI," *World Neurosurgery*, vol. 149, pp. 461–469, 2011.
- [50] M. Zuo, Y. Xu, X. Zhang et al., "Aberrant brain regional homogeneity and functional connectivity of entorhinal cortex in vascular mild cognitive impairment: a resting-state functional MRI study," *Frontiers in Neurology*, vol. 9, no. 1177, 2018.
- [51] X. Zhou, X. Hu, C. Zhang et al., "Aberrant functional connectivity and structural atrophy in subcortical vascular cognitive impairment: relationship with cognitive impairments," *Frontiers in Aging Neuroscience*, vol. 8, no. 14, 2016.
- [52] L. Ni, R. Liu, Z. Yin et al., "Aberrant spontaneous brain activity in patients with mild cognitive impairment and concomitant lacunar infarction: a resting-state functional MRI study," *Journal of Alzheimer's Disease*, vol. 50, no. 4, pp. 1243–1254, 2016.

## Research Article

# Effect of Acupuncture Stimulation of Hegu (LI4) and Taichong (LR3) on the Resting-State Networks in Alzheimer's Disease: Beyond the Default Mode Network

Shaozhen Ji <sup>1</sup>, Hao Zhang <sup>2</sup>, Wen Qin,<sup>3</sup> Ming Liu,<sup>2</sup> Weimin Zheng,<sup>4</sup> Ying Han,<sup>5</sup> Haiqing Song,<sup>5</sup> Kuncheng Li <sup>6</sup>, Jie Lu <sup>6</sup> and Zhiqun Wang <sup>4</sup>

<sup>1</sup>Department of Neurology, Dongfang Hospital, Beijing University of Chinese Medicine, Beijing 100078, China

<sup>2</sup>Department of Radiology, Dongfang Hospital, Beijing University of Chinese Medicine, Beijing 100078, China

<sup>3</sup>Department of Radiology and Tianjin Key Laboratory of Functional Imaging, Tianjin Medical University General Hospital, Tianjin 300052, China

<sup>4</sup>Department of Radiology, Aerospace Center Hospital, Beijing 100049, China

<sup>5</sup>Department of Neurology, Xuanwu Hospital of Capital Medical University, Beijing 100053, China

<sup>6</sup>Department of Radiology, Xuanwu Hospital of Capital Medical University, Beijing 100053, China

Correspondence should be addressed to Kuncheng Li; [likuncheng1955@126.com](mailto:likuncheng1955@126.com), Jie Lu; [imaginglu@hotmail.com](mailto:imaginglu@hotmail.com), and Zhiqun Wang; [wangzhiqun@126.com](mailto:wangzhiqun@126.com)

Received 26 May 2020; Revised 2 December 2020; Accepted 25 February 2021; Published 8 March 2021

Academic Editor: Malgorzata Kossut

Copyright © 2021 Shaozhen Ji et al. This is an open access article distributed under the Creative Commons Attribution License, which permits unrestricted use, distribution, and reproduction in any medium, provided the original work is properly cited.

It was reported that acupuncture could treat Alzheimer's disease (AD) with the potential mechanisms remaining unclear. The aim of the study is to explore the effect of the combination stimulus of Hegu (LI4) and Taichong (LR3) on the resting-state brain networks in AD, beyond the default network (DMN). Twenty-eight subjects including 14 AD patients and 14 healthy controls (HCs) matched by age, gender, and educational level were recruited in this study. After the baseline resting-state MRI scans, the manual acupuncture stimulation was performed for 3 minutes, and then, another 10 minutes of resting-state fMRI scans was acquired. In addition to the DMN, five other resting-state networks were identified by independent component analysis (ICA), including left frontal parietal network (IFPN), right frontal parietal network (rFPN), visual network (VN), sensorimotor network (SMN), and auditory network (AN). And the impaired connectivity in the IFPN, rFPN, SMN, and VN was found in AD patients compared with those in HCs. After acupuncture, significantly decreased connectivity in the right middle frontal gyrus (MFG) of rFPN ( $P = 0.007$ ) was identified in AD patients. However, reduced connectivity in the right inferior frontal gyrus (IFG) ( $P = 0.047$ ) and left superior frontal gyrus (SFG) ( $P = 0.041$ ) of IFPN and some regions of the SMN (the left inferior parietal lobula ( $P = 0.004$ ), left postcentral gyrus (PoCG) ( $P = 0.001$ ), right PoCG ( $P = 0.032$ ), and right MFG ( $P = 0.010$ )) and the right MOG of VN ( $P = 0.003$ ) was indicated in HCs. In addition, after controlling for the effect of acupuncture on HCs, the functional connectivity of the right cerebellum crus I, left IFG, and left angular gyrus (AG) of IFPN showed to be decreased, while the left MFG of IFPN and the right lingual gyrus of VN increased in AD patients. These findings might have some reference values for the interpretation of the combination stimulus of Hegu (LI4) and Taichong (LR3) in AD patients, which could deepen our understanding of the potential mechanisms of acupuncture on AD.

## 1. Introduction

Alzheimer's disease (AD) is the most common type of dementia and a progressive neurodegenerative disease, which is characterized by two mainly pathological changes includ-

ing amyloid-beta plaques and neurofibrillary tangles, finally resulting in neuronal degeneration and loss [1, 2]. The disease affected millions of elderly subjects worldwide causing remarkable costs to the society. However, there is no effective method for early diagnosis and treatment of AD in the world



[3]. Acupuncture, an alternative and complementary treatment of traditional Chinese medicine, to date, has been widely used to ameliorate impairments in neuropsychiatric symptoms in AD patients and rodent models [4]. However, the potential mechanisms of acupuncture on AD remain unclear.

Neuroplasticity is the ability of the brain's response to intrinsic or environmental demands and reorganizing its structure and function, which is engaged in brain development, learning, and self-healing of neural injuries [5]. Neurogenesis, dendritic remodeling and synapse turnover, and modulation of the structure and function of neuronal networks were involved in this physiological process [5–7]. It was reported that neural plasticity dysfunction may contribute to brain network disruption in AD [8]. Abnormal functional connectivity was demonstrated to be a candidate biomarker for AD, and its severity correlates with clinical disease severity in AD [9]. Previous studies have revealed abnormal large-scale functional brain networks in AD patients, which include the default mode network (DMN) [9], the salience network (SN), frontal parietal network (FPN) [10], visual network (VN) [11], sensorimotor network (SMN) [12], and auditory network (AN) [13]. We previously found that enhanced functional connectivity (FC) in some regions of the DMN caused by the acupuncture stimulation of Hegu (LI4) and Taichong (LR3) might be associated with improvement of cognitive function in AD patients [14]. According to traditional Chinese medicine, both Hegu (LI4) and Taichong (LR3) are known as hubs for internal and external energy gathering and transforming. And the combination stimulus of Hegu (LI4) and Taichong (LR3) is defined as “the four gates,” which is usually applied to promote the circulation of “Qi” and blood throughout the whole body [14]. Besides the DMN, the effect of acupuncture on other large-scale resting-state networks remains unknown in AD.

Herein, we aim to explore the effect of combination stimulus of Hegu (LI4) and Taichong (LR3) on other resting-state networks including the salience network (SN), frontal parietal network (FPN), visual network (VN), sensorimotor network (SMN), and auditory network (AN) in the AD patients. Our finding could enrich the understanding of mechanisms of acupuncture on AD.

## 2. Materials and Methods

**2.1. Subjects.** This study was approved by Xuanwu Hospital Medical Ethics Committee of Capital Medical University. Fourteen patients diagnosed with AD were recruited from Xuanwu Hospital of Capital Medical University and underwent professional and complete physical and neurological examinations, standard laboratory tests, and specific neuropsychological evaluations. The diagnosis of AD fulfilled the Diagnostic and Statistical Manual of Mental Disorders (Fourth Edition) criteria [15] for dementia and the National Institute of Neurological and Communicative Disorders and Stroke/Alzheimer's Disease and Related Disorders Association (NINCDS-ADRDA) criteria [16] for clinically probable AD. Subjects with AD have a global score of clinical dementia rating scale (CDR) of 1 or 2 [17]. Fourteen healthy controls

(HCs) with normal cognitive function matched by age, gender, and educational level were included as a healthy control (HC) group for neuroimaging comparisons.

Individuals with psychosis, stroke, tumors, trauma, severe hypertension, epilepsy, substance abuse, mental retardation, or contraindications for MRI (cardiac defibrillators, pacemakers, electromagnetic system implants, mechanical heart valves or vascular clips, cochlear implants, or claustrophobia) were excluded. All participants provided their written informed consent before being involved in the study.

**2.2. Acupuncture Timeline.** Cloud & Dragon brand (Cloud & Dragon Medical Device Co., Ltd, Jiangsu, China) disposable acupuncture needles (size  $0.30 \times 25$  mm) were used. After baseline MRI scans, all participants received manual acupuncture at bilateral Hegu (LI4, located in the hand dorsum) and Taichong (LR3, located in the dorsalis of the foot) (Figure 1 for all point locations). After skin disinfection, acupuncture needles were inserted 10 to 15 mm into the skin. Following needle insertion, manual stimulations such as small, equal manipulations of twirling, lifting, and thrusting were performed on all needles to induce characteristic sensation “de qi” (a composite of sensations including soreness, numbness, distention, heaviness, and other sensations), which is assigned as an essential component for acupuncture efficacy [18]. The process of acupuncture stimulation lasted for three minutes, and then, all needles were withdrawn.

**2.3. MRI Acquisition.** The baseline resting-state MRI data were acquired before the process of acupuncture stimulation. Participants firstly had rest for three minutes and then received manual acupuncture stimulation for three minutes. After the needles were withdrawn, another 10 minutes of resting-state fMRI scans was acquired (Figure 1).

MRI data acquisition was performed on a 3.0 T MR scanner (Siemens, Erlangen, Germany). Foam padding and headphones were used to control head motion and scanner noise. The data scan parameters of resting-state fMRI were as follows: repetition time (TR) = 2,000 ms, echo time (TE) = 40 ms, flip angle (FA) =  $90^\circ$ , matrix =  $64 \times 64$ , field of view (FOV) =  $240 \times 240$  mm<sup>2</sup>, slice thickness = 3 mm, slice gap = 1 mm, voxel size =  $3.75 \times 3.75 \times 3$  mm<sup>3</sup>, and bandwidth = 2232 Hz/pixel. Rapid collection gradient echo (MP-RAGE) sequence prepared by magnetization method was used to acquire sagittal T1-weighted MR images (TR/TE = 1,900/2.2 ms; FA =  $9^\circ$ ; matrix =  $256 \times 256$ ; inversion time = 900 ms; slice thickness = 1 mm, no gap; 176 slices).

All image data were analyzed using the Data Processing Assistant for Resting-State fMRI (DPARSFA) [19]. The first 10 volumes of each subject were removed, to make the signal to reach equilibrium and participants' adaptation to the scanning noise. The remaining volumes were corrected for within-scan acquisition time differences between slices, and the images with head movement greater than 2 mm in any direction or head rotation greater than  $2^\circ$  were excluded. To spatially normalize the fMRI data, the realigned volumes were spatially standardized into the MNI space using the EPI template. The functional images were resampled into a

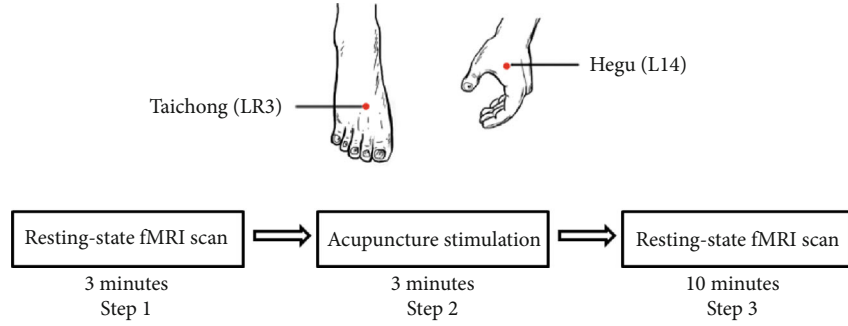


FIGURE 1: Timeline of fMRI acquisition and acupuncture.

voxel size of  $3 \times 3 \times 3 \text{ mm}^3$ . Then, the functional images were smoothed with a Gaussian kernel of  $4 \times 4 \times 4 \text{ mm}^3$  full width at half maximum (FWHM) to reduce the spatial noise.

**2.4. Independent Component Analysis (ICA).** The putative resting-state networks analysis was conducted by the group independent component analysis (ICA) of the GIFT software (<http://icatb.sourceforge.net>, version 1.3i) [20], and the minimum component length (MDL) criterion was used to determine the number of independent components (ICs) [21]. The fMRI data of all participants were concatenated into one group, the temporal dimension of the aggregate dataset was reduced through principal component analysis (PCA), and the separation of data was performed by the IC estimation of the infomax algorithm (with time course and spatial maps) [22, 23]. We further compared the stability of IC estimates of image data to account for spatial correlation at order estimated by minimum description length (MDL) criterion, based on the filtered and unfiltered data by using the software package ICASSO. ICs and time courses of each participant were back-reconstructed by GICA [24].

We identified the brain network by visual inspection, which was previously described [25]. The individual-level components were extracted from back-reconstruction and were converted into  $z$ -scores, which reflect the degree of correlation between the time series of a given voxel and the mean time series of its components. For each network component, the  $z$ -score of each voxel was defined as the resting-state intranetwork FC.

**2.5. Statistics Analysis.** Continuous variables of demographics and neuropsychological scores were presented as mean  $\pm$  standard deviation (SD) and compared by Student's  $t$ -tests or Mann-Whitney  $U$  test based on distributional properties. Categorical variables were described as percentages and compared by chi-square tests. The statistical tests were two-sided, and a  $P$  value  $< 0.05$  was considered statistically significant. Analyses were conducted with SPSS version 25.0 (IBM Corp, Armonk, NY, USA).

The statistics analysis of images was performed using Statistical Parametric Mapping software (SPM12; <http://www.fil.ion.ucl.ac.uk/spm/software/spm12>). First, one-sample  $t$ -test was used to achieve the brain network  $z$ -statistic map for each condition (HC\_before, HC\_after, AD\_before, and AD\_after). We use a family-wise error (FWE) correction

TABLE 1: Characteristics of the patients with AD and HCs.

	AD ( $N = 12$ )	HCs ( $N = 12$ )	$P$ value
Gender, female/male	7/5	7/5	1.00
Age (year)*	$67.58 \pm 9.05$	$64.83 \pm 6.94$	0.259
Education (year)*	$9.17 \pm 3.19$	$11.58 \pm 4.60$	0.178
Course (month)*	$11.5 \pm 5.16$	—	—
MoCA*	$14.83 \pm 3.41$	$27.75 \pm 0.62$	$<0.01$
CDR*	$1.04 \pm 0.33$	$0.00 \pm 0.00$	$<0.01$
AVLT (immediate)*	$12.17 \pm 3.61$	$25.50 \pm 5.39$	$<0.01$
AVLT (short time)*	$2.58 \pm 1.56$	$10.83 \pm 3.01$	$<0.01$
AVLT (long time)*	$3.25 \pm 1.82$	$12.92 \pm 1.73$	$<0.01$

\*Mean  $\pm$  SD. AD: Alzheimer's disease; HCs: healthy controls; MoCA: Montreal Cognitive Assessment; CDR: clinical dementia rating scale; AVLT: auditory verbal learning test; immediate: immediate recall of learning verbal; delayed: delayed recall of learning verbal; recognition: recognition of learning verbal; SD: standard deviation.

with a threshold of  $P < 0.05$  for multiple comparisons. Then, the statistics mask was made by combining the 4 conditions (i.e., HC\_before, HC\_after, AD\_before, and AD\_after), which were applied to compare the between-group differences (HC\_before vs AD\_before) and the interaction effect of acupuncture by group ( $[AD\_before > AD\_after] > [HC\_before > HC\_after]$ ,  $[AD\_after > AD\_before] > [HC\_after > HC\_before]$ ). Second, two-sample  $t$ -test was used to indicate the differences of the whole brain network ( $P < 0.05$ , FWE correction) between-group difference in AD and HC groups before acupuncture (NC\_before vs. AD\_before) controlling for gender and age as covariates. Based on the group differences before acupuncture (HC\_before vs. AD\_before), regions of interest (ROIs) were defined according to the activated clusters. To determine the effect of acupuncture on modulating brain network connectivity, we extracted the  $z$  values for the regions with different connections. Then, a paired  $t$ -test was involved in comparing the effects of acupuncture on the HC and AD groups in each ROI. Finally, a general linear model (GLM) [26] of covariance was used to compare the interaction effect ( $P < 0.05$ , FWE correction) of acupuncture (before vs. after) by group (AD vs. HC). In addition, we calculated the respective simple main effects (i.e., AD\_before vs. AD\_after and HC\_before vs. HC\_after).



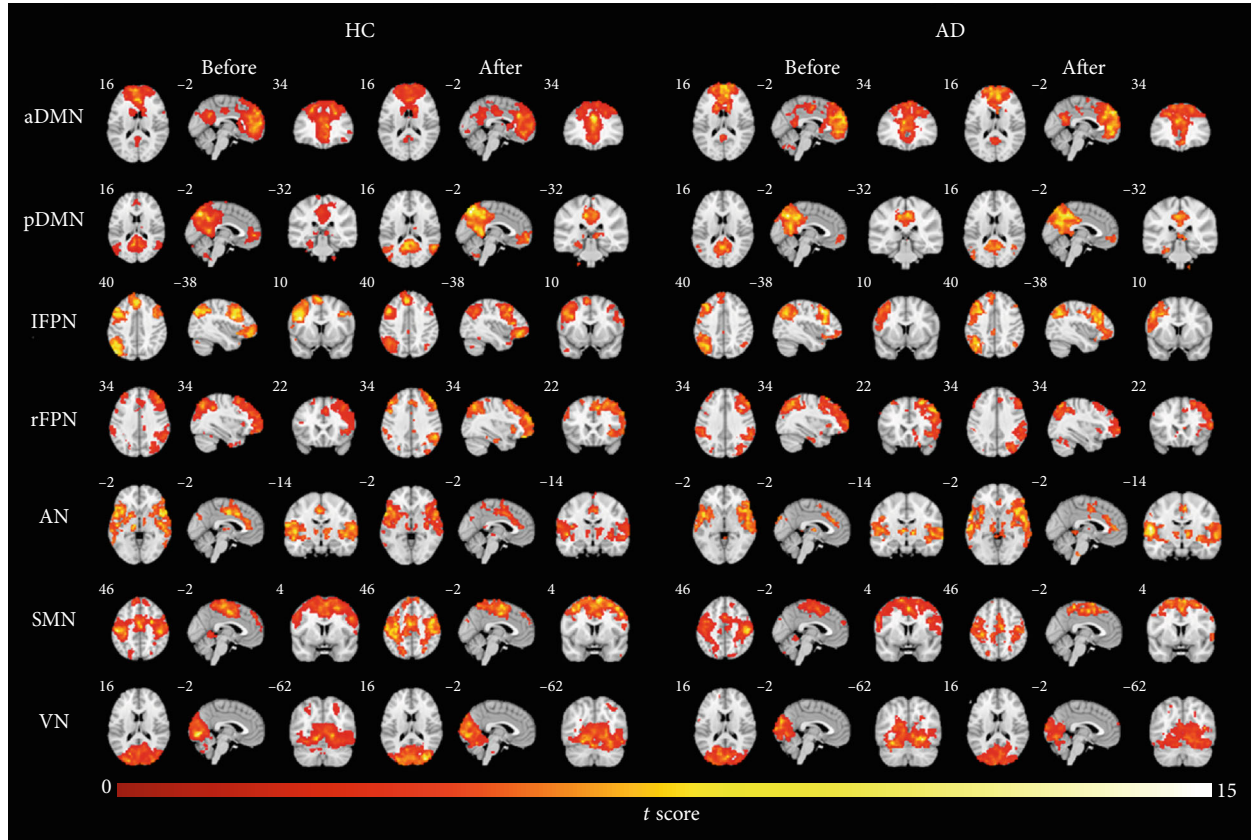


FIGURE 2: Within-condition anterior DMN (aDMN), posterior DMN (pDMN), left frontal parietal network (IFPN), right frontal parietal network (rFPN), auditory network (AN), sensorimotor network (SMN), and visual network (VN) connectivity patterns identified by independent component analysis (ICA), including patterns for the 2 conditions before acupuncture (i.e., HC\_before and AD\_before) and 2 conditions after acupuncture (i.e., HC\_after and AD\_after).

### 3. Results

**3.1. Clinical Data and Neuropsychological Test.** In the study, both two HCs and two AD patients were excluded from the study due to the head motions ( $>2$  mm and  $2^\circ$ ). Then, the clinical information of 24 participants who underwent the MRI scans is shown in Table 1. There was no significant difference of age and gender between the AD patients and HCs. And lower scores of CDR, Montreal Cognitive Assessment (MoCA), and auditory verbal learning test (AVLT) were investigated in AD patients compared with those of HCs ( $P < 0.01$ ).

**3.2. The Identification of Large-Scale Brain Networks in AD Patients and HCs.** Figure 2 showed some intrinsic network maps for 4 conditions (HC\_before, HC\_after, AD\_before, and AD\_after). Besides the DMN, five components of interest including left frontal parietal network (IFPN), right frontal parietal network (rFPN), auditory network (AN), sensorimotor network (SMN), and visual network (VN) were revealed by visual inspection [27].

**3.3. Comparison of Functional Connectivity of the Large-Scale Resting-State Networks between AD Patients and HCs before Acupuncture.** Before acupuncture, except the functional connectivity in the AN without significant difference, the con-

nectivity of other identified networks including IFPN, rFPN, SMN, and VN showed to be decreased in AD patients, compared with those of HCs. Some clusters included the left superior frontal gyrus (SFG), the left middle frontal gyrus (MFG), left precuneus, the left inferior frontal gyrus (IFG), and right MFG located in the IFPN; the right angular gyrus (AG) and right MFG in the rFPN; the left IPL, bilateral post-central gyrus (PoCG), and right MFG in the SMN; and the right middle occipital gyrus (MOG) of VN and presented to be significantly decreased in AD patients (Figure 3 and Table 2).

**3.4. The Effect of Acupuncture on These Networks Separately in HCs and AD Patients.** Then, we explored the associated pattern of the acupuncture's influence on these networks above described, separately in HCs and AD patients. Eight ROIs showed changes related to acupuncture, which included the right IFG and left SFG of IFPN; the right MFG of rFPN; the left IPL, left PoCG, right PoCG, and right MFG of SMN; and the right MOG of VN. Among these ROIs, significantly decreased activity in the right MFG of rFPN ( $P = 0.007$ ) was identified in AD patients, not in the HCs. Significantly decreased FC in the right IFG ( $P = 0.047$ ) and left SFG ( $P = 0.041$ ) of IFPN; the left IPL ( $P = 0.004$ ), left PoCG ( $P = 0.001$ ), right PoCG ( $P = 0.032$ ), and right MFG

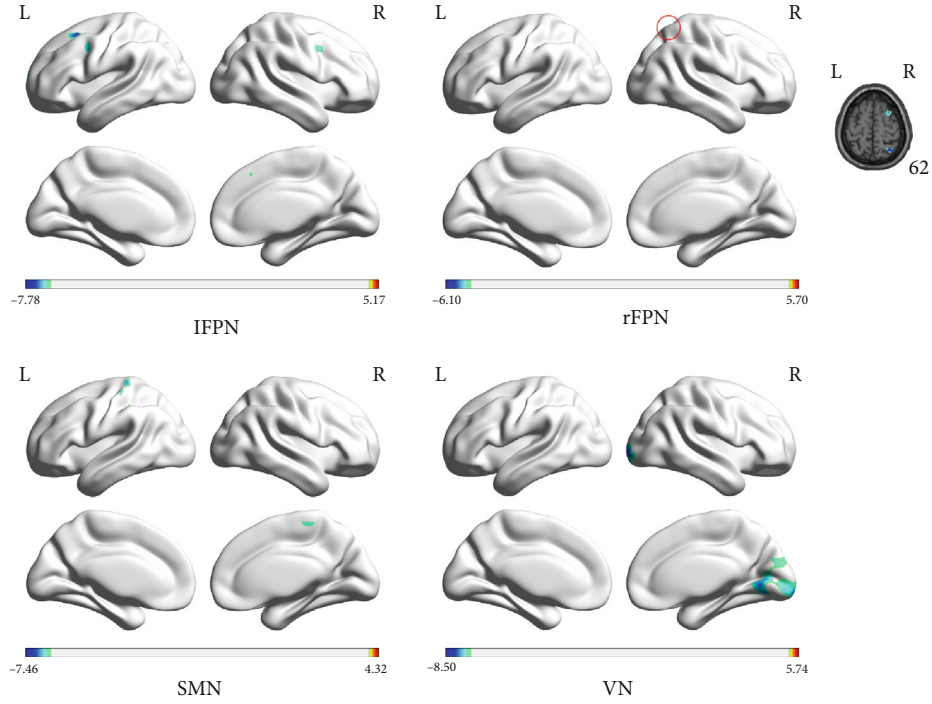


FIGURE 3: The large-scale resting state networks with different activities of FC between AD patients and HCs before acupuncture (the color scale represents  $t$  values). FC: functional connectivity; AD: Alzheimer's disease; HCs: healthy controls; IFPN: left frontal parietal network; rFPN: right frontal parietal network; SMN: sensorimotor network; VN: visual network; L: left; R: right.

TABLE 2: Comparison of large-scale networks before acupuncture between AD patients and HCs.

Networks	Brain regions	MNI coordinate			BA	Cluster size	$t$ score
		$x$	$y$	$z$			
IFPN	Left SFG	-30	60	21	10	44	5.77
	Left MFG	-48	9	42	8	88	6.53
	Left precuneus	-36	-78	36	19	34	4.65
	Right IFG	45	6	39	9	37	5.73
	Right MFG	3	24	48	8	28	5.28
	Left SFG	-24	15	54	8	31	7.79
rFPN	Right AG	42	-60	54	40	63	6.1
	Right MFG	30	9	60	6	38	5.19
SMN	Left IPL	-42	-30	42	40	36	4.27
	Left PoCG	-36	-30	69	3	121	7.46
	Right PoCG	48	-36	60	40	63	5.35
	Right MFG	3	-27	63	6	57	4.94
VN	Right MOG	21	-99	0	18	752	8.5

FC: functional connectivity; AD: Alzheimer's disease; HCs: healthy controls; BA: Brodmann area; MNI: Montreal Neurological Institute;  $x$ ,  $y$ , and  $z$ : coordinates of primary peak locations in the MNI space; IFPN: left frontal parietal network; rFPN: right frontal parietal network; SMN: sensorimotor network; VN: visual network; SFG: superior frontal gyrus; MFG: middle frontal gyrus; IFG: inferior frontal gyrus; AG: angular gyrus; IPL: inferior parietal lobule; PoCG: postcentral gyrus; MOG: middle occipital gyrus.

( $P = 0.010$ ) of SMN; and the right MOG of VN ( $P = 0.003$ ) were identified in HCs, not in the AD patients. (Figure 4).

3.5. *The Explorations of the Acupuncture Effect on Large-Scale Resting-State Networks in AD.* Figure 5 shows the interaction effect of acupuncture by group, and details of related changes in the FC are shown in Table 3. After controlling for the effect of acupuncture on HCs, decreased FC in the right cerebellum crus I, left IFG, and left AG of IFPN was identified, while the increased FC in the left MFG of IFPN and the right lingual gyrus of VN was found in AD patients.

#### 4. Discussion

AD is a progressive and complicated neurodegenerative disease caused by neuronal degeneration and cell loss of the whole brain [28]. And its symptoms included memory loss, disorientation, mood and behavior changes, confusion, unfounded suspicions, and eventually, difficulty speaking, swallowing, and walking. In our study, we found decreased FC in some identified large-scale networks including IFPN, rFPN, SMN, and VN in AD patients, which suggested that AD might be related to changes of FC in larger-scale functional networks responsible for these abnormal behaviors [13, 29–31]. Interestingly, we did not find the significant effect of the combination stimulus of Hegu (LI4) and Tai-chong (LR3) on all of the identified networks in AD patients. After controlling for the effect of acupuncture on HCs, we found the decreased FC in some regions of the IFPN, while increased FC in some regions of IFPN and VN in AD

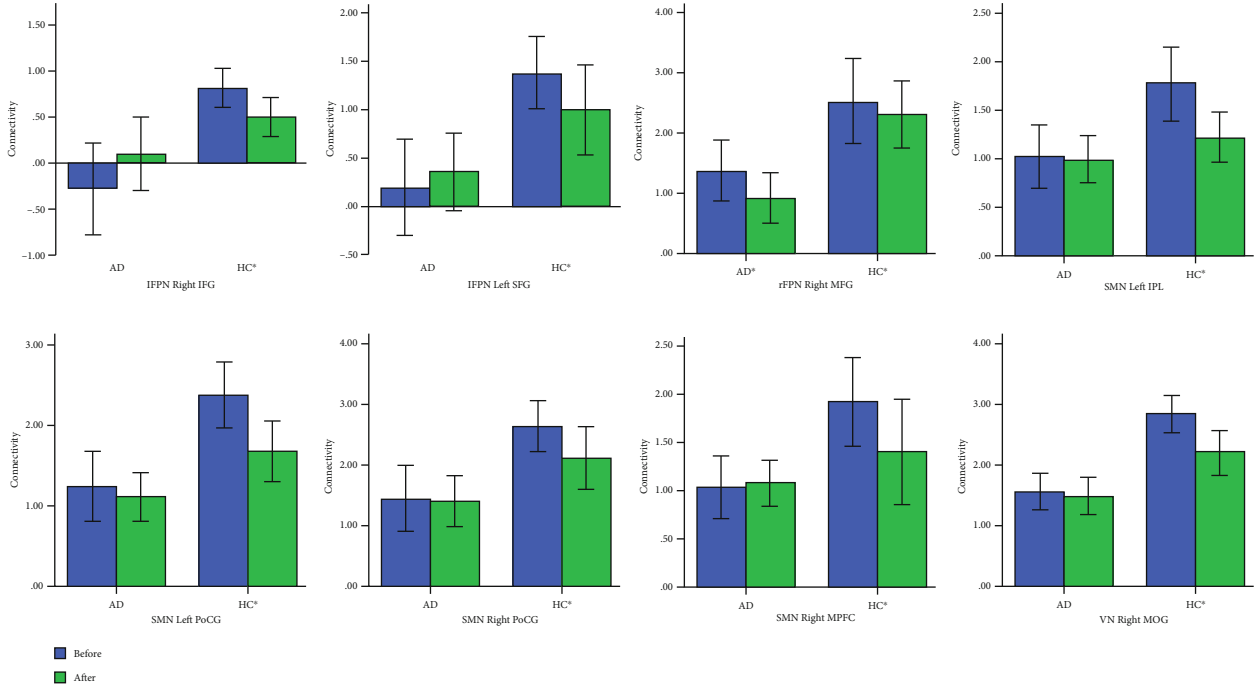


FIGURE 4: Eight regions of large-scale networks with changes of FC after acupuncture. AD: Alzheimer's disease; HCs: healthy controls; IFPN: left frontal parietal network; rFPN: right frontal parietal network; SMN: sensorimotor network; VN: visual network; IFG: inferior frontal gyrus; SFG: superior frontal gyrus; MFG: middle frontal gyrus; IPL: inferior parietal lobule; PoCG: postcentral gyrus; MOG: middle occipital gyrus.

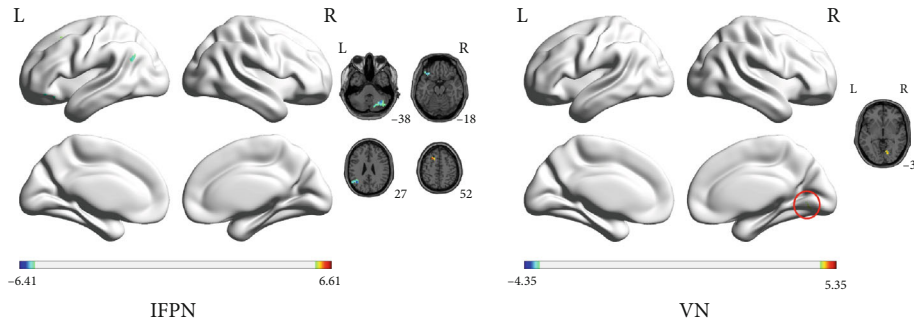


FIGURE 5: Decreased or increased FC possibly related to acupuncture in some regions of IFPN and VN in AD patients (the color scale represents  $t$  values). FC: functional connectivity; IFPN: left frontal parietal network; VN: visual network; L: left; R: right.

TABLE 3: Brain regions with decreased or increased FC possibly related to acupuncture in the AD patients.

Networks	Brain regions	MNI coordinate			BA	Cluster size	$t$ score
		$x$	$y$	$z$			
Decreased: (AD_before > AD_after) > (HC_before > HC_after)							
IFPN	Right cerebellum crus I	36	-63	39	—	111	5.37
	Left IFG	-45	30	-15	47	48	5.81
	Left AG	-39	-63	33	39	90	6.42
Increased: (AD_after > AD_before) > (HC_after > HC_before)							
IFPN	Left MFG	-24	18	51	8	30	5.68
VN	Right LG	15	-72	-6	18	29	4.73

FC: functional connectivity; AD: Alzheimer's disease; HCs: healthy controls; BA: Brodmann area; MNI: Montreal Neurological Institute;  $x$ ,  $y$ , and  $z$ : coordinates of primary peak locations in the MNI space; IFPN: left frontal parietal network; VN: visual network; IFG: inferior frontal gyrus; AG: angular gyrus; MFG: middle frontal gyrus; LG: lingual gyrus.

patients, which might suggest the effect of acupuncture on some restricted regions of specific brain networks selectively in AD. These results revealed the effect of the acupuncture stimulation of Hegu (LI4) and Taichong (LR3) on some large-scale brain networks of AD patients beyond DMN and might suggest the potential mechanism of acupuncture's effect on AD.

The FPN was reported to play an important role in the executive control function and language [32]. Many studies indicated that the functional disconnection and compensation in the FPN might coexist in AD [33]. Zhao et al. found that the superior parietal gyrus (SPG) regions and left paracentral lobule (PCL) of FPN presented increased FC, while the left supramarginal gyrus (SMG) and left inferior parietal (IPL.L) regions showed decreased FC in AD patients [34]. Although our results showed FC reduced within the FPN in AD patients, we found both disrupted and excessive enhanced FC of different regions in IFPN after combination stimulus of Hegu (LI4) and Taichong (LR3). It is possible that during acupuncture, the region was activated to preserve and compensate for losses in function attributable to the degenerative effects of the disease; conversely, the region was reduced to restrain the excessive enhance due to the disease. All these findings might have coincided with the theory of dynamic functional reorganization.

Usually, visual cortices are activated not only by visual stimuli but also by visual mental imaginary and remembering [35]. Previous studies suggested that acupuncture at Taichong (LR3) could specifically perform the bidirectional regulation (excitation and inhibition) on vision-related brain areas [36, 37], which might be a mechanism for treating vision-related diseases. This observation confirmed reduced FC of VN in the healthy olds and further verified that acupuncture stimulus of Taichong (LR3) might specifically regulate the VN. Moreover, complex visual disturbances are observed in AD patients, including constructional and visuo-perceptual disorientation, specifically difficulties in searching for objects (figure-ground discrimination), finding their way in familiar surroundings (environmental agnosia) [38, 39]. Many studies found that the reduced FC of ventral/dorsal VN could play a crucial role in the visuospatial disorder of patients with AD pathology [9, 40–42], which may associate with amyloid-beta and neurofibrillary tangle (NFT) aggregation as well as neurodegeneration and axonal damage in visual cortical regions in AD pathology [43]. We found that combination stimulus of Hegu (LI4) and Taichong (LR3) activated FC of some regions in the VN of AD patients, which suggested acupuncture at Hegu (LI4) and Taichong (LR3) might treat visual disturbances in AD.

Many evidences suggested that stimulation at Hegu (LI4) and Taichong (LR3) induced distinct response patterns. For example, it was reported that acupuncture at Hegu (LI4) mainly specifically deactivated right frontal areas [37]. And many researches showed that acupuncture at Taichong (LR3) mainly specifically activated the brain functional network that participates in visual function, associative function, and emotion cognition [37, 44]. This observation identified decreased FC of the rFPN in AD patients and significantly reduced FC of the SMN, IFPN, and VN in the HCs after ac-

puncture at Hegu (LI4) and Taichong (LR3). These results coincided with previous findings, which suggested that acupuncture at Hegu (LI4) and Taichong (LR3) may regulate the neuroplasticity of specific brain networks to induce therapeutic effects. But we only find acupuncture at Hegu (LI4) and Taichong (LR3) effect in the VN and IFPN in AD patients, after controlling for the effect of acupuncture on HCs. This might be partly explained by pathology and characteristics of AD; that is, the destruction of the SMN and rFPN due to AD might be so severe that acupuncture failed to preserve their integrality. Thus, FC in more regions were significantly changed in HC than AD. Moreover, a relatively small sample size might provide another explanation.

Previous studies have found that acupuncture could modulate the synaptic plasticity in AD patients or animal model [45], by enhancing long-term potentiation (LTP) and long-term depression (LTD) of the hippocampus [46], increasing the synapse number and postsynaptic density thickness [47], and modulating regional spontaneous activity [48, 49]. It is well known that neuroplasticity might contribute to preserve the integrality of brain networks. In this study, the neurophysiology mechanism of this influence on the IFPN and VN of AD patients remains unclear, which remains to be established.

There are still some limitations in our study. First, we did not demonstrate whether the enhancement or reduction was associated with acupoint specificity due to the lack of the sham acupuncture needle. Second, we did not find the correlation between changes of functional connectivity of these networks after acupuncture and behaviors in AD patients. Third, a relatively small sample size was included in this study. Furthermore, despite controlling the sequence of scan and using the ICA method, the influence of the scan lengths on the reliability and similarity of FC would be inescapable [50, 51]. The changes in FC after a few minutes of stimulation may be merely a transient change in reactivity, which might not completely equal to the effect of acupuncture on neuroplasticity. Given that the sustained effect of acupuncture on the network is unclear, in the future, we will design a longitudinal study to trace these patients at different time points and explore the alteration of brain network in patients with AD after acupuncture for a period time. Therefore, future longitudinal studies with a much larger sample are warranted to elucidate the progressive functional changes caused by acupuncture in AD patients and its relationship with the clinical performances.

## 5. Conclusion

In conclusion, by using the ICA method, our study found that the activity of large-scale brain networks in AD patients could be mediated by the acupuncture stimulation on Hegu (LI4) and Taichong (LR3). These findings have important implications for the underlying neurobiology of AD and the effect of acupuncture on the disease, which might have some reference values for the interpretation of the therapeutic effects of acupuncture at Hegu (LI4) and Taichong (LR3) on AD in the future.



## Data Availability

The clinical and image data used to support the findings of this study are available from the corresponding author upon request.

## Conflicts of Interest

The authors declare that they have no conflict of interest.

## Authors' Contributions

Dr. Zhiqun Wang, Dr. Jie Lu, and Dr. Kuncheng Li had full access to all of the data in the study and take responsibility for the integrity of the data and the accuracy of the data analysis. Shaozhen Ji, Hao Zhang, and Zhiqun Wang were responsible for the study concept and design. Shaozhen Ji, Hao Zhang, Wen Qin, Zhiqun Wang, Kuncheng Li, and Jie Lu were responsible for the acquisition, analysis, or interpretation of data. Shaozhen Ji, Hao Zhang, and Zhiqun Wang were responsible for the drafting of the manuscript. Kuncheng Li, Jie Lu, and Zhiqun Wang were responsible for the critical revision of the manuscript for important intellectual content. Hao Zhang and Wen Qin were responsible for the statistical analysis. Zhiqun Wang obtained funding. Ming Liu, Weimin Zheng, Ying Han, Haiqing Song, Kuncheng Li, Jie Lu, and Zhiqun Wang provided administrative, technical, or material support. Zhiqun Wang was responsible for the study supervision. Shaozhen Ji and Hao Zhang contributed equally to this work.

## Acknowledgments

The authors sincerely thank the participants for their help and willingness to participate in this study. This study was supported by the National Natural Scientific Foundation of China (Grant Nos. 81370037, 81571648, and 81471649) and the Fundamental Research Funds for the Central Universities (Grant No. 2021-JYB-XSJJ071).

## References

- [1] A. W. Bero, P. Yan, J. H. Roh et al., "Neuronal activity regulates the regional vulnerability to amyloid- $\beta$  deposition," *Nature Neuroscience*, vol. 14, no. 6, pp. 750–756, 2011.
- [2] H. Braak and E. Braak, "Staging of Alzheimer's disease-related neurofibrillary changes," *Neurobiology of Aging*, vol. 16, no. 3, pp. 271–278, 1995, discussion 278–284.
- [3] R. J. Perry, P. Watson, and J. R. Hodges, "The nature and staging of attention dysfunction in early (minimal and mild) Alzheimer's disease: relationship to episodic and semantic memory impairment," *Neuropsychologia*, vol. 38, no. 3, pp. 252–271, 2000.
- [4] C. H. Tu, I. MacDonald, and Y. H. Chen, "The effects of acupuncture on glutamatergic neurotransmission in depression, anxiety, schizophrenia, and Alzheimer's disease: a review of the literature," *Frontiers in Psychiatry*, vol. 10, p. 14, 2019.
- [5] C. Z. Liu, J. Kong, and K. Wang, "Acupuncture therapies and neuroplasticity," *Neural Plasticity*, vol. 2017, Article ID 6178505, 2 pages, 2017.
- [6] S. H. Bennett, A. J. Kirby, and G. T. Finnerty, "Rewiring the connectome: evidence and effects," *Neuroscience and Biobehavioral Reviews*, vol. 88, pp. 51–62, 2018.
- [7] L. Y. Xiao, X. R. Wang, Y. Yang et al., "Applications of acupuncture therapy in modulating plasticity of central nervous system," *Neuromodulation*, vol. 21, no. 8, pp. 762–776, 2018.
- [8] M. Stampanoni Bassi, E. Iezzi, L. Gilio, D. Centonze, and F. Buttari, "Synaptic plasticity shapes brain connectivity: implications for network topology," *International Journal of Molecular Sciences*, vol. 20, no. 24, p. 6193, 2019.
- [9] M. Pievani, N. Filippini, M. P. van den Heuvel, S. F. Cappa, and G. B. Frisoni, "Brain connectivity in neurodegenerative diseases—from phenotype to proteinopathy," *Nature Reviews. Neurology*, vol. 10, no. 11, pp. 620–633, 2014.
- [10] E. D. Vidoni, G. P. Thomas, R. A. Honea, N. Loskutova, and J. M. Burns, "Evidence of altered corticomotor system connectivity in early-stage Alzheimer's disease," *Journal of Neurologic Physical Therapy*, vol. 36, no. 1, pp. 8–16, 2012.
- [11] M. S. E. Sendi, E. Zendeirouh, R. L. Miller et al., "Alzheimer's disease projection from normal to mild dementia reflected in functional network connectivity: a longitudinal study," *Frontiers in Neural Circuits*, vol. 14, article 593263, 15 pages, 2021.
- [12] F. Agosta, M. A. Rocca, E. Pagani et al., "Sensorimotor network rewiring in mild cognitive impairment and Alzheimer's disease," *Human Brain Mapping*, vol. 31, no. 4, pp. 515–525, 2010.
- [13] F. Agosta, M. Pievani, C. Geroldi, M. Copetti, G. B. Frisoni, and M. Filippi, "Resting state fMRI in Alzheimer's disease: beyond the default mode network," *Neurobiology of Aging*, vol. 33, no. 8, pp. 1564–1578, 2012.
- [14] P. Liang, Z. Wang, T. Qian, and K. Li, "Acupuncture stimulation of Taichong (Liv3) and Hegu (LI4) modulates the default mode network activity in Alzheimer's disease," *American Journal of Alzheimer's Disease and Other Dementias*, vol. 29, no. 8, pp. 739–748, 2014.
- [15] G. Lewis, *DSM-IV: Diagnostic and Statistical Manual of Mental Disorders*, American Psychiatric Association, Washington, DC, 4th ed edition, 1994.
- [16] G. McKhann, D. Drachman, M. Folstein, R. Katzman, D. Price, and E. M. Stadlan, "Clinical diagnosis of Alzheimer's disease: report of the NINCDS-ADRDA Work Group under the auspices of Department of Health and Human Services Task Force on Alzheimer's Disease," *Neurology*, vol. 34, no. 7, pp. 939–944, 1984.
- [17] J. C. Morris, "The Clinical Dementia Rating (CDR): current version and scoring rules," *Neurology*, vol. 43, no. 11, pp. 2412–2414, 1993.
- [18] J. Kong, R. Gollub, T. Huang et al., "Acupuncture de qi, from qualitative history to quantitative measurement," *Journal of Alternative and Complementary Medicine*, vol. 13, no. 10, pp. 1059–1070, 2007.
- [19] Y. Chao-Gan and Z. Yu-Feng, "DPARF: a MATLAB toolbox for "pipeline" data analysis of resting-state fMRI," *Frontiers in Systems Neuroscience*, vol. 4, p. 13, 2010.
- [20] C. F. Beckmann, M. DeLuca, J. T. Devlin, and S. M. Smith, "Investigations into resting-state connectivity using independent component analysis," *Philosophical Transactions of the Royal Society of London. Series B, Biological Sciences*, vol. 360, no. 1457, pp. 1001–1013, 2005.
- [21] Y. O. Li, T. Adali, and V. D. Calhoun, "Estimating the number of independent components for functional magnetic

- resonance imaging data,” *Human Brain Mapping*, vol. 28, no. 11, pp. 1251–1266, 2007.
- [22] V. D. Calhoun, T. Adali, G. D. Pearlson, and J. J. Pekar, “A method for making group inferences from functional MRI data using independent component analysis,” *Human Brain Mapping*, vol. 14, no. 3, pp. 140–151, 2001.
- [23] M. J. Jafri, G. D. Pearlson, M. Stevens, and V. D. Calhoun, “A method for functional network connectivity among spatially independent resting-state components in schizophrenia,” *NeuroImage*, vol. 39, no. 4, pp. 1666–1681, 2008.
- [24] E. B. Erhardt, S. Rachakonda, E. J. Bedrick, E. A. Allen, T. Adali, and V. D. Calhoun, “Comparison of multi-subject ICA methods for analysis of fMRI data,” *Human Brain Mapping*, vol. 32, no. 12, pp. 2075–2095, 2011.
- [25] W. W. Seeley, V. Menon, A. F. Schatzberg et al., “Dissociable intrinsic connectivity networks for salience processing and executive control,” *The Journal of Neuroscience*, vol. 27, no. 9, pp. 2349–2356, 2007.
- [26] E. Bagarinao, K. Matsuo, T. Nakai, and S. Sato, “Estimation of general linear model coefficients for real-time application,” *NeuroImage*, vol. 19, no. 2, pp. 422–429, 2003.
- [27] A. R. Laird, P. M. Fox, S. B. Eickhoff et al., “Behavioral interpretations of intrinsic connectivity networks,” *Journal of Cognitive Neuroscience*, vol. 23, no. 12, pp. 4022–4037, 2011.
- [28] Y. Vyas, J. M. Montgomery, and J. E. Cheyne, “Hippocampal deficits in amyloid- $\beta$ -related rodent models of Alzheimer’s disease,” *Frontiers in Neuroscience*, vol. 14, p. 266, 2020.
- [29] S. H. Joo, H. K. Lim, and C. U. Lee, “Three large-scale functional brain networks from resting-state functional MRI in subjects with different levels of cognitive impairment,” *Psychiatry Investigation*, vol. 13, no. 1, pp. 1–7, 2016.
- [30] M. R. Brier, J. B. Thomas, A. Z. Snyder et al., “Loss of intranetwork and internetwork resting state functional connections with Alzheimer’s disease progression,” *The Journal of Neuroscience*, vol. 32, no. 26, pp. 8890–8899, 2012.
- [31] Q. Zhao, H. Lu, H. Metmer, W. X. Y. Li, and J. Lu, “Evaluating functional connectivity of executive control network and frontoparietal network in Alzheimer’s disease,” *Brain Research*, vol. 1678, pp. 262–272, 2018.
- [32] E. A. Crone, C. Wendelken, S. E. Donohue, and S. A. Bunge, “Neural evidence for dissociable components of task-switching,” *Cerebral Cortex*, vol. 16, no. 4, pp. 475–486, 2006.
- [33] Z. Wang, M. Xia, Z. Dai et al., “Differentially disrupted functional connectivity of the subregions of the inferior parietal lobule in Alzheimer’s disease,” *Brain Structure & Function*, vol. 220, no. 2, pp. 745–762, 2015.
- [34] Q. Zhao, X. Sang, H. Metmer, Z. N. N. K. Swati, J. Lu, and Alzheimer’s Disease Neuroimaging Initiative, “Functional segregation of executive control network and frontoparietal network in Alzheimer’s disease,” *Cortex*, vol. 120, pp. 36–48, 2019.
- [35] S. M. Kosslyn, G. Ganis, and W. L. Thompson, “Neural foundations of imagery,” *Nature Reviews Neuroscience*, vol. 2, no. 9, pp. 635–642, 2001.
- [36] C. Wu, S. Qu, J. Zhang et al., “Correlation between the effects of acupuncture at Taichong (LR3) and functional brain areas: a resting-state functional magnetic resonance imaging study using true versus sham acupuncture,” *Evidence-based Complementary and Alternative Medicine*, vol. 2014, Article ID 729091, 7 pages, 2014.
- [37] B. Yan, K. Li, J. Xu et al., “Acupoint-specific fMRI patterns in human brain,” *Neuroscience Letters*, vol. 383, no. 3, pp. 236–240, 2005.
- [38] M. A. Cerquera-Jaramillo, M. O. Nava-Mesa, R. E. González-Reyes, C. Tellez-Conti, and A. de-la-Torre, “Visual Features in Alzheimer’s Disease: From Basic Mechanisms to Clinical Overview,” *Neural Plasticity*, vol. 2018, Article ID 2941783, 21 pages, 2018.
- [39] L. Krajcovicova, M. Barton, N. Elfmarkova-Nemcova, M. Mikl, R. Marecek, and I. Rektorova, “Changes in connectivity of the posterior default network node during visual processing in mild cognitive impairment: staged decline between normal aging and Alzheimer’s disease,” *Journal of Neural Transmission (Vienna)*, vol. 124, no. 12, pp. 1607–1619, 2017.
- [40] L. Wang, Y. Zang, Y. He et al., “Changes in hippocampal connectivity in the early stages of Alzheimer’s disease: evidence from resting state fMRI,” *NeuroImage*, vol. 31, no. 2, pp. 496–504, 2006.
- [41] L. Pini, C. Geroldi, S. Galluzzi et al., “Age at onset reveals different functional connectivity abnormalities in prodromal Alzheimer’s disease,” *Brain Imaging and Behavior*, vol. 14, no. 6, pp. 2594–2605, 2020.
- [42] X. Ma, Z. Zhuo, L. Wei, et al., “Altered temporal organization of brief spontaneous brain activities in patients with Alzheimer’s disease,” *Neuroscience*, vol. 425, pp. 1–11, 2020.
- [43] Y. Kusne, A. B. Wolf, K. Townley, M. Conway, and G. A. Peyman, “Visual system manifestations of Alzheimer’s disease,” *Acta Ophthalmologica*, vol. 95, no. 8, pp. e668–e676, 2017.
- [44] Y. Zheng, Y. Wang, Y. Lan et al., “Imaging of brain function based on the analysis of functional connectivity-imaging analysis of brain function by fMRI after acupuncture at LR3 in healthy individuals,” *African Journal of Traditional, Complementary, and Alternative Medicines*, vol. 13, no. 6, pp. 90–100, 2016.
- [45] C. C. Yu, C. Y. Ma, H. Wang et al., “Effects of acupuncture on Alzheimer’s disease: evidence from neuroimaging studies,” *Chinese Journal of Integrative Medicine*, vol. 25, no. 8, pp. 631–640, 2019.
- [46] W. Li, L. H. Kong, H. Wang et al., “High-frequency electroacupuncture evidently reinforces hippocampal synaptic transmission in Alzheimer’s disease rats,” *Neural Regeneration Research*, vol. 11, no. 5, pp. 801–806, 2016.
- [47] C. C. Yu, Y. Wang, F. Shen et al., “High-frequency (50 Hz) electroacupuncture ameliorates cognitive impairment in rats with amyloid beta 1-42-induced Alzheimer’s disease,” *Neural Regeneration Research*, vol. 13, no. 10, pp. 1833–1841, 2018.
- [48] Y. Shan, J. J. Wang, Z. Q. Wang et al., “Neuronal Specificity of Acupuncture in Alzheimer’s Disease and Mild Cognitive Impairment Patients: A Functional MRI Study,” *Evidence-based Complementary and Alternative Medicine*, vol. 2018, Article ID 7619197, 10 pages, 2018.
- [49] Z. Wang, B. Nie, D. Li et al., “Effect of acupuncture in mild cognitive impairment and Alzheimer disease: a functional MRI study,” *PLoS One*, vol. 7, no. 8, article e42730, 2012.
- [50] R. M. Birn, E. K. Molloy, R. Patriat et al., “The effect of scan length on the reliability of resting-state fMRI connectivity estimates,” *NeuroImage*, vol. 83, pp. 550–558, 2013.
- [51] X. Liu and J. H. Duyn, “Time-varying functional network information extracted from brief instances of spontaneous brain activity,” *Proceedings of the National Academy of Sciences of the United States of America*, vol. 110, no. 11, pp. 4392–4397, 2013.



## Review Article

# The Role of Neuroglial Crosstalk and Synaptic Plasticity-Mediated Central Sensitization in Acupuncture Analgesia

Zhongxi Lyu,<sup>1,2,3</sup> Yongming Guo<sup>1,2,3</sup>, Yinan Gong<sup>1</sup>, Wen Fan<sup>1,4</sup>, Baomin Dou,<sup>1</sup>  
Ningcen Li,<sup>1</sup> Shenjun Wang,<sup>1,2,3</sup> Yuan Xu,<sup>1,2,3</sup> Yangyang Liu<sup>1,2,3</sup>, Bo Chen<sup>1,2,3</sup>,  
Yi Guo<sup>1,3,5</sup>, Zhifang Xu<sup>1,2,3</sup> and Xiaowei Lin<sup>1,3,5</sup>

<sup>1</sup>Research Center of Experimental Acupuncture Science, Tianjin University of Traditional Chinese Medicine, Tianjin 301617, China

<sup>2</sup>School of Acupuncture & Moxibustion and Tuina, Tianjin University of Traditional Chinese Medicine, Tianjin 301617, China

<sup>3</sup>National Clinical Research Center for Chinese Medicine Acupuncture and Moxibustion, Tianjin 300381, China

<sup>4</sup>Suzuka University of Medical Science, Suzuka 5100293, Japan

<sup>5</sup>School of Traditional Chinese Medicine, Tianjin University of Traditional Chinese Medicine, Tianjin 301617, China

Correspondence should be addressed to Zhifang Xu; xuzhifangmsn@hotmail.com and Xiaowei Lin; linxiaoweiqhzh@163.com

Zhongxi Lyu and Yongming Guo contributed equally to this work.

Received 23 June 2020; Revised 30 December 2020; Accepted 7 January 2021; Published 18 January 2021

Academic Editor: Zhen Zheng

Copyright © 2021 Zhongxi Lyu et al. This is an open access article distributed under the Creative Commons Attribution License, which permits unrestricted use, distribution, and reproduction in any medium, provided the original work is properly cited.

Although pain is regarded as a global public health priority, analgesic therapy remains a significant challenge. Pain is a hypersensitivity state caused by peripheral and central sensitization, with the latter considered the culprit for chronic pain. This study summarizes the pathogenesis of central sensitization from the perspective of neuroglial crosstalk and synaptic plasticity and underlines the related analgesic mechanisms of acupuncture. Central sensitization is modulated by the neurotransmitters and neuropeptides involved in the ascending excitatory pathway and the descending pain modulatory system. Acupuncture analgesia is associated with downregulating glutamate in the ascending excitatory pathway and upregulating opioids,  $\gamma$ -aminobutyric acid, norepinephrine, and 5-hydroxytryptamine in the descending pain modulatory system. Furthermore, it is increasingly appreciated that neurotransmitters, cytokines, and chemokines are implicated in neuroglial crosstalk and associated plasticity, thus contributing to central sensitization. Acupuncture produces its analgesic action by inhibiting cytokines, such as interleukin-1 $\beta$ , interleukin-6, and tumor necrosis factor- $\alpha$ , and upregulating interleukin-10, as well as modulating chemokines and their receptors such as CX3CL1/CX3CR1, CXCL12/CXCR4, CCL2/CCR2, and CXCL1/CXCR2. These factors are regulated by acupuncture through the activation of multiple signaling pathways, including mitogen-activated protein kinase signaling (e.g., the p38, extracellular signal-regulated kinases, and c-Jun-N-terminal kinase pathways), which contribute to the activation of nociceptive neurons. However, the responses of chemokines to acupuncture vary among the types of pain models, acupuncture methods, and stimulation parameters. Thus, the exact mechanisms require future clarification. Taken together, inhibition of central sensitization modulated by neuroglial plasticity is central in acupuncture analgesia, providing a novel insight for the clinical application of acupuncture analgesia.

## 1. Introduction

Pain is mediated by nociceptive nerve fibers and is a physiological alarm response to protect the body by reducing tissue damage from injury [1]. Thirty to fifty percent of patients with pathological pain suffer from anxiety and depression long after wound healing. Both the pain and unpleasant emotions affect

their quality of life and cause serious social and economic consequences [2, 3]. However, the solution for chronic pain remains a major challenge throughout the world. Oral drugs are often the first choice, and their usage has expanded exponentially in recent years [4]. Unfortunately, the extensive application of analgesic drugs may result in organ damage and abuse, together with causing serious social problems [5].

For example, long-term overuse of opioids, the most common class of prescribed painkillers, can lead to side effects such as addiction, tolerance, and drowsiness, as well as impaired memory, attention, and judgment. Opioid abuse can also potentially cause respiratory depression [6, 7]. Therefore, a natural analgesic that can also regulate pain-related moods and cognitive disorders is necessary.

Acupuncture therapy is a well-known treatment that originated in China and has been applied in 183 countries and regions all over the world [8, 9]. Long-term clinical practice has proved that acupuncture is an effective treatment to relieve pain. The World Health Organization has recommended acupuncture for more than 30 types of pain conditions, including lumbago, headache, sciatica, and postoperative pain [10]. Referring to the National Guideline Clearinghouse (<http://www.guidelines.gov/>), there are 49 specific medical recommendations for acupuncture, of which 37 (75.51%) are pain-related diseases [11]. At present, many clinical randomized controlled trials (RCTs) have demonstrated the analgesic effect of acupuncture [12]. As shown in a 16-week RCT, compared with sham acupuncture treatment and awaiting-treatment groups, acupuncture treatment could significantly reduce the incidence of migraine without premonitory migraine, an effect that lasted at least 24 weeks [13]. A meta-analysis by Vickers et al. analyzed the individual data of patients in RCTs with nonspecific musculoskeletal pain, osteoarthritis, shoulder pain, and chronic headache, concluding that acupuncture is effective for the treatment of chronic pain and has long-lasting therapeutic effects [12]. These studies have indicated that acupuncture analgesia is effective and safe and can improve the quality of life of patients suffering from pain.

Pain is caused by tissue damage or similar pathophysiological causes. Pain sensitization plays a key role in pain occurrence and maintenance. Pain sensitization starts from the sensitization of peripheral nerves and involves a series of neuroplastic changes in the spinal cord and brain [14, 15], namely, central sensitization. Neurotransmitters, neurotrophic factors, lipids, and cytokines/chemokines play important roles in the communication between neurons and glial cells in both peripheral and central sensitization [16, 17]. Interestingly, increasing evidence suggests that acupuncture can alleviate central sensitization induced by glial cell-mediated inflammation to achieve analgesia [18, 19]. Therefore, we have summarized the analgesic mechanisms of acupuncture in terms of neuroglial crosstalk and neuroplasticity-mediated central sensitization, highlighting the central neuroimmunological regulating mechanisms and providing novel evidence and insights for the clinical application of acupuncture.

## 2. Methods

**2.1. Search Strategy.** We searched the PubMed database for published studies, from January 2010 to April 2020. The keywords included ["acupuncture" or "electroacupuncture" or "manual acupuncture"] and ["pain" or "analgesia" or "analgesic"]. The language was limited to English. The filter process was done firstly by the website's search engine which initially identified 2888 articles.

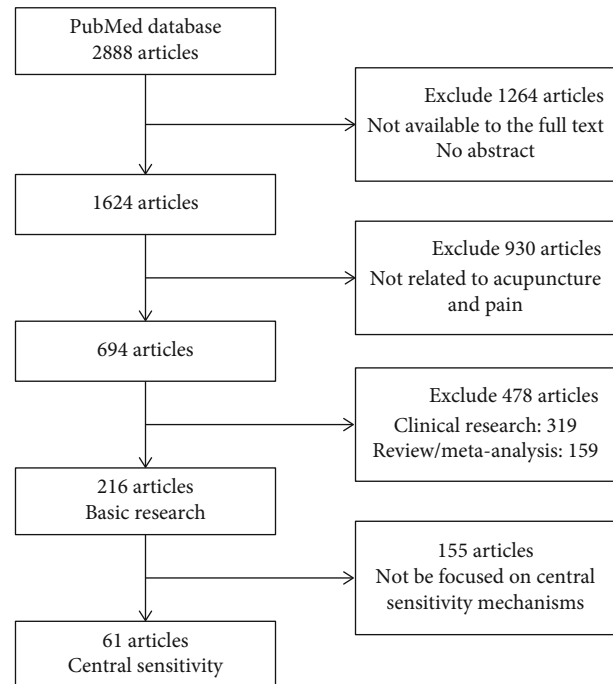


FIGURE 1: Flow chart of the search processes.

**2.2. Study Selection.** Of these articles, we excluded 1264 articles due to the absence of an abstract or unavailability of the full text, leaving 1624 articles. Hand searching was performed by screening the reference lists of articles that met our inclusion criteria based on the titles and abstracts. Of these, we excluded 930 articles as not related to acupuncture and pain in the titles and abstracts before full-text assessments resulting in 694 articles. These included 216 basic research articles, 319 clinical research articles, and 159 review articles or meta-analyses. The full texts of 216 basic research articles meeting the inclusion criteria were obtained and read carefully. Of these, 155 articles were excluded from 216 basic researches due to not be focused on central sensitivity mechanisms, resulting in 61 articles. A flowchart of the search process is shown in Figure 1.

**2.3. Data Extraction.** Of 61 basic researches on the central mechanism, the information from 35 typical and recently published studies are listed in Table 1 due to similarities in some of the studies, to analyze the central sensitization-related mechanisms of acupuncture analgesia. The study design data were extracted and classified using a predefined data extraction form that designated the pain model type, the intervention (methods, acupoints, acupuncture parameters), and the outcome measures (pain-related behavior, mechanism indexes). The data were extracted mainly by one author and were checked by the other authors.

## 3. Role of Neural-Immune Crosstalk in Peripheral Sensitization

The basic process of pain generation occurs when nociceptors located in the periphery of peptidergic and nonpeptidergic primary nociceptive neurons selectively respond to thermal, mechanical nociception, and irritating chemicals.

TABLE 1: Central sensitization regulatory mechanism of acupuncture analgesia.

Refs.	Pain model	Intervention methods	Acupoints	Acupuncture parameter	Pain-related behavior	Test site	Biochemical measurements
<i>4.1 Acupuncture inhibits the ascending excitatory pathway</i>							
Zhao et al. [42]	CCI	EA	ST36, SP6	2 Hz, 2 mA for 30 mins	Mechanical allodynia	Spinal cord	NR2B↓
Lee et al. [43]	CFA	EA	ST36, SP6	2 Hz, 1 mA for 30 mins	Thermal hyperalgesia	Spinal cord	Phospho-GluR2↓
Han et al. [44]	CFA	EA	ST36, SP6	2-15 Hz, 1 mA for 30 mins	Mechanical allodynia, thermal hyperalgesia	Spinal cord	GluR2 phosphorylation↓
Kim et al. [45]	CFA	EA	ST36, SP6	2 Hz, 1 mA for 30 mins	Thermal hyperalgesia	Spinal cord	GFAP↓, GLAST↑, GLT-1↑
Zeng et al. [46]	SNI	EA	ST36, SP6	2 Hz, 3 mA for 30 mins	Mechanical allodynia	Spinal cord	GLAST↑, GLT-1↓
Zhou et al. [47]	CFA	EA	ST36, BL60	Alternative 2 Hz/120 Hz, 1-2 mA for 30 mins	—	Spinal cord	Calcium voltage-gated channel subunit ↓, calcium voltage-gated channel auxiliary subunit gamma ↓
<i>4.2 Acupuncture regulates the descending pain modulatory system</i>							
Hu et al. [48]	CFA	EA	ST36, BL60	2 Hz/100 Hz, 1-2 mA for 30 mins	Mechanical allodynia	RVM	p38MAPK↓
Yuan et al. [49]	KOA	EA	Ex-LE4, ST35	2 Hz, 15 Hz or 100 Hz, 1 mA/0.1 mA for 30 mins	Mechanical allodynia, thermal hyperalgesia	vPAG	Endocannabinoid-CB1R-GABA-5-HT↑
Li et al. [50]	Hyperalgesia during ethanol withdrawal	EA	ST36	2 Hz, 0.2-0.3 mA for 20 mins	Thermal hyperalgesia	Habenula	MORs↑
Meng et al. [51]	Pacitaxel-induced neuropathic pain	EA	GB30	10 Hz, 2 mA for 30 mins	Mechanical allodynia	Spinal cord	μ and δ opioid receptor↑
Huang et al. [52]	CCI	EA	GV20, GV14	15 Hz, 1 mA for 20 mins	Mechanical allodynia and thermal hyperalgesia	PAG	GABA <sub>A</sub> ↑, GABA↑, GLU↓
Jiang et al. [53]	CCI	EA	EX-B2	2/15 Hz, 2 mA for 30 mins	Mechanical allodynia, thermal hyperalgesia	Spinal cord	GABA <sub>A</sub> ↑
Li et al. [54]	CCI	EA	ST36, GB34	Alternative 2 Hz/100 Hz, 1.5 mA for 30 mins	Mechanical allodynia, thermal hyperalgesia	Spinal cord	KCC2↑, GABAA receptor γ2↑

TABLE 1: Continued.

Refs.	Pain model	Intervention methods	Acupoints	Acupuncture parameter	Pain-related behavior	Test site	Biochemical measurements
Choi et al. [55]	PTX-induced neuropathic pain	EA	ST36	2 Hz, 2 mA for 30 mins	Mechanical allodynia and thermal hyperalgesia	Spinal cord	alpha2- and beta-adrenoceptors↑
Choi et al. [56]	PTX-induced neuropathic pain	BVA	LI11, ST36	—	Mechanical allodynia	Spinal cord	α2-adrenoceptor↑
Kim et al. [57]	Ankle sprain pain	EA	SI6	10 Hz, 2 mA for 30 mins	Weight-bearing force on the affected foot	Spinal cord	α2-adrenoceptor↑
Zhang et al. [58]	CFA	EA	GB30	10 Hz, 3 mA for 40 mins	Thermal hyperalgesia	Spinal cord	α2-ARs↑, 5-HTRs↑
da Silva et al. [59]	Uninjured rats	EA	ST36, SP6	2, 100, or 2/100 Hz, 1.4-1.5 mA for 20 mins	Thermal hyperalgesia	Spinal cord	Norepinephrine, acetylcholine, endogenous opioids, or GABA
Wu et al. [60]	Pain-depression dyad	EA	ST36, SP6	100 Hz, 1.0, 1.5, and 2.0 mA, each for 15 min	Mechanical allodynia	Dorsal raphe nucleus	5-HT↑
Zhang et al. [61]	CFA	EA	GB30	10 Hz, 3 mA, twice for 20 min each	Thermal hyperalgesia	Spinal cord	5-HT↑, 5-HT1AR↑
Zhang et al. [62]	CIP	EA	GB30	10 Hz, 2 mA for 30 mins	Mechanical allodynia and thermal hyperalgesia	Spinal cord	5-HT1AR↑, p-CaMKII↓
Li et al. [63]	Osteoarthritis-induced pain	EA	ST36, GB30	10 Hz, 2 mA for 30 mins	Weight-bearing force on the affected foot	Spinal cord	5-HT2A/2C↑
<i>4.3 Role of the tripartite synapse in acupuncture analgesia</i>							
Liang et al. [64]	SNL	EA	ST36, BL60	2, 100, or 2/100 Hz, 1-2 mA for 30 mins	Mechanical allodynia	Spinal cord	GFAP↓, OX-42↓
Choi et al. [65]	SCI	MA	GV26, GB34	Turned at a rate of 2 spins per second for 30 s, and retained for 30 mins	Mechanical allodynia, thermal hyperalgesia	Spinal cord	p38MAPK↓, ERK↓, PGE2↓
Lee et al. [66]	SCI	MA	GV26, GB34	Turned at a rate of two spins per second for 30 s, retained for 30 mins	Mechanical allodynia, thermal hyperalgesia	Spinal cord	JNK↓, CCL2↓, CCL4↓, and CCL20↓
Wang et al. [67]	CCI	EA	ST36, GB34	Alternative 2 Hz/100 Hz, 1 mA for 30 mins	—	Spinal cord	IL-1↑, TNF-α↓, BDNF↓, NT3/4↓, NGF↓
Yu et al. [68]	CFA	EA	ST36, SP6	Alternative 2 Hz/100 Hz, 2 mA for 20 mins	Mechanical allodynia, thermal hyperalgesia	Spinal cord	IL-10↑, IL-1β↓, NLRP3↓, TNF-α↓
Dai et al. [69]	Paw incision pain	EA	SP6, GB34	Alternative 2 Hz/100 Hz, 1-2-3 mA for 30 mins	Mechanical allodynia	Spinal cord	IL-10↑, LTP↓

TABLE 1: Continued.

Refs.	Pain model	Intervention methods	Acupoints	Acupuncture parameter	Pain-related behavior	Test site	Biochemical measurements
Ali et al. [70]	SNL	EA	ST36, SP6	2 Hz, 2-3 mA for 20 mins	Mechanical allodynia	Spinal cord	IL-10↑, $\beta$ -endorphin↑
Zhao et al. [71]	PTX-induced neuropathic pain	EA	ST36	10 Hz, 1 mA for 30 mins	Mechanical allodynia	Spinal cord	TMEM119↓, GFAP↓, TLR-4/NF- $\kappa$ b↓, TNF- $\alpha$ , and IL-1 $\beta$ ↓
Hsu et al. [72]	CFA	EA	ST36	2 Hz, 1 mA for 15 mins	Mechanical allodynia, thermal hyperalgesia	Spinal cord/thalamus	TLR2↓, pP13K↓, pAkt↓, pmTOR↓, pERK↓, pp38↓, pJNK↓, pCREB↓, pNF $\kappa$ B↓, Nav1.7↓, Nav1.8↓
<i>4.4 Role of chemokines and their receptors in acupuncture analgesia</i>							
Gao et al. [73]	Neck-incision pain	EA	LI18, LI4, PC6, or ST36, GB34	Alternative 2 Hz/100 Hz, 1 mA, 30 mins	Thermal pain	Spinal cord	ATP↓, P2X7R↓, CX3CL1↓, CX3CR1↓, p38 MAPK proteins↓
Li et al. [74]	CFA	EA	ST36	2 Hz for 30 mins	Mechanical allodynia, thermal hyperalgesia	Spinal cord	CX3CL1↓, p38 MAPK phosphorylation↓, IL-1↓, IL-6↓, and TNF- $\alpha$ ↓
Li et al. [75]	Paw incision pain	ACA	GB34, SP6	Alternative 2 Hz/100 Hz, 1, 2, 3 mA per 10 mins	Mechanical allodynia, thermal pain	Spinal cord	CX3CR signaling
Hu et al. [76]	CPIP	EA	ST36, BL60	Alternative 2 Hz/100 Hz, 0.5-1.5 mA, 30 mins	Mechanical hyperalgesia	Spinal cord	CXCL12/CXCR4↓, ERK↓

ACA: acupuncture-combined anesthesia; BVA: bee venom acupuncture; CCI: chronic constriction injury; CFA: complete Freund's adjuvant; CIP: chronic postschemic pain; EA: electroacupuncture; MA: manual acupuncture; SNL: spinal nerve ligation; SCI: spinal cord injury; TENS: transcutaneous electric nerve stimulation; RVM: rostral ventromedial medulla; PAG: periaqueductal gray; vPAG: ventral lateral periaqueductal gray.



During this process, related neurons in the dorsal root ganglia depolarize and generate receptor potentials, converting physical or chemical information to electrical information. The electrical information is transmitted along the sensory pathway to the spinal cord and other primary centers. The integrated information from the primary center can be transmitted to higher centers in the brain to form the pain sensation, or to the motor neurons in the anterior horn to produce a reflex [20].

Pain sensitization is a remodeling mechanism of the central and peripheral nociceptive receptors. Continuous stimulation such as tissue and nerve injury remodels the nociceptor to produce pain sensitization, specifically, peripheral sensitization, is indicative of primary hyperalgesia, including peripheral nociceptive receptors and dorsal root ganglion DRG [21]. Neuroimmune interactions are essential for peripheral sensitization [22]. There are two types of peripheral inflammation: tissue and neurogenic inflammation. Tissue damage can cause the local release of histamine, vascular dilatation, increased blood flow, and vascular exudation, as well as the release of various cytokines/chemokines and agglutination factors. The immune cells (including macrophages, mast cells, neutrophils, and lymphocytes) release inflammatory mediators to aggravate pain and, at the same time, release endogenous opioid peptides to inhibit peripheral inflammatory pain [23]. In recent years, cytokines/chemokines have been found to be involved in regulating and sensitizing the excitability of nociceptors. Inflammatory cytokines (interleukin- $1\beta$  (IL- $1\beta$ ), IL-6 and tumor necrosis factor- $\alpha$  (TNF- $\alpha$ )) mediate allodynia (pain resulting from a stimulus that would not normally provoke pain), hyperalgesia (increased response to noxious stimulation), and increasing the expression levels of substance P (SP) and prostaglandin E2 (PGE2) in neurons and glial cells in the DRG. Structurally, chemokines are similar to cytokines, and their receptors are expressed in the DRG. For instance, monocyte chemoattractant protein-1 (CCL2) and its receptor, C-C chemokine receptor type 2 (CCR2), were both increased in the nerve injury model. Moreover, CCL2 can promote the interaction between immune cells and nociceptors, thus playing a key role in inflammatory and neuropathic pain [20]. At the same time, the excitatory effect of cytokines/chemokines on nociceptive neurons is manifested by regulating the opening of ion channels; specifically, the activation of chemokine receptors can regulate the current in voltage-gated calcium channels (VGCCs) [20].

Neurogenic inflammation is caused by chemicals, such as SP and calcitonin gene-related peptide (CGRP), that are released from primary nociceptive neurons [24]. Upon peripheral tissue injury, sustained nociceptive stimulation or inflammation sensitizes the nociceptors. These discharges activate  $\gamma$ -aminobutyric acid (GABA) neurons by acting on *N*-methyl-D-aspartate (NMDA) or non-NMDA receptors in the intermediate neurons of the spinal cord and cause depolarization by acting on adjacent primary afferent terminals. The discharge also produces a dorsal root reflex by retrograde conduction, leading to the resensitization of the injury receptors mediated by neurogenic inflammation and finally inducing paresthesia and allodynia [20]. In addition, the sympathetic nervous system participates in strengthening

the neurogenic inflammatory process, and neuroimmune crosstalk plays an important role in peripheral sensitivity.

#### 4. Central Sensitization in Pain Transmission and Modulation Pathways Is a Crucial Target for Acupuncture Analgesia

Central sensitization, namely secondary hyperalgesia, including the disbalance of the ascending excitatory pathway and descending pain modulatory system, plays a vital role in the development and maintenance of chronic pain [25]. In the ascending excitatory pathway, amplification of neural signaling within the central nervous system (CNS) produces a state of neuronal hyperactivity and hyperexcitability in the spinal cord and brain, leading to hyperalgesia [26]. This occurs mainly in the lamina I and lamina V neurons of the spinal cord, as well as in medullary reticular formation, thalamus, hypothalamus, cerebellum, amygdala, basal ganglia, hippocampus, cortexes S1 and S2, insula, anterior cingulate cortex (ACC), prefrontal cortex, and some related cortical areas in the parietal and temporal lobes [27–30]. The descending pain modulatory system arises from a number of supraspinal sites, including the midbrain periaqueductal gray (PAG) that projects indirectly to the spinal cord via the rostral ventromedial medulla (RVM), lateral and caudal dorsal reticular nucleus (DRN), and ventrolateral medulla, of which the PAG-RVM system has been most studied [31].

As shown in Table 1, the neuropathic pain models, including pain generated by chronic constriction injury, chemotherapy-induced pain, spinal nerve ligation, and spinal cord injury, have been widely used in the study of central sensitization-mediated acupuncture analgesia. Inflammatory pain induced by the administration of complete Freund's adjuvant also causes central sensitization, including the dual mechanisms of peripheral and central sensitization. Many of these studies have used electroacupuncture (EA) rather than manual acupuncture, and the acupressure points ST36 and SP6 have been most used. Both low frequencies at 2–15 Hz and, alternatively, higher frequencies between 2 Hz and 100 Hz were effective in EA analgesia, providing useful information for maximizing the effects of acupuncture analgesia in clinical settings.

*4.1. Acupuncture Inhibits the Ascending Excitatory Pathway.* As described in Section 1, nociceptive receptors are composed of types A $\delta$  and C sensory fibers which transduce noxious stimuli from damaged peripheral tissues to the spinal cord. Neuroplasticity in the dorsal horn of the spinal cord assists and enhances pain perception by the nociceptive neurons. Central sensitization includes three processes: activation, sensitization, and modification of the CNS [32]. These are characterized by increases in the excitatory postsynaptic current (EPSC), including windup, long-term potentiation (LTP), and disinhibition. Among these, LTP caused by both high- and low-frequency electrical stimulation, nerve damage, or tissue damage is a process in which a transient synaptic activity can produce a long-lasting increase in synaptic strength. LTP relies on NMDA receptors (NMDARs) and voltage-dependent calcium channels, and

results in calcium influx, thereby activating protein kinase A, protein kinase C, and calcium/calmodulin-dependent protein kinase II (CaMKII) [33]. Protein synthesis is necessary for late-phase LTP (L-LTP), and administration of brain-derived neurotrophic factor (BDNF) in the spinal dorsal horn and the hippocampus can induce L-LTP of C-fiber potentials [34]. Disinhibition includes a reduction of GABAergic and/or glycinergic inhibition and an enhancement of A $\beta$  and C fiber sensitivity. The loss of inhibitory interneurons, impaired storage and/or release of inhibitory neurotransmitters, and impaired postsynaptic receptor activity have been proposed as the mechanisms underlying disinhibition [35]. Finally, the integrated signals travel through the spinal cord to the thalamus, where the location and intensity of the pain is processed. The signal then travels to the classic pain nerve circuit, the cerebral sensory cortex (S1, S2), which distinguishes the location and duration of the pain [36]. Apart from S1 and S2, neuronal activities in the ACC, insular cortex, and amygdala also contribute to various aspects of pain perception, including the experience of discomfort [37].

In terms of the molecular mechanisms, primary nociceptive neurons release glutamate, SP, CGRP, adenosine triphosphate (ATP), and neurokinin-1 (NK1) into the spinal cord. These molecules interact with their receptors, including NMDARs,  $\alpha$ -amino-3-hydroxy-5-methyl-4-isoxazolepropionic acid receptors (AMPA), metabotropic glutamate receptors (mGluR), SP receptors (NK1R), calcitonin receptor-like receptors (CRLR), and purinergic receptors (P2X, P2Y) of the spinal nociceptive projection neurons. This induces an influx of Ca<sup>2+</sup> into the pain neurons of the spinal cord [38], activating calcium-dependent intracellular cascades, inducing NMDAR phosphorylation [39], ultimately resulting in the generation of nociceptive information throughout the spinothalamic pain pathway [40, 41]. Thus, these mediators released by nociceptive neurons cause neural hyperexcitability and nociceptive transmission.

Glutamate is the most important and widely distributed excitatory neurotransmitter in the CNS and plays a critical role in the ascending excitatory pathway. Glutamate receptors are broadly divided into two groups, metabotropic glutamate receptors (mGluRs), and cation-permeable ionotropic glutamate receptors (iGluRs), which are, in turn, subdivided into NMDAR, Kainate-type iGluR, and AMPAR. Excitatory glutamatergic transmission plays a crucial role in the onset of chronic pain and is characterized by an increase in glutamate concentrations and receptor stimulation, leading to the transmission of pain messages [77, 78]. Somers et al. investigated the effects and potential mechanisms of transcutaneous electrical nerve stimulation (TENS) on neuropathic pain caused by chronic constriction injury (CCI). The mechanical allodynia was relieved by decreased concentrations of excitatory glutamate in the dorsal horn with a combination of low- and high-frequency TENS [79]. Recent evidence has shown that 2 Hz EA bilateral stimulation on the *Zusanli* (ST36) and *Sanyinjiao* (SP6) acupressure points produced analgesic effects through the downregulation of the N-methyl-D-aspartate receptor type 2B (NR2B, NMDAR subunit), inhibiting the transmission of pain messages in a CCI

rat model [42]. AMPAR consists of four subunits (GluR1-R4). EA has been demonstrated to prevent phosphorylation of AMPAR, especially the GluR2 subunit, in a Complete Freund's Adjuvant (CFA) model [43, 44]. In addition, the antinociceptive effect of EA is proposed to be related to the recovery of glutamate transporter (GT) expression, which can remove excess glutamate from the synaptic clefts. Both the spinal glutamate-aspartate transporter and GT1, which are mainly distributed in glial cells, were increased after EA treatment in CFA-injected rats as a result of proteasome downregulation [45]. A similar response has also been observed in a neuropathic pain model of spared nerve injury treated with EA [46]. Glutamatergic synaptic transmission is coupled with excess Ca<sup>2+</sup> entry into projection neurons and results in the activation of the Ca<sup>2+</sup>-dependent enzyme Ca<sup>2+</sup>/calmodulin-dependent protein kinase II (CamKII) and phosphorylation of the NR2B subunit of NMDAR at postsynaptic sites in the ACC, thus modulating visceral pain in a viscerally hypersensitive model [80]. It was reported that EA at ST36 and *Kunlun* (BL60) could reverse the actions of the calcium voltage-gated channel subunit and calcium voltage-gated channel auxiliary subunit  $\gamma$ , thus reducing chronic inflammatory pain (CIP) in the CFA rats [47].

**4.2. Acupuncture Regulates the Descending Pain Modulatory System.** It is now clear that the descending pain modulatory pathway can be both facilitatory and inhibitory, with a dynamic balance between the two functions. When acute pain turns to chronic pain, the descending facilitation function is dominant, leading to enhanced pain sensitization and even "mirror pain," in which the rostral RVM plays a key role. Descending projections from the RVM, identified as ON and OFF cells, facilitate and inhibit spinal nociceptive transmission, respectively. For example, RVM lesions or functional silencing can prevent pain sensitization induced by nerve injury. Excitatory amino acids, AMPAR, NMDAR, and the BDNF/TrkB signaling pathway are also involved in the process of descending facilitation. Several neurotransmitters (e.g., opioid, GABA, norepinephrine, and 5-hydroxytryptamine (5-HT)) are involved in these descending pathways [20]. It has been demonstrated that acupuncture functions mainly through facilitating the descending inhibitory system to ease pain, while the regulation of acupuncture on the descending facilitation system is poorly understood. Limited results have suggested that EA relieves inflammatory pain via inhibiting the activation of p38 mitogen-activated protein kinases (MAPK) in the central descending facilitation system [48]. In addition, EA potentiates the descending inhibitory control of 5-HT in the medulla via cannabinoid receptors on GABAergic but not glutamatergic neurons, thus inhibiting knee osteoarthritis pain [49].

**4.2.1. Regulation of Opioids and Their Receptors by Acupuncture.** Opioids and their receptors help reduce the excitatory transmitter release in the midbrain descending pathway, especially in the PAG-RVM system [81]. Kissiwa et al. found that opioid receptors, mainly the  $\mu$  opioid receptors (MORs), could inhibit glutamate release at synapses in

the amygdala [82]. In addition, the analgesic capacity of MORs in the PAG was negatively regulated by glutamate-binding NMDAR NR1 subunits [83]. Until now, the activation of endogenous opioids (e.g., enkephalin,  $\beta$ -endorphin, and dynorphin)/opioid receptor (e.g.,  $\mu$  and  $\delta$  opioid receptors) is the best-understood mechanism of acupuncture analgesia [50, 84–87]. Although different frequencies of EA can be reversed by the opioid antagonist naloxone, the types of opioids that mediate EA effects vary according to the EA frequency. For example, a single administration of 2 Hz EA at ST36 for 20 minutes can alleviate hyperalgesia during ethanol withdrawal through the mediation of MORs in the lateral habenula (LHb), an epithalamic structure rich in MORs. Activation of MORs may inhibit the release of glutamate in the LHb, which can block the descending nociceptive signal from the LHb to the PAG, thus reducing pain [50]. Besides MORs, 10 Hz EA at *Huantiao* (GB30) can significantly relieve paclitaxel-induced mechanical allodynia and hyperalgesia via the  $\delta$  or  $\kappa$  opioid receptors [51].

#### 4.2.2. Regulation of Nonopioid Neurotransmitters by Acupuncture

(1) *GABAergic Inhibitory Interneuron Network*. GABA is an important inhibitory neurotransmitter that is involved in the reduction of pain sensation through presynaptic inhibition [88]. The imbalance between excitatory glutamatergic and inhibitory GABAergic transmission, particularly decreased inhibition of GABAergic synaptic transmission in the spinal pain circuit, has been considered to underlie the development of central sensitization [23, 27, 52, 89, 90]. It was also found that RVM GABAergic neurons could facilitate mechanical pain by inhibiting dorsal horn enkephalinergic/GABAergic interneurons [91]. EA may initiate analgesia by increasing GABA expression on the descending pain modulatory pathways in the PAG [52]. Furthermore, the GABA receptor, a ligand-gated ionotropic receptor, is located mainly in postsynaptic neurons and contributes to the initiation of fast synaptic inhibition, thus being the major target for producing sedation [92]. EA at the bilateral L4 and L6 of *Hua Tuo Jia Ji* points (EX-B2) [53] or ST36 and *Yanglingquan* (GB34) points can significantly reduce neuropathic pain by increasing the GABA receptors in the spinal cord [54]. Moreover, EA can support the GABAergic system by reducing the rate of GABA reuptake. GABA transporter-1 (GAT1), the dominant neuronal GABA transporter, controls GABA concentrations, and EA was found to reduce GAT1 activity via activating the  $\delta$ -opioid receptor in the PAG [93]. Taken together, acupuncture can modulate the GABAergic system by increasing GABA expression, activating the GABA receptor, and inhibiting GABA reuptake.

(2) *Norepinephrine*. Norepinephrine is released from descending projection into the dorsal horn and helps to evoke an antinociceptive effect. The depletion of spinal norepinephrine caused mechanical hypersensitivity in a dose-dependent manner in a chronic pain rat model [94]. Studies have clearly shown that norepinephrine is involved in acupuncture analgesia. A previous report by Choi et al. demon-

strated that EA stimulation (2 mA, 2 Hz, 30 min, once every two days) at bilateral ST36 could significantly diminish paclitaxel-induced neuropathic pain. Further studies have shown that the antinociceptive effect of EA was mediated by spinal descending adrenergic pathways through the activation of the  $\alpha$ 2- and  $\beta$ -spinal adrenoceptors in mice [55, 56]. Consistent with these results, studies have shown that EA-induced analgesia in a rat model of an ankle sprain is mediated mainly by suppressing dorsal horn neuron activity through  $\alpha$ -adrenoceptors [57]. In addition, studies have shown that the analgesic effect of 10-Hz-EA was regulated by the spinal  $\alpha$ 2a-adrenoceptor, compared to the  $\alpha$ 2b-adrenoceptor in a CFA-induced inflammatory pain model [58]. It has also been found that intrathecal injection of desipramine, a selective noradrenaline uptake inhibitor, increased the availability of spinal noradrenaline and prolonged the antinociception effect of EA [59].

(3) *5-Hydroxytryptamine*. 5-HT (also called serotonin) arises largely from the RVM to the spinal cord and exerts biphasic modulation in the descending facilitation and inhibitory pathways. The facilitatory and inhibitory influence on the spinal processing of nociceptive information were mediated through recruitment of RVM ON or OFF cells, respectively, and depended on acute or chronic pain states and the type of receptor acted upon [60, 95]. A low dose of 5-HT produces facilitation of fast EPSCs in the spinal cord, while a high dose of 5-HT induces inhibition of AMPA/kainite-receptor-mediated EPSCs [88, 96]. Numerous studies have shown the involvement of the 5-HT and 5-HT receptors in acupuncture analgesia effects [60, 97–99]. EA at 100 Hz, but not 2, 50, or 2/100 Hz, was effective in alleviating the pain-depression dyad and upregulating 5-HT in the DRN of reserpine-injected rats [60]. In a CFA-inflammatory pain model, 10 Hz EA inhibited thermal hyperalgesia through the activation of spinal 5-hydroxytryptamine 1A receptors (5-HT<sub>1A</sub>) but not 5-HT<sub>2BR</sub>, 5-HT<sub>2CR</sub>, or 5-HT<sub>3R</sub> [58, 61]. Consistent with these results, EA activated spinal 5-HT<sub>1A</sub> to alleviate both allodynia and hyperalgesia in CIP rats [62]. In an osteoarthritis model, the effectiveness and mechanisms of EA were focused on the involvement of spinal 5-HT<sub>2A/2C</sub> receptors [63]. Taken together, these data suggest that spinal 5-HT and its receptors are involved in acupuncture analgesia but the effects differ according to both animal models and EA frequencies.

#### 4.3. Role of the Tripartite Synapse in Acupuncture Analgesia

4.3.1. *Neuroglial Crosstalk Regulates the Neural Plasticity*. Vladimir Parpura first proposed the concept of the “tripartite synapse” in 1994 [100]. This concept added glial cells (astrocytes and microglia) to the original classic pre- and postsynaptic neuronal cells, thus emphasizing the important roles of glial cells in synaptic transmission and regulation. It is noteworthy that recent studies have shown that central sensitization driven by neuroinflammation in the CNS is accompanied by glial activation, including the activation of astrocytes, microglia, and oligodendrocytes in the spinal cord and brain [101]. Lau and coworkers found that



L5 spinal nerve ligation (SNL) caused the upregulation of cyclooxygenase-1 (COX-1) and COX-2 in spinal microglial and neuronal cells; these enzymes are involved in the production of prostaglandins (PGs) via arachidonic acid pathways and, in turn, lead to the development of neuropathic pain [102]. Functional imaging also showed elevated cerebral levels of the translocator protein, a marker of glial activation, in patients with chronic low back pain [103]. Therefore, chronic pain may also be the result of “gliopathy” [104].

It is increasingly clear that neural plasticity is regulated by neuroglial crosstalk. After peripheral tissue or nerve damage, neurotransmitters such as glutamate, SP, and CGRP released from nociceptive primary afferent fibers in the dorsal horn not only cause intense high-frequency activation of the neural postsynaptic receptors and amplification of the postsynaptic current but also interact with their corresponding receptors on microglia and astrocytes [105–107], activating the voltage-dependent calcium channel and inducing calcium entry into the neuron. Glia-derived substances are termed gliotransmitters and include cytokines (IL-1, IL-6, and TNF- $\alpha$ ), chemokines (CCL2 [108] and CXCL1 [109]), and inflammatory mediators (e.g., bradykinin, PGs, and nitric oxide). These chemicals promote an inflammatory environment [101] and act as chemical mediators to amplify neuroglial reactivity in a paracrine manner, favoring the elevation of these mediators in the dorsal horn of the spinal cord [110]. As an example, TNF- $\alpha$  acting at the TNF- $\alpha$  receptor 1 (TNFR1) functions in the development of pain by facilitating excitatory synaptic signaling in the acute phases after nerve injury in CCI mice compared with sham control mice [111]. TNF- $\alpha$  contributes to neural plasticity through mechanisms involving the downregulation of GTs, upregulation of the glutamate concentration in the synapse, and phosphorylation of NMDAR. TNF- $\alpha$  subsequently promotes the facilitation of excitatory synaptic transmission and downregulates the expression of GABA receptors, thus reducing the inhibition of excitatory transmission [112]. Chemokines can also regulate the interactions of neurons and glial cells, e.g., CCL2 derived from astrocytes can “talk to” neurons by regulating neuronal activity via c-Jun-N-terminal kinase (JNK) MAPK [108]. These mediators produced by active glial cells contribute to neural plasticity. During the process, the activated glia can release prostaglandin, BDNF, nitric oxide, and other neuroactive substances; reduce the inhibitory effects of GABA; and upregulate the expression of NMDARs, thereby increasing nerve excitability and maintaining neuropathic pain [22, 113]. Moreover, modification of glial cell numbers in the brain is likely correlated with the emotional experience of pain, as well as mood disorders such as depression and anxiety [114]. Once activated, the glial cells in the spinal cord release cytokines that provide positive feedback, further enhancing excitatory synaptic transmission.

**4.3.2. Inhibition of Glial Activity by Acupuncture.** It has been shown that in the neuropathic pain model induced by SNL, the inhibition of spinal microglia and astrocytes mediates the immediate and long-term EA analgesia, respectively [64]. It has also been reported that the analgesic efficacy of

EA might be related to the modulation of microglial and astrocyte activation [115–117]. Acupuncture has been reported to suppress signal transduction pathways and key molecules, including p38 MAPK, extracellular regulated kinases (ERK), and JNK, in microglial and astrocyte activation in pain processing [65, 66, 118–120]. Previous results observed that the acupuncture analgesic effect is related to spinal cytokines and neurotrophic factors released by glial cells [67, 121, 122]. Repeated EA treatment at the bilateral ST36 and GB34 points once a day can relieve chronic pain and suppress the elevated mRNA expression of TNF $\alpha$  and IL-1 $\beta$  in the spinal cord of CCI rats [67]. EA (2/100 Hz, 2 mA) for five consecutive days can significantly increase the mechanical threshold and thermal latency after CFA injection. This could be partially associated with the suppression of proinflammatory cytokines (e.g., TNF- $\alpha$  and IL-1 $\beta$ ) and the stimulation of IL-10 in the spinal cord. IL-10, produced by the spinal cord, is the key anti-inflammatory cytokine for relieving both inflammatory pain [68, 69] and neuropathic pain [70]. Paclitaxel significantly activates both microglia and astrocytes and increases the expression of inflammatory cytokines (IL-1 $\beta$  and TNF- $\alpha$ ) in the lumbar spinal cord. EA treatment (10 Hz, 1 mA) at the bilateral ST36 point in rats suppressed the expression of inflammatory cytokines through the downregulation of the TLR4/NF- $\kappa$ B pathway as well as suppressing activated microglia and astrocytes [71]. Besides TLR4, increased expression of TLR2 in the spinal cord and thalamus was also reportedly suppressed by EA in a CFA model [72]. Therefore, the downregulation of gliotransmitters by acupuncture can prevent the activation of neuroglial crosstalk, thus contributing to the easing of chronic pain. However, the evidence on how acupuncture modulates glial cells to inhibit excitatory synaptic transmission is still incomplete.

#### 4.4. Role of Chemokines and Their Receptors in Acupuncture Analgesia

**4.4.1. Introduction to the Chemokine System.** Chemokines, 8–12 kDa secreted proteins, constitute the largest family of cytokines. According to the number and spacing of cysteines, chemokines consist of two major families, CC (CC<sub>1–28</sub>) and CXC (CXC<sub>1–16</sub>) chemokines, as well as two minor families, XC (XC<sub>1–2</sub>) and CX3C (CX3CL1) chemokines [123]. All chemokines bind to the members of a family of seven transmembrane-spanning heterotrimeric G protein-coupled receptors (GPCRs). Chemokines are regarded as important mediators of inflammation and help to control the positioning and migratory patterns of immune cells. Immune cell residence in primary (T cells, B cells), secondary (lymph nodes, spleen, Peyer’s patches), and tertiary lymphoid organs are under the fine control of this complex system of approximately 50 endogenous chemokines [123]. The development of T cells in the thymus depends on the interaction of epithelial-derived CCL21, CCL25, and CXCL12 with CCR7, CCR9, and CXCR4, respectively, expressed on T cell progenitors [124]. In contrast to the thymus, the homeostasis and development of immune cells in the bone marrow seems to be governed by the opposing forces of interactions between

CXCL12/CXCR4 and CCL2/CCR2 [123]. Chemokines, considered as regulators of peripheral immune cell transport, are capable of inducing the migration of T, NK cells, dendritic cells, and/or macrophages [125]. There has been growing recognition that the chemokine system orchestrates immune cell migration (e.g., macrophages [126] and lymphocytes [127]) into the DRG and CNS. This plays a critical role in the central sensitization in the early initiation of pain perception [128]. Besides, chemokines and their receptors expressed by neurons and glial cells in the CNS have been shown to mediate neuroglial communication and nociceptive signal transmission at different anatomical locations, including nerves, the DRG, spinal cord, and brain [129, 130].

*4.4.2. Acupuncture Analgesia via Regulation Chemokine and Their Receptors.* Concomitant with the increasing use of acupuncture to alleviate pain, attention has been paid in recent years to the mechanism of acupuncture analgesia from the perspective of chemokines.

(1) *CX3CL1/CX3CR1.* CX3CL1 is specifically expressed in neurons and binds to the CX3CR1 receptor on the microglial cell membrane [125], activating the MAPK pathway. MAPKs play important roles in information transmission between neurons and glial cells as well as the genesis of pain hypersensitivity induced by CX3CL1/CX3CR1 [131, 132]. Gao et al. reported that peripheral injury to the primary afferent nociceptive neurons caused the release of CX3CL1 into the spinal cord, which activated the production of TNF $\alpha$  in a p38 MAPK-dependent mechanism in microglia. In turn, the activation of TNF- $\alpha$  regulates CCL2 expression in astrocytes in a JNK MAPK-dependent manner. CCL2 subsequently activates central neurons through CCR2, eventually leading to neuropathic pain [133]. Neutralizing antibodies to CX3CL1 or CX3CR1 could attenuate mechanical hyperalgesia in neuropathic pain models [134, 135]. It has been demonstrated that neuron-microglia interactions are mediated by purinergic receptors, and, subsequently, by CX3CL1/CX3CR1. The purinergic P2X7R/CX3CL1/CX3CR1 pathway, following intracellular phosphorylation of microglial p38 MAPK [136] which subsequently stimulates the release of IL-6 and IL-1 $\beta$  [137], plays a key role in nociceptive signal transmission [138].

In a rat neck-incision pain model, Gao et al. found that two sessions of EA at *Futu* (LI18), *Hegu* (LI4), *Neiguan* (PC6), or ST36, GB34 could significantly relieve thermal pain, followed by the downregulation of ATP/P2X7R/CX3CL1/CX3CR1 signaling and suppression of its downstream p38 MAPK pathway in the upper cervical spinal cord after three sessions. Thereby, EA suppressed ATP/P2X7R/CX3CL1/CX3CR1/p38 MAPK-induced neuroglial crosstalk in pain processing [73]. The results are consistent with the reports by Li that 2 Hz EA at ST36 for 30 mins reduced the overexpression of CX3CL1 other than CX3CR1 in the spinal cord of the CFA model rats. EA inhibited the activation of neuronal and microglial cells and decreased p38 MAPK signaling and the downstream proinflammatory cytokines IL-1, IL-6, and TNF- $\alpha$ . They also found that EA did not

inhibit the expression of p38 MAPK but inhibited its phosphorylation [74]. Slightly different from their results, the report by Li et al. [75] demonstrated that mechanical allodynia and thermal pain induced hyperalgesia by paw incision was significantly suppressed by acupuncture-combined anesthesia (ACA). However, the analgesic effect of ACA was not apparent in CX3CR1 knockout mice and was also blocked when a neutralizing antibody to CX3CR1 was intrathecally injected 1 h before ACA in C57BL/6J mice, suggesting that CX3CR1 in microglia is not only involved in postincision pain, but also in ACA-induced analgesia.

(2) *CXCL12/CXCR4.* CXCL12 and CXCR4 are, respectively, expressed in neurons and glial cells in the central nervous system [139], and the CXCL12/CXCR4 activation leads to increased pain sensitivity in the spinal cord. A study by Luo et al. demonstrated that CXCL12 and CXCR4 are upregulated in the spinal cord dorsal horn in chronic posts ischemic pain (CPIP) mice. Intrathecal blocking of CXCR4 improved mechanical allodynia, suggesting an important role of spinal CXCL12/CXCR4 signaling in ameliorating the pain response [140]. Hu et al. found that EA exerted an analgesic effect on the same rat model of CPIP by suppressing the overexpression of CXCL12/CXCR4 in the spinal cord dorsal horn. Furthermore, they found that EA can effectively inhibit excessive activation of glial cells in the spinal cord and markedly reduce downstream ERK pathway activation, thus reducing the central sensitization and exerting an analgesic effect [76].

(3) *CCL2/CCR2.* CCL2 is expressed in spinal astrocytes and induces neuronal activation via CCR2 to increase excitatory synaptic transmission (astrocyte-to-neuron signaling), contributing to central sensitization and neuropathic pain development. It has been shown that CCL2/CCR2 was upregulated in the spinal cord via the JNK pathway after SNL [108]. CCL2 can also rapidly increase NMDA-induced current and spontaneous EPSCs [108] or inhibit GABA-induced currents [141] in dorsal horn neurons, all of which are critically involved in the maintenance of pain. Furthermore, spinal administration of CCL2 induced thermal hyperalgesia via activating the spinal transient receptor potential vanilloid 1 (TRPV1) receptors [142]. Lee et al. demonstrated acupuncture at *Shuigou* (GV26) and GB34 significantly alleviated both mechanical allodynia and thermal hyperalgesia after spinal cord injury at L4-L5. It is noteworthy that acupuncture inhibited the astrocyte expression of CCL2, which is known to be mediated through the JNK pathway and contributes to excitatory synaptic transmission. Apart from the findings on CCL2, Lee also showed that JNK-dependent CCL4 and CCL20 expression was significantly decreased by acupuncture treatment [66].

(4) *CXCL1/CXCR2.* CXCL1 and CXCR2 are expressed in astrocytes and neurons, respectively, in the spinal cord, and CXCL1/CXCR2 in the lumbar spinal cord has been demonstrated to play key roles in pain processing. The application of CXCL1 in the spinal cord acted on CXCR2, inducing the expression of phosphorylated ERK and cAMP-response element-binding protein, c-fos, and COX-2 in the spinal cord

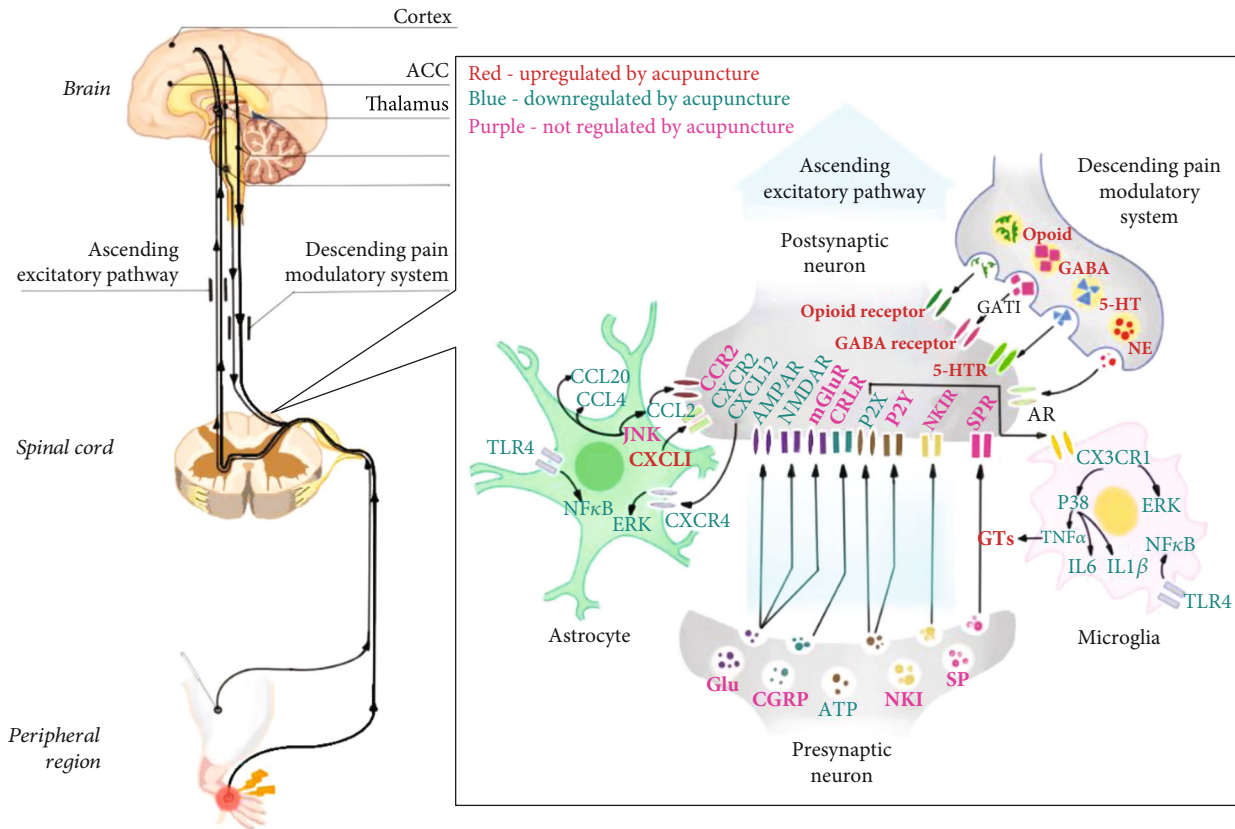


FIGURE 2: Role of neuroglial crosstalk and synaptic plasticity mediated central sensitization in acupuncture analgesia. The titles of neurotransmitters, neuropeptides, and immune factors are presented in red, blue, and purple, as the figure shows. Factors in red are upregulated by acupuncture, while factors in blue are downregulated by acupuncture. Factors in purple are activated or inhibited in the central sensitization process but are not regulated by acupuncture. ACC: anterior cingulate cortex; PAG: periaqueductal gray; RVM: rostral ventromedial medulla; GABA:  $\gamma$ -aminobutyric acid; 5-HT: 5-hydroxytryptamine; 5-HTR: 5-hydroxytryptamine receptor; NE: norepinephrine; AR: adrenergic receptor; GAT1: GABA transporter 1; Glu: glutamate; AMPAR:  $\alpha$ -amino-3-hydroxy-5-methyl-4-isoxazolepropionic acid receptor; NMDAR: *N*-methyl-*D*-aspartate receptor; mGluR: metabotropic glutamate receptors; CGRP: calcitonin gene-related peptide; CRLR: calcitonin receptor-like receptor; ATP: adenosine triphosphate; P2X: P2X receptor; P2Y: P2Y receptor; NK1: neurokinin-1; NK1 receptor: neurokinin-1 receptor; SP: substance P; SPR: substance P receptor; CX3CL1: C-X3-C motif chemokine ligand 1; CX3CR1: C-X3-C chemokine receptor 1; ERK: extracellular signal-regulated kinases; TNF- $\alpha$ : tumor necrosis factor- $\alpha$ ; IL-6: interleukin-6; IL-1 $\beta$ : interleukin-1 $\beta$ ; GT: glutamate transporter; TLR4: toll-like receptor 4; JNK: c-Jun-N-terminal kinase; CCL2: C-C motif chemokine ligand 2; CCL4: C-C motif chemokine ligand 4; CCL20: C-C motif chemokine ligand 20; CCR2: C-C chemokine receptor 2; CXCL1: C-X-C motif chemokine ligand 1; CXCR2: C-X-C chemokine receptor 2; CXCL12: C-X-C motif chemokine ligand 12; CXCR4: C-X-C chemokine receptor 4. Red, promoted by acupuncture; blue, inhibited by acupuncture.

neurons and leading to the subsequent maintenance of neuropathic pain [109]. Similarly, Cao and coworkers showed that astrocytes were activated after inflammation and released CXCL1 in the spinal cord, which could then act on CXCR2 to induce ERK activation, synaptic transmission, and COX-2 expression in dorsal horn neurons, ultimately contributing to the pathogenesis of CFA-induced inflammatory pain [143]. In addition, Xu et al. found that astrocyte-secreted CXCL1 activated spinal cord dorsal horn neurons to express CXCR2 in cancer pain models [144]. Taken together, CXCL1/CXCR2 is involved in the development of neuropathic, inflammatory, and cancer pain.

However, it has also been demonstrated that CXCL1/CXCR2 is involved in pain relief. Previously, a study by Cao et al. demonstrated intrathecal administration of recombinant CXCL1 in wild-type mice significantly reduced

spinal nerve L5 transection- (L5Tx-) induced mechanical hypersensitivity. Due to CXCL1's chemotaxis, it is capable of associating with the increased number of opioid peptides produced by infiltrating neutrophils in the lumbar spinal cord [145]. Similarly, Guo and his colleagues showed that bone marrow stromal cell-induced monocytes secrete CXCL1 which could cross the blood-brain barrier and contribute to pain relief. The CXCL1/CXCR2 signaling triggers opioid release by activation of central  $\mu$ -opioid receptors in the RVM [146]. Furthermore, we have observed a novel function of acupuncture-derived CXCL1 in the CFA rat model. In our unpublished data, it was found that acupuncture at ST36 could induce high CXCL1 levels in CFA rat serum. CXCL1 neutralizing antibodies reduced the acupuncture analgesic effect by 20%. Our results demonstrated that acupuncture-derived CXCL1 can induce spinal cord CXCR2 desensitization, blocking COX2 production in the spinal cord. These

phenomena showed that the same chemokines involved in pain sensitization may also be neuroprotective and promote pain relief under certain conditions.

## 5. Conclusion

To conclude (as shown in Figure 2), it is well established that pain is a hypersensitivity state caused by peripheral and central sensitization. Central sensitization is modulated by the ascending excitatory pathway and the descending pain modulatory system. With the emergence of the “tripartite synapse” concept, neuroglial cells are considered as active partners of neurons at the synapse and can contribute to central sensitization. It is increasingly appreciated that neurotransmitters (e.g., glutamate, opioid, GABA, norepinephrine, and 5-HT), inflammatory cytokines, and chemokines are implicated in this crosstalk. Acupuncture analgesia involves the ascending excitatory pathway and the descending pain modulatory system through the downregulation of glutamate and upregulation of opioids, GABA, norepinephrine, and 5-HT. Evidence indicates that the occurrence and maintenance of pain are closely related to immune responses, and the role of cytokines/chemokines in mediating neuroglial communication has attracted much attention in recent years. Acupuncture analgesia has also been demonstrated to inhibit cytokines such as IL-1 $\beta$ , IL-6, and TNF- $\alpha$  and upregulate IL-10, as well as modulating chemokines and their receptors such as CX3CL1/CX3CR1, CXCL12/CXCR4, CCL2/CCR2, and CXCL1/CXCR2. Furthermore, acupuncture has been found to regulate downstream neural MAPK signaling (e.g., p38, ERK, and JNK pathways), which contribute to the activation of nociceptive neurons. However, the responses of chemokines to acupuncture differ between pain model types, acupuncture methods, and parameters, requiring future clarification of the exact mechanisms. Taken together, the inhibition of neuroglial plasticity-mediated central sensitization is one of the critical mechanisms in acupuncture analgesia, contributing to the wider application of acupuncture, alone or in combination with pain medication, in the enhancement of treatment effectiveness and the lowering of pain medication dosages and decreasing the risk of debilitating adverse effects. The acupuncture parameters described in these studies, particularly those of EA stimulation, also provide significant information for maximizing the effect of acupuncture in the clinical setting.

## Abbreviations

RTCs:	Randomized controlled trials
IL-1 $\beta$ :	Interleukin-1 $\beta$
TNF- $\alpha$ :	Tumor necrosis factor- $\alpha$
SP:	Substance P
PGE2:	Prostaglandin E2
DRG:	Dorsal root ganglion
VGCCs:	Voltage-gated calcium channels
CGRP:	Calcitonin gene-related peptide
GABA:	$\gamma$ -Aminobutyric acid
NMDA:	N-methyl-D-aspartate

CNS:	Central nervous system
EPSC:	Excitatory postsynaptic current
LTP:	Long-term potentiation
NMDARs:	N-methyl-D-aspartate receptors
CaMKII:	Calcium/calmodulin-dependent protein kinase II
L-LTP:	Late-phase LTP
BDNF:	Brain-derived neurotrophic factor
ACC:	Anterior cingulate cortex
ATP:	Adenosine triphosphate
NK1:	Neurokinin-1
AMPA:	$\alpha$ -Amino-3-hydroxy-5-methyl-4-isoxazolepropionic acid receptors
mGluR:	Metabotropic glutamate receptors
SPR:	SP receptor
CRLR:	Like receptor
NK1R:	NK1 receptor
iGluR:	$\alpha$ -Amino-3-hydroxy-5-methyl-4-isoxazolepropionic acid receptor, ionotropic glutamate receptors
TENS:	Transcutaneous electrical nerve stimulation
CCI:	Chronic constriction injury
EA:	Electroacupuncture
NR2B:	N-methyl-D-aspartate receptor type 2B
CFA:	Complete Freund's adjuvant
GT:	Glutamate transporter
CIP:	Chronic inflammatory pain
PAG:	Periaqueductal gray
RVM:	Rostral ventromedial medulla
DRN:	Dorsal reticular nucleus
5-HT:	5-Hydroxytryptamine
MOR:	$\mu$ opioid receptor
LHb:	Lateral habenula
GAT1:	GABA transporter 1
5-HT1AR:	5-Hydroxytryptamine 1A receptors
SNL:	Spinal nerve ligation
COX-1:	Cyclooxygenase-1
PGs:	Prostaglandins
TNFR1:	TNF- $\alpha$ receptor 1
MAPK:	Mitogen-activated protein kinase
ERK:	Extracellular signal-regulated kinase
MA:	Manual acupuncture
GPCRs:	G protein-coupled receptors
JNK:	c-Jun-N-terminal kinase
ACA:	Acupuncture-combined anesthesia
CPIP:	Chronic posts ischemic pain
TRPV1:	Transient receptor potential1 vanilloid 1
L5Tx:	L5 transection

## Data Availability

The generated or analyzed data used to support the findings of this study are included within the article.

## Conflicts of Interest

The authors have no conflict of interest regarding this paper.



## Authors' Contributions

The authors contributed in the following manner: Zhongxi Lyu and Yongming Guo contributed to the concept design, data collection, and paper writing; Wen Fan and Baomin Dou contributed to the figures and graphic abstract edit; Yinan Gong contributed to the data collection and analysis; Ningcen Li, Shenjun Wang, Yuan Xu, Yangyang Liu, Bo Chen, and Yi Guo contributed to the language modification and text check; and Xiaowei Lin and Zhifang Xu contributed to the concept design and paper review. Zhongxi Lyu and Yongming Guo contributed equally to this work.

## Acknowledgments

This study was financially supported by the National Key R&D Program of China No. 2019YFC1709003; the National Natural Science Foundation of China (NSFC) No. 81704146, 81873369, and 81873368; the Natural Science Foundation of Tianjin No. 20JQNJC00280.

## References

- [1] L. J. Crofford, "Chronic pain: where the body meets the brain," *Transactions of the American Clinical and Climatological Association*, vol. 126, pp. 167–183, 2015.
- [2] A. Vincent, M. O. Whipple, S. J. McAllister, K. M. Aleman, and J. L. St Sauver, "A cross-sectional assessment of the prevalence of multiple chronic conditions and medication use in a sample of community-dwelling adults with fibromyalgia in Olmsted County, Minnesota," *BMJ Open*, vol. 5, no. 3, article e006681, 2015.
- [3] P. Baral, S. Udit, and I. M. Chiu, "Pain and immunity: implications for host defence," *Nature Reviews Immunology*, vol. 19, no. 7, pp. 433–447, 2019.
- [4] B. I. Martin, R. A. Deyo, S. K. Mirza et al., "Expenditures and health status among adults with back and neck problems," *JAMA*, vol. 299, no. 6, pp. 656–664, 2008.
- [5] M. Verret, F. Lauzier, R. Zarychanski et al., "Perioperative use of gabapentinoids for the management of postoperative acute pain: protocol of a systematic review and meta-analysis," *Systematic Reviews*, vol. 8, no. 1, p. 24, 2019.
- [6] N. B. Finnerup, "Nonnarcotic methods of pain management," *The New England Journal of Medicine*, vol. 380, no. 25, pp. 2440–2448, 2019.
- [7] K. Kingwell, "Screening for cleaner pain relief," *Nature Reviews Drug Discovery*, vol. 15, no. 10, p. 677, 2016.
- [8] NIN Consensus Development Panel on Acupuncture, "Acupuncture," *JAMA: The Journal of the American Medical Association*, vol. 280, no. 17, pp. 1518–1524, 1998.
- [9] Q. Zhang, A. Sharan, S. A. Espinosa, D. Gallego-Perez, and J. Weeks, "The path toward integration of traditional and complementary medicine into health systems globally: the World Health Organization report on the implementation of the 2014–2023 strategy," *Journal of Alternative and Complementary Medicine*, vol. 25, no. 9, pp. 869–871, 2019.
- [10] M. Abou el Hassan, K. Huang, M. B. K. Esvara et al., "Cancer cells hijack PRC2 to modify multiple cytokine pathways," *PLoS One*, vol. 10, no. 6, article e0126466, 2015.
- [11] Y. Guo, H. Zhao, F. Wang et al., "Recommendations for acupuncture in clinical practice guidelines of the national guideline clearinghouse," *Chinese Journal of Integrative Medicine*, vol. 23, no. 11, pp. 864–870, 2017.
- [12] A. J. Vickers, E. A. Vertosick, G. Lewith et al., "Acupuncture for Chronic Pain: Update of an Individual Patient Data Meta-Analysis," *The Journal of Pain*, vol. 19, no. 5, pp. 455–474, 2018.
- [13] L. Zhao, J. Chen, Y. Li et al., "The long-term effect of acupuncture for migraine prophylaxis," *JAMA Internal Medicine*, vol. 177, no. 4, pp. 508–515, 2017.
- [14] E. Deval, J. Noel, N. Lay et al., "ASIC3, a sensor of acidic and primary inflammatory pain," *The EMBO Journal*, vol. 27, no. 22, pp. 3047–3055, 2008.
- [15] S. Wang, Y. Dai, K. Kobayashi et al., "Potentiation of the P2X3 ATP receptor by PAR-2 in rat dorsal root ganglia neurons, through protein kinase-dependent mechanisms, contributes to inflammatory pain," *The European Journal of Neuroscience*, vol. 36, no. 3, pp. 2293–2301, 2012.
- [16] R. L. Silva, A. H. Lopes, R. M. Guimaraes, and T. M. Cunha, "CXCL1/CXCR2 signaling in pathological pain: role in peripheral and central sensitization," *Neurobiology of Disease*, vol. 105, pp. 109–116, 2017.
- [17] R. R. Ji, Z. Z. Xu, and Y. J. Gao, "Emerging targets in neuroinflammation-driven chronic pain," *Nature Reviews Drug Discovery*, vol. 13, no. 7, pp. 533–548, 2014.
- [18] F. A. Pinho-Ribeiro, W. A. Verri Jr., and I. M. Chiu, "Nociceptor sensory neuron-immune interactions in pain and inflammation," *Trends in Immunology*, vol. 38, no. 1, pp. 5–19, 2017.
- [19] S. Talbot, S. L. Foster, and C. J. Woolf, "Neuroimmunity: physiology and pathology," *Annual Review of Immunology*, vol. 34, no. 1, pp. 421–447, 2016.
- [20] J. H. Jun Chen, B. Fan, S. Yu, and J. Wang, "The underlying mechanisms of chronic pain: from basic to clinical," *Chinese Journal of Pain Medicine*, vol. 20, no. 2, pp. 70–80, 2014.
- [21] C. J. Woolf and Q. Ma, "Nociceptors—noxious stimulus detectors," *Neuron*, vol. 55, no. 3, pp. 353–364, 2007.
- [22] K. Ren and R. Dubner, "Interactions between the immune and nervous systems in pain," *Nature Medicine*, vol. 16, no. 11, pp. 1267–1276, 2010.
- [23] A. I. Basbaum, D. M. Bautista, G. Scherrer, and D. Julius, "Cellular and molecular mechanisms of pain," *Cell*, vol. 139, no. 2, pp. 267–284, 2009.
- [24] W. D. Willis Jr., "Dorsal root potentials and dorsal root reflexes: a double-edged sword," *Experimental Brain Research*, vol. 124, no. 4, pp. 395–421, 1999.
- [25] P. Boadas-Vaello, S. Castany, J. Homs, B. Alvarez-Perez, M. Deulofeu, and E. Verdu, "Neuroplasticity of ascending and descending pathways after somatosensory system injury: reviewing knowledge to identify neuropathic pain therapeutic targets," *Spinal Cord*, vol. 54, no. 5, pp. 330–340, 2016.
- [26] C. J. Woolf, "Central sensitization: implications for the diagnosis and treatment of pain," *Pain*, vol. 152, Supplement, pp. S2–15, 2011.
- [27] A. Latremoliere and C. J. Woolf, "Central sensitization: a generator of pain hypersensitivity by central neural plasticity," *The Journal of Pain*, vol. 10, no. 9, pp. 895–926, 2009.
- [28] X. M. Shao, J. Sun, Y. L. Jiang et al., "Inhibition of the cAMP/PKA/CREB pathway contributes to the analgesic effects of electroacupuncture in the anterior cingulate cortex in a rat pain memory model," *Neural Plasticity*, vol. 2016, Article ID 5320641, 16 pages, 2016.

- [29] Z. J. Weng, L. Y. Wu, C. L. Zhou et al., "Effect of electroacupuncture on P2X3 receptor regulation in the peripheral and central nervous systems of rats with visceral pain caused by irritable bowel syndrome," *Purinergic Signal*, vol. 11, no. 3, pp. 321–329, 2015.
- [30] Y. Qiao, F. Wu, J. Wang, X. Cui, C. Liu, and X. Zhu, "Effects of injection of anti-corticotropin release hormone serum in the lateral ventricles and electroacupuncture analgesia on pain threshold in rats with adjuvant arthritis," *Neural Regeneration Research*, vol. 7, no. 21, pp. 1630–1636, 2012.
- [31] M. M. Heinricher, I. Tavares, J. L. Leith, and B. M. Lumb, "Descending control of nociception: specificity, recruitment and plasticity," *Brain Research Reviews*, vol. 60, no. 1, pp. 214–225, 2009.
- [32] A. Kumar, H. Kaur, and A. Singh, "Neuropathic pain models caused by damage to central or peripheral nervous system," *Pharmacological Reports*, vol. 70, no. 2, pp. 206–216, 2018.
- [33] J. Lisman, R. Yasuda, and S. Raghavachari, "Mechanisms of CaMKII action in long-term potentiation," *Nature Reviews Neuroscience*, vol. 13, no. 3, pp. 169–182, 2012.
- [34] L. J. Zhou, Y. Zhong, W. J. Ren, Y. Y. Li, T. Zhang, and X. G. Liu, "BDNF induces late-phase LTP of C-fiber evoked field potentials in rat spinal dorsal horn," *Experimental Neurology*, vol. 212, no. 2, pp. 507–514, 2008.
- [35] A. J. Todd, "Neuronal circuitry for pain processing in the dorsal horn," *Nature Reviews Neuroscience*, vol. 11, no. 12, pp. 823–836, 2010.
- [36] L. J. Cole, K. L. Bennell, Y. Ahamed et al., "Determining brain mechanisms that underpin analgesia induced by the use of pain coping skills," *Pain Medicine*, vol. 19, no. 11, pp. 2177–2190, 2018.
- [37] M. Zhuo, "Cortical excitation and chronic pain," *Trends in Neurosciences*, vol. 31, no. 4, pp. 199–207, 2008.
- [38] S. Doolen, C. B. Blake, B. N. Smith, and B. K. Taylor, "Peripheral nerve injury increases glutamate-evoked calcium mobilization in adult spinal cord neurons," *Molecular Pain*, vol. 8, 2012.
- [39] C. Ultenius, B. Linderoth, B. A. Meyerson, and J. Wallin, "Spinal NMDA receptor phosphorylation correlates with the presence of neuropathic signs following peripheral nerve injury in the rat," *Neuroscience Letters*, vol. 399, no. 1–2, pp. 85–90, 2006.
- [40] C. K. Tong, E. J. Kaftan, and A. B. Macdermott, "Functional identification of NR2 subunits contributing to NMDA receptors on substance P receptor-expressing dorsal horn neurons," *Molecular Pain*, vol. 4, 2008.
- [41] V. Neugebauer, "Metabotropic glutamate receptors—important modulators of nociception and pain behavior," *Pain*, vol. 98, no. 1, pp. 1–8, 2002.
- [42] W. S. Zhao, Z. N. Jiang, H. Shi, L. L. Xu, Y. Yang, and Y. C. Wang, "Low-frequency electroacupuncture alleviates chronic constrictive injury-induced mechanical allodynia by inhibiting NR2B upregulation in ipsilateral spinal dorsal horn in rats," *Chinese Journal of Integrative Medicine*, vol. 25, no. 6, pp. 462–467, 2019.
- [43] Y. S. Lee, J. H. Lee, I. S. Lee, and B. T. Choi, "Effects of electroacupuncture on spinal  $\alpha$ -amino-3-hydroxy-5-methyl-4-isoxazole propionic acid receptor in rats injected with complete Freund's adjuvant," *Molecular Medicine Reports*, vol. 8, no. 4, pp. 1130–1134, 2013.
- [44] K. Han, A. Zhang, Y. Mo et al., "Islet-cell autoantigen 69 mediates the antihyperalgesic effects of electroacupuncture on inflammatory pain by regulating spinal glutamate receptor subunit 2 phosphorylation through protein interacting with C-kinase 1 in mice," *Pain*, vol. 160, no. 3, pp. 712–723, 2019.
- [45] H. N. Kim, Y. R. Kim, J. Y. Jang, H. K. Shin, and B. T. Choi, "Electroacupuncture confers antinociceptive effects via inhibition of glutamate transporter downregulation in complete Freund's adjuvant-injected rats," *Evidence-based Complementary and Alternative Medicine*, vol. 2012, Article ID 643973, 11 pages, 2012.
- [46] J. Zeng, L. Y. Cui, Y. Feng, and M. X. Ding, "Electroacupuncture relieves neuropathic pain via upregulation of glutamate transporters in the spinal cord of rats," *Neuroscience Letters*, vol. 620, pp. 38–42, 2016.
- [47] J. Zhou, Y. Jin, R. Ma et al., "Electroacupuncture alleviates experimental chronic inflammatory pain by inhibiting calcium voltage-gated channel-mediated inflammation," *Evidence-Based Complementary and Alternative Medicine*, vol. 2020, Article ID 7061972, 10 pages, 2020.
- [48] M. L. Hu, F. Y. Zhou, J. J. Liu, Y. Ding, J. M. Zhong, and M. X. Ding, "Electroacupuncture inhibits the activation of p38MAPK in the central descending facilitatory pathway in rats with inflammatory pain," *Evidence-Based Complementary and Alternative Medicine*, vol. 2017, Article ID 7531060, 10 pages, 2017.
- [49] X. C. Yuan, B. Zhu, X. H. Jing et al., "Electroacupuncture potentiates cannabinoid receptor-mediated descending inhibitory control in a mouse model of knee osteoarthritis," *Frontiers in Molecular Neuroscience*, vol. 11, p. 112, 2018.
- [50] J. Li, C. Fu, H. Liu et al., "Electroacupuncture attenuates hyperalgesia in rats withdrawn from chronic alcohol drinking via habenular mu opioid receptors," *Alcoholism, Clinical and Experimental Research*, vol. 41, no. 3, pp. 637–643, 2017.
- [51] X. Meng, Y. Zhang, A. Li et al., "The effects of opioid receptor antagonists on electroacupuncture-produced anti-allodynia/hyperalgesia in rats with paclitaxel-evoked peripheral neuropathy," *Brain Research*, vol. 1414, pp. 58–65, 2011.
- [52] C. P. Huang, Y. W. Lin, D. Y. Lee, and C. L. Hsieh, "Electroacupuncture relieves CCI-induced neuropathic pain involving excitatory and inhibitory neurotransmitters," *Evidence-Based Complementary and Alternative Medicine*, vol. 2019, Article ID 6784735, 9 pages, 2019.
- [53] S. W. Jiang, Y. W. Lin, and C. L. Hsieh, "Electroacupuncture at Hua Tuo Jia Ji Acupoints reduced neuropathic pain and increased GABAA receptors in rat spinal cord," *Evidence-Based Complementary and Alternative Medicine*, vol. 2018, Article ID 8041820, 10 pages, 2018.
- [54] S. S. Li, W. Z. Tu, C. Q. Jia et al., "KCC2-GABAA pathway correlates with the analgesic effect of electro-acupuncture in CCI rats," *Molecular Medicine Reports*, vol. 17, no. 5, pp. 6961–6968, 2018.
- [55] J. W. Choi, S. Y. Kang, J. G. Choi et al., "Analgesic effect of electroacupuncture on paclitaxel-induced neuropathic pain via spinal opioidergic and adrenergic mechanisms in mice," *The American Journal of Chinese Medicine*, vol. 43, no. 1, pp. 57–70, 2015.
- [56] J. Choi, C. Jeon, J. H. Lee et al., "Suppressive effects of bee venom acupuncture on paclitaxel-induced neuropathic pain in rats: mediation by spinal  $\alpha$ 2-Adrenergic receptor," *Toxins*, vol. 9, no. 11, p. 351, 2017.
- [57] J. H. Kim, H. Y. Kim, K. Chung, and J. M. Chung, "Electroacupuncture reduces the evoked responses of the spinal dorsal



- horn neurons in ankle-sprained rats,” *Journal of Neurophysiology*, vol. 105, no. 5, pp. 2050–2057, 2011.
- [58] Y. Zhang, R. X. Zhang, M. Zhang et al., “Electroacupuncture inhibition of hyperalgesia in an inflammatory pain rat model: involvement of distinct spinal serotonin and norepinephrine receptor subtypes,” *British Journal of Anaesthesia*, vol. 109, no. 2, pp. 245–252, 2012.
- [59] J. R. da Silva, M. L. da Silva, and W. A. Prado, “Electroacupuncture at 2/100 hz activates antinociceptive spinal mechanisms different from those activated by electroacupuncture at 2 and 100 hz in responder rats,” *Evidence-Based Complementary and Alternative Medicine*, vol. 2013, Article ID 205316, 14 pages, 2013.
- [60] Y. Y. Wu, Y. L. Jiang, X. F. He et al., “5-HT in the dorsal raphe nucleus is involved in the effects of 100-Hz electroacupuncture on the pain-depression dyad in rats,” *Experimental and Therapeutic Medicine*, vol. 14, no. 1, pp. 107–114, 2017.
- [61] Y. Zhang, A. Li, J. Xin et al., “Involvement of spinal serotonin receptors in electroacupuncture anti-hyperalgesia in an inflammatory pain rat model,” *Neurochemical Research*, vol. 36, no. 10, pp. 1785–1792, 2011.
- [62] Y. Zhang, A. Li, J. Xin et al., “Electroacupuncture alleviates chemotherapy-induced pain through inhibiting phosphorylation of spinal CaMKII in rats,” *European Journal of Pain*, vol. 22, no. 4, pp. 679–690, 2018.
- [63] A. Li, Y. Zhang, L. Lao et al., “Serotonin receptor 2A/C is involved in electroacupuncture inhibition of pain in an osteoarthritis rat model,” *Evidence-Based Complementary and Alternative Medicine*, vol. 2011, Article ID 619650, 6 pages, 2011.
- [64] Y. Liang, Y. Qiu, J. du et al., “Inhibition of spinal microglia and astrocytes contributes to the anti-allodynic effect of electroacupuncture in neuropathic pain induced by spinal nerve ligation,” *Acupuncture in Medicine*, vol. 34, no. 1, pp. 40–47, 2016.
- [65] D. C. Choi, J. Y. Lee, E. J. Lim, H. H. Baik, T. H. Oh, and T. Y. Yune, “Inhibition of ROS-induced p38MAPK and ERK activation in microglia by acupuncture relieves neuropathic pain after spinal cord injury in rats,” *Experimental Neurology*, vol. 236, no. 2, pp. 268–282, 2012.
- [66] J. Y. Lee, D. C. Choi, T. H. Oh, and T. Y. Yune, “Analgesic effect of acupuncture is mediated via inhibition of JNK activation in astrocytes after spinal cord injury,” *PLoS One*, vol. 8, no. 9, article e73948, 2013.
- [67] J. Wang, Y. Gao, S. Chen et al., “The effect of repeated electroacupuncture analgesia on neurotrophic and cytokine factors in neuropathic pain rats,” *Evidence-Based Complementary and Alternative Medicine*, vol. 2016, Article ID 8403064, 11 pages, 2016.
- [68] M. L. Yu, R. D. Wei, T. Zhang et al., “Electroacupuncture relieves pain and attenuates inflammation progression through inducing IL-10 production in CFA-induced mice,” *Inflammation*, vol. 43, no. 4, pp. 1233–1245, 2020.
- [69] W. J. Dai, J. L. Sun, C. Li et al., “Involvement of Interleukin-10 in analgesia of electroacupuncture on incision pain,” *Evidence-Based Complementary and Alternative Medicine*, vol. 2019, Article ID 8413576, 11 pages, 2019.
- [70] U. Ali, E. Apriyani, H. Y. Wu, X. F. Mao, H. Liu, and Y. X. Wang, “Low frequency electroacupuncture alleviates neuropathic pain by activation of spinal microglial IL-10/ $\beta$ -endorphin pathway,” *Biomedicine & Pharmacotherapy*, vol. 125, p. 109898, 2020.
- [71] Y. X. Zhao, M. J. Yao, Q. Liu, J. J. Xin, J. H. Gao, and X. C. Yu, “Electroacupuncture treatment attenuates paclitaxel-induced neuropathic pain in rats via inhibiting spinal glia and the TLR4/NF- $\kappa$ B pathway,” *Journal of Pain Research*, vol. - Volume 13, pp. 239–250, 2020.
- [72] H. C. Hsu, C. L. Hsieh, S. Y. Wu, and Y. W. Lin, “Toll-like receptor 2 plays an essential role in electroacupuncture analgesia in a mouse model of inflammatory pain,” *Acupuncture in Medicine*, vol. 37, no. 6, pp. 356–364, 2019.
- [73] Y. H. Gao, C. W. Li, J. Y. Wang et al., “Effect of electroacupuncture on the cervicospinal P2X7 receptor/fractalkine/CX3CR1 signaling pathway in a rat neck-incision pain model,” *Purinergic Signal*, vol. 13, no. 2, pp. 215–225, 2017.
- [74] Y. Li, Z. Fang, N. Gu et al., “Inhibition of chemokine CX3CL1 in spinal cord mediates the electroacupuncture-induced suppression of inflammatory pain,” *Journal of Pain Research*, vol. Volume 12, pp. 2663–2672, 2019.
- [75] C. Li, W. Mao, Y. K. Huang, Z. Q. Zhao, and N. Lyu, “Roles of CX3CR1 in mediation of post-incision induced mechanical pain hypersensitivity: effects of acupuncture-combined anesthesia,” *Sheng Li Xue Bao*, vol. 70, no. 3, pp. 237–244, 2018.
- [76] Q. Hu, X. Zheng, X. Li et al., “Electroacupuncture alleviates mechanical allodynia in a rat model of complex regional pain syndrome type-I via suppressing spinal CXCL12/CXCR4 signaling,” *The Journal of Pain*, vol. 21, no. 9–10, pp. 1060–1074, 2020.
- [77] X. Yan and H. R. Weng, “Endogenous interleukin-1 $\beta$  in neuropathic rats enhances glutamate release from the primary afferents in the spinal dorsal horn through coupling with pre-synaptic N-methyl-D-aspartic acid receptors,” *The Journal of Biological Chemistry*, vol. 288, no. 42, pp. 30544–30557, 2013.
- [78] M. Swartjes, A. Morariu, M. Niesters, L. Aarts, and A. Dahan, “Nonselective and NR2B-selective N-methyl-D-aspartic acid receptor antagonists produce antinociception and long-term relief of allodynia in acute and neuropathic pain,” *Anesthesiology*, vol. 115, no. 1, pp. 165–174, 2011.
- [79] D. L. Somers and F. R. Clemente, “Contralateral high or a combination of high- and low-frequency transcutaneous electrical nerve stimulation reduces mechanical allodynia and alters dorsal horn neurotransmitter content in neuropathic rats,” *The Journal of Pain*, vol. 10, no. 2, pp. 221–229, 2009.
- [80] Y. Li, X. Zhang, H. Liu et al., “Retracted: phosphorylated CaMKII post-synaptic binding to NR2B subunits in the anterior cingulate cortex mediates visceral pain in visceral hypersensitive rats,” *Journal of Neurochemistry*, vol. 121, no. 4, pp. 662–671, 2012.
- [81] R. H. Dworkin, A. B. O’Connor, J. Audette et al., “Recommendations for the pharmacological management of neuropathic pain: an overview and literature update,” *Mayo Clinic Proceedings*, vol. 85, no. 3, pp. S3–14, 2010.
- [82] S. A. Kissiwa, S. D. Patel, B. L. Winters, and E. E. Bagley, “Opioids differentially modulate two synapses important for pain processing in the amygdala,” *British Journal of Pharmacology*, vol. 177, no. 2, pp. 420–431, 2020.
- [83] M. Rodriguez-Munoz, P. Sanchez-Blazquez, A. Vicente-Sanchez, E. Berrocoso, and J. Garzon, “The mu-opioid receptor and the NMDA receptor associate in PAG neurons: implications in pain control,” *Neuropsychopharmacology*, vol. 37, no. 2, pp. 338–349, 2012.

- [84] H. P. Li, W. Su, Y. Shu et al., "Electroacupuncture decreases Netrin-1-induced myelinated afferent fiber sprouting and neuropathic pain through  $\mu$ -opioid receptors," *Journal of Pain Research*, vol. Volume 12, pp. 1259–1268, 2019.
- [85] H. Y. Liao, C. L. Hsieh, C. P. Huang, and Y. W. Lin, "Electroacupuncture attenuates induction of inflammatory pain by regulating opioid and adenosine pathways in mice," *Scientific Reports*, vol. 7, no. 1, p. 15679, 2017.
- [86] S. Zhang, H. Tang, J. Zhou, and Y. Gu, "Electroacupuncture attenuates neuropathic pain after brachial plexus injury," *Neural Regeneration Research*, vol. 9, no. 14, pp. 1365–1370, 2014.
- [87] Y. Zhang, A. Li, L. Lao et al., "Rostral ventromedial medulla  $\mu$ , but not  $\kappa$ , opioid receptors are involved in electroacupuncture anti-hyperalgesia in an inflammatory pain rat model," *Brain Research*, vol. 1395, pp. 38–45, 2011.
- [88] T. Chen, W. W. Zhang, Y. X. Chu, and Y. Q. Wang, "Acupuncture for pain management: molecular mechanisms of action," *The American Journal of Chinese Medicine*, vol. 48, no. 4, pp. 793–811, 2020.
- [89] H. Zhu, H. C. Xiang, H. P. Li, et al., "Inhibition of GABAergic neurons and excitation of glutamatergic neurons in the ventrolateral periaqueductal gray participate in electroacupuncture analgesia mediated by cannabinoid receptor," *Frontiers in Neuroscience*, vol. 13, p. 484, 2019.
- [90] J. Yowtak, J. Wang, H. Y. Kim, Y. Lu, K. Chung, and J. M. Chung, "Effect of antioxidant treatment on spinal GABA neurons in a neuropathic pain model in the mouse," *Pain*, vol. 154, no. 11, pp. 2469–2476, 2013.
- [91] A. François, S. A. Low, E. I. Sypek et al., "A brainstem-spinal cord inhibitory circuit for mechanical pain modulation by GABA and Enkephalins," *Neuron*, vol. 93, no. 4, pp. 822–839.e6, 2017.
- [92] D. Nutt, "GABAA receptors: subtypes, regional distribution, and function," *Journal of Clinical Sleep Medicine*, vol. 2, no. 2, pp. S7–11, 2006.
- [93] L. Pu, N. Xu, P. Xia et al., "Inhibition of Activity of GABA Transporter GAT1 by  $\mu$ -Opioid Receptor," *Evidence-Based Complementary and Alternative Medicine*, vol. 2012, Article ID 818451, 12 pages, 2012.
- [94] R. Tamano, M. Ishida, T. Asaki, M. Hasegawa, and S. Shinohara, "Effect of spinal monoaminergic neuronal system dysfunction on pain threshold in rats, and the analgesic effect of serotonin and norepinephrine reuptake inhibitors," *Neuroscience Letters*, vol. 615, pp. 78–82, 2016.
- [95] W. Rahman, C. S. Bauer, K. Bannister, J. L. Vonsy, A. C. Dolphin, and A. H. Dickenson, "Descending serotonergic facilitation and the antinociceptive effects of pregabalin in a rat model of osteoarthritic pain," *Molecular Pain*, vol. 5, pp. 1744–8069, 2009.
- [96] M. Zhuo, "Descending facilitation," *Molecular Pain*, vol. 13, pp. 17448069–17699212, 2017.
- [97] P. Pei, L. Liu, L. P. Zhao et al., "Electroacupuncture exerts an anti-migraine effect via modulation of the 5-HT7 receptor in the conscious rat," *Acupuncture in Medicine*, vol. 37, no. 1, pp. 47–54, 2019.
- [98] J. C. Wu, E. T. Ziea, L. Lao et al., "Effect of electroacupuncture on visceral hyperalgesia, serotonin and fos expression in an animal model of irritable bowel syndrome," *Journal of Neurogastroenterology and Motility*, vol. 16, no. 3, pp. 306–314, 2010.
- [99] L. Liu, P. Pei, L. P. Zhao, Z. Y. Qu, Y. P. Zhu, and L. P. Wang, "Electroacupuncture pretreatment at GB20 exerts antinociceptive effects via peripheral and central serotonin mechanism in conscious migraine rats," *Evidence-Based Complementary and Alternative Medicine*, vol. 2016, Article ID 1846296, 10 pages, 2016.
- [100] V. Parpura, T. A. Basarsky, F. Liu, K. Jęftinija, S. Jęftinija, and P. G. Haydon, "Glutamate-mediated astrocyte-neuron signalling," *Nature*, vol. 369, no. 6483, pp. 744–747, 1994.
- [101] R. R. Ji, A. Nackley, Y. Huh, N. Terrando, and W. Maixner, "Neuroinflammation and central sensitization in chronic and widespread pain," *Anesthesiology*, vol. 129, no. 2, pp. 343–366, 2018.
- [102] Y. M. Lau, S. C. Wong, S. W. Tsang, W. K. Lau, A. P. Lu, and H. Zhang, "Cellular sources of cyclooxygenase-1 and -2 up-regulation in the spinal dorsal horn after spinal nerve ligation," *Neuropathology and Applied Neurobiology*, vol. 40, no. 4, pp. 452–463, 2014.
- [103] M. L. Loggia, D. B. Chonde, O. Akeju et al., "Evidence for brain glial activation in chronic pain patients," *Brain*, vol. 138, no. 3, pp. 604–615, 2015.
- [104] R. R. Ji, T. Berta, and M. Nedergaard, "Glia and pain: is chronic pain a gliopathy?," *Pain*, vol. 154, Supplement 1, pp. S10–S28, 2013.
- [105] J. M. Pocock and H. Kettenmann, "Neurotransmitter receptors on microglia," *Trends in Neurosciences*, vol. 30, no. 10, pp. 527–535, 2007.
- [106] D. Schomberg and J. K. Olson, "Immune responses of microglia in the spinal cord: contribution to pain states," *Experimental Neurology*, vol. 234, no. 2, pp. 262–270, 2012.
- [107] J. Cao, J. S. Wang, X. H. Ren, and W. D. Zang, "Spinal sample showing p-JNK and P38 associated with the pain signaling transduction of glial cell in neuropathic pain," *Spinal Cord*, vol. 53, no. 2, pp. 92–97, 2015.
- [108] Y. J. Gao, L. Zhang, O. A. Samad et al., "JNK-induced MCP-1 production in spinal cord astrocytes contributes to central sensitization and neuropathic pain," *The Journal of Neuroscience*, vol. 29, no. 13, pp. 4096–4108, 2009.
- [109] Z. J. Zhang, D. L. Cao, X. Zhang, R. R. Ji, and Y. J. Gao, "Chemokine contribution to neuropathic pain: respective induction of CXCL1 and CXCR2 in spinal cord astrocytes and neurons," *Pain*, vol. 154, no. 10, pp. 2185–2197, 2013.
- [110] M. Zhuo, G. Wu, and L. J. Wu, "Neuronal and microglial mechanisms of neuropathic pain," *Molecular Brain*, vol. 4, no. 1, p. 31, 2011.
- [111] H. Zhang, H. Zhang, and P. M. Dougherty, "Dynamic effects of TNF- $\alpha$  on synaptic transmission in mice over time following sciatic nerve chronic constriction injury," *Journal of Neurophysiology*, vol. 110, no. 7, pp. 1663–1671, 2013.
- [112] B. Sung, G. Lim, and J. Mao, "Altered expression and uptake activity of spinal glutamate transporters after nerve injury contribute to the pathogenesis of neuropathic pain in rats," *The Journal of Neuroscience*, vol. 23, no. 7, pp. 2899–2910, 2003.
- [113] C. J. Woolf and M. W. Salter, "Neuronal plasticity: increasing the gain in pain," *Science*, vol. 288, no. 5472, pp. 1765–1768, 2000.
- [114] G. Rajkowska and J. J. Miguel-Hidalgo, "Gliogenesis and glial pathology in depression," *CNS & Neurological Disorders Drug Targets*, vol. 6, no. 3, pp. 219–233, 2007.

- [115] S. S. Ballon Romero, Y. C. Lee, L. J. Fuh, H. Y. Chung, S. Y. Hung, and Y. H. Chen, "Analgesic and neuroprotective effects of electroacupuncture in a dental pulp injury model—a basic research," *International Journal of Molecular Sciences*, vol. 21, no. 7, p. 2628, 2020.
- [116] W. Z. Tu, S. S. Li, X. Jiang et al., "Effect of electroacupuncture on the BDNF-TrkB pathway in the spinal cord of CCI rats," *International Journal of Molecular Medicine*, vol. 41, no. 6, pp. 3307–3315, 2018.
- [117] J. Y. Wang, Y. H. Gao, L. N. Qiao et al., "Repeated electroacupuncture treatment attenuated hyperalgesia through suppression of spinal glial activation in chronic neuropathic pain rats," *BMC Complementary and Alternative Medicine*, vol. 18, no. 1, p. 74, 2018.
- [118] J. Q. Fang, J. Y. Du, Y. Liang, and J. F. Fang, "Intervention of electroacupuncture on spinal p38 MAPK/ATF-2/VR-1 pathway in treating inflammatory pain induced by CFA in rats," *Molecular Pain*, vol. 9, p. 13, 2013.
- [119] J. Q. Fang, J. F. Fang, Y. Liang, and J. Y. Du, "Electroacupuncture mediates extracellular signal-regulated kinase 1/2 pathways in the spinal cord of rats with inflammatory pain," *BMC Complementary and Alternative Medicine*, vol. 14, no. 1, p. 285, 2014.
- [120] P. Han, S. Liu, M. Zhang et al., "Inhibition of spinal interleukin-33/ST2 signaling and downstream ERK and JNK pathways in electroacupuncture analgesia in formalin mice," *PLoS One*, vol. 10, no. 6, article e0129576, 2015.
- [121] Q. Liu, Y. Liu, J. Bian, Q. Li, and Y. Zhang, "The preemptive analgesia of pre-electroacupuncture in rats with formalin-induced acute inflammatory pain," *Molecular Pain*, vol. 15, article 1744806919866529, 2019.
- [122] W. Tu, W. Wang, H. Xi, R. He, L. Gao, and S. Jiang, "Regulation of Neurotrophin-3 and Interleukin-1 and Inhibition of Spinal Glial Activation Contribute to the Analgesic Effect of Electroacupuncture in Chronic Neuropathic Pain States of Rats," *Evidence-based Complementary and Alternative Medicine*, vol. 2015, Article ID 642081, 9 pages, 2015.
- [123] J. W. Griffith, C. L. Sokol, and A. D. Luster, "Chemokines and chemokine receptors: positioning cells for host defense and immunity," *Annual Review of Immunology*, vol. 32, no. 1, pp. 659–702, 2014.
- [124] P. E. Love and A. Bhandoola, "Signal integration and cross-talk during thymocyte migration and emigration," *Nature Reviews. Immunology*, vol. 11, no. 7, pp. 469–477, 2011.
- [125] C. Savarin-Vuaillet and R. M. Ransohoff, "Chemokines and chemokine receptors in neurological disease: raise, retain, or reduce?," *Neurotherapeutics*, vol. 4, no. 4, pp. 590–601, 2007.
- [126] J. M. Dawes, H. Kiesewetter, J. R. Perkins, D. L. Bennett, and S. B. McMahon, "Chemokine expression in peripheral tissues from the monosodium Lodoacetate model of chronic joint pain," *Molecular Pain*, vol. 9, pp. 1744–8069, 2013.
- [127] M. de Miguel, D. C. Kraychete, and R. J. Meyer Nascimento, "Chronic pain: cytokines, lymphocytes and chemokines," *Inflammation & Allergy Drug Targets*, vol. 13, no. 5, pp. 339–349, 2014.
- [128] M. A. Thacker, A. K. Clark, F. Marchand, and S. B. McMahon, "Pathophysiology of peripheral neuropathic pain: immune cells and molecules," *Anesthesia and Analgesia*, vol. 105, no. 3, pp. 838–847, 2007.
- [129] R. J. Miller, W. Rostene, E. Apartis et al., "Chemokine action in the nervous system," *The Journal of Neuroscience*, vol. 28, no. 46, pp. 11792–11795, 2008.
- [130] A. Jaerve and H. W. Muller, "Chemokines in CNS injury and repair," *Cell and Tissue Research*, vol. 349, no. 1, pp. 229–248, 2012.
- [131] J. H. Hu, J. P. Yang, L. Liu et al., "Involvement of CX3CR1 in bone cancer pain through the activation of microglia p38 MAPK pathway in the spinal cord," *Brain Research*, vol. 1465, pp. 1–9, 2012.
- [132] Y. Q. Zhou, H. Y. Gao, X. H. Guan et al., "Chemokines and their receptors: potential therapeutic targets for bone cancer pain," *Current Pharmaceutical Design*, vol. 21, no. 34, pp. 5029–5033, 2015.
- [133] Y. J. Gao and R. R. Ji, "Chemokines, neuronal-glia interactions, and central processing of neuropathic pain," *Pharmacology & Therapeutics*, vol. 126, no. 1, pp. 56–68, 2010.
- [134] Z. Y. Zhuang, Y. Kawasaki, P. H. Tan, Y. R. Wen, J. Huang, and R. R. Ji, "Role of the CX3CR1/p38 MAPK pathway in spinal microglia for the development of neuropathic pain following nerve injury-induced cleavage of fractalkine," *Brain, Behavior, and Immunity*, vol. 21, no. 5, pp. 642–651, 2007.
- [135] K. M. Lee, S. M. Jeon, and H. J. Cho, "Interleukin-6 induces microglial CX3CR1 expression in the spinal cord after peripheral nerve injury through the activation of p38 MAPK," *European Journal of Pain*, vol. 14, no. 7, pp. 682.e1–682.e12, 2010.
- [136] A. K. Clark, P. K. Yip, J. Grist et al., "Inhibition of spinal microglial cathepsin S for the reversal of neuropathic pain," *Proceedings of the National Academy of Sciences of the United States of America*, vol. 104, no. 25, pp. 10655–10660, 2007.
- [137] E. Milligan, V. Zapata, D. Schoeniger et al., "An initial investigation of spinal mechanisms underlying pain enhancement induced by fractalkine, a neuronally released chemokine," *The European Journal of Neuroscience*, vol. 22, no. 11, pp. 2775–2782, 2005.
- [138] A. K. Clark and M. Malcangio, "Fractalkine/CX3CR1 signaling during neuropathic pain," *Frontiers in Cellular Neuroscience*, vol. 8, 2014.
- [139] N. D. Jayaraj, B. J. Bhattacharyya, A. A. Belmadani et al., "Reducing CXCR4-mediated nociceptor hyperexcitability reverses painful diabetic neuropathy," *The Journal of Clinical Investigation*, vol. 128, no. 6, pp. 2205–2225, 2018.
- [140] X. Luo, W. L. Tai, L. Sun et al., "Crosstalk between astrocytic CXCL12 and microglial CXCR4 contributes to the development of neuropathic pain," *Molecular Pain*, vol. 12, p. 174480691663638, 2016.
- [141] R. D. Gosselin, C. Varela, G. Banisadr et al., "Constitutive expression of CCR2 chemokine receptor and inhibition by MCP-1/CCL2 of GABA-induced currents in spinal cord neurons," *Journal of Neurochemistry*, vol. 95, no. 4, pp. 1023–1034, 2005.
- [142] D. Spicarova, P. Adamek, N. Kalynovska, P. Mrozkova, and J. Palecek, "TRPV1 receptor inhibition decreases CCL2-induced hyperalgesia," *Neuropharmacology*, vol. 81, pp. 75–84, 2014.
- [143] D. L. Cao, Z. J. Zhang, R. G. Xie, B. C. Jiang, R. R. Ji, and Y. J. Gao, "Chemokine CXCL1 enhances inflammatory pain and increases NMDA receptor activity and COX-2 expression in spinal cord neurons via activation of CXCR2," *Experimental Neurology*, vol. 261, pp. 328–336, 2014.

- [144] J. Xu, M. D. Zhu, X. Zhang et al., “NF $\kappa$ B-mediated CXCL1 production in spinal cord astrocytes contributes to the maintenance of bone cancer pain in mice,” *Journal of Neuroinflammation*, vol. 11, no. 1, p. 38, 2014.
- [145] L. Cao and J. T. Malon, “Anti-nociceptive role of CXCL1 in a murine model of peripheral nerve injury-induced neuropathic pain,” *Neuroscience*, vol. 372, pp. 225–236, 2018.
- [146] W. Guo, S. Imai, J. L. Yang et al., “*In vivo* immune interactions of multipotent stromal cells underlie their long-lasting pain-relieving effect,” *Scientific Reports*, vol. 7, no. 1, p. 10107, 2017.



## Review Article

# The Role of Acupuncture Improving Cognitive Deficits due to Alzheimer's Disease or Vascular Diseases through Regulating Neuroplasticity

Shaozhen Ji <sup>1,2,3</sup>, Jiayu Duan,<sup>1,4</sup> Xiaobing Hou,<sup>5</sup> Li Zhou,<sup>6</sup> Weilan Qin,<sup>6</sup> Huanmin Niu,<sup>5</sup> Shuyun Luo,<sup>5</sup> Yunling Zhang,<sup>7</sup> Piu Chan <sup>2,3</sup> and Xianglan Jin <sup>1</sup>

<sup>1</sup>Department of Neurology, Dongfang Hospital, Beijing University of Chinese Medicine, Beijing 100078, China

<sup>2</sup>Department of Neurobiology, Xuanwu Hospital of Capital Medical University, Beijing 100053, China

<sup>3</sup>National Clinical Research Center for Geriatric Disorders, Capital Medical University, Beijing 100053, China

<sup>4</sup>Beijing University of Chinese Medicine, Beijing 100029, China

<sup>5</sup>Department of Neurology, Beijing First Hospital of Integrated Chinese and Western Medicine, Beijing 100039, China

<sup>6</sup>Department of Acupuncture and Moxibustion, Dongfang Hospital, Beijing University of Chinese Medicine, Beijing 100078, China

<sup>7</sup>Xiyuan Hospital, China Academy of Chinese Medical Sciences, Beijing 100091, China

Correspondence should be addressed to Piu Chan; pbchan@hotmail.com and Xianglan Jin; jxlan2001@126.com

Received 24 June 2020; Revised 29 November 2020; Accepted 15 December 2020; Published 12 January 2021

Academic Editor: Zhen Zheng

Copyright © 2021 Shaozhen Ji et al. This is an open access article distributed under the Creative Commons Attribution License, which permits unrestricted use, distribution, and reproduction in any medium, provided the original work is properly cited.

Dementia affects millions of elderly worldwide causing remarkable costs to society, but effective treatment is still lacking. Acupuncture is one of the complementary therapies that has been applied to cognitive deficits such as Alzheimer's disease (AD) and vascular cognitive impairment (VCI), while the underlying mechanisms of its therapeutic efficiency remain elusive. Neuroplasticity is defined as the ability of the nervous system to adapt to internal and external environmental changes, which may support some data to clarify mechanisms how acupuncture improves cognitive impairments. This review summarizes the up-to-date and comprehensive information on the effectiveness of acupuncture treatment on neurogenesis and gliogenesis, synaptic plasticity, related regulatory factors, and signaling pathways, as well as brain network connectivity, to lay ground for fully elucidating the potential mechanism of acupuncture on the regulation of neuroplasticity and promoting its clinical application as a complementary therapy for AD and VCI.

## 1. Introduction

As the population ages, the prevalence of dementia is increasing worldwide with an annual incidence of nearly 10 million [1], which leads to threats and challenges to global health and wellbeing. Dementia is characterized as a syndrome with myriad and complex causes, including primary neurologic, neuropsychiatric, and medical conditions and genetic and environmental factors [2, 3]. In the elderly, neurodegenerative dementias are most common [2], among which Alzheimer's disease (AD) is believed to be the leading cause of dementia, and vascular cognitive impairment (VCI) is the second utmost cause [4, 5]. Unprecedented advancements have been made in molecular neuroimaging, clinicopatho-

logic correlation, and the development of novel biomarkers in recent decades. However, effective therapeutics remain limited and even absent to date [4, 5]. Acupuncture, as one of complementary therapies for AD and VCI, is gradually applied to alleviate suffering, aggressively treating contributing symptoms and improving overall quality of life [6–10]. However, the underlying mechanisms remain elusive.

Neuroplasticity refers to the capacity of the nervous system to adapt to internal and external environmental changes by reorganizing its structure, function, and connections [11–14], which occurs at various levels of the nervous system from tissue to cellular to molecular [13]. It is known that dysregulated or disrupted neuroplasticity is implicated as a pathological mechanism in AD [15] and VCI [16].

Furthermore, some treatments that stimulate or modulate neuroplasticity have been indicated as effective in improving cognition [12, 17, 18], and might be potential therapy in cognitive impairments such as AD and VCI.

Acupuncture signals are recognized as a potent form of sensory stimulation that ascend mainly through the spinal ventrolateral funiculus to the brain [19]. The mechanisms of acupuncture-mediated neuroplasticity have recently attracted increased interest. Accordingly, acupuncture modulation over several cognition- or aging-related gene expressions [20], plasticity signaling pathways [21, 22], and brain functional connectivities [23] has been studied. Herein, we review the application of different protocols of acupuncture in animal models and humans, and their effectiveness on neuroplasticity in various sections: neurogenesis and gliogenesis, synaptic plasticity, related proteins and signaling pathways, and brain network connectivity. This review is aimed at laying the ground for elucidating the potential mechanism of acupuncture on AD and VCI to promote its clinical application as a complementary treatment.

## 2. Neurogenesis and Gliogenesis

The proliferation and differentiation of neurons and glial cells, also known as neurogenesis and gliogenesis, contribute to some neurorepair and improve brain function [24, 25]. Many previous results demonstrated that cerebral amyloidosis in AD mouse models caused neuronal proliferation inhibition and marked gliogenesis [26–28], and that stroke could trigger striatal and cortical neurogenesis and gliogenesis in murine models [29]. Mounting evidence indicates that adult hippocampal neurogenesis is implicated in cognitive processes, and that neurogenesis deficits may impair learning and memory. In states of brain injury such as AD and VCI, compensatory neurogenesis and gliogenesis mediate a balance between initial injury processes and endogenous repair processes [24]. Regulation of neurogenesis and gliogenesis is possibly associated with improving cognitive impairment and, consequently, may be attractive therapeutic targets for AD and VCI.

It is known that neurogenesis in the adult mammalian brain mostly takes place in specific brain regions harboring adult neuro stem and precursor cells, such as the subgranular zone (SGZ) of the hippocampal dentate gyrus (DG) and the ventricular/subventricular zone (VZ/SVZ) of the lateral ventricles [25]. Cognitive impairment due to AD or ischemic injury is recognized as partly related with neuron loss, impairment of cell proliferation, and imbalance between neuron loss and proliferation in the above regions [30]. Some studies showed that both manual acupuncture (MA) and electroacupuncture (EA) could ameliorate the learning and memory deficits of AD mice models through inducing the enhancement of neuron proliferation and migration in hippocampal DG and VZ/SVZ [31–33]. And the effect of MA and EA on improving cognitive dysfunction through the proliferation and differentiation of hippocampal neuro stem cells (NSCs) was also identified in murine models for vascular dementia (VaD) [34–36]. In addition, neurogenesis could take place in other brain areas in pathological conditions,

such as the cortex [37], where the promotion of neurogenesis related to EA was also detected in the transgenic mice model for AD [33].

VCI is recognized to be associated with pathological changes in white matter degeneration and demyelination [38]. Oligodendrocyte (OL), as one predominant cell type in white matter, mediates myelination that is an essential process for the appropriate propagation of action potentials along axons [39]. Myelination participates in the restoration of damaged white matter in the adult brain [40], which may provide potential utility for the treatment of VCI. In a mouse model of VaD, EA was indicated to enhance the differentiation of oligodendrocyte precursor cells (OPCs) into mature OLs and ameliorate white matter damage in the corpus callosum (CC) [41]. Moreover, astrocytes also perform critical impacts on promoting neovascularization, regulating neuronal activity, and supporting synaptogenesis and neurogenesis, which may influence recovery following ischemic lesion [39, 42]. Experimental studies have reported that acupuncture was able to influence the proliferation and differentiation of astrocytes; however, the results were discrepant. One study revealed that MA was able to inhibit astrocyte activation and proliferation in VaD rat models [36]. Conversely, Kim et al. found that EA stimulation could induce NSCs differentiated into astrocytes in a VaD mouse model [35]. These results may be caused by differential acupoints or acupuncture methods. The differential influence of the acupuncture method (i.e., MA vs. EA) on neurogenesis has been demonstrated. And one study found that MA vs. EA stimulation at the same acupoints might induce differential cell proliferation and neuroblast differentiation in healthy rats [43]. And further investigation of the compared impact of differential acupuncture methods and acupoints on gliogenesis in AD and VCI models is required.

In addition to the direct effect on endogenous neurogenesis and gliogenesis, acupuncture was able to promote the survival, proliferation, migration, and differentiation of exogenous NSCs in the hippocampal microenvironment by regulating components of the cerebral microenvironment [44] or the related cytokine levels [45] in an AD mice model. All these findings demonstrated the influence of acupuncture on endogenous and exogenous neurogenesis and gliogenesis in AD and VCI, which deepen our understanding of acupuncture modulating neuroplasticity. There remain some limitations and even discrepancies in these results possibly caused by acupoints or models or observation times, or even acupuncture methods (i.e., MA vs. EA). And the mechanisms underlying the impact of acupuncture on neurogenesis and gliogenesis in different states, especially molecular mechanisms, need to be investigated.

## 3. Synaptic Plasticity

Synapses, the most sensitive and plastic structures, are directly involved in the integration and transfer of information within the neuro system. Previous studies demonstrated that synapse loss and dysfunction was a key feature in AD [46] and VCI [47] and positively correlates with cognitive damage. Impaired dendritic structure, spine density, and



synaptic ultrastructure of neurons have been identified in brain tissue of AD patients and murine models, caused by soluble amyloid beta ( $A\beta$ ) in the hippocampus [48, 49]. And ischemia-induced synapse reduction was also recognized to be the major pathological causes of VaD [50]. Synaptic plasticity, also defined as activity-dependent synaptic modifications of the strength of synaptic connections, is widely recognized to be fundamental to the formation and maintenance of learning and memory [51]. Synaptic plasticity in the neuro network, an important basis for cortical plasticity, is associated with learning and memory and sensorimotor dysfunction and recovery [51, 52]. Synaptic plasticity mainly includes modulation of the morphological structure of synapses and the synaptic strength and transmission, in which some synaptic protein markers, neurotransmitters, and receptors participate. Recently, modulation of synaptic plasticity is believed to be a promising approach for treating AD and VCI.

Synapse-structure parameters, such as synaptic curvatures, the width of the synaptic cleft, and the thickness of the postsynaptic density, are proposed to be important indicators that reflect synaptic morphological plasticity and greatly affect synaptic transmission [53]. Many studies revealed that MA and EA treatments had positive effects on the recovery of the learning and memory abilities not only in AD rat models but also in VCI, through increasing synaptic curvatures, decreasing the width of synaptic clefts, and thickening the postsynaptic densities in the hippocampus [49, 54]. In addition, MA was able to reverse the learning and memory impairments in AD mice models through enhancing the conjunction among the synapses and promoting synaptic formation [20] and regeneration [55], reducing ultrastructural degradation of synapses [56], and increasing the number and length of dendrites [57] and neurite fibers [58].

Long-term potentiation (LTP) and long-term depression (LTD) are considered as two indicators and forms of synaptic transmission [59]. As a cellular model of synaptic plasticity, LTP is the long-lasting enhancement in signal transmission between two neurons after synchronous stimulation associated with memory formation and storage, reflecting an increase of synaptic strength [60]. LTD is relevant to memory integration, forgetting, and recovery of LTP production at desaturation state [61]. And converging studies supported a crucial role of LTD in some types of learning and memory and in situations where cognitive demands require a flexible response [59]. Many electrophysiological studies showed that acupuncture could apparently improve the recovery from cognitive deficits by promoting LTP and/or LTD [61–63] and preventing or restoring the impaired LTP [64–69] in AD or VCI rat models. In addition to LTP and LTD, EA could also ameliorate the synaptic transmission by raising the slope of excitatory postsynaptic potential (EPSP) and the amplitude of population spikes (PS) in an AD mouse model [70].

Synaptophysin (SYN) is a major integral membrane protein of the presynaptic vesicle, and postsynaptic density 95 (PSD-95) and growth-associated protein 43 (GAP-43) are postsynaptic markers [71]. As important protein markers of regeneration and remodeling, they are widely found in all

nerve terminals and used for quantifying the number of axon terminals, reflecting the occurrence, density, and strength of synapses [49, 72]. Many previous studies reported reduced expression of SYN and PSD-95 in the hippocampus in AD and VaD [73, 74]. It was demonstrated that acupuncture was able to promote synapse-structure damage rehabilitation by upregulating the expression of SYN [44, 54, 55], PSD-95 [56, 75, 76], and GAP-43 [77] to improve the learning and memory abilities of AD and VCI murine models.

Furthermore, accumulated evidence indicates that the effect of acupuncture on modulating synaptic structure and function in AD and VCI is achieved by changing the releasing of the presynaptic neurotransmitter or the function of the postsynaptic receptor [67, 68, 78]. As one of the major neurotransmitters, dopamine (D) plays an essential role in modulating hippocampal LTP and memory processes [79, 80]. Ye et al. found that MA could activate D1/D5 receptors to ameliorate cognitive function and LTP impairments in VaD rats [67]. The central cholinergic pathway and the norepinephrine- (NE) adrenergic receptor (AR) system are known for their critical roles in learning acquisition and synaptic plasticity in the mammalian limbic system. It was demonstrated that MA not only could alleviate memory-associated decreases in the levels of choline acetyltransferase (ChAT) and restore the expression of choline transporter 1 (CHT1) as well as vesicular acetylcholine transporter (AChT), resulting eventually in the recovery of the entire cholinergic system circulation pathway [81], but also was able to enhance norepinephrine (NE) levels and the activation of  $\beta$ 1-AR in the hippocampus [68]. In addition,  $\gamma$ -aminobutyric acid (GABA) is one main inhibitory neurotransmitter in the central nervous system inhibiting the excessive release of glutamate (Glu). And GABA receptor-mediated inhibitory inputs modulate hippocampal LTP [82]. EA could elevate the excitability of granule cells by decreasing GABA from interneurons, which resulted in increasing LTP [78].

Glutamate receptors (GluRs) are the main receptors of the postsynaptic neurotransmitter area and modulate synaptic plasticity; they are divided into metabotropic GluRs and ionotropic GluRs. Among the three types of ionotropic GluRs, N-methyl-D-aspartate receptor (NMDAR) is the most widely distributed regulator of synaptic plasticity, which plays an important role in inducing and maintaining LTP and LTD closely associated with learning and memory [83]. NMDARs are comprised of NMDAR subtype 1 (NMDAR1) subunits plus at least one type of NMDAR2 subunit [84]. It was reported that EA could reduce the deficit of LTP in VaD rat models via reversal of NMDAR1- and transient receptor potential vanilloid subtype 1- (TRPV1-) mediated neurotoxicity [62]. NMDAR2 seems to have complex properties, and different NMDAR2 subunits confer distinct electrophysiological and pharmacological properties on the receptors and couple themselves with opposing signaling pathways and influences on the direction of synaptic plasticity [85]. Specifically, NMDAR2A activation is beneficial for neuronal regeneration and neuroprotection, while NMDAR2B induces neurotoxicity and neuronal apoptosis [85]. One study found that EA could alleviate cognitive

dysfunction caused by ischemic injury through downregulation of NMDAR2B and upregulation of NMDAR2A [86].

The effect of EA on synaptic plasticity might be related to the parameter of stimulation. One study has found that high-frequency EA may yield a stronger protective effect on hippocampal synaptic plasticity compared with low- or medium-frequency EA in AD rat models [61]. Further research focusing on ascertaining the optimum acupuncture parameter is required. Moreover, besides these mechanisms described above, many synaptic-related proteins or signaling pathways were required in maintaining synaptic structural plasticity and synaptic transmission. Investigations of synaptic plasticity-related regulatory factors and signaling mechanisms have been performed in many studies, and these are going to be described in Section 4.

#### 4. Neuroplasticity-Related Regulatory Factors and Signaling Pathways

Multiple crucial steps are involved in the process of neuroplasticity, which include many layers of regulation, composed of both intrinsic and extrinsic mechanisms. For example, there are a number of coordinated cell-intrinsic programs and external signals involved in distinct stages of adult neurogenesis, including proliferation and lineage differentiation of NSCs, migration of neuroblasts, and integration of newborn neurons [87]. Given the important role of related factors and signaling pathways in neuroplasticity, ascertaining acupuncture's effect on them may be vital to understanding the mechanisms of its treatment for AD and VCI.

As one of the morphogens that are critical during embryonic development of the nervous system, Notch is highly conserved and serves as niche signals to regulate the proliferation of adult NSCs [88]. The regeneration of neurons from neural progenitors may be impaired due to the abnormal elevated Notch signal pathway. EA treatment suppressed neuronal apoptosis and improved cognitive impairment in AD rat models possibly via the downregulation of an abnormal elevated Notch signaling pathway [89]. Moreover, EA also was able to enhance hippocampal NSC proliferation in VaD rat models via the activation of the Notch signaling pathway [34].

In addition to the neurotransmitters described above, the survival and synaptic integration of newly born cells are subject to regulation by neurotrophic factors. As a member of the neurotrophic factor family, the BDNF protein is synthesized as pre-pro-BDNF and cleaved intracellularly into a pro-BDNF protein encompassing two domains: the pro-domain and the mature BDNF domain [90]. BDNF is actually secreted in the pro- and mature form [91], which had distinct receptors and signaling cascades resulting in opposing biological functions [92–94]. The mature BDNF preferentially binds to phosphorylated tropomyosin receptor kinase B (Trk-B) receptors leading to cell survival and differentiation as well as hippocampal LTP, whereas pro-BDNF preferentially binds to p75 neurotrophin receptor (p75NTR) leading to apoptosis and hippocampal LTD [95]. It was observed that acupuncture could upregulate the expression of Trk-B receptors and could decrease the expression level of p75NTR in

AD and VaD murine models, influence the modulation and processing of the BDNF protein from pro-BDNF to mature BDNF [33, 96, 97], and eventually enhance the mRNA expression levels of mature BDNF [35, 45, 54, 81]. One clinical trial showed that combined scalp acupuncture and cognitive training could improve the cognitive function and BDNF levels of peripheral blood in patients with stroke during the recovery stage [98]. Other extrinsic factors such as neurotrophin 3 (NT3), NT4, and NT5 also play an important role in the regulation of neuronal integration [99]. EA treatment has been reported to increase the expression of NT4/5 and their receptor, tyrosine receptor Trk-B, and promote OL regeneration in association with cognitive functional improvements in a VaD mice model [41]. In addition, acupuncture also could regulate intrinsic factors associated with neuronal integration. For instance, MA was demonstrated to restore the expression of cAMP-response element-binding protein (CREB) mRNA in the hippocampus of rats with cognitive impairment [81].

The typical pathological hallmarks of AD include extracellular A $\beta$  plaques and intracellular neurofibrillary tangles (NFTs) composed of hyperphosphorylated tau proteins, both of which resulted in the loss and morphological changes of dendritic spines, directly leading to the damage of neuronal synaptic function and neuroplasticity [100]. Many studies showed that acupuncture could regulate neuroplasticity by directly reducing A $\beta$  deposition [56, 101], and some related proteins and signaling pathways participated in this process. Glycogen synthase kinase 3 beta (GSK3 $\beta$ ) is a serine/threonine protein kinase that plays a crucial role in AD pathogenesis, and its hyperactivity or overexpression is increasingly shown to be closely related to A $\beta$  generation, tau hyperphosphorylation, and synaptic plasticity [102]. Inhibition of GSK3 $\beta$  has been indicated to increase the number of synapses and postsynaptic density thickness, and rescue the reduction of spine density in the hippocampus of an AD model. It has been revealed that EA could promote synapse-structure damage rehabilitation by downregulating GSK3 $\beta$  to improve the learning and memory abilities of AD rat models [49, 77]. As the downstream target of GSK3 $\beta$ , the reactivation of mTOR restored the acidification of the autophagy lysosome, further promoting the autophagy clearance of pathological A $\beta$  plaque load [103]. Yu et al. found that EA rescued structural and functional synaptic plasticity impairments and memory deficits in AD rat models through the inactivation of GSK3 $\beta$ /mTOR signaling [21]. Moreover,  $\beta$ -site amyloid precursor protein cleaving enzyme 1 (BACE1) is the key protein involved in A $\beta$  peptide generation. One study indicated that EA could downregulate the expression of BACE1 in one AD mouse model [64].

There are some regulated factors and signaling pathways directly involved in the modulation of LTP. Protein kinase A (PKA) is a predominantly positive modulator of LTP in the hippocampus and has been demonstrated to indispensably participate in the efficacy of hippocampus-based memory [104]. Tang et al. found that EA could upregulate PKA activation, enhance synaptic plasticity, and improve memory in an AD mice model [64]. The p70 ribosomal protein S6 (p70S6) kinase/ribosomal protein S6 signaling pathway has

TABLE 1: The mechanisms of acupuncture regulating neurogenesis, gliogenesis, and synaptic plasticity.

Acupuncture intervention		EA parameters Intensity, frequency	Model/participants	Mechanisms	Refs.
MA	Qihai (CV6), Zhongwan (CV12), Danzhong (CV17), bilateral Xuehai (SP10), bilateral Zusanli (ST36)	—	SAMP 8 mice	Induce different cell proliferation in different brain regions, and increase neuron density in hippocampal CA3 and DG. Promote the proliferation, migration, and differentiation of exogenous neural stem cells via increasing SYN mRNA and protein levels. Increase the number of apical and basal dendritic branches and total length of apical and basal dendrites. Improve the distribution and arrangement of nerve fibers.	[31, 32, 44, 57, 58]
MA	Bilateral Zusanli (ST36)	—	Multi-infarction dementia modeled in rats with 3% microemboli saline suspension injected into the internal carotid artery	Increase the number of pyramidal neurons, and tend to decrease the number of astrocytes in the hippocampal CA1 area.	[36]
EA	Baihui (GV20)	1 mA, 2/15 Hz	APP/PS1 transgenic mice	Attenuate A $\beta$ deposits, upregulate the expression of BDNF, and promote neurogenesis in both the hippocampus and cortex.	[33]
EA	Baihui (GV20), Dazhui (GV14)	2 V, 2 Hz	MCAO mice	Increase the number of proliferative cells and differentiated cells in the hippocampus and SVZ of the ipsilateral hemisphere, promote differentiation of proliferated cells into neurons or astrocytes, and upregulate mRNA expression of BDNF and VEGF.	[35]
EA	Bilateral Quchi (LI11), bilateral Zusanli (ST36)	NA, 1 or 20 Hz	MCAO rats	Activate the crucial signaling molecules in the notch signaling pathway, increase the secretion of BDNF and GDNF, and promote the proliferation of hippocampal NSCs.	[34]
EA	Baihui (GV20), Dazhui (GV14)	2 V, 2 Hz	BCAS mice	Promote the differentiation of OPCs into OLs, and mediate positive changes in the expression of NT4/5 and its receptor Trk-B.	[41]
MA	Qihai (CV6), Zhongwan (CV12), Danzhong (CV17), bilateral Xuehai (SP10), bilateral Zusanli (ST36)	—	SAMP 8, coculture model of hippocampal tissue specimens, and NSCs in vitro	Increase the count of NeuN- and GFAP-positive cells, regulate the cytokine levels associated with survival, proliferation, and differentiation of NSCs (upregulate the expression of basic FGF, EGF, and BDNF).	[45]
MA	Qihai (CV6), Zhongwan (CV12), Danzhong (CV17), bilateral Xuehai (SP10), bilateral Zusanli (ST36)	—	SAMP 10 mice	Enhance the conjunction among the synapses and hasten the new synapse formation by upregulating YB-1 expression.	[20]
EA	Baihui (GV20), Shenshu (BL23)	NA, 2, 30 and 50 Hz	Rat models of AD induced by injecting A $\beta$ 1-42 into the bilateral lateral ventricles	Increase synaptic curvatures, decrease the width of synaptic clefts, thicken postsynaptic densities, and downregulate the expression of GSK3 $\beta$ , amyloid precursor protein, and A $\beta$ 1-40. Promote synaptic damage rehabilitation by downregulating GSK3 $\beta$ and upregulating GAP-43.	[49, 77]

TABLE 1: Continued.

Acupuncture intervention		EA parameters Intensity, frequency	Model/participants	Mechanisms	Refs.
	Acupoint				
MA+EA	Yintang (GV29), bilateral Yingxiang (LI20)	1.5 mA, 15 Hz (bilateral LI20)	SAMP 8 mice	Inhibit the phosphorylation of p38MAPK and the excessive activation of MG in the hippocampus to reduce the neuroinflammatory response and neurotoxicity of A $\beta$ and promote synaptic regeneration.	[55]
EA	Bilateral Taixi (KI3)	1 mA, 2 Hz	5XFAD mice	Alleviate neuroinflammation, reduce ultrastructural degradation of synapses via upregulation of SYN and PSD-95 protein, and decrease MG-mediated A $\beta$ deposition.	[56]
MA	Bilateral Taixi (KI3), bilateral Taichong (LR3)	—	MCAO rats	Promote the expression of BDNF and SYN, and synaptic structure reconstruction by increasing the postsynaptic density, narrowing the synapse cleft width.	[54]
EA	Baihui (GV20), Shenshu (BL23)	NA, 2 or 50 Hz	Rat models of AD induced by injecting A $\beta$ 1-42 into the bilateral lateral ventricles	Increase the ranges of LTP and LTD.	[61]
EA	Baihui (GV20), Yintang (GV29), Shuigou (GV26)	1 mA, 1 Hz	APP/PS1 transgenic mice	Reduce BACE1 deposition and regulate PKA and LTP.	[64]
EA	Baihui (GV20), Dazhui (GV14), bilateral Shenshu (BL23), bilateral Yongquan (KI1)	1-2 mA, 4 Hz	AD model rats established by injecting A $\beta$ 25-35 into the bilateral dentate gyri of the hippocampal CA1 area	Raise the slope of EPSP and the amplitude of PS.	[70]
EA	Baihui (GV20), bilateral Zusanli (ST36)	NA, 2 Hz	Diabetes mellitus and cerebral ischemia model rats	Restore impaired LTP.	[65]
EA	Baihui (GV20)	2 mA, 2 Hz	MACO rats	Reduce the deficit of LTP via reversal of NMDAR1- and TRPV1-mediated neurotoxicity.	[62]
EA	Baihui (GV20), Dazhui (GV14), bilateral Shenshu (BL23)	4 mA, 2 Hz	MACO rats	Promote LTP and upregulate expression of p70S6 kinase and ribosomal protein S6 in the hippocampus. Decrease ROS production, increase neural cell survival, and improve LTP.	[63]
MA	Baihui (GV20), Zusanli (ST36)	—	2VO rats by bilateral common carotid artery occlusion	Upregulate DBH expression in hippocampus. Prevent impairments of LTP, promote the release of dopamine and its major metabolites in the hippocampus, and decrease D1 receptors and D5 receptors in the hippocampal DG region. Enhance LTP and NE levels and increase $\beta$ 1-ARs in the hippocampus.	[66-69]
EA	Baihui (GV20), bilateral Yongquan (KI1)	0.5 mA, 1/50 Hz	APP/PS1 transgenic mice	Reduce the expression of A $\beta$ in the hippocampus and increase the expression of PSD-95 and SYN.	[75]
EA	Baihui (GV20), Dazhui (GV14), Shenshu (BL23)	1 mA, 2 Hz	SAMP 8 mice	Increase the expression of SYN and PSD-95, and inhibit AMPK activation and eEF2K activity.	[76]
EA	Zusanli (ST36), Sanyinjiao (SP6)	2 mV, 2 Hz	Anesthetized rats	Elevate excitability of granule cells by decreasing GABA from interneurons, which result in increasing LTP.	[78]

TABLE 1: Continued.

Acupuncture intervention		EA parameters Intensity, frequency	Model/participants	Mechanisms	Refs.
EA	Acupoint				
MA	Baihui (GV20)	—	Memory defects rats caused by SCO administration	Restore the expression of CHT1, vesicular AChT, BDNF and CREB mRNA in the hippocampus.	[81]
EA	Baihui (GV20), Shenting (GV24)	NA, 1-20 Hz	MCAO rats	Reduce Ca <sup>2+</sup> influx via inhibition of Glu neurotoxicity and downregulation of NMDAR2B expression.	[86]
EA	Baihui (GV20)	NA, 1 and 20 Hz	APP/PS1 transgenic mice	Enhance the expression levels of mature BDNF and pro-BDNF, and BDNF/pro-BDNF ratio, upregulate the expression levels of phosphorylated Trk-B, and decrease the expression level of p75NTR. Upregulate NAA, Glu and mI metabolism, increase the surviving neurons in the hippocampus, and promote the expression of BDNF and Trk-B.	[96, 97]
MA	Baihui (GV20), Sishencong (EX-HN1), bilateral Fengchi (GB20), Shenting (GV24)	—	Patients with PSCI	Improve BDNF and NGF levels in peripheral blood.	[98]
EA	Baihui (GV20), Shenshu (BL23)	1 mA, 50 Hz	D-galactose-induced aged rats	Attenuate the hippocampal loss of dendritic spines, ameliorate neuronal microtubule injuries, increase the expressions of postsynaptic PSD-95 and presynaptic SYN, and inhibit the GSK3 $\beta$ /mTOR signaling pathway.	[21]
EA	Baihui (GV20), bilateral Shenshu (BL23), bilateral Neiguan (PC6), bilateral Zusanli (ST36), bilateral Sanyinjiao (SP6)	NA, 5 Hz	Al/D-gal-OLETF rats	Increase the protein level of p-GSK3 $\beta$ .	[22]
EA	Baihui (GV20), Dazhui (GV14), bilateral Shenshu (BL23)	2 mA, 4 Hz	2VO rats by bilateral common carotid artery occlusion	Upregulate expression of mTOR and eIF4E in the hippocampus.	[109]
EA	Baihui (GV20), Shenshu (BL23)	$\leq$ 2 mA, 20 Hz	Intrahippocampally injected A $\beta$ 1-40 rat model	Alleviate the cell apoptosis resulting from A $\beta$ infusion in hippocampal CA1 regions through upregulating the expression of Bcl-2 and downregulating the expression of Bax, promote the expression of synapsin-1 and SYN, and downregulate the level of Notch1 and Hes1 mRNA in the hippocampus.	[89]
MA	Baihui (GV20), Yintang (GV29), Shuigou (GV26)	—	SAMP 8 mice	Improve the level of glucose metabolism in the brain, and the content of A $\beta$ amyloid in the cortex.	[101]

NA: not available. Abbreviations are found in Supplementary Table 3. The locations of acupoints are shown in Figure 1.



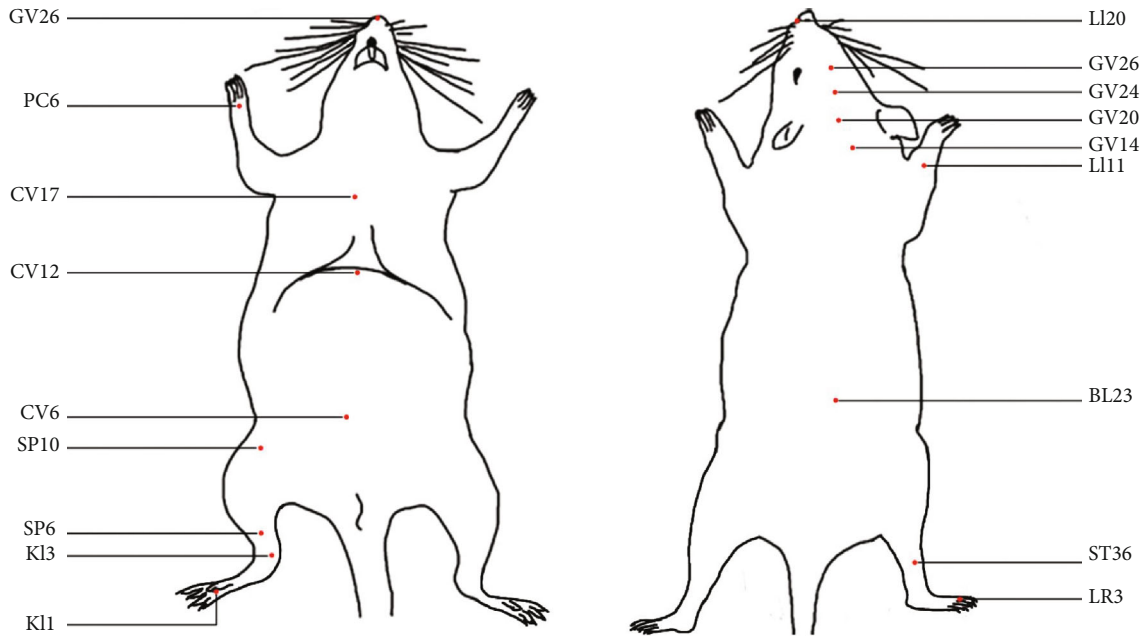


FIGURE 1: The locations of acupoints in mice.

been shown to promote neuronal growth and LTP [105, 106]. One study showed reduced expression of p70S6 kinase and ribosomal protein S6 in the hippocampus of VaD rats, which suggested that the p70S6 kinase/ribosomal protein S6 pathway was involved in the pathogenesis of VaD [63]. EA was demonstrated to improve the learning and spatial memory abilities of VaD rats and facilitate LTP in the hippocampus by upregulating expression of p70S6 kinase and ribosomal protein S6 [63]. The p70S6 kinase was phosphorylated by activation of the mammalian target of rapamycin (mTOR) signal pathway, which has been shown to promote neuronal growth and LTP [107, 108]. Acupuncture stimulation has been indicated to promote neuroplasticity by regulating the mTOR signal pathway in AD or VaD rats [21, 109]. Moreover, it was reported that MA could reverse the learning and memory impairments in an AD mouse model through upregulating eukaryotic Y-box-binding protein (YB-1) expression [20], which enhanced the conjunction among the synapses and promoted synaptic formation indirectly [110]. The eukaryotic elongation factor-2 kinase/eukaryotic elongation factor-2 (eEF2K/eEF2) pathway is also associated with synaptic plasticity and its inhibition prevents synaptic failure in AD. One study showed that EA improved the synaptic function in AD by inhibiting the AMPK/eEF2K/eEF2 pathway in an AD mouse model [76].

Besides the above-related factors and signaling pathways, other mechanisms, such as oxidative stress, glucose metabolism, and inflammatory responses, were considered to play a key role in acupuncture treating AD or VCI and modulating neuroplasticity (Table 1 and Figure 1). These molecular mechanisms support acupuncture as a potentially promising therapy for the treatment of cognitive dysfunction in patients with VD or VCI.

## 5. Brain Network Connectivity

Some previous neuroimaging researches have revealed neuropathological changes and/or structural-functional reorganization in AD and VCI resulting in altered connectivity patterns in brain networks [14, 111–113]. For example, some rapidly and reversibly increased or decreased strengths of brain network connections, also known as altered recruitments of functional connections normally devoted to performing a given task or the recruitment of additional network connections that are not typically activated by healthy people. And the alteration of network connectivity is a form of neuroplasticity that could indicate compensatory mechanisms engaged to maintain a normal level of cognitive function or promote the recovery from cognitive dysfunction due to the primary white matter lesions and neuronal loss [14, 114, 115].

Many neuroimaging studies showed that acupuncture could induce neuroplastic reorganization of brain functional networks in AD or mild cognitive impairment (MCI), the prophase state of AD [116] (Table 2 and Figure 2). There were several regions showing increased or decreased activities in MCI and AD patients after short-term MA or EA stimulation, including cognitive-related areas, visual-related areas, sensorimotor-related areas, emotion-related areas, the basal ganglia, and the cerebellum [23, 113, 117–123]. However, there remains a lack of correlation between the changes in cognitive function and alteration in functional connectivity. In two other long-term studies, MCI patients exhibited improvement of cognitive performance after MA, as well as extensive activation and deactivation in brain networks [123, 124]. And functional connectivity strength in some regions was negatively correlated with the changes in

TABLE 2: The mechanisms of acupuncture modulating brain network connectivity.

Acupuncture intervention	Acupoint	Intervention parameters	Participants	Mechanisms	Refs.
MA	Bilateral Taichong (LR3), bilateral Hegu (LI4)	3 minutes	AD patients vs. HCs	Modulate DMN activity in AD patients, with increased cluster in the left PCC, the right MTG, together with the right IPL and decreased bilateral CG and left PCu within DMN connectivity. Enhance the functional connectivity between the hippocampus and the precentral gyrus in AD patients.	[23, 117]
MA	Bilateral Taichong (LR3), bilateral Hegu (LI4)	3 minutes	MCI patients vs. AD patients vs. HCs	Induce increased or decreased activities in regions of MCI, AD subjects, most of which were involved in the temporal lobe and the frontal lobe closely related to memory and cognition. Induce similar activations in cognitive-related brain areas (inferior frontal gyrus, supramarginal gyrus, and rolandic operculum) as well as deactivations in cognitive-related areas, visual-related areas, basal ganglia, and cerebellum in AD and MCI patients, which were not found in HCs.	[113, 118]
MA	Bilateral Taichong (LR3), bilateral Hegu (LI4)	A total of 4 courses in 6 months (3 times a week, 4 weeks as a course)	MCI patients vs. HCs	Enhance hippocampal FC with ITG and MTG in aMCI subjects. Enhance the correlations related with the temporal regions in MCI patients. Increase the correlations related with the temporal regions for the deep acupuncture condition, compared to superficial acupuncture. Deep acupuncture induces the strongest and most extensive effective connectivities related to the therapeutic effect of acupuncture in MCI patients.	[125]
MA	Taixi (KI3) on the right side	3 minutes (deep acupuncture vs. superficial acupuncture)	MCI patients vs. HCs	Activate 20 brain regions in both MCI and HC participants, including the bilateral anterior cingulate gyrus (BA 32, 24), left medial frontal cortex (BA 9, 10, 11), left cuneus (BA 19), left middle frontal gyrus (BA 11), left lingual gyrus (BA 18), right medial frontal gyrus (BA 11), bilateral inferior frontal gyrus (BA 47), left superior frontal gyrus (BA 11), right cuneus (BA 19, 18), right superior temporal gyrus (BA 38), left subcallosal gyrus (BA 47), bilateral precuneus (BA 19), right medial frontal gyrus (BA 10), right superior frontal (BA 11), left cingulate gyrus (BA 32), left precentral gyrus (BA 6), and right fusiform gyrus (BA 19).	[119–121]
MA	Sishencong (EX-HN1), Yintang (GV29), Neiguan (PC6), Taixi (KI3), Fenglong (ST40), Taichong (LR3)	5 times a week, 4 consecutive weeks (acupoint acupuncture vs. sham acupoint acupuncture)	MCI patients	Increase the connections between cognition-related regions such as the insula, dorsolateral prefrontal cortex, hippocampus, thalamus, inferior parietal lobule, and anterior cingulate cortex.	[124]
EA	Neiguan (PC6) on right side	6 minutes, 1 Hz	AD patients vs. HCs	Activate functions of different brain regions in the HC vs. AD patients, including activation of the frontal lobe, the temporal lobe, and the cingulate gyrus as well as the cerebellum in AD patients, and the frontal lobe and the temporal lobe activated in HCs.	[122]
MA	Shenmen (HT 7), Zusanli (ST36), Fenglong (ST 40) Taixi (KI 3)	NA	AD patients	Induce right main hemisphere activations (temporal lobe, such as hippocampal gyrus, insula, and some area of parietal lobe) and left activated regions (temporal lobe, parietal lobule, some regions of cerebellum)	[123]

NA: not available. Abbreviations are found in Supplementary Table 3. The locations of acupoints are shown in Figure 2.

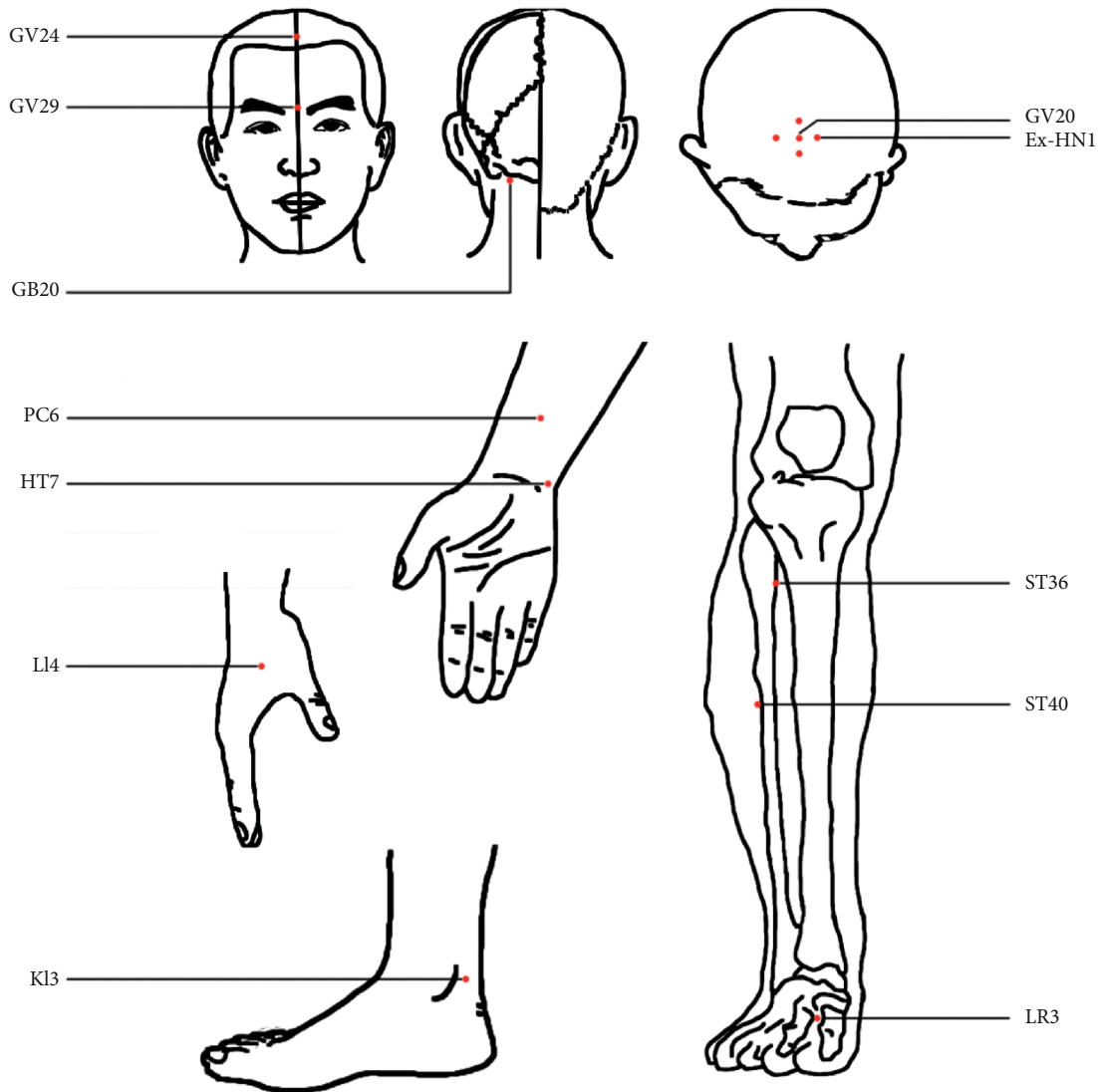


FIGURE 2: The locations of acupoints in humans.

memory scores [125], which offered evidence in support of compensatory mechanisms triggered to overcome cognitive deficits in MCI. These findings might provide a deep understanding of acupuncture's therapeutic effect in AD.

Acupuncture's influence on brain network connectivity might be correlated to acupoints, depth of stimulation, and frequency of EA stimulation in AD and MCI. The synergistic effects of different single acupoints or combined acupoints could activate different brain areas and impact the therapeutic effects of acupuncture [116]. And deep stimulation at appropriate acupoints could perform stronger or more extensive effective connectivity related to the therapeutic effect compared with superficial stimulation [119, 121, 126]. Furthermore, high-frequency EA may induce more specific targeted brain response or strengthen the functional connectivity of brain networks associated with memory and cognition. Thus, the impact of acupoint specificity, needling depth specificity, and EA parameter specificity on brain network connectivity in future neuroimaging studies also needs to be elucidated. Since few fMRI imaging studies have been

reported regarding acupuncture in patients with VCI, the effect of acupuncture on neuroplastic reorganization of brain functional networks in VCI is still to be established.

## 6. Discussion

In addition to directly attenuating the deposition, neuroinflammatory response, and neurotoxicity of  $A\beta$  [127] and increasing cerebral blood flow [128], acupuncture also could improve cognitive abilities through regulation of neuroplasticity (Figure 3). The improvement of the cellular/molecular microenvironment and recruitment of unaffected or additional brain networks might play important roles in this process. For example, the modulation of the neurotransmitter system involved in the improvement of the cellular/molecular microenvironment may be another candidate potential mechanism through which acupuncture could regulate neuroplasticity [44]. Moreover, it has been demonstrated that other methods in popular practice could increase cognitive reserve and resilience by regulating neuroplasticity, e.g.,

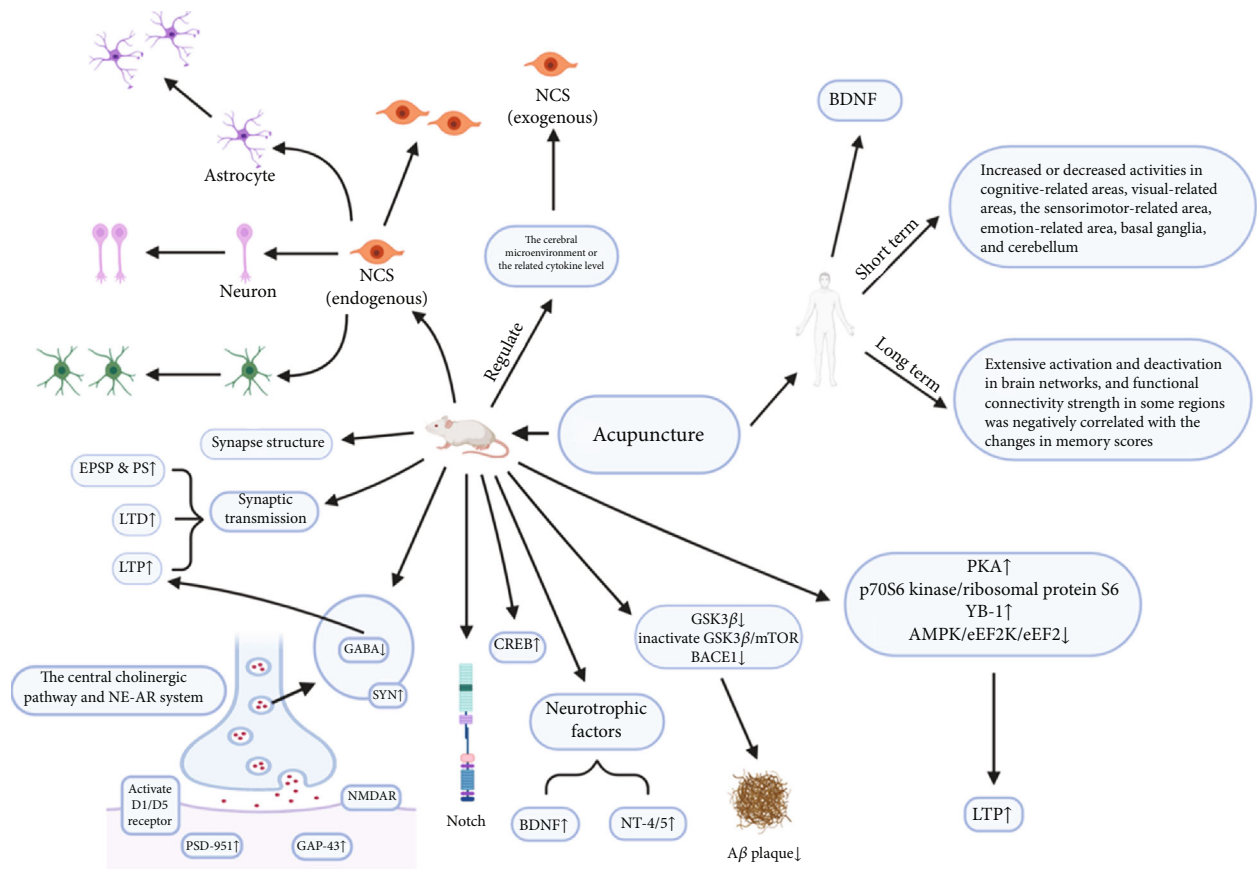


FIGURE 3: Mechanisms involved in acupuncture regulating neuroplasticity to improve cognitive function.

physical exercises, stimulating psychosocial experiences, meditation, mind games/puzzles, or dietary changes. It will be interesting to investigate whether acupuncture could increase cognitive reserve and resilience in the elderly. And the results would greatly expand the clinical application of acupuncture. Furthermore, identification of differential impacts of manipulation on brain networks may contribute to understanding the mechanisms of acupuncture in neuroplasticity. The comparison between acupuncture and sham/placebo acupuncture occurred in few clinical studies [124], which indicated increased connections between cognition-related regions by acupuncture not sham/placebo acupuncture. In the further researches, diffusion tensor imaging (DTI) of white matter microstructure adjacent to the primary somatosensory cortex and magnetic resonance spectroscopy (MRS) would be used to explore potential differential mechanisms of manipulation.

There are still some inevitable limitations in this review. First of all, because of differences in the quality of included animal studies, such as sample size calculations, experimental animals and procedures, housing and husbandry conditions, intervention, and assessment of experimental outcomes, the heterogeneities cannot be totally avoided (Supplementary Table 1). Second, it is well known that the efficacy of acupuncture stimulation was partly defined by the characteristic sensation “de qi” clinically (a composite of sensations including soreness, numbness, distention, heaviness, and other sensations) [129]. The efficacy of

interventions could not be estimated in animal studies. Third, there are differential influences on neuroplasticity due to acupuncture manipulation. For instance, experimental outcomes may be differently attributed to intervention performed by the acupuncture method (i.e., MA vs. EA) and acupoints [35, 36]. Since the number of studies was small, some pathways affected by the manipulation of acupuncture were not discussed, for instance, synaptophysin expression, modulation of neurotransmitter, and neuroplastic reorganization of brain functional networks (Supplementary Table 2).

## 7. Conclusion

A growing number of contemporary studies have gradually validated acupuncture’s traditional uses in treating AD and VCI. In view of acupuncture’s therapeutic efficiency and regulation of neuroplasticity, it may be beneficial to develop acupuncture as a potentially promising therapy for AD and VCI. However, the exact mechanisms underlying acupuncture’s influence on neuroplasticity is still unknown. In addition, identification of differential impacts of acupoint specificity, acupuncture method specificity, depth specificity, cognitive state specificity, and EA parameter specificity on neuroplasticity may contribute to understanding the mechanisms of acupuncture in AD and VCI. These may be important future challenges in standardized clinical applications.

## Data Availability

Previously reported data were used to support this study and are cited at relevant places within the text as references.

## Conflicts of Interest

The authors declare that they have no conflicts of interest.

## Authors' Contributions

Shaozhen Ji, Piu Chan, and Xianglan Jin contributed in study concept and design. Shaozhen Ji and Jiayu Duan contributed in literature search. Shaozhen Ji contributed in drafting the manuscript. Shaozhen Ji, Jiayu Duan, Xiaobing Hou, Li Zhou, Weilan Qin, Piu Chan, and Xianglan Jin contributed in critical revision of the manuscript for important intellectual content. Piu Chan and Xianglan Jin contributed in obtaining funding. Xiaobing Hou, Li Zhou, Weilan Qin, Huanmin Niu, Shuyun Luo, Yunling Zhang, Piu Chan, and Xianglan Jin contributed in administrative, technical, or material support. Yunling Zhang, Piu Chan, and Xianglan Jin contributed in study supervision. Shaozhen Ji and Jiayu Duan contributed equally to this work.

## Acknowledgments

The study was supported by grants 2018YFC1312001 and 2017YFC0840105 from the National Key R&D Program of China; grant SML20150803 from the Beijing Municipal Administration of Hospitals' Mission Plan; grant Z171100000117013 from the Beijing Municipal Science & Technology Commission; and grants 2020-JYB-ZDGG-124 and 2021-JYB-XSJJ071 from the Fundamental Research Funds for the Central Universities of China. Xianglan Jin is supported by the Talent Cultivation Plan for Inheritance of Clinical Characteristic Technology of Chinese Medicine.

## Supplementary Materials

We describe characteristics of included animal studies in Supplementary Table 1 referring to the new ARRIVE guidelines, as well as characteristics of included human studies in Supplementary Table 2. Some abbreviations included in this review are listed in Supplementary Table 3. (*Supplementary Materials*)

## References

- [1] H. Zhang, L. Hardie, A. O. Bawajeeh, and J. Cade, "Meat consumption, cognitive function and disorders: a systematic review with narrative synthesis and meta-analysis," *Nutrients*, vol. 12, no. 5, p. 1528, 2020.
- [2] S. A. Gale, D. Acar, and K. R. Daffner, "Dementia," *The American Journal of Medicine*, vol. 131, no. 10, pp. 1161–1169, 2018.
- [3] L. Fratiglioni, A. Marseglia, and S. Dekhtyar, "Ageing without dementia: can stimulating psychosocial and lifestyle experiences make a difference?," *The Lancet Neurology*, vol. 19, no. 6, pp. 533–543, 2020.

- [4] C. Iadecola, M. Duering, V. Hachinski et al., "Vascular Cognitive Impairment and Dementia," *Journal of the American College of Cardiology*, vol. 73, no. 25, pp. 3326–3344, 2019.
- [5] M. Revi, "Alzheimer's disease therapeutic approaches," *Advances in Experimental Medicine and Biology*, vol. 1195, pp. 105–116, 2020.
- [6] C. Y. Hung, X. Y. Wu, V. C. Chung, E. C. Tang, J. C. Wu, and A. Y. Lau, "Overview of systematic reviews with meta-analyses on acupuncture in post-stroke cognitive impairment and depression management," *Integrative Medicine Research*, vol. 8, no. 3, pp. 145–159, 2019.
- [7] Z. B. Liu, W. M. Niu, X. H. Yang, and X. M. Niu, "Clinical investigation on electroacupuncture treatment of vascular dementia with "Xiusanzhen"," *Zhen Ci Yan Jiu*, vol. 33, no. 2, pp. 131–134, 2008.
- [8] S. Wang, H. Yang, J. Zhang et al., "Efficacy and safety assessment of acupuncture and nimodipine to treat mild cognitive impairment after cerebral infarction: a randomized controlled trial," *BMC Complementary and Alternative Medicine*, vol. 16, no. 1, p. 361, 2016.
- [9] Y. Y. Wang, S. F. Yu, H. Y. Xue, Y. Li, C. Zhao, and Y. H. Jin, "Effectiveness and safety of acupuncture for the treatment of Alzheimer's disease: a systematic review and meta-analysis," *Frontiers in Aging Neuroscience*, vol. 12, p. 98, 2020.
- [10] J. W. Yang, G. X. Shi, S. Zhang et al., "Effectiveness of acupuncture for vascular cognitive impairment no dementia: a randomized controlled trial," *Clinical Rehabilitation*, vol. 33, no. 4, pp. 642–652, 2019.
- [11] J. D. Sweatt, "Neural plasticity and behavior—sixty years of conceptual advances," *Journal of Neurochemistry*, vol. 139, Suppl 2, pp. 179–199, 2016.
- [12] S. C. Cramer, M. Sur, B. H. Dobkin et al., "Harnessing neuroplasticity for clinical applications," *Brain*, vol. 134, no. 6, pp. 1591–1609, 2011.
- [13] R. von Bernhardi, L. E. Bernhardi, and J. Eugenin, "What is neural plasticity?," *Advances in Experimental Medicine and Biology*, vol. 1015, pp. 1–15, 2017.
- [14] A. F. Arnsten, C. D. Paspalas, N. J. Gamo, Y. Yang, and M. Wang, "Dynamic network connectivity: a new form of neuroplasticity," *Trends in Cognitive Sciences*, vol. 14, no. 8, pp. 365–375, 2010.
- [15] J. Jackson, E. Jambrina, J. Li et al., "Targeting the synapse in Alzheimer's disease," *Frontiers in Neuroscience*, vol. 13, p. 735, 2019.
- [16] B. Liu, J. Liu, J. Zhang, W. Mao, and S. Li, "Effects of autophagy on synaptic-plasticity-related protein expression in the hippocampus CA1 of a rat model of vascular dementia," *Neuroscience Letters*, vol. 707, article 134312, 2019.
- [17] E. Dayan and L. G. Cohen, "Neuroplasticity subserving motor skill learning," *Neuron*, vol. 72, no. 3, pp. 443–454, 2011.
- [18] C. Cavaleiro, J. Martins, J. Goncalves, and M. Castelo-Branco, "Memory and cognition-related neuroplasticity enhancement by transcranial direct current stimulation in rodents: a systematic review," *Neural Plasticity*, vol. 2020, Article ID 4795267, 23 pages, 2020.
- [19] Z. Q. Zhao, "Neural mechanism underlying acupuncture analgesia," *Progress in Neurobiology*, vol. 85, no. 4, pp. 355–375, 2008.
- [20] X. Ding, J. Yu, T. Yu, Y. Fu, and J. Han, "Acupuncture regulates the aging-related changes in gene profile expression of



- the hippocampus in senescence-accelerated mouse (SAMP10),” *Neuroscience Letters*, vol. 399, no. 1-2, pp. 11–16, 2006.
- [21] C. C. Yu, J. Wang, S. S. Ye et al., “Preventive Electroacupuncture Ameliorates D-Galactose-Induced Alzheimer’s Disease-Like Pathology and Memory Deficits Probably via Inhibition of GSK3 $\beta$ /mTOR Signaling Pathway,” *Evidence-based Complementary and Alternative Medicine*, vol. 2020, Article ID 1428752, 12 pages, 2020.
- [22] X. Huang, K. Huang, Z. Li et al., “Electroacupuncture improves cognitive deficits and insulin resistance in an OLETF rat model of Al/D-gal induced aging model via the PI3K/Akt signaling pathway,” *Brain Research*, vol. 1740, article 146834, 2020.
- [23] P. Liang, Z. Wang, T. Qian, and K. Li, “Acupuncture stimulation of Taichong (Liv3) and Hegu (LI4) modulates the default mode network activity in Alzheimer’s disease,” *American Journal of Alzheimer’s Disease and Other Dementias*, vol. 29, no. 8, pp. 739–748, 2014.
- [24] J. Frisen, “Neurogenesis and gliogenesis in nervous system plasticity and repair,” *Annual Review of Cell and Developmental Biology*, vol. 32, no. 1, pp. 127–141, 2016.
- [25] C. Zhao, W. Deng, and F. H. Gage, “Mechanisms and functional implications of adult neurogenesis,” *Cell*, vol. 132, no. 4, pp. 645–660, 2008.
- [26] D. Baglietto-Vargas, E. Sánchez-Mejias, V. Navarro et al., “Dual roles of A $\beta$  in proliferative processes in an amyloidogenic model of Alzheimer’s disease,” *Scientific Reports*, vol. 7, no. 1, article 10085, 2017.
- [27] L. Bondolfi, M. Calhoun, F. Ermini et al., “Amyloid-associated neuron loss and gliogenesis in the neocortex of amyloid precursor protein transgenic mice,” *The Journal of Neuroscience*, vol. 22, no. 2, pp. 515–522, 2002.
- [28] L. Verret, J. L. Jankowsky, G. M. Xu, D. R. Borchelt, and C. Rampon, “Alzheimer’s-type amyloidosis in transgenic mice impairs survival of newborn neurons derived from adult hippocampal neurogenesis,” *The Journal of Neuroscience*, vol. 27, no. 25, pp. 6771–6780, 2007.
- [29] O. Lindvall and Z. Kokaia, “Neurogenesis following stroke affecting the adult brain,” *Cold Spring Harbor Perspectives in Biology*, vol. 7, no. 11, 2015.
- [30] G. Li, H. Cheng, X. Zhang et al., “Hippocampal neuron loss is correlated with cognitive deficits in SAMP8 mice,” *Neurological Sciences*, vol. 34, no. 6, pp. 963–969, 2013.
- [31] G. Li, X. Zhang, H. Cheng et al., “Acupuncture improves cognitive deficits and increases neuron density of the hippocampus in middle-aged SAMP8 mice,” *Acupuncture in Medicine*, vol. 30, no. 4, pp. 339–345, 2012.
- [32] H. Cheng, J. Yu, Z. Jiang et al., “Acupuncture improves cognitive deficits and regulates the brain cell proliferation of SAMP8 mice,” *Neuroscience Letters*, vol. 432, no. 2, pp. 111–116, 2008.
- [33] X. Li, F. Guo, Q. Zhang et al., “Electroacupuncture decreases cognitive impairment and promotes neurogenesis in the APP/PS1 transgenic mice,” *BMC Complementary and Alternative Medicine*, vol. 14, no. 1, p. 37, 2014.
- [34] J. Tao, B. Chen, Y. Gao et al., “Electroacupuncture enhances hippocampal NSCs proliferation in cerebral ischemia-reperfusion injured rats via activation of notch signaling pathway,” *The International Journal of Neuroscience*, vol. 124, no. 3, pp. 204–212, 2013.
- [35] Y. R. Kim, H. N. Kim, S. M. Ahn, Y. H. Choi, H. K. Shin, and B. T. Choi, “Electroacupuncture promotes post-stroke functional recovery via enhancing endogenous neurogenesis in mouse focal cerebral ischemia,” *PLoS One*, vol. 9, no. 2, article e90000, 2014.
- [36] F. Li, C. Q. Yan, L. T. Lin et al., “Acupuncture attenuates cognitive deficits and increases pyramidal neuron number in hippocampal CA1 area of vascular dementia rats,” *BMC Complementary and Alternative Medicine*, vol. 15, no. 1, p. 133, 2015.
- [37] R. Lin and L. Iacovitti, “Classic and novel stem cell niches in brain homeostasis and repair,” *Brain Research*, vol. 1628, pp. 327–342, 2015.
- [38] P. B. Gorelick, A. Scuteri, S. E. Black et al., “Vascular contributions to cognitive impairment and dementia: a statement for healthcare professionals from the American Heart Association/American Stroke Association,” *Stroke*, vol. 42, no. 9, pp. 2672–2713, 2011.
- [39] A. M. Ibrahim, F. H. Pottou, E. S. Dahiya, F. A. Khan, and J. S. Kumar, “Neuron-glia interactions: molecular basis of Alzheimer’s disease and applications of neuroproteomics,” *The European Journal of Neuroscience*, vol. 52, no. 2, pp. 2931–2943, 2020.
- [40] R. J. Franklin and C. French-Constant, “Remyelination in the CNS: from biology to therapy,” *Nature Reviews Neuroscience*, vol. 9, no. 11, pp. 839–855, 2008.
- [41] S. M. Ahn, Y. R. Kim, H. N. Kim, Y. I. Shin, H. K. Shin, and B. T. Choi, “Electroacupuncture ameliorates memory impairments by enhancing oligodendrocyte regeneration in a mouse model of prolonged cerebral hypoperfusion,” *Scientific Reports*, vol. 6, no. 1, article 28646, 2016.
- [42] M. Santello, N. Toni, and A. Volterra, “Astrocyte function from information processing to cognition and cognitive impairment,” *Nature Neuroscience*, vol. 22, no. 2, pp. 154–166, 2019.
- [43] I. K. Hwang, J. Y. Chung, D. Y. Yoo et al., “Comparing the effects of acupuncture and electroacupuncture at Zusanli and Baihui on cell proliferation and neuroblast differentiation in the rat hippocampus,” *The Journal of Veterinary Medical Science*, vol. 72, no. 3, pp. 279–284, 2010.
- [44] C. L. Zhou, L. Zhao, H. Y. Shi et al., “Combined acupuncture and HuangDiSan treatment affects behavior and synaptophysin levels in the hippocampus of senescence-accelerated mouse prone 8 after neural stem cell transplantation,” *Neural Regeneration Research*, vol. 13, no. 3, pp. 541–548, 2018.
- [45] L. Zhao, C. Zhou, L. Li et al., “Acupuncture improves cerebral microenvironment in mice with Alzheimer’s disease treated with hippocampal neural stem cells,” *Molecular Neurobiology*, vol. 54, no. 7, pp. 5120–5130, 2017.
- [46] C. R. Jack Jr., D. S. Knopman, W. J. Jagust et al., “Hypothetical model of dynamic biomarkers of the Alzheimer’s pathological cascade,” *Lancet Neurology*, vol. 9, no. 1, pp. 119–128, 2010.
- [47] F. Wang, Y. Cao, L. Ma, H. Pei, W. D. Rausch, and H. Li, “Dysfunction of cerebrovascular endothelial cells: prelude to vascular dementia,” *Frontiers in Aging Neuroscience*, vol. 10, p. 376, 2018.
- [48] E. Falke, J. Nissanov, T. W. Mitchell, D. A. Bennett, J. Q. Trojanowski, and S. E. Arnold, “Subicular dendritic arborization in Alzheimer’s disease correlates with neurofibrillary tangle density,” *The American Journal of Pathology*, vol. 163, no. 4, pp. 1615–1621, 2003.

- [49] C. C. Yu, Y. Wang, F. Shen et al., "High-frequency (50 Hz) electroacupuncture ameliorates cognitive impairment in rats with amyloid beta 1-42-induced Alzheimer's disease," *Neural Regeneration Research*, vol. 13, no. 10, pp. 1833–1841, 2018.
- [50] H. Y. Yang, Y. Liu, J. C. Xie, N. N. Liu, and X. Tian, "Effects of repetitive transcranial magnetic stimulation on synaptic plasticity and apoptosis in vascular dementia rats," *Behavioural Brain Research*, vol. 281, pp. 149–155, 2015.
- [51] S. A. Buffington, W. Huang, and M. Costa-Mattioli, "Translational control in synaptic plasticity and cognitive dysfunction," *Annual Review of Neuroscience*, vol. 37, no. 1, pp. 17–38, 2014.
- [52] G. Neves, S. F. Cooke, and T. V. Bliss, "Synaptic plasticity, memory and the hippocampus: a neural network approach to causality," *Nature Reviews Neuroscience*, vol. 9, no. 1, pp. 65–75, 2008.
- [53] J. N. Bourne and K. M. Harris, "Balancing structure and function at hippocampal dendritic spines," *Annual Review of Neuroscience*, vol. 31, no. 1, pp. 47–67, 2008.
- [54] W. G. Xia, C. J. Zheng, X. Zhang, and J. Wang, "Effects of "nourishing liver and kidney" acupuncture therapy on expression of brain derived neurotrophic factor and synaptophysin after cerebral ischemia reperfusion in rats," *Journal of Huazhong University of Science and Technology. Medical Sciences*, vol. 37, no. 2, pp. 271–278, 2017.
- [55] Y. Wang, Q. Wang, B. Ren et al., "'Olfactory three-needle" enhances spatial learning and memory ability in SAMP8 mice," *Behavioural Neurology*, vol. 2020, Article ID 2893289, 11 pages, 2020.
- [56] M. Cai, J. H. Lee, and E. J. Yang, "Electroacupuncture attenuates cognition impairment via anti-neuroinflammation in an Alzheimer's disease animal model," *Journal of Neuroinflammation*, vol. 16, no. 1, p. 264, 2019.
- [57] B. H. Kan, J. C. Yu, L. Zhao et al., "Acupuncture improves dendritic structure and spatial learning and memory ability of Alzheimer's disease mice," *Neural Regeneration Research*, vol. 13, no. 8, pp. 1390–1395, 2018.
- [58] T. Liu, X. Z. Zhang, J. X. Han, and K. Nie, "Using bioinformatics tools to explore cellular biological mechanisms of "triple energizer acupuncture method" in treating senile dementia," *Zhen Ci Yan Jiu*, vol. 44, pp. 424–429, 2019.
- [59] G. L. Collingridge, S. Peineau, J. G. Howland, and Y. T. Wang, "Long-term depression in the CNS," *Nature Reviews. Neuroscience*, vol. 11, no. 7, pp. 459–473, 2010.
- [60] E. N. van den Broeke, C. M. van Rijn, J. A. Biurrin Manresa, O. K. Andersen, L. Arendt-Nielsen, and O. H. Wilder-Smith, "Neurophysiological correlates of nociceptive heterosynaptic long-term potentiation in humans," *Journal of Neurophysiology*, vol. 103, no. 4, pp. 2107–2113, 2010.
- [61] L.-h. Kong, W. Li, H. Wang et al., "High-frequency electroacupuncture evidently reinforces hippocampal synaptic transmission in Alzheimer's disease rats," *Neural Regeneration Research*, vol. 11, no. 5, pp. 801–806, 2016.
- [62] Y. W. Lin and C. L. Hsieh, "Electroacupuncture at Baihui acupoint (GV20) reverses behavior deficit and long-term potentiation through N-methyl-D-aspartate and transient receptor potential vanilloid subtype 1 receptors in middle cerebral artery occlusion rats," *Journal of Integrative Neuroscience*, vol. 9, no. 3, pp. 269–282, 2010.
- [63] Y. Zhu, X. Wang, X. Ye, C. Gao, and W. Wang, "Effects of electroacupuncture on the expression of p70 ribosomal protein S6 kinase and ribosomal protein S6 in the hippocampus of rats with vascular dementia," *Neural Regeneration Research*, vol. 7, no. 3, pp. 207–211, 2012.
- [64] Y. Tang, S. Shao, Y. Guo et al., "Electroacupuncture mitigates hippocampal cognitive impairments by reducing BACE1 deposition and activating PKA in APP/PS1 double transgenic mice," *Neural Plasticity*, vol. 2019, Article ID 2823679, 12 pages, 2019.
- [65] X. H. Jing, S. L. Chen, H. Shi, H. Cai, and Z. G. Jin, "Electroacupuncture restores learning and memory impairment induced by both diabetes mellitus and cerebral ischemia in rats," *Neuroscience Letters*, vol. 443, no. 3, pp. 193–198, 2008.
- [66] J. W. Yang, X. R. Wang, M. Zhang et al., "Acupuncture as a multifunctional neuroprotective therapy ameliorates cognitive impairment in a rat model of vascular dementia: a quantitative iTRAQ proteomics study," *CNS Neuroscience & Therapeutics*, vol. 24, no. 12, pp. 1264–1274, 2018.
- [67] Y. Ye, H. Li, J. W. Yang et al., "Acupuncture attenuated vascular dementia-induced hippocampal long-term potentiation impairments via activation of D1/D5 receptors," *Stroke*, vol. 48, no. 4, pp. 1044–1051, 2017.
- [68] L. Y. Xiao, X. R. Wang, J. W. Yang et al., "Acupuncture prevents the impairment of hippocampal LTP through  $\beta$ 1-AR in vascular dementia rats," *Molecular Neurobiology*, vol. 55, no. 10, pp. 7677–7690, 2018.
- [69] L.-Y. Xiao, J.-W. Yang, X.-R. Wang et al., "Acupuncture Rescues Cognitive Impairment and Upregulates Dopamine-Hydroxylase Expression in Chronic Cerebral Hypoperfusion Rats," *BioMed Research International*, vol. 2018, Article ID 5423961, 8 pages, 2018.
- [70] M. H. Shen, Q. Q. Tang, Z. R. Li, and C. Ma, "Effect of electroacupuncture on hippocampal LTP in Alzheimer's disease rats induced by Abeta(25-35)," *Zhen Ci Yan Jiu*, vol. 35, no. 1, pp. 3–7, 2010.
- [71] P. Greengard, F. Valtorta, A. J. Czernik, and F. Benfenati, "Synaptic vesicle phosphoproteins and regulation of synaptic function," *Science*, vol. 259, no. 5096, pp. 780–785, 1993.
- [72] A. Citri and R. C. Malenka, "Synaptic plasticity: multiple forms, functions, and mechanisms," *Neuropsychopharmacology*, vol. 33, no. 1, pp. 18–41, 2008.
- [73] S. B. Martin, A. L. S. Dowling, J. Lianekhammy et al., "Synaptophysin and synaptotagmin-1 in Down syndrome are differentially affected by Alzheimer's disease," *Journal of Alzheimer's Disease*, vol. 42, no. 3, pp. 767–775, 2014.
- [74] J. Dong, J. Zhao, Y. Lin et al., "Exercise improves recognition memory and synaptic plasticity in the prefrontal cortex for rats modelling vascular dementia," *Neurological Research*, vol. 40, pp. 68–77, 2017.
- [75] G. Yang, Y.-N. Pei, S.-J. Shao et al., "Effects of electroacupuncture at "Baihui" and "Yongquan" on the levels of synaptic plasticity related proteins postsynaptic density-95 and synaptophysin in hippocampus of APP/PS1 mice," *Zhen Ci Yan Jiu*, vol. 45, no. 4, pp. 310–314, 2020.
- [76] W. Dong, W. Yang, F. Li et al., "Electroacupuncture improves synaptic function in SAMP8 mice probably via inhibition of the AMPK/eEF2K/eEF2 signaling pathway," *Evidence-based Complementary and Alternative Medicine*, vol. 2019, Article ID 8260815, 10 pages, 2019.
- [77] Y. Wang, L. Kong, W. Li et al., "Effects and mechanisms of different frequencies of electroacupuncture for learning and

- memory ability of Alzheimer's rats," *Zhongguo Zhen Jiu*, vol. 37, no. 6, pp. 629–636, 2017.
- [78] X. He, T. Yan, R. Chen, and D. Ran, "Acute effects of electroacupuncture (EA) on hippocampal long term potentiation (LTP) of perforant path-dentate gyrus granule cells synapse related to memory," *Acupunct Electrother Res*, vol. 37, no. 2, pp. 89–101, 2012.
- [79] N. A. Otmakhova and J. E. Lisman, "D1/D5 dopamine receptor activation increases the magnitude of early long-term potentiation at CA1 hippocampal synapses," *The Journal of Neuroscience*, vol. 16, no. 23, pp. 7478–7486, 1996.
- [80] N. X. Tritsch and B. L. Sabatini, "Dopaminergic modulation of synaptic transmission in cortex and striatum," *Neuron*, vol. 76, no. 1, pp. 33–50, 2012.
- [81] B. Lee, B. Sur, J. Shim, D. H. Hahm, and H. Lee, "Acupuncture stimulation improves scopolamine-induced cognitive impairment via activation of cholinergic system and regulation of BDNF and CREB expressions in rats," *BMC Complementary and Alternative Medicine*, vol. 14, no. 1, p. 338, 2014.
- [82] F. Arima-Yoshida, A. M. Watabe, and T. Manabe, "The mechanisms of the strong inhibitory modulation of long-term potentiation in the rat dentate gyrus," *The European Journal of Neuroscience*, vol. 33, no. 9, pp. 1637–1646, 2011.
- [83] P. C. Kind and P. E. Neumann, "Plasticity: downstream of glutamate," *Trends in Neurosciences*, vol. 24, no. 10, pp. 553–555, 2001.
- [84] L. Liu, T. P. Wong, M. F. Pozza et al., "Role of NMDA receptor subtypes in governing the direction of hippocampal synaptic plasticity," *Science*, vol. 304, no. 5673, pp. 1021–1024, 2004.
- [85] T. E. Bartlett, N. J. Bannister, V. J. Collett et al., "Differential roles of NR2A and NR2B-containing NMDA receptors in LTP and LTD in the CA1 region of two-week old rat hippocampus," *Neuropharmacology*, vol. 52, no. 1, pp. 60–70, 2007.
- [86] Y. Zhang, X. Mao, R. Lin, Z. Li, and J. Lin, "Electroacupuncture ameliorates cognitive impairment through inhibition of Ca<sup>2+</sup>-mediated neurotoxicity in a rat model of cerebral ischaemia-reperfusion injury," *Acupuncture in Medicine*, vol. 36, no. 6, pp. 401–407, 2018.
- [87] Y. Mu, S. W. Lee, and F. H. Gage, "Signaling in adult neurogenesis," *Current Opinion in Neurobiology*, vol. 20, no. 4, pp. 416–423, 2010.
- [88] T. Iso, L. Kedes, and Y. Hamamori, "HES and HERP families: multiple effectors of the Notch signaling pathway," *Journal of Cellular Physiology*, vol. 194, no. 3, pp. 237–255, 2003.
- [89] H.-d. Guo, J.-x. Tian, J. Zhu et al., "Electroacupuncture suppressed neuronal apoptosis and improved cognitive impairment in the AD model rats possibly via downregulation of Notch signaling pathway," *Evidence-based Complementary and Alternative Medicine*, vol. 2015, Article ID 393569, 9 pages, 2015.
- [90] D. K. Binder and H. E. Scharfman, "Brain-derived neurotrophic factor," *Growth Factors*, vol. 22, pp. 123–131, 2009.
- [91] M. F. Egan, M. Kojima, J. H. Callicott et al., "The BDNF val66met polymorphism affects activity-dependent secretion of BDNF and human memory and hippocampal function," *Cell*, vol. 112, pp. 257–269, 2003.
- [92] Z. Y. Chen, P. D. Patel, G. Sant et al., "Variant brain-derived neurotrophic factor (BDNF) (Met66) alters the intracellular trafficking and activity-dependent secretion of wild-type BDNF in neurosecretory cells and cortical neurons," *The Journal of Neuroscience*, vol. 24, no. 18, pp. 4401–4411, 2004.
- [93] P. T. Pang, H. K. Teng, E. Zaitsev et al., "Cleavage of proBDNF by tPA/plasmin is essential for long-term hippocampal plasticity," *Science*, vol. 306, no. 5695, pp. 487–491, 2004.
- [94] B. Lu, P. T. Pang, and N. H. Woo, "The yin and yang of neurotrophin action," *Nature Reviews. Neuroscience*, vol. 6, no. 8, pp. 603–614, 2005.
- [95] R. Lee, P. Kermani, K. K. Teng, and B. L. Hempstead, "Regulation of cell survival by secreted proneurotrophins," *Science*, vol. 294, no. 5548, pp. 1945–1948, 2001.
- [96] R. Lin, J. Chen, X. Li et al., "Electroacupuncture at the Baihui acupoint alleviates cognitive impairment and exerts neuroprotective effects by modulating the expression and processing of brain-derived neurotrophic factor in APP/PS1 transgenic mice," *Molecular Medicine Reports*, vol. 13, no. 2, pp. 1611–1617, 2016.
- [97] R. Lin, L. Li, Y. Zhang et al., "Electroacupuncture ameliorate learning and memory by improving N-acetylaspertate and glutamate metabolism in APP/PS1 mice," *Biological Research*, vol. 51, no. 1, p. 21, 2018.
- [98] J. Xiong, Z. Zhang, Y. Ma et al., "The effect of combined scalp acupuncture and cognitive training in patients with stroke on cognitive and motor functions," *NeuroRehabilitation*, vol. 46, pp. 75–82, 2020.
- [99] Z. C. Hesp, E. Z. Goldstein, C. J. Miranda, B. K. Kaspar, and D. M. McTigue, "Chronic oligodendrogenesis and remyelination after spinal cord injury in mice and rats," *The Journal of Neuroscience*, vol. 35, no. 3, pp. 1274–1290, 2015.
- [100] T. Arendt, J. T. Stieler, and M. Holzer, "Tau and tauopathies," *Brain Research Bulletin*, vol. 126, pp. 238–292, 2016.
- [101] J. Jiang, G. Liu, S. Shi, Y. Li, and Z. Li, "Effects of manual acupuncture combined with donepezil in a mouse model of Alzheimer's disease," *Acupuncture in Medicine*, vol. 37, no. 1, pp. 64–71, 2019.
- [102] P. H. Reddy, "Amyloid beta-induced glycogen synthase kinase 3 $\beta$  phosphorylated VDAC1 in Alzheimer's disease: implications for synaptic dysfunction and neuronal damage," *Biochimica et Biophysica Acta-Molecular Basis of Disease*, vol. 1832, no. 12, pp. 1913–1921, 2013.
- [103] L. Avrahami, D. Farfara, M. Shaham-Kol, R. Vassar, D. Frenkel, and H. Eldar-Finkelman, "Inhibition of glycogen synthase kinase-3 ameliorates  $\beta$ -amyloid pathology and restores lysosomal acidification and mammalian target of rapamycin activity in the Alzheimer disease mouse model: in vivo and in vitro studies," *The Journal of Biological Chemistry*, vol. 288, no. 2, pp. 1295–1306, 2013.
- [104] S. N. Duffy, K. J. Craddock, T. Abel, and P. V. Nguyen, "Environmental enrichment modifies the PKA-dependence of hippocampal LTP and improves hippocampus-dependent memory," *Learning & Memory*, vol. 8, no. 1, pp. 26–34, 2001.
- [105] S. J. Raiker, H. Lee, K. T. Baldwin, Y. Duan, P. Shrager, and R. J. Giger, "Oligodendrocyte-myelin glycoprotein and Nogo negatively regulate activity-dependent synaptic plasticity," *The Journal of Neuroscience*, vol. 30, pp. 12432–12445, 2010.
- [106] L. Sui, J. Wang, and B. M. Li, "Role of the phosphoinositide 3-kinase-Akt-mammalian target of the rapamycin signaling pathway in long-term potentiation and trace fear conditioning memory in rat medial prefrontal cortex," *Learning & Memory*, vol. 15, no. 10, pp. 762–776, 2008.



- [107] C. A. Hoeffler, W. Tang, H. Wong et al., "Removal of FKBP12 enhances mTOR-Raptor interactions, LTP, memory, and perseverative/repetitive behavior," *Neuron*, vol. 60, no. 5, pp. 832–845, 2008.
- [108] L. Swiech, M. Perycz, A. Malik, and J. Jaworski, "Role of mTOR in physiology and pathology of the nervous system," *Biochimica et Biophysica Acta*, vol. 1784, no. 1, pp. 116–132, 2008.
- [109] Y. Zhu, Y. Zeng, X. Wang, and X. Ye, "Effect of electroacupuncture on the expression of mTOR and eIF4E in hippocampus of rats with vascular dementia," *Neurological Sciences*, vol. 34, no. 7, pp. 1093–1097, 2013.
- [110] T. Fukada and N. K. Tonks, "Identification of YB-1 as a regulator of PTP1B expression: implications for regulation of insulin and cytokine signaling," *The EMBO Journal*, vol. 22, no. 3, pp. 479–493, 2003.
- [111] L. Sang, C. Liu, L. Wang et al., "Disrupted brain structural connectivity network in subcortical ischemic vascular cognitive impairment with no dementia," *Frontiers in Aging Neuroscience*, vol. 12, p. 6, 2020.
- [112] R. A. Sperling, P. S. LaViolette, K. O'Keefe et al., "Amyloid deposition is associated with impaired default network function in older persons without dementia," *Neuron*, vol. 63, no. 2, pp. 178–188, 2009.
- [113] Z. Wang, B. Nie, D. Li et al., "Effect of acupuncture in mild cognitive impairment and Alzheimer disease: a functional MRI study," *PLoS One*, vol. 7, no. 8, article e42730, 2012.
- [114] Y. Tang, Y. Xing, Z. Zhu et al., "The effects of 7-week cognitive training in patients with vascular cognitive impairment, no dementia (the Cog-VACCINE study): a randomized controlled trial," *Alzheimers Dement*, vol. 15, no. 5, pp. 605–614, 2019.
- [115] M. Stampanoni Bassi, E. Iezzi, L. Gilio, D. Centonze, and F. Buttari, "Synaptic plasticity shapes brain connectivity: implications for network topology," *International Journal of Molecular Sciences*, vol. 20, no. 24, p. 6193, 2019.
- [116] C.-c. Yu, C.-y. Ma, H. Wang et al., "Effects of acupuncture on Alzheimer's disease: evidence from neuroimaging studies," *Chinese Journal of Integrative Medicine*, vol. 25, no. 8, pp. 631–640, 2019.
- [117] W. Zheng, Z. Su, X. Liu et al., "Modulation of functional activity and connectivity by acupuncture in patients with Alzheimer disease as measured by resting-state fMRI," *PLoS One*, vol. 13, article e0196933, 2018.
- [118] Y. Shan, J.-J. Wang, Z.-Q. Wang et al., "Neuronal specificity of acupuncture in Alzheimer's disease and mild cognitive impairment patients: a functional MRI study," *Evidence-based Complementary and Alternative Medicine*, vol. 2018, Article ID 7619197, 10 pages, 2018.
- [119] Y. Feng, L. Bai, Y. Ren et al., "fMRI connectivity analysis of acupuncture effects on the whole brain network in mild cognitive impairment patients," *Magnetic Resonance Imaging*, vol. 30, no. 5, pp. 672–682, 2012.
- [120] L. Zhao, F. Zhu, S. Chen et al., "Acupuncture at the Taixi (KI3) acupoint activates cerebral neurons in elderly patients with mild cognitive impairment," *Neural Regeneration Research*, vol. 9, pp. 1163–1168, 2014.
- [121] S. Chen, L. Bai, M. Xu et al., "Multivariate granger causality analysis of acupuncture effects in mild cognitive impairment patients: an fMRI study," *Evidence-based Complementary and Alternative Medicine*, vol. 2013, Article ID 127271, 12 pages, 2013.
- [122] P. Fu, J. P. Jia, J. Zhu, and J. J. Huang, "Effects of acupuncture at Neiguan (PC 6) on human brain functional imaging in different functional states," *Zhongguo Zhen Jiu*, vol. 25, pp. 784–786, 2005.
- [123] Y. Zhou and J. Jia, "Effect of acupuncture given at the HT 7, ST 36, ST 40 and KI 3 acupoints on various parts of the brains of Alzheimer's disease patients," *Acupuncture & Electro-Therapeutics Research*, vol. 33, no. 1, pp. 9–17, 2008.
- [124] T. T. Tan, D. Wang, J. K. Huang et al., "Modulatory effects of acupuncture on brain networks in mild cognitive impairment patients," *Neural Regeneration Research*, vol. 12, no. 2, pp. 250–258, 2017.
- [125] H. Li, Z. Wang, H. Yu et al., "The long-term effects of acupuncture on hippocampal functional connectivity in aMCI with hippocampal atrophy: a randomized longitudinal fMRI study," *Neural Plasticity*, vol. 2020, 9 pages, 2020.
- [126] L. Bai, M. Zhang, S. Chen et al., "Characterizing acupuncture de qi in mild cognitive impairment: relations with small-world efficiency of functional brain networks," *Evidence-based Complementary and Alternative Medicine*, vol. 2013, Article ID 304804, 8 pages, 2013.
- [127] L. Y. Xiao, X. R. Wang, Y. Yang et al., "Applications of acupuncture therapy in modulating plasticity of central nervous system," *Neuromodulation*, vol. 21, no. 8, pp. 762–776, 2018.
- [128] N. Ding, J. Jiang, A. Xu, Y. Tang, and Z. Li, "Manual acupuncture regulates behavior and cerebral blood flow in the SAMP8 mouse model of Alzheimer's disease," *Frontiers in Neuroscience*, vol. 13, p. 37, 2019.
- [129] J. Kong, R. Gollub, T. Huang et al., "Acupuncture de qi, from qualitative history to quantitative measurement," *Journal of Alternative and Complementary Medicine*, vol. 13, no. 10, pp. 1059–1070, 2007.

## Research Article

# Electroacupuncture Ameliorates Neuroinflammation-Mediated Cognitive Deficits through Inhibition of NLRP3 in Presenilin1/2 Conditional Double Knockout Mice

Kun Li,<sup>1,2</sup> Guoqi Shi,<sup>2</sup> Yang Zhao,<sup>1,2</sup> Yiwen Chen,<sup>2</sup> Jie Gao,<sup>1,3</sup> Lin Yao,<sup>4</sup> Jiaying Zhao,<sup>2</sup> Hongzhu Li,<sup>2</sup> Ying Xu <sup>1</sup> and Yongjun Chen <sup>2,5,6</sup>

<sup>1</sup>Department of Physiology, School of Basic Medicine, Shanghai University of Traditional Chinese Medicine, 1200 Cailun Road, Shanghai 201203, China

<sup>2</sup>South China Research Center for Acupuncture and Moxibustion, Medical College of Acu-Moxi and Rehabilitation, Guangzhou University of Chinese Medicine, Guangzhou 510006, China

<sup>3</sup>School of Rehabilitation Science, University of Traditional Chinese Medicine, 1200 Cailun Road, Shanghai 201203, China

<sup>4</sup>School of Pharmaceutical Sciences, Guangzhou University of Chinese Medicine, Guangzhou 510006, China

<sup>5</sup>Center for Brain Science and Brain-Inspired Intelligence, Guangdong-Hong Kong-Macao Greater Bay Area, Guangzhou 510515, China

<sup>6</sup>Guangdong Province Key Laboratory of Psychiatric Disorders, Southern Medical University, Guangzhou 510515, China

Correspondence should be addressed to Ying Xu; [yingxu612@shutcm.edu.cn](mailto:yingxu612@shutcm.edu.cn) and Yongjun Chen; [ychen@gzucm.edu.cn](mailto:ychen@gzucm.edu.cn)

Received 20 June 2020; Revised 16 December 2020; Accepted 27 December 2020; Published 6 January 2021

Academic Editor: J. Michael Wyss

Copyright © 2021 Kun Li et al. This is an open access article distributed under the Creative Commons Attribution License, which permits unrestricted use, distribution, and reproduction in any medium, provided the original work is properly cited.

Neuroinflammation is considered as one of the crucial pathogenesis in promoting neurodegenerative progress of Alzheimer's disease (AD). As complementary and alternative therapy, electroacupuncture (EA) stimulation has been widely used in clinical practice for anti-inflammation. However, whether EA promotes the cognitive deficits resulting from neuroinflammation in AD remains unclear. In this study, the presenilin 1 and 2 conditional double knockout (PS cDKO) mice, exhibited a series of AD-like pathology, robust neuroinflammatory responses, and memory deficits, were used to evaluate the potential neuroprotective effect of EA at *Baihui* (GV 20) and *Shenting* (GV 24) by behavioral testing, electrophysiology recording, and molecular biology analyzing. First, we observed that EA improved memory deficits and impaired synaptic plasticity. Moreover, EA possesses an ability to suppress the hyperphosphorylated tau and robust elevated NLRP3, ASC, Caspase-1, IL-1 $\beta$ , and IL-18 in PS cDKO mice. Importantly, MCC950, a potent and selective inhibitor of NLRP3 inflammasome, has similar effects on inhibiting the hyperphosphorylated tau and the robust elevated NLRP3 components and neuroinflammatory responses of PS cDKO mice as well as EA treatment. Furthermore, EA treatment is not able to further improve the AD-like phenotypes of PS cDKO mice in combination with the MCC950 administration. Therefore, EA stimulation at GV 20 and GV 24 acupoints may be a potential alternative therapy for deterring cognitive deficits in AD through suppression of NLRP3 inflammasome activation.

## 1. Introduction

Alzheimer's disease (AD) is the most common type of dementia in the elderly population [1], characterized by progressive decline in the cognitive and psychomotor function. The extracellular deposition of amyloid- $\beta$  plaques, hyperphosphorylation of tau-associated neurofibrillary tangles, and neuroinflammation caused by the innate immune sys-

tem in the brain are considered as the major pathological hallmarks of AD and have gained much attention [2–4]. Previous studies show that plaques, tangles, and neuronal debris persistently activate primed microglia, which results in a constant production of proinflammatory mediators, such as interleukin-1 beta (IL-1 $\beta$ ), tumor necrosis factor alpha (TNF- $\alpha$ ), nitric oxide, chemokines, and complements [5, 6]. These mediators maintain microglial activation and induce



neuroinflammatory responses in early phase of AD, which aggravate tau pathology, synaptic, and neuronal dysfunction. With the continuity of neuroinflammation, the neurodegenerative progress of AD also accelerated [7]. Therefore, blockage of neuroinflammation-mediated synaptic and neural dysfunction may be potential therapeutic strategies for preventing the occurrence of AD, delaying its process, or improving its symptoms.

The inflammasome is a critical protein complex of the innate immune system, which consists of pyrin domain-containing protein 3 (NLRP3) receptor, the adaptor apoptosis-associated speck-like protein (ASC), and the cysteine protease caspase-1 [8]. Activation of NLRP3 inflammasome mediates the maturation of caspase-1 and the secretion of proinflammatory cytokines IL-1 $\beta$  and IL-18 [9]. Previous research suggested that the role of NLRP3 inflammasome activation by amyloid-beta (A $\beta$ ) may be critical for IL-1 $\beta$  processing and subsequent inflammatory responses [10, 11]. Recent studies provide evidence that the NLRP3 inflammasome are essential for both the progression of A $\beta$  and tau pathology directly in AD [12, 13]. These findings indicate that NLRP3 inflammasome may be a potential therapeutic target for AD (or neurodegenerative disorders).

As the subunits of  $\gamma$ -secretase, the presenilin (PS)1/2 are responsible for the proteolytic processing of amyloid precursor proteins (APPs) and other proteins involved in apoptosis and neuronal adhesion [14]. Previous reports indicated that the mutations in the PS1 and PS2 were discovered in brain of early-onset AD patients [15]. To investigate the therapeutic effect and underlying mechanism in AD, we used the PS1 and PS2 conditional double knockout (PS cDKO) mice as an animal model with deletion of PS1 in the forebrain and PS2 in the whole body [16, 17]. PS cDKO mice displayed obvious AD-like phenotypes, including tau hyperphosphorylation, synaptic and neuronal loss, brain atrophy, and memory deficits, especially glia activation and neuroinflammatory responses but no distinct change in deposition of A $\beta$  plaques [18–20]. Since PS cDKO mice exhibit robust inflammatory responses from young adults (3 months), they have been chosen as a suitable animal model to mimic the progress of AD and study the pharmacological mechanisms of neuroinflammation-mediated neurodegenerative disorders.

As one of the most recognized alternative therapies, acupuncture has been widely used to treat cognitive impairment and neurodegenerative disorders including AD [21, 22]. Both *Baihui* (GV 20) and *Shenting* (GV 24) are located on the midline of the head, which are most commonly used acupoints for the treatment of neurological and psychiatric disorders such as mania, epilepsy, depression, and dementia [23–25]. However, whether EA stimulus can attenuate the cognitive impairment resulting from neuroinflammation in AD remains unclear. Here, we applied EA at GV 20 and GV 24 acupoints to four months old PS cDKO mice for three weeks. Specifically, we studied the effects of EA on behavioral changes, synaptic plasticity, inflammation response, and NLRP3 inflammasome component analyses. We found that EA treatment ameliorated cognitive deficits, impaired long-term potentiation (LTP) induction, and abnormal expression of NMDA receptors of PS cDKO mice, which might be asso-

ciated with the antineuroinflammatory effects of EA through blockage of the NLRP3 inflammasome signaling pathway in hippocampus. This study suggested that EA at GV20 and GV24 acupoints should be considered as an effective therapeutic strategy against neuroinflammation-mediated neurodegenerative disease.

## 2. Materials and Methods

**2.1. Animals.** The PS cDKO mice were generated and genotyped as previously described [18]. Briefly, the cDKO mice were acquired by crossing the forebrain-specific PS1 heterozygous knockout mice with conventional PS2 heterozygous knockout mice based on the C57BL/6J genetic background. Mice with the transgene Cre, fPS1/fPS1, and PS2<sup>-/-</sup> served as PS cDKO mice, and their littermates (Cre<sup>-</sup>, PS1<sup>+/+</sup>, and PS2<sup>+/+</sup>) served as control wild-type (WT) mice. Mice were group-housed (four per cage) at a temperature of 22  $\pm$  2°C, 40–70% humidity on a 12-h light/dark cycle (the lights were on from 7 a.m. to 7 p.m.), with ad libitum access to food and water. PS cDKO mice and their littermate WT mice at 4 months were used in this study. All the experiments were approved by the Institutional Animal Care and Use Committee at Guangzhou University of Chinese Medicine (GZUCM).

**2.2. Electroacupuncture and MCC950 Treatment.** Four-month-old PS cDKO mice and their littermates were randomly divided into four groups: WT, WT+EA, PS cDKO (cDKO), and cDKO+EA. Disposable acupuncture needles (0.16  $\times$  7 mm) were purchased from Beijing Zhongyan Taihe Medical Instrument Co., Ltd (Zhongyan Taihe, Beijing, China). To avoid the side effects of anesthetic, EA stimulation was applied to the mice in EA treatment groups in the awakened state. The self-made fixing device is made of 50 mL epoxy tube and thin insulated iron wire. Enough holes were left on the epoxy tube to make sure mice inside could not move but breathe normally. There was a bigger hole on the top of the mouse head to facilitate the EA stimulation. Mice were fixed in the self-made fixing devices. The needles were inserted to a depth of 4 mm at the *Baihui* (GV 20) and *Shenting* (GV 24) acupoints after the skin had been cleaned with alcohol wipes. Then, the mice were connected to a Master-8 Stimulator (Master-8, AMPI, Israel), and electrical current (2 Hz, 1 mA) was given to the needles. As shown in (Figure 1(a)), mice received EA stimulation for 15 min at 10:00 a.m. each day for 5 consecutive days per week, and the whole course of treatment lasted 3 consecutive weeks. To avoid this and minimize the effect, all the mice were put into self-made fixing devices for adaptation two weeks before EA stimulation as described previously [26]. During the three weeks for EA stimulation, mice in the WT group and in the cDKO group were fixed in the same devices in the awakened state and treated the same way without giving EA stimulation.

MCC950 is a kind of NLRP3 inflammasome inhibitor used for the interventional study, and it was purchased from Sigma-Aldrich (St. Louis, MO, USA). Four-month-old mice and their littermates were randomly divided into five groups:

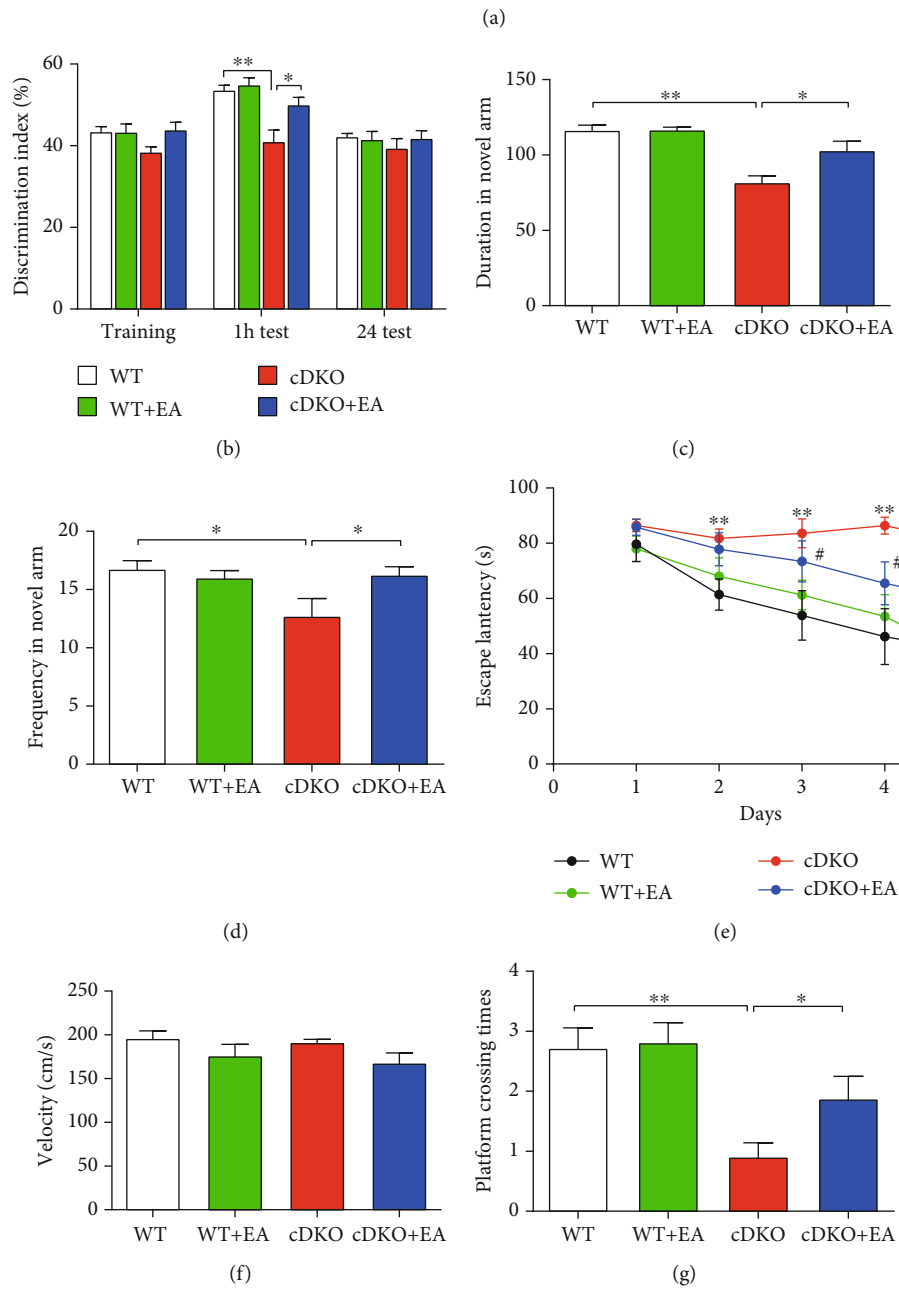
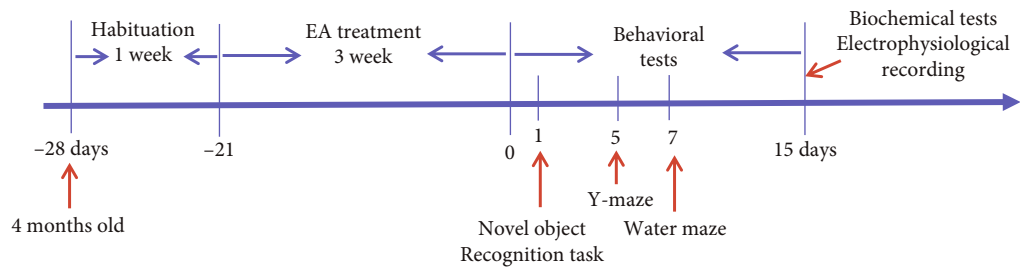


FIGURE 1: Continued.

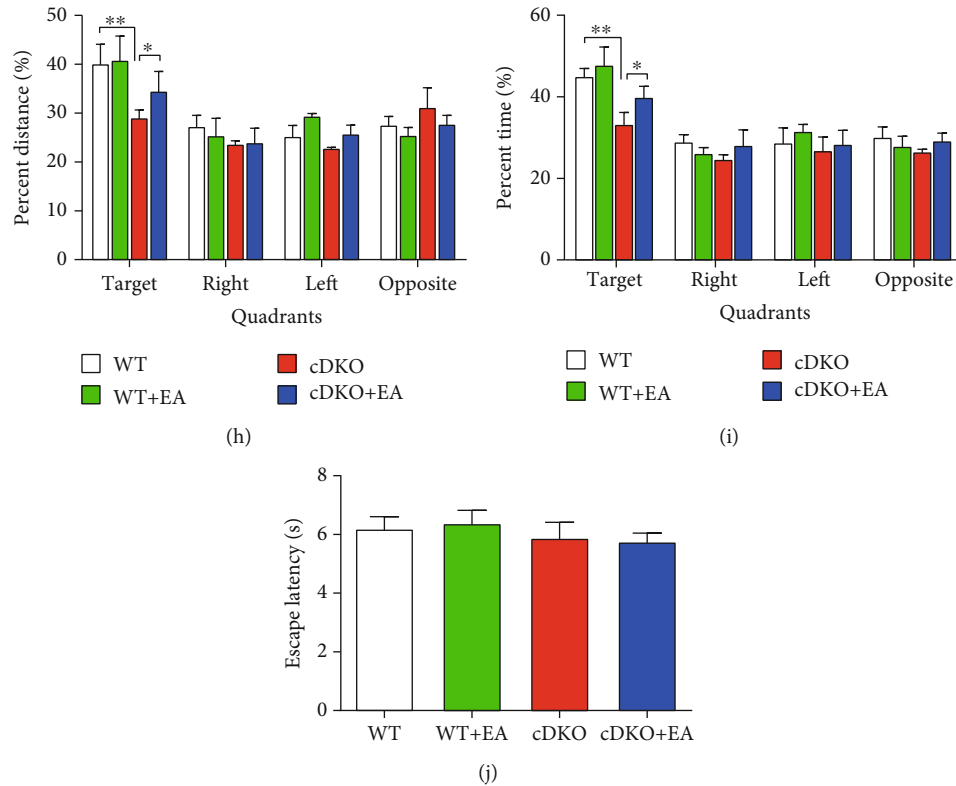


FIGURE 1: EA treatment ameliorates impaired memory in PS cDKO mice. (a) The experimental timeline of habituation, EA stimulation, and behavioral tests. (b) Effects of EA treatment on recognition memory in PS cDKO mice by NOR task. (c, d) The duration spent and frequency visited in the novel arm of the Y-maze. (e) The escape latency to the hidden platform in target quadrant during the first phase of 5 consecutive training days of the MWM test. (f) Mice of four groups exhibited no differences in swimming speed in the MWM test. (g) Platform crossing times in the second phase, probe trial on day 6 of the MWM test. (h, i) Percentage of distance swim and time spent in the target quadrant during the probe trial of the MWM test. (j) Escape latency to the visible platform without differences among the four groups in the MWM test. ( $n = 8$  mice for each group). Data are the mean  $\pm$  S.E.M., \* $p < 0.05$ , \*\* $p < 0.01$  vs WT mice. # $p < 0.05$ , ## $p < 0.01$  vs cDKO mice.

wild-type (WT), PS cDKO (cDKO), cDKO + EA, cDKO + MCC950, and cDKO + EA + MCC950. The mice in WT and PS cDKO groups were fed normally, and the mice in cDKO + EA and cDKO + EA + MCC950 groups were given EA treatment for three consecutive weeks as describe above. MCC950 was dissolved in sterile saline. After three weeks of EA treatment, three times of intraperitoneal injection (IP) of MCC950 (20 mg/kg) with or without EA or vehicle were given once every two days. Mice were killed in the next day after the last intraperitoneal injection of MCC950. Hippocampus was dissected on ice and stored at  $-80^{\circ}\text{C}$  until being processed to analyze the protein and gene expression.

### 2.3. Behavior Analysis

**2.3.1. Novel Object Recognition (NOR) Task.** The experiment was performed as we previously described [27], and each mouse was placed in a new object recognition box ( $40\text{ cm} \times 40\text{ cm} \times 25\text{ cm}$ ) for 3 days to adapt to the environment. During the training phase, two toys with the same color and shape were placed in the experimental box, and each group of mice was allowed to explore freely for 15 min. In the tests 1 and 24 h after the training, the mice were put back in the same experimental box, and one of the familiar toys was

replaced with a new one with different colors and shapes. Mice were allowed to explore two objects freely for 15 min. Noldus software and tracking systems (Noldus, Wageningen, Netherland) were used to record and analyze behavior. The calculation of the preference index is used to evaluate recognition memory: the ratio of the time spent exploring any identical or novel object to the total time spent exploring two objects.

**2.3.2. Y-Maze.** The Y-maze consists of three identical arms ( $30\text{ cm} \times 6\text{ cm} \times 15\text{ cm}$ ), which are arranged in  $120^{\circ}$  order. In the training phase, a movable baffle is used to seal one arm of the Y-maze as a closed arm, and the other two arms are kept unblocked as a starting arm and an open arm, respectively. First, the mice were placed face to the center of the maze in the starting arm, so that the mice could explore freely in the maze for 8 min, and then the mice were taken out. After 1 h, remove the movable baffle, open the closed arm, place the mouse in the starting arm in the same way again (keep the three arms clear), let the mouse explore freely in the three arms for 8 min, take out the mouse to clean the fecal urine after the observation and record, wipe the maze with 75% alcohol, clear the residual smell, and then continue the record of the next mouse. The spatial memory ability of

mice was measured by observing and recording the time of staying in each arm and the times of entering the closed arm.

**2.3.3. Morris Water Maze (MWM).** The MWM experiment was used to measure the hippocampal-dependent spatial memory in mice, and the protocol was as described before [28]. The MWM experimental swimming pool has a diameter of 120 cm, a height of 60 cm, and a temperature of  $22 \pm 1^\circ\text{C}$ . We placed the round platform 10 cm in diameter in the center of the target quadrant and set its height 2 cm below the water surface to hide the platform position. In the training phase, the time of finding the hidden platform in 90 s was recorded for 5 consecutive days, and the position of the hidden platform in the target quadrant remained unchanged during the recording period. On day 6, the space exploration test was carried out, the platform was removed, and the mice were allowed to swim freely in the pool for 90 s. Then, the percentage of time spent in each quadrant and the swimming distance, the frequency of crossing the original position of the platform, and the swimming speed were recorded. The escape latency within 90 s was recorded at the visual platform stage on day 7 to evaluate whether the visual acuity of the mice affected the experiment.

#### 2.4. Electrophysiological Recording

**2.4.1. Slice Preparation.** The experimental scheme was as described in the previous study [29]. In short, we anesthetized the mice with ether then decapitated them. Cut the hippocampus into  $400\ \mu\text{m}$  slices and prepared with Vibroslice (Leica VT1000s, Wetzlar, Germany) in ice-cold artificial cerebrospinal fluid (ACSF). ACSF (in mM): 120 NaCl, 2.5 KCl, 2 CaCl<sub>2</sub>, 2 MgSO<sub>4</sub>, 1.2 NaH<sub>2</sub>PO<sub>4</sub>, 26 NaHCO<sub>3</sub>, and 10 D-glucose. After cutting, hippocampal slices were left inside a holding chamber with ACSF at temperature ( $33 \pm 1^\circ\text{C}$ ) for recovery for 30 min. Then, hippocampal slices maintained for 2–8 h at room temperature ( $25 \pm 1^\circ\text{C}$ ). All the solutions were saturated with 95% O<sub>2</sub>/5% CO<sub>2</sub> (vol/vol).

**2.4.2. Electrophysiology Recordings.** The slices were transferred from the holding chamber to a recording chamber with superfusion of ACSF (3 mL/min) at constant  $32\text{--}33^\circ\text{C}$ . The Schaffer collateral (SC) was stimulated with a two-concentric bipolar stimulating electrode (FHC, Bowdoinham, ME, USA) to evoke the field excitatory postsynaptic potentials (fEPSPs). Monophasic pulse (0.1 ms duration) of the constant current was used to test the stimuli at a frequency of 0.033 Hz, the intensity of which was adjusted to produce 30% of the maximum response. Axon MultiClamp 700B (Molecular Devices, Sunnyvale, CA, USA) amplifier with ACSF filled glass pipettes (1–3 M $\Omega$ ) was put in the stratum radiatum of CA1 to record stable fEPSPs at SC-CA1 synapse for 20 min. Next, high frequency stimulus (HFS, 100 Hz, 1 s) was given to induce LTP, and evoked fEPSPs were recorded for 60 min with the same intensity of the test stimulus. The strength of synaptic transmission could be determined by measuring the initial (10–60% rising phase) slope of the fEPSPs. Clampex version 10.3 software (Axon, US) was applied to get the data. LTP levels were based on the slopes of fEPSPs at an average of 50–60 min after tetanus

stimulation, which was normalized to the slopes of the last 10 min fEPSPs before tetanus stimulation.

**2.5. mRNA Analysis.** Quantitative real-time PCR (qRT-PCR) was performed as we described in the previously published paper [30]. In short, after behavioral tests, mice were sacrificed. The hippocampal tissue of mice was dissected and removed and immediately froze in liquid nitrogen. Total RNA of mice from the hippocampus was isolated by using a E.Z.N.A<sup>®</sup> Total RNA Kit (Omega Bio-Tek, Inc., Norcross, GA). To obtain cDNA, the reversed transcription of total RNA was achieved by using a PrimeScript<sup>™</sup>TMRT reagent Kit (Takara, Japan). Quantitative PCR with SYBR Green Dye Gene Expression Assays was applied to determine the gene expression by using the ABI7500 system (Applied Biosystems, Carlsbad, CA, USA). The required primers were synthesized by Shanghai Sangon Biological Engineering Technology Company (Shanghai, China). Required primers sequences were as follows: TNF- $\alpha$  (forward: 5'-GAAC TGGC AGAA GAGG CACT; reverse: 5'-AGGG TCTG GGCC ATAG AACT), IL-1 $\beta$  (forward: 5'-CAGG CAGG CAGT ATCA CTCA; reverse: 5'-AGCT CATA TGGG TCCG ACAG), ASC (forward: 5'-TCCA ACCC CTAA AACT GCGT; reverse: 5'-CACG AACT GCCT GGTA CTGT), IL-18 (forward: 5'-CTGG CTGT GACC CTCT CTGT; reverse: 5'-CTGG AACA CGTT TCTG AAAG), caspase-1 (forward: 5'-TCTC ACCG CTTC GGAC AT; reverse: 5'-ACAT CTGG GACT TCTT CG), NLRP3 (forward: 5'-AGTG GATG GGTT TGCT GGG; reverse: 5'-GCGT GTAG CGAC TGTT GAGG),  $\beta$ -actin (forward: 5'-AGCCCATGTACGTAGCCATCC; reverse: 5'-TCTCAG CTGTGGTGGTGAAG). The cycle threshold was determined for each sample as the initial increase in fluorescence above background.  $\beta$ -Actin was used as internal control for normalization.

**2.6. Western Blot Analysis.** After behavioral tests, mice were sacrificed. The hippocampal tissue of mice was dissected and removed and immediately froze in liquid nitrogen. Homogenized the frozen tissues with tissue lysate in ice-cold RIPA buffer (composition: 50 mM Tris-HCl pH 7.4, 150 mM NaCl, 1% Triton X-100, 1 mM EDTA, 1% sodium deoxycholate, 0.1% SDS, 1 mM sodium fluoride, 2 mM sodium orthovanadate) supplemented with 1 mM phenylmethane sulfonyl fluoride and inhibitors of protease and phosphatase (aprotinin, leupeptin, and pepstatin A, 10  $\mu\text{g}/\text{mL}$  for each). Centrifugation at 15,000 rpm and  $4^\circ\text{C}$  for 30 min to obtain the lysates. Electrophoresed 40  $\mu\text{g}$  proteins of tissue lysate on 10% SDS-PAGE gels, then the proteins were transferred to nitrocellulose membrane (Amersham Biosciences, Buckinghamshire, UK). The proteins on the membrane were incubated with primary antibodies at  $4^\circ\text{C}$  overnight. Washed the membranes three times and then incubated them with HRP-conjugated secondary antibodies (1:3000, Cell Signaling Technology, Danvers, MA, USA) at room temperature for 1 h. Then, a SuperSignal West Femto Kit (ThermoFisher Scientific, Waltham, MA, USA) was used to develop the membranes. Image



Quant software (Tanon, Shanghai, China) and Image J were applied to scan the films and quantified the intensities of protein bands. The relative protein levels were normalized to  $\beta$ -actin. The following primary antibodies were used in the Western blot analyses: rabbit anti-NR1 (1:1000, CST), rabbit anti-NR2A (1:1000, CST), rabbit anti-NR2B (1:1000, Abcam), mouse anti-p-tau (396) (1:1000, Santa Cruz, Biotechnology, Dallas, Texas, USA), mouse anti-p-tau (404) (1:1000, Santa Cruz), mouse anti-tau (1:1000, Santa Cruz), rabbit anti-NLRP3 (1:1000, CST), mouse anti-ASC (1:1000, Santa Cruz), mouse anti-caspase-1 (1:1000, Santa Cruz), and anti- $\beta$ -actin (1:1000, CST).

**2.7. Statistical Analysis.** All the data were presented as the mean  $\pm$  standard error of mean (S.E.M) and were analyzed by using SPSS 21.0 (Chicago, IL, USA) and GraphPad Prism version 5.0 (San Diego, CA, USA). One-way or two-way ANOVA with post hoc Bonferroni's multiple comparison tests were used to analyze the results.  $p < 0.05$  was considered statistically significant. When carrying out data analyses, the experimenters were blind to the grouping of mice.

### 3. Results

**3.1. EA Treatment Ameliorates Memory Deficits in PS cDKO Mice.** According to previous studies, 5 months old PS cDKO mice have exhibited severe impaired recognition and spatial memory [18]. Thus, NOR, Y-maze, and MWM test were performed to assess the effects of EA on impaired memory in PS cDKO mice. The experimental timeline of behavioral tests is shown in Figure 1(a). NOR is usually used to analyze the hippocampus-dependent recognition memory function. During the training session of NOR, the mice from four groups showed no difference in their preference for two same objects. After an hour, we found that PS cDKO mice spent less time exploring new objects than the WT mice in the retention test. However, EA treatment enhanced the preference degree and cognitive index of new objects in the PS cDKO mice (Figure 1(b)). Thus, our experimental results indicated that EA treatment could improve the short-term recognition memory deficits in PS cDKO mice.

The Y-maze is an effective way to measure the spatial memory ability of animals by using the nature of mice to explore new and different environments. As shown in Figures 1(c) and 1(d), we observed that PS cDKO mice displayed lower preference for new arms compared with WT mice. However, EA treatment significantly increased the duration (Figure 1(c)) and frequency (Figure 1(d)) of entering the new arm in PS cDKO mice, suggesting that EA could improve the spatial memory deficits in PS cDKO mice.

Subsequently, the MWM test were conducted to evaluate the spatial reference memory of animals. During the first phase (5 consecutive days) for training, the escape latency of PS cDKO mice was longer compared with WT mice, indicating that PS cDKO mice might spend more time finding the hidden platform. However, EA treatment significantly shortened their escape latency time in PS cDKO mice (Figure 1(e)). In the second phase (day 6), the probe trial was carried out to measure the memory retention of these

mice in the target quadrant. There were also no significant differences in their swimming velocities among four groups (Figure 1(f)). It was found that the WT group showed a strong preference in the target quadrant, but the PS cDKO group exhibited no discrimination in the distance and time occupancies among the four quadrants, and they crossed fewer times in the target quadrant comparing to other quadrants. Afterwards, PS cDKO mice with EA treatment spent longer time, crossed more times, and swam further in target quadrant. In the meantime, when comparing the duration of stay in other quadrants, there were no differences among the four groups (Figures 1(g)–1(i)). During the second phase, day 7, mice in four groups exhibited no differences in the visible platform test (Figure 1(j)), indicating that EA treatment can improve the spatial reference memory deficits of PS cDKO mice, but has no impact on their sensorimotor abilities. The above results suggest that EA treatment may have positive therapeutic effect on ameliorating impaired recognition and spatial memory in the PS cDKO mice.

**3.2. EA Treatment Improves Impaired Synaptic Plasticity in the Hippocampus of PS cDKO Mice.** Since synaptic plasticity may be one of the basic underlying mechanisms for improving ability of learning and memory, we observed the effects of EA treatment on alternation of LTP induction by determining fEPSPs at SC-CA1 synapses of PS cDKO mice. As shown in Figure 2(a), their slopes under different stimulation intensities were similar among four groups, suggesting that EA treatment had no impact on basal synaptic transmission at SC-CA1 synapse of PS cDKO mice. Likewise, the magnitude of LTP induced by HFS in PS cDKO mice was also decreased expressively in comparison with WT mice, in accordance with our previous study [27]. Interestingly, the decreased LTP magnitude induced by HFS was ameliorated by EA treatment (Figures 2(b)–2(d)). Taken together, these results manifest that EA treatment can moderate the impaired synaptic plasticity in PS cDKO mice.

The role of NMDA receptors in the LTP induction at SC-CA1 synapses in the hippocampus is well established. We next determine whether EA treatment can recover their deficiency, which are known as playing key roles in synaptic plasticity and memory of PS cDKO mice in our previous study [27]. Western blot analysis showed that expression levels of NR1, NR2A, and NR2B in the hippocampus of PS cDKO mice were decreased when compared to WT mice, while EA treatment reversed those (Figures 2(e)–2(h)). The above results suggest that EA treatment reverse the downregulation in the expression of synaptic plasticity-associated proteins involved in the neuropathology of PS cDKO mice.

**3.3. Hyperphosphorylated Tau and Neuroinflammatory Responses of PS cDKO Mice Are Reduced by EA Treatment.** Previous research has shown that tau hyperphosphorylation and neuroinflammatory responses are linked with synaptic plasticity and memory dysfunction in AD [31, 32]. Firstly, we assessed the effect of EA treatment on the expression of hyperphosphorylated tau in the hippocampus of PS cDKO mice. The Western blot analysis showed that there was obvious elevation in the expression levels of phosphorylated tau



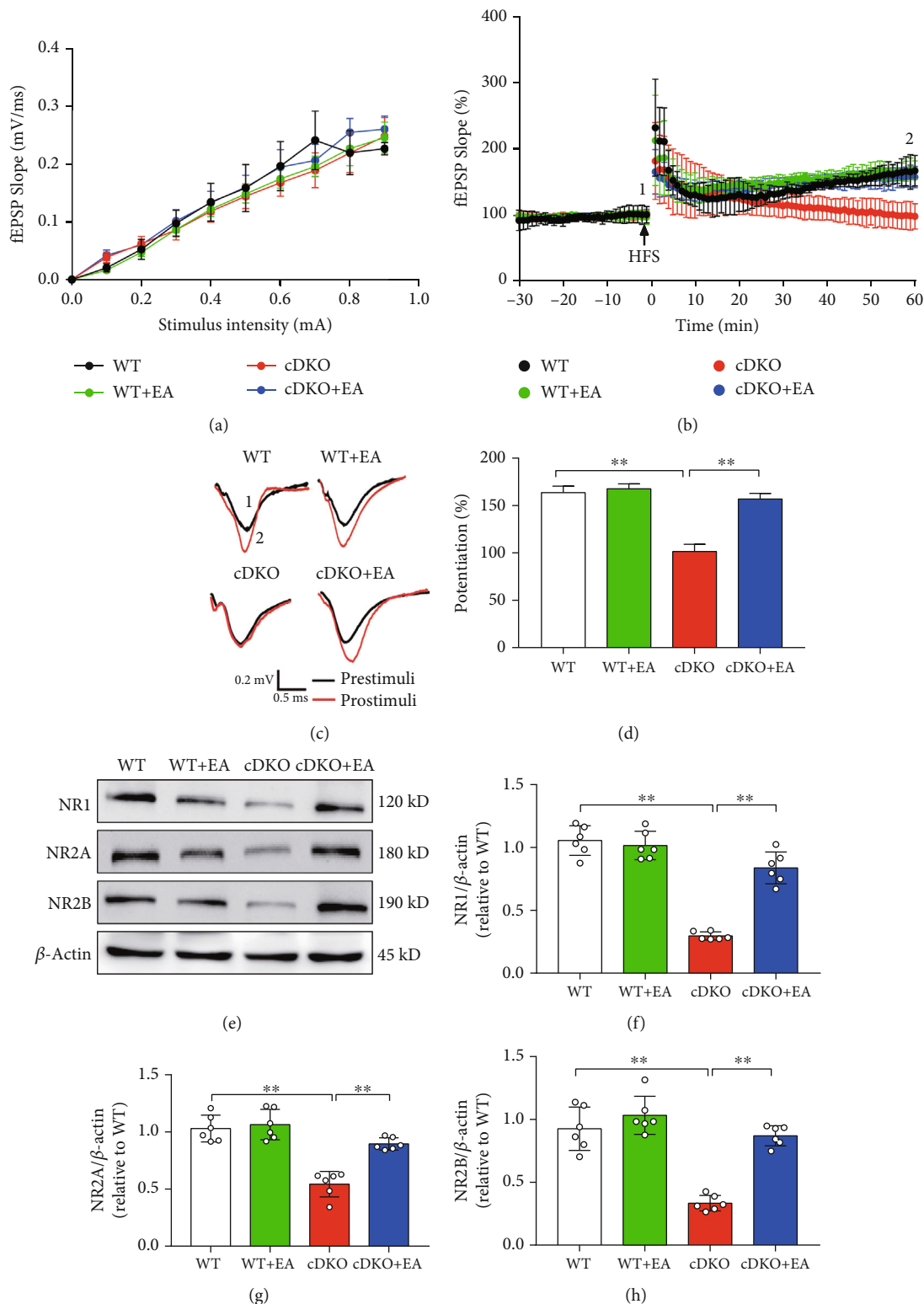


FIGURE 2: EA treatment improves impaired LTP at SC-CA1 synapses and level of NMDA receptors in the hippocampus of PS cDKO mice. (a) Quantitative data of I/O curves obtained at different stimulus intensities. (b) Normalized fEPSP slopes in SC-CA1 synapses from hippocampal slices of indicated mice. (c) Representative fEPSP traces taken before (1, black lines) and 60 min after tetanus stimulation (2, red lines) from each group. Scale bar: 0.5 mV, 10 ms. (d) Quantitative data of potentiation at 60 min after tetanus stimulation ( $n = 7$  slices from 5 mice for each group). (e) Representative Western blot of synapse-associated proteins in the hippocampus. (f)–(h) Quantification of Western blot of the synapse-associated proteins in the hippocampus ( $n = 6$  mice for each group). The levels of synapse-associated proteins were standardized based on the respective level of  $\beta$ -actin. The values were expressed as relative changes to the respective WT mice, which was set to 1. Data are the mean  $\pm$  S.E.M., \* $p < 0.05$ , \*\* $p < 0.01$ .

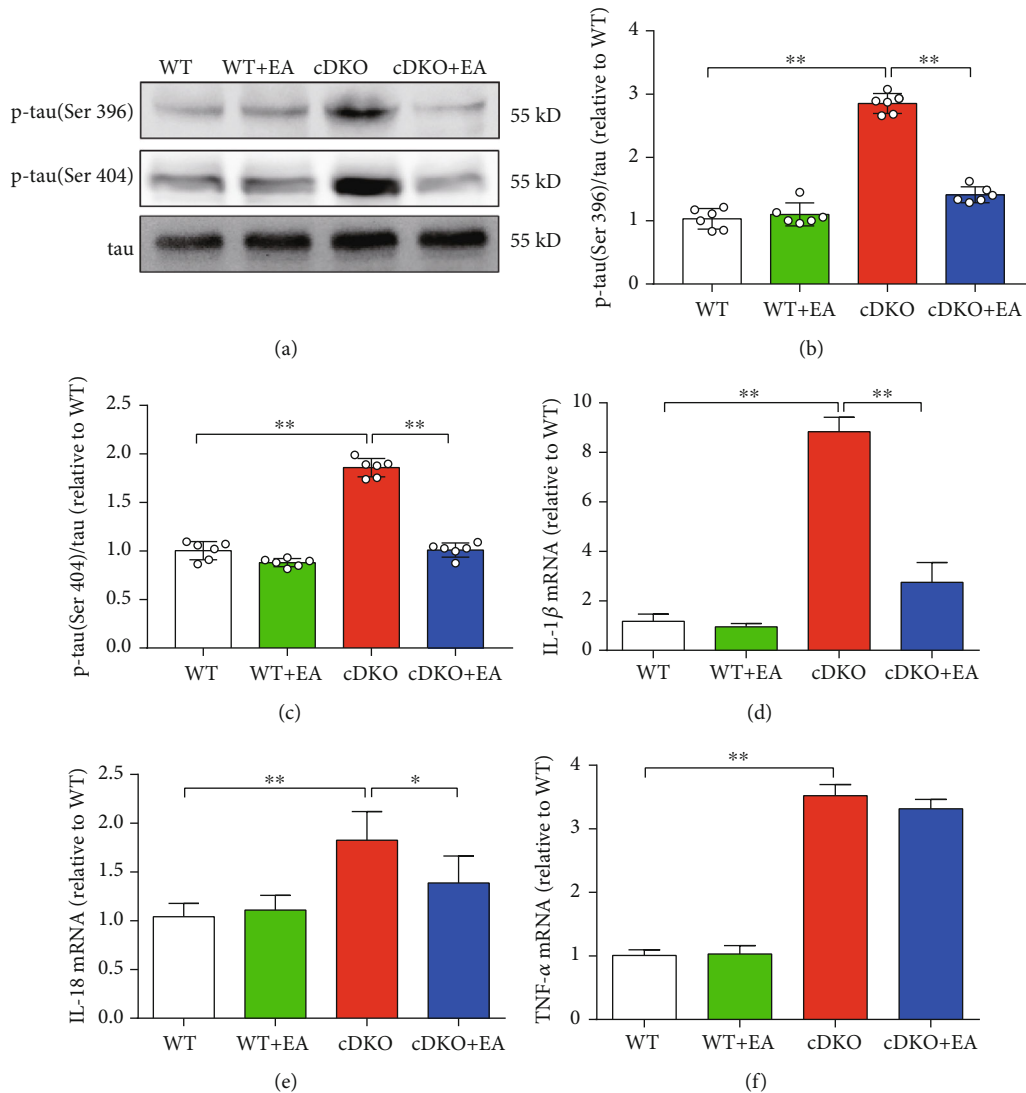


FIGURE 3: EA treatment inhibits tau hyperphosphorylation and elevated inflammatory response in the hippocampus of PS cDKO mice. (a) Representative Western blot of phosphor-tau (Ser396/Ser404) in the hippocampus. (b, c) Quantification of Western blot for p-tau in the hippocampus ( $n = 6$  mice for each group). The protein levels of p-tau were normalized with the levels of their respective total tau. The values were expressed as relative changes to the respective WT mice, which was set to 1. (d)–(f) Quantitative mRNA levels of IL-1 $\beta$ , IL-18, and TNF- $\alpha$  in the hippocampus by qRT-PCR ( $n = 5$  mice for each group). The mRNA levels were standardized based on the respective level of  $\beta$ -actin. Values were expressed as relative changes to WT mice, which was set to 1. Data are the mean  $\pm$  S.E.M., \* $p$  < 0.05, \*\* $p$  < 0.01.

(Ser396/Ser404) in the hippocampus of PS cDKO mice, which could be reversed by EA treatment (Figures 3(a)–3(c)). Moreover, we also determined the effects of EA treatment on the mRNA levels of proinflammatory cytokines in the hippocampus of PS cDKO mice, such as IL-1 $\beta$ , IL-18, and TNF- $\alpha$  by qRT-PCR analyses. The results showed that the mRNA levels of IL-1 $\beta$ , IL-18, and TNF- $\alpha$  were significantly upregulated in the hippocampus of PS cDKO mice. Notably, EA treatment could suppress the mRNA levels of IL-1 $\beta$  and IL-18 (Figures 3(d) and 3(e)), but no effect on the TNF- $\alpha$  mRNA expression (Figure 3(f)). These results above indicate that EA treatment has the ability to exert neuroprotective effects on synaptic plasticity and memory deficits in PS cDKO mice by inhibiting hyperphosphorylated tau and some proinflammatory cytokines in hippocampus.

**3.4. EA Treatment Reverses the Robust Upregulated Levels of NLRP3 Inflammasome in the Hippocampus of PS cDKO Mice.** Inflammatory corpuscles are innate immune system sensors, which can regulate the activation of microglia to induce inflammation according to risk signals. In this process, NLRP3 inflammasome is activated by double stimulations, which leads to the heterogenesis of ASC and the activation of caspase-1 [8, 9]. Here, we analyzed the mRNA expression of NLRP3, ASC, and caspase-1. The results showed that EA treatment significantly inhibited the mRNA level of these inflammasome-related proteins in the hippocampus of PS cDKO mice (Figures 4(a)–4(c)). Similarly, Western blot analysis showed that the expression of NLRP3, ASC, and caspase-1 was significantly increased in the hippocampus of PS cDKO mice, while EA

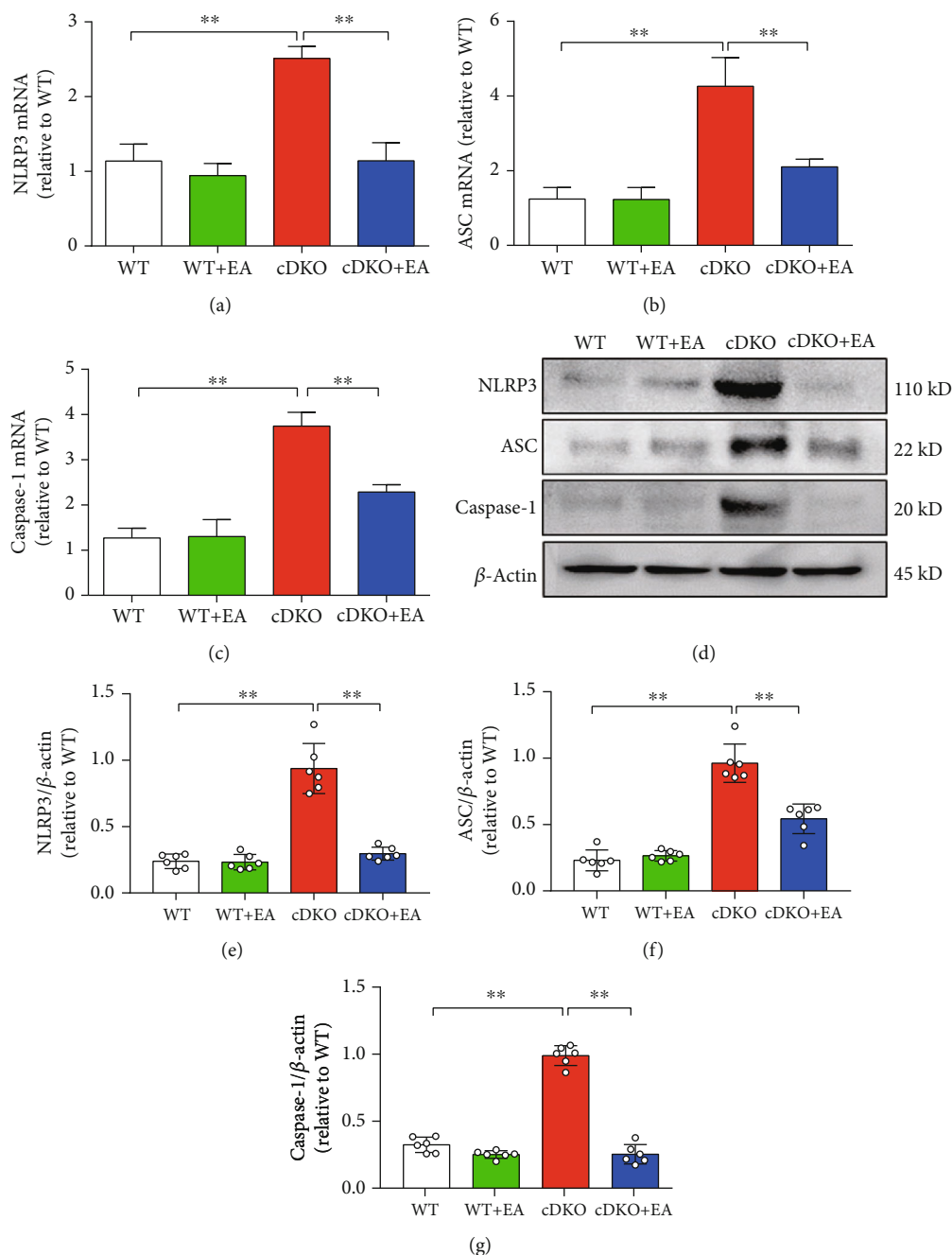


FIGURE 4: EA treatment reverses the robust upregulated levels of NLRP3 inflammasome in the hippocampus of PS cDKO mice. (a)–(c) Total RNA was isolated and subjected to quantitate the mRNA levels of NLRP3, ASC, and caspase-1 in the hip by qRT-PCR ( $n = 5$  mice for each group). The mRNA levels were standardized based on the respective level of  $\beta$ -actin. Values were expressed as relative changes to WT mice, which was set to 1. (d) Representative Western blot of NLRP3, ASC, and caspase-1 in the hippocampus. (e)–(g) Quantification of Western blot for NLRP3, ASC, and caspase-1 in the hippocampus ( $n = 6$  mice for each group). The protein levels of NLRP3, ASC, and caspase-1 were normalized with the levels of  $\beta$ -actin. The values were expressed as relative changes to the respective WT mice, which was set to 1. Data are the mean  $\pm$  S.E.M., \* $p < 0.05$ , \*\* $p < 0.01$ .

treatment significantly inhibited the expression of NLRP3 and ASC (Figures 4(d)–4(g)).

**3.5. EA Treatment Inhibits the Neuroinflammatory Response in the Hippocampus of PS cDKO Mice through Inhibiting NLRP3 Inflammasome.** In order to better understand the molecular mechanism of cognitive and memory deficits in

PS cDKO mice, we thus studied the effect of EA treatment on neuroinflammation, using MCC950, a NLRP3 inhibitor, to inhibit the expression of NLRP3 in the hippocampus of PS cDKO mice. Western blot analysis showed that the protein expression of NLRP3, ASC, and caspase-1 in the hippocampus could be significantly reduced by MCC950 treatment alone (Figures 5(a)–5(d)). Meanwhile, MCC950

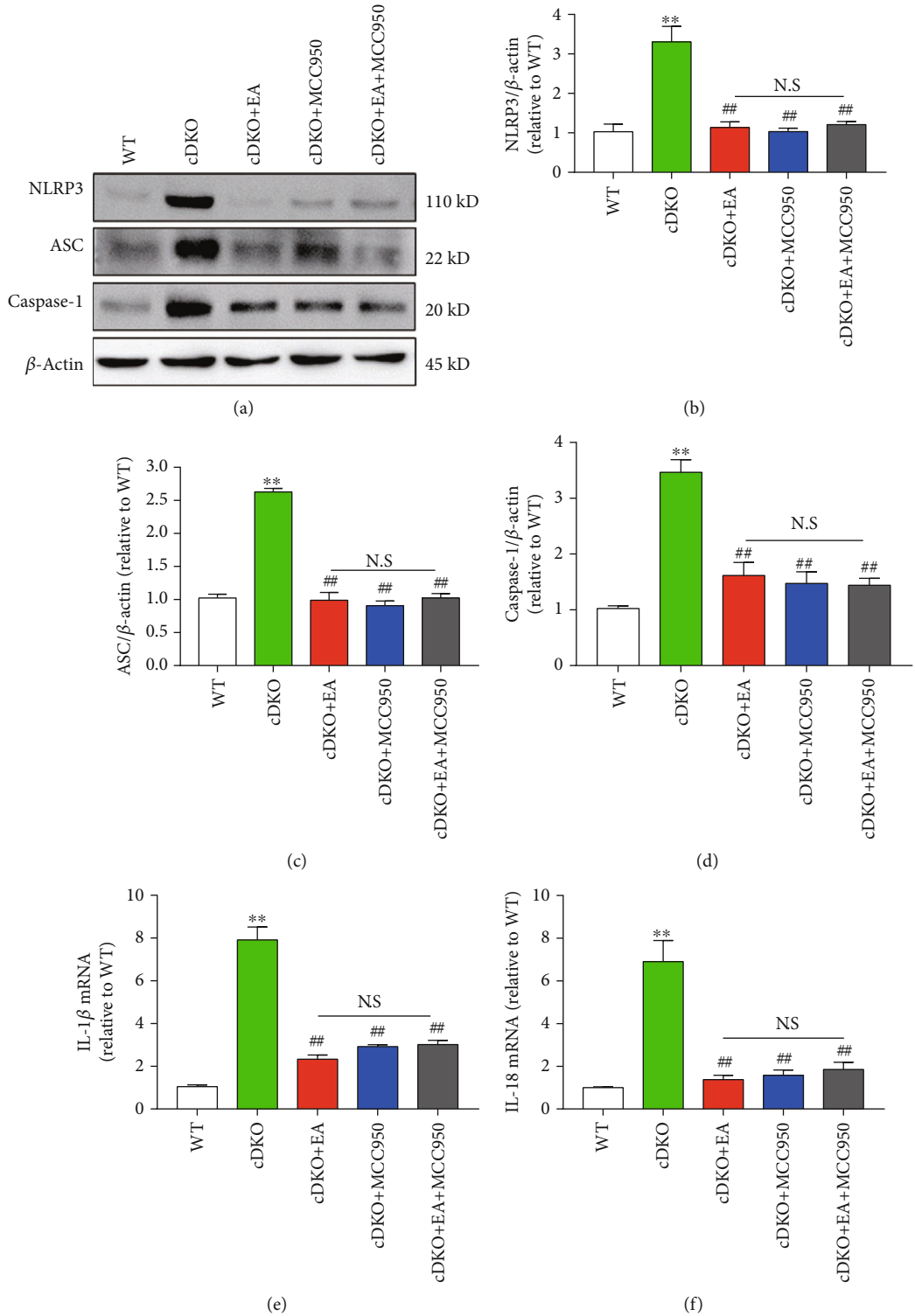


FIGURE 5: MCC950 does not further increase the effect of EA on inhibiting NLRP3 inflammasome and neuroinflammatory responses in the hippocampus of PS cDKO mice. (a) Representative Western blot of NLRP3, ASC, and caspase-1 in the hippocampus. (b)–(d) Quantitative analysis of NLRP3, ASC, and caspase-1 in the hippocampus were standardized based on the respective level of β-actin ( $n = 6$  mice for each group). (e, f) Total RNA was isolated and subjected to quantitate the mRNA levels of IL-1β and IL-18 in the hippocampus by qRT-PCR ( $n = 5$  mice for each group). The mRNA levels were standardized based on the respective level of β-actin. Values were expressed as relative changes to WT mice, which was set to 1.0. Data are the mean ± S.E.M., \* $p < 0.05$ , \*\* $p < 0.01$  vs WT mice. # $p < 0.05$ , ## $p < 0.01$  vs cDKO mice.

also significantly reduced the mRNA levels of IL-1 $\beta$  and IL-18. Strikingly, we found that EA and MCC950 treatment exhibited similar effects on the level of IL-1 $\beta$ , IL-18, NLRP3, ASC, and caspase-1 (Figures 5(a)–5(f)). In order to determine whether they work in the same way, we combined EA and MCC950 treatment for PS cDKO mice. The experimental results showed that the combined treatment did not further reduce the expression of NLRP3 (Figures 5(a)–5(d)) and the mRNA levels of IL-1 $\beta$  and IL-18 (Figure 5(e) and 5(f)) in the hippocampus of PS cDKO mice. Together, these findings provide further evidence that EA treatment may inhibit neuroinflammatory responses by blocking the NLRP3-ASC signaling pathway.

**3.6. EA Treatment Ameliorates Tau Pathology and NMDA Receptor Damage of PS cDKO Mice through Inhibiting NLRP3 Inflammasome.** To further investigate the correlation between EA treatment, NLRP3 inflammation, and AD-like phenotypes, Western blot was performed to evaluate the effects of EA, MCC950, and combination of two treatments. As shown in Figure 6, both EA treatment and MCC950 treatment alone could significantly rescue synaptic proteins in the hippocampus PS cDKO mice, including NR1, NR2A, and NR2B. In addition, the increase of phosphorylated tau levels of Ser396 and Ser404 was significantly inhibited by MCC950 or EA treatment alone. However, we found that the combined therapy did not further improve the NMDA receptor function damage in the hippocampus of PS cDKO mice (Figures 6(b)–6(d)) or further reduce the phosphorylated tau level of Ser396 and Ser404 (Figures 6(e) and 6(f)). These results further indicate that EA has the neuroprotective effect on PS cDKO mice through inhibiting NLRP3 inflammasome, reducing hyperphosphorylated tau and improving the expression of NMDA receptors.

#### 4. Discussion

In this study, we found that 3 weeks EA stimulation at GV 20 and GV 24 acupoints could effectively ameliorate the memory deficits, improve the expression of NMDA receptors and LTP induction, inhibit hyperphosphorylated tau, and robust elevated neuroinflammatory responses in the PS cDKO mice. Furthermore, EA treatment reversed the robust upregulated levels of NLRP3 inflammasome in the hippocampus of PS cDKO mice, and the MCC950 administration did not further increase the effects of EA treatment on inhibiting the upregulated levels of NLRP3 inflammasome in the hippocampus of PS cDKO mice.

Our results showed that PS cDKO mice in 5 months old exhibited significant memory deficits in NOR, Y-maze, and MWM test, which was consistent with previous studies [28, 33]. Furthermore, EA stimulation at GV 20 and GV 24 acupoints could effectively ameliorate the cognitive deficits of PS cDKO mice (Figure 1). Consistent with our result, previous study proved that EA treatment could improve learning-memory ability of the AD mice model and ameliorate post-stroke cognitive impairments via inhibition periinfarct astroglia and microglial/macrophage P2 purinoceptors-mediated neuroinflammation [34–36]. In addition, PS cDKO mice

exhibited obvious deficits in LTP induction at SC-CA1 synapses, and impaired magnitude of LTP in PS cDKO mice was ameliorated by EA treatment (Figure 2). Similarly, our previous study proved the efficacy of EA at GV 20 and GV 24 on promoting LTP induction and cognitive deficits in rat exposed to maternal separation [37]. Other studies also proved that EA stimulation could improve the spatial learning and memory of AD animal models induced by ethanol or vessel occlusion [38–40]. Clinically, EA or acupuncture therapy has been widely used to treat cognitive impairment of neurodegenerative disorders including AD and dementia [41, 42]. Both results of AD animal models and clinical practice support the efficacy of EA on treating cognitive deficits.

The ionotropic receptors of glutamate NMDA receptors are spread in postsynaptic membranes of the hippocampus, and NMDA receptor stimulation elicits the translocation of CaMKII to postsynaptic sites, where CaMKII is activated by NMDAR-triggered calcium influx and plays an important role in LTP induction and memory formation [35, 43]. In our study, Western blot analysis showed that the expression levels of NR1, NR2A, and NR2B in the hippocampus of PS cDKO mice were all increased after EA treatment (Figure 3). Similarly, our previous study has proved that these PS cDKO mice exhibited the impaired expression of NMDA receptors and dramatic decrease in the NMDAR/AMPA ratio in comparison with WT mice [27]. Consistent with our results, one recent study indicated that EA at GV 20 and GV 24 acupoints improved increased intracellular calcium concentrations regulated by the activation of NMDA receptors [44]. Taken together, these results provide further evidence that restoration of the NMDA receptors in PS cDKO mice by EA at GV 20 and GV 24, which may relate to the deficits of the cognitive function and synaptic plasticity in PS cDKO mice.

Besides of significant age-related AD-like symptoms, previous studies showed that PS cDKO mice exhibited a series of pathology, such as elevated hyperphosphorylated tau [18, 27, 33, 45]. Abnormal phosphorylation of tau, the major component of the neurofibrillary tangle, has been associated with synaptic plasticity and memory deficits in AD [32]. We found that there was an obvious hyperphosphorylation of tau at Ser396 and Ser404 in the hippocampus of PS cDKO mice, and the hyperphosphorylated tau in the hippocampus was reversed after the EA treatment (Figure 3). These results above indicate that EA treatment can protect neurons in the hippocampus of PS cDKO mice by lowering the hyperphosphorylation of tau. Consistent with our results, recent evidence suggested that EA could counteract diabetes-associated tau hyperphosphorylation in adult rat and had a possible beneficial effect on the brain cholinergic system in diabetes [46]. These results agree with our observations in this study, which suggests that EA stimulation at GV 20 and GV24 ameliorates learning and cognitive deficit in PS cDKO mice via lowering the tau pathology.

Neuroinflammation is also critical in progression of AD [47]. Except for hyperphosphorylated tau and impaired synaptic plasticity, PS cDKO mice showed the increased mRNA levels of IL-1 $\beta$  and TNF- $\alpha$  (Figure 3), which are consistent with our previous studies [27]. Strikingly, this study is the



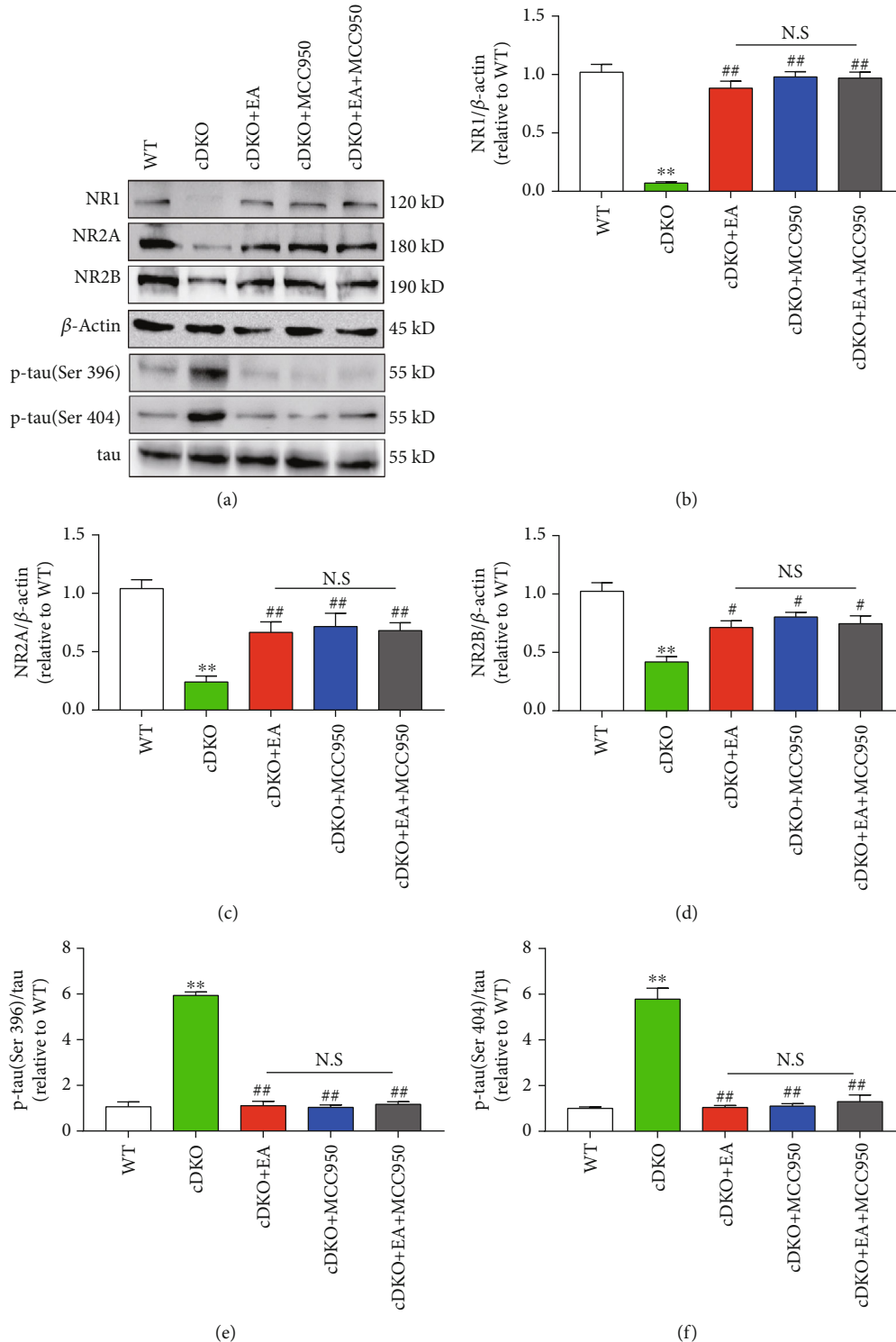


FIGURE 6: MCC950 does not further increase the effect of EA on ameliorated hyperphosphorylated tau and impaired NMDA receptors in the hippocampus of PS cDKO mice. (a) Representative Western blot of NR1, NR2A, NR2B, p-tau (Ser396), and p-tau (Ser404) in the hippocampus. (b)–(f) Quantification of NR1, NR2A, NR2B, p-tau (Ser396), and p-tau (Ser404) in the hippocampus according to the respective levels of  $\beta$ -actin or total tau ( $n = 6$  mice for each group). The values were expressed as relative changes to the respective WT mice, which was set to 1. Data are the mean  $\pm$  S.E.M., \* $p < 0.05$ , \*\* $p < 0.01$  vs WT mice. # $p < 0.05$ , ## $p < 0.01$  vs cDKO mice.

first to show that PS cDKO caused the robust to increase in the expression of NLRP3, ASC, and caspase-1 at both the protein and mRNA levels (Figure 3). Consistent with our results, the levels of NLRP3 inflammasome are substantially

elevated both in brains from AD patients [10] and several rodent AD models [10, 12, 13, 48], since previous studies have shown that NLRP3 inflammasome activation induces the cleavages of cytokine precursors to generate active IL-

1 $\beta$  and IL-18 [9]. In addition, NLRP3 inflammasome was also been found to drive the tau pathology in a recent study [13]. Therefore, it is likely that our study provides a strong correlation between hyperphosphorylated tau, neuroinflammation, and NLRP3 inflammation in PS cDKO mice, which is in accordance with accumulated evidences that NLRP3 inflammasome has been implicated in the pathogenesis of AD [49].

Meaningfully, our studies exhibited that EA treatment significantly inhibited the robust elevated levels of components and products of NLRP3 inflammasome components in PS cDKO mice (Figures 4 and 5). Specially, we provide further evidence that inhibiting NLRP3 inflammasome by MCC950 reduces the robust elevated tau, IL-1 $\beta$ , and IL-18 as well as NLRP3 components (Figures 5 and 6). Intriguingly, we found that EA at GV20 and GV24 acupoints has similar effect on NLRP3 inflammation components and neuroinflammation responses as MCC950 administration (Figures 5 and 6). In accordance with our results, other studies found that using both EA and manual acupuncture could ameliorate the upregulation of NLRP3 inflammasome as well as their synaptic and cognitive dysfunction in senescence-accelerated (SAMP8) mice [50, 51]. Furthermore, our results demonstrated that EA treatment fail to further enhance the inhibiting effect of MCC950 on NLRP3 components and products (Figures 5 and 6). Together, these results provide further support to the idea that EA suppresses the IL-1 $\beta$  and IL-18 via inhibiting the NLRP3 inflammasome. It is conceivable that the findings of this study could shed light on the mechanisms of EA therapy on the neuroinflammatory-mediated cognitive impairment in AD.

## Data Availability

The data used to support the findings of this study are available from the corresponding author upon request.

## Conflicts of Interest

The authors declare no conflicts of interest.

## Authors' Contributions

Yongjun Chen and Ying Xu designed the experiments. Kun Li, Guoqi Shi, and Jie Gao conducted the behavioral test, Western blot, EA treatment, and MCC950 administration. Yang Zhao conducted electrophysiology experiments. Yiwen Chen, Hongzhu Li, and Jiaying Zhao conducted the data analysis. Yongjun Chen and Ying Xu written the manuscript. Lin Yao helped revise the manuscript. All authors read and approved the final manuscript. Kun Li, Guoqi Shi, and Yang Zhao contributed equally to this work.

## Acknowledgments

This work was supported, in part, by the National Key R&D Program of China (2019YFC1712100 to Y Chen), Guangdong Province Universities and Colleges Pearl River Scholar Funded Scheme (China, Grant 2016 A1-AFD018181Z3903

to Y Chen), General Program of National Natural Science Foundation of China (81773927 to Y Xu), National Natural Science Foundation of China (81704168 to JY Zhao), and Science and Technology Program of Guangzhou (China, Grant to L Yao).

## References

- [1] J. Gaugler, B. James, T. Johnson, K. Scholz, and J. Weuve, "2015 Alzheimer's disease facts and figures," *Alzheimer's & dementia : the journal of the Alzheimer's Association*, vol. 11, no. 3, pp. 332–384, 2015.
- [2] P. L. McGeer, J. Rogers, and E. G. McGeer, "Inflammation, antiinflammatory agents, and Alzheimer's disease: the last 22 years," *Journal of Alzheimer's Disease*, vol. 54, no. 3, pp. 853–857, 2016.
- [3] C. Ballard et al., "Alzheimer's disease," *The Lancet*, vol. 377, no. 9770, pp. 1019–1031, 2011.
- [4] S. A. Small and K. Duff, "Linking Abeta and tau in late-onset Alzheimer's disease: a dual pathway hypothesis," *Neuron*, vol. 60, no. 4, pp. 534–542, 2008.
- [5] F. L. Heppner, R. M. Ransohoff, and B. Becher, "Immune attack: the role of inflammation in Alzheimer disease," *Nature Reviews Neuroscience*, vol. 16, no. 6, pp. 358–372, 2015.
- [6] T. Wyss-Coray, "Inflammation in Alzheimer disease: driving force, bystander or beneficial response?," *Nature Medicine*, vol. 12, no. 9, pp. 1005–1015, 2006.
- [7] B. A. In'T Veld, A. Ruitenber, A. Hofman et al., "Nonsteroidal antiinflammatory drugs and the risk of Alzheimer's disease," *The New England Journal of Medicine*, vol. 345, no. 21, pp. 1515–1521, 2001.
- [8] M. S. J. Mangan, E. J. Olhava, W. R. Roush, H. M. Seidel, G. D. Glick, and E. Latz, "Targeting the NLRP3 inflammasome in inflammatory diseases," *Drug Discovery*, vol. 17, no. 8, pp. 588–606, 2018.
- [9] M. T. Heneka, R. M. McManus, and E. Latz, "Inflammasome signalling in brain function and neurodegenerative disease," *Nature Reviews Neuroscience*, vol. 19, no. 10, pp. 610–621, 2018.
- [10] M. T. Heneka, M. P. Kummer, A. Stutz et al., "NLRP3 is activated in Alzheimer's disease and contributes to pathology in APP/PS1 mice," *Nature*, vol. 493, no. 7434, pp. 674–678, 2013.
- [11] O. Qazi, P. T. Parthasarathy, R. Lockey, and N. Kolliputi, "Can microRNAs keep inflammasomes in check?," *Frontiers in Genetics*, vol. 4, p. 30, 2013.
- [12] C. Venegas, S. Kumar, B. S. Franklin et al., "Microglia-derived ASC specks cross-seed amyloid- $\beta$  in Alzheimer's disease," *Nature*, vol. 552, no. 7685, pp. 355–361, 2017.
- [13] C. Ising, C. Venegas, S. Zhang et al., "NLRP3 inflammasome activation drives tau pathology," *Nature*, vol. 575, no. 7784, pp. 669–673, 2019.
- [14] T. Li, G. Ma, H. Cai, D. L. Price, and P. C. Wong, "Nicastrin is required for assembly of presenilin/gamma-secretase complexes to mediate Notch signaling and for processing and trafficking of beta-amyloid precursor protein in mammals," *The Journal of Neuroscience*, vol. 23, no. 8, pp. 3272–3277, 2003.
- [15] C. Czech, G. Tremp, and L. Pradier, "Presenilins and Alzheimer's disease: biological functions and pathogenic mechanisms," *Progress in Neurobiology*, vol. 60, no. 4, pp. 363–384, 2000.

- [16] R. Feng, C. Rampon, Y. P. Tang et al., "Deficient neurogenesis in forebrain-specific presenilin-1 knockout mice is associated with reduced clearance of hippocampal memory traces," *Neuron*, vol. 32, no. 5, pp. 911–926, 2001.
- [17] D. B. Donoviel, A. K. Hadjantonakis, M. Ikeda, H. Zheng, P. S. G. Hyslop, and A. Bernstein, "Mice lacking both presenilin genes exhibit early embryonic patterning defects," *Genes & Development*, vol. 13, no. 21, pp. 2801–2810, 1999.
- [18] C. A. Saura, S. Y. Choi, V. Beglopoulos et al., "Loss of presenilin function causes impairments of memory and synaptic plasticity followed by age-dependent neurodegeneration," *Neuron*, vol. 42, no. 1, pp. 23–36, 2004.
- [19] R. Feng, H. Wang, J. Wang, D. Shrom, X. Zeng, and J. Z. Tsien, "Forebrain degeneration and ventricle enlargement caused by double knockout of Alzheimer's presenilin-1 and presenilin-2," *Proceedings of the National Academy of Sciences of the United States of America*, vol. 101, no. 21, pp. 8162–8167, 2004.
- [20] X. Jiang, D. Zhang, J. Shi, Y. Chen, P. Zhang, and B. Mei, "Increased inflammatory response both in brain and in periphery in presenilin 1 and presenilin 2 conditional double knock-out mice," *Journal of Alzheimer's Disease*, vol. 18, no. 3, pp. 515–523, 2009.
- [21] B. Lee, B. Sur, J. Shim, D.-H. Hahm, and H. Lee, "Acupuncture stimulation improves scopolamine-induced cognitive impairment via activation of cholinergic system and regulation of BDNF and CREB expressions in rats," *BMC Complementary and Alternative Medicine*, vol. 14, no. 1, p. 338, 2014.
- [22] Q. Zhang, Y. N. Li, Y. Y. Guo et al., "Effects of preconditioning of electro-acupuncture on postoperative cognitive dysfunction in elderly: a prospective, randomized, controlled trial," *Medicine*, vol. 96, no. 26, article e7375, 2017.
- [23] Q. Liu, B. Li, H. Y. Zhu, Y. Q. Wang, J. Yu, and G. C. Wu, "Glia atrophy in the hippocampus of chronic unpredictable stress-induced depression model rats is reversed by electroacupuncture treatment," *Journal of Affective Disorders*, vol. 128, no. 3, pp. 309–313, 2011.
- [24] X. Zhang, Y. Song, T. Bao et al., "Antidepressant-like effects of acupuncture involved the ERK signaling pathway in rats," *BMC Complementary and Alternative Medicine*, vol. 16, no. 1, p. 380, 2016.
- [25] Y. Lie, *Skill with Illustrations of Chinese Acupuncture and Moxibustion*, Hunan Science and Technology Press, Changsha, China, 1992.
- [26] Y. Zheng, J. He, L. Guo et al., "Transcriptome analysis on maternal separation rats with depression-related manifestations ameliorated by electroacupuncture," *Frontiers in Neuroscience*, vol. 13, p. 314, 2019.
- [27] Y. Zhao, H. Deng, K. Li et al., "Trans-cinnamaldehyde improves neuroinflammation-mediated NMDA receptor dysfunction and memory deficits through blocking NF- $\kappa$ B pathway in presenilin1/2 conditional double knockout mice," *Brain, Behavior, and Immunity*, vol. 82, pp. 45–62, 2019.
- [28] L. Zhang, Z. Zhang, Y. Fu et al., "Trans-cinnamaldehyde improves memory impairment by blocking microglial activation through the destabilization of iNOS mRNA in mice challenged with lipopolysaccharide," *Neuropharmacology*, vol. 110, Part A, pp. 503–518, 2016.
- [29] Y.-J. Chen, M. Zhang, D. M. Yin et al., "ErbB4 in parvalbumin-positive interneurons is critical for neuregulin 1 regulation of long-term potentiation," *Proceedings of the National Academy of Sciences of the United States of America*, vol. 107, no. 50, pp. 21818–21823, 2010.
- [30] L. Yao, A. Bhatta, Z. Xu et al., "Obesity-induced vascular inflammation involves elevated arginase activity," *Regulatory, Integrative and Comparative Physiology*, vol. 313, no. 5, pp. R560–R571, 2017.
- [31] M. T. Heneka, M. J. Carson, J. E. Khoury et al., "Neuroinflammation in Alzheimer's disease," *The Lancet Neurology*, vol. 14, no. 4, pp. 388–405, 2015.
- [32] T. L. Spire-Jones, W. H. Stoothoff, A. de Calignon, P. B. Jones, and B. T. Hyman, "Tau pathophysiology in neurodegeneration: a tangled issue," *Trends in Neurosciences*, vol. 32, no. 3, pp. 150–159, 2009.
- [33] Q. Chen, A. Nakajima, S. H. Choi, X. Xiong, and Y. P. Tang, "Loss of presenilin function causes Alzheimer's disease-like neurodegeneration in the mouse," *Journal of Neuroscience Research*, vol. 86, no. 7, pp. 1615–1625, 2008.
- [34] R. G. M. Morris, P. Garrud, J. N. P. Rawlins, and J. O'Keefe, "Place navigation impaired in rats with hippocampal lesions," *Nature*, vol. 297, no. 5868, pp. 681–683, 1982.
- [35] T. V. P. Bliss and G. L. Collingridge, "A synaptic model of memory: long-term potentiation in the hippocampus," *Nature*, vol. 361, no. 6407, pp. 31–39, 1993.
- [36] J. Jiang, K. Gao, Y. Zhou et al., "Electroacupuncture Treatment Improves Learning-Memory Ability and Brain Glucose Metabolism in a Mouse Model of Alzheimer's Disease: Using Morris Water Maze and Micro-PET," *Evidence-Based Complementary and Alternative Medicine*, vol. 2015, Article ID 142129, 7 pages, 2015.
- [37] L. Guo, X. Liang, Z. Liang et al., "Electroacupuncture ameliorates cognitive deficit and improves hippocampal synaptic plasticity in adult rat with neonatal maternal separation," *Evidence-Based Complementary and Alternative Medicine*, vol. 2018, Article ID 2468105, 9 pages, 2018.
- [38] B. Lu, Z. Ma, F. Cheng et al., "Effects of electroacupuncture on ethanol-induced impairments of spatial learning and memory and Fos expression in the hippocampus in rats," *Neuroscience Letters*, vol. 576, pp. 62–67, 2014.
- [39] Y. Ye, H. Li, J. W. Yang et al., "Acupuncture attenuated vascular dementia-induced hippocampal long-term potentiation impairments via activation of D1/D5 receptors," *Stroke*, vol. 48, no. 4, pp. 1044–1051, 2017.
- [40] Y. She, J. Xu, Y. Duan et al., "Possible antidepressant effects and mechanism of electroacupuncture in behaviors and hippocampal synaptic plasticity in a depression rat model," *Brain Research*, vol. 1629, pp. 291–297, 2015.
- [41] X.-W. Fan, H. H. Liu, H. B. Wang et al., "Electroacupuncture improves cognitive function and hippocampal neurogenesis after brain irradiation," *Radiation Research*, vol. 187, no. 6, pp. 672–681, 2017.
- [42] S. Wang, H. Yang, J. Zhang et al., "Efficacy and safety assessment of acupuncture and nimodipine to treat mild cognitive impairment after cerebral infarction: a randomized controlled trial," *BMC Complementary and Alternative Medicine*, vol. 16, no. 1, p. 361, 2016.
- [43] J. Lisman, H. Schulman, and H. Cline, "The molecular basis of CaMKII function in synaptic and behavioural memory," *Nature Reviews Neuroscience*, vol. 3, no. 3, pp. 175–190, 2002.
- [44] Z. Wang, B. Lin, W. Liu et al., "Electroacupuncture ameliorates learning and memory deficits via hippocampal 5-HT<sub>1A</sub> receptors and the PKA signaling pathway in rats with ischemic stroke," *Metabolic Brain Disease*, vol. 35, no. 3, pp. 549–558, 2020.

- [45] A. Takashima, M. Murayama, O. Murayama et al., "Presenilin 1 associates with glycogen synthase kinase-3beta and its substrate tau," *Proceedings of the National Academy of Sciences of the United States of America*, vol. 95, no. 16, pp. 9637–9641, 1998.
- [46] M. L. Rocco, A. Pristerà, L. Pistillo, L. Aloe, N. Canu, and L. Manni, "Brain cholinergic markers and tau phosphorylation are altered in experimental type 1 diabetes: normalization by electroacupuncture," *Journal of Alzheimer's Disease*, vol. 33, no. 3, pp. 767–773, 2013.
- [47] C. Ising and M. T. Heneka, "Functional and structural damage of neurons by innate immune mechanisms during neurodegeneration," *Cell Death & Disease*, vol. 9, no. 2, p. 120, 2018.
- [48] A. Halle, V. Hornung, G. C. Petzold et al., "The NALP3 inflammasome is involved in the innate immune response to amyloid-beta," *Nature Immunology*, vol. 9, no. 8, pp. 857–865, 2008.
- [49] M. Saresella, F. La Rosa, F. Piancone et al., "The NLRP3 and NLRP1 inflammasomes are activated in Alzheimer's disease," *Molecular Neurodegeneration*, vol. 11, no. 1, p. 23, 2016.
- [50] J. Jiang, N. Ding, K. Wang, and Z. Li, "Electroacupuncture Could Influence the Expression of IL-1 $\beta$  and NLRP3 Inflammasome in Hippocampus of Alzheimer's Disease Animal Model," *Evidence-Based Complementary and Alternative Medicine*, vol. 2018, Article ID 8296824, 7 pages, 2018.
- [51] N. Ding, J. Jiang, M. Lu et al., "Manual acupuncture suppresses the expression of proinflammatory proteins associated with the NLRP3 Inflammasome in the Hippocampus of SAMP8 mice," *Evidence-based Complementary and Alternative Medicine*, vol. 2017, Article ID 3435891, 8 pages, 2017.

## Research Article

# Transcutaneous Electrical Acupoint Stimulation in Early Life Changes Synaptic Plasticity and Improves Symptoms in a Valproic Acid-Induced Rat Model of Autism

Xiaoxi Wang<sup>1,2,3</sup>, Rui Ding<sup>4</sup>, Yayue Song<sup>5</sup>, Juan Wang<sup>4</sup>, Chen Zhang<sup>6</sup>, Songping Han<sup>7</sup>, Jisheng Han<sup>1,2,3</sup> and Rong Zhang<sup>1,2,3,8</sup>

<sup>1</sup>Department of Neurobiology, School of Basic Medical Sciences, Peking University, Beijing, China

<sup>2</sup>Neuroscience Research Institute, Peking University, Beijing, China

<sup>3</sup>Key laboratory for Neuroscience, Ministry of Education/National Health and Family Planning Commission, Peking University, Beijing, China

<sup>4</sup>Department of Bioinformatics, School of Basic Medical Sciences, Peking University, Beijing, China

<sup>5</sup>School of Basic Medical Sciences, Tianjin Medical University, Tianjin, China

<sup>6</sup>Department of Neurobiology, School of Basic Medical Sciences, Beijing Key Laboratory of Neural Regeneration and Repair, Advanced Innovation Center for Human Brain Protection, Capital Medical University, Beijing, China

<sup>7</sup>Wuxi HANS Health Medical Technology Co., Ltd., Wuxi, China

<sup>8</sup>Department of Integration of Chinese and Western Medicine, School of Basic Medical Sciences, Peking University, Beijing 100191, China

Correspondence should be addressed to Jisheng Han; [hanjisheng@bjmu.edu.cn](mailto:hanjisheng@bjmu.edu.cn) and Rong Zhang; [zhangrong@bjmu.edu.cn](mailto:zhangrong@bjmu.edu.cn)

Received 14 September 2020; Accepted 12 December 2020; Published 30 December 2020

Academic Editor: Lu Wang

Copyright © 2020 Xiaoxi Wang et al. This is an open access article distributed under the Creative Commons Attribution License, which permits unrestricted use, distribution, and reproduction in any medium, provided the original work is properly cited.

Autism spectrum disorder (ASD) is a developmental disorder characterized by social behavior deficit in childhood without satisfactory medical intervention. Transcutaneous electrical acupoint stimulation (TEAS) is a noninvasive technique derived from acupuncture and has been shown to have similar therapeutic effects in many diseases. Valproic acid- (VPA-) induced ASD is a known model of ASD in rats. The therapeutic efficacy of TEAS was evaluated in the VPA model of ASD in the present study. The offspring of a VPA-treated rat received TEAS in the early life stage followed by a series of examinations conducted in their adolescence. The results show that following TEAS treatment in early life, the social and cognitive ability in adolescence of the offspring of a VPA rat were significantly improved. In addition, the abnormal pain threshold was significantly corrected. Additional studies demonstrated that the dendritic spine density of the primary sensory cortex was decreased with Golgi staining. Results of the transcriptomic study showed that expression of some transcription factors such as the neurotrophic factor were downregulated in the hypothalamus of the VPA model of ASD. The reduced gene expression was reversed following TEAS. These results suggest that TEAS in the early life stage may mitigate disorders of social and recognition ability and normalize the pain threshold of the ASD rat model. The mechanism involved may be related to improvement of synaptic plasticity.

## 1. Introduction

Autism spectrum disorder (ASD) is a developmental disorder. The core symptoms include social and communication deficits and stereotypic behavior. Together with its core symptoms, ASD patients also suffer from a lot of other cooccurring problems, especially hyperactivity or hyporeactiv-

ity to sensory inputs and intellectual disability [1]. In the past few decades, the prevalence of ASD has increased dramatically. It is higher in boys than in girls, with an estimated ratio of 4 : 1 [2]. In DSM-V, the diagnostic criteria for perception appeared for the first time. As an earlier study reported, 90% of ASD children had an abnormal response to sensory stimulation [3]. Several studies have strongly implicated that



an abnormal response to perception was one of the most obvious characteristics to distinguish ASD from other children with developmental disabilities [4–6]. Unfortunately, the etiology of ASD is still unclear, and the medical therapy is often one used to treat some associated symptoms, such as irritability and comorbidities [7]. Among the available methods for the treatment of ASD, rehabilitation training is most widely used for ASD intervention [7, 8]. But rehabilitation training often puts a heavy economic burden on families and society [9]. Besides, rehabilitation training has limitations, especially for infants with ASD [10].

The hypothesis for ASD pathogenesis mainly focuses on genetics and environment [11]. The molecular and cellular mechanisms mainly involve structural and functional abnormalities of the brain and synaptic plasticity abnormalities. Synapse generation and maturation is one of the key links in the development of brain neural circuits. In the early life stage, the number of dendritic spines increases rapidly. After reaching a peak, the density of dendritic spines in the brain stops increasing and gradually decreases, which is called “spine pruning” [12–14]. Spine pruning is considered to be related to neural circuit refinement which may be related to the pathogenesis of ASD [15]. In previous studies, dendritic spine density of ASD elder patients was significantly higher than that of the control [15–17].

Some evidence indicates that there is a relationship between the modulatory functions of the endocrine system and social behavior [18, 19]. As a part of the endocrine system, the hypothalamus can release a variety of neurotransmitters, such as oxytocin (OXT) and arginine-vasopressin (AVP). Because OXT and AVP were beneficial for regulating socio-emotional responses, they have attracted great interest for their critical implications for ASD [20–22]. Furthermore, the hypothalamus can also improve the emotional behavior by gut/axis and microbiota [23]. So, we pay more attention to hypothalamus in our current etiology study for ASD.

Acupuncture appears to be effective for treating many diseases and/or disorders by regulating the functions of the autonomic nervous system. Some research suggests that acupuncture could help ASD children to relieve their symptoms [24–26]. Moreover, meta-analysis results show that acupuncture could help ASD children reduce their Childhood Autism Rating Scale (CARS) and their Autism Behavior Checklist (ABC) score [27]. Transcutaneous electrical acupoint (TEAS) combines traditional acupuncture therapy with transcutaneous electrical nerve stimulation, which can produce effects similar to acupuncture [28].

Because TEAS is noninvasive stimulation, it is easier for children to accept. Consistent with our study, previous work in our lab also showed that TEAS would reduce part of ASD children’s CARS and ABC total score, thereby improving their condition [29]. This previous study also demonstrated that TEAS simultaneously improved plasma levels of oxytocin and arginine-vasopressin [29]. Results in an animal study also done in our lab were similar to our clinical studies, showing that electro-acupuncture improved the social interaction behavior of rats [30].

However, few investigations have focused on the effect and mechanism of TEAS in early life. In this study, we use

an autistic rat model to study the behavioral effect of TEAS in the early life stage and its influence on transcriptomics and synapse plasticity.

## 2. Material and Method

Male and female Wistar rats (270 g–350 g) were obtained from the Department of Experimental Animal Sciences, Peking University Health Science Center. Animals were housed individually with access to food and water. The humidity was  $50\% \pm 10\%$ , and temperature was  $23 \pm 2^\circ\text{C}$ . The animals were maintained with a 12–12 h light-dark cycle. This study was carried out following USA National Institutes of Health Guide for the Care and Use of Laboratory Animals. The protocol was approved by Peking University Animal Care and Use Committee (ethics approval ID, LA2015204).

Female and male rats were placed in the same cage to mate overnight. The day was considered embryonic day 0.5 (E0.5) in the presence of a vaginal plug. The pregnant rats were randomly divided into two groups: VPA group and control (NS-control) group. In the VPA group, pregnant rats were intraperitoneally injected with VPA (Sigma: P4543, diluted with normal saline to a concentration of 200 mg/ml) at a dose of 450 mg/kg at embryonic day 12.5 (E12.5). The pregnant rats in the control group received the same concentration of normal saline at E12.5. After weaning at postnatal day 21 (PND21), offspring of the same sex were housed separately with 2–6 per cage.

On the postnatal day of 7th (PND7), the offspring of the VPA group were randomly divided into two groups: sham group (VPA-sham) and TEAS group (VPA-TEAS). The VPA-TEAS group was given transcutaneous electrical acupoint stimulation (JS-502-A manufactured at Wuxi HANS Health Medical Technology Company, Wuxi), with 6 mm electrodes attached on the acupoint of Zusanli (Figure 1(b)). TEAS duration was 7 days, from PND7 to PND13. Each day treatment duration was 30 minutes (Figure 1(a)). The current intensity of PND7 was 2 mA, PND8–10 was 3 mA, and PND11–13 was 4 mA. To be consistent with our previous clinical study, we chose 2/15 Hz as frequency (pulse width: 0.6 ms in 2 Hz and 0.4 ms in 15 Hz, each lasting for 3 s) [29].

The electrode was attached to the VPA-sham group on the same acupoint but without electrical stimulation. During stimulation, all of the offspring were placed in a clear plastic chamber, and a  $37^\circ\text{C}$  heating pad was placed under the box to maintain their body temperature.

### 2.1. Behavior Test

*2.2. Developmental Milestone and Pup Separation-Induced Ultrasonic Vocalization Test.* The developmental milestones of offspring were tested beginning from postnatal days 7 to 21 (PND7–21). The parameters of physical developmental milestones included body weight and eye-opening. A pup separation-induced ultrasonic vocalization (USV) test was performed on postnatal days 7 (PND7) and 13 (PND13). A pup was randomly chosen and gently removed from the home cage and then transported to a clear plastic chamber

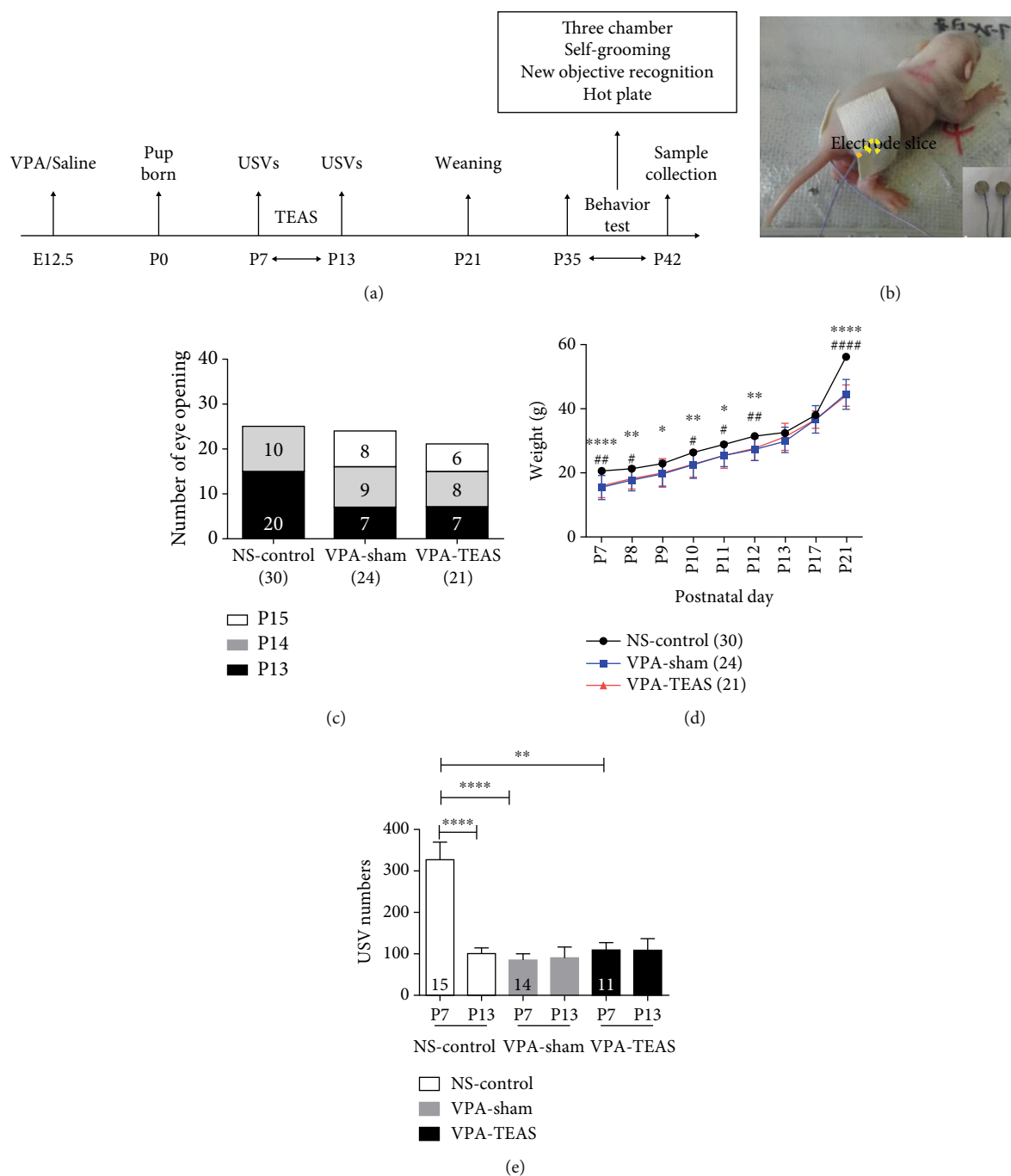


FIGURE 1: TEAS on PND7-PND13 did not improve the development and USVs of VPA-induced offspring. (a) Experimental design of TEAS intervention and behavior tests. (b) The photo is the offspring receiving TEAS. (c) The number of pups with eye-opened on certain days (two-way ANOVA, NS-control  $n = 30$ , VPA-sham  $n = 24$ , VPA-TEAS  $n = 21$ ). (d) Body weight of pups from PND2 to PND21 (one-way ANOVA, NS-control  $n = 30$ , VPA-sham  $n = 24$ , VPA-TEAS  $n = 21$ ). (e) Total USV numbers (PND7 vs. PND13: paired  $t$ -test, NS-control vs. VPA-sham vs. VPA-TEAS: one-way ANOVA, NS-control  $n = 15$ , VPA-sham  $n = 14$ , VPA-TEAS  $n = 11$ ). Data are presented as the mean  $\pm$  SEM. \* $P < 0.05$ , \*\* $P < 0.01$ , \*\*\* $P < 0.001$ ; NS-control vs. VPA-TEAS, # $P < 0.05$ , ## $P < 0.01$ .

(39 cm  $\times$  25 cm  $\times$  20 cm) on a heating pad (37°C) in a separate room. The USVs were recorded for 5 min by a condenser microphone (CM16/CPMA, Avisoft Bioacoustics, Germany) which hung 25 cm above the cage floor (AUSG-116H, Avisoft Bioacoustics, Germany). The sampling rate was set at 250 kHz. The connected amplifier (AUSG-116H, Avisoft Bioacoustics, Berlin, Germany) was set at a sampling rate of

250 kHz with a 125 kHz low-pass filter [31]. The USV data were analyzed by Avisoft SASLab Pro (Version 4.52).

**2.2.1. Three-Chamber Test.** A three-chamber test was performed on postnatal days 35-42 (PND35-42) during the dark cycle [30]. The apparatus for testing was a rectangular Plexiglas box, which was divided into three chambers

(40 cm × 34 cm × 24 cm), with the side chambers each connected to the middle chamber by a corridor (10 cm × 10 cm × 15 cm). The test included three stages: adaptive stage, stage 1 (social preference), and stage 2 (social novelty).

During the adaptive stage, the subject rat was allowed to explore the entire apparatus freely for 5 min. During stage 1, a weight and sex-matched unfamiliar model rat was retained in a small cage as a social stimulus and then placed in one of the side chambers. Then, an identical empty cage was placed on the other side of the chamber. The subject rat was allowed to explore the entire apparatus freely with the corridors open to allow interaction with the model rat and empty cage for 10 min. The social preference index was calculated as:  $(\text{time in stranger side} - \text{time in empty cage side}) / (\text{time in stranger side} + \text{time in empty cage side})$  [32].

During stage 2, another weight and sex-matched unfamiliar model rat was placed in the empty cage as a novel social stimulus. The subject rat was also allowed to explore the entire apparatus and interact with the familiar and novel model rats for 10 min. The social novelty index was calculated as:  $(\text{time in new stranger side} - \text{time in familiar stranger side}) / (\text{time in new stranger side} + \text{time in familiar stranger side})$ . The entire apparatus was cleaned with 75% ethanol after each trial was completed to eliminate the impact of residual rat odors.

**2.2.2. Self-Grooming Test.** The self-grooming test is a paradigm which measures the level of stereotyped behavior of rodents. During the dark period under dim red illumination, the subject rat was placed into an empty cage (39 cm × 25 cm × 20 cm), which was similar to the home cage, and encouraged to explore it for 10 min. In this study, self-grooming behaviors included (1) wiping the nose, face, head, and ears with forepaws and (2) licking the body, anogenital area, and tail [33]. The test consisted of a 10 min habituation and a following 10 min test. The test stage was videotaped, and the duration of self-grooming was analyzed.

**2.2.3. Novel Object Recognition Test.** Learning and memory ability were evaluated by a novel object recognition test during the dark period under dim red illumination. A subject rat was placed in the test arena (60 cm × 40 cm × 40 cm) for 10 min of habituation on the first and second day. The training stage was on the third day. During the training stage, the rat was allowed to explore two identical objects in the arena for 20 min. 1 hour after training stage, the test stage started. One of the two objects would be replaced by a new object (with a similar size but with different colors and shapes). The rat was placed into the arena again to allow the animal to explore freely for 10 min and videotaped. The sniffing time for each of the two objects was determined by an observer blinded to the treatment group. Object exploration behavior was defined as the nose of the rat touching the object or being oriented toward the object within 2 cm.

**2.2.4. Hot Plate Test.** The thermal nociception threshold was examined by a hot plate test. A solid aluminum plate was used for heating and maintaining a constant temperature. A

Perspex cylinder which was transparent and removable was used. The temperature of the hot plate was set at 3 levels: 50°C, 53°C, and 56°C. After a rat was placed on the hot plate, the latent period was recorded for any of the behaviors: licking or lifting paws or jumping off the hot plate at each temperature. The paw withdrawal latency was intended to reflect the nociception threshold. A cut-off time of 60 s was set to avoid tissue damage. The subject rat was tested three times with 15 min intervals, and the mean of three recordings was the final result.

**2.3. Golgi Staining.** After the behavior tests, Golgi staining was used to evaluate neuron development of rats by the Hito Golgi-Cox OptimStain™ kit (HTKNS1125, Hitobiotec). Solution 1 and solution 2 of the kit were mixed in equal volumes at room temperature in a dark place 24 h before the experiment. The brain was removed and transferred into the mixed solution and remained for 2 weeks at room temperature in the dark. The brain tissue was transferred into solution 3 at 4°C for 24–72 h in the dark. After immersion in solution 3, the brain was frozen at 60°C. Coronal sections (150 μm) were prepared with a freezing microtome (Leica-1950, Germany). The sections were stained using solutions 4 and 5 after mounting the sections onto the slides with gelatin. Finally, the stained sections were imaged using a confocal microscope (TCS-SP8 STED 3X, Leica, Germany) equipped with a 40x oil immersion. Images were analyzed using the Fiji/Image J. For each rat, nine different neurons were quantified from three slides. The spine density from the three neuron segments (70 μm) was averaged to provide a single value for each type of neuron.

## 2.4. Transcriptomics

**2.4.1. Library Preparation for Transcriptome Sequencing.** After behavior tests, the hypothalamus of the rat was collected for transcriptomics. A total amount of 1 μg RNA per sample was used as input material for the RNA sample preparations. Sequencing libraries were generated using NEBNext® Ultra™ RNA Library Prep Kit for Illumina® (NEB, USA) following the manufacturer's recommendations; index codes were added to attribute sequences to each sample. Briefly, mRNA was purified from total RNA using poly-T oligo-attached magnetic beads. Fragmentation was carried out using divalent cations under elevated temperature in NEBNext First Strand Synthesis Reaction Buffer (5x). First strand cDNA was synthesized using random hexamer primer and M-MuLV Reverse Transcriptase (RNase H-). Second strand cDNA synthesis was subsequently performed using DNA Polymerase I and RNase H. Remaining overhangs were converted into blunt ends via exonuclease/polymerase activities. After adenylation of 3' ends of DNA fragments, the NEBNext Adaptor with hairpin loop structure was ligated to prepare for hybridization. In order to select cDNA fragments, preferentially of 250~300 bp in length, the library fragments were purified with the AMPure XP system (Beckman Coulter, Beverly, USA). Then, 3 μl USER Enzyme (NEB, USA) was used with size-selected, adaptor-ligated cDNA at 37°C for 15 min followed by 5 min at 95°C before

PCR. Then, PCR was performed with Fusion High-Fidelity DNA polymerase, Universal PCR primers, and Index (X) Primer. At last, PCR products were purified (AMPure XP system), and the quality was assessed on the Agilent Bioanalyzer 2100 system.

**2.4.2. Clustering and Sequencing.** The clustering of the indexed samples was performed on a cBot Cluster Generation System using TruSeq PE Cluster Kit v3-cBot-HS (Illumina) according to the manufacturer's instructions. After cluster generation, the library preparations were sequenced on an Illumina Nova seq platform, and 150 bp paired-end reads were generated.

**2.4.3. Differential Expression Analysis.** Differential expression analysis of two conditions/groups (two biological replicates per condition) was performed using the DESeq2 R package (1.16.1). The DESeq2 provided statistical routines for determining differential expression in digital gene expression data using a model based on the negative binomial distribution. The resulting  $P$  values were adjusted using the Benjamin and Hochberg's approach for controlling the false discovery rate. Genes with  $P$  value  $< 0.05$  found by DESeq2 were assigned as differentially expressed.

**2.4.4. GO and KEGG Enrichment Analysis of Expressed Genes.** The Rattus norvegicus PPI network was downloaded from the BioGRID database (<https://thebiogrid.org/>, v3.5.184). Gene Ontology (GO) enrichment analysis of differentially expressed genes and neighbor nodes were implemented by python package NetworkX [34]. GO terms with  $P$  value less than 0.05 were considered significantly enriched by differentially expressed genes.

KEGG is a database resource for understanding high-level functions and utilities of a biological system, such as the cell, the organism, and the ecosystem. It is based on molecular-level information, especially large-scale molecular datasets generated by genome sequencing and other high-throughput experimental technologies (<https://www.genome.jp/kegg/>). We used DAVID v6.8 (<https://david.ncifcrf.gov/>) to test the statistical enrichment of differential expression genes in KEGG pathways [35, 36].

**2.5. Statistics.** IBM SPSS Statistics 19 (SPSS Inc., Chicago, IL, USA) and GraphPad Prism 5.0 (GraphPad Software Inc., San Diego, CA, USA) were used for statistical analyses and generating graphs. For the comparisons, parametric tests including  $t$ -tests and one-way analysis of variance (ANOVA) were used if the data was normally distributed (distribution tested by the Shapiro-Wilk normality test), and nonparametric approaches, including the Wilcoxon test and Kruskal-Wallis test, were used for data with a nonnormal distribution. Pearson's chi-squared test was used to assess rank variables. For all data, the results were expressed as the mean  $\pm$  standard error of the mean (SEM), and  $P < 0.05$  (two-tailed) was considered statistically significant.

### 3. Result

**3.1. TEAS Effect on Development Milestone and USVs.** To evaluate the therapeutic effect, the TEAS treatment was administered from PND7 to PND13. There were no statistical differences in eye-opening time among the NS-control group, VPA-sham group, and VPA-TEAS group (two-way ANOVA, Figure 1(c)). The body weight of the NS-control group was higher than the VPA group (one-way ANOVA,  $P < 0.05$ , Figure 1(d)). The total number of USVs was lower in the VPA-sham and the VPA-TEAS group compared with that in the NS-control group on PND7. And the USV number was significantly lower in the NS-control group on PND13 compared with that on PND7 (paired  $t$ -test,  $P < 0.05$ , Figure 1(e)). But there were no differences between the VPA-sham and VPA-TEAS group on PND7 or PND13 (Figure 1(e)). These results showed that TEAS in early life did not improve the development and communication ability of the VPA-induced offspring.

**3.2. Early TEAS Produced a Long-Term Behavioral Effect in Adolescence.** Sociability, self-grooming, and cognition ability were evaluated during adolescence.

- (1) *Social preference*: in stage 1 of the three-chamber tests, the NS-control group and the VPA-TEAS group spent more time on the stranger rat side than on the empty cage side (paired  $t$ -test,  $P < 0.05$ , Figure 2(b)). On the contrary, there was no difference between the stranger rat side and the empty cage side of the VPA-sham group (paired  $t$ -test,  $P = 0.95$ , Figure 2(b)). The sniffing time of the stranger rat in the VPA-sham group was lower than that in the NS-control group and the VPA-TEAS group (one-way ANOVA,  $P < 0.001$ , Figure 2(c)). The result in the social index was consistent with sniffing time, which for the VPA-sham group was lower than for the NS-control group and the VPA-TEAS group (one-way ANOVA,  $P < 0.05$ , Figure 2(d)). These results suggested that offspring of the VPA-treated rat had social preference deficits, and early TEAS intervention would repair the social preference deficits in this VPA-induced rat model of ASD
- (2) *Social novelty*: in stage 2 of the three-chamber tests, all of the three groups (NS-control group, VPA-sham group, and VPA-TEAS group) showed a preference for the new stranger rat (paired  $t$ -test,  $P < 0.05$ , Figure 2(f)). No differences in sniffing time of the new stranger rat or the social index of social memory were observed among the three groups
- (3) *Repetitive behavior*: repetitive behavior manifested as self-grooming behavior was analyzed. The results suggested that the VPA-sham and the VPA-TEAS group had more repetitive behavior (one-way ANOVA,  $P < 0.001$ , Figure 2(i))



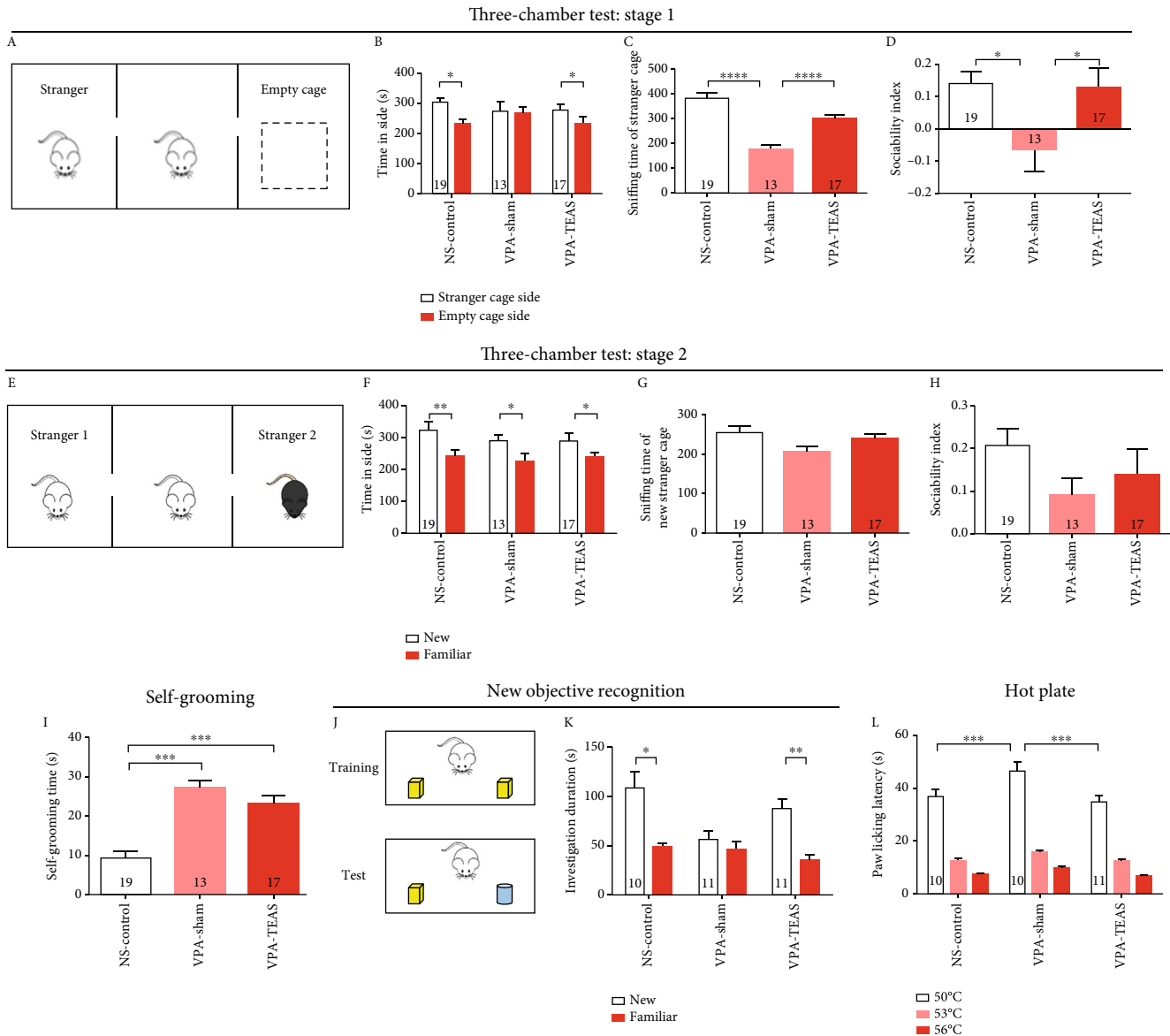


**FIGURE 2:** TEAS treatment in early life stage had long-term behavior effects on offspring of VPA treated rats. (a) Schematic diagram of three-chamber test in stage 1 (social preference). (b) The time the animal spent investigating either on the stranger cage side or empty cage side in stage 1 of the three-chamber test (paired *t*-test, NS-control *n* = 19, VPA-sham *n* = 13, VPA-TEAS *n* = 17). (c) The sniffing time of the stranger cage in stage 1 of the three-chamber test (one-way ANOVA). (d) The social preference index (one-way ANOVA). (e) Schematic diagram of the three-chamber test in stage 2 (social novelty). (f) The time spent investigating either the new stranger or the familiar stranger in stage 1 of the three-chamber test (paired *t*-test, NS-control *n* = 19, VPA-sham *n* = 13, VPA-TEAS *n* = 17). (g) The sniffing time on new stranger in stage 2 of the three-chamber test (one-way ANOVA). (h) The social preference index (one-way ANOVA). (i) The time of self-grooming test (one-way ANOVA, NS-control *n* = 19, VPA-sham *n* = 13, VPA-TEAS *n* = 17). (j) Schematic diagram of new objective recognition. (k) The time spent on investigating either familiar or novel object in novel object recognition test (one-way ANOVA, NS-control *n* = 10, VPA-sham *n* = 10, VPA-TEAS *n* = 11). (l) The withdrawal latency in the hot plate test for heat sensitivity (one-way ANOVA for same temperature, NS-control *n* = 10, VPA-sham *n* = 10, VPA-TEAS *n* = 11). Data was presented as the mean ± SEM. \**P* < 0.05, \*\**P* < 0.01, \*\*\**P* < 0.001.

(4) *Cognitive ability*: cognitive ability was examined with a novel object recognition test. During the test stage, the NS-control and the VPA-TEAS group spent more time sniffing the new object than the VPA-sham group (paired *t*-test, *P* < 0.05, Figure 2(k)). This result indicated that early TEAS would improve the cognitive ability of the VPA rat in adolescence

(5) *Hot plate*: in the hot-plate experiment, the data showed that paw withdrawal latency increased significantly for the VPA-sham group compared with the NS-control and VPA-TEAS group at 50°C (one-way ANOVA, *P* < 0.001, Figure 2(l)). At 53°C and 56°C, there was no difference in the paw withdrawal latency among the three groups. This result suggested



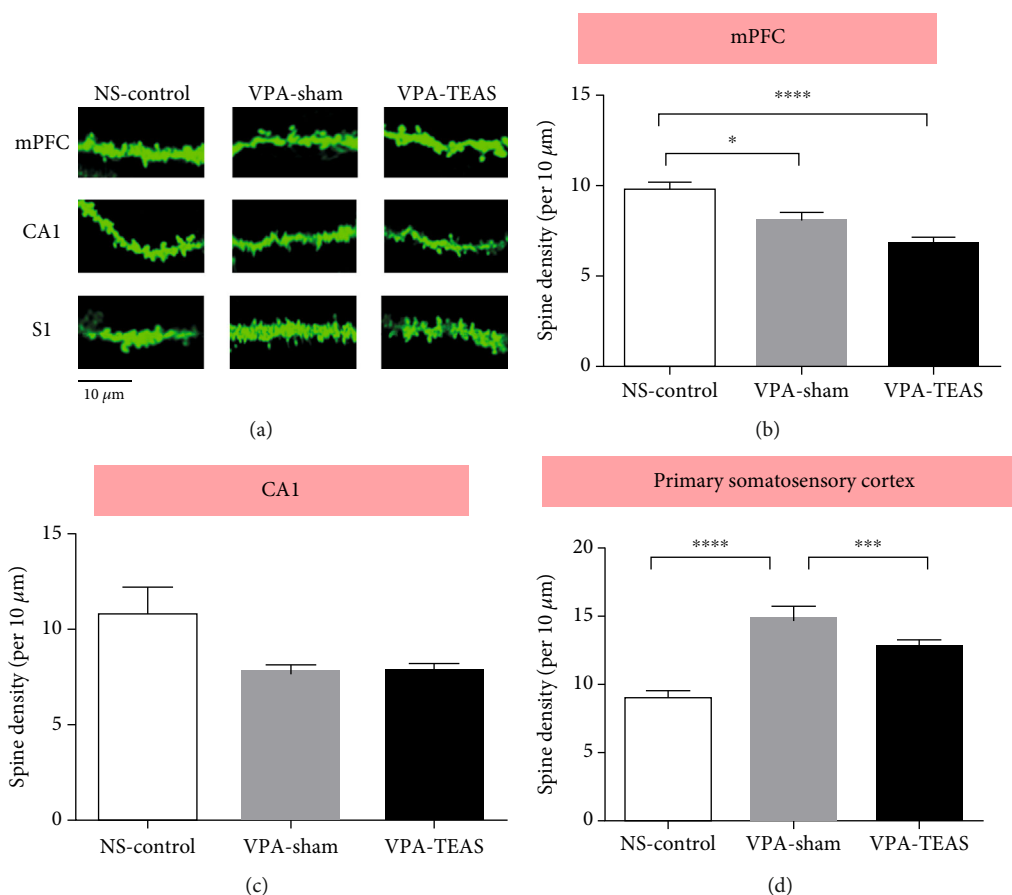


FIGURE 3: TEAS in early life would repair the deficit of spine pruning on VPA rats in S1 neurons. (a) Representative images of dendritic spines from mPFC, CA1, and S1 neurons (scale bar = 10 μm). (b) The spine density of mPFC in PND42 (one-way ANOVA). (c) The spine density of CA1 in PND42 (one-way ANOVA). (d) The spine density of primary somatosensory cortex (S1) in PND42 (one-way ANOVA,  $n = 4$  rats for each group, nine neurons per rat). Data was presented as mean  $\pm$  SEM. \* $P < 0.05$ , \*\*\* $P < 0.001$ , \*\*\*\* $P < 0.0001$ .

that pain perception impaired in this VPA rat model of ASD and TEAS intervention in the early stage would mitigate the abnormal pain perception in adolescence

**3.3. Improvement by Early TEAS on Dendritic Spine Pruning in S1.** Dendritic spine density in medial prefrontal cortex (mPFC), hippocampus CA1, and primary somatosensory cortex (S1) were analyzed by Golgi staining after behavior tests. In mPFC, spine density of the VPA-sham and VPA-TEAS groups was lower than that of the NS-control group (one-way ANOVA,  $P < 0.05$ , Figure 3(b)). In CA1, a tendency towards a lower spine density was seen in the VPA-sham and VPA-TEAS groups (one-way ANOVA,  $P = 0.09$ , Figure 3(c)). Interestingly, the spine density was increased in the VPA-sham group compared with the NS-control in PND42. The increased spine density was partially reversed in the VPA-TEAS group (one-way ANOVA,  $P < 0.001$ , Figure 3(d)). This finding indicated that early TEAS would be beneficial for facilitating spine pruning in certain brain regions.

**3.4. Transcriptome Analysis.** The hypothalamus is located under the cerebral cortex that can release a variety of neuro-

transmitters. Hypothalamic neurons have extensive synaptic connections with nerve fibers from other parts. To detect the synaptic changes produced by TEAS, we chose transcriptome to analyze the hypothalamus changes.

**3.4.1. Differential Gene Analysis.** Transcriptome referred to the total of all RNA transcribed by a specific tissue or cell at a certain time or state. Differential gene analysis revealed that compared with the NS-control group, the VPA-sham group had 1158 genes with changed expression patterns, including 621 upregulated genes and 537 downregulated genes (Figures 4(a), 4(b), and 4(d)). Furthermore, the VPA-TEAS group had 801 genes changed in comparison with the VPA-sham group, including 330 genes upregulated and 471 genes downregulated (Figures 4(a), 4(b), and 4(e)). As shown in Figure 4(a), 251 changed genes were commonly found among three groups.

**3.4.2. GO Analysis.** GO analysis included the biological process (BP), cell component (CC), and molecular function (MF). In BP terms (Figure 5(a)), the autism-related GO terms were regulation of neuron apoptotic process (GO:0043523), sensory perception of pain (GO:0019233), regulation of neuronal synaptic plasticity (GO:0048168), and regulation of

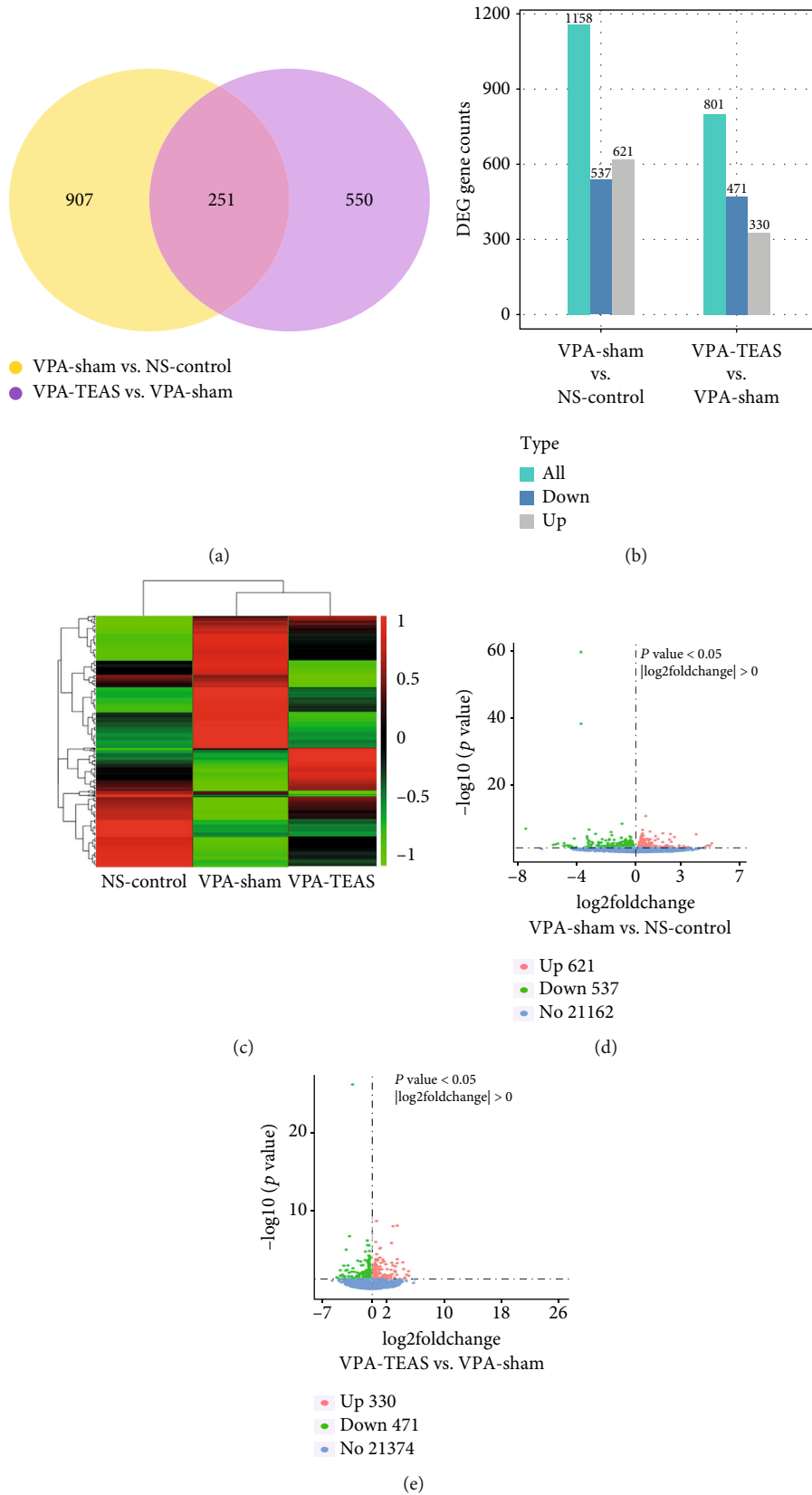


FIGURE 4: Differential gene analysis of the hypothalamus. (a) The Venn chart of differential gene among NS-control, VPA-sham, and VPA-TEAS group ( $n = 3$  for each group). (b) Distribution of differential genes of NS-control, VPA-sham, and VPA-TEAS group. (c) Clustering of NS-control, VPA-sham, and VPA-TEAS group in heat map diagram. (d) Volcano plot of differential genes between VPA-sham and NS-control. (e) Volcano plot of differential genes between VPA-TEAS and VPA-sham.

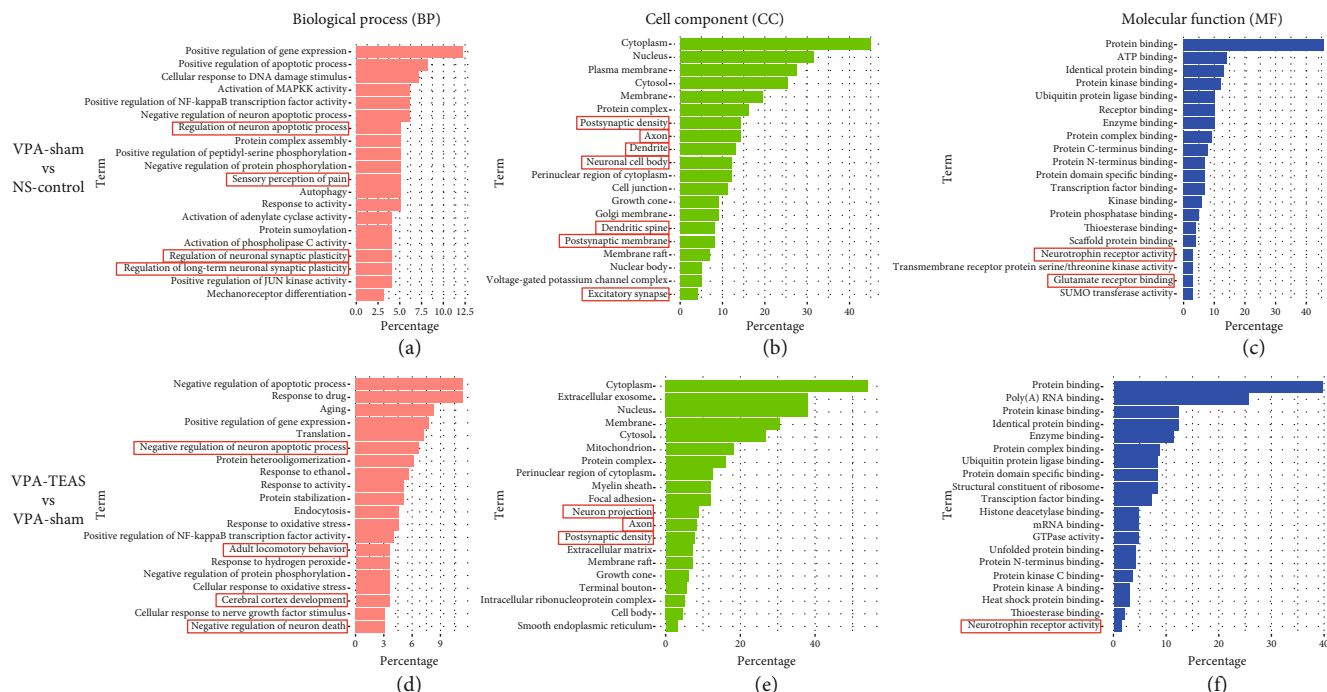


FIGURE 5: GO analysis of differential terms in BP, CC, and MF terms: (a–c) downregulated terms in BP, CC, and MF frequency between the VPA-sham and the NS-control; (d–f) upregulated terms in BP, CC, and MF frequency between the VPA-TEAS and the VPA-sham. (The red color presents biological process terms. The green color presents cell component terms. The blue color presents molecular function terms.)

long-term neuronal synaptic plasticity (GO:0048169). In CC terms (Figure 5(b)), autism-related GO terms were postsynaptic density (GO:0014069), axon (GO:0030424), dendritic spine (GO:0043197), neuronal cell body (GO:0043025), postsynaptic membrane (GO:0045211), and excitatory synapse (GO:0060076). In MF terms (Figure 5(c)), the autism-related GO terms are neurotrophin receptor binding (GO:0005168) and glutamate receptor binding (GO:0035254). These findings suggested that the VPA-induced rat model would experience autism-like behavior through synaptic dysfunction.

Between the VPA-TEAS and the VPA-sham group in BP terms (Figure 5(d)), biological process terms which related to autism were negative regulation of neuron apoptotic process (GO:0043524), cerebral cortex development (GO:0021987), and negative regulation of neuron death (GO:1901215). In CC terms (Figure 5(e)), autism-related GO terms were neuron projection (GO:0043005), axon (GO:0030424), and postsynaptic density (GO:0014069). In MF terms (Figure 5(f)), the autism-related GO term was neurotrophin receptor activity (GO:0005030). These results showed that early TEAS would improve neuron development of the VPA rats.

**3.4.3. KEGG.** KEGG pathway analysis of the integrated differentially expressed genes was performed using the DAVID database, and the results of the analysis are shown in Figure 6. Compared with the NS-control group, the downregulated differentially expressed genes were mainly enriched in the oxytocin pathway, neurotrophic signaling pathway, glutamatergic synapse, and dopaminergic synapse, which were related to the ASD pathogen (Figure 6(a)). And then, we found that the upregulated differentially expressed genes

of the VPA-TEAS group were mainly enriched in the neurotrophic signaling pathway (Figure 6(b)). Thus, the neurotrophic signaling pathway would be a potential target for ASD intervention.

#### 4. Discussion

Our findings showed that the VPA-induced rat model had impaired social, cognition, and sensory functions. Moreover, TEAS in early life could repair the above deficits in adolescence. Finally, early TEAS would be beneficial to spine pruning and neuron development of the VPA-induced rat model.

Epidemiology demonstrated that the offspring of mothers taking VPA during pregnancy would be three times more likely to suffer ASD than those not taking VPA [37]. So VPA is commonly used in the autism-like animal model. In our study, prenatal exposure to VPA was found to lead to social, cognition, and sensory impairment of offspring, which was consistent with previous research [38].

In the previous ASD animal studies, the time of acupuncture intervention was usually selected after PND21 [39–41], but in our study, we chose PND7 to PND13 as the TEAS time. That was because PND7 to PND13 was about 1-2 years old in humans. Firstly, we chose this period to be consistent with our previous clinic study [29]. Secondly, TEAS had a better effect in 3-6 years old ASD children than those above 7 [37]. More importantly, according to the Centers for Disease Control and Prevention (CDC) recommendation, early intervention can significantly improve the development of ASD children [7]. Treatment for ASD children should be started as soon as possible, when ASD symptoms appear.

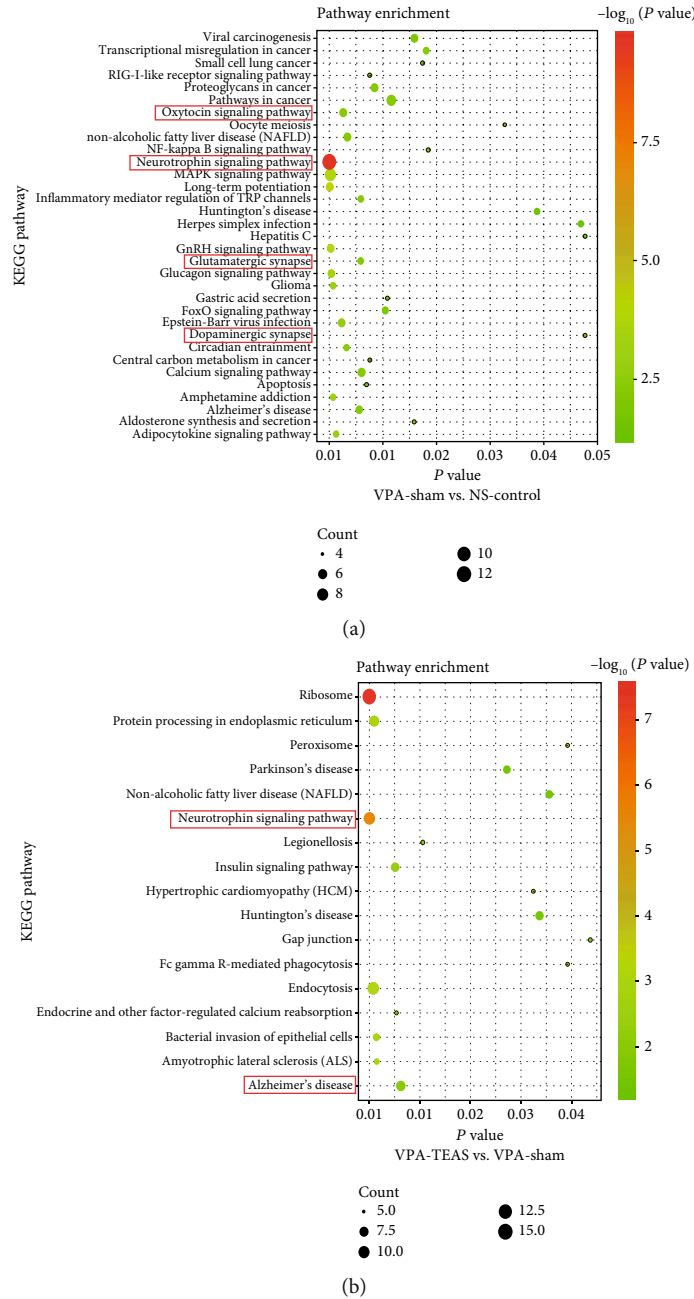


FIGURE 6: The Kyoto Encyclopedia of Genes and Genomes (KEGG) pathways enrichment: (a) KEGG enrichment pathway of downregulation in the VPA-sham compared with the NS-control; (b) KEGG enrichment pathway of upregulated in the VPA-TEAS compared with VPA-sham. (The black points present the number of enriched genes. The color from red to green presents  $P$  value of pathway analysis).

The earliest appearance of ASD symptoms is at 18-24 months after birth [42]. This period met the CDC’s recommendation for the early intervention stage of ASD.

In parameters selection, we used 2/15 Hz as the frequency, which is the same one used in our clinical study. And 2/15 Hz TEAS was also effective for treating the ASD children according to our previous work [29]. In this study, we observed that early TEAS would repair the deficits of social, cognition, and abnormal heat sensation. As a noninvasive stimulus, TEAS would be more suitable for young animals than manual or electrical acupuncture.

Several lines of evidence from our study suggested that the etiology of ASD was related to genetic and environmental risk factors [1, 11] which would affect synaptic function and neuron development. The density of dendritic spines changed dynamically, increasing in early life and starting to decrease in adolescence. And this kind of dendritic spine change has been called spine pruning, which is related to precision functioning of the central nervous system [38, 43]. The change of spine pruning was roughly the same in different brain regions, but time and extent were different [14, 44].

Acupuncture has been practiced in China for over 2000 years to treat a variety of diseases [45]. The methods of acupuncture were integrated into electrical acupuncture and TEAS. Physiological effects of TEAS are similar to manual acupuncture in analgesia, etc. [46]. Cumulative evidences have demonstrated that acupuncture could induce neural plasticity in rodents [47]. And our Golgi staining results showed that TEAS would decrease the spine density of the VPA rat model in S1 at adolescence.

But we did not observe the same phenomenon in mPFC and CA1. In the previous studies, acupuncture has been found to play a positive role in improving the expression levels of synaptophysin and PSD-95 [48, 49]. Most of the brain area acupuncture research is concerned with the hippocampus and cortex [50–53]. For example, in the previous study, it was found that acupuncture modulated the excitability of the motor cortex, and the plasticity was time-dependent [54]. Furthermore, it was suggested that the synaptic effect may be due to the changes in the synaptic structure of the brain, the detection time, and the acupoint [47]. Our results may give a hint that TEAS may have brain region specificity in the ASD animal model. Simultaneously, the synaptic effect of TEAS, such as spine pruning, may be distinct in different life periods. Moreover, it is plausible that TEAS in early life might repair the deficit of spine pruning at adolescence in the VPA rat model, which would help the ASD animal model to repair abnormal neural circuits. In the future study, we will seek related molecular factors to analyze the TEAS synaptic effect in different brain areas and at different life times.

The synaptic function changes are accompanied by molecular changes. Because of the difficulty of brain tissue collection, there is limited data on transcriptomics of ASD patients. The prior work has suggested that there was dysregulation of the AMPA receptor subunit expression in the cerebellum of ASD patients [55]. Meanwhile, ASD patient brain research found that the gene expression of the immune response was upregulated, while that involved in the synaptic function was downregulated [56]. In an ASD animal study, many genes and proteins were found to be changed, such as the autism-related susceptibility genes BDNF, Shank3, and ERK1 [57]. In the study of the VPA mouse model, Neu2 and Mt2a had a significant decrease in the amygdala [58]. Besides, transcriptomics found that the impairment in the VPA model in the brain area involved the orbital frontal lobe and cerebellar vermis [59].

But there was little information about the hypothalamus of ASD transcriptomics in previous studies. This study indicated that some genes significantly changed in the VPA rat model, like the genes postsynaptic density, the excitatory synapse, and sensory perception of pain. Moreover, our present KEGG study showed that the pathways related to ASD in the VPA rat model included the oxytocin signaling pathway, the neurotrophic signaling pathway, the glutamatergic synapse, and the dopaminergic synapse. These pathways were related to the synapse, indicating that VPA was associated with the occurrence and development of synapses in offspring.

Transcriptomic studies provide only limited information regarding medical treatment of ASD at this time. The possi-

ble targeted intervention goals from other previous studies included synapse function, chromatin modification and transcriptional regulation, neuron projection, and neurogenesis [60, 61]. Our findings indicated that early TEAS will improve the postsynaptic density, axon, and neuron projection of the VPA rat model. These results were related to the pathogenesis of ASD and might provide potential targets for treatment.

Nerve growth factor is the earliest discovered neurotrophic factor and can provide nutrition for neurons and induce neurite outgrowth [62]. It was reported that the neurotrophic factor level of an ASD rat was lower than that of the control [63, 64]. There was also a report that spine maturation required the neurotrophic factor [65]. Previously, other studies reported that acupuncture or electrical acupuncture would increase the expression of the neurotrophic factor [66–68]. In line with these results, we could infer that TEAS would promote spine maturation by increasing the expression of neurotrophic factors.

A possible limitation of our study is the potential relation between spine maturation and transcript factor which should be explored more deeply. And our transcriptomic results showed that early TEAS would not only improve the synapse function but also other pathways, such as ribosome and peroxisome. In the future, we hope to find more evidence to support the therapeutic effect of TEAS on ASD.

## 5. Conclusions

The present study demonstrates that a VPA-induced rat will have autistic like behavior deficits. The reason for the behavior deficits is related to spine pruning and synaptic impairment. Equally important, TEAS in early life can repair the social, cognition, and heat insensitivity impairments and have a long-term positive effect on the synapse function in adolescence.

## Data Availability

The data used to support the findings of this study are available from the corresponding author upon request.

## Conflicts of Interest

The authors declare no competing interests.

## Authors' Contributions

XW performed the experiments, wrote the manuscript, and analyzed the data. RD and JW analyzed the data of transcriptomics. YS helped perform the experiments. RZ, JH, and SH helped to design the study and contributed to the analysis with constructive discussions. All authors approved the final version.

## Acknowledgments

This work was supported by grants from the Beijing Municipal Science and Technology Commission (Z181100001518005), the National Basic Research Program of China (2017YFA0105201), the National Science



Foundation of China (81925011), and the Key Realm R&D Program of GuangDong Province (2019B030335001).

## References

- [1] C. Lord, T. S. Brugha, T. Charman et al., "Autism spectrum disorder," *Nature Reviews. Disease Primers*, vol. 6, no. 1, p. 5, 2020.
- [2] Center for Disease Control and Prevention, "Screening and diagnosis of autism spectrum disorder | CDC[EB/OL]," 2020, <https://www.cdc.gov/ncbddd/autism/screening.html>.
- [3] S. R. Leekam, C. Nieto, S. J. Libby, L. Wing, and J. Gould, "Describing the sensory abnormalities of children and adults with autism," *Journal of Autism and Developmental Disorders*, vol. 37, no. 5, pp. 894–910, 2007.
- [4] A. Ben-Sasson, L. Hen, R. Fluss, S. A. Cermak, B. Engel-Yeger, and E. Gal, "A meta-analysis of sensory modulation symptoms in individuals with autism spectrum disorders," *Journal of Autism and Developmental Disorders*, vol. 39, no. 1, pp. 1–11, 2009.
- [5] L. D. Wiggins, D. L. Robins, R. Bakeman, and L. B. Adamson, "Brief report: sensory abnormalities as distinguishing symptoms of autism spectrum disorders in young children," *Journal of Autism and Developmental Disorders*, vol. 39, no. 7, pp. 1087–1091, 2009.
- [6] L. Y. Tsai and M. Ghaziuddin, "DSM-5 ASD moves forward into the past," *Journal of Autism and Developmental Disorders*, vol. 44, no. 2, pp. 321–330, 2014.
- [7] Center for Disease Control and Prevention, "Treatment and intervention services for autism spectrum disorder | NCBDDD | CDC[EB/OL]," 2020, <https://www.cdc.gov/ncbddd/autism/treatment.html#Complementary>.
- [8] S. L. Hyman, S. E. Levy, and S. M. Myers, "Identification, evaluation, and management of children with autism spectrum disorder," *Pediatrics*, vol. 145, no. 1, 2020.
- [9] M. L. Ganz, "The lifetime distribution of the incremental societal costs of autism," *Archives of Pediatrics & Adolescent Medicine*, vol. 161, no. 4, pp. 343–349, 2007.
- [10] S. Lindgren, D. Wacker, A. Suess et al., "Telehealth and autism: treating challenging behavior at lower cost," *Pediatrics*, vol. 137, pp. S167–S175, 2016.
- [11] P. Chaste and M. Leboyer, "Autism risk factors: genes, environment, and gene-environment interactions," *Dialogues in Clinical Neuroscience*, vol. 14, no. 3, pp. 281–292, 2012.
- [12] J. De Felipe, P. Marco, A. Fairen, and E. G. Jones, "Inhibitory synaptogenesis in mouse somatosensory cortex," *Cerebral Cortex*, vol. 7, no. 7, pp. 619–634, 1997.
- [13] P. R. Huttenlocher, "Synaptic density in human frontal cortex – Developmental changes and effects of aging," *Brain Research*, vol. 163, no. 2, pp. 195–205, 1979.
- [14] G. N. Elston, T. Oga, and I. Fujita, "Spinogenesis and pruning scales across functional hierarchies," *The Journal of Neuroscience*, vol. 29, no. 10, pp. 3271–3275, 2009.
- [15] P. Penzes, M. E. Cahill, K. A. Jones, J. E. VanLeeuwen, and K. M. Woolfrey, "Dendritic spine pathology in neuropsychiatric disorders," *Nature Neuroscience*, vol. 14, no. 3, pp. 285–293, 2011.
- [16] H. Y. Zoghbi and M. F. Bear, "Synaptic dysfunction in neurodevelopmental disorders associated with autism and intellectual disabilities," *Cold Spring Harbor Perspectives in Biology*, vol. 4, no. 3, 2012.
- [17] G. Tang, K. Gudsnuk, S. H. Kuo et al., "Loss of mTOR-dependent macroautophagy causes autistic-like synaptic pruning deficits," *Neuron*, vol. 83, no. 5, pp. 1131–1143, 2014.
- [18] N. Torres, D. Martins, A. J. Santos, D. Prata, and M. Verissimo, "How do hypothalamic nonapeptides shape youth's sociality? A systematic review on oxytocin, vasopressin and human socio-emotional development," *Neuroscience and Biobehavioral Reviews*, vol. 90, pp. 309–331, 2018.
- [19] C. E. Hostinar, R. M. Sullivan, and M. R. Gunnar, "Psychobiological mechanisms underlying the social buffering of the hypothalamic-pituitary-adrenocortical axis: a review of animal models and human studies across development," *Psychological Bulletin*, vol. 140, no. 1, pp. 256–282, 2014.
- [20] H. Higashida, T. Yuhi, S. Akther et al., "Oxytocin release via activation of TRPM2 and CD38 in the hypothalamus during hyperthermia in mice: implication for autism spectrum disorder," *Neurochemistry International*, vol. 119, pp. 42–48, 2018.
- [21] E. E. Storm and L. H. Tecott, "Social circuits: peptidergic regulation of mammalian social behavior," *Neuron*, vol. 47, no. 4, pp. 483–486, 2005.
- [22] M. Nakajima, A. Gorlich, and N. Heintz, "Oxytocin modulates female sociosexual behavior through a specific class of prefrontal cortical interneurons," *Cell*, vol. 159, no. 2, pp. 295–305, 2014.
- [23] E. A. Mayer, K. Tillisch, and A. Gupta, "Gut/brain axis and the microbiota," *The Journal of Clinical Investigation*, vol. 125, no. 3, pp. 926–938, 2015.
- [24] A. H. Abo, A. Gelewkhan, and Z. Mahdi, "Analysis of evidence-based autism symptoms enhancement by acupuncture," *Journal of Acupuncture and Meridian Studies*, vol. 10, no. 6, pp. 375–384, 2017.
- [25] J. Hofer, F. Hoffmann, I. Kamp-Becker et al., "Complementary and alternative medicine use in adults with autism spectrum disorder in Germany: results from a multi-center survey," *BMC Psychiatry*, vol. 19, no. 1, p. 53, 2019.
- [26] C. H. Yau, C. L. Ip, and Y. Y. Chau, "The therapeutic effect of scalp acupuncture on natal autism and regressive autism," *Chinese Medicine*, vol. 13, no. 1, p. 30, 2018.
- [27] B. Lee, J. Lee, J. H. Cheon, H. K. Sung, S. H. Cho, and G. T. Chang, "The efficacy and safety of acupuncture for the treatment of children with autism spectrum disorder: a systematic review and meta-analysis," *Evidence-based Complementary and Alternative Medicine*, vol. 2018, Article ID 1057539, 21 pages, 2018.
- [28] F. Qu, R. Li, W. Sun et al., "Use of electroacupuncture and transcutaneous electrical acupoint stimulation in reproductive medicine: a group consensus," *Journal of Zhejiang University. Science. B*, vol. 18, no. 3, pp. 186–193, 2017.
- [29] R. Zhang, M. X. Jia, J. S. Zhang et al., "Transcutaneous electrical acupoint stimulation in children with autism and its impact on plasma levels of arginine-vasopressin and oxytocin: a prospective single-blinded controlled study," *Research in Developmental Disabilities*, vol. 33, no. 4, pp. 1136–1146, 2012.
- [30] H. F. Zhang, H. X. Li, Y. C. Dai et al., "Electro-acupuncture improves the social interaction behavior of rats," *Physiology & Behavior*, vol. 151, pp. 485–493, 2015.
- [31] X. J. Xu, H. F. Zhang, X. J. Shou et al., "Prenatal hyperandrogenic environment induced autistic-like behavior in rat offspring," *Physiology & Behavior*, vol. 138, pp. 13–20, 2015.
- [32] K. C. Kim, P. Kim, H. S. Go et al., "Male-specific alteration in excitatory post-synaptic development and social interaction in

- pre-natal valproic acid exposure model of autism spectrum disorder," *Journal of Neurochemistry*, vol. 124, no. 6, pp. 832–843, 2013.
- [33] A. V. Kalueff, A. M. Stewart, C. Song, K. C. Berridge, A. M. Graybiel, and J. C. Fentress, "Neurobiology of rodent self-grooming and its value for translational neuroscience," *Nature Reviews. Neuroscience*, vol. 17, no. 1, pp. 45–59, 2016.
- [34] A. Chatr-Aryamontri, R. Oughtred, L. Boucher et al., "The BioGRID interaction database: 2017 update," *Nucleic Acids Research*, vol. 45, no. D1, pp. D369–D379, 2017.
- [35] I. Thanseem, A. Anitha, K. Nakamura et al., "Elevated transcription factor specificity protein 1 in autistic brains alters the expression of autism candidate genes," *Biological Psychiatry*, vol. 71, no. 5, pp. 410–418, 2012.
- [36] S. Rose, S. C. Bennuri, J. E. Davis et al., "Butyrate enhances mitochondrial function during oxidative stress in cell lines from boys with autism," *Translational Psychiatry*, vol. 8, no. 1, p. 42, 2018.
- [37] J. S. Zhang, X. T. Zhang, L. P. Zou, R. Zhang, S. P. Han, and J. S. Han, "A preliminary study on effect of transcutaneous electrical acupoint stimulation for children with autism," *Zhen Ci Yan Jiu*, vol. 42, no. 3, pp. 249–253, 2017.
- [38] P. Rakic, J. P. Bourgeois, and P. S. Goldman-Rakic, "Synaptic development of the cerebral cortex: implications for learning, memory, and mental illness," *Progress in Brain Research*, vol. 102, pp. 227–243, 1994.
- [39] J. Khongrum and J. Wattanathorn, "Laser acupuncture at HT7 improves the cerebellar disorders in valproic acid-rat model of autism," *Journal of Acupuncture and Meridian Studies*, vol. 10, no. 4, pp. 231–239, 2017.
- [40] J. Khongrum and J. Wattanathorn, "Laser acupuncture improves behavioral disorders and brain oxidative stress status in the valproic acid rat model of autism," *Journal of Acupuncture and Meridian Studies*, vol. 8, no. 4, pp. 183–191, 2015.
- [41] Y. Z. Hong, X. J. Zhang, L. Hong, Q. R. Huang, and Q. Wu, "Influence of acupuncture of "Changqiang" (GV 1) on learning-memory ability and gap junction-related protein expression in the prefrontal cortex in autism rats," *Zhen Ci Yan Jiu*, vol. 39, no. 3, pp. 173–179, 2014.
- [42] R. Sturmer, B. Howard, P. Bergmann et al., "Accurate autism screening at the 18-month well-child visit requires different strategies than at 24 months," *Journal of Autism and Developmental Disorders*, vol. 47, no. 10, pp. 3296–3310, 2017.
- [43] G. Yang, F. Pan, and W. B. Gan, "Stably maintained dendritic spines are associated with lifelong memories," *Nature*, vol. 462, no. 7275, pp. 920–924, 2009.
- [44] P. R. Huttenlocher and R. M. Raichelson, "Effects of neonatal hemispherectomy on location and number of corticospinal neurons in the rat," *Brain Research. Developmental Brain Research*, vol. 47, no. 1, pp. 59–69, 1989.
- [45] W. Zhou and P. Benharash, "Effects and mechanisms of acupuncture based on the principle of meridians," *Journal of Acupuncture and Meridian Studies*, vol. 7, no. 4, pp. 190–193, 2014.
- [46] J. Zhang, Y. Zhang, X. Huang et al., "Different acupuncture therapies for allergic rhinitis: overview of systematic reviews and network meta-analysis," *Evidence-based Complementary and Alternative Medicine*, vol. 2020, Article ID 8363027, 18 pages, 2020.
- [47] L. Y. Xiao, X. R. Wang, Y. Yang et al., "Applications of acupuncture therapy in modulating plasticity of central nervous system," *Neuromodulation*, vol. 21, no. 8, pp. 762–776, 2018.
- [48] W. Yi, N. G. Xu, and G. B. Wang, "Experimental study on effects of electro-acupuncture in improving synaptic plasticity in focal cerebral ischemia rats," *Zhongguo Zhong Xi Yi Jie He Za Zhi*, vol. 26, no. 8, pp. 710–714, 2006.
- [49] W. G. Xia, C. J. Zheng, X. Zhang, and J. Wang, "Effects of "nourishing liver and kidney" acupuncture therapy on expression of brain derived neurotrophic factor and synaptophysin after cerebral ischemia reperfusion in rats," *Journal of Huazhong University of Science and Technology. Medical Sciences*, vol. 37, no. 2, pp. 271–278, 2017.
- [50] Y. Yang, I. Eisner, S. Chen, S. Wang, F. Zhang, and L. Wang, "Neuroplasticity changes on human motor cortex induced by acupuncture therapy: a preliminary study," *Neural Plasticity*, vol. 2017, Article ID 4716792, 8 pages, 2017.
- [51] R. Lin, X. Li, W. Liu et al., "Electro-acupuncture ameliorates cognitive impairment via improvement of brain-derived neurotrophic factor-mediated hippocampal synaptic plasticity in cerebral ischemia-reperfusion injured rats," *Experimental and Therapeutic Medicine*, vol. 14, no. 3, pp. 2373–2379, 2017.
- [52] L. M. Chavez, S. S. Huang, I. MacDonald, J. G. Lin, Y. C. Lee, and Y. H. Chen, "Mechanisms of acupuncture therapy in ischemic stroke rehabilitation: a literature review of basic studies," *International Journal of Molecular Sciences*, vol. 18, no. 11, p. 2270, 2017.
- [53] B. Y. Zeng, S. Salvage, and P. Jenner, "Effect and mechanism of acupuncture on Alzheimer's disease," *International Review of Neurobiology*, vol. 111, pp. 181–195, 2013.
- [54] X. K. He, Q. Q. Sun, H. H. Liu, X. Y. Guo, C. Chen, and L. D. Chen, "Timing of acupuncture during LTP-like plasticity induced by paired-associative stimulation," *Behavioural Neurology*, vol. 2019, Article ID 9278270, 10 pages, 2019.
- [55] A. E. Purcell, O. H. Jeon, A. W. Zimmerman, M. E. Blue, and J. Pevsner, "Postmortem brain abnormalities of the glutamate neurotransmitter system in autism," *Neurology*, vol. 57, no. 9, pp. 1618–1628, 2001.
- [56] I. Voineagu, "Gene expression studies in autism: moving from the genome to the transcriptome and beyond," *Neurobiology of Disease*, vol. 45, no. 1, pp. 69–75, 2012.
- [57] C. M. Daimon, J. M. Jasien, W. R. Wood et al., "Hippocampal transcriptomic and proteomic alterations in the BTBR mouse model of autism spectrum disorder," *Frontiers in Physiology*, vol. 6, p. 324, 2015.
- [58] A. Oguchi-Katayama, A. Monma, Y. Sekino, T. Moriguchi, and K. Sato, "Comparative gene expression analysis of the amygdala in autistic rat models produced by pre- and postnatal exposures to valproic acid," *The Journal of Toxicological Sciences*, vol. 38, no. 3, pp. 391–402, 2013.
- [59] O. S. Cohen, E. I. Varlinskaya, C. A. Wilson, S. J. Glatt, and S. M. Mooney, "Acute prenatal exposure to a moderate dose of valproic acid increases social behavior and alters gene expression in rats," *International Journal of Developmental Neuroscience*, vol. 31, no. 8, pp. 740–750, 2013.
- [60] N. Sestan and M. W. State, "Lost in translation: traversing the complex path from genomics to therapeutics in autism spectrum disorder," *Neuron*, vol. 100, no. 2, pp. 406–423, 2018.
- [61] Y. Gao, F. Wang, B. E. Eisinger, L. E. Kelnhofner, E. M. Jobe, and X. Zhao, "Integrative single-cell transcriptomics reveals molecular networks defining neuronal maturation during postnatal neurogenesis," *Cerebral Cortex*, vol. 27, no. 3, pp. 2064–2077, 2017.
- [62] H. Yu, J. Liu, J. Ma, and L. Xiang, "Local delivery of controlled released nerve growth factor promotes sciatic nerve

- regeneration after crush injury,” *Neuroscience Letters*, vol. 566, pp. 177–181, 2014.
- [63] K. Skogstrand, C. M. Hagen, N. Borbye-Lorenzen et al., “Reduced neonatal brain-derived neurotrophic factor is associated with autism spectrum disorders,” *Translational Psychiatry*, vol. 9, no. 1, p. 252, 2019.
- [64] K. R. Bou, “The growth factors/neuropeptides axis in the pathogenesis of autism spectrum disorder and schizophrenia,” *Asian Journal of Psychiatry*, vol. 44, pp. 170-171, 2019.
- [65] L. L. Orefice, C. C. Shih, H. Xu, E. G. Waterhouse, and B. Xu, “Control of spine maturation and pruning through proBDNF synthesized and released in dendrites,” *Molecular and Cellular Neurosciences*, vol. 71, pp. 66–79, 2016.
- [66] T. Gui-Hua, S. Kai, H. Ping et al., “Long-term stimulation with electroacupuncture at DU20 and ST36 rescues hippocampal neuron through attenuating cerebral blood flow in spontaneously hypertensive rats,” *Evidence-Based Complementary and Alternative Medicine*, vol. 2013, Article ID 482947, 10 pages, 2013.
- [67] L. Zhen-huan, Q. Yan-chao, P. Pei-guang et al., “Effect of acupuncture-moxibustion combined with nerve growth factor on compensation of cerebral function in the children of cerebral palsy,” *Zhongguo Zhen Jiu = Chinese Acupuncture & Moxibustion*, vol. 27, no. 8, 2007.
- [68] L. Dan, C. Qiu-Xin, Z. Wei et al., “Acupuncture promotes functional recovery after cerebral hemorrhage by upregulating neurotrophic factor expression,” *Neural Regeneration Research*, vol. 15, no. 8, 2020.

## Research Article

# The Instant Effects of Continuous Transcutaneous Auricular Vagus Nerve Stimulation at Acupoints on the Functional Connectivity of Amygdala in Migraine without Aura: A Preliminary Study

Wenting Luo <sup>1,2</sup>, Yue Zhang <sup>1</sup>, Zhaoxian Yan <sup>1</sup>, Xian Liu <sup>1</sup>, Xiaoyan Hou <sup>1</sup>,  
Weicui Chen <sup>1</sup>, Yongsong Ye <sup>1</sup>, Hui Li <sup>3</sup>, and Bo Liu <sup>1</sup>

<sup>1</sup>Department of Radiology, The Second Affiliated Hospital of Guangzhou University of Chinese Medicine, Guangzhou 510120, China

<sup>2</sup>The Second Clinical College, Guangzhou University of Chinese Medicine, Guangzhou 510405, China

<sup>3</sup>Department of Neurology, The Second Affiliated Hospital of Guangzhou University of Chinese Medicine, Guangzhou 510120, China

Correspondence should be addressed to Hui Li; [lihuicm@126.com](mailto:lihuicm@126.com) and Bo Liu; [liubogzcm@163.com](mailto:liubogzcm@163.com)

Received 26 June 2020; Revised 21 October 2020; Accepted 28 October 2020; Published 10 December 2020

Academic Editor: Lu Wang

Copyright © 2020 Wenting Luo et al. This is an open access article distributed under the Creative Commons Attribution License, which permits unrestricted use, distribution, and reproduction in any medium, provided the original work is properly cited.

**Background.** A growing body of evidence suggests that both auricular acupuncture and transcutaneous auricular vagus nerve stimulation (taVNS) can induce antinociception and relieve symptoms of migraine. However, their instant effects and central treatment mechanism remain unclear. Many studies proved that the amygdalae play a vital role not only in emotion modulation but also in pain processing. In this study, we investigated the modulation effects of continuous taVNS at acupoints on the FC of the bilateral amygdalae in MwoA. **Methods.** Thirty episodic migraineurs were recruited for the single-blind, crossover functional magnetic resonance imaging (fMRI) study. Each participant attended two kinds of eight-minute stimulations, taVNS and sham-taVNS (staVNS), separated by seven days in random order. Finally, 27 of them were included in the analysis of seed-to-voxel FC with the left/right amygdala as seeds. **Results.** Compared with staVNS, the FC decreased during taVNS between the left amygdala and left middle frontal gyrus (MFG), left dorsolateral superior frontal gyrus, right supplementary motor area (SMA), bilateral paracentral lobules, bilateral postcingulum gyrus, and right frontal superior medial gyrus, so did the FC of the right amygdala and left MFG. A significant positive correlation was observed between the FC of the left amygdala and right SMA and the frequency/total time of migraine attacks during the preceding four weeks. **Conclusion.** Continuous taVNS at acupoints can modulate the FC between the bilateral amygdalae and pain-related brain regions in MwoA, involving the limbic system, default mode network, and pain matrix, with obvious differences between the left amygdala and the right amygdala. The taVNS may produce treatment effects by modulating the abnormal FC of the amygdala and pain networks, possibly having the same central mechanism as auricular acupuncture.

## 1. Introduction

Migraine without aura (MwoA), the most common type of migraine, is the second-largest neurological disorder affecting the global disability-adjusted lifespan year, causing a severe burden on the health system and budgets [1]. However, its conventional medical treatments for migraines are far from satisfactory [2]. It is essential to find more effective and safe treatments.

A recent study [3] suggested that the occurrence of migraine was related to the imbalance of the autonomic nervous system, and increasing parasympathetic (mainly including vagal) nerve activity could alleviate the symptoms of migraine [4]. However, there are only a few indirect ways to regulate the vagal nerve tension, such as breathing regulation and yoga [5]. It is worth noting that noninvasive vagus nerve stimulation (nVNS) can directly regulate vagal nerve activity to treat migraines effectively [6, 7]. It has been



approved for treating episodic migraines by the Food and Drug Administration (FDA) of the USA in 2017, reducing the severity and frequency of headache [8, 9], improving the quality of life and reducing the cost of treatment [10], and being well-tolerated [11]. Notably, transcutaneous auricular vagus nerve stimulation (taVNS), a kind of simpler and effective nVNS [12], may have the same treatment effect and mechanism as auricular acupuncture [13]. A growing body of evidence suggests that both auricular acupuncture and taVNS can induce antinociception and relieve symptoms of migraine. However, the instant effects and central mechanism of electrical stimulation at auricular points innervated by the vagal nerve in MwoA are still unclear.

Previous neuroimaging evidences [14–17] suggested that migraine was associated with abnormal structure and function of brain regions involved in pain and emotional processing, such as the prefrontal cortex (PFC), cingulate gyrus, supplementary motor area (SMA), amygdala, hippocampus, insula, precuneus, periaqueductal gray matter (PAG), thalamus, cerebellum, and et al. Among them, the vital functions of the amygdalae in migraine have already attracted many researchers' attentions [18, 19]. Recent studies [20–22] demonstrated that the amygdalae were also involved in pain processing and modulation. A neuroimaging study found that the amygdala was activated during the headache, and its decreased volume was related to the frequency of headache attacks [23]. The FC of the left amygdala and left middle cingulate gyrus increased in episodic migraine compared with healthy controls, and there were obvious differences between the left amygdala and the right amygdala [24]. These results suggested that the dysfunction of the amygdala might be a potential mechanism of MwoA. However, little has known about the FC of the bilateral amygdalae and other regions in MwoA patients before and during taVNS so far.

Based on the above argument, we hypothesized that continuous taVNS at auricular points could modulate the abnormal FC of the left/right amygdala in MwoA patients. Then, the voxel-wise FC was analyzed during continuous stimulation, using the left/right amygdala as seeds, respectively.

## 2. Materials and Methods

**2.1. Participants.** Thirty episodic migraineurs without aura were recruited for the single-blind, crossover functional magnetic resonance imaging (fMRI) study from the neurology clinic outpatient of the Second Affiliated Hospital of Guangzhou University of Chinese Medicine from January to December in 2018. Each participant attended two fMRI scan sessions during the eight-minute continuous stimulation at auricular points separated by seven days, one for taVNS and another for sham-taVNS in random order. Informed consent was obtained from all participants. This study protocol was approved by the Institutional Review Board of the Second Affiliated Hospital of Guangzhou University of Chinese Medicine.

Similar to our previous study [25], the diagnosis of migraine was based on the International Classification of Headache Disorders 2<sup>nd</sup> Edition (ICHD-II) [21, 26], as diag-

nosed by a specialist working at the neurology outpatient service.

The inclusion criteria were as follows: (1) aged 18–45 years old, (2) right-handed, (3) at least six months of migraine duration, (4) having at least one attack per month, (5) having no prophylactic headache medicine during the past one month, and (6) having no psychoactive or vasoactive drugs during the past three months.

The participants were excluded if any of the following criteria were met: (1) was caused by other diseases or special types of migraine, (2) attacked within 48 hours before and during the scan, (3) had pregnancy or lactation, (4) had severe head deformity or intracranial lesions, (5) had other chronic pain diseases, and (6) had the standard score of self-rating anxiety or depression scale greater than 50.

### 2.2. Intervention Program

**2.2.1. Stimulator.** Huatuo auricular vagus nerve stimulators were from SDZ-II, Suzhou Medical Appliance Factory, China.

**2.2.2. Stimulation Parameters.** The stimulation parameters are as follows: constant voltage, continuous wave, 1 Hz, 0.2 ms, and the current intensity below the pain threshold, lasting 8 minutes. taVNS points: CO11 and CO14, left cymba concha (abundant in vagal afferent fibers). StaVNS points: SF2 and SF4–5, left scapha (no vagal afferent fibers) (Figure 1) [25, 27].

**2.3. Clinical Assessments.** The demographic information and clinical scale data of all patients were collected, including Migraine Specific Quality-of-Life Questionnaire (MSQ), Self-rating Depression Scale (SDS), Self-rating Anxiety Scale (SAS), Visual Analog Scale (VAS), the frequency, and total duration time of migraine attacks during the past four weeks preceding the fMRI scans.

**2.4. MRI Data Acquisition.** All MRI scans were conducted on a 3.0T Siemens MRI scanner (Siemens MAGNETOM Verio 3.0T, Erlangen, Germany) with a 24-channel phased-array head coil. All subjects were told to stay awake and remained motionless during the scan, keeping their eyes closed. Each scan session lasted approximately 20 minutes. The orders of MRI scans were as follows: a high-resolution anatomical image (MPRAGE), an eight-minute resting-state functional MRI, and an eight-minute continuous real or sham-taVNS (fMRI was applied during this continuous stimulation period).

T1-weighted MPRAGE was applied with the following parameters: TR = 1900 ms, TE = 2.27 ms, FOV = 256 mm × 256 mm, flip angle = 9°, matrix = 256 × 256, thickness = 1.0 mm, and 176 slices. The eight-minute resting state and eight-minute continuous real or sham-taVNS fMRI scan were acquired with the following parameters: TR = 2000 ms, TE = 30 ms, FOV = 224 mm × 224 mm, flip angle = 90°, matrix = 64 × 64, thickness = 3.5 mm, 31 slices, and 240 time points.

### 2.5. fMRI Data Analysis

**2.5.1. fMRI Data Preprocessing.** The fMRI data preprocessing was performed using DPABI 3.0 and SPM 12.0 based on



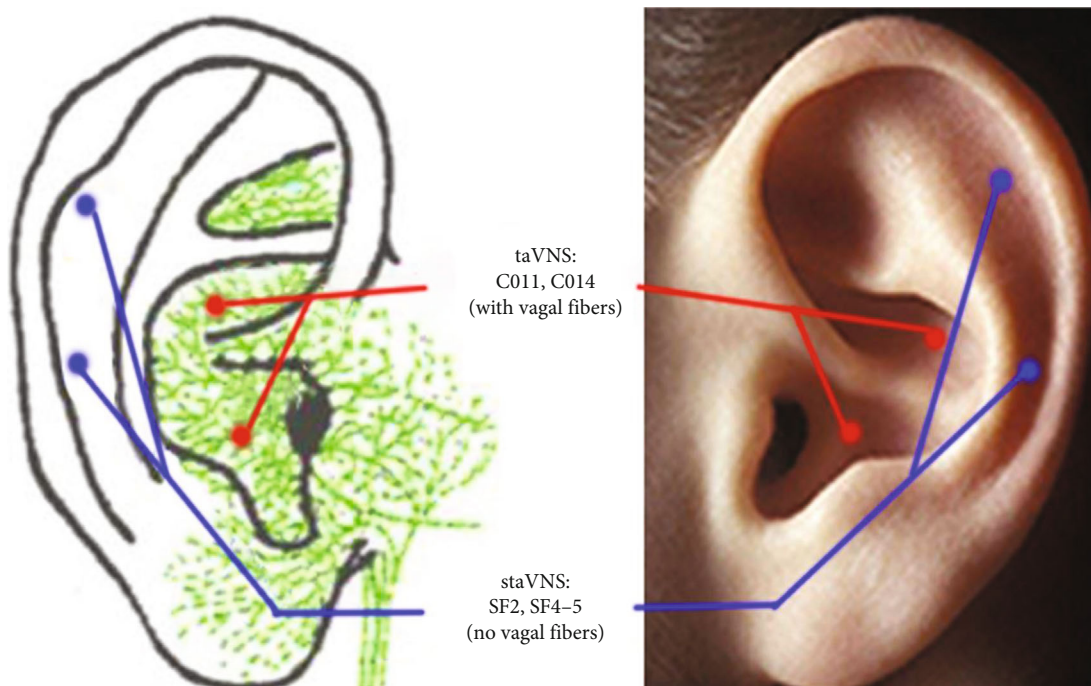


FIGURE 1: The innervations of the auricular branch of the vagal nerve and the points stimulated at the ear. The vagal nerve branch is marked by green color, the taVNS points by red, and the staVNS points by blue.

MATLAB (The MathWorks, Natick, MA, USA). After removing the first ten volumes of each participant, the functional images were corrected for the intravolume acquisition time delay using slice timing and realignment. One of the participants was excluded based on the criteria of displacement  $> 2.5$  mm or angular rotation  $> 2.5^\circ$  in any direction. Then, all corrected functional data were normalized to the Montreal Neurological Institute (MNI) space and resampled to a 3 mm isotropic resolution. The resulting images were further temporally band-pass filtered (0.01–0.08 Hz) to remove the effects of low-frequency drift and high-frequency physiological noise. Finally, 24 head-motion parameters, white matter signals, and cerebrospinal fluid signals were regressed using a general linear model, and linear trends were removed from the fMRI data. Spatial smoothing was also performed before the functional connection analysis using a Gaussian filter (6 mm full-width half maximum; full width at half maximum [FWHM]).

**2.5.2. Seed-to-Voxel FC Analysis.** The seeds of the left amygdala and right amygdala were defined separately, using the AAL template (Figure 2) (same to the previous literature [24]). Then, the amygdalae were resliced with the brain mask template with  $63 \times 71 \times 63$  size. The FC calculation was performed in DPABI (V3.0). The averaged time courses of the left/right amygdala were extracted, respectively. Next, Pearson correlation was used to calculate the FC between the extracted time courses and the time courses of the whole brain in a voxel-wise manner, respectively. The correlation coefficient map was then converted into a Fisher-Z map by Fisher's  $r$ -to- $z$  transformation to improve normality.

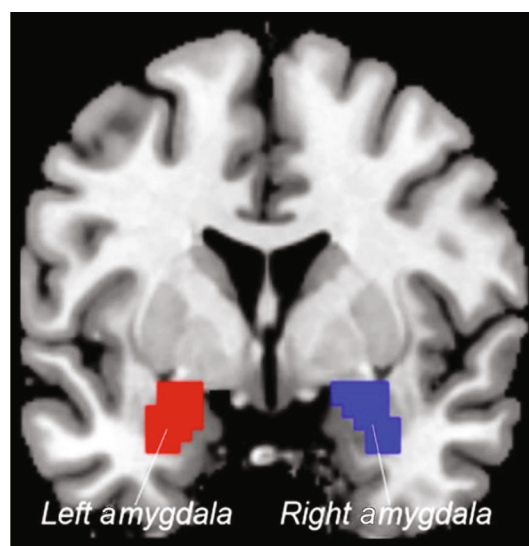


FIGURE 2: The left and right amygdalae were, respectively, generated based on the AAL template as seeds. Red: the left amygdala; blue: the right amygdala.

**2.6. Statistical Analysis.** The intergroup analysis (taVNS vs. staVNS) of the FC was performed using a paired  $t$ -test, with the mean head-motion value (mean FD Jenkinson) as covariate variables. A threshold of voxel-wise  $p$  uncorrected and cluster-level  $p$  corrected by familywise error corrected (FWE) were applied for multiple comparison correction. If voxel-wise  $p < 0.001$  and cluster-level  $p < 0.05$ , the difference was statistically significant.

TABLE 1: The demographic and clinical data during the past four weeks ( $n = 27$ ).

Characteristics	(Frequency/mean $\pm$ SD)
Gender (male/female)	2/25
Age	29.85 $\pm$ 8.09
Disease duration in years	9.22 $\pm$ 7.26
Frequency per month	1.22 $\pm$ 0.51
Total time per month	18.93 $\pm$ 15.61
VAS	42.99 $\pm$ 17.01
MSQ	72.52 $\pm$ 9.41
SDS score	45.96 $\pm$ 9.69
SAS score	42.63 $\pm$ 9.87

VAS: Visual Analog Scale; MSQ: Migraine Specific Quality-of-Life Questionnaire; SDS: Self-rating Depression Scale; SAS: Self-rating Anxiety Scale. Frequency/total time per month: The frequency/the total time of migraine attacks during the past four weeks.

Besides, in the baseline resting state and continuous stimulation state, we, respectively, extracted the average  $z$  values of significantly altered clusters of the left/right amygdala (taVNS vs. staVNS). Then, the differences of the  $z$ FC values were compared using a paired  $t$ -test between taVNS and staVNS in the two states, and  $p < 0.05$  was considered to be statistically significant [28]. We also explored the association between the initial clinical assessments and the altered  $z$ FC values (taVNS minus staVNS) in continuous stimulation state across all subjects after Bonferroni correction.

### 3. Results

**3.1. Clinical Results.** Twenty-seven patients completed the study and were included in the data analysis, because the two participants did not finish the fMRI scan, and one was excluded for displacement  $> 2.5$  mm or angular rotation  $> 2.5^\circ$  in any direction. The demographics are shown in Table 1.

#### 3.2. fMRI Results

**3.2.1. Left Amygdala as Seed.** The brain regions with decreased FC of the left amygdala mainly located in the left middle frontal gyrus (MFG), left dorsolateral superior frontal gyrus (SFG), right supplementary motor area (SMA), and bilateral paracentral lobule during continuous stimulation of taVNS compared with sham-taVNS (Table 2 and Figure 3(a)). No significant increased FC was observed.

Since the postcingulum cortex (PCC) and frontal medial gyrus are important nodes in the default mode network (DMN) [29, 30] and endogenous pain-inhibitory circuits [31, 32]. They play a very important role in the migraine pathogenesis [29–32]. Similar to the previous study [33], the small volume correction with a threshold of voxel-wise  $p < 0.001$  and cluster-level  $p < 0.05$  was used in ROI analysis. The direct intergroup comparison revealed more decreased FC in taVNS compared with the sham, in the bilateral PCC and the right frontal superior medial gyrus (small-volume corrected at  $p_{\text{FWE}} < 0.001$ ) (Table 2 and Figure 3(b)).

During stimulation, there were statistical significances for the FC in left MFG and SFG, right SMA and bilateral paracentral lobule, PCC, and right medial superior frontal gyrus (taVNS vs. staVNS) ( $t [1, 26] = -6.149$ ,  $p < 0.001$ , Figure 4(a);  $t [1, 26] = -4.143$ ,  $p < 0.001$ , Figure 4(b);  $t [1, 26] = -3.157$ ,  $p < 0.001$ , Figure 4(c);  $t [1, 26] = -4.734$ ,  $p < 0.001$ , Figure 4(d)), while there was no significant difference before stimulation ( $t [1, 26] = -1.134$ ,  $p = 0.267$ , Figure 4(a);  $t [1, 26] = -0.765$ ,  $p = 0.451$ , Figure 4(b);  $t [1, 26] = 0.271$ ,  $p = 0.789$ , Figure 4(c);  $t [1, 26] = -0.428$ ,  $p = 0.672$ , Figure 4(d)) (Supplementary table 1). All the changing trend of these FC were opposite between taVNS and staVNS.

The FC between the left amygdala and right SMA was correlated with the frequency ( $p = 0.017$  and  $r = 0.455$ ) and the total time ( $p = 0.011$  and  $r = 0.482$ ) of migraine attacks during the preceding four weeks before treatment (Supplementary table 2 and Figure 5), and there was no significant association for other FCs.

**3.2.2. Right Amygdala as Seed.** Compared with the staVNS, the FC significantly decreased between the right amygdala and left MFG in continuous taVNS (Table 3 and Figure 6). The value of the FC between the right amygdala and left MFG does not correlate with the migraine attacks.

The FC of the right amygdala and the left middle frontal gyrus had no significant difference before stimulation ( $t [1, 26] = -0.410$  and  $p = 0.685$ ), with significant difference during stimulation ( $t [1, 26] = -5.789$  and  $p < 0.001$ ) (taVNS vs. staVNS) (Supplementary table 3 and Figure 7). The changing trend of the FC was opposite between taVNS and staVNS.

### 4. Discussion

In this trial, we explored the altered FC of the bilateral amygdalae in MwoA during continuous taVNS and staVNS. To summarize, we found that the FCs significantly decreased during taVNS compared with staVNS between the amygdala and DMN (bilateral PCC), prefrontal cortex (PFC: left dorso-lateral SFG, left MFG, and right superior medial frontal gyrus), pain matrix (right SMA), and sensorimotor network (bilateral paracentral lobule), with different changes in the FC between the left amygdala and the right amygdala. Moreover, the value of the FC between the left amygdala and right SMA was positively correlated with the frequency and total time of migraine attacks during the preceding four weeks before treatment. Our research suggests that taVNS at auricular points may modulate the function of the limbic system and pain-related networks via adjusting abnormal FC of the amygdalae to treat migraines. We were the first to report the FC of the bilateral amygdalae during continuous taVNS at acupoints and staVNS in MwoA.

The amygdala played a crucial role in the pathogenesis, chronicity, and recurrence of migraines [24, 34], not only in emotion modulation but also in pain processing. Firstly, animal experiments have proved that the amygdala played an essential role in the regulation of synaptic transmission of neurons related to cortical spreading depression (CSD) and the neuropathic pain in migraine [35]. Secondly,

TABLE 2: The functional connectivity results using the left amygdala as a seed in 27 MwoA patients.

Contrast	Cluster	Brain region	Peak $T$ value	Peak $Z$ value	MNI coordinates		
					X	Y	Z
Real>sham		No brain region above the threshold					
	178	Left middle frontal gyrus	6.10	4.73	-27	48	30
	68	Left superior frontal gyrus	5.22	4.25	-21	60	6
Real<sham	18	Right supplementary motor area	5.37	4.34	3	-9	72
	18	Bilateral paracentral lobule	5.00	4.12	-3	-21	75
	17	Bilateral post cingulum gyrus*	4.47	3.80	3	-51	27
	15	Right frontal superior medial gyrus*	4.59	3.87	3	63	0

\*Small-volume correction at  $p_{FWE} < 0.001$ .

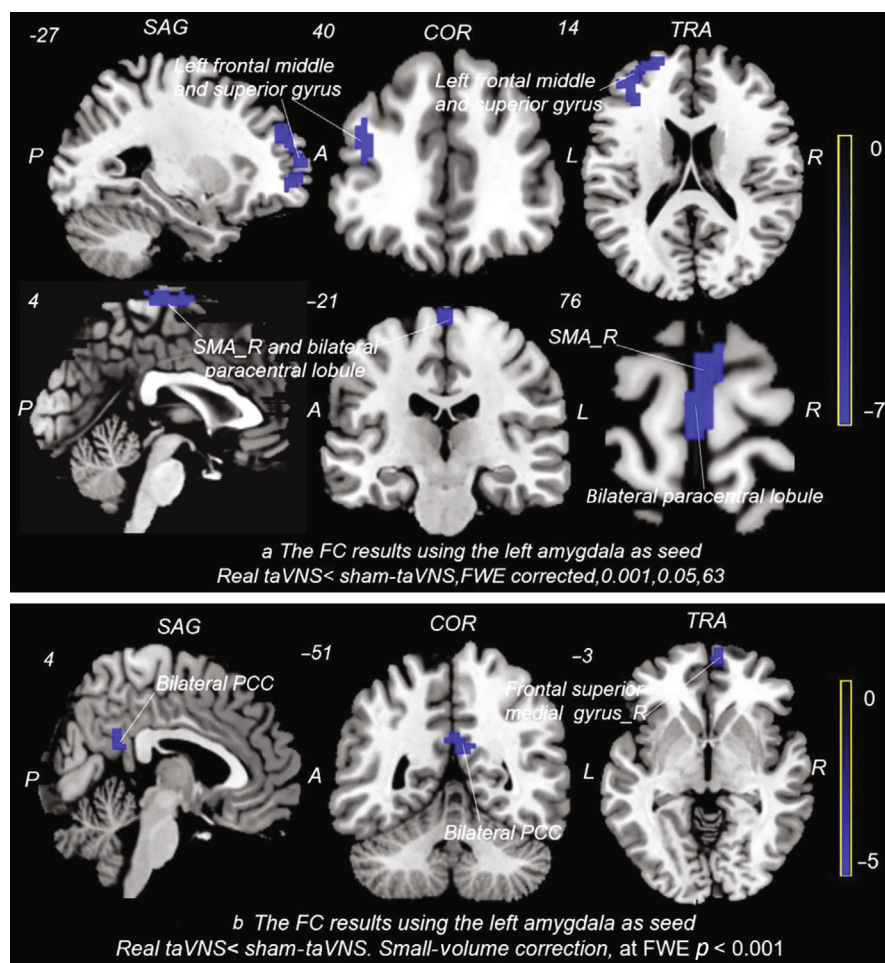
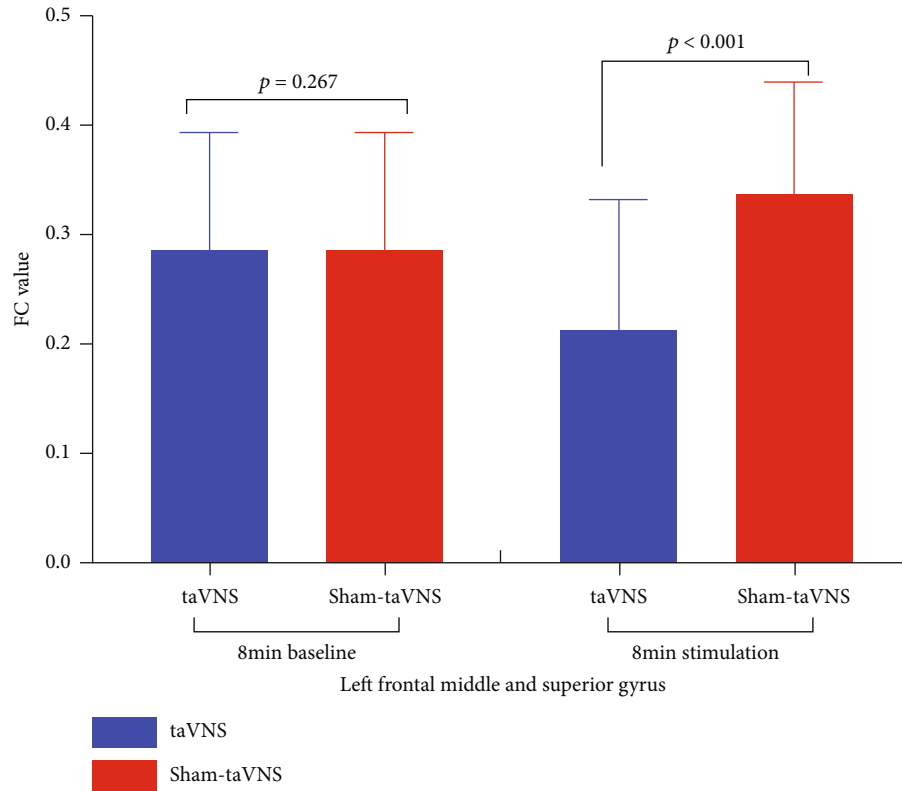


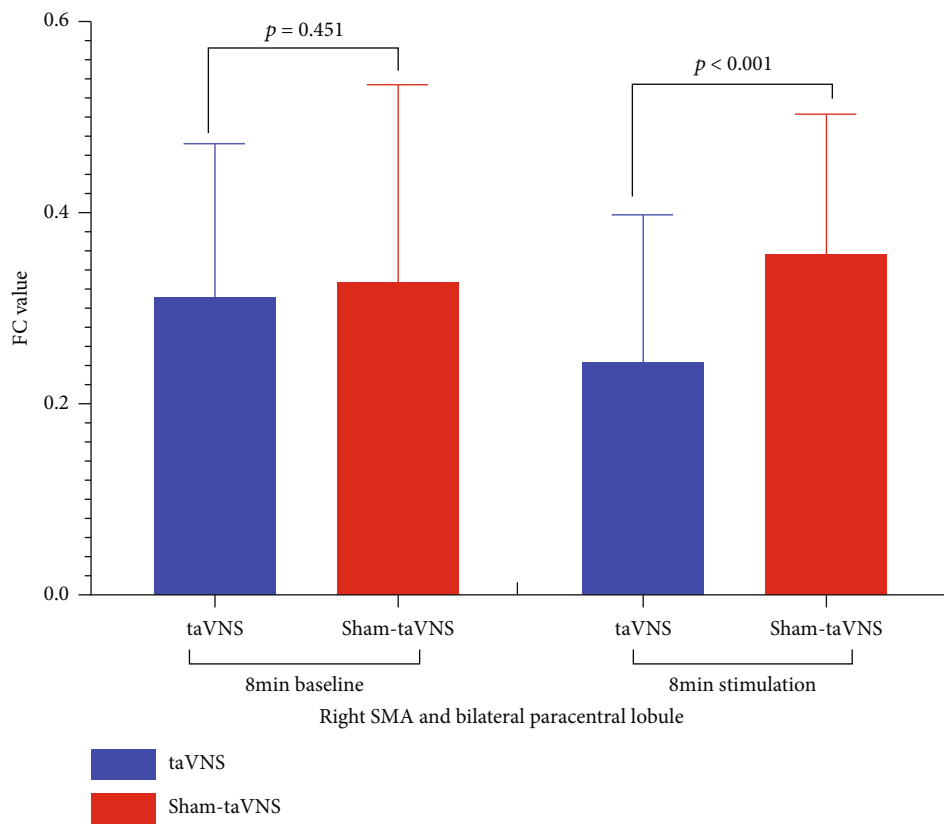
FIGURE 3: The functional connectivity (FC) of the left amygdala in MwoA during continuous stimulation (taVNS vs. staVNS). L: left; R: right; P: posterior; A: anterior; SAG: sagittal; COR: coronal; TRA: transverse; PCC: postcingulum gyrus; SMA: supplementary motor area; FWE: familywise error correction. Compared with sham-taVNS, the FC significantly decreased between the left amygdala and left frontal middle gyrus, left frontal superior gyrus, right SMA, bilateral paracentral lobule ((a) FWE multiple comparison correction, voxel-level  $p < 0.001$  and cluster-level  $p < 0.05$ ), bilateral PCC, and right frontal superior medial gyrus ((b) small-volume correction, FWE  $p < 0.001$ ) in taVNS.

migraine patients are often accompanied by negative emotions such as aversion, anxiety, fear, and avoiding pain behavior, which are closely related to the function of the amygdala [26, 28]. Finally, there are a large number of fibrous connections and the FC between the amygdala and pain-related brain regions [24] and networks [21]. Therefore,

modulating the dysfunctional FC of the amygdala might be a potential treatment mechanism in MwoA. Meanwhile, our recent study demonstrated that taVNS can modulate the resting-state FC between the bilateral LC and left amygdala and certain pain-related brain regions consistent with the vagus nerve central projections [25]. So, exploring the

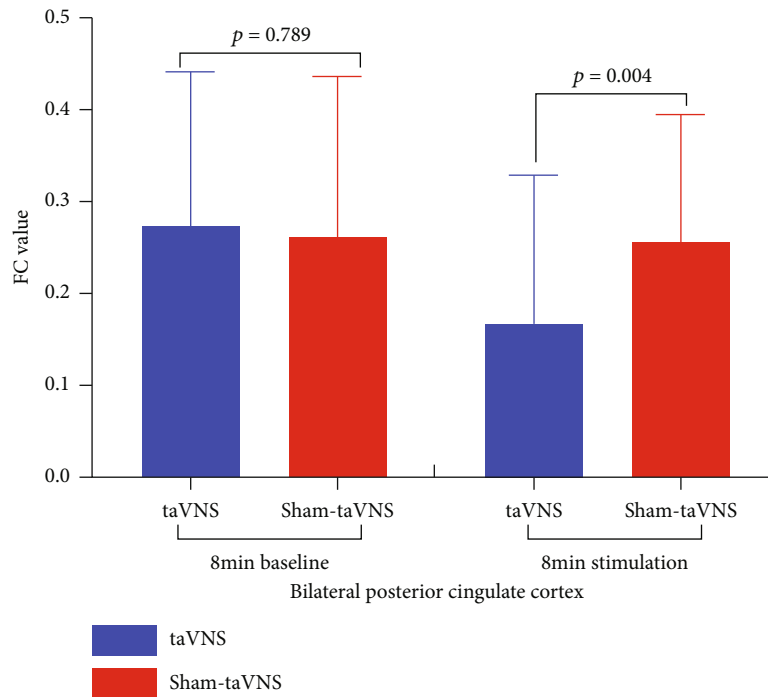


(a)

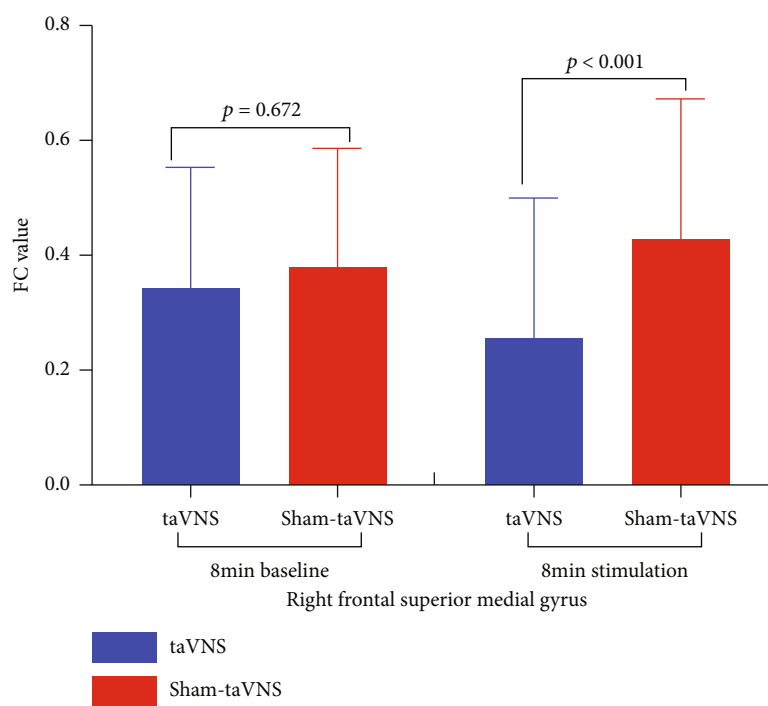


(b)

FIGURE 4: Continued.



(c)



(d)

FIGURE 4: The effects on the functional connectivity (FC) of the left amygdala between stimulations and time factors. SMA: supplementary motor area. A paired *t*-test was used. If  $p < 0.05$ , the difference was statistically significant. Before stimulation, there was no statistical significance for the FC of (a) the left amygdala and left MFG and SFG, (b) right SMA and paracentral lobule, (c) posterior cingulate cortex, (d) and frontal superior medial gyrus (taVNS versus staVNS). During stimulation, their differences were significant. The intensity of the FC decreased in taVNS and increased in staVNS (prestimulation vs. during stimulation). Therefore, the trend of the changed FC was opposite between taVNS and staVNS.

changed FC of the amygdala in the MwoA during continuous stimulation helps us to understand the mechanism and intervention effects of taVNS.

Antinociceptive effects of the taVNS were demonstrated in numerous animal experiments [36, 37] and clinical studies [38–40]. The taVNS may reduce nociception and pain



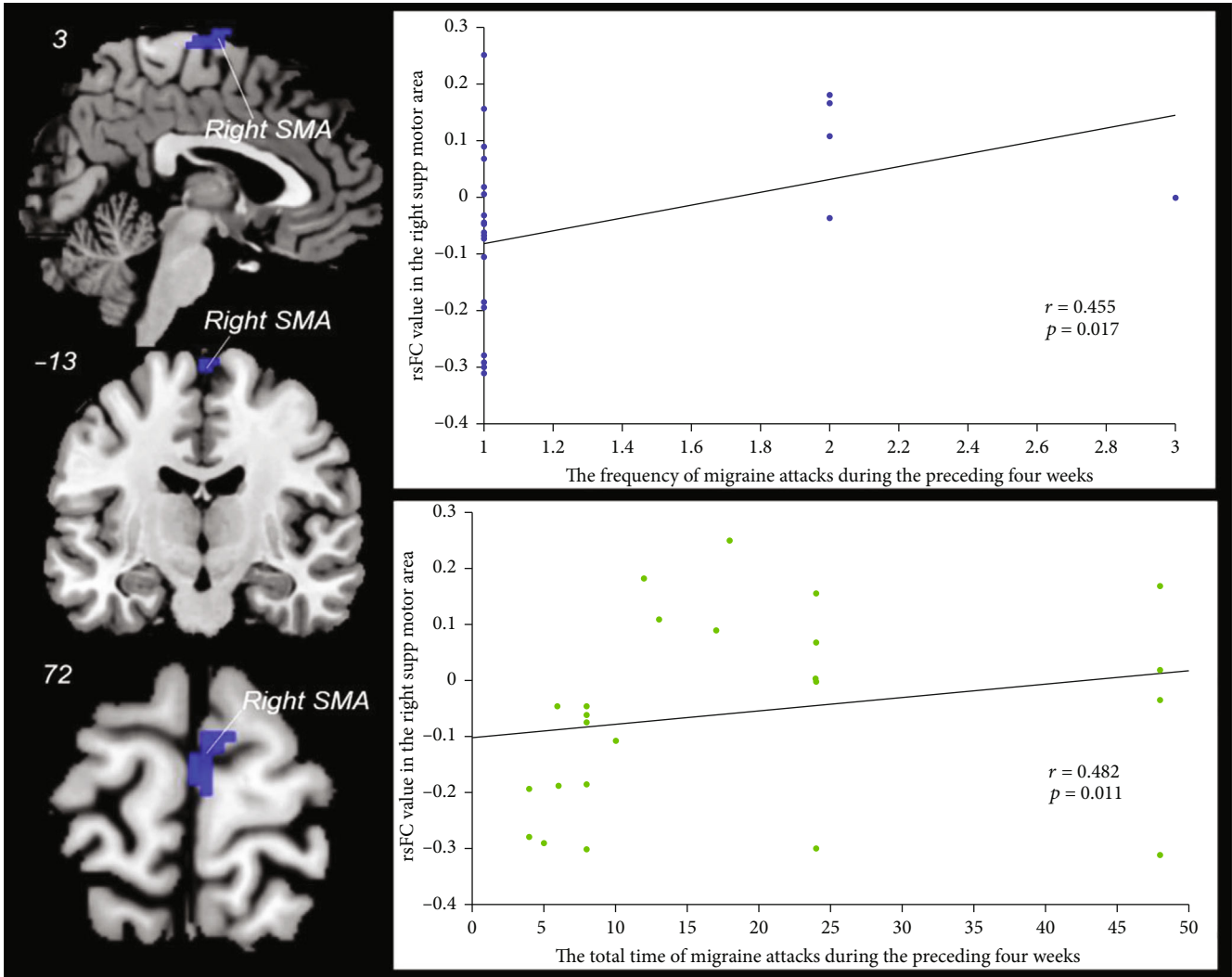


FIGURE 5: Correlation analysis between migraine attacks and the functional connectivity (FC) of the left amygdala during taVNS. SMA: supplementary motor area; rsFC: resting-state FC; suppt: superior. The FC between the left amygdala and the right SMA was correlated with the frequency ( $p = 0.017$  and  $r = 0.455$ ) and the total time ( $p = 0.011$  and  $r = 0.482$ ) of migraine attacks during the preceding four weeks.

TABLE 3: The functional connectivity results using the right amygdala as a seed in 27 MwoA patients.

Contrast	Cluster	Brain region	Peak $T$ value	Peak $Z$ value	MNI coordinates		
					X	Y	Z
Real>sham		No brain region above the threshold					
Real<sham	131	Left middle frontal gyrus	5.54	4.43	-38	45	21

through multiple mechanisms [41, 42], such as adjusting the autonomic nervous system, suppressing pain neurons, affecting the behavioral pain response, and modulating the pain networks. Reducing the sympathetic hyperactivity and increasing the parasympathetic activity may help manage pain via taVNS [43], with its anti-inflammatory effect together [44]. In animal models, VNS could inhibit nociceptive activation of trigeminal cervical neurons [45] and Fos protein expression [46]. In addition, Pena found that the VNS facilitated the extinction of conditioned fear responses by promoting plasticity of the amygdala and infralimbic area

[47]. Furthermore, its effects on the pain networks will be discussed in detail below.

The most interesting finding was that taVNS is capable of regulating the endogenous analgesia loop and descending pain inhibitory system. The FCs decreased between the amygdala and SFG, MFG, and superior medial frontal gyrus during continuous taVNS. This is consistent with the observation from our previous block-designed study that taVNS produced widespread fMRI signal decreased in the bilateral SFG, MFG, and medial prefrontal gyrus on MwoA [29]. As we all know, the medial frontal gyrus

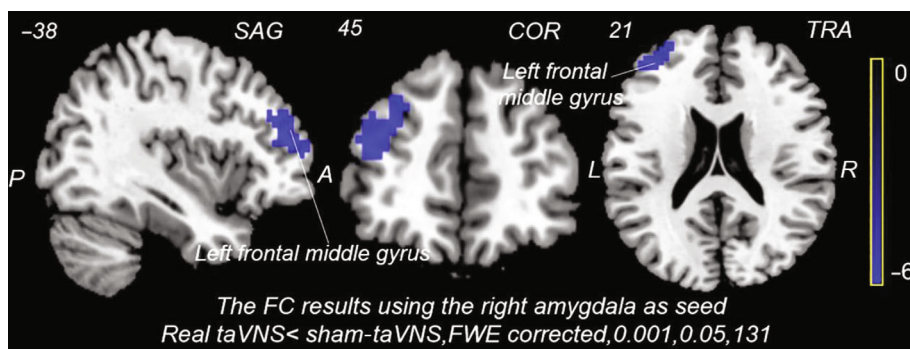


FIGURE 6: The functional connectivity (FC) of the right amygdala in MwoA during continuous stimulation (taVNS vs. staVNS). SAG: sagittal; COR: coronal; TRA: transverse; FWE: familywise error correction. Compared with staVNS, the FC of the right amygdala and left frontal middle gyrus significantly decreased during taVNS (voxel-level  $p < 0.001$  and cluster-level  $p_{FWE} < 0.05$ ).

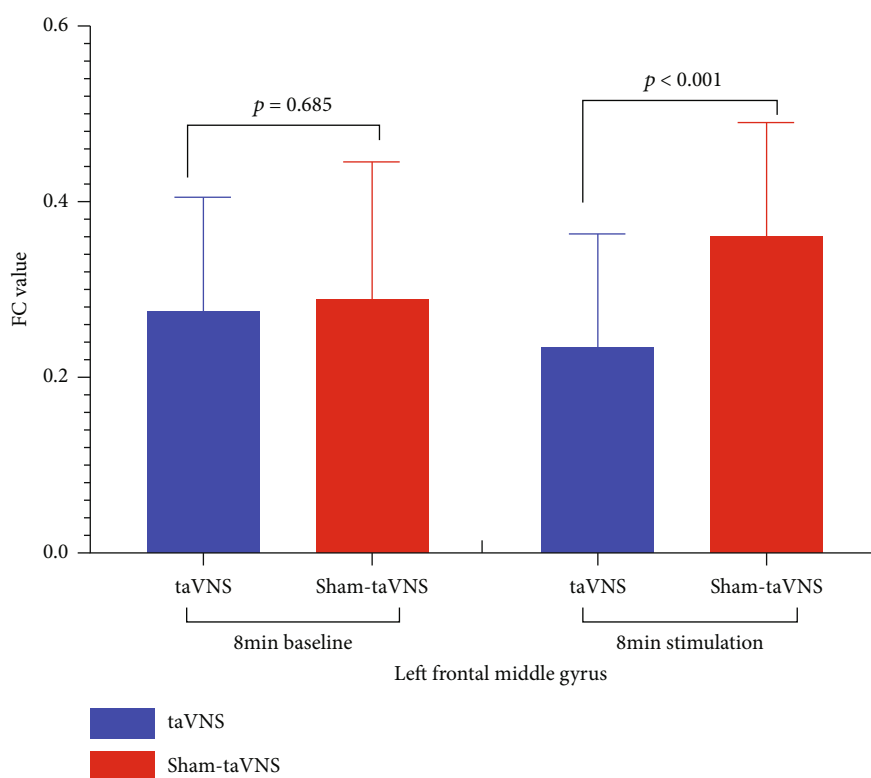


FIGURE 7: The functional connectivity (FC) comparisons of the right amygdala in different states and stimulations. A paired  $t$ -test was used. If  $p < 0.05$ , the difference was statistically significant. Before stimulation, there was no statistical significance for the FC of the right amygdala and left middle frontal gyrus (taVNS vs. staVNS), but the difference was significant during stimulation. The FC decreased in taVNS and increased in staVNS (prestimulation vs. during stimulation). Therefore, the changing trend of the FC was opposite between taVNS and staVNS.

belongs to the medial prefrontal cortex, a key node of the endogenous analgesia loop, and descending pain inhibitory system [19]. Meanwhile, the SFG and MFG are parts of the prefrontal cortex which is of great importance for pain perception and response [28]. Both the amygdala and prefrontal cortex were essential for the limbic system widely connected with other nervous systems and participated in pain and emotional regulation. Neuroimaging studies [24] have reported that the FCs were damaged in migraine between the limbic system and pain-related brain areas. Some researchers [19] even put forward the neurological dysfunction

model of the limbic pain network in migraine, highlighting the importance of the limbic system in the pathological mechanism of migraine. Notably, migraine patients have abnormal increases in FC within and around the limbic system. For example, Wei and colleagues [48] found that the FC of the limbic system (bilateral amygdala and right hippocampus) and left middle occipital gyrus (MOG) significantly increased in MwoA patients compared with healthy controls, and the FC between the left amygdala and MOG was positively correlated with the duration of migraine. Therefore, limbic system dysfunction plays an

important role in the occurrence, development, and regulation of migraines. Further study of acupuncture analgesia [49] found that the amplitude of low-frequency fluctuation (ALFF) in left insula decreased in patients with chronic low back pain after acupuncture, and the decrease of average ALFF was positively related to the decrease of VAS value, which confirms that regulating the function of limbic system may be one of the mechanisms for endogenous analgesia. The taVNS could regulate amygdala activity from a recent study [50] and caused extensive negative activation in the limbic system [30]. Therefore, we speculated that taVNS may modulate the function of the limbic system through the amygdalae, regulating the pain networks, and exerting an analgesic effect.

Another important finding was that DMN is crucial to migraine and can be affected by taVNS. The FC decreased between the left amygdala and bilateral PCC after taVNS compared with staVNS in our current trial. Similarly, we found that taVNS decreased the fMRI signal in the bilateral PCC on MwoA in our previous block-designed study [29]. It is noteworthy that PCC is one core area of DMN closely related to pain perception response [31] and inhibition [51]. Neuroimaging studies [52] have found that headache was associated with a reduced volume of the mPFC. Husoy et al. [24] also found the FC of the left amygdala and DMN increased in MwoA, and the increased FC was associated with the development of headaches. More and more studies confirmed that abnormal FC between the limbic system and DMN was related to pain, so regulating their FC could alleviate pain, which is supported by the results of analgesic treatment research. Zou [53] suggested acupuncture could reduce the FC within DMN to a healthy control level in chronic migraine patients, and the FC between DMN and limbic system also decreased in chronic pain patients after cognitive behavioral therapy [54]. Furthermore, Fang [55] found that compared with staVNS, the FC decreased between the DMN and limbic system after one-month taVNS, suggesting that taVNS can regulate the FC between the limbic system and DMN. Hence, taVNS is a valuable choice for pain treatment.

Last but not least, taVNS can modulate the pain matrix. Our result indicated that the FC between the left amygdala and right SMA decreased after taVNS. It is generally accepted that the SMA contributes to the pain matrix. Imaging studies [56] found that there were functional connections between the amygdala and SMA, indicating that the function of the pain matrix was related to the amygdala. The pain matrix and limbic system had high regional homogeneity (ReHo) [57] in pain. Solstrand [58] indicated that the resting-state FC (rsFC) of SMA and the amygdala increased in migraine patients, and the increased rsFC was negatively correlated with migraine frequency, which revealed that the pain matrix and limbic system worked together in pain perception and regulation, and their increased functional activities were closely related to pain. Fortunately, the abnormally increased functional activity of the amygdala and the pain matrix can be reversed by interventions. For example, Shi [57] found extensive negative activation of brain regions of the limbic system and the pain matrix after acupuncture. It is worth

noting that the FC between the amygdala and pain matrix decreased after taVNS in our study. Therefore, taVNS can adjust the abnormal FC between the limbic system and the pain matrix in MwoA patients.

However, there are some limitations in our research. Firstly, we only studied the instant effects of taVNS; thus, more studies are needed to evaluate the long-term impact of taVNS. Secondly, although crossover-control design can save the sample size and eliminate the influence of the differences between individuals, it increased the false-positive rate of the experiment, and randomized controlled studies will be considered. Thirdly, we just explored the altered FC using the seed-to-voxel analysis (same to the published article [24]) during taVNS compared with sham-taVNS. It is a very good idea and very important to explore the effects of taVNS on the pain matrix using the ROI-to-ROI analysis in the follow-up study. Finally, the outcome of this small sample study maybe not enough to be extended to the public, so larger samples are needed in the future.

## 5. Conclusions

From the above discussion, we can conclude that continuous taVNS at auricular points can modulate the FC between the bilateral amygdalae and pain-related regions in MwoA, involving the limbic system, DMN, and pain matrix, with obvious differences between the left amygdala and the right amygdala. The taVNS may produce treatment effects by modulating the abnormal FC of the amygdala and pain networks, possibly having the same central mechanism as auricular acupuncture.

## Data Availability

The data (fMRI) used to support the findings of this study are included within the article and the supplementary information files.

## Conflicts of Interest

The authors declare that there is no conflict of interest regarding the publication of this paper.

## Authors' Contributions

Experimental design was done by Bo Liu, Yue Zhang, and Xian Liu. Yue Zhang, Wenting Luo, Hui Li, Zhaoxian Yan, and Weicui Chen contributed to the data collection. Data analysis was done by Yue Zhang, Wenting Luo, and Xiaoyan Hou. Wenting Luo, Bo Liu, and Yue Zhang contributed to the manuscript preparation. All authors have approved the final manuscript. Wenting Luo and Yue Zhang are co-first authors.

## Acknowledgments

This research was supported by the Medical Scientific Research Foundation of Guangdong Province of China (A2017234) and the Administration of Traditional Chinese Medicine of Guangdong Province of China (20182047).

## Supplementary Materials

Supplementary Table 1: the functional connectivity comparisons of the left amygdala in different states and stimulations. Supplementary Table 2: correlations of the functional connectivity and clinical data. Supplementary Table 3: the functional connectivity comparisons of the right amygdala in different states and stimulations. (*Supplementary Materials*)

## References

- [1] GBD 2016 Neurology Collaborators, "Global, regional, and national burden of neurological disorders, 1990–2016: a systematic analysis for the Global Burden of Disease Study 2016," *Lancet Neurology*, vol. 18, no. 5, pp. 459–480, 2019.
- [2] P. J. Goadsby, "Bench to bedside advances in the 21st century for primary headache disorders: migraine treatments for migraine patients," *Brain*, vol. 139, no. 10, pp. 2571–2577, 2016.
- [3] S. Grassini and S. Nordin, "Comorbidity in migraine with functional somatic syndromes, psychiatric disorders and inflammatory diseases: a matter of central sensitization?," *Behavioral Medicine*, vol. 43, no. 2, pp. 91–99, 2016.
- [4] M. S. Vasudha, N. K. Manjunath, and H. R. Nagendra, "Changes in MIDAS, perceived stress, frontalis muscle activity and non-steroidal anti-inflammatory drugs usage in patients with migraine headache without aura following ayurveda and yoga compared to controls: an open labeled non-randomized study," *Annals of Neurosciences*, vol. 25, no. 4, pp. 250–260, 2019.
- [5] E. Toschi-Dias, E. Tobaldini, M. Solbiati et al., "Sudarshan Kriya Yoga improves cardiac autonomic control in patients with anxiety-depression disorders," *Journal of Affective Disorders*, vol. 214, pp. 74–80, 2017.
- [6] J. L. Hawkins, L. E. Cornelison, B. A. Blankenship, and P. L. Durham, "Vagus nerve stimulation inhibits trigeminal nociception in a rodent model of episodic migraine," *Pain Reports*, vol. 2, no. 6, article e628, 2017.
- [7] E. Tobaldini, E. Toschi-Dias, L. A. de Souza et al., "Cardiac and peripheral autonomic responses to orthostatic stress during transcutaneous vagus nerve stimulation in healthy subjects," *Journal of Clinical Medicine*, vol. 8, no. 4, p. 496, 2019.
- [8] S. R. Chaudhry, I. S. Lendvai, S. Muhammad et al., "Inter-ictal assay of peripheral circulating inflammatory mediators in migraine patients under adjunctive cervical non-invasive vagus nerve stimulation (nVNS): a proof-of-concept study," *Brain Stimulation*, vol. 12, no. 3, pp. 643–651, 2019.
- [9] P. Martelletti, on Behalf of the PRESTO Study Group, P. Barbanti et al., "Consistent effects of non-invasive vagus nerve stimulation (nVNS) for the acute treatment of migraine: additional findings from the randomized, sham-controlled, double-blind PRESTO trial," *The Journal of Headache and Pain*, vol. 19, no. 1, p. 101, 2018.
- [10] M. Mwamburi, E. J. Liebler, and A. T. Tenaglia, "Review of non-invasive vagus nerve stimulation (gammaCore): efficacy, safety, potential impact on comorbidities, and economic burden for episodic and chronic cluster headache," *The American Journal of Managed Care*, vol. 23, 17 Supplement, pp. S317–S325, 2017.
- [11] T. M. Kiefe, B. Pinteá, S. Muhammad et al., "Cervical non-invasive vagus nerve stimulation (nVNS) for preventive and acute treatment of episodic and chronic migraine and migraine-associated sleep disturbance: preliminary findings from a prospective observational cohort study," *The Journal of Headache and Pain*, vol. 16, no. 1, 2015.
- [12] H. M. Hamer and S. Bauer, "Lessons learned from transcutaneous vagus nerve stimulation (tVNS)," *Epilepsy Research*, vol. 153, pp. 83–84, 2019.
- [13] T. Usichenko, H. Hacker, and M. Lotze, "Transcutaneous auricular vagal nerve stimulation (taVNS) might be a mechanism behind the analgesic effects of auricular acupuncture," *Brain Stimulation*, vol. 10, no. 6, pp. 1042–1044, 2017.
- [14] B. M. Ellingson, C. Hesterman, M. Johnston, N. R. Dudeck, A. C. Charles, and J. P. Villablanca, "Advanced imaging in the evaluation of migraine headaches," *Neuroimaging Clinics of North America*, vol. 29, no. 2, pp. 301–324, 2019.
- [15] M. J. Lee, B. Y. Park, S. Cho, S. T. Kim, H. Park, and C. S. Chung, "Increased connectivity of pain matrix in chronic migraine: a resting-state functional MRI study," *The Journal of Headache and Pain*, vol. 20, no. 1, p. 29, 2019.
- [16] Z. Chen, X. Chen, M. Liu et al., "Altered functional connectivity of the marginal division in migraine: a resting-state fMRI study," *The Journal of Headache and Pain*, vol. 17, no. 1, p. 89, 2016.
- [17] X. M. Androulakis, K. A. Krebs, C. Jenkins et al., "Central executive and default mode network Intra-network functional connectivity patterns in chronic migraine," *Journal of Neurological Disorders*, vol. 6, no. 5, 2018.
- [18] N. Hadjikhani, N. Ward, J. Boshyan et al., "The missing link: enhanced functional connectivity between amygdala and viscerosensitive cortex in migraine," *Cephalalgia*, vol. 33, no. 15, pp. 1264–1268, 2013.
- [19] M. Maizels, S. Aurora, and M. Heinricher, "Beyond neurovascular: migraine as a dysfunctional neurolimbic pain network," *Headache*, vol. 52, no. 10, pp. 1553–1565, 2012.
- [20] S. Dehbandi, E. J. Speckmann, H. C. Pape, and A. Gorji, "Cortical spreading depression modulates synaptic transmission of the rat lateral amygdala," *The European Journal of Neuroscience*, vol. 27, no. 8, pp. 2057–2065, 2008.
- [21] C. Mainero, J. Boshyan, and N. Hadjikhani, "Altered functional magnetic resonance imaging resting-state connectivity in periaqueductal gray networks in migraine," *Annals of Neurology*, vol. 70, no. 5, pp. 838–845, 2011.
- [22] D. Akcali, A. Sayin, Y. Sara, and H. Bolay, "Does single cortical spreading depression elicit pain behaviour in freely moving rats?," *Cephalalgia*, vol. 30, no. 10, pp. 1195–1206, 2010.
- [23] Z. Jia and S. Yu, "Grey matter alterations in migraine: a systematic review and meta-analysis," *NeuroImage: Clinical*, vol. 14, pp. 130–140, 2017.
- [24] A. K. Husøy, C. Pintzka, L. Eikenes et al., "Volume and shape of subcortical grey matter structures related to headache: a cross-sectional population-based imaging study in the Nord-Trøndelag health study," *Cephalalgia*, vol. 39, no. 2, pp. 173–184, 2019.
- [25] Y. Zhang, J. Liu, H. Li et al., "Transcutaneous auricular vagus nerve stimulation at 1 Hz modulates locus coeruleus activity and resting state functional connectivity in patients with migraine: an fMRI study," *NeuroImage: Clinical*, vol. 24, p. 101971, 2019.
- [26] Headache Classification Subcommittee of the International Headache Society, "The international classification of headache disorders," *Cephalalgia*, vol. 24 Supplement 1, pp. 9–160, 2004.



- [27] P. J. Rong, J. L. Fang, L. P. Wang et al., "Transcutaneous vagus nerve stimulation for the treatment of depression: a study protocol for a double blinded randomized clinical trial," *BMC Complementary and Alternative Medicine*, vol. 12, p. 255, 2012.
- [28] Y. Tu, J. Fang, J. Cao et al., "A distinct biomarker of continuous transcutaneous vagus nerve stimulation treatment in major depressive disorder," *Brain Stimulation*, vol. 11, no. 3, pp. 501–508, 2018.
- [29] B. W. Badran, L. T. Dowdle, O. J. Mithoefer et al., "Neurophysiologic effects of transcutaneous auricular vagus nerve stimulation (taVNS) via electrical stimulation of the tragus: a concurrent taVNS/fMRI study and review," *Brain Stimulation*, vol. 11, no. 3, pp. 492–500, 2018.
- [30] M. L. Loggia, R. R. Edwards, J. Kim et al., "Disentangling linear and nonlinear brain responses to evoked deep tissue pain," *Pain*, vol. 153, no. 10, pp. 2140–2151, 2012.
- [31] B. A. Vogt, S. Derbyshire, and A. K. P. Jones, "Pain processing in four regions of human cingulate cortex localized with co-registered PET and MR imaging," *The European Journal of Neuroscience*, vol. 8, no. 7, pp. 1461–1473, 1996.
- [32] Y. Argaman, L. B. Kisler, Y. Granovsky et al., "The endogenous analgesia signature in the resting brain of healthy adults and migraineurs," *The Journal of Pain*, vol. 21, no. 7–8, pp. 905–918, 2020.
- [33] J. Fang, N. Egorova, P. Rong et al., "Early cortical biomarkers of longitudinal transcutaneous vagus nerve stimulation treatment success in depression," *Neuroimage Clinical*, vol. 14, pp. 105–111, 2017.
- [34] L. Garcia-Larrea and R. Peyron, "Pain matrices and neuropathic pain matrices: a review," *Pain*, vol. 154, Suppl 1, pp. S29–S43, 2013.
- [35] Z. Chen, X. Chen, M. Liu, Z. Dong, L. Ma, and S. Yu, "Altered functional connectivity of amygdala underlying the neuromechanism of migraine pathogenesis," *The Journal of Headache and Pain*, vol. 18, no. 1, p. 7, 2017.
- [36] R. Babygirija, M. Sood, P. Kannampalli, J. N. Sengupta, and A. Miranda, "Percutaneous electrical nerve field stimulation modulates central pain pathways and attenuates post-inflammatory visceral and somatic hyperalgesia in rats," *Neuroscience*, vol. 356, pp. 11–21, 2017.
- [37] S.-P. Chen, I. Ay, A. L. de Moraes et al., "Vagus nerve stimulation inhibits cortical spreading depression," *Pain*, vol. 157, no. 4, pp. 797–805, 2016.
- [38] R. Laqua, B. Leutzow, M. Wendt, and T. Usichenko, "Transcutaneous vagal nerve stimulation may elicit anti- and pronociceptive effects under experimentally-induced pain - a crossover placebo-controlled investigation," *Autonomic Neuroscience*, vol. 185, pp. 120–122, 2014.
- [39] A. Straube, J. Ellrich, O. Eren, B. Blum, and R. Ruscheweyh, "Treatment of chronic migraine with transcutaneous stimulation of the auricular branch of the vagal nerve (auricular t-VNS): a randomized, monocentric clinical trial," *The Journal of Headache and Pain*, vol. 16, no. 1, p. 543, 2015.
- [40] R. G. Garcia, R. L. Lin, J. Lee et al., "Modulation of brainstem activity and connectivity by respiratory-gated auricular vagal afferent nerve stimulation in migraine patients," *Pain*, vol. 158, no. 8, pp. 1461–1472, 2017.
- [41] H. Yuan and S. D. Silberstein, "Vagus nerve and vagus nerve stimulation, a comprehensive review: part III," *Headache*, vol. 56, no. 3, pp. 479–490, 2016.
- [42] E. Kaniusas, S. Kampusch, M. Tittgemeyer et al., "Current directions in the auricular vagus nerve stimulation I - a physiological perspective," *Frontiers in Neuroscience*, vol. 13, p. 854, 2019.
- [43] S. A. Deuchars, V. K. Lall, J. Clancy et al., "Mechanisms underpinning sympathetic nervous activity and its modulation using transcutaneous vagus nerve stimulation," *Experimental Physiology*, vol. 103, no. 3, pp. 326–331, 2018.
- [44] B. Bonaz, V. Sinniger, and S. Pellissier, "Anti-inflammatory properties of the vagus nerve: potential therapeutic implications of vagus nerve stimulation," *The Journal of Physiology*, vol. 594, no. 20, pp. 5781–5790, 2016.
- [45] S. Akerman, B. Simon, and M. Romero-Reyes, "Vagus nerve stimulation suppresses acute noxious activation of trigeminocervical neurons in animal models of primary headache," *Neurobiology of Disease*, vol. 102, pp. 96–104, 2017.
- [46] C. Bohotin, M. Scholsem, V. Bohotin, R. Franzen, and J. Schoenen, "Vagus nerve stimulation attenuates heat- and formalin-induced pain in rats," *Neuroscience Letters*, vol. 351, no. 2, pp. 79–82, 2003.
- [47] D. F. Peña, J. E. Childs, S. Willett, A. Vital, C. K. McIntyre, and S. Kroener, "Vagus nerve stimulation enhances extinction of conditioned fear and modulates plasticity in the pathway from the ventromedial prefrontal cortex to the amygdala," *Frontiers in Behavioral Neuroscience*, vol. 8, 2014.
- [48] H.-L. Wei, J. Chen, Y.-C. Chen et al., "Impaired functional connectivity of limbic system in migraine without aura," *Brain Imaging and Behavior*, vol. 14, no. 5, pp. 1805–1814, 2020.
- [49] A. Xiang, Y. Yu, X. Jia et al., "The low-frequency BOLD signal oscillation response in the insular associated to immediate analgesia of ankle acupuncture in patients with chronic low back pain," *Journal of Pain Research*, vol. Volume 12, pp. 841–850, 2019.
- [50] J. Liu, J. Fang, Z. Wang et al., "Transcutaneous vagus nerve stimulation modulates amygdala functional connectivity in patients with depression," *Journal of Affective Disorders*, vol. 205, pp. 319–326, 2016.
- [51] I. Morrison, M. V. Peelen, and P. E. Downing, "The sight of others' pain modulates motor processing in human cingulate cortex," *Cerebral Cortex*, vol. 17, no. 9, pp. 2214–2222, 2007.
- [52] S. Soheili-Nezhad, A. Sedghi, F. Schweser et al., "Structural and functional reorganization of the brain in migraine without aura," *Frontiers in Neurology*, vol. 10, p. 442, 2019.
- [53] Y. Zou, W. Tang, X. Li, M. Xu, and J. Li, "Acupuncture reversible effects on altered default mode network of chronic migraine accompanied with clinical symptom relief," *Neural Plasticity*, vol. 2019, Article ID 5047463, 10 pages, 2019.
- [54] M. Shpaner, C. Kelly, G. Lieberman et al., "Unlearning chronic pain: a randomized controlled trial to investigate changes in intrinsic brain connectivity following cognitive behavioral therapy," *NeuroImage: Clinical*, vol. 5, pp. 365–376, 2014.
- [55] J. Fang, P. Rong, Y. Hong et al., "Transcutaneous vagus nerve stimulation modulates default mode network in major depressive disorder," *Biological Psychiatry*, vol. 79, no. 4, pp. 266–273, 2016.
- [56] N. Toschi, A. Duggento, and L. Passamonti, "Functional connectivity in amygdalar-sensory/(pre)motor networks at rest: new evidence from the human connectome project," *The European Journal of Neuroscience*, vol. 45, no. 9, pp. 1224–1229, 2017.



- [57] Y. Shi, Z. Liu, S. Zhang et al., "Brain network response to acupuncture stimuli in experimental acute low back pain: an fMRI study," *Evidence-based Complementary and Alternative Medicine*, vol. 2015, Article ID 210120, 13 pages, 2015.
- [58] L. S. Dahlberg, C. N. Linnman, D. Lee, R. Burstein, L. Becerra, and D. Borsook, "Responsivity of periaqueductal gray connectivity is related to headache frequency in episodic migraine," *Frontiers in Neurology*, vol. 9, 2018.

## Review Article

# The Effectiveness and Safety of Manual Acupuncture Therapy in Patients with Poststroke Cognitive Impairment: A Meta-analysis

Wei Liu , Chang Rao , Yuzheng Du , Lili Zhang , and Jipeng Yang 

First Teaching Hospital of Tianjin University of Traditional Chinese Medicine, Tianjin, China

Correspondence should be addressed to Yuzheng Du; drduyuzheng@163.com

Wei Liu and Chang Rao contributed equally to this work.

Received 19 June 2020; Revised 7 October 2020; Accepted 28 October 2020; Published 25 November 2020

Academic Editor: Zhen Zheng

Copyright © 2020 Wei Liu et al. This is an open access article distributed under the Creative Commons Attribution License, which permits unrestricted use, distribution, and reproduction in any medium, provided the original work is properly cited.

**Background.** Poststroke cognitive impairment (PSCI) is a common cause of disability among patients with stroke. Meanwhile, acupuncture has increasingly been used to improve motor and cognitive function for stroke patients. The aim of the present study was to summarize and evaluate the evidence on the effectiveness of acupuncture in treating PSCI. **Methods.** Eight databases (PubMed, The Cochrane Library, CNKI, WanFang Data, VIP, CBM, Medline, Embase databases) were searched from January 2010 to January 2020. Meta-analyses were conducted for the eligible randomized controlled trials (RCTs). Assessments were performed using Mini-Mental State Examination (MMSE), Montreal Cognitive Assessment (MoCA), Barthel Index (BI), or modified Barthel Index (MBI). **Results.** A total of 657 relevant RCTs were identified, and 22 RCTs with 1856 patients were eventually included. Meta-analysis showed that acupuncture appeared to be effective for improving cognitive function as assessed by MMSE (mean difference (MD) = 1.73, 95% confidence interval (CI) (1.39, 2.06),  $P < 0.00001$ ) and MoCA (MD = 2.32, 95% CI (1.92, 2.73),  $P < 0.00001$ ). Furthermore, it also suggested that acupuncture could improve the activities of daily life (ADL) for PSCI patients as assessed by BI or MBI (SMD = 0.97, 95% CI (0.57, 1.38),  $P < 0.00001$ ). **Conclusions.** Compared with nonacupuncture group, acupuncture group showed better effects in improving the scores of MMSE, MoCA, BI, and MBI. This meta-analysis provided positive evidence that acupuncture may be effective in improving cognitive function and activities of daily life for PSCI patients. Meanwhile, long retention time of acupuncture may improve cognitive function and activities of daily life, and twist technique may be an important factor that could influence cognitive function. However, further studies using large samples and a rigorous study design are needed to confirm the role of acupuncture in the treatment of PSCI.

## 1. Introduction

Stroke ranks only second to ischemic heart disease as the leading cause of death and the third leading cause of disability-adjusted life-years (DALYs) lost worldwide [1]. In China, with over 2 million new cases annually, stroke has a close relationship with the highest DALYs lost of any disease [2]. Cognitive decline is a major cause of disability in stroke survivors [3]. It is estimated that 11.8 million patients who have had a stroke, 9.5 million of whom have had cognitive impairments after their stroke [4].

Poststroke cognitive impairment (PSCI) contains two different degrees of cognitive impairment, including post-stroke cognitive impairment with no dementia (PSCIND) and poststroke dementia (PSD) [5]. In the study [6] which enrolled 620 patients in 12 hospitals with ischemic stroke, of the 506 patients who were followed-up at 3 months after stroke, 353 patients (69.8%) suffered cognitive impairment as measured by the Korean Vascular Cognitive Impairment Harmonization Standards neuropsychological protocol (K-VCIHS-NP). In America, the study on 212 subjects from the Framingham Study suggested that 19.3% of cases

developed into dementia in 10 years after stroke [7]. PSCI is strongly related to a higher risk of mortality [8], poor functional outcome [9], and poor quality of life [10]. Identifying patients at risk of cognitive impairment is, therefore, important as well as targeting interventions to this group.

Unfortunately, treatment of PSCI has not been standardized [11]. So far, there are many drugs to improve cognitive, including acetylcholinesterase inhibitors, memantine [12], and nicergoline [13]. But because of the unclear efficacy and side effect, until now, there is a none drug that has been approved by the Food and Drug Administration (FDA) to treat vascular cognitive impairment [14].

In recent years, the spectrum of diseases suitable for acupuncture abroad has been significantly broader, like nervous system, muscular tissue, skeletal system, connective tissue, mental and behavioral disorders, digestive system, and respiratory system [15]. The World Health Organization has also recommended acupuncture as an alternative and complementary strategy for stroke treatment and improvement [16]. In the treatment of apoplexy sequelae, acupuncture is mainly used to treat dyspraxia [17], enhance life quality [18], improve cognition [19], and deal with depression and anxiety [20]. Animal experiments [21] showed that acupuncture could improve cognitive function by stimulating cholinergic enzyme activity and regulating brain-derived neurotrophic factor (BDNF) and cAMP-response element-binding protein (CREB) expression in the rats' brain; Cai et al. [22] demonstrated that electroacupuncture can improve cognitive impairment in Alzheimer's disease mice by inhibiting synaptic degeneration and neuroinflammation.

After searching the database, we found that there were few systematic reviews or meta-analysis focused on the effectiveness of acupuncture in treating PSCI recently, although the number of papers related to this area has an upward trend in the last five years. For instance, the latest meta-analyses on acupuncture treating PSCI were published in 2014 [23] and 2016 [24]. But due to the limitation of sample size and the quality of trials included in the former one, the effectiveness of acupuncture in treating PSCI has not been fully determined. Meanwhile, the later one which also lacked quality randomized controlled trials (RCTs) was merely focused on the effectiveness of scalp acupuncture. Therefore, the purpose of this study is to evaluate the clinical efficacy of acupuncture in the treatment of PSCI by meta-analysis and provide evidence for its rational clinical application.

## 2. Methods

**2.1. Search Methods for Identification of Studies.** We searched CNKI, WanFang Data, VIP, CBM, PubMed, Medline, Embase, and The Cochrane Library to collect randomized controlled trials of acupuncture in the treatment of PSCI published in both Chinese and English. The retrieval time was from January 2010 to January 2020. Searching terms included stroke, cerebral infarction, encephalorrhagia, cognitive impairment and so on. For example, the searching strategy we used on Pubmed is (((cognitive[Title/Abstract]) OR Cognition[Title/Abstract])) AND (((((stroke[Title/Abstract]) OR cerebral infarction[Title/Abstract]) OR apoplex-

y[Title/Abstract]) OR hematencephalon[Title/Abstract]) OR encephalorrhagia[Title/Abstract]) OR cerebral hemorrhage[Title/Abstract]) OR infarct of brain[Title/Abstract])) AND acupuncture[Title/Abstract].

**2.2. Inclusion/exclusion Criteria.** Relevant clinical trials were included if the following criteria were met: (1) they were randomized controlled trials (RCTs); (2) they included patients diagnosed with poststroke cognitive impairment; (3) they use cognitive function as an outcome measure; (4) the difference of interventions between experimental and control groups is whether they use acupuncture or not. To be more precise, the intervention of experimental group is acupuncture therapy plus another therapy or standard treatment; the intervention of control group is standard treatment or the therapy which also be used in the experimental group except acupuncture therapy. If trials which met above criteria contained more than two groups, the group receiving acupuncture was chosen as the experimental group, and the nonacupuncture treatment group was chosen as the control group.

Trials were excluded if they met any of the following criteria: (1) acupuncture were used in the control group; (2) neither the Mini-Mental State Examination (MMSE) nor the Montreal Cognitive Assessment (MoCA) was used as cognitive function evaluation scale; (3) specific type of acupuncture treatment was used in the experimental group, such as electroacupuncture and laser needles for acupuncture.

**2.3. Data Extraction.** Two reviewers (L.W. and R.C.) independently extracted the general information of the included trials and reached consensus on all items. Extracted data included authors, year of publication, sample size, source of diagnosis, interventions, main outcomes, and information about acupuncture treatment (including course, frequency, and retention time).

Measures of the outcome evaluation that were reported in the included studies were Mini-Mental State Examination (MMSE), Montreal Cognitive Assessment (MoCA), Barthel Index (BI), or modified Barthel Index (MBI). MMSE which contains domains of orientation, memory, attention, language, and visuospatial ability is the most common used screening scale [25, 26]. MoCA, which is also a cognitive screening and tracking tool, is more useful for the mild stages of the cognitive impairment [27]. It is composed of several cognitive domains such as memory, executive function, attention, language, abstraction, naming, delayed recalls, and orientation [28]. BI is one of the most widely used outcome measures to assess functioning for the patients who have neurological disorders [29, 30]. It consists of 10 others' rated questions which are for the purpose of evaluating the ability of daily life [31].

**2.4. Quality Assessment.** The methodological quality and the risk of bias of the included studies were evaluated by the risk of bias 2.0 (ROB 2.0) tool. One author assessed the risk of bias of included studies by using ROB 2.0, and the other author confirmed the judgment. The following items were categorized as having high, low, or unclear risk of bias:

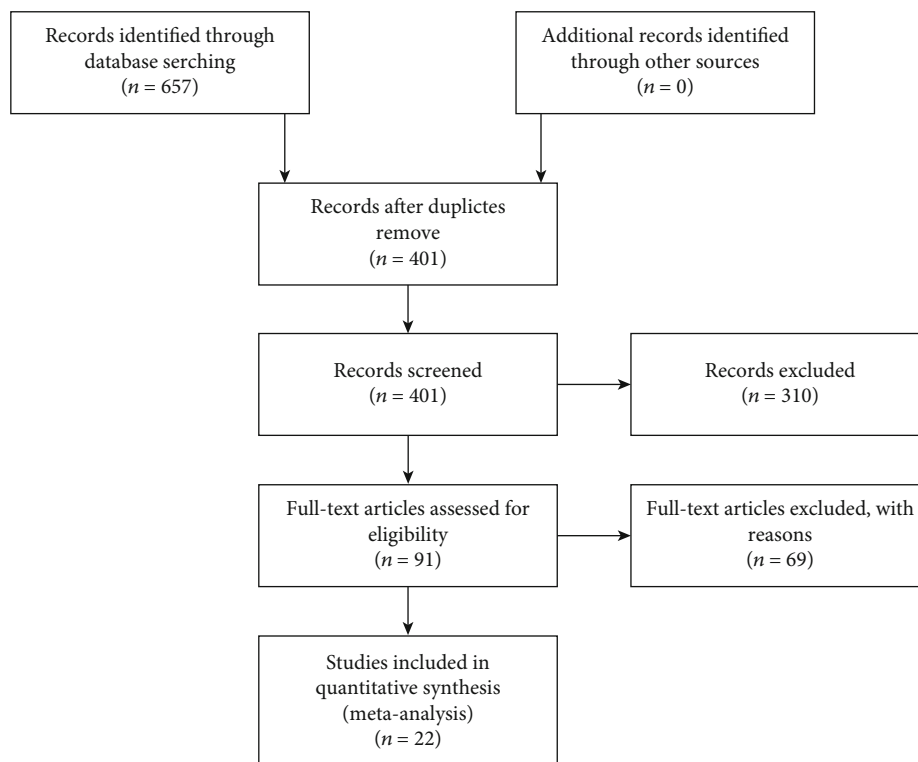


FIGURE 1: Flow diagram of the systematic review.

randomization process, deviations from intended interventions, missing outcome data, measurement of the outcome, and selection of the reported result and overall.

**2.5. Statistical Analysis.** The Review Manager software (version 5.3 Cochrane Collaboration, Oxford, United Kingdom) was used to perform most of the statistical analysis. The mean difference (MD) which was used as the effect analysis statistics for continuous data was calculated with a 95% confidence interval (CI).

The  $I^2$  statistic was used to analyze the heterogeneity between the data of included trials. If the figure of  $I^2$  was above 50%, which means significant heterogeneity, sensitivity analysis would be performed to analysis the source of heterogeneity. Random-effects model was applied to calculate the study results with significant heterogeneity, while a fixed effect model is used if the statistical heterogeneity was inapparent. Publication bias was detected using a funnel plot.

### 3. Results

**3.1. Study Description.** Our search identified 657 articles after removing duplicates. Among them, 22 RCTs met our inclusion criteria and were included in this study (Figure 1). The articles included in the analysis are summarized in Table 1. There are 2 in English [32, 33] and 20 articles in Chinese [34–53].

**3.2. Study Quality.** The risk of bias assessment of the included RCTs is illustrated in Figure 2. With regard to randomization process, 4 studies had a low ROB, and 18 studies had an unclear ROB. With regard to deviations from intended inter-

ventions, all RCTs had a low ROB. With regard to missing outcome data, 16 studies had a low ROB, and 6 studies had a high ROB. With regard to measurement of the outcome, 2 studies had a low ROB, and 20 studies had an unclear ROB. With regard to selection of the reported result, 1 study had a low ROB, and 21 studies had an unclear ROB.

**3.3. Descriptions of Acupuncture Treatment.** The acupuncture interventions of the included trials varied across the 22 trials. The majority of the studies [32, 35–39, 42–45] used acupuncture with medicine, such as cholinesterase inhibitor or lipid-lowering medication, as the intervention of the experiment group. Eight studies [34, 41, 46–48, 50–52] used acupuncture with cognitive training; two studies [33, 53] used acupuncture alone; two studies [42, 49] used acupuncture with rehabilitation training.

In terms of acupoint selecting, single area acupoint points were used in five studies [39, 40, 45, 49, 50], including the eye, ear, and scalp acupuncture. Special acupuncture therapy, Jin three-needle therapy, and tri-jiao therapy were also used in three studies [46, 47, 53]. Apart from that, a total of 33 acupoints were selected in other 14 studies. Acupoints used for cognitive impairment in most trials were DU 20 (Bai Hui) and DU24 (Shen Ting) (Figure 3).

**3.4. Effects of Acupuncture Treatment According to MMSE Assessment Scales.** A total of 17 studies reported MMSE scores, including 1389 patients. Heterogeneity test results showed high heterogeneity between groups ( $I^2 = 95%$ ,  $P < 0.00001$ ). Sensitivity analysis was done by using the leave-one-out approach; five studies [40, 46, 48, 51, 53] were found

TABLE 1: Summary of randomized controlled trials of acupuncture for PSCI.

Author (year)	Sample size	Participants Average age (years) <sup>(i)</sup>	Sex (male/female)	Source of diagnostic	Intervention group regimen	Control group regimen	Main outcomes	Acupuncture course	Acupuncture frequency	Acupuncture retention time
Wang 2016 [32]	79	<sup>a</sup> 65.2 ± 7.1	<sup>a</sup> 26/14	Stroke: CT or MRI	Acupuncture	Nimodipine	1. MoCA	12 weeks	5 times per week	30 min
Jiang 2016 [33]	101	<sup>b</sup> 60.6 ± 6.7	<sup>b</sup> 26/13	CI: MoCA	Nimodipine	Conventional treatment	1. MMSE 2. MoCA 3. FIM	12 weeks	5 times per week	30 min
		<sup>a</sup> 61.58 ± 9.71	<sup>a</sup> 25/27	Stroke: clinical diagnosis	Acupuncture					
Wang 2018 [34]	115	<sup>b</sup> 60.53 ± 9.19	<sup>b</sup> 24/25	CI: MMSE	Conventional treatment	Conventional treatment Cognitive training	1. MMSE 2. TCD 3. NO 4. TG, HDL-C, LDL-C, TC	3 months	Daily	Scalp acupuncture: 6 h Body acupuncture: 0.5 h
		<sup>a</sup> 52.37 ± 8.43	<sup>a</sup> 30/25	Stroke: CT or MRI	Acupuncture					
Bao 2012 [35]	60	<sup>b</sup> 64 ± 6	<sup>b</sup> 21/9	CI: MMSE	Donepezil	Donepezil	1. MMSE 2. MESS 3. Barthel	2 months	6 times per week	50 min
		<sup>a</sup> 63 ± 6	<sup>a</sup> 19/11	Stroke: CT or MRI	Acupuncture					
Zhang 2017 [36]	84	<sup>b</sup> 63.07 ± 10.59	<sup>b</sup> 28/14	CI: complain of memory loss	Atorvastatin	Atorvastatin	1. MMSE 2. WBV, HBV LBV	4 weeks	5 times per week	20 min
		<sup>a</sup> 63.28 ± 10.68	<sup>a</sup> 27/15	Stroke: CT or MRI	Acupuncture					
Wang Q 2019 [37]	118	<sup>b</sup> 67.71 ± 3.02	<sup>b</sup> 32/27	CI: complain of memory loss	Atorvastatin	Atorvastatin	1. MMSE 2. WBV, HBV LBV, FIB 3. SAS	30 days	Daily	30 min
		<sup>a</sup> 68.88 ± 3.64	<sup>a</sup> 36/23	Stroke: CT or MRI	Acupuncture					
Yang 2015 [38]	72	<sup>b</sup> 65.97 ± 3.308	<sup>b</sup> 21/15	CI: MoCA	Nimodipine	Nimodipine	1. MoCA	3 months	6 times per week	30 min
		<sup>a</sup> 65.89 ± 3.276	<sup>a</sup> 25/11	Stroke: CT or MRI	Acupuncture					
Du 2017 [39]	60	<sup>b</sup> 64.43 ± 3.27	<sup>b</sup> 14/16	CI: MMSE, CDR	Donepezil	Donepezil	1. MMSE 2. Barthel 3. Hcy	6 weeks	7 times per week	30 min
		<sup>a</sup> 64.60 ± 2.84	<sup>a</sup> 16/14	Stroke: CT or MRI	Acupuncture					
110	<sup>a</sup> 59.47 ± 8.62	<sup>a</sup> 36/19	Stroke: CT or MRI	Eye acupuncture	Eye acupuncture	1. MMSE	4 weeks	Daily	5 min	



TABLE 1: Continued.

Author (year)	Sample size	Participants Average age (years) <sup>[i]</sup>	Sex (male/female)	Source of diagnostic	Intervention group regimen	Control group regimen	Main outcomes	Acupuncture course	Acupuncture frequency	Acupuncture retention time
Teng 2018 [40]										
Qiu 2018 [41]	60	<sup>b</sup> 58.65 ± 8.17	<sup>b</sup> 35/20	CI: MMSE and LOTCA	Standard treatment Cognitive training	Cognitive training	2. LOTCA	1 month	5 times per week	30 min
		<sup>a</sup> 54.18 ± 4.137	<sup>a</sup> 17/11	Stroke: MRI	Acupuncture	Standard treatment	1. MoCA	1 month	5 times per week	30 min
		<sup>b</sup> 54.93 ± 3.443	<sup>b</sup> 19/10	CI: MoCA, NCSE	Standard treatment Rehabilitation	Rehabilitation	2. EEG signal			
Li 2019 [42]	80	<sup>a</sup> 66.9 ± 5.9	<sup>a</sup> 18/22	Stroke: CT or MRI	Acupuncture	Standard treatment	1. MoCA	6 weeks	5 times per week	30 min
		<sup>b</sup> 67.4 ± 6.1	<sup>b</sup> 22/18	CI: MoCA, MMSE	Donepezil Standard treatment	Donepezil	2. MMSE			
		<sup>a</sup> 66.9 ± 11.1	<sup>a</sup> 39/19	Stroke: standard <sup>[ii]</sup>	Acupuncture	Compound musk injection	1. GCS	3 weeks	5 times per week	30 min
		<sup>b</sup> 65.9 ± 11.5	<sup>b</sup> 29/26	CI: standard <sup>[iii]</sup>	Compound musk injection	Compound musk injection	2. MoCA			
							3. Barthel			
							4. Assessment of scores for TCM			
							5. Hematoma volume			
Nie 2019 [44]	63	---	<sup>a</sup> 16/14	Stroke: CT or MRI	Acupuncture	Butyphthalide	1. MoCA	40 days	Daily	30 min
			<sup>b</sup> 18/12	CI: MoCA, MMSE	Butyphthalide Standard treatment	Standard treatment	2. MMSE			
		<sup>a</sup> 60 ± 6	<sup>a</sup> 16/14	Stroke: CT or MRI	Acupuncture	Piracetam	3. ADL			
		<sup>b</sup> 60 ± 6	<sup>b</sup> 18/12	CI: CCSE	Piracetam	Piracetam	4. Ngb			
							1. MMSE	4 weeks	5 times per week	6 h
							2. Plasma cortisol			



TABLE 1: Continued.

Author (year)	Sample size	Participants Average age (years) <sup>[i]</sup>	Sex (male/female)	Source of diagnostic	Intervention group regimen	Control group regimen	Main outcomes	Acupuncture course	Acupuncture frequency	Acupuncture retention time
Song 2017 [51]	62	<sup>a</sup> 56.37 ± 1.27	<sup>a</sup> 24/7	Stroke: CT or MRI	Acupuncture	Standard treatment	1. MMSE	12 weeks	5 times per week	30 min
Zhang 2018 [52]	63	<sup>b</sup> 58.19 ± 1.24	<sup>b</sup> 19/12	CI: MMSE	Standard treatment	Cognitive training	2. miR-124, miR-132, miR-134, miR-138 expression levels	4 weeks	6 times per week	30 min
					Acupuncture	Cognitive training				
Li 2012 [53]	60	<sup>a</sup> 67.31 ± 10.98	—	Stroke: CT or MRI	Standard treatment	Standard treatment	1. MMSE	3 weeks	6 times per week	30 min
					Acupuncture	Cognitive training				
		<sup>b</sup> 66.24 ± 12.53		CI: MMSE	Standard treatment		3. Barthel			
							1. MMSE			
							2. ADL			

<sup>[i]</sup>Experimental group; <sup>[ii]</sup>control group. <sup>[iii]</sup>Key points for diagnosis of various cerebrovascular diseases. <sup>[iv]</sup>National Institute of Neurological Disorders and Stroke-Canadian stroke network vascular cognitive impairment harmonization standards. <sup>[v]</sup>Spectrum of disease in vascular cognitive impairment.

	Randomization process	Deviations from intended interventions	Missing outcome data	Measurement of the outcome	Selection of the reported result	Overall
Zhang 2019	?	+	+	?	?	!
Wang Z 2019	?	+	+	?	?	!
Wang Q 2019	?	+	?	?	?	?
Nie 2019	?	+	+	?	?	!
Mao 2019	?	+	?	?	?	?
Li 2019	?	+	+	?	?	!
Ding 2019	?	+	+	?	?	!
Zhang 2018	?	+	+	?	?	!
Wang 2018	?	+	?	?	?	!
Tang 2018	?	+	+	?	?	?
Qiu 2018	?	+	+	+	?	!
Zeng 2018	?	+	+	?	?	!
Zhang 2017	?	+	+	?	?	!
Song 2017	+	+	?	?	?	!
Du 2017	?	+	?	?	?	?
Liu 2016	?	+	+	?	?	!
Wang 2016	+	+	+	+	?	!
Jiang 2016	+	+	?	+	+	+
Yang 2015	+	+	+	?	?	?
Li 2012	?	+	+	?	?	!
Bao 2012	?	+	+	?	?	!
Bai 2012	?	+	+	?	?	!

+ Low risk  
 ? Some concerns  
 ? High risk

FIGURE 2: Risk of bias assessment for included studies.

which could vary the direction of the combined estimates. Three [40, 48, 51] of them were removed for incorrect using of MMSE. The score of MMSE should be related to education level when detecting cognitive impairment [54], but these studies used same scoring criteria for people with different educational levels in the inclusion criteria which could cause that patients without cognitive impairment, but low educa-

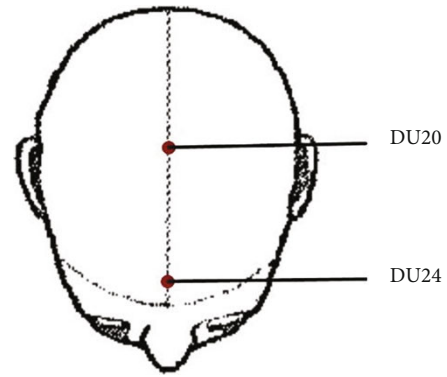


FIGURE 3: DU 20 (Bai Hui) and DU24 (Shen Ting).

tional level were included in the studies. In addition, another two [46, 53] of them that we removed could significantly vary the direction of the combined estimates (test for subgroup differences:  $\chi^2 = 187.08$ ,  $df = 1$  ( $P < 0.00001$ ),  $I^2 = 99.5\%$ ) (Figure 4). After studying the full articles carefully, we found that the difference between these two and other article is that they both used Jin 3-needle technique which has a unique twist technique. This indicated that the source of heterogeneity might be related to the frequency and duration of twist technique. It also illustrated that twist technique may influence the effect of improving cognitive function, as the studies used Jin 3-needle technique (MD = 11.82, 95% CI (10.41, 13.23),  $P < 0.00001$ ,  $I^2 = 0\%$ ) had better outcomes than the studies did not (MD = 1.73, 95% CI (1.39, 2.06),  $P < 0.00001$ ,  $I^2 = 50\%$ ). However, further research is still needed due to the small number of included studies using Jin 3-needle technique.

Finally, after sensitivity analysis, a total of 12 studies were included for evaluating the effect of acupuncture treatment according to MMSE. The fixed effect model was used for analysis on the basis of heterogeneity test ( $I^2 = 50\%$ ). The results of meta-analysis showed that the MMSE score of the acupuncture treatment group was higher than that of the control group (MD = 1.73, 95% CI (1.39, 2.06),  $P < 0.00001$ ). According to subgroup analysis based on treatment duration, meta-analysis results showed that MMSE score of the acupuncture treatment group was higher than that of the treatment group in  $\leq 7$ -week subgroup (MD = 1.63, 95% CI (1.28, 1.99),  $P < 0.00001$ ,  $I^2 = 60\%$ ). MMSE score in the  $> 7$ -week subgroup was higher than that in the treatment group (MD = 2.36, 95% CI (1.43, 3.29),  $P < 0.00001$ ,  $I^2 = 0\%$ ) (Figure 5). It illustrated that the duration of acupuncture treatment was also a factor that could influence heterogeneity but have few effect on the outcomes. We also conducted subgroup analysis based on retention time and frequency of acupuncture, but those did not have much influence on heterogeneity or outcomes.

3.5. Effects of Acupuncture Treatment According to MoCA Assessment Scales. There are nine [32, 33, 38, 41–44, 49, 52] trials that used MoCA to compare the cognitive function between acupuncture group and nonacupuncture group. A high statistical heterogeneity was observed ( $I^2 = 84\% > 50\%$ ).

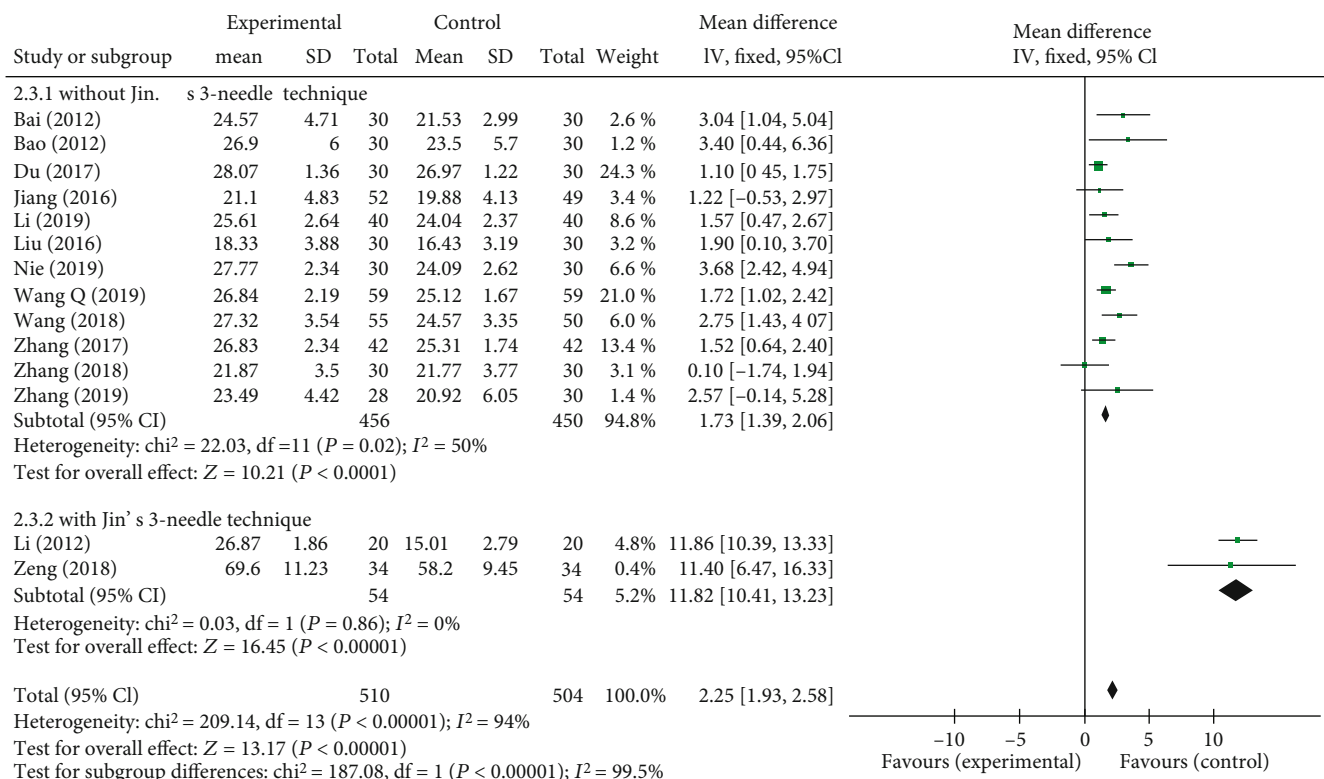


FIGURE 4: The forest plots of MMSE (subgroup: with or without Jin 3-needle technique).

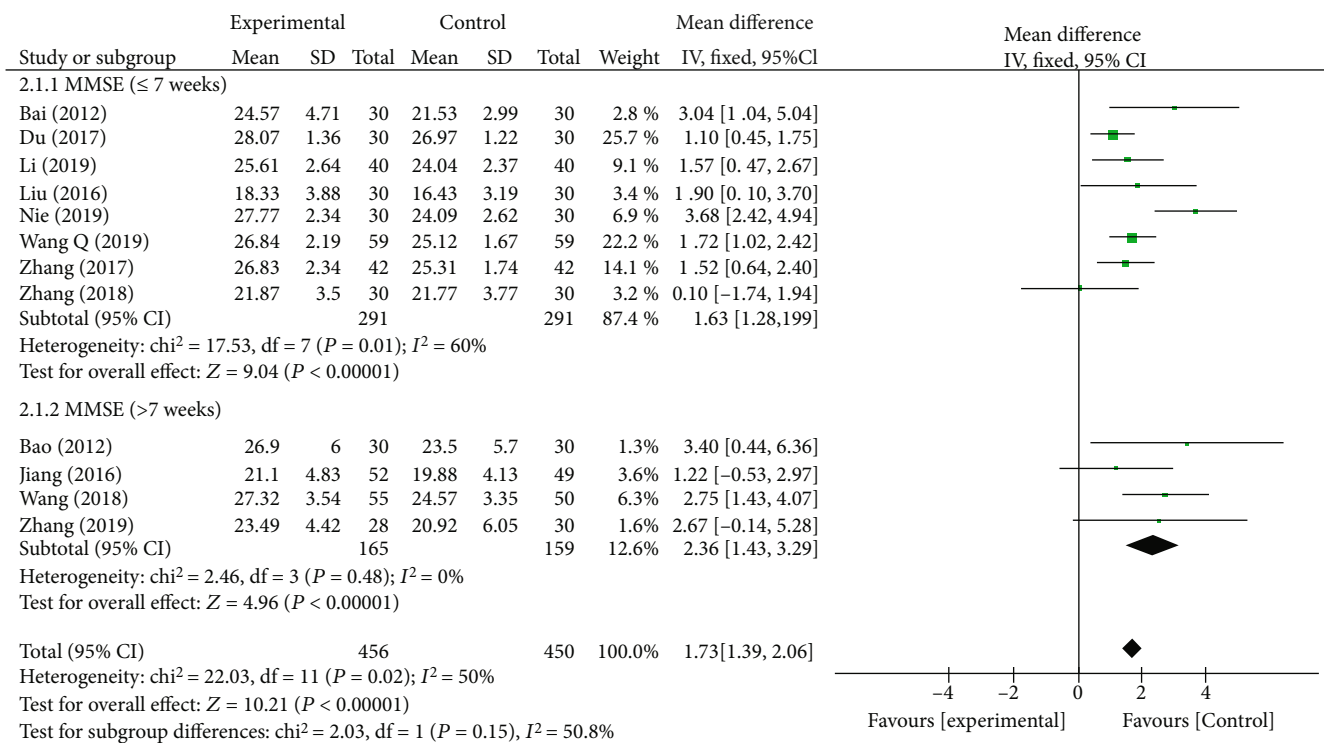


FIGURE 5: The forest plots of MMSE (subgroup: course  $\leq 7$  weeks or course  $> 7$  weeks).

After using sensitivity analysis of studies, we found one article [49] that had relatively large impact on statistical heterogeneity. What distinguishes it from other studies is the retention

time of acupuncture, so we conducted subgroup analysis based on retention time (Figure 6). It shows that the score of MoCA in the acupuncture group was observed to be higher than that



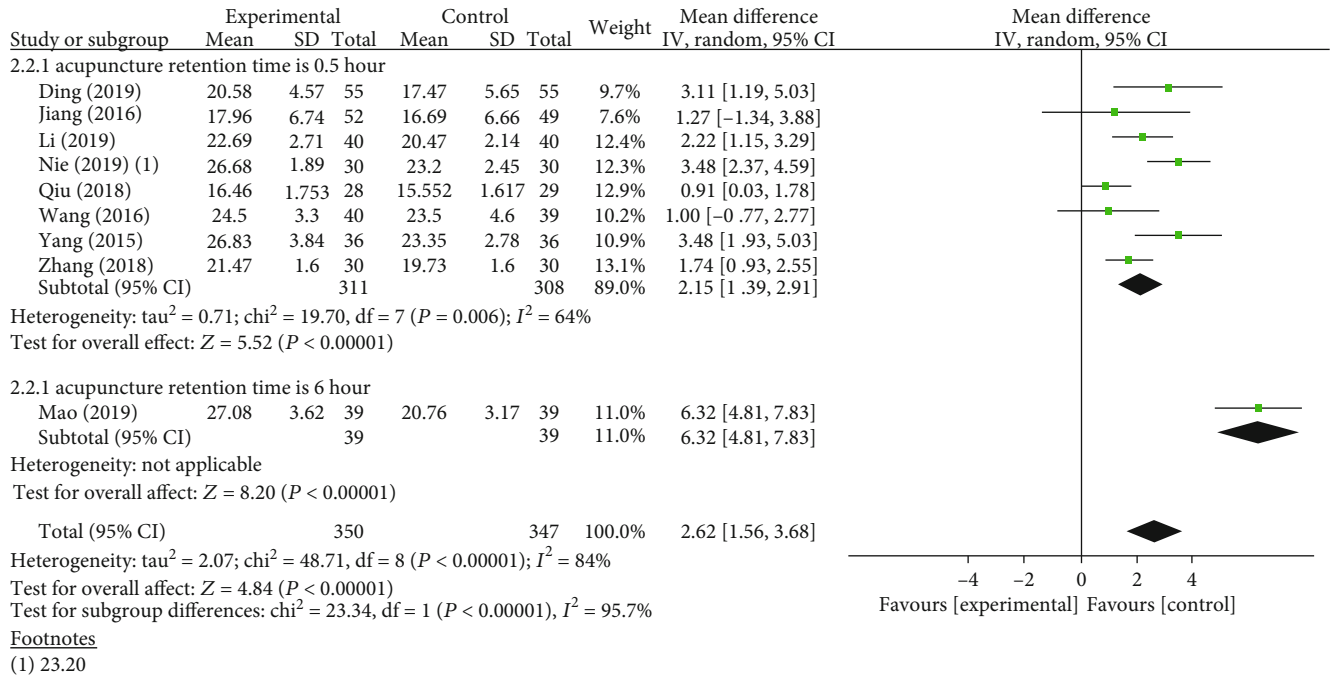


FIGURE 6: The forest plots of MoCA.

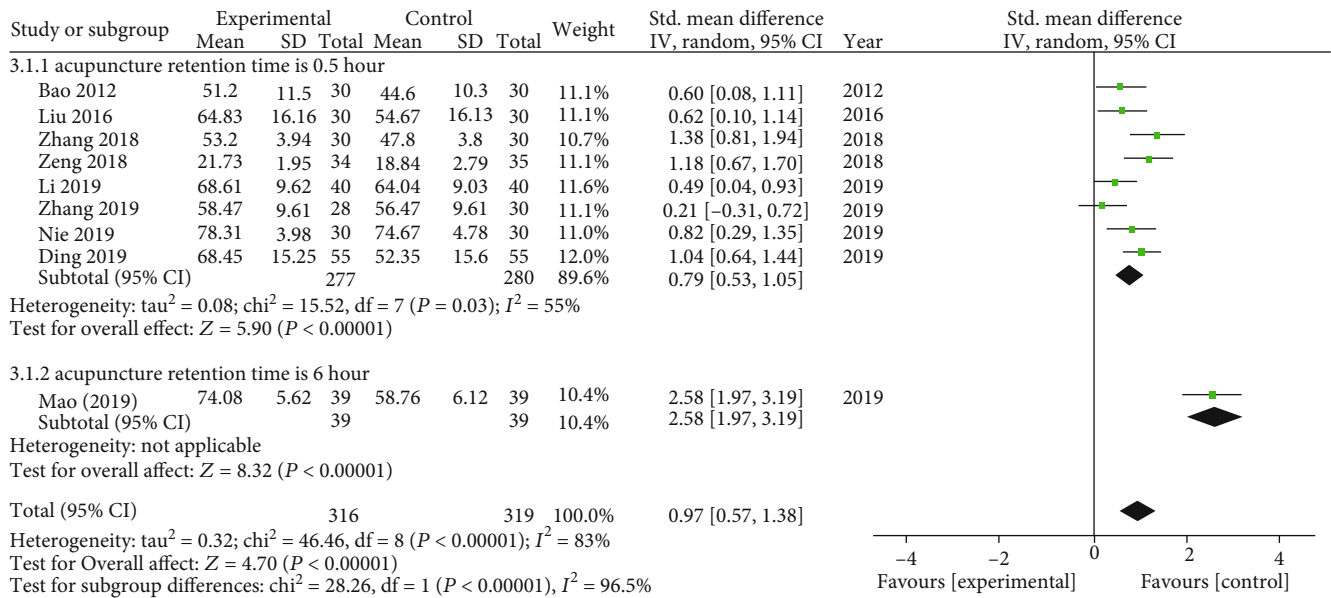


FIGURE 7: The forest plots of activities of daily life.

in the nonacupuncture group (MD = 2.32, 95% CI (1.92, 2.73), P < 0.00001); the difference is statistically significant. It also illustrated that retention time may also influence the effect of improving MoCA score, as the study with retention time of 6h (MD = 6.32, 95% CI (4.81, 7.83), P < 0.00001) had better outcomes than the studies with retention time of 0.5h (MD = 2.15, 95% CI (1.39, 2.91), P < 0.00001, I<sup>2</sup> = 64%). However, further research is still needed due to the small number of included studies with long retention time.

3.6. *Effects of Acupuncture Treatment According to Activities of Daily Living.* There are nine [35, 42–44, 46, 47, 49, 50, 52] trials that used Barthel Index or modified Barthel Index to compare ADL between acupuncture group and nonacupuncture group. The other two trials [48, 53] also mentioned they evaluated ADL but did not specified what kind of scale they used; therefore, we did not include them in this analysis. A high statistical heterogeneity was observed (I<sup>2</sup> = 83% > 50%). Therefore, random-effects model analysis

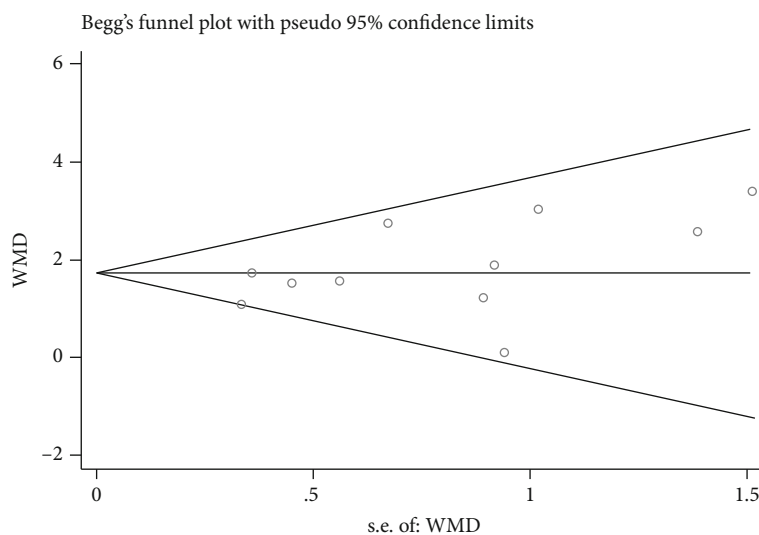


FIGURE 8: Begg's funnel plot.

Begg's test			
adj. Kendall's score (P-Q)	=		16
Std. dev. of score	=		14.58
Number of studies	=		12
$z$	=		1.10
Pr > $ z $	=		0.273
$z$	=		1.03 (continuity corrected)
Pr > $ z $	=		0.304 (continuity corrected)

FIGURE 9: Begg's test.

was chosen to conduct meta-analysis. After using sensitivity analysis of studies, we found one article [49] that had relatively large impact on statistical heterogeneity. What distinguishes it from other studies was the retention time of acupuncture, so we conducted subgroup analysis based on retention time (Figure 7). Therefore, we divided the 9 articles into 2 groups according to the acupuncture retention time. It shows that the score in the acupuncture group was observed to be higher than that in the nonacupuncture group (SMD = 0.97, 95% CI (0.57, 1.38),  $P < 0.00001$ ); the difference is statistically significant. It also showed that longer acupuncture retention time may lead to better result in activities of daily life (0.5 hours: SMD = 0.79, 95% CI (0.53, 1.05),  $P < 0.00001$ ; 6 hours subgroup: SMD = 2.58, 95% CI (1.97, 3.19),  $P < 0.00001$ ).

**3.7. Safety.** Safety of acupuncture therapy was reported in nine [32, 33, 37, 39, 42–44, 48, 50] of the included articles. Six [32, 33, 37, 39, 43, 48] of the articles reported no adverse events related to acupuncture therapy happened during the trials. One article [50] reported one case of adverse event but did not mention the reason. One article [42] reported one case of subcutaneous hematoma in the experiment group and three cases of fainting in the control group. Another article [44] reported one case of fainting during acupuncture and two cases of subcutaneous hematoma.

**3.8. Publication Bias.** We used STATA V.15.1 to evaluate publication bias. For MMSE, publication bias was assessed using Begg's test (Figures 8 and 9) and Egger's test (Figures 10 and 11), which did not show significant publication bias in the included studies. For MoCA and Barthel, the publication bias could not be assessed as less than ten articles were included.

## 4. Discussion

After searching PubMed, the Cochrane Library, CNKI, Wan-Fang Data, VIP, CBM, Medline, and Embase databases, 657 relevant RCTs were found in this meta-analysis, and 22 RCTs with 1856 patients were eventually included. According to this study, more evidence was provided to prove that acupuncture treatment is beneficial to PSCI patients in terms of cognitive function and ability of daily life. PSCI, which has high prevalence rate, is a result of mixed damage mechanisms [55]. Jeremy's study [56] suggested that ongoing ischemic vascular processes were the main mechanism which also emphasized the importance of management for vascular risk factor. Apart from that, there is no established therapy for prevention for PSCI so far. Hence, it is of vital importance for us to explore an effective and highly compliant treatment for PSCI patients.

There were a few relevant meta-analyses about acupuncture treatment for cognitive impairment. Liu et al. [57] searched RCTs that used acupuncture in the treatment of PSCI before February 2012 and included 21 RCTs with a total of 1421 patients. Due to the high risk of bias and lack of unified scale for evaluating cognitive function of the included studies, it is hard to reach reliable conclusions on the effect of acupuncture. Furthermore, it did not focus on analyzing the effects of acupuncture alone but on the combined treatment with acupuncture, which made it difficult to objectively evaluate the effect of acupuncture treatment for PSCI. Kim et al. [58] searched the RCTs on mild cognitive impairment (MCI) patients from October 2007 to August 2017 and

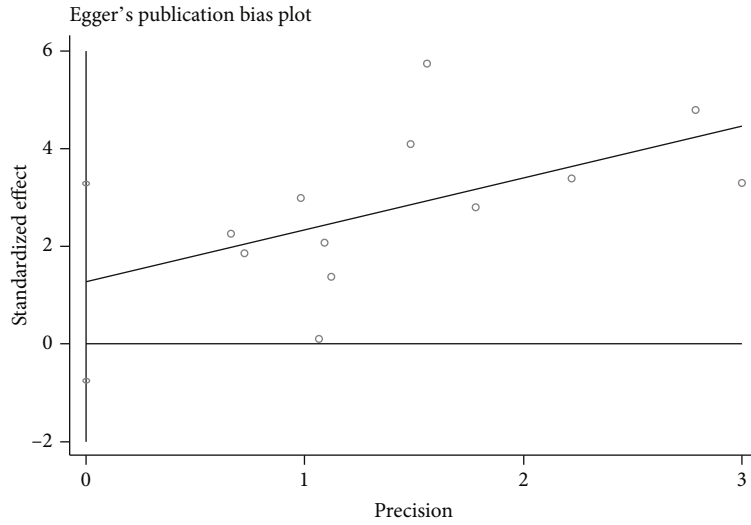


FIGURE 10: Egger's publication bias plot.

Egger's test

Std_Eff	Coef.	Std. err.	t	P >  t	(95% conf. interval)	
Slope	1.059989	.5298442	2.00	0.073	-.1205776	2.240555
Bias	1.262201	.9052232	1.39	0.193	-.7547619	3.279164

FIGURE 11: Egger's test.

compared the effect of electroacupuncture (EA) to western medication. Their study, which included 5 RCTs with 257 patients, showed that EA had a higher score on MMSE and MoCA than western medications. But the weak methodological quality of the studies and small sample size may affect the reliability of the results.

This present review offered several significant perspectives. Firstly, a common deficiency of previous RCTs and reviews is the lack of attention to ADL. There were only 9 RCTs that we included used BI or MBI to evaluate ADL on PSCI patients. ADL is one of the most important measures to evaluate how serve PSCI is and an essential measure to distinguish PSCIND and PSD [12]. Moreover, PSD has a significant higher fatality rate than PSCIND [55]. Therefore, we strongly recommend future studies to focus on the ability of daily life for PSCI patients and explore if acupuncture has the benefit of preventing PSCIND progressing to PSD whenever possible. Secondly, it may cause false increase in patients' test results by using the same version of scale to evaluate cognitive function before and after the treatment. In order to ensure accuracy of MoCA test, we completed MoCA's official standardized training and certification program online. We learned from the official website (<https://www.mocatest.org/training-certification/>) that the delay between administration should be sufficient to decrease the risk of a possible learning effect when administering the MoCA to the same subject; the alternative/equivalent versions of the MoCA should be used to decreased possible learning effects when the MoCA is administered, respectively. Therefore, we suggest using different versions of MoCA, such as 7.1, 7.2, or 7.3 versions at different stages of

assessment. Thirdly, more attention should be paid to the standardized use of the scale. For instance, in this review, three articles were found incorrect using of MMSE. The wrong use of the scale may lead to serious errors in screening and evaluation of patients. Furthermore, most of the included RCTs have unclear bias of randomization process, measurement of the outcome, and selection of the reported results, which have a significant impact on the evaluation of the results. It is true that the nature of the acupuncture made it difficult for investigators to blind participants and almost impossible to blind the therapists; all the RCTs we included likewise did not blind the participants or therapists. However, we should attach more importance to the blinding on outcome assessors, especially the scale evaluators whose judgement may have a large influence on the outcome. We also advise that all the RCTs which study the effect of acupuncture should have a protocol with complete information prior to the start of trials. The protocol should provide detailed information according to the CONSORT statement and STRICTA recommendations in order to minimize the performance and assessment bias of RCTs.

This review also had certain limitations. Firstly, although we searched the trials written in Chinese or English, all the trials included were conducted in China. This is related to the less application of using acupuncture treatment on PSCI in countries other than China, and it may limit the universality of the results. Moreover, our study mainly focused on the effect of acupuncture alone but neglected the synergistic effect between acupuncture and other effective treatment, such as medication or cognitive training. In addition, this study did not consider the possible placebo effect of

acupuncture as no sham/placebo-controlled trials were included. Furthermore, significant heterogeneities were observed in our study. Experimental design, various acupoint selecting, and therapist skill difference can contribute to the high heterogeneity. Problems about which acupoints are most effective for PSCI and how long the treatment should last need to be resolved in future studies.

## 5. Conclusions

Compared with the nonacupuncture group, the acupuncture group showed better effects in improving the scores of MMSE, MoCA, BI, and MBI. This meta-analysis provided positive evidence that acupuncture may be effective in improving cognitive function and activities of daily life for PSCI patients. Meanwhile, long retention time of acupuncture may improve cognitive function and activities of daily life, and twist technique may be an important factor that could influence cognitive function. However, further studies using large samples and a rigorous study design are needed to confirm the role of acupuncture in the treatment of PSCI.

## Abbreviations

DALYs:	Disability-adjusted life-years
PSCI:	Poststroke cognitive impairment
PSCIND:	Poststroke cognitive impairment with no dementia
PSD:	Poststroke dementia
K-VCIHS-NP:	Korean Vascular Cognitive Impairment Harmonization Standards neuropsychological protocol
RCTs:	Randomized controlled trials
FDA:	The Food and Drug Administration
BDNF:	Brain-derived neurotrophic factor
CREB:	cAMP-response element-binding protein
CNKI:	China National Knowledge Infrastructure
CBM:	China Science Medicine disc
VIP:	China Science and Technology Journal Database
RCT:	Randomized controlled trial
MMSE:	Mini-Mental State Examination
MoCA:	Montreal Cognitive Assessment
BI:	Barthel Index
MBI:	Modified Barthel Index
MD:	Mean difference
CI:	Confidence interval
ROB 2.0:	Risk of bias 2.0
CI:	Confidence interval.

## Data Availability

The datasets generated during and analysed during the current study are available from the corresponding author on reasonable request.

## Conflicts of Interest

The authors declare that there is no conflict of interest regarding the publication of this article.

## Authors' Contributions

Wei Liu and Chang Rao developed the study concept and design, performed the data acquisition and analysis, and drafted the manuscript. Jipeng Yang and Lili Zhang modified the manuscript. Yuzheng Du read, modified, and approved the final manuscript for submission.

## Acknowledgments

This study was financially supported by the Tianjin Science and Technology Project (NO. 18PTLCSY00060).

## Supplementary Materials

Supplemental Files: PRISMA Checklist (the 27 checklist items pertain to the content of a systematic review and meta-analysis, which include the title, abstract, methods, results, discussion, and funding). (*Supplementary Materials*)

## References

- [1] G. J. Hankey, "Stroke," *Lancet*, vol. 389, no. 10069, pp. 641–654, 2017.
- [2] S. Wu, B. Wu, M. Liu et al., "Stroke in China: advances and challenges in epidemiology, prevention, and management," *Lancet Neurology*, vol. 18, no. 4, pp. 394–405, 2019.
- [3] D. A. Levine, A. T. Galecki, K. M. Langa et al., "Trajectory of cognitive decline after incident stroke," *Journal of the American Medical Association*, vol. 314, no. 1, pp. 41–51, 2015.
- [4] L. Jia, M. Quan, Y. Fu et al., "Dementia in China: epidemiology, clinical management, and research advances," *Lancet Neurology*, vol. 19, no. 1, pp. 81–92, 2020.
- [5] Q. Guo, Q. Guo, B. Luo et al., "Expert consensus on the management of cognitive impairment after stroke," *Chinese Journal of Stroke*, vol. 12, no. 6, pp. 519–531, 2017.
- [6] K. H. Yu, S. J. Cho, M. S. Oh et al., "Cognitive impairment evaluated with vascular cognitive impairment harmonization standards in a multicenter prospective stroke cohort in Korea," *Stroke*, vol. 44, no. 3, pp. 786–788, 2013.
- [7] C. S. Ivan, S. Seshadri, A. Beiser et al., "Dementia after stroke: the Framingham study," *Stroke*, vol. 35, no. 6, pp. 1264–1268, 2004.
- [8] K. B. Rajan, N. T. Aggarwal, R. S. Wilson, S. A. Everson-Rose, and D. A. Evans, "Association of cognitive functioning, incident stroke, and mortality in older adults," *Stroke*, vol. 45, no. 9, pp. 2563–2567, 2014.
- [9] H. Jokinen, S. Melkas, R. Ylikoski et al., "Post-stroke cognitive impairment is common even after successful clinical recovery," *European Journal of Neurology*, vol. 22, no. 9, pp. 1288–1294, 2015.
- [10] J. H. Park, B. J. Kim, H. J. Bae et al., "Impact of post-stroke cognitive impairment with no dementia on health-related quality of life," *Journal of Stroke*, vol. 15, no. 1, pp. 49–56, 2013.

- [11] J. H. Sun, L. Tan, and J. T. Yu, "Post-stroke cognitive impairment: epidemiology, mechanisms and management," *Annals of Translational Medicine*, vol. 2, no. 8, p. 80, 2014.
- [12] M. D. Mijajlović, A. Pavlović, M. Brainin et al., "Post-stroke dementia - a comprehensive review," *BMC Medicine*, vol. 15, no. 1, p. 11, 2017.
- [13] M. Fioravanti, L. Flicker, and Cochrane Dementia and Cognitive Improvement Group, "Nicergoline for dementia and other age associated forms of cognitive impairment," *Cochrane Database of Systematic Reviews*, vol. 2001, no. 4, article CD003159, 2001.
- [14] P. B. Gorelick, A. Scuteri, S. E. Black et al., "Vascular contributions to cognitive impairment and dementia: a statement for healthcare professionals from the American Heart Association/American Stroke Association," *Stroke*, vol. 42, no. 9, pp. 2672–2713, 2011.
- [15] Y. Guo, M. Xiangwen, L. Yihong et al., "Comparison and analysis on the development of acupuncture and moxibustion medicine in recent years," *Chin J Inf Tradit Chin Med*, vol. 20, no. 4, pp. 1–5, 2013.
- [16] L. M. Chavez, S. S. Huang, I. MacDonald, J. G. Lin, Y. C. Lee, and Y. H. Chen, "Mechanisms of acupuncture therapy in ischemic stroke rehabilitation: a literature review of basic studies," *International Journal of Molecular Sciences*, vol. 18, no. 11, p. 2270, 2017.
- [17] M. Mukherjee, L. K. McPeak, J. B. Redford, C. Sun, and W. Liu, "The effect of electro-acupuncture on spasticity of the wrist joint in chronic stroke survivors," *Archives of Physical Medicine and Rehabilitation*, vol. 88, no. 2, pp. 159–166, 2007.
- [18] P. Chou, H. Chu, and J. G. Lin, "Effects of electroacupuncture treatment on impaired cognition and quality of life in Taiwanese stroke patients," *Journal of Alternative and Complementary Medicine*, vol. 15, no. 10, pp. 1067–1073, 2009.
- [19] U. Ghafoor, J. H. Lee, K. S. Hong, S. S. Park, J. Kim, and H. R. Yoo, "Effects of acupuncture therapy on MCI patients using functional near-infrared spectroscopy," *Frontiers in Aging Neuroscience*, vol. 11, 2019.
- [20] Z. J. Zhang, H. Y. Chen, K. C. Yip, R. Ng, and V. T. Wong, "The effectiveness and safety of acupuncture therapy in depressive disorders: systematic review and meta-analysis," *Journal of Affective Disorders*, vol. 124, no. 1-2, pp. 9–21, 2010.
- [21] B. Lee, B. Sur, J. Shim, D. H. Hahm, and H. Lee, "Acupuncture stimulation improves scopolamine-induced cognitive impairment via activation of cholinergic system and regulation of BDNF and CREB expressions in rats," *BMC Complementary and Alternative Medicine*, vol. 14, no. 1, 2014.
- [22] M. Cai, J. H. Lee, and E. J. Yang, "Electroacupuncture attenuates cognition impairment via anti-neuroinflammation in an Alzheimer's disease animal model," *Journal of Neuroinflammation*, vol. 16, no. 1, p. 264, 2019.
- [23] Z. Dan, L. Zuowei, and L. Ping, "Systematic review of different acupuncture methods in the treatment of post-stroke cognitive impairment," *Journal of Sichuan of Traditional Chinese Medicine*, vol. 32, no. 6, pp. 155–158, 2014.
- [24] C. Lizao, L. Wu, J. Wang et al., "Meta-analysis on the treatment of post-stroke cognitive impairment with head acupuncture," *Guiding Journal of Traditional Chinese Medicine and Pharmacy*, vol. 22, no. 22, pp. 84–87, 2016.
- [25] H. Brodaty, M. H. Connors, C. Loy et al., "Screening for dementia in primary care: a comparison of the GPCOG and the MMSE," *Dementia and Geriatric Cognitive Disorders*, vol. 42, no. 5-6, pp. 323–330, 2016.
- [26] M. F. Folstein, S. E. Folstein, and P. R. McHugh, "“Mini-mental state”. A practical method for grading the cognitive state of patients for the clinician," *Journal of Psychiatric Research*, vol. 12, no. 3, pp. 189–198, 1975.
- [27] Z. S. Nasreddine, N. A. Phillips, V. Bédirian et al., "The Montreal cognitive assessment, MoCA: a brief screening tool for mild cognitive impairment," *Journal of the American Geriatrics Society*, vol. 53, no. 4, pp. 695–699, 2005.
- [28] Y. L. Chang, M. W. Bondi, L. K. McEvoy et al., "Global clinical dementia rating of 0.5 in MCI masks variability related to level of function," *Neurology*, vol. 76, no. 7, pp. 652–659, 2011.
- [29] S. Kwon, A. G. Hartzema, P. W. Duncan, and S. Min-Lai, "Disability measures in stroke," *Stroke*, vol. 35, no. 4, pp. 918–923, 2004.
- [30] H. Houlden, M. Edwards, J. McNeil, and R. Greenwood, "Use of the Barthel index and the functional Independence measure during early inpatient rehabilitation after single incident brain injury," *Clinical Rehabilitation*, vol. 20, no. 2, pp. 153–159, 2016.
- [31] B. Proding, R. O'Connor, G. Stucki, and A. Tennant, "Establishing score equivalence of the functional Independence measure motor scale and the Barthel index, utilising the international classification of functioning, disability and health and Rasch measurement theory," *Journal of Rehabilitation Medicine*, vol. 49, no. 5, pp. 416–422, 2017.
- [32] S. Wang, H. Yang, J. Zhang et al., "Efficacy and safety assessment of acupuncture and nimodipine to treat mild cognitive impairment after cerebral infarction: a randomized controlled trial," *BMC Complementary and Alternative Medicine*, vol. 16, no. 1, p. 361, 2016.
- [33] C. Jiang, S. Yang, J. Tao et al., "Clinical efficacy of acupuncture treatment in combination with RehaCom cognitive training for improving cognitive function in stroke: a 2 × 2 factorial design randomized controlled trial," *Journal of the American Medical Directors Association*, vol. 17, no. 12, pp. 1114–1122, 2016.
- [34] W. Lina and L. Fang, "Effect of atorvastatin combined with acupuncture on patients with mild cognitive impairment after stroke," *GuangDong Medical Journal*, vol. 39, no. 23, pp. 3557–3561, 2018.
- [35] B. Yu, Z. Wei, and S. Xiaowei, "Therapeutic observation on acupuncture for mild cognitive impairment after cerebral infarction," *Shanghai Journal of Acupuncture and Moxibustion*, vol. 31, no. 7, pp. 470–472, 2012.
- [36] Z. Xiaojian, Z. Yuan, G. Zechun et al., "Effect of acupuncture at cervical Jiaji point and Du Channel point combined with atorvastatin on hemodynamics in patients with mild cognitive impairment after stroke," *Journal of Hunan Normal University (Medical Sciences)*, vol. 14, no. 2, pp. 131–134, 2017.
- [37] W. Qin, D. Juncheng, and S. Liangying, "Effects of acupuncture combined with atorvastatin on Hemorheology and cognitive status of elderly patients with mild cognitive impairment after ischemic stroke," *Chinese Journal of Gerontology*, vol. 39, no. 21, pp. 5180–5183, 2019.
- [38] Y. Hongling, Z. Jiangang, L. Tao et al., "Therapeutic observation on acupuncture combined with Nimodipine for mild cognitive impairment after cerebral infarction," *Journal of Clinical Acupuncture and Moxibustion*, vol. 31, no. 3, pp. 33–36, 2015.



- [39] D. Nini, *Observation on the Curative Effect of Acupuncture of Ear-Well Acupoint on Treating Mild Vascular Cognitive Impairment after Stroke*, Master, Anhui University of Chinese Medicine, Anhui, China, 2017.
- [40] T. Xin, Z. Bingfeng, and L. Gao, "Clinical study on post stroke cognitive impairment by eye acupuncture," *Guid J Tradit Chin Med Pharm*, vol. 24, no. 12, pp. 67–69, 2018.
- [41] Q. Churui, *Effect of Acupuncture on Attention Function in Post-Stroke Patients with Cognitive Impairment Based on EEG Signal*, Fujian University of Traditional Chinese Medicine, Fujian, China, Master, 2018.
- [42] L. Lei, X. Pei, C. Qiao et al., "Effects of acupuncture combined with donepezil on cognitive impairment after stroke in elderly patients. Chinese journal of prevention and control of chronic," *Diseases*, vol. 27, no. 8, pp. 617–620, 2019.
- [43] D. Hezheng, Z. Xuezheng, C. Xiyuan et al., "Kidney and medullary acupuncture combined with compound musk injection for the treatment of cognitive impairment after stroke," *Chinese Journal of General Practice*, vol. 17, no. 3, pp. 416–418 +499, 2019.
- [44] N. Yapeng, *Study on the Effect and Therapeutic Effect of Tongdu Tiaoshen Acupuncture on Platelet Microparticles in Patients with Ischemic Stroke*, Master, Anhui University of Chinese Medicine, Anhui, China, 2019.
- [45] B. Jing, L. Baodong, and Q. Wang, "Therapeutic observation on cluster needling at scalp Acupoints plus cognition training for post-stroke cognitive impairment," *Shanghai J Acup Moxib*, vol. 31, no. 10, pp. 711–713, 2012.
- [46] Z. Lilan, Z. Xiaolan, H. Zhen et al., "Clinical effects of Jin's 3-needle combined with cognitive rehabilitation training in the treatment of convalescent cerebral apoplexy with cognitive impairment," *Shandong Journal of Traditional Chinese Medicine*, vol. 37, no. 5, pp. 367–370, 2018.
- [47] Z. Yuanyuan, S. Bin, H. Guilan et al., "Clinical observation of triple energizer acupuncture combined with computer aided cognitive training in treatment of cognitive impairment after acute stroke," *Shandong Journal of Traditional Chinese Medicine*, vol. 38, no. 12, pp. 1118–1122, 2019.
- [48] W. Zhenyao, Z. Hu, W. Xinwei et al., "Efficacy of acupuncture plus cognitive rehabilitation training for post-stroke cognitive impairment and its effect on cytokines," *Shanghai J Acup Moxib*, vol. 38, no. 10, pp. 1098–1102, 2019.
- [49] C. Mao and F. Cheng, "Treatment of 39 patients with cognitive impairment after stroke with acupuncture combined with modern rehabilitation training," *Traditional Chinese Medicinal Research*, vol. 32, no. 10, pp. 47–49, 2019.
- [50] L. Shuo, *Effect of Eye Acupuncture Combined with Cognitive Training on Vascular Cognitive Impairment after Stroke*, Master, Liaoning University of Traditional Chinese Medicine, Liaoning, China, 2016.
- [51] S. Haiyan, *Effects of Acupuncture Combined with Cognitive Training on the Expression of Synapse Related miRNAs in Patients with Post-Stroke Cognitive Impairment*, Master, Fujian University of Traditional Chinese Medicine, Fujian, China, 2017.
- [52] Z. Jiyun, *Acupuncture Combined with Cognitive Rehabilitation in the Treatment of Cognitive Impairment after Stroke*, Master, Shanxi University of Chinese Medicine, Shanxi, China, 2018.
- [53] L. Fei, C. Hongliang, Z. Wending et al., "Efficacy observation of Bianjing Cijing combined with Nie's 3-needle in the treatment of cognitive impairment in acute stroke. Clinical," *Journal of Traditional Chinese Medicine*, vol. 24, no. 11, pp. 1059–1061, 2012.
- [54] C. Fu, X. Jin, B. Chen et al., "Comparison of the mini-mental state examination and Montreal cognitive assessment executive subtests in detecting post-stroke cognitive impairment," *Geriatrics & Gerontology International*, vol. 17, no. 12, pp. 2329–2335, 2017.
- [55] Y. Qu, L. Zhuo, N. Li et al., "Prevalence of post-stroke cognitive impairment in China: a community-based, cross-sectional study," *PLoS One*, vol. 10, no. 4, article e0122864, 2015.
- [56] J. Molad, H. Hallevi, A. D. Korczyn et al., "Vascular and neurodegenerative markers for the prediction of post-stroke cognitive impairment: results from the TABASCO study," *Journal of Alzheimer's Disease*, vol. 70, no. 3, pp. 889–898, 2019.
- [57] F. Liu, Z. M. Li, Y. J. Jiang, and L. D. Chen, "A meta-analysis of acupuncture use in the treatment of cognitive impairment after stroke," *The Journal of Alternative and Complementary Medicine*, vol. 20, no. 7, pp. 535–544, 2014.
- [58] H. Kim, H. K. Kim, S. Y. Kim, Y. I. Kim, H. R. Yoo, and I. C. Jung, "Cognitive improvement effects of electro-acupuncture for the treatment of MCI compared with Western medications: a systematic review and meta-analysis," *BMC Complementary and Alternative Medicine*, vol. 19, no. 1, p. 13, 2019.

## Review Article

# Acupuncture for Adults with Diarrhea-Predominant Irritable Bowel Syndrome or Functional Diarrhea: A Systematic Review and Meta-Analysis

Jianbo Guo,<sup>1,2</sup> Xiaoxiao Xing,<sup>2</sup> Jiani Wu,<sup>1</sup> Hui Zhang,<sup>3</sup> Yongen Yun,<sup>2</sup> Zongshi Qin ,<sup>4</sup> and Qingyong He <sup>1</sup>

<sup>1</sup>Guang'anmen Hospital, China Academy of Chinese Medical Sciences, Beijing, China

<sup>2</sup>Beijing University of Chinese Medicine, Beijing, China

<sup>3</sup>Henan University of Chinese Medicine, Henan, China

<sup>4</sup>Faculty of Medicine, The University of Hong Kong, Hong Kong, China

Correspondence should be addressed to Zongshi Qin; [arisq@connect.hku.hk](mailto:arisq@connect.hku.hk) and Qingyong He; [heqingyong@163.com](mailto:heqingyong@163.com)

Received 29 July 2020; Revised 27 October 2020; Accepted 29 October 2020; Published 23 November 2020

Academic Editor: Zhen Zheng

Copyright © 2020 Jianbo Guo et al. This is an open access article distributed under the Creative Commons Attribution License, which permits unrestricted use, distribution, and reproduction in any medium, provided the original work is properly cited.

**Objective.** To evaluate the clinical effectiveness and safety of acupuncture therapy in the treatment of diarrhea-predominant irritable bowel syndrome (IBS-D) or functional diarrhea (FD) in adults. **Method.** Five electronic databases—PubMed, EMBASE, CNKI, VIP, and Wanfang—were searched, respectively, until June 8, 2020. The literature of clinical randomized controlled trials of acupuncture for the treatment of IBS-D or FD in adults were collected. Meta-analysis was conducted by Using Stata 16.0 software, the quality of the included studies was assessed by the RevMan ROB summary and graph, and the results were graded by GRADE. **Result.** Thirty-one studies with 3234 patients were included. Most of the studies were evaluated as low risk of bias related to selection bias, attrition bias, and reporting bias. Nevertheless, seven studies showed the high risk of bias due to incomplete outcome data. GRADE's assessments were either moderate certainty or low certainty. Compared with loperamide, acupuncture showed more effectiveness in weekly defecation (SMD = -0.29, 95% CI [-0.49, -0.08]), but no significant improvement in the result of the Bristol stool form (SMD = -0.28, 95% CI [-0.68, 0.12]). In terms of the drop-off rate, although the acupuncture group was higher than the bacillus licheniformis plus beanxit group (RR = 2.57, 95% CI [0.24, 27.65]), loperamide group (RR = 1.11, 95% CI [0.57, 2.15]), and trimebutine maleate group (RR = 1.19, 95% CI [0.31, 4.53]), respectively, it was lower than the dicetel group (RR = 0.83, 95% CI [0.56, 1.23]) and affected the overall trend (RR = 0.93, 95% CI [0.67, 1.29]). Besides, acupuncture produced more significant effect than dicetel related to the total symptom score (SMD = -1.17, 95% CI [-1.42, -0.93]), IBS quality of life (SMD = 2.37, 95% CI [1.94, 2.80]), recurrence rate (RR = 0.43, 95% CI [0.28, 0.66]), and IBS Symptom Severity Scale (SMD = -0.75, 95% CI [-1.04, -0.47]). Compared to dicetel (RR = 1.25, 95% CI [1.18, 1.32]) and trimebutine maleate (RR = 1.35, 95% CI [1.13, 1.61]), acupuncture also showed more effective at total efficiency. The more adverse effect occurred in the acupuncture group when comparing with the dicetel group (RR = 11.86, 95% CI [1.58, 89.07]) and loperamide group (RR = 4.42, 95% CI [0.57, 33.97]), but most of the adverse reactions were mild hypodermic hemorrhage. **Conclusion.** Acupuncture treatment can improve the clinical effectiveness of IBS-D or FD, with great safety, but the above conclusions need to be further verified through the higher quality of evidence.

## 1. Introduction

Diarrhea-predominant irritable bowel syndrome (IBS-D) or functional diarrhea (FD) is a disease with high incidence rates, which affects the lives of people in China, America,

and even the world, often accompanied by mental illness [1–3]. The main clinical manifestations of IBS-D and FD are passing water samples three or more times daily, accompanied by abdominal pain and discomfort [4, 5]. It was considered to be a functional disease closely related to the

physiological or mental status of patients, but a gradually in-depth study of pathophysiological mechanisms can explain these symptoms [6]. Calprotectin and fecal lactoferrin both are markers of an inflammatory response in IBS-D or FD. In particular, the psychological symptoms and visceral hypersensitivity of IBS-D or FD patients have been shown to be closely related to parasympathetic dysfunction, which may affect the severity of the disease [7, 8].

At present, anticholinergic drugs, antispasmodic drugs, antitomotility, and antidiarrheal drugs are commonly used to treat IBS-D and FD, but adverse effects include dizziness, nausea, vomiting, and even respiratory inhibition. It is difficult to obtain the satisfactory effect of these drugs in IBS-D and FD patients. Probiotics are effective and safe in IBS patients, but studies on the detection of strains, dose, and duration of treatment are inconsistent. [9] Therefore, it is particularly important to find a treatment method that can effectively reduce pain in patients with fewer side effects [10].

Acupuncture, as a special nondrug technology in traditional Chinese medicine, is used to treat diseases by inserting fine needles or stimulating acupoints manually [11]. Previous studies have found that acupuncture treatment is closely related to the central nervous system and the intestinal nervous system; besides, acupuncture points cover the main nerve bundles of the body [12]. Evidence suggests that acupuncture can produce curative effects on gastrointestinal motility through nerve and body fluid channels [13–17]. This study explores the effectiveness and safety of acupuncture in the treatment of IBS-D or FD by systematic review and meta-analysis.

## 2. Methods

**2.1. Search Strategy.** This meta-analysis was conducted by guidelines [18, 19] set out in the PRISMA statement (Supplementary material 1: PRISMA Checklist) and was registered with PROSPERO (CRD42015017574). We conducted a literature search (using PubMed), the Chinese Science and Technology Periodical Database (Embase), the Chinese National Knowledge Infrastructure Database (CNKI), China Scientific Journal Database (VIP), and Wanfang Database. The retrieval time was from the establishment of the database to June 8, 2020. The search method combined MeSH subject words and free search words as follows: “diarrhea OR irritable bowel syndrome OR functional diarrhea” AND “acupuncture” AND “randomly” AND “controlled.” Supplementary material 2 outlines the search strategy of the PubMed database. This study protocol has been published previously [Qin et al. 2018].

**2.2. Inclusion and Exclusion Criteria.** The literature included in our study met the following requirements: (1) study type: clinical randomized controlled trials of acupuncture treatment for IBS-D or FD, blinded or nonblinded, written in Chinese or English, and available online before June 8, 2020; (2) intervention measures: the treatment group was treated with penetrating acupuncture, or combined with a control group, and the control group was treated with conventional medicine, sham acupuncture, or conventional ac-

puncture; (3) participants: patients aged 18 years and over, with unlimited gender and case source, who were definitively diagnosed with IBS-D or FD; and (4) outcome indicators: weekly defecation rate, patient drop off rate, Bristol stool form, total symptom score, IBS quality of life (IBS-QOL), total efficiency, recurrence rate, IBS Symptom Severity Scale (IBS-SSS) and adverse effect. The exclusion criteria were as follows: (1) studies of non-IBS-D or FD cases; (2) the intervention measures of the treatment group were nonpenetrating acupuncture, such as laser acupuncture, acupoint pressing, percutaneous, or percutaneous electrical nerve stimulation; (3) the control group and the experimental group were used for different types of acupuncture (i.e., acupuncture and electroacupuncture); (4) conference papers; (5) the literature on the effectiveness evaluation index did not meet the inclusion requirements; (6) literature published multiple times; and (7) literature with Western medicine or other therapies as the main research objective.

**2.3. Literature Quality Assessment.** According to the Cochrane criteria, we assessed the quality of the included studies in six domains: (1) random treatment assignment; (2) treatment assignment concealment; (3) treatment blinding (including blinding for patients, study implementers, and study outcome assessors); (4) data integrity of the study results; (5) selective reporting in the study; and (6) other biases. From the above domains, two researchers (J.G and X.X) evaluated the risk of bias in the included literature according to the three criteria of “low risk,” “high risk,” or “unknown risk.” In case of disagreement during the evaluation, the decision was made through consultation or discussion with a third researcher (Z.Q). GRADE (grades of recommendation, assessment, development, and evaluation) was used to grade and evaluate weekly defecation, Bristol stool form, total symptom score, IBS-QOL, and IBS-SSS analysis results.

**2.4. Data Extraction and Analyses.** Data extraction included (1) basic information of the study including the first author, year of publication, study time, sample size, and patient age; (2) treatment information of the study including treatment methods, outcome indicators, and adverse events, of the observation group, and the control group. If the data included in the study were incomplete, we tried to contact the original author for supplementation.

Stata 16.0 software was used for data analysis. A random-effect model was used, as different acupuncture points or intervention cycles in each study may affect the therapeutic effect. Cohen’s  $d$  and 95% confidence interval (CI) were used for continuous variables, and RR (relative risk) was used for secondary variables.  $Q$  statistics and  $I^2$  were used to judge the heterogeneity of the study (i.e., when the  $P$  value of  $Q$  statistics  $< 0.1$  or  $I^2 > 50\%$ , there is a large heterogeneity between the studies). A L’Abbe’s chart was used to test the heterogeneity of binary variables. A meta-regression method and a bubble chart were used to evaluate the impact of related factors on outcome indicators and determine the source of heterogeneity. A funnel graph and an Egger test were used to evaluate publication bias. Finally, if there was significant

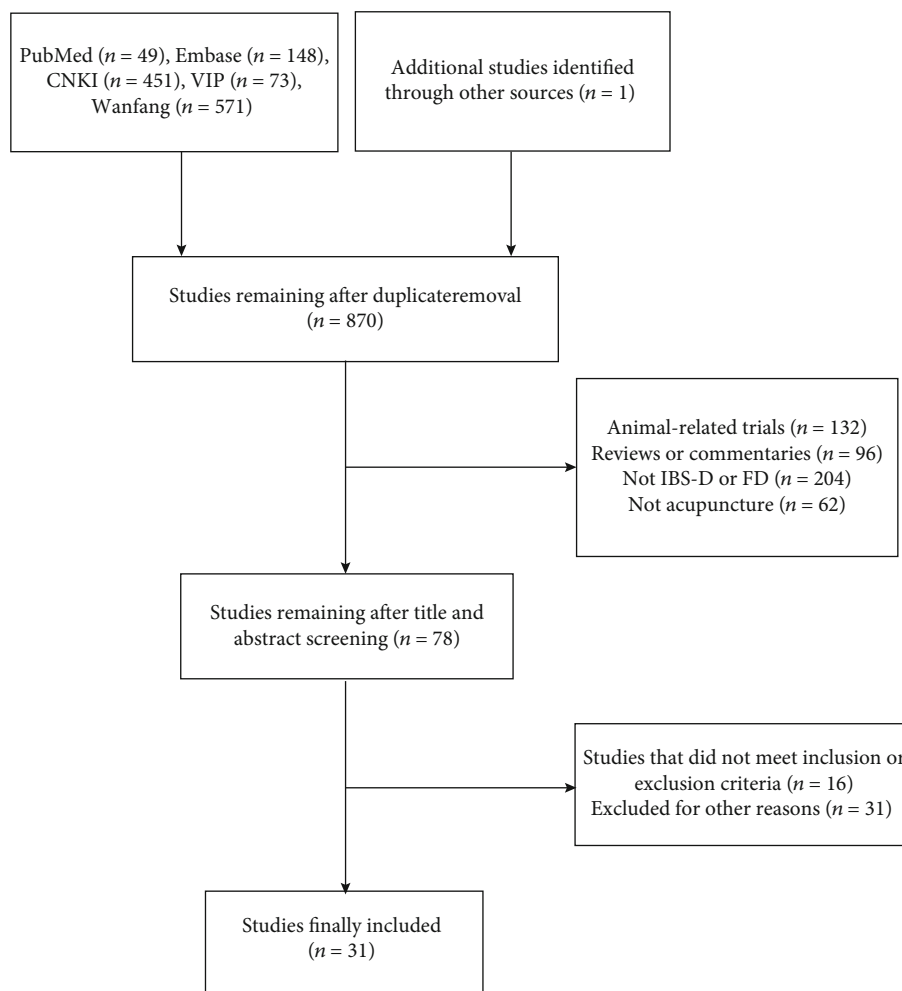


FIGURE 1: Flow chart of literature search.

heterogeneity between studies, a sensitivity analysis was conducted, and then meta-analysis was conducted by excluding the studies that induced heterogeneity.

### 3. Result

**3.1. Literature Selection.** Altogether, 1293 documents were retrieved, 870 of which were obtained after removing multiples of the same publication or publications with the same data, 78 of which were left after reading the title and abstract to address the inclusion criteria. After reading the full text, 31 studies met the inclusion standards and were finally included, all of which were published in journals. Figure 1 shows the inclusion and exclusion flow chart.

**3.2. Literature Characteristics.** Among the 31 studies [20–50] included, 5 studies [24, 28, 30, 38, 41] used the random allocation method, which was evaluated as high risk or unknown risk; 5 studies [20, 32, 34, 47, 50] used the allocation hidden method, which was evaluated as low risk; 5 studies [22, 32, 34, 48, 50] used the blind method, which was evaluated as low risk; 12 studies [30, 31, 33, 34, 37, 39–42, 45, 46, 48] did not mention the completeness of the results, so were evaluated as high risk or unknown risk; 3 studies [25, 33, 37] did

not use the selective report and were evaluated as a high risk or unknown risk; 3 studies [20, 32, 50] did not have any significant other sources of bias. Table 1 presents the basic information about the included studies. Figures 2 and 3 present the risk of bias summary and graph related to the included studies, respectively. 26 studies reported methods of random sequence generation that were evaluated as low risk of bias, but 3 studies used nonstandard random grouping methods existed at the high risk of bias. As to allocation concealment of selection bias, performance bias, and detection bias, evaluations of numerous studies were regarded as unclear risk of bias. 18 studies with complete outcome data were evaluated as low risk of bias, but 7 studies existed at the high risk of bias due to incomplete outcome data. 28 studies with rarely selective reporting were evaluated as low risk of bias, and other biases in most of the included studies were unclear. Table 2 presents the results of GRADE: weekly defecation, Bristol stool form, total symptom score, IBS-QOL, and IBS-SSS.

(1): weekly defecation; (2): patient drop-off rate; (3): Bristol stool form; (4): total efficiency; (5): IBS-QOL; (6): total symptom score; (7): recurrence rate; (8): IBS-SSS; (9): adverse reactions; NR: not reported; T: treatment group; C: control group

TABLE 1: Basic information of the included studies.

Study ID	Sample size (T/C)	Mean age (years)	Diagnostic standards	Intervention	Comparison	Duration (weeks)	Outcome	Adverse effects
Qian et al. 2011 [20]	120 (60/60)	T: 42.5 ± 7.3 C: 43.5 ± 7.6	Roman III	Acupuncture plus dicetel	Sham acupuncture plus dicetel	4	(2)(4)(6)	NR
Sun et al. 2011 [21]	63 (31/32)	T: 38.8 ± 11.8 C: 38.6 ± 11.5	Roman III	Acupuncture	Dicetel	4	(2)(4) (5)(6)	None
Wang et al. 2011 [22]	120 (60/60)	T: 37.2 ± 10.2 C: 40.1 ± 11.7	Roman III	Eye acupuncture	Dicetel	4	(2)(4) (7)(9)	T: 6 C: 0
Chen et al. 2012 [23]	64 (34/30)	T: 41.9 ± 10.0 C: 40.5 ± 8.8	Roman III	Electroacupuncture	Bacillus licheniformis plus deaxxit	4	(2)(4)(7)	NR
Li et al. 2012 [24]	64 (32/32)	T: 55.5 ± 5.4 C: 55.3 ± 5.5	Roman III	Acupuncture	Dicetel	4	(2)(4)	NR
Pei et al. 2012 [25]	65 (33/32)	T: 39.1 ± 11.8 C: 37.9 ± 11.5	Roman III	Acupuncture	Dicetel	4	(2)(4)	NR
Wu et al. 2013 [26]	48 (24/24)	T: 41.0 ± 13.0 C: 39.0 ± 13.0	Roman III	Acupuncture	Dicetel	4	(2)(4)(6)	NR
Li et al. 2012 [27]	70 (35/35)	T: 39.1 ± 11.8 C: 37.9 ± 11.5	Roman II	Acupuncture	Dicetel	4	(2)(4) (6)(7)	NR
Liu 2013 [28]	60 (30/30)	T: 37.0 ± 10.1 C: 39.7 ± 10.6	Roman III	Acupuncture	Dicetel	4	(2)(4)(9)	T: 5 C: 0
Zhan et al. 2013 [29]	66 (33/33)	T: 42.5 ± 13.6 C: 37.3 ± 12.7	Roman III	Acupuncture	Dicetel	4	(2)(4) (5)(6)	NR
Wu et al. 2014 [30]	73 (36/37)	T: 39.6 ± 12.8 C: 36.5 ± 14.2	Roman III	Warm acupuncture	Bacillus licheniformis plus deaxxit	4	(2)(4)	NR
Li et al. 2014 [31]	60 (30/30)	T: 31.5 C: 33.8	Roman III	Acupuncture	Dicetel	4	(2)	NR
Zheng et al. 2014 [32]	348 (261/87)	T: 41.2 ± 17.1 C: 42.3 ± 18.4	Roman III	Acupuncture	Loperamide	4	(1)(2) (3)(9)	T: 3 C: 0
Li et al. 2015 [33]	40 (24/16)	T: 37.5 ± 16.4 C: 36.9 ± 14.7	Roman III	Electroacupuncture	Loperamide	4	(1)(2) (3)(4)	NR
Zheng et al. 2016 [34]	448 (336/112)	T: 40.5 ± 16.9 C: 40.6 ± 16.7	Roman III	Electroacupuncture	Loperamide	4	(1)(2) (3)(9)	T: 11 C: 0
Qin et al. 2017 [35]	61 (31/30)	T: 41 ± 11 C: 39 ± 12	Roman III	Acupuncture	Dicetel	4	(2)(4)(8)	None
Li et al. 2017 [36]	81 (54/27)	T: 46 ± 13 C: 48 ± 13	Roman III	Acupuncture	Dicetel	6	(2)(4) (8)(9)	T: 0 C: 1
Nie 2017 [37]	100 (50/50)	T: 35.2 ± 6.2 C: 34.2 ± 9.9	Roman III	Acupuncture	Dicetel	6	(2)(4)	NR



TABLE 1: Continued.

Study ID	Sample size (T/C)	Mean age (years)	Diagnostic standards	Intervention	Comparison	Duration (weeks)	Outcome	Adverse effects
Huang 2017 [38]	56 (38/18)	T: 36.3 ± 7.4 C: 38.8 ± 9.9	Roman III	Acupuncture	Dicetel	6	(2)(4)(7)	None
Liang 2017 [39]	34 (22/12)	T: 46.5 ± 11.4 C: 50.8 ± 14.2	Roman III	Acupuncture	Dicetel	6	(2)(4)(8)	NR
Zhong et al. 2018 [40]	60 (30/30)	T: 31.6 ± 12.3 C: 30.2 ± 14.0	Roman III	Electroacupuncture	Loperamide	9	(1)(2)(3)	NR
Yang et al. 2018 [41]	180 (120/60)	T: 40.0 ± 15.4 C: 40.0 ± 15.0	Roman III	Acupuncture	Trimebutine maleate	4	(2)(4)	NR
Zou et al. 2019 [42]	72 (36/36)	T: 42.2 ± 11.2 C: 43.7 ± 12.5	Roman III	Warm acupuncture	Eosinophil-lactobacillus compound tablet	3	(2)(4)(6)	NR
Meng 2019 [43]	70 (35/35)	T: 39.3 ± 11.5 C: 38.4 ± 13.5	Roman IV	Acupuncture	Dicetel	4	(2)(4) (8)(9)	T: 1 C: 5
Zhang 2019 [44]	65 (33/32)	T: 39.5 ± 2.1 C: 39.9 ± 2.1	Roman III	Warm acupuncture	Dicetel	4	(2)(4)(8)	NR
Lu 2019 [45]	76 (38/38)	T: 51.0 ± 9.5 C: 48.0 ± 10.5	Roman III	Acupuncture	Dicetel	4	(2)(4)(6)	NR
Mao 2019 [46]	80 (40/40)	T: 46.4 ± 11.5 C: 47.5 ± 12.4	Roman III	Acupuncture	Dicetel	6	(2)(4)(5) (8)(9)	T: 2 C: 4
Lin 2019 [47]	68 (34/34)	T: 39.9 ± 12.2 C: 40.1 ± 11.2	Compliant with Roman III	Acupuncture plus Dicetel	Dicetel	4	(2)(4)(5)	None
Li 2019 [48]	60 (30/30)	T: 45.0 ± 10.5 C: 45.0 ± 10.0	Roman IV	Warm acupuncture	Dicetel	8	(2)(4)	NR
Liu 2020 [49]	70 (35/35)	T: 42.5 ± 17.5 C: 41.5 ± 8.8	Roman III	Acupuncture	Trimebutine maleate	8	(2)(4)(8)	NR
Li et al. 2020 [50]	392 (261/131)	T: 45.9 ± 13.0 C: 47.0 ± 12.7	Roman III	Acupuncture	Dicetel	6	(2)	NR

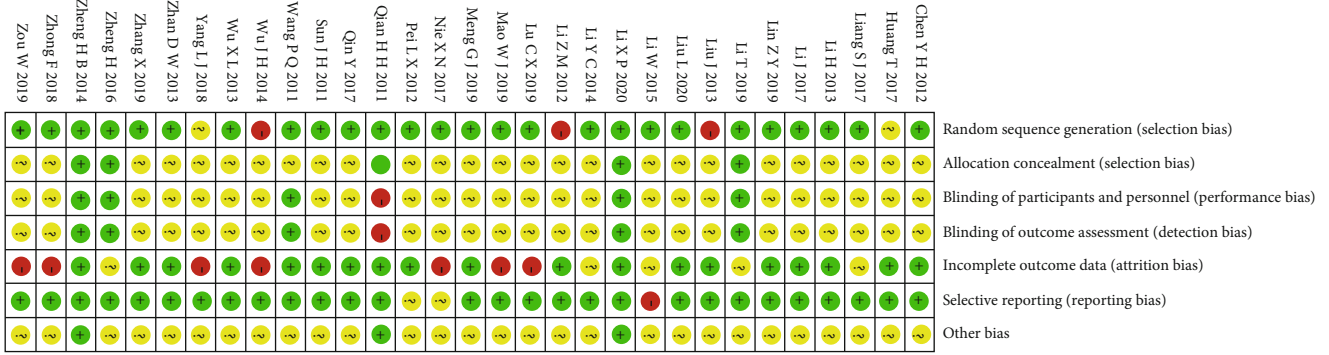


FIGURE 2: Risk of bias summary.

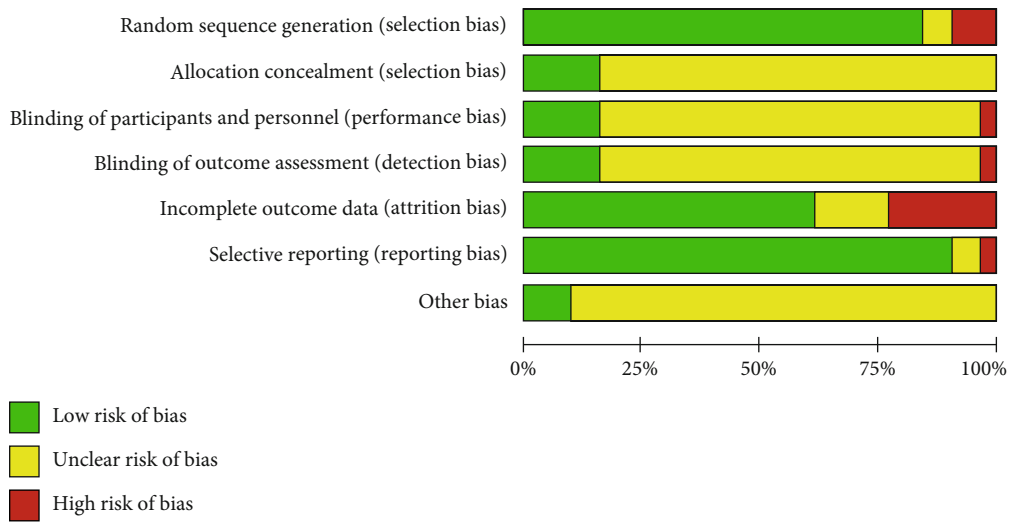


FIGURE 3: Risk of bias graph.

RCTs: randomized controlled trials; LOW (low certainty): our confidence in the effect estimate is limited: the true effect may be substantially different from the estimate of the effect; MODERATE (moderate certainty): we are moderately confident in the effect estimate: the true effect is likely to be close to the estimate of the effect, but there is a possibility that it is substantially different.

### 4. Result of Meta-Analysis

4.1. *Weekly Defecation.* Four studies [32–34, 40] reported participants’ number of defecations every week after treatment. The intervention methods of the control group were all loperamide. The results of the heterogeneity test demonstrated that there was no statistical significance ( $P = 0.19$ ) between the studies and a significant heterogeneity existed between the studies ( $Q(3) = 24.65, P \leq 0.01, I^2 = 96.03\%$ ). Sensitivity analysis and meta-analysis removed studies [32, 33] that lead to this heterogeneity. One study [32] applied the form of electroacupuncture as the intervention which was different from comparative studies caused heterogeneity. The other study [33] selected fewer acupoints than comparative caused the heterogeneity. The updated forest plot is

shown in Figure 4, demonstrating no heterogeneity among studies ( $Q(1) = 0.40, P = 0.53, I^2 = 0.00\%$ ), while maintaining a statistically significant difference between studies (SMD =  $-0.29, 95\% \text{ CI } [-0.49, -0.08], P = 0.01$ ).

4.2. *Patient Drop-off Rate.* Thirty-one studies [20–50] reported the patient drop-off rate. Due to the different intervention methods of the control groups, we compared and analyzed some of the studies [21–41, 43–46, 48–50] through the subgroup. The results of the heterogeneity test showed that there was no significant difference in comparing the acupuncture group with the bacillus licheniformis plus deanxit group (RR = 2.57, 95% CI [0.24, 27.65],  $P > 0.05$ ), the acupuncture group with the dicetel group (RR = 0.83, 95% CI [0.56, 1.23],  $P > 0.05$ ), the acupuncture group with the loperamide group (RR = 1.11, 95% CI [0.57, 2.15],  $P > 0.05$ ), the acupuncture group with the trimebutine maleate group (RR = 1.19, 95% CI [0.31, 4.53],  $P > 0.05$ ), and no heterogeneity between these studies ( $Q(27) = 4.28, P = 1.00, I^2 = 0.00\%$ ). Figure 5 presents this data in a forest plot. Combined with shear complement analysis, Egger test results showed that there is no published bias ( $\beta_1 = 0.03, \text{SE of } \beta_1 = 0.35$ ,

TABLE 2: GRADE summary of comparing the acupuncture group with different nonacupuncture groups.

Outcomes	Anticipated absolute effects* (95% CI) Assumed risk: nonacupuncture	Corresponding risk: acupuncture	Relative effect (95% CI)	N <sup>o</sup> of participants (studies)	Certainty of the evidence (GRADE)
Weekly defecation	The mean weekly defecation in the control groups was -5.2	The mean weekly defecation in the intervention groups was 0.29 lower (0.49 lower to 0.08 lower)	—	471 (2 RCTs)	⊕⊕⊕○ MODERATE
Bristol stool form	The mean Bristol stool form in the control groups was -4.16	The mean Bristol stool form in the intervention groups was 0.28 lower (0.68 lower to 0.12 higher)	—	100 (2 RCTs)	⊕⊕○○ LOW
Total symptom score	The mean total symptom score in the control groups was -4.1	The mean total symptom score in the intervention groups was 1.17 lower (1.42 lower to 0.93 lower)	—	303 (5 RCTs)	⊕⊕⊕○ MODERATE
IBS-QOL	The mean IBS-QOL in the control groups was 71.15	The mean IBS-QOL in the intervention groups was 2.37 higher (1.94 higher to 2.80 higher)	—	143 (2 RCTs)	⊕⊕○○ LOW
IBS-SSS	The mean IBS-SSS in the control groups was -95.7	The mean IBS-SSS in the intervention groups was 0.75 lower (1.04 lower to 0.47 lower)	—	319 (5 RCTs)	⊕⊕⊕○ MODERATE

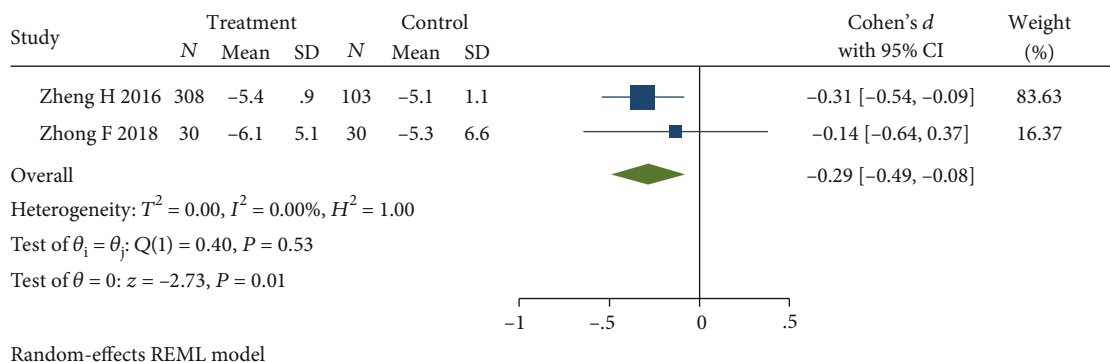


FIGURE 4: Forest plot of comparison of weekly defecation between the acupuncture group and loperamide group.

$z = 0.10, P = 0.92$ ). The L'Abbe plot of the heterogeneity test and funnel plot are presented in Figure 6.

4.3. *Bristol stool form.* Four studies [32–34, 40] reported the stool form using Bristol's chart, and the intervention methods of the control group were all loperamide. The result showed that there was no statistical significance between studies ( $P = 0.31$ ), but an obvious heterogeneity between the studies ( $Q(3) = 790.23, P \leq 0.01, I^2 = 99.91\%$ ). Sensitivity analysis and then a meta-analysis were carried out by removing studies [32, 34] that lead to this heterogeneity. One study [32] caused the heterogeneity still from the difference in acupuncture and electroacupuncture, and the other study [34] applied a different scoring method that resulted in heterogeneity. Figure 7 presents a forest map demonstrating no heterogeneity among studies ( $Q(1) = 0.00, P = 0.17, I^2 = 0.00\%$ ), and that there is no statistical signifi-

cance between studies (SMD =  $-0.28, 95\% \text{ CI } [-0.68, 0.12], P = 0.17$ ).

4.4. *Total Symptom Score.* Seven studies [20, 21, 26, 27, 29, 42, 45] reported the total symptom score. The meta-analysis was completed by removing the studies [20, 42] which caused the high heterogeneity. One study [20] applied acupuncture plus dicetel as an intervention different from comparative studies, which could cause the heterogeneity. The other study [42] selected warm acupuncture as an intervention that could still cause heterogeneity. Figure 8 presents a forest plot, which demonstrates no heterogeneity ( $Q(4) = 2.92, P = 0.57, I^2 = 0.00\%$ ) among the studies which used dicetel in control groups, and that the differences among studies continue to be significantly different (SMD =  $-1.17, 95\% \text{ CI } [-1.42, -0.93], P \leq 0.01$ ). Across studies, the total score of symptoms in the treatment group was lower than that in the control

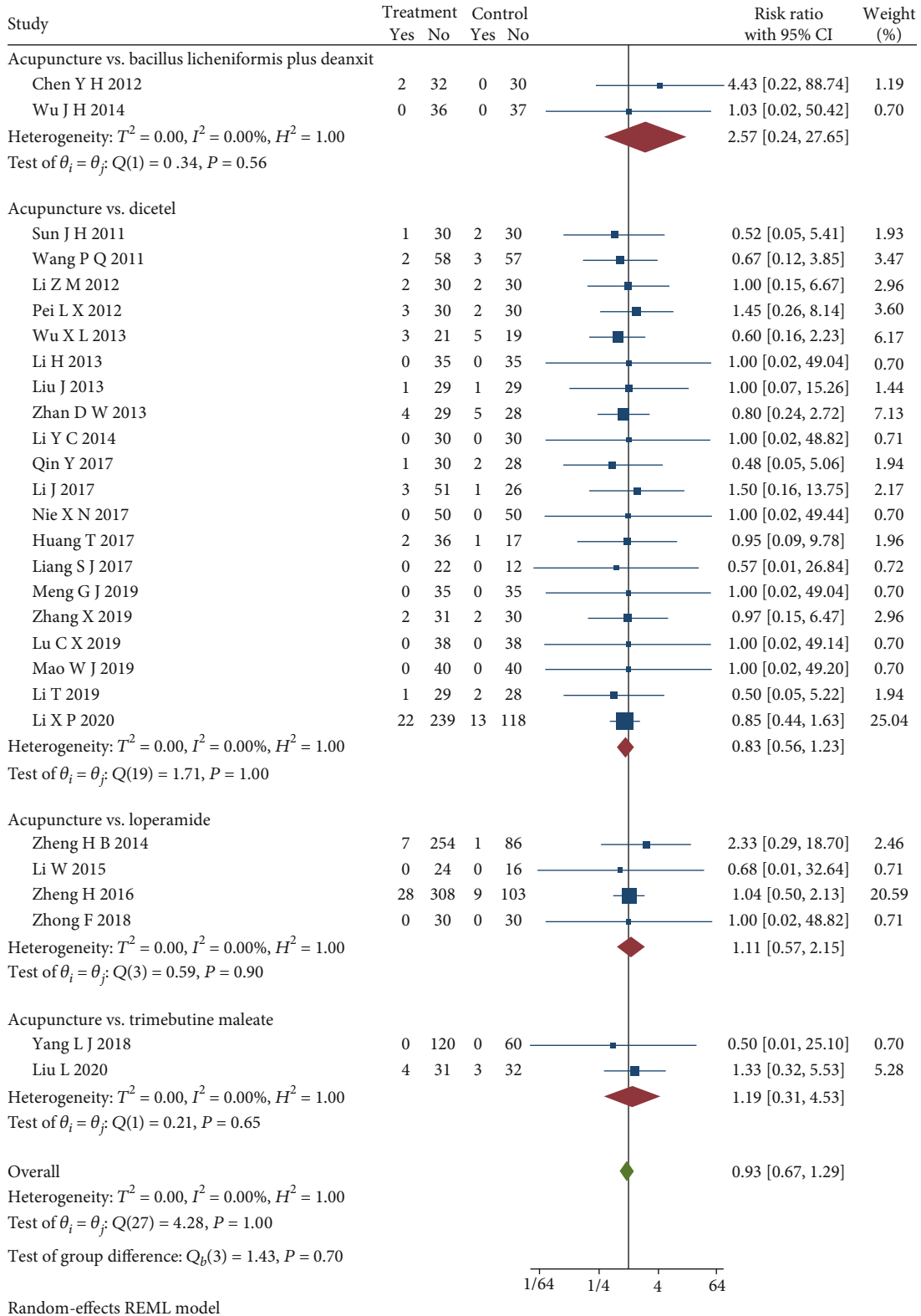


FIGURE 5: Forest plot of subgroup analysis on the patient drop-off rate.

group. Combined with the shear and complement analysis, Egger test results demonstrate that there was no publication bias ( $\beta_1 = -0.16, SE \text{ of } \beta_1 = 4.37, z = -0.04, P = 0.97$ ).

4.5. **IBS-QOL.** Four studies [21, 29, 46, 47] reported the IBS-QOL and the intervention methods of the control group were all dicetel. The results showed that there was

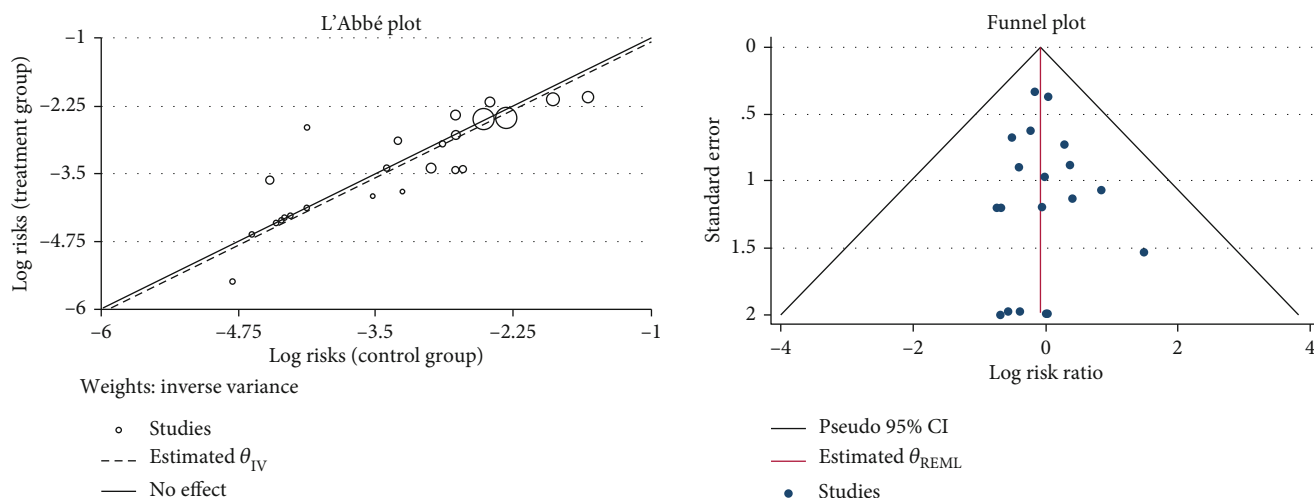


FIGURE 6: L'Abbe and funnel plots of the patient drop-off rate.

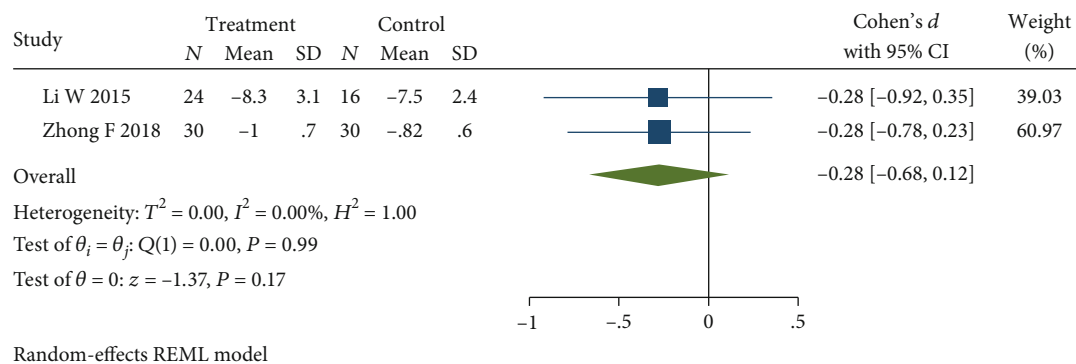


FIGURE 7: Forest plot of comparison of the Bristol stool form between the acupuncture group and loperamide group.

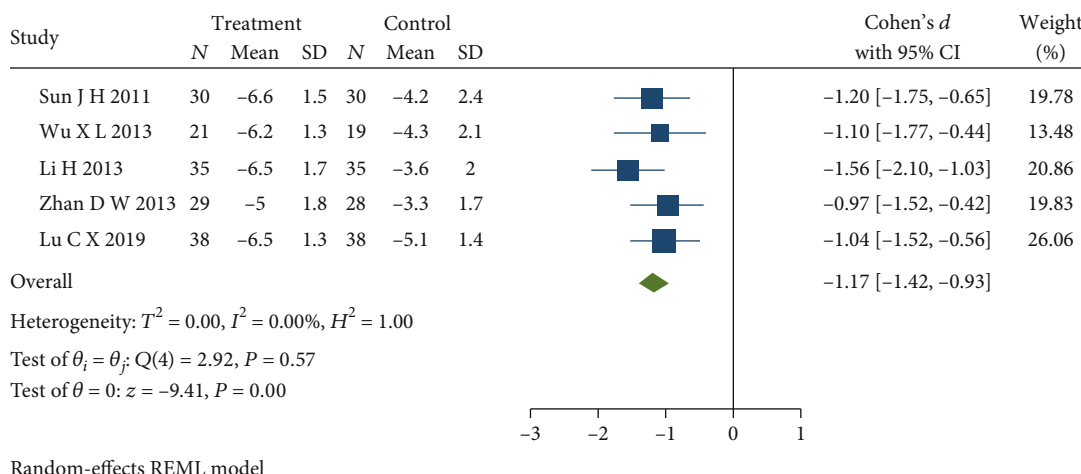


FIGURE 8: Forest plot of comparison of the total symptom score between the acupuncture group and dicetel group.

a significant statistical difference among studies ( $P \leq 0.01$ ) but obvious heterogeneity between studies ( $Q(3) = 32.75, P \leq 0.01, I^2 = 90.95\%$ ). After meta-analysis and eliminating studies [21, 29] which selected a different scoring method

leading to this heterogeneity, the forest plot presented in Figure 9 demonstrates that there is no heterogeneity ( $Q(1) = 0.15, P = 0.7, I^2 = 0.00\%$ ) among studies, and the differences between studies remain statistically significant



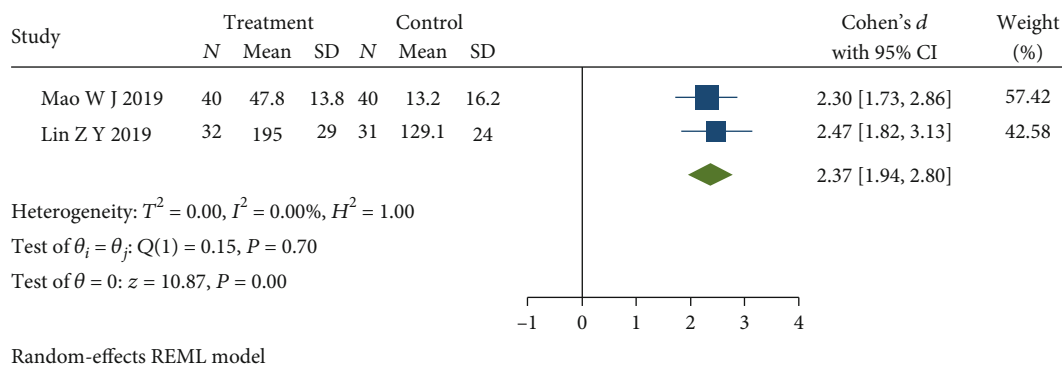


FIGURE 9: Forest plot of comparison of IBS-QOL between the acupuncture group and dicetel group.

(SMD = 2.37, 95% CI [1.94, 2.80],  $P \leq 0.01$ ). The quality of life in the treatment group was better than that in the control group.

**4.6. Total Efficiency.** Twenty-seven studies [20–30, 26–30, 33, 35–39, 41–49] reported the total effective treatment rate. We can analyze 22 studies [21–30, 35–39, 41, 43–46, 48, 49] through the subgroup because of different western medicine in control groups. Sensitivity analysis removed two studies [23, 30] which caused obvious heterogeneity in a subgroup. One study applied electroacupuncture as an intervention, and the other study applied warm acupuncture that could cause heterogeneity. Updated subgroup analysis showed a significant statistical difference in comparing the acupuncture group with dicetel (RR = 1.25, 95% CI [1.18, 1.32],  $P < 0.05$ ), the acupuncture group with the trimebutine maleate group (RR = 1.35, 95% CI [1.13, 1.61],  $P < 0.05$ ), the acupuncture group with the pinaverium bromide tablet group (RR = 1.40, 95% CI [1.16, 1.69],  $P < 0.05$ ), and no heterogeneity among studies ( $Q(19) = 10.51$ ,  $P = 0.94$ ,  $I^2 = 0.00\%$ ). Figure 10 presents the forest plot of the results. The total effective rate of the treatment group was greater than that of the control group. Combined with the shear complement analysis, funnel plots demonstrated that 7 published studies were missing. The Egger test showed that there were published biases ( $\beta_1 = 1.98$ , SE of  $\beta_1 = 0.90$ ,  $z = 2.21$ ,  $P = 0.03$ ). The L'Abbe plot of the heterogeneity test and funnel plot both are shown in Figure 11.

**4.7. Recurrence Rate.** Four studies [22, 23, 27, 38] reported the recurrence rate. Sensitivity analysis and then a meta-analysis were carried out by removing the study [23] which used a different oral medication that could cause the obvious heterogeneity in the control group. Figure 12 presents the forest plot, which demonstrates that there is no heterogeneity ( $Q(2) = 1.51$ ,  $P = 0.47$ ,  $I^2 = 0.00\%$ ) among the studies which used dicetel in control groups, and the differences between the studies remain statistically significant (RR = 0.43, 95% CI [0.28, 0.66],  $P \leq 0.01$ ). The recurrence rate of the treatment group was lower than that of the control group. Combined with the shear and complement analysis, there were two missing published biases in the funnel plot. Egger test results show that there is no published bias ( $\beta_1 = -1.78$ , SE of  $\beta_1 = 1.46$ ,  $z = -1.22$ ,  $P = 0.22$ ).

**4.8. IBS-SSS.** IBS-SSS was reported in 7 studies [35, 36, 39, 43, 44, 46, 49]. Subgroup analysis was completed after it removed one study [49] which used a different oral medication in the control group, but still the obvious heterogeneity among the left studies ( $Q(5) = 107.80$ ,  $P \leq 0.01$ ,  $I^2 = 99.60\%$ ). Sensitivity analysis and meta-analysis were conducted by removing the study [44] lead to this heterogeneity, which applied a different form of acupuncture that caused the result. The updated forest plot of meta-analysis is shown in Figure 13 and demonstrates that there is low heterogeneity among studies ( $Q(4) = 6.19$ ,  $P = 0.19$ ,  $I^2 = 31.60\%$ ) which used dicetel in the control group, and the difference between the studies is statistically significant (SMD =  $-0.75$ , 95% CI [ $-1.04$ ,  $-0.47$ ],  $P \leq 0.01$ ). Combined with shear complement analysis, Egger test results showed that there were no biased publications ( $\beta_1 = 3.91$ , SE of  $\beta_1 = 3.81$ ,  $z = 1.03$ ,  $P = 0.30$ ).

**4.9. Adverse Effect.** Adverse events were reported in 7 studies [22, 28, 32, 34, 36, 43, 46]. Subgroup analysis completed with these studies, but one subgroup showed an obvious heterogeneity ( $Q(4) = 9.79$ ,  $P = 0.04$ ,  $I^2 = 61.60\%$ ). One study applied a different form of acupuncture that caused the obvious heterogeneity. Sensitivity analysis and then a meta-analysis were carried out after removing the study [22]. Figure 14 presents the updated forest plot and demonstrates that there is no heterogeneity: acupuncture group versus dicetel group ( $Q(3) = 5.68$ ,  $P = 0.13$ ,  $I^2 = 46.12\%$ ) and acupuncture group versus loperamide group ( $Q(1) = 0.32$ ,  $P = 0.57$ ,  $I^2 = 0.00\%$ ). There were more adverse events in the acupuncture group than in the control group. The comparing acupuncture group with dicetel group is no statistically significant (RR = 0.59, 95% CI [0.12, 2.90],  $P > 0.05$ ), but comparing the acupuncture group with the loperamide group is no statistically significant (RR = 4.42, 95% CI [0.57, 33.97],  $P > 0.05$ ). Combined with shear complement analysis, Egger test results showed no biased publications ( $\beta_1 = 2.40$ , SE of  $\beta_1 = 2.36$ ,  $z = 1.02$ ,  $P = 0.31$ ).

## 5. Discussion

In this systematic review and meta-analysis, the effectiveness and safety of 31 acupuncture concerned studies for patients with IBS-D or FD were evaluated. We found that acupuncture can significantly reduce the number of stools per week

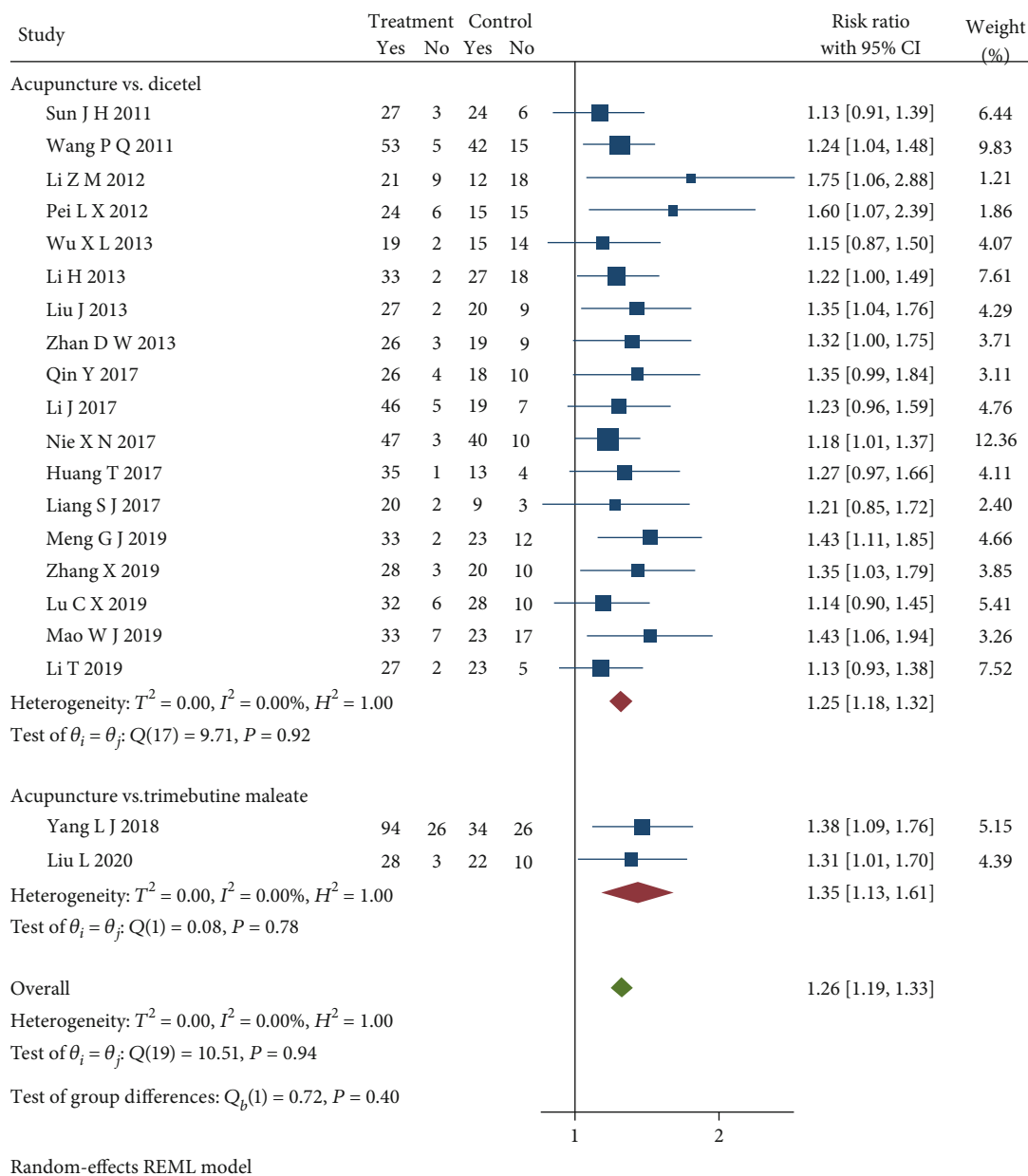


FIGURE 10: Forest plot of subgroup analysis on total efficiency.

in IBS-D or FD patients, improve patients' overall symptoms, improve the total effective rate, decrease the recurrence rate, and reduce the pain level of patients. Based on the results, we believe that acupuncture can improve the quality of life of patients with IBS-D or FD. Although the number of adverse events in the acupuncture group was similar to that in the control group, the majority of adverse events in the acupuncture group were subcutaneous hemorrhage. With such slight adverse events, we have observed that acceptance among patients has not been reduced. Moreover, the withdrawal rate of patients in the acupuncture group was still slightly lower than that in the control group. Previous studies ignored the importance of the FD which should be related to chronic diarrhea and lack of standard, high-quality clinical trials. This study combined the IBS-D with the FD as the object of research included one standard, high-quality clinical trial

[50] which improved the quality of evidence-based medicine. Besides, the patient drop-off rate was reported in our results which showed the comparison of patient receptivity. Unlike previous methods, our study made an advanced analysis through applied the Stata 16.0 software, and some results were evaluated by GRADE that exhibited a more compelling piece of evidence.

The quality of life of IBS-D or FD patients is generally not high that has been demonstrated [51]. Also, the consistency of stool in patients with IBS-D or FD is between type 5 and type 7 on the Bristol stool scale [52]. Among them, abdominal pain is the main diagnostic standard of IBS-D, while FD is mainly diagnosed by excluding the possibility of other diseases [53]. The prevalence of FD and IBS-D in China is 1.72% and 1.54%, respectively [54]. Despite conventional drugs that can temporarily alleviate symptoms, many

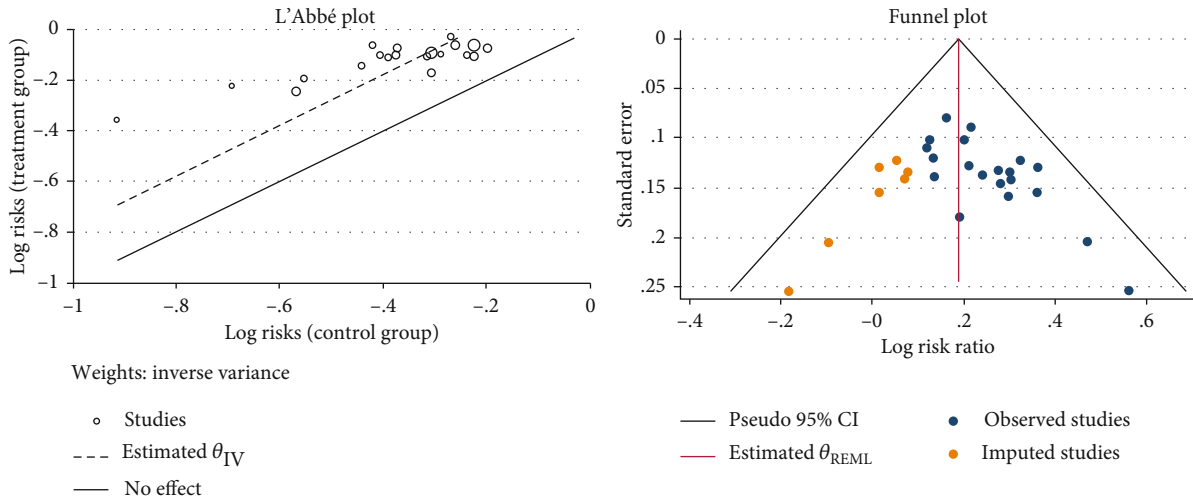


FIGURE 11: L'Abbe and funnel plots of total efficiency.

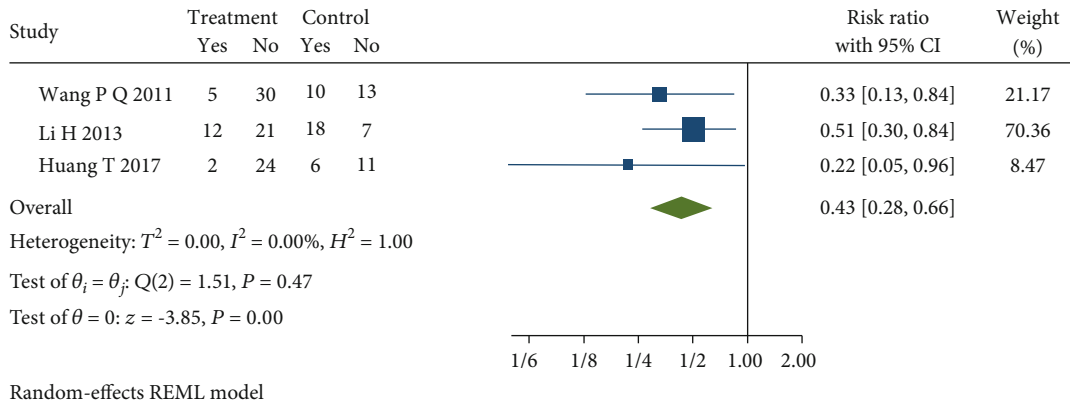


FIGURE 12: Forest plot of comparison of the recurrence rate between the acupuncture group and dicetel group.

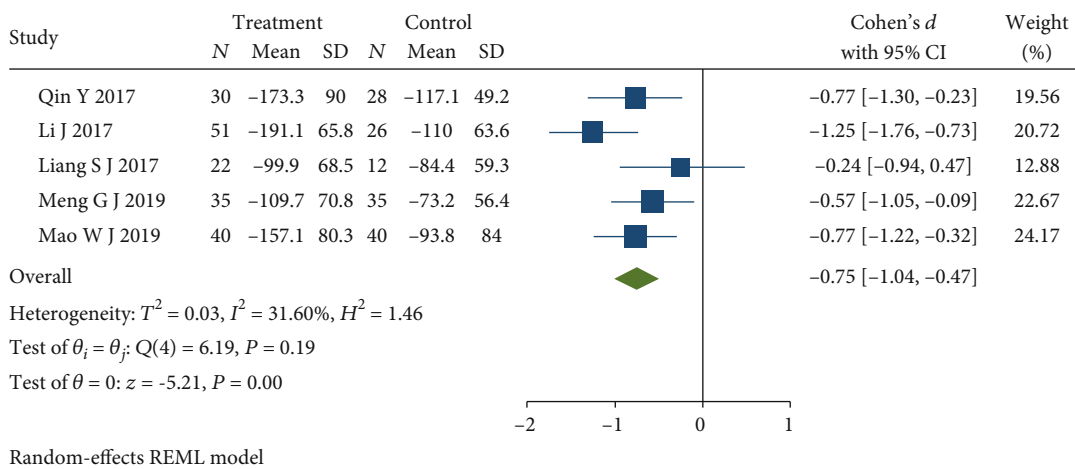


FIGURE 13: Forest plot of comparison of IBS-SSS between the acupuncture group and dicetel group.

patients still suffer from the IBS-D or FD, and the recurrence rate was as high as 40% after 3 months. It has been reported that approximately 60.1% of the drug treatment patients stop

taking drugs on their own due to the lack of obvious symptom improvement [55, 56]. At present, the etiology and pathogenesis of IBS-D or FD are not clear, but there is growing

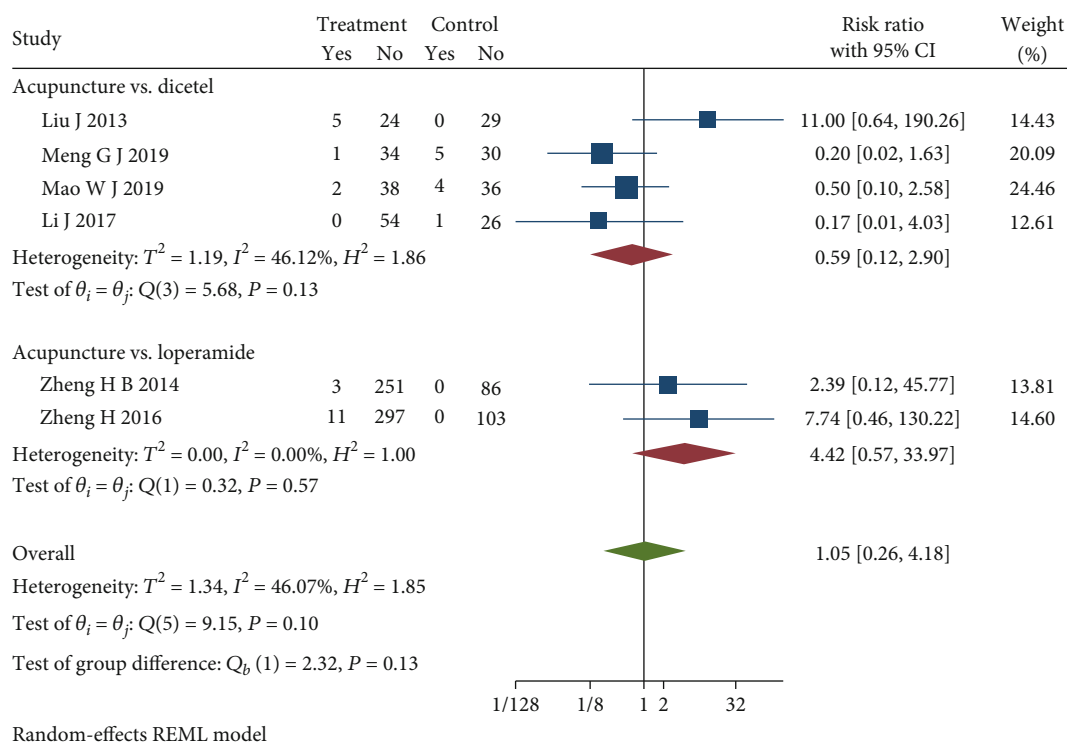


FIGURE 14: Forest plot of comparison of the adverse effect.

evidence that pathogenic factors may be related to inflammation, central nervous system disorders, and brain-gut interaction [57]. Serum vasoactive intestinal peptide (VIP) is a neurotransmitter that inhibits gastrointestinal motility and promotes the secretion of intestinal water and electrolytes [58]. 5-hydroxytryptamine (5-HT) as a neurotransmitter also widely exists in the central nervous system and gastrointestinal tract and can regulate gastrointestinal function [59, 60]. Acupuncture, as an alternative therapy for a variety of diseases [61–63], may have achieved the effect of treating IBS-D and FD by regulating nerve-related functions [64]. From the studies included in this review, we also found that acupuncture could improve clinical reports of VIP and 5-HT levels [31].

According to the risk of bias summary and graph, the overall quality of our study is still low. Many studies were regarded as unclear risk of bias in terms of selection bias, performance bias, detection bias, and other bias. Incomplete outcome data in some studies led to a high bias, and we tried to contact authors but got no available datum. The inconsistent diagnostic standards of some studies may lead to the nonstandard diagnosis of FD and IBS-D. Only six studies [22, 32, 34, 48, 50] describe randomized methods and use blinding methods. The remaining studies do not specifically describe randomized or blind treatment methods, which could cause selection bias under the subjective choice of subjects or researchers. And most studies lacked the group of sham acupuncture, and only one study selected the acupuncture plus dicetel compared with sham acupuncture plus dicetel. So, the results of this study were merely a comparison between acupunc-

ture and western medicine, and studies of sham acupuncture groups are still needed. Sensitivity analysis revealed the form of acupuncture, the method of scale scoring, the difference of acupuncture points, and the difference of oral medication in the control group that could be the sources of heterogeneity. In this study, electroacupuncture, warm acupuncture, and eye acupuncture were regarded as the same intervention, even the difference of acupuncture points was hard to keep consistent. Besides, in the clinic, different forms of acupuncture may have different stimulation and patient receptivity. So, potential biases could affect the accuracy of some results. Although our results avoided the high heterogeneity through removed some studies, the reduction in the number of patients affected the quality of the results.

The clinical effect of acupuncture on IBS-D or FD cannot be ignored. It has great safety, can avoid adverse reactions caused by western medicine, and has the advantages of simple operation and low cost [65]. This study objectively explored the effectiveness and safety of acupuncture in the treatment of IBS-D or FD and provided preliminary and reliable evidence-based medicine for clinical practice and decision-making.

## 6. Conclusion

Our systematic review and meta-analysis can prove the effectiveness of acupuncture in the treatment of IBS-D or FD, but it still needs to be verified by a clinical standard large sample test.

## Conflicts of Interest

All authors declare that they have no conflict of interests.

## Authors' Contributions

Jianbo Guo and Xiaoxiao Xing contributed equally to this article and wrote the draft. Qingyong He and Zongshi Qin designed the study. Jiani Wu modified this article. Hui Zhang and Yongen Yun participated in the statistical analysis. All authors read and approved the final manuscript. Jianbo Guo and Xiaoxiao Xing contributed equally to this manuscript.

## Acknowledgments

The current work was supported by the Beijing Science and Technology Nova Program (Z181100006218035).

## Supplementary Materials

Supplementary 1. S1: PRISMA Checklist.

Supplementary 2. S2: search strategy of the PubMed database.

## References

- [1] M. I. Pinto-Sanchez, G. B. Hall, K. Ghajar et al., "Probiotic bifidobacterium longum NCC3001 reduces depression scores and alters brain activity: a pilot study in patients with irritable bowel syndrome," *Gastroenterology*, vol. 153, no. 2, pp. 448–459.e8, 2017.
- [2] X. Q. Li, M. Chang, D. Xu, and X. C. Fang, "Status analysis of an epidemiological survey of irritable bowel syndrome in China," *Journal of Gastroenterology and Hepatology*, vol. 22, no. 8, pp. 734–739, 2013.
- [3] R. S. Sandler, W. F. Stewart, J. N. Liberman, J. A. Ricci, and N. L. Zorich, "Abdominal pain, bloating, and diarrhea in the United States: prevalence and impact," *Digestive Diseases and Sciences*, vol. 45, no. 6, pp. 1166–1171, 2000.
- [4] The Cochrane Collaboration, B. Lim, E. Manheimer et al., "Acupuncture for treatment of irritable bowel syndrome," *Cochrane Database of Systematic Reviews*, vol. 18, no. 4, pp. 1–104, 2006.
- [5] Z. Qin, B. Li, J. Wu et al., "Acupuncture for chronic diarrhea in adults: protocol for a systematic review," *Medicine*, vol. 96, no. 4, article e5952, 2017.
- [6] A. Hadjivasilis, C. Tsioutis, A. Michalinos, D. Ntourakis, D. K. Christodoulou, and A. P. Agouridis, "New insights into irritable bowel syndrome: from pathophysiology to treatment," *Annals of Gastroenterology*, vol. 32, no. 6, pp. 554–564, 2019.
- [7] W. Smalley, C. Falck-Ytter, A. Carrasco-Labra, S. Wani, L. Lytvyn, and Y. Falck-Ytter, "AGA clinical practice guidelines on the laboratory evaluation of functional Diarrhea and Diarrhea-predominant irritable bowel syndrome in adults (IBS-D)," *Gastroenterology*, vol. 157, no. 3, pp. 851–854, 2019.
- [8] X. Xu, L. Liu, S. Yao, and Y. Zhang, "Visceral sensitivity, gut barrier function and autonomic nerve function in patients with diarrhea-predominant irritable bowel syndrome," *Zhong Nan Da Xue Xue Bao. Yi Xue Ban*, vol. 42, no. 5, pp. 522–528, 2017.
- [9] D. J. Cangemi and B. E. Lacy, "Management of irritable bowel syndrome with diarrhea: a review of nonpharmacological and pharmacological interventions," *Therapeutic Advances in Gastroenterology*, vol. 12, 2019.
- [10] E. S. Dellon and Y. Ringel, "Treatment of functional diarrhea," *Current Treatment Options in Gastroenterology*, vol. 9, no. 4, pp. 331–342, 2006.
- [11] D. N. Juurlink and L. A. Dhalla, "Dependence and addiction during chronic opioid therapy," *Journal of Medical Toxicology*, vol. 8, no. 4, pp. 393–399, 2012.
- [12] W. Zhou and P. Benharash, "Effects and mechanisms of acupuncture based on the principle of meridians," *Journal of Acupuncture and Meridian Studies*, vol. 7, no. 4, pp. 190–193, 2014.
- [13] J. Yin and J. D. Chen, "Gastrointestinal motility disorders and acupuncture," *Autonomic Neuroscience*, vol. 157, no. 1–2, pp. 31–37, 2010.
- [14] T. Takahashi, "Acupuncture for functional gastrointestinal disorders," *Journal of Gastroenterology*, vol. 41, no. 5, pp. 408–417, 2006.
- [15] E. Noguchi, "Mechanism of reflex regulation of the gastroduodenal function by acupuncture," *Evidence-based Complementary and Alternative Medicine*, vol. 5, no. 3, pp. 251–256, 2008.
- [16] T. Takahashi, "Mechanism of acupuncture on neuromodulation in the Gut-A review," *Neuromodulation*, vol. 14, no. 1, pp. 8–12, 2011.
- [17] Y. Q. Li, B. Zhu, P. J. Rong, H. Ben, and Y. H. Li, "Neural mechanism of acupuncture-modulated gastric motility," *World Journal of Gastroenterology*, vol. 13, no. 5, pp. 709–716, 2007.
- [18] K. Knobloch, U. Yoon, and P. M. Vogt, "Preferred reporting items for systematic reviews and meta-analyses (PRISMA) statement and publication bias," *Journal of Cranio-Maxillofacial Surgery*, vol. 39, no. 2, pp. 91–92, 2011.
- [19] A. Liberati, D. G. Altman, J. Tetzlaff et al., "The PRISMA statement for reporting systematic reviews and meta-analyses of studies that evaluate health care interventions: explanation and elaboration," *Annals of Internal Medicine*, vol. 151, no. 4, pp. W–W94, 2009.
- [20] H. H. Qian, Y. P. Zhu, S. Meng, G. H. Qi, and X. X. Zhao, "Randomized controlled trial of acupuncture treatment for diarrheal irritable bowel syndrome," *World Journal of Chinese Digestion*, vol. 19, no. 3, pp. 257–261, 2011.
- [21] J. H. Sun, X. L. Wu, C. Xia et al., "Clinical evaluation of soothing liver and invigorating spleen of acupuncture treatment on diarrhea-predominant irritable bowel syndrome," *Chinese Journal of Integrative Medicine*, vol. 17, no. 10, pp. 780–785, 2011.
- [22] P. Q. Wang, S. N. Chen, Y. D. Liu, X. Y. Chen, and J. Wang, "Clinical study of 60 cases of diarrheal irritable bowel syndrome treated with eye acupuncture," *Journal of Traditional Chinese Medicine*, vol. 52, no. 14, pp. 1203–1206, 2011.
- [23] Y. H. Chen, X. K. Chen, X. J. Yin, and Y. Shi, "Comparative study on efficacy of electroacupuncture combined with probiotics in the treatment of diarrheal irritable bowel syndrome," *Chinese Journal Of Integrated Traditional Chinese and Western Medicine*, vol. 32, no. 5, pp. 594–598, 2012.
- [24] Z. Li, *Clinical Study on Acupuncture Treatment of Diarrhea-Type Irritable Bowel Syndrome (Liver Depression and Spleen Deficiency Syndrome)*, Liaoning University of Traditional Chinese Medicine, 2012.



- [25] L. X. Pei, J. H. Sun, C. Xia et al., "Clinical study on acupuncture therapy for the syndrome of liver depression and spleen deficiency in diarrhea with irritable bowel syndrome," *Journal of Nanjing University of Chinese Medicine*, vol. 28, no. 1, pp. 27–29, 2012.
- [26] X. L. Wu, Y. L. Wang, J. H. Sun et al., "Clinical observation of liver depression and spleen deficiency syndrome in diarrheal irritable bowel syndrome treated with acupuncture and its effect on Th1/Th2," *Chinese Acupuncture*, vol. 33, no. 12, pp. 1057–1060, 2013.
- [27] H. Li, L. X. Pei, and J. L. Zhou, "Comparative observation of acupuncture and western medicine in the treatment of diarrheal irritable bowel syndrome," *Chinese Acupuncture & Moxibustion*, vol. 32, no. 8, pp. 679–682, 2012.
- [28] J. Liu, *Efficacy Evaluation and Mechanism of Eye Acupuncture in the Treatment of Diarrhea Type of Irritable Bowel Syndrome (Liver Depression and Spleen Syndrome)*, Liaoning University of Traditional Chinese Medicine, 2013.
- [29] D. W. Zhan, *Effect of Acupuncture on Serum 5-HT, NPY and CGRP Levels in Patients with Diarrhoeal Irritable Bowel Syndrome*, Nanjing University of Chinese Medicine, 2013.
- [30] J. H. Wu, "Observation on therapeutic effect of warm acupuncture on diarrhea type irritable bowel syndrome," *Chinese Journal of Traditional Chinese Medicine Information*, vol. 21, no. 11, pp. 98–99, 2014.
- [31] Y. C. Li, "Effect of acupuncture on serum brain-gut peptide in patients with spleen deficiency and diarrhea with irritable bowel syndrome," *Chinese Journal of Clinical Acupuncture*, vol. 30, no. 10, pp. 19–20, 2014.
- [32] H. B. Zheng, *Multi-Center, Large Sample Randomized Controlled Study on Acupuncture Treatment of Diarrheal Irritable Bowel Syndrome*, Chengdu University of Traditional Chinese Medicine, 2014.
- [33] W. Li and W. Zhang, "Effect of electroacupuncture on fecal symptoms in patients with functional diarrhea," *Liaoning Journal of Traditional Chinese Medicine*, vol. 42, no. 10, pp. 1974–1976, 2015.
- [34] H. Zheng, Y. Li, W. Zhang et al., "Electroacupuncture for patients with diarrhea-predominant irritable bowel syndrome or functional diarrhea: a randomized controlled trial," *Medicine*, vol. 95, no. 24, p. e3884, 2016.
- [35] Y. Qin, W. Yi, S. X. Lin, C. F. Yang, and Z. M. Zhuang, "Clinical efficacy observation of abdominal acupuncture therapy in the treatment of diarrheal irritable bowel syndrome," *Chinese Acupuncture*, vol. 37, no. 12, pp. 1265–1268, 2017.
- [36] J. Li, J. Lu, J. H. Sun et al., "Tiaoshen Jianpi combined with acupoint acupuncture to improve symptoms and sleep quality of diarrhea-type irritable bowel syndrome: a randomized controlled trial," *Chinese Acupuncture*, vol. 37, no. 1, pp. 9–13, 2017.
- [37] X. N. Nie, Y. Li, and Z. M. Shi, "A randomized controlled study on the treatment of diarrhea-type irritable bowel syndrome with acupuncture and acupuncture on the head and body," *Journal of Chengdu University of Chinese Medicine*, vol. 40, no. 4, pp. 48–51, 2017.
- [38] T. Huang, *Clinical Study on Acupuncture Treatment of Diarrheal Irritable Bowel Syndrome*, Nanjing University of Chinese Medicine, 2017.
- [39] S. J. Liang, *Effect of Tiaoshenjianpi Acupuncture on the Hypothalamus-Pituitary-Adrenal Axis in Patients with Diarrhea-Type Irritable Bowel Syndrome*, Nanjing University of Traditional Chinese Medicine, 2017.
- [40] F. Zhong, Y. Cao, R. Luo et al., "Observation on the therapeutic effect of electroacupuncture on Duozhonghezhiyu point in the treatment of diarrheal irritable bowel syndrome," *Journal of Hunan University of Chinese Medicine*, vol. 38, no. 4, pp. 435–438, 2008.
- [41] L. J. Yang, X. X. Wang, B. Li et al., "Effect of acupuncture on acupoint pain threshold in patients with irritable bowel syndrome," *Shanghai Journal of Acupuncture*, vol. 37, no. 9, pp. 1030–1036, 2016.
- [42] W. Zou, L. Y. Mao, M. Liu, and T. Yu, "Clinical study on the treatment of diarrheal irritable bowel syndrome with spleen and stomach weakness by warm acupuncture," *Shaanxi Traditional Chinese Medicine*, vol. 40, no. 12, pp. 1786–1788, 2019.
- [43] G. J. Meng, "A randomized controlled study of acupuncture treatment for depressive symptoms in diarrheal irritable bowel syndrome," *Chinese Journal of Acupuncture and Massage*, vol. 17, no. 6, pp. 422–426, 2017.
- [44] X. Zhang, M. Ding, and H. Feng, "Du's heat tonic method of acupuncture treatment of diarrheal irritable bowel syndrome: a randomized controlled study," *Acupuncture and Massage Medicine*, vol. 2, pp. 124–130, 2019.
- [45] C. X. Lu, "Effect of acupuncture therapy on diarrhea type irritable bowel syndrome with liver depression and spleen deficiency," *Contemporary Medical Journal*, vol. 17, no. 19, pp. 43–45, 2019.
- [46] W. J. Mao, "Clinical study on acupuncture treatment of 40 cases of diurnal irritable bowel syndrome," *Jiangsu Chinese Medicine*, vol. 51, no. 9, pp. 63–65, 2019.
- [47] Z. Y. Lin, *Clinical Observation of Acupuncture Treatment of Spleen Deficiency and Dampness-Sheng Type Irritable Bowel Syndrome (Diarrheal Type)*, Fujian University of Traditional Chinese Medicine, 2019.
- [48] T. Li, *Clinical Effect Observation of Relieving Liver Depression and Warming Acupuncture on Diarrhea Type Irritable Bowel Syndrome (Liver Depression and Spleen Deficiency Type)*, Beijing University of Chinese Medicine, 2019.
- [49] L. Liu, L. J. Hao, and Z. M. Shi, "Clinical observation on acupuncture of foot jue Yin liver meridian for treatment of diarrheal irritable bowel syndrome," *Journal of Guangzhou University of Chinese Medicine*, vol. 37, no. 2, pp. 279–284, 2020.
- [50] L. Pei, H. Geng, J. Guo et al., "Effect of acupuncture in patients with irritable bowel syndrome: a randomized controlled trial," *Mayo Clinic Proceedings*, vol. 95, no. 8, pp. 1671–1683, 2020.
- [51] L. M. Mena Bares, E. Carmona Asenjo, M. V. García Sánchez et al., "SGammagrafía con <sup>75</sup>SeHCAT en la diarrea crónica por malabsorción de ácidos biliares," *Revista Española De Medicina Nuclear E Imagen Molecular*, vol. 36, no. 1, pp. 37–47, 2017.
- [52] R. P. Arasaradnam, S. Brown, A. Forbes et al., "Guidelines for the investigation of chronic diarrhoea in adults: British Society of Gastroenterology, 3rd edition," *Gut*, vol. 67, no. 8, pp. 1380–1399, 2018.
- [53] J. Hammer, G. D. Eslick, S. C. Howell, E. Altiparmak, and N. J. Talley, "Diagnostic yield of alarm features in irritable bowel syndrome and functional dyspepsia," *Gut*, vol. 53, no. 5, pp. 666–672, 2004.
- [54] Y.-F. Zhao, X.-J. Guo, Z.-S. Zhang et al., "Epidemiology of functional diarrhea and comparison with diarrhea-predominant irritable bowel syndrome: a population-based survey in China," *PLoS One*, vol. 7, no. 8, p. e43749, 2012.

- [55] J. K. Triantafyllidis and G. Malgarinos, "Long-term efficacy and safety of otilonium bromide in the management of irritable bowel syndrome: a literature review," *Clinical and Experimental Gastroenterology*, vol. 7, pp. 75–82, 2014.
- [56] J. J. Mira, G. Lacima, and X. Cortes Gil, "Perceptions of the public healthcare system from private-care patients with irritable bowel syndrome with constipation in Spain," *Revista Española de Enfermedades Digestivas*, vol. 110, no. 10, pp. 612–620, 2018.
- [57] L. Saha, "Irritable bowel syndrome: pathogenesis, diagnosis, treatment, and evidence-based medicine," *World Journal of Gastroenterology*, vol. 20, no. 22, pp. 6759–6773, 2014.
- [58] A. W. Mangel, J. D. Bornstein, L. R. Hamm et al., "Clinical trial: asimadoline in the treatment of patients with irritable bowel syndrome," *Alimentary Pharmacology & Therapeutics*, vol. 28, no. 2, pp. 239–249, 2008.
- [59] J. H. Sellin, "A practical approach to treating patients with chronic diarrhea," *Reviews in Gastroenterological Disorders*, vol. 7, no. 3, pp. S19–S26, 2007.
- [60] E. A. Salsitz, "Chronic pain, chronic opioid addiction: a complex nexus," *Journal of Medical Toxicology*, vol. 12, no. 1, pp. 54–57, 2016.
- [61] S. S. Magge and J. L. Wolf, "Complementary and alternative medicine and mind-body therapies for treatment of irritable bowel syndrome in women," *Women's Health*, vol. 9, no. 6, pp. 557–567, 2013.
- [62] A. S. Cheifetz, R. Gianotti, R. Lubert, and P. R. Gibson, "Complementary and alternative medicines used by patients with inflammatory bowel diseases," *Gastroenterology*, vol. 152, no. 2, pp. 415–429.e15, 2017.
- [63] B. Kligler, R. Teets, and M. Quick, "Complementary/integrative therapies that work: a review of the evidence," *American Family Physician*, vol. 94, no. 5, pp. 369–374, 2016.
- [64] C. Zhou, D. R. Nie, A. H. Yuan, and J. Yang, "Professor YANG Jun's clinical characteristics in the treatment of chronic diarrhea with acupuncture and herbal medicine based on qi activity theory in *Huangdi Neijing*," *Zhongguo Zhen Jiu*, vol. 40, no. 2, pp. 207–210, 2020.
- [65] D. X. Deng, K. K. Guo, J. Tan et al., "Meta-analysis of clinical research on acupuncture treatment of diarrheal irritable bowel syndrome," *Chinese Acupuncture*, vol. 37, no. 8, pp. 907–912, 2017.

## Research Article

# EA Improves the Motor Function in Rats with Spinal Cord Injury by Inhibiting Signal Transduction of Semaphorin3A and Upregulating of the Peripheral Nerve Networks

Rong Hu <sup>1</sup>, Haipeng Xu,<sup>1</sup> Yaheng Jiang,<sup>1</sup> Yi Chen,<sup>1</sup> Kelin He,<sup>1,2</sup> Lei Wu,<sup>2</sup> XiaoMei Shao <sup>1</sup> and Ruijie Ma <sup>1,2</sup>

<sup>1</sup>Department of Neurobiology and Acupuncture Research, The Third Clinical Medical College, Zhejiang Chinese Medical University, Key Laboratory of Acupuncture and Neurology of Zhejiang Province, Hangzhou, China

<sup>2</sup>Department of Acupuncture, The Third Affiliated Hospital of Zhejiang Chinese Medical University, Zhejiang Province, Hangzhou, China

Correspondence should be addressed to Ruijie Ma; maria7878@sina.com

Rong Hu and Haipeng Xu contributed equally to this work.

Received 19 May 2020; Revised 22 September 2020; Accepted 31 October 2020; Published 21 November 2020

Academic Editor: Lu Wang

Copyright © 2020 Rong Hu et al. This is an open access article distributed under the Creative Commons Attribution License, which permits unrestricted use, distribution, and reproduction in any medium, provided the original work is properly cited.

Peripheral nerve networks (PNNs) play a vital role in the neural recovery after spinal cord injury (SCI). Electroacupuncture (EA), as an alternative medicine, has been widely used in SCI and was proven to be effective on neural functional recovery. In this study, the interaction between PNNs and semaphrin3A (Sema3A) in the recovery of the motor function after SCI was observed, and the effect of EA on them was evaluated. After the establishment of the SCI animal model, we found that motor neurons in the ventral horn of the injured spinal cord segment decreased, Nissl bodies were blurry, and PNNs and Sema3A as well as its receptor neuropilin1 (NRP1) aggregated around the central tube of the gray matter of the spinal cord. When we knocked down the expression of Sema3A at the damage site, NRP1 also downregulated, importantly, PNNs concentration decreased, and tenascin-R (TN-R) and aggrecan were also reduced, while the Basso-Beattie-Bresnahan (BBB) motor function score dramatically increased. In addition, when conducting EA stimulation on Jiaji (EX-B2) acupoints, the highly upregulated Sema3A and NRP1 were reversed post-SCI, which can lessen the accumulation of PNNs around the central tube of the spinal cord gray matter, and simultaneously promote the recovery of motor function in rats. These results suggest that EA may further affect the plasticity of PNNs by regulating the Sema3A signal and promoting the recovery of the motor function post-SCI.

## 1. Introduction

Spinal cord injury (SCI) and its secondary complications have become a significant social and economic burden on the health care system and patient's families, which mainly leads to irreversible neurological impairment [1]. Although SCI shows some spontaneous recovery of the motor and sensory function, recovery in patients with complete SCI is quite limited and predictable [2]. As an alternative therapy, Electroacupuncture (EA) has been proven to be particularly effective in the rehabilitation of spinal cord injury. According to Dorsher [3], EA can significantly improve the long-term neurological

recovery of patients with SCI in the acute stage. Moreover, a previous meta-analysis [4] by our team showed that EA played an active role in the recovery of the neurological function and motor function post-SCI. Additionally, EA on Jiaji (EX-B2) acupoints with the stimulation parameter from 2 Hz/100 Hz has been shown as an antioxidant, anti-inflammation, and antiapoptosis agent, thus promoting axonal regeneration, nerve growth factor improvement, and some gene expressions [5–8]. These effects of EA may have a positive effect on functional recovery post-SCI and can be acknowledged to reduce the risk of secondary spinal cord damage.

Spinal cord injury not only destroys the connectivity of neural circuits but also causes a series of secondary

pathological processes, such as inflammation and glial fiber scar, which are chemical barriers to prevent axon regeneration and limit nerve function repair. Nevertheless, the function of the adult spinal cord could be restored by promoting the germination and regeneration of axons and rebuilding the neural circuits [9, 10]. However, the adult central nervous system (CNS) limits the ability of injured neurons to germinate and regenerate [11]. Perineuronal nets (PNNs), a highly structured portion of the extracellular matrix, mostly surround the soma and dendrites of specific type of neurons and play a critical role in protecting nerve growth and regulating neural plasticity [12]. After injury of the CNS, the abnormal accumulation of PNNs can limit the neuroplasticity or axonal regeneration by participating in the formation of glial scar [13, 14]. Therefore, the intervention and regulation of PNNs after SCI may be helpful to the recovery of nerve function and can mediate the spontaneous motor recovery.

Semaphorin3A (Sema3A), as an essential member of the semaphore family, is mainly produced by neurons or astrocytes in the adult CNS, and its polypeptides and neuropeptide receptors are widespread [15]. Recent studies have found that Sema3A is involved in the growth of axons and the formation of new synaptic connections during embryonic development, which is highly aggregated, and migrates to the injured site after SCI [16, 17]. Sema3A can bind to PNNs by chondroitin sulfate-E (CS-E) to prevent the synapses of neurons from crossing the damaged area and prevent the formation of new neuronal connections [18]. Previous studies have shown that EA can alleviate the expression of myelin growth inhibitor and promote nerve regeneration after SCI, and the changes in the connections between these neurons can effectively promote the recovery of the nerve function. So far, our understanding of whether EA can influence neuronal connections and specific mechanisms by interfering with PNN is still very limited.

In order to explore the changes of PNNs mediated by the signaling of Sema3A after SCI, we observed the disintegration of PNNs after the degradation of the Sema3A signal by microinjection of viral vector. Meanwhile, the therapeutic effect of EA was consistent with it.

## 2. Materials and Methods

**2.1. Reagent and Chemicals.** The modified Allen device for a model of spinal cord injury was the Model II-NYU/MASCIS impactor device (W.M.Keck, USA) from the Key Laboratory of Acupuncture and Neurology of Zhejiang Province. The sterilized needles were 0.25 mm × 25 mm from Suzhou Medical Co. Ltd. (Jiangsu, China). Acupuncture point nerve stimulator was the HANS-200A from Huawei Co. Ltd. (Beijing, China). Nikon A1R laser scanning confocal microscope was from Nikon Corporation (Nikon, Japan). Frozen microtome was the Thermo NX50 from American Thermo Corporation. The stereotaxic apparatus and isoflurane inhalation were from RWD Life Science Co., Ltd. (Shenzhen, China). The mini-protean vertical electrophoresis and membrane transfer systems were from the U.S. Bio-Rad company. The gel imaging system was Image Quant LAS4000

from the Germany GE Corporation. Microplate Reader was Spectra Max M4 from MeiGu Molecular Co. Ltd.

Sodium chloride, paraformaldehyde, isopropanol, methanol, sucrose, ethanol, penicillin, and Nissl staining solution were from Hanpusi Biotechnology Co., Ltd. (Zhejiang, China). Ponceau S Solution, SDS, Tris, glycine, and ECL Western Blotting Substrate Kit were from Beyotime Science & Technology Co., Ltd. Nembutal and N,N,N',N'-tetramethyl ethylenediamine (TEMED) were obtained from Sigma-Aldrich (Missouri, USA). The 20 protease inhibitor cocktail tablets were from Roche Diagnostics GmbH (Mannheim, Germany). Pierce™ BCA Protein Assay Kit was from Thermo Fisher Scientific Inc. (NJ, USA). Difco™ Skim milk was from Becton, Dickinson, and Company (NJ, USA). The PVDF membrane was from Merck Millipore Ltd. (Billerica, USA). Antibodies to neuropilin1 (WB), HAPLN1, aggrecan, β-actin, and Alexa Fluor 488-AffiniPure donkey anti-goat were purchased from Abcam PLC; tenascin-R and neuropilin1 (IF) were from R&D Technology Inc; semaphorin3A was from Genetex Technology Inc; Wisteria floribunda lectin was from Vectorlabs Technology Inc. Anti-rabbit IgG, HRP-linked antibody was from CST, and anti-mouse IgG, HRP-linked antibody was from Jackson. Streptavidin Alexa Fluor Conjugate was from Invitrogen.

**2.2. Animals.** Healthy adult male SD rats (eight weeks old, 200–220 g body weight) were purchased from the Shanghai Xipu Bikai experimental animal Company (animal license No.: SCXK(Shanghai) 2018-0006) and housed in the Laboratory Animal Center of Zhejiang Chinese Medical University accredited by the Association for Assessment and Accreditation of Laboratory Animal Care (AAALAC, animal license No.: SYXK (Zhejiang) 2018-0012). Rats were maintained under controlled conditions with access to food and water ad libitum. All animal experiments were performed in compliance with all relevant ethical regulations for animal testing and research and in accordance with animal protocols approved by the animal ethics committee of Zhejiang Chinese Medical University (ZSLL, 2017-183). All the experimental protocols strictly followed the guidelines of the National Institutes of Health (NIH) on the use of laboratory animals (NIH Publication No. 8023).

**2.3. SCI Rat Model.** To produce a contusive SCI model at T10, rats were placed on their ventral surface in a U-shaped stabilizer, then received a T10 contusion using the MASCIS weight-drop device with a 5 × 10 g/cm gravitational potential energy [19] after a T10 laminectomy. The severity and consistency of the injury were verified by checking the bruise on the spinal cord or tail-flick of rats after weight drop. Rats in the sham group only underwent laminectomy. All animals were injected penicillin (100 U/d) intraperitoneally for 3 days. Then, the rats were returned to clean home cages that were partially placed on a heating pad until they fully recovered from the anesthesia. The manual bladder expression was performed twice daily until the bladder emptying.

**2.4. Acupuncture Treatment.** Rats were submitted to EA treatment at the T9-T11 Jiaji (EX-B2) acupoints [20] which



located on the two sides of the spinous process of the dorsal part. All sterilized disposable stainless steel acupuncture needles with a 0.25 mm diameter were inserted as deep as 4–5 mm until the tip of the needle touches the vertebral lamina and then connected with a pair of electrodes from acupuncture point nerve stimulator. The parameters were set as follows: an alternating wave current output (2 Hz/100 Hz), with the intensities remaining at 1 mA that causing slight vibration of the muscles around the treatment areas, was started from the first day after operation, 20 min once daily, for 7 or 14 consecutive days. The rats of the sham group, model group, and AAV group were only bound in the prone position for 20 minutes when the EA group received treatment.

**2.5. Behavioral Testing.** The Basso-Beattie-Bresnahan (BBB) test [21] is judged on a scale of 0–21 (0, complete hind limb paralysis; 21, normal locomotion, Table 1), is based on hind limb movements made in an open field including hind limb joint movement, weight support, plantar stepping, coordination, paw position, and trunk and tail control, and is performed to evaluate the overall basic locomotor performance. Briefly, each rat was placed in an open field and evaluated more than 3 min by two experimenters who were blinded to experimental groups, and one of them counts the total number of scores. Additionally, all rats were assessed before modeling to ensure that there were no baseline defects and averaged into a final score per session.

**2.6. Sema3A Targets Screening.** In order to obtain the effective interference target for Sema3A, the six Sema3A targets of wy2884-2889, the overexpression plasmid wy2890, and the control plasmid wy1720 with the EGFP cDNAs were cloned into plasmid pAAV-MCS. AAV 293 cells were cultured in Dulbecco's modified Eagle medium and transport to collect the fraction containing AAV. Then, the target sequences were screened by fluorescence subtracting and Western blot.

**2.7. AAV Viral Injections.** To inhibit the *ema3A* expression, 0.5  $\mu$ l AAV2/9-U6-shRNA (*Sema3A*)-CAG-tdtomato or a negative control AAV2/9-U6-shRNA(luciferase)-CAG-tdtomato virus was injected into the bilateral of the T9 spinal cord using a 10  $\mu$ l Hamilton syringe, after rats anesthetized with pentobarbital sodium (40 mg/kg, i.p.). The depth of the injection tip was 1.5 mm and keeps in place for another 5 minutes to avoid virus leakage. Vessel and nerve were avoided while injection was done, and virus ultimately titer was  $7.5E + 12$  v.g./ml.

**2.8. Nissl Staining.** For Nissl staining, 25- $\mu$ m-thick frozen section was subjected to stain with cresyl violet and dehydrated with different concentrations of ethanol. The number of positive cells in the ventral horn at the epicenter of the lesion 0.5 mm to the injury epicenter was calculated and analyzed by ImageJ software which was averaged into a final score per session.

**2.9. Western Blotting.** Spinal cord tissues of rats were homogenized with radioimmunoprecipitation assay (RIPA) buffer containing proteinase inhibitors, and then the total protein concentration of each sample was determined by using the

bicinchoninic acid (BCA) method according to the kit's instruction. Furthermore, equal amounts of protein from each sample were divorced on 10% SDS-PAGE gels and transferred to polyvinyl difluoride (PVDF) membranes. The membranes were blocked with 5% nonfat milk in TBST containing 0.1% Tween 20 at room temperature for 1 h and then incubated overnight at 4°C with primary antibody: semaphorin3A (1:500), neuropilin1 (1:1000), HAPLN1 (1:1000), aggrecan (1:500), Tenascin R (1:200), and  $\beta$ -actin (1:5000). The following day, the membrane was incubated at room temperature for 2 h with the 2 antibodies: anti-rabbit IgG, HRP-linked antibody (1:2000) or anti-mouse IgG, HRP-linked antibody (1:2000). Finally, the immunoreactivity was detected using enhanced chemiluminescence and visualized with an Image Quant LAS 4000. The density of each band was measured by ImageJ analysis software. The relative expression of the target protein is the target protein (absorbance value)/the internal reference factor of actin (absorbance value), and the results were expressed as mean  $\pm$  standard deviation.

**2.10. Immunofluorescence Staining.** Transverse spinal cord sections (25  $\mu$ m) were cut on a frozen microtome, installed on gelatin-coated glass slides as 8 sets of every 5th serial section. Above 25- $\mu$ m-thick frozen sections were incubated with the following primary antibodies: semaphorin3A (1:200), neuropilin1 (1:50), and Wisteria floribunda lectin (1:100). Signal was detected with the corresponding second antibodies conjugated to Streptavidin Alexa Fluor 555 Conjugate (1:200) or Streptavidin, Alexa Fluor 488 conjugate (1:200) or Alexa Fluor 488-AffiniPure Goat Anti-rabbit IgG (H + L) (1:600) or Alexa Fluor 488-AffiniPure donkey anti-goat IgG (H + L) (1:500) and viewed by Nikon A1R laser scanning confocal microscope. In order to quantize the image and keep the uniform microscope setting in the entire image acquisition process, 3–5 images were randomly selected per rat tissue, averaged, and analyzed by ImageJ software.

**2.11. Statistical Analyses.** The statistical significance of the difference between control and experimental groups was determined by one-way ANOVA followed by Tukey Kramer tests which were performed with SPSS.20 (Statistic package for social science) (SPSS Inc., Chicago, USA). Data is shown as mean  $\pm$  SEM and considered to indicate statistically significant if  $P < 0.05$ .

### 3. Results

**3.1. Motor Dysfunction after SCI.** Firstly, we established the modified rat model of SCI via Allen's method described previously. As shown in Figure 1(a), the BBB score was used to observe the motor function of hind limbs on the 7th, 14th, and 21st days after SCI in rats, and we found the hind limbs of rats completely paralyzed following SCI, while its performance was improved gradually from the second post-SCI week. Specifically, the lower limb motor function was normal with the score of 21 points in the sham group. Unfortunately, the BBB score was among 0–2 points on the 7th day post-SCI which had severe motor dysfunction, and the motor function



TABLE 1: Basso-Beattie-Bresnahan locomotor rating score.

Score	The ability of the lower limb motor
0	There is no visible hindlimb (HL) movement
1	Light movement of one or both joints, usually hip and/or knee
2	Broad movement of one joint or joint and slight movement of the other
3	Extensive movement of the two joints
4	Light movement of three joints
5	Light movement of two joints and wide movement of the third
6	Broad movement of the two joints and light movement of the third
7	The extensive movement of all three joints of HL
8	The ball of the foot without weight support or without weight support
9	The soles of the feet occasionally bear the weight of the ground (for example, when stationary), frequent or consistent load-bearing movements of the dorsal claw, without the soles of the feet supporting the movement
10	Paw surface occasionally moves with load bearing without FL-HL coordination
11	Paw surface has more load-bearing movement and no FL-HL coordination
12	More load-bearing movement and occasional FL-HL coordination on the paw surface
13	Common paw-bearing movement and frequent FL-HL coordination
14	Continuous palm-surface-bearing movement with consistent FL-HL coordination, or common palm-surface movement, continuous fore-hind limb coordination, and occasionally dorsal claw movement
15	Continuous paw and palm-bearing movement and consistent FL-HL coordination, no or occasional ground grasping movement in the forward motion of the forelimbs, and the position of the main claw parallel to the body at the initial contact
16	In the gait, the continuous paw landing and the coordinated movement of the front and rear limbs are common in the process of grasping the ground; the main claw position is parallel to the body at initial contact and rotates after load transfer
17	In the gait, the continuous paw landing and the coordinated movement of the front and rear limbs are common in the process of grasping the ground; the main claw position is parallel to the body at initial contact and load transfer
18	In the gait, the continuous paw touches the ground in a coordinated manner with the front and rear limbs. In the process of progress, the continuous paw grasps the ground. The position of the main paw is parallel to the body at the initial contact
19	In the gait, the continuous paw touches the ground in a coordinated manner with the front and rear limbs. The continuous paw grasps the ground in the process of advancing. The position of the main paw is parallel to the body at the initial contact and load transfer
20	The position of the main claw is parallel to the body during initial contact and weight transfer. The trunk is unstable, and the tail kept cocking up
21	The position of the main claw is parallel to the body at the initial contact and load transfer, and the trunk is stable and the tail kept cocking up

of hind limbs began to gradually recover after 14 days (Figure 2(c)). Therefore, it can be predicted that the motor function of the hind limbs was obviously impaired after SCI, whereas it can be slightly recovered on account of the limited self-healing ability.

**3.2. Morphological Changes of the Spinal Cord after SCI.** We carried out Nissl staining to evaluate the changes of neuron morphology in the sham group and on the 7th, 14th, and 21st days after SCI. The results showed, compared with the sham group, that Nissl-positive motor neuron number in the ventral horn of the spinal cord after SCI was significantly reduced, and Nissl bodies became fuzzy and gradually recovered on the 21st day after SCI (Figures 2(a) and 2(b)).

**3.3. The Expression of *Sema3A* and *NRP1* after SCI.** To quantify the expression of the *Sema3A* signal in the injury site of spinal cord, *Sema3A* and *NRP1* immunotherapy were performed. Subsequently, our immunofluorescence study showed that the *Sema3A* signal around the central canal of

the spinal cord gray matter increased abnormally compared with the sham group on the 7th day post-SCI, but there was no significant differences on the 14th and 21st day after SCI. *NRP1* also significantly increased around the central canal on the 7th day post-SCI, and it was downregulated on the 14th day after SCI while still higher than that of the sham group; however, no significant difference was observed on the 21st day after SCI compared with the 14th day in the post-SCI group (Figures 3(a) and 3(b)). We further examined the expression of *Sema3A* and *NRP1* in the SCI rats by Western blotting, and the results were consistent with that of immunofluorescence (Figures 3(c) and 3(d)).

**3.4. The Expression of PNNs after SCI.** It has been demonstrated that the aggregation of PNNs wrapping around soma and dendrites after the CNS injury hinders the neuronal axon regeneration and limits the nerve plasticity. We labeled PNNs in the spinal cord by wisteria floribunda agglutinin (WFA) which can be bind to *N*-acetylgalactosamine (GalNAc) in most PNN polysaccharide chains. Importantly,

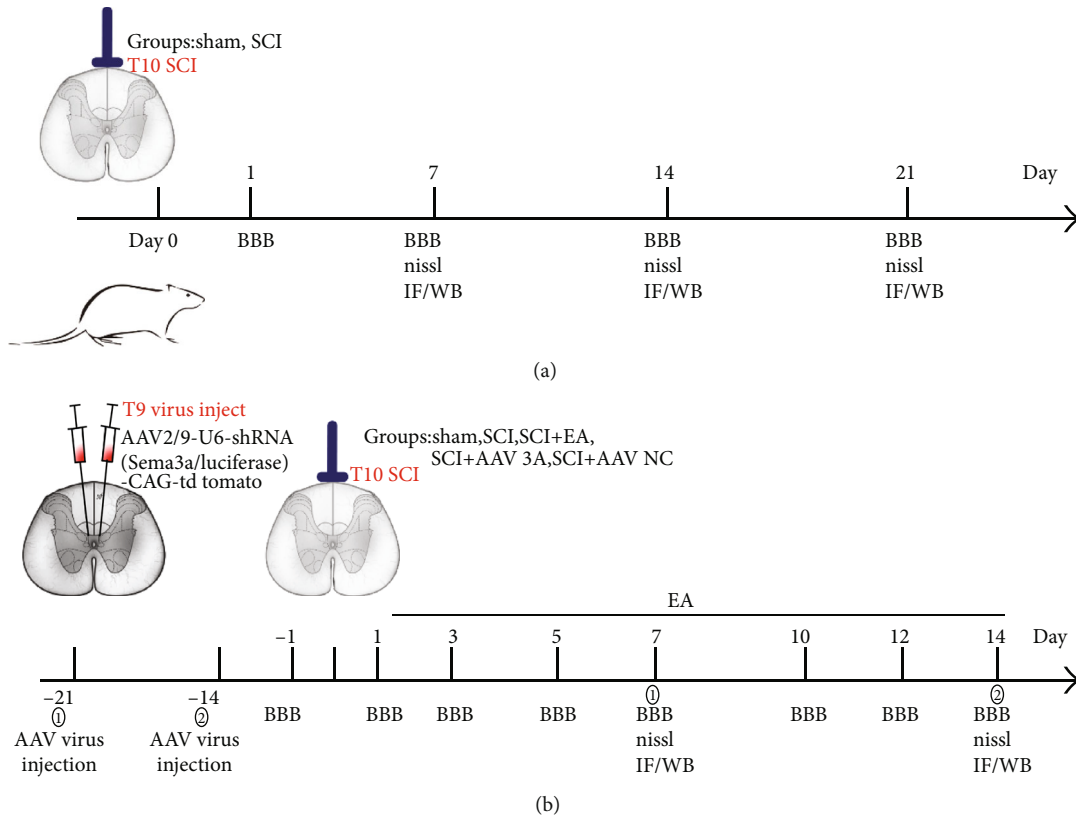


FIGURE 1: (a, b) Timeline of the experimental protocol.

immunofluorescence results were similar to previously reported which showed that WFA was upregulated around the central canal of the spinal cord gray matter post-SCI and reached the peak on the 14th day (Figures 4(a) and 4(b)). In addition, we examined the expression of the main structural proteins in PNNs, including TN-R, HAPLN1, and aggrecan by Western blotting. We found HAPLN1 was not significantly changed after SCI, while TN-R and aggrecan were significantly upregulated on the 14th day after SCI compared to the sham group (Figures 4(c)–4(e)).

**3.5. *Sema3A* Targets Screenings.** To further verify the impact of *Sema3A* post-SCI, we designed 6 sets of SNCA-shRNA sequence plasmids with GFP fluorescent tags and integrated them into an adeno-associated virus (AAV), then transfected them into HEK293 cells to observe the degree of translated. We utilized fluorescence attenuation detection cotransfect 293 T cells in vitro with the interference group, the interference control sample wy2884–2889, the interference control sample WY1720, and the overexpressed sample WY2890. It was found that the negative control WY1720 of the interference target had no ability to knockdown, while the target sequences of WY2886, WY2887, and WY2889 in the experimental group had a strong knockdown ability (Figure 5(c)). Western blotting was further used to check the efficiency of each target, and the result displayed WY2887 had the least amount of protein as well as the best interference effect (Figure 5(b)). Therefore, we considered wy2887 is the most suitable one among the six sequences of wy2884–2889

(Table 2). Hence, we chose wy2887 to package AAV2/9-U6-shRNA (*Sema3A*)-CAG-tdtomato for the following experiment. To verify the knockdown efficiency of *Sema3A* shRNA in rats, AAV2/9-U6-shRNA(*Sema3A*)-CAG-tdtomato was injected into the T9 spinal cord by stereoscopic microinjection for 21 days before modeling (Figure 6(a) and 6(b)), AAV2/9-U6-shRNA(luciferase)-CAG-tdtomato was used as a comparison, and samples were extracted on the 7th day after SCI for Western blotting. It was displayed that AAV2/9-U6-shRNA (*Sema3A*)-CAG-tdtomato could significantly decrease the expression of *Sema3A* after SCI (Figure 6(c)).

**3.6. *Inhibition of Sema3A Promotes Functional Recovery after SCI by Reducing the Accumulation of PNNs at the Injury Site.*** To clarify the role of *Sema3A*, we injected AAV2/9-U6-shRNA (*Sema3A*)-CAG-tdtomato into T9 spinal cord rats 21 days or 14 days before modeling according to the experimental plan to knock down the expression of *Sema3A* (Figure 1(b)). AAV2/9-U6-shRNA(luciferase)-CAG-tdtomato was used as negative control, then observed the changes of PNNs around the central canal of the spinal cord at the injured area and the motor function of the hindlimbs of the rats. Immunofluorescence and Western blotting both recovered that knockdown *Sema3A* could significantly downregulate the expression of *Sema3A* and its receptor NRP1 (Figure 7). Indeed, WFA around the central canal was downregulated after knocking down *Sema3A* (Figures 8(a) and 8(b)), and the expressions of TN-R and aggrecan in the SCI

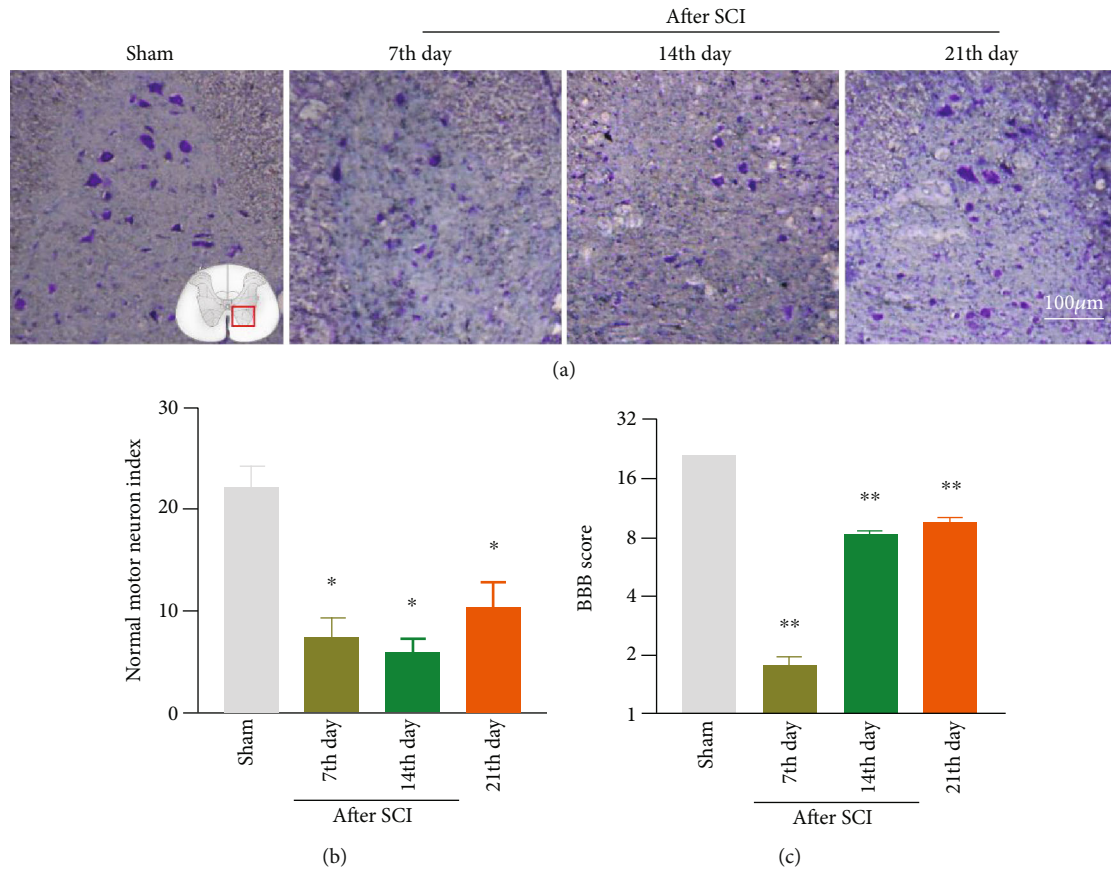


FIGURE 2: Establishment of the SCI model in rat. After SCI, the motor neurons in the ventral horn of the spinal cord decreased, the Nissl's body became fuzzy, and the motor function decreased. (a) The Nissl staining of the ventral horn of the spinal cord in the sham group and the SCI group represents the figure. (b) The number of surviving motoneurons in the ventral horn of the spinal cord was quantified,  $n = 3$ . (c) BBB function scores of rats in the sham group and the SCI group,  $n = 10$ , compared with the sham group, \* $P < 0.05$ , \*\* $P < 0.01$ . All data are presented as the mean  $\pm$  SEM.

area were also deregulated, but the control virus group had no significant effect (Figures 8(d) and 8(e)).

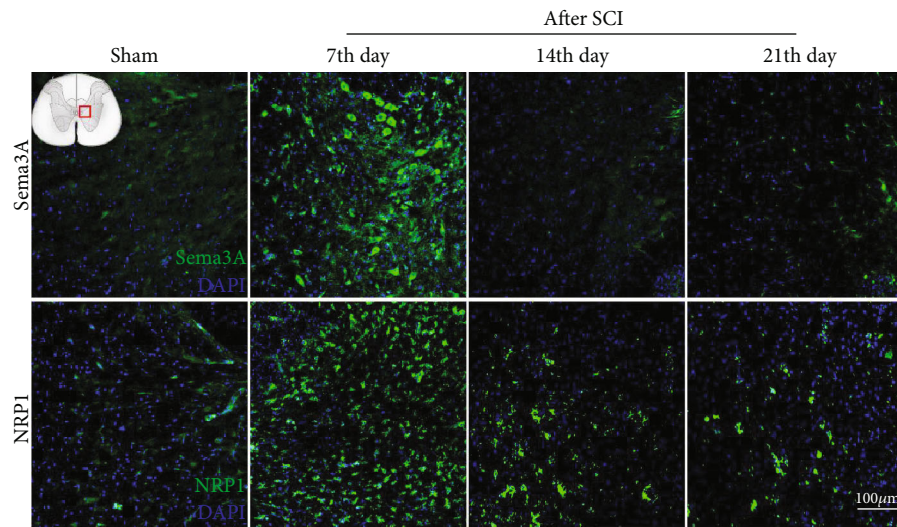
Morphologically, the Nissl staining result was reminded that the number of Nissl-positive motor neurons in the ventral horn of the spinal cord about the group of knocking down *Sema3A* was notably increased compared with the SCI group (Figures 9(a) and 9(b)). Functionally, we found that the BBB score was significantly higher than the SCI group when we deliberately downregulated the expression of *Sema3A* in the injured spinal cord, except for the control virus group, which suggested that downregulation of *Sema3A* could promote the recovery of the lower limb motor function in the SCI rats (Figures 8(c) and 9(c)).

**3.7. EA Treatment Promotes Functional Recovery after SCI, Possibly by Regulating *Sema3A* to Reduce the Accumulation of PNNs.** To evaluate whether EA could meliorate the abnormal aggregation of PNNs and *Sema3A*, we used immunofluorescence and Western blotting to detect the influence of EA treated on SCI. Excitingly, the changes of molecular biology in the injured spinal cord of SCI rats after EA treatment were similar to that of knockdown *Sema3A*. Immunofluorescence showed that the aggregation of Nrp1, *Sema3A*, and WFA around the central canal of the spinal cord gray matter in

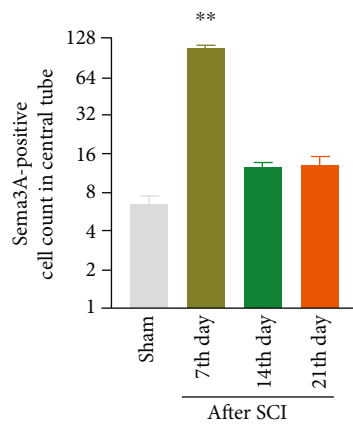
the EA-treated group was lower than that in the SCI-treated group (Figures 7(a)–7(c) and 8(a) and 8(b)). Furthermore, these results were verified by Western blotting which wonderfully demonstrated that the protein expression of *Sema3A*, Nrp1, TN-R, and aggrecan in the spinal cord of the EA-treated group was evidently less than the SCI group (Figures 7(d) and 7(e) and 8(d) and 8(e)).

In addition, damaged motor neurons in the ventral horn of the injured spinal cord were properly repaired after EA treatment. Specifically, as far as histomorphology is concerned that the number of Nissl-positive motoneurons in the ventral horn of the spinal cord, compared to the SCI group, was significantly augmented by EA treatment (Figures 9(a) and 9(b)). In terms of the motor function, EA has the same effect as those who were knocked down the expression of *Sema3A* in the injury spinal cord, which can actively improve the motor function of hind limbs in rats with SCI. Although the BBB score of the EA group was slightly lower than the *Sema3A* knockdown group, it was still visibly greater than the SCI group, especially after the 5th day under intervened (Figures 8(c) and 9(c)).

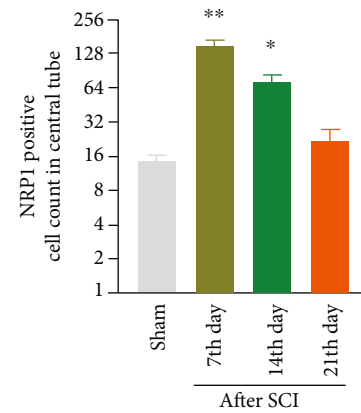
**3.8. Discussion.** PNNs and *Sema3A* are widely known for their capacity to limit nerve plasticity after CNS injury. In



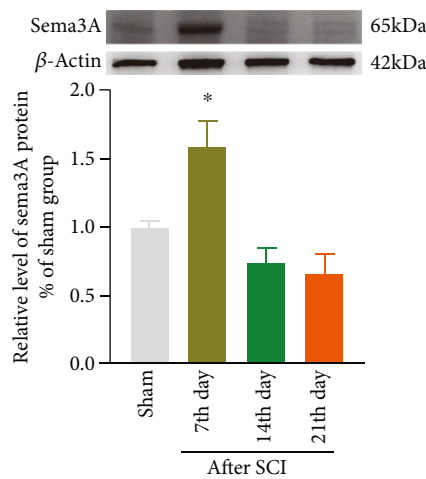
(a)



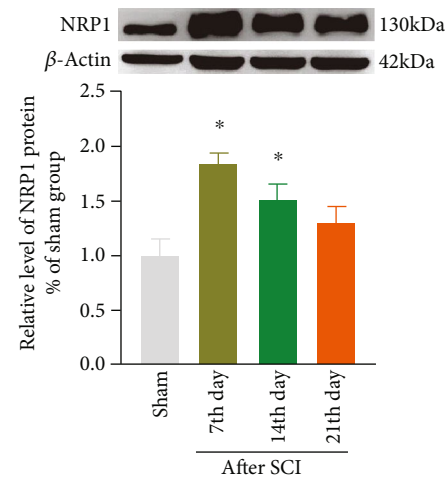
(b)



(c)



(d)



(e)

FIGURE 3: The expression of Sema3A and its receptor NRP1 were upregulated around the central gray matter of the spinal cord after SCI. (a) The results of immunofluorescence showed the expression of Sema3A and its receptor NRP1 around the central canal of the spinal cord gray matter in the sham group and the SCI group. (b, c) Quantification of immunofluorescence data in panel (a),  $n = 3$ . (d, e) Representative bands and statistics of Sema3A and NRP1 in the spinal cord by Western blotting,  $n = 5$ , compared with the sham group, \* $P < 0.05$ , \*\* $P < 0.01$ . All data are presented as the mean  $\pm$  SEM.



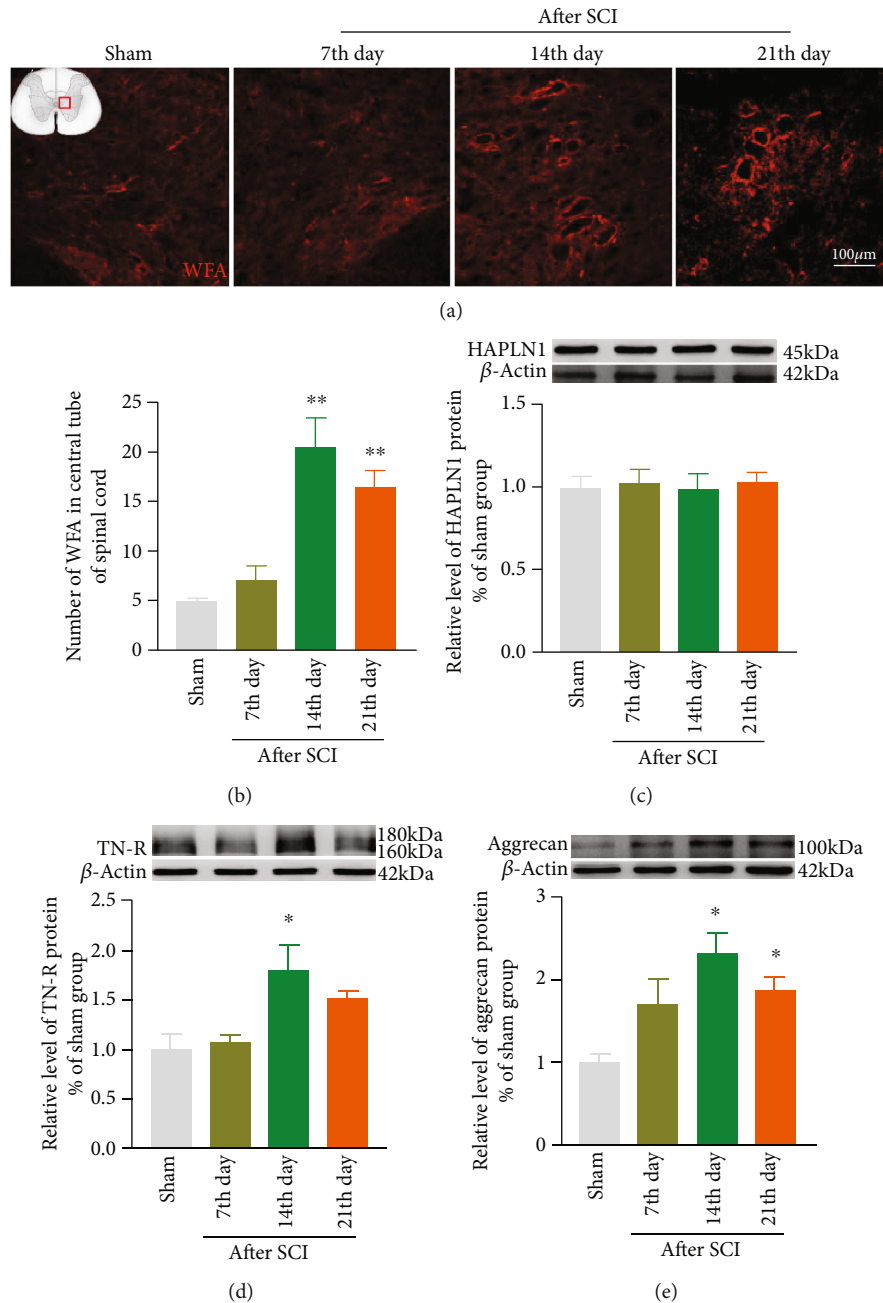


FIGURE 4: Expression changes of PNNs and their related proteins TN-R, HAPLN1, and aggrecan in the spinal cord after SCI. (a) Immunofluorescence representative diagram of changes in expression levels of WFA around the central tube of the spinal cord in the SCI group and sham group. (b) Quantification of the immunofluorescence data in panel (a),  $n = 3$ . (c) Representative bands and statistics of TN-R, HAPLN1, and aggrecan in the spinal cord by Western blotting, compared with the sham group, \* $P < 0.05$ , \*\* $P < 0.01$ . All data are presented as the mean  $\pm$  SEM.

this study, we found that motor neurons in the ventral horn of the injured spinal cord segment decreased, and PNNs and Sema3A as well as its receptor NRP1 aggregated around the central tube of the gray matter of the spinal cord. When the expression of Sema3A at the damage site was knocked down, NRP1's expression was also downregulated, accompanied by the PNNs concentration decreased. The expression of TN-R and aggrecan was also reduced; meanwhile, the BBB motor function score dramatically increased. In addition, Electroacupuncture can reverse the high upregulation

of Sema3A and NRP1 after spinal cord injury, reduce the accumulation of PNNs around the central canal of gray matter, and promote the recovery of the motor function.

It is worth noting that PNNs, as the main external environment of the central nervous system, are mainly composed of hyaluronic acid (HA), proteoglycan 1 (hapln1), tenascin-r (TN-R), and chondroitin sulfate proteoglycan (CSPG) [22]. They are activity dependent and form around the soma and proximal neurites presenting at the closure of critical periods during development and involve many homeostasis



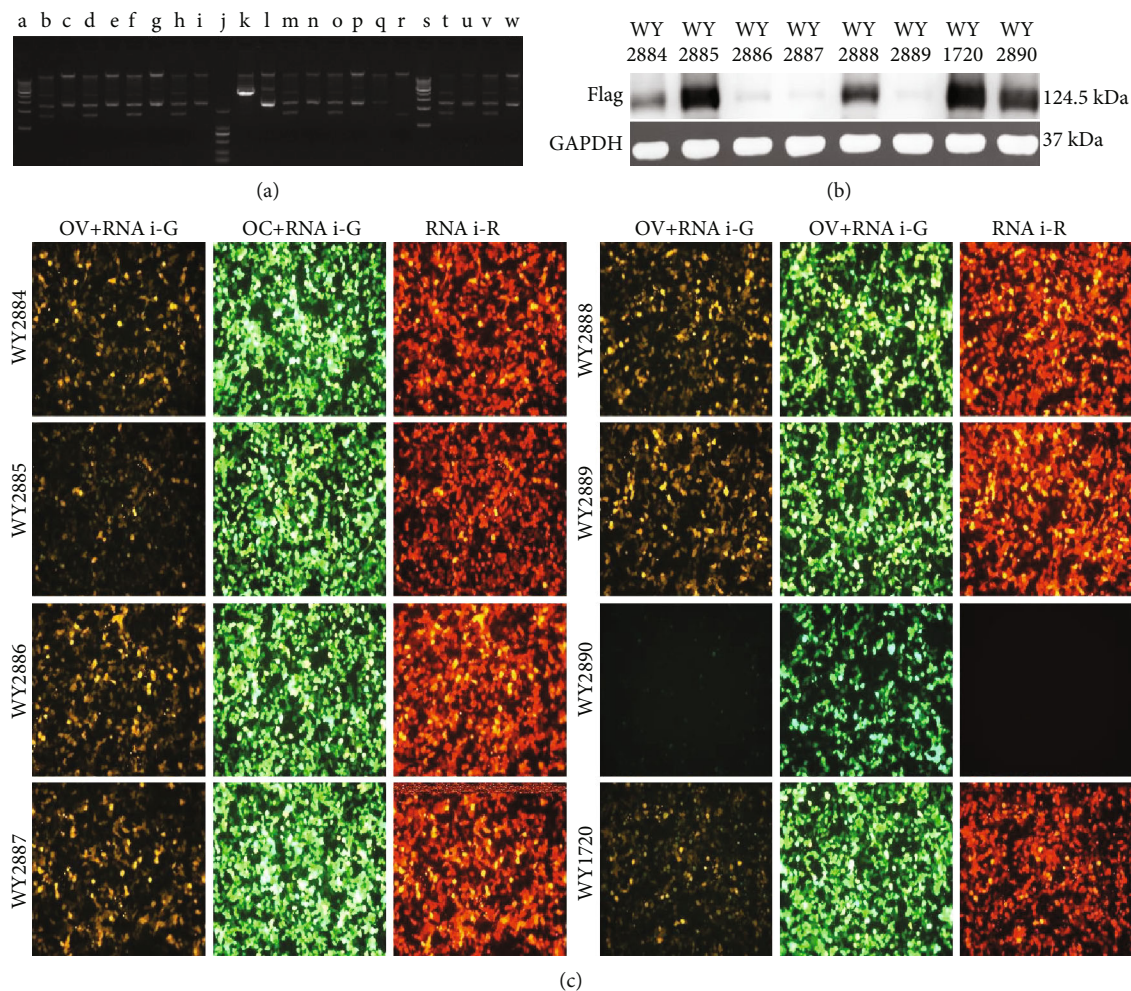


FIGURE 5: Sema3A in vitro target screening. (a) wy2884-2889 plasmid enzymatic digestion validation, using the enzymatic digestion site: SmaI, (a and s: 1Kb DNA ladder, the bands from bottom to top are 1Kb, 2Kb, 3Kb, 4Kb, 5Kb, 6Kb, 7Kb, 8Kb, 9Kb, and 10Kb; J: DL 2000 DNA marker, the bands from bottom to top are 100 bp, 250 bp, 500 bp, 750 bp, 1Kb, and 2Kb; b, d, f, h, k, m, o, q, t, and v were, respectively, the bands after wy2884-2889 plasmid digestion, and a, c, e, g, i, l, n, p, r, u, and w were the control bands of wy2884-2889 plasmid without enzyme digestion, and the size of each band was in line with the expectation). (b) The interference group sample wy2884-2889, the interference control samples WY1720, and the overexpressed samples WY2890 Western blotting bands. The Flag signal was obvious, and the size was 124.5 kDa. As a whole, the wy2887 group had the least protein and the best interference effect. The WY2886 and WY2889 groups also had less protein. (c) Representative diagram of the interference group wy2884-2889, the interference control sample WY1720, and the overexpressed sample WY2890 were cotransfected into 293 T cells in vitro of fluorescence attenuation detection. The results showed that the negative control wy1720 of the interfering target had no knockdown ability. The target sequences of WY2886, WY2887, and WY2889 in the experimental group wy2884-2889 had a strong knockout ability. (OV: wy2890: pAAV-CMV\_bGI-Sema3A-EGFP-3Flag-WPRE-hGHPA; OC: wx963: pAAV-CMV\_bGI-EGFP-3Flag-WPRE-hGHPA).

TABLE 2: Sema3A target screening sequence.

No.	Target sequence	Plasmid
1	GGAAAAGAACAATGTGCCAA	WY2884
2	CCATCCAATTTGCACCTAT	WY2885
3	CCTGAAGATGACAAAGTAT	WY2886
4	GCTAGAATAGTTCAGATAT	WY2887
5	GCAATGGAGCTTTCTACTA	WY2888
6	GGATGAGTTCTGTGAACAA	WY2889

functions, for example, neuroprotection. Biochemical analysis suggests that PNNs are present in 30% of ventral horn motor neurons in the spinal cord [23–25]. TN-R as a member of the tenascin family in the CNS is closely related to the development and plasticity of nervous and the migration of nerve cells. Aggrecan is one type of CSPGs. It can be connected with the lectin domain of CSPGs to form an organized PNN backbone, which is crucial for the structure of PNNs [26, 27]. Studies have shown [28, 29] that in SCI models, the expression of CSPGs is upregulated and gradually migrated to the injury site, interacting with astrocytes, microglia, and macrophages to form a glial scar and inhibit axonal regeneration. In addition, inhibition of the expression

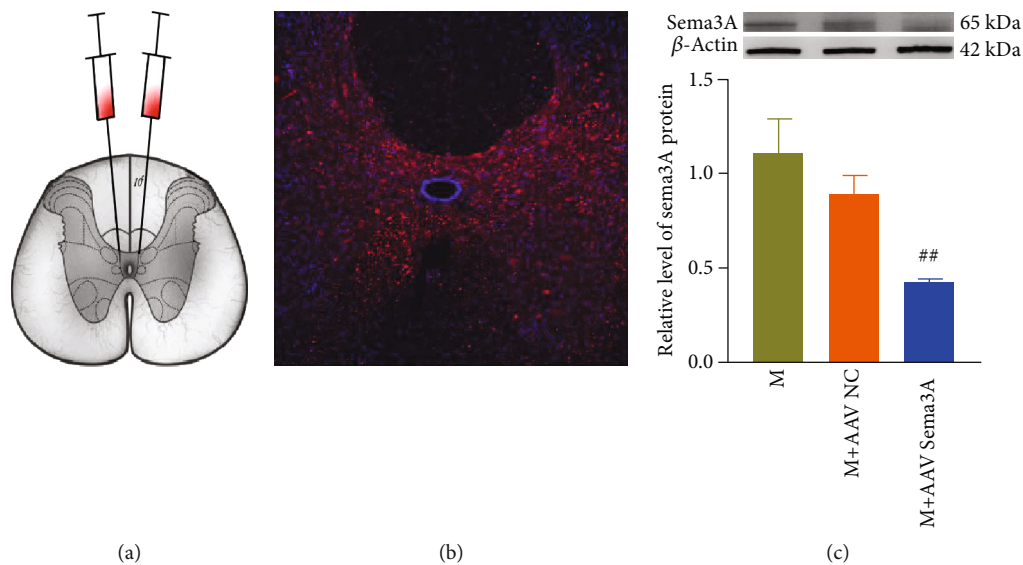


FIGURE 6: The expression of Sema3A around the central tube of the spinal cord is decreased after knockdown Sema3A. (a) Schematic diagram of virus injection. (b) The microscopic representative diagram of the T10 expression at 4 weeks after virus injection. (c) The quantitative diagram represents bands of Sema3A Western blotting in the T10 spinal cord at 4 weeks after virus injection,  $n = 3$ , compared with the SCI group,  $##P < 0.01$ . All data are presented as the mean  $\pm$  SEM.

of TN-R and aggrecan is conducive to the reconstruction of synapses between neurons and the repair of the spinal cord function after SCI [30, 31].

Interestingly, PNNs constitute a physical barrier between neurons and extracellular cells which impede nerve repair in the model of SCI, while enzymatic removal of PNNs can promote functional recovery [32]. Massey and coworkers [33, 34] found that PNNs were obviously upregulated around dorsal column nuclei neurons of rats following a mid-cervical dorsal column tract lesion postinjury, while these upregulated PNNs restricted the plasticity and allowed sprouting into its denervated portions from the intact sensory axons with their degrade via injection of ChABC which can acutely remove CS-GAGs. So, changes in the PNN may be beneficial to regulating the remodeling and plasticity that occur in SCI for the animal to acquire some degree of locomotor functional recovery.

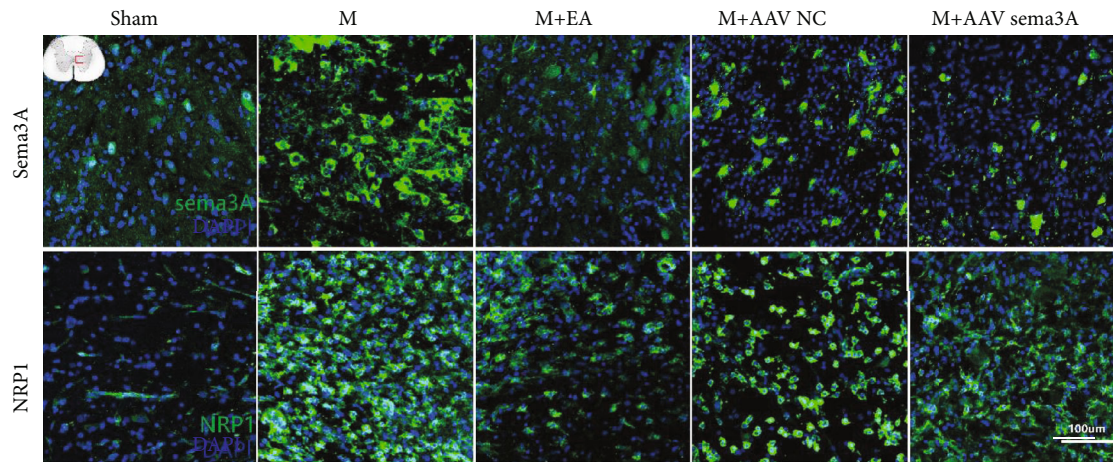
Recent finding [35] indicates that Sema3A, as an inhibitor of axon connection, contains receptor neuropilin1 (NRP1) which is the extracellular receptor and expressed on the dendrites and axons of neurons. It is rarely expressed in normal conditions, but significantly increased after SCI, leading to the collapse of nerve growth cone and inhibiting the connection between neurons only under the action of NRP1 [36, 37]. Studies on the relationship between Sema3A and PNNs have shown that [38–40] Sema3A may possible be a potentially part of PNNs in regulating neuronal plasticity after SCI, which plays a key role in nerve remodeling by highly affinity binding to PNNs through chondroitin sulfate E.

In this experiment, we first evaluated the changes of the Sema3A signal and PNNs in SCI rats and further studied the potential relationship between them and the effect of EA. We found that the number of motor neurons decreased and motor dysfunction after SCI, accompanied by signifi-

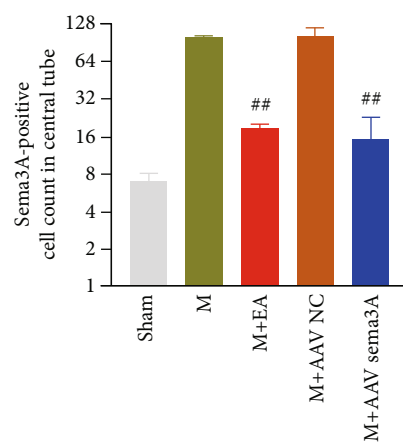
cantly increases in the expressions of PNNs, TN-R and aggrecan, Sema3A, and NRP1, but no significant changes in HAPLN1, compared to the sham group. Subsequently, in order to further study the correlation between the Sema3A signal and PNNs in the rat spinal cord tissue after SCI, as well as the effect of EA intervention, we packaged the Sema3A target sequence selected in vitro and injected it into the injured site to knock down the expression of Sema3A as a positive control for the EA intervention. We found that when rats passively reduce the expression of Sema3A around the central canal of gray matter or receive EA at Jiaji points, the Sema3A signal, WFA, TN-R, and aggrecan aggregation in the spinal cord tissue are significantly reduced and with the recovery of the motor function of both lower limbs.

EA as a complementary method to treat SCI has been widely used and is known for its benefits in synapse formation, neural rehabilitation, and restoration, which may be attributed to its enhancement of neurotrophic factor secretion, antioxidation, anti-inflammation, and antiapoptosis [8, 41, 42]. The frequency and wave type of EA are of great importance for functional recovery of patients with SCI. EA with loose-dense wave can significantly promote nerve regeneration and repair of SCI rats, speed up the removal of free radicals, enhance blood circulation, and reduce the secondary injury of SCI to promote the recovery of the motor function significantly [43]. Importantly, there is increasing evidence that [44] 2 Hz/100 Hz loose-dense wave EA plays a positive role in motor functional recovery of SCI which can promote nerve regeneration and repair.

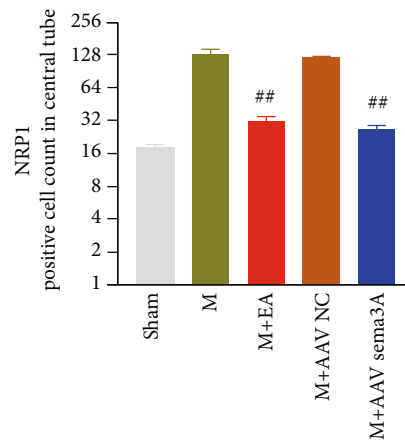
In the theory of traditional Chinese medicine, Jiaji points are located between the governor vessel (GV) and the bladder meridian of foot-taiyang (BL). In the human body, there are 34 acupoints belong to huatuo Jiaji points which locate on 0.5 inch lateral from the first thoracic vertebra to the fifth lumbar vertebra. Therefore, needling insert into Jiaji points can not



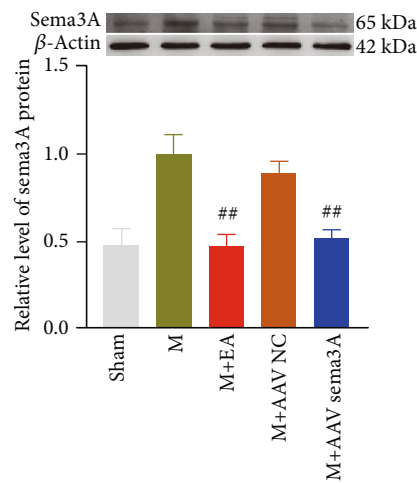
(a)



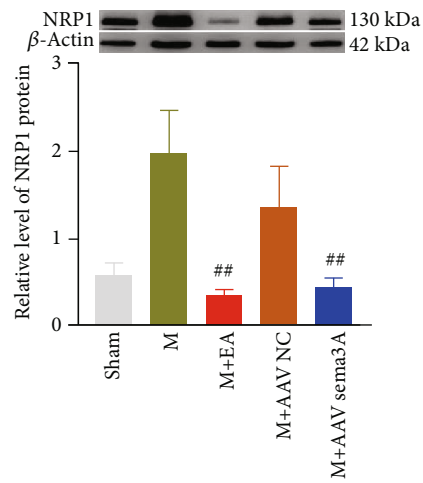
(b)



(c)



(d)



(e)

FIGURE 7: EA and Sema3A knockdown downregulated the expression of Sema3A and its receptor NRP1 around the central canal of the spinal cord. (a) A representative diagram of Sema3A and its receptor NRP1 expression around the central tube of gray matter in the spinal cord in the sham group, M + EA group, M + AAV Sema3A group, and M + AAV NC group was shown by immunofluorescence. (b, c) Quantification of the immunofluorescence data in panel (a),  $n = 3$ . (d, e) The representative band and statistic of Sema3A and NRP1 in the spinal cord,  $n = 5$ , compared with the SCI group,  $##P < 0.01$ . All data are presented as the mean  $\pm$  SEM.



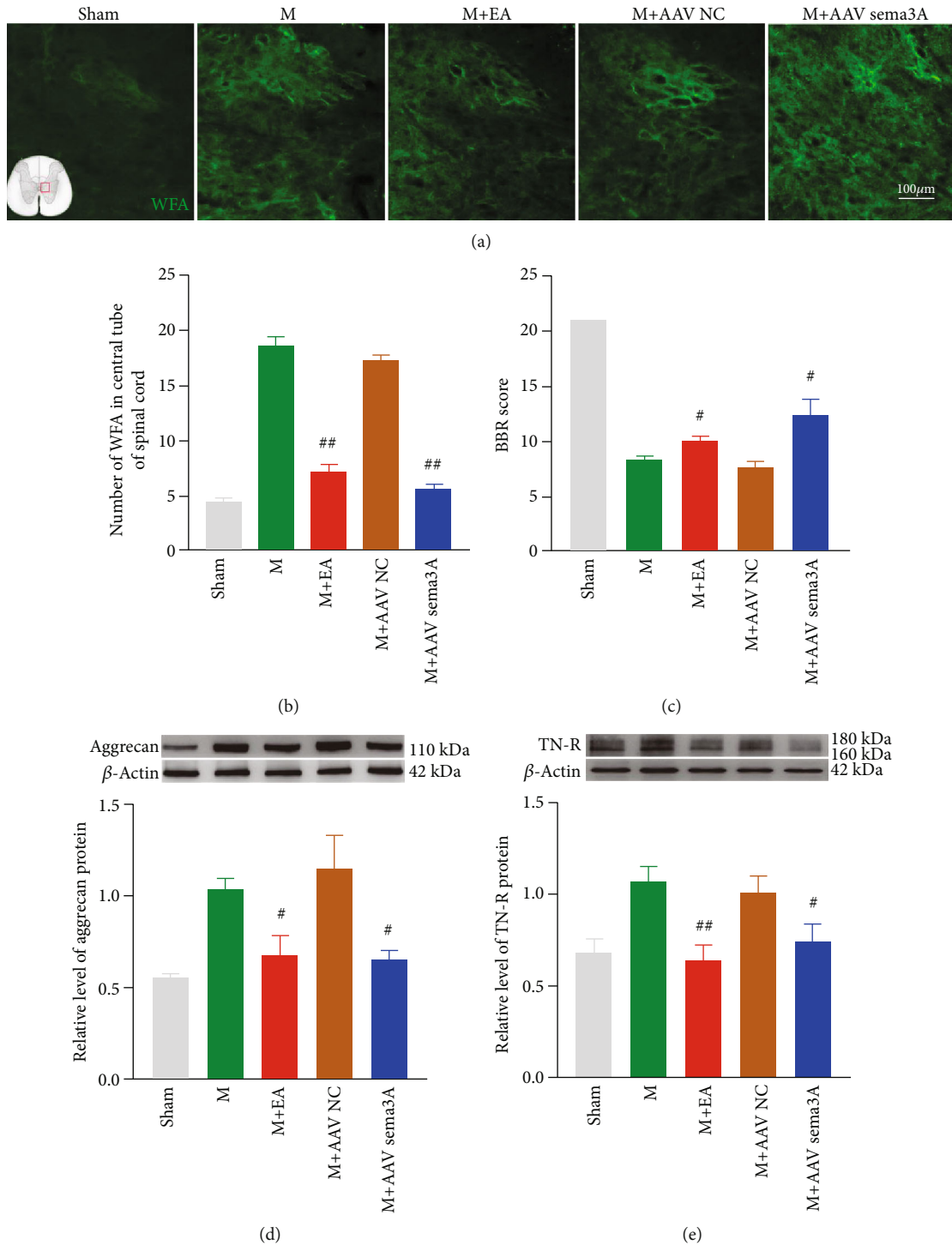


FIGURE 8: The expressions of WFA and TN-R and aggrecan in the spinal cord were downregulated by EA and Sema3A knocking. (a) A representative chart of the changes of the WFA expression around the central tube of the spinal cord in the sham group, 14 days after SCI, M+EA group, M+AAV Sema3A group, and M+AAV NC group, was shown by immunofluorescence. (b) Quantification of the immunofluorescence data in panel (a),  $n = 3$ . (c) The motor function score of each group at day 14. (d, e) The representative band and statistics of aggrecan and TN-R in the spinal cord,  $n = 5$ , compared with the M group,  $\#P < 0.05$ ,  $\#\#P < 0.01$ . All data are presented as the mean  $\pm$  SEM.

only regulate the qi of the GV and the BL but also adjust the balance of qi and blood in the zang-fu organs, so as to dredge and smooth the passage of the meridian. From the anatomy structure, EA on Jiaji points can stimulate the corresponding

posterior ramus of the spinal nerve arising from the lower vertebrae. Our previous results also confirmed that 2 Hz/100 Hz EA stimulation of Jiaji points can reduce the expression of myelin growth inhibitor and effectively

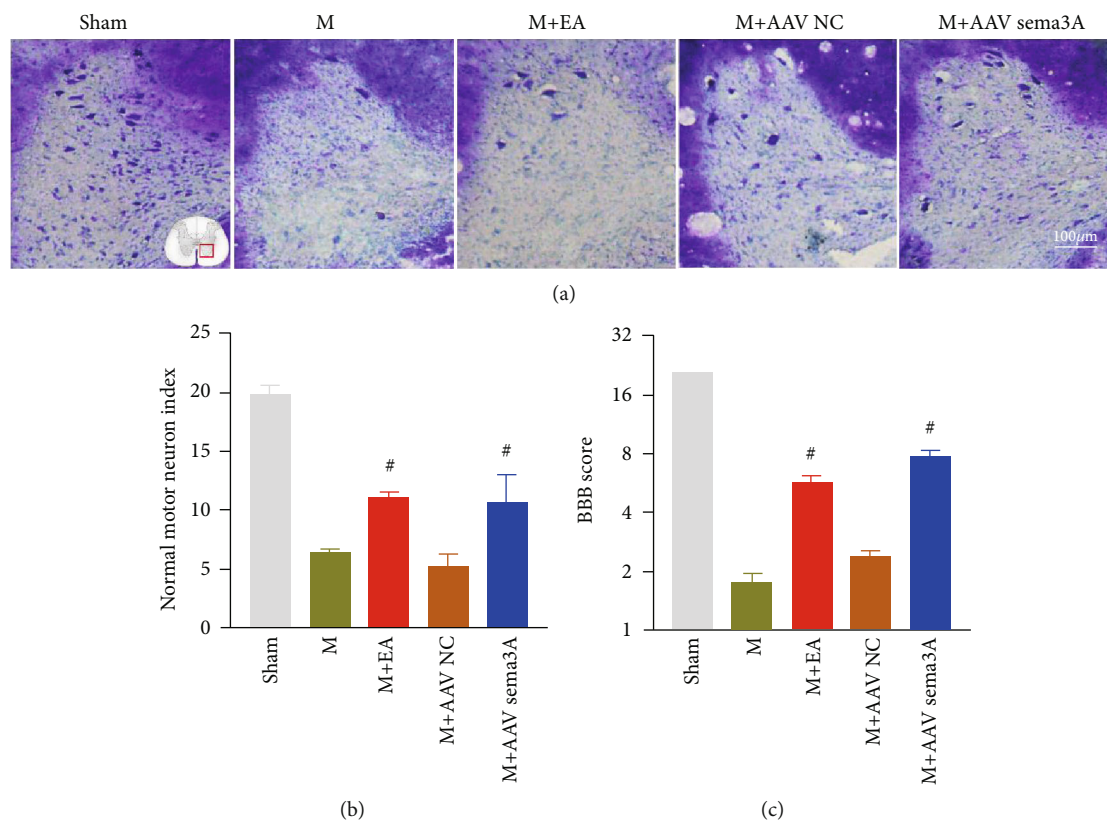


FIGURE 9: EA or Sema3A knockdown can promote the functional recovery after SCI in rats. (a) The figure represents the Nissl staining of the ventral horn of the spinal cord (b) The number of surviving motoneurons in the ventral horn of the spinal cord was quantified by Nissl staining, compared with the SCI group,  $\#P < 0.05$ ,  $n = 3$ . (c) The motor function score of each group at day 7, compared with the SCI group,  $\#P < 0.05$ ,  $n = 10$ . All data are presented as the mean  $\pm$  SEM.

promote the regeneration of nerve and axon after SCI [45, 46]. Despite the fact that some previous studies have confirmed the role of EA in promoting functional recovery after SCI, the mechanism of whether EA can promote neurological recovery by interfering with PNN changes after SCI is still in the exploratory stage.

In this study, we found the expression levels of aggrecan and TNR protein in PNNs were dramatically reduced, as well as Sema3A and NRP1, after 2 Hz/100 Hz alternating wave acupuncture treatment, which was consistent with the trend after the knocking down of Sema3A in the damaged site. Taken together, the data of our study have showed that regulating the expression of Sema3A after SCI can affect the plasticity of PNN and is beneficial to the repair of the motor function, and Jiaji EA may regulate PNN plasticity through Sema3A and improve the locomotor function of the paralyzed hind limbs finally.

#### 4. Conclusions

In summary, the results showed that EA at Jiaji points could improve the recovery of the motor function after SCI and has a positive therapeutic effect on SCI. EA therapy for SCI may affect the plasticity of PNNs by regulating the Sema3A signal transduction. This study ultimately reveals a new sight for the intervention effect of EA on spinal cord injury; however, the precise mechanism of the negative correlation between PNNs

and motor function recovery post-SCI remains to be further explored.

#### Data Availability

All the data used to support the findings of this study are included within the article.

#### Additional Points

*Author statements.* The manuscript is original, has not been submitted to or is not under consideration by another publication, has not been previously published in any language or any form, including electronic, and contains no disclosure of confidential information or authorship/patent application/funding source disputations.

#### Ethical Approval

All experimental procedures were approved by the Animal Ethics Committee of Zhejiang Chinese Medical University in China.

#### Conflicts of Interest

The authors declare that there is no conflict of interest regarding the publication of this paper.



## Authors' Contributions

Rong Hu and Haipeng Xu contributed equally to this work as co-first authors. Ruijie Ma designed this study. Rong Hu, Haipeng Xu, Yaheng Jiang, Kelin He, and Lei Wu completed this study. Rong Hu and Haipeng Xu analyzed the data. Rong Hu, Haipeng Xu, and Yi Chen wrote the manuscript. Xiao-Mei Shao participated in the revision of the article. Ruijie Ma validated the manuscript. All authors had read and approved the final version of the paper.

## Acknowledgments

We sincerely thank The third clinical college of Zhejiang Chinese Medical University, Hangzhou, Zhejiang, China, for offering the experimental areas and instruments. We also thank all teachers and students there for directing empirical methods. The project was supported by the project funding: funded by the Zhejiang Provincial Natural Science Foundation of China (LY19H270009) and (LQ19H270003) and Key Traditional Chinese Medicine Discipline of Zhejiang Province (2017-XK-A18).

## References

- [1] Y. Wu, H. Chen, Z. Tan, D. Li, and C. Liang, "Therapeutic effects of Erbin inhibitor on spinal cord contusion in mice," *American Journal of Translational Research*, vol. 11, no. 4, pp. 2570–2579, 2019.
- [2] J. W. Fawcett, A. Curt, J. D. Steeves et al., "Guidelines for the conduct of clinical trials for spinal cord injury as developed by the ICCP panel: spontaneous recovery after spinal cord injury and statistical power needed for therapeutic clinical trials," *Spinal Cord*, vol. 45, no. 3, pp. 190–205, 2007.
- [3] P. T. Dorsher and P. M. McIntosh, "Acupuncture's effects in treating the sequelae of acute and chronic spinal cord injuries: a review of allopathic and traditional chinese medicine literature," *Evidence-Based Complementary and Alternative Medicine*, vol. 2011, Article ID 428108, 8 pages, 2011.
- [4] R. Ma, X. Liu, J. Clark, G. M. Williams, and S. A. Doi, "The impact of acupuncture on neurological recovery in spinal cord injury: a systematic review and meta-analysis," *Neurotrauma*, vol. 32, no. 24, pp. 1943–1957, 2015.
- [5] X. Y. Wang, X. L. Li, S. Q. Hong, Y. B. Xi-Yang, and T. H. Wang, "Electroacupuncture induced spinal plasticity is linked to multiple gene expressions in dorsal root deafferented rats," *Journal of Molecular Neuroscience*, vol. 37, no. 2, pp. 97–110, 2009.
- [6] R. J. Ma, L. Zhang, J. Bai, and W. Gao, "Effects of electroacupuncture combining with herbs on expressions of GAP-43mRNA and BDNF mRNA in the rats with spinal cord injury," *Chinese Archives of Traditional Chinese Medicine*, vol. 3, no. 27, pp. 576–578, 2009.
- [7] R. J. Ma, L. J. Zhang, L. Z. Sun, X. F. Nie, K. L. He, and C. H. Zhu, "The study on OMgp expression of ASCI rats treated by Jia-Ji electroacupuncture," *Chinese Archives of Traditional Chinese Medicine*, vol. 32, pp. 1283–1286, 2014.
- [8] S.-h. Jiang, W.-z. Tu, E.-m. Zou et al., "Neuroprotective effects of different modalities of acupuncture on traumatic spinal cord injury in rats," *Evidence-Based Complementary and Alternative Medicine*, vol. 2014, Article ID 431580, 9 pages, 2014.
- [9] R. Kumar, J. Lim, R. A. Mekary et al., "Traumatic spinal injury: global epidemiology and worldwide volume," *World Neurosurgery*, vol. 113, pp. e345–e363, 2018.
- [10] M. Wyndaele and J. J. Wyndaele, "Incidence, prevalence and epidemiology of spinal cord injury: what learns a worldwide literature survey?," *Spinal Cord*, vol. 44, no. 9, pp. 523–529, 2006.
- [11] L. M. Ramer, M. S. Ramer, and E. J. Bradbury, "Restoring function after spinal cord injury: towards clinical translation of experimental strategies," *The Lancet Neurology*, vol. 13, no. 12, pp. 1241–1256, 2014.
- [12] T. H. Hutson and S. di Giovanni, "The translational landscape in spinal cord injury: focus on neuroplasticity and regeneration," *Nature Reviews Neurology*, vol. 15, no. 12, pp. 732–745, 2019.
- [13] D. A. McCreedy and S. E. Sakiyama-Elbert, "Combination therapies in the CNS: engineering the environment," *Neuroscience Letters*, vol. 519, no. 2, pp. 115–121, 2012.
- [14] N. Lipachev, N. Arnst, A. Melnikova et al., "Quantitative changes in perineuronal nets in development and posttraumatic condition," *Journal of Molecular Histology*, vol. 50, no. 3, pp. 203–216, 2019.
- [15] A. Williams, G. Piaton, M.-S. Aigrot et al., "Semaphorin 3A and 3F: key players in myelin repair in multiple sclerosis?," *Brain*, vol. 130, no. 10, pp. 2554–2565, 2007.
- [16] C. M. Galtrey and J. W. Fawcett, "The role of chondroitin sulfate proteoglycans in regeneration and plasticity in the central nervous system," *Brain Research Reviews*, vol. 54, no. 1, pp. 1–18, 2007.
- [17] Y. Goshima, Y. Sasaki, T. Nakayama, T. Ito, and T. Kimura, "Current Perspective. Functions of semaphorins in axon guidance and neuronal regeneration," *Japanese Journal of Pharmacology*, vol. 82, no. 4, pp. 273–279, 2000.
- [18] F. de Winter, M. Oudega, A. J. Lankhorst et al., "Injury-induced class 3 semaphorin expression in the rat spinal cord," *Experimental Neurology*, vol. 175, no. 1, pp. 61–75, 2002.
- [19] B. C. Jongbloets and R. J. Pasterkamp, "Semaphorin signalling during development," *Development*, vol. 141, no. 17, pp. 3292–3297, 2014.
- [20] J. A. Gruner, "A monitored contusion model of spinal cord injury in the rat," *Journal of Neurotrauma*, vol. 9, no. 2, pp. 123–128, 1992.
- [21] Z. Wei, Y. Wang, W. Zhao, and M. Schachner, "Electroacupuncture modulates I1 adhesion molecule expression after mouse spinal cord injury," *The American Journal of Chinese Medicine*, vol. 45, no. 1, pp. 37–52, 2017.
- [22] S. W. Scheff, D. A. Saucier, and M. E. Cain, "A statistical method for analyzing rating scale data: the BBB locomotor score," *Journal of Neurotrauma*, vol. 19, no. 10, pp. 1251–1260, 2002.
- [23] J. L. Quintanar, D. Calderon-Vallejo, and I. Hernandez-Jasso, "Effects of GnRH on neurite outgrowth, neurofilament and spinophilin proteins expression in cultured spinal cord neurons of rat embryos," *Neurochemical Research*, vol. 41, no. 10, pp. 2693–2698, 2016.
- [24] A. M. Wong, C. P. Leong, T. Y. Su, S. W. Yu, W. C. Tsai, and C. P. C. Chen, "Clinical trial of acupuncture for patients with spinal cord injuries," *American Journal of Physical Medicine & Rehabilitation*, vol. 82, no. 1, pp. 21–27, 2003.
- [25] C. C. Smith, R. Mauricio, L. Nobre et al., "Differential regulation of perineuronal nets in the brain and spinal cord with

- exercise training," *Brain Research Bulletin*, vol. 111, pp. 20–26, 2015.
- [26] S. Miyata, S. Nadanaka, M. Igarashi, and H. Kitagawa, "Structural variation of chondroitin sulfate chains contributes to the molecular heterogeneity of perineuronal nets," *Frontiers in Integrative Neuroscience*, vol. 12, p. 3, 2018.
- [27] G. Brückner, J. Grosche, S. Schmidt et al., "Postnatal development of perineuronal nets in wild-type mice and in a mutant deficient in tenascin-R," *The Journal of Comparative Neurology*, vol. 428, no. 4, pp. 616–629, 2000.
- [28] D. Carulli, T. Pizzorusso, J. C. F. Kwok et al., "Animals lacking link protein have attenuated perineuronal nets and persistent plasticity," *Brain*, vol. 133, no. 8, pp. 2331–2347, 2010.
- [29] A. Buss, K. Pech, B. A. Kakulas et al., "Ng2 and phosphacan are present in the astroglial scar after human traumatic spinal cord injury," *BMC Neurology*, vol. 9, no. 1, p. 32, 2009.
- [30] D. Wang, R. M. Ichiyama, R. Zhao, M. R. Andrews, and J. W. Fawcett, "Chondroitinase combined with rehabilitation promotes recovery of forelimb function in rats with chronic spinal cord injury," *Journal of Neuroscience*, vol. 31, no. 25, pp. 9332–9344, 2011.
- [31] E. J. Bradbury, L. D. Moon, R. J. Popat et al., "Chondroitinase ABC promotes functional recovery after spinal cord injury," *Nature*, vol. 416, no. 6881, pp. 636–640, 2002.
- [32] P. Pesheva, S. Gloor, and R. Probstmeier, "Tenascin-R as a regulator of CNS glial cell function," *Progress in Brain Research*, vol. 132, pp. 103–114, 2001.
- [33] E. Muir, F. de Winter, J. Verhaagen, and J. Fawcett, "Recent advances in the therapeutic uses of chondroitinase ABC," *Experimental Neurology*, vol. 321, article 113032, 2019.
- [34] J. M. Massey, J. Ams, M. S. Viapiano et al., "Increased chondroitin sulfate proteoglycan expression in denervated brainstem targets following spinal cord injury creates a barrier to axonal regeneration overcome by chondroitinase ABC and neurotrophin-3," *Experimental Neurology*, vol. 209, no. 2, pp. 426–445, 2008.
- [35] J. M. Massey, C. H. Hubscher, M. R. Wagoner et al., "Chondroitinase ABC digestion of the perineuronal net promotes functional collateral sprouting in the cuneate nucleus after cervical spinal cord injury," *Journal of Neuroscience*, vol. 26, no. 16, pp. 4406–4414, 2006.
- [36] S. Kaneko, A. Iwanami, M. Nakamura et al., "A selective sema3A inhibitor enhances regenerative responses and functional recovery of the injured spinal cord," *Nature Medicine*, vol. 12, no. 12, pp. 1380–1389, 2006.
- [37] M. Shelly, L. Cancedda, B. K. Lim et al., "Semaphorin3a regulates neuronal polarization by suppressing axon formation and promoting dendrite growth," *Neuron*, vol. 71, no. 3, pp. 433–446, 2011.
- [38] R. J. Pasterkamp, "Getting neural circuits into shape with semaphorins," *Nature Reviews. Neuroscience*, vol. 13, no. 9, pp. 605–618, 2012.
- [39] D. Carulli, S. Foscarin, A. Faralli, E. Pajaj, and F. Rossi, "Modulation of semaphorin3A in perineuronal nets during structural plasticity in the adult cerebellum," *Molecular and Cellular Neurosciences*, vol. 57, pp. 10–22, 2013.
- [40] T. Vo, D. Carulli, E. M. Ehlert et al., "The chemorepulsive axon guidance protein semaphorin3A is a constituent of perineuronal nets in the adult rodent brain," *Molecular and Cellular Neurosciences*, vol. 56, pp. 186–200, 2013.
- [41] F. de Winter, J. C. Kwok, J. W. Fawcett, T. T. Vo, D. Carulli, and J. Verhaagen, "The chemorepulsive protein semaphorin 3a and perineuronal net-mediated plasticity," *Neural Plasticity*, vol. 2016, Article ID 3679545, 14 pages, 2016.
- [42] Q. Renfu, C. Rongliang, D. Mengxuan et al., "Anti-apoptotic signal transduction mechanism of electroacupuncture in acute spinal cord injury," *Acupuncture in Medicine*, vol. 32, no. 6, pp. 463–471, 2014.
- [43] Y. Zhang, Y. B. Qiu, Z. Yang et al., "The effect of electroacupuncture with different waveforms on the motor function recovery of spinal cord injury rats," *Chinese Journal of Rehabilitation Medicine*, vol. 27, no. 12, pp. 1097–1101, 2012.
- [44] H. Y. Luo, Z. W. Zeng, X. B. Yu, J. He, J. Cao, and B. Xu, "Effect of electroacupuncture with different frequencies on hindlimb locomotor function and expression of LC3, Beclin1 and cleaved Caspase-3 proteins in spinal cord injury rats," *Journal of Acupuncture Research*, vol. 44, no. 9, pp. 625–631, 2019.
- [45] R. Hu, Y. Chen, H. P. Xu, K. L. He, L. Wu, and R. J. Ma, "Effect of electroacupuncture at "Jiaji"(EX-B 2) points on the proliferation and differentiation of oligodendrocyte precursor cells in rats with acute spinal cord injury," *Journal of Chinese Acupuncture*, vol. 40, no. 5, pp. 519–525, 2020.
- [46] L. Z. Sun, R. Ma, L. Z. Zhang, and K. He, "Study of Jia Ji electroacupuncture intervention on remyelination of spinal cord injury in rats," *Journal of Zhejiang University of Chinese medicine*, vol. 38, no. 5, pp. 626–630, 2014.

## Research Article

# Early Electroacupuncture Extends the rtPA Time Window to 6h in a Male Rat Model of Embolic Stroke via the ERK1/2-MMP9 Pathway

Xin-chang Zhang <sup>1,2</sup>, Ya-hui Gu,<sup>1,2</sup> Wen-tao Xu,<sup>1,2</sup> Yang-yang Song,<sup>1,2</sup> Ao Zhang,<sup>1,2</sup> Zhi-hui Zhang,<sup>1,2</sup> Si-yuan Jiang,<sup>1,2</sup> Si-qi Chang,<sup>1,2</sup> and Guang-xia Ni <sup>1,2</sup>

<sup>1</sup>College of Acupuncture-Moxibustion and Tuina, Nanjing University of Chinese Medicine, Nanjing 210023, China

<sup>2</sup>Key Laboratory of Acupuncture and Medicine Research of Ministry of Education, Nanjing University of Chinese Medicine, Nanjing 210023, China

Correspondence should be addressed to Guang-xia Ni; [xgn66@163.com](mailto:xgn66@163.com)

Received 26 June 2020; Revised 10 October 2020; Accepted 14 October 2020; Published 11 November 2020

Academic Editor: Lu Wang

Copyright © 2020 Xin-chang Zhang et al. This is an open access article distributed under the Creative Commons Attribution License, which permits unrestricted use, distribution, and reproduction in any medium, provided the original work is properly cited.

**Background.** Recombinant tissue plasminogen activator (rtPA) is the only recommended pharmacological treatment for acute ischemic stroke, but it has a restricted therapeutic time window. When administered at time points greater than 4.5 h after stroke onset, rtPA disrupts the blood-brain barrier (BBB), which leads to serious brain edema and hemorrhagic transformation. Electroacupuncture (EA) exerts a neuroprotective effect on cerebral ischemia; however, researchers have not clearly determined whether EA increases the safety of thrombolysis and extends the therapeutic time window of rtPA administration following ischemic stroke. **Objective.** The present study was conducted to test the hypothesis that EA extends the therapeutic time window of rtPA for ischemic stroke in a male rat model of embolic stroke. **Methods.** SD rats were randomly divided into the sham operation group, model group, rtPA group, EA+rtPA group, and rtPA+MEK1/2 inhibitor group. An injection of rtPA was administered 6 h after ischemia. Rats were treated with EA at the Shuigou (GV26) and Neiguan (PC6) acupoints at 2 h after ischemia. Neurological function, infarct volume, BBB permeability, brain edema, and hemorrhagic transformation were assessed at 24 h after ischemia. Western blotting and immunofluorescence staining were performed to detect the levels of proteins involved in the ERK1/2 signaling pathway (MEK1/2 and ERK1/2), tight junction proteins (Claudin5 and ZO-1), and MMP9 in the ischemic penumbra at 24 h after stroke. **Results.** Delayed rtPA treatment aggravated hemorrhagic transformation and brain edema. However, treatment with EA plus rtPA significantly improved neurological function and reduced the infarct volume, hemorrhagic transformation, brain edema, and EB leakage in rats compared with rtPA alone. EA increased the levels of tight junction proteins, inhibited the activation of the ERK1/2 signaling pathway, and reduced MMP9 overexpression induced by delayed rtPA thrombolysis. **Conclusions.** EA potentially represents an effective adjunct method to increase the safety of thrombolytic therapy and extend the therapeutic time window of rtPA administration following ischemic stroke. This neuroprotective effect may be mediated by the inhibition of the ERK1/2-MMP9 pathway and alleviation of the destruction of the BBB.

## 1. Introduction

Stroke is a leading cause of mortality and disability worldwide [1]; approximately 13.7 million new stroke cases, 5.5 million deaths, and 116.4 million disability-adjusted life-years due to stroke were reported in 2016 [2]. Acute ischemic

stroke, the most common subtype, accounts for 87% of all strokes [3] and primarily results from occlusion of the cerebral arteries by thrombosis or embolism [4]. Currently, intravenous thrombolysis with recombinant tissue plasminogen activator (rtPA) has been proven to be the most effective pharmacological treatment for acute ischemic stroke when

administered within 3–4.5 h after ischemia onset [5]. Unfortunately, the use of rtPA is restricted by its narrow thrombolytic time window, because it may cause thrombolytic complications, such as brain edema and hemorrhagic transformation, particularly when delayed thrombolysis is initiated after 4.5 h [6, 7]. Due to these limitations, only 3.8–8% of patients with ischemic stroke benefit from rtPA-mediated thrombolysis [8]. Therefore, any neuroprotective strategy designed to reduce complications and extend the thrombolytic time window will be very important.

Based on accumulating evidence from clinical and animal studies, the disruption of the blood-brain barrier (BBB) is the key event that leads to brain edema and hemorrhagic transformation during thrombolysis for ischemic stroke [9–11]. The BBB is composed of endothelial cells, tight junctions (TJs), pericytes, astrocytic endfeet, and extracellular matrix (ECM) [12]. Matrix metalloproteinases (MMPs) are a family of zinc-dependent endopeptidases that are best known for their role in the degradation and remodeling of ECM components [13]. The level of the matrix metalloproteinase 9 (MMP9) protein has consistently been shown to increase after ischemic stroke, and it plays an important role in BBB destruction by degrading ECM and TJ proteins [14–16]. More importantly, rtPA may cross the BBB, enter the brain parenchyma, and thereby damage the neurovascular matrix by promoting MMP9 production and activation [17, 18]. Consequently, selective inhibition of MMP9 reduces brain injury, particularly the degradation of the BBB, after rtPA thrombolysis for ischemic stroke [14, 19].

Extracellular signal-regulated kinase 1/2 (ERK1/2), a critical member of mitogen-activated protein kinase (MAPK) cascades, is activated by dual phosphorylation catalyzed by MAPK kinase (MAPKK, also known as MEK1/2). The ERK1/2 signaling pathway is involved in the inflammatory response and apoptosis and plays an important role in the repair of the BBB after brain injury [20, 21]. MMP9 expression is induced by ERK1/2 signaling, and inhibition of ERK1/2 signaling reduces the hemorrhagic transformation and brain edema caused by overexpression of MMP9 following cerebral ischemia [14, 22–24].

Electroacupuncture (EA), a type of acupuncture with electronic stimulation, is a well-known complementary and alternative medical treatment for ischemic stroke in China. Based on both clinical and experimental studies, EA, a safe and effective treatment, significantly reduces the infarct volume and neurological deficit score following cerebral ischemia [25–27]. EA stimulation exerts a neuroprotective effect by increasing the expression of TJ proteins (Claudin5 and ZO-1), reducing MMP9 expression and protecting the BBB integrity in various animal models of ischemic stroke [28–30]. In addition, EA alleviates cerebral ischemia and reperfusion injury by modulating the ERK1/2 signaling pathway [31]. However, researchers have not yet clearly determined whether EA improves the safety of thrombolysis and extends the therapeutic time window during rtPA thrombolysis for ischemic stroke. Therefore, the present study was conducted to test the hypothesis that EA represents an adjunct therapy that will extend the therapeutic time window of rtPA for ischemic stroke by alleviating BBB damage and reducing

the risk of complications induced by delayed rtPA thrombolysis. Moreover, we further elucidated whether this neuroprotective effect was associated with the modulation of the ERK1/2-MMP9 signaling pathway, as well as the underlying mechanisms.

## 2. Materials and Methods

**2.1. Animals.** Adult male Sprague-Dawley (SD) rats weighing  $320 \pm 20$  g were supplied by Shanghai Xipuer-Bikai Experimental Animal Co., Ltd. (Shanghai, China; license no. SCXK (Hu): 2018-0006). All rats were housed in a temperature- and humidity-controlled room on a 12 h light/dark cycle at the Experimental Animal Centre of Nanjing University of Chinese Medicine. This study was approved by the Institutional Animal Care and Use Committee of Nanjing University of Chinese Medicine, and all procedures were strictly conducted in accordance with the guidelines of the National Institutes of Health Animal Care and Use Committee. The experiments reported here were performed in accordance with the ARRIVE guidelines.

**2.2. Establishment of the Embolic Stroke Model.** An embolic stroke model was induced by placing a blood clot into the middle cerebral artery (MCA) using the methods described by Zhang et al. [32].

- (a) *Preparation of Embolus.* The external carotid artery (ECA) of the donor rat was catheterized; blood was transferred into 20 cm long PE-50 tubing, allowed to clot for 2 h at 37°C, and then stored at 4°C for 22 h. A 5 cm segment of clot-filled PE-50 tubing was cut, and the clot was then drawn into a PE-10 tubing connected to a saline-filled syringe via a 30 G needle. The clot was drawn into and flushed out of the PE-10 tubing repeatedly to remove the red blood cells. A 4 cm segment of clot was cut and transferred to a modified PE-50 catheter (outer diameter of 0.35 mm) connected to a 100  $\mu$ l syringe and the clot was then injected into the MCA.
- (b) *Embolic Stroke Model Establishment.* Rats were anesthetized with isoflurane (5% for induction and 1.5–2% for maintenance), and then, an embolic stroke was induced. The rectal temperature ( $37 \pm 0.5^\circ\text{C}$ ) was maintained throughout surgery with an electric blanket. The right common carotid artery (CCA), internal carotid artery (ICA), and ECA were exposed via a midline cervical incision. The distal end and branches of the ECA were ligated, and the CCA and the ICA were temporarily clamped with a microvascular clip. Immediately thereafter, a partial arteriotomy on the ECA was performed, and the tip of a modified PE-50 catheter containing the clot was inserted into the ECA lumen and advanced 19–22 mm from the ECA into the lumen of the ICA until it reached the origin of the MCA. Then, the catheter was retracted 1–2 mm, and the clot was slowly injected with 5–10  $\mu$ l of saline at a rate of 10  $\mu$ l/min. The catheter was withdrawn from the arteriotomy



5 min after the injection. The cerebral blood flow (CBF) was monitored with laser Doppler flowmetry (LDF, MoorVMS-LDF1) by gently attaching an LDF probe to the dura mater. The successful obstruction of CBF by the thrombus was defined as a reduction in perfusion greater than 70% of the baseline CBF [33] (Supplementary Figure 1). The successful establishment of the model was judged based on the obstruction of CBF and neurological deficit score at 2 h after stroke. For sham-operated rats, the same surgery was performed, except that 5-10  $\mu$ l saline was injected into the MCA

**2.3. Experimental Design and Groups.** Two sets of experiments were performed, and the animals were randomly divided into various groups.

In the first experiment, rats were randomly assigned to the following groups: (1) sham, (2) model, (3) rtPA, and (4) rtPA+EA. A tail vein injection of rtPA (Boehringer Ingelheim, Germany) was administered at 6 h after stroke induction, and the doses of rtPA (10 mg/kg) were determined based on previous studies [34, 35]. An equal volume of normal saline was injected intravenously at the corresponding times in rats that did not receive rtPA. These animals were used to measure the infarct volume, brain edema, neurological deficit score, hemorrhagic transformation, BBB permeability, and expression of ZO-1, Claudin5, ERK1/2, and MMP9. In this experiment, we determined that EA attenuated delayed rtPA-induced BBB disruption and hemorrhagic transformation and improved neurological function by preventing the activation of ERK1/2 and MMP9.

We conducted a second experiment to determine whether ERK1/2 signaling affects the expression of MMP9 in rats with embolic stroke. The rats were randomly divided into the sham group, rtPA group, and rtPA+MEK1/2 inhibitor (U0126). U0126 (5  $\mu$ l, 0.2  $\mu$ g/ $\mu$ l) [36] or vehicle (0.1 M PBS containing 0.4% DMSO) was administered intracerebroventricularly (ICV) 30 min prior to embolic stroke. The ICV injection site was chosen at the following coordinates from the bregma according to the rat brain in stereotaxic coordinates: anteroposterior, 1.2 mm; lateral, 2.0 mm; and depth, 3.8 mm.

At 24 h after stroke, all animals were euthanized, and their brains were harvested for further experiments.

**2.4. Electroacupuncture Treatment.** Rats in the rtPA+EA group received EA at the Shuigou (GV26) and left Neiguan (PC6) acupoints at 2 h postembolic stroke. GV26 was located at the junction of the upper 1/3 and middle 1/3 of the upper lip. PC6 was located approximately 3 mm proximal to the palm crease above the median nerve. Stainless steel acupuncture needles (outer diameter 0.3 mm) were inserted 2-3 mm into GV26 and PC6. Then, the needles were connected to an electrical stimulator (HANS-200, Nanjing Jisheng Medical Technology Company, China) with an intensity of 1 mA and frequency of 2/15 Hz for 30 min.

**2.5. Measurement of Neurological Function.** The neurological deficit score was recorded at 2 h and 24 h after embolic stroke

and determined with a modified 6-point scoring system [37, 38] as follows: 0, no apparent deficits; 1, contralateral forelimb flexion; 2, decreased grip of the contralateral forelimb while pulled by tail; 3, spontaneous movement in all directions, contralateral circling only if pulled by tail; 4, spontaneous contralateral circling; and 5, death. The successful establishment of the embolic stroke model was confirmed by the obstruction of CBF and a neurological deficit score of no less than 2 points at 2 h after stroke.

**2.6. Measurement of the Infarct Volume and Brain Edema.** TTC staining was performed 24 h after ischemia onset to determine the infarct volume. Rats were euthanized, and the brains were rapidly removed and frozen at -30°C for 15 min. Then, brain tissues were sectioned into 2-mm-thick coronal slices and immersed in a 2% solution of TTC (Sigma) at 37°C in the dark for 30 min. Normal regions were stained red, whereas infarct regions appeared white. Finally, the stained slices were fixed with a 4% paraformaldehyde solution for 24 hours and scanned to measure the ratio of infarct area to the whole brain using an image analysis system (ImageJ software).

Brain edema was assessed at 24 h after ischemia onset by measuring the brain water content using the wet-dry weight technique. The cerebellum and olfactory bulb were removed. Then, the injured right hemisphere was weighed to obtain its wet weight and subsequently dried at 100°C for 24 hours to obtain the dry weight. The percentage of the brain water content was calculated as (wet weight - dry weight)/(wet weight)  $\times$  100%.

**2.7. Evaluation of BBB Permeability.** BBB permeability was assessed by measuring the extravasation of Evans Blue (EB, Sigma) dye in the rat brain at 24 h after embolic stroke [39, 40]. Two hours before decapitation, 2% EB was injected into rats via the tail vein at 4 mL/kg (body weight). The rats were deeply anesthetized and transcardially perfused with normal saline through the left ventricle until an outflow of clear perfusion fluid from the right atrium was observed. After decapitation, the brain tissue was removed, and the right hemisphere was weighed. The brain tissue was homogenized in a formamide solution (1 mL/100 mg) and then incubated in a water bath (60°C) for 24 h before being centrifuged at 1000  $\times$  g for 30 min. Finally, the absorbance of EB in the supernatants was measured at 620 nm using a spectrophotometer. The EB content was reported as micrograms per gram of brain tissue and was calculated from a standard curve.

**2.8. Measurement of Hemorrhagic Transformation.** Hemorrhagic transformation was determined by detecting hemoglobin levels on the ischemic side of the brain using a method reported in a previous study [41]. At 24 h after embolic stroke, rats were anesthetized and perfused transcardially with 0.1 M phosphate-buffered saline (PBS). The ischemic hemisphere was separated, homogenized in 0.1 M PBS, and then centrifuged for 30 min (13000 rpm). Thereafter, the supernatant was collected, and the hemoglobin level was measured with a hemoglobin assay kit (QuantiChrom™



Hemoglobin Assay Kit, Hayward, USA) according to the manufacturer's protocol. The optical density value of each sample was measured at 400 nm using a microplate reader.

**2.9. Western Blot Analysis.** All rats were sacrificed at 24 h poststroke, and the ischemic penumbra was separated based on a previous study [42]. Total protein was extracted using a protein extraction kit (Beyotime Biotech) according to the manufacturer's protocol. The protein content was determined using the quantitative BCA protein assay. Equal amounts of protein (30  $\mu$ g) were separated by electrophoresis on 10% SDS-PAGE gels and transferred to PVDF membranes. The membranes were blocked with 5% BSA for 2 h at room temperature, followed by an overnight incubation at 4°C with the following specific primary antibodies: ERK1/2 (1:1000, ab17942, Abcam), MEK1/2 (1:1000, ab178876, Abcam), MMP9 (1:2000, ab76003, Abcam), p-MEK1/2 (1:1000, CST9154, CST), p-ERK1/2 (1:2000, CST4370, CST), Claudin5 (1:2000, ab131259, Abcam), and ZO-1 (1:1000, 21773-1-AP, Proteintech). After washes with TBST, the membranes were incubated with HRP-labeled goat anti-rabbit IgG (1:1000, A0208, Beyotime Biotech) at room temperature for one hour. The bands were detected using an enhanced chemiluminescent substrate (ECL, Thermo Scientific) and visualized using a Bioshine ChemiQ4800 imaging system (Shanghai Bioshine Scientific Instrument Co., Ltd). Finally, the gray level ratio of target proteins was obtained using the ImageJ software, and  $\beta$ -tubulin (1:2000, 30302ES20, Yeasen) was used as the internal control.

**2.10. Immunofluorescence Staining.** The animals were perfused transcardially with a 4% paraformaldehyde solution, and the brains were dissected and fixed with paraformaldehyde for 24 h at 4°C. After dehydration with a 40% sucrose solution and embedding in OTC, the brain tissues were cut into 12- $\mu$ m frozen sections for staining using a cryostat (Leica CM1950, Germany). Next, tissue sections were washed three times with PBS, permeabilized, and blocked with PBS containing 0.1% Tween 20, 0.3% Triton X-100, and 5% BSA. Then, the sections were incubated overnight at 4°C with the following specific primary antibodies: MMP9 (1:300, ab76003, Abcam), Claudin5 (1:500, ab131259, Abcam), and ZO-1 (1:50, 21773-1-AP, Proteintech). Sections were then washed with PBS and incubated for 1 h with secondary antibodies (Alexa Fluor 594, ab150080, Abcam and Alexa Fluor 488, ab150077, Abcam) at room temperature. Nuclear counterstaining was performed using DAPI (C0065, Solarbio, China). Images of ischemic penumbral sections were randomly captured using an Olympus BX63 fluorescence microscope (Olympus, Tokyo, Japan). Fluorescence intensity was quantified using the ImageJ software, and the results are presented as average optical density (AOD) values.

**2.11. Statistical Analysis.** All data were analyzed using the SPSS 24 and GraphPad Prism 7 software, and the data are reported as mean values  $\pm$  standard deviations. Data with a normal distribution and homogeneity of variance were ana-

lyzed using analysis of variance (ANOVA). The nonparametric Mann-Whitney  $U$  test was used to analyze nonnormally distributed data. Statistical significance was defined as  $p < 0.05$ , and a high level of statistical significance was defined as  $p < 0.01$ .

### 3. Results

**3.1. EA Improved Brain Injury following Delayed rtPA Thrombolysis for Ischemic Stroke.** We evaluated neurological deficits and the cerebral infarct volume at 24 hours after stroke to determine the effects of EA on delayed rtPA thrombolysis for ischemic stroke. The neurological deficit score and infarct volume in rats with rtPA thrombolysis did not differ from the model group ( $p > 0.05$ , Figures 1(a) and 1(c)). However, the combination of EA and 6 h rtPA resulted in significant reductions in the neurological deficit score and infarct volume compared to the model group and to the group treated with 6 h rtPA alone ( $p < 0.05$ ,  $p < 0.01$ , Figures 1(a) and 1(c)). Based on the results, EA improved brain injury following delayed rtPA thrombolysis for ischemic stroke.

**3.2. EA Decreased Hemorrhagic Transformation and Brain Edema Induced by Delayed rtPA Thrombolysis for Ischemic Stroke.** We evaluated hemorrhagic transformation and brain edema at 24 hours after stroke to examine the potential effect of EA on delayed rtPA-induced complications. As depicted in Figure 2, we did not detect any significant hemorrhagic transformation in the model group compared to the sham group ( $p > 0.05$ , Figure 2(a)). The rtPA treatment at 6 h after stroke significantly increased the hemoglobin level compared with the model group; however, the combination of EA and 6 h rtPA significantly decreased the hemoglobin level compared to the 6 h rtPA alone group ( $p < 0.01$ , Figure 2(a)). In addition, the rtPA treatment at 6 h after stroke significantly increased the brain water content compared with the model group, but the combination of EA and 6 h rtPA significantly decreased the brain water content compared to the model group and to the 6 h rtPA alone group ( $p < 0.01$ , Figure 2(b)). Thus, rtPA thrombolysis beyond the time window after acute ischemic stroke aggravated the incidence and severity of hemorrhagic transformation and brain edema, but EA decreased hemorrhagic transformation and brain edema induced by delayed rtPA thrombolysis.

**3.3. EA Reduced BBB Permeability Induced by Delayed rtPA Thrombolysis for Ischemic Stroke.** We assessed BBB permeability by measuring the amount of EB leakage in the ischemic hemisphere to investigate the effect of EA on the BBB integrity in the postischemic brains subjected to delayed rtPA thrombolysis. As depicted in Figure 3, rtPA thrombolysis at 6 h after ischemia significantly increased EB leakage compared to the model group ( $p < 0.01$ , Figure 3). However, the combination of EA and 6 h rtPA significantly decreased EB leakage compared to the model group and to the 6 h rtPA alone group ( $p < 0.01$ , Figure 3). Based on these results, the administration of rtPA thrombolysis beyond the time window after acute ischemic stroke increased BBB permeability,

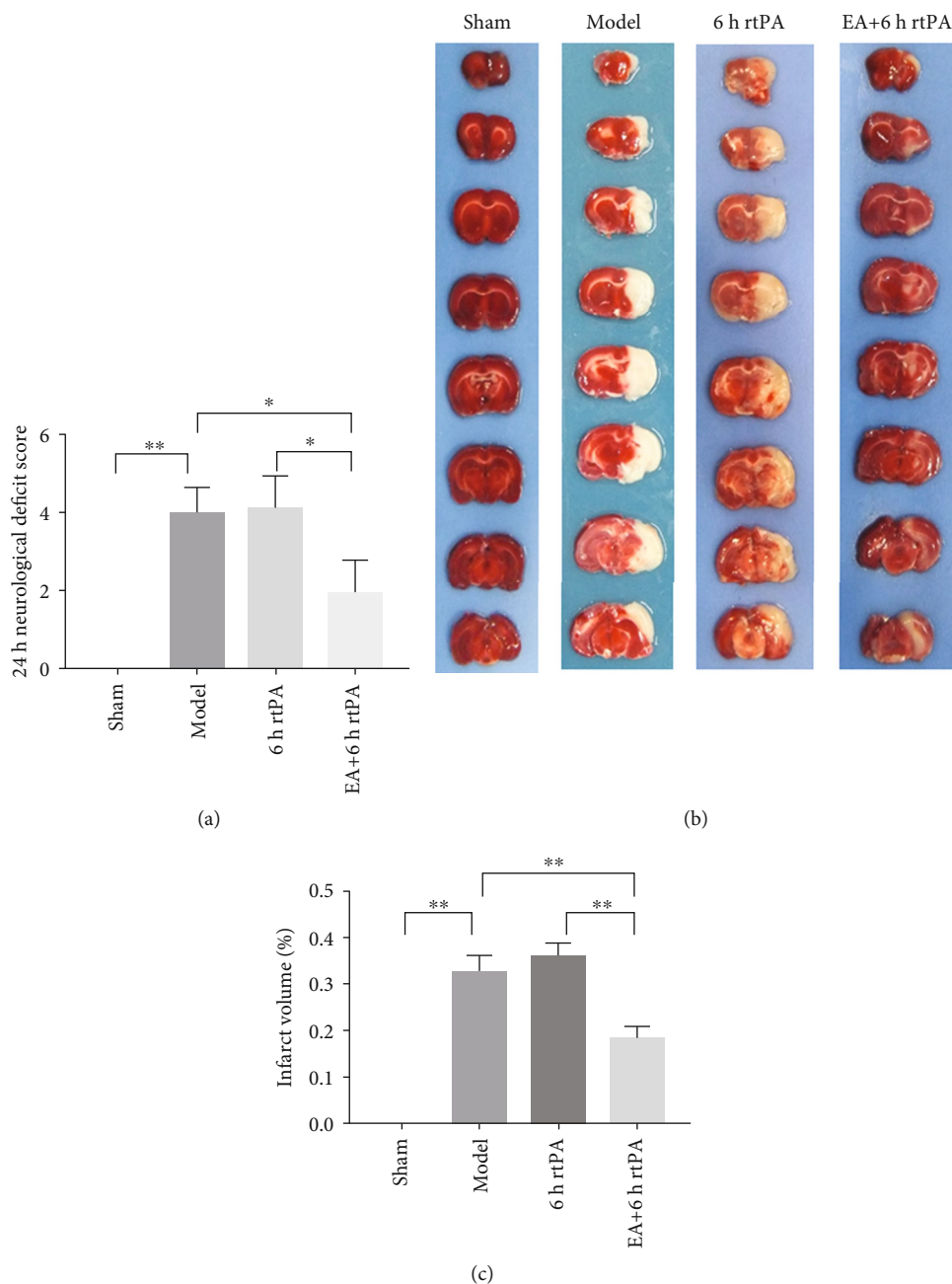


FIGURE 1: The neurological deficit score ( $n = 10$  rats) and infarct volume ( $n = 6$  rats) in each group. (a) Neurological deficit score. (b) Representative images of brain slices stained with TTC. (c) Brain infarct volume. \* indicates  $p < 0.05$ ; \*\* indicates  $p < 0.01$ .

but EA preserved the BBB integrity and reduced BBB permeability induced by delayed rtPA thrombolysis.

**3.4. EA Attenuated the Loss of Tight Junction Proteins Induced by Delayed rtPA Thrombolysis for Ischemic Stroke.** Because tight junctions play an important role in maintaining BBB integrity, we examined whether EA increased the levels of TJ proteins (Claudin5 and ZO-1) using immunofluorescence staining and Western blot analysis. As depicted in Figures 4 and 5, rtPA thrombolysis at 6 h after ischemia significantly decreased the levels of the Claudin5 and ZO-1 proteins compared to the model group. However, compared with the model group and the 6 h rtPA alone group, the com-

bination of EA and 6 h rtPA significantly increased the levels of the Claudin5 and ZO-1 proteins ( $p < 0.01$ , Figures 4(b), 4(d), 5(b), and 5(d)). Therefore, the administration of rtPA beyond the time window after acute ischemic stroke substantially disrupted the BBB, but EA increased the levels of TJ proteins and alleviated the impairment of the BBB induced by delayed rtPA thrombolysis.

**3.5. EA Attenuated MMP9 Overexpression Induced by Delayed rtPA Thrombolysis for Ischemic Stroke.** MMP9 plays a pivotal role in BBB disruption, leading to brain edema and hemorrhagic transformation [43], and rtPA enhances the activation of MMP9 [44]. Therefore, we investigated the

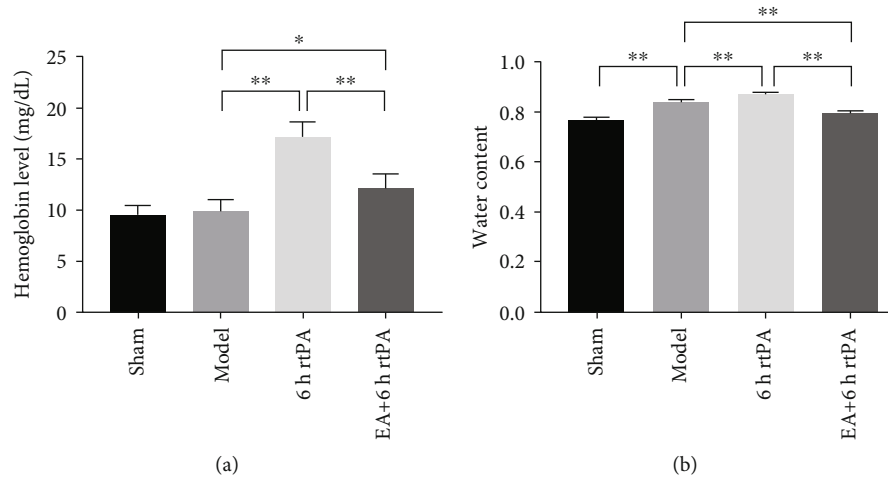


FIGURE 2: Hemorrhagic transformation and brain edema in each group ( $n = 6$  rats). (a) Hemoglobin level. (b) Brain water content. \* indicates  $p < 0.05$ ; \*\* indicates  $p < 0.01$ .

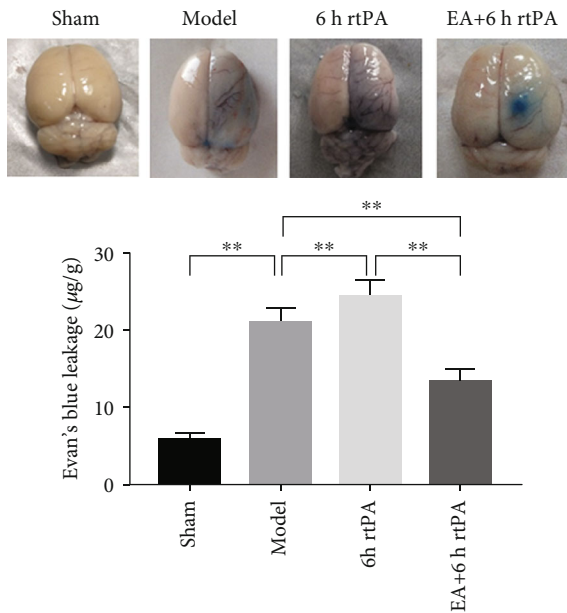


FIGURE 3: BBB permeability in each group ( $n = 6$  rats). \*\* indicates  $p < 0.01$ .

effects of EA on MMP9 activation induced by delayed rtPA thrombolysis for ischemic stroke. As depicted in Figure 6, rtPA thrombolysis at 6 h after ischemia significantly increased the levels of the MMP9 protein compared to the model group ( $p < 0.01$ , Figure 6(b)). However, compared with the model group and 6 h rtPA alone group, the combination of EA and 6 h rtPA significantly decreased the levels of the MMP9 protein ( $p < 0.01$ , Figure 6(b);  $p < 0.05$ , Figure 6(d)). Based on these results, the administration of rtPA thrombolysis beyond the time window after acute ischemic stroke caused MMP9 overexpression, but EA reduced the high levels of the MMP9 protein induced by delayed rtPA thrombolysis.

**3.6. EA Ameliorated BBB Disruption by Inhibiting the ERK1/2-MMP9 Pathway following Delayed rtPA Thrombolysis for Ischemic Stroke.** The levels of phosphorylated MER1/2 (p-MER1/2) and phosphorylated ERK1/2 (p-ERK1/2) were analyzed at 24 h after stroke using Western blot analyses to evaluate the potential relationship between the protective effects of EA on the BBB integrity and ERK1/2 signaling. As depicted in Figure 7(a), the levels of p-MER1/2 and p-ERK1/2 in the model group were significantly elevated compared with the sham group. In the 6 h rtPA group, the levels of p-MER1/2 and p-ERK1/2 were further elevated and did not differ from the levels in the model group ( $p > 0.05$ , Figures 7(b) and 7(c)). However, compared with the model group and the 6 h rtPA alone group, the combination of EA and 6 h rtPA significantly decreased the levels of p-MER1/2 and p-ERK1/2 ( $p < 0.01$ , Figures 7(b) and 7(c)). Therefore, ERK1/2 signaling was activated after acute ischemic stroke. Thrombolysis beyond the time window did not decrease the level of phosphorylated ERK1/2. However, EA inhibited the activation of the ERK1/2 signaling pathway and reduced the high level of phosphorylated ERK1/2 following delayed rtPA thrombolysis for ischemic stroke.

We randomly divided the rats into a sham group, a 6 h rtPA group and a 6 h rtPA+MEK1/2 inhibitor (U0126) to determine whether ERK1/2 signaling modulates MMP9 expression in rats with embolic stroke. Levels of p-ERK1/2 and MMP9 were analyzed at 24 h after stroke using Western blot analyses. As depicted in Figure 7(d), compared with the sham operation, levels of p-ERK1/2 and MMP9 were significantly increased in the 6 h rtPA group ( $p < 0.01$ , Figures 7(e) and 7(f)); compared with the 6 h rtPA group, levels of p-ERK1/2 and MMP9 were significantly decreased in the 6 h rtPA+U0126 group ( $p < 0.01$ , Figures 7(e) and 7(f)). Thus, MMP9 was the downstream target of the ERK1/2 signaling pathway, and inhibition of ERK1/2 further reduced the level of MMP9 in rats with embolic stroke. Based on these findings, EA ameliorated BBB disruption by inhibiting the ERK1/2-MMP9 pathway following delayed rtPA thrombolysis for ischemic stroke.

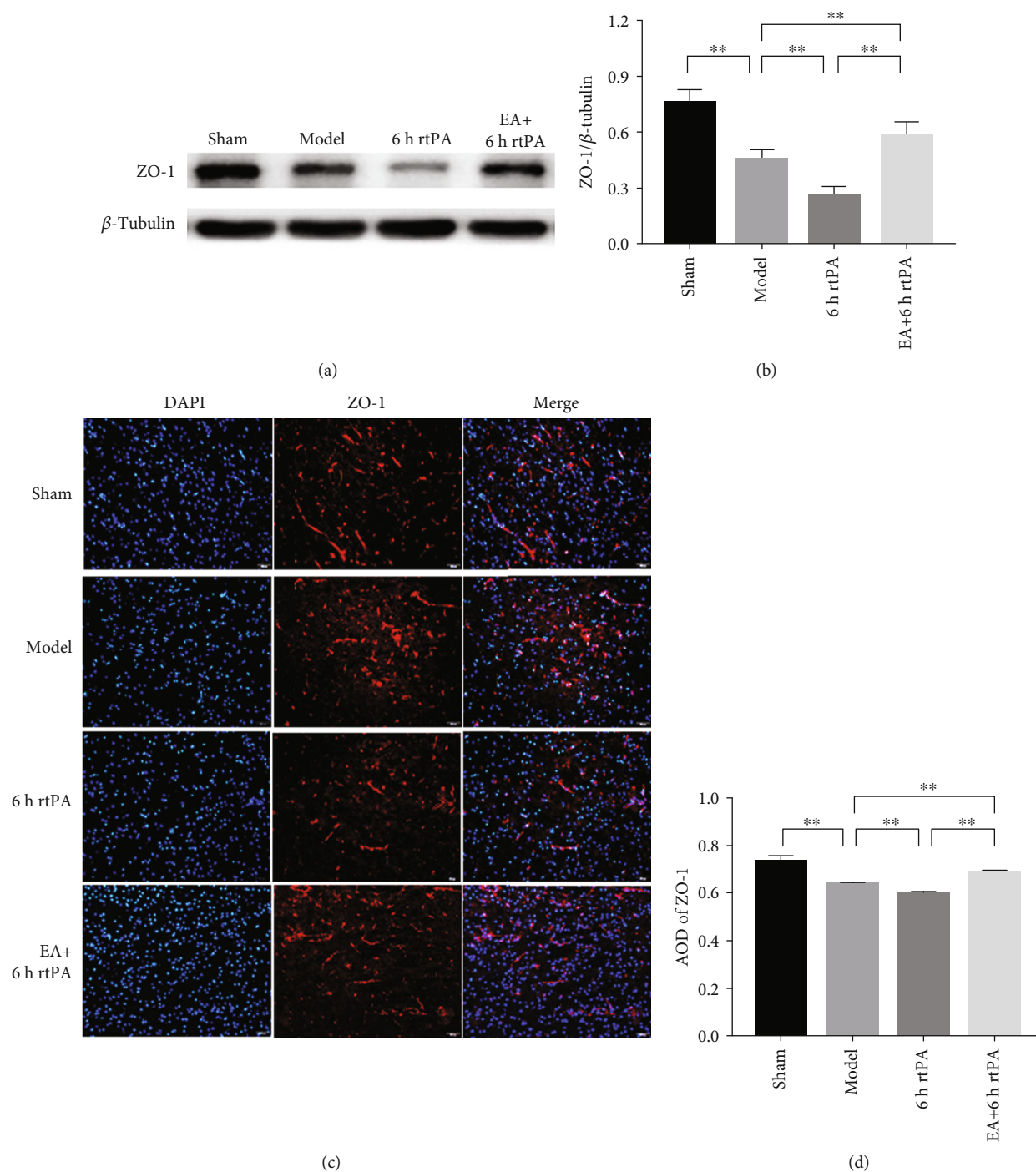


FIGURE 4: Western blot and immunofluorescence staining for ZO-1 in each group ( $n = 6$  rats). (a) Representative immunoblot showing the level of ZO-1 in the ischemic penumbra area. (b) Relative levels of the ZO-1 protein. (c) Representative images of ZO-1 staining in the ischemic penumbra area. Bar = 50  $\mu$ m. (d) Average optical density of ZO-1. \*\* indicates  $p < 0.01$ .

## 4. Discussion

**4.1. Overview of Findings.** This study was the first to investigate the important question of whether early EA extends the thrombolytic time window of rtPA by alleviating the BBB disruption and rtPA-associated complications after delayed rtPA treatment in a male rat model of embolic stroke. EA significantly improved neurological function and reduced the

infarct size, hemorrhagic transformation, brain edema, and EB leakage in rats that received EA at 2 h and rtPA at 6 h after ischemic stroke. Moreover, these protective effects were probably related to the amelioration of BBB disruption by attenuating the degradation of TJ proteins and inhibiting the ERK1/2-MMP9 pathway. Our study described a potentially effective adjunct therapy to increase the safety and thrombolytic time window of rtPA following ischemic stroke.



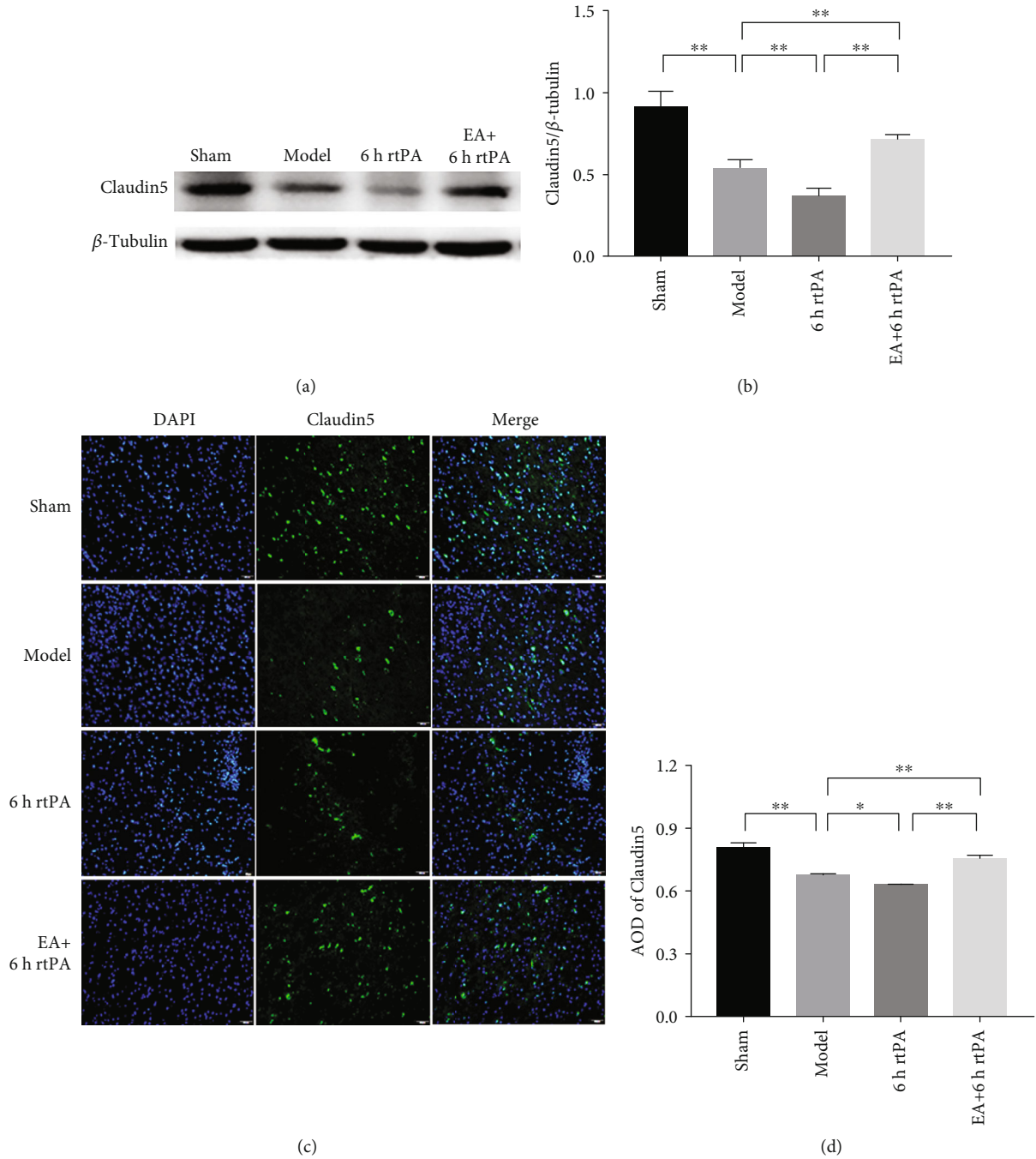


FIGURE 5: Western blot and immunofluorescence staining for Claudin5 in each group ( $n = 6$  rats). (a) Representative immunoblot showing Claudin5 levels in the ischemic penumbra area. (b) Relative levels of the Claudin5 protein. (c) Representative images of Claudin5 staining in the ischemic penumbra area. Bar = 50  $\mu$ m. (d) Average optical density of Claudin 5. \* indicates  $p < 0.05$ ; \*\* indicates  $p < 0.01$ .

**4.2. EA Application during rtPA Thrombolysis for Acute Ischemic Stroke.** Acupuncture is a traditional therapy derived from ancient China that has been used for more than 3000 years. EA is derived from the combination of traditional acupuncture and modern electrical stimulation, which has been recommended as a complementary therapy for ischemic stroke in both Asian and Western countries [26]. Additionally, EA is widely used in clinical practice and experimental studies of ischemic stroke due to its repeatability and the standardization of the frequency, intensity and duration.

According to the theory of traditional Chinese medicine, the basic mechanism of ischemic stroke is an imbalance between Ying and Yang, as well as an obstruction of Qi and blood. Shuigou (GV26) is the acupoint of the governor meridian, which collects Yang from peripheral regions and transports it to the brain. Neiguan (PC6) is the acupoint of the pericardium meridian, which exists in a close physiological and pathological relationship with the brain and promotes the circulation of Qi and blood. Consequently, the GV26 and PC6 acupoints were chosen for EA stimulation.



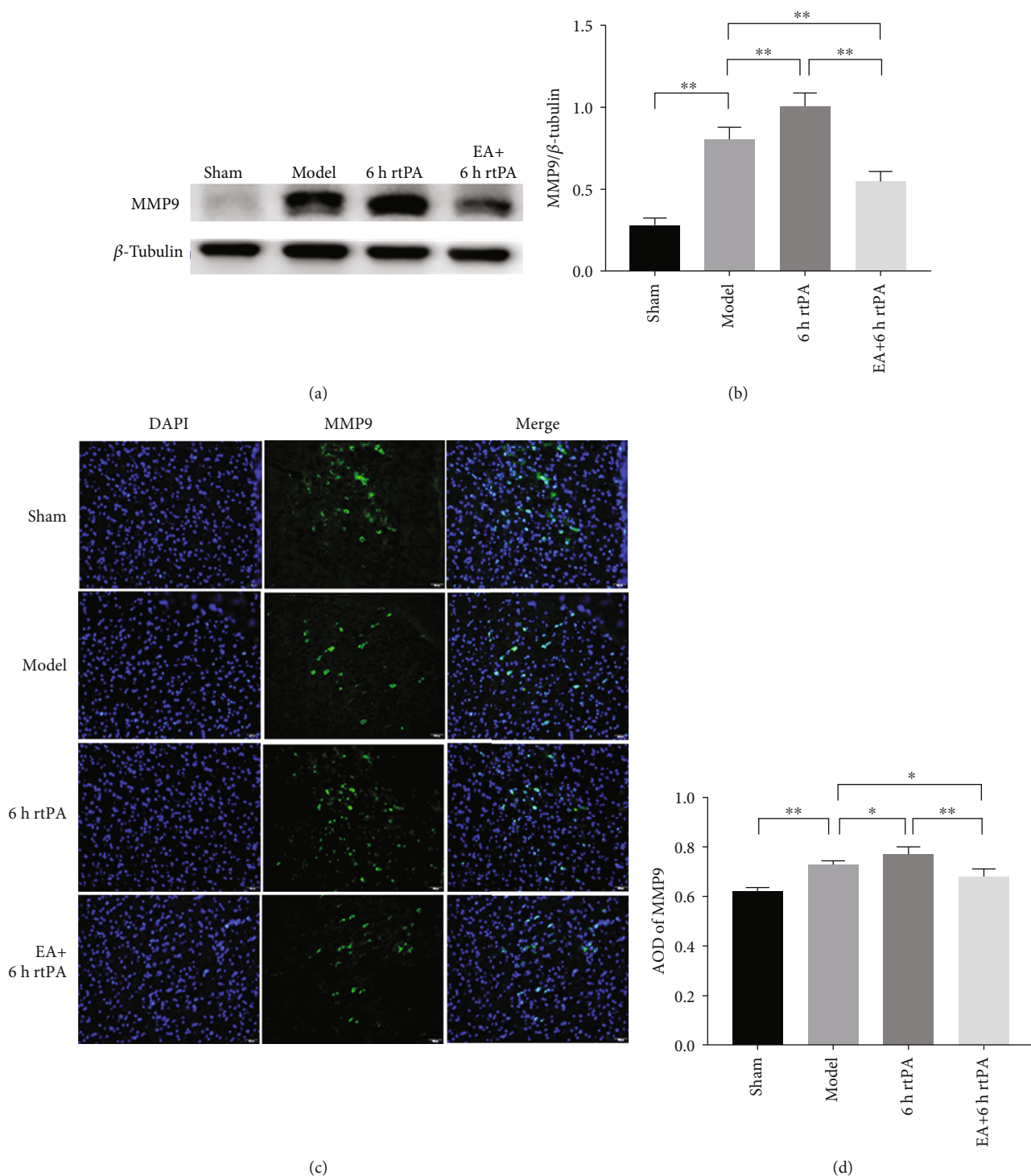


FIGURE 6: Western blot and immunofluorescence staining for MMP9 in each group ( $n = 6$  rats). (a) Representative immunoblot showing the levels of MMP9 in the ischemic penumbra area. (b) Relative levels of the MMP9 protein. (c) Representative images of MMP9 staining in the ischemic penumbra area. Bar = 50  $\mu$ m. (d) Average optical density of MMP9. \*indicates  $p < 0.05$ ; \*\*indicates  $p < 0.01$ .

In addition, many researchers have reported that EA at GV26 and PC6 facilitates the resuscitation of the brain, increases cerebral blood flow, reduces the infarct volume, and alleviates brain injury after ischemic stroke [45–47]. In our study, an embolic stroke model was used to study thrombolytic therapy, because it resembles the pathological condition of cere-

bral thrombosis in the clinic. Within 1 hour after clot injection, spontaneous clot dissolution and vascular recanalization are observed [48]. Maximum neurological deficit scores were recorded for rats as early as 2 h after the induction of ischemia [49]. Therefore, the 2-hour occlusion of the middle cerebral artery produces a large infarct volume

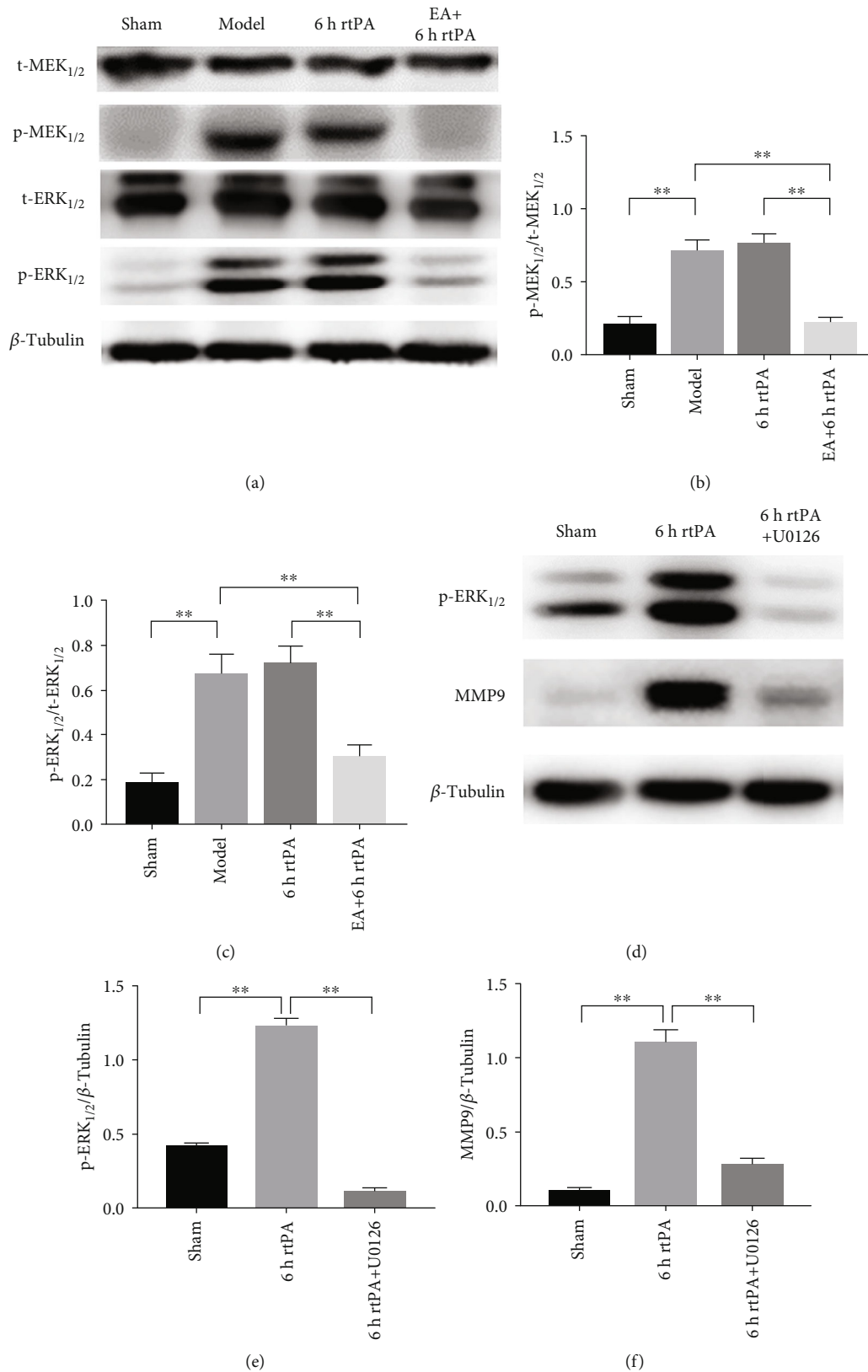


FIGURE 7: Western blots showing the effects of EA on the ERK1/2-MMP9 pathway in each group ( $n = 6$  rats). (a) Representative immunoblots showing the levels of t-MEK<sub>1/2</sub>, p-MEK<sub>1/2</sub>, t-ERK<sub>1/2</sub>, and p-ERK<sub>1/2</sub> in the sham, model, 6 h rtPA, and EA+6 h rtPA groups. (b) Relative levels of p-MEK<sub>1/2</sub>/t-MEK<sub>1/2</sub>. (c) Relative levels of p-ERK<sub>1/2</sub>/t-ERK<sub>1/2</sub>. (d) Representative immunoblots showing the levels of p-ERK<sub>1/2</sub> and MMP9 in the sham, 6 h rtPA, and 6 h rtPA+U0126 groups. (e) Relative levels of p-ERK<sub>1/2</sub>. (f) Relative levels of MMP9. \*\*indicates  $p < 0.01$ .

that is reliable and stable during the first 24 h after cerebral ischemia [50]. Moreover, this study aimed to observe the effect of early EA on thrombolytic complications, and another study confirmed that the application of EA at 2 h after ischemic stroke reduced the cerebral infarct size and neuronal damage in rats with cerebral ischemia-reperfusion injury [51]. Therefore, we delivered EA at 2 h after the onset of cerebral ischemia. However, no study has examined the effect of EA on thrombolysis in subjects with acute ischemic stroke, and the effect of EA on thrombolysis remains unclear. Therefore, our study investigated whether early EA improved the safety of thrombolysis and extended the thrombolytic time window during rtPA thrombolysis for acute ischemic stroke.

**4.3. MMP9 and rtPA-Associated Thrombolytic Complications.** Currently, the intravenous infusion of rtPA within 3–4.5 h is the most efficient pharmacological therapy for acute ischemic stroke [5]. However, based on accumulating data, rtPA also exerts deleterious effects on the ischemic brain that potentially compromise the overall benefit of thrombolysis during stroke [52]. In multiple animal studies, rtPA has been reported to cause neurotoxicity and brain damage after cerebral ischemia [52–54]. Moreover, delayed treatment with rtPA beyond 4.5 h generates serious hemorrhagic transformation and brain edema due to the degradation of ECM components and increased BBB permeability [6, 7]. As shown in the present study, rats treated with rtPA at 6 h after the onset of embolic stroke presented severe neurological deficits and large cerebral infarct volumes, similar to rats with embolic stroke alone. However, delayed rtPA-associated hemorrhagic transformation and brain edema were significantly increased, consistent with previous studies [55, 56]. Thus, rtPA thrombolysis for ischemic stroke at a delayed time point did not improve neurological outcomes, but increased the risk of thrombolytic complications. BBB disruption is a critical pathological process that occurs after cerebral ischemia-reperfusion and is thought to be a prerequisite for hemorrhagic transformation, brain edema, and poor treatment outcomes [10, 11, 44]. Therefore, the maintenance of BBB integrity has been one of the major targets for protecting the brain from ischemic stroke. Claudin5 and ZO-1 are important TJ proteins that are located in the tightly sealed monolayer of brain endothelial cells comprising the BBB and are sensitive markers of BBB disruption [57]. MMP9 is expressed in many cell types, including vascular endothelial cells, and plays a vital role in rtPA-mediated neurotoxicity after stroke thrombolytic therapy [58]. Based on accumulating evidence, delayed rtPA treatment activates MMP9 in ischemic brains, and the activation of MMP9 subsequently degrades the ECM and TJ proteins, leading to BBB opening, brain edema, and hemorrhagic transformation [17, 19, 56, 59]. Consistent with these studies, delayed rtPA treatment significantly increased MMP9 levels and aggravated the loss of TJ proteins (Claudin5 and ZO-1) in the ischemic penumbra of rats following cerebral ischemia compared to the model group in the present study.

**4.4. Role of ERK1/2 Signaling in rtPA Thrombolysis for Acute Ischemic Stroke.** ERK1/2 is widely expressed in the nervous system and activated in the early stage after brain injury. Activated ERK1/2 phosphorylates substrates in the cytoplasm or nucleus, thereby inducing the expression or activation of specific proteins, leading to cell proliferation, differentiation, apoptosis, and other processes [60]. ERK1/2 is immediately activated in the ischemic region after the occlusion of the middle cerebral artery, and the expression of ERK1/2 in neural stem cells of rats with ischemic stroke increases in a time-dependent manner [61]. The ERK1/2 signaling pathway regulates the inflammatory response and apoptosis and participates in the repair of BBB disruption after cerebral ischemia [20]. The role of the ERK1/2 signaling pathway in cerebral ischemic injury has become a hot topic in recent years; however, two contradictory views have been described. The ERK1/2 signaling pathway has been shown to alleviate brain injury and exert neuroprotective effects after cerebral ischemia [21, 61, 62]. Nevertheless, more studies have shown that activation of the ERK1/2 signaling pathway promotes inflammation, aggravates nerve cell death, and eventually leads to the deterioration of neurological function following cerebral ischemia [36, 63–65]. Meanwhile, a substantial loss of TJ proteins is observed in the rat brain tissue, and blocking the activation of ERK1/2 with the MEK inhibitor U0126 protects the integrity of the BBB and mitigates brain damage in rat models of ischemic stroke [66]. These dual roles of the ERK1/2 signaling pathway may be attributed to the use of different stimuli, cerebral ischemic models, and periods of ischemic stroke. Therefore, we first clarified the role of the ERK1/2 signaling pathway in ischemic brain injury during thrombolytic therapy in a male rat model of embolic stroke. ERK1/2 signaling was activated during delayed rtPA thrombolysis for acute ischemic stroke in the present study. Moreover, the decrease in ERK1/2 phosphorylation improved neurological function and reduced the infarct size following delayed rtPA thrombolysis.

**4.5. Possible Mechanisms Underlying the Effects of EA on Acute Ischemic Stroke.** EA significantly reduced the infarct size, hemorrhagic transformation, brain edema, and EB leakage and extended the therapeutic time window of rtPA in a male rat model of embolic stroke. Moreover, we further explored the potential molecular mechanism of EA treatment. The activation of ERK1/2 is accompanied by MMP9 overexpression in ischemic brain tissue, which leads to BBB destruction and brain edema in rats subjected to cerebral ischemia-reperfusion; however, U0126 reverses these changes and improves neurological function [14, 23]. U0126, a selective inhibitor of MEK1/2, was administered to inhibit the activation of ERK1/2 signaling and to determine whether ERK1/2 signaling modulates MMP9 expression in rats with embolic stroke during delayed rtPA thrombolysis. MMP9 was the downstream target of the ERK1/2 signaling pathway. In addition, EA decreased rtPA-induced MMP9 overexpression by inhibiting the ERK1/2 pathway and reduced thrombolytic complications of delayed rtPA thrombolysis for ischemic stroke in rats.

According to numerous experimental studies, the beneficial effects of EA treatment for ischemic stroke have been confirmed to be achieved by regulating a series of pathological reactions. EA administered early after cerebral ischemia protects cells against neuronal injury in cerebral ischemia-reperfusion by ameliorating nitro/oxidative stress-induced mitochondrial dysfunction and decreasing the accumulation of damaged mitochondria via Pink1/Parkin-mediated mitophagy clearance [67]. An EA pretreatment regime has also been shown to effectively reduce the cerebral infarct volume and the level of neuronal apoptosis in the hippocampal CA1 region after cerebral ischemia-reperfusion injury, and its mechanism may be related to the inhibition of the GluN2B/m-calpain/p38 MAPK proapoptotic pathway [68]. Another study found that EA reduced neurological deficit scores, impeded oxidative stress injury, inhibited inflammatory cytokine production, curbed P38 phosphorylation, and suppressed TRPV-1 expression, indicating a neuroprotective effect of the EA pretreatment on rats with cerebral ischemia-reperfusion injury [69]. Moreover, EA stimulation has been shown to reduce MMP9 expression, preserve BBB integrity, and alleviate cerebral ischemic injury by modulating the ERK1/2 signaling pathway in ischemic stroke models [28–31]. Similar to the results from the aforementioned studies, EA increased the levels of the Claudin5 and ZO-1 proteins and alleviated the impairment of the BBB induced by delayed rtPA thrombolysis in the present study. Furthermore, EA inhibited the activation of the ERK1/2 signaling pathway and reduced MMP9 overexpression induced by delayed rtPA thrombolysis.

**4.6. Limitations and Implications.** The present study has a limitation in that we only examined the neurological function, infarct size, hemorrhagic transformation, brain edema, and EB leakage at 24 h after ischemic stroke. The acute neuroprotective effect appears to be good, but the long-term effect remains unclear. For animal experiments and clinical applications, further studies are needed to determine whether the protective effect of EA on rtPA thrombolysis for ischemic stroke in the acute phase would be sustained for longer periods.

## 5. Conclusions

In conclusion, early administration of EA before the rtPA infusion improved stroke outcomes and reduced hemorrhagic transformation and brain edema associated with late thrombolysis. EA potentially represents an effective adjunct method to enhance the safety of thrombolytic therapy and extend the therapeutic time window of rtPA to 6 h in a male rat model of embolic stroke. This neuroprotective effect may be mediated by the inhibition of the ERK1/2-MMP9 pathway and alleviation of the destruction of the BBB. The findings provide a reliable theoretical basis for the clinical treatment of acute ischemic stroke with thrombolytic therapy within a broadened therapeutic window.

## Data Availability

The data that support the finding of the study are available from the corresponding author upon reasonable request.

## Conflicts of Interest

The authors declare that there is no conflict of interests regarding the publication of this paper.

## Acknowledgments

This study was supported by the National Natural Science Foundation of China (NO. 81674067) and the Open Projects of the Discipline of Chinese Medicine of Nanjing University of Chinese Medicine Supported by the Subject of Academic priority discipline of Jiangsu Higher Education Institutions (NO. ZYX03KF013).

## Supplementary Materials

Supplementary Figure 1: cerebral blood flow was monitored during the induction of embolic stroke model. (*Supplementary Materials*)

## References

- [1] M. Naghavi, A. A. Abajobir, C. Abbafati et al., “Global, regional, and national age-sex specific mortality for 264 causes of death, 1980–2016: a systematic analysis for the Global Burden of Disease Study 2016,” *The Lancet*, vol. 390, no. 10100, pp. 1151–1210, 2017.
- [2] C. O. Johnson, M. Nguyen, G. A. Roth et al., “Global, regional, and national burden of stroke, 1990–2016: a systematic analysis for the Global Burden of Disease Study 2016,” *The Lancet Neurology*, vol. 18, no. 5, pp. 439–458, 2019.
- [3] E. J. Benjamin, P. Muntner, A. Alonso et al., “Heart disease and stroke statistics—2019 update: a report from the American Heart Association,” *Circulation*, vol. 139, no. 10, pp. e56–e528, 2019.
- [4] P. Deb, S. Sharma, and K. M. Hassan, “Pathophysiologic mechanisms of acute ischemic stroke: an overview with emphasis on therapeutic significance beyond thrombolysis,” *Pathophysiology*, vol. 17, no. 3, pp. 197–218, 2010.
- [5] W. J. Powers, A. A. Rabinstein, T. Ackerson et al., “Guidelines for the Early Management of Patients With Acute Ischemic Stroke: 2019 Update to the 2018 Guidelines for the Early Management of Acute Ischemic Stroke: A Guideline for Healthcare Professionals From the American Heart Association/American Stroke Association,” *Stroke*, vol. 50, no. 12, pp. e344–e418, 2019.
- [6] J. S. Balami, B. A. Sutherland, and A. M. Buchan, “Complications associated with recombinant tissue plasminogen activator therapy for acute ischaemic stroke,” *CNS & Neurological Disorders Drug Targets*, vol. 12, no. 2, pp. 155–169, 2013.
- [7] M. Kanazawa, T. Takahashi, M. Nishizawa, and T. Shimohata, “Therapeutic strategies to attenuate hemorrhagic transformation after tissue plasminogen activator treatment for acute ischemic stroke,” *Journal of Atherosclerosis and Thrombosis*, vol. 24, no. 3, pp. 240–253, 2017.



- [8] Y. Zhou, S. Yan, X. Song et al., "Intravenous thrombolytic therapy for acute ischemic stroke in Hubei, China: a survey of thrombolysis rate and barriers," *BMC Neurology*, vol. 19, no. 1, p. 202, 2019.
- [9] M. Yepes, B. D. Roussel, C. Ali, and D. Vivien, "Tissue-type plasminogen activator in the ischemic brain: more than a thrombolytic," *Trends in Neurosciences*, vol. 32, no. 1, pp. 48–55, 2009.
- [10] M.-X. Dong, Q.-C. Hu, P. Shen et al., "Recombinant tissue plasminogen activator induces neurological side effects independent on thrombolysis in mechanical animal models of focal cerebral infarction: a systematic review and meta-analysis," *PLOS ONE*, vol. 11, no. 7, article e158848, 2016.
- [11] F. Simão, T. Ustunkaya, A. C. Clermont, and E. P. Feener, "Plasma kallikrein mediates brain hemorrhage and edema caused by tissue plasminogen activator therapy in mice after stroke," *Blood*, vol. 129, no. 16, pp. 2280–2290, 2017.
- [12] J. Keane and M. Campbell, "The dynamic blood-brain barrier," *The FEBS Journal*, vol. 282, no. 21, pp. 4067–4079, 2015.
- [13] M. Matusiewicz, K. Neubauer, M. Mierzchala-Pasierb, A. Gamian, and M. Krzystek-Korpacka, "Matrix metalloproteinase-9: its interplay with angiogenic factors in inflammatory bowel diseases," *Disease Markers*, vol. 2014, 8 pages, 2014.
- [14] A. Maddahi, Q. Chen, and L. Edvinsson, "Enhanced cerebrovascular expression of matrix metalloproteinase-9 and tissue inhibitor of metalloproteinase-1 via the MEK/ERK pathway during cerebral ischemia in the rat," *BMC Neuroscience*, vol. 10, no. 1, p. 56, 2009.
- [15] Y. Yang, E. Y. Estrada, J. F. Thompson, W. Liu, and G. A. Rosenberg, "Matrix metalloproteinase-mediated disruption of tight junction proteins in cerebral vessels is reversed by synthetic matrix metalloproteinase inhibitor in focal ischemia in rat," *Journal of Cerebral Blood Flow and Metabolism*, vol. 27, no. 4, pp. 697–709, 2006.
- [16] A. Kalani, P. K. Kamat, A. Famil'tseva et al., "Role of MicroRNA29b in blood-brain barrier dysfunction during hyperhomocysteinemia: an epigenetic mechanism," *Journal of Cerebral Blood Flow & Metabolism*, vol. 34, no. 7, pp. 1212–1222, 2014.
- [17] B. Piccardi, V. Palumbo, M. Nesi et al., "Unbalanced metalloproteinase-9 and tissue inhibitors of metalloproteinases ratios predict hemorrhagic transformation of lesion in ischemic stroke patients treated with thrombolysis: results from the MAGIC study," *Frontiers in Neurology*, vol. 6, 2015.
- [18] X. Yi, G. Sui, Q. Zhou et al., "Variants in matrix metalloproteinase-9 gene are associated with hemorrhagic transformation in acute ischemic stroke patients with atherothrombosis, small artery disease, and cardioembolic stroke," *Brain and Behavior*, vol. 9, no. 6, article e1294, p. e01294, 2019.
- [19] M. Chaturvedi and L. Kaczmarek, "MMP-9 inhibition: a therapeutic strategy in ischemic stroke," *Molecular Neurobiology*, vol. 49, no. 1, pp. 563–573, 2014.
- [20] J. Sun and G. Nan, "The extracellular signal-regulated kinase 1/2 pathway in neurological diseases: a potential therapeutic target (review)," *International Journal of Molecular Medicine*, vol. 39, no. 6, pp. 1338–1346, 2017.
- [21] Z. Yu, M. Cai, X. Li et al., "Neuroprotective effects of Tongxinluo on focal cerebral ischemia and reperfusion injury in rats associated with the activation of the MEK1/2/ERK1/2/p90RSK signaling pathway," *Brain Research*, vol. 1685, pp. 9–18, 2018.
- [22] K. Arai, S. Lee, and E. H. Lo, "Essential role for ERK mitogen-activated protein kinase in matrix metalloproteinase-9 regulation in rat cortical astrocytes," *Glia*, vol. 43, no. 3, pp. 254–264, 2003.
- [23] H. Sang, Z. Qiu, J. Cai et al., "Early increased bradykinin 1 receptor contributes to hemorrhagic transformation after ischemic stroke in type 1 diabetic rats," *Translational Stroke Research*, vol. 8, no. 6, pp. 597–611, 2017.
- [24] K. Chaudhry, R. Rogers, M. Guo et al., "Matrix metalloproteinase-9 (MMP-9) expression and extracellular signal-regulated kinase 1 and 2 (ERK1/2) activation in exercise-reduced neuronal apoptosis after stroke," *Neuroscience Letters*, vol. 474, no. 2, pp. 109–114, 2010.
- [25] L. Chi, K. Du, D. Liu, Y. Bo, and W. Li, "Electroacupuncture brain protection during ischemic stroke: a role for the parasympathetic nervous system," *Journal of Cerebral Blood Flow & Metabolism*, vol. 38, no. 3, pp. 479–491, 2018.
- [26] A.-J. Liu, J.-H. Li, H.-Q. Li et al., "Electroacupuncture for acute ischemic stroke: a meta-analysis of randomized controlled trials," *The American Journal of Chinese Medicine*, vol. 43, no. 8, pp. 1541–1566, 2016.
- [27] Y. Xing, M. Zhang, W.-B. Li, F. Dong, and F. Zhang, "Mechanisms involved in the neuroprotection of electroacupuncture therapy for ischemic stroke," *Frontiers in Neuroscience*, vol. 12, 2018.
- [28] R. Lin, K. Yu, X. Li et al., "Electroacupuncture ameliorates post-stroke learning and memory through minimizing ultrastructural brain damage and inhibiting the expression of MMP-2 and MMP-9 in cerebral ischemia-reperfusion injured rats," *Molecular Medicine Reports*, vol. 14, no. 1, pp. 225–233, 2016.
- [29] Y. S. Jung, S. Lee, J. H. Park, H. B. Seo, B. T. Choi, and H. K. Shin, "Electroacupuncture preconditioning reduces ROS generation with NOX4 down-regulation and ameliorates blood-brain barrier disruption after ischemic stroke," *Journal of Biomedical Science*, vol. 23, no. 1, p. 32, 2016.
- [30] R. Zou, Z. Wu, and S. Cui, "Electroacupuncture pretreatment attenuates bloodbrain barrier disruption following cerebral ischemia/reperfusion," *Molecular Medicine Reports*, vol. 12, no. 2, pp. 2027–2034, 2015.
- [31] Y. Xing, S. Yang, M. Wang, F. Dong, Y. S. Feng, and F. Zhang, "Electroacupuncture alleviated neuronal apoptosis following ischemic stroke in rats via midkine and ERK/JNK/p38 signaling pathway," *Journal of Molecular Neuroscience*, vol. 66, no. 1, pp. 26–36, 2018.
- [32] L. Zhang, R. L. Zhang, Q. Jiang, G. Ding, M. Chopp, and Z. G. Zhang, "Focal embolic cerebral ischemia in the rat," *Nature Protocols*, vol. 10, no. 4, pp. 539–547, 2015.
- [33] V. A. DiNapoli, C. L. Rosen, T. Nagamine, and T. Crocco, "Selective MCA occlusion: a precise embolic stroke model," *Journal of Neuroscience Methods*, vol. 154, no. 1-2, pp. 233–238, 2006.
- [34] Z. Si, J. Liu, K. Hu, Y. Lin, J. Liu, and A. Wang, "Effects of thrombolysis within 6 hours on acute cerebral infarction in an improved rat embolic middle cerebral artery occlusion model for ischaemic stroke," *Journal of Cellular and Molecular Medicine*, vol. 23, no. 4, pp. 2468–2474, 2019.
- [35] T. Yamashita, T. Kamiya, K. Deguchi et al., "Dissociation and protection of the neurovascular unit after thrombolysis and reperfusion in ischemic rat brain," *Journal of Cerebral Blood Flow & Metabolism*, vol. 29, no. 4, pp. 715–725, 2009.



- [36] J. Li, D. Yan, X. Liu et al., "U0126 protects hippocampal CA1 neurons against forebrain ischemia-induced apoptosis via the ERK1/2 signaling pathway and NMDA receptors," *Neurological Research*, vol. 40, no. 4, pp. 318–323, 2018.
- [37] T. Engelhorn, S. Goerike, A. Doerfler et al., "The angiotensin II type 1-receptor blocker candesartan increases cerebral blood flow, reduces infarct size, and improves neurologic outcome after transient cerebral ischemia in rats," *Journal of Cerebral Blood Flow and Metabolism*, vol. 24, no. 4, pp. 467–474, 2004.
- [38] J. B. Bederson, L. H. Pitts, M. Tsuji, M. C. Nishimura, R. L. Davis, and H. Bartkowski, "Rat middle cerebral artery occlusion: evaluation of the model and development of a neurologic examination," *Stroke*, vol. 17, no. 3, pp. 472–476, 1986.
- [39] M. Allahtavakoli, F. Amin, A. Esmaeeli-Nadimi, A. Shamsizadeh, M. Kazemi-Arababadi, and D. Kennedy, "Ascorbic acid reduces the adverse effects of delayed administration of tissue plasminogen activator in a rat stroke model," *Basic & Clinical Pharmacology & Toxicology*, vol. 117, no. 5, pp. 335–339, 2015.
- [40] L. Belayev, R. Busto, W. Zhao, and M. D. Ginsberg, "Quantitative evaluation of blood-brain barrier permeability following middle cerebral artery occlusion in rats," *Brain Research*, vol. 739, no. 1-2, pp. 88–96, 1996.
- [41] Z. Qin, M. Karabiyikoglu, Y. Hua et al., "Hyperbaric oxygen-induced attenuation of hemorrhagic transformation after experimental focal transient cerebral ischemia," *Stroke*, vol. 38, no. 4, pp. 1362–1367, 2007.
- [42] S. Ashwal, B. Tone, H. R. Tian, D. J. Cole, and W. J. Pearce, "Core and penumbral nitric oxide synthase activity during cerebral ischemia and reperfusion," *Stroke*, vol. 29, no. 5, pp. 1037–1047, 1998.
- [43] J. Copin, D. J. Bengualid, R. F. da Silva, O. Kargiotis, K. Schaller, and Y. Gasche, "Recombinant tissue plasminogen activator induces blood-brain barrier breakdown by a matrix metalloproteinase-9-independent pathway after transient focal cerebral ischemia in mouse," *The European Journal of Neuroscience*, vol. 34, no. 7, pp. 1085–1092, 2011.
- [44] R.-H. Jiang, Q.-Q. Zu, X.-Q. Xu et al., "A canine model of hemorrhagic transformation using recombinant tissue plasminogen activator administration after acute ischemic stroke," *Frontiers in Neurology*, vol. 10, 2019.
- [45] H. Zheng, W. Jiang, X. Zhao et al., "Electroacupuncture induces acute changes in cerebral cortical miRNA profile, improves cerebral blood flow and alleviates neurological deficits in a rat model of stroke," *Neural Regeneration Research*, vol. 11, no. 12, pp. 1940–1950, 2016.
- [46] H. Zhao, Y. Lu, Y. Wang et al., "Electroacupuncture contributes to recovery of neurological deficits in experimental stroke by activating astrocytes," *Restorative Neurology and Neuroscience*, vol. 36, no. 3, pp. 301–312, 2018.
- [47] F. Zhou, J. Guo, J. Cheng, G. Wu, J. Sun, and Y. Xia, "Electroacupuncture and brain protection against cerebral ischemia: specific effects of acupoints," *Evidence-based Complementary and Alternative Medicine*, vol. 2013, Article ID 804397, 14 pages, 2013.
- [48] C. Kleinschnitz, F. Fluri, and M. Schuhmann, "Animal models of ischemic stroke and their application in clinical research," *Drug Design, Development and Therapy*, vol. 9, pp. 3445–3454, 2015.
- [49] D. Reglödi, A. Tamás, and I. Lengvári, "Examination of sensorimotor performance following middle cerebral artery occlusion in rats," *Brain Research Bulletin*, vol. 59, no. 6, pp. 459–466, 2003.
- [50] S. Liu, G. Zhen, B. P. Meloni, K. Campbell, and H. R. Winn, "Rodent stroke model guidelines for preclinical stroke trials (1ST edition)," *Journal of Experimental Stroke and Translational Medicine*, vol. 2, no. 2, pp. 2–27, 2009.
- [51] Y.-m. Zhang, H. Xu, H. Sun, S.-h. Chen, and F.-m. Wang, "Electroacupuncture treatment improves neurological function associated with regulation of tight junction proteins in rats with cerebral ischemia reperfusion injury," *Evidence-based Complementary and Alternative Medicine*, vol. 2014, 10 pages, 2014.
- [52] M. Fan, H. Xu, L. Wang et al., "Tissue plasminogen activator neurotoxicity is neutralized by recombinant ADAMTS 13," *Scientific Reports*, vol. 6, no. 1, 2016.
- [53] E. H. Lo, J. P. Broderick, and M. A. Moskowitz, "tPA and proteolysis in the neurovascular unit," *Stroke*, vol. 35, no. 2, pp. 354–356, 2004.
- [54] Y. F. Wang, S. E. Tsirka, S. Strickland, P. E. Stieg, S. G. Soriano, and S. A. Lipton, "Tissue plasminogen activator (tPA) increases neuronal damage after focal cerebral ischemia in wild-type and tPA-deficient mice," *Nature Medicine*, vol. 4, no. 2, pp. 228–231, 1998.
- [55] S. Won, J. H. Lee, B. Wali, D. G. Stein, and I. Sayeed, "Progesterone attenuates hemorrhagic transformation after delayed tPA treatment in an experimental model of stroke in rats: involvement of the VEGF–MMP pathway," *Journal of Cerebral Blood Flow & Metabolism*, vol. 34, no. 1, pp. 72–80, 2014.
- [56] H. Chen, B. Guan, X. Chen et al., "Baicalin attenuates blood-brain barrier disruption and hemorrhagic transformation and improves neurological outcome in ischemic stroke rats with delayed t-PA treatment: involvement of ONOO(-)-MMP-9 pathway," *Translational Stroke Research*, vol. 9, no. 5, pp. 515–529, 2018.
- [57] B. T. Hawkins and T. P. Davis, "The blood-brain barrier/neurovascular unit in health and disease," *Pharmacological Reviews*, vol. 57, no. 2, pp. 173–185, 2005.
- [58] M. Zarisfi, F. Allahtavakoli, M. Hassanipour et al., "Transient brain hypothermia reduces the reperfusion injury of delayed tissue plasminogen activator and extends its therapeutic time window in a focal embolic stroke model," *Brain Research Bulletin*, vol. 134, pp. 85–90, 2017.
- [59] H. Chen, X. Chen, Y. Luo, and J. Shen, "Potential molecular targets of peroxynitrite in mediating blood-brain barrier damage and haemorrhagic transformation in acute ischaemic stroke with delayed tissue plasminogen activator treatment," *Free Radical Research*, vol. 52, no. 11-12, pp. 1220–1239, 2018.
- [60] T. Kong, M. Liu, B. Ji, B. Bai, B. Cheng, and C. Wang, "Role of the extracellular signal-regulated kinase 1/2 signaling pathway in ischemia-reperfusion injury," *Frontiers in Physiology*, vol. 10, 2019.
- [61] Q. C. Wang, L. Lu, and H. J. Zhou, "Relationship between the MAPK/ERK pathway and neurocyte apoptosis after cerebral infarction in rats," *European Review for Medical and Pharmacological Sciences*, vol. 23, no. 12, pp. 5374–5381, 2019.
- [62] S. K. Mohamed, A. Ahmed, E. M. Elmersy, and S. Nofal, "ERK activation by zanolol has neuroprotective effect in cerebral ischemia reperfusion," *Life Sciences*, vol. 227, pp. 137–144, 2019.
- [63] M. Mostajeran, L. Edvinsson, K. Warfvinge, R. Singh, and S. Ansar, "Inhibition of mitogen-activated protein kinase 1/2

- in the acute phase of stroke improves long-term neurological outcome and promotes recovery processes in rats,” *Acta Physiologica*, vol. 219, no. 4, pp. 814–824, 2017.
- [64] W. Chen, J. Feng, and W. Tong, “Phosphorylation of astrocytic connexin43 by ERK1/2 impairs blood–brain barrier in acute cerebral ischemia,” *Cell & Bioscience*, vol. 7, no. 1, 2017.
- [65] Y. Lu, J. Kang, Y. Bai et al., “Hyperbaric oxygen enlarges the area of brain damage in MCAO rats by blocking autophagy via ERK1/2 activation,” *European Journal of Pharmacology*, vol. 728, pp. 93–99, 2014.
- [66] J. A. Shin, Y. A. Kim, S. I. Jeong, K. E. Lee, H. S. Kim, and E. M. Park, “Extracellular signal-regulated kinase1/2-dependent changes in tight junctions after ischemic preconditioning contributes to tolerance induction after ischemic stroke,” *Brain Structure and Function*, vol. 220, no. 1, pp. 13–26, 2015.
- [67] H. Wang, S. Chen, Y. Zhang, H. Xu, and H. Sun, “Electroacupuncture ameliorates neuronal injury by Pink1/Parkin-mediated mitophagy clearance in cerebral ischemia-reperfusion,” *Nitric Oxide*, vol. 91, pp. 23–34, 2019.
- [68] B.-y. Zhang, G.-r. Wang, W.-h. Ning et al., “Electroacupuncture pretreatment elicits tolerance to cerebral ischemia/reperfusion through inhibition of the GluN2B/m-Calpain/p38 MAPK proapoptotic pathway,” *Neural Plasticity*, vol. 2020, Article ID 8840675, 14 pages, 2020.
- [69] M. Long, Z. Wang, D. Zheng et al., “Electroacupuncture pretreatment elicits neuroprotection against cerebral ischemia-reperfusion injury in rats associated with transient receptor potential vanilloid 1-mediated anti-oxidant stress and anti-inflammation,” *Inflammation*, vol. 42, no. 5, pp. 1777–1787, 2019.

## Review Article

# The Electric Shock during Acupuncture: A Normal Needling Sensation or a Warning Sign

Yongsong Guo <sup>1</sup>, Ke Zhu <sup>1</sup>, Jing Guo <sup>2</sup>, Yongbing Kuang <sup>3</sup>, Zhihui Zhao <sup>1</sup>,  
and Weihong Li <sup>1,4</sup>

<sup>1</sup>Basic Medical College, Chengdu University of Traditional Chinese Medicine, Chengdu 610075, China

<sup>2</sup>Acupuncture College, Chengdu University of Traditional Chinese Medicine, Chengdu 610075, China

<sup>3</sup>Department of Tuina, Hospital of Chengdu University of Traditional Chinese Medicine, Chengdu 610075, China

<sup>4</sup>Department of Pneumology, Hospital of Chengdu University of Traditional Chinese Medicine, Chengdu 610075, China

Correspondence should be addressed to Weihong Li; [liweihong@cdutcm.edu.cn](mailto:liweihong@cdutcm.edu.cn)

Received 25 June 2020; Revised 10 October 2020; Accepted 19 October 2020; Published 3 November 2020

Academic Editor: Lu Wang

Copyright © 2020 Yongsong Guo et al. This is an open access article distributed under the Creative Commons Attribution License, which permits unrestricted use, distribution, and reproduction in any medium, provided the original work is properly cited.

The electric shock has been proposed as one of the new needling sensations in recent years. In acupuncture sensation scales, the electric shock is included by ASS and SNQS, but not SASS, MASS, and C-MMASS. Some scholars argue that the electric shock is a normal needling sensation, but some researchers do not agree with this view. This problem has not been resolved due to a lack of evidence from basic research. Literature and research point out that the electric shock is caused by inserting a needle into the nerve directly. A question of considerable scientific and practical interest is whether the electric shock should be a normal needling sensation. In this article, we review the historical documentation of the needling sensation and the process of formulating and improving acupuncture sensation scales to suggest that the electric shock may not be a normal needling sensation. Secondly, we collected and analyzed cases of nerve injury caused by acupuncture accompanied by the electric shock and why acupuncture caused the electric shock without nerve injury. It suggests that there may be a correlation between the electric shock and peripheral nerve injury, and acupuncture manipulation is an essential factor in adverse acupuncture events. Finally, we put forward that the electric shock during acupuncture is a warning sign that the peripheral nerve may be injured, rather than a normal needling sensation. In the future, we hope to have experimental studies on the mechanism of the electric shock or observational studies on the correlation between the electric shock and peripheral nerve injury to verify.

## 1. Introduction

The needling sensation refers to the subjective feeling that the recipient obtains in the acupoint after the acupuncturist inserts a needle into the acupoint or other acupuncture induction point and applies specific acupuncture techniques. The needling sensation is closely related to acupuncture treatment's therapeutic effect in traditional Chinese medicine [1–3]. Research has shown that the needling sensation may be an essential variable in acupuncture treatment studies' efficacy and mechanism [4]. The needling sensation can be briefly summarized as sourness, numbness, heaviness, or distension. The electric shock has been proposed as one of the new needling sensations in recent years. Shanghai and Sichuan Research Institute of Acupuncture and Meridian

found in observational, experimental studies that acupuncture on nerves can produce the electric shock and proposed that the electric shock is a needling sensation [5, 6]. There is a special acupuncture treatment method called nerve trunk stimulation therapy in China, which uses the electric shock generated during the acupuncture process as the standard for Deqi. Some acupuncturists sum up their clinical acupuncture experience repeatedly and hold the same view [7–11].

However, other researchers suggested that the needle be stopped when the electric shock occurs during acupuncture to avoid nerve injury [12–14]. Patients provide the electric shock as a kind of needling sensation to the maker of acupuncture sensation scales. In the current representative acupuncture sensation scales, the electric shock is only included by ASS and SNQS. Now, due to the lack of basic

research on the generation mechanism of the electric shock, we cannot answer positively whether the electric shock should be classified as a normal needling sensation. However, we discussed the historical literature records of needling sensation, the development process of acupuncture sensation scale, the adverse acupuncture events related to the electric shock, and nerve trunk stimulation therapy. And then, we put forward the point that there may be a correlation between the acupuncture and peripheral nerve injury. Acupuncture manipulation is an important influencing factor. Whether the electric shock is included in the scale needs more experimental evidence.

## 2. The Phenomenon of the Electric Shock

The electric shock appears on acupuncture sensation scales or needling sensation research, while we failed to find a specific description of the electric shock. Due to cultural and language background differences, there are other electric shock expressions, such as radiation and shock [15]. Therefore, based on relevant literature, we describe electric shock as an intense stimulation. It is produced by acupuncture into the human body at a certain depth or after lifting, twisting, and twirling manipulations, which can be instantaneously transmitted to the distal limbs. Within the stimulus conduction range, the limbs may appear numbness, severe pain, and other discomforts. Through summarizing the clinical literature on acupuncture, it is found that the electric shock only occurs when the needle penetrates the acupoint and reaches a certain depth [9, 10, 16].

Furthermore, according to the researcher's report [7, 17, 18], the electric shock will be quickly transmitted to the distal end of the limb, and its transmission range is consistent with the innervation area of the nerve trunk or branch around those acupoints. For instance, the researchers summarized the needling sensation of acupuncture at Huantiao (GB30). They pointed out that sciatic nerve trunks stabbed at different angles and depths will produce the electric shock, which can quickly be conducted to different innervation areas of the lower extremities [19].

## 3. Records Related to the Electric Shock in Acupuncture Ancient Literature

Acupuncture has a history of more than two thousand years in China, and all generations of acupuncture scholars have summarized the needling sensation. Since the ancients did not know about electricity, we took the radiation (the feeling of radiating to the far end in an instant) that must exist in the electric shock as the literature search object. However, we did not find any related records. On the contrary, in *The Miraculous Pivot*, the transmission phenomenon of needling sensation is described as "Under the acupuncture manipulation, the feeling of Deqi will be transmitted to the affected area like insects and ants crawling." This conveys an important message to us that the transmission of needling sensation is slow and will not be transmitted to the far end instantly. *The Miraculous Pivot* records process of Deqi as "The feeling of Deqi during acupuncture is slow and comfortable." In general, the needling sensation is slowly produced and gradually

transmitted to the affected area under acupuncture manipulation. As *Plain Questions* mentioned, "Deqi needs to be obtained after correct acupuncture manipulation." Besides, *The A-B Classic of Acupuncture and Moxibustion* records, "Febrile disease can be treated with acupuncture ST 43. Acupuncture ST 43 makes the feet feel cool through acupuncture manipulation. After the cooling sensation is transmitted from the foot to the knee joint, the needle is removed." It is showed that the needling sensation is conducted to the affected area with acupoints as the center. This rule is also summarized in *Great Compendium of Acupuncture and Moxibustion* and *Willful Intercept of Acupuncture*.

On the contrary, the conduction direction of the electric shock is fixed. The electric shock is conducted from the location where the nerve is punctured to the distal limb. The electric shock does not conform to acupuncture scholars' summary of the content of needling sensation in the past dynasties. Ancient Chinese medical literature does not support that the electrical shock is a normal needling sensation.

## 4. Opinions of the Maker of Acupuncture Sensation Scales

The makers of needle-sense scales are divided on whether the needling sensation should include the electric shock. Under the background of the international popularization of acupuncture, it is necessary to establish objective and unified standards of the needling sensation to evaluate acupuncture research and treatment more scientific. The researchers have developed several representative acupuncture sensation scales, including acupuncture sensation scale (ASS) [20], the subjective acupuncture sensation scale (SASS) [21], MGH acupuncture sensation scale (MASS) [22], Southampton needle sensation questionnaire (SNSQ) [23], visual analog scales (VAS) [24], and the Modified MASS-Chinese version (C-MMASS) [25] (Table 1). The content of needling sensation comes from acupuncture experiments and needling sensation questionnaire research [26, 27].

ASS: acupuncture sensation scale; SASS: the subjective acupuncture sensation scale; MASS: MGH acupuncture sensation scale; SNSQ: Southampton needle sensation questionnaire; C-MMASS: the Modified MASS-Chinese version.

Vincent et al. [20] developed the ASS by providing a list of adjectives describing pain in the McGill Pain Questionnaire (MPQ) [28] to acupuncturists and patients for selection. Kong et al. [21] developed SASS through acupuncture experiments. The MASS was upgraded from the SASS and perfected by referring to the ASS. White et al. [23] developed the SNSQ after interviewing patients based on the existing scales and acupuncture experts' reviewing. Yu et al. [25] developed an acupuncture sensation scale suitable for the Chinese population through acupuncture experiments based on MASS. Examining the process of formulating and gradually improving these scales, we found that the electric shock was included in ASS and SNSQ but not in SASS, MASS, and C-MMASS. Furthermore, the electric shock is a weak factor in the ASS. SNSQ left the electric shock because some patients have experienced acupuncture treatment, and White et al. pointed out that the electric shock should be viewed as

TABLE 1: The contents of representative acupuncture sensation scales.

Group	Scale	Year	Content about needling sensation
Vincent et al. [20]	ASS	1989	Dull-heavy sensations, a general intensity dimension, spreading, stinging, hot, sharp, and electric sensations
Kong et al. [21]	SASS	2005	Heaviness, stabbing, tingling, throbbing, burning, fullness, numbness, soreness, and aching
Kong et al. [22]	MASS	2007	Heaviness, deep pressure, soreness, aching, sharp pain, warmth, cold, fullness/distension, tingling, numbness, dull pain, and throbbing
White et al. [23]	SNSQ	2008	Heavy, pressure, spreading, stinging, tingling, deep ache, dull ache, warm, uncomfortable, bruised, fading, numb, twinge, throbbing, pricking, and electric shock
Yu et al. [25]	C-MMASS	2012	Soreness, aching, pressure, heaviness, fullness, tingling numbness, sharp pain, dull pain, warmth, cold, and throbbing

TABLE 2: Peripheral nerve injury associated with acupuncture.

Case	Acupoint	Patient sensation during acupuncture	Patients sensation or symptoms after acupuncture	Result of examine	Damaged nerve
(1) Wang [32]	Neiguan (PC6)	Electric shock, burning and radiated to the hand	The thumb, index finger, and middle finger could not flex and had difficulty in straightening	The affected limb has limited movement, skin temperature, thermesthesia, and pain are weaker than the healthy side	Median nerve
(2) Sobel et al. [33]	Yanglingquan (GB34)	Pain and radiated to the right lower limb	Burning, pain, unable to move the right foot	The extensor hallucis longus, extensor digitorum longus, and peroneal muscles were all graded as 2/5, and the anterior tibialis muscle was graded as 4/5	Peroneal nerve
(3) Sato et al. [34]	Yanglingquan (GB34)	Pain and radiated to the left leg	Pain, burning, numbness, and weakness in the left leg	EMG: compound muscle action potentials of the peroneal nerve in the left leg showed a remarkable decrease in amplitude distal to the level of the fibular head	Peroneal nerve
(4) Ruan et al. [35]	Yanglingquan (GB34)	Electric shock, pain, and radiated to the left lower leg	Pain, burning in the calf to the back of the foot, weakness in the lower extremities	EMG examination revealed injury of the common peroneal nerve	Peroneal nerve
(5) Wang [36]	Huantiao (GB30)	Electric shock, pain, and radiated down to the right foot	Numbness and weakness in the right leg	No record	Sciatic nerve

EMG: electromyogram.

separate or individual items describing needle sensation in the SNSQ. The electric shock of ASS and SNQS mainly comes from experienced acupuncturists and patients' subjective feelings on needling sensation, and the maker cannot be sure whether the information obtained is correct. Based on the current information, whether the electric shock should be classified as a normal needling sensation requires basic research evidence to prove it.

## 5. Case Reports of Peripheral Nerve Injury Caused by Acupuncture with the Electric Shock

Reviewing the literature [29–31], adverse events of acupuncture mainly include internal organs, tissue, or nerve injury, especially for pneumothorax and central nervous system

injury. We searched the following databases to find the case reports published from 1990 to 2019: VIP science and technology periodical database (CQVIP), China National Knowledge Infrastructure (CNKI), Wanfang Database (WF), and PubMed. Search terms included “acupuncture, electroacupuncture” combined with “adverse event, adverse reaction, and peripheral nerve injury.” We found 11 documents related to peripheral nerve injury caused by acupuncture. After excluding needle breakage and unrecorded needling sensation, five documents are remaining related to the occurrence of the electric shock (or similar expression) during acupuncture. Those articles reported one case of median nerve injury caused by acupuncture at Neiguan (PC6) [32], three cases of common peroneal nerve injury caused by acupuncture at Yanglingquan (GB34) [33–35], and one case of sciatic nerve injury caused by acupuncture at Huantiao (GB30) [36]. We will briefly describe in Table 2.



In those adverse events, patients had different degrees of electric shock and other discomforts during acupuncture. The operator continued applying acupuncture while they did not realize that the electric shock would cause adverse consequences. In case one, case four, and case five, the operators believe that the electric shock is a strong reflection of Deqi. When the patient has the electric shock during acupuncture, the operator strengthens the electric shock's intensity through acupuncture manipulation. In the above cases, the conclusions from the neurological examination or electromyography examination suggested peripheral nerve injury. Doctors pointed out that it was caused by the peripheral nerve being stabbed by the needle.

## 6. The Electric Shock and Nerve Trunk Stimulation Therapy

In China, the direct acupuncture method, the nerve trunk to treat diseases, is called nerve trunk stimulation therapy. This therapy emerged in the 1970s and became popular in the 1980s to 1990s. It is a research result combining meridian and neuroanatomy. Traditional acupoints are interpreted as nerve trunk stimulation points [37, 38]. In the clinical application of nerve trunk stimulation therapy, the operator uses a needle to directly acupuncture the nerve trunk to cause the patient to generate the electric shock. In order to cause the patient to produce the electric shock, the operator will perform acupuncture manipulation for stimulating Qi of meridians at the corresponding nerve trunk stimulation point. Researchers using this therapy have given relevant points for attention. In the process of acupuncture, when the patient feels the electric shock, the needle should be slightly lifted to make the needle tip away from the nerve trunk; immediately afterward, other acupuncture operations were no longer used. This kind of electric shock will be converted to other needling sensation [39, 40]. The points for attention are also reflected in the xingnao kaiqiao acupuncture therapy by Professor Shi Xuemin to avoid nerve injury [12, 41–43]. Researchers of nerve trunk stimulation therapy and Professor Shi Xuemin emphasize that the electric shock should not be sought too much, as they think it may injure the nerves. These two acupuncture therapies make the needle tip to leave the nerve trunk after the electric shock is generated during acupuncture, and the basic acupuncture operation of lifting, twisting, and twirling is no longer applied to avoid repeated puncture of the nerve.

Streitberger et al. [44, 45] conducted an observational, experimental study of acupuncture. During the process of acupuncture P6 (pericardium 6) and puncturing the median nerve with the needle, it was found that the subject had already Deqi before the needle touched the median nerve (the recorded needling sensation did not contain the electric shock). In the experiment, the median nerve was punctured in 14 cases, abnormal sensations were reported in 10 cases, radioactive needling sensation was reported in 8 cases, and the needle was immediately removed due to intractable electric pain in 1 case. The experimental study results suggest no connection between Deqi and acupuncture nerves, but it is necessary to avoid puncturing nerves through relevant train-

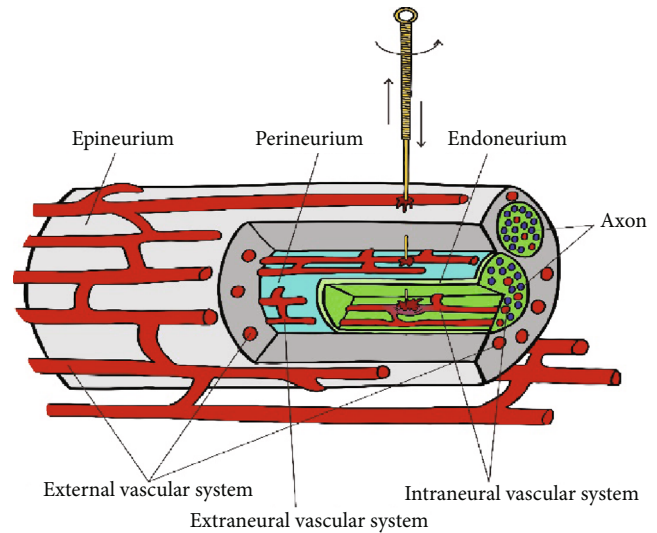


FIGURE 1: Microvascular injury on peripheral nerves.

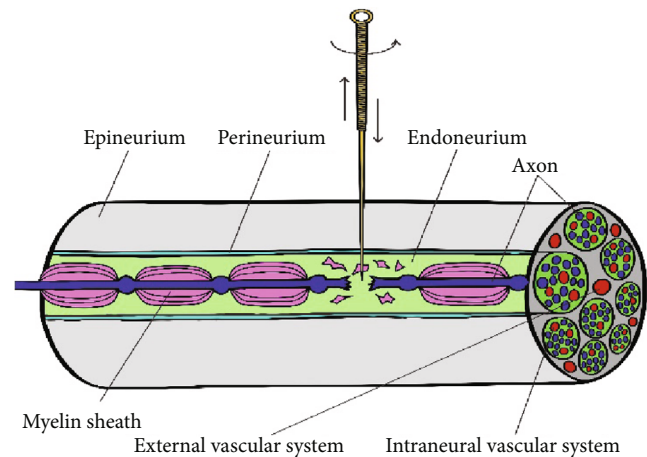


FIGURE 2: Traumatic demyelination and axonotmesis about peripheral nerve.

ing. Although the electric shock occurred during the experiment, a follow-up one week later showed no nerve injury in the subjects whose nerves were punctured. A peripheral nerve consists of 50% neurons, 50% fat, and connective tissue. The experiment did not use acupuncture manipulation to repeatedly puncture the nerve, reducing the possibility of the needle puncturing the nerve tract. The possibility of nerve injury is low in a single nerve puncture accompanied by the electric shock, but the probability will increase if the nerve is punctured multiple times.

## 7. The Possible Consequences of Repeated Puncturing Nerves by Acupuncture Manipulation

Repeatedly piercing the nerve in seeking the Electric Shock by lifting, twisting, and twirling is crucial to nerve injury. At present, there is no basic experimental study on puncturing nerves with acupuncture needles. Therefore, we refer to

the situation of nerve injury caused by injection needles to explore the possible injury caused by acupuncture repeatedly puncturing the nerve. The nerve is regarded as a unique organ composed of nerve tissue, connective tissue, and microvasculature. There is no significant difference in the nerve's local inflammation caused by needles of different diameters [46, 47]. Both extraneural and intraneural vascular systems are likely to be punctured when needles stab the nerve. In particular, extraneural vascular has more opportunities of being injured than intraneural vascular [48, 49] (Figure 1). Acupuncture may also cause nerve fiber injury during twirling, lifting, and thrusting (Figure 2).

During twirling, lifting, and thrusting, the extraneural and intraneural vascular system nerve may be punctured. Moreover, the hematoma can cause inflammation and squeeze the surrounding nerve tissue.

During twirling, lifting, and thrusting, myelin sheath and axon may be destroyed, and then, the injury triggers classic inflammation and neuropathic inflammation.

## 8. Summary

By reviewing ancient Chinese medicine books, the formulation process of acupuncture sensation scale, adverse events of acupuncture, and the related literature of nerve stem stimulation therapy, our view is that the electric shock in the acupuncture process is a warning sign to indicate that the peripheral nerve may have been injured. Furthermore, acupuncture manipulation is an essential factor in causing nerve injury. The reason is as follows: no record of the needling sensation similar to the electric shock is found in ancient Chinese medicine books; the electric shock is inconsistent with the documented needling sensation in the conduction speed and direction; the scale makers that included the electric shock into the acupuncture sensation scales have doubts about whether the electric shock is a normal needling sensation; moreover, the electric shock is not derived from acupuncture experiments, but from the self-summary of acupuncturists and patients. Analyzing the case of nerve injury caused by acupuncture accompanied by the electric shock and comparing it with the nerve stem stimulation therapy in which the electric shock appears but there are no acupuncture accidents have been reported. We propose that obtaining electrical shock through acupuncture manipulation during acupuncture may cause nerve injury. However, the current studies supporting that the sense of electric shock belongs to normal needle sensation or that the sense of electric shock indicates nerve injury are limited to expert experience and adverse acupuncture case reports. In the future, it is necessary to conduct clinical observational studies or experimental studies on the correlation between the electric shock and nerve injury.

## Data Availability

The data supporting this systematic review are from previously reported studies and datasets, which have been cited. The picture used to support this systematic review are included within the article.

## Conflicts of Interest

The authors declare no conflict of interest.

## Acknowledgments

Funding statement grants are from the National Key R&D Program of China (2017YFC1703304), the National Natural Science Foundation of China (81873204), and the International Science and Technology Cooperation Project of the Science and Technology Department of Sichuan Province, China (18GJHZ0235).

## References

- [1] Y. Chae and H. Olausson, "The role of touch in acupuncture treatment," *Acupuncture in Medicine*, vol. 35, no. 2, pp. 148–152, 2018.
- [2] Y.-l. Ren, T.-p. Guo, H.-b. Du et al., "A survey of the practice and perspectives of Chinese acupuncturists on Deqi," *Evidence-based Complementary and Alternative Medicine*, vol. 2015, Article ID 684708, 8 pages, 2015.
- [3] N. J. Hu, C. Lin, J. Li et al., "Remarks on the relationship between deqi and effect of acupuncture," *Zhongguo Zhen Jiu*, vol. 34, no. 4, pp. 413–416, 2014.
- [4] X.-Y. Yang, G.-X. Shi, Q.-Q. Li, Z.-H. Zhang, Q. Xu, and C.-Z. Liu, "Characterization of Deqi sensation and acupuncture effect," *Evidence-based Complementary and Alternative Medicine*, vol. 2013, Article ID 319734, 7 pages, 2013.
- [5] Shanghai Research Institute of Acupuncture and Meridian, "Morphological observation of acupuncture sensation in human body," *Acupuncture Research*, vol. 2, no. z1, pp. 11–12, 1977.
- [6] Q. S. Dong, X. Q. Wang, and R. T. Zhang, "Exploring the material basis of acupuncture points from the relationship between acupuncture and sensory function," *Journal of Sichuan of Traditional Chinese Medicine*, vol. 25, no. 1, pp. 92–97, 2007.
- [7] F. Y. Lu, Y. Y. Wang, C. Zhou et al., "Relationship between acupuncture sensations of *deqi* and different organizational structures of acupoint area," *Zhongguo Zhen Jiu*, vol. 39, no. 5, pp. 523–527, 2019.
- [8] W. Zou, L. Wang, X. Yu, X. Sun, and J. Liu, "Operation and essence of Toutianliang manipulation by professor ZHANG Jin," *Zhongguo Zhen Jiu*, vol. 36, no. 1, pp. 53–55, 2016.
- [9] J. J. Huang and P. Fu, "Discussion on the Depth of the Acupoint and the Depth of the Acupuncture Needle Insertion," *Acupuncture Research*, vol. 31, no. 4, pp. 246–248, 2006.
- [10] D. Chen, "Relationship between needling layers and needling sensations in acupuncture," *Zhongguo Zhen Jiu*, vol. 37, no. 11, pp. 1219–1222, 2017.
- [11] Y. Song, H. Sun, X. Li, J. E. Zhong, L. Bu, and X. Sun, "Own experience on acupuncture sensation," *Zhongguo Zhen Jiu*, vol. 38, no. 8, pp. 853–856, 2018.
- [12] X. Meng, W. Gu, F. Ma, Y. Du, and Q. Zhao, "Acupuncture therapy for regaining consciousness in terms of acupoint location, needle insertion and needle manipulation," *Zhongguo Zhen Jiu*, vol. 35, no. 3, pp. 249–251, 2015.
- [13] M. H. Li, Z. D. Li, and Z. H. Meng, "Discussion on the elements and the clinical application of needling sensation

- manipulation," *Zhongguo Zhen Jiu*, vol. 33, no. 1, pp. 43–45, 2013.
- [14] C. Q. Guo and Y. L. Chen, "Analysis of peripheral nerve injury due to point injection," *Shanghai Journal of Acupuncture and Moxibustion*, vol. 26, no. 4, pp. 29–31, 2007.
- [15] H. MacPherson and A. Asghar, "Acupuncture needle sensations associated with De Qi: a classification based on experts' ratings," *Journal of Alternative and Complementary Medicine*, vol. 12, no. 7, pp. 633–637, 2006.
- [16] J. J. Park, M. Akazawa, J. Ahn et al., "Acupuncture sensation during ultrasound guided acupuncture needling," *Acupuncture in Medicine*, vol. 29, no. 4, pp. 257–265, 2011.
- [17] R. He and B. X. Zhao, "Progress of researches on mechanisms of needling and moxibustion sensations and their related sensation transmission," *Zhen Ci Yan Jiu*, vol. 44, no. 4, pp. 307–311, 2019.
- [18] L. P. Guan and C. Z. Liu, "Progresses of study on correlativity of qi-arrival of needling with clinical therapeutic effect and its action mechanism," *Zhongguo Zhen Jiu*, vol. 29, no. 11, pp. 945–948, 2009.
- [19] J. Bai, J. Han, D. Zhu et al., "Research and thinking on needling sensation of acupoint Huantiao (GB 30)," *Zhongguo Zhen Jiu*, vol. 35, no. 3, pp. 253–256, 2015.
- [20] C. A. Vincent, P. H. Richardson, J. J. Black, and C. E. Pither, "The significance of needle placement site in acupuncture," *Journal of Psychosomatic Research*, vol. 33, no. 4, pp. 489–496, 1989.
- [21] J. Kong, D. T. Fufa, A. J. Gerber et al., "Psychophysical outcomes from a randomized pilot study of manual, electro, and sham acupuncture treatment on experimentally induced thermal pain," *The Journal of Pain*, vol. 6, no. 1, pp. 55–64, 2005.
- [22] J. Kong, R. Gollub, T. Huang et al., "Acupuncture de qi, from qualitative history to quantitative measurement," *Journal of Alternative and Complementary Medicine*, vol. 13, no. 10, pp. 1059–1070, 2007.
- [23] P. White, F. Bishop, H. Hardy et al., "Southampton needle sensation questionnaire: development and validation of a measure to gauge acupuncture needle sensation," *Journal of Alternative and Complementary Medicine*, vol. 14, no. 4, pp. 373–379, 2008.
- [24] W. Kou, I. Gareus, J. D. Bell et al., "Quantification of DeQi sensation by visual analog scales in healthy humans after immunostimulating acupuncture treatment," *The American Journal of Chinese Medicine*, vol. 35, no. 5, pp. 753–765, 2007.
- [25] D. T. Yu, A. Y. Jones, and M. Y. Pang, "Development and validation of the Chinese version of the Massachusetts General Hospital Acupuncture Sensation Scale: an exploratory and methodological study," *Acupuncture in Medicine*, vol. 30, no. 3, pp. 214–221, 2012.
- [26] J. J. Mao, J. T. Farrar, K. Armstrong, A. Donahue, J. Ngo, and M. A. Bowman, "De qi: Chinese acupuncture patients' experiences and beliefs regarding acupuncture needling sensation—an exploratory survey," *Acupuncture in Medicine*, vol. 25, no. 4, pp. 158–165, 2007.
- [27] J. E. Park, Y. H. Ryu, Y. Liu et al., "A literature review of de qi in clinical studies," *Acupuncture in Medicine*, vol. 31, no. 2, pp. 132–142, 2013.
- [28] R. Melzack, "The McGill Pain Questionnaire: major properties and scoring methods," *Pain*, vol. 1, no. 3, pp. 277–299, 1975.
- [29] M. W. C. Chan, X. Y. Wu, J. C. Y. Wu, S. Y. S. Wong, and V. C. H. Chung, "Safety of acupuncture: overview of systematic reviews," *Scientific Reports*, vol. 7, no. 1, article 3369, 2017.
- [30] C. M. Witt, D. Pach, B. Brinkhaus et al., "Safety of acupuncture: results of a prospective observational study with 229,230 patients and introduction of a medical information and consent form," *Forschende Komplementärmedizin*, vol. 16, no. 2, pp. 91–97, 2009.
- [31] J. Wu, Y. Hu, Y. Zhu, P. Yin, G. Litscher, and S. Xu, "Systematic review of adverse effects: a further step towards modernization of acupuncture in China," *Evidence-Based Complementary and Alternative Medicine*, vol. 2015, Article ID 432467, 9 pages, 2015.
- [32] L. Wang, "Acupuncture at Neiguan causes contracture of hand muscles," *Shanghai Journal of Acupuncture and Moxibustion*, vol. 10, no. 2, p. 45, 1991.
- [33] E. Sobel, E. Y. Huang, and C. B. Wieting, "Drop foot as a complication of acupuncture injury and intragluteal injection," *Journal of the American Podiatric Medical Association*, vol. 87, no. 2, pp. 52–59, 1997.
- [34] M. Sato, H. Katsumoto, K. Kawamura, H. Sugiyama, and T. Takahashi, "Peroneal nerve palsy following acupuncture treatment. A case report," *The Journal of Bone and Joint Surgery American Volume*, vol. 85, no. 5, pp. 916–918, 2003.
- [35] J. W. Ruan, S. M. Li, M. Wen, Z. D. Rao, and Y. H. Hu, "Analysis on adverse effects of acupuncture in clinical practices," *Zhongguo Zhen Jiu*, vol. 29, no. 11, pp. 939–942, 2009.
- [36] K. F. Wang, "Some thoughts about acupuncture accidents," *Journal of Clinical Acupuncture and Moxibustion*, vol. 15, no. 5, pp. 57–58, 1999.
- [37] Z. C. Yang, *Nerve Trunk Stimulation Therapy*, Liaoning People's Publishing House, Shenyang, 1978.
- [38] Y. Qu, *Practical Nerve Trunk Stimulation Therapy*, People's Military Medical Publishing House, Beijing, 2008.
- [39] L. Qiu, X. L. Hu, X. Y. Zhao et al., "A randomized controlled clinical trial of treatment of lumbar disc herniation-induced sciatica by acupuncture stimulation of sciatic nerve trunk," *Zhen Ci Yan Jiu*, vol. 41, no. 5, pp. 447–450, 2016.
- [40] G. J. Pang, "Overview of nerve trunk stimulation therapy for stroke," *Journal of Clinical Acupuncture and Moxibustion*, vol. 24, no. 3, pp. 50–51, 2008.
- [41] L. F. Chen, J. Q. Fang, L. N. Chen, and C. Wang, "Achievements and enlightenment of modern acupuncture therapy for stroke based on the neuroanatomy," *Zhen Ci Yan Jiu*, vol. 39, no. 2, pp. 164–168, 2014.
- [42] C. C. Mi, "Analysis on acupuncture method of some acupoints in the method of Xingnao Kaiqiao," *Tianjin Journal of Traditional Chinese Medicine*, vol. 26, no. 1, pp. 50–51, 2009.
- [43] X. M. Shi, *Stroke and the Xingnao Kaiqiao Acupuncture Therapy*, Science Press, Beijing, 2007.
- [44] K. Streitberger, U. Eichenberger, A. Schneider, S. Witte, and M. Greher, "Ultrasound measurements of the distance between acupuncture needle tip at P6 and the median nerve," *Journal of Alternative and Complementary Medicine*, vol. 13, no. 5, pp. 585–592, 2007.
- [45] J. Kessler and K. Streitberger, "Perforation of the median nerve with an acupuncture needle guided by ultrasound," *Acupuncture in Medicine*, vol. 26, no. 4, pp. 231–233, 2008.
- [46] T. Steinfeldt, W. Nimphius, T. Werner et al., "Nerve injury by needle nerve perforation in regional anaesthesia: does size matter?," *British Journal of Anaesthesia*, vol. 104, no. 2, pp. 245–253, 2010, Epub 2009 Dec 22.
- [47] A. S. Rice and S. B. McMahon, "Peripheral nerve injury caused by injection needles used in regional anaesthesia: influence of




bevel configuration, studied in a rat model," *British Journal of Anaesthesia*, vol. 69, no. 5, pp. 433–438, 1992.

- [48] S. Geuna, S. Raimondo, G. Ronchi et al., "Chapter 3: histology of the peripheral nerve and changes occurring during nerve regeneration," *International Review of Neurobiology*, vol. 87, pp. 27–46, 2009.
- [49] B. Rydevik and G. Lundborg, "Permeability of intraneural microvessels and perineurium following acute, graded experimental nerve compression," *Scandinavian Journal of Plastic and Reconstructive Surgery*, vol. 11, no. 3, pp. 179–187, 1977.



## Research Article

# Effects of Transcutaneous Auricular Vagus Nerve Stimulation on Peripheral and Central Tumor Necrosis Factor Alpha in Rats with Depression-Chronic Somatic Pain Comorbidity

Xiao Guo <sup>1,2</sup>, Yuanyuan Zhao,<sup>3</sup> Feng Huang,<sup>1,4</sup> Shaoyuan Li,<sup>1</sup> Man Luo,<sup>1</sup> Yu Wang,<sup>1</sup> Jinling Zhang,<sup>1</sup> Liang Li,<sup>1</sup> Yue Zhang,<sup>1</sup> Yue Jiao,<sup>1</sup> Bin Zhao,<sup>1</sup> Junying Wang,<sup>1</sup> Hong Meng,<sup>5</sup> Zhangjin Zhang <sup>6</sup>, and Peijing Rong <sup>1</sup>

<sup>1</sup>Institute of Acupuncture and Moxibustion, China Academy of Chinese Medical Sciences, Beijing 100700, China

<sup>2</sup>Department of Scientific Research Management, China Academy of Chinese Medical Sciences, Beijing 100700, China

<sup>3</sup>Department of Psychiatry, First Hospital of Hebei Medical University, Shijiazhuang 050031, China

<sup>4</sup>Beijing Hospital of Traditional Chinese Medicine, Capital Medical University, Beijing 100010, China

<sup>5</sup>Key Laboratory of Cosmetic, China National Light Industry, Beijing Technology and Business University, Beijing 100048, China

<sup>6</sup>The School of Chinese Medicine, LKS Faculty of Medicine, The University of Hong Kong, Hong Kong, China

Correspondence should be addressed to Zhangjin Zhang; zhangzj@hku.hk and Peijing Rong; drrongpj@163.com

Received 6 June 2020; Revised 6 September 2020; Accepted 24 September 2020; Published 22 October 2020

Academic Editor: Yongjun Chen

Copyright © 2020 Xiao Guo et al. This is an open access article distributed under the Creative Commons Attribution License, which permits unrestricted use, distribution, and reproduction in any medium, provided the original work is properly cited.

Depression and pain disorders share a high degree of comorbidity. Inflammatory mechanisms play an important role in the pathogenesis of depression-chronic somatic pain comorbidity. In this study, we investigated the effects of acupuncture on blood and brain regional tumor necrosis factor alpha (TNF- $\alpha$ ) in rats with depression and chronic somatic pain comorbidity. Forty Sprague-Dawley rats were randomly divided into the following 4 groups with 10 each: control, model, model treated with transcutaneous auricular vagus nerve stimulation (taVNS), and model treated with electroacupuncture (EA). Chronic unpredictable mild stress (CUMS) with chronic constriction injury of the sciatic nerve (CCI) was used to produce depression and chronic somatic pain comorbidity in the latter 3 groups. The rats of the taVNS and EA groups received, respectively, taVNS and EA at ST 36 for 28 days. Pain intensity was measured using a mechanical withdrawal threshold and thermal stimulation latency once biweekly. Depressive behavior was examined using a sucrose preference test at baseline and the end of modeling and intervention. The level of plasma TNF- $\alpha$  and the expression of TNF- $\alpha$  in the prefrontal cortex (PFC), hippocampus, amygdala, and hypothalamus were measured. While CUMS plus CCI produced remarkable depression-like behavior and pain disorders, EA and taVNS significantly improved depression and reduced pain intensity. CUMS plus CCI also resulted in a significant increase in plasma TNF- $\alpha$  level and the expression in all brain regions examined compared to the intact controls. Both EA and taVNS interventions, however, suppressed the elevated level of TNF- $\alpha$ . These results suggest that EA and taVNS have antidepressant and analgesic effects. Such effects may be associated with the suppression of TNF- $\alpha$ -related neuroinflammation.

## 1. Introduction

Depression is a common mental disorder and often accompanied with unexplained painful physical symptoms [1]. The prevalence of chronic pain is about 51.8% to 59.1% among patients with depression [2]. Pain and depression share a complex reciprocal relationship [3]. (1) More severe

depression is accompanied with greater pain. (2) Improvement in pain correlates with improvement in depression [4]. (3) Pain affects the prognosis and treatment of depression, and vice versa [2]. In short, when chronic pain and depression occur concomitantly, the prognosis is worse than in either case, leading to greater functional impairment, longer duration, and less effective medication [5]. The



comorbidity increases the socioeconomic cost, and the direct medical costs of comorbid patients are more than twice as high as those with a single disease [3]. Therefore, finding out the underlying mechanisms in order to ensure appropriate treatment and promote the development of new treatments for depression and comorbid pain is urgently needed [6].

Many potential common pathways and neurotransmitters have been proposed to underlie the comorbidity of pain and depression. A growing body of evidences suggested that pain and depression may work in the similar brain regions that manage both mood and noxious sensory pathways of body pains, including the PFC, insular cortex, anterior cingulate, thalamus, hippocampus, and amygdala, which form an anatomical basis for the coexistence of pain and depression [7, 8]. Increasingly, neuroimmune and neuroinflammatory mechanisms are considered to play a key role in the association between depression and pain. An experiment shows that among 37 outpatients with major depression and 48 healthy controls, increased pain sensitivity (by pressure pain thresholds test) in depression may link to increased TNF- $\alpha$  concentration [6]. Moreover, in animal models of depression, the increased expression of proinflammatory cytokines in the area of the brain which is responsible for the disposing of emotion and pain is accompanied by inflammation or neuropathic pain [3]. In brief, depression-pain comorbidity is associated with an elevated level of proinflammatory cytokines, including interleukin (IL)-1, IL-6, and TNF- $\alpha$  [9]. By affecting chronic pain and depression-related pathophysiological functional areas via the blood-brain barrier, the elevated level of proinflammatory cytokines can result in changes in neurotransmitter metabolism, neuroendocrine function, and neuroplasticity, thus inducing the occurrence of the depression-chronic somatic pain comorbidity [7].

The vagus nerve has been shown to reflexively limit the innate immune response through the binding of its neurotransmitter acetylcholine (ACh) to the  $\alpha 7$  nicotinic acetylcholine receptor ( $\alpha 7$ nAChR) present on immune cells [10]. Conchae is the only region on our body surface where the vagus nerve innervates. The vagus afferent fibers can project to other brain regions such as the hypothalamus and amygdala via the nucleus tractus solitari (NTS). In consequence, the auricular branch of the vagus nerve is a peripheral pathway to the central nervous system (CNS) [11]. Electric stimuli might follow an inverse path from peripheral nerves toward the brain stem and central structures [12]. Therefore, taVNS can produce a similar effect to the classic vagus nerve stimulation (VNS) on improving the inflammation. Based on the above findings, we postulate an idea that taVNS can improve depression combined with chronic somatic pain by reducing the level of proinflammatory cytokines, such as TNF- $\alpha$ . In addition, it was reported that EA at ST 36 can effectively relieve chronic pain [13, 14] and improve depression-like behaviors in rats [15]. Therefore, we select the intervention of EA at ST 36 as the positive control.

## 2. Materials and Methods

*2.1. Experimental Animals.* 40 adult male Sprague-Dawley rats ( $200 \pm 20$  g) were obtained from China Food and Drug

Testing and Research Institute (Beijing, China, Animal License Key No. 2014-0013). They were fed ad libitum and kept at a  $23 \pm 1^\circ\text{C}$  temperature and  $50\% \pm 10\%$  humidity with an alternating 12 h light/dark cycle. The rats were randomly divided into four groups in conformity to the random digital tables: control group, model group, taVNS group, and EA group, with 10 rats in each group. The rats in the latter 3 groups were single cage rearing. Before modeling, all rats were kept adaptively for seven days. The protocol of the experiment was approved by the Animal Care and Use Committee of the Institute of Acupuncture and Moxibustion, China Academy of Chinese Medical Sciences (D2017-07-31-1).

*2.2. Instruments, Drugs, and Reagents.* Instruments include plantar analgesia meter (IITC Life Science, USA), von Frey filaments (Ugo Basile, Italy), matrix animal anesthesia ventilator system (Midmark, USA), electronic scale (JJ test instrument factory, Changshu, China), HANS instrument (HANS-100A, Nanjing, China), high-speed refrigerated centrifuge (Eppendorf, Germany), mini-protean 3 Dodeca (Bio-Rad, USA), PowerPac HC Power Supply (Bio-Rad, USA), shaker (Kylin-Bell, Haimen, China), homogenizer (IKA, Germany), automatic ice machine (Grant, USA), Multiskan Microplate reader (Thermo, USA), pH meter (Sartorius, Germany), and electrothermal constant temperature incubator (Taisite, Tianjin, China). Glycine, SDS, and Trizma base were purchased from Sigma (Louis, USA). APS, TEMED, Tween-20, Bromphenol Blue, DTT, Acrylamide, and Bis-Acrylamide were obtained from AMRESCO (Washington, USA). Methanol (dried) and NaCl were from Sinopharm (Beijing, China). Goat antirabbit IgG (H+L), HRP, and goat antimouse IgG (H+L), HRP, were obtained from Jackson (West Baltimore Pike, West Grove, PA, USA). Protein lysis buffer was purchased from Ukzybiotech (Beijing, China). BCA Protein Assay Kit was obtained from Beijing Biosynthesis Biotechnology Co., LTD (Beijing, China). The protease inhibitor cocktail was from Roche (Basel, Switzerland). Immobilon ECL was from Millipore (Massachusetts, USA). Nonfat milk was obtained from Dingguo Changsheng Biotechnology (Beijing, China). Isoflurane was purchased from Jiupai (Shijiazhuang, China). The rat TNF- $\alpha$  ELISA kit was from Neobioscience (Shenzhen, China). The protein ladder was from Biomed (Beijing, China).

*2.3. Experimental Procedure.* Four groups of rats were given a week of adaptive rearing at -35 day. CUMS was conducted in the latter 3 groups for 28 day. At 0 day, two rats with lower sucrose preference in the control group and two rats with higher sucrose preference in the model, taVNS, and EA groups were, respectively, removed. Then, CCI was performed in the latter 3 groups, with 8 rats in each group. The success of the CUMS combined with CCI model was evaluated by the sucrose preference test, mechanical withdrawal threshold, and thermal stimulation latency. After the modeling is completed, the intervention is carried out. The taVNS and EA groups were intervened for 28 consecutive days, respectively. Plasma and brain tissues in the PFC, hippocampus, amygdala, and hypothalamus were collected

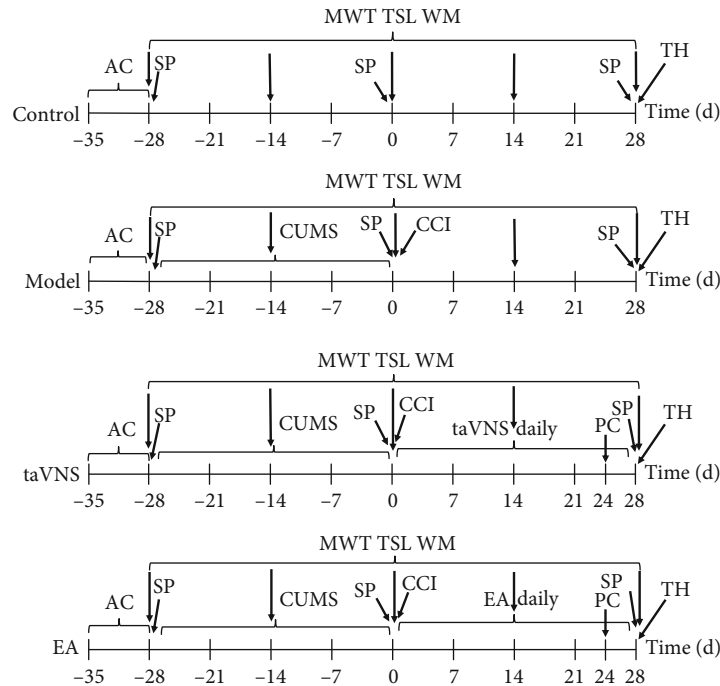


FIGURE 1: Experimental procedure: AC: acclimatization; SP: sucrose preference; CUMS: chronic unpredictable mild stress; taVNS: transcutaneous vagus nerve stimulation; CCI: chronic constriction injury of the sciatic nerve; MWT: mechanical withdrawal threshold; TSL: thermal stimulation latency; WM: weight measurement; EA: electroacupuncture at ST 36; PC: plasma collection; TH: tissue harvest.

in each group at 28 day. The sucrose preference test was performed at -28 day, 0 day, and 28 day. The mechanical withdrawal threshold, thermal stimulation latency, and weight measurement were performed at -28 day, -14 day, 0 day, 14 day, and 28 day. The plasma was taken from the rats in the taVNS and EA groups at 0 min, 15 min, and 30 min to test the immediate effects of the interventions at 24 day. The interventions of taVNS and EA lasted 30 min; therefore, 0 min, 15 min, and 30 min represent before the intervention, during the intervention, and after the intervention, respectively. Unfortunately, two rats from the control and EA groups died accidentally while being taken blood from the tail vein at 24 day (Figure 1).

**2.4. Chronic Unpredictable Mild Stress Model.** The CUMS model is a widely recognized depression modeling method at home and abroad, which can preferably simulate the pathogenesis of human depression. In this experiment, the rats in the latter 3 groups received seven kinds of CUMS, including upside-down day and night (12/12 h), hot plate test (52°C, 5 min), swimming at 8°C–10°C (5 min), in a wet cage (24 h), tail pinch (3 min), food deprivation (24 h), and water deprivation (24 h). The modeling time is 28 days. The different stressors were randomly distributed, with an interval of seven days between repetitions. All stressors were administered four times within 28 days [16].

**2.5. Chronic Constriction Injury of the Sciatic Nerve Model.** After 28 days of chronic unpredictable mild stress, chronic constriction injury of the sciatic nerve model was made in the latter 3 groups of rats. Before the operation, the rats were

anesthetized with isoflurane gas and placed on the operating table of the animals in the prone position. Remove the hair in the middle of the left thigh of rats, cut open the skin in the outer margin of the thigh femur, blunt and separate the muscles, and expose the sciatic nerve trunk. Wrap the 4-0 chrome gut around the middle of the sciatic nerve stem and tie a knot. Tighten the knot at a constant speed until it is just on either side of the nerve stem, creating a slight compression. Tie the second knot carefully to avoid any effect on the tightness of the first knot. In this way, the sciatic nerve trunk is evenly three knots with an interval of about 1 mm [17]. The skin wound was nailed with metal nails to prevent rats from gnawing. Each operator is fixed to ensure that the ligation force is comparable [18].

**2.6. Intervention.** After modeling, the taVNS and EA groups were treated with an electrical stimulator for 28 consecutive days. The intervention time was from 15:00 to 17:00 every day, and each time the electrical stimulation lasted 30 min. The intensity and frequency of electrical stimulation were set at 2 mA and 15 Hz. The waveform was selected as a disperse-dense wave. The intervention was operated under anesthesia with isoflurane gas. The taVNS group was connected with a positive and negative electrode self-adsorption conductive magnet which was noninvasively fixed in the bilateral cavity of the auricular concha of rats. The auricle of rats was observed to maintain slight vibration. If there was no vibration, a cotton swab was used to wipe the auricular concha with normal saline to enhance the conductive effect. The EA was inserted perpendicularly into the skin 5 mm apart at bilateral ST 36 in the EA group. ST 36 locates

5 mm below the humeral head [19]. The stimulation intensity, frequency, and waveform were the same as those of the taVNS group.

**2.7. Sucrose Preference Test.** All the rats were singly housed in a cage when the sucrose preference test began. Two bottles of 1% sucrose solution were placed in each cage at the same time for 24 h, and the animals were trained to adapt to drink sucrose water. Replace one of the bottles with pure water for the next 24 hours. After 23 h of food and water deprivation, each cage was given two bottles of water quantified in advance: one bottle of 1% sucrose water and one bottle of pure water. Sucrose and water bottles were placed in randomly assigned sides of the cage. After 60 min, remove two bottles and weigh them. The results of sucrose preference test were calculated according to the following equation: sucrose solution (g)/(sucrose solution (g) + water (g)) × 100%.

**2.8. Mechanical Withdrawal Threshold.** The mechanical pain threshold was measured by using the von Frey filaments. The rat was placed in the plastic cages on a perforated metal platform to habituate the environment for one hour the day before the first test and no measurements were made. Allow the rat to adapt to the environment for 15 min before each test. The stimulation force of von Frey filaments can provide a range of 0.008 g to 300 g. The Von Frey filaments were used to vertically stimulate the intermetatarsal bones of the 4th and 5th posterior feet of the rats. Brisk withdraw or paw flinching was considered as the effective stimulation which was recorded. The bilateral hind paw mechanical withdrawal threshold was tested three times, and the average values were calculated.

**2.9. Thermal Stimulation Latency.** The thermal stimulation latency was measured by using the Plantar Analgesia Meter. Each rat was placed in the individual plexiglass enclosure compartment on the glass surface to habituate the environment for one hour the day before the first test, and no measurements were made. Allow the rat to adapt to the environment for 5 min before each test. The thermal stimulus was emitted from a movable radiant heat source under the glass surface and was focused on the plantar surface of the hind paw. The source output temperature was set at 52°C. The cutoff time was set at 25 s to prevent potential tissue damage caused by continuous heating. Move the trigger with both hands, so that the radiant heat source is focused on the 4th and 5th tibia of the hind paw of the rat. Press the trigger button to heat the rat's foot. When the rat is withdrawing the paw, the instrument automatically records the latency time. Bilateral hind paw thermal withdrawal latencies were tested three times, and the average values were calculated.

**2.10. ELISA Analysis.** The plates were coated with the TNF- $\alpha$  and SP antigen (100  $\mu$ l/well) and incubated overnight at 4°C. The plates were washed with PBS-0.05% Tween20 (PBST) and blocked with PBST-1% BSA (200  $\mu$ l/well) at 37°C for one hour. The plates were washed, and the plasma samples diluted to different multiples were added and incubated at 37°C for two hours. The plates were washed, and the rabbit antirat IgG (H+L) was added and incubated at 37°C for one

hour. The plates were washed, and a chromogenic solution was allowed to react for 20 min. The optical density (OD) value of each well was measured using a microplate reader at wavelengths of 562 nm. The standard curve was prepared according to the standard solution and corresponding OD value, and thus, the concentrations of TNF- $\alpha$  and SP of each sample could be calculated.

**2.11. Western Blot Analysis.** The total protein of brain samples was extracted using the extraction kit according to the manufacturer's instructions and analyzed with a bicinchoninic acid (BCA) protein concentration assay kit. Proteins (30  $\mu$ g/well) and protein ladder were separated by gel electrophoreses running on PowerPac HC Power Supply for approximately 20 min at 90 V in running buffer (250 mM Tris base, 2.5 M glycine, 1% SDS, pH 8.3) and transferred to polyvinylidene difluoride (PVDF) membranes at 300 mA for 90 min. The membranes were blocked with 5% nonfat dry milk in TBST (TBS containing 20% Tween-20, pH 7.5) for 1 h at room temperature. The primary antibodies (1:1000 dilution for TNF- $\alpha$ ) were then incubated overnight at 4°C in TBST with 5% nonfat dry milk. After three 10-min washes in TBST, the secondary antibody was incubated in a 1:10000 dilution in TBST with 5% nonfat dry milk for 40 min at room temperature followed by three 10-min washes in TBST. The membranes were exposed to clarity enhanced chemiluminescence (ECL) reagent for 3 min at room temperature. The detection of immunoreactive bands was performed by image scan using a Gel Image system ver.4.00.

**2.12. Statistical Analysis.** The data were analyzed by using SPSS version 22.0 (SPSS Inc., Chicago, IL, USA) and GraphPad Prism 5.0 (GraphPad Software Inc., San Diego, CA, USA). The data is expressed as mean  $\pm$  standard deviation. The paired *t*-test was used for the before-and-after comparison of data in the group. One-way analysis of variance was used for comparison of data between the groups. A value of  $P < 0.05$  was considered statistically significant.

### 3. Results

**3.1. The Weight in Each Group at Different Time Points.** There was no significant difference in the weight between the four groups at -28 day ( $P > 0.05$ ). Compared with the control group, the weight decreased significantly in the taVNS, EA, and model groups at -14 day and 0 day ( $P < 0.01$ ), indicating the weight of rats were affected by CUMS. Compared with the model group, the weight decreased significantly in the taVNS group at 28 day ( $P < 0.05$ ). The weight decreased in the taVNS group at 28 day compared with the EA group, but no statistical difference was found between them ( $P > 0.05$ ) (Table 1).

**3.2. Sucrose Preference in Each Group at Different Time Points.** There was no significant difference in the sucrose preference between the four groups at -28 day ( $P > 0.05$ ). Compared with the control group, the sucrose preference decreased significantly in the taVNS, EA, and model groups at 0 day ( $P < 0.05$ ), suggesting that the CUMS model has

TABLE 1: Comparison of weight in each group at different time points ( $\bar{x} \pm s$ ).

Group	-28 day		-14 day		0 day		14 day		28 day	
	<i>n</i>	Weight (g)	<i>n</i>	Weight (g)	<i>n</i>	Weight (g)	<i>n</i>	Weight (g)	<i>n</i>	Weight (g)
Control	10	219.4 ± 15.9	10	341.3 ± 30.3	8	386.0 ± 40.5	8	450.4 ± 42.7	7	459.7 ± 47.4
Model	10	219.0 ± 11.8	10	279.9 ± 18.0***	8	338.6 ± 32.5**	8	431.7 ± 43.4	8	452.1 ± 46.7
taVNS	10	213.0 ± 11.4	10	271.5 ± 23.3***	8	319.6 ± 25.4***	8	396.5 ± 25.3*	8	406.5 ± 26.5*#
EA	10	220.0 ± 13.2	10	285.5 ± 15.2***	8	340.1 ± 28.2**	8	409.5 ± 43.4*	7	434.1 ± 29.8

At 0 day, two rats were removed from each group. At 24 day, two rats from the control and EA groups died when experimenters took blood from the caudal vein. \*\*\* $P < 0.001$ , vs. the control group; \*\* $P < 0.01$ , vs. the control group; \* $P < 0.05$ , vs. the control group; # $P < 0.05$ , vs. the model group.

TABLE 2: Comparison of sucrose preference in each group at different time points ( $\bar{x} \pm s$ ).

Group	-28 day		0 day		28 day	
	<i>n</i>	SP (%)	<i>n</i>	SP (%)	<i>n</i>	SP (%)
Control	10	0.62 ± 0.19	8	0.76 ± 0.12	7	0.80 ± 0.12
Model	10	0.57 ± 0.22	8	0.59 ± 0.12*	8	0.63 ± 0.13
taVNS	10	0.71 ± 0.21	8	0.60 ± 0.15*	8	0.81 ± 0.16#
EA	10	0.62 ± 0.21	8	0.60 ± 0.16*	7	0.80 ± 0.25

SP: sucrose preference. \* $P < 0.05$ , vs. the control group; # $P < 0.05$ , vs. the model group.

been successfully built. Compared with the model group, the sucrose preference increased significantly in the taVNS group at 28 day ( $P < 0.05$ ), the sucrose preference increased in the EA group at 28 day, but no statistical difference was found between them ( $P > 0.05$ ). The difference in sucrose preference between the taVNS and model groups was similar to those between the EA and model groups ( $P > 0.05$ ) (Table 2).

**3.3. Mechanical Withdrawal Threshold in Each Group at Different Time Points.** There was no significant difference in the mechanical withdrawal threshold between the four groups at -28 day ( $P > 0.05$ ). Compared with the control group, the mechanical withdrawal threshold decreased significantly in the taVNS, EA, and model groups at 0 day ( $P < 0.001$ ). Compared with the model group, the mechanical withdrawal threshold increased in the EA and taVNS groups at 28 day, but no statistical difference was found between them ( $P > 0.05$ ). Compared with the EA group, the mechanical withdrawal threshold decreased in the taVNS group at 28 day, but no statistical difference was found between them ( $P > 0.05$ ) (Table 3).

**3.4. Thermal Stimulation Latency in Each Group at Different Time Points.** There was no significant difference in the thermal stimulation latency between the four groups at -28 day ( $P > 0.05$ ). Compared with the control group, the thermal stimulation latency decreased significantly in the taVNS, EA, and model groups at 0 day ( $P < 0.05$ ). Compared with the model group, the thermal stimulation latency increased significantly in the EA and taVNS groups at 28 day ( $P < 0.05$ ). Compared with the EA group, the thermal stimulation latency decreased in the taVNS group at 28 day, but no statistical difference was found between them ( $P > 0.05$ ) (Table 4).

**3.5. The Concentration of TNF- $\alpha$  and SP in Plasma for Each Group.** Compared with the control group, the plasma concentration of TNF- $\alpha$  increased significantly in the model group at 28 day ( $P < 0.05$ ). Compared with the model group, the TNF- $\alpha$  level decreased significantly in the EA group at 28 day ( $P < 0.01$ ), the concentration of TNF- $\alpha$  decreased in the taVNS group at 28 day, but no statistical difference was found between them ( $P > 0.05$ ) (Table 5). Compared with that at 0 min, the concentration of TNF- $\alpha$  in plasma decreased in the taVNS and EA groups at 15 and 30 min, but no statistical difference was found between them ( $P > 0.05$ ). Compared with that at 15 min, the concentration of TNF- $\alpha$  decreased continuously in the EA group at 30 min, but no statistical difference was found between them ( $P > 0.05$ ). There was a large difference between 0 min and 30 min in the EA group than those in the taVNS group (Figure 2(a)).

Compared with the control group, the concentration of SP in plasma decreased in the model group and taVNS group at 28 day, but no statistical difference was found between them ( $P > 0.05$ ). The concentration of SP was higher in the EA group compared with the other three groups at 28 day, but no statistical difference was found between them ( $P > 0.05$ ) (Table 5). Compared with that at 0 min, the concentration of SP decreased continuously in the taVNS group at 15 and 30 min, but no statistical difference was found between them ( $P > 0.05$ ). Compared with that at 0 min, the plasma concentration of SP in the EA group decreased at 15 min and increased at 30min, but no statistical difference was found between them ( $P > 0.05$ ) (Figure 2(b)).

**3.6. The Expression of TNF- $\alpha$  in the PFC, Hippocampus, Amygdala, and Hypothalamus for Each Group at 28 Day.** Compared with the control group, the expression level of TNF- $\alpha$  in the hippocampus, amygdala, and hypothalamus increased significantly in the model group ( $P < 0.05$ ). The expression level of TNF- $\alpha$  in PFC increased in the model group, but no statistical difference was found between them ( $P = 0.058$ ). Compared with the model group, the expression level of TNF- $\alpha$  in the amygdala decreased significantly in the EA group ( $P < 0.05$ ), the expression level of TNF- $\alpha$  in the hypothalamus and hippocampus decreased in the taVNS group, but no statistical difference was found between them ( $P = 0.054, 0.052$ ). The expression level of TNF- $\alpha$  in the PFC, hypothalamus, and hippocampus decreased in the EA group, but no statistical difference was found between them ( $P > 0.05$ ). Compared with the EA group, the expression level of TNF- $\alpha$  in the PFC and amygdala were higher in the taVNS



TABLE 3: Comparison of the mechanical withdrawal threshold in each group at different time points ( $\bar{x} \pm s$ ).

Group	-28 day		-14 day		0 day		14 day		28 day	
	<i>n</i>	MWT (g)	<i>n</i>	MWT (g)	<i>n</i>	MWT (g)	<i>n</i>	MWT (g)	<i>n</i>	MWT (g)
Control	10	8.0 ± 1.6	10	6.7 ± 3.9	8	6.8 ± 1.8	8	6.3 ± 2.3	7	7.4 ± 2.2
Model	10	7.7 ± 2.7	10	4.9 ± 2.3	8	2.3 ± 2.8***	8	3.6 ± 2.9*	8	4.6 ± 2.9*
taVNS	10	7.8 ± 2.6	10	5.2 ± 2.5	8	1.2 ± 1.3***	8	3.4 ± 2.1*	8	5.3 ± 2.6
EA	10	8.4 ± 1.8	10	5.8 ± 2.4	8	1.2 ± 0.6***	8	4.0 ± 2.6	7	6.0 ± 2.3

MWT: mechanical withdrawal threshold. \*\*\* $P < 0.001$ , vs. the control group; \* $P < 0.05$ , vs. the control group.

TABLE 4: Comparison of thermal stimulation latency in each group at different time points ( $\bar{x} \pm s$ ).

Group	-28 day		14 day		0 day		14 day		28 day	
	<i>n</i>	TSL (sec)	<i>n</i>	TSL (sec)	<i>n</i>	TSL (sec)	<i>n</i>	TSL (sec)	<i>n</i>	TSL (sec)
Control	10	12.03 ± 3.42	10	12.42 ± 1.41	8	11.82 ± 2.76	8	11.14 ± 2.25	7	12.12 ± 2.87
Model	10	11.30 ± 2.85	10	11.52 ± 2.46	8	7.57 ± 2.08**	8	9.56 ± 1.60	8	9.47 ± 1.27*
taVNS	10	11.17 ± 2.72	10	11.26 ± 2.57	8	8.84 ± 2.26*	8	10.58 ± 2.20	8	11.88 ± 1.30 <sup>#</sup>
EA	10	10.73 ± 2.98	10	9.94 ± 1.92*	8	8.76 ± 2.03*	8	10.07 ± 3.08	7	12.20 ± 1.60 <sup>#</sup>

TSL: thermal stimulation latency. \*\* $P < 0.01$ , vs. the control group; \* $P < 0.05$ , vs. the control group; <sup>#</sup> $P < 0.01$ , vs. the model group; <sup>#</sup> $P < 0.05$ , vs. the model group.

TABLE 5: Comparison of plasma concentration of TNF- $\alpha$  and SP in each group at 28 day ( $\bar{x} \pm s$ ).

Group	<i>n</i>	TNF- $\alpha$ (pg/ml)	SP (pg/ml)
Control	7	29.94 ± 32.11	114.86 ± 58.77
Model	8	76.24 ± 39.74*	85.34 ± 44.63
taVNS	8	49.88 ± 29.70	84.34 ± 54.84
EA	7	25.16 ± 26.99 <sup>#</sup>	124.08 ± 45.24

\* $P < 0.05$ , vs. the control group; <sup>#</sup> $P < 0.01$ , vs. the model group.

group ( $P > 0.05$ ), the expression level of TNF- $\alpha$  in the hippocampus and hypothalamus was lower in the taVNS group, but no statistical difference was found between them ( $P > 0.05$ ) (Figure 3).

#### 4. Discussion

Our researches have shown that taVNS is a promising potential treatment that can improve the severity of major depression [20–22] and taVNS can relieve neuropathic pain in Zucker Diabetes Fat rats by promoting melatonin secretion [18]. Acupuncture is recognized worldwide as a treatment with analgesic effect [23]. It is reported that EA at ST 36 can relieve the neuropathic pain induced by CCI [24]. Moreover, EA at DU 20 and ST 36 has a therapeutic effect on depression [25].

Based on previous research, we choose taVNS and EA at ST 36 as the intervention for comorbidity of depression and pain in our experiment. Compared to the general drug treatment, taVNS and EA have the advantages of obvious treatment effect, low treatment cost, convenient operation, and safety. In our experiment, we found that both taVNS and EA at ST 36 can improve the depressive behavior and relieve chronic pain in rats with depression-chronic pain comorbid-

ity after 28 consecutive days of intervention. In comparison, taVNS is good at improving depression-like behavior, and EA at ST 36 is good at relieving the pain symptoms. No adverse reactions occurred in the taVNS and EA groups during the intervention, indicating the treatments in the two groups were safe.

In our experiment, we also found induction and alleviation of depression-like behavior and chronic somatic pain symptoms was closely associated with the change of TNF- $\alpha$  level in the peripheral blood and brain regions, suggesting the inflammatory and immune processes play an important role in the biological mechanisms of depression-chronic somatic pain comorbidity. In the inflammatory mechanism of comorbidity of depression and pain, the peripheral proinflammatory cytokines can access the brain and activate local CNS inflammatory networks to affect the function of neurotransmitters involved in the pathophysiology of depression and pain [9]. To be specific, the peripheral production of TNF- $\alpha$ , IL-1, and IL-6 by monocytes results in a subsequent production of TNF- $\alpha$  and other mediators in the brain via toll-like receptor 4 (TLR4) present on circumventricular organs and peripheral vagal nerve afferents, leading to the activation of microglia. Activated microglia are the main source of TNF- $\alpha$  within the brain, while neuronal cells and astrocytes can produce it at a lower level. Thus, the crosstalk between peripheral immune cells and immune cells in the CNS may induce a positive feedback loop that further increases the production of TNF- $\alpha$  and other proinflammatory cytokines [9, 26, 27]. In our experiment, we found that TNF- $\alpha$  was increased in the PFC, hippocampus, amygdala, hypothalamus, and plasma in rats with depression-chronic pain comorbidity. The change of TNF- $\alpha$  in the brain was in accordance with those in plasma, indicating the probable existence of crosstalk between the peripheral immune cells and immune cells in the CNS.



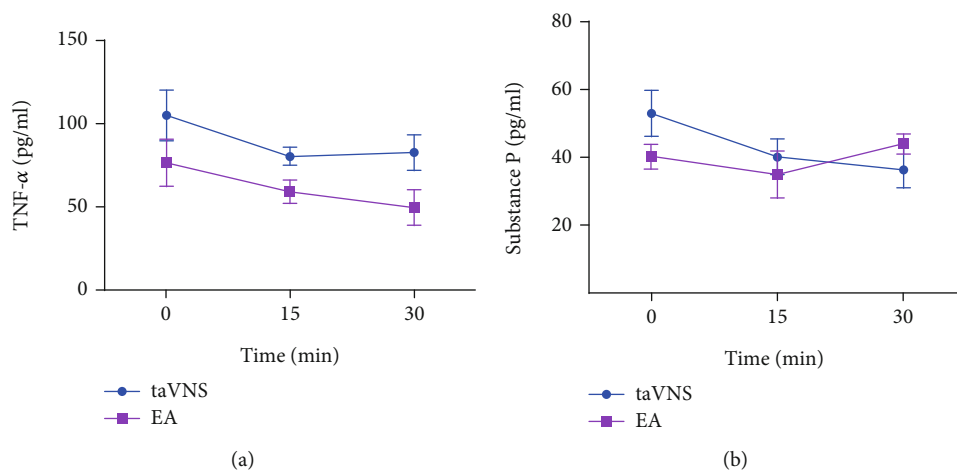


FIGURE 2: Comparison of plasma concentration of TNF- $\alpha$  and SP in taVNS and EA groups before, during, and after intervention. (a) Comparison of plasma concentration of TNF- $\alpha$  in taVNS and EA groups before, during, and after intervention. (b) Comparison of plasma concentration of SP in the taVNS and EA groups before, during, and after intervention.

The cholinergic anti-inflammatory pathway (CAP) is a physiological mechanism whereby the CNS regulates or inhibits local or systemic inflammatory response with cholinergic nerves and their neurotransmitters [28]. It is an endogenous anti-inflammatory pathway that links the nervous system and the immune system via the vagus nerve. The CAP can be activated by VNS or cholinergic agonists [29]. Ach is a neurotransmitter mainly released by vagus nerve endings. And  $\alpha 7$ nAChR is a key protein of signals triggered by VNS to induce the endogenous CAP [28]. Ach activates  $\alpha 7$ nAChR on macrophages, lymphocytes, and other inflammatory cells, regulating the synthesis and release of inflammatory cytokines and relieving the systemic inflammatory reaction [30]. The anti-inflammatory effects of taVNS and EA at ST 36 are closely related to the vagus-mediated cholinergic pathway. Previous studies have shown that EA at ST 36 also can reduce the serum TNF- $\alpha$  level in septic rats. Moreover, abdominal vagotomy or  $\alpha 7$ nAChR inhibitor can reverse the suppressive role of EA [31]. It proves that the anti-inflammatory role of EA at ST 36 is likely to depend on an intact vagus nerve and might exert its effects by the cholinergic  $\alpha 7$ nAChR [32]. EA at ST 36 activates the somatic fiber endings around ST 36 points, which send the acupuncture signals to the spinal cord via somatic sensory nerve fibers. In the spinal cord, the nerve impulses are transmitted to the NTS. After relayed and integrated by NTS, the nerve impulses activate CAP via efferent vagus nerve [33, 34]. Auricular concha is the only region on the surface of mammals where vagal afferent fibers are distributed. Nerve impulses can be transmitted to the NTS relay along the auricular branches of the vagus nerve, and then exert cholinergic anti-inflammatory effects via the efferent vagus nerve [33, 35]. Our experimental results showed that EA at ST 36 and taVNS have their anti-inflammatory effect mainly by decreasing TNF- $\alpha$  in plasma and brain regions. Among them, EA at ST 36 plays a more significant role.

In addition to TNF- $\alpha$ , SP is also an indicator of our study. SP is an eleven-amino acid long neuropeptide, widely distributed in the CNS and peripheral nervous system [36, 37]. It is a member of the tachykinin family and is involved in many biological processes, including nociception and neurogenic inflammation [38, 39]. In the aspect of nociception, pain-sensing fibers (nociceptors) release SP to increase pain sensitivity through its actions in the dorsal horn of the spinal cord. SP transmits and integrates nociceptive signals; accumulating studies found that SP also has an antinociceptive effect [40, 41]. In the aspect of inflammation, SP plays a critical role in its ability to stimulate and/or modulate the production of various cytokines by a wide range of immune cells [39]. We found SP showed a tendency to decline before, during, and after taVNS. However, the results of the SP content in the four groups showed confusion at 28 day, which cannot be explained for a reasonable reason. The only reason may be that the plasma SP was stored in the refrigerator at  $-80^{\circ}\text{C}$  for too long before the detection, resulting in the change of the content of SP during the storage process. In the future, we need to strictly control each step of SP detection to ensure the reliability of the experimental data. What is more, the lack of pathological images in the experiment is unable to provide the evidence of microglia activation in related brain regions. In the future, we need to use morphological methods to observe the activation of immune cells in peripheral plasma and related brain regions. Fortunately, we have found the important role of TNF- $\alpha$  in the inflammatory mechanism of depression-chronic somatic pain comorbidity, which lays the foundation for TNF- $\alpha$  regulator as a new drug target for the treatment of the disease. At the same time, we also found that EA at ST 36 and taVNS can improve the depression and relieve chronic somatic pain in model rats, which provides new and effective treatment methods for the disease. In a word, we need a large sample size, multi-indicators experiment to further research the

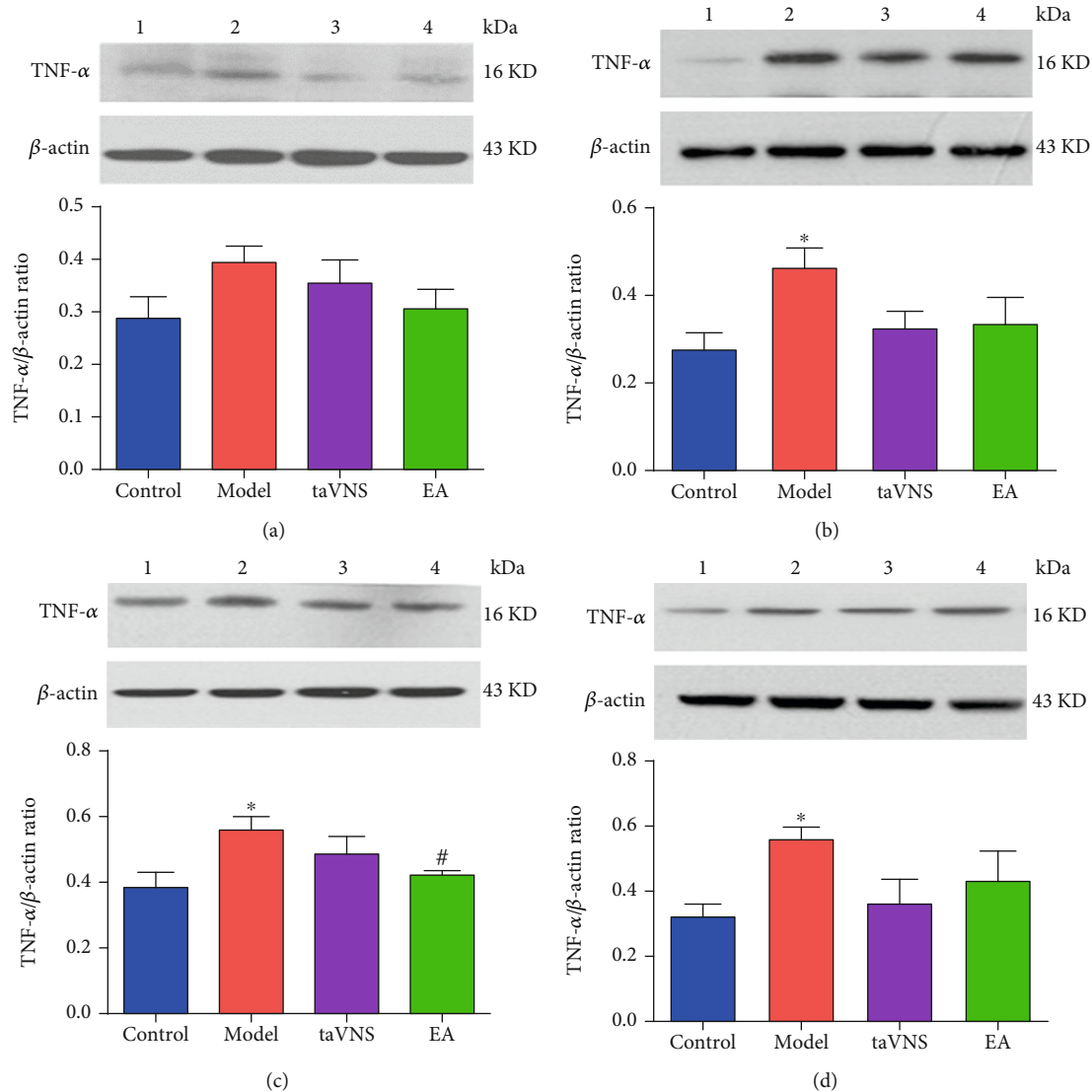


FIGURE 3: Expressions of TNF- $\alpha$  in PFC, hippocampus, amygdala, and hypothalamus. (a) Comparison of the TNF- $\alpha$  expression in the PFC for each group at 28 day. (b) Comparison of the TNF- $\alpha$  expression in the hippocampus for each group at 28 day. (c) Comparison of the TNF- $\alpha$  expression in the amygdala for each group at 28 day. (d) Comparison of TNF- $\alpha$  expression in the hypothalamus for each group at 28 day. 1: control group; 2: model group; 3: taVNS group; 4: EA group. \* $P < 0.05$ , vs. the control group. # $P < 0.05$ , vs. the model group.

anti-inflammatory mechanism of acupuncture in the comorbidity of depression and pain in the future.

## 5. Conclusion

CUMS combined CCI can induce depression-like behavior and chronic somatic pain disorders under solitary care for 28 consecutive days. After 28 consecutive days of intervention, both taVNS and EA at ST 36 can improve depression-like behavior and relieve chronic somatic pain. Compared with the control group, the levels of TNF- $\alpha$  in plasma, PFC, hippocampus, hypothalamus, and amygdala increased in rats with depression-chronic somatic pain comorbidity, and the elevated expression of TNF- $\alpha$  can be downregulated by taVNS and EA at ST 36.

## Data Availability

The data used to support the findings of this study are available from the corresponding author upon request.

## Conflicts of Interest

The authors declare that there are no conflicts of interest regarding the publication of this paper.

## Authors' Contributions

Xiao Guo, Yuanyuan Zhao, and Feng Huang contributed equally to this work as co-first authors. Peijing Rong, Zhangjin Zhang, and Hong Meng designed the study and contributed to the writing of the manuscript. Xiao Guo,

Yuanyuan Zhao, and Feng Huang wrote the first draft. Xiao Guo, Shaoyuan Li, Man Luo, and Yue Zhang performed the experiments. Yu Wang, Yue Jiao, Bin Zhao, and Junying Wang analyzed the data. Jinling Zhang and Liang Li contributed reagents and instruments. All authors reviewed and approved the final manuscript.

## Acknowledgments

This work was supported by the National Basic Research Program of China (2018YFC1705800), International Cooperation Project of Traditional Chinese Medicine in China Academy of Chinese Medical Sciences (GH2017-07), Guangdong Province Higher Vocational Colleges and Schools Pearl River Scholar Funded Scheme (2018) (A1-AFD018181Z3905), Beijing Key Laboratory of Plant Resources Research and Development, Beijing Technology and Business University Innovation (PRRD-2016-ZD2), Fundamental Research Funds for Beijing Municipal Science & Technology Commission (Z161100002616003), and Joint Sino-German Research Project (GZ1236).

## References

- [1] N. Rijavec and V. N. Grubic, "Depression and pain: often together but still a clinical challenge: a review," *Psychiatria Danubina*, vol. 24, no. 4, pp. 346–352, 2012.
- [2] L. Doan, T. Manders, and J. Wang, "Neuroplasticity underlying the comorbidity of pain and depression," *Neural Plasticity*, vol. 2015, Article ID 504691, 16 pages, 2015.
- [3] N. N. Burke, D. P. Finn, and M. Roche, "Chronic administration of amitriptyline differentially alters neuropathic pain-related behaviour in the presence and absence of a depressive-like phenotype," *Behavioural Brain Research*, vol. 278, pp. 193–201, 2015.
- [4] D. A. Fishbain, B. Cole, J. E. Lewis, and J. Gao, "Does pain interfere with antidepressant depression treatment response and remission in patients with depression and pain? An evidence-based structured review," *Pain Medicine*, vol. 15, no. 9, pp. 1522–1539, 2014.
- [5] L. Bravo, J. A. Mico, R. Rey-Brea, B. Pérez-Nievas, J. C. Leza, and E. Berrocoso, "Depressive-like states heighten the aversion to painful stimuli in a rat model of comorbid chronic pain and depression," *Anesthesiology*, vol. 117, no. 3, pp. 613–625, 2012.
- [6] N. N. Burke, D. P. Finn, and M. Roche, "Neuroinflammatory mechanisms linking pain and depression," *Modern Trends in Pharmacopsychiatry*, vol. 30, pp. 36–50, 2015.
- [7] J. Y. Sheng, S. Liu, Y. C. Wang, R. Cui, and X. Zhang, "The link between depression and chronic pain: neural mechanisms in the brain," *Neural Plasticity*, vol. 2017, Article ID 9724371, 10 pages, 2017.
- [8] C. H. Lin, Y. C. Yen, M. C. Chen, and C. C. Chen, "Depression and pain impair daily functioning and quality of life in patients with major depressive disorder," *Journal of Affective Disorders*, vol. 166, pp. 173–178, 2014.
- [9] B. Bortolato, A. F. Carvalho, J. K. Soczynska, G. I. Perini, and R. S. McIntyre, "The involvement of TNF- $\alpha$  in cognitive dysfunction associated with major depressive disorder: an opportunity for domain specific treatments," *Current Neuropharmacology*, vol. 13, no. 5, pp. 558–576, 2015.
- [10] M. Kox, M. Vaneker, J. G. van der Hoeven, G. J. Scheffer, C. W. Hoedemaekers, and P. Pickkers, "Effects of vagus nerve stimulation and vagotomy on systemic and pulmonary inflammation in a two-hit model in rats," *PLoS One*, vol. 7, no. 4, article e34431, 2012.
- [11] Y. T. Yu, P. J. Rong, and B. Zhu, "Present situation and prospect of transcutaneous auricular vagus nerve stimulation in encephalopathy treatment," *Modernization of Traditional Chinese Medicine and Materia Medica-World Science and Technology*, vol. 19, no. 3, pp. 462–468, 2017.
- [12] P. Shiozawa, M. E. Silva, T. C. Carvalho, Q. Cordeiro, A. R. Brunoni, and F. Fregni, "Transcutaneous vagus and trigeminal nerve stimulation for neuropsychiatric disorders: a systematic review," *Arquivos de Neuro-Psiquiatria*, vol. 72, no. 7, pp. 542–547, 2014.
- [13] J. Y. Du, J. Fang, C. Wen, X. Shao, Y. Liang, and J. Fang, "The effect of electroacupuncture on PKMzeta in the ACC in regulating anxiety-like behaviors in rats experiencing chronic inflammatory pain," *Neural Plasticity*, vol. 2017, Article ID 3728752, 13 pages, 2017.
- [14] H. Sun and Y. Z. Zhang, "Effect of acupuncture and moxibustion at Baihui and Zusanli on behavior of mouse and rat depression model," *Journal of Clinical Acupuncture and Moxibustion*, vol. 19, no. 2, pp. 47–49, 2003.
- [15] Y. H. Gao, J. Y. Wang, L. H. Tan et al., "High mobility group box 1/CD 24 receptor/ $\beta$ -EP signaling in "Zusanli" (ST 36) region contributes to electroacupuncture analgesia in rats with neuropathic pain," *Acupuncture Research*, vol. 43, no. 9, pp. 537–542, 2018.
- [16] X. H. Yang, S. Q. Song, and Y. Xu, "Resveratrol ameliorates chronic unpredictable mild stress-induced depression-like behavior: involvement of the HPA axis, inflammatory markers, BDNF, and Wnt/ $\beta$ -catenin pathway in rats," *Neuropsychiatric Disease and Treatment*, vol. 13, pp. 2727–2736, 2017.
- [17] C. Ma, C. X. Li, J. L. Yi, and L. P. Yan, "Comparison of the chronic constriction injury of the sciatic nerve (CCI) models performed by different materials in neuropathic pain of rats," *Chinese Pharmacological Bulletin*, vol. 24, no. 4, pp. 555–557, 2008.
- [18] X. Zhai, *The Study of Electroacupuncture Auricular Concha Region Regulating Plasma Melatonin of Zucker Diabetes Fat Rat to Relieve Neuralgia and Hypoglycemia*, Doctoral Dissertation of China Academy of Chinese Medical Sciences, 2013.
- [19] C. Bingyan, L. Rui, T. Huanhuan et al., "Effect on glycinemia in rats with type 2 diabetes induced by streptozotocin: low-frequency electro-pulse needling stimulated Weiwanshiu (EX-B 3) and Zusanli (ST 36)," *Journal of Traditional Chinese Medicine*, vol. 36, no. 6, pp. 768–778, 2016.
- [20] Y. Tu, J. Fang, J. Cao et al., "A distinct biomarker of continuous transcutaneous vagus nerve stimulation treatment in major depressive disorder," *Brain Stimulation*, vol. 11, no. 3, pp. 501–508, 2018.
- [21] Z. Wang, J. Fang, J. Liu et al., "Frequency-dependent functional connectivity of the nucleus accumbens during continuous transcutaneous vagus nerve stimulation in major depressive disorder," *Journal of Psychiatric Research*, vol. 102, pp. 123–131, 2018.
- [22] J. Kong, J. Fang, J. Park, S. Li, and P. Rong, "Treating depression with transcutaneous auricular vagus nerve stimulation: state of the art and future perspectives," *Frontiers in Psychiatry*, vol. 9, p. 20, 2018.

- [23] Y. Y. Wu, Y. L. Jiang, X. F. He et al., "Effects of electroacupuncture with dominant frequency at SP 6 and ST 36 based on meridian theory on pain-depression dyad in rats," *Evidence-Based Complementary and Alternative Medicine*, vol. 2015, Article ID 732845, 10 pages, 2015.
- [24] H. C. Hsu, N. Y. Tang, Y. W. Lin, T. C. Li, H. J. Liu, and C. L. Hsieh, "Effect of electroacupuncture on rats with chronic constriction injury-induced neuropathic pain," *The Scientific World Journal*, vol. 2014, Article ID 129875, 9 pages, 2014.
- [25] H. Sun, H. Zhao, J. Zhang et al., "Effect of acupuncture at Baihui (GV 20) and Zusanli (ST 36) on the level of serum inflammatory cytokines in patients with depression," *Chinese Acupuncture & Moxibustion*, vol. 30, no. 3, pp. 195–199, 2010.
- [26] A. K. Walker, A. Kavelaars, C. J. Heijnen, and R. Dantzer, "Neuroinflammation and comorbidity of pain and depression," *Pharmacological Reviews*, vol. 66, no. 1, pp. 80–101, 2014.
- [27] J. C. Felger and F. E. Lotrich, "Inflammatory cytokines in depression: neurobiological mechanisms and therapeutic implications," *Neuroscience*, vol. 246, pp. 199–229, 2013.
- [28] X. X. Lu, Z. Q. Hong, Z. Tan et al., "Nicotinic acetylcholine receptor alpha7 subunit mediates vagus nerve stimulation-induced neuroprotection in acute permanent cerebral ischemia by a7nAChR/JAK2 pathway," *Medical Science Monitor*, vol. 23, pp. 6072–6081, 2017.
- [29] D. Liu, T. Li, H. Luo, X. Zuo, S. Liu, and S. Wu, "The effect of the cholinergic anti-inflammatory pathway on collagen-induced arthritis involves the modulation of dendritic cell differentiation," *Arthritis Research & Therapy*, vol. 20, no. 1, p. 263, 2018.
- [30] Z. De-Pu, G. Li-Sha, C. Guang-Yi et al., "The cholinergic anti-inflammatory pathway ameliorates acute viral myocarditis in mice by regulating CD4<sup>+</sup> T cell differentiation," *Virulence*, vol. 9, no. 1, pp. 1364–1376, 2018.
- [31] Y. Geng, D. Chen, J. Zhou, H. Jiang, and H. Zhang, "Role of cholinergic anti-inflammatory pathway in treatment of intestinal ischemia-reperfusion injury by electroacupuncture at Zusanli," *Evidence-Based Complementary and Alternative Medicine*, vol. 2017, Article ID 6471984, 5 pages, 2017.
- [32] H. Wang, L. Wang, X. Shi et al., "Electroacupuncture at Zusanli prevents severe scalds-induced gut ischemia and paralysis by activating the cholinergic pathway," *Evidence-Based Complementary and Alternative Medicine*, vol. 2015, Article ID 787393, 6 pages, 2015.
- [33] Y. X. Zhao, W. He, X. H. Jing et al., "Transcutaneous auricular vagus nerve stimulation protects endotoxemic rat from lipopolysaccharide-induced inflammation," *Evidence-Based Complementary and Alternative Medicine*, vol. 2012, Article ID 627023, 10 pages, 2012.
- [34] Q. Song, S. Hu, H. Wang et al., "Electroacupuncture at Zusanli point (ST36) attenuates pro-inflammatory cytokine release and organ dysfunction by activating cholinergic anti-inflammatory pathway in rat with endotoxin challenge," *African Journal of Traditional Complementary and Alternative Medicines*, vol. 11, no. 2, pp. 469–474, 2014.
- [35] P. J. Rong, W. Wei, J. D. Chen et al., "Establishment and explanation of the theory of 'enlightening the Spirit by modulating pivot' on depression treatment," *Journal of Traditional Chinese Medicine*, vol. 60, no. 4, pp. 295–298, 2019.
- [36] G. M. Zhao and J. S. Yin, "Study on relationship between substance P and its receptor Neurokinin-1 receptor with pain," *Medical Recapitulate*, vol. 21, no. 16, pp. 2890–2893, 2015.
- [37] S. Suvas, "Role of substance P neuropeptide in inflammation, wound healing, and tissue homeostasis," *Journal of Immunology*, vol. 199, no. 5, pp. 1543–1552, 2017.
- [38] M. B. Johnson, A. D. Young, and I. Marriott, "The therapeutic potential of targeting substance P/NK-1R interactions in inflammatory CNS disorders," *Frontiers in Cellular Neuroscience*, vol. 10, p. 296, 2017.
- [39] A. Mashaghi, A. Marmalidou, M. Tehrani, P. M. Grace, C. Pothoulakis, and R. Dana, "Neuropeptide substance P and the immune response," *Cellular and Molecular Life Sciences*, vol. 73, no. 22, pp. 4249–4264, 2016.
- [40] C. T. Chang, B. Y. Jiang, and C. C. Chen, "Ion channels involved in substance P-mediated nociception and antinociception," *International Journal of Molecular Sciences*, vol. 20, no. 7, p. 1596, 2019.
- [41] M. Yang, G. C. Zhu, and Z. X. Liu, "Advances in roles of substance P and substance P receptor in neuropathic pain," *Journal of Nanchang University*, vol. 53, no. 7, pp. 80–82+85, 2013.

## Research Article

# Effect of Electroacupuncture on Pain Perception and Pain-Related Affection: Dissociation or Interaction Based on the Anterior Cingulate Cortex and S1

Yan Shi,<sup>1,2</sup> Shujing Yao,<sup>1</sup> Zui Shen,<sup>1</sup> Lijiao She,<sup>3</sup> Yingling Xu,<sup>1</sup> Boyi Liu,<sup>1</sup> Yi Liang,<sup>1</sup> Yongliang Jiang,<sup>1</sup> Jing Sun,<sup>1</sup> Yuanyuan Wu,<sup>1</sup> Junying Du,<sup>1</sup> Yilin Zhu,<sup>1</sup> Zemin Wu,<sup>1</sup> Jianqiao Fang <sup>1</sup> and Xiaomei Shao <sup>1</sup>

<sup>1</sup>Department of Neurobiology and Acupuncture Research, The Third Clinical College, Zhejiang Chinese Medical University, Key Laboratory of Acupuncture and Neurology of Zhejiang Province, Hangzhou 310053, China

<sup>2</sup>Department of Acupuncture and Massage, Affiliated Hangzhou First People's Hospital, Zhejiang University School of Medicine, Hangzhou 310006, China

<sup>3</sup>Department of Rehabilitation Medicine, Changxing People's Hospital, Huzhou 313100, China

Correspondence should be addressed to Jianqiao Fang; [fangjianqiao7532@163.com](mailto:fangjianqiao7532@163.com) and Xiaomei Shao; [13185097375@163.com](mailto:13185097375@163.com)

Received 21 June 2020; Revised 1 September 2020; Accepted 23 September 2020; Published 14 October 2020

Academic Editor: Jing-Wen Yang

Copyright © 2020 Yan Shi et al. This is an open access article distributed under the Creative Commons Attribution License, which permits unrestricted use, distribution, and reproduction in any medium, provided the original work is properly cited.

Electroacupuncture (EA) can effectively modulate pain perception and pain-related negative affect; however, we do not know whether the effect of EA on sensation and affect is parallel, or dissociated, interactional. In this study, we observed the effects of the anterior cingulate cortex (ACC) lesion and the primary somatosensory cortex (S1) activation on pain perception, pain-related affection, and neural oscillation in S1. ACC lesions did not affect pain perception but relieved pain-paired aversion. S1 activation increased pain perception and anxious behavior. EA can mitigate pain perception regardless of whether there is an ACC lesion. Chronic pain may increase the delta and theta band oscillatory activity in the S1 brain region and decrease the oscillatory activity in the alpha, beta, and gamma bands. EA intervention may inhibit the oscillatory activity of the alpha and beta bands. These results suggest that EA may mitigate chronic pain by relieving pain perception and reducing pain-related affection through different mechanisms. This evidence builds upon findings from previous studies of chronic pain and EA treatment.

## 1. Introduction

For a long time, it was generally believed that pain perception was well understood, while the pain related affection was yet unclear. Recently, the dissociation theory of pain sensation and affection was put forward [1, 2]. Many studies have indicated that chronic pain not only aggravates pain perception but also induces negative affective states (e.g., aversiveness, anxiety, depression, and anhedonia), sleep disorders, abnormal decision-making, and even suicide [3–7]. Approximately 20–30% of chronic pain patients have a negative affect [8, 9]. Pain and related affection influence each other

and demonstrate reciprocal causation. Experimental studies have indicated that emotional interventions, such as meditation, not only alleviate pain perception and negative affection but also have a beneficial protective effect on the brain's gray matter and pain regulation pathways [10, 11]. Mitigating chronic pain by modulating negative affect is a new research direction, and the mechanism of the interaction between chronic pain and negative affect remains unclear.

Pain processing involves multiple cortices. In the imaging studies of chronic pain in the human brain, researchers have found that the most frequently activated brain regions include the anterior cingulate cortex (ACC), the primary



somatosensory cortex (S1), insula cortex, prefrontal cortex, and thalamus, among others [12]. Most reports have made it clear that the ACC plays a key role in pain-related emotion. Some studies have shown that the ACC and amygdala are involved in the direct representation of the bodily state. Moreover, S1 and the insula are also related to emotion processing [13–16]. Researchers found that damage to the right S1 had subtle effects on emotional tasks and experiences [17, 18]. Brain regions associated with pain may interact with each other during the processing of pain information [19]. In response to this view, some studies have found that the integration of excitatory neurons in S1 originates from pain information from the peripheral nerves and is transmitted to other pain-related brain regions [20, 21]. Using the two-photon calcium ion imaging technology, it has been found that the spontaneous activity and sensory response in S1 and stimulation of S1 can increase chronic pain [22]. Inhibition of S1 activity can attenuate chronic pain. In addition, they found that the electrical response of the ACC to peripheral stimulation was consistent with the activity of S1 neurons. The inhibition of ACC activity can reduce the mechanical touch and pain, indicating that the excitatory neuronal activity in S1 increases responses to pain behavior by promoting activation of the ACC. Early studies on pain affection focused on psychological research; with the remarkable development of human imaging research, we have a deeper insight into the brain network which regulates pain and affection interaction. Pain perception and affection interact with each other. S1 and ACC are the main brain regions regulating pain and affection, respectively, so S1 and ACC may be closely correlated.

Electroacupuncture (EA) is an important treatment method developed based on improving traditional Chinese medicine. It has good analgesic effects and is widely used clinically [23, 24]. Related animal studies have shown that EA can increase the pain threshold and can effectively regulate pain-related emotion and cognitive behavior disorder [25, 26]. At the same time, in clinical research, EA not only alleviates various kinds of acute and chronic pain [27] but also significantly improves emotional symptoms [28]. However, whether the mechanism of the effect of EA on pain perception and pain-related affect is similar is still unclear.

Therefore, in the present study, we examined chronic inflammatory pain perception, pain-paired aversion, and pain-related anxiety in rats with and without an ACC lesion and S1 activated and synchronous neural oscillations in S1, to explore whether pain perception and negative affection influence each other based on ACC and/or S1, and if the effect of EA on chronic pain is a result of the effect of EA on negative affect.

## 2. Material and Methods

**2.1. Animals and Groups.** Seventy adult male Sprague-Dawley rats (Animal Experiment Center, Zhejiang Chinese Medical University, Zhejiang, China), weighing 250–280 g, were group-housed, with 3–4 rats per cage, in an environmentally controlled room (24–26°C, 40–50% humidity) and kept on a 12 h light-dark cycle with free access to rodent chow and water. The whole experiment was performed under

the guidelines of the International Association for the Study of Pain and the Institutional Animal Ethical Committee (IAEC).

The 50 rats were randomly divided into a blank control group (control group), complete Freund's adjuvant- (CFA-) induced chronic pain model group (model group), model+EA group, model+ACC lesion group (ACC lesion group), and ACC lesion+EA group (ACC lesion+EA group). This part was to explore whether pain perception and negative affect influence each other based on ACC.

The other 20 rats were divided into the control-hM3D-saline (C-hM3D-saline group) and the control-hM3D-clozapine-N-oxide (C-hM3D-CNO group). This part was to explore whether pain perception and negative affect influence each other based on S1.

### 2.2. Surgeries

**2.2.1. ACC Lesion.** The rats were anesthetized using urethane (1.2 g/kg i.p., Sigma-Aldrich, St. Louis, MO, USA), fixed to a stereotaxic apparatus (68025, RWD Life Science, China), and maintained at a constant body temperature of 37°C with real-time monitoring of temperature changes. After using iodine to disinfect the head of the rats, we cut the scalp and exposed the anterior fontanelle, posterior fontanelle, and frontal bone of the skull. A dental drill was used to drill holes in the surface of the rat skull, and one cranial nail was fixed on each side with dental cement. According to *The Rat Brain in Stereotaxic Coordinates* by Paxinos and Watson, the electrodes were slowly inserted into the ACC using a stereotaxic apparatus (+2.7 mm rostrocaudal, +1 mm mediolateral, and 2.0 mm dorsoventral). The biaxial electrode in the ACC was connected to the lesion-making device; 1 mA direct current was supplied for 60 s to create the lesion. After the surgery, the rats were rested for a week.

**2.2.2. S1 Electrode Implantation.** To record the electrophysiological signals, we implanted array electrodes in S1. The pre-operative procedure was the same as that for an ACC lesion surgery. The recording electrode array was positioned according to the rat brain atlas (-1.32 mm rostrocaudal, +2.5 mm mediolateral, and 2.35 mm dorsoventral).

**2.3. Electroacupuncture Treatment.** The model+EA and lesion+EA groups received EA intervention from the second day to the fourteenth day after model induction using the Master-9 electric pulse stimulator made in USA, seven times, every other day. The fine needle was 0.25 mm in diameter and 13 mm in length. The EA treatment was performed at bilateral Housanli acupoints and the reference electrode (1 cm inferior to the Housanli acupoint); the following stimulation parameters were used: frequency, 2/100 Hz; duration, 30 min; and intensity range, 0.5–1.5 mA (set at 0.5 mA initially and increased by 0.5 mA every 10 min). The other groups were given constraints as EA but not EA treatment.

### 2.4. Behavioral Tests

**2.4.1. Paw Withdrawal Thresholds.** After the paw withdrawal threshold (PWT) was stable, the baseline PWT before model

induction and the mechanical pain threshold of rats at 26 h and day 16 (16 d) after model induction were measured, excluding those with an abnormal pain threshold before the experiment (pain threshold < 10 g or >40 g). The measurement method was using a dynamic plantar tactile instrument (model 37450; Ugo Basile, Comerio, Italy) following a previously described method [29].

**2.4.2. Conditioned Place Aversion Testing.** The CFA-induced pain-paired aversive behavior was tested using a modified conditioned place aversion (CPA) paradigm. Rats in each group were free to move and train in two equally sized cabinets (A and B, each sized 35 cm × 28 cm × 45 cm), with a removable and installable baffle between the two cabinets. The walls of the two cabinets were composed of wallpaper strips of varying widths (3 cm vs. 9 cm) and colors (black vs. white). The bottom of the apparatus was hollowed out and could be placed on a pain measuring rack. A camera was installed above the apparatus and connected to the animal video tracking system software to adjust the video picture to facilitate subsequent tracking and recording. The surrounding environment (temperature, 24–25°C; humidity, 40–60%; noise, <40 dB) before the experiment was controlled carefully, thus maintaining a quiet environment. The modified CPA paradigm was divided into three parts. First, on the free behavior day, the baffle between two cabinets was removed, and the rats were allowed to move freely in both cabinets for 30 min (a 1 min preparatory period was given and not included in the final data). The retention time of the rats spent in cabinet A and cabinet B was recorded. The conditional and nonconditional boxes of rats were randomly determined. Second, on the preconditioning day, the baffle was installed, and rats that had not undergone model induction were placed in the previously determined nonconditioned box for 30 min. Third, on the conditional day, the control group was injected with 50  $\mu$ l saline; the other four groups were injected with 50  $\mu$ l CFA. Two and twenty-six hours after model induction, the rats underwent mechanical plantar stimulation with a dynamic plantar tactile instrument (model 37450; Ugo Basile) as part of the conditioned training for 30 min. The rats were first placed in the conditioning cabinet for 5 min to adapt; the left foot of the rats was subjected to mechanical PWT testing (the methods and parameters were the same as the mechanical pain measurement) for 6–10 min. After PWT values were obtained, the control group was subjected to mechanical foot stimulation at  $(\text{PWT} \times 0.5)/5$  s (i.e., maximum stimulation is half of the PWT and is reached over 5 s). The number of times the rat lifted its foot during the 5 s period was recorded. Stimulation was performed once every min, and the number of foot lifts within 20 min was recorded. The mechanical pain threshold was measured using  $(\text{PWT} \times 1.5)/5$  s for the last 20 min in the other groups (i.e., the maximum stimulation was 1.5 times the PWT); the remaining procedures were performed the same as those in the control group. Fourth, on the second, ninth, and fifteenth postconditioning days after model induction, the rats were placed in open cabinets freely for 30 min. The activity time in each cabinet was recorded.

Aversive behavior was calculated using the CPA score, which is the difference in time between the test day (2 d, 9 d, and 15 d) and baseline for the pain-paired cabinet. The formula was as follows:  $T_{\text{score}} = T_{\text{preconditioning}} - T_{\text{postconditioning}}$ .

At the beginning of the experiment, the rat was gently lifted by the tail and placed in the center of the two cabinets. After a 1 min acclimation period, the activity of the rat in the cabinets was monitored and observed using the Smart 3.0 software (Panlab, USA), and data were collected for 30 min. After each experiment, the apparatus was thoroughly scrubbed with 10% alcohol to eliminate feces and prevent residual odor from interfering with the activities of the next rat.

**2.5. Local Field Potentials (LFPs).** LFPs in S1 were recorded during the free period before and 2 h, 2 d, 9 d, and 15 d after modeling, using the implanted array electrode with a Cerebus neural signal processing system (Blackrock Microsystems, Salt Lake City, UT, USA). Behavioral tasks and LFP signals were linked using the ANY-maze interface system (Stoelting, CO, USA) to synchronously record behavioral monitoring and LFP signals. The extracellular LFPs in S1 were recorded using the array microelectrode embedded in the rat S1 with the Cerebus 128 multichannel in vivo recording system (Blackrock Microsystems, Salt Lake City, UT, USA). The LFP signal was amplified using a preamplifier ( $\times 300$ ), band-pass filtered at 0.3–250 Hz, and sampled at 1 kHz. After the signal acquisition, the LFP signal data collected from each channel in the S1 brain region were band-pass filtered and processed at 2–45 Hz through the NeuroExplorer 5.021 (NEX, Plexon Inc., USA) and MATLAB analysis software (MathWorks, Natick, MA, USA), and the average power spectral densities (PSD) of each group and the PSD percentage of each frequency band were compared.

**2.6. Open Field Testing.** A black Plexiglas chamber (100 cm × 100 cm × 50 cm) formed the apparatus, which was divided evenly into 16 small squares (25 × 25 cm/each). The four squares in the center were defined as the central areas and the other twelve as the peripheral areas. Before testing, the rats were put into the experimental environment for an hour to adapt to it. Then, the rats were gently placed into the central areas with their heads facing away from the experimenter. The behavior was videotaped for 5 min by the Smart 3.0 system (Panlab, USA). The whole apparatus was wiped with 75% ethanol before each trail.

**2.7. Chemical Genetic Method.** The preoperative procedure was the same as that for the S1 electrode implantation. Then, viruses were injected into S1, rAAV-hSyn-hM3D(Gq)-EGFP-WPRE-pA (virus titer:  $2.79 \times 10^{12}$  vg/ml, 60 nl/min, 350 nl/injection; BrainVTA, Wuhan, China). Thirty minutes before the behavioral assessment, the designer drug CNO (10 mg/kg, i.p.; C0832, Sigma-Aldrich, St. Louis, MO, USA) was administered. The same volume of saline was administered to the C-hM3D-saline group.

**2.8. Data Analysis.** The experimental data are presented as the mean  $\pm$  standard error of the mean. One-way or two-

way repeated measures analysis of variance (rm-ANOVA) with the Bonferroni post hoc analysis was used when the variances were equal. One-way ANOVA was used for multi-group comparison, and the LSD test was used for two-to-two comparisons between groups. In the case of an uneven variance, Dunnett's T3 test was used for two-to-two comparisons between groups. Results were considered statistically significant at  $P < 0.05$ .

### 3. Results

**3.1. Pain Perception.** As shown in Figure 1, there was no significant difference before CFA injection between the control, model, model+EA, ACC lesion, and ACC lesion+EA groups (two-way rm-ANOVA;  $P > 0.05$ ). Compared with the control group 26 h after CFA injection, the PWTs significantly decreased in the other four groups ( $P < 0.05$ , Bonferroni test). On 16 d, compared with that in the control group, the PWTs in the model group and ACC lesion group were significantly lower ( $P < 0.05$ , Bonferroni test). Compared with that in the model group, the PWTs in the model+EA group and ACC lesion+EA group were significantly higher ( $P < 0.05$ , Bonferroni test) (Figure 1).

We also detected the lifted foot times of the rats' left foot after CFA injection. Compared with that in the control group, the lifted foot times in the four groups was significantly higher at 2 h, 26 h, and 16 d ( $P < 0.05$ , Bonferroni test). Compared with that in the model group at 16 d, the shrinkage sufficient times in the model+EA group and ACC lesion+EA group were significantly lower ( $P < 0.05$ , Bonferroni test). The ACC lesion+EA group had a significantly lower lifted foot times than the ACC lesion group ( $P < 0.01$ , Bonferroni test) (Figure 2).

Then, we measured the PWTs in rats after the activation of S1 by the chemical genetic method. Compared with the C-hM3D-saline group, the PWTs in C-hM3D-CNO rats were significantly decreased ( $P < 0.05$ , Bonferroni test) (Figure 3).

### 3.2. Pain-Related Emotional Behavior

**3.2.1. Pain-Related Emotional Behavior after an ACC Lesion.** The experimental results showed that there was no significant difference between the five groups of the rats in the conditioning cabinet or nonconditioning cabinet before the injection of CFA. On 2 d, the CPA scores in the model and model+EA groups were significantly higher than those in the control group ( $P < 0.05$ , Bonferroni test). Compared with the CPA score in the model group, the ACC lesion group and ACC lesion+EA group had significantly lower values ( $P < 0.05$ , Bonferroni test). Nine days after CFA injection, compared with that in the control group, the CPA score in the model and model+EA groups was significantly higher ( $P < 0.05$ , Bonferroni test); compared with the model group, the ACC lesion and ACC lesion+EA groups had significantly lower scores ( $P < 0.05$ , Bonferroni test); compared with the model+EA group, the ACC lesion+EA group had significantly lower scores ( $P < 0.01$ ). Fifteen days after CFA injection, compared with the CPA score in the control group, the model group had a significantly higher

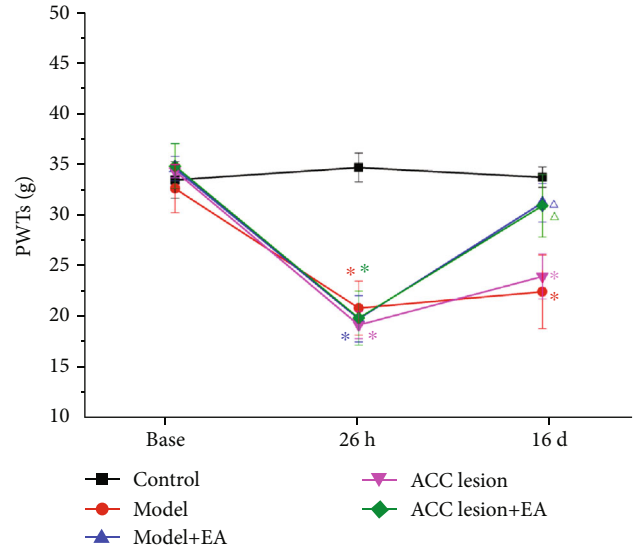


FIGURE 1: PWT of the ipsilateral (left) hind paw in each group. \* $P < 0.05$  compared with the control group.  $\Delta P < 0.05$  compared with the model group.  $n = 8$ . Abbreviations: PWT: paw withdrawal threshold; EA: electroacupuncture; ACC: anterior cingulate cortex.

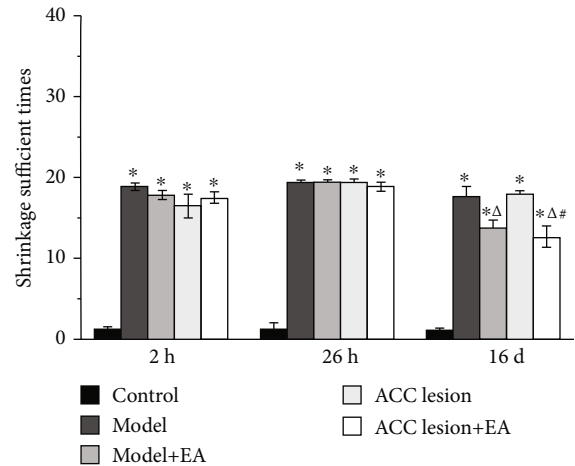


FIGURE 2: The shrinkage sufficient times for the left hind paw in each group. \* $P < 0.05$  compared with the control group.  $\Delta P < 0.05$  compared with the model group.  $\#P < 0.05$  compared with the ACC lesion group. Abbreviations: EA: electroacupuncture; ACC: anterior cingulate cortex.

score ( $P < 0.05$ , Bonferroni test), but the model+EA group showed no significant difference. Compared with the model group, the ACC lesion group had a significantly lower score ( $P < 0.01$ , Bonferroni test). There was no significant difference in the score between the model+EA group and ACC lesion+EA group (Figure 4).

**3.2.2. Pain-Related Emotional Behavior after S1 Activation.** The results showed that the time in the center of the C-hM3D-CNO rats was significantly increased in the open field testing (OFT) ( $P < 0.05$ , Bonferroni test), compared with the C-hM3D-saline group (Figure 5).



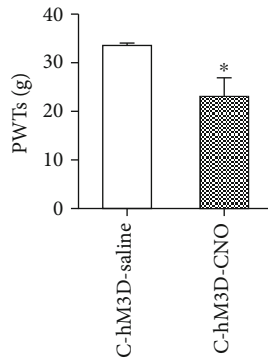


FIGURE 3: Paw withdrawal thresholds decreased by the specific activation of S1 glutamergic neurons in the control rats. \* $P < 0.05$  compared with the C-hM3D-saline group. Abbreviations: PWT: paw withdrawal threshold; S1: primary somatosensory cortex.

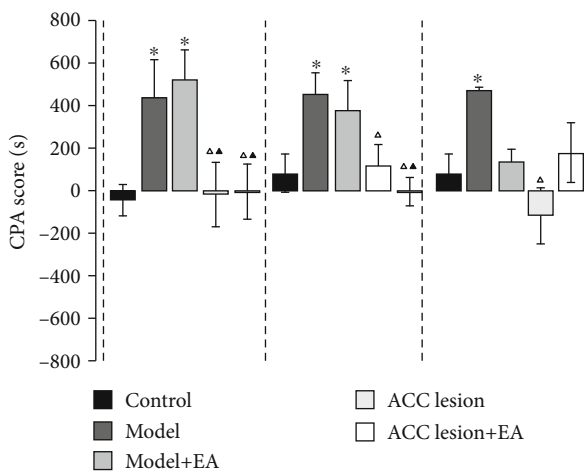


FIGURE 4: Values of aversive behavioral testing. \* $P < 0.05$  compared with the control group. ▲ $P < 0.05$  compared with the model group. ▲▲ $P < 0.05$  compared with the model+EA group. Abbreviations: CPA: conditioned place aversion; EA: electroacupuncture; ACC: anterior cingulate cortex.

**3.3. LFP Signals in S1.** Different frequency bands in the S1 brain activity of the model group changed at different time points relative to those in the model group. Compared with the baseline, the delta frequency PSD was significantly higher at 2 d, 9 d, and 15 d (one-way rm-ANOVA,  $P < 0.01$ ). Compared with the baseline value, the theta band PSD two days after CFA injection was significantly higher (one-way rm-ANOVA,  $P < 0.05$ ); PSDs at 9 d and 15 d were significantly lower than those at 2 d (one-way rm-ANOVA,  $P < 0.05$ ). Compared with the values at baseline and 2 d, the PSDs of the alpha, beta, and gamma bands were significantly lower at 9 d and 15 d (one-way rm-ANOVA,  $P < 0.05$ ) (Figure 6).

In the model+EA group, the delta band in the S1 brain region at different time points was significantly different. Compared with that at the baseline, the delta band PSD was significantly lower at 2 d (one-way rm-ANOVA,  $P < 0.05$ ). Compared with that at 2 d, the PSD of the delta band was significantly higher at 15 d (one-way rm-ANOVA,  $P < 0.05$ ). For the theta band, compared with that at the baseline, the

PSD was significantly higher at 2 d (one-way rm-ANOVA,  $P < 0.05$ ); the value at 15 d was significantly lower than that at 2 d (one-way rm-ANOVA,  $P < 0.05$ ). The gamma band PSD was significantly lower at 9 d and 15 d compared with that at 2 d (one-way rm-ANOVA,  $P < 0.05$ ). In addition, the alpha and beta bands were not significantly different at any of the time points (Figure 7).

Furthermore, we analyzed the alpha and beta bands for changes in the S1 brain region at different times. There was no significant difference in the PSD of each band at the baseline. Compared with that in the control group, the PSD of the alpha band in the model+EA group was significantly lower at 2 d (one-way rm-ANOVA,  $P < 0.01$ ), and the PSD of the model group was significantly lower at 9 d and 15 d after CFA injection (one-way rm-ANOVA,  $P < 0.05$ ). Compared with that in the model group, the alpha band PSD in the model+EA group was significantly higher at 9 d and 15 d (one-way rm-ANOVA,  $P < 0.05$ ) (Figure 8(a)).

Compared with that in the control group, the PSD percentage of the beta band in the model group and model+EA group was significantly lower at 2 d, 9 d, and 15 d after CFA injection (one-way rm-ANOVA  $P < 0.01$ ). Compared with that in the model group, the PSD percentage of the beta band in the model+EA group was significantly higher at 9 d and 15 d (one-way rm-ANOVA,  $P < 0.01$ ) (Figure 8(b)).

## 4. Discussion

The results showed that ACC lesions have no effect on pain perception, but they relieve pain-paired aversion. EA can mitigate pain perception, regardless of the presence or absence of an ACC lesion. However, ACC lesions and EA have a similar effect on pain-related aversion. S1 activation induced lower pain threshold and anxiety disorder. CFA-induced chronic pain may increase the delta and theta band oscillatory activity in S1 and decrease the oscillatory activity of the alpha, beta, and gamma bands. EA intervention may inhibit the oscillatory activity of the alpha and beta bands. These results suggest that ACC is involved in the dissociation of pain perception and pain-related affection, while S1 may be related to the interaction of pain perception and pain-related negative affection. EA may improve pain-related aversion by influencing ACC activity and regulating theta power in S1.

**4.1. ACC Lesion Induced Changes in Pain-Related Aversion in CFA Rats.** ACC is a highly heterogeneous cortical region that connects the lateral and medial pain pathways, providing a physiological basis for the interaction between pain and affect [30]. Studies have found that synaptic transmission and plasticity in ACC play a vital role in pain, fear, learning, and memory. Joshua et al. were the first to propose the use of conditioned position aversion to study behavioral responses to pain-related emotions and successfully established the formalin-induced CPA (F-CPA) model, laying a foundation for studying the mechanism of negative emotions caused by pain [31]. Subsequently, Joshua et al. showed, for the first time, that rostral ACC (rACC) damage can weaken CPA. Researchers [32] further proved that the ACC was a brain

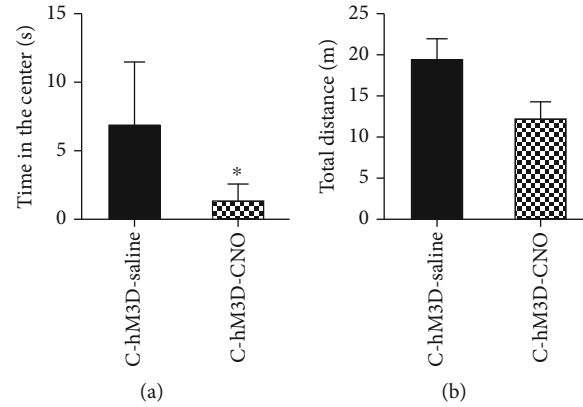


FIGURE 5: Anxiety disorders induced by the specific activation of S1 glutaminergic neurons in control rats. (a) Time in the center. (b) Total distance. \* $P < 0.05$  compared with C-hM3D-saline group. Abbreviations: C: control; CNO: clozapine-N-oxide.

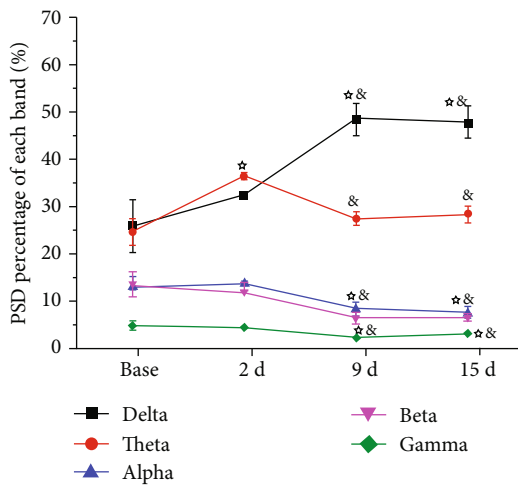


FIGURE 6: Synchronous LFPs observed during nociceptive behavioral testing in the model group. \* $P < 0.05$  compared with the baseline.  $\&$   $P < 0.05$  compared with 2 d. Abbreviations: PSD: power spectral density; LFP: local field potential.

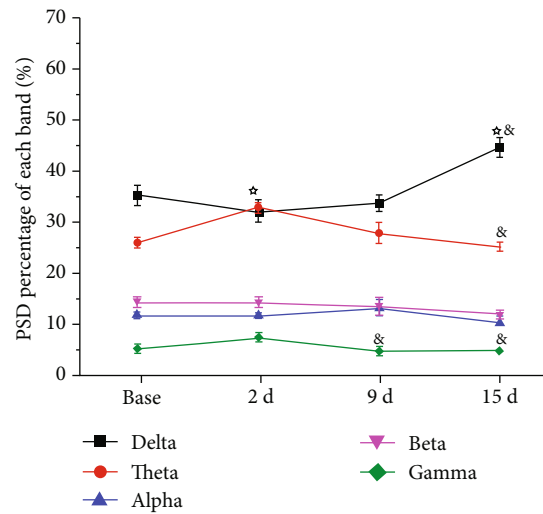


FIGURE 7: Synchronous LFPs observed during nociceptive behavioral testing in the model+EA group. \* $P < 0.05$  compared with the baseline.  $\&$   $P < 0.05$  compared with 2 d. Five frequency band intervals were considered: delta (2-4 Hz), theta (4-9 Hz), alpha (9-15 Hz), beta (15-30 Hz), and gamma (30-45 Hz). Abbreviations: PSD: power spectral density; LFP: local field potential.

region closely linked to pain-related emotions. It has been found that the long-term enhancement of ACC activity may be one of the mechanisms of persistent emotional change in patients with chronic pain caused by nerve injury or peripheral inflammation [33–36]. Our data showed that the PWT of the model group was significantly lower than that of the control group at 16 d. The group with the ACC lesion did not differ from the control group at 16 d. However, the pain-related aversion developed from 2 d to 16 d, and there was no manifestation of aversion after ACC lesioning. This suggests that pain perception and pain-related aversion are separate process in some specific brain areas, and ACC plays a key role in pain-related aversion.

Notably, pain-related aversion could be triggered easily and persisted for 16 days in this study. A prior study reported that neural activity in the ACC correlated with noxious intensities, and modulation of ACC neurons can regulate the aversive response to acute pain [37]. The manifestation of aversion enhances the progress of the primary disease

and chronicity. It is necessary to inhibit the earlier pain-paired aversion behavior by controlling ACC activity.

**4.2. After EA, ACC Lesion Induced Changes in Pain Aversion in CFA Rats.** Compared with that in the model group, the PWT of the EA group and ACC lesion+EA group was significantly higher at 16 d; however, the ACC lesion showed no significant difference. This means that EA can relieve pain perception, and the effect is not the result of the ACC activity. The aversive behavior was improved in the EA, ACC lesion, and ACC lesion+EA groups relative to that in the model group. It suggests that EA can improve pain-related aversion, and the effect is similar in the presence of an ACC lesion. Remarkably, the effect of EA on pain-paired aversion gradually increased from 9 d to 16 d; thus, the cumulative effect of EA on pain-paired aversion is pivotal. EA can effectively



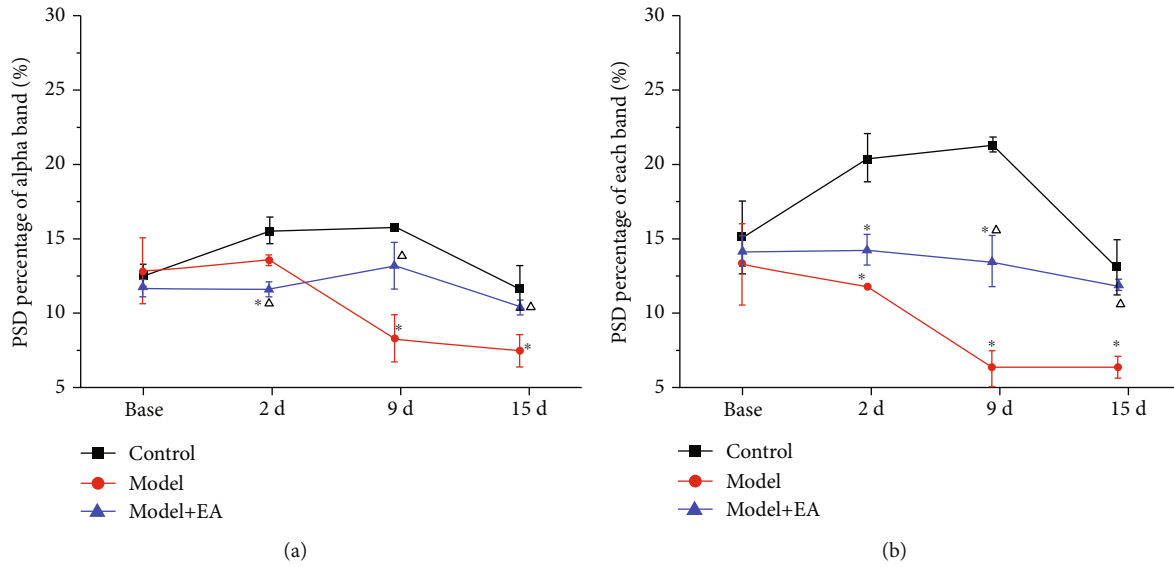


FIGURE 8: The effect of EA on the PSD percentage of the alpha (a) and beta (b) bands in the S1 of CFA rats. \* $P < 0.05$  compared with the control group.  $^{\wedge}P < 0.05$  compared with the model group. Abbreviations: PSD: power spectral density; EA: electroacupuncture; S1: primary somatosensory cortex; CFA: complete Freund's adjuvant.

relieve the negative emotions associated with pain, in which the ACC may be involved in the EA effect.

The effect in the ACC lesion group was different from that in the ACC lesion+EA group at 9 d. This suggests that EA may regulate pain-paired aversion through other mechanisms barring the ACC activity. As a higher structure, the ACC may integrate affective signals directly or indirectly through the projection of other regions, such as S1, the amygdala, insular cortex, medial prefrontal cortex, and hippocampus, among others [38]. The ACC has strong connections to multiple brain regions, which overlap with the regions that regulate pain [39]. The extensive connections prove that an interaction exists between pain perception and pain-related aversion. Human clinical studies have found [40] that surgical removal of ACC not only alleviates various pain-related feelings but also significantly alleviates depression, anxiety, and other emotions caused by pain in patients. According to our results, we did not find an influence of ACC lesions on pain perception, which demonstrates that pain perception and pain-paired aversion are separate processes.

**4.3. Changes in S1 Neural Oscillations in Model Rats and after EA Intervention.** Pain is a perception that is affected by an immense brain regional network, which involves multiple brain regions. The coding of various information, such as cognition, memory, and emotion, by the brain requires transmission and processing in multiple brain regions, while the neural oscillation produced by the brain can closely associate the activity of neurons in each brain region, which can strengthen interregional synergistic operations and information processing efficiency. It has been discovered that neural oscillation is associated with five frequency bands, comprising delta (2-4 Hz), theta (4-9 Hz), alpha (9-15 Hz), beta (15-30 Hz), and gamma (30-45 Hz).

In this study, there was no significant difference in the neural oscillation between various frequency bands in S1 before model induction between the groups. However, on the second day after constructing the chronic pain model using CFA injection, the PSD of the theta frequency band was remarkably enhanced, while that of the beta and gamma frequency bands was markedly reduced. On the ninth day after model induction, the PSD of the delta frequency band increased to a peak, while that of the alpha, beta, and gamma frequency bands decreased. This finding suggests that the delta frequency band might not be involved in the early formation of pain perception but gradually increases during the development of chronic pain. The PSD of the theta frequency band was dramatically enhanced immediately after the second day of model induction, which was gradually reduced to the level before model induction at 9 d and 15 d after model induction, indicating that the theta frequency band might participate in related information processing during the early formation of pain perception; however, the influence of the theta frequency band gradually reduced with the development of chronic inflammatory pain. Moreover, the PSD of the alpha, beta, and gamma frequency bands showed an apparent decreasing trend after model induction, demonstrating that the reduction in rhythmic oscillation activity of these three frequency bands in S1 was closely correlated with the formation of chronic pain.

It has been reported that reinforcement learning and feedback locking reward motivation are related to specific activity in the delta frequency band [41]. The theta frequency band is generally regarded as the neural oscillation frequency band that is related to pain perception, cognition, and memory [40, 42, 43]. The alpha frequency band is related to spontaneous and top-down visual-spatial allocation, which is markedly enhanced when attention is completely transferred but is gradually reduced when attention is

balanced across the field of view [44]. The beta frequency band plays a distinct role during the perception process, and a marked reduction in the beta frequency band energy can be detected during the brain activity of perception conversion [45]. The gamma frequency band is also closely related to pain [46]. In our results, EA could reverse the decrease of PSD in the alpha and beta bands. Some studies have reported that the effect of EA on chronic pain is through regulating pain perception and pain-paired aversion.

The effect of EA in treating various pain-related diseases has been extensively recognized, and its analgesic effect can last for a long time after treatment. Neuroimaging research has indicated that the application of acupuncture or EA may induce extensive [47, 48] that mainly participate in the overlapping neural networks of pain transmission and perception. Moreover, acupuncture can also directly affect electroencephalographic activity in both healthy human populations and animals [49, 50]. EA intervention can reduce the amplitude of high-frequency band activity in rats with postoperative pain (especially for that of the beta frequency band) and reverse the increased strength of coupling of the crossover frequency between the beta and low-frequency band [51], demonstrating that EA may exert analgesia by regulating rhythmic intracerebral neural oscillation.

## 5. Conclusion

Our research reveals that ACC is involved in the dissociation of pain perception and pain-related affection, while S1 may be related to the interaction of pain perception and pain-related negative affection. EA may improve pain-related affection by influencing the ACC activity and regulating theta power in S1. These results suggest that EA may mitigate chronic pain by relieving pain perception and improving pain-related affection through different mechanisms. This evidence builds upon findings from previous studies of chronic pain and EA treatment.

## Data Availability

The figure types of the data used to support the findings of this study are included within the supplementary information file(s).

## Conflicts of Interest

The authors have no conflicts of interest to declare.

## Authors' Contributions

Yan Shi and Shujing Yao contributed equally to this work as co-first authors. Xiaomei Shao and Jianqiao Fang contributed equally to this work as co-corresponding authors. Xiaomei Shao and Jianqiao Fang designed the experimental protocols. Yan Shi and Zui Shen performed data analysis and ACC lesioning. Lijiao She and Yilin Zhu made the electrode arrays and performed the implantation surgeries. Jing Sun and Shujing Yao performed paw withdrawal threshold testing. Yuanyuan Wu and Yingling Xu performed the elevated zero

test. Zemin Wu and Yongliang Jiang performed the recording of LFPs. Junying Du performed data analysis. Boyi Liu and Yi Liang performed manuscript writing.

## Acknowledgments

This study was supported by the National Natural Science Foundation of China (81873360, 81804183, and 81704141), the Basic Public Welfare Research of Zhejiang Province (LY19H270007), and the Experimental Animal Science and Technology Project of Zhejiang Province (2018C37083).

## References

- [1] H. Haller, H. Cramer, R. Lauche, and G. Dobos, "Somatoform disorders and medically unexplained symptoms in primary care," *Deutsches Ärzteblatt International*, vol. 112, no. 16, pp. 279–287, 2015.
- [2] Z. Y. Tao, P. X. Wang, S. Q. Wei, R. J. Traub, J. F. Li, and D. Y. Cao, "The role of descending pain modulation in chronic primary pain: potential application of drugs targeting serotonergic system," *Neural Plasticity*, vol. 2019, Article ID 1389296, 16 pages, 2019.
- [3] S. E. E. Mills, K. P. Nicolson, and B. H. Smith, "Chronic pain: a review of its epidemiology and associated factors in population-based studies," *British Journal of Anaesthesia*, vol. 123, no. 2, pp. e273–e283, 2019.
- [4] I. Elbinoune, B. Amine, S. Shyen, S. Gueddari, R. Abouqal, and N. Hajjaj-Hassouni, "Chronic neck pain and anxiety-depression: prevalence and associated risk factors," *The Pan African Medical Journal*, vol. 24, p. 89, 2016.
- [5] E. L. Zale and J. W. Ditre, "Pain-related fear, disability, and the fear-avoidance model of chronic pain," *Current Opinion in Psychology*, vol. 5, pp. 24–30, 2015.
- [6] E. Navratilova, K. Morimura, J. Y. Xie, C. W. Atcherley, M. H. Ossipov, and F. Porreca, "Positive emotions and brain reward circuits in chronic pain," *The Journal of Comparative Neurology*, vol. 524, no. 8, pp. 1646–1652, 2016.
- [7] M. Keilani, R. Crevenna, and T. E. Dorner, "Sleep quality in subjects suffering from chronic pain," *Wiener Klinische Wochenschrift*, vol. 130, no. 1–2, pp. 31–36, 2018.
- [8] R. R. Edwards, R. H. Dworkin, M. D. Sullivan, D. C. Turk, and A. D. Wasan, "The role of psychosocial processes in the development and maintenance of chronic pain," *The Journal of Pain*, vol. 17, Supplement 9, pp. T70–T92, 2016.
- [9] H. Ahn, M. Weaver, D. Lyon, E. Choi, and R. B. Fillingim, "Depression and pain in Asian and white Americans with knee osteoarthritis," *The Journal of Pain*, vol. 18, no. 10, pp. 1229–1236, 2017.
- [10] B. K. Holzel, J. Carmody, M. Vangel et al., "Mindfulness practice leads to increases in regional brain gray matter density," *Psychiatry Research*, vol. 191, no. 1, pp. 36–43, 2011.
- [11] A. Lutz, D. R. McFarlin, D. M. Perlman, T. V. Salomons, and R. J. Davidson, "Altered anterior insula activation during anticipation and experience of painful stimuli in expert meditators," *NeuroImage*, vol. 64, pp. 538–546, 2013.
- [12] C. M. Kaplan, A. Schrepf, D. Vatansever et al., "Functional and neurochemical disruptions of brain hub topology in chronic pain," *Pain*, vol. 160, no. 4, pp. 973–983, 2019.
- [13] C. A. Webb, E. A. Olson, W. D. S. Killgore, D. A. Pizzagalli, S. L. Rauch, and I. M. Rosso, "Rostral anterior cingulate cortex

- morphology predicts treatment response to internet-based Cognitive Behavioral Therapy for depression,” *Biological Psychiatry: Cognitive Neuroscience and Neuroimaging*, vol. 3, no. 3, pp. 255–262, 2018.
- [14] A. L. Bauernfeind, A. A. de Sousa, T. Avasthi et al., “A volumetric comparison of the insular cortex and its subregions in primates,” *Journal of Human Evolution*, vol. 64, no. 4, pp. 263–279, 2013.
- [15] S. Wang, R. Yu, J. M. Tyszka et al., “The human amygdala parametrically encodes the intensity of specific facial emotions and their categorical ambiguity,” *Nature Communications*, vol. 8, no. 1, article 14821, 2017.
- [16] E. Kropf, S. K. Syan, L. Minuzzi, and B. N. Frey, “From anatomy to function: the role of the somatosensory cortex in emotional regulation,” *Braz J Psychiatry*, vol. 41, no. 3, pp. 261–269, 2019.
- [17] P. A. Kragel and K. S. LaBar, “Somatosensory representations link the perception of emotional expressions and sensory experience,” *eNeuro*, vol. 3, no. 2, 2016.
- [18] L. Nummenmaa, E. Glerean, R. Hari, and J. K. Hietanen, “Bodily maps of emotions,” *Proceedings of the National Academy of Sciences of the United States of America*, vol. 111, no. 2, pp. 646–651, 2014.
- [19] M. Moayedi, T. V. Salomons, and L. Y. Atlas, “Pain neuroimaging in humans: a primer for beginners and non-imagers,” *The Journal of Pain*, vol. 19, no. 9, pp. 961.e1–961.e21, 2018.
- [20] K. Fox, “Experience-dependent plasticity mechanisms for neural rehabilitation in somatosensory cortex,” *Philosophical Transactions of the Royal Society of London Series B, Biological Sciences*, vol. 364, no. 1515, pp. 369–381, 2009.
- [21] H.-H. Liu, D. B. McClatchy, L. Schiapparelli, W. Shen, J. R. Yates III, and H. T. Cline, “Role of the visual experience-dependent nascent proteome in neuronal plasticity,” *Elife*, vol. 7, 2018.
- [22] K. Eto, H. Wake, M. Watanabe et al., “Inter-regional contribution of enhanced activity of the primary somatosensory cortex to the anterior cingulate cortex accelerates chronic pain behavior,” *The Journal of Neuroscience*, vol. 31, no. 21, pp. 7631–7636, 2011.
- [23] C. A. Paley and M. I. Johnson, “Acupuncture for the relief of chronic pain: a synthesis of systematic reviews,” *Medicina*, vol. 56, no. 1, p. 6, 2020.
- [24] I. S. Lee, H. Lee, Y. H. Chen, and Y. Chae, “Bibliometric analysis of research assessing the use of acupuncture for pain treatment over the past 20 years,” *Journal of Pain Research*, vol. 13, pp. 367–376, 2020.
- [25] J.-Q. Fang, J. Y. du, Y. Liang, and J. F. Fang, “Intervention of electroacupuncture on spinal p38 MAPK/ATF-2/VR-1 pathway in treating inflammatory pain induced by CFA in rats,” *Molecular Pain*, vol. 9, no. 13, pp. 1744–8069-9-13–1744-8069-9-14, 2013.
- [26] Y. Wu, Y. Jiang, X. Shao et al., “Proteomics analysis of the amygdala in rats with CFA-induced pain aversion with electro-acupuncture stimulation,” *Journal of Pain Research*, vol. 12, pp. 3067–3078, 2019.
- [27] Z. Y. Ju, K. Wang, H. S. Cui et al., “Acupuncture for neuropathic pain in adults,” *Cochrane Database of Systematic Reviews*, vol. 12, article CD012057, 2017.
- [28] C. A. Smith, M. Armour, M. S. Lee, L. Q. Wang, and P. J. Hay, “Acupuncture for depression,” *Cochrane Database of Systematic Reviews*, vol. 3, article CD004046, 2018.
- [29] Z. Shen, Y. Zhu, B. Liu et al., “Effects of electroacupuncture on pain memory-related behaviors and synchronous neural oscillations in the rostral anterior cingulate cortex in freely moving rats,” *Neural Plasticity*, vol. 2019, Article ID 2057308, 12 pages, 2019.
- [30] H. Zhou, Q. Zhang, E. Martinez et al., “Ketamine reduces aversion in rodent pain models by suppressing hyperactivity of the anterior cingulate cortex,” *Nature Communications*, vol. 9, no. 1, article 3751, 2018.
- [31] J. P. Johansen, H. L. Fields, and B. H. Manning, “The affective component of pain in rodents direct evidence for a contribution of the anterior cingulate cortex,” *Proceedings of the National Academy of Sciences of the United States of America*, vol. 98, no. 14, pp. 8077–8082, 2001.
- [32] T. T. Li, W. H. Ren, X. Xiao et al., “NMDA NR2A and NR2B receptors in the rostral anterior cingulate cortex contribute to pain-related aversion in male rats,” *Pain*, vol. 146, no. 1, pp. 183–193, 2009.
- [33] H. Toyoda, M. G. Zhao, and M. Zhuo, “Enhanced quantal release of excitatory transmitter in anterior cingulate cortex of adult mice with chronic pain,” *Molecular Pain*, vol. 5, p. 4, 2009.
- [34] M. Zhuo, “Long-term potentiation in the anterior cingulate cortex and chronic pain,” *Philosophical Transactions of the Royal Society B: Biological Sciences*, vol. 369, no. 1633, article 20130146, 2014.
- [35] J. Sellmeijer, V. Mathis, S. Hugel et al., “Hyperactivity of anterior cingulate cortex areas 24a/24b drives chronic pain-induced anxiodepressive-like consequences,” *The Journal of Neuroscience*, vol. 38, no. 12, pp. 3102–3115, 2018.
- [36] Z. Chen, X. Shen, L. Huang, H. Wu, and M. Zhang, “Membrane potential synchrony of neurons in anterior cingulate cortex plays a pivotal role in generation of neuropathic pain,” *Scientific Reports*, vol. 8, no. 1, article 1691, 2018.
- [37] Q. Zhang, T. Manders, A. P. Tong et al., “Chronic pain induces generalized enhancement of aversion,” *Elife*, vol. 6, 2017.
- [38] S. Gu, F. Wang, C. Cao, E. Wu, Y. Y. Tang, and J. H. Huang, “An integrative way for studying neural basis of basic emotions with fMRI,” *Frontiers in Neuroscience*, vol. 13, p. 628, 2019.
- [39] M. C. Bushnell, M. Ceko, and L. A. Low, “Cognitive and emotional control of pain and its disruption in chronic pain,” *Nature Reviews Neuroscience*, vol. 14, no. 7, pp. 502–511, 2013.
- [40] M. J. Euler, T. J. Wiltshire, M. A. Niermeyer, and J. E. Butner, “Working memory performance inversely predicts spontaneous delta and theta-band scaling relations,” *Brain Research*, vol. 1637, pp. 22–33, 2016.
- [41] J. F. Cavanagh, “Cortical delta activity reflects reward prediction error and related behavioral adjustments, but at different times,” *NeuroImage*, vol. 110, pp. 205–216, 2015.
- [42] J. F. Cavanagh and M. J. Frank, “Frontal theta as a mechanism for cognitive control,” *Trends in Cognitive Sciences*, vol. 18, no. 8, pp. 414–421, 2014.
- [43] Y. Huang, L. Chen, and H. Luo, “Behavioral oscillation in priming: competing perceptual predictions conveyed in alternating theta-band rhythms,” *The Journal of Neuroscience*, vol. 35, no. 6, pp. 2830–2837, 2015.
- [44] I. Dombrowe and C. C. Hilgetag, “Occipitoparietal alpha-band responses to the graded allocation of top-down spatial attention,” *Journal of Neurophysiology*, vol. 112, no. 6, pp. 1307–1316, 2014.
- [45] T. Minami, Y. Noritake, and S. Nakachi, “Decreased beta-band activity is correlated with disambiguation of hidden figures,” *Neuropsychologia*, vol. 56, pp. 9–16, 2014.

- [46] J. H. Kim, J. H. Chien, C. C. Liu, and F. A. Lenz, "Painful cutaneous laser stimuli induce event-related gamma-band activity in the lateral thalamus of humans," *Journal of Neurophysiology*, vol. 113, no. 5, pp. 1564–1573, 2015.
- [47] G. T. Lewith, P. J. White, and J. Pariente, "Investigating acupuncture using brain imaging techniques: the current state of play," *Evidence-Based Complementary and Alternative Medicine*, vol. 2, no. 3, pp. 315–319, 2005.
- [48] J. Fang, X. Wang, H. Liu et al., "The Limbic-Prefrontal Network Modulated by Electroacupuncture at CV4 and CV12," *Evidence-Based Complementary and Alternative Medicine*, vol. 2012, Article ID 515893, 2012.
- [49] S. F. Hsu, C. Y. Chen, M. D. Ke, C. H. Huang, Y. T. Sun, and J. G. Lin, "Variations of brain activities of acupuncture to TE5 of left hand in normal subjects," *The American Journal of Chinese Medicine*, vol. 39, no. 4, pp. 673–686, 2011.
- [50] G. Litscher, "Ten Years Evidence-based High-Tech Acupuncture Part 3: A Short Review of Animal Experiments," *Evidence-Based Complementary and Alternative Medicine*, vol. 7, no. 2, pp. 151–155, 2010.
- [51] J. Wang, J. Wang, X. Li et al., "Modulation of brain electroencephalography oscillations by electroacupuncture in a rat model of postincisional pain," *Evidence-Based Complementary and Alternative Medicine*, vol. 2013, Article ID 160357, 11 pages, 2013.

## Research Article

# Electroacupuncture Pretreatment Elicits Tolerance to Cerebral Ischemia/Reperfusion through Inhibition of the GluN2B/m-Calpain/p38 MAPK Proapoptotic Pathway

Bao-yu Zhang,<sup>1</sup> Guan-ran Wang,<sup>2</sup> Wen-hua Ning,<sup>1</sup> Jian Liu,<sup>1,3,4</sup> Sha Yang,<sup>1,3,5</sup> Yan Shen,<sup>1,3,5</sup> Yang Wang,<sup>1,6</sup> Meng-xiong Zhao,<sup>1</sup> and Li Li <sup>1,3,7</sup>

<sup>1</sup>First Teaching Hospital of Tianjin University of Traditional Chinese Medicine, Tianjin, China

<sup>2</sup>Heilongjiang University of Chinese Medicine, Harbin, China

<sup>3</sup>National Clinical Research Center for Chinese Medicine Acupuncture and Moxibustion, Tianjin, China

<sup>4</sup>Key Laboratory of Cerebrovascular Disease Acupuncture Therapy of State Administration of Traditional Chinese Medicine, Tianjin, China

<sup>5</sup>Tianjin Key Laboratory of Acupuncture and Moxibustion, Tianjin, China

<sup>6</sup>Tianjin Key Laboratory of Translational Research of Prescription and Syndrome, Tianjin, China

<sup>7</sup>Academy for Advanced Interdisciplinary Studies, Peking University, Beijing, China

Correspondence should be addressed to Li Li; [lilitcm@foxmail.com](mailto:lilitcm@foxmail.com)

Received 26 June 2020; Revised 29 August 2020; Accepted 7 September 2020; Published 29 September 2020

Academic Editor: Yongjun Chen

Copyright © 2020 Bao-yu Zhang et al. This is an open access article distributed under the Creative Commons Attribution License, which permits unrestricted use, distribution, and reproduction in any medium, provided the original work is properly cited.

**Background.** As one of the first steps in the pathology of cerebral ischemia, glutamate-induced excitotoxicity progresses too fast to be the target of postischemic intervention. However, ischemic preconditioning including electroacupuncture (EA) might elicit cerebral ischemic tolerance through ameliorating excitotoxicity. **Objective.** To investigate whether EA pretreatment based on TCM theory could elicit cerebral tolerance against ischemia/reperfusion (I/R) injury, and explore its potential excitotoxicity inhibition mechanism from regulating proapoptotic pathway of the NMDA subtype of glutamate receptor (GluN2B). **Methods.** The experimental procedure included 5 consecutive days of pretreatment stage and the subsequent modeling stage for one day. All rats were evenly randomized into three groups: sham MCAO/R, MCAO/R, and EA+MCAO/R. During pretreatment procedure, only rats in the EA+MCAO/R group received EA intervention on GV20, SP6, and PC6 once a day for 5 days. Model preparation for MCAO/R or sham MCAO/R started 2 hours after the last pretreatment. 24 hours after model preparation, the Garcia neurobehavioral scoring criteria was used for the evaluation of neurological deficits, TTC for the measurement of infarct volume, TUNEL staining for determination of neural cell apoptosis at hippocampal CA1 area, and WB and double immunofluorescence staining for expression and the cellular localization of GluN2B and m-calpain and p38 MAPK. **Results.** This EA pretreatment regime could improve neurofunction, decrease cerebral infarction volume, and reduce neuronal apoptosis 24 hours after cerebral I/R injury. And EA pretreatment might inhibit the excessive activation of GluN2B receptor, the GluN2B downstream proapoptotic mediator m-calpain, and the phosphorylation of its transcription factor p38 MAPK in the hippocampal neurons after cerebral I/R injury. **Conclusion.** The EA regime might induce tolerance against I/R injury partially through the regulation of the proapoptotic GluN2B/m-calpain/p38 MAPK pathway of glutamate.

## 1. Introduction

Stroke is the second leading cause of death and the third leading cause of disability worldwide [1]. Stroke is estimated to cause 12 million deaths per year by 2030 [2]. Ischemic stroke, induced by occlusion of cerebral blood flow mainly in the

middle cerebral artery (MCA), accounts for about 87.9% of all strokes and often leads to severe central nervous system injury or even death [3]. Currently, recombinant tissue plasminogen activator (rt-PA) is the only FDA-approved agent for the hyperacute phase of ischemic stroke [2]. However, application of such therapy is limited by the narrow



therapeutic time window (3-4.5 h) and strict indications [3]. Therefore, only 2-5% of patients attacked by acute ischemic stroke have received rt-PA treatment [2]. Furthermore, rt-PA-treated patients had an absolute risk of symptomatic intracerebral hemorrhage at 2.3% per year over 10 years [4, 5]. Moreover, there was no significant reduction in mortality at 3 to 6 months after intravenous thrombolysis compared with the aspirin-control group (17.9% vs. 16.5%), and two-thirds of survivors still suffer from certain disability [6].

Since current status of stroke management has always been far below expectation, stroke neurobiologists have advanced a considerable body of evidence supporting the hypothesis that, with certain preconditioning, the mammalian brain can adapt to injurious insults such as cerebral ischemia to promote cell survival in the face of subsequent injury [7]. Such neuroprotective effect triggered by certain “preconditioning” stimuli has been referred as “cerebral ischemic tolerance.”

The candidate stimuli should be a nonlethal stimulus strong enough to initiate a response inducing tolerance against subsequent lethal attacks but not so much as to cause permanent tissue damage [8]. Various preconditioning paradigms such as hypoxia, nonlethal ischemia, and pharmacological anesthetics have been explored for providing a unique window into the brain’s endogenous protective mechanisms [9]. Most of the pretreatment methods are double-edged, producing nonlethal harmful stimuli to the body for ischemic tolerance. Remote ischemic pretreatment might be the only regime that has been studied in clinical research. However, this multicenter clinical trial conducted in 2015 suggested that remote ischemic pretreatment did not improve patient outcomes [10].

Even though acupuncture and moxibustion had been applied for disease prevention since ancient time, the first evidence supporting its role for inducing cerebral ischemic tolerance in an animal model was provided by Xiong’s team in 2003 [11]. The study confirmed that electroacupuncture (EA) at GV20 before cerebral ischemia can reduce the degree of postischemic neural deficit in an animal model [11]. Until now, the mechanism of cerebral ischemic tolerance induced by EA pretreatment has been explored from various aspects, such as inhibition of inflammation, oxidative stress, endoplasmic reticulum stress, regulation of cannabinoid system, autophagy, protection of blood-brain barrier, and antiapoptosis [12–14]. Nevertheless, superiority of preconditioning should contribute to its rapid response to lethal injury. Glutamate-induced excitotoxicity was identified as one of the first steps in the pathology of cerebral ischemia [15]. Under the pathological conditions such as cerebral ischemia, glutamate would be overreleased to the synaptic cleft and then activated the NR2B-containing NMDA receptor (GluN2B), followed by calcium overload in the cell. The overloaded calcium would activate the m-calpain in the cytoplasm and then induce the endonuclease reaction of STEP61, which further inhibit the dephosphorylation of p38 MAPKs and finally lead to cell apoptosis through signal transduction [16, 17]. The occurrence and progression of such process is too fast to be the target of postischemic intervention [18]. However, ischemic preconditioning was

found to ameliorate excitotoxicity by inhibiting glutamate release [19, 20].

So, this study will focus on whether EA pretreatment could decrease excitotoxicity by regulating downstream of glutamate receptor in an animal model of cerebral ischemia/reperfusion (I/R) injury.

## 2. Material and Methods

**2.1. Animals.** Specific pathogen-free male Sprague-Dawley rats (aged 6 weeks old and weighing  $250 \pm 20$  g) were supplied by Beijing Vital River Laboratory Animal Technology Co. Ltd. (Beijing, China; license no. SCXK(Jing)2016-0006). All rats were bred and housed in the SPF animal facility at the Institute of Radiation Medicine, Chinese Academy of Medical Sciences and Peking Union Medical College (Tianjin, China; license no. SYXK (Jin) 2019-0002) under controlled conditions in a 12-hour light/dark cycle with a ambient temperature of 20-25°C and a humidity at 40-70% for at least 3 days before preconditioning. Rats were allowed free access to a standard rodent diet and clean water. All procedures were approved by the Ethics Committee of Tianjin University of Traditional Chinese Medicine (TCM-LAEC2019018).

### 2.2. Experimental Protocol

**2.2.1. Experiment I: Cerebral Protective Effect of EA Pretreatment for Middle Cerebral Artery Ischemia/Reperfusion Injury (MCAO/R).** To determine the neuroprotective effect of EA pretreatment for cerebral I/R, rats were evenly randomized into three groups: sham MCAO/R, MCAO/R, and EA+MCAO/R (Figure 1(a)). The experimental procedure included 5 consecutive days of pretreatment stage and the subsequent modeling stage for one day. During pretreatment procedure, all rats were constrained by handmade cloth and only rats in the EA +MCAO/R group are receiving EA intervention. MCAO/R or sham MCAO/R procedure started after 2 hours of the last pretreatment. For all MCAO/R rats, blood flow of MCA was monitored during the modeling procedure to illustrate the validity of cerebral I/R. At 24-hour postsham-MCAO/R or MCAO/R, an independent personnel blinded to group allocation evaluates neurological deficits of all animal using the Garcia neurobehavioral scoring criteria [21]. Afterwards, all rats were sacrificed under anesthesia and the brain tissue was collected for the measurement of infarct volume or neural cell apoptosis at hippocampal CA1 area using TTC and TUNEL staining.

**2.2.2. Experiment II: Effect of EA Pretreatment on GluN2B and Its Downstream Pathway of MCAO/R.** To determine the effect of EA pretreatment on glutamate receptor GluN2B and its downstream pathway postcerebral I/R, rats were evenly randomized into three groups: sham MCAO/R, MCAO/R, and EA+MCAO/R. All pretreatment procedures and the subsequent modeling procedure coincide with Experiment I. At 24-hour postsham-MCAO/R or MCAO/R, all rats were sacrificed under anesthesia and the right hippocampi were taken to determine the expression of GluN2B, m-

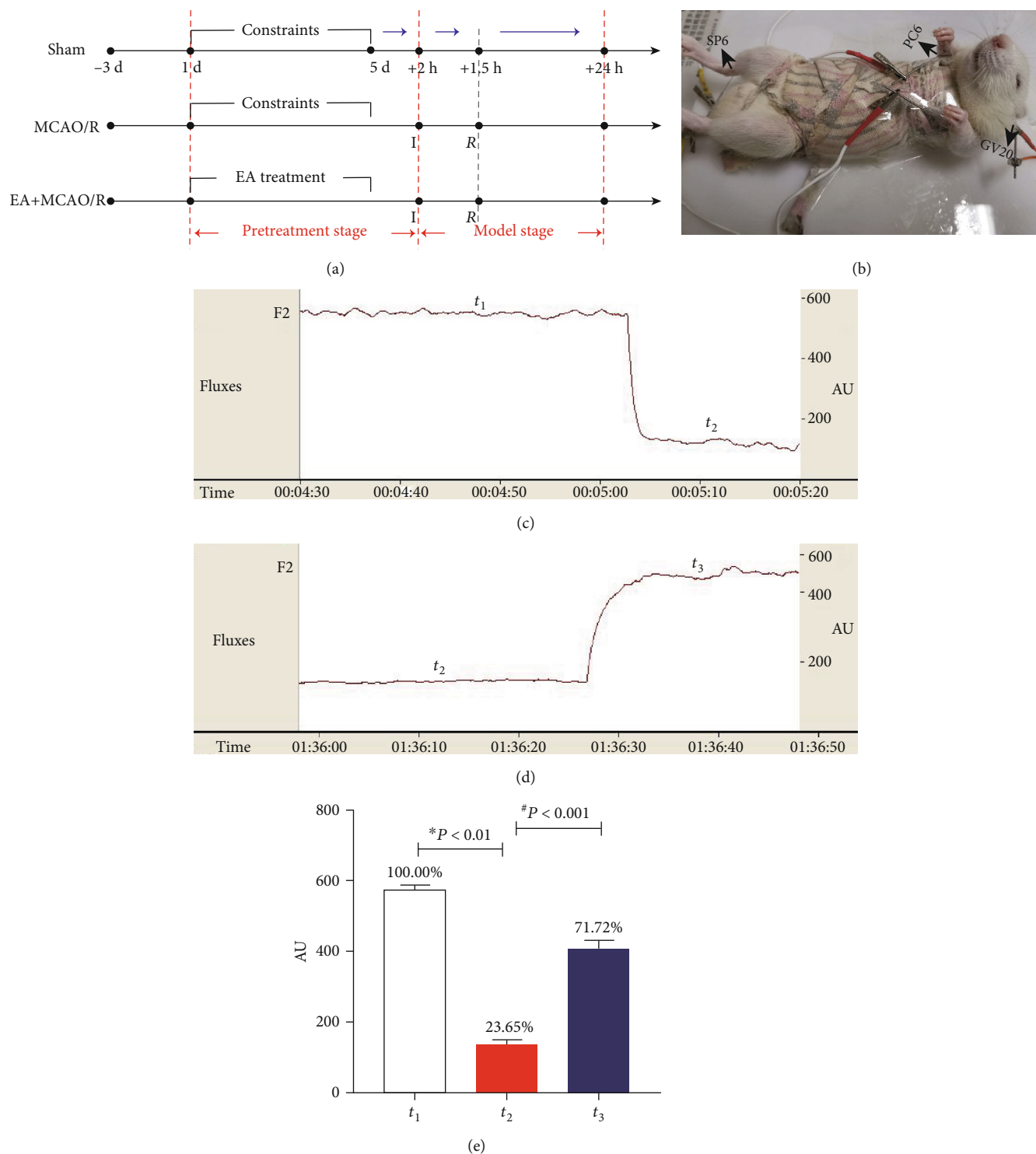


FIGURE 1: EA pretreatment and model preparation for rats in three groups. (a) The experimental procedure included 5 consecutive days of pretreatment stage and the subsequent modeling stage for one day (I: ischemia, insertion of suture to block the blood flow; R: reperfusion, withdrawal of the suture to restore blood flow at 90 minutes after ischemia). (b) EA stimulation. (c) Cerebral blood flow of the baseline ( $t_1$ ) and postischemia ( $t_2$ ). (d) Blood flow after reperfusion ( $t_3$ ). (e) Comparison of cerebral blood flow at different time points ( $n = 8$ ). The unit of blood flow “AU” is the unit determined by the manufacturer. The blood flow at three time points was compared using one-way ANOVA for repeated measurement. The results did not meet the sphericity test (Mauchly  $W = 0.252$ ,  $P < 0.05$ ), so the differences among groups were examined using MANOVA ( $F = 470464.634$ ,  $P < 0.001$ ) followed by LSD for post hoc multiple comparisons.  $*P$  vs. sham;  $^{\#}P$  vs. MCAO/R.

calpain, and p38 MAPK by Western blot (WB) and the cellular localization of GluN2B and m-calpain using double immunofluorescence staining.

**2.3. EA Pretreatment.** During EA pretreatment, all rats were constrained by handmade cloth and fixed at the desk using adhesive tape (Figure 1(b)). Location of GV20, PC6, and SP6 in rats was referred to “Experimental acupuncture science” [22]. GV20 was selected at the midpoint between the tips of the ears and punctured backward with depth of 2 mm. Bilateral PC6 were selected 3 mm above the wrist joint on the medial side of the forelimb between the ulna and the radius and were punctured vertically with depth of 1 mm; SP6 was selected 10 mm above the tip of the medial malleolus at the hind limbs and was punctured vertically with depth of 5 mm. Five sites of acupoints were needled using sterile acupuncture needles of 0.25 mm \* 25 mm (*Huatu*, Suzhou Medical Supplies Factory, China). Then, all needles were connected to the electrodes. Unilateral PC6 and SP6 were connected to the positive and negative end of the same electrode, and GV20 and the tip of the ear were connected to the positive and negative end of the same electrode to form a current circuit using EA therapeutic apparatus (*HANS-100A*, Nanjing Jisheng Medical Technology, China). All acupoints were stimulated with the parameters of 2/15 Hz, 1 mA for 20 min/d for 5 consecutive days. Limbs and head would slightly tremor during electrical stimulation which was considered as the sign of *Deqi*.

**2.4. The Model of Cerebral I/R Was Prepared Using Suture Method under the Monitoring of Laser Doppler Flowmeter.** Focal cerebral ischemia was induced by a transient right middle cerebral artery occlusion and subsequent blood reperfusion 90 minutes later in a rat model. Before model preparation, SD rats would be fasted yet drank water freely for 12 hours. During anesthesia process, the rats were placed in the anesthesia induction chamber of the small animal anesthesia system, and the concentration of 3% isoflurane (isoflurane, RWD Life Science Co., Ltd., China) was set to induce anesthesia. After the basal reflex of the rats disappeared, the rats were fixed on the board with rubber bands with a breathing mask connected to the anesthesia system, and then, a midline incision was cut on the neck to adequately expose the right common carotid artery (CCA), external carotid artery (ECA), and internal carotid artery (ICA). After the ligation of the right CCA and ECA, a suture was inserted from the CCA into the ICA up to a depth of 18 to 20 mm. After 90 min of occlusion, the filament was withdrawn for reperfusion.

The regional cerebral blood flow (rCBF) was monitored using a Laser Doppler Flowmeter (DRT-4, Moor, UK). The cerebral blood flow after the separation of the carotid artery ( $t_1$ ) was set as the baseline value of blood flow. Blood flow after ischemia ( $t_2$ ) and reperfusion ( $t_3$ ) was also recorded to evaluate the effect of model preparation (Figures 1(c) and 1(d)). In each time point, when the blood flow was relatively stable, the value would be recorded and preserved for 1 min without interruption. The model was successful when local cerebral blood flow in the middle cerebral artery decreased

to 30% below the baseline blood flow after ischemia [23]. The modeling process in our study could produce a representative model of cerebral I/R since local cerebral blood flow decreased to 23.65% of the baseline value after ischemia and returned to 71.72% after suture withdrawal (Figure 1(e)).

**2.5. Garcia Score.** The neurobehavioral scoring was performed according to the methods of Garcia et al. [21], which includes six aspects: spontaneous activity (in cage for 5 min, 0-3 scores), symmetry of movements (four limbs, 0-3 scores), symmetry of forelimbs (outstretching while held by tail, 0-3 scores), climbing wall of wire cage (1-3 scores), reaction to touch on either side of trunk (1-3 scores), and response to vibrissae touch (1-3 scores). Total value of Garcia is 18, with lower score for more impaired neurologic function.

**2.6. TTC Staining.** Animals were anesthetized and sacrificed to extract brain tissue. After rinsing with ice brine, the brain tissue was quickly frozen in -20°C refrigerator for 20 min to harden the brain tissue for cutting. Sections were made along the coronal plane with a thickness of 2 mm, and 5-6 slices were cut for each brain. Put the brain slices into a petri dish wrapped with tinfoil and containing 2% TTC (Solarbio, China) and then dye them in a 37°C incubator for 30 minutes. During this period, gently turn the brain slices so that they can be fully exposed to the reaction. Take out the petri dish, suck out the TTC solution with 1 ml needle tube, inject 4% paraformaldehyde solution to fix it for 5 min, and then take out and place the slices in order for pictures. Finally, the cerebral infarction volume ratio of each brain slice was calculated by Image-Pro Plus image software. In order to reduce the error caused by cerebral ischemic hemispheric edema, the infarct volume was used to subtract the ipsilateral normal tissue volume from the contralateral normal tissue volume, and the result was expressed by the percentage of infarct volume: infarct volume percentage = (contralateral tissue volume - ipsilateral normal tissue volume) / contralateral normal tissue volume \* 100%.

**2.7. TUNEL Staining.** After dewaxed by xylene and dehydrated with ethanol, paraffin sections were added with 20 µg/ml protease K working solution (Solarbio, China) for 15 min at room temperature. Then, 51 µl of TUNEL detection solution (45 µl equilibrium buffer : 5 µl nucleotide mixture : 1 µl rTdT enzyme) was added to each sample and incubated in the dark for 1 h. 2× SSC was incubated at room temperature for 15 min to terminate the reaction (Everbright Inc., USA). Add DAPI containing antfluorescence quench to incubate for 5 min in the dark and then cover the coverslip. 200x images of hippocampal CA1 were obtained by a fluorescence microscope (Leica, Germany). The percentage of apoptotic positive cells in different visual fields was calculated, and the mean value was taken for statistical analysis. To represent the results of TUNEL staining, we calculated the apoptosis rate using the following formula: apoptosis rate = positive cells / total cells per field \* 100%.

**2.8. Western Blot (WB).** The total protein was lysed with histiocyte lysate. The lysate buffer was prepared as follows: 1 ml RIPA buffer containing 10 µl protease inhibitor (PMSF) and 10 µl protein phosphatase inhibitor (Solarbio, Beijing,

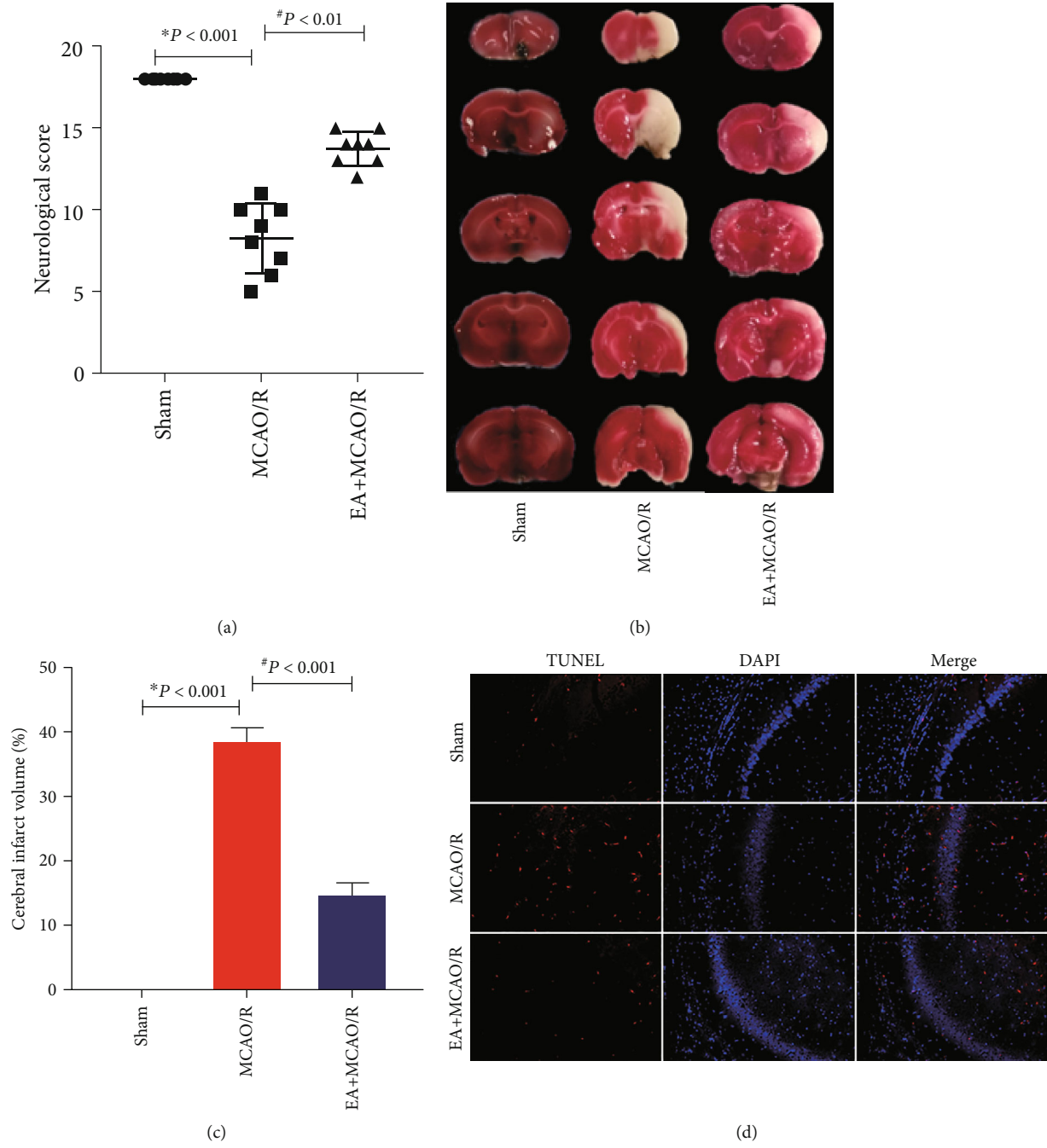


FIGURE 2: Continued.



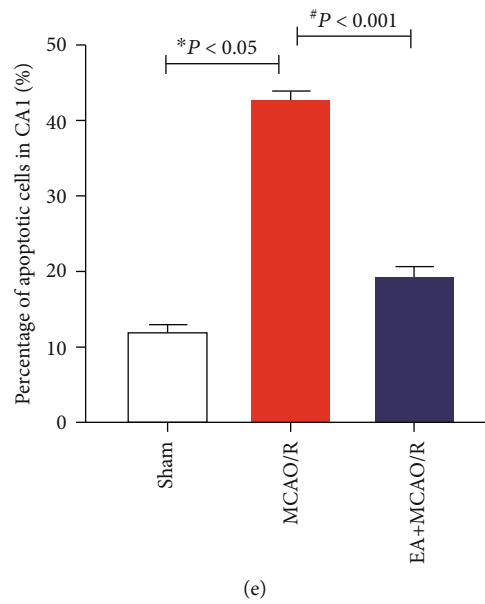


FIGURE 2: Effect of EA pretreatment on Garcia score, cerebral infarction volume, and the number of neuron apoptosis in the hippocampal CA1 region of MCAO/R rats. After cerebral I/R injury for 24 h, the neural behavior of the rats was evaluated by the Garcia score ( $n = 8$ ), the infarct volume was detected by TTC staining of the brain slices ( $n = 4$ ), and the cellular outcome was detected by TUNEL fluorescence staining ( $n = 4$ ). (a) Comparison of Garcia score. The results conformed to the normal distribution yet with heterogenous variance. Differences among groups were examined using the Kruskal-Wallis test ( $H = 21.324$ ,  $P < 0.001$ ) followed by the Dunn test for post hoc multiple comparisons. (b) Representative slice of TTC staining. (c) Comparison of infarct volume. The results conformed to the normal distribution with homogeneous variance. Differences among groups were examined using AVONA ( $F(2, 9) = 513.909$ ,  $P < 0.001$ ) followed by LSD for post hoc multiple comparisons. (d) Representative immunofluorescence staining of TUNEL-positive cells (red) in brain sections. Scale bars =  $100 \mu\text{m}$ . (e) Comparison of apoptotic cell. The results conformed to the normal distribution and homogeneous variances. Differences among groups were examined using AVONA ( $F(2, 7) = 517.694$ ,  $P < 0.001$ ) followed by LSD for post hoc multiple comparisons. \* $P$  vs. sham; # $P$  vs. MCAO/R.

China). The hippocampal tissue of the affected side was incubated in the buffer on ice for 30 min and centrifuged at 12,000 g for 10 min. Then, BCA kit (Solarbio, Beijing, China) was used to measure the protein concentration of the supernatant. Afterwards, protein samples were split by 8% (GluN2B and m-calpain) or 15% (p38 MAPK and p-p38 MAPK) SDS-PAGE, and the electrophoretic voltage was 80 V to 120 V. The protein is then transferred to the PVDF membrane by a 200 mA current, and the action time was 70 min (p38 MAPK and p-p38 MAPK), 90 min (m-calpain), and 120 min (GluN2B), respectively. The following primary antibodies were used: Rabbit anti-GluN2B (65783, 1:1000, Abcam, USA); Rabbit anti-m-calpain (39165, 1:1000, Abcam, USA); Mouse anti-p38 (31828, 1:1000, Abcam, USA); Rabbit anti-p-p38 (4511, 1:1000, CST, USA); and Mouse anti- $\beta$ -tubulin (HC101-01, 1:5000, TransGen, China). Secondary HRP-Conjugated Goat Anti-Rabbit or Goat Anti-Mouse antibody (1:5000, TransGen, China) was used. The optical density of the bands was determined by gel imaging system (Jena, Germany) with chemiluminescence reagent (Millipore, USA) as a developer solution. The intensity of chemiluminescence was measured using Visionworks 8.0.

**2.9. Double Immunofluorescence Staining.** Paraffin sections were dewaxed, rehydrated, antigen repaired (EDTA, Solarbio, C1034, China), and sealed with 5% goat serum (Solarbio, SL038, China) at room temperature for 30 min. The follow-

ing primary antibodies were used: Rabbit anti-GluN2B (65783, 1:100, Abcam, USA); Rabbit anti-m-calpain (39165, 1:100, Abcam, USA); and Mouse anti-NeuN (104224, 1:100, Abcam, USA). The secondary antibody used was PE-labeled Goat Anti-Rabbit IgG (1:200, TransGen, China) and AF488-labeled Goat Anti-Mouse IgG (1:200, TransGen, China). The nuclei were labeled after incubated away from the light with DAPI for 2 min. Finally, images of sections were captured using a fluorescence microscope (Leica, Germany).

**2.10. Statistical Analysis.** SPSS21.0 was used for data processing and statistical analysis. The measurement data were expressed as the mean  $\pm$  standard error. The measurement data at different time points were compared using one-way ANOVA for repeated measurement. The measurement data without time sequence was compared using one-way ANOVA or the Kruskal-Wallis test according to data distribution.  $P$  values of 0.05 were considered to indicate statistical significance.

### 3. Results

**3.1. EA Pretreatment Induced Neuroprotection against Cerebral I/R.** This EA pretreatment regime proposed based on TCM theory has never been explored for inducing cerebral ischemic tolerance. In order to evaluate the neuroprotective effect of this new EA pretreatment protocol on cerebral



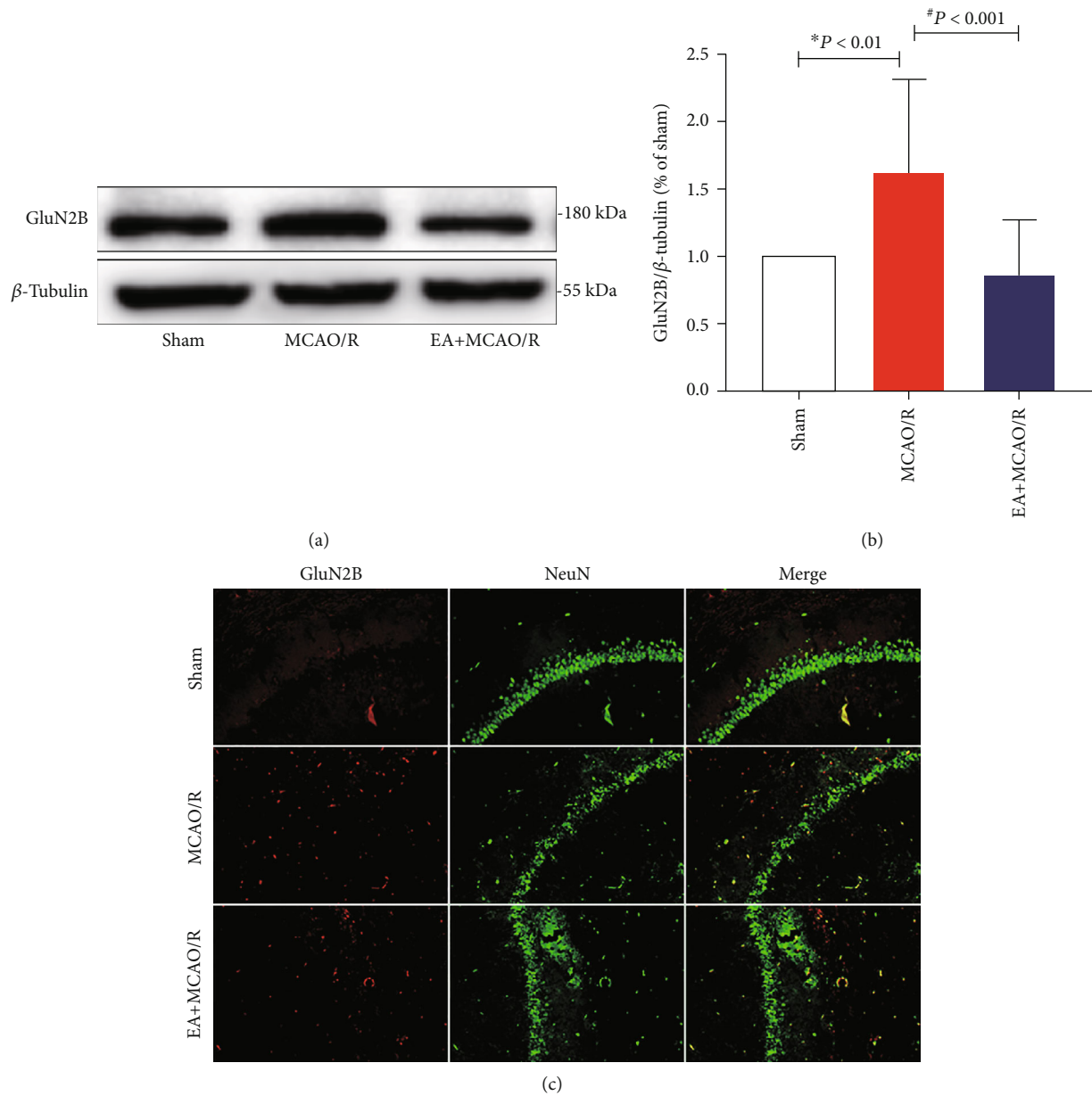


FIGURE 3: Effect of EA pretreatment on GluN2B expression ( $n = 4$ ). GluN2B protein expression and cell localization were detected at 24 h after cerebral I/R by WB and double immunofluorescence staining. (a) Representative WB bands showing GluN2B expression in the rat hippocampus of three groups. (b) Comparison of the GluN2B expression. The results conformed to the normal distribution with heterogenous variance. Differences among groups were examined using the Kruskal-Wallis test ( $H = 18.598$ ,  $P < 0.001$ ) followed by the Dunn test for post hoc multiple comparisons. (c) Representative double immunofluorescence staining (yellow) of GluN2B-positive cells (red) and NeuN-positive cells (green) in brain sections. Scale bars = 100  $\mu$ m. \* $P$  vs. sham; # $P$  vs. MCAO/R.

I/R, neurological behavior, infarct volume, and apoptosis in the hippocampal CA1 area were measured using Garcia score, TTC staining, and TUNEL fluorescence staining, respectively. The results confirmed the beneficial effect of this 5-day EA pretreatment on cerebral I/R injury. Compared with the sham group, rats of the MCAO/R model presented impaired neurological dysfunction ( $8.25 \pm 2.12$ ,  $P < 0.001$ ; Figure 2(a)) and increased infarct volume ( $38.51 \pm 2.21$ ,  $P < 0.001$ ; Figures 2(b) and 2(c)), and cells with positive TUNEL fluorescence suggested that apoptosis in the hippocampal CA1 area was also exacerbated in MCAO/R rats

( $42.76 \pm 1.20$ ,  $P = 0.019 < 0.05$ ; Figures 2(d) and 2(e)). Meanwhile, pretreatment with EA might improve neurological deficit ( $13.75 \pm 1.04$ ,  $P = 0.001 < 0.01$ ; Figure 2(a)), decrease infarct volume ( $14.57 \pm 2.00$ ,  $P < 0.001$ ; Figures 2(b) and 2(c)), and reduce TUNEL-positive apoptotic cells in hippocampal CA1 area ( $19.33 \pm 1.40$ ,  $P < 0.001$ ; Figures 2(d) and 2(e)).

**3.2. EA Pretreatment Downregulated Neuronal Expression of GluN2B in Hippocampal CA1 Region Postcerebral I/R Injury.** In order to test whether the glutamate proapoptotic

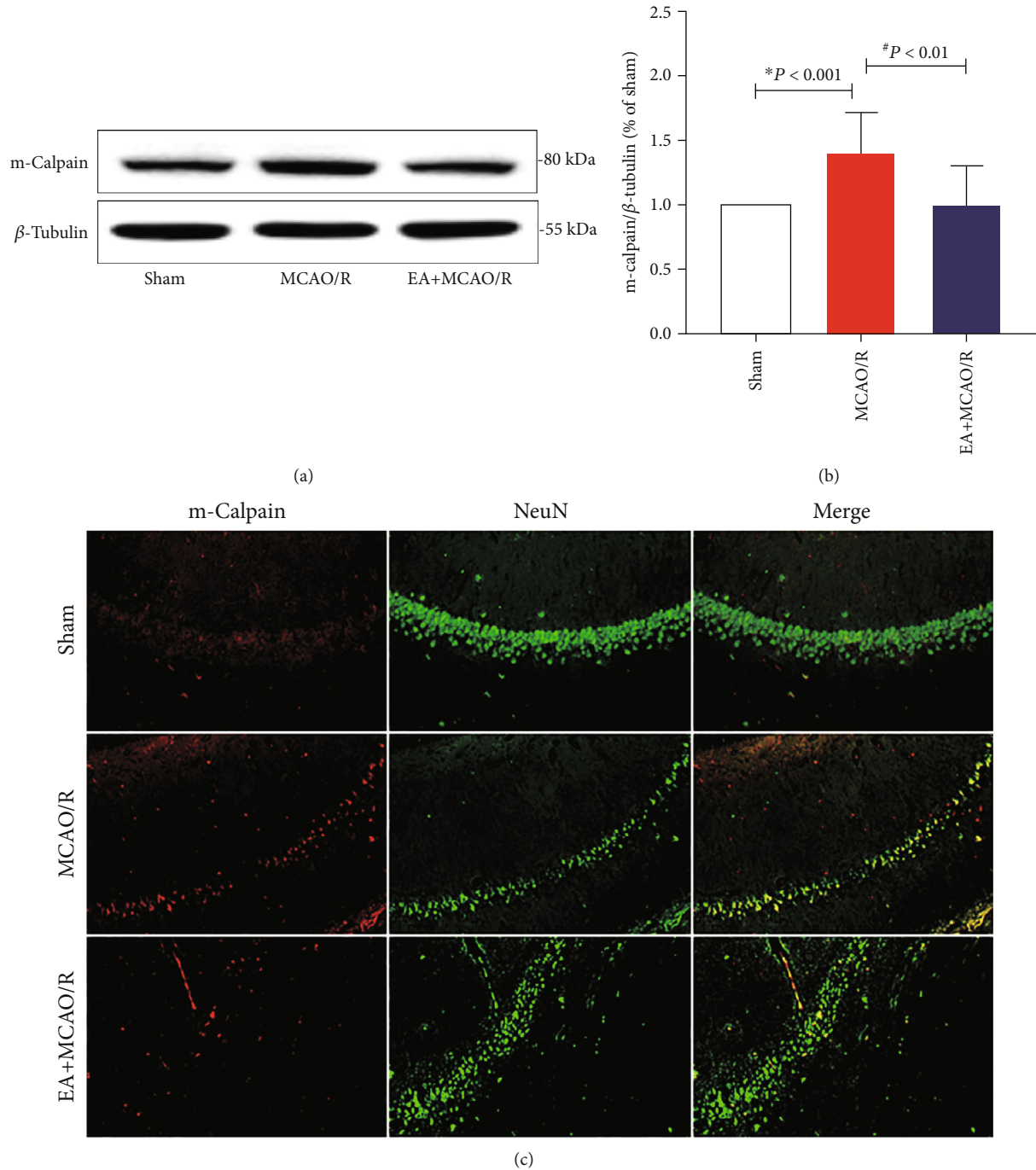


FIGURE 4: Effect of EA pretreatment on m-calpain expressed in the rat hippocampal CA1 neurons ( $n = 4$ ). The expression and cell localization of m-calpain at 24 h after cerebral I/R were detected by WB and double-standard immunofluorescence staining. (a) Representative WB bands showing m-calpain expression in rats among the three groups. (b) Comparison of the m-calpain expression. The result did not conform to the normal distribution. Differences among groups were examined using the Kruskal-Wallis test ( $H = 21.421$ ,  $P < 0.001$ ) followed by the Dunn test for post hoc multiple comparisons. (c) Representative double immunofluorescence staining (yellow) of m-calpain-positive cells (red) and NeuN-positive cells (green) in brain sections. Scale bars = 100  $\mu$ m.  $*P$  vs. sham;  $\#P$  vs. MCAO/R.

receptor GluN2B might mediate the ischemic tolerance of EA pretreatment, overall expression of GluN2B in the hippocampus of the affected side was detected using WB, and the expression of GluN2B in neurons at the CA1 region was further observed using GluN2B and NeuN colabeling immunofluorescence staining.

The overall expression of GluN2B in the hippocampus of rats in the MCAO/R model group was significantly increased ( $1.62 \pm 0.70$ ,  $P = 0.002 < 0.01$ ; Figures 3(a) and 3(b)) compared to sham rats, and EA pretreatment could reverse this reaction ( $0.86 \pm 0.41$ ,  $P < 0.001$ ; Figures 3(a) and 3(b)). Moreover, when the labels of GluN2B and NeuN were

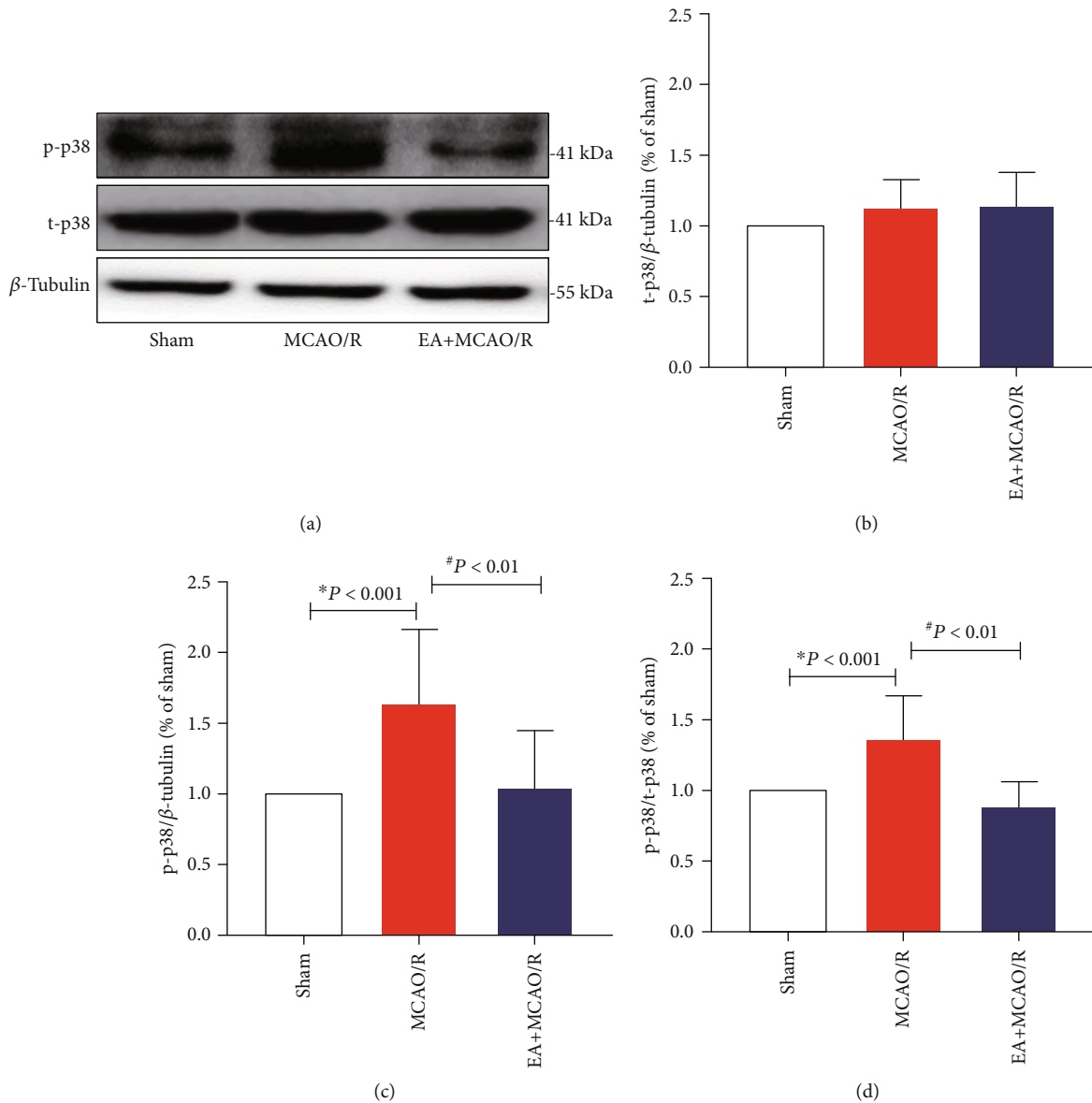


FIGURE 5: Effect of EA pretreatment on t-p38 and p-p38 expression in the hippocampal CA1 neurons ( $n = 4$ ). The expression of p38 and p-p38 in the hippocampal neurons was detected by WB at 24 h after cerebral I/R. (a) Representative WB bands showing p38 MAPK expression in the rat hippocampus of three groups. (b, c) Comparison of total p38 (t-p38) and phosphorylated p38 (p-p38) expression. The result of t-p38/ $\beta$ -tubulin conformed to normal distribution with homogeneous variance. Differences among groups were examined using AVONA ( $F(2, 33) = 1.941$ ,  $P = 0.160 > 0.05$ ). The result of p-p38/ $\beta$ -tubulin conformed to normal distribution with homogeneous variance. Differences among groups were examined using AVONA ( $F(2, 33) = 10.380$ ,  $P < 0.001$ ). (d) Comparison of p-p38/t-p38 ratio. The result of p-p38/t-p38 conformed to normal distribution with homogeneous variance. Differences among groups were examined using AVONA ( $F(2, 33) = 18.015$ ,  $P < 0.001$ ) followed by LSD for post hoc multiple comparisons. \* $P$  vs. sham; # $P$  vs. MCAO/R.

merged, the number of colabeled cells in the EA+MCAO/R group was significantly lower than that in the MCAO/R group (Figure 3(c)). This suggested that EA pretreatment might inhibit the excessive activation of GluN2B receptor in neurons at the hippocampal CA1 region postcerebral I/R injury.

**3.3. EA Pretreatment Downregulated the Neuronal Expression of m-Calpain in Hippocampal CA1 Region Postcerebral I/R Injury.** In order to test whether m-calpain might also contribute to be the ischemic tolerance of EA pretreatment, overall

expression of m-calpain in the hippocampus of the affected side was detected using WB, and the expression of m-calpain in the neurons at the CA1 region was further observed using m-calpain and NeuN double immunofluorescence staining.

It was found that overall expression of m-calpain in the hippocampus of rats in the MCAO/R group was significantly increased compared with the sham rats ( $1.40 \pm 0.31$ ,  $P < 0.001$ ; Figures 4(a) and 4(b)), and overall expression of m-calpain was significantly decreased in the EA+MCAO/R group compared with that in the MCAO/R group

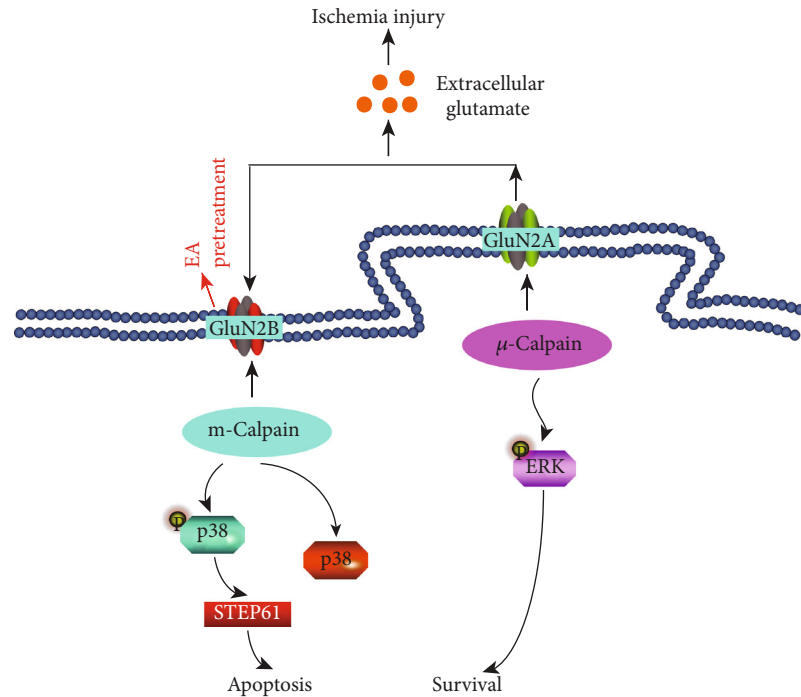


FIGURE 6: Bidirectional action of glutamate NMDA receptors during ischemic injury and role of EA pretreatment. GluN2B: the NR2B-containing NMDA receptors; GluN2A: the NR2A-containing NMDA receptors; STEP61: striatal-enriched protein tyrosine phosphatase; ERK: extracellular signal-regulated kinase.

( $0.99 \pm 0.31$ ,  $P = 0.001 < 0.01$ ; Figures 4(a) and 4(b)). m-Calpain and NeuN colabeled image showed the same intergroup change pattern (Figure 4(c)). This indicated that EA pretreatment might also inhibit the GluN2B downstream proapoptotic mediator m-calpain in the hippocampal neurons for rats' postcerebral I/R injury.

**3.4. EA Pretreatment Downregulated the Phosphorylation of p38 MAPK in Hippocampal Region Postcerebral I/R Injury.** Mitogen-activated protein kinases (MAPKs) are downstream targets of calpain in neurons. After ischemic injury, activated m-calpain would activate p38 MAPK to initiate the cell apoptosis signaling pathway [17]. It was also a key issue that whether p38 MAPK activation might lead to ischemic tolerance of EA pretreatment. Therefore, the ratio of phosphate p38 to total p38 was also calculated after quantitation test using WB.

The expression of total p38 protein (t-p38) was stable among all groups (Figures 5(a) and 5(b)), but the level of phosphorylated p38 (p-p38) and the p-p38/t-p38 ratio were significantly different between each group. The expression and proportion of p-p38 in the hippocampal tissue of rats in the MCAO/R group was significantly higher than that in the sham group ( $1.59 \pm 0.50$ ,  $1.49 \pm 0.45$ ,  $P < 0.001$ ,  $P < 0.001$ ; Figures 5(a), 5(c), and 5(d)), and the expression and proportion of p-p38 in the EA+MCAO/R group was significantly lower than that in the MCAO/R group ( $1.06 \pm 0.37$ ,  $0.99 \pm 0.34$ ,  $P = 0.002 < 0.01$ ,  $P = 0.001 < 0.01$ ; Figures 5(a), 5(c), and 5(d)). This suggests that EA pretreatment may mitigate hippocampal cell apoptosis induced by excitatory neu-

rotoxicity postcerebral I/R through inhibiting the phosphorylated activation of p38 MAPK.

#### 4. Discussion

Proper preconditioning could protect against cerebral ischemia through activating several endogenous signaling pathways [8, 24]. It is applicable not only for people at high risk of stroke or stroke recurrence but also for patients with anticipated cerebral ischemia, such as invasive cerebral surgery. The anticipation of such preconditioning lies in reducing severity of ischemia injury, prolonging treatment window for other postattack intervention such as rt-PA, and promoting recovery capability [25]. Since the severity of neurological deficit is independently associated with an increased risk of symptomatic intracerebral hemorrhage post-t-PA, ischemic tolerance might also affect the occurrence of postthrombolysis hemorrhage through decrease severity of neurological deficit [26]. EA is considered as the combination of traditional Chinese medicine and modern electrical stimulation. Among all regimes of preconditioning, EA should be valued for its feasibility, practicability, and safety in clinical practice. Furthermore, acupuncture has already been widely used for poststroke management on motor, cognitive, and swallowing function [27–29]. It is highly possible that acupuncture could be recruited into the health delivery of systemic stroke management. Therefore, exploring the role and mechanism of EA in inducing cerebral ischemia is of great importance.

The majority of previous studies only stimulate GV20 for eliciting cerebral ischemic tolerance [11, 30, 31]. Our team



proposed another acupuncture regime, i.e., stimulating GV20, SP6, and PC6 at the same time based on theory of traditional Chinese medicine (TCM). Ischemic tolerance could be induced with holistic adaptation through regulating spirit, activating collaterals, harmonizing *Qi* and blood, and nourishing the liver, spleen, and kidney. GV20, the most common used acupoint, mainly regulate spirit and activate local collaterals for ischemic tolerance. The addition of SP6 and PC6 could improve the efficacy in complementary of GV20 to fulfill the goal of holistic adaptation. Therefore, the combined EA protocol might present more stable and effective performance. It turned out that in comparison with the rats in MCAO/R, 5 days of repeated EA intervention on GV20, SP6, and PC6 could decrease neurological dysfunction, decrease infarct volume, and reduce apoptosis in hippocampal CA1 area. Therefore, this part of experiment could provide an effective EA prescription based on theory of TCM for further mechanism exploration and clinical efficacy validation. For the convenience of similar studies by other researchers who might be interested in cerebral ischemic tolerance, we listed all details of EA pretreatment in Methods, including acupoint location, electrical stimulation, and sign of *Qeqi*.

When ischemic injury attacks, rapid release of glutamate from presynaptic neuron would induce excitotoxicity and finally leading to neuronal death [32], whereas neurotransmitters including glutamate have been validated as the mediators of acupuncture therapeutic effect in neurological diseases [33] and the activators of EA pretreatment in stimulating endogenous cerebral protection. Previous studies suggested that EA pretreatment can reduce glutamate concentration in the striatum [34] and hippocampus [35] of rats, respectively, in animal mode of cerebral I/R injury and vascular dementia. Reduction of extracellular glutamate by EA pretreatment might achieve through reabsorption by overexpression of glutamate transporter type 2 [36]. Neurotoxicity mainly depends on postsynaptic calcium overload. The NMDA subtype of glutamate receptors has attracted much attention in recent years due to its higher permeability to  $Ca^{2+}$  compared with voltage-gated channels when inducing calcium overload [1, 37]. Well-documented experimental evidence from both in vitro and in vivo models of stroke strongly supports that overactivation of the NMDA receptors is the primary step leading to neuronal injury after insults of stroke [38, 39]. As is shown in Figure 6, NR2A- and NR2B-containing NMDA receptor subtypes (GluN2B and GluN2A) have opposing roles in influencing the direction of synaptic plasticity when mediating cell death and cell survival in vivo rat model of ischemic stroke [39]. Namely, contrary to the role of neuroprotective GluN2A, activation of synaptic or extrasynaptic GluN2B receptor results in excitotoxicity, increasing neuronal apoptosis. Inhibition of NMDA receptor through intracranial [40] or intravenous [41] injection before ischemia can also reduce the infarct volume and prevent neuronal damage after cerebral ischemia. Furthermore, blocking GluN2B-mediated cell death was effective in reducing infarct volume only when the receptor antagonist was given before the onset of stroke [39]. Therefore, GluN2B could be a key to elicit cerebral ischemia tolerance. EA was found to

improve cognitive impairment in rats through inhibiting GluN2B expression [42]. So, we tested the hypothesis that EA pretreatment might elicit cerebral tolerance to ischemia by regulating level of GluN2B using WB and double immunofluorescence staining. In concordance with the previous study [42], our results suggested that repeated EA before ischemia can inhibit GluN2B expression in hippocampal CA1 region. Therefore, glutamate proapoptotic receptor GluN2B might contribute to the reduction of post-I/R neural injury by mitigating excitotoxicity.

As is shown in Figure 6, apoptosis induced by GluN2B receptor is mediated by enzyme digestion reaction of m-calpain and the subsequent phosphorylation of the transcription factor [43]. Calpain activation is the intracellular calcium-dependent event with the greatest contribution to excitotoxicity [44]. When triggered by overloaded intracellular  $Ca^{2+}$ , the  $Ca^{2+}$ -dependent proteases m-calpain can cause degradation of cytoskeleton and structural proteins, and ultimately initiate the pathway leading to neuronal death [45]. Many previous studies had shown that focal cerebral ischemia can activate m-calpain in the hippocampus, cortex, and striatum through upregulating its protein expression at 1 h after cerebral ischemia [46], and then trigger calpain-mediated STEP (striatal-enriched protein tyrosine phosphatase) lysis and induce neurotoxicity [47]. Therefore, as the key downstream mediator of GluN2B, m-calpain activation is the most critical intracellular calcium-dependent event that is contributing to neurotoxicity [48]. At present, the regulatory effect of acupuncture on m-calpain has never been reported. Our study showed that m-calpain in the hippocampus was activated at 24 h after cerebral I/R injury, and EA pretreatment can decrease the expression of m-calpain in the hippocampal CA1 region neurons. This suggested that EA pretreatment might block the most important intracellular calcium activation pathway of excitotoxicity induced by I/R injury.

NMDA receptor-mediated death signaling is transcription-dependent [43]. The key transcription factor of GluN2B-mediated proapoptotic pathway is p38 MAPK [43]. A large number of studies had shown that the p38 MAPK signal transduction pathway is closely related to cerebral I/R injury and ischemia tolerance [49–51]. Level of phosphorylated p38 MAPK reached a peak at 24 hours after cerebral ischemia [52]. Previous studies had found that EA can reduce the relative density of phosphorylated p38 MAPK in an animal model of cerebral ischemia [51]. Our results showed that there was no marked difference in the expression level of the total p38 in each group at 24 h after cerebral I/R, but there was a significant difference in the ratio of phosphorylated p38 to total p38 in each group. The increased ratio in the model group indicated that p38 MAPK protein played a damaging role through phosphorylation activation after cerebral ischemia, which was consistent with previous studies. Our study also showed that EA pretreatment can inhibit p38 MAPK phosphorylation in the hippocampus in rats with cerebral I/R injury.

Some limitations also restrict interpretation of our study. Firstly, we only focused on the GluN2B-mediated proapoptotic pathway of excitotoxicity. However, the GluN2A-



mediated prosurvival pathway also could contribute to the regulation of excitotoxicity. Previous study showed that EA pretreatment could also upregulate the expression of GluN2A [42]. Therefore, the synergic action of the GluN2B proapoptotic and GluN2A prosurvival pathways in excitotoxicity could be further elucidated in future studies. Secondly, the process of neurotoxicity postcerebral ischemia should be highly time-sensitive. So, further study should be conducted to illustrate the time-variant property of EA pretreatment on postschismic excitotoxicity from the perspective of extracellular glutamate.

## 5. Conclusion

This study suggested that our EA pretreatment regime could effectively increase the neurofunction and reduce the volume of cerebral infarction and the level of neuronal apoptosis in the hippocampal CA1 region for an animal model of cerebral I/R injury, and its mechanism may be related to the inhibition of the GluN2B/m-calpain/p38 MAPK proapoptotic pathway.

## Data Availability

The data used to support the findings of this study are available from the corresponding author upon request.

## Disclosure

Bao-yu Zhang, Guan-ran Wang, and Wen-hua Ning are regarded as co-first authors.

## Conflicts of Interest

The authors declare that they have no competing interests.

## Authors' Contributions

Bao-yu Zhang, Guan-ran Wang, Wen-hua Ning, and Li Li had full access to all of the data in the study and took responsibility for the integrity of the data and the accuracy of the data analysis. Li Li designed the study and revised the manuscript. Bao-yu Zhang, Guan-ran Wang, and Wen-hua Ning conducted the experiments and drafted the manuscript. Jian Liu, Sha Yang, and Yan Shen gave their valuable advice about data analysis and interpretation. Yang Wang and Meng-xiong Zhao provided the technique support for the experiment. All authors approved the final version of the paper. Bao-yu Zhang, Guan-ran Wang, and Wen-hua Ning contributed equally to the manuscript.

## Acknowledgments

This work was supported by the National Natural Science Foundation of China (81804189), the Tianjin Natural Science Foundation (18JCZDJC99200), the Developmental Program for Changjiang Scholars and Innovative Research Team Program (IRT1167), and the Program of Tianjin Municipal Commission of Health and Family Planning for Research

on Traditional Chinese Medicine and Integrative Medicine (2017130).

## References

- [1] G. J. Hankey, "Stroke," *Lancet*, vol. 389, no. 10069, pp. 641–654, 2017.
- [2] B. M. Demaerschalk, D. O. Kleindorfer, O. M. Adeoye et al., "Scientific rationale for the inclusion and exclusion criteria for intravenous alteplase in acute ischemic stroke: a statement for healthcare professionals from the American Heart Association/American Stroke Association," *Stroke*, vol. 47, no. 2, pp. 581–641, 2016.
- [3] W. J. Powers, A. A. Rabinstein, T. Ackerson et al., "2018 guidelines for the early management of patients with acute ischemic stroke: a guideline for healthcare professionals from the American Heart Association/American Stroke Association," *Stroke*, vol. 49, no. 3, 2018.
- [4] H. Kim, R. A.-S. Salman, C. E. McCulloch, C. Stapf, W. L. Young, and For the MARS Coinvestigators, "Untreated brain arteriovenous malformation: patient-level meta-analysis of hemorrhage predictors," *Neurology*, vol. 83, no. 7, pp. 590–597, 2014.
- [5] C. P. Derdeyn, G. J. Zipfel, F. C. Albuquerque et al., "Management of brain arteriovenous malformations: a scientific statement for healthcare professionals from the American Heart Association/American Stroke Association," *Stroke*, vol. 48, no. 8, pp. e200–200e224, 2017.
- [6] J. Emberson, K. R. Lees, P. Lyden et al., "Effect of treatment delay, age, and stroke severity on the effects of intravenous thrombolysis with alteplase for acute ischaemic stroke: a meta-analysis of individual patient data from randomised trials," *Lancet*, vol. 384, no. 9958, pp. 1929–1935, 2014.
- [7] J. M. Gidday, "Cerebral preconditioning and ischaemic tolerance," *Nature Reviews. Neuroscience*, vol. 7, no. 6, pp. 437–448, 2006.
- [8] N. Thushara Vijayakumar, A. Sangwan, B. Sharma, A. Majid, and G. K. Rajanikant, "Cerebral ischemic preconditioning: the road so far..." *Molecular Neurobiology*, vol. 53, no. 4, pp. 2579–2593, 2016.
- [9] S. V. Narayanan, K. R. Dave, and M. A. Perez-Pinzon, "Ischemic preconditioning and clinical scenarios," *Current Opinion in Neurology*, vol. 26, no. 1, pp. 1–7, 2013.
- [10] P. Meybohm, B. Bein, O. Brosteanu et al., "A multicenter trial of remote ischemic preconditioning for heart surgery," *The New England Journal of Medicine*, vol. 373, no. 15, pp. 1397–1407, 2015.
- [11] L. Xiong, Z. Lu, L. Hou et al. et al., "Pretreatment with repeated electroacupuncture attenuates transient focal cerebral ischemic injury in rats," *Chinese Medical Journal*, vol. 116, no. 1, pp. 108–111, 2003.
- [12] Z. Liu, X. Chen, Y. Gao et al., "Involvement of GluR2 up-regulation in neuroprotection by electroacupuncture pretreatment via cannabinoid CB1 receptor in mice," *Scientific Reports*, vol. 5, no. 1, 2015.
- [13] L. Chavez, S.-S. Huang, I. MacDonald, J.-G. Lin, Y.-C. Lee, and Y.-H. Chen, "Mechanisms of acupuncture therapy in ischemic stroke rehabilitation: a literature review of basic studies," *International Journal of Molecular Sciences*, vol. 18, no. 11, p. 2270, 2017.

- [14] Q. Y. Chang, Y. W. Lin, and C. L. Hsieh, "Acupuncture and neuroregeneration in ischemic stroke," *Neural Regeneration Research*, vol. 13, no. 4, pp. 573–583, 2018.
- [15] O. Revah, E. Lasser-Katz, I. A. Fleidervish, and M. J. Gutnick, "The earliest neuronal responses to hypoxia in the neocortical circuit are glutamate-dependent," *Neurobiology of Disease*, vol. 95, pp. 158–167, 2016.
- [16] K. L. Simpkins, R. P. Guttman, Y. Dong et al., "Selective activation induced cleavage of the NR2B subunit by calpain," *The Journal of Neuroscience: the official journal of the Society for Neuroscience*, vol. 23, no. 36, pp. 11322–11331, 2003.
- [17] J. Y. Jang, Y. W. Choi, H. N. Kim et al., "Neuroprotective effects of a novel single compound 1-methoxyoctadecan-1-ol isolated from *Uncaria sinensis* in primary cortical neurons and a photothrombotic ischemia model," *PLOS One*, vol. 9, no. 1, p. e85322, 2014.
- [18] D. Purves, G. J. Augustine, D. Fitzpatrick et al., *Neuroscience*, Sinauer Associates, 2004.
- [19] K. R. Dave, C. Lange-Asschenfeldt, A. P. Raval et al., "Ischemic preconditioning ameliorates excitotoxicity by shifting glutamate/gamma-aminobutyric acid release and biosynthesis," *Journal of Neuroscience Research*, vol. 82, no. 5, pp. 665–673, 2005.
- [20] A. G. Douen, K. Akiyama, M. J. Hogan et al., "Preconditioning with cortical spreading depression decreases inraischemic cerebral glutamate levels and down-regulates excitatory amino acid transporters EAAT1 and EAAT2 from rat cerebral cortex plasma membranes," *Journal of Neurochemistry*, vol. 75, no. 2, pp. 812–818, 2000.
- [21] J. H. Garcia, S. Wagner, K. F. Liu, and X. J. Hu, "Neurological deficit and extent of neuronal necrosis attributable to middle cerebral artery occlusion in rats. Statistical validation," *Stroke*, vol. 26, no. 4, pp. 627–635, 1995.
- [22] Y. Guo, "Experimental acupuncture science," *Zhong Guo Zhong Yi Yao Chu Ban She*, 2016.
- [23] Y. Yang, "Study on behavior and neurovascular regeneration mechanism of acupuncture in rats with cerebral ischemia-reperfusion injury," *Peking Union Medical College*, 2016.
- [24] S. L. Stevens, K. B. Vartanian, and M. P. Stenzel-Poore, "Reprogramming the response to stroke by preconditioning," *Stroke*, vol. 45, no. 8, pp. 2527–2531, 2014.
- [25] F. R. Bahjat, R. Gesuete, and M. P. Stenzel-Poore, "Steps to translate preconditioning from basic research to the clinic," *Translational Stroke Research*, vol. 4, no. 1, pp. 89–103, 2013.
- [26] The NINDS t-PA Stroke Study Group, "Intracerebral Hemorrhage After Intravenous t-PA Therapy for Ischemic Stroke," *Stroke*, vol. 28, no. 11, pp. 2109–2118, 1997.
- [27] A. Yang, H. M. Wu, J.-L. Tang, L. Xu, M. Yang, and G. J. Liu, "Acupuncture for stroke rehabilitation," *The Cochrane Database of Systematic Reviews*, vol. 8, 2016.
- [28] S. Shariffar, J. J. Shuster, and M. D. Bishop, "Adding electrical stimulation during standard rehabilitation after stroke to improve motor function. A systematic review and meta-analysis," *Annals of Physical and Rehabilitation Medicine*, vol. 61, no. 5, pp. 339–344, 2018.
- [29] L. X. Li, K. Deng, and Y. Qu, "Acupuncture treatment for post-stroke dysphagia: an update meta-analysis of randomized controlled trials," *Chinese Journal of Integrative Medicine*, vol. 24, no. 9, pp. 686–695, 2018.
- [30] F. Wang, Z. Gao, X. Li et al., "NDRG2 is involved in anti-apoptosis induced by electroacupuncture pretreatment after focal cerebral ischemia in rats," *Neurological Research*, vol. 35, no. 4, pp. 406–414, 2013.
- [31] Z. Q. Wu, S. Y. Cui, L. Zhu, and Z. Q. Zou, "Study on the mechanism of mTOR-mediated autophagy during electroacupuncture pretreatment against cerebral ischemic injury," *Evidence-Based Complementary and Alternative Medicine: eCAM*, vol. 2016, pp. 1–8, 2016.
- [32] S. E. Khoshnam, W. Winlow, M. Farzaneh, Y. Farbood, and H. F. Moghaddam, "Pathogenic mechanisms following ischemic stroke," *Neurological Sciences: official journal of the Italian Neurological Society and of the Italian Society of Clinical Neurophysiology*, vol. 38, no. 7, pp. 1167–1186, 2017.
- [33] L. Manni, M. Albanesi, M. Guaragna, S. B. Paparo, and L. Aloe, "Neurotrophins and acupuncture," *Autonomic Neuroscience: Basic & Clinical*, vol. 157, no. 1-2, pp. 9–17, 2010.
- [34] Z. Y. J. Z. M. GUO, "Effect of electroacupuncture pretreatment on glutamate and  $\gamma$ -amino butyric acid in rats following middle cerebral artery occlusion," *Shi Yong Lao Nian Yi Xue*, vol. 27, 2013.
- [35] P. Y. Meng, G. J. Sun, S. H. Liu, and H. M. Yan, "Effect of electroacupuncture pretreatment on glutamate-NMDAR signal pathway in hippocampal neurons of vascular dementia rats," *Zhen Ci Yan Jiu*, vol. 33, no. 2, pp. 103–106, 2008.
- [36] X. Zhu, J. Yin, L. Li et al., "Electroacupuncture preconditioning-induced neuroprotection may be mediated by glutamate transporter type 2," *Neurochemistry International*, vol. 63, no. 4, pp. 302–308, 2013.
- [37] M. Tymianski, M. P. Charlton, P. L. Carlen, and C. H. Tator, "Source specificity of early calcium neurotoxicity in cultured embryonic spinal neurons," *The Journal of Neuroscience: the official journal of the Society for Neuroscience*, vol. 13, no. 5, pp. 2085–2104, 1993.
- [38] K. Furukawa, W. Fu, Y. Li, W. Witke, D. J. Kwiatkowski, and M. P. Mattson, "The actin-severing protein gelsolin modulates calcium channel and NMDA receptor activities and vulnerability to excitotoxicity in hippocampal neurons," *The Journal of Neuroscience: the official journal of the Society for Neuroscience*, vol. 17, no. 21, pp. 8178–8186, 1997.
- [39] Y. Liu, T. P. Wong, M. Aarts et al., "NMDA receptor subunits have differential roles in mediating excitotoxic neuronal death both in vitro and in vivo," *The Journal of Neuroscience: the official journal of the Society for Neuroscience*, vol. 27, no. 11, pp. 2846–2857, 2007.
- [40] R. Simon, J. Swan, T. Griffiths, and B. Meldrum, "Blockade of N-methyl-D-aspartate receptors may protect against ischemic damage in the brain," *Science*, vol. 226, no. 4676, pp. 850–852, 1984.
- [41] I. Margail, S. Parmentier, J. Callebert, M. Allix, R. G. Boulu, and M. Plotkine, "Short therapeutic window for MK-801 in transient focal cerebral ischemia in normotensive rats," *Journal of Cerebral Blood Flow and Metabolism*, vol. 16, no. 1, pp. 107–113, 1996.
- [42] M. H. Shen, C. B. Zhang, J. H. Zhang, and P. F. Li, "Electroacupuncture attenuates cerebral ischemia and reperfusion injury in middle cerebral artery occlusion of rat via modulation of apoptosis, inflammation, oxidative stress, and excitotoxicity," *Evidence-Based Complementary and Alternative Medicine: eCAM*, vol. 2016, article 9438650, pp. 1–15, 2016.
- [43] T. W. Lai, S. Zhang, and Y. T. Wang, "Excitotoxicity and stroke: identifying novel targets for neuroprotection," *Progress in Neurobiology*, vol. 115, pp. 157–188, 2014.

- [44] G. Y. Wu, K. Deisseroth, and R. W. Tsien, "Activity-dependent CREB phosphorylation: convergence of a fast, sensitive calmodulin kinase pathway and a slow, less sensitive mitogen-activated protein kinase pathway," *Proceedings of the National Academy of Sciences of the United States of America*, vol. 98, no. 5, pp. 2808–2813, 2001.
- [45] R. T. Bartus, N. J. Hayward, P. J. Elliott et al., "Calpain inhibitor AK295 protects neurons from focal brain ischemia. Effects of postocclusion intra-arterial administration," *Stroke*, vol. 25, no. 11, pp. 2265–2270, 1994.
- [46] R. W. Neumar, F. H. Meng, A. M. Mills et al., "Calpain activity in the rat brain after transient forebrain ischemia," *Experimental Neurology*, vol. 170, no. 1, pp. 27–35, 2001.
- [47] C. M. Gladding, M. D. Sepers, J. Xu et al., "Calpain and STriatal-enriched protein tyrosine phosphatase (STEP) activation contribute to extrasynaptic NMDA receptor localization in a Huntington's disease mouse model," *Human Molecular Genetics*, vol. 21, no. 17, pp. 3739–3752, 2012.
- [48] M. Curcio, I. L. Salazar, M. Mele, L. M. T. Canzoniero, and C. B. Duarte, "Calpains and neuronal damage in the ischemic brain: the Swiss knife in synaptic injury," *Progress in Neurobiology*, vol. 143, pp. 1–35, 2016.
- [49] H. C. Lai, Q. Y. Chang, and C. L. Hsieh, "Signal transduction pathways of acupuncture for treating some nervous system diseases," *Evidence-Based Complementary and Alternative Medicine: eCAM*, vol. 2019, article 2909632, pp. 1–37, 2019.
- [50] T. Wang, F. Wang, L. Yu, and Z. Li, "Nobiletin alleviates cerebral ischemic-reperfusion injury via MAPK signaling pathway," *American Journal of Translational Research*, vol. 11, no. 9, pp. 5967–5977, 2019.
- [51] Y. Xing, S. D. Yang, M. M. Wang, F. Dong, Y. S. Feng, and F. Zhang, "Electroacupuncture alleviated neuronal apoptosis following ischemic stroke in rats via Midkine and ERK/JNK/p38 signaling pathway," *Journal of Molecular Neuroscience: MN*, vol. 66, no. 1, pp. 26–36, 2018.
- [52] K. M. Walton, R. DiRocco, B. A. Bartlett et al., "Activation of p38<sup>MAPK</sup> in microglia after ischemia," *Journal of Neurochemistry*, vol. 70, no. 4, pp. 1764–1767, 1998.

## Research Article

# Electroacupuncture Involved in Motor Cortex and Hypoglossal Neural Control to Improve Voluntary Swallowing of Poststroke Dysphagia Mice

Shuai Cui,<sup>1,2</sup> Shuqi Yao,<sup>1</sup> Chunxiao Wu ,<sup>1</sup> Lulu Yao,<sup>1</sup> Peidong Huang,<sup>3</sup> Yongjun Chen ,<sup>1</sup> Chunzhi Tang ,<sup>1</sup> and Nenggui Xu <sup>1</sup>

<sup>1</sup>South China Research Center for Acupuncture and Moxibustion, Medical College of Acupuncture Moxibustion and Rehabilitation, Guangzhou University of Chinese Medicine, 510006 Guangzhou, China

<sup>2</sup>Research Institute of Acupuncture and Meridian, Anhui University of Chinese Medicine, 230038 Hefei, China

<sup>3</sup>Acupuncture Massage and Rehabilitation Institute, Yunnan University of Chinese Medicine, 650500 Kunming, China

Correspondence should be addressed to Nenggui Xu; [ngxu8018@163.com](mailto:ngxu8018@163.com)

Received 11 April 2020; Revised 20 July 2020; Accepted 6 September 2020; Published 27 September 2020

Academic Editor: Stuart C. Mangel

Copyright © 2020 Shuai Cui et al. This is an open access article distributed under the Creative Commons Attribution License, which permits unrestricted use, distribution, and reproduction in any medium, provided the original work is properly cited.

The descending motor nerve conduction of voluntary swallowing is mainly launched by primary motor cortex (M1). M1 can activate and regulate peripheral nerves (hypoglossal) to control the swallowing. Acupuncture at “Lianquan” acupoint (CV23) has a positive effect against poststroke dysphagia (PSD). In previous work, we have demonstrated that electroacupuncture (EA) could regulate swallowing-related motor neurons and promote swallowing activity in the essential part of central pattern generator (CPG), containing nucleus ambiguus (NA), nucleus of the solitary tract (NTS), and ventrolateral medulla (VLM) under the physiological condition. In the present work, we have investigated the effects of EA on the PSD mice *in vivo* and sought evidence for PSD improvement by electrophysiology recording and laser speckle contrast imaging (LSCI). Four main conclusions can be drawn from our study: (i) EA may enhance the local field potential in noninfarction area of M1, activate the swallowing-related neurons (pyramidal cells), and increase the motor conduction of noninfarction area in voluntary swallowing; (ii) EA may improve the blood flow in both M1 on the healthy side and deglutition muscles and relieve PSD symptoms; (iii) EA could increase the motor conduction velocity (MCV) in hypoglossal nerve, enhance the EMG of mylohyoid muscle, alleviate the paralysis of swallowing muscles, release the substance P, and restore the ability to drink water; and (iv) EA can boost the functional compensation of M1 in the noninfarction side, strengthen the excitatory of hypoglossal nerve, and be involved in the voluntary swallowing neural control to improve PSD. This research provides a timely and necessary experimental evidence of the motor neural regulation in dysphagia after stroke by acupuncture in clinic.

## 1. Introduction

“Dysphagia” is defined as an obstacle to the flow of liquid-s/pills from the mouth to the esophagus. Dysphagia is a serious problem in various neurologic diseases, and it is associated with an increase in morbidity and mortality [1–6]. Stroke is the most common neurologic cause of dysphagia. Severe dysphagia is usually observed during the first 2–4 weeks after stroke, and a prevalence of 29%–81% has been documented. However, minor disorders of swallowing have been reported at a prevalence of 91% in the stroke patients

[5, 7–9]. Dysphagia can result in significant complications, such as malnutrition, aspiration pneumonia, and poor quality of life [10–12]. A large number of functional and structural abnormalities are present in dysphagia patients in each of its phases, such as the oral cavity, pharynx, larynx, or esophagus [13–15].

To initiate and regulate swallowing, a combination of feedback and motor planning is required [16]. Most scholars believe that the cortical swallowing center is concentrated mainly in the primary sensorimotor cortex, anterior cingulate gyrus, and insula [17]. The characteristics of injury to



the cortical swallowing center are multifocal and bilateral, damage to which can affect the subthreshold excitability of nucleus tractus solitarius and nucleus ambiguus in the central pattern generator (CPG) for swallowing and reduce its regulation of swallowing function [18]. M1 can regulate the processing and transmission of neural information in the brain. Yuan and his colleagues found that the excitability and area of the motor cortex associated with swallowing were increased in the left hemisphere and alleviated the swallowing dysfunction of patients if the right motor cortex was injured [19]. That result showed that dysphagia improvement required maintenance of bilateral pathways. However, most studies mainly involved in healthy people or a small sample of patients with dysphagia, while experimental studies exploring the underlying mechanisms are so limited. Therefore, further research is required to understand how the motor cortex conducts through the descending motor nerves, affects swallowing function, and how blood flow changes in the brain and deglutition-muscle groups after dysphagia occurring.

The life quality of the patients suffering from poststroke dysphagia (PSD) can be affected severely if the PSD is caused by cortical ischemic injury, but various early rehabilitation programs can improve this situation [20]. Interventions for patients with dysphagia include electromyographic biofeedback, Mendelsohn maneuver, repetitive transcranial magnetic stimulation, and surface neuromuscular electrical stimulation. The mechanism underpinning neural regulation of swallowing is poorly understood. Hence, the relevant treatment and research methods are limited to only local changes in neural regulation of swallowing function, and the efficacy of some treatment methods has not been demonstrated. However, as a conventional therapy for stroke rehabilitation in China, acupuncture has been used extensively as a complementary or alternative therapy worldwide [21]. In PSD patients with cortical hemisphere injury, several studies have suggested that acupuncture may be helpful for patients' recovery [22, 23]. Animal experiments have shown that electrical stimulation can induce continuous swallowing [24]. In previous work, we have demonstrated that electroacupuncture (EA) could regulate swallowing-related motor neurons and promote swallowing activity in the essential part of central pattern generator (CPG), containing nucleus ambiguus (NA), nucleus of the solitary tract (NTS), and ventrolateral medulla (VLM) under the physiological condition ([25]; You H et al., 2018; [26]). Some researchers have also found that electrical stimulation can reorganize the motor-cortex neurons involved in swallowing. Only M1, thalamus, and insula are activated after transcutaneous electrical stimulation in pharyngeal muscle; in addition, cortical recombination mediated by electrical stimulation improves swallowing function, which is closely correlated to the occurrence and parameters of electrical stimulation [27–29]. M1 has a crucial role in the neural pathway that controls voluntary swallowing. Although its role in the voluntary oral phase of swallowing is undisputed [30], its precise role in motor control of the pharyngeal phase is not clearly defined, and the descending neural regulation of swallowing is also not clear.

In the present study, the mice suffering swallowing dysfunction after stroke were treated by EA. We aimed to observe the descending motor nerve regulation mechanism and blood flow changes involved in voluntary swallowing, so we could further illuminate how EA intervene the motor neural control of voluntary swallowing to improve PSD in mice.

## 2. Materials and Methods

**2.1. Ethical Approval of the Study Protocol.** This study was carried out in accordance with the principles of the Basel Declaration and recommendations of the guidelines of the Guangzhou University of Chinese Medicine Committee for Care and Use of Research Animals. The protocol was approved by the Guangzhou University of Chinese Medicine Committee for Care and Use of Research Animals.

**2.2. Animals.** Animals were provided by the Animal Laboratory Center of Guangzhou University of Chinese Medicine (Guangzhou, China; experimental animal certificate number: 44005800008103; animal license number: SCXK (Yue) 2013-0034).

Male C57BL/6J mice (8 months, specific pathogen-free, 25–33 g) were housed in individual cages under standard laboratory conditions. Food and water were supplied ad libitum.

A total of 12 mice from 67 mice were randomly selected as a normal group to test laser speckle contrast imaging (LSCI), electroencephalogram (EEG), electromyography (EMG), water intake, and substance P (SP) concentration.

The rest 55 mice were used to build a PSD model by photochemical method. EA and sham EA were applied on the PSD model. For EA, the needle was retaining, and electric stimulation lasted 15 min, but for sham EA, no electric stimulation was given. EA (acute) was only stimulated for one day; EA (chronic) was stimulated continuously for three days. 18 mice were randomly selected into three groups: sham EA, EA (acute), and EA (chronic) to test LSCI and electrophysiology recording, which were compared before and after stimulation. 24 mice randomly selected four groups: model, sham EA, EA (acute), and EA (chronic) to test electromyography (EMG), water intake, and SP concentration. 7 mice from 67 mice were excluded because the model was not successful.

**2.3. PSD Model.** We referred to the modeling method of Michael Schroeter [31]. Mice were fixed with a holder. Tail veins were injected with Rose Bengal solution (1.5%; Sigma–Aldrich, Saint Louis, MO, USA) at 10  $\mu$ L/g body weight. After injection, anesthesia was induced with 4% isoflurane. Then, anesthesia was maintained with 2% isoflurane using a mask.

Mice were fixed on stereotaxic apparatus (RWD Biotechnology, Shenzhen, China). The skull was exposed, and the correct M1 coordinates were located (1 mm lateral and 0.16 mm posterior to the bregma; depth from the brain surface, 1 mm). A laser (wave length: 530 nm; power: 15 mW) was used to irradiate an area of  $\sim$ 2 mm<sup>2</sup>. After 8 min of irradiation, the scalp was sutured, and mice were placed back in



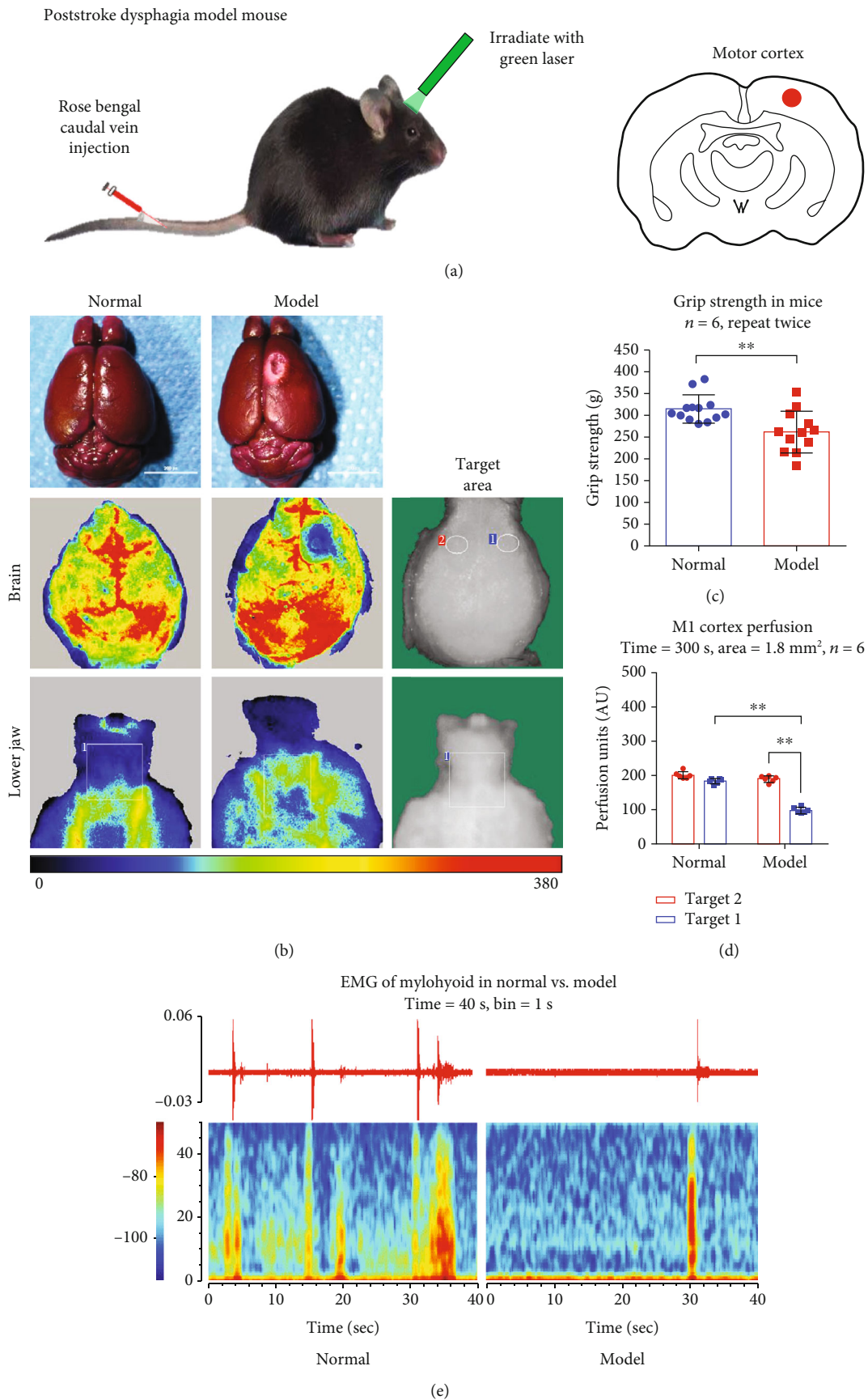


FIGURE 1: Continued.

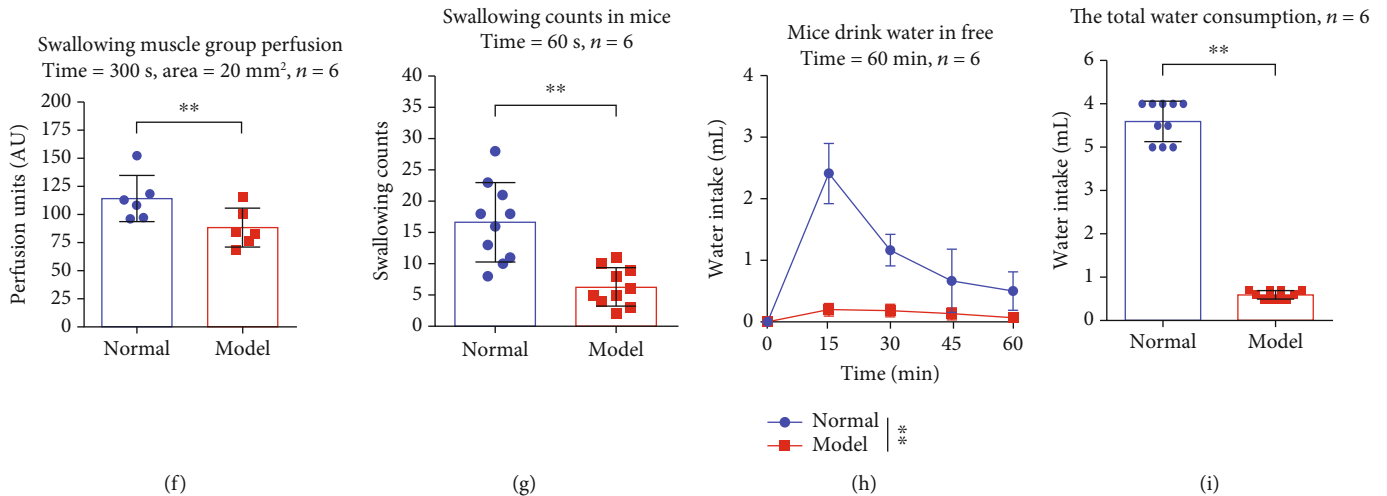


FIGURE 1: Evaluation of some indexes between the poststroke dysphagia (PSD) model and normal mice. (a) The PSD model process and cerebral infarcts position. (b) Laser speckle contrast imaging (LSCI): the brain and lower jaw in normal and the model group. (c) Grip strength test: normal vs. model:  $**p < 0.01$ . (d) Motor cortex perfusion: time = 300 s, target 1 = noninfarction, target 2 = infarction, target area = 1.8 mm<sup>2</sup>, normal vs. model (target 1):  $**p < 0.01$ , target 2 vs. target 1 (model):  $**p < 0.01$ . (e) Electromyography (EMG) of mylohyoid and real-time spectrum in normal vs. model group, time = 40 s, bin = 1 s. (f) Swallowing muscle perfusion: time = 300 s, target area = 20 mm<sup>2</sup>, normal vs. model:  $**p < 0.01$ . (g) Swallowing counts: time = 60 s, normal vs. model:  $**p < 0.01$ . (h) Drink water at different times: time = 0 min, 15 min, 30 min, 45 min, and 60 min. Normal vs. model:  $**p < 0.01$ . (i) Total water consumption: normal vs. model:  $**p < 0.01$ .

their cages to recover from anesthesia. Swallowing-related muscle function and water intake were evaluated in conscious mice (Figures 1(a) and 1(g)–1(i)).

**2.4. EA Parameters.** Anesthesia was induced using 4% isoflurane. Mice were laid supine and fixed. Anesthesia was maintained with 2% isoflurane using a mask. First routinely sterilized neck skin, then we located CV23. We inserted an acupuncture needle to the upper margin of the midline of the mandible. Another needle was inserted 2 mm adjacent to CV23. The needling depth of CV23 is 5 mm. An EA apparatus (continuous wave; current, 1 mA; frequency, 2 Hz; time, 15 min per day; HANS-200A/100B; HANS, Beijing, China) was attached to the acupuncture needle: acute EA treatment for 1 day and chronic EA treatment for continuous 3 days (Figure 2(a)).

**2.5. Grip Strength Test.** The grasping power of mice limbs was measured by a grip tester (YLS-13A1; YiyanTechnology & Development, Shandong, China). Mice of identical age were employed in this experiment only if their toes were not damaged.

Mice were placed carefully on a grip power board. Their tails were held, and mice were pulled back gently in the horizontal direction. The mice were pulled back with even greater force after they grasped the plate, causing them to loosen their claws. The instrument recorded the maximum grip strength of mice limbs automatically. This experiment was repeated twice for each mouse in each group, and the average value was taken.

**2.6. LSCI.** Mice were anesthetized with 2% isoflurane and then fixed on stereotaxic apparatus (RWD Biotechnology).

The skull was exposed. A laser was focused on the target area. Recording was lasted for 5 min. We observed changes in total cerebral blood flow to selected infarction area and noninfarction area (area: 1.8 mm<sup>2</sup>) of the motor cortex and compared blood perfusion changes in each group.

Mice were laid supine and fixed. Fur near the mylohyoid muscle was removed by using depilatory cream. The laser was focused on the swallowing muscles (area: 20 mm<sup>2</sup>). Recording was lasted for 5 min. We observed the blood perfusion changes around the swallowing muscles.

**2.7. Recording of the Discharge of M1 Neurons In Vivo.** Anesthesia was maintained with 2% isoflurane, and mice were fixed on stereotaxic apparatus. The skull was exposed after routine sterilization. The left M1 coordinates were located (bregma: -0.16 mm; LR: 1 mm; H: 1 mm). Then, 2 × 4 + 1 matrix electrodes were implanted in the target brain region to observe spontaneous discharges through a multichannel recording system (Plexon, Dallas, TX, USA). Spikes and LFP were recorded for 5 min in each group. An offline sorter (Plexon) was used to filter signals. Processed signals were analyzed statistically using NeuroExplorer™ (Nex Technologies, Lexington, MA, USA).

**2.8. Recording of Hypoglossal Nerves In Vivo.** Mice were fixed supine. Anesthesia was maintained with 2% isoflurane. The cervical hypoglossal nerve was isolated carefully and then drawn out with a thin wire (Figure 3(e)). Bipolar platinum recording electrodes were hooked up to the hypoglossal nerve. A drop of paraffin oil was placed over the surface of the nerve. The reference electrode was inserted into nearby subcutaneous tissue. After waking from anesthesia, water feeding was initiated with a 5 mL microsyringe. Changes in

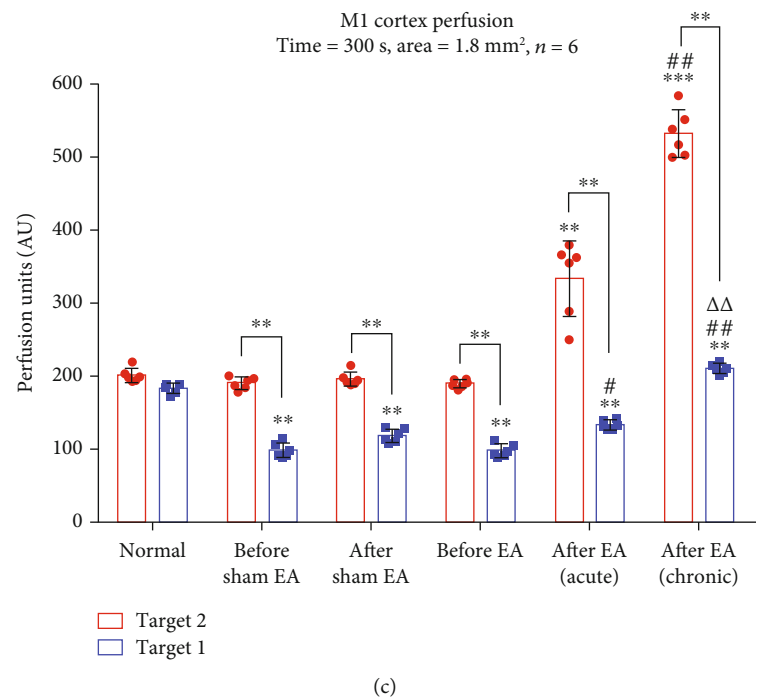
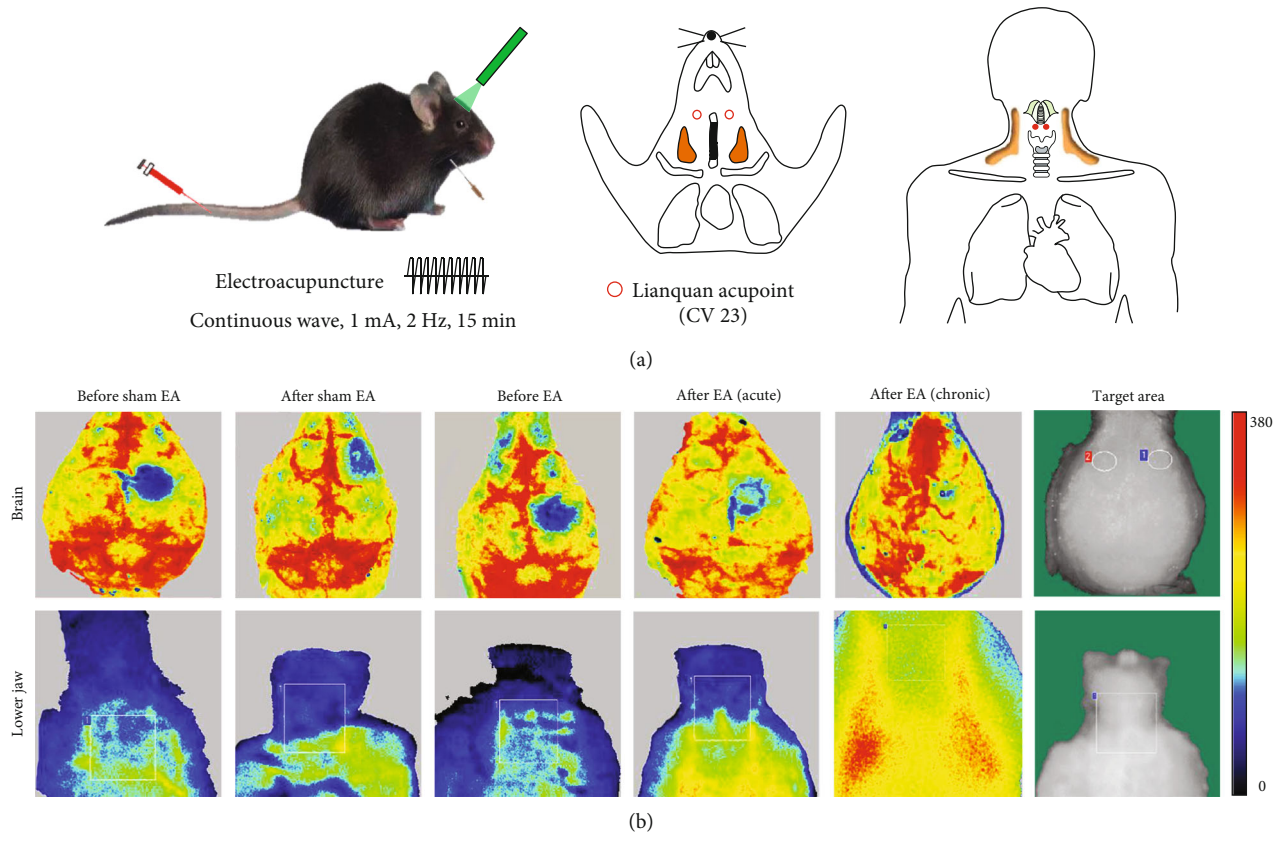


FIGURE 2: Continued.

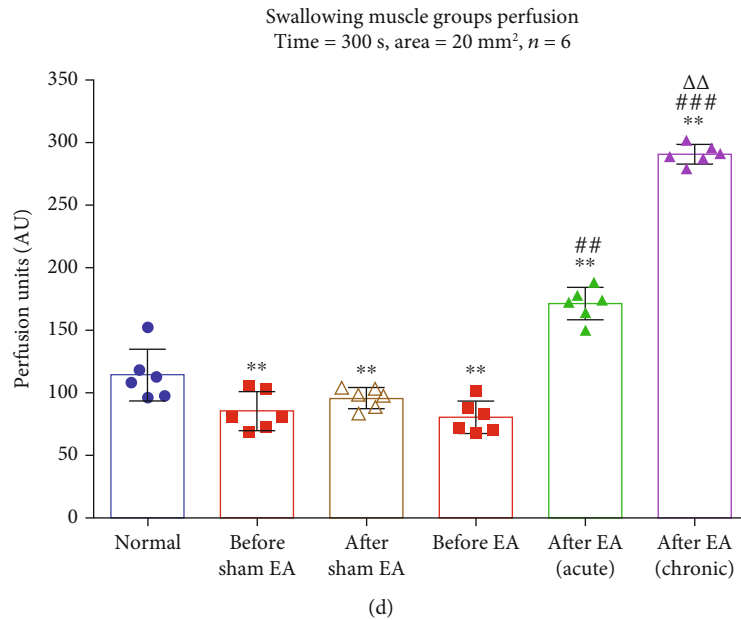


FIGURE 2: The brain and lower jaw blood perfusion changes at before and after electroacupuncture in the PSD model. (a) Electroacupuncture parameters: continuous wave, 1 mA, 2 Hz, and 15 min. Acupoint: Lianquan (CV 23). (b) The brain and lower jaw of LSCI in each group: sham EA = lack of electric stimulation, after EA (acute) = EA stimulation once, and after EA (chronic) = EA stimulation for 3 days. (c) Motor cortex perfusion: time = 300 s, target 1 = noninfarction, target 2 = infarction, target area = 1.8 mm<sup>2</sup>, normal vs. others group (target 1):  $**p < 0.01$ . Target 2 vs. target 1:  $**p < 0.01$  in others group except normal. Before EA vs. after EA (acute) (target 1):  $^{\#}p < 0.05$ ; before EA vs. after EA (chronic) (target 1):  $^{##}p < 0.01$ . Before EA vs. after EA (acute) (target 2):  $**p < 0.01$ , before EA vs. after EA (chronic) (target 2):  $^{***}p < 0.001$ . After EA (acute) vs. after EA (chronic) (target 2):  $^{##}p < 0.01$ . After EA (acute) vs. after EA (chronic) (target 2):  $^{\Delta\Delta}p < 0.01$ . (d) Swallowing muscle perfusion: time = 300 s, target area = 20 mm<sup>2</sup>, compared with normal,  $**p < 0.01$  in others group. Before EA vs. after EA (acute):  $^{\#}p < 0.01$ . Before EA vs. after EA (chronic):  $^{***}p < 0.001$ . After EA (acute) vs. after EA (chronic):  $^{\Delta\Delta}p < 0.01$ .

activity of hypoglossal nerve was evoked and recorded by Spike2 in mice swallowing (Fig. S4).

**2.9. EMG Recording in the Mylohyoid Muscle In Vivo.** Anesthesia was induced with 4% isoflurane. Mice were fixed supine on stereotaxic apparatus at 45°. Pure water (4 mL) was extracted with a 5 mL intragastric syringe and placed in a microinjection pump (Stoelting, Wood Dale, IL, USA). The angle of the lavage needle was adjusted for placement under the tongue. A recording electrode was inserted into the mylohyoid muscle. The reference electrode was inserted into the masseter muscle. After waking up from anesthesia, mice were given water (2  $\mu$ L/s, 5 s). The EMG activity of the mylohyoid muscle was evoked and recorded by the Spike2 software (CED, Cambridge, UK) when mice were swallowing water.

**2.10. MCV.** Mice were placed under 2% isoflurane anesthesia in the supine position. One side of the hypoglossal nerve was separated, and the mylohyoid muscle was exposed. The hook-shaped stimulation electrode was placed in the hypoglossal nerve trunk, the recording electrode was placed in the mylohyoid muscle, and the reference electrode was placed in the nearby tissue. Pulling the hook electrode of hypoglossal nerve trunk for 1 second, the evoked EMG was observed (threshold: 0.02 mV, duration: 30 ms). The time from the stimulation point to the first evoked action potential was the latency:  $t$ , the distance from the nerve trunk to the

mylohyoid muscle:  $s$ , and conduction velocity:  $v = s/t$  (Figure 4(a)).

**2.11. Water Intake.** Five groups of mice ( $n = 6$ ) were fed separately and were deprived of water for 1 day. On day 2, each group was given drinking water *ad libitum*, and we recorded the changes in water intake at 15, 30, 45, and 60 min, as well as the total water intake in 1 day.

**2.12. SP Concentration in Serum.** Blood was obtained from the eyeballs of mice in each group after relevant experimental recording was completed. The extracted blood was placed at room temperature for 2 h and centrifuged at approximately 3500  $\times$  g for 15 min (at 4°C or room temperature for pre-chilled samples). After centrifugation, the supernatant was collected. The SP concentration was measured using an ELISA kit (ENZO Life Sciences, Farmingdale, NY, USA). Changes in the serum SP concentration in each group were compared.

**2.13. Linear Correlation Analysis.** Linear regression analysis was carried out on swallowing counts, water intake, SP concentration, swallowing-related pyramidal cell spike counts, and hypoglossal nerve spike counts.

**2.14. Statistical Analyses.** Statistical analyses were undertaken using SPSS 23.0 (IBM, Armonk, NY, USA). The difference between groups was analyzed by one-way ANOVA. The homogeneity of the variance was tested before comparisons

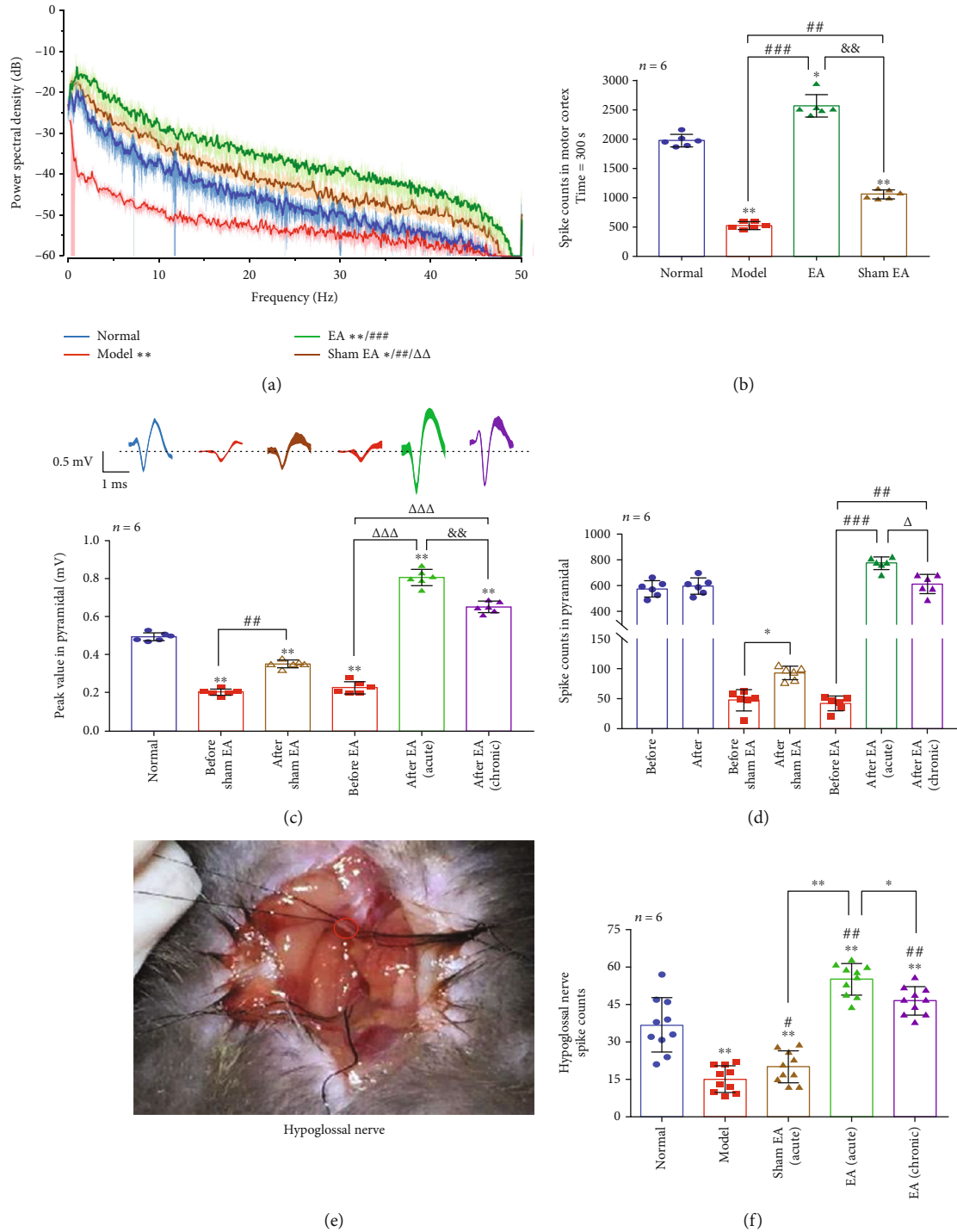


FIGURE 3: Electroacupuncture stimulation affects central and peripheral neurons activities. (a) Power spectral density in each group. Normal vs. model,  $**p < 0.01$ ; normal vs. EA,  $**p < 0.01$ ; normal vs. sham EA,  $*p < 0.05$ . Model vs. EA,  $###p < 0.001$ ; model vs. sham EA,  $##p < 0.01$ . EA vs. sham EA,  $\Delta\Delta p < 0.01$ . (b) Spike counts in motor cortex: time = 300 s, compared with normal,  $*p < 0.05$  in EA and  $**p < 0.01$  in the model and sham EA. Compared with the model,  $###p < 0.001$  in EA and  $##p < 0.01$  in sham EA. Compared with EA,  $\&\&p < 0.01$  in sham EA. (c) Pyramidal peak value in each group: compared with normal,  $**p < 0.01$  in others group. Before sham EA vs. after sham EA:  $##p < 0.01$ . Before EA vs. after EA (acute):  $\Delta\Delta\Delta p < 0.001$ , before EA vs. after EA (chronic):  $\Delta\Delta\Delta p < 0.001$ . After EA (acute) vs. after EA (chronic):  $\&\&p < 0.01$ . (d) Pyramidal spike counts in each group: before sham EA vs. after sham EA:  $*p < 0.05$ , before EA vs. after EA (acute):  $###p < 0.001$ , before EA vs. after EA (chronic):  $##p < 0.01$ , and after EA (acute) vs. after EA (chronic):  $\Delta p < 0.05$ . (e) Photograph was shown that hypoglossal nerve has been separated. (f) Hypoglossal nerve spike counts: compared with normal,  $**p < 0.01$  in others group. Compared with model,  $*p < 0.05$  in sham EA (acute) and  $**p < 0.01$  in EA (acute) and EA (chronic). Compared with sham EA (acute),  $**p < 0.01$  in EA (acute). Compared with EA (acute),  $*p < 0.05$  in EA (chronic).



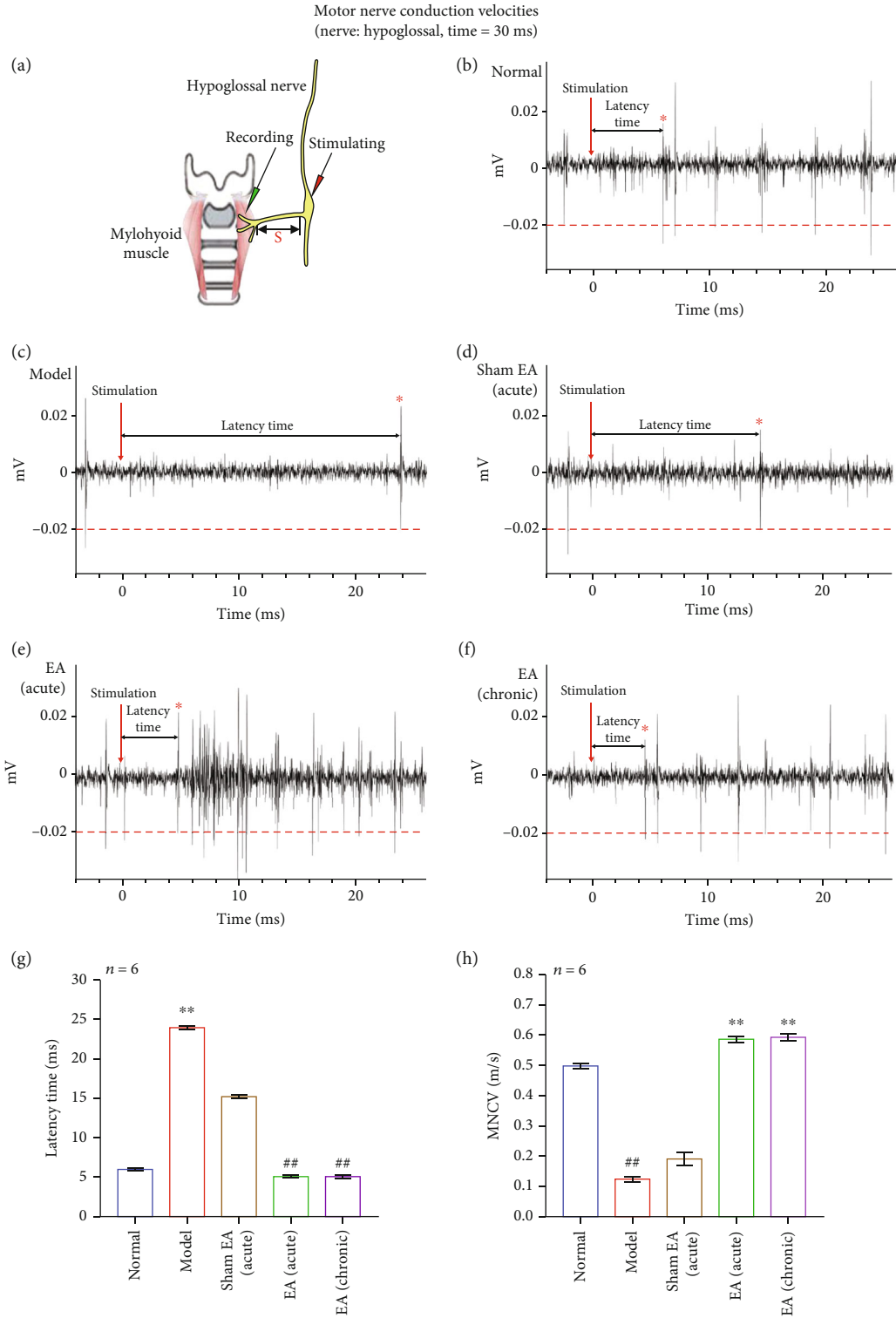


FIGURE 4: Motor conduction velocity of hypoglossal nerve. (a) Stimulation electrode: hypoglossal nerve trunk; recording electrode: mylohyoid muscle; the distance between nerve trunk and muscle:  $s$ ; the latency between stimulation point and the first EMG evoked by mylohyoid muscle:  $t$ ; MCV:  $v = s/t$ . (b–f) The latency between the stimulation point and the first induced EMG (marked with an asterisk) in each group. Model: PSD; sham EA: acupuncture without electric; EA acute: EA for 1 day; EA chronic: EA for 3 days. MCV was detected after treatment in each group. (g) Difference of latency in each group. Compared with the normal, the model increased significantly (\*\* $p < 0.01$ ); compared with the model, EA (acute) and EA (chronic) have obviously decreased (\*\* $p < 0.01$ ). (h) Difference of MNCV in each group. Compared with the normal, the model increased significantly (\*\* $p < 0.01$ ); compared with the model, EA (acute) and EA (chronic) have obviously decreased (\*\* $p < 0.01$ ).

between groups were made. The least-square difference test was used for homogeneity of variance, and the Tamhane's T2 test for heterogeneity of variance.  $p < 0.05$  was considered as statistically significant.

M1 neurons were analyzed by Offline Sorter™ and NeuroExplorer. Analyze methods including Raster, PCA, auto-correlation, and power spectral density were used.

The method of identifying neurons in M1 through auto-correlation analysis [32] and the characteristics of pyramidal cells were as follows: (1) low mean discharge frequency (0.5–10 Hz) and irregular discharge pattern; (2) the ISI histogram showed that the short ISI (3–10 ms) was dominant, and exponential attenuation was present after 3–5 ms ISI; and (3) wide waveform ( $>300 \mu\text{s}$ ). The characteristics of interneurons were as follows: (1) high mean discharge frequency ( $>5 \text{ Hz}$ ); (2) the ISI histogram presented delayed spikes and slower attenuation; and (3) narrow waveform ( $<250 \mu\text{s}$ ).

### 3. Results

**3.1. Impaired Blood Flow and Swallowing Function in PSD Mice Model.** To induce the PSD model, we used the photochemical method to cause infarction area in right M1, then to evaluate the model (Figure 1(a)). Compared with the control group, the grip power in the model decreased significantly in the grip strength test ( $n = 6$  mice/group,  $p < 0.01$ ), which suggested that symptoms of stroke caused by ischemia in the motor cortex (Figure 1(c)). By observing the brain and the lower jaw with laser speckle contrast imaging (LSCI), we found the right of M1 showed an obvious focal ischemia, and the blood perfusion of lower jaw was lower in the model (Figure 1(b)). Compared the target 1 (infarction area) with the target 2 (noninfarction area), the M1 perfusion was significantly different ( $n = 6$  mice/group,  $p < 0.01$ ). Compared with normal, the target 1 of the model was obviously decreased ( $n = 6$  mice/group,  $p < 0.01$ ), and swallowing muscle perfusion was significantly decreased ( $n = 6$  mice/group,  $p < 0.01$ ) (Figures 1(d) and 1(f)), which suggested that the blood flow in the brain was changed in the PSD model. Observing the EMG of mylohyoid in the model, we found that the real-time power spectrum and swallowing counts were reduced ( $n = 6$  mice/group,  $p < 0.01$ ) (Figures 1(e) and 1(g)), and water intake and total water consumption were also decreased, compared with the control group ( $n = 6$  mice/group,  $p < 0.01$ ) (Figures 1(h) and 1(i)). These results indicate swallowing and water intake dysfunction were caused by the PSD model.

**3.2. Effect of EA at CV23 on Cerebral Blood Flow and Lower Jaw in PSD Mice.** LSCI showed different cerebral blood flow and lower jaw at before and after EA or sham EA change (Figure 2(b)). The blood flow showed significant difference between infarction (target 1) and noninfarction (target 2) group ( $n = 6$  mice/group,  $p < 0.01$ ). After EA (acute), blood perfusion was increased in the noninfarction area ( $n = 6$  mice/group,  $p < 0.01$ ), and after EA (chronic), it was significantly increased, compared to before EA ( $p < 0.001$ ) and after EA (acute) group ( $p < 0.01$ ). These results illustrate EA could promote the blood perfusion of M1 in the noninfarction area.

The infarction area of M1 perfusion showed significant difference between each group ( $n = 6$  mice/group,  $p < 0.01$ ). After EA (acute) was increased than before EA in the infarction area ( $n = 6$  mice/group,  $p < 0.05$ ); after EA (chronic) was significantly increased than before EA ( $p < 0.01$ ) and after EA (acute) ( $p < 0.01$ ) (Figure 2(c)). These results show EA could supply blood perfusion in the infarction area and alleviate the infarction area.

In the lower jaw, swallowing muscle perfusion showed significant difference between each group ( $n = 6$  mice/group,  $p < 0.01$ ). Compared with before EA, the blood perfusion of after EA (acute) was increased ( $n = 6$  mice/group,  $p < 0.01$ ), after EA (chronic) was dramatically increased ( $p < 0.001$ ); compared with after EA (acute), after EA (chronic) was significantly increased ( $p < 0.01$ ) (Figure 2(d)). These results demonstrate EA could improve the blood flow of the lower jaw.

**3.3. The Neurons in Noninfarction Area of M1 Were Activated by EA in PSD Mice.** We implanted the multichannel electrodes into the noninfarction area of M1, compared spike counts in each group at before and after condition (Fig. S3A, S3B). First, we observed the normal group ( $n = 6$ ) at before and after recording: in total 5 units, 2 units were defined as interneurons, and 3 units were defined as pyramidal cells (Fig. S1A, S2A). Before vs. after, spike continuous (SPKC) and local field potential (LFP) showed no difference (before: interneurons account for 70.35%, and pyramidal cells account for 29.65%; after: interneurons account for 64.90%, and pyramidal cells account for 35.10% (Fig S3D)). In addition, we stimulated the model group ( $n = 6$ ) with sham EA (lack of electric). In total recording 3 units, 2 units were interneurons, and 1 unit was pyramidal cell (Fig. S1B, S1C; Fig.S2B, S2C). Before sham EA vs. after sham EA, SPKC and LFP were obviously decreased (before sham EA: interneurons account for 82.99%, and pyramidal cells account for 17.01%; after sham EA: interneurons account for 81.75%, and pyramidal cells account for 18.25% (Fig. S3E)). Third, we stimulated the model group ( $n = 6$ ) with EA (acute: 1 day): recording 3 units, 2 units were interneurons, and 1 unit was pyramidal cell (Fig. S1D, S2D). Before EA vs. after EA, SPKC and LFP were obviously increased. Before EA, interneurons account for 15.73%; after EA (acute), interneurons account for 66.38%, and pyramidal cells account for 33.62% (Fig. S3F). Finally, we sustained EA (chronic: 3 days) to stimulate the model group: recording 3 units, 2 units were interneurons, and 1 unit was pyramidal cell (Fig. S1E, S2E). After EA (acute) vs. after EA (chronic), SPKC and LFP were relatively stable. After (chronic), interneurons account for 65.40%, and pyramidal cells account for 34.60% (Figure S3F). These results indicate EA could evoke noninfarction neurons activities; the effect of chronic EA was lasting and stable than acute EA.

In the power spectral density, compared with the model, sham EA was different ( $p < 0.01$ ); EA was significantly different ( $p < 0.001$ ); compared with sham EA, EA was different ( $p < 0.01$ ). The results show that EA increased the energy of LFP (Figure 3(a)). At the same time, we found that the total spike counts of each group in M1 ( $n = 6$ , time = 300 s) were

TABLE 1: The different number of response neurons in each group of mice.

Groups ( $n = 6$ )	Model	Sham EA (acute)	EA (acute)	EA (chronic)	Normal
Interneuron	8	9	10	13	14
Pyramidal	2	4	8	10	15
Total	10	13	18	23	29

also changed; model was obviously decreased than normal ( $p < 0.01$ ), but after EA, the spike counts were significantly increased ( $p < 0.001$ ); it shows that EA can promote population neuronal activity of M1 in PSD mice (Figure 3(b)).

We identified the number of pyramidal cells in the motor cortex and observed their peak value and spike counts. The number of pyramidal cells in each group ( $n = 6$ ) was normal = 15, model = 2, sham EA = 4, EA (acute) = 8, and EA (chronic) = 10 (Table 1). Compared with peak value at before and after in each group (0.5 mV, 1 ms,  $n = 6$ ), each group was significantly different, compared with normal ( $p < 0.01$ ); after sham EA of peak value and spike counts were increased than before sham EA ( $p < 0.01$  and  $p < 0.05$ , separately); after EA (acute) and after EA (chronic) of peak value and spike counts were obviously increased than before EA ( $p < 0.001$  and  $p < 0.01$ , separately); after EA (chronic) of peak value and spike counts were decreased than after EA (acute) ( $p < 0.01$  and  $p < 0.05$ , separately). These demonstrated that EA could promote the potential intensity of pyramidal cells, chronic EA flattens the potential intensity of them (Figures 3(c) and 3(d)).

**3.4. The Effects of EA on Hypoglossal Nerve in PSD Mice.** To observe spike counts of hypoglossal nerve, we found that each group ( $n = 6$ ) was significantly different than normal ( $p < 0.01$ ). Compared the model, spike counts of sham EA, EA (acute), and EA (chronic) were increased ( $p < 0.05$ ,  $p < 0.01$ , and  $p < 0.01$ , separately). Compared with sham EA, EA (acute) and EA (chronic) were obvious increased ( $p < 0.01$ ). Compared with EA (acute), EA (chronic) was decreased ( $p < 0.05$ ) (Figure 3(f)). These results show that EA could excite the swallowing-related (hypoglossal) nerves, and chronic EA may inhibit peripheral nerves overexcitation and restore them to a nearly normal level.

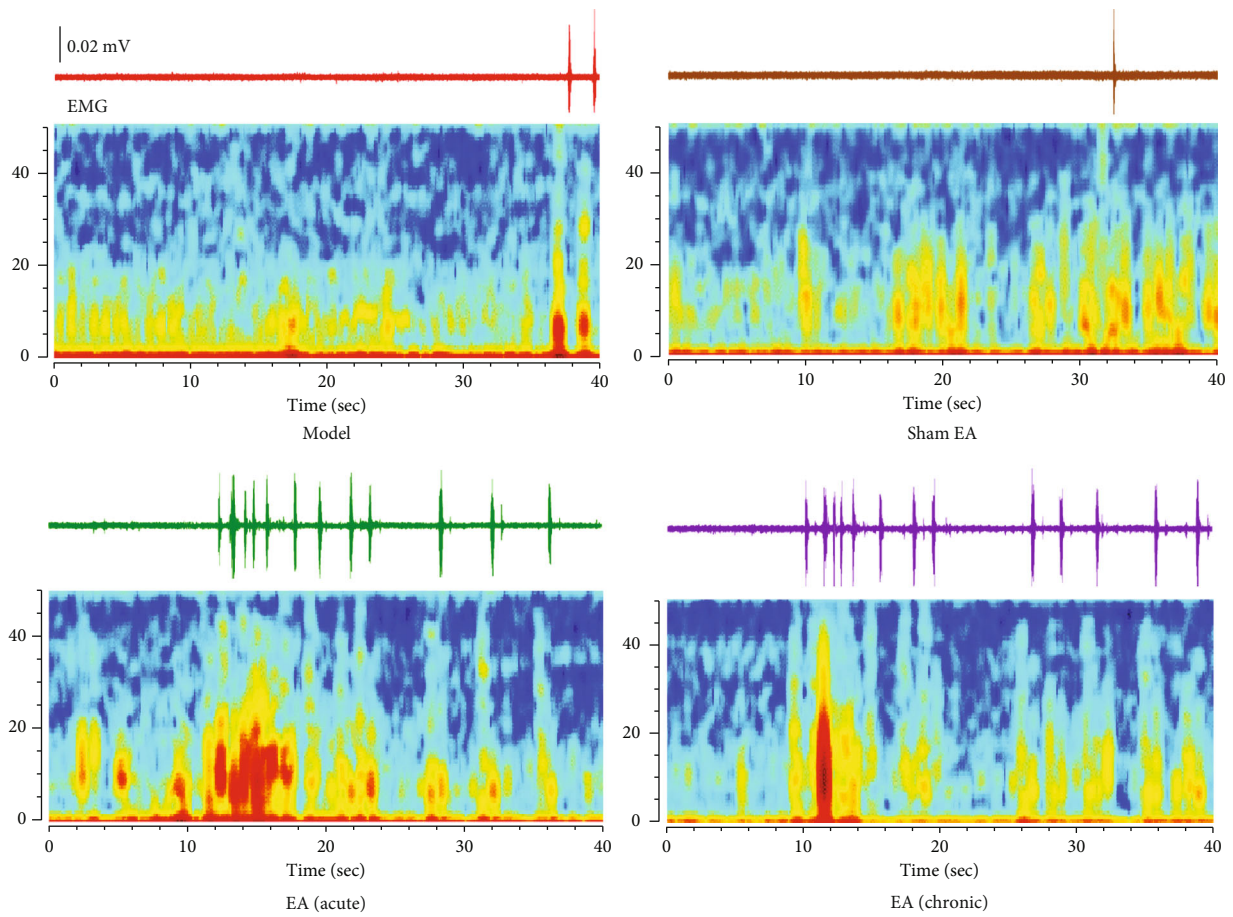
**3.5. The Effects of EA on MCV in PSD Mice.** The hypoglossal nerve is one of the peripheral nerves innervating the swallowing of the mylohyoid muscle. We verified the effect of motor cortex injury on peripheral nerve discharges by stimulating the hypoglossal nerve trunk to induce the EMG of the muscle. It was found that the latency of action potential induced by dysphagia after stroke was significantly prolonged ( $p < 0.01$ ) (Figures 4(c) and 4(g)), indicating that the motor conduction ability of hypoglossal nerve decreased significantly due to the M1 injury ( $p < 0.01$ ) (Figure 4(h)). However, both acute and chronic EA treatment could obviously shorten the latency of the motor conduction ( $p < 0.01$ ) (Figures 4(e)–4(g)), gradually increase the MNCV ( $p < 0.01$ ) (Figure 4(h)), and recover the hypoglossal nerve function.

It is inferred that dysphagia after stroke can affect the swallowing-related peripheral motor nerve, and EA could improve the conduction disorder caused by M1 injury, thus promoting the swallowing function recovery.

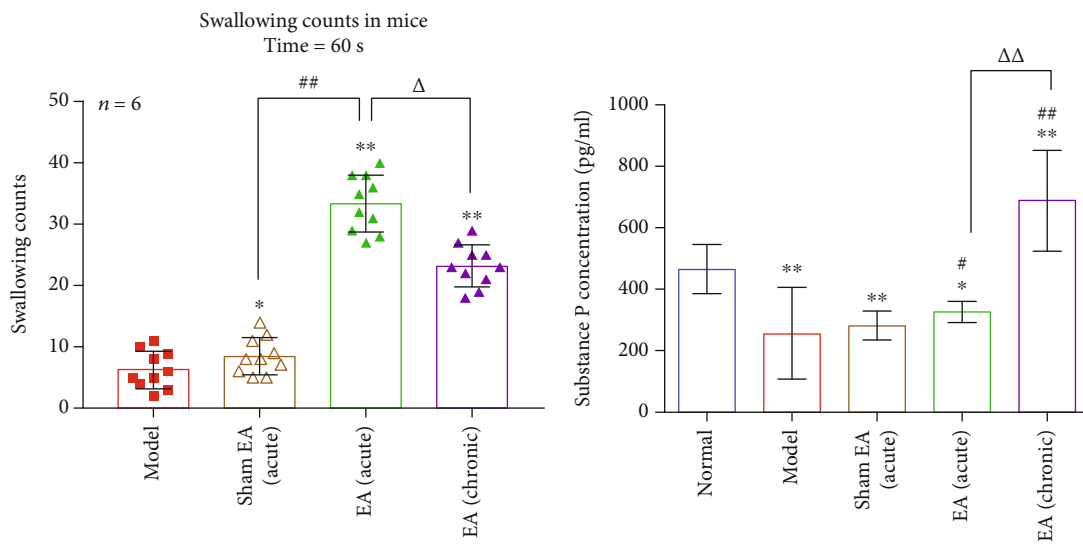
**3.6. The Effects of EA on Swallowing Counts and EMG in PSD Mice.** Compared the EMG and real-time spectrum in each group (0.02 mV, time = 40 s), we found EMG, and power spectrum in the model and sham EA were lower than EA (acute) and EA (chronic). There was no little difference between EA (acute) and EA (chronic) in EMG, but power spectrum of EA (acute) was stronger than EA (chronic) (Figure 5(a)). In swallowing counts ( $n = 6$ , time = 60 s), the model was lower than any other groups ( $p < 0.05$  and  $p < 0.01$ , separately). Compared with sham EA, EA (acute) was significantly increased ( $p < 0.01$ ); compared with EA (acute), EA (chronic) was decreased ( $p < 0.05$ ) (Figure 5(b)). These results illustrated that EA could enhance the swallowing-related muscle and increase the swallowing counts in PSD mice.

**3.7. The Effects of EA on Drink Water and SP Release in PSD Mice.** All of mice were deprived of water for 1 day. On day 2, each group was given drinking water *ad libitum* ( $n = 6$ ), and we found the obvious changes in water intake at 15, 30, 45, and 60 min (Figure 5(d) and Table 2). In total water consumption, the water intake of model was the lowest than any other group ( $p < 0.001$ ,  $p < 0.05$ , and  $p < 0.01$ , separately). Compare with sham EA, EA (acute) was significantly increased ( $p < 0.01$ ); compared with EA (acute), EA (chronic) was obviously increased (Figure 5(e)). The SP concentration of the model was decreased compared with normal ( $p < 0.01$ ). After EA (acute) and EA (chronic), the SP release was increased than the model ( $p < 0.05$  and  $p < 0.01$ , separately) (Figure 5(c)). The results were confirmed that EA could promote the SP release and water intake and improve the swallowing function of PSD mice.

**3.8. Swallowing Counts and Water Intake Are Correlated with Pyramidal Cell of M1 and Hypoglossal Nerve in PSD Mice.** We undertook linear correlation analysis of swallowing counts, spike counts in pyramidal cell, hypoglossal nerve spike counts, water intake, and SP in PSD mice by EA. First, we found the swallowing counts were positively correlated with water intake ( $p < 0.001$ ,  $r = 0.6451$ ) and SP ( $p < 0.001$ ,  $r = 0.6737$ ) (Figures 6(a1) and 6(a2)); it shows that the more swallowing counts, the more water intake and SP release in PSD mice. In addition, we found the pyramidal cell spike counts in M1 were positively correlated with swallowing counts ( $p < 0.001$ ,  $r = 0.6213$ ), water intake ( $p < 0.001$ ,  $r = 0.9105$ ), and hypoglossal spike counts ( $p < 0.001$ ,  $r = 0.6311$ ) (Figures 6(b1), 6(b2), and 6(c1)); it demonstrates that pyramidal cell in M1 affects hypoglossal nerve to increase the swallowing counts, which could promote SP release and recover the amount of water when the PSD mice swallowed. At last, hypoglossal nerve spike counts were positively correlated with swallowing counts ( $p < 0.0001$ ,  $r = 0.8244$ ) and water intake ( $p < 0.0001$ ,  $r = 0.6583$ ) (Figures 6(c2) and 6(c3)); it shows that swallowing-related peripheral nerves



(a)



(b)

(c)

FIGURE 5: Continued.



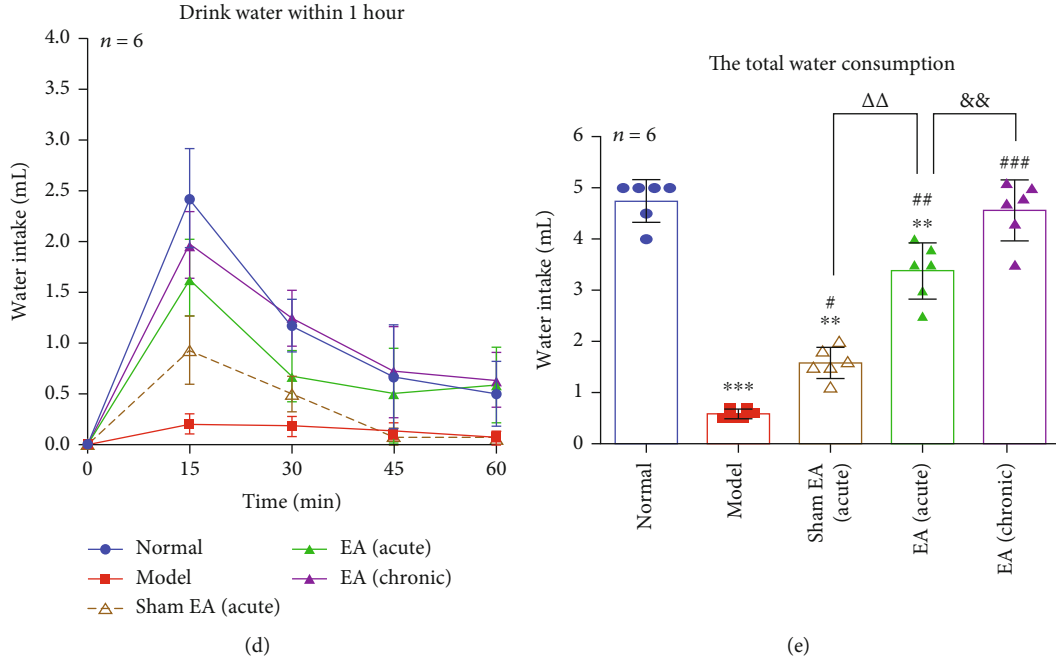


FIGURE 5: Electroacupuncture stimulation improves swallowing counts, SP release, and water intake in mice. (a) The changes of EMG and real-time spectrum in each group: EA (acute) > EA (chronic) > sham EA > model, time = 40 s, peak value = 0.02 mV. (b) Swallowing counts in each group: time = 60 s, compared with the model,  $*p < 0.05$  in sham EA (acute) and  $**p < 0.01$  in EA (acute) and EA (chronic). Compared with sham EA (acute),  $^{##}p < 0.01$  in EA (acute). Compared with EA (acute),  $^{\Delta}p < 0.05$  in EA (chronic). (c) Substance P: compared with normal,  $*p < 0.05$  in EA (acute) and  $**p < 0.01$  in the model, sham EA (acute), and EA (chronic). Compared with the model,  $^{#}p < 0.05$  in EA (acute),  $^{##}p < 0.01$  in EA (chronic). EA (acute) vs. EA (chronic):  $^{\Delta\Delta}p < 0.01$ . (d) Mice drink water within 1 hour: normal > EA (chronic) > EA (acute) > sham EA (acute) > model. (e) Total water consumption: compared with normal,  $***p < 0.001$  in the model and  $**p < 0.01$  in sham EA (acute) and EA (acute). Compared with model,  $*p < 0.05$  in sham EA (acute),  $**p < 0.01$  in EA (acute), and  $***p < 0.001$  in EA (chronic). Compared with sham EA (acute),  $**p < 0.01$  in EA (acute). Compared with EA (acute),  $**p < 0.01$  in EA (chronic).

TABLE 2: Water intake changes at different time periods in each group of mice.

Groups ( $n = 6$ )	Model	Sham EA (acute)	EA (acute)	EA (chronic)	Normal
0 min	0	0	0	0	0
15 min	$0.2 \pm 0.089^{**}$	$0.993 \pm 0.333^{**/##}$	$1.633 \pm 0.383^{**/##/\Delta\Delta}$	$1.967 \pm 0.327^{**/##/\Delta\Delta}$	$2.417 \pm 0.491$
30 min	$0.183 \pm 0.098^{**}$	$0.5 \pm 0.179^{**/##}$	$0.667 \pm 0.258^{**/##}$	$1.25 \pm 0.274^{##/\Delta\Delta/\Delta\Delta}$	$1.167 \pm 0.258$
45 min	$0.133 \pm 0.082^{*}$	$0.083 \pm 0.075^{*}$	$0.5 \pm 0.447$	$0.717 \pm 0.449^{#/\Delta}$	$0.667 \pm 0.516$
60 min	$0.067 \pm 0.052^{**}$	$0.067 \pm 0.052^{**}$	$0.583 \pm 0.376^{##/\Delta\Delta}$	$0.633 \pm 0.273^{##/\Delta\Delta}$	$0.5 \pm 0.316$

Notes:  $*p < 0.05$  and  $**p < 0.01$  versus normal;  $^{#}p < 0.05$  and  $^{##}p < 0.01$  versus model;  $^{\Delta}p < 0.05$  and  $^{\Delta\Delta}p < 0.01$  versus sham EA;  $^{\Delta\Delta\Delta}p < 0.01$  versus EA (acute).

(hypoglossal) directly affect the swallowing counts and water intake in PSD mice. Based on the above correlation results, we conclude that EA could activate the swallowing-related pyramidal cell of the noninfarction area in M1, then directly affect hypoglossal nerve to neural regulate the swallowing counts and promote SP release, ultimately improved swallowing dysfunction in PSD mice.

#### 4. Discussion

Stimulation the “Lianquan” acupoint (CV 23) by EA and feeding water induce the excitability of voluntary swallowing, in order to promote the motor cortex noninfarction neurons excitement and compensation the motor cortex function on

the infarction side. The motor cortex on the noninfarction side transmitted motion excited to NTS and NA of the central pattern generator (CPG) that generate the swallowing reflex. At the same time, EA effects were exciting peripheral hypoglossal nerve, restoring the swallowing function of mylohyoid muscle, thereby to improve the dysphagia in oropharyngeal phase (Figure 7).

Dysphagia is characterized as being worse for liquids than solids [33]. M1 has a substantial role in the neural control the voluntary swallowing. Deglutition initiation and especially the oral phase of voluntary swallowing require the integrity of the motor areas of the cerebral cortex. We found that pyramidal cells were activated in noninfarction area of M1 by EA and that this action was associated with



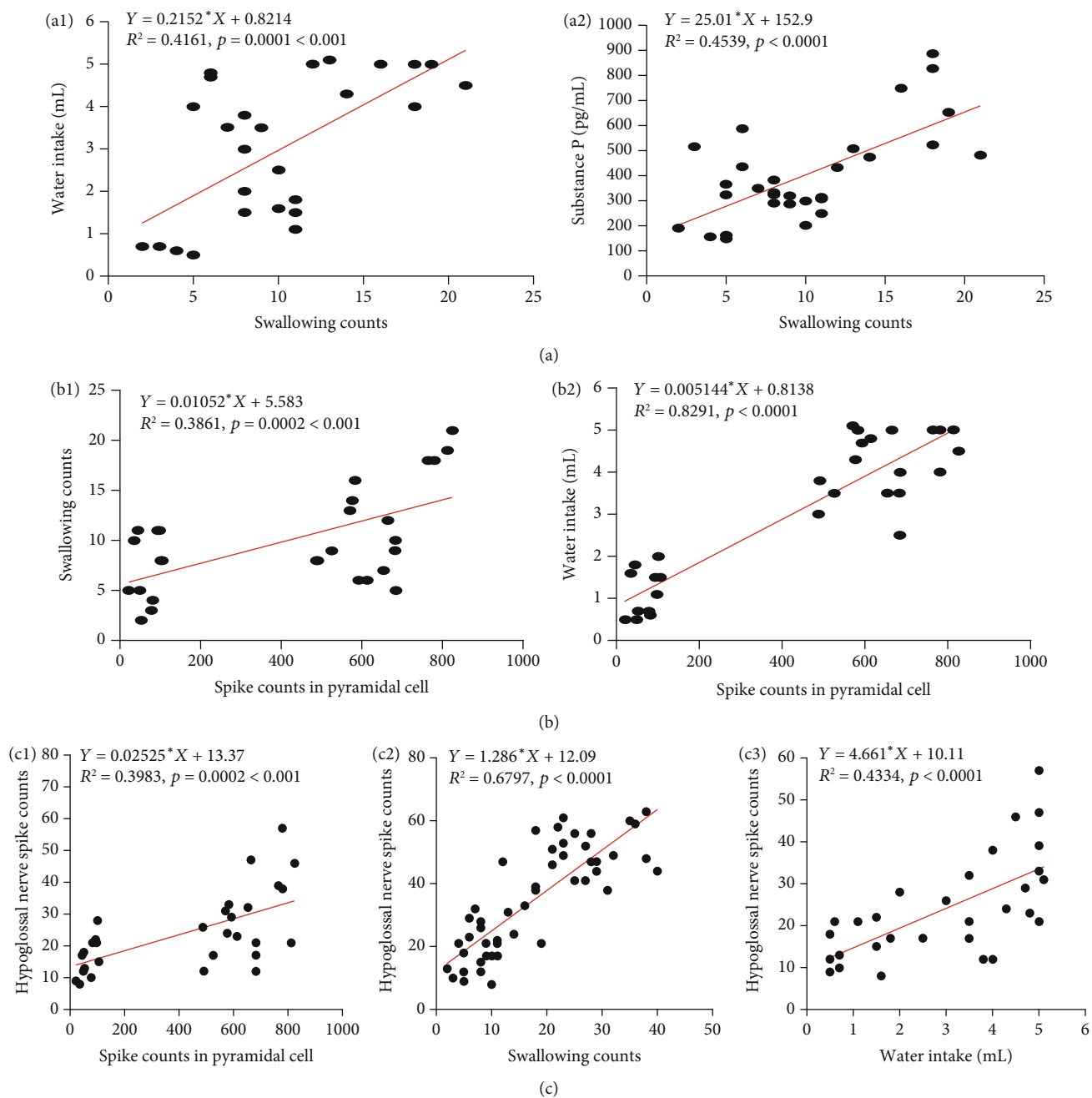


FIGURE 6: Linear correlation analysis of related-swallowing indicators in PSD mice. (a1) Swallowing counts were positively correlated with water intake, \*\*\*  $p < 0.001$ ,  $r = 0.6451$ . (a2) Swallowing counts were positively correlated with substance P, \*\*\*  $p < 0.001$ ,  $r = 0.6737$ . (b1) Spike counts in pyramidal cell were positively correlated with swallowing counts, \*\*\*  $p < 0.001$ ,  $r = 0.6213$ . (b2) Spike counts in pyramidal cell were positively correlated with water intake, \*\*\*  $p < 0.001$ ,  $r = 0.9105$ . (c1) Spike counts in pyramidal cell were positively correlated with hypoglossal nerve spike counts, \*\*\*  $p < 0.001$ ,  $r = 0.6311$ . (c2) Swallowing counts were positively correlated with hypoglossal nerve spike counts, \*\*\*\*  $p < 0.0001$ ,  $r = 0.8244$ . (c3) Water intake was positively correlated with hypoglossal nerve spike counts, \*\*\*\*  $p < 0.0001$ ,  $r = 0.6583$ .

swallowing. In addition, stimulation of conception vessel (CV) 23 by EA could improve the blood flow in M1 and around deglutition-muscle groups, promote blood supplementation in tissue, and restore voluntary swallowing. Also, EA may reactivate peripheral nervous of voluntary swallowing, strengthen neural control of the hypoglossal nerve, release relevant neurotransmitters, recover voluntary swal-

lowing gradually, and improve the PSD caused by unilateral M1 injury.

During voluntary swallowing, the cortex and subcortical areas play important roles in triggering and controlling the sequence of swallowing movements, especially in the oral phase [34]. Researchers have recognized the function of the cerebral cortex in swallowing control by observing patients

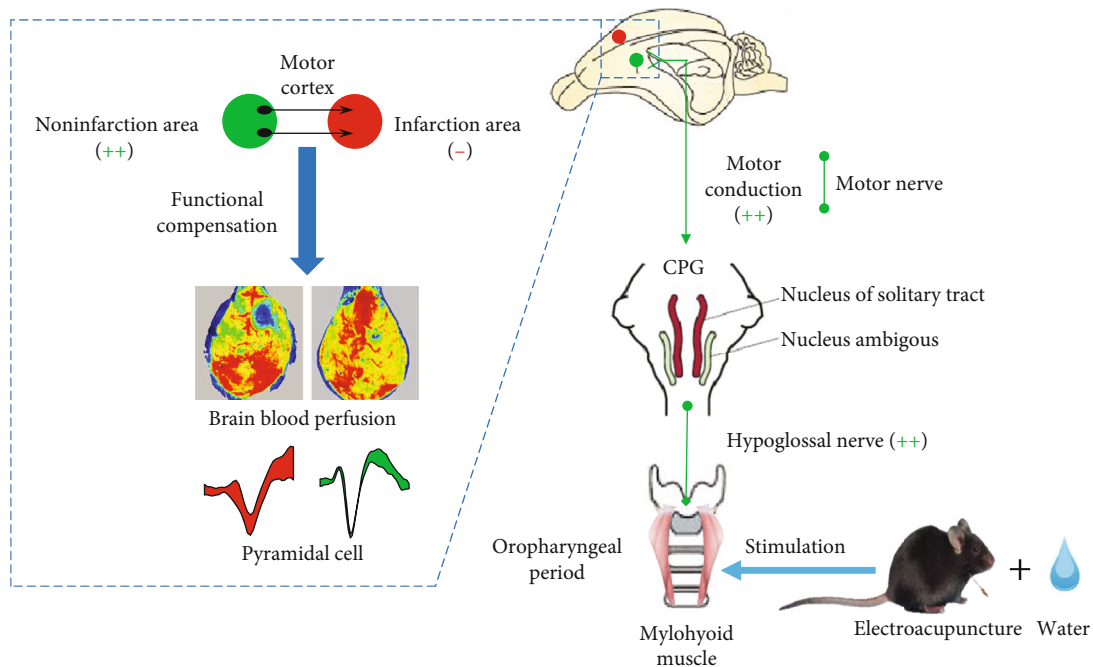


FIGURE 7: The EA stimulation involves in the motor neural control of motor cortex and hypoglossal nerves to improve the voluntary swallowing in poststroke dysphagia mice.

with cortical dysphagia. However, the compensatory mechanism and functional recombination of dysphagia are not clear. Several experimental studies have suggested that the cerebral cortex has obvious hemisphere lateralization in response to swallowing. The locus of cortical control of swallowing lies anterior caudal to M1. The motor cortex is a crucial area for planning swallowing, and the oropharyngeal motor area is the central area which initiates swallowing [1, 3, 19, 35–40]. Therefore, patients with PSD may experience compensatory neurologic recombination in M1.

Consistent with this hypothesis, we found that the number and kind of neurons, spike counts in the noninfarction side of M1 in PSD mice reduced significantly (Figure 3(b); Table 1), so the compensatory mechanism could not be activated. After EA therapy immediately (acute) and EA for 3 days (chronic), pyramidal cells (which are the main projection neurons in the cerebral cortex) in the noninfarction side were activated to compensate the role of M1 in the infarction side (Figures 3(c) and 3(d)). Moreover, the activation of pyramidal cells promoted the increase in swallowing counts and water intake in PSD mice (Figures 6(b1) and 6(b2)). These data demonstrated that CV23 stimulation may activate the swallowing-related neurons (pyramidal cells) of M1 in the healthy side and improve voluntary swallowing.

The submental musculature offers the opportunity to assess M1 excitability during the different motor components of swallowing because it has a central role in the oral and pharyngeal phases of swallowing [30]. We recorded and compared the EMG of the mandibular swallowing muscles when drinking water in each group. Both acute and chronic EA treatment could stimulate the swallowing muscles in PSD mice, promote an increase in swallowing counts, and

change water intake significantly (Figures 5(b), 5(d), and 5(e)). Simultaneously, stimulation of CV23 by EA could also improve the local blood flow of swallowing muscles, and blood perfusion in the noninfarction side in M1 was also increased significantly (Figure 2). The pharyngeal musculature is thought to be represented bilaterally but asymmetrically, suggesting hemispheric dominance in the motor control of these muscles [41]. For a healthy person, when swallowing water, the peak activation was occurred  $\geq 12$  s after the onset of swallowing, but, in patients with cortical dysphagia, peak activation occurs much later than 12 s [6]. We have observed this phenomenon in animal experiments. Hamdy et al. showed that to induce changes in excitation of the motor cortex with prolonged electrical stimulation of the pharynx for  $\leq 15$  min [3], the sensory input to the cortex must be manipulated, and compensatory recombination of the intact hemisphere must be undertaken to restore swallowing function in the pharynx [3, 28]. Hence, we undertook specific stimulation conduction of CV23 to strengthen PSD treatment using EA for 15 min.

Some studies have shown that acupuncture has a certain effect in this respect. Acupuncture at the corresponding acupoints can not only enhance nerve reflex but also promote muscle coordination and flexibility and achieve the purpose of improving swallowing [42–44]. “Lianquan” acupoint is between hyoid bone and thyroid cartilage, and the branches of swallowing nerve and hypoglossal nerve are located in its deep part. Deep needling can directly stimulate the swallowing muscle group and glossopharyngeal terminal nerve, and the reflex enhances the excitability of medulla oblongata, which is beneficial to the recovery of swallowing reflex arc. “Lianquan” acupoint is located in the control area of motor

fibers of hypoglossal and swallowing nerves. Therefore, we choose “Lianquan” acupoint to observe the effect of post-stroke dysphagia with theoretical basis.

The peripheral nervous receives signal from the central motor nerves and plays an important role in the voluntary swallowing. Pharyngeal phase starts by action of the pharyngeal plexus (which comprises the glossopharyngeal (IX), vagus (X), and accessory (XI) nerves) and the hypoglossal nerves on each side from the ansa cervicalis [45]. During swallowing, the hypoglossal (XII) nerves are responsible for the extrinsic and intrinsic muscles of the tongue. In addition, fibers from the cervical plexus in association with the hypoglossal nerve forms the ansa cervicalis will innervate the geniohyoid muscle [46, 47]. Jean suggested that the main motor nuclei involved in swallowing motor activity are the hypoglossal nucleus, and the nucleus ambiguus, hypoglossal, glossopharyngeal, and trigeminal nerves are the main motor nerves [48]. A lesion of the hypoglossal nerve can cause dysarthria, dysphagia, and tongue paralysis [49]. Sundman et al. suggested that the three mechanisms underlying dysphagia were delayed initiation of the swallowing reflex, impaired pharyngeal muscle function, and impaired coordination [50]; these symptoms of dysphagia are attributed to the damage of several central nuclei associated with swallowing [51, 52]. Related studies show that the loss of innervation of these muscles which the hyoid and anterior digastric muscles help to open the jaw and raise the hyoid during swallowing may be one of the causes of dysphagia in rats [53]. Therefore, there must be a certain relationship between the M1 responsible for initiating the swallowing reflex and the hypoglossal nerve innervating the digastric and lingual protrudor muscles in the neural regulation of dysphagia after stroke.

In this experiment, we found that the hypoglossal nerve activity has significantly decreased ( $p < 0.01$ , Figure 3(f)); the EMG of mylohyoid muscle was also inhibited ( $p < 0.01$ , Figures 5(a) and 5(b)), and the latency of evoked EMG activity by stimulation the hypoglossal nerve trunk was obviously prolonged ( $p < 0.01$ , Figures 4(c) and 4(g)) after the M1 injury, suggesting that the damage of motor cortex could affect the muscles innervated by hypoglossal nerve. Electrical stimulation of the hypoglossal nerve trunk cannot quickly induce action potentials, indicating that the central nervous regulation of swallowing is much greater than the peripheral local innervation. Acute or chronic EA could activate this nerve in PSD mice ( $p < 0.01$ , Figure 3(f)). The excitability of hypoglossal nerves was related to the spike counts of pyramidal cells in M1 on the healthy side (Figure 6(c1)), illustrating that EA promotes the excitation of M1, especially pyramidal cells, and then increases the discharge of hypoglossal nerve ( $p < 0.01$ ), which has significantly shorten the latency of mylohyoid muscle and increases the MCV ( $p < 0.01$ ); thus, the swallowing counts and water intake were further improved in dysphagia mice (Figures 3(f), 4(e)–4(h), 5(b), and 5(e)). It is revealed that EA could enhance the MCV of swallowing-related and help the body recover the swallowing function.

SP is a neurotransmitter that promotes the swallowing reflex in animals, and reduction of its secretion is related to inhibition of the swallowing reflex [54]. We showed that

the SP concentration in serum was reduced dramatically in PSD mice, but after EA, it increased significantly (Figures 5(c) and 6(a2)). These data suggested that EA could promote SP release to improve swallowing function. Scholars have reported that SP can enhance swallow and cough reflexes and may also have a role in the response of the pharyngeal mucosa to local stimulation [55, 56]. Paul and colleagues showed that 78.6% of patients treated successfully by pharyngeal electrical stimulation showed a poststimulation increase in SP levels, whereas 88.9% of cases without clinical improvement of dysphagia had stable or decreased SP levels [57]. We postulate that pharyngeal electrical stimulation and EA stimulation have a close relationship in terms of the increase in SP levels. Thus, EA may trigger SP release, which results in peripheral sensitization of sensory neurons. This action would facilitate the motor swallowing response in the upstream swallowing network and enhance the excitability of the noninfarction side in M1 to aid recovery from PSD.

This study only observed the role of motor conduction and neural control of motor cortex-hypoglossal nerve by EA in PSD mice, but the ascending sensory conduction of EA stimulation is not involved. How EA involving sensory nerve conduction regulates the swallowing disorders may become the potential study in the future.

## Abbreviations

CPG:	Central pattern generator
CV:	Conception vessel
EA:	Electroacupuncture
EEG:	Electroencephalogram
EMG:	Electromyography
LFP:	Local field potential
LSCI:	Laser speckle contrast imaging
M1:	Motor cortex 1
MCV:	Motor conduction velocity
NA:	Nucleus ambiguus
NTS:	Nucleus of the solitary tract
PCA:	Principal component analysis
PSD:	Post-stroke dysphagia
SP:	Substance P
SPKC:	Spike continuous
VLM:	Ventrolateral medulla.

## Data Availability

The data used to support the findings of this study are included within the article.

## Conflicts of Interest

The authors declare no potential conflicts of interest with respect to the research, authorship, and/or publication of this article.

## Authors' Contributions

S. Cui, L. Y. Y. Chen, C. Tang, and N. Xu designed the research. S. Cui, S. Yao, and C. Wu contributed to the data

acquisition and data analysis; S. Cui and L. Yao designed and drew the diagrams. All authors have approved the final version of the manuscript. Shuai Cui and Shuqi Yao contributed equally to this work.

## Acknowledgments

We thank Professor Yiping Zhou for assistance with manuscript preparation, and the present work was supported by grants from National Natural Science Foundation of China (81774406).

## Supplementary Materials

Supplementary 1: PCA in each group, time = 300 s. (A) Normal: 5 units. (B) Model: 3 units. (C) Sham EA: 3 units. (D) EA acute: 3 units. (E) EA chronic: 3 units. Supplementary 2: autocorrelograms in each group, bin = 1 ms. (A) Normal: 2 interneurons (unit a and unit b) and 3 pyramidal cells (unit c, unit d, and unit e). (B) Model: 1 interneuron (unit a) and 2 pyramidal cells (unit b and unit c). (C) Sham EA: 1 interneuron (unit a) and 2 pyramidal cells (unit b and unit c). (D) EA acute: 1 interneuron (unit a) and 2 pyramidal cells (unit b and unit c). (E) EA chronic: 1 interneuron (unit a) and 2 pyramidal cells (unit b and unit c). Supplementary 3: the motor cortex neuron changes of noninfarction area were recorded by multichannel electrophysiology *in vivo*. (A) Multichannel recording electrode:  $2 \times 4 + 1$  matrix electrode implantation. (B) Electrode recording site: bregma:  $-0.16$  mm; left: 1 mm; depth: 1 mm. (C) Photograph showing the site of the recording electrode: M1, bar =  $500 \mu\text{m}$ . (D) Normal: recording 5 units. Normal-before vs. normal-after: time = 5 min in each phase, interval = stop recording 15 min. Interneuron vs. pyramidal: before = 29.65% vs. 70.35%, after = 35.1% vs. 64.9%. (E) Model: recording 3 units. Before sham EA vs. after sham EA: time = 5 min in each phase, interval = lack of electric stimulation 15 min. Interneuron vs. pyramidal: before sham EA = 17.01% vs. 82.99%, after sham EA = 18.25% vs. 81.75%. (F) Model: recording 3 units. Before EA vs. after EA (acute) vs. after EA (chronic): time = 5 min in each phase, interval 1 = EA stimulation 15 min, interval 2 = EA stimulation for 3 days interneuron vs. pyramidal: before EA = 15.73% vs. 84.27%, after EA (acute) = 33.62% vs. 66.38%, and after EA (chronic) = 34.6% vs. 65.4%. Supplementary 4: the hypoglossal nerve was recorded *in vivo*. (Supplementary Materials)

## References

- [1] S. Hamdy, Q. Aziz, D. G. Thompson, and J. C. Rothwell, "Physiology and pathophysiology of the swallowing area of human motor cortex," *Neural Plasticity*, vol. 8, no. 1-2, Article ID 293195, 97 pages, 2001.
- [2] S. Hamdy, D. J. Mikulis, A. Crawley et al., "Cortical activation during human volitional swallowing: an event-related fMRI study," *The American Journal of Physiology*, vol. 277, no. 1, pp. G219–G225, 1999.
- [3] S. Hamdy, J. C. Rothwell, Q. Aziz, and D. G. Thompson, "Organization and reorganization of human swallowing motor cortex: implications for recovery after stroke," *Clinical Science*, vol. 99, no. 2, pp. 151–157, 2000.
- [4] S. Hamdy, J. C. Rothwell, D. J. Brooks, D. Bailey, Q. Aziz, and D. G. Thompson, "Identification of the cerebral loci processing human swallowing with  $\text{H}_2^{15}\text{O}$  PET activation," *Journal of Neurophysiology*, vol. 81, no. 4, pp. 1917–1926, 1999.
- [5] A. M. Mourao, S. M. Lemos, E. O. Almeida, L. C. Vicente, and A. L. Teixeira, "Frequency and factors associated with dysphagia in stroke," *Codas*, vol. 28, no. 1, pp. 66–70, 2016.
- [6] H. Yang, K. K. Ang, C. Wang, K. S. Phua, and C. Guan, "Neural and cortical analysis of swallowing and detection of motor imagery of swallow for dysphagia rehabilitation – a review," *Progress in Brain Research*, vol. 228, pp. 185–219, 2016.
- [7] D. L. Cohen, C. Roffe, J. Beavan et al., "Post-stroke dysphagia: a review and design considerations for future trials," *International Journal of Stroke*, vol. 11, no. 4, pp. 399–411, 2016.
- [8] P. Falsetti, C. Acciai, R. Palilla et al., "Oropharyngeal dysphagia after stroke: incidence, diagnosis, and clinical predictors in patients admitted to a neurorehabilitation unit," *Journal of Stroke and Cerebrovascular Diseases*, vol. 18, no. 5, pp. 329–335, 2009.
- [9] E. K. Umay, E. Unlu, G. K. Saylam, A. Cakci, and H. Korkmaz, "Evaluation of dysphagia in early stroke patients by bedside, endoscopic, and electrophysiological methods," *Dysphagia*, vol. 28, no. 3, pp. 395–403, 2013.
- [10] S. Y. Chen, W. C. Chie, Y. N. Lin, Y. C. Chang, T. G. Wang, and I. N. Lien, "Can the aspiration detected by videofluoroscopic swallowing studies predict long-term survival in stroke patients with dysphagia?," *Disability and Rehabilitation*, vol. 26, no. 23, pp. 1347–1353, 2004.
- [11] R. Ding and J. A. Logemann, "Pneumonia in stroke patients: a retrospective study," *Dysphagia*, vol. 15, no. 2, pp. 51–57, 2000.
- [12] R. Teasell, N. Foley, J. Fisher, and H. Finestone, "The incidence, management, and complications of dysphagia in patients with medullary strokes admitted to a rehabilitation unit," *Dysphagia*, vol. 17, no. 2, pp. 115–120, 2002.
- [13] K. Matsuo and J. B. Palmer, "Anatomy and physiology of feeding and swallowing: normal and abnormal," *Physical Medicine and Rehabilitation Clinics of North America*, vol. 19, no. 4, pp. 691–707, 2008.
- [14] M. J. Mckeown, D. C. Torpey, and W. C. Gehm, "Non-invasive monitoring of functionally distinct muscle activations during swallowing," *Clinical Neurophysiology*, vol. 113, no. 3, pp. 354–366, 2002.
- [15] H. You, S. Hu, Q. Ye et al., "Role of 5-HT1A in the nucleus of the solitary tract in the regulation of swallowing activities evoked by electroacupuncture in anesthetized rats," *Neuroscience Letters*, vol. 687, pp. 308–312, 2018.
- [16] P. L. Furlong, A. R. Hobson, Q. Aziz et al., "Dissociating the spatio-temporal characteristics of cortical neuronal activity associated with human volitional swallowing in the healthy adult brain," *NeuroImage*, vol. 22, no. 4, pp. 1447–1455, 2004.
- [17] E. Michou and S. Hamdy, "Cortical input in control of swallowing," *Otolaryngology and Head and Neck Surgery*, vol. 17, no. 3, pp. 166–171, 2009.
- [18] S. Li, C. Luo, B. Yu et al., "Functional magnetic resonance imaging study on dysphagia after unilateral hemispheric stroke a preliminary study," *Journal of Neurology, Neurosurgery, and Psychiatry*, vol. 80, no. 12, pp. 1320–1329, 2009.
- [19] X. D. Yuan, L. F. Zhou, S. J. Wang et al., "Compensatory recombination phenomena of neurological functions in



- central dysphagia patients,” *Neural Regeneration Research*, vol. 10, no. 3, pp. 490–497, 2015.
- [20] K. Bahceci, E. Umay, I. Gundogdu, E. Gurcay, E. Ozturk, and S. Alicura, “The effect of swallowing rehabilitation on quality of life of the dysphagic patients with cortical ischemic stroke,” *Iranian journal of neurology*, vol. 16, no. 4, pp. 178–184, 2017.
- [21] L. Li, K. Deng, and Y. Qu, “Acupuncture treatment for post-stroke dysphagia: an update meta-analysis of randomized controlled trials,” *Chinese Journal of Integrative Medicine*, vol. 24, no. 9, pp. 686–695, 2018.
- [22] H. Cai, B. Ma, X. Gao, and H. Gao, “Tongue acupuncture in treatment of post-stroke dysphagia,” *International Journal of Clinical and Experimental Medicine*, vol. 8, no. 8, pp. 14090–14094, 2015.
- [23] Y. Wang, J. Shen, X. M. Wang et al., “Scalp acupuncture for acute ischemic stroke: a meta-analysis of randomized controlled trials,” *Evidence-based Complementary and Alternative Medicine*, vol. 2012, Article ID 480950, 9 pages, 2012.
- [24] R. K. Goyal, R. Padmanabhan, and Q. Sang, “Neural circuits in swallowing and abdominal vagal afferent-mediated lower esophageal sphincter relaxation,” *The American Journal of Medicine*, vol. 111, no. 8, Supplement 1, pp. 95–105, 2001.
- [25] J. Shi, Q. Ye, J. Zhao et al., “EA promotes swallowing via activating swallowing-related motor neurons in the nucleus ambiguus,” *Brain Research*, vol. 1718, pp. 103–113, 2019.
- [26] Q. Ye, C. Liu, J. Shi et al., “Effect of electro-acupuncture on regulating the swallowing by activating the interneuron in ventrolateral medulla (VLM),” *Brain Research Bulletin*, vol. 144, pp. 132–139, 2019.
- [27] S. H. Doeltgen, J. Dalrymple-Alford, M. C. Ridding, and M. L. Huckabee, “Differential effects of neuromuscular electrical stimulation parameters on submental Motor-Evoked Potentials,” *Neural Repair*, vol. 24, no. 6, pp. 519–527, 2010.
- [28] S. Hamdy, J. C. Rothwell, Q. Aziz, K. D. Singh, and D. G. Thompson, “Long-term reorganization of human motor cortex driven by short-term sensory stimulation,” *Nature Neuroscience*, vol. 1, no. 1, pp. 64–68, 1998.
- [29] I. A. Humbert and S. Joel, “Tactile, gustatory, and visual bio-feedback stimuli modulate neural substrates of deglutition,” *NeuroImage*, vol. 59, no. 2, pp. 1485–1490, 2012.
- [30] H. D. Sebastian, C. R. Michael, D. A. John, and M. L. Huckabee, “Task-dependent differences in corticobulbar excitability of the submental motor projections: implications for neural control of swallowing,” *Brain Research Bulletin*, vol. 84, no. 1, pp. 88–93, 2011.
- [31] S. Michael, J. Sebastian, and S. Guido, “Non-invasive induction of focal cerebral ischemia in mice by photothrombosis of cortical microvessels: characterization of inflammatory responses,” *Journal of neuroscience methods*, vol. 117, no. 1, pp. 43–49, 2002.
- [32] G. Pang and G. L. Zhang, “Subcellular localization of serotonin 2A receptor in dorsal hippocampal CA1 area and its effect on neuronal firing,” *Chinese Pharmacological Bulletin*, vol. 30, no. 9, pp. 1262–1266, 2014.
- [33] J. Lancaster, “Dysphagia: its nature, assessment and management,” *British Journal of Community Nursing*, vol. 20, no. -Sup6a, pp. S28–S32, 2015.
- [34] C. Ertekin, “Voluntary versus spontaneous swallowing in man,” *Dysphagia*, vol. 26, no. 2, pp. 183–192, 2011.
- [35] S. D. Forman, J. D. Cohen, M. Fitzgerald, W. F. Eddy, M. A. Mintun, and D. C. Noll, “Improved assessment of significant activation in functional magnetic resonance imaging (fMRI): use of a cluster-size threshold,” *Magnetic Resonance in Medicine*, vol. 33, no. 5, pp. 636–647, 1995.
- [36] M. G. Lacourse, E. L. Orr, S. C. Cramer, and M. J. Cohen, “Brain activation during execution and motor imagery of novel and skilled sequential hand movements,” *NeuroImage*, vol. 27, no. 3, pp. 505–519, 2005.
- [37] B. R. Komisaruk, K. M. Mosier, W. C. Liu et al., “Functional localization of brainstem and cervical spinal cord nuclei in humans with fMRI,” *American Journal of Neuroradiology*, vol. 23, no. 4, pp. 609–617, 2002.
- [38] M. Lotze, P. Montoya, M. Erb et al., “Activation of cortical and cerebellar motor areas during executed and imagined hand movements: an fMRI study,” *Journal of Cognitive Neuroscience*, vol. 11, no. 5, pp. 491–501, 1999.
- [39] Z. S. Saad, G. Chen, R. C. Reynolds et al., “Functional imaging analysis contest (FIAC) analysis according to AFNI and SUMA,” *Human brain mapping*, vol. 27, no. 5, pp. 417–424, 2006.
- [40] A. J. Szameitat, S. Shen, and A. Sterr, “Motor imagery of complex everyday movements: an fMRI study,” *NeuroImage*, vol. 34, no. 2, pp. 702–713, 2007.
- [41] S. Mistry, E. S. Verin, S. Singh et al., “Unilateral suppression of pharyngeal motor cortex to repetitive transcranial magnetic stimulation reveals functional asymmetry in the hemispheric projections to human swallowing,” *The Journal of Physiology*, vol. 585, no. 2, pp. 525–538, 2007.
- [42] Y. X. Chen, “Therapeutic effect of acupuncture combined with swallowing training on patients with dysphagia after cerebral infarction,” *Chinese Journal of Modern Drug Application*, vol. 12, no. 1, pp. 70–71, 2018.
- [43] L. Wang and Y. Pei, “Acupuncture for dysphagia after stroke,” *Journal of Practical Traditional Chinese Internal Medicine*, vol. 30, no. 8, pp. 92–94, 2016.
- [44] F. X. Yang and L. Chen, “A clinical study of tongue needle combined with catheter balloon dilatation in the treatment of dysphagia after stroke,” *Shanghai journal of acupuncture and moxibustion*, vol. 36, no. 3, pp. 261–264, 2017.
- [45] M. M. B. Costa, “Neural control of swallowing,” *Arquivos de Gastroenterologia*, vol. 55, supplement 1, pp. 61–75, 2018.
- [46] J. G. Chusid, *Neuroanatomicorrelativa e Neurologiafuncional*, Guanabara Koogan, Rio de Janeiro, 18th edition, 1985.
- [47] A. C. Guyton and J. E. Hall, *Textbook of Medical Physiology*, Saunders Elsevier, Philadelphia, PA, 10th edition, 2011.
- [48] A. Jean, “Brain stem control of swallowing: neuronal network and cellular mechanisms,” *Physiological Reviews*, vol. 81, no. 2, pp. 929–969, 2001.
- [49] S. Meng, L. F. Reissig, C. H. Tzou, K. Meng, W. Grisold, and W. Weninger, “Ultrasound of the hypoglossal nerve in the neck: visualization and initial clinical experience with patients,” *American Journal of Neuroradiology*, vol. 37, no. 2, pp. 354–359, 2016.
- [50] E. Sundman, H. Witt, R. Olsson, O. Ekberg, R. Kuylenstierna, and L. I. Eriksson, “The incidence and mechanisms of pharyngeal and upper esophageal dysfunction in partially paralyzed humans: pharyngeal videoradiography and simultaneous manometry after atracurium,” *Anesthesiology*, vol. 92, no. 4, pp. 977–984, 2000.
- [51] T. E. Lever, A. Gorsek, K. T. Cox et al., “An animal model of oral dysphagia in amyotrophic lateral sclerosis,” *Dysphagia*, vol. 24, no. 2, pp. 180–195, 2009.



- [52] T. E. Lever, E. Simon, K. T. Cox et al., "A mouse model of pharyngeal dysphagia in amyotrophic lateral sclerosis," *Dysphagia*, vol. 25, no. 2, pp. 112–126, 2010.
- [53] J. B. Travers and L. M. Jackson, "Hypoglossal neural activity during licking and swallowing in the awake rat," *Journal of Neurophysiology*, vol. 67, no. 5, pp. 1171–1184, 1992.
- [54] T. Nakashima, N. Hattori, M. Okimoto, J. Yanagida, and N. Kohno, "Nicergoline improves dysphagia by upregulating substance P in the elderly," *Medicine*, vol. 90, no. 4, pp. 279–283, 2011.
- [55] Y. Imoto, A. Kojima, Y. Osawa, H. Sunaga, and S. Fujieda, "Cough reflex induced by capsaicin inhalation in patients with dysphagia," *Acta Oto-Laryngologica*, vol. 131, no. 1, pp. 96–100, 2011.
- [56] Y. Jin, K. Sekizawa, T. Fukushima, M. Morikawa, H. Nakazawa, and H. Sasaki, "Capsaicin desensitization inhibits swallowing reflex in guinea pigs," *American Journal of Respiratory and Critical Care Medicine*, vol. 149, no. 1, pp. 261–263, 1994.
- [57] M. Paul, S. K. Sonja, B. Stefan et al., "Increase of substance P concentration in saliva after pharyngeal electrical stimulation in severely dysphagic stroke patients – an indicator of decannulation success?," *Neurosignals*, vol. 25, pp. 74–87, 2017.

## Review Article

# Effects and Mechanisms of Acupuncture Combined with Mesenchymal Stem Cell Transplantation on Neural Recovery after Spinal Cord Injury: Progress and Prospects

Huiling Tang,<sup>1,2</sup> Yi Guo<sup>1,3,4</sup>, Yadan Zhao,<sup>1</sup> Songtao Wang,<sup>1</sup> Jiaqi Wang,<sup>1</sup> Wei Li,<sup>1</sup> Siru Qin,<sup>1</sup> Yinan Gong,<sup>1</sup> Wen Fan,<sup>5</sup> Zelin Chen,<sup>1,4,6</sup> Yongming Guo<sup>1,4,6</sup>, Zhifang Xu<sup>1,6</sup>, and Yuxin Fang<sup>1,6</sup>

<sup>1</sup>Research Center of Experimental Acupuncture Science, Tianjin University of Traditional Chinese Medicine, Tianjin 301617, China

<sup>2</sup>Shanghai Minhang Traditional Chinese Medicine Hospital, Shanghai 201103, China

<sup>3</sup>School of Traditional Chinese Medicine, Tianjin University of Traditional Chinese Medicine, Tianjin 301617, China

<sup>4</sup>National Clinical Research Center for Chinese Medicine Acupuncture and Moxibustion, Tianjin 300381, China

<sup>5</sup>Suzuka University of Medical Science, Suzuka 5100293, Japan

<sup>6</sup>School of Acupuncture & Moxibustion and Tuina, Tianjin University of Traditional Chinese Medicine, Tianjin 301617, China

Correspondence should be addressed to Zhifang Xu; xuzhifangmsn@hotmail.com and Yuxin Fang; meng99\_2006@126.com

Received 23 June 2020; Revised 29 August 2020; Accepted 5 September 2020; Published 25 September 2020

Academic Editor: Lu Wang

Copyright © 2020 Huiling Tang et al. This is an open access article distributed under the Creative Commons Attribution License, which permits unrestricted use, distribution, and reproduction in any medium, provided the original work is properly cited.

Spinal cord injury (SCI) is a structural event with devastating consequences worldwide. Due to the limited intrinsic regenerative capacity of the spinal cord in adults, the neural restoration after SCI is difficult. Acupuncture is effective for SCI-induced neurologic deficits, and the potential mechanisms responsible for its effects involve neural protection by the inhibition of inflammation, oxidation, and apoptosis. Moreover, acupuncture promotes neural regeneration and axon sprouting by activating multiple cellular signal transduction pathways, such as the Wnt, Notch, and Rho/Rho kinase (ROCK) pathways. Several studies have demonstrated that the efficacy of combining acupuncture with mesenchymal stem cells (MSCs) transplantation is superior to either procedure alone. The advantage of the combined treatment is dependent on the ability of acupuncture to enhance the survival of MSCs, promote their differentiation into neurons, and facilitate targeted migration of MSCs to the spinal cord. Additionally, the differentiation of MSCs into neurons overcomes the problem of the shortage of endogenous neural stem cells (NSCs) in the acupuncture-treated SCI patients. Therefore, the combination of acupuncture and MSCs transplantation could become a novel and effective strategy for the treatment of SCI. Such a possibility needs to be verified by basic and clinical research.

## 1. Introduction

Spinal cord injury (SCI) is a structural event with devastating consequences, such as permanent loss of motor, sensory, and autonomic functions and, in severe cases, paraplegia or quadriplegia below the level of injury [1]. The incidence of SCI tends to increase worldwide, with 17,000 new cases each year [2]. The pathophysiology of SCI can be categorized as primary injury and secondary injury. The secondary injury involves apoptosis and necrosis of damaged neurons, dislocation and demyelination of axons resulting from the loss of

oligodendrocyte-derived myelin, local nerve inflammation caused by tissue edema or ischemia, and formation of a parenchymal cavity or glial scar in the spinal cord after hemorrhage [3, 4]. Currently, no effective treatment to reverse the trauma of SCI is available. This limitation is mostly due to the extremely limited capacity of the spinal cord to regenerate and enable the recovery of neurologic deficits [5]. The main strategies for the treatment of SCI include pharmacologic interventions, surgery, stem cell transplantation, behavioral therapy, physical stimulation, and supportive therapy. Among them, the current first-line treatment is the

administration of high-dose corticosteroids, such as methylprednisolone sodium succinate, which can inhibit local inflammation and oxidative stress, protect the blood-spinal cord barrier, and prevent the death of neurons [6]. However, since multiple potential risks and equivocal clinical results have been reported, there is no consensus on the standardized application of corticosteroids in SCI treatment. Therefore, the development of safer and more effective therapies promoting neural restoration and functional recovery after SCI is of great clinical relevance.

Acupuncture is a procedure involving the insertion of a fine needle into the skin or deeper tissues at specific locations of the body (acupoints) to prevent and treat diseases [7]. Several lines of neuroanatomical and neurological evidence have demonstrated the abundant distribution of nerve endings in human meridians and acupoints, and the involvement of the nervous system is indispensable for the effects of acupuncture [8]. An increasing number of clinical studies have shown that acupuncture can effectively improve the functional recovery of neurons after various types of central nervous system injuries (CNSIs), including SCI [9]. The potential mechanisms mediating the effects of acupuncture include the prevention of inflammatory and oxidant stress, suppression of apoptosis, and stimulation of proliferation and differentiation of endogenous NSCs [10, 11]. However, there are still several obstacles to the application of acupuncture for the promotion of neural regeneration, such as an insufficient number of endogenous NSCs capable of differentiating into functional neurons. Thus, further research is needed to achieve progress in this field.

Mesenchymal stem cells (MSCs) are multipotential stem cells derived from the mesoderm. They are capable of self-renewal and multilineage differentiation and maintain these biological characteristics after large-scale expansion *in vitro*. MSCs have been regarded as pluripotent “seed cells” with two main therapeutic effects. One effect is the migration of cells to the damaged tissue and differentiation into tissue-specific cell types, thus restoring the function of target tissues and organs. The other effect is the inhibition of local inflammation, apoptosis, and fibrosis; promotion of angiogenesis; and stimulation of regeneration and differentiation of resident tissue progenitor cells by secreting soluble growth and trophic factors [12, 13]. Moreover, MSCs have several advantages, such as the ability to differentiate into multiple lineages, low immunogenicity, abundant sources, simplicity of preparation, and low tumorigenicity [14]. Many clinical and basic studies have documented that while MSC transplantation is effective for SCI, it is associated with certain problems, such as unpredictable cell viability, low efficiency of differentiation into corresponding tissue cells, and insufficient ability to migrate to target organs [15–17]. In recent years, studies in China and abroad have demonstrated that the combination of acupuncture and MSC transplantation provides a greater benefit in SCI patients than either procedure alone. Therefore, the present analysis addresses the clinical efficacy and potential mechanisms of acupuncture and acupuncture combined with MSC transplantation in the treatment of SCI, utilizing the data generated during the past 20 years. The objective of this work was to critically evaluate

the underlying evidence and provide novel insights for the clinical application of acupuncture in SCI therapy.

## 2. The Effect of Acupuncture on Neural Restoration in Spinal Cord Injury and Its Mechanism

**2.1. Clinical Efficacy of Acupuncture in Neurological Rehabilitation of SCI Patients.** Several randomized controlled trials have demonstrated that different acupuncture methods can improve the sensory and motor function of SCI patients (Table 1). Pooled analyses in a meta-analysis showed that acupuncture had a beneficial effect on neurological recovery (relative risk: 1.28, 95% confidence interval (CI): 1.12-1.50), motor function (weighted mean difference: 6.86, 95% CI: 0.41-13.31), and functional recovery (standardized mean difference: 0.88, 95% CI: 0.56-1.21). Moreover, acupuncture improved the activity of daily living (ADL) in SCI patients, particularly if applied at the back of the Governor Vessel (GV) and bladder channel acupoints [9, 18]. Wong et al. [19] performed an RCT evaluating the efficacy of acupuncture in 100 patients with SCI and demonstrated that acupuncture implemented early in acute SCI increased Functional Independence Measure scores. Wang et al. [20] conducted a prospective RCT with 48 SCI patients to compare the efficacy of paraplegia-triple-needling method (GV and the Back-shu) and the conventional acupuncture at GB30 (*Huantiao*), ST36 (*Zusanli*), GB39 (*Xuanzhong*), and SP6 (*Sanyinjiao*). The results indicated that both therapies improved the ADL score and the comprehensive function in patients with traumatic SCI of the thoracic and lumbar vertebrae. The paraplegia-triple-needling combined with the rehabilitation training provided a better long-term improvement [20]. Also, it has been reported that acupuncture can effectively ameliorate various complications of SCI, such as pain, neurogenic bladder, pressure sores, spasm, and osteoporosis [2, 21–23]. However, the above-indicated meta-analysis identified several limitations of the performed studies, such as the lack of high-quality multicenter large-size trials, the lack of uniform acupuncture methods, the bias of clinical trials, and the incidence of adverse events caused by acupuncture [18, 24]. Therefore, the standardization of acupuncture procedures may facilitate the evaluation of their efficacy and clinical outcomes.

**2.2. Neuroprotective and Neurogenerative Mechanisms of Acupuncture in SCI.** The pathological processes after SCI can be divided into three stages: acute, subacute, and chronic. The first stage includes a local inflammatory response, which mainly involves infiltration of immune cells such as macrophages, T lymphocytes, neutrophils, and microglia, and the release of proinflammatory cytokines, such as tumor necrosis factor- $\alpha$  (TNF- $\alpha$ ), interleukin-1 $\beta$  (IL-1 $\beta$ ), and interleukin-6 (IL-6). At the mitochondrial level, insufficient reduction of oxygen and nitrogen molecules generates high levels of reactive oxygen species (ROS) and reactive nitrogen species (RNS), respectively. ROS and RNS trigger neuronal DNA damage and oxidative stress-induced cell death [25]. Additionally, the activation of astrocytes leads to the deposition of a high amount of the extracellular matrix, inhibiting cell

TABLE 1: Effect of acupuncture on the repair of spinal cord injury.

Study	Number of patients	Randomized, type of clinical trial	Acupuncture intervention	Control intervention	Effect indicators
[19]	100	Yes, RCT	EA (SI3 and B62; 75 Hz, 10 mV)	Usual SCI rehabilitation care	Neurologic and functional recovery $\uparrow$ , ASIA and FIM scores $\uparrow$
[20]	48	Yes, RCT	Acupuncture (GV and the Back-shu acupoints according to the injury region)+electric pulsing stimulation (0.1~1 mA, 20 minutes)	Acupuncture (GB30, ST36, GB39, and SP6)+rehabilitation training	Modified Barthel index $\uparrow$ , function comprehensive assessment $\uparrow$
[2]	1	No, a case report	Scalp acupuncture (DU24, DU19, DU18, DU21)	Not applicable	Motor function $\uparrow$ , neural plasticity $\uparrow$
[21]	10	No, controlled trial	EA (LI4 and LI11; 5 Hz)	Not applicable	Activated C6 and C2 cervical spinal cord levels, functional MRI

Abbreviations: RCT: randomized controlled trial; SI3: *Houxu*; B62: *Shenmai*; ASIA: American Spinal Injury Association; GV: *Dumai*; GB30: *Huantiao*; ST36: *Zusanli*; GB39: *Xuanzhong*; SP6: *Sanyinjiao*; Ex-B2: *Jiaji*; LI4: *Hegu*; LI11: *Quchi*; DU24: *Shenting*; DU19: *Houding*; DU18: *Qiangjian*; DU21: *Qiangding*.

migration and axon growth and repair, and forms a large cystic cavity in the injured region. Together, these mechanisms contribute to the progressive damage of the primary injured tissue, producing a “secondary injury”. The secondary injury is followed by the subacute phase, which lasts for approximately 1 year after the initial event. During the subacute phase, various factors lead to a further expansion of the injured area and the development of the chronic stage [26]. In addition, these complex pathological changes engender several complications, such as respiratory and cardiac dysfunction, abnormal temperature control, hypo- and hypertension, neurogenic bladder, and sexual dysfunction [22].

In the past 20 years, the mechanism of the action of acupuncture on SCI has been extensively studied using standardized acupuncture methods, such as electroacupuncture (EA) (Table 2). The most frequently used acupoints include the GV and bladder channel acupoints, such as Ex-B05 (*Jiaji* acupoints), GV14 (*Dazhui*), GV4 (*Mingmen*), and a few other meridian acupoints, such as ST36. When acupuncture is applied to the back acupoints, the needle is directed mostly toward the dura mater, indicating that EA may act directly on the meningeal branches of the spinal cord at the corresponding nerve segments, including the spinal dura mater, vertebra, dura mater, and ligaments [27]. The neural plasticity defines the ability of the nervous system to repair itself, structurally and functionally. Acupuncture provides a kind of physical peripheral stimulation and central sensory feedback to promote functional recovery, which could be essential for the formation of new synapses after SCI [27]. The potential mechanisms by which acupuncture modulates the neural plasticity and promotes neural restoration and functional recovery are summarized below.

**2.2.1. Neuroprotective Effect of Acupuncture.** SCI causes the loss of a large number of neurons, oligodendrocytes, astrocytes, and microglia, leading to various functional disorders. Therefore, a timely and effective prevention of nerve cell death is critical for the treatment of SCI [28]. It has been demonstrated that acupuncture provides neuroprotection

by inhibiting oxidative stress and inflammatory response after SCI. Juarez Becerril et al. [29] reported that EA stimulation of GV4 reduced the level of ROS by 15%, decreased the extent of spinal cord tissue damage by 25%, and improved the motor function of hindlimbs in paralyzed rats by 18.1%. Jiang et al. [30] demonstrated that EA of GV26 (*Shuigou*) and GV16 (*Fengfu*) reduced the synthesis and release of pro-inflammatory factors such as TNF- $\alpha$ , IL-1, and IL-6 in the damaged area of acute SCI in rats. Moreover, EA at GV6 (*Jizhong*) and GV9 (*Zhiyang*) not only reduced the population of M1 macrophages and the expression of their marker CD86 and associated cytokines TNF- $\alpha$ , IL-1 $\beta$ , and IL-6 but also increased the proportion of M2 macrophages and upregulated the expression of their marker CD206 and released cytokine IL-10, indicating that EA could promote macrophage polarization from proinflammatory M1 phenotypes to anti-inflammatory M2 phenotypes. Moreover, M2 macrophage polarization induced the synthesis and secretion of neurotrophic factor-3 (NT-3) that has a neuroprotective activity [31]. Choi et al. [32] showed that EA at GV26 and GB34 (*Yanglingquan*) in rats with acute SCI inhibited the apoptosis and demyelination of spinal cord neurons. The mechanism of this effect involves the suppression of inflammation induced by the activation of microglia through the downregulation of p38 mitogen-activated protein kinase (MAPK) phosphorylation. Apoptosis signaling involves endogenous pathways mediated by mitochondria and exogenous pathways mediated by death receptors. The endogenous pathway is activated by the change in mitochondrial membrane permeability, the release of proapoptotic molecules such as cytochrome c into the cytoplasm, and the activation of caspase-9 cascade. Conversely, the exogenous pathway is initiated by the stimulation of caspase-8 after the apoptotic signal activates death receptors FAS, TRAIL-Rs, and TNF receptor 1 and the related death domain [33–35]. These two pathways eventually converge at caspase-3, which executes apoptosis by cleaving the cytoskeleton and activating DNA-degrading enzymes. Du et al. [36] documented that the penetrating acupuncture at BL54 (*Zhibian*) and ST28

TABLE 2: Mechanism of acupuncture on the repair of spinal cord injury.

Study	Acupuncture intervention	Control intervention	Effect indicators	Mechanism index
Neuroprotective effect of acupuncture				
[29]	EA (GV4; 2-100 Hz, 2.5 mA, 30 minutes)	EA (GV26)	Motor function $\uparrow$ , Basso-Beattie-Bresnahan (BBB) locomotor rating scale scores $\uparrow$	Hydroxyl radical concentration $\downarrow$ , lipid peroxidation $\downarrow$
[30]	EA (DU26, DU16; 2 Hz, 0.2 mA, 30 minutes) MA (DU26, DU16; 2 revolutions per second for 10 s, every 10 minutes, 30 minutes)	No treatment	Neuronal function recovery $\uparrow$ , antioxidation $\uparrow$ , anti-inflammation $\uparrow$ , antiapoptosis effects $\uparrow$	IL-1 $\beta$ $\downarrow$ , IL-6 $\downarrow$ , TNF- $\alpha$ $\downarrow$
[31]	EA (GV6, GV9; 60 Hz for 1.05 s and 2 Hz for 2.85 s, $\leq$ 1 mA, 20 minutes, once every other day, 4 weeks)	No treatment	BBB functional $\uparrow$	M1 (TNF- $\alpha$ $\downarrow$ , IL-1 $\beta$ $\downarrow$ , IL-6 $\downarrow$ ), M2 (IL-10 $\uparrow$ , CD206 $\uparrow$ ), NT-3 expression $\uparrow$ , the polarization of M2 microglia/macrophages $\uparrow$
[32]	Acupuncture (GV26, GB34; two spins/second, 30 s, 30 minutes, once a day, 2 weeks)	Not received any acupuncture treatment	Functional recovery $\uparrow$	Caspase-3 $\downarrow$ , p38 MAPK $\downarrow$ , resident microglia $\downarrow$ , TNF- $\alpha$ $\downarrow$ , IL-1 $\beta$ $\downarrow$ , IL-6 $\downarrow$ , nitric oxide synthase $\downarrow$ , cyclooxygenase-2 $\downarrow$ , matrix metalloprotease-9 $\downarrow$
[33]	Elongated needle (BL54, ST28, CV6, CV3; 20-40 times/min, 1.5-3 V, 15 minutes)	No acupuncture stimulation	Decrease spinal injury $\downarrow$ , cell apoptosis $\downarrow$	p-Akt and p-ERK1/2 $\uparrow$ , Cyt c and caspase-3 $\downarrow$
[34]	EA (ST36, KI3; 60 Hz for 1.05 s and 2 Hz for 2.85 s, $\leq$ 2 mA, 20 minutes)	No electrical stimulation	Locomotor skills $\uparrow$ , ultrastructural features of the myelin sheath $\uparrow$	Caspase-12 $\uparrow$ , Cyt c $\uparrow$ , oligodendrocyte proliferation $\uparrow$ , oligodendrocyte death $\downarrow$
[35]	EA (GV6, GV9; 60 Hz, 20 minutes)	No acupuncture stimulation	Functional recovery $\uparrow$ , tissue loss and neuronal apoptosis $\downarrow$	Proapoptotic proteins (cleaved caspase-3/9 $\downarrow$ and cleaved PARP $\downarrow$ ), antiapoptotic protein Bcl-2 $\uparrow$ , miR-214 $\uparrow$
[36]	Elongated needle (BL54, ST28; 20-40beats/min, 1.5-3 V, 15 minutes)	Control group	Cell apoptosis $\downarrow$	FAS $\rightarrow$ caspase-3 cascade $\downarrow$
[37]	Elongated needle therapy (BL54, ST28; 2 Hz, 1-3 mA, 15 minutes)	Not received acupuncture treatment	BBB locomotor scale $\uparrow$	PI3K/Akt and MAPK/ERK signaling pathways $\uparrow$ , Bax protein $\downarrow$ , Bcl-2 $\uparrow$ , mitochondrial apoptosis pathway $\downarrow$
[38]	EA (BL54, ST28, CV6, CV3; 20 Hz/40 Hz, 15 minutes)	Elongated needle EA	Promote repair $\uparrow$	PI3K/Akt $\uparrow$ , ERK1/2 $\uparrow$ , Cyt c $\downarrow$ , caspase-3 $\downarrow$
[29]	EA (GV4; 2.5 mA, 2-100 Hz, 30 minutes)	EA (GV26)	Motor function $\uparrow$ , BBB locomotor scale $\uparrow$	Hydroxyl radical concentration $\downarrow$ , lipid peroxidation $\downarrow$
Acupuncture modulates neural plasticity and promotes neural regeneration				
Wnt signaling pathway				
[39]	EA (GV14, GV4; 2 Hz, 1 mA, 20 minutes)	Not received EA treatment	Hindlimb motor functions $\uparrow$ , neuroprotective effects $\uparrow$ , proliferation and differentiation of neural stem cells $\uparrow$	Wnt/ $\beta$ -catenin signaling pathway $\uparrow$ , proliferation and differentiation of neural stem cells $\uparrow$
[40]	Fire needle acupuncture (T7, T8, T11, T12; 1/3 s, 3-5 mm, once a day)	Not treated by fire needle acupuncture	Lower limb locomotor function $\uparrow$	Wnt/ $\beta$ -catenin $\uparrow$ , ERK $\downarrow$ , nestin $\uparrow$ , NSE $\uparrow$ , Gal-C $\uparrow$ , GFAP $\downarrow$ ; Wnt-3a $\uparrow$ , GSK3 $\beta$ $\uparrow$ , $\beta$ -catenin $\uparrow$ , ngn1 $\uparrow$ , ERK1/2 $\downarrow$ , cyclin D1 gene and protein $\downarrow$
Notch signaling pathway				
[42]	EA (GV14, GV4; 2 Hz, 2 V, 30 minutes, once a day)	Without any treatment	Morphological recovery $\uparrow$	Notch signaling pathway $\downarrow$ , promoting the proliferation of endogenous neural stem cells $\uparrow$
[43]				



TABLE 2: Continued.

Study	Acupuncture intervention	Control intervention	Effect indicators	Mechanism index
	EA (GB30, Ex-B05; 100 Hz/2 s and 2 Hz/2 s, 3 mA, 5 mm)	Not received EA treatment	Spontaneous regeneration↑, remyelination↑, recovery of function↑	BrdU(+)/NG2(+) cells↑, the proliferation of endogenous neural stem cells and oligodendrocytes↑
	Rho/ROCK signaling			
[46]	EA (DU14, DU4, SP6, GB30, ST36, BL60; 4 Hz, 30 minutes, once a day, 7 days)	No acupuncture stimulation	Tissue repair and neurological functional recovery↑, BBB locomotor scale and inclined plane test scores↑	Neuronal apoptosis↓, decreases RhoA↓, Nogo-A mRNA↓
[47]	EA (GV3, GV14, ST36, BL32; 100 Hz for 1.5 ms and 2 Hz for 1.5 ms)	Blocking agent Y27632	Spinal cord tissue morphology↑, BBB score of lower limb movement function↑	Rho/ROCK signaling pathway↓, axonal growth and inflammatory reaction↓
[48]	EA (Ex-B2; 100 Hz, 30 minutes, once daily for 14 days and 28 days)	ROCK inhibitor groups	Hindlimb locomotor function↑	RhoA/ROCK signaling pathway↓ (RhoA↓, ROCK II↓, MLC proteins↓)
[49]	EA (GV3, GV14, ST36, BL32; 100 Hz for 1.5 ms and 2 Hz for 1.5 ms, 2 V, 20 minutes, 14 days)	Blocking agent Y27632 EA+Y	Lower limb movement function↑	Nogo/NgR and Rho/ROCK signaling pathway↓ (mRNA and protein expression of Nogo-A↓, NgR↓, LINGO-1↓, RhoA and ROCK II↓)
[57]	EA (GV3, GV14, ST36, BL32; 2 Hz, 2 V, 20 minutes, 14 days)	Monosialoganglioside treatment	Hindlimb motor functions↑	Rho-A and Rho-associated kinase II (ROCK II)↓, Rho/ROCK signaling pathway↓
	Neurotrophic factors			
[58]	EA (ST36, GB39, ST32, SP6; 2 Hz, 98 pulses per minute, 15 minutes, ST36 and GB39, first day, ST32 and SP6, second day, each pair of acupoints was stimulated on alternate days)	Not received EA treatment	Sensory functional↑	CNTF↓, p75-like apoptosis-(death domain protein)↓, IGF-1↓, transforming growth factor-beta 2↓, FGF-4↓
[53]	EA (ST36, GB39, ST32, SP6; alternating stimulus, 98 Hz, 30 minutes, the stimulating electrodes were changed and their polarity reversed after 15 minutes)	Not received EA treatment	Hindlimb locomotor and sensory functions↑	CNTF↑, FGF-2↑, TrkB mRNA↑; NGF, PDGF↓, TGF-β1↓, IGF-1↓, TrkA↓, TrkC mRNA↓
[50]	EA (GV1; 2 Hz, 2 mA, 20 minutes, once a day)	Not received EA treatment	BBB↑	NGF↑, BDNF↑
[59]	EA (ST36, GB39, ST32, SP6; 75 cycles/minute, 40-50 μA, 30 minutes, once a day)	No treatment	BBB locomotor rating scale scores↑, motor neuron function↑	AChE activity↑, GDNF↑
[51]	EA (GV14, GV4; 2 Hz, 1 mA, 20 minutes)	No treatment	Motor function↑, neuronal function↑	NT-3↑
[52]	EA-2 group (GV20, GV16, GV14, GV4; GV14 and GV4, 2 Hz, 0.2 mA, 30 minutes, once every 2 days, 6 weeks)	EA-1 group	BBB locomotor rating scale scores↑, locomotor function↑	BDNF↑, NT-3↑
[54]	EA (GV14, GV4, GV7, GV5; alternating stimulus, 2 Hz, 10 minutes, 6 days EA-1 day interval-6 days EA)	No treatment	Movement function↑	BDNF↑, CREB↑
[38]	EA (BL54, ST28, CV6, CV3; 20 Hz/40 Hz)	Only performed a laminectomy	Promote repair↑	PI3K/Akt↑, ERK1/2↑, cytochrome c↓, caspase-3↓
[60]	EA (GV4, GV14; GV9, GV6; 2 Hz, 20 minutes)	Not received EA treatment	Hindlimb locomotor↑ and sensory functions↑	IGF-1↓, FGF-2↓, CNTF↓, PDGF↓, TGF-β1↓, TrkA↓, TrkB↓, TrkC↓, NTFs↑
[55]	EA (Ex-B2, 2 Hz; 3, 7, and 14 days)	Not received EA treatment	BBB locomotor scoring↑, hindlimb locomotor function↑	EGFR↓, GFAP↓, nerve axon regeneration↑

TABLE 2: Continued.

Study	Acupuncture intervention	Control intervention	Effect indicators	Mechanism index
[56]	EA (Ex-B2, 2/100 Hz, 0.2 mA, 15 minutes)	Not received EA treatment	Locomotor function↑	LI↑, GFAP↑, (early phase)-(GFAP)↓, (later stages), nestin↑
[58]	EA (ST36, GB39, ST32, SP6; alternating stimulus, 2 Hz, 98 pulses/minute, 15 minutes, after the third day, stimulate every other day)	Not received EA treatment	Sensory functional↑	CNTF↓, p75-like apoptosis-(death domain protein)↓, IGF-1↓, transforming growth factor-beta 2↓, FGF-4↓

Abbreviation: GV4: *Mingmen*; GV26: *Shuigou*; BBB: Basso-Beattie-Bresnahan; DU16: *Fengfu*; IL-1 $\beta$ : interleukin-1 $\beta$ ; IL-6: interleukin-6; TNF- $\alpha$ : tumor necrosis factor- $\alpha$ ; GV6: *Jizhong*; GV9: *Zhiyang*; NT-3: neurotrophin-3; GB34: *Yanglingquan*; MAPK: mitogen-activated protein kinase; BL54: *Zhibian*; ST28: *Shuidao*; CV6: *Qihai*; CV3: *Zhongji*; Cyt c: cytochrome c; ST36: *Zusanli*; KI3: *Taixi*; GV4: *Mingmen*; GV14: *Dazhui*; SCI: spinal cord injury; ERK: extracellular signal-regulated kinase; GSK3 $\beta$ : glycogen synthase kinase 3 $\beta$ ; GB30: *Huantiao*; Ex-B05: *Huatuojiaji*; BL32: *Ciliao*; ST32: *Futu*; GV1: *Changqiang*; NGF: nerve growth factor; BDNF: brain-derived neurotrophic factor; AChE: acetylcholinesterase; GDNF: glial cell line-derived neurotrophic factor; GV20: *Baihui*; GV7: *Zhongshu*; GV5: *Xuanshu*; Ex-B2: *Jiaji*; CREB: cAMP response element-binding; NTFs: neurotrophic factors; EGFR: epidermal growth factor receptor; GFAP: glial fibrillary acidic protein.

(*Shuidao*) inhibited exogenous death receptor-mediated apoptosis of neurons in acute SCI and downregulated the local expression of FAS and caspase-3. Shi et al. [37] showed that the elongated needle therapy at BL54 and ST28 promoted the recovery from SCI. This beneficial effect was associated with the suppression of inflammation via the phosphoinositide 3-kinase/Akt (PI3K/Akt) and MAPK/extracellular signal-regulated kinase (ERK) signaling pathways, which resulted in the downregulation of the Bax protein, upregulation of Bcl-2, and inhibition of the mitochondria-mediated apoptosis. Therefore, acupuncture may promote the survival of neurons after SCI by blocking both the endogenous and exogenous apoptosis pathways, facilitating the activation of SCI repair and functional recovery [38].

**2.2.2. Acupuncture Modulates Neural Plasticity and Promotes Neural Regeneration.** A growing body of evidence indicates the crucial role of intracellular signaling cascades, such as the Wnt, Notch, and ROCK pathways, in neural plasticity and regeneration after SCI. Thus, the development of therapeutic agents targeting these pathways is expected to contribute to the treatment of SCI.

The Wnt signaling pathway plays an important role in the proliferation, differentiation, and axon orientation of NSCs. Wnt-1, the key element in the Wnt pathway, and the critical transcription factor  $\beta$ -catenin are highly expressed in the early stage of SCI, which is consistent with the reactive proliferation of endogenous NSCs of the spinal cord [39, 40]. Xu et al. [40] demonstrated that a fire needle at the Ex-B05 points promoted lower limb locomotor function in SCI rats. Moreover, they documented that the potential mechanism underlying the effect of acupuncture involves the stimulation of proliferation and differentiation of NSCs into neurons by the activation of the Wnt/ $\beta$ -catenin pathway (Wnt-3a, GSK3,  $\beta$ -catenin, and *ngn1*) and inhibition of the overexpression of MAPK-ERK kinase/extracellular signal-regulated protein kinases 1 and 2 (ERK1/2) and cyclin D1. Wang et al. [39] found that the expression of Wnt-1, Wnt-3a, and  $\beta$ -catenin in the injured area was increased at 1, 7, and 14 days after SCI, while the expression of Wnt-1, Wnt-3a, and  $\beta$ -catenin was increased by EA at GV14 and GV4. These results suggest that GV EA may promote the regeneration of neurons by activating the Wnt/ $\beta$ -catenin signaling pathway. The above studies only

mentioned that acupuncture improves locomotor function as well as regulates these pathway proteins, where changes expressed by NSCs need to be clarified, and additional supporting data generated by the loss-of-function methodology are needed to reach a definitive conclusion.

Notch signaling is a classical pathway controlling the proliferation and differentiation of endogenous NSCs. There are four types of Notch receptors, named Notch1 through Notch4; their ligands are members of the Delta/Serrate/Lag2 protein family, such as Delta. The activation of Notch receptors induces the transcription and expression of downstream repressor genes, such as Hes 1 and Hes 5, which regulate cell proliferation and differentiation [41]. After SCI, the Notch signaling is activated, stimulating endogenous NSC proliferation and differentiation predominantly into astrocytes, hindering SCI repair. Geng et al. [42] documented that EA at GV14 and GV4 promoted the proliferation of endogenous NSCs in the spinal cord and inhibited the local expression of Notch1, Notch3, and Notch4, preventing endogenous NSCs from differentiating into astrocytes. It has also been shown that EA at GV and the bladder channel in SCI rats inhibited Notch signaling and increased the number of BrdU/neuron-glia antigen 2 (NG2) double-positive cells around SCI. Additionally, this procedure promoted the proliferation of endogenous NSCs and the differentiation of oligodendrocytes in the injured spinal cord [43].

Rho/ROCK signaling is mainly responsible for regulating cytoskeleton organization, cell growth, cell migration, proliferation, and development [44]. The RhoA/ROCK pathway mediates the effects of myelin-associated axon growth inhibitors (Nogo), myelin-associated glycoprotein, oligodendrocyte-myelin glycoprotein, and repulsive guidance molecule. Blocking RhoA/ROCK signaling reverses the inhibitory effects of these molecules on axon outgrowth and promotes axonal sprouting and functional recovery in CNSI models [45]. Wu et al. [46] demonstrated that EA treatment at GV14, GV4, SP6, GB30, ST36, and BL60 (*Kunlun*) for 7 days improved tissue repair and neurological functional recovery, reduced neuronal apoptosis, and suppressed the expression of RhoA and Nogo-A at the SCI lesion. It has also been shown that EA downregulated the expression of RhoA, ROCK II, myosin light chain, Nogo-A, NgR, and LINGO-1 in the anterior horn of the spinal cord, resulting in an improvement of the motor function

of the hindlimb in SCI rats [47–49]. These data suggest that acupuncture can improve SCI neural restoration by enhancing the Rho/ROCK signaling. However, the specific mechanism underlying the effects of acupuncture on axon growth and regeneration mediated by the Rho/ROCK signaling has not been fully elucidated. Whether the regulation of local inflammation and cell migration by acupuncture involves this signaling pathway remains to be determined.

Endogenous neurotrophic factors (NTFs), such as the nerve growth factor (NGF) [50], brain-derived neurotrophic factor (BDNF), and NT-3 [51, 52], act by binding to their receptors, respectively, TrkA, TrkB, and TrkC [53]. These factors are essential to promote axon sprouting and neuronal regeneration in the injured site. NGF/tropomyosin receptor kinase A (TrkA) signaling can prevent apoptosis by the activation of the PI3K/Akt pathway. Acupuncture has been shown to increase the expression of the BDNF receptor kinase B (TrkB) [54] by activating tropomyosin through the PI3K/Akt and ERK1/2 signaling. These processes lead to the phosphorylation and activation of the cyclic AMP (cAMP) response element-binding transcription factor, which upregulates the transcription of the BDNF gene [54]. In addition to affecting NTFs and their receptors, acupuncture can modulate neural plasticity by inhibiting the expression of the epidermal growth factor receptor [55] and glial fibrillary acidic protein (GFAP) [56] in the spinal cord, thus promoting axon regeneration and preventing the formation of the glial scar.

In summary, the current researches on the mechanism of acupuncture in SCI are focused mostly on the level of single molecules and/or signaling pathways. However, a wide range of interactive communication exists between different signaling pathways, and acupuncture may regulate a complex network of multiple signaling molecules and pathways. This notion is consistent with the holistic regulation characteristics of acupuncture, involving multiple targets, links, approaches, and levels. How acupuncture affects this complex network requires further investigation. Moreover, due to the small number of endogenous NSCs and the unfavorable microenvironment of the injured region of SCI, the proliferation and differentiation of endogenous NSCs may not be sufficient to replace the damaged central nervous system. Thus, it is crucial to identify treatments that could be combined with acupuncture to achieve a better promotion of the restoration of neurons after SCI.

### **3. The Effects of Acupuncture Combined with Mesenchymal Stem Cells on SCI and Their Mechanism**

*3.1. Effects of Mesenchymal Stem Cells on Neural Restoration after SCI and Their Mechanisms.* MSCs are important members of the stem cell family; they are derived from the early developmental mesoderm and belong to pluripotent stem cells [61]. Given their strong proliferation ability and multilineage differentiation potential, MSCs can be induced to generate neurons and glial cells [15, 62]. Clinical studies have confirmed that MSC transplantation is effective in the treatment of post-SCI dysfunction [14]. In the first longitudinal study of the effect of MSCs on the outcomes in SCI patients, autolo-

gous MSCs were isolated from each patient's bone marrow, amplified, and implanted by intramedullary or intradural injection [63]. Within 6 months after implantation, motor function was significantly improved in 7 of 10 patients. After 3 years of follow-up, motor function continued to improve, and no other complications or signs of tumor formation were present [64]. Similarly, a recent clinical trial showed that in 10 of 14 SCI patients, the treatment with MSCs ameliorated the sensory impairment, as documented by the improvement in the American Spinal Injury Association (ASIA) motor and sensory scores [65]. Recently, clinical trials of MSC transplantation for the treatment of acute and subacute SCI patients have been systematically reviewed, and the conclusion was reached that this therapy can safely and effectively improve SCI-related symptoms such as dyskinesia [66, 67]. A retrospective study of acute SCI showed that 19 (70%) of the completed ( $n = 18$ ) and ongoing ( $n = 9$ ) clinical trials were focused on the intrathecal injection of MSCs for the treatment of SCI [66]. However, the exploration of other transplantation methods was also underway and will provide a clinical basis for the optimal route of MSC transplantation for the treatment of SCI. Moreover, it is generally considered that to improve the survival rate of MSCs, the best time window for transplantation is within 1-2 weeks after the injury [68]. Also, implantation of MSCs results in a short-term improvement of autonomic nerve function and relieves from sweat gland secretion disorder and orthostatic hypotension, i.e., goals that could not be achieved by the traditional treatment.

The mechanisms underlying the effects of MSC transplantation in the treatment of SCI include the activation of multiple paracrine or autocrine NGFs, neuron regeneration, nerve loop reconstruction, integration of transplanted cells and host cells, and prevention or reduction of glial scar formation at the site of injury [66]. After migrating to the lesion, implanted MSCs can differentiate into functional neurons, which can form synapses with host neurons [68]. They also can improve axonal regeneration, inhibit demyelination while promoting myelin regeneration [16, 69–72], and reconstruct functional neural networks [15]. It has been proposed that the therapeutic action of implanted MSC in SCI is based on the secretion of a variety of factors, such as NGF, NT-3, and BDNF [73, 74]. Furthermore, paracrine immunomodulatory mediators secreted by MSCs can reduce harmful inflammation by inhibiting the differentiation of macrophages and microglia into neurotoxic, proinflammatory M1 subsets and promoting the generation of immunomodulatory M2 subsets which contribute to axonal growth and myelin regeneration [75]. The paracrine factors also help to promote the differentiation of MSCs, creating an environment facilitating the survival of transplanted MSCs, axonal regeneration, and integration of implanted cells with host cells.

In summary, MSC transplantation appears to represent an effective treatment for SCI patients, but large-scale phase III clinical trials are needed. The mechanism of the beneficial effects of MSCs involves neuroprotection, immune regulation, neuron regeneration, and the restoration of nerve conduction. Together, these processes contribute to structural repair and functional recovery of the injured spinal cord. However, some studies have shown that MSCs located in the lesion cannot differentiate into neurons due to an unfavorable microenvironment in the injured

TABLE 3: Effects of the combination of acupuncture and MSC implantation on spinal cord injury and their mechanisms.

Study	Intervention & acupuncture parameters	Control intervention	Effect indicators	Comparison of effects between groups	Mechanism index
[78]	MSCs ( $1 \times 10^6$ viable cells/mL), EA (Ex-B2; H1 = 2 Hz, H2 = 50 Hz, 20 minutes, 14 days), MSCs+EA	PBS group	Combined behavioral score $\uparrow$	BMSC+acupuncture > acupuncture > BMSC > PBS	Differentiation of BMSC into neuronal cells $\uparrow$ , NSE $\uparrow$ , GFAP $\uparrow$
[77]	MSCs ( $1 \times 10^5$ viable cells/mL)+EA (GV1, GV2, GV6, GV9; 60 Hz for 1.05 s and 2 Hz for 2.85 s, $\leq 1$ mA, 20 minutes), MSCs+EA	Sham-control Op-control	BBB locomotion test $\uparrow$ , differentiation of MSCs $\uparrow$ , regeneration of nerve fibers $\uparrow$	MSCs+EA > EA > MSCs > control	GFAP $\downarrow$ , CSPGs $\downarrow$
[81]	MSCs ( $5 \times 10^5$ cells/mL)+EA (T9, T11; 39 A/h, 20 Hz, 15 minutes, twice a day), MSCs+EA	Normal group	Functional deficits $\uparrow$ , axonal regeneration $\uparrow$	MSCs+EA > MSCs > EA > normal	GFAP $\downarrow$ , CSPGs $\downarrow$ , G-CSF $\uparrow$ , BDNF $\uparrow$ , VEGF $\uparrow$ , IL-6 $\uparrow$
[83]	MSCs ( $1 \times 10^5$ cells/ $\mu$ L, 5 $\mu$ L)+EA (GV1, GV2, GV6, GV9; 60 Hz for 1.05 s and 2 Hz for 2.85 s, once every other day, 7 weeks), MSCs+EA	Op-control	Axonal regeneration $\uparrow$ , partial locomotor functional $\uparrow$	MSCs+EA > MSCs > EA > Op-control	NT-3 $\uparrow$ , cAMP level $\uparrow$ , 5-HT $\uparrow$ , CGRP-positive nerve fibers $\uparrow$
[85]	TrkC-MSCs ( $1 \times 10^5$ cells/ $\mu$ L, 5 $\mu$ L)+EA (GV6, GV9; 60 Hz for 1.05 s and 2 Hz for 2.85 s, $\leq 1$ mA, 20 minutes), MSCs+EA	PBS group	Remyelination $\uparrow$ , functional $\uparrow$	TrkC-MSCs+EA > MSCs+EA > TrkC-MSCs > MSCs	NT-3 $\uparrow$
[84]	MSCs ( $1 \times 10^5$ cells/mL, 5 mL)+EA (GV9, GV6, GV2, GV1; 60 Hz for 1.05 s and 2 Hz for 2.85 s, 1 mA, 20 minutes); MSCs+EA	Normal group	BBB locomotion test $\uparrow$	MSCs+EA > EA > MSCs > Op-control	Endogenous NT-3 $\uparrow$ , 5-HT-positive nerve fibers $\uparrow$

Abbreviations: BMSCs: bone marrow stromal cells; PBS group: PBS injection in the injured area; Ex-B2: *Jiaji*; PBS: phosphate-buffered saline; GV1: *Changqiang*; GV2: *Yaoshu*; GV6: *Jizhong*; GV9: *Zhiyang*; MSCs: mesenchymal stem cells; Sham-control: received a laminectomy without spinal cord transection; Op-control: operated control received a spinal cord transection only without any treatments; GFAP: glial fibrillary acidic protein; BBB: Basso-Beattie-Bresnahan; CSPGs: chondroitin sulfate proteoglycans; normal group: normal rats; G-CSF: granulocyte colony-stimulating factor; BDNF: brain-derived neurotrophic factor; VEGF: vascular endothelial growth factor; IL-6: interleukin-6; NT-3: neurotrophin-3.

spinal cord and their low survival rate. Therefore, an improvement in the survival and directional differentiation of MSCs is essential to achieve progress in clinical applications of these cells in SCI treatment.

**3.2. Effects and Mechanisms of the Combined Acupuncture/MSCTherapy for SCI.** In recent years, extensive research has been performed, and some progress has been achieved, on the efficacy and mechanisms of acupuncture combined with MSC transplantation in the treatment of acute CNSIs such as SCI, traumatic brain injury, stroke, and cerebral palsy [76]. The combination of acupuncture and MSC transplantation resulted in an improvement of the SCI comprehensive functional score and the BBB motor score. Importantly, the curative effect of the combination therapy was better than that of either acupuncture or MSC implantation alone (Table 3).

The mechanism responsible for the effect of the combined therapy appears to depend on the promotion of the survival and differentiation of MSCs. Ding et al. [77] documented that

10 weeks of combination therapy increased the formation of descending corticospinal tract projections into the lesion and showed improved Basso-Beattie-Bresnahan (BBB) scores and enhanced motor-evoked potentials in rats with spinal cord transection. Sun et al. [78] have shown that the combination therapy increased the expression of neuron- and glial-specific markers (neuron-specific enolase (NSE) and GFAP, respectively) more than MSC transplantation alone, suggesting that acupuncture promotes the differentiation of MSCs into neurons and glial cells. The structural and functional recovery after the combination treatment may also be due to the downregulation of expression of GFAP and chondroitin sulfate proteoglycans (CSPGs), which could prevent axonal degeneration and improve axonal regeneration.

The neurotrophic factor NT-3 has an important function in the development, differentiation, and survival of neurons and in signal transduction. NT-3 also induces the growth of axons from the intact corticospinal tract across the midline to the innervated side [79, 80]. Liu et al. [81] documented that



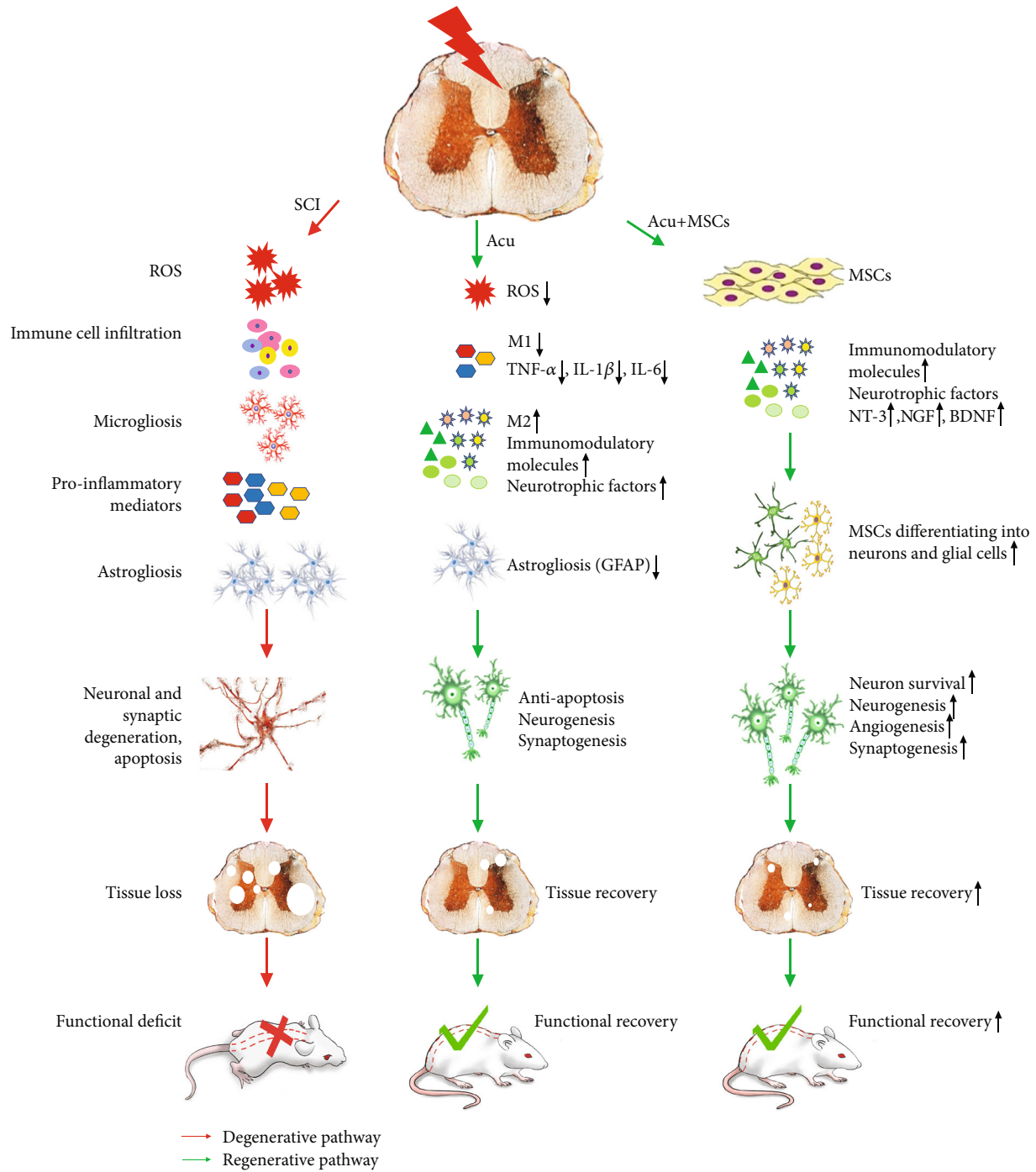


FIGURE 1: Effects of the combination of acupuncture and MSC transplantation on neural recovery after spinal cord injury (SCI) and the underlying mechanisms. ROS: reactive oxygen species; TNF- $\alpha$ : tumor necrosis factor- $\alpha$ ; IL-1 $\beta$ : interleukin-1 $\beta$ ; IL-6: interleukin-6; MSCs: mesenchymal stem cells; GFAP: glial fibrillary acidic protein; NT-3: neurotrophic factor-3; NGF: nerve growth factor; BDNF: brain-derived neurotrophic factor.

the combination treatment increased the number of surviving MSCs, an effect that may be related to the acupuncture-induced increase in the cAMP level in the SCI area. cAMP, in turn, can increase the expression of endogenous NT-3, promoting the differentiation of MSCs into neuron-like cells and oligodendrocytes; these cells replace the injured tissue and fill the cystic area [82–84]. Ding et al. [85] grafted TrkC (NT-3 receptor)-modified MSCs (TrkC-MSCs) into the demyeli-

nated spinal cord and applied EA. In this experiment, EA increased NT-3 expression, promoting the differentiation of TrkC-MSCs into oligodendrocyte-like cells, remyelination, and functional improvement of the demyelinated spinal cord. Additional effects of acupuncture involve the inhibition of GFAP secretion, promotion of the synthesis of laminin, and regeneration of calcitonin gene-related peptide-positive and serotonin-positive nerve fibers and corticospinal tract nerve



fibers. Also, acupuncture reduces the size of the nerve cavity to prevent further expansion of the nerve scar and creates a favorable microenvironment for nerve fiber regeneration and penetration into the injured area. Ultimately, these effects can lead to an improvement in motor function. Moreover, acupuncture can enhance the migration of MSCs by increasing the phosphorylation of Akt and ERK. Finally, unpublished data obtained in our laboratory showed that the expression of chemokines (such as CXCL1) and their receptors (such as CXCR2) in target organs increased significantly after acupuncture. We have raised the possibility that the chemotactic effect of acupuncture may enhance the homing ability of MSCs, which is critical for the targeted migration of these cells.

In summary, we advance a hypothesis that the biological mechanism underlying the beneficial impact of acupuncture combined with MSCs transplantation involves the improvement in the local microenvironment at the site of injury through the neuroprotective and immunomodulatory effects of acupuncture. The combination therapy can improve the survival rate and direct the differentiation of MSCs, promoting the differentiation of exogenous MSCs into oligodendrocyte-like or neuron-like cells. Secondly, the combined treatment promotes targeted migration of MSCs to the spinal cord. Thirdly, transplanted MSCs can release a large amount of neurotrophic and immunomodulatory factors that, through paracrine mechanisms, can enhance acupuncture neuroprotection, nutrition, and axonal budding, counteracting problems such as the small number of host endogenous NSCs and the limited ability of acupuncture to promote their differentiation.

#### 4. Conclusion

In conclusion, the recovery of patients after SCI is difficult due to the complex pathological sequelae of the injury and limited regenerative capacity of neurons (Figure 1). Acupuncture is effective for SCI-induced neurologic deficits. The potential mechanisms of acupuncture actions involve the protection of neurons against inflammation, oxidation, and apoptosis and the improvement of the local microenvironment. Additionally, acupuncture can promote neural regeneration and axon sprouting via multiple cellular signal transduction pathways, such as ROCK, Wnt, and Notch. Although MSC transplantation alleviates neural deficits and related complications, low survival and differentiation rates of MSCs limit the effects of their use in SCI. Several studies have documented that the combination of acupuncture and MSC transplantation is superior to each procedure alone. The combination therapy can enhance the survival of MSCs, promote their differentiation into neurons, and facilitate their targeted migration to the spinal cord by stimulating the secretion of neurotrophic factors such as NT-3. Ultimately, these processes lead to the improvement of the microenvironment and generation of a functional neural network. Additionally, the differentiation of MSCs into neurons can overcome the shortage of endogenous NSCs in SCI patients. Therefore, acupuncture combined with MSC transplantation could become a novel and effective strategy for the treatment of SCI. This possibility needs to be verified by basic and clinical research.

#### Abbreviations

ADL:	Activity of daily living
ASIA:	American Spinal Injury Association
BDNF:	Brain-derived neurotrophic factor
CNSIs:	Central nervous system injuries
CSPGs:	Chondroitin sulfate proteoglycans
cAMP:	Cyclic AMP
EA:	Electroacupuncture
NTFs:	Endogenous neurotrophic factors
ERK:	Extracellular signal-regulated kinase
GFAP:	Glial fibrillary acidic protein
GV:	Governor Vessel
IL-1 $\beta$ :	Interleukin-1 $\beta$
IL-6:	Interleukin-6
MSCs:	Mesenchymal stem cells
MAPK:	Mitogen-activated protein kinase
NGF:	Nerve growth factor
NSCs:	Neural stem cells
NG2:	Neuron-glia antigen 2
NT-3:	Neurotrophic factor-3
RNS:	Reactive nitrogen species
ROS:	Reactive oxygen species
ROCK:	Rho/Rho kinase
SCI:	Spinal cord injury
TNF- $\alpha$ :	Tumor necrosis factor- $\alpha$ .

#### Data Availability

All data used during the study are available from the corresponding author by request “xuzhifangmsn@hotmail.com”.

#### Conflicts of Interest

The authors have no conflict of interest regarding this paper.

#### Authors' Contributions

Huiling Tang and Yi Guo contributed equally to this work.

#### Acknowledgments

This study was financially supported by the National Natural Science Foundation of China (NSFC) (Nos. 81973944, 81704146, 81873369, 81873368, and 81503636), National Key R&D Program of China (Nos. 2019YFC1712200 and 2019YFC1712204), and Youth Talent Promotion Project of the China Association for Science and Technology (No. 2019-2021ZGZJXH-QNRC001).

#### References

- [1] K. Y. Nam, H. J. Kim, B. S. Kwon, J. W. Park, H. J. Lee, and A. Yoo, “Robot-assisted gait training (Lokomat) improves walking function and activity in people with spinal cord injury: a systematic review,” *Journal of Neuroengineering and Rehabilitation*, vol. 14, no. 1, p. 24, 2017.
- [2] C. Widrin, “Scalp acupuncture for the treatment of motor function in acute spinal cord injury: a case report,” *Journal of*

- Acupuncture and Meridian Studies*, vol. 11, no. 2, pp. 74–76, 2018.
- [3] M. T. Fitch and J. Silver, “CNS injury, glial scars, and inflammation: inhibitory extracellular matrices and regeneration failure,” *Experimental Neurology*, vol. 209, no. 2, pp. 294–301, 2008.
  - [4] A. D. Gaudet and P. G. Popovich, “Extracellular matrix regulation of inflammation in the healthy and injured spinal cord,” *Experimental Neurology*, vol. 258, pp. 24–34, 2014.
  - [5] L. M. Ramer, M. S. Ramer, and E. J. Bradbury, “Restoring function after spinal cord injury: towards clinical translation of experimental strategies,” *The Lancet Neurology*, vol. 13, no. 12, pp. 1241–1256, 2014.
  - [6] M. G. Fehlings, J. R. Wilson, L. A. Tetreault et al., “A clinical practice guideline for the management of patients with acute spinal cord injury: recommendations on the use of methylprednisolone sodium succinate,” *Global Spine Journal*, vol. 7, 3\_suppl, pp. 203S–211S, 2017.
  - [7] L. M. Chavez, S. S. Huang, I. Mac Donald, J. G. Lin, Y. C. Lee, and Y. H. Chen, “Mechanisms of acupuncture therapy in ischemic stroke rehabilitation: a literature review of basic studies,” *International Journal of Molecular Sciences*, vol. 18, no. 11, p. 2270, 2017.
  - [8] A. H. Li, J. M. Zhang, and Y. K. Xie, “Human acupuncture points mapped in rats are associated with excitable muscle/skin-nerve complexes with enriched nerve endings,” *Brain Research*, vol. 1012, no. 1-2, pp. 154–159, 2004.
  - [9] F. Xiong, C. Fu, Q. Zhang et al., “The effect of different acupuncture therapies on neurological recovery in spinal cord injury: a systematic review and network meta-analysis of randomized controlled trials,” *Evidence-Based Complementary and Alternative Medicine*, vol. 2019, Article ID 2371084, 12 pages, 2019.
  - [10] W. Cai and W. D. Shen, “Anti-apoptotic mechanisms of acupuncture in neurological diseases: a review,” *The American Journal of Chinese Medicine*, vol. 46, no. 3, pp. 515–535, 2018.
  - [11] Y. Y. Chen, W. Zhang, Y. L. Chen, S. J. Chen, H. Dong, and Y. S. Zeng, “Electro-acupuncture improves survival and migration of transplanted neural stem cells in injured spinal cord in rats,” *Acupuncture & Electro-Therapeutics Research*, vol. 33, no. 1, pp. 19–31, 2008.
  - [12] J. P. Antonios, G. J. Farah, D. R. Cleary, J. R. Martin, J. D. Ciacci, and M. H. Pham, “Immunosuppressive mechanisms for stem cell transplant survival in spinal cord injury,” *Neurosurgical Focus*, vol. 46, no. 3, article E9, 2019.
  - [13] M.-J. Tsai, D. Y. Liou, Y. R. Lin et al., “Attenuating spinal cord injury by conditioned medium from bone marrow mesenchymal stem cells,” *Journal of Clinical Medicine*, vol. 8, no. 1, p. 23, 2019.
  - [14] M. Farzaneh, A. Anbiyaiee, and S. E. Khoshnam, “Human pluripotent stem cells for spinal cord injury,” *Current Stem Cell Research & Therapy*, vol. 15, no. 2, pp. 135–143, 2020.
  - [15] M. Alishahi, A. Anbiyaiee, M. Farzaneh, and S. E. Khoshnam, “Human mesenchymal stem cells for spinal cord injury,” *Current Stem Cell Research & Therapy*, vol. 15, no. 4, pp. 340–348, 2020.
  - [16] X. Liu, W. Xu, Z. Zhang et al., “Vascular endothelial growth factor-transfected bone marrow mesenchymal stem cells improve the recovery of motor and sensory functions of rats with spinal cord injury,” *Spine*, vol. 45, no. 7, article E372, pp. E364–E372, 2020.
  - [17] Y. Yang, M. Pang, Y. Y. Chen et al., “Human umbilical cord mesenchymal stem cells to treat spinal cord injury in the early chronic phase: study protocol for a prospective, multicenter, randomized, placebo-controlled, single-blinded clinical trial,” *Neural Regeneration Research*, vol. 15, no. 8, pp. 1532–1538, 2020.
  - [18] R. Ma, X. Liu, J. Clark, G. M. Williams, and S. A. Doi, “The impact of acupuncture on neurological recovery in spinal cord injury: a systematic review and meta-analysis,” *Journal of Neurotrauma*, vol. 32, no. 24, pp. 1943–1957, 2015.
  - [19] A. M. K. Wong, C. P. Leong, T. Y. Su, S. W. Yu, W. C. Tsai, and C. P. C. Chen, “Clinical trial of acupuncture for patients with spinal cord injuries,” *American Journal of Physical Medicine & Rehabilitation*, vol. 82, no. 1, pp. 21–27, 2003.
  - [20] W. C. Wang, J. C. Lu, Q. Wang et al., “Effect on the activities of daily life of the patients with traumatic spinal cord injury treated by the paraplegia-triple-needling method,” *Zhongguo zhen jiu = Chinese Acupuncture & Moxibustion*, vol. 32, no. 10, pp. 877–881, 2012.
  - [21] Y. X. Chen, K. M. Kong, W. D. Wang, C. H. Xie, and R. H. Wu, “Functional MR imaging of the spinal cord in cervical spinal cord injury patients by acupuncture at LI 4 (Hegu) and LI 11(Quchi),” in *2007 29th Annual International Conference of the IEEE Engineering in Medicine and Biology Society*, pp. 3388–3391, Lyon, France, August 2007.
  - [22] Q. Fan, O. Cavus, L. Xiong, and Y. Xia, “Spinal cord injury: how could acupuncture help,” *Journal of Acupuncture and Meridian Studies*, vol. 11, no. 4, pp. 124–132, 2018.
  - [23] Q. H. Qi, “Study on acupuncture and moxibustion for treatment of spinal cord injury at the rehabilitation stage,” *Zhongguo zhen jiu = Chinese Acupuncture & Moxibustion*, vol. 27, no. 7, pp. 533–535, 2007.
  - [24] F. A. Paola and M. Arnold, “Acupuncture and spinal cord medicine,” *The Journal of Spinal Cord Medicine*, vol. 26, no. 1, pp. 12–20, 2016.
  - [25] P. G. Sullivan, S. Krishnamurthy, S. P. Patel, J. D. Pandya, and A. G. Rabchevsky, “Temporal characterization of mitochondrial bioenergetics after spinal cord injury,” *Journal of Neurotrauma*, vol. 24, no. 6, pp. 991–999, 2007.
  - [26] C. A. Oyinbo, “Secondary injury mechanisms in traumatic spinal cord injury: a nugget of this multiply cascade,” *Acta Neurobiologiae Experimentalis*, vol. 71, no. 2, pp. 281–299, 2011.
  - [27] Z. Liu, Y. Ding, and Y. S. Zeng, “A new combined therapeutic strategy of governor vessel electro-acupuncture and adult stem cell transplantation promotes the recovery of injured spinal cord,” *Current Medicinal Chemistry*, vol. 18, no. 33, pp. 5165–5171, 2011.
  - [28] L. L. Horvay, F. Galimi, F. H. Gage, and P. J. Horner, “Fate of endogenous stem/progenitor cells following spinal cord injury,” *The Journal of Comparative Neurology*, vol. 498, no. 4, pp. 525–538, 2006.
  - [29] O. Juarez Becerril, H. Salgado Ceballos, C. Anguiano Solis et al., “Electro-acupuncture at GV4 improves functional recovery in paralyzed rats after a traumatic spinal cord injury,” *Acupuncture & Electro-Therapeutics Research*, vol. 40, no. 4, pp. 355–369, 2015.
  - [30] S. H. Jiang, W. Z. Tu, E. M. Zou et al., “Neuroprotective effects of different modalities of acupuncture on traumatic spinal cord injury in rats,” *Evidence-Based Complementary and Alternative Medicine*, vol. 2014, Article ID 431580, 9 pages, 2014.
  - [31] J. Zhao, L. Wang, and Y. Li, “Electroacupuncture alleviates the inflammatory response via effects on M1 and M2 macrophages

- after spinal cord injury," *Acupuncture in Medicine*, vol. 35, no. 3, pp. 224–230, 2017.
- [32] D. C. Choi, J. Y. Lee, Y. J. Moon, S. W. Kim, T. H. Oh, and T. Y. Yune, "Acupuncture-mediated inhibition of inflammation facilitates significant functional recovery after spinal cord injury," *Neurobiology of disease*, vol. 39, no. 3, pp. 272–282, 2010.
- [33] R. L. Chen, R. F. Quan, S. C. Xu, Y. M. Ni, X. Zheng, and S. J. Xie, "Effect of elongated-needle penetration intervention on spinal apoptosis and cell signal transduction in acute spinal cord injury rabbits," *Zhen ci yan jiu = Acupuncture Research*, vol. 39, no. 4, pp. 259–66, 277, 2014.
- [34] S. Huang, C. Tang, S. Sun et al., "Protective effect of electroacupuncture on neural myelin sheaths is mediated via promotion of oligodendrocyte proliferation and inhibition of oligodendrocyte death after compressed spinal cord injury," *Molecular Neurobiology*, vol. 52, no. 3, pp. 1870–1881, 2015.
- [35] J. Liu and Y. Wu, "Electro-acupuncture-modulated miR-214 prevents neuronal apoptosis by targeting Bax and inhibits sodium channel Nav1.3 expression in rats after spinal cord injury," *Bio-medicine & Pharmacotherapy*, vol. 89, pp. 1125–1135, 2017.
- [36] M. du, R. Chen, R. Quan et al., "A brief analysis of traditional chinese medical elongated needle therapy on acute spinal cord injury and its mechanism," *Evidence-Based Complementary and Alternative Medicine*, vol. 2013, Article ID 828754, 7 pages, 2013.
- [37] Y. Shi, R. Quan, C. Li et al., "The study of traditional Chinese medical elongated-needle therapy promoting neurological recovery mechanism after spinal cord injury in rats," *Journal of Ethnopharmacology*, vol. 187, pp. 28–41, 2016.
- [38] Q. Renfu, C. Rongliang, D. Mengxuan et al., "Anti-apoptotic signal transduction mechanism of electroacupuncture in acute spinal cord injury," *Acupuncture in Medicine*, vol. 32, no. 6, pp. 463–471, 2014.
- [39] X. Wang, S. H. Shi, H. J. Yao et al., "Electroacupuncture at Dazhui (GV14) and Mingmen (GV4) protects against spinal cord injury: the role of the Wnt/ $\beta$ -catenin signaling pathway," *Neural Regeneration Research*, vol. 11, no. 12, pp. 2004–2011, 2016.
- [40] J. Xu, S. Cheng, Z. Jiao et al., "Fire needle acupuncture regulates Wnt/ERK multiple pathways to promote neural stem cells to differentiate into neurons in rats with spinal cord injury," *CNS & Neurological Disorders Drug Targets*, vol. 18, no. 3, pp. 245–255, 2019.
- [41] R. Schwanbeck, T. Schroeder, K. Henning et al., "Notch signaling in embryonic and adult myelopoiesis," *Cells, Tissues, Organs*, vol. 188, no. 1-2, pp. 91–102, 2008.
- [42] X. Geng, T. Sun, J. H. Li, N. Zhao, Y. Wang, and H. L. Yu, "Electroacupuncture in the repair of spinal cord injury: inhibiting the Notch signaling pathway and promoting neural stem cell proliferation," *Neural Regeneration Research*, vol. 10, no. 3, pp. 394–403, 2015.
- [43] H. Wu, M. Hu, D. Yuan et al., "Electroacupuncture promotes the proliferation of endogenous neural stem cells and oligodendrocytes in the injured spinal cord of adult rats," *Neural Regeneration Research*, vol. 7, no. 15, pp. 1138–1144, 2012.
- [44] J. Shi and L. Wei, "Rho kinases in cardiovascular physiology and pathophysiology: the effect of fasudil," *Journal of Cardiovascular Pharmacology*, vol. 62, no. 4, pp. 341–354, 2013.
- [45] Y. Fujita and T. Yamashita, "Axon growth inhibition by RhoA/ROCK in the central nervous system," *Frontiers in Neuroscience*, vol. 8, p. 338, 2014.
- [46] M. F. Wu, S. Q. Zhang, J. B. Liu, Y. Li, Q. S. Zhu, and R. Gu, "Neuroprotective effects of electroacupuncture on early- and late-stage spinal cord injury," *Neural Regeneration Research*, vol. 10, no. 10, pp. 1628–1634, 2015.
- [47] E. S. Hong, H. H. Yao, Y. J. Min et al., "The mechanism of electroacupuncture for treating spinal cord injury rats by mediating Rho/Rho-associated kinase signaling pathway," *The Journal of Spinal Cord Medicine*, vol. 2019, Article ID 31596180, pp. 1–11, 2019.
- [48] X. N. Li, X. S. Liang, L. Wu et al., "Electroacupuncture improves limb locomotor function possibly by suppressing Rho-ROCK II pathway related factors in anterior horns of spinal cord in rats with acute spinal cord injury," *Zhen ci yan jiu = Acupuncture Research*, vol. 43, no. 7, pp. 445–449, 2018.
- [49] W. P. Xiao, L. L. Q. Ding, Y. J. Min et al., "Electroacupuncture promoting axonal regeneration in spinal cord injury rats via suppression of Nogo/NgR and Rho/ROCK signaling Pathway," *Neuropsychiatric Disease and Treatment*, vol. 15, pp. 3429–3442, 2019.
- [50] Z. Huang, Y. Liu, Z. Su, J. Su, and Q. Wu, "Effects of electroacupuncture at "Changqiang" (GV 1) on expression of nerve growth factor and brain derived neurotrophic factor in rats after acute spinal cord injury," *Zhongguo zhen jiu = Chinese Acupuncture & Moxibustion*, vol. 38, no. 4, pp. 399–404, 2018.
- [51] Y. P. Mo, H. J. Yao, W. Lv et al., "Effects of electroacupuncture at governor vessel acupoints on neurotrophin-3 in rats with experimental spinal cord injury," *Neural Plasticity*, vol. 2016, Article ID 2371875, 9 pages, 2016.
- [52] W. Z. Tu, S. H. Jiang, L. Zhang et al., "Electro-acupuncture at governor vessel improves neurological function in rats with spinal cord injury," *Chinese Journal of Integrative Medicine*, vol. 2017, Article ID 28762132, 7 pages, 2017.
- [53] X. Wang, S. Ju, S. Chen et al., "Effect of electro-acupuncture on neuroplasticity of spinal cord-transected rats," *Medical Science Monitor*, vol. 23, pp. 4241–4251, 2017.
- [54] X. F. Zhang, Y. Zou, Y. Zhao, T. H. Wang, and W. Zhang, "Effects of electroacupuncture of "governor vessel" acupoints on changes of BDNF in the cortical motor area of mice with spinal cord transection," *Sichuan da xue xue bao. Yi xue ban = Journal of Sichuan University. Medical science edition*, vol. 43, no. 2, pp. 250–253, 2012.
- [55] B. Peng, X. F. Meng, M. Li et al., "Effects of electroacupuncture on the expression of epidermal growth factor receptor and glial fibrillary acidic protein after spinal cord injury in rats," *Zhen ci yan jiu = Acupuncture Research*, vol. 32, no. 4, pp. 219–223, 2007.
- [56] Z. Wei, Y. Wang, W. Zhao, and M. Schachner, "Electro-acupuncture modulates L1 adhesion molecule expression after mouse spinal cord injury," *The American Journal of Chinese Medicine*, vol. 45, no. 1, pp. 37–52, 2017.
- [57] Y. J. Min, L. L. Ding, L. H. Cheng et al., "Effect of electroacupuncture on the mRNA and protein expression of Rho-A and Rho-associated kinase II in spinal cord injury rats," *Neural Regeneration Research*, vol. 12, no. 2, pp. 276–282, 2017.
- [58] X. Y. Wang, X. L. Li, S. Q. Hong, Y. B. Xi-Yang, and T. H. Wang, "Electroacupuncture induced spinal plasticity is linked to multiple gene expressions in dorsal root deafferented rats," *Journal of Molecular Neuroscience*, vol. 37, no. 2, pp. 97–110, 2009.
- [59] J. H. Yang, J. G. Lv, H. Wang, and H. Y. Nie, "Electroacupuncture promotes the recovery of motor neuron function in the anterior horn of the injured spinal cord," *Neural Regeneration Research*, vol. 10, no. 12, pp. 2033–2039, 2015.



- [60] S. J. Liu, S. S. Zheng, Q. Q. Dan, J. Liu, and T. H. Wang, "Effects of governor vessel electroacupuncture on the systematic expressions of NTFs in spinal cord transected rats," *Neuropeptides*, vol. 48, no. 4, pp. 239–247, 2014.
- [61] D. van der Kooy and S. Weiss, "Why stem cells," *Science*, vol. 287, no. 5457, pp. 1439–1441, 2000.
- [62] Z. Gong, K. Xia, A. Xu et al., "Stem cell transplantation: a promising therapy for spinal cord injury," *Current Stem Cell Research & Therapy*, vol. 15, no. 4, pp. 321–331, 2020.
- [63] S. K. Oh, K. H. Choi, J. Y. Yoo, D. Y. Kim, S. J. Kim, and S. R. Jeon, "A phase III clinical trial showing limited efficacy of autologous mesenchymal stem cell therapy for spinal cord injury," *Neurosurgery*, vol. 78, no. 3, pp. 436–447, 2016.
- [64] J. H. Park, D. Y. Kim, I. Y. Sung et al., "Long-term results of spinal cord injury therapy using mesenchymal stem cells derived from bone marrow in humans," *Neurosurgery*, vol. 70, no. 5, pp. 1238–1247, 2012.
- [65] P. Phedy, Y. P. Djaja, L. Gatam et al., "Motoric recovery after transplantation of bone marrow derived mesenchymal stem cells in chronic spinal cord injury: a case report," *The American Journal of Case Reports*, vol. 20, pp. 1299–1304, 2019.
- [66] M. C. Jin, Z. A. Medress, T. D. Azad, V. M. Doulames, and A. Veeravagu, "Stem cell therapies for acute spinal cord injury in humans: a review," *Neurosurgical Focus*, vol. 46, no. 3, article E10, 2019.
- [67] P. Xu and X. Yang, "The efficacy and safety of mesenchymal stem cell transplantation for spinal cord injury patients: a meta-analysis and systematic review," *Cell Transplantation*, vol. 28, no. 1, pp. 36–46, 2018.
- [68] J. P. Li, D. W. Wang, and Q. H. Song, "Transplantation of erythropoietin gene-transfected umbilical cord mesenchymal stem cells as a treatment for limb ischemia in rats," *Genetics and Molecular Research*, vol. 14, no. 4, pp. 19005–19015, 2015.
- [69] Y. T. Chen, M. J. Tsai, N. Hsieh et al., "The superiority of conditioned medium derived from rapidly expanded mesenchymal stem cells for neural repair," *Stem Cell Research & Therapy*, vol. 10, no. 1, p. 390, 2019.
- [70] R. Hakim, R. Covacu, V. Zachariadis et al., "Mesenchymal stem cells transplanted into spinal cord injury adopt immune cell-like characteristics," *Stem Cell Research & Therapy*, vol. 10, no. 1, p. 115, 2019.
- [71] Y. O. Mukhamedshina, O. A. Gracheva, D. M. Mukhutdinova, Y. A. Chelyshev, and A. A. Rizvanov, "Mesenchymal stem cells and the neuronal microenvironment in the area of spinal cord injury," *Neural Regeneration Research*, vol. 14, no. 2, pp. 227–237, 2019.
- [72] X. Wang, L. Ye, K. Zhang, L. Gao, J. Xiao, and Y. Zhang, "Upregulation of microRNA-200a in bone marrow mesenchymal stem cells enhances the repair of spinal cord injury in rats by reducing oxidative stress and regulating Keap1/Nrf2 pathway," *Artificial Organs*, vol. 44, no. 7, pp. 744–752, 2020.
- [73] H. J. Chung, W. H. Chung, J. H. Lee et al., "Expression of neurotrophic factors in injured spinal cord after transplantation of human-umbilical cord blood stem cells in rats," *Journal of Veterinary Science*, vol. 17, no. 1, pp. 97–102, 2016.
- [74] A. B. Spejo, G. B. Chiarotto, A. D. F. Ferreira et al., "Neuroprotection and immunomodulation following intraspinal axotomy of motoneurons by treatment with adult mesenchymal stem cells," *Journal of Neuroinflammation*, vol. 15, no. 1, p. 230, 2018.
- [75] C. Mo, L. Ren, Z. Zhenfu et al., "Effects of bone marrow mesenchymal stem cells transplantation for treating rat spinal cord injury and cytokine expression at injury sites," *Zhongguo xiufu chongjian waike zazhi = Chinese Journal of Reparative and Reconstructive Surgery*, vol. 30, no. 3, pp. 265–271, 2016.
- [76] A. M. Martinez, C. O. Goulart, S. Ramalho Bdos, J. T. Oliveira, and F. M. Almeida, "Neurotrauma and mesenchymal stem cells treatment: from experimental studies to clinical trials," *World Journal of Stem Cells*, vol. 6, no. 2, pp. 179–194, 2014.
- [77] Y. Ding, Q. Yan, J. W. Ruan et al., "Bone marrow mesenchymal stem cells and electroacupuncture downregulate the inhibitor molecules and promote the axonal regeneration in the transected spinal cord of rats," *Cell Transplantation*, vol. 20, no. 4, pp. 475–491, 2011.
- [78] Z. Sun, X. Li, Z. Su, Y. Zhao, L. Zhang, and M. Wu, "Electroacupuncture-enhanced differentiation of bone marrow stromal cells into neuronal cells," *Journal of Sport Rehabilitation*, vol. 18, no. 3, pp. 398–406, 2009.
- [79] I. Jean, C. Lavialle, A. Barthelaix-Pouplard, and C. Fressinaud, "Neurotrophin-3 specifically increases mature oligodendrocyte population and enhances remyelination after chemical demyelination of adult rat CNS," *Brain Research*, vol. 972, no. 1–2, pp. 110–118, 2003.
- [80] C. Leite, N. T. Silva, S. Mendes et al., "Differentiation of human umbilical cord matrix mesenchymal stem cells into neural-like progenitor cells and maturation into an oligodendroglial-like lineage," *PLoS One*, vol. 9, no. 10, article e111059, 2014.
- [81] H. Liu, K. Yang, T. Xin, W. Wu, and Y. Chen, "Implanted electro-acupuncture electric stimulation improves outcome of stem cells' transplantation in spinal cord injury," *Artificial Cells, Blood Substitutes, and Immobilization Biotechnology*, vol. 40, no. 5, pp. 331–337, 2012.
- [82] Y. Ding, Q. Yan, J. W. Ruan et al., "Electroacupuncture promotes the differentiation of transplanted bone marrow mesenchymal stem cells overexpressing TrkC into neuron-like cells in transected spinal cord of rats," *Cell Transplantation*, vol. 22, no. 1, pp. 65–86, 2013.
- [83] Y. Ding, Q. Yan, J. W. Ruan et al., "Electro-acupuncture promotes survival, differentiation of the bone marrow mesenchymal stem cells as well as functional recovery in the spinal cord-transected rats," *BMC Neuroscience*, vol. 10, no. 1, p. 35, 2009.
- [84] Q. Yan, J. W. Ruan, Y. Ding, W. J. Li, Y. Li, and Y. S. Zeng, "Electro-acupuncture promotes differentiation of mesenchymal stem cells, regeneration of nerve fibers and partial functional recovery after spinal cord injury," *Experimental and Toxicologic Pathology*, vol. 63, no. 1–2, pp. 151–156, 2011.
- [85] Y. Ding, R. Y. Zhang, B. He et al., "Combination of electroacupuncture and grafted mesenchymal stem cells overexpressing TrkC improves remyelination and function in demyelinated spinal cord of rats," *Scientific Reports*, vol. 5, no. 1, article 9133, 2015.

## Review Article

# Applications of Acupuncture Therapy in Modulating the Plasticity of Neurodegenerative Disease and Depression: Do MicroRNA and Neurotrophin BDNF Shed Light on the Underlying Mechanism?

Xia Li,<sup>1</sup> Jun Zhao,<sup>1</sup> Zhigang Li <sup>1</sup>, Li Zhang <sup>1</sup>, and Zejun Huo <sup>2</sup>

<sup>1</sup>*School of Acupuncture-Moxibustion and Tuina, Beijing University of Chinese Medicine, Beijing 100029, China*

<sup>2</sup>*Department of Chinese Medicine, Peking University 3rd Hospital, Beijing 100191, China*

Correspondence should be addressed to Li Zhang; zhangli1572@sina.com and Zejun Huo; huozejun@163.com

Received 9 June 2020; Revised 12 August 2020; Accepted 5 September 2020; Published 22 September 2020

Academic Editor: Yongjun Chen

Copyright © 2020 Xia Li et al. This is an open access article distributed under the Creative Commons Attribution License, which permits unrestricted use, distribution, and reproduction in any medium, provided the original work is properly cited.

As the global population ages, the incidence of neurodegenerative diseases has risen. Furthermore, it has been suggested that depression, especially in elderly people, may also be an indication of latent neurodegeneration. Stroke, Alzheimer's disease (AD), and Parkinson's disease (PD) are usually accompanied by depression. The urgent challenge is further enforced by psychiatric comorbid conditions, particularly the feeling of despair in these patients. Fortunately, as our understanding of the neurobiological substrates of maladies affecting the central nervous system (CNS) has increased, more therapeutic options and novel potential biological mechanisms have been presented: (1) Neurodegenerative diseases share some similarities in their pathological characteristics, including changes in neuron structure or function and neuronal plasticity. (2) MicroRNAs (miRNAs) are small noncoding RNAs that contribute to the pathogenesis of diverse neurological disease. (3) One ubiquitous neurotrophin, brain-derived neurotrophic factor (BDNF), is crucial for the development of the nervous system. Accumulating data have indicated that miRNAs not only are related to BDNF regulation but also can directly bind with the 3'-UTR of BDNF to regulate BDNF and participate in neuroplasticity. In this short review, we present evidence of shared biological substrates among stroke, AD, PD, and depression and summarize the possible influencing mechanisms of acupuncture on the neuroplasticity of these diseases. We discuss neuroplasticity underscored by the roles of miRNAs and BDNF, which might further reveal the potential biological mechanism of neurodegenerative diseases and depression by acupuncture.

## 1. Introduction

Neurodegenerative diseases, including stroke, Alzheimer's disease (AD), and Parkinson's disease (PD), are chronic progressive diseases caused by the apoptosis, loss, and degeneration of neurons in the central nervous system (CNS) and alter neuroplasticity [1]. Moreover, major depressive disorder has strong relationships with neurodegenerative diseases and the natural processes of ageing: they have not only overlapping clinical features, such as mood disorder [2], but also neuroplasticity mediated by neurotrophic factors that also orchestrate adaptive defensive behaviours [3]. Hence, the links

among brain plasticity, neurodegenerative diseases, and depression are of interest to researchers [4].

Neuroplasticity is the ability of the brain's neural network system to adapt to changes in internal and external environments and to alter the structure and function of neurons accordingly. In other words, neuroplasticity can be defined as "the ability of the nervous system to respond to intrinsic or extrinsic stimuli by reorganizing its structure, connections, and function" [5]. Neuroplasticity includes structural plasticity and functional plasticity of the nervous system, which makes up the physiological basis for repair when the nervous system is damaged [6]. Brain structural plasticity is



an extraordinary tool that allows the mature brain to adapt to environmental changes and repair itself after lesions or disease and slow ageing. Its function involves behavioural performance, learning and memory, mental activity, and other neurobiological processes.

Brain-derived neurotrophic factor (BDNF) stands out due to its high level of expression in the brain and its potent effects on synapses [7]. BDNF regulates the structural plasticity of nerves not only by promoting the growth, reconstruction, and synaptic formation of axons and dendrites but also by changing synaptic transmission and affecting the functional plasticity of nerves through presynaptic and postsynaptic mechanisms. BDNF also regulates activity-dependent forms of synaptic plasticity, such as long-term potentiation (LTP), which is thought to underlie learning and memory [8]. Simultaneously, converging evidence strongly suggests that deficits in BDNF signalling or decreased BDNF leads to the pathogenesis of several major diseases and disorders, such as AD and PD [7, 9]. BDNF has emerged as a key facilitator of neuroplasticity involved in motor learning and rehabilitation after stroke [10]. In addition, BDNF has been shown to be critically involved in the regulation of synaptic plasticity and the pathophysiology of mood disorders [11, 12]. Remarkably, according to the published literature, AD, stroke, and PD are usually accompanied by depression, and these neurodegenerative diseases and depression are related to BDNF. If a common way to regulate BDNF was determined, it could be used to regulate neuroplasticity to delay the progression of diseases.

Fortunately, emerging studies have shown that microRNAs (miRNAs) not only contribute to the pathogenesis of neurological disease but also play important roles in neurogenesis, neurodevelopment, and neural plasticity [13, 14]. miRNAs can posttranscriptionally degrade mRNA or inhibit the translation of mRNA by binding the 3'-UTR section of mRNAs, further influencing the expression of target genes [15]. In a limited number of studies published thus far, we searched electronic bibliographic databases and found that some miRNAs not only are related to BDNF regulation but also can directly bind with the 3'-UTR of BDNF to regulate BDNF and participate in neuroplasticity [16]. Hence, miRNA/BDNF regulatory networks may be closely related to neural plasticity. Numerous previous studies have shown that acupuncture has positive clinical effects on stroke, AD, PD, and depression. We reviewed recent publications related to acupuncture on related miRNAs and BDNF in neurodegenerative diseases and depression. The aim of this study was to explore the biological mechanisms underlying the comorbidity of these diseases and the effect of acupuncture on regulating neural plasticity.

## 2. Main Text

### 2.1. Stroke

**2.1.1. BDNF Plays Important Roles in Stroke.** A previous study identified that several therapeutic interventions, such as exercise and rehabilitation, enhance functional recovery after stroke. The beneficial effects of these therapies include

improved learning and memory, improved motor function, and increased expression of proteins involved in brain plasticity, such as BDNF [17]. A clinical study showed an increased number of BDNF-producing Treg cells after stroke, suggesting the possibility that Treg cells may be able to supply BDNF to the site of injury to confer neuroprotection after stroke [18]. Similarly, in middle cerebral artery occlusion (MCAO) model rats, strategies that widely increase BDNF within the nervous system were found to enhance neuroplasticity processes involved in motor relearning during stroke rehabilitation, whereas attenuating BDNF levels in the brain completely negated the recovery of skilled motor movements [19]. Hence, capitalizing on the beneficial effects of BDNF in the CNS may be effective for facilitating recovery after stroke.

**2.1.2. miRNAs Play Important Roles in Stroke.** miRNAs are increasingly believed to play important roles in neuroprotection and synaptic plasticity during and after ischaemia. For instance, miR-124 is highly specific to neurons in cerebral ischaemic injury and may play a dual role in regulating apoptosis and exerting detrimental effects on synaptic plasticity and axonal growth [20]. Upregulation of miR-191a-5p exacerbated neuronal injury in ischaemic stroke. Conversely, downregulation of miR-191a-5p expression in the cortex partly reversed this injury [21]. Similarly, miR-195 downregulated Kruppel-like factor 5 (KLF5) and blocked the JNK signalling pathway, ultimately inhibiting neuronal apoptosis in rats with ischaemic stroke [22]. Additionally, miR-133b can regulate gene expression, promote neurite remodelling, and improve functional recovery in rats subjected to MCAO [23]. Intracerebroventricular injection of miR-494 agomir reduced neuronal apoptosis and infarct volume during the acute stage of MCAO and promoted axonal plasticity and long-term outcomes during the recovery stage [24]. Similarly, miR-181a can regulate synaptic function in stroke recovery, and the dendrites of miR-181a-overexpressing neurons have fewer and smaller spines [25]. Consistent with these general observations, miR-134 was enriched in the neuronal dendrites of a rat model of stroke hippocampal CA1 and negatively controlled the size of dendritic spines; thus, regulating synaptic-dendritic plasticity may ameliorate cognitive impairment in rats with MCAO-induced cognitive deficits [26]. According to the above results, miRNAs could potentially predict stroke outcomes as novel biomarkers.

**2.1.3. miRNAs May Regulate Stroke via Influencing BDNF.** The miRNA-related BDNF signalling pathway plays a significant role in the pathogenesis of stroke and seems to be a promising therapeutic target, as summarized in Table 1. In acute ischaemic stroke patients, miR-124 was targeted by the 3'-UTR of BDNF mRNA [27]. Additionally, a dual-luciferase reporter assay identified BDNF as the direct target of miR-210, which is a crucial ischaemic stroke-associated miRNA and a potential target for stroke therapy [28]. Interestingly, the SNP rs7124442 in the 3'-UTR of BDNF might also act as a protective factor in patients with ischaemic stroke by affecting the regulatory role of miR-922 in BDNF expression [29]. Similarly, in MCAO brain tissues, bioinformatic analysis showed that miR-10b-5p could bind directly

TABLE 1: Deregulated miRNAs and target genes of stroke and summary of related acupuncture literatures.

Study	Species/tissue	miRNA	Result/target genes	
Wang et al. [27]	Stroke patient	miR-124	BDNF	
Zeng et al. [28]	Striatum	miR-210	BDNF	
Liu et al. [29]	Stroke patient	miR-922	The SNP rs7124442 in BDNF 3'-UTR, through affecting the regulatory role of miR-922 in BDNF expression	
Lu et al. [31]	Hippocampus	miR-10b-5p	BDNF	
Varendi et al. [32]	Cellular model	miR-155	BDNF	
Summary of related acupuncture literatures				
Study	Species/tissue	Method/acupoint	Stimulation parameter	Result
Tao et al. [34]	Cortex and striatum	EA at LI11, ST36	1 Hz/20 Hz, 30 min	BDNF ↑
Kim et al. [35]	Striatum and hippocampus	EA at GV20, GV14	2 Hz, 1 mA, 20 min	BDNF ↑
Jiang [36]	Whole brain	EA at GV20, GV16	2 Hz/30 Hz, 30 min, 2 V	BDNF ↑
Kim et al. [37]	Whole brain	EA at GV20, GB7	3 Hz, 5 min	BDNF ↑
Zhou [38]	Cortex	EA at PC6, ST36	2 Hz/30 Hz, 30 min, 5 mA	BDNF ↑
Teng. [39]	Whole brain	MA at GV20-GB7 scalp cave	Needles were turned at a rate of three revolutions per second, twirled 3 times for 5 min, and retained for 30 min	BDNF ↑
Zhang et al. [40]	Hippocampus	MA at nape cluster acupoints	15 min/day	BDNF ↑
Ye et al. [41]	Cortex	EA at LI11, ST36	1 Hz/20 Hz, 30 min, 6 V	BDNF ↑
Liu [42]	Hippocampus	EA at GV20, GV24	2 Hz/20 Hz, 30 min, 6 V	miR-219a ↓
Zhou et al. [21]	Neurons and cortexes	EA at GV20	1 mA, 30 min	miR-191a-5p ↓
Zhao et al. [43]	Ischaemic penumbra	EA at GV20	2 Hz/10 Hz, 1-2 mA, 30 min	miR-132 ↑
Liu et al. [26]	Peri-infarct cortex	EA at GV20, GV24	1 Hz/20 Hz, 0.2 mA, 6 V, 30 min	miR-134 ↓
Liu et al. [44]	Peri-infarct cortex	EA at LI11, ST36	1 Hz/20 Hz, 4 V, 30 min	miR-9 ↑
Zheng et al. [45]	Cortex	EA at GV26, PC6	2 Hz, 3 mA, 1 min	miR-494 ↓, miR-206 ↑
Deng et al. [46]	Ischaemic penumbra	EA at GV20	2 Hz/10 Hz, 1-2 mA, 30 min	miR-181b ↑

MA: manual acupuncture; EA: electroacupuncture.

to the 3'-UTR sites of BDNF and negatively regulate its expression [30]. In a recent study, miR-155 targeted BDNF, and downregulation of miR-155-targeted BDNF transcripts protected against ischaemic brain injury [31]. Another study reported a similar conclusion: miR-155, miR-1, miR-10b, and miR-191 directly repressed BDNF by binding to their predicted sites in the 3'-UTR of BDNF [32]. Although we found that miR-9 regulates axon extension and branching by targeting Map 1b (not BDNF) in mouse cortical neurons, the associations are intriguing (short stimulation with BDNF decreases miR-9 expression, whereas prolonged stimulation with a high concentration of BDNF increases miR-9 expression in the axon) [33]. The potential regulatory signalling pathway between miRNA and BDNF acts in a biphasic manner and is worthy of being analysed and studied further.

*2.1.4. Acupuncture Plays a Therapeutic Role in Stroke by Regulating the Expression of BDNF and miRNAs.* Previous studies have shown that the number of BDNF-positive neurons or neurons with localized BDNF expression was

downregulated in the peri-infarct cortex, the striatum, the subventricular zone, and the hippocampus of ischaemia and reperfusion- (I/R-) injured rats [34, 35]. However, Jiang reported that electroacupuncture (EA) can increase the synthesis and release of BDNF after ischaemia [36]. As summarized in Table 1, Min et al. reported that EA at GV20 increased the expression of BDNF associated with motor recovery [37]. Zhou further explored a possible compensatory part of the functional mechanism of EA that involves regulation of the contralateral cerebral cortex. It was revealed that EA can improve the symptoms of neurological deficits and motor function recovery in rats [38]. In addition, Teng showed the mechanism of acupuncture at the GV20-GB7 scalp cave on intracerebral haemorrhage. According to their results, acupuncture can play a role in protecting the brain [39]. Similarly, nape cluster acupuncture exerts protective and reparative effects on the brain tissue in rats with post-ischaemic stroke sequelae [40]. EA was administered at acupoints LI11 and ST36 to promote the repair of ischaemic injured neurons and reduce their apoptosis [41]. The above

studies all showed that after administration of acupuncture, neurological deficits and cerebral infarcts were also improved, and the mechanism of action of EA may involve effective upregulation of rat brain tissue BDNF protein expression.

Many studies have reported how acupuncture can regulate the expression of miRNAs in stroke. Liu published a study in which a bioinformatic analysis of 48 miRNAs in the ischaemic hippocampus CA1 was used to test the underlying mechanism of EA in ischaemic stroke. According to the results, miR-132, miR-134, miR-125b, miR-181a, etc. were downregulated, which was related to learning memory. In addition, miR-219a, which is closely related to synaptic plasticity, was also downregulated by EA treatment at the GV20 and GV24 acupoints [42]. However, upregulation of miR-191a-5p exacerbated neuronal injury and partly reversed the neuroprotective effect of EA treatment after I/R injury [21]. Zhao et al. aimed to identify whether upregulation of miR-132 by EA improved the damaged nerves after stroke. After administration of EA, upregulated miR-132 suppressed SOX2 in primary neurons after oxygen-glucose deprivation, which promoted neurite outgrowth [43]. Liu et al. found that the density of dendritic spines and the number of synapses in hippocampal CA1 pyramidal cells were obviously reduced in stroke model rats. In this study, EA decreased the expression of miR-134, thereby negatively regulating LIMK1 to enhance synaptic-dendritic plasticity [26]. Intriguingly, Liu et al. also investigated the neuroprotective mechanism of miR-9-mediated activation of the nuclear factor- $\kappa$ B signalling pathway by EA at acupoints LI11 and ST36. Compared with pre-EA treatment conditions, the expression of miR-9 in the peri-infarct cortex was increased; conversely, miR-9 inhibitors suppressed the cerebral protective efficacy of EA treatment [44]. Zheng et al. evaluated changes in the cerebral cortical miRNA profile, cerebral blood flow, and neurological function induced by EA in a rat model of stroke. In that study, miR-494 was downregulated, and miR-206 was upregulated in the penumbra. Simultaneously, EA increased cerebral blood flow and alleviated neurological impairment in rats [45]. Similarly, Deng et al. treated acupoint GV20 after ischaemic stroke. EA increased miR-181b levels in the penumbras and improved neurobehavioural function [46].

In summary, the above studies indicated that acupuncture may play an important role in the neural plasticity of stroke by regulating the expression levels of miRNAs and BDNF. These studies also suggest that epigenetic regulation is critical for synaptic plasticity and warrants specific investigations in the setting of stroke recovery.

## 2.2. PD

**2.2.1. BDNF Plays Important Roles in PD.** PD is a disabling neurodegenerative disease that may be associated with non-motor symptoms, such as cognitive deficits, and is often accompanied by altered BDNF production [47]. Neurons expressing particularly low levels of BDNF may be at greatest risk of injury in PD and possibly a trigger for degeneration itself [48]. BDNF was positively correlated with a longer time

span of disease, the severity of PD symptoms, and more advanced stages of disease [49]. These findings suggest that BDNF may be implicated in the pathogenic mechanisms of PD. Excitingly, in recent years, clinical studies have demonstrated that treatment with antiparkinsonian drugs may increase BDNF levels [50]. Similarly, exercise therapy can trigger several plasticity-related events in the human PD brain, including corticomotor excitation and changes in BDNF levels [51]. In general, BDNF may be a potential biomarker for evaluating cognitive changes in PD and other neurological syndromes associated with cognitive decline [47].

**2.2.2. miRNAs Play Important Roles in PD.** Over the past decade, many studies have reported dysregulation of miRNA expression in PD [52]. Specific miRNAs of interest that have been implicated in PD pathogenesis include miR-29, miR-26, miR-485, miR-30, and let-7 [53]. For instance, miR-29 has been shown to regulate various processes that are important in PD development, such as apoptosis, neuronal survival, and epigenetic modulation [54]. Similarly, miR-26 can modulate processes such as DNA repair and LTP maintenance [55]. One study further identified a developmentally and activity-regulated miR-485 that controls dendritic spine number and synapse formation in an activity-dependent homeostatic manner [56]. Furthermore, miR-132 widely participates in axon growth, neural migration, and plasticity. However, dysregulation of miR-132 results in the occurrence and exacerbation of neural developmental degenerative diseases, such as AD and PD. Regulating miR-132 expression relieves symptoms, alleviates severity, and finally affects a cure [57]. Hence, it is important to identify and validate these miRNAs in the ageing PD brain.

**2.2.3. miRNAs May Regulate PD via Influencing BDNF.** The analysis of miRNA expression in biopsy specimens from the PD brains combined with target mRNA identification might provide new therapeutic options. As summarized in Table 2, previous studies have shown that miR-494-3p plays a role in promoting the development of PD [58], and the online starBase database predicted the existence of complementary sequences between miR-494-3p and BDNF, indicating that BDNF might be a target of miR-494-3p. According to their results, abnormally expressed miR-494-3p and BDNF might be associated with the development of PD [59]. On the other hand, it has been reported that miR-30a-5p is a potential biomarker for PD [60], targeting and suppressing BDNF expression in the prefrontal cortex [61], and a lower BDNF level is associated with greater cognitive impairments in PD patients [9]. In addition, a recent study reported that miR-7 was upregulated in the brain tissue of rats with atrazine-induced PD. The study also identified that miR-7 regulated the expression of BDNF through an autoregulatory mechanism [62]. Similarly, it has been reported that miR-210-3p targets BDNF mRNA. Therefore, according to the study conclusion, interfering with miRNA expression could be a strategy for BDNF regulation in PD pathogenesis [63].

TABLE 2: Deregulated miRNAs and target genes of Parkinson and summary of related acupuncture literatures.

Study	Species/tissue	miRNA	Result/target genes	
Deng et al. [59]	Cellular model	miR-494-3p	BDNF	
Mellios et al. [61]	Prefrontal cortex	miR-30a-5p	BDNF	
Li et al. [62]	Whole brain	miR-7	BDNF	
Zhang et al. [63]	Cellular model	miR-210-3p	BDNF	
Summary of related acupuncture literatures				
Study	Species/tissue	Method/acupoint	Stimulation parameter	Result
Huang et al. [66]	Nigra	EA at LR3, GV16	100 Hz, 0.5 mA, 30 min	BDNF ↑
Yang et al. [67]	Nigra	EA at GV20, GV16	100 Hz, 1 mA, 30 min	BDNF ↑
Pak et al. [68]	Nigra and striatum	EA at GV20, GV14	2 Hz, 1 mA, 20 min	BDNF ↑
Feng et al. [69]	Whole brain	MA at chorea-tremble controlled zone	20 min/day	BDNF ↑
Zhang [70]	Nigra	EA at GV20, GV21	2 Hz/100 Hz, 1 V, 20 min	BDNF mRNA ↑
Wang [71]	Nigra and striatum	EA at EX-HN1, EX-HN5, CV12, ST25, LR3, HT7, SP6	20 Hz, 1 mA, 20 min	BDNF ↑
Sun et al. [72]	Midbrain and hippocampus	EA at GV20, GV14	0 Hz/100 Hz, 1 mA, 10 min→2 mA, 10 min→3 mA, 10 min	BDNF ↑
Liang et al. [73]	Nigra and ventral tegmental area	EA at GV20, GV14	2 Hz/100 Hz, 30 min 1 mA, 10 min→2 mA, 10 min→3 mA, 10 min	BDNF mRNA ↑, BDNF ↑
Liu [75]	Striatum	MA at GB34, LR3	2 Hz, 1 mA, 20 min	miR-124 ↑

MA: manual acupuncture; EA: electroacupuncture.

**2.2.4. Acupuncture Plays a Therapeutic Role in PD by Regulating the Expression of BDNF and miRNAs.** Accumulating clinical evidence has shown that using EA as a complementary therapy ameliorates motor and nonmotor symptoms of PD and improves the plasticity of synaptic activity [64]. Acupuncture can cause changes in the neuroplasticity of PD, manifested by increasing BDNF expression levels and promoting nerve regeneration [65], as summarized in Table 2. On the one hand, BDNF may change the mechanism of synaptic plasticity, which is critical for cognition and memory. EA responsiveness to PD was studied by Huang et al., whereby EA was administered to acupoints LR3 and GV16 in a PD rat model. After EA treatment, learning and memory abilities were significantly improved, and BDNF was increased compared with the model group [66]. On the other hand, PD is characterized by dopaminergic neuron loss in the substantia nigra. EA therapy may attenuate this loss by promoting the expression of endogenous BDNF [67]. For instance, in a rat model of PD, EA treatment ameliorated motor impairments and dopaminergic neuron loss, and these changes were accompanied by significantly upregulated BDNF expression in both the substantia nigra and the striatum [68]. Furthermore, acupuncture, especially combined therapy with medoba, at the control area of dancing tremors in PD mice improved the absence of dopaminergic neurons in the substantia nigra by enhancing the expression of BDNF in the brain [69]. In addition, 6-hydroxydopamine (6-OHDA) lesion rat models of PD were used by Zhang, who reported that EA induced an increase in BDNF mRNA expression in PD model rats [70]. Moreover, Wang tested the effects of different amounts of electricity on the positive cell count of black striatum BDNF in PD model

rats which were compared, and the related mechanism was discussed. According to their results, one of the therapeutic mechanisms of music and pulse EA in PD model rats was achieved by regulating the number of black striatum BDNF-positive cells [71]. Interestingly, Sun et al. and Liang et al. compared the effects of different frequencies of chronic EA stimulation in a rat model of PD. The results indicated that 4 weeks of EA treatment at 100 Hz reversed the 6-OHDA-induced abnormal expression of BDNF on the lesioned side in the ventral midbrain and the hippocampus [72]. Similarly, compared with pre-EA treatment conditions, the levels of BDNF mRNA in the SN and the ventral tegmental area of the lesioned side were significantly increased in the 100 Hz EA group but unchanged in the 0 and 2 Hz groups. The authors also suggested that activation of endogenous BDNF by long-term high-frequency EA may be involved in the regeneration of injured dopaminergic neurons, which may underlie the effectiveness of EA in the treatment of PD [73].

Previous studies have shown that miR-124 is closely related to PD [74], and the overexpression of miR-124 diminished the production of CDK5 by inhibiting the calpain1/p25/CDK5 pathway. Furthermore, CDK5 silencing could give rise to upregulated BDNF and relieve synaptic failure in PD [20]. Liu further studied whether acupuncture could regulate the expression of miR-124 in the striatum of transgenic mice with PD. Acupuncture was performed on acupoints GB34 and LR3. Compared with preacupuncture treatment conditions, the expression of miR-124 and BDNF protein was upregulated. The author also suggested that the miR-124/BDNF signalling pathway may be involved in the pathogenesis of PD [75].



To summarize, acupuncture treatment appears to be a promising approach for the management of PD. Acupuncture regulated miRNA levels and promoted BDNF expression, which seem to play important roles in the development of PD.

### 2.3. AD

**2.3.1. BDNF Plays Important Roles in AD.** AD is a progressive neurodegenerative disorder resulting in memory loss and eventually dementia [76]. BDNF is required for learning and memory, and this crucial protein is significantly reduced in the brains of AD patients, leading to reduced plasticity and neuronal death [77]. Accumulating data have also indicated that there is a general reduction in BDNF mRNA and protein in AD animal models [76]. These findings have contributed to the development of BDNF treatment regimens for AD.

**2.3.2. miRNAs Play Important Roles in AD.** There is now considerable evidence that the dysregulation of miRNAs correlates with the progression and severity of AD [78]. The differential expression of miRNAs has been reported in many brain regions [79]. miRNAs can also regulate synaptic transmission and plasticity in the hippocampus and neocortex and regulate memory formation [80]. It has been reported that miR-132 exerts neuroprotective function as it has been shown to regulate both neuron morphogenesis and plasticity, and it is the most significantly reduced miRNA in the brains of AD patients. Research has further confirmed that genetic deletion of miR-132 in mice promotes A $\beta$  deposition, leading to impaired memory and enhanced Tau pathology [81]. However, the upregulation of miR-142-5p and miR-134-5p expression contributes to the pathogenesis of AD by triggering synaptic dysfunction associated with A $\beta$ -mediated pathophysiology [79, 82]. In learning memory aspects, miR-124 and miR-181a, which are two miRNAs that are upregulated in the hippocampus, are directly associated with deficits in synaptic plasticity [83, 84]. Similarly, overexpression of miR-338-5p and miR-181 functionally prevented impairments in synaptic plasticity, learning ability, and memory retention in an animal model of AD [85, 86]. Furthermore, overexpression of miR-153 has provided new insight into the molecular mechanism of presynaptic plasticity impairment at the miRNA level and suggests that chronic brain hypoperfusion obstructs presynaptic vesicle fusion with the presynaptic membrane via miR-153-mediated downregulation of multiple synaptic vesicle-related proteins [87]. Previously, miR-34a and miR-34c were confirmed to be involved in synaptic deficits in AD pathological development, to influence synaptic plasticity and to play key roles in AD pathogenesis [88, 89]. Evidence from a recent study indicated that the miR-34a gene and miR-34a-mediated concurrent repression of its target genes in neural networks may result in dysfunction of synaptic plasticity, energy metabolism, and resting state network activity [90]. In addition, the dysregulation of certain miRNAs is also strongly correlated with the presence of AD-type neuropathological changes. There are notable miRNAs that are regulated in AD. For example, in postmortem AD brains, three miRNAs were upregulated—miR-30a-

5p, miR-206, and miR-92b-3p [61, 91]—and four miRNAs were downregulated—miR-132/212 cluster, miR-9, miR-129, and miR-136 [78, 92]. In summary, our results provide insights into polygenetic AD mechanisms and reveal that miRNAs may be involved in neural plasticity as potential therapeutic targets for AD.

**2.3.3. miRNAs May Regulate AD via Influencing BDNF.** The miRNA-related BDNF signalling pathway seems to be both profitable and promising for AD treatment, as summarized in Table 3. Two previous studies confirmed that BDNF exerts its beneficial effects on CNS neurons via upregulation of miR-132 [93, 94]. A later study pointed out that both AD patients and AD models have high levels of miR-206 in the brain, which contributes to memory impairments by suppressing the expression of BDNF [95, 96]. Similarly, recent evidence suggests that the miR-134-5p-mediated posttranscriptional regulation of CREB-1 and BDNF is an important molecular mechanism underlying plasticity deficits in AD [79]. Luciferase assays confirmed that miR-30a-5p, miR-195, and miR-613 can target specific sequences surrounding the proximal polyadenylation site within the BDNF 3'-untranslated region [61, 97]. Neuronal overexpression of miR-30a-5p resulted in downregulation of BDNF protein [61]. Another dual-luciferase reporter gene assay demonstrated that miR-10a targeted BDNF, and the authors indicated that miR-10a restrains synapse remodelling and neuronal cell proliferation while promoting apoptosis in AD rats by inhibiting the BDNF-TrkB signalling pathway [98]. Furthermore, miR-322 is significantly increased with the decrease in BDNF in the AD mouse brain, and a luciferase reporter assay identified that miR-322 can directly conjugate to the 3'-UTR of BDNF [16]. As such, there is a novel miRNA-dependent mechanism of BDNF degradation in AD pathogenesis, which may drive miRNA- or BDNF-based therapeutic strategies against AD.

**2.3.4. Acupuncture Plays a Therapeutic Role in AD by Regulating the Expression of BDNF.** Previous studies have shown that electrotherapy can repair the synaptic form and inhibit synaptic degeneration of hippocampal neurons in AD rats [99]. More importantly, the efficacy of EA was demonstrated by regulating the expression of BDNF, as summarized in Table 3. Both studies showed that EA can upregulate the expression of hippocampal BDNF, maintain hippocampal LTP to a certain extent [100], and enhance neurogenesis to improve learning and memory in AD rats [101]. Similarly, Li et al. also showed that repeated EA stimulation may improve cognitive function, upregulate the expression of BDNF, and promote neurogenesis in AD [102]. Moreover, Lin et al. showed that EA at acupoint GV20 can significantly increase the expression levels of mature BDNF and a precursor protein, proBDNF, in APP/PS1 mice. EA may serve as a promising treatment strategy for AD, which may exert neuroprotective effects by adjusting the expression and processing of BDNF [103].

Intriguingly, Keifer et al. published a study aimed at exploring the interrelationship of the miRNA-BDNF signalling loop in the AD brain. According to their results, the

TABLE 3: Deregulated miRNAs and target genes of Alzheimer's disease and summary of related electroacupuncture literatures.

Study	Species/tissue	miRNA	Result/target genes	
Vo et al. [93]	Cortical neurons	miR-132	BDNF triggered the rapid induction and persistent expression of mature miR-132	
Numakawa et al. [94]	Cortical neurons	miR-132	BDNF increased levels of synaptic proteins via upregulation of miR-132	
Tian et al. [96]	Hippocampus	miR-206	BDNF	
Mellios et al. [61]	Prefrontal cortex	miR-30a-5p miR-195	Both miR-30a-5p and miR-195 targeted BDNF	
Li et al. [97]	AD patients and mouse model	miR-613	BDNF	
Wu et al. [98]	Neuronal cells	miR-10a	BDNF	
Zhang et al. [16]	Mouse brain	miR-322	BDNF	
Summary of related electroacupuncture literatures				
Study	Species/tissue	Method/acupoint	Stimulation parameter	Result
Wang et al. [100]	Hippocampus	EA at BL23, GV14, PC6	2 Hz, 1 mA, 20 min	BDNF ↑
Zhang et al. [101]	Hippocampus and cortex	EA at GV20, GV16	150 Hz, 15 min	BDNF ↑
Li et al. [102]	Hippocampus and cortex	EA at GV20	2 Hz/15 Hz, 1 mA, 30 min	BDNF ↑
Lin et al. [103]	Hippocampus	EA at GV20	1 Hz/20 Hz, 30 min	BDNF ↑

EA: electroacupuncture.

reduction in BDNF that occurs in the AD brain is the result of two independent mechanisms: (1) a failure in the proteolytic conversion of BDNF precursor protein to its functional mature form and (2) posttranscriptional inhibition of target BDNF gene expression by miRNAs [76]. Hence, the role of miRNAs in BDNF regulation should be considered when developing BDNF-based therapeutic acupuncture treatments for AD.

#### 2.4. Depression

**2.4.1. BDNF Plays Important Roles in Depression.** Depression affects a growing number of patients both physically and mentally. Depression can result in cognitive impairment in addition to mood changes. Severe depression not only results in impaired learning and memory but also compromises the structural and functional integrity of the brain and exhibits maladaptive synaptic plasticity and degenerative changes in the hippocampus and amygdala [104]. Many studies have shown that BDNF is closely related to depression and that BDNF mediates neurogenesis and synaptic plasticity [105]. In animal models of stress, BDNF levels are reduced in both the cortex and the hippocampus [106, 107]. Similarly, the expression of BDNF was significantly decreased in postmortem brain samples of depressed patients [108, 109], whereas the expression of BDNF in the hippocampus of subjects who took antidepressants was higher than that of subjects who did not take antidepressants. Further study revealed that antidepressant-dependent BDNF levels may prevent or minimize hippocampal changes in human samples [110]. Hence, the BDNF imbalance expression in the brain may help to clarify the relationship between neuroplasticity and the pathophysiology of depression.

**2.4.2. miRNAs Play Important Roles in Depression.** By analysing the above literature, we found that miR-132 and miR-124

participate in neural plasticity. miR-132 dysregulation in major depressive disorder is associated with multiple facets of brain function and structure in the frontolimbic network (the key network for emotional regulation and memory) [111]. Additionally, miR-124 contributes to chronic ultra-mild stress- (CUMS-) induced dendritic hypotrophy and reduced spine density of dentate gyrus granule neurons, which controls resilience/susceptibility to chronic stress-induced depression-like behaviours [112]. Further research has revealed that miR-124-3p-mediated stress is also related to synaptic plasticity [113]. Similarly, the combined effect of miR-92a and miR-485 on transcription factors, along with histone-modifying enzymes, may have functional relevance by producing changes in gene regulatory networks that modify the neuroplastic capacity of the adult dorsal hippocampus under stress [114]. In the depression model, miR-137 loss-of-function results in altered synaptic transmission and plasticity and anxiety and depression-like behaviour in mice [115]. Moreover, amelioration of depression-like behaviour also involves modulation of the synapse-associated factor miR-134 within the basolateral amygdala [116]. The literature also suggests that late-life depressive symptoms are associated with downregulation of prefrontal cortex miR-484, which is related to synaptic transmission [117]. In addition, miR-99a may be involved in the regulation of hypothalamic synaptic plasticity and might be a potential therapeutic target for peri/postmenopausal depression [118].

**2.4.3. miRNAs May Regulate Depression via Influencing BDNF.** In vivo or in vitro rat experiments, miR-206 has been proven to be an important regulator and participator in depression via its direct target gene BDNF [119]. Additionally, inhibition of miR-124 may be a strategy for treating depression by activating the BDNF-TrkB signalling pathway in the hippocampus [120]. Intriguingly, a previous study demonstrated that miR-16 mediates the action of the

TABLE 4: Deregulated miRNAs and target genes of depression and summary of related acupuncture literatures.

Study	Species/tissue	miRNA	Result/target genes	
Yang et al. [119]	Hippocampus	miR-206	BDNF	
Wang et al. [120]	Hippocampus	miR-124	miR-124 produced antidepressant-like effects by activating the BDNF-TrkB signalling pathway	
Sun et al. [122]	Cellular model	miR-16	BDNF	
Varendi et al. [32]	Cellular model	miR-155	BDNF	
Summary of related acupuncture literatures				
Study	Species/tissue	Method/acupoint	Stimulation parameter	Result
Zhang et al. [126]	Hippocampus	MA at GV20, GV29	Needles were twirled for 1 min and retained for 10 min	BDNF ↑
Luo et al. [127]	Hippocampus	EA at GV20, GV29	2 Hz, 2 mA, 20 min	BDNF mRNA ↑, BDNF ↑
Duan et al. [128]	Hippocampus	EA at GV20, GV29	2 Hz, 0.6 mA, 30 min	BDNF ↑
Jiang et al. [129]	Hippocampus	MA at GV20, GV29	20 min/day	BDNF ↑
Yang et al. [130]	Hippocampus	EA at GV20 and GV29 combined with citalopram	2 Hz/100 Hz	BDNF ↑
Park et al. [131]	Prefrontal cortex	MA at HT7	Needles were turned at two revolutions per second for 15 s and removed immediately afterward	BDNF ↑
Zhao et al. [132]	Hippocampus	EA at GV20 and GV29	2 Hz, 1 mA, 20 min	miR-16 ↓

MA: manual acupuncture; EA: electroacupuncture.

antidepressant fluoxetine by acting as a micromanager of hippocampal neurogenesis [121]. The 3'-UTR of BDNF was found to be targeted by miR-16 using miRNA analysis software [122]. Hence, the miR-16/BDNF signalling pathway is involved in depressive disorder and seems to be promising [121]. One study that employed *in silico* approaches, reporter systems, and analysis of endogenous BDNF showed that miR-1, miR-10b, miR-155, and miR-191 directly repress BDNF expression by binding to their predicted sites in the BDNF 3'-UTR [32]. Simultaneously, evidence revealed that BDNF performs antidepressant functions and can be regulated by miR-155 [123]. Thus, miR-155 may affect the depressant status of patients via BDNF, as summarized in Table 4.

**2.4.4. Acupuncture Plays a Therapeutic Role in Depression by Regulating the Expression of BDNF and miRNAs.** Acupuncture therapy has been shown not only to be an effective treatment modality for depression but also to improve depression-like behaviours and reverse the impairment of LTP [124]. The neuroprotective effects include upregulating the gene and protein expression of BDNF in the hippocampus [125]. Acupuncture markedly increased BDNF protein levels, which provided further evidence supporting its positive effects [126]. As summarized in Table 4, Luo et al. performed EA at acupoints GV20 and GV29 in animals with depression induced by CUMS. Compared with preacupuncture treatment conditions, depression-like behaviours were ameliorated and induced an increase in BDNF expression in the hippocampus after treatment [127]. Acupuncture may exert neuroprotective effects in several nervous system diseases through the modulation of BDNF. Duan et al. further investigated the antidepressant mechanism of EA at GV20 and GV29. According to their results, EA increased

BDNF levels by regulating multiple targets in the cyclic adenosine monophosphate response element-binding protein signalling pathway, thereby promoting nerve regeneration [128]. Similarly, Jiang et al. published a study suggesting that the antidepressant effect of acupuncture might be mediated by regulating the DNA methylation and histone modifications of BDNF [129]. Interestingly, Yang et al. revealed that 2 Hz EA plus 5 mg/kg citalopram produced a remarkably increased expression of BDNF in the hippocampus [130]. In addition, in maternally separated depression rat pups, acupuncture stimulation at HT7 significantly increased the BDNF level of the prefrontal cortex [131].

Interestingly, based on previous studies, miR-16 is closely related to depression, and the 3'-UTR of BDNF was found to be targeted by miR-16 [122]. Zhao et al. evaluated the underlying epigenetic mechanism of EA in depression. The CUMS rat model was used, and EA was administered at acupoints GV20 and GV29. After the administration of EA, depression-like behaviours were improved, and high expression of miR-16 in the hippocampus was inhibited as well [132]. Regrettably, this study did not directly explore the relationship between EA regulation of BDNF and neural plasticity. In summary, acupuncture-promoted plasticity protein BDNF expression seems to play an important role in the development of depression. However, further studies are required to investigate the effects of acupuncture on miRNA expression in depression, as acupuncture could target BDNF and related plasticity mechanisms.

### 3. Discussion

We reviewed various studies that have shown neuroplasticity effects caused by regulation of BDNF and miRNAs in different neurodegenerative diseases. The results of the

abovementioned studies suggest that the expression levels of BDNF and various miRNAs, which are thought to play significant roles in various diseases, are changed by acupuncture treatment.

Analysing the literature on stroke suggested that miR-219a and miR-134, which are closely related to synaptic plasticity, were downregulated by EA treatment [26, 42]. Similarly, EA increased miR-181b levels in the penumbra and improved neurobehavioural function [46]. miR-494 was downregulated and miR-206 was upregulated in the penumbra [45]. EA increased cerebral blood flow and alleviated neurological impairment in rats. Moreover, upregulated miR-132 suppressed SOX2 in primary neurons after oxygen-glucose deprivation, which promoted neurite outgrowth [43]. Intriguingly, miR-9 responds locally to BDNF. The expression level of miR-9 in the peri-infarct cortex was increased by EA in stroke rat models [44]. However, upregulation of miR-191a-5p exacerbated neuronal injury and partly reversed the neuroprotective effect of EA treatment after ischaemia/reperfusion injury [21]. Other miRNAs are also potentially associated with stroke. For instance, miR-124, miR-210, miR-10b-5p, and miR-155 were shown to directly target BDNF [27, 28, 30, 31]. Numerous studies have reported that the expression levels of BDNF in rat brain tissue surrounding the haematoma, the cerebral cortex, the peri-infarct cortex, the subventricular zone, the striatum, the hippocampus, etc. are significantly increased after acupuncture [34–41]. Simultaneously, acupuncture has protective and reparative effects on brain tissue, which can improve the symptoms of cerebral infarct, neurological deficits, and motor function in rats. Its mechanism may be related to the upregulation of BDNF and the promotion of nerve cell growth. These changes and distinct roles of many miRNAs may provide an intriguing connection between the effect of acupuncture on stroke and BDNF.

Remarkably, one of the characteristics of PD is the loss of dopaminergic neurons in the substantia nigra. EA therapy may attenuate this loss by promoting the expression of endogenous BDNF [67]. Similarly, the learning and memory abilities of PD rats were significantly improved compared with those of the model group after EA, accompanied by increased BDNF expression levels [66–73], which may underlie the effectiveness of EA in the treatment of PD. Another study investigated whether acupuncture could regulate the expression of miR-124 in the striatum of transgenic mice with PD. According to the study conclusions, the expression levels of miR-124 and BDNF protein were upregulated after treatment [75]. More significantly, many studies have shown that there are complementary sequences among miR-494-3p, miR-30a-5p, miR-7, and miR-210-3p and BDNF [59, 61–63], suggesting that interfering with the expression of these miRNAs could be a strategy for BDNF regulation in PD pathogenesis. Therefore, miRNAs that can directly target BDNF genes might be associated with the potential acupuncture treatment mechanism in PD.

With regard to AD and its link with miRNAs and BDNF, the expression level of miR-132 was increased via BDNF regulation [93, 94]. Furthermore, miR-322, miR-30a-5p, miR-206, miR-195, miR-10a, and miR-163 were identified to tar-

get BDNF [16, 61, 96–98]. Interestingly, EA improved learning and memory in AD rats, promoted neurogenesis in AD, and maintained hippocampal LTP to a certain extent. Almost all studies have suggested that EA can increase BDNF expression levels in the brains of AD model animals [100–103]. Hence, the role of miRNAs in BDNF regulation should be considered when developing BDNF-based acupuncture treatment for AD.

Other miRNAs are also potentially associated with depression. For instance, miR-132, miR-124, miR-124-3p, and miR-137 loss-of-function resulted in altered synaptic transmission and plasticity [113, 115]. Similarly, miR-134, miR-92a, and miR-485 are involved in depression brain neuroplastic capacity [114, 116]. Interestingly, miR-206 and miR-155 were shown to directly regulate BDNF in depression studies [32, 119]. The 3'-UTR of BDNF was also targeted by miR-16, which mediates the action of the antidepressant fluoxetine by acting as a micromanager of hippocampal neurogenesis [122]. Most interestingly, numerous studies have shown that EA can not only inhibit the expression of miR-16 in the hippocampus [132] but also increase the levels of BDNF in the brains of depression model rats [126–130]. Therefore, acupuncture promoted synaptic plasticity via BDNF protein expression and regulated a few miRNAs that were found to target BDNF, which seem to play important roles in the development of depression.

Based on the current analysis of the published literature, we summarize that acupuncture treatment seemingly restores the level of BDNF, which is thought to play significant roles in depression and neurodegenerative diseases such as AD, stroke, and PD. Although it should be critically considered that there are methodological and conclusion differences among the studies, the associations are intriguing and worthy of further analysis and study, especially with respect to neuroplasticity.

Major depressive disorder is a highly prevalent psychiatric disorder that is commonly associated with neurodegenerative diseases. In the actual clinical situation, poststroke depression is one of the most common and well-studied phenomena in poststroke patients. Depression worsens the course of poststroke neurological disorders, with poorer functional recovery [133]. Similarly, psychiatric and mood disturbances are common comorbidities with AD and PD. Depressive symptoms increase the overall burden of illness, mainly due to the negative impact on the quality of life of patients (increased disability and morbidity) [134]. In addition, stroke patients also exhibit an increased risk of depression and dementia [135]. A high comorbidity between stroke, AD, PD, and depression suggests there might be similar mechanisms underlying the course of these diseases, and their shared comorbidity mechanism is worth exploring.

Although the structural and functional changes implicated in the relationship between depression and neurodegeneration seem to be highly complex, excitingly, several studies have shown altered BDNF production and secretion in a variety of neurodegenerative diseases as well as in depression [136]. Overall, BDNF is one of the key molecules modulating and linking brain plasticity, and the neuroplasticity hypothesis postulates that the loss of BDNF plays a major



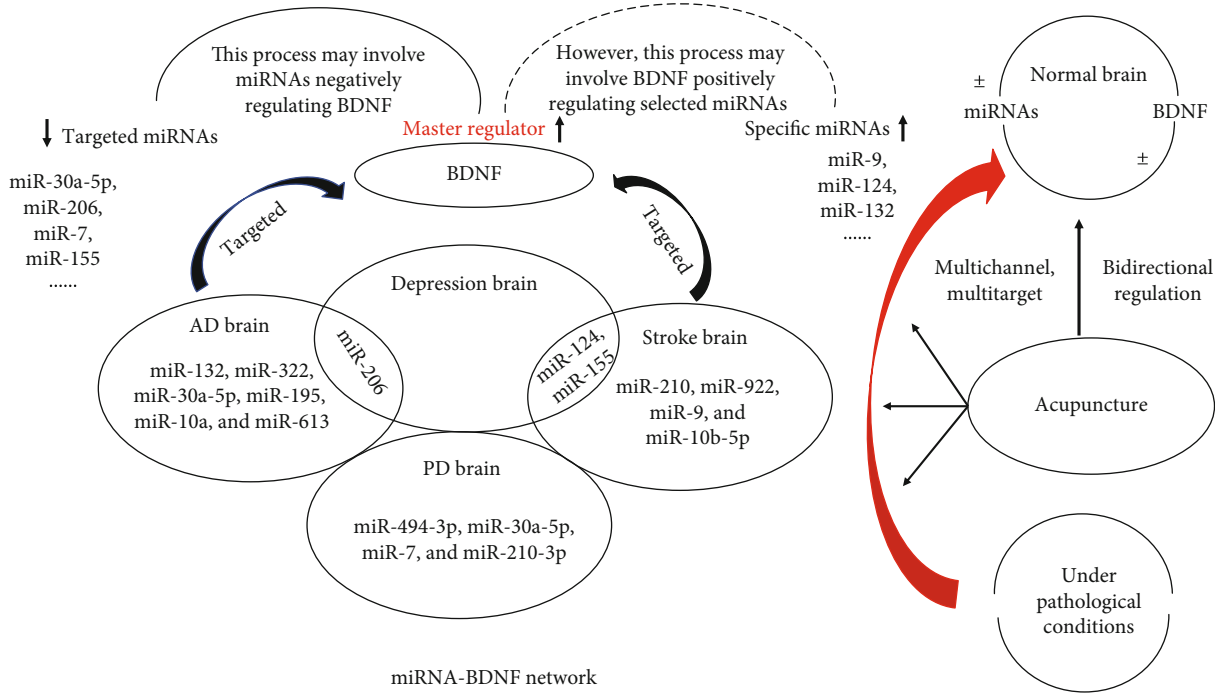


FIGURE 1: Model illustrating the biological mechanism by which acupuncture regulates the miRNA-BDNF network.

role in the pathophysiology of poststroke depression and depression with AD [137, 138]. Similarly, in a short review, while providing evidence of shared biological substrates between PD and depression, neuroplasticity was underscored by the roles of BDNF [139]. Hence, it is possible that depression and neurodegenerative diseases could be improved by a common neuroplasticity mechanism by regulating BDNF expression.

In addition to the coestablished roles of BDNF in modulating neuroplasticity in neurodegenerative diseases and depression, a few other fundamental factors that may have a profound effect in such diseases are currently being explored, such as miRNAs, a class of small noncoding RNAs that can typically bind to the 3'-UTRs of mRNAs to induce repression or degradation. Evidence indicates that the 3'-UTR of BDNF is a significant target of miRNAs, and an in silico analysis suggested that it may have 17 binding sites potentially recognized by as many as 26 miRNAs [61]. In this study, we identified that the expression of BDNF in AD brain neurons is controlled by miR-132, miR-206, miR-30a-5p, miR-195, miR-10a, miR-322, and miR-613; in stroke, the expression of BDNF in brain neurons is controlled by miR-124, miR-210, miR-922, miR-9, miR-10b-5p, and miR-155; in PD brain neurons, the expression of BDNF is controlled by miR-494-3p, miR-30a-5p, miR-7, and miR-210-3p; and in depression brain neurons, it is controlled by miR-206, miR-124, and miR-155. Intriguingly, miR-206 has been proven to be a coregulator in AD and depression. Simultaneously, miR-124 and miR-155 have been shown to be coparticipants in stroke and depression. It is therefore intriguing to speculate that miRNAs might participate in a molecular network involving multiple diseases as the miR-

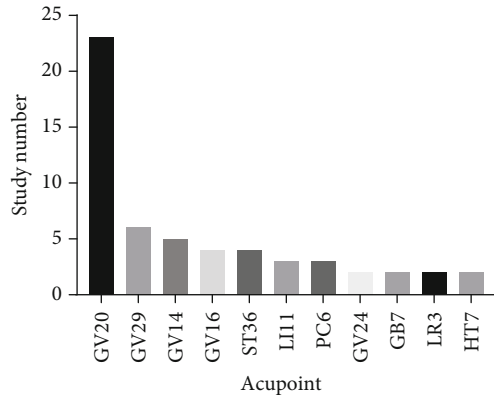


FIGURE 2: Individual acupoint frequency. If the acupoint is present in no more than two studies, the data is not shown.

NAs that are abundantly expressed seem to overlap between neurodegenerative diseases and depression brain states. We further speculate that BDNF is referred to as a “master regulator” because BDNF can be regulated by various miRNAs; thus, the gene expression networks can exert a substantial effect on BDNF. Based on the above multiple regulatory mechanisms, miRNAs build a complex point-to-surface regulatory network, which can not only relate to numerous neurodegenerative diseases and depression states by regulating individual miRNAs but also finely regulate the expression of BDNF by combining several miRNAs. The characteristics of miRNA-BDNF network regulation are highly consistent with the characteristics of multichannel, multitarget, multi-level regulation of acupuncture (Figure 1).

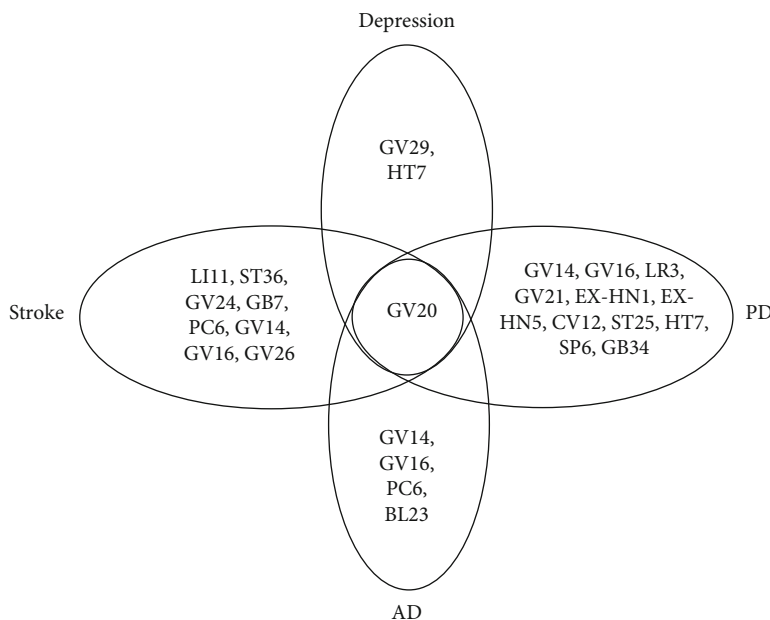


FIGURE 3: Venn diagram showing acupoints that were differentially administered across the stroke, Alzheimer’s disease (AD), Parkinson’s disease (PD), and depression relevant studies.

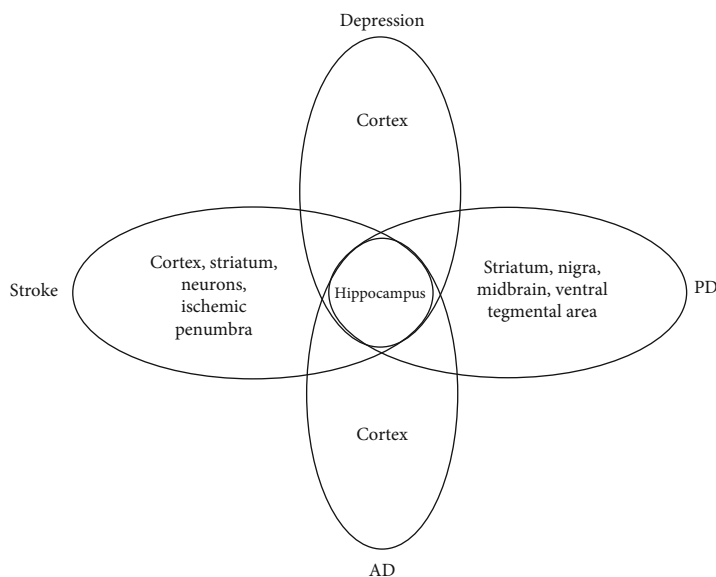


FIGURE 4: Venn diagram showing brain areas that were differentially selected across the stroke, Alzheimer’s disease (AD), Parkinson’s disease (PD), and depression relevant studies.

Acupuncture has been practiced in China for over 2000 years to regain the dynamic balance of the organism based on the “meridian theory” as described in the Yellow Emperor’s Classic of Internal Medicine. Two types of acupuncture treatment, MA and EA, are distinguished by its treatment method. By manual manipulation or stimulation using a low current and frequency, acupuncture has been shown to modulate neurogenesis and synaptogenesis [140]. According to studies investigating the diseases, the most frequently applied acupoints are GV20, GV29, and GV14 (Figure 2), which are localized on the Governor

Vessel (GV). GV runs along the middle of the back and connects with the brain; thus, GV acupoints have always been used for brain and nervous system disorders. Although GV acupoints are frequently used, there are few studies comparing the overlapped molecular outcomes of them with each other or other acupoints among different diseases. In our study, we identified that GV20 elicited the best effects on plasticity (Figure 3), which may contribute to understanding the mechanisms of acupuncture. Overall, the associations are intriguing and worthy of being analysed and studied further.

In summary, we propose that it should be critically considered that there are methodological and hypothetical differences between the studies: (1) the regulatory impact of miRNAs on BDNF expression in the brain needs to be strongly considered in the development of therapeutic treatments for neurodegenerative diseases and depression. (2) Although we briefly reviewed the evidence for a positive action of BDNF on miRNA expression and a negative action of miRNAs on BDNF, the miRNA-BDNF pathway may not be a closed loop system, and many other regulatory elements are at play that control specificity of miRNA expression. Hence, this manuscript highlighted the effect of acupuncture and in what way miRNAs have taken part in elucidating mechanism of acupuncture and neuroplasticity. (3) Based on the analysis of the published literature, we summarized that acupuncture treatment seemingly has a bidirectional regulatory ability to restore levels of diverse miRNAs and BDNF to their normal states (Figure 1). (4) Intriguingly, when the same acupoint was used in all four diseases, the underlying effects on the hippocampus may show similar and overlapping molecular outcome among different diseases (Figures 3 and 4). New findings could lead to the discovery of the biological mechanism by which acupuncture regulates the miRNA-BDNF network and could identify the underlying neurodegenerative disease-depression comorbidity mechanism of acupuncture treatment in the near future.

## Conflicts of Interest

There are no conflicts of interest among all authors.

## Authors' Contributions

All authors were involved in designing the study. Xia Li and Jun Zhao are co-first authors, and they contributed equally to this manuscript.

## Acknowledgments

This work was supported by grants from the National Natural Science Foundation of China (no. 81973938 and no. 81574052).

## References

- [1] J. N. Mazon, A. H. de Mello, G. K. Ferreira, and G. T. Rezin, "The impact of obesity on neurodegenerative diseases," *Life Sciences*, vol. 182, pp. 22–28, 2017.
- [2] M. G. Erkinen, M. O. Kim, and M. D. Geschwind, "Clinical neurology and epidemiology of the major neurodegenerative diseases," *Cold Spring Harbor Perspectives in Biology*, vol. 10, no. 4, 2018.
- [3] G. R. Villas Boas, R. Boerngen de Lacerda, M. M. Paes et al., "Molecular aspects of depression: a review from neurobiology to treatment," *European Journal of Pharmacology*, vol. 851, pp. 99–121, 2019.
- [4] G. Z. Réus, S. E. Titus, H. M. Abelaira et al., "Neurochemical correlation between major depressive disorder and neurodegenerative diseases," *Life Sciences*, vol. 158, pp. 121–129, 2016.
- [5] S. C. Cramer, M. Sur, B. H. Dobkin et al., "Harnessing neuroplasticity for clinical applications," *Brain*, vol. 134, no. 6, pp. 1591–1609, 2011.
- [6] C. La Rosa, R. Parolisi, and L. Bonfanti, "Brain structural plasticity: from adult neurogenesis to immature neurons," *Frontiers in Neuroscience*, vol. 14, p. 75, 2020.
- [7] B. Lu, G. Nagappan, and Y. Lu, "BDNF and synaptic plasticity, cognitive function, and dysfunction," *Handbook of Experimental Pharmacology*, vol. 220, pp. 223–250, 2014.
- [8] G. Leal, C. R. Bramham, and C. B. Duarte, "BDNF and hippocampal synaptic plasticity," *Vitamins and Hormones*, vol. 104, pp. 153–195, 2017.
- [9] Y. Wang, H. Liu, B. S. Zhang, J. C. Soares, and X. Y. Zhang, "Low BDNF is associated with cognitive impairments in patients with Parkinson's disease," *Parkinsonism & Related Disorders*, vol. 29, pp. 66–71, 2016.
- [10] C. S. Mang, K. L. Campbell, C. J. Ross, and L. A. Boyd, "Promoting neuroplasticity for motor rehabilitation after stroke: considering the effects of aerobic exercise and genetic variation on brain-derived neurotrophic factor," *Physical Therapy*, vol. 93, no. 12, pp. 1707–1716, 2013.
- [11] H. K. Manji, J. A. Quiroz, J. Sporn et al., "Enhancing neuronal plasticity and cellular resilience to develop novel, improved therapeutics for difficult-to-treat depression," *Biological Psychiatry*, vol. 53, no. 8, pp. 707–742, 2003.
- [12] A. Caviedes, C. Lafourcade, C. Soto, and U. Wyneken, "BDNF/NF-kappa B signaling in the neurobiology of depression," *Current Pharmaceutical Design*, vol. 23, no. 21, pp. 3154–3163, 2017.
- [13] P. Jin, D. C. Zarnescu, S. Ceman et al., "Biochemical and genetic interaction between the fragile X mental retardation protein and the microRNA pathway," *Nature Neuroscience*, vol. 7, no. 2, pp. 113–117, 2004.
- [14] K. Saavedra, A. M. Molina-Marquez, N. Saavedra, T. Zambrano, and L. A. Salazar, "Epigenetic modifications of major depressive disorder," *International Journal of Molecular Sciences*, vol. 17, no. 8, 2016.
- [15] J. Tavakolizadeh, K. Roshanaei, A. Salmaninejad et al., "MicroRNAs and exosomes in depression: potential diagnostic biomarkers," *Journal of Cellular Biochemistry*, vol. 119, no. 5, pp. 3783–3797, 2018.
- [16] J. Zhang, Z. Liu, Y. Pei, W. Yang, C. Xie, and S. Long, "RETRACTED ARTICLE: MicroRNA-322 cluster promotes tau phosphorylation via targeting brain-derived neurotrophic factor," *Neurochemical Research*, vol. 43, no. 3, pp. 736–744, 2018.
- [17] M. Ploughman, S. Granter-Button, G. Chernenko, B. A. Tucker, K. M. Mearow, and D. Corbett, "Endurance exercise regimens induce differential effects on brain-derived neurotrophic factor, synapsin-I and insulin-like growth factor I after focal ischemia," *Neuroscience*, vol. 136, no. 4, pp. 991–1001, 2005.
- [18] A. Chan, J. Yan, P. Csurhes, J. Greer, and P. McCombe, "Circulating brain derived neurotrophic factor (BDNF) and frequency of BDNF positive T cells in peripheral blood in human ischemic stroke: effect on outcome," *Journal of Neuroimmunology*, vol. 286, pp. 42–47, 2015.
- [19] M. Ploughman, V. Windle, C. L. MacLellan, N. White, J. J. Dore, and D. Corbett, "Brain-derived neurotrophic factor contributes to recovery of skilled reaching after focal ischemia in rats," *Stroke*, vol. 40, no. 4, pp. 1490–1495, 2009.

- [20] X. Liu, Z. Feng, L. Du et al., "The potential role of microRNA-124 in cerebral ischemia injury," *International Journal of Molecular Sciences*, vol. 21, no. 1, 2020.
- [21] H. Zhou, C. Yang, F. Bai et al., "Electroacupuncture alleviates brain damage through targeting of neuronal calcium sensor 1 by miR-191a-5p after ischemic stroke," *Rejuvenation Research*, vol. 20, no. 6, pp. 492–505, 2017.
- [22] L. Chang, W. Zhang, S. Shi et al., "microRNA-195 attenuates neuronal apoptosis in rats with ischemic stroke through inhibiting KLF5-mediated activation of the JNK signaling pathway," *Molecular Medicine*, vol. 26, no. 1, p. 31, 2020.
- [23] H. Xin, Y. Li, Z. Liu et al., "MiR-133b promotes neural plasticity and functional recovery after treatment of stroke with multipotent mesenchymal stromal cells in rats via transfer of exosome-enriched extracellular particles," *Stem Cells*, vol. 31, no. 12, pp. 2737–2746, 2013.
- [24] H. Zhao, G. Li, S. Zhang et al., "Inhibition of histone deacetylase 3 by MiR-494 alleviates neuronal loss and improves neurological recovery in experimental stroke," *Journal of Cerebral Blood Flow and Metabolism*, vol. 39, no. 12, pp. 2392–2405, 2019.
- [25] R. Saba, P. H. Storchel, A. Aksoy-Aksel et al., "Dopamine-regulated microRNA MiR-181a controls GluA2 surface expression in hippocampal neurons," *Molecular and Cellular Biology*, vol. 32, no. 3, pp. 619–632, 2012.
- [26] W. Liu, J. Wu, J. Huang et al., "Electroacupuncture regulates hippocampal synaptic plasticity via miR-134-Mediated LIMK1 function in rats with ischemic stroke," *Neural Plasticity*, vol. 2017, Article ID 9545646, 11 pages, 2017.
- [27] J. Wang, Q. Huang, J. Ding, and X. Wang, "Elevated serum levels of brain-derived neurotrophic factor and miR-124 in acute ischemic stroke patients and the molecular mechanism," *3 Biotech*, vol. 9, no. 11, p. 386, 2019.
- [28] L. L. Zeng, X. S. He, J. R. Liu, C. B. Zheng, Y. T. Wang, and G. Y. Yang, "Lentivirus-mediated overexpression of microRNA-210 improves long-term outcomes after focal cerebral ischemia in mice," *CNS Neuroscience & Therapeutics*, vol. 22, no. 12, pp. 961–969, 2016.
- [29] B. Liu, W. He, and D. Liu, "Functional BDNF rs7124442 variant regulated by miR-922 is associated with better short-term recovery of ischemic stroke," *Therapeutics and Clinical Risk Management*, vol. Volume 15, pp. 1369–1375, 2019.
- [30] L. Wang, W. Liu, Y. Zhang et al., "Dexmedetomidine had neuroprotective effects on hippocampal neuronal cells via targeting lncRNA SHNG16 mediated microRNA-10b-5p/BDNF axis," *Molecular and Cellular Biochemistry*, vol. 469, no. 1-2, pp. 41–51, 2020.
- [31] Y. Lu, Z. Huang, Y. Hua, and G. Xiao, "Minocycline promotes BDNF expression of N2a cells via inhibition of miR-155-mediated repression after oxygen-glucose deprivation and reoxygenation," *Cellular and Molecular Neurobiology*, vol. 38, no. 6, pp. 1305–1313, 2018.
- [32] K. Varendi, A. Kumar, M. A. Harma, and J. O. Andressoo, "miR-1, miR-10b, miR-155, and miR-191 are novel regulators of BDNF," *Cellular and Molecular Life Sciences*, vol. 71, no. 22, pp. 4443–4456, 2014.
- [33] F. Dajas-Bailador, B. Bonev, P. Garcez, P. Stanley, F. Guillemot, and N. Papalopulu, "MicroRNA-9 regulates axon extension and branching by targeting Map1b in mouse cortical neurons," *Nature Neuroscience*, vol. 15, no. 5, pp. 697–699, 2012.
- [34] J. Tao, Y. Zheng, W. Liu et al., "Electro-acupuncture at LI11 and ST36 acupoints exerts neuroprotective effects via reactive astrocyte proliferation after ischemia and reperfusion injury in rats," *Brain Research Bulletin*, vol. 120, pp. 14–24, 2016.
- [35] Y. R. Kim, S. M. Ahn, M. E. Pak et al., "Potential benefits of mesenchymal stem cells and electroacupuncture on the trophic factors associated with neurogenesis in mice with ischemic stroke," *Scientific Reports*, vol. 8, no. 1, p. 2044, 2018.
- [36] C. Jiang, *From BDNF, NGF and Nestin angle to study the protection and repair mechanism of electroacupuncture on the neural damage of brain ischemia*, Heilongjiang University of Chinese Medicine, 2006.
- [37] M. W. Kim, Y. C. Chung, H. C. Jung et al., "Electroacupuncture enhances motor recovery performance with brain-derived neurotrophic factor expression in rats with cerebral infarction," *Acupuncture in Medicine*, vol. 30, no. 3, pp. 222–226, 2012.
- [38] L. Zhou, *Effects of electroacupuncture on the expression of BDNF, Sema3A, and NRP-1 in rats with focal cerebral infarction*, Guangxi Medicine University, 2019.
- [39] W. Teng, *The experimental influences of Baihui-Qubin acupuncture on brain-derived neurotrophic factor expression of rats with intracerebral hemorrhage*, Heilongjiang University of Chinese Medicine, 2009.
- [40] W. Xiao, X. Zhang, Z. Wang, Y. Wang, X. Guo, and H. E. Ling, "Effect of nape cluster acupuncture on BDNF, NGF and neurobehaviors in rats with post-ischemic stroke sequelae," *Shanghai Journal of Acupuncture and Moxibustion*, vol. 33, no. 2, pp. 181–184, 2014.
- [41] X. Ye, Y. Jiang, Y. You et al., "The effect of electroacupuncture the expression of brain-derived neurotrophic factor in cerebral ischemia-reperfusion injury model rats," *Chinese Journal of Rehabilitation Medicine*, vol. 29, no. 3, pp. 204–207, 2014.
- [42] W. Liu, *Based on miRNAs mediating synaptic plasticity to investigate the mechanism of electroacupuncture improving learning and memory in a rat model of ischemic stroke*, Fujian University of Traditional Chinese Medicine, 2017.
- [43] X. Zhao, F. Bai, E. Zhang et al., "Electroacupuncture improves neurobehavioral function through targeting of SOX2-mediated axonal regeneration by microRNA-132 after ischemic stroke," *Frontiers in Molecular Neuroscience*, vol. 11, p. 471, 2018.
- [44] W. Liu, X. Wang, Y. Zheng et al., "Electroacupuncture inhibits inflammatory injury by targeting the miR-9-mediated NF- $\kappa$ B signaling pathway following ischemic stroke," *Molecular Medicine Reports*, vol. 13, no. 2, pp. 1618–1626, 2016.
- [45] H. Z. Zheng, W. Jiang, X. F. Zhao et al., "Electroacupuncture induces acute changes in cerebral cortical miRNA profile, improves cerebral blood flow and alleviates neurological deficits in a rat model of stroke," *Neural Regeneration Research*, vol. 11, no. 12, pp. 1940–1950, 2016.
- [46] B. Deng, F. Bai, H. Zhou et al., "Electroacupuncture enhances rehabilitation through miR-181b targeting PirB after ischemic stroke," *Scientific Reports*, vol. 6, no. 1, p. 38997, 2016.
- [47] A. Costa, A. Peppe, G. A. Carlesimo et al., "Brain-derived neurotrophic factor serum levels correlate with cognitive performance in Parkinson's disease patients with mild cognitive impairment," *Frontiers in Behavioral Neuroscience*, vol. 9, p. 253, 2015.



- [48] D. W. Howells, M. J. Porritt, J. Y. F. Wong et al., "Reduced BDNF mRNA expression in the Parkinson's disease substantia nigra," *Experimental Neurology*, vol. 166, no. 1, pp. 127–135, 2000.
- [49] P. Scalzo, A. Kümmer, T. L. Bretas, F. Cardoso, and A. L. Teixeira, "Serum levels of brain-derived neurotrophic factor correlate with motor impairment in Parkinson's disease," *Journal of Neurology*, vol. 257, no. 4, pp. 540–545, 2010.
- [50] T. Gyárfás, J. Knuuttila, P. Lindholm, T. Rantamäki, and E. Castrén, "Regulation of brain-derived neurotrophic factor (BDNF) and cerebral dopamine neurotrophic factor (CDNF) by anti-parkinsonian drug therapy in vivo," *Cellular and Molecular Neurobiology*, vol. 30, no. 3, pp. 361–368, 2010.
- [51] M. A. Hirsch, S. S. Iyer, and M. Sanjak, "Exercise-induced neuroplasticity in human Parkinson's disease: what is the evidence telling us?," *Parkinsonism & Related Disorders*, vol. 22, Suppl 1, pp. S78–S81, 2016.
- [52] F. Gillardon, M. Mack, W. Rist et al., "MicroRNA and proteome expression profiling in early-symptomatic  $\alpha$ -synuclein(A30P)-transgenic mice," *Proteomics. Clinical Applications*, vol. 2, no. 5, pp. 697–705, 2008.
- [53] S. Y. Goh, Y. X. Chao, S. T. Dheen, E. K. Tan, and S. S. Tay, "Role of microRNAs in Parkinson's disease," *International Journal of Molecular Sciences*, vol. 20, no. 22, p. 5649, 2019.
- [54] G. Lyu, Y. Guan, C. Zhang et al., "TGF- $\beta$  signaling alters H4K20me3 status via miR-29 and contributes to cellular senescence and cardiac aging," *Nature Communications*, vol. 9, no. 1, p. 2560, 2018.
- [55] Q. H. Gu, D. Yu, Z. Hu et al., "miR-26a and miR-384-5p are required for LTP maintenance and spine enlargement," *Nature Communications*, vol. 6, no. 1, p. 6789, 2015.
- [56] J. E. Cohen, P. R. Lee, S. Chen, W. Li, and R. D. Fields, "MicroRNA regulation of homeostatic synaptic plasticity," *Proceedings of the National Academy of Sciences*, vol. 108, no. 28, pp. 11650–11655, 2011.
- [57] Y. Qian, J. Song, Y. Ouyang et al., "Advances in roles of miR-132 in the nervous system," *Frontiers in Pharmacology*, vol. 8, p. 770, 2017.
- [58] L. Geng, T. Zhang, W. Liu, and Y. Chen, "miR-494-3p modulates the progression of in vitro and in vivo Parkinson's disease models by targeting SIRT3," *Neuroscience Letters*, vol. 675, pp. 23–30, 2018.
- [59] C. Deng, J. Zhu, J. Yuan, Y. Xiang, and L. Dai, "Pramipexole inhibits MPP<sup>+</sup>-induced neurotoxicity by miR-494-3p/BDNF," *Neurochemical Research*, vol. 45, no. 2, pp. 268–277, 2020.
- [60] C. Schwienbacher, L. Foco, A. Picard et al., "Plasma and white blood cells show different miRNA expression profiles in Parkinson's disease," *Journal of Molecular Neuroscience*, vol. 62, no. 2, pp. 244–254, 2017.
- [61] N. Mellios, H. S. Huang, A. Grigorenko, E. Rogaev, and S. Akbarian, "A set of differentially expressed miRNAs, including miR-30a-5p, act as post-transcriptional inhibitors of BDNF in prefrontal cortex," *Human Molecular Genetics*, vol. 17, no. 19, pp. 3030–3042, 2008.
- [62] B. Li, Y. Jiang, Y. Xu, Y. Li, and B. Li, "Identification of miRNA-7 as a regulator of brain-derived neurotrophic factor/ $\alpha$ -synuclein axis in atrazine-induced Parkinson's disease by peripheral blood and brain microRNA profiling," *Chemosphere*, vol. 233, pp. 542–548, 2019.
- [63] S. Zhang, S. Chen, A. Liu et al., "Inhibition of BDNF production by MPP<sup>+</sup> through up-regulation of miR-210-3p contributes to dopaminergic neuron damage in MPTP model," *Neuroscience Letters*, vol. 675, pp. 133–139, 2018.
- [64] H. Wang, X. Liang, X. Wang, D. Luo, J. Jia, and X. Wang, "Electro-acupuncture stimulation improves spontaneous locomotor hyperactivity in MPTP intoxicated mice," *PLoS One*, vol. 8, no. 5, p. e64403, 2013.
- [65] S. Wang, J. Fang, J. Ma et al., "Electroacupuncture-regulated neurotrophic factor mRNA expression in the substantia nigra of Parkinson's disease rats," *Neural Regeneration Research*, vol. 8, no. 6, pp. 540–549, 2013.
- [66] P. Huang, J. Ma, Y. Wang, S. Gan, H. Li, and T. Lei, "Effect of Taichong and Fengfu on learning and memory ability and brain-derived neurotrophic factor in a rat model of Parkinson's disease," *Traditional Chinese Medicine Journal*, vol. 9, no. 2, pp. 55–57, 2010.
- [67] D. Yang, M. Cai, X. Chen, and H. Ou, "Effect of electroacupuncture scalp points on the expression of the brain-derived neurotrophic factor in substantia nigra in the Parkinson's disease rat model," *Journal of Zhejiang Chinese Medical University*, vol. 38, no. 3, pp. 327–332, 2014.
- [68] M. E. Pak, S. M. Ahn, D. H. Jung et al., "Electroacupuncture therapy ameliorates motor dysfunction via brain-derived neurotrophic factor and glial cell line-derived neurotrophic factor in a mouse model of Parkinson's disease," *The Journals of Gerontology. Series A, Biological Sciences and Medical Sciences*, vol. 75, no. 4, pp. 712–721, 2020.
- [69] J. Feng, H. M. Sun, Y. Y. Wang et al., "Influences of needling chorea-tremble controlled zone on expressions of dopaminergic neurons and BDNF in mice with Parkinson's disease," *Journal of Beijing University of Traditional Chinese Medicine*, vol. 37, no. 1, pp. 53–57, 2014.
- [70] J. Zhang, *Experimental studies on the intervention of electroacupuncture 'Baihui through Qinding' in Parkinson's disease mice*, Heilongjiang University of Chinese Medicine, 2010.
- [71] H. Wang, *Effects of different electricity on serum and black striatum BDNF in Parkinsonism model rats*, Heilongjiang College of traditional Chinese Medicine, 2018.
- [72] M. Sun, K. Wang, Y. Yu et al., "Electroacupuncture alleviates depressive-like symptoms and modulates BDNF signaling in 6-hydroxydopamine rats," *Evidence-based Complementary and Alternative Medicine*, vol. 2016, Article ID 7842362, 11 pages, 2016.
- [73] X.-B. Liang, X.-Y. Liu, F.-Q. Li et al., "Long-term high-frequency electro-acupuncture stimulation prevents neuronal degeneration and up-regulates BDNF mRNA in the substantia nigra and ventral tegmental area following medial forebrain bundle axotomy," *Molecular Brain Research*, vol. 108, no. 1-2, pp. 51–59, 2002.
- [74] Y. Sun, Z.-M. Luo, X.-M. Guo, D.-F. Su, and X. Liu, "An updated role of microRNA-124 in central nervous system disorders: a review," *Frontiers in Cellular Neuroscience*, vol. 9, p. 193, 2015.
- [75] Y. Liu, *Effect of acupuncture on behaviour and expression of miRNA-124 in the striatum of transgenic mice with Parkinson's disease*, University of South China, 2018.
- [76] J. Keifer, Z. Zheng, and G. Ambigapathy, "A microRNA-BDNF negative feedback signaling loop in brain: implications for Alzheimer's disease," *Microna*, vol. 4, no. 2, pp. 101–108, 2015.

- [77] S. Arora, D. Sharma, and J. Singh, "GLUT-1: an effective target to deliver brain-derived neurotrophic factor gene across the blood brain barrier," *ACS Chemical Neuroscience*, vol. 11, no. 11, pp. 1620–1633, 2020.
- [78] P. Lau, K. Bossers, R. Janky et al., "Alteration of the microRNA network during the progression of Alzheimer's disease," *EMBO Molecular Medicine*, vol. 5, no. 10, pp. 1613–1634, 2013.
- [79] N. Baby, N. Alagappan, S. T. Dheen, and S. Sajikumar, "MicroRNA-134-5p inhibition rescues long-term plasticity and synaptic tagging/capture in an A $\beta$  (1-42)-induced model of Alzheimer's disease," *Aging Cell*, vol. 19, no. 1, article e13046, 2020.
- [80] J. Remenyi, M. W. M. van den Bosch, O. Palygin et al., "miR-132/212 knockout mice reveal roles for these miRNAs in regulating cortical synaptic transmission and plasticity," *PLoS One*, vol. 8, no. 4, article e62509, 2013.
- [81] N. Xu, A.-D. Li, L.-L. Ji, Y. Ye, Z.-Y. Wang, and L. Tong, "miR-132 regulates the expression of synaptic proteins in APP/PS1 transgenic mice through C1q," *European Journal of Histochemistry*, vol. 63, no. 2, 2019.
- [82] J. Song and Y. K. Kim, "Identification of the role of miR-142-5p in Alzheimer's disease by comparative bioinformatics and cellular analysis," *Frontiers in Molecular Neuroscience*, vol. 10, p. 227, 2017.
- [83] X. Wang, D. Liu, H. Z. Huang et al., "A novel microRNA-124/PTPN1 signal pathway mediates synaptic and memory deficits in Alzheimer's disease," *Biological Psychiatry*, vol. 83, no. 5, pp. 395–405, 2018.
- [84] C. J. Rodriguez-Ortiz, G. A. Prieto, A. C. Martini et al., "miR-181a negatively modulates synaptic plasticity in hippocampal cultures and its inhibition rescues memory deficits in a mouse model of Alzheimer's disease," *Aging Cell*, vol. 19, no. 3, article e13118, 2020.
- [85] Q. Qian, J. Zhang, F.-P. He et al., "Down-regulated expression of microRNA-338-5p contributes to neuropathology in Alzheimer's disease," *The FASEB Journal*, vol. 33, no. 3, pp. 4404–4417, 2019.
- [86] C. J. Rodriguez-Ortiz, D. Baglietto-Vargas, H. Martinez-Coria, F. M. LaFerla, and M. Kitazawa, "Upregulation of miR-181 decreases c-Fos and SIRT-1 in the hippocampus of 3xTg-AD mice," *Journal of Alzheimer's Disease*, vol. 42, no. 4, pp. 1229–1238, 2014.
- [87] M.-L. Yan, S. Zhang, H.-M. Zhao et al., "MicroRNA-153 impairs presynaptic plasticity by blocking vesicle release following chronic brain hypoperfusion," *Cell Communication and Signaling*, vol. 18, no. 1, p. 57, 2020.
- [88] Y. Xu, P. Chen, X. Wang, J. Yao, and S. Zhuang, "miR-34a deficiency in APP/PS1 mice promotes cognitive function by increasing synaptic plasticity via AMPA and NMDA receptors," *Neuroscience Letters*, vol. 670, pp. 94–104, 2018.
- [89] Y. C. Kao, I. F. Wang, and K. J. Tsai, "miRNA-34c overexpression causes dendritic loss and memory decline," *International Journal of Molecular Sciences*, vol. 19, no. 8, p. 2323, 2018.
- [90] S. Sarkar, S. Jun, S. Rellick, D. D. Quintana, J. Z. Cavendish, and J. W. Simpkins, "Expression of microRNA-34a in Alzheimer's disease brain targets genes linked to synaptic plasticity, energy metabolism, and resting state network activity," *Brain Research*, vol. 1646, pp. 139–151, 2016.
- [91] S. T. Lee, K. Chu, K. H. Jung et al., "miR-206 regulates brain-derived neurotrophic factor in Alzheimer disease model," *Annals of Neurology*, vol. 72, no. 2, pp. 269–277, 2012.
- [92] J. P. Cogswell, J. Ward, I. A. Taylor et al., "Identification of miRNA changes in Alzheimer's disease brain and CSF yields putative biomarkers and insights into disease pathways," *Journal of Alzheimer's Disease*, vol. 14, no. 1, pp. 27–41, 2008.
- [93] N. Vo, M. E. Klein, O. Varlamova et al., "From the cover: a cAMP-response element binding protein-induced microRNA regulates neuronal morphogenesis," *Proceedings of the National Academy of Sciences*, vol. 102, no. 45, pp. 16426–16431, 2005.
- [94] T. Numakawa, M. Richards, N. Adachi, S. Kishi, H. Kunugi, and K. Hashido, "MicroRNA function and neurotrophin BDNF," *Neurochemistry International*, vol. 59, no. 5, pp. 551–558, 2011.
- [95] B. Xie, Z. Liu, L. Jiang et al., "Increased serum miR-206 level predicts conversion from amnesic mild cognitive impairment to Alzheimer's disease: a 5-year follow-up study," *Journal of Alzheimer's Disease*, vol. 55, no. 2, pp. 509–520, 2017.
- [96] N. Tian, Z. Cao, and Y. Zhang, "MiR-206 decreases brain-derived neurotrophic factor levels in a transgenic mouse model of Alzheimer's disease," *Neuroscience Bulletin*, vol. 30, no. 2, pp. 191–197, 2014.
- [97] W. Li, X. Li, X. Xin, P. C. Kan, and Y. Yan, "MicroRNA-613 regulates the expression of brain-derived neurotrophic factor in Alzheimer's disease," *Bioscience Trends*, vol. 10, no. 5, pp. 372–377, 2016.
- [98] B. W. Wu, M. S. Wu, and J. D. Guo, "Effects of microRNA-10a on synapse remodeling in hippocampal neurons and neuronal cell proliferation and apoptosis through the BDNF-TrkB signaling pathway in a rat model of Alzheimer's disease," *Journal of Cellular Physiology*, vol. 233, no. 7, pp. 5281–5292, 2018.
- [99] L. Song, Y. Shu-guang, and H. Ting, "Effects of electroacupuncture on synaptic plasticity of hippocampal neurons in model rats with Alzheimer disease," *Chinese Journal of Clinical Rehabilitation*, vol. 27, pp. 187–189, 2006.
- [100] X. Wang, F. Shen, L. Kong et al., "Effects of low frequency electroacupuncture on expression of BDNF in hippocampus of Alzheimer's disease model rats," *Journal of Hubei University of Chinese Medicine*, vol. 17, no. 5, pp. 7–9, 2015.
- [101] D. Zhang, Y. Sun, and L. Wang, "The influence of electroacupuncture Baihui and Fengfu on behavior and the expression of brain BDNF in rats model of learning and memory impairment," *Acta Chinese Medicine and Pharmacology*, vol. 39, no. 3, pp. 113–115, 2011.
- [102] X. Li, F. Guo, Q. Zhang et al., "Electroacupuncture decreases cognitive impairment and promotes neurogenesis in the APP/PS1 transgenic mice," *BMC Complementary and Alternative Medicine*, vol. 14, no. 1, p. 37, 2014.
- [103] R. Lin, J. Chen, X. Li et al., "Electroacupuncture at the Baihui acupoint alleviates cognitive impairment and exerts neuroprotective effects by modulating the expression and processing of brain-derived neurotrophic factor in APP/PS1 transgenic mice," *Molecular Medicine Reports*, vol. 13, no. 2, pp. 1611–1617, 2016.
- [104] K. Mahati, V. Bhagya, T. Christofer, A. Sneha, and B. S. Shankaranarayana Rao, "Enriched environment ameliorates depression-induced cognitive deficits and restores abnormal hippocampal synaptic plasticity," *Neurobiology of Learning and Memory*, vol. 134, no. Part B, pp. 379–391, 2016.
- [105] J. O. Groves, "Is it time to reassess the BDNF hypothesis of depression?," *Molecular Psychiatry*, vol. 12, no. 12, pp. 1079–1088, 2007.

- [106] R. S. Duman and L. M. Monteggia, "A neurotrophic model for stress-related mood disorders," *Biological Psychiatry*, vol. 59, no. 12, pp. 1116–1127, 2006.
- [107] R. Molteni, F. Calabrese, A. Cattaneo et al., "Acute stress responsiveness of the neurotrophin BDNF in the rat hippocampus is modulated by chronic treatment with the antidepressant duloxetine," *Neuropsychopharmacology*, vol. 34, no. 6, pp. 1523–1532, 2009.
- [108] J. P. Guilloux, G. Douillard-Guilloux, R. Kota et al., "Molecular evidence for BDNF- and GABA-related dysfunctions in the amygdala of female subjects with major depression," *Molecular Psychiatry*, vol. 17, no. 11, pp. 1130–1142, 2012.
- [109] A. Tripp, H. Oh, J. P. Guilloux, K. Martinowich, D. A. Lewis, and E. Sibille, "Brain-derived neurotrophic factor signaling and subgenual anterior cingulate cortex dysfunction in major depressive disorder," *The American Journal of Psychiatry*, vol. 169, no. 11, pp. 1194–1202, 2012.
- [110] B. Chen, D. Dowlatshahi, G. M. MacQueen, J. F. Wang, and L. T. Young, "Increased hippocampal BDNF immunoreactivity in subjects treated with antidepressant medication," *Biological Psychiatry*, vol. 50, no. 4, pp. 260–265, 2001.
- [111] S. Qi, X. Yang, L. Zhao et al., "MicroRNA132 associated multimodal neuroimaging patterns in unmedicated major depressive disorder," *Brain*, vol. 141, no. 3, pp. 916–926, 2018.
- [112] F. Higuchi, S. Uchida, H. Yamagata et al., "Hippocampal microRNA-124 enhances chronic stress resilience in mice," *The Journal of Neuroscience*, vol. 36, no. 27, pp. 7253–7267, 2016.
- [113] B. Roy, M. Dunbar, R. C. Shelton, and Y. Dwivedi, "Identification of microRNA-124-3p as a putative epigenetic signature of major depressive disorder," *Neuropsychopharmacology*, vol. 42, no. 4, pp. 864–875, 2017.
- [114] M. Muñoz-Llanos, M. A. García-Pérez, X. Xu et al., "MicroRNA profiling and bioinformatics target analysis in dorsal hippocampus of chronically stressed rats: relevance to depression pathophysiology," *Frontiers in Molecular Neuroscience*, vol. 11, p. 251, 2018.
- [115] H. L. Yan, X. W. Sun, Z. M. Wang et al., "MiR-137 deficiency causes anxiety-like behaviors in mice," *Frontiers in Molecular Neuroscience*, vol. 12, p. 260, 2019.
- [116] H. Yu, C. Fan, L. Yang et al., "Ginsenoside Rg1 prevents chronic stress-induced depression-like behaviors and neuronal structural plasticity in rats," *Cellular Physiology and Biochemistry*, vol. 48, no. 6, pp. 2470–2482, 2018.
- [117] T. S. Wingo, J. Yang, W. Fan et al., "Brain microRNAs associated with late-life depressive symptoms are also associated with cognitive trajectory and dementia," *NPJ Genomic Medicine*, vol. 5, no. 1, p. 6, 2020.
- [118] J. Yang, L. Zhang, L. L. Cao et al., "MicroRNA-99a is a potential target for regulating hypothalamic synaptic plasticity in the peri/postmenopausal depression model," *Cells*, vol. 8, no. 9, p. 1081, 2019.
- [119] X. Yang, Q. Yang, X. Wang et al., "MicroRNA expression profile and functional analysis reveal that miR-206 is a critical novel gene for the expression of BDNF induced by ketamine," *Neuromolecular Medicine*, vol. 16, no. 3, pp. 594–605, 2014.
- [120] S.-S. Wang, R.-H. Mu, C.-F. Li et al., "MicroRNA-124 targets glucocorticoid receptor and is involved in depression-like behaviors," *Progress in Neuro-Psychopharmacology and Biological Psychiatry*, vol. 79, no. Part B, pp. 417–425, 2017.
- [121] J. M. Launay, S. Mouillet-Richard, A. Baudry, M. Pietri, and O. Kellermann, "Raphe-mediated signals control the hippocampal response to SRI antidepressants via miR-16," *Translational Psychiatry*, vol. 1, no. 11, article e56, 2011.
- [122] Y.-X. Sun, J. Yang, P.-Y. Wang, Y.-J. Li, S.-Y. Xie, and R.-P. Sun, "Cisplatin regulates SH-SY5Y cell growth through downregulation of BDNF via miR-16," *Oncology Reports*, vol. 30, no. 5, pp. 2343–2349, 2013.
- [123] N. Xu, H. Meng, T. Liu et al., "Blueberry phenolics reduce gastrointestinal infection of patients with cerebral venous thrombosis by improving depressant-induced autoimmune disorder via miR-155-mediated brain-derived neurotrophic factor," *Frontiers in Pharmacology*, vol. 8, p. 853, 2017.
- [124] Y. She, J. Xu, Y. Duan et al., "Possible antidepressant effects and mechanism of electroacupuncture in behaviors and hippocampal synaptic plasticity in a depression rat model," *Brain Research*, vol. 1629, pp. 291–297, 2015.
- [125] D. Lin, Q. Wu, X. Lin et al., "Brain-derived neurotrophic factor signaling pathway: modulation by acupuncture in telomerase knockout mice," *Alternative Therapies in Health and Medicine*, vol. 21, no. 6, pp. 36–46, 2015.
- [126] X. Zhang, Y. Song, T. Bao et al., "Antidepressant-like effects of acupuncture involved the ERK signaling pathway in rats," *BMC Complementary and Alternative Medicine*, vol. 16, no. 1, p. 380, 2016.
- [127] T. Luo, H. Tian, H. Song et al., "Possible involvement of tissue plasminogen activator/brain-derived neurotrophic factor pathway in anti-depressant effects of electroacupuncture in chronic unpredictable mild stress-induced depression in rats," *Frontiers in Psychiatry*, vol. 11, p. 63, 2020.
- [128] D. M. Duan, Y. Tu, P. Liu, and S. Jiao, "Antidepressant effect of electroacupuncture regulates signal targeting in the brain and increases brain-derived neurotrophic factor levels," *Neural Regeneration Research*, vol. 11, no. 10, pp. 1595–1602, 2016.
- [129] H. Jiang, X. Zhang, J. Lu et al., "Antidepressant-like effects of acupuncture—insights from DNA methylation and histone modifications of brain-derived neurotrophic factor," *Frontiers in Psychiatry*, vol. 9, p. 102, 2018.
- [130] J. Yang, Y. Pei, Y. L. Pan et al., "Enhanced antidepressant-like effects of electroacupuncture combined with citalopram in a rat model of depression," *Evidence-based Complementary and Alternative Medicine*, vol. 2013, Article ID 107380, 12 pages, 2013.
- [131] H. Park, D. Yoo, S. Kwon et al., "Acupuncture stimulation at HT7 alleviates depression-induced behavioral changes via regulation of the serotonin system in the prefrontal cortex of maternally-separated rat pups," *The Journal of Physiological Sciences*, vol. 62, no. 4, pp. 351–357, 2012.
- [132] J. Zhao, H. Tian, H. Song et al., "Effect of electroacupuncture on reuptake of serotonin via miRNA-16 expression in a rat model of depression," *Evidence-based Complementary and Alternative Medicine*, vol. 2019, Article ID 7124318, 16 pages, 2019.
- [133] I. Loubinoux, G. Kronenberg, M. Endres et al., "Post-stroke depression: mechanisms, translation and therapy," *Journal of Cellular and Molecular Medicine*, vol. 16, no. 9, pp. 1961–1969, 2012.
- [134] C. P. C. Galts, L. E. B. Bettio, D. C. Jewett et al., "Depression in neurodegenerative diseases: common mechanisms and current treatment options," *Neuroscience and Biobehavioral Reviews*, vol. 102, pp. 56–84, 2019.

- [135] K. Filipka, A. Wisniewski, M. Biercewicz, and R. Slusarz, "Are depression and dementia a common problem for stroke older adults? A review of chosen epidemiological studies," *Psychiatric Quarterly*, vol. 91, no. 3, pp. 807–817, 2020.
- [136] N. Pluchino, M. Russo, A. N. Santoro, P. Litta, V. Cela, and A. R. Genazzani, "Steroid hormones and BDNF," *Neuroscience*, vol. 239, pp. 271–279, 2013.
- [137] M. Fukuchi, "Identifying inducers of BDNF gene expression from pharmacologically validated compounds; antipyretic drug dipyrone increases BDNF mRNA in neurons," *Biochemical and Biophysical Research Communications*, vol. 524, no. 4, pp. 957–962, 2020.
- [138] C. Chen, Y. Dong, F. Liu et al., "A study of antidepressant effect and mechanism on intranasal delivery of BDNF-HA2TAT/AAV to rats with post-stroke depression," *Neuropsychiatric Disease and Treatment*, vol. Volume 16, pp. 637–649, 2020.
- [139] Y. Tizabi, B. Getachew, A. B. Csoka, K. F. Manaye, and R. L. Copeland, "Novel targets for parkinsonism-depression comorbidity," *Progress in Molecular Biology and Translational Science*, vol. 167, pp. 1–24, 2019.
- [140] L. Y. Xiao, X. R. Wang, Y. Yang et al., "Applications of acupuncture therapy in modulating plasticity of central nervous system," *Neuromodulation*, vol. 21, no. 8, pp. 762–776, 2018.



## Research Article

# EA Ameliorated Depressive Behaviors in CUMS Rats and Was Related to Its Suppressing Autophagy in the Hippocampus

Zhinan Zhang <sup>1</sup>, Xiaowen Cai,<sup>1</sup> Zengyu Yao,<sup>1</sup> Feng Wen,<sup>1</sup> Zhiyi Fu,<sup>1</sup> Jiping Zhang,<sup>1</sup> Zheng Zhong,<sup>2</sup> Yong Huang <sup>1</sup>, and Shanshan Qu <sup>1</sup>

<sup>1</sup>School of Traditional Chinese Medicine, Southern Medical University, Guangzhou, Guangdong Province, 510515, China

<sup>2</sup>Nanfang Hospital, Southern Medical University, Guangzhou, Guangdong Province, 510515, China

Correspondence should be addressed to Yong Huang; [nanfanglihuang@163.com](mailto:nanfanglihuang@163.com) and Shanshan Qu; [s2qu@163.com](mailto:s2qu@163.com)

Received 11 June 2020; Revised 7 September 2020; Accepted 11 September 2020; Published 22 September 2020

Academic Editor: Lu Wang

Copyright © 2020 Zhinan Zhang et al. This is an open access article distributed under the Creative Commons Attribution License, which permits unrestricted use, distribution, and reproduction in any medium, provided the original work is properly cited.

Autophagy is confirmed to be involved in the onset and development of depression, and some antidepressants took effect by influencing the autophagic process. Electroacupuncture (EA), as a common complementary treatment for depression, may share the mechanism of influencing autophagy in the hippocampus like antidepressants. To investigate that, sixty Sprague-Dawley rats firstly went through chronic unpredictable mild stress (CUMS) model establishment, and 15 rats were assigned to a control group. After modeling, 45 successfully CUMS-induced rats were randomly divided to 3 groups: CUMS, selective serotonin reuptake inhibitor (SSRI), and EA groups (15 rats per group), to accept different interventions for 2 weeks. A sucrose preference test (SPT), weighing, and open field test (OFT) were measurement for depressive behaviors of rats. Transmission electron microscope (TEM), immunohistochemistry (IHC), and western blot analysis were used to evaluate the autophagic changes. After that, depression-like behaviors were successfully induced in CUMS models and reversed by SSRI and EA treatments (both  $p < 0.05$ ), but these two therapies had nonsignificant difference between each other ( $p > 0.05$ ). Autolysosomes observed through TEM in the CUMS group were more than that in the control group. Their number and size in the SSRI and EA groups also decreased significantly. From IHC, the CUMS group showed enhanced positive expression of both Beclin1 and LC3 in CA1 after modeling ( $p < 0.05$ ), and the LC3 level declined after EA treatments, which was verified by decreased LC3-II/LC3-I in western blot analysis. We speculated that CUMS-induced depression-like behavior was interacted with an autophagy process in the hippocampus, and EA demonstrated antidepressant effects by partly inhibiting autophagy with a decreased number of autolysosomes and level of LC3 along with LC3-II/LC3-I.

## 1. Introduction

Depression is a common mental disorder that severely limits psychosocial functioning and diminishes quality of life [1], affecting over 300 million people worldwide [2]. It contributes the most global all years lived with disability ranked by the WHO as well as the main reason blamed for suicide [2]. Many molecular mechanisms are involved in the etiology of the disorder, among which autophagy has been put forward as one of them [3].

Autophagy is a widely existed protein degradation method in eukaryotic cells, which is usually induced and upregulated by external stimuli. Three forms of autophagy are mainly described: macroautophagy, microautophagy,

and chaperone-mediated autophagy, among which the macroautophagy is the most common type. In macroautophagy, expendable cytoplasmic constituents are targeted and isolated from the rest of the cell in the form of autophagosomes. After that, autolysosomes fused with available lysosomes and autophagosomes are degraded and recycled.

A variety of proteins are involved in the regulation of autophagy, among which the Beclin1 and LC3 are the typical ones. Beclin1, a homologous of yeast ATG6, is a regulatory gene of autophagy. Besides, the modification process of LC3, microtubule-associated protein 1 light chain 3, is very important for the formation of autophagosomes. The precursor of LC3 was processed into LC3-I by cysteine protease Atg4B. After the catalyzing of Atg7,

intracytoplasmic LC3-I transformed into a form of membrane bound, namely, LC3-II [4]. The number of autophagosomes is associated with the ratio of LC3-II/LC3-I. Therefore, Beclin1 and LC3 are important markers when autophagy occurs.

Autophagy is in fact a conserved lysosomal degradation pathway essential for the central nervous system. It plays an important role in neuronal development and synaptic plasticity. The dysfunction of autophagic degradation leading to accumulation of abnormal protein inside the neuronal cells is the common basis of neurodegenerative diseases, such as Parkinson's disease, Alzheimer's disease, and Huntington's disease [5]. There is increasing evidence showing that stressors can induce autophagy [6]. Exposure to various kinds of environmental stressors is a convincing cause to depression, by which a depression animal model, chronic unpredictable mild stress (CUMS) model, has been established and widely used [7]. Some recent researches showed autophagy alteration in CUMS animals with the reversal of behavioral effect [8, 9].

Autophagy has been frequently discussed in the researches of depression about human and animal. A small sample-size study found higher expression of autophagy genes in blood mononuclear cells from depression patients than that from healthy controls [10], and another study presented the positive correlation between the expression of Beclin1 in these cells and clinical treatment success [11]. Since the hippocampus is one of the key brain areas where depression develops, autophagy is often discovered in this location. Liu et al. observed the autophagy activation of the hippocampus in the depression model of rats, such as increased autophagosomes, LC3-II/LC3-I ratio, and Beclin1 level in neurons and the atrophied brain area [12]. Hence, autophagy was inhibited in the hippocampus of OBX rats (a depression animal model) and upregulated by fluoxetine (a widely used antidepressant belonging to selective serotonin reuptake inhibitors (SSRIs)) with reversal of depressive-like behavior and enhanced expression of LC3-II, Beclin1, etc. [13]. Other studies also presented decreased autophagic markers [14, 15].

Acupuncture and electroacupuncture (EA) are effective complementary therapies for depression based on antidepressant treatment [16]. The effect on autophagy of acupuncture or electroacupuncture (EA) has been proven in several diseases. Tian et al. found that acupuncture could clear  $\alpha$ -synuclein in the substantia nigra par compacta of the brain in a PD mouse model [17]. With decreased levels of LC3 and Beclin1, EA may alleviate the cerebral ischemia/reperfusion by inhibiting neurons' excessive autophagy [18]. Meanwhile, autophagy may be beneficial that the LC3 expression of autophagy had positive correlation with neurologic function in a hemorrhagic stroke rat model [19].

However, although the investigation of autophagy in depression is comparatively thorough and a certain number of studies about acupuncture and autophagy have published, the comprehensive research discussing the acupuncture impact on autophagy in depression is still limited. Therefore, this experiment was designed to investigate the autophagy phenomenon in hippocampus neurons of CUMS rats and

TABLE 1: The stressors of the 21-day CUMS procedure.

Stressor	Duration
Water deprivation	24 h
Food deprivation	24 h
Immobilization	6 h
Level shaking	5 min
Tail clamping	3 min

attempt to find out the antidepressant mechanism of EA underneath.

## 2. Materials and Methods

**2.1. Animals.** Seventy-five male Sprague-Dawley rats weighing 180-220 g, provided by Southern Medical University Experimental Animal Center (Guangdong, China; license No. SYXK (Yue) 2016-0167), were housed individually in the SPF facility (temperature  $24 \pm 2^\circ\text{C}$ , humidity 50-60%) at Southern Medical University, China. After 3-day adaption, CUMS models began to be established in all rats except for 15 rats in the control group. The study protocol was approved by Southern Medical University Experimental Animal Ethics Committee (NO. L2017178) and followed the United States National Institutes of Health Guide for the Care and Use of Laboratory Animals (NIH Publication No. 85-23, revised 1986).

**2.2. Chronic Unpredictable Mild Stress (CUMS) Model Establishment.** The CUMS model was established referring to previous studies [20-23] that evaluate biological effects of antidepressants. Except for the control group, the remaining 60 rats underwent a 21-day CUMS procedure modified on Zhang et al. [24], during which the rats were exposed to different stressors including water deprivation (24 h), food deprivation (24 h), immobilization (2 h), level shaking (5 min), and tail clamping (3 min; 3 cm from the end of the tail). These stressors were processed randomly as one stressor per day on rats, and the same stressor was not applied consecutively over two days to avoid animals' prediction of the occurrence of stimulation (Table 1). According to our former experiment, about 75-80% CUMS rats could be successfully induced, which was similar to the literature [25], and these CUMS-induced rats were then randomly and equally assigned to the CUMS, SSRI, and groups, followed by respective interventions. Besides, the control group received normal breeding.

**2.3. Intervention.** The whole intervention lasted for 14 days after CUMS modeling [24]. After CUMS modeling, rats in the EA group underwent EA at GV20 (at the midpoint between the auricular apices) and GV29 (at the midpoint between the medial ends of the two eyebrows) [26]. Disposable acupuncture needles (0.30 mm  $\times$  25 mm, Hwato Appliance Factory) were inserted in both acupoints horizontally to 5 mm depth. Following the insertions, the needles were connected to electrodes for electrical simulation with sparse waves (1 mA in electric current, 2 Hz in frequency, and 5 V

in voltage). The stimulus intensity was preferable when the rat's head slightly trembled. The whole EA treatment was implemented for 30 min each time, once per day. Rats in the SSRI group were given paroxetine (1.8 mg/kg/d, i.g.) [27] after 30-minute gentle immobilization. The same volume of saline (per kg as paroxetine) was also applied on the EA group. For the control and CUMS groups, only gentle immobilization and saline administration were used once per day during the same period.

**2.4. Behavioral Analysis.** Three parameters including sucrose preference test (SPT), weighing, and open field test (OFT) were examined at the end of intervention to evaluate the depression-like behavior of rats. The rats were scheduled for euthanasia the day after OFT.

**2.4.1. Sucrose Preference Test (SPT) and Weighing.** The procedure of SPT was performed as described previously [20, 28]. Firstly, rats were trained to adapt 1% sucrose solution (weight in volume ( $w/v$ )) in their home cages with two bottles of 1% sucrose solution placed in each cage. Twenty-four hours later, 1% sucrose in one bottle was replaced with tap water and continued adapting for 24 h. After adaptation, rats were deprived of water and food for 24 h, followed by rats weighing. During the 1 h SPT, rats were housed in individual cages and had free access to two bottles containing 200 ml of sucrose solution (1%  $w/v$ ) and 200 ml of water, respectively. Each bottle was weighed before and after the test, and two bottles were changed randomly to prevent place preference. The sucrose preference was calculated as the percentage of the consumed 1% sucrose solution relative to the total amount of liquid intake. At the end of the test, all animals were returned to their home group housing with normal breeding.

**2.4.2. Open Field Test (OFT).** The OFT is often employed to evaluate the effects of antidepressant treatment in animals [29]. In this study, it was used to measure exploratory behavior and general activity in rats, performed as previous research [20]. The apparatus was a 100 cm  $\times$  100 cm  $\times$  38 cm black wooden box which was kept in an isolated room with normal lighting and temperature. The floor of the arena was divided into 25 cm  $\times$  10 cm  $\times$  10 cm squares. A video recording system was stationed above the apparatus to capture the movement of rats within the box. Subsequently, each rat was placed in the center of the open field without any agitation, and their explorative movement was measured for 5 min using the video recorder. After one test of a rat, the apparatus was cleaned to abolish the odor of the former tested rat. A neutral observer stayed away from the apparatus during the test. When OFT was finished, the video was analyzed using SMART 3.0, and the time in the center area and total distance traveled were assessed.

**2.5. Transmission Electron Microscope (TEM).** Eight rats from each group were anesthetized with 10% chloral hydrate anesthesia (3 ml/kg, intraperitoneal injection), followed by perfusion with a mixture of 2.5% glutaraldehyde and 2.5% paraformaldehyde. Then, the left CA1 of each hippocampal tissue was separated immediately, and immersion fixation

was completed at around 1 mm<sup>3</sup> size. Samples were rinsed in cold phosphate-buffered saline (PBS, 4x for 15 min) and placed in 2.5% glutaraldehyde until the operation of TEM. First, they were immersed in 1% osmium for 1 hour and rinsed in PBS (3x for 15 min). Next, they were immersed in ascending concentrations of acetone (50, 70, and 90%, each for 15 min; 100%, 3x for 15 min). After being immersed in mixed liquor of acetone and Spurr's resin (acetone : Spurr's resin = 1 : 1 for 1 h; acetone : Spurr's resin = 1 : 2 for 2 h), they were quickly immersed in Spurr's resin at room temperature overnight and then embedded in coffin molds in Spurr's resin, curing for 8 h at 70°C in an oven (Shanghai Yiheng, DHG-9053A). 60-nm-thick ultrathin sections were cut (Leica, UC7) and counterstained with saturated aqueous uranyl acetate and Reynolds' lead citrate (3x for 5 min). Sections were photographed with TEM (Hitachi, H-7500) at 10,000x and 40,000x magnifications.

**2.6. Immunohistochemistry (IHC).** For IHC, the left CA1 region of random 24 rats from each group was fixed with 4% paraformaldehyde, embedded in paraffin, and sectioned. After being rehydrated, the samples were immersed with 3% H<sub>2</sub>O<sub>2</sub> at room temperature for 10 min to block endogenous horseradish peroxidase (HRP) activity, and antigen retrieval was performed by microwave for 8 min in citrate buffer. Each section was incubated with normal goat serum in PBS for 30 min at room temperature and then incubated with primary antibody (1:100; anti-Beclin1 antibody, Abcam; anti-LC3 antibody, Abcam) at 4°C overnight. After phosphate-buffered saline (PBS) washing, the slides were then incubated with a corresponding second antibody (Abcam) at room temperature for 30 min and stained with diaminobenzidine (DAB; ChemMate TM DAKO Envision TM Detection Kit, DAKO). The slides were then counterstained with hematoxylin, dehydrated, and mounted. The degree of staining was controlled by microscopic observation (Olympus) with 200x magnification. The IHC scores were calculated by the software ImageJ which showed percent contribution of different grades of positive.

**2.7. Western Blot Analysis.** The left CA1 tissues of random 16 rats from each group were homogenized in lysis buffer, and the lysis process was continued for 30 min at 4°C. After being centrifuged at 12000 rpm for 15 min, the protein contents were determined by bicinchoninic acid protein assay (Beyotime Institute of Biotechnology, Shanghai, China). 20  $\mu$ g of proteins of each sample was loaded into wells of 12% SDS-PAGE gel, electrophoretically separated, and transferred on to PVDF membrane. After being blocked in 5% skim milk/TBST at room temperature for 3 h, the membranes were incubated with specific primary antibodies including anti-Beclin1 (1:1000; Abcam), anti-LC3 (1:2000; Abcam), and anti-GAPDH (1:2000; Proteintech) in incubation boxes at 4°C for 16 h. The membranes were washed with TBST for 3 times with 5 min each before and after the incubation of secondary antibody [1:2000; HRP-conjugated Affinipure Goat Anti-Rabbit IgG (H+L)]. Finally, images were acquired using

TABLE 2: Comparison of SPT, weight, and OFT among 4 groups (mean  $\pm$  SD).

Group	SPT-sucrose preference (%)	Weight (g)	OFT-time in the center area (s)	OFT-total distance traveled (cm)
Control ( $n = 15$ )	80.87 $\pm$ 8.53	441.02 $\pm$ 38.19	18.72 $\pm$ 16.43	4124.67 $\pm$ 941.30
CUMS ( $n = 15$ )	54.05 $\pm$ 22.35*	363.18 $\pm$ 28.32*	0.04 $\pm$ 0.10*	2925.52 $\pm$ 1197.65*
SSRI ( $n = 15$ )	77.15 $\pm$ 7.94 <sup>#</sup>	394.44 $\pm$ 24.40* <sup>#</sup>	12.87 $\pm$ 13.80 <sup>#</sup>	6267.50 $\pm$ 2387.70* <sup>#</sup>
EA ( $n = 15$ )	79.54 $\pm$ 9.08 <sup>#</sup>	388.99 $\pm$ 31.24* <sup>#</sup>	12.17 $\pm$ 17.61 <sup>#</sup>	6287.90 $\pm$ 755.56* <sup>#</sup>
$F$	16.455	4.795	19.310	13.400
$p$	<0.05	0.05	<0.05	<0.05

darkroom development techniques for chemiluminescence (ProteinSimple, FluorChem E, USA).

**2.8. Statistical Analysis.** All data were presented as mean  $\pm$  SD both complied with normal distribution. One-way ANOVA followed by LSD post hoc tests was used to evaluate differences for behavioral analysis, IHC, and TEM results among groups. A  $p$  value < 0.05 was considered to be statistically significant. All calculations were made using SPSS 22.0 and GraphPad Prism 8.0 (GraphPad Software, Inc., San Diego, CA, USA).

### 3. Results

**3.1. Behavior Analysis.** Firstly, excluding the modeling failure, there were 45 remaining rats presented CUMS-induced depressive behaviors according to evaluation of SPT, weight, and OFT, with a successful modeling rate of about 75%. They were then immediately divided into the CUMS, SSRI, and EA groups (15 per group) and accepted different treatments. CUMS models were stable in the course of treatment with significantly different behavioral results compared with the control group ( $p < 0.05$ ). No rats died during the model establishment or intervention period. Secondly, the SSRI and EA groups also showed positive results compared with the CUMS group, which indicated the improvement of depression-like behavior of rats after both treatments ( $p < 0.05$ ), but they were nonsignificantly different between each other ( $p > 0.05$ ) (Table 2 and Figure 1).

Difference among groups was analyzed with one-way ANOVA as normal distribution complied, and LSD was used for a post hoc test with homogeneity of variance satisfied. \* $p < 0.05$  vs. the control group; <sup>#</sup> $p < 0.05$  vs. the CUMS group.

**3.2. TEM.** Autolysosomes (vacuum-like bilayer structures enveloping the cell contents) of five rats from each group were observed through TEM and highlighted by yellow arrows in Figure 2. The size and number both increased in the CUMS group than those in the control group, which proved the activation of autophagy after modeling. Compared with those in the CUMS group, the number and size of autolysosomes in the SSRI and EA groups decreased significantly, but it was hard to distinguish the difference among them from Figure 2.

**3.3. IHC.** With ImageJ, we chose the sum of percent contribution of positive to compare the expression intensity of

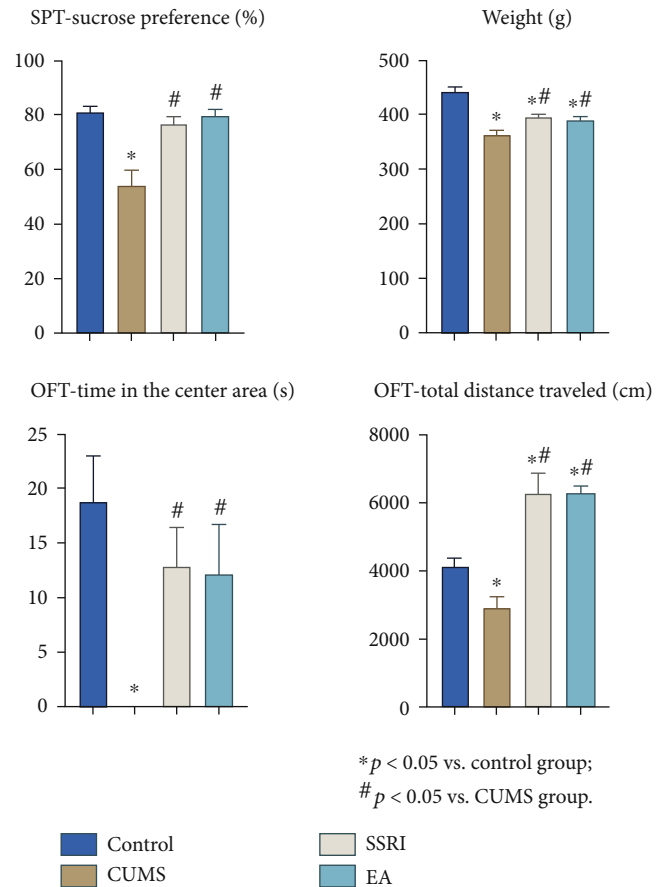


FIGURE 1: Comparison of SPT, weight, and OFT among 4 groups (mean  $\pm$  SEM) (the OFT-time in the center area of the CUMS group was too much shorter than those of the other groups to show in the bar graph, but the specific number is listed in Table 2) ( $n = 15$ ).

two targets in CA1. The difference of Beclin1 and LC3 among groups was significant ( $p < 0.05$ ). During the post hoc test, the CUMS group showed significant higher positive expression of Beclin1 and LC3 than the control group, indicating the activation of autophagy in CA1 after modeling ( $p < 0.05$ ). The Beclin1 level in the SSRI or EA group was higher compared with that in the control group, respectively ( $p < 0.05$ ), but there was no significant difference between these two groups ( $p > 0.05$ ). Moreover, the LC3 level declined after SSRI and EA treatments, and the effect of



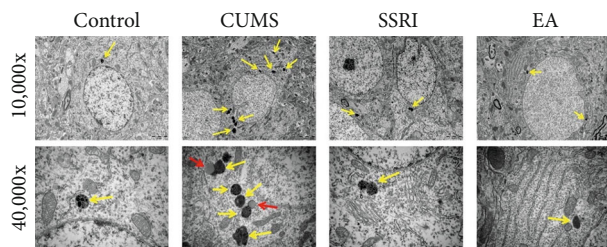


FIGURE 2: Number and size of autolysosomes in hippocampus CA1 neurons in each group (yellow arrows, autolysosomes; red arrows, autophagosomes; magnification, 10,000 $\times$  (2  $\mu$ m) and 40,000 $\times$  (500 nm)) ( $n = 2$ ).

EA in regulating LC3 expression was greater than that of SSRI ( $p < 0.05$ ) (Table 3 and Figure 3).

Difference among groups was analyzed with one-way ANOVA as normal distribution complied, and LSD was used for the post hoc test with homogeneity of variance satisfied. \* $p < 0.05$  vs. the control group; # $p < 0.05$  vs. the CUMS group;  $\Delta p < 0.05$  vs. the SSRI group.

**3.4. Western Blot Analysis.** The difference of relative normalized Beclin1 and LC3-II/LC3-I expression among groups was significant ( $p < 0.05$ ). During the post hoc test, Beclin1 level trend was in accordance with IHC results. The CUMS, SSRI, and EA groups all showed significant higher positive expression of Beclin1 than the control group ( $p < 0.05$ ), but they did not significantly distinguish with each two of them ( $p > 0.05$ ). As for LC3-II/LC3-I, this ratio was significantly higher in the CUMS, SSRI, and EA groups compared with the control group, respectively. LC3-II/LC3-I also declined after EA treatments ( $p < 0.05$ ), which agreed with IHC results. Moreover, the difference between the SSRI and CUMS or EA groups did not reach statistical significance ( $p > 0.05$ ) (Figure 4).

## 4. Discussion

As a widely applied animal model for depression, the CUMS model presents depressive behaviors like anhedonia and decreased locomotor activity. Anhedonia is the core symptom of depression with the characteristic as lacking enjoyment of food in human or animal models. Loss of weight may then result from the reduced food intake. SPT is recognized as a common method to evaluate the anhedonia in animals, and the reduced preference for sucrose in the test is a key indicator of depression in rodents [28]. Besides, the OFT measured locomotor activity, with reduced locomotor activity indicating anxiety-like behaviors associated with depression [30]. Hence, we used SPT, weighing, and OFT in the evaluation of depressive behaviors of CUMS rats in this study. After modeling, the CUMS rats displayed conspicuous depressive-like symptoms such as anhedonia, decline in spontaneous locomotor functions, and weight loss. The results were consistent with findings in previous reports [31], supporting the success of the modeling.

From the results of TEM in our experiment, autolysosomes in the hippocampus neurons observed in CUMS rats

TABLE 3: Positive expression of Beclin1 and LC3 (mean  $\pm$  SD, percent).

Group	Beclin1	LC3
Control ( $n = 6$ )	37.04 $\pm$ 12.87	1.02 $\pm$ 0.46
CUMS ( $n = 6$ )	73.92 $\pm$ 7.63*	5.61 $\pm$ 1.63*
SSRI ( $n = 6$ )	73.27 $\pm$ 1.27*	2.33 $\pm$ 0.90* <sup>#</sup>
EA ( $n = 6$ )	66.40 $\pm$ 11.71*	1.05 $\pm$ 0.61 <sup>#,Δ</sup>
$F$	20.081	27.757
$P$	<0.05	<0.05

were more than those in the control ones. What is more, EA or SSRI also reduced the number and size of autolysosomes compared with the CUMS group. Considering all the results above, SSRI and EA may improve depressive behaviors through impacting the autophagy level of hippocampus neurons. Although there are limited depression researches learning the relationship between autophagy and EA, the correlation of autophagy in the hippocampus and depression has attracted growing attention. Autophagosomes, the form before autolysosomes, were reported to increase in the hippocampus of chronic restraint stress-exposed rats, another widely used depression animal model [32]. Notably, autophagosomes could also exert a protective effect in alleviating hippocampus neuronal apoptosis along with amelioration of depressive-like behaviors [33]. So, the specific mechanism of autolysosomes changes induced by EA in the hippocampus of CUMS rats still waits for further investigation.

Autophagy is essential for basal homeostasis. Beclin1 is a key regulator of autophagy in mammalian cells [34], and LC3 is a reliable marker of autophagosomes [35]. Both expression levels can reflect the autophagy activity of cells. To firstly provide the direct evidence linking the interaction between EA and autophagy to depression, we assessed the expression of autophagic biomarkers, including Beclin1 and LC3, in the CA1 of rats' hippocampus following CUMS.

Given by our study, CUMS rats presented depressive behaviors and enhanced expression of Beclin1 and LC3 according to IHC. When Beclin1 is activated, a lot of membrane sources (the production center of autophagosomes) are formed in the cytoplasm. In the process from phagophore to autolysosomes, LC3-I transferred from the cytoplasm to LC3-II on the membrane of autophagosomes. LC3 functions in autophagy substrate selection and autophagosome biogenesis [36]. Its membrane-located form LC3-II has a positive correlation with the amount of autophagosomes [37], and it is degraded by lysosomal enzyme after autophagosomes fusing with lysosomes into autolysosomes [38]. The higher expression of Beclin1 and LC3 in the CUMS group suggested the activation of autophagy in this depression animal model. In addition, the ratio of LC3-II/LC3-I that closely related to the number of autophagosomes could be tested as additional research to verify the changes of LC3 [39]. In the western blot analysis, the ratio decreased in the EA group after treatment but not in the SSRI group. Hence, both positive results from IHC and western blot analysis supported the effect of EA on LC3 expression in CUMS models.

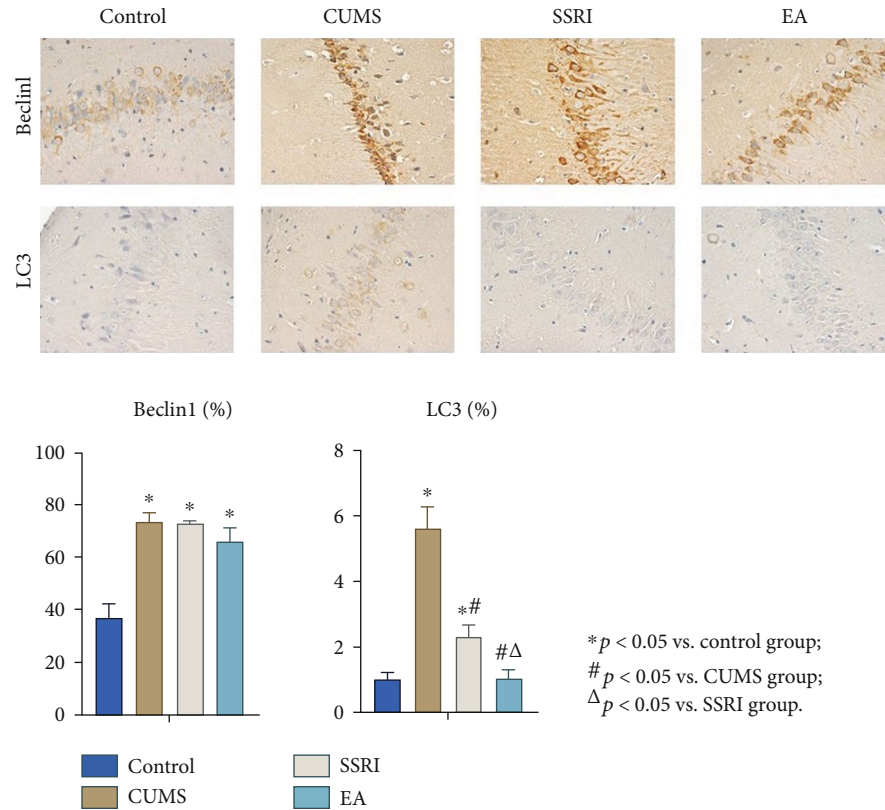


FIGURE 3: Expression of Beclin1 and LC3 in hippocampus CA1 of each group (IHC, 200x magnification; mean  $\pm$  SEM;  $n = 6$ ).

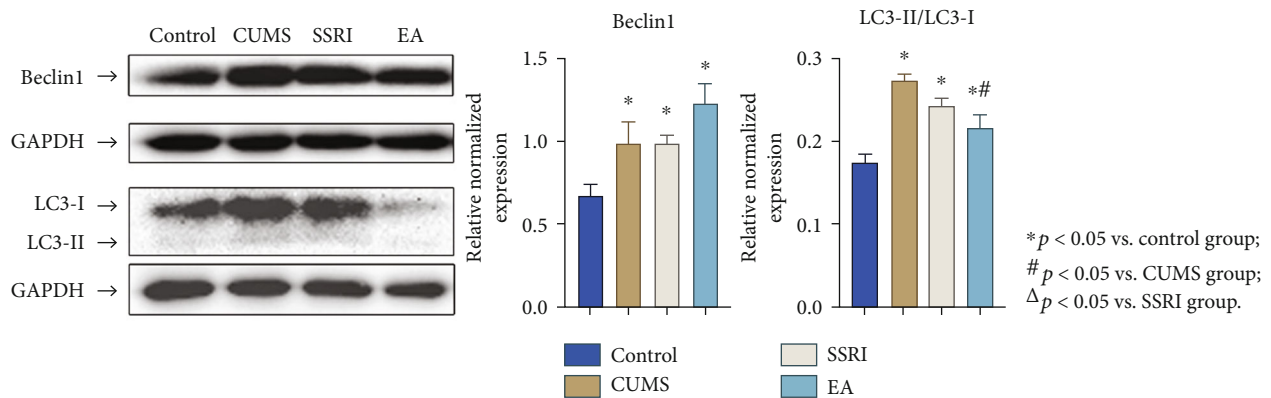


FIGURE 4: Expression of Beclin1 and LC3-II/LC3-I in hippocampus CA1 of each group (relative normalized; mean  $\pm$  SEM;  $n = 4$ ).

Actually, CUMS can either activate the pathway involving Beclin1 and LC3 in hippocampus [40] or inhibit it [14, 15, 41]. In addition, these two markers can also be differently influenced in other models or types of depression. For example, Beclin1 and LC3 were upregulated in electroconvulsive shock-induced depressive rats [42] and downregulated in pain- or LPS-induced depression rats as well as maternal separation rats which were accompanied with depressive behaviors [43–45]. The function of autophagy in the nervous system is still controversial. In the circumstances, the effect of autophagy on depression may be bilateral. For example, hydrogen sulfide, an antidepressant-

like compound for diabetic rats, could improve the depression-like behavior of rats by enhancing hippocampal autophagy through BDNF-TrkB pathway [46], but the similar improvement was explained by opposite mechanism in another research, in which the upregulating BDNF-TrkB pathway was along with the decreasing autophagy in hippocampus [47]. Maybe the effect of autophagy on depression varies from different types or treatments.

One of the major brain areas where EA ameliorates depressive behaviors of animals is the hippocampus, in which several mechanisms have been confirmed, such as synaptic plasticity, neuroinflammation, and neurotransmitter

upregulation [48–50]. However, whether and how autophagy participates in the regulation of EA on depression are unclear yet. Furthermore, apoptosis is closely relevant to autophagy as they, respectively, constitute distinct mechanisms for the turnover or destruction of cytoplasmic structures within cells and of cells within organisms. An apoptosis-related research discovered that acupuncture could improve depressive behaviors of psychological stress-induced depression rats by suppressing oxidative stress-mitochondrial apoptotic pathway in the hippocampus [51]. It is likely that EA could affect autophagy in the hippocampus of depression models.

Treatments that rescued behavioral deficits of CUMS animals by autophagy were mostly based on the Beclin1 and/or LC3 pathway in the hippocampus, accompanied with the changes of autophagosomes or autolysosomes. Animal studies have showed the activation of Beclin1 and LC3-II following fluoxetine treatment in the hippocampus, and this alteration could be observed in microglia [40, 52]. Additionally, some other brain regions were involved in the regulation of autophagy in CUMS animal models, such as the prefrontal cortex, in which andrographolide may produce antidepressant-like effects in CUMS-induced mice by upregulating autophagy [53]. Collecting the evidence above, these mentioned therapies may reverse inhibited autophagy in the hippocampus or other brain areas under CUMS-induced depression state.

EA has been proven to interact with critical autophagic markers or autolysosomes. Although the influence of autophagy in depression is waiting to be verified, EA has shown neural protection against or with autophagy in other neural degenerated diseases. The regulation of acupuncture or EA on autophagy has been mainly discussed in cerebral ischemia reperfusion (CIR). Autophagy is a crucial part in the impairment of CIR and could be improved or suppressed by EA dependent on time in CIR animal models [18, 54, 55], indicating that EA may play a dual role in CIR autophagy. Besides, in central poststroke pain rat models, EA could relieve symptoms by inhibiting autophagy in the hippocampus [56], which could enlighten the study of EA on autophagy in depression.

In this present study, SSRI and EA did not yet influence Beclin1 increase triggered by CUMS, but reduced the level of LC3 in the hippocampus after modeling where EA showed advantage over SSRI. As mentioned above, LC3 is closely relative to the number of autolysosomes; thus, the autolysosome decline from TEM was connected with the lower LC3 level of the EA group than the SSRI or CUMS group. The results of TEM and IHC suggested that EA probably participated in the formation of autolysosomes related with LC3. Furthermore, both Beclin1 and LC3 are involved in the regulation of autophagy intensity and duration [18]. Collecting the different variations of Beclin1 and LC3, we considered that EA took effect on relieving depressive behaviors through inhibition of LC3-involved autolysosomes formation, but not Beclin1.

Although this article is a preliminary observation about EA's influence on the autophagy process in the hippocampus of CUMS rats, many remarkable characteristics of acupuncture therapy have been explained from the perspective of

autophagy mechanism. For example, acupuncture induces an increase in autophagy in the brain by inserting needles into the legs and avoids the difficulty of crossing the blood-brain barrier for conventional drugs [55], which provides a new idea for green medicine.

There are still some limitations in the study. Based on the inconsistent autophagic changes in the hippocampus of CUMS animal models and the close relationship with apoptosis, the neural apoptosis could be added to verify the effect of autophagy. This is a primary research about EA's effect on autophagy in depression models; hence, research about investigation of apoptosis and the specificity of EA with sham-acupoint control is considerable in the future.

## 5. Conclusion

Although the interrelationship among EA, autophagy, and depression is interesting and blank, our data preliminarily provided the evidence that the occurrence of CUMS-induced depression-like behavior may be concerned with autophagy, and EA demonstrated antidepressant effects by partly inhibiting autophagy with the decreased level of LC3 and number of autolysosomes. This study raised the possibility that EA ameliorated depressive behaviors in CUMS rats by suppressing the autophagic level in the hippocampus.

## Data Availability

All data that support the findings are included in the article.

## Conflicts of Interest

The authors declare that there is no conflict of interest regarding the publication of this paper.

## Authors' Contributions

Zhinan Zhang and Xiaowen Cai contributed equally to this work.

## Acknowledgments

This study was supported by the National Natural Science Foundation of China (Grant nos. 81873359 and 81603474), Natural Science Foundation of Guangdong Province (Grant nos. 2016A030313522 and 2016A030310383), Science and Technology Program of Guangzhou (Grant no. 201707010041), and Dean's Funding Project of 2018, Nanfang Hospital, Southern Medical University (Grant no. 2018Z023).

## References

- [1] G. S. Malhi and J. J. Mann, "Depression," *Lancet (London, England)*, vol. 392, no. 10161, pp. 2299–2312, 2018.
- [2] Organization, W H, *Depression and Other Common Mental Disorders: Global Health Estimates*, World Health Organization, 2017.



- [3] J. Jia and W. Le, "Molecular network of neuronal autophagy in the pathophysiology and treatment of depression," *Neuroscience Bulletin*, vol. 31, no. 4, pp. 427–434, 2015.
- [4] S. Barth, D. Glick, and K. F. Macleod, "Autophagy: Assays and artifacts," *The Journal of Pathology*, vol. 221, no. 2, pp. 117–124, 2010.
- [5] S. Saha, D. P. Panigrahi, S. Patil, and S. K. Bhutia, "Autophagy in health and disease: a comprehensive review," *Biomedicine & Pharmacotherapy*, vol. 104, pp. 485–495, 2018.
- [6] P. Ravanan, I. F. Srikumar, and P. Talwar, "Autophagy: the spotlight for cellular stress responses," *Life Sciences*, vol. 188, pp. 53–67, 2017.
- [7] D. A. Slattery and J. F. Cryan, "Modelling depression in animals: at the interface of reward and stress pathways," *Psychopharmacology*, vol. 234, no. 9–10, pp. 1451–1465, 2017.
- [8] X. Xiao, X. Shang, B. Zhai, H. Zhang, and T. Zhang, "Nicotine alleviates chronic stress-induced anxiety and depressive-like behavior and hippocampal neuropathology via regulating autophagy signaling," *Neurochemistry International*, vol. 114, pp. 58–70, 2018.
- [9] H. Woo, C. J. Hong, S. Jung, S. Choe, and S. W. Yu, "Chronic restraint stress induces hippocampal memory deficits by impairing insulin signaling," *Molecular Brain*, vol. 11, no. 1, p. 37, 2018.
- [10] E. Alcocer-Gómez, N. Casas-Barquero, J. Núñez-Vasco, J. M. Navarro-Pando, and P. Bullón, "Psychological status in depressive patients correlates with metabolic gene expression," *CNS neuroscience & Therapeutics*, vol. 23, no. 10, pp. 843–845, 2017.
- [11] N. C. Gassen, J. Hartmann, M. V. Schmidt, and T. Rein, "Fkbp5/fkbp51 enhances autophagy to synergize with antidepressant action," *Autophagy*, vol. 11, no. 3, pp. 578–580, 2015.
- [12] H. Liu, H.-T. Wang, A.-J. Xu, D. Chen, J.-G. Liu, and A. Q. Kan, "Change of autophagy in hippocampal neurons of depression model rats and its mechanism," *Journal of Jilin University*, vol. 39, no. 4, pp. 672–675, 2013.
- [13] Y. Zhou, X. Tao, Z. Wang et al., "Hippocampus metabolic disturbance and autophagy deficiency in olfactory bulbectomized rats and the modulatory effect of fluoxetine," *International Journal of Molecular Sciences*, vol. 20, no. 17, p. 4282, 2019.
- [14] Y. Yang, Z. Hu, X. Du, H. Davies, X. Huo, and M. Fang, "Mir-16 and fluoxetine both reverse autophagic and apoptotic change in chronic unpredictable mild stress model rats," *Frontiers in Neuroscience*, vol. 11, p. 428, 2017.
- [15] X. Huang, H. Wu, R. Jiang et al., "The antidepressant effects of  $\alpha$ -tocopherol are related to activation of autophagy via the ampk/mTOR pathway," *European Journal of Pharmacology*, vol. 833, pp. 1–7, 2018.
- [16] B. Zhao, Z. Li, Y. Wang et al., "Can acupuncture combined with SSRIs improve clinical symptoms and quality of life in patients with depression? Secondary outcomes of a pragmatic randomized controlled trial," *Complementary Therapies in Medicine*, vol. 45, pp. 295–302, 2019.
- [17] T. Tian, Y. Sun, H. Wu et al., "Acupuncture promotes mTOR-independent autophagic clearance of aggregation-prone proteins in mouse brain," *Scientific Reports*, vol. 6, no. 1, p. 19714, 2016.
- [18] Z. Ting, Z. Jianbin, and H. Luqi, "Protective effect of electroacupuncture on neuronal autophagy in perfusion period of cerebral ischemia," *Neuroscience Letters*, vol. 661, pp. 41–45, 2017.
- [19] H. Liu, B. Zhang, X.-W. Li et al., "penetrative needling improves neurological function by up-regulating expression of autophagy related protein lc3 in rats with hemorrhagic stroke," *Acupuncture Research*, vol. 44, no. 9, pp. 637–642, 2019.
- [20] B. Chen, J. Li, Y. Xie et al., "Cang-ai volatile oil improves depressive-like behaviors and regulates da and 5-HT metabolism in the brains of cums-induced rats," *J Ethnopharmacol*, vol. 244, p. 112088, 2019.
- [21] Y. Lu, C. S. Ho, X. Liu et al., "Chronic administration of fluoxetine and pro-inflammatory cytokine change in a rat model of depression," *PLoS One*, vol. 12, no. 10, article e0186700, 2017.
- [22] Y. Lu, C. S. Ho, R. S. McIntyre, W. Wang, and R. C. Ho, "Effects of vortioxetine and fluoxetine on the level of brain derived neurotrophic factors (BDNF) in the hippocampus of chronic unpredictable mild stress-induced depressive rats," *Brain Research Bulletin*, vol. 142, pp. 1–7, 2018.
- [23] Y. Lu, C. S. Ho, R. S. McIntyre, W. Wang, and R. C. Ho, "Ago-melatonin-induced modulation of brain-derived neurotrophic factor (BDNF) in the rat hippocampus," *Life Sciences*, vol. 210, pp. 177–184, 2018.
- [24] Y.-Q. Zhang, X.-B. Wang, R.-R. Xue, X.-X. Gao, and W. Li, "Ginsenoside Rg1 attenuates chronic unpredictable mild stress-induced depressive-like effect via regulating NF- $\kappa$ B/NLRP3 pathway in rats," *Neuroreport*, vol. 30, no. 13, pp. 893–900, 2019.
- [25] P. Willner, "Reliability of the chronic mild stress model of depression: a user survey," *Neurobiology of Stress*, vol. 6, pp. 68–77, 2017.
- [26] J. Cao, Y. Tang, Y. Li, K. Gao, X. Shi, and Z. Li, "Behavioral changes and hippocampus glucose metabolism in app/ps1 transgenic mice via electro-acupuncture at governor vessel acupoints," *Frontiers in Aging Neuroscience*, vol. 9, no. 5, 2017.
- [27] Y. L. Ye, K. Zhong, D. D. Liu et al., "Huanglian-jie-du-tang extract ameliorates depression-like behaviors through BDNF-TrkB-CREB pathway in rats with chronic unpredictable stress," *Evidence-Based Complementary Alternative Medicine*, vol. 2017, article 7903918, 13 pages, 2017.
- [28] M. Y. Liu, C. Y. Yin, L. J. Zhu et al., "Sucrose preference test for measurement of stress-induced anhedonia in mice," *Nature Protocols*, vol. 13, no. 7, pp. 1686–1698, 2018.
- [29] Y. J. Shyong, M. H. Wang, L. W. Kuo et al., "Mesoporous hydroxyapatite as a carrier of olanzapine for long-acting antidepressant treatment in rats with induced depression," *Journal of Control Release*, vol. 255, pp. 62–72, 2017.
- [30] S. Liu, T. Li, H. Liu et al., "Resveratrol exerts antidepressant properties in the chronic unpredictable mild stress model through the regulation of oxidative stress and mTOR pathway in the rat hippocampus and prefrontal cortex," *Behavioural Brain Research*, vol. 302, pp. 191–199, 2016.
- [31] Z. Yan, H. Jiao, X. Ding et al., "Xiaoyaosan improves depressive-like behaviors in mice through regulating apelin-APJ system in hypothalamus," *Molecules*, vol. 23, no. 5, p. 1073, 2018.
- [32] Q. Tian, L. Chen, B. Luo et al., "Hydrogen sulfide antagonizes chronic restraint stress-induced depressive-like behaviors via upregulation of adiponectin," *Frontiers in Psychiatry*, vol. 9, p. 399, 2018.
- [33] M. Wang, Y. Bi, S. Zeng et al., "Modified Xiaoyao San ameliorates depressive-like behaviors by triggering autophagosome



- formation to alleviate neuronal apoptosis,” *Biomedicine & Pharmacotherapy*, vol. 111, pp. 1057–1065, 2019.
- [34] L. Galluzzi, F. Pietrocola, B. Levine, and G. Kroemer, “Metabolic control of autophagy,” *Cell*, vol. 159, no. 6, pp. 1263–1276, 2014.
- [35] Y. Feng, S. K. Backues, M. Baba, J. M. Heo, J. W. Harper, and D. J. Klionsky, “Phosphorylation of atg9 regulates movement to the phagophore assembly site and the rate of autophagosome formation,” *Autophagy*, vol. 12, no. 4, pp. 648–658, 2016.
- [36] D. J. Klionsky, K. Abdelmohsen, A. Abe et al., “Guidelines for the use and interpretation of assays for monitoring autophagy (3rd edition),” *Autophagy*, vol. 12, no. 1, 2016.
- [37] I. Tanida, “Autophagosome formation and molecular mechanism of autophagy,” *Antioxidants & Redox Signaling*, vol. 14, no. 11, pp. 2201–2214, 2011.
- [38] I. Tanida, T. Ueno, E. Kominami, and V. Deretic, “Lc3 and autophagy,” in *Autophagosome and phagosome*, pp. 77–88, Humana Press, Totowa, NJ, 2008.
- [39] X. Li, M.-H. Wang, C. Qin, W. H. Fan, D. S. Tian, and J. L. Liu, “Fingolimod suppresses neuronal autophagy through the mtor/p70s6k pathway and alleviates ischemic brain damage in mice,” *PLoS One*, vol. 12, no. 11, p. e0188748, 2017.
- [40] P. Wang, Y.-B. Feng, L. Wang et al., “Interleukin-6: its role and mechanisms in rescuing depression-like behaviors in rat models of depression,” *Brain, Behavior, and Immunity*, vol. 82, pp. 106–121, 2019.
- [41] Z. Huang, X. Huang, Q. Wang et al., “Extract of euryale ferox salisb exerts antidepressant effects and regulates autophagy through the adenosine monophosphate-activated protein kinase-unc-51-like kinase 1 pathway,” *IUBMB life*, vol. 70, no. 4, pp. 300–309, 2018.
- [42] P. Li, X.-C. Hao, J. Luo, F. Lv, K. Wei, and S. Min, “Propofol mitigates learning and memory impairment after electroconvulsive shock in depressed rats by inhibiting autophagy in the hippocampus,” *Medical Science Monitor : International Medical Journal of Experimental and Clinical Research*, vol. 22, pp. 1702–1708, 2016.
- [43] J. Zong, X. Liao, B. Ren, and Z. Wang, “The antidepressant effects of rosiglitazone on rats with depression induced by neuropathic pain,” *Life Sciences*, vol. 203, pp. 315–322, 2018.
- [44] C. Liu, S. Hao, M. Zhu, Y. Wang, T. Zhang, and Z. Yang, “Maternal separation induces different autophagic responses in the hippocampus and prefrontal cortex of adult rats,” *Neuroscience*, vol. 374, pp. 287–294, 2018.
- [45] P. Jiang, Y. Guo, R. Dang et al., “Salvianolic acid b protects against lipopolysaccharide-induced behavioral deficits and neuroinflammatory response: involvement of autophagy and nlrp3 inflammasome,” *Journal of Neuroinflammation*, vol. 14, no. 1, p. 239, 2017.
- [46] H.-Y. Liu, H.-J. Wei, L. Wu et al., “Bdnf-trkb pathway mediates antidepressant-like roles of H2S in diabetic rats via promoting hippocampal autophagy,” *Clinical and Experimental Pharmacology & Physiology*, vol. 47, no. 2, pp. 302–312, 2019.
- [47] X. Song, B. Liu, L. Cui et al., “Silibinin ameliorates anxiety/depression-like behaviors in amyloid  $\beta$ -treated rats by upregulating bdnf/trkb pathway and attenuating autophagy in hippocampus,” *Physiology & Behavior*, vol. 179, pp. 487–493, 2017.
- [48] X. Han, H. Wu, P. Yin et al., “Electroacupuncture restores hippocampal synaptic plasticity via modulation of 5-HT receptors in a rat model of depression,” *Brain Research Bulletin*, vol. 139, pp. 256–262, 2018.
- [49] N. Yue, B. Li, L. Yang et al., “Electro-acupuncture alleviates chronic unpredictable stress-induced depressive- and anxiety-like behavior and hippocampal neuroinflammation in rat model of depression,” *Frontiers in Molecular Neuroscience*, vol. 11, p. 149, 2018.
- [50] J. Zhao, H. Tian, H. Song et al., “Effect of electroacupuncture on reuptake of serotonin via mirna-16 expression in a rat model of depression,” *Evidence-based Complementary and Alternative Medicine : eCAM*, vol. 2019, article 7124318, pp. 1–6, 2019.
- [51] Y. Sun, Y. Tu, Y. Guo et al., “Acupuncture improved depressive behavior by regulating expression of hippocampal apoptosis-related factors in psychological stress-induced depression rats,” *Acupuncture Research*, vol. 44, no. 6, pp. 412–418, 2019.
- [52] X. Tan, X. Du, Y. Jiang, B. O. A. Botchway, Z. Hu, and M. Fang, “Inhibition of autophagy in microglia alters depressive-like behavior via bdnf pathway in postpartum depression,” *Frontiers in Psychiatry*, vol. 9, p. 434, 2018.
- [53] J. Geng, J. Liu, X. Yuan, W. Liu, and W. Guo, “Andrographolide triggers autophagy-mediated inflammation inhibition and attenuates chronic unpredictable mild stress (cums)-induced depressive-like behavior in mice,” *Toxicology and Applied Pharmacology*, vol. 379, p. 114688, 2019.
- [54] Z. Wu, Z. Zou, R. Zou, X. Zhou, and S. Cui, “Electroacupuncture pretreatment induces tolerance against cerebral ischemia/reperfusion injury through inhibition of the autophagy pathway,” *Molecular Medicine Reports*, vol. 11, no. 6, pp. 4438–4446, 2015.
- [55] Y.-G. Huang, S.-B. Yang, L.-P. Du, S.-J. Cai, Z.-T. Feng, and Z.-G. Mei, “electroacupuncture pretreatment alleviated cerebral ischemia-reperfusion injury via suppressing autophagy in cerebral cortex tissue in rats,” *Acupuncture Research*, vol. 44, no. 12, pp. 867–872, 2019.
- [56] L. Zheng, X.-Y. Li, F.-Z. Huang et al., “Effect of electroacupuncture on relieving central post-stroke pain by inhibiting autophagy in the hippocampus,” *Brain Research*, vol. 1733, p. 146680, 2020.

## Research Article

# Electroacupuncture on Trigeminal Nerve-Innervated Acupoints Ameliorates Poststroke Cognitive Impairment in Rats with Middle Cerebral Artery Occlusion: Involvement of Neuroprotection and Synaptic Plasticity

Yu Zheng,<sup>1</sup> Zongshi Qin,<sup>1</sup> Bun Tsoi,<sup>1</sup> Jiangang Shen,<sup>1</sup> and Zhang-Jin Zhang <sup>1,2</sup>

<sup>1</sup>School of Chinese Medicine, LKS Faculty of Medicine, The University of Hong Kong, Hong Kong, China

<sup>2</sup>Department of Chinese Medicine, The University of Hong Kong Shenzhen Hospital (HKU-SZH), Shenzhen, Guangdong 518053, China

Correspondence should be addressed to Zhang-Jin Zhang; zhangzj@hku.hk

Received 8 June 2020; Revised 13 August 2020; Accepted 18 August 2020; Published 7 September 2020

Academic Editor: Yongjun Chen

Copyright © 2020 Yu Zheng et al. This is an open access article distributed under the Creative Commons Attribution License, which permits unrestricted use, distribution, and reproduction in any medium, provided the original work is properly cited.

Poststroke cognitive impairment (PSCI) is a severe sequela of stroke. There are no effective therapeutic options for it. In this study, we evaluated whether electroacupuncture (EA) on the trigeminal nerve-innervated acupoints could alleviate PSCI and identified the mechanisms in an animal model. The male Sprague-Dawley rat middle cerebral artery occlusion (MCAO) model was used in our study. EA was conducted on the two scalp acupoints, *EX-HN3* (*Yintang*) and *GV20* (*Baihui*), innervated by the trigeminal nerve, for 14 sessions, daily. Morris water maze and novel object recognition were used to evaluate the animal's cognitive performance. Neuroprotection and synaptic plasticity biomarkers were analyzed in brain tissues. Ischemia-reperfusion (I/R) injury significantly impaired spatial and cognition memory, while EA obviously reversed cognitive deterioration to the control level in the two cognitive paradigms. Moreover, EA reversed the I/R injury-induced decrease of brain-derived neurotrophic factor, tyrosine kinase B, N-methyl-D-aspartic acid receptor 1,  $\alpha$ -amino-3-hydroxy-5-methyl-4-isoxazole propionic acid receptor,  $\gamma$ -aminobutyric acid type A receptors,  $Ca^{2+}$ /calmodulin-dependent protein kinase II, neuronal nuclei, and postsynaptic density protein 95 expression in the prefrontal cortex and hippocampus. These results suggest that EA on the trigeminal nerve-innervated acupoints is an effective therapy for PSCI, in association with mediating neuroprotection and synaptic plasticity in related brain regions in the MCAO rat model.

## 1. Introduction

Stroke is the second leading cause of disability-related death worldwide [1]. Increasing numbers of stroke patients suffer from poststroke cognitive impairment (PSCI), characterized by poor performance on abstract thinking, memory, orientation, and similar functions. However, the mechanism of PSCI has not been fully elucidated. Thus, the therapeutic options for it are limited. Some commonly used drugs in Alzheimer's disease (AD) have shown positive effects in PSCI patients, such as cholinesterase inhibitors in which one of them is donepezil [2]. But the benefits in global and daily cognitive

function are inconsistent, making it difficult to assess the efficacy [3].

In cerebral ischemia, multiple pathophysiological changes can be observed, including brain edema, neuronal loss, and changes in synaptic plasticity [4]. Most synapses are found in the dendrites, which are the primary determinants of neuronal integration and information processing [5]. The primary activities of the neurotrophic factor are improving synaptic transfer, promoting synaptic plasticity, developing synaptogenesis, and neuroprotection, which could ameliorate synaptic dysfunction [6]. Synaptic plasticity can also be altered by changing the quantity of synaptic

neurotransmitter receptors [7], such as N-methyl-D-aspartate receptor (NMDAR),  $\alpha$ -amino-3-hydroxy-5-methyl-4-isoxazole propionic acid receptor (AMPA), and  $\gamma$ -aminobutyric acid type A receptor (GABA<sub>A</sub>R) which are associated with neuronal development, synaptic plasticity, learning, and memory [8, 9]. Note that NMDAR is activated by Ca<sup>2+</sup> influx [10]. Therefore, the intracellular Ca<sup>2+</sup>/calmodulin-dependent protein kinase II (CaMKII) is also a critical molecular determinant of neuroprotection and cognitive function [11].

The hippocampus, one of the most intensely studied areas of the brain, is assumed to be involved in spatial memory [12]. In addition to spatial memory, nonspatial recognition memory is the ability to distinguish whether something is familiar or not. Evidence from human neuroimaging has indicated that the prefrontal cortex (PFC) contributes to recognition memory [13, 14]. Both the hippocampus and PFC have a strong association with cognitive function in different kinds of memories, which have been chosen to be the related brain regions in our study.

In the past decades, complementary medicine has become popular in clinical services and one of them is acupuncture. Acupuncture is gradually gaining popularity for the treatment of neurological diseases, including vascular dementia [15], vascular cognitive impairment no dementia [16], PSCI [17], and stroke [18]. However, more evidence is needed to evaluate its clinical effects. We have explored a novel acupuncture regimen named electroacupuncture trigeminal nerve stimulation (EA/TNS) [19]. Recently, we have published one directly related clinical trials of EA/TNS on PSCI patients, suggesting that EA on forehead acupoints could reduce cognitive deterioration of stroke patients [20]. We want to explore the mechanism of it through this study.

Therefore, we hypothesize that acupuncture could reverse PSCI in animal models by neuroprotection and regulating synaptic plasticity in the hippocampus and PFC. One classical PSCI animal model (middle cerebral artery occlusion (MCAO)) was used in our study. Corresponding behavior tests were conducted to evaluate cognitive performance. Biomarkers for neuroprotective activity and synaptic plasticity-related proteins were tested.

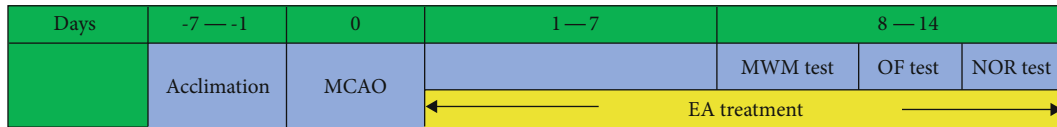
## 2. Materials and Methods

**2.1. Animals and Experimental Procedure.** The experiment protocol was approved by the Committee on the Use of Live Animals in Teaching and Research (CULATR: 4840-18) of LKS Faculty of Medicine of the University of Hong Kong. The male Sprague-Dawley rats weighing  $270 \pm 20$  g were housed three to four per cage and maintained on a 12 h light/dark cycle at 23°C with water and food available ad libitum. Animals that were dying before the experimental endpoint were replaced to ensure  $n = 10$  each group for quantification according to some previous studies [21, 22]. Body weight was monitored during the whole experiment. The whole experimental procedure was conducted in the lab animal unit (LAU) of the University of Hong Kong, and the animals were monitored by a veterinarian every day to assess their welfare. The whole experimental timeline is shown in Figure 1.

**2.2. MCAO Procedure.** The MCAO operation was established according to the previous protocol [23]. Briefly, rats were anaesthetized with 4% isoflurane (Abbott, IL, USA) and maintained at 2% isoflurane via inhalation. Rats were then placed on a warm pad to maintain body temperature. Under an operating microscope, after creating a 2 cm width incision in the neck, the common carotid artery (CCA) was located under the muscles. The CCA, internal carotid artery (ICA), and external carotid artery (ECA) were separated and ligated with a 6/0 nylon thread (Ningbo Medical Needle Co. Ltd., Ningbo, China) under an operating microscope. A nylon thread with a diameter of 0.36 mm with a silicone tip (L3600, Jialing Co. Ltd., Guangzhou, China) was inserted into the ICA from a stump on the ECA. The thread bolt was set into the bifurcation point of the left middle cerebral artery (MCA), inducing the blockage of blood flow. The CCA was transiently ligated during these processes. After 2 hours of occlusion, the bolt was taken out such that the CCA was unobstructed to allow blood reperfusion to the ischemic area. The muscle layer was sutured with a 5/0 polyglactin suture, and the layers were incised with a 3/0 nylon suture. Sham-operated rats were subjected to the same procedure as above without suture insertion into the MCA. All rats were kept on the warm pad until they awoke when they were returned to their cages. Liquid food was provided if needed. Intraoperative monitoring (IOM) forms were required during the operation.

**2.3. Treatment.** After 24 h recovery from the operation, in the EA group, acupuncture needles ( $0.25 \times 15$  mm, MOCM, China) were inserted tangentially to the skin into the acupoints, *EX-HN3 (Yintang)* and *GV20 (Baihui)* to a depth of 10 mm. Electroacupuncture on these two acupoints is the most commonly used regimen in the acupuncture treatment of various psychiatric disorders [24]. The needle handles were taped onto the surface at the two acupoints. The rats could move freely in the box during the treatment (Supplementary File 1). The needles were connected to the output terminals of the electroacupuncture instrument (ITO Physiotherapy & Rehabilitation Co., Tokyo, Japan) with continuous-wave stimulation at a frequency of 2 Hz, intensity of 1 mA, pulse width of 100  $\mu$ s for 10 min, for 14 days. The determination of the low frequency is used because it could exert broader modulatory effects on central neurochemical systems compared to that of the high frequency and has been widely used in clinical practice and animal studies [25]. The same wire stabilization without acupuncture needle procedure was used during the treatment, to minimize potential confounders in the model and sham-operated groups. As such, all three groups of animals experienced similar handling-induced stress. All EA treatment was conducted in the morning.

**2.4. Behavioral Test.** The Morris water maze and novel object recognition tests were performed to evaluate rats' spatial learning and memory and cognition memory abilities, respectively. The open field test was used in this research to evaluate the anxiety level and locomotor level. All testing was conducted in the morning, videotaped, and analyzed with video tracking software (EthoVision, Noldus, Netherlands).



MCAO: middle cerebral artery occlusion

EA: electroacupuncture

MWM: morris water maze

NOR: novel object recognition

OF: open field

FIGURE 1: The experimental timeline.

**2.4.1. Morris Water Maze Test.** The water maze test was conducted in a circular diameter of a 150 cm tank with a height of 50 cm water. Four different markers, equally spaced along the circumference of the tank, were pasted on the tank to divide it into 4 quadrants. Subsequently, water at  $24 \pm 2^\circ\text{C}$  was poured into the water maze. The tank was positioned in a well-lit testing room. The test was conducted for six consecutive days within two parts, training and probe testing. On the first day, a transparent cylinder platform was above the water level so that the rat could find that there exist a platform in the tank and posited in one quadrant. The rat in each group facing the wall was lowered gently into the water for free swimming for 60 seconds twice, respectively, and randomly selected from the other three quadrants. On the second to the fifth day, the platform was submerged and hidden from the rat's view but still in the same quadrant as the first day. The similar layout and training method would be employed. If the rat could find and rest on the platform within 60 seconds, the time would be recorded. If the rat could not find the platform within 60 seconds, it would be guided to the platform for 10 seconds, and the time would be recorded as 60 seconds. The average time was recorded in these two training.

The probe test was carried out one day after the last training trial. The platform was removed, and the rat would be placed in a new start position for freely swimming 60 seconds. The duration spent in the targeted quadrant in which the arena platform was located and the frequency into the targeted quadrant was recorded.

After each day swimming test, the rats would be dried and put under an infrared lamp to keep them warm.

**2.4.2. Novel Object Recognition Test.** The apparatus is a  $100 \times 100 \times 60$  cm Plexiglas arena with black walls and floor. During the training phase, the rat has encountered two equal sample objects (cube with water, made of plastic) in opposite corners for 10 min. 24 hours later, the rat was returned to the same apparatus and presented with a familiar object and a novel object (cylinder with water, made of plastic) for 10 min. Exploration is defined as exploring the object at a distance  $\leq 2$  cm or touching with its nose. The total exploring time for objects was calculated, and the discrimination index was calculated and analyzed through the following formula [26]:

$$\text{Index} = \frac{(\text{Time spent exploring novel object} - \text{time spent exploring unchanged object})}{(\text{Time spent exploring novel object} + \text{time spent exploring unchanged object})} \quad (1)$$

**2.4.3. Open Field Test.** The open field apparatus is a  $100 \times 100 \times 60$  cm Plexiglas arena with black walls and floor with a  $30 \times 30$  cm central zone. Testing followed in a dim-light condition without the presence of experimenters. The total duration time between the central and surrounding zones was recorded in a 10 min test period. The apparatus was cleaned with 75% alcohol between tests.

**2.5. Tissue Preparation and Sections.** The rats were transcranially perfused with PBS under anesthesia to collect brain tissue for further examination after the above behavior tests. The hippocampus and PFC were extracted with radioimmuno-precipitation assay (RIPA) buffer (Sigma-Aldrich, USA) supplemented with 1% protein inhibitor phenylmethanesulfonyl fluoride (PMSF, Sigma-Aldrich, USA). After centrifugation, the supernatants were collected for Western blot.

**2.6. Western Blot Analysis.** The mentioned supernatants were analyzed according to the standard Western blot protocol. Equal amounts of proteins were separated by 10% SDS-PAGE gel, transferred onto polyvinylidene difluoride membranes (PVDF,  $0.22 \mu\text{M}$ , Bio-Rad Laboratories, Inc.), and blocked with 5% BSA blocking buffer. Immunodetection was performed with primary antibodies against PSD-95 (1:2000, Abcam), NeuN, AMPAR (1:2000, Cell Signaling Technology),  $\beta$ -actin (1:5000, Cell Signaling Technology), CaMKII, BDNF, GABA<sub>A</sub>R, NMDAR1, and TrkB (1:2000, Santa Cruz Biotechnology, Inc.) at  $4^\circ\text{C}$  overnight. This was followed by coinubation with related secondary antibodies for 2 h at  $4^\circ\text{C}$ . Bands were detected by enhanced chemiluminescence staining (GE Healthcare, IL, USA). The images were captured by Gel-Doc System (Bio-Rad, Laboratories, Inc.). The intensity of protein bands was quantified by scanning densitometry with Image Lab 5.1 software (Bio-Rad, Laboratories, Inc.).

**2.7. Immunofluorescence.** After phosphate-buffered saline perfusion under anesthesia, the rat was continuously perfused with 4% paraformaldehyde (PFA), and the whole brain was removed and fixed in 4% PFA for at least one week. Then, the brains were immersed with 30% sucrose solution for dehydration until the tissue reached the bottom of the tube totally at  $4^\circ\text{C}$ . The fixed and dehydrated brain was mounted with OCT compound (Leica, Germany), and coronal brain sections ( $30 \mu\text{m}$  thick) were cut using a microtome cryostat (Leica, Germany) at  $-20^\circ\text{C}$ . The cerebral slices were blocked for 1 hour and incubated at  $4^\circ\text{C}$  overnight in the



following primary antibodies: mouse anti-NeuN (1:200, Millipore) and rabbit anti-PSD-95 (1:200, Cell signaling technology). The slices were then incubated with fluorescent-dye-conjugated secondary antibodies (DyLight 594-conjugated goat anti-mouse, 1:200, Abcam; DyLight 488-conjugated goat anti-rabbit, 1:200, Invitrogen) for 1 h at room temperature. The slides were stained with 4',6-diamidino-2-phenylindole (DAPI) for 15 min. Images were captured using a Zeiss confocal microscope (Zeiss, LSM 780, Germany).

**2.8. Statistical Analysis.** Values were expressed as the mean  $\pm$  standard error of the mean and subjected to one-way analysis of variance (ANOVA) followed by Dunnett's multiple comparison test for multiple comparisons to detect a between-group statistical difference in behavioral variables (duration in the water maze test, novel object recognition test, and open field test), using Western blot analysis. Two-way ANOVA was used for the body weight during the 5-day training latency data of water maze. The group, time point, and the interaction between the group and time point were treated as fixed effects. GraphPad Prism 7.0 software was used for the statistical analysis. Statistical significance was defined as  $p < 0.05$  with a two-sided test.

### 3. Results

**3.1. Body Weight Change during the Experiment.** Firstly, we investigated the effect of EA on the recovery of I/R injury rats, especially on the body weight. The MCAO operation induced body weight loss (Figure 2). During the whole treatment period, a significant between-group difference ( $F_{2,378} = 258.7$ ,  $p < 0.0001$ ), not only to the time effect ( $F_{13,378} = 7.54$ ,  $p < 0.0001$ ) but also to the interaction effect between group and time, is detected ( $F_{26,378} = 2.534$ ,  $p < 0.0001$ ), while the body weight increased significantly in the EA group compared to the model group during most of the treatment days.

**3.2. Cognitive Performance in the Water Maze.** Then, we explored one of the main effect indicators, spatial learning and memory ability, of rat by the Morris water maze test. During the 5-day training latency data of the water maze, two-way ANOVA revealed that there is a significant between-group difference ( $F_{2,135} = 19.07$ ,  $p < 0.0001$ ), in either time effect ( $F_{4,135} = 13.89$ ,  $p < 0.0001$ ). From training day 2 to day 4, a significant difference between the model and control group has been found ( $p_{\text{day}2} = 0.0175$ ,  $p_{\text{day}3} = 0.0171$ , and  $p_{\text{day}4} = 0.0003$ ), but no difference between the model and EA treatment group ( $p_{\text{day}2} = 0.8896$ ,  $p_{\text{day}3} = 0.9579$ , and  $p_{\text{day}4} = 0.059$ ). At day 5, multiple comparisons further showed that significantly longer latency was found in the comparison between the model group and the control group ( $p = 0.0068$ ) and the EA treatment group ( $p = 0.025$ ). No interaction effect between group and time is detected ( $F_{8,135} = 1.18$ ,  $p = 0.3157$ ). Significant effects were revealed on the duration spent in the targeted quadrant among these groups after one-way ANOVA ( $F_{2,27} = 11.69$ ,  $p = 0.0002$ ).

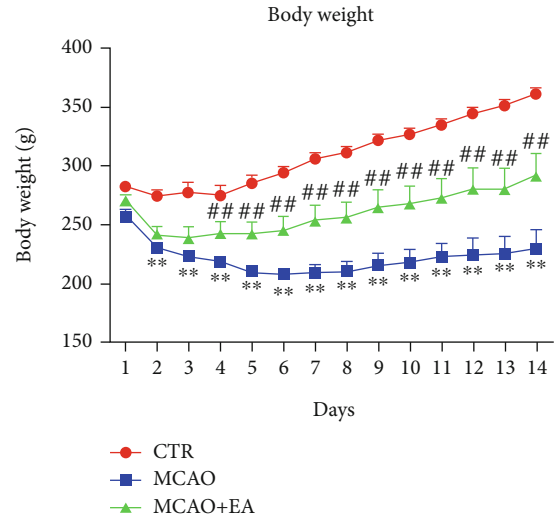


FIGURE 2: Body weight change during the experiment. Data are expressed as mean  $\pm$  SEM, where \*\* $p < 0.01$  compared to the control group and ## $p < 0.01$  compared to the model group ( $n = 10$  each group). CTR: control; MCAO: middle cerebral artery occlusion; EA: electroacupuncture.

Dunnett's multiple comparisons indicated that operation decreased the time in the quadrant compared to the control group ( $p = 0.0001$ ), while EA could apparently increase it compared to the MCAO group. But there is no significant difference in frequency in the targeted quadrant ( $F_{2,27} = 0.8151$ ,  $p = 0.4532$ ) and velocity ( $F_{2,27} = 3.195$ ,  $p = 0.0568$ ) in the probe test ( $p = 0.0087$ ) (Figure 3). The results above indicate that there is a decline in the spatial learning and memory in the MCAO group and could be reversed by EA treatment.

**3.3. Cognitive Performance in Novel Object Recognition.** Unlike orientation in the Morris water maze test, the novel object recognition test uses the innate animal preference for novelty, if they could recognize the novel object compared to the familiar objects [26]. This function is dominated by the PFC rather than by the hippocampus in the water maze test [27]. In the novel object recognition test, one-way ANOVA indicated significant effects in the discrimination index ( $F_{2,27} = 4.388$ ,  $p = 0.0224$ ). The discrimination index of the MCAO group was negative, which means the rats in this group preferred to explore the familiar object than the control ( $p = 0.0332$ ), and EA could increase this index compared to the MCAO group ( $p = 0.0273$ ). These results indicate that the recognition function is affected in the MCAO group, and EA could ameliorate this dysfunction. However, there is no difference in the total exploring time ( $F_{2,27} = 1.218$ ,  $p = 0.3115$ ) (Figure 4), indicating that there is no neophobia among these groups.

**3.4. Anxiety Level in the Open Field Test.** It has been indicated that anxiety could disrupt cognitive function [28]. Therefore, we determined whether these operations, including the MCAO surgical operation and EA treatment, would influence the rats' anxiety. The open field test is a well-known

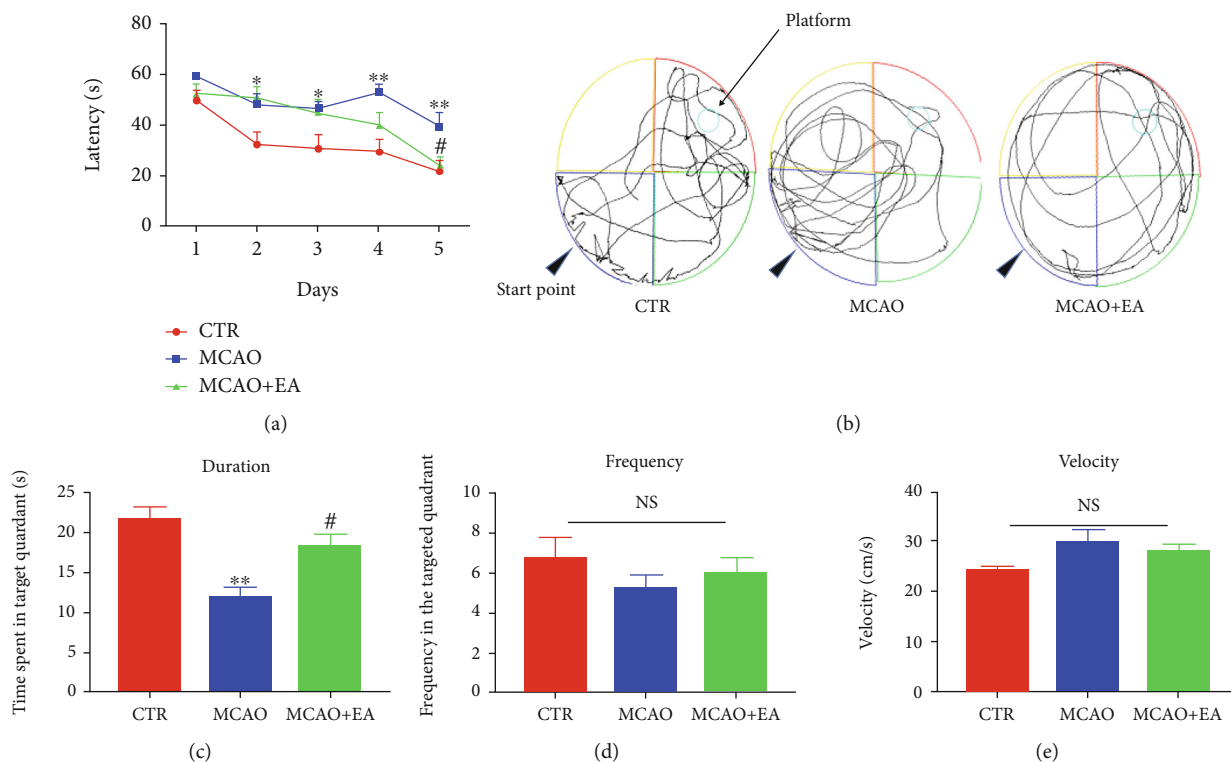


FIGURE 3: Effects of the MCAO and EA in the water maze test. Escape latency to the invisible platform in the training phase (a), representative swimming track (b), time spent in targeted quadrant (c), frequency in the targeted quadrant (d), and velocity in the water maze (e). Data are expressed as mean ± SEM, where \* $p < 0.05$  and \*\* $p < 0.01$  compared to the control group and # $p < 0.05$  compared to the MCAO group ( $n = 10$  each group). NS: no significance; CTR: control; MCAO: middle cerebral artery occlusion; EA: electroacupuncture.

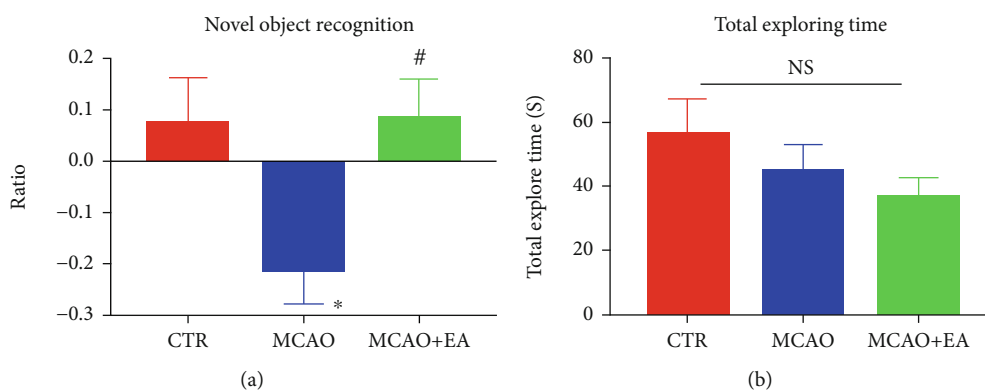


FIGURE 4: Effects of the MCAO and EA in the novel object recognition test. The discrimination index of the novel object (a). Negative ratio means the rats preferred to explore the familiar object rather than the novel object. Total exploring time in test phases (b). Data are expressed as mean ± SEM, where \* $p < 0.05$ , compared to the control group, and # $p < 0.05$  compared to the MCAO group ( $n = 10$  each group). NS: no significance; CTR: control; MCAO: middle cerebral artery occlusion; EA: electroacupuncture.

behavioral test to assess rodents' anxiety [29]. Typically, rodents prefer to stay near the walls rather than the central region while exploring the box, a behavior called thigmotaxis. Spending less time in the periphery is a sign of anxiolysis [30]. Results showed that no significant differences were found in the time spent ( $F_{2,27} = 1.578, p = 0.2248$ ) and frequency in the central zone ( $F_{2,27} = 0.8632, p = 0.4331$ ) and total distance travelled ( $F_{2,27} = 0.09577, p = 0.9090$ ) in the open field test (Figure 5), indicating that the surgery and

EA treatment affect neither anxiety level nor locomotor function.

3.5. The Expression of Biomarkers for Neuroprotective Activity and Functional Neuroplasticity in Brain Tissues. Summarizing the above behavioral test results, EA treatment could ameliorate the cognitive function. Molecular mechanism would be explored to understand the underlying mechanisms. There are 6 related biomarker expressions detected

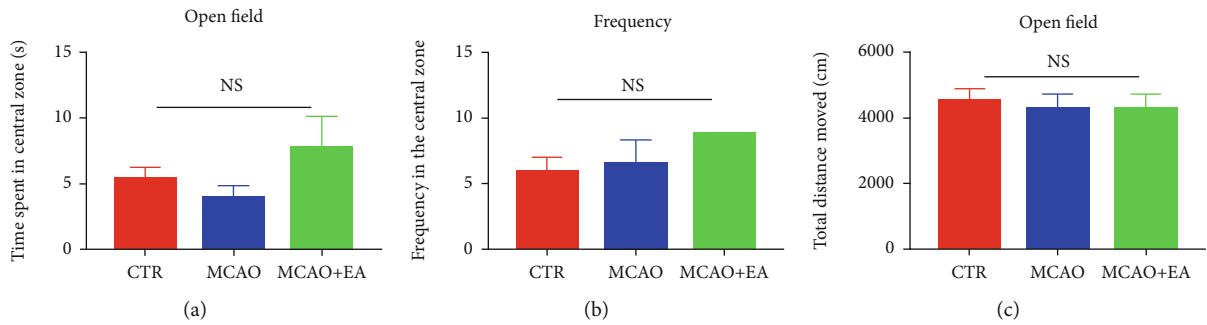


FIGURE 5: Effects of the MCAO and EA in the open field test. Time spent in the central zone (a), frequency in the central zone (b), and total distance moved (c). Data are expressed as mean  $\pm$  SEM ( $n = 10$  each group). NS: no significance; CTR: control; MCAO: middle cerebral artery occlusion; EA: electroacupuncture.

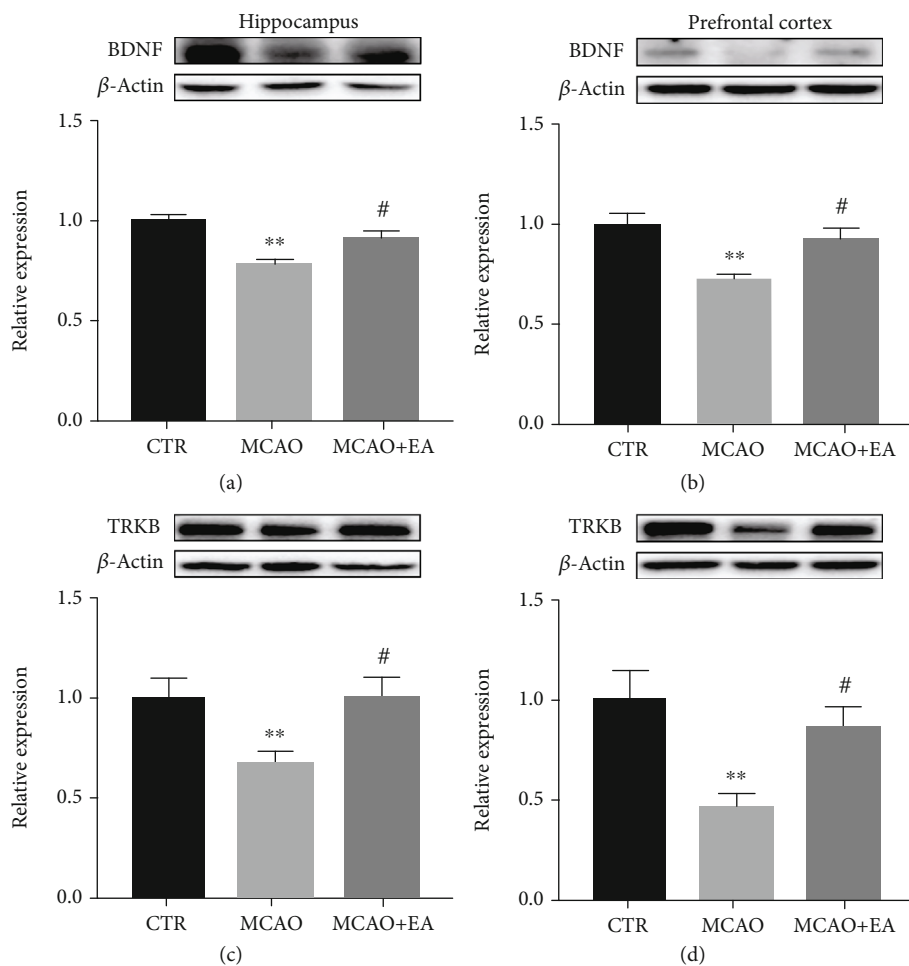


FIGURE 6: Effects of the MCAO and EA in neuroprotective-related proteins. BDNF (a, b) and TrkB (c, d) expressions in the hippocampus and PFC. Value is expressed as mean  $\pm$  SEM, where  $*p < 0.05$  and  $**p < 0.01$  compared to control group and  $\#p < 0.05$  compared to the MCAO group ( $n \geq 5$  each group). CTR: control; MCAO: middle cerebral artery occlusion; EA: electroacupuncture.

in the hippocampus and PFC with Western blot. These biomarkers were the proteins on the BDNF/TrkB signaling pathway as well as neurotransmitter receptors and its downstream protein.

One-way ANOVA revealed marked effects on the BDNF/TrkB signaling pathway in the hippocampus

( $F_{2,21} \geq 4.134$ ,  $p \leq 0.0306$ ) and in the PFC ( $F_{2,15} \geq 5.901$ ,  $p \leq 0.0129$ ) (Figure 6). The MCAO surgery significantly downregulated the expression of these two proteins in both brain regions than the control group ( $p < 0.0421$ ). However, the EA treatment could reverse these biomarker levels almost back to the control group level ( $p < 0.0461$ ).

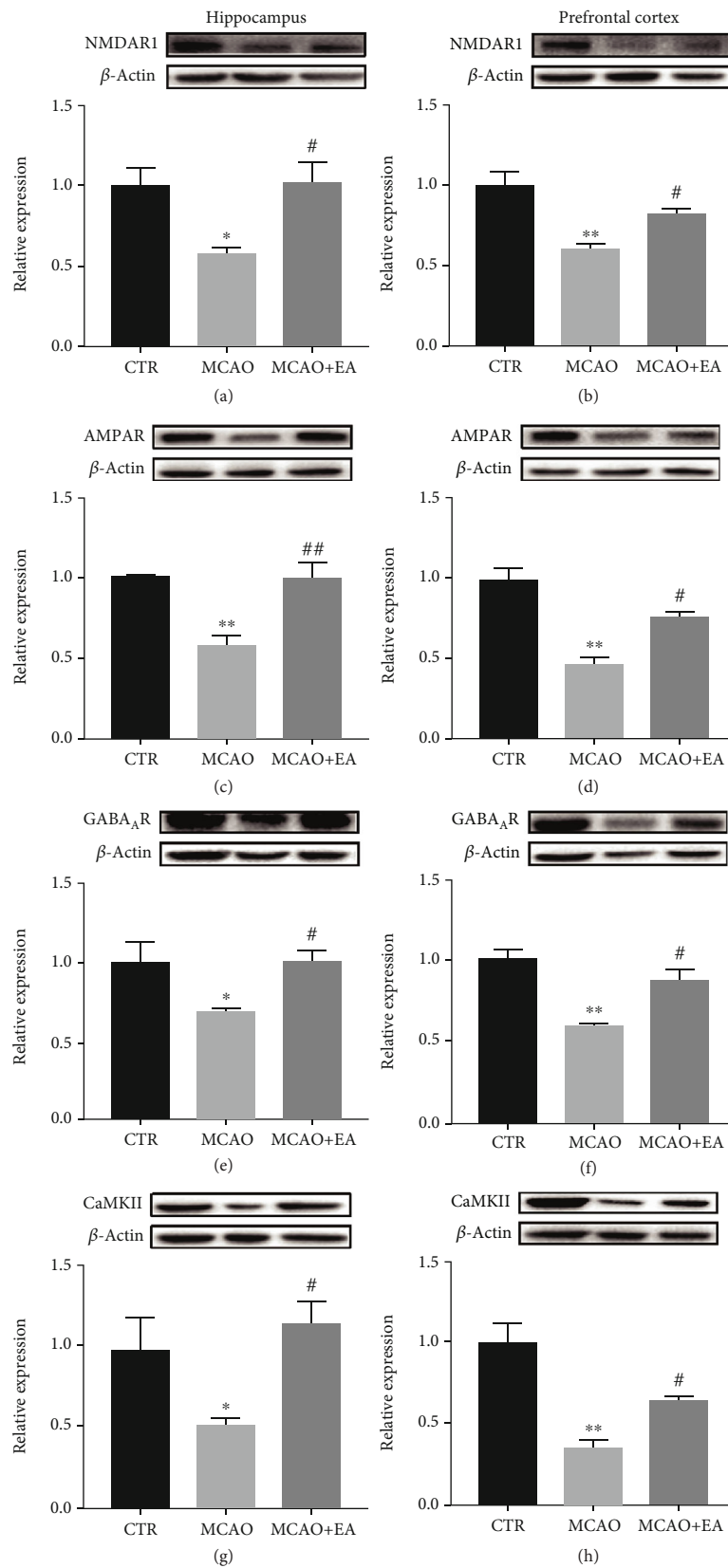


FIGURE 7: Effects of the MCAO and EA in neurotransmitter receptor proteins. NMDAR1 (a, b), AMPAR (c, d), GABA<sub>A</sub>R (e, f), and CaMKII (g, h) in the hippocampus and PFC, measured using Western blot analysis. Value is expressed as mean ± SEM, where \**p* < 0.05 and \*\**p* < 0.01 compared to the control group and #*p* < 0.05 and ##*p* < 0.01 compared to the MCAO group (*n* ≥ 3 each group). CTR: control; MCAO: middle cerebral artery occlusion; EA: electroacupuncture.



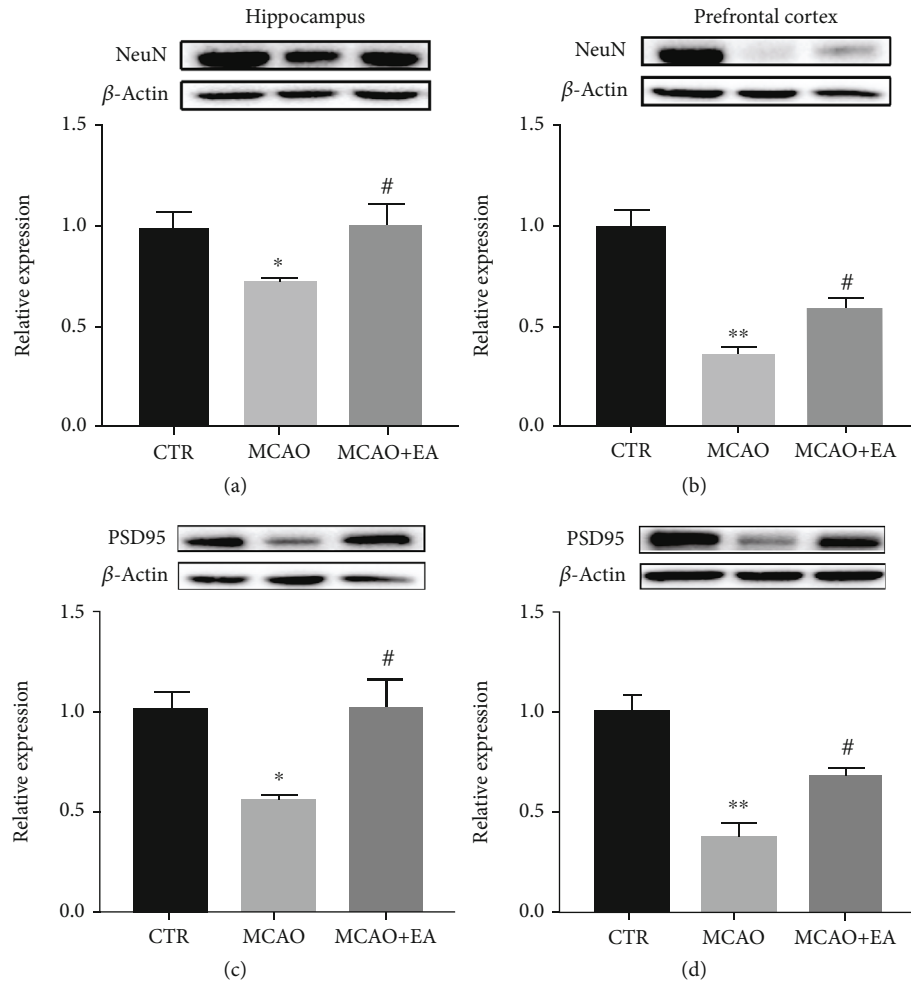


FIGURE 8: Effects of the MCAO and EA in synaptic-related proteins. Effects of MCAO and EA on the expression of the neuroplasticity biomarkers, NeuN (a, b) and PSD-95 (c, d) in the hippocampus and PFC. Value is expressed as mean  $\pm$  SEM, where \* $p < 0.05$  and \*\* $p < 0.01$  compared to the control group and # $p < 0.05$  and ## $p < 0.01$  compared to the MCAO group ( $n \geq 5$  each group). CTR: control; MCAO: middle cerebral artery occlusion; EA: electroacupuncture.

Meanwhile, significant effects could be found on the expression of functional neuroplasticity biomarkers, NMDAR1, AMPAR, GABA<sub>A</sub>R, and CaMKII, in the hippocampus ( $F_{2,12} \geq 4.138$ ,  $p \leq 0.0387$ ) and PFC ( $F_{2,12} \geq 10.53$ ,  $p \leq 0.038$ ) (Figure 7). The MCAO operation markedly decreased the expression of these proteins in the brain regions ( $p < 0.0478$ ). Furthermore, EA significantly reversed these expressions to the control level ( $p < 0.0483$ ). These results show that stroke could downregulate the neurotrophin signaling pathway as well as the expression of neurotransmitter receptors. However, EA could reverse these biomarkers.

**3.6. The Expression of the Structural Synaptic Plasticity-Related Protein in Brain Tissues.** Apart from functional neuroplasticity biomarkers, some structural neuroplasticity biomarkers were also investigated. One-way ANOVA revealed a significant difference among the expression of the biomarker for neurons, NeuN, ( $F_{2,12} \geq 4.283$ ,  $p \leq 0.0338$ ), and synaptic plasticity-related protein PSD-95, in the hippocam-

pus and PFC ( $F_{2,12} \geq 6.567$ ,  $p \leq 0.0118$ ) (Figure 8). The results above suggest that suppressions of the neuronal nuclear biomarker and structural synaptic protein could be found in the operation group and EA could restore these.

**3.7. Immunofluorescence of the Synaptic Plasticity-Related Protein in the Hippocampus.** In parallel to Western blotting, PSD-95 spatial information was measured in the hippocampus by immunofluorescence (Figure 9(a)). Significant treatment effects were present on the PSD-95 in the hippocampus ( $F_{2,6} = 26.98$ ,  $p = 0.001$ ). EA could restore the PSD-95 expression after the MCAO operation. The results are consistent with the above Western blotting results.

## 4. Discussion

In China, the prevalence of PSCI is 41.8% in ischemic stroke survivors aged  $\geq 40$  [31]. It has an adverse influence on their daily life and a growing economic burden on their family [32]. However, most current therapies, such as

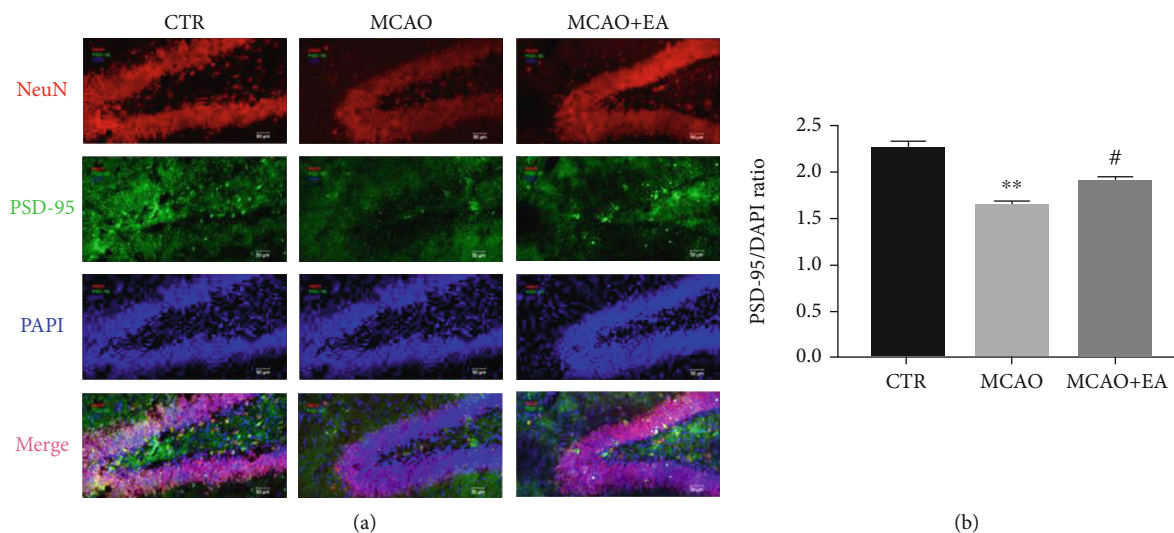


FIGURE 9: Effects of MCAO and EA on the fluorescence intensity ratio of PSD-95/DAPI in the hippocampus. The fluorescence intensity ratio of PSD-95/DAPI (b) was analyzed. Data are expressed as mean  $\pm$  SEM, where \*\* $p < 0.01$  compared to the control group and # $p < 0.05$  compared to the MCAO group ( $n = 3$  each group). CTR: control; MCAO: middle cerebral artery occlusion; EA: electroacupuncture.

pharmacological treatment and cognitive training, lack of sufficient evidence [33]. Systematic reviews have proposed that acupuncture may be effective on cognitive function after stroke [34, 35]. This novel EA/TNS has applied into different kinds of cognitive impairment in clinical studies [20, 36].

In our study, the body weight of the animal was decreased after the MCAO operation, which was similar to some other studies [23, 37]. The EA treatment promoted the recovery of body weight in the I/R injury rats. This result could be mainly attributed to the multiple effects of acupuncture. In fact, similar multiple effects were observed in our clinical study [20]. EA could reduce not only cognitive deterioration of stroke patients but also some other sequelae of stroke, such as post-stroke depression and functional disability [20].

According to previous studies [38–40], MCAO can induce cognitive impairment in animal behavior tests. In the current study, the rats in the MCAO group required much longer time to find the platform during the training phase and spent less time in the targeted quadrant in the probe phase, compared with the sham-operated rats. In the novel object recognition test, the MCAO group spent less time on the novel object than the control group. However, EA/TNS reversed the above phenomena in both tests. These results indicate that the MCAO group rats had not only impaired spatial learning and memory but also recognition decline, while the EA/TNS treatment could ameliorate these dysfunctions in both cognitive tests. This could provide additional animal behavior evidence to support the findings in our clinical study [20].

However, in the open field test, we found no intergroup differences in the time spent or the frequency of entry into the central zone. There was also no difference between these groups in the velocity of movement or the frequency of entry into the targeted quadrant in the water maze test, as well as the total exploration time in the novel object recognition test. These results suggest that neither the MCAO operation nor the EA treatment affected the anxiety levels or locomotor

function in these three groups, which implied that the longer latency and shorter duration in the water maze test were the consequences of cognitive dysfunction, rather than of locomotor abnormality. Furthermore, these dysfunctions were the direct impact of stroke rather than anxiety.

BDNF, as a member of the neurotrophin family, is a critical molecular determinant of cell proliferation, differentiation, and synaptic modulation [41]. BDNF exerts its neuroprotective functions via binding to the TrkB receptor [42]. It can affect cognitive function via long-term potentiation (LTP), which is a powerful regulator of plasticity-related processes in long-term memory [43]. In one clinical study, BDNF levels in the serum were discovered to be much lower in patients with a history of acute ischemic stroke than in healthy individuals [44]. Likewise, in this study, we found that the BDNF level in the MCAO group was lower than that in the control group. This is also consistent with some other animal experiments [45, 46]. Meanwhile, at the downstream of the BDNF/TrkB signaling pathway, the changes in the TrkB level reflected those of BDNF in both our study and others [47, 48]. EA/TNS was found to reverse these changes in our study, suggesting that it restores cognitive function by enhancing the BDNF/TrkB pathway to contribute to neuroprotection.

Apart from its neuroprotective effects, acupuncture was also found to alter the quantity of neurotransmitter receptors; then, it might improve synaptic plasticity in this study [7]. However, overactive NMDAR [49] and AMPAR [50] can bring about excitotoxicity and neurotoxicity. Excitotoxicity appeared in the early stage of reperfusion. One study indicated that the numbers of NMDAR and AMPAR were suppressed for up to 3 days after reperfusion [51]. Nevertheless, in the long term, these receptors play decisive roles in synaptic plasticity. Our results revealed that the MCAO operation downregulated the expression of NMDAR, AMPAR, GABAAR, and CaMKII, suggesting that stroke promotes cognitive deterioration. Cotreatment with EA prevented

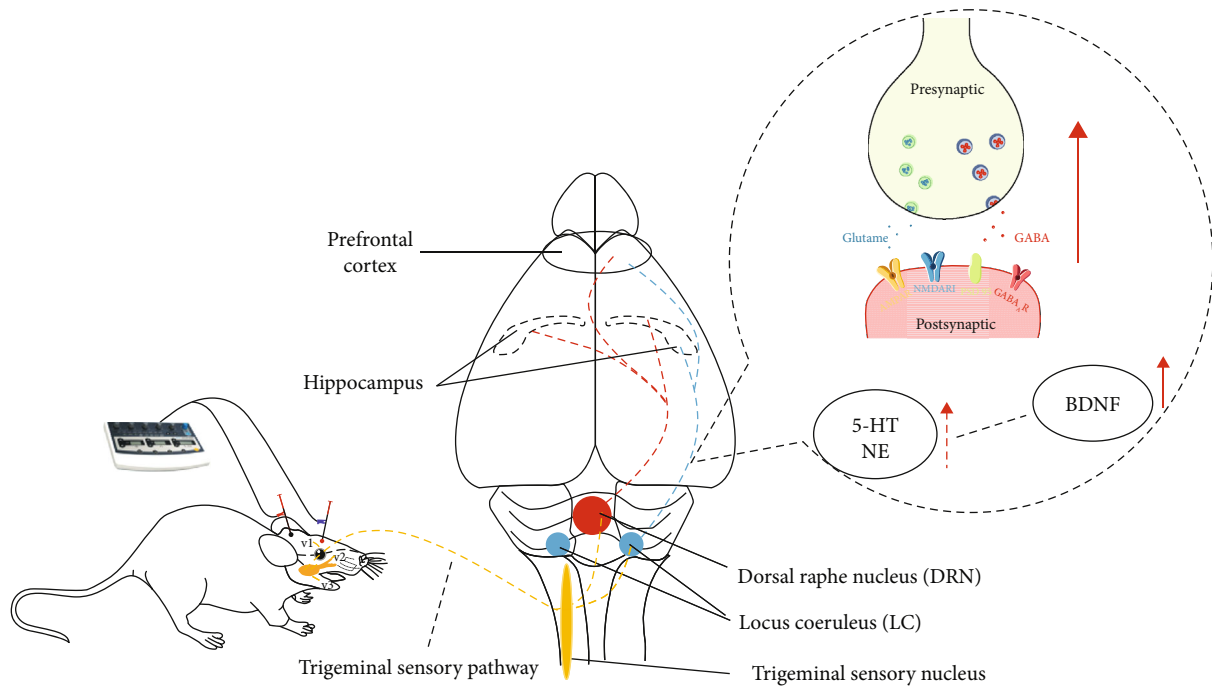


FIGURE 10: Schematic chart of the possible pathway for EA at GV20 and EX-HN3 against poststroke cognitive impairment in a rat model.

these adverse effects of MCAO but did not induce overexpression of NMDAR or AMPAR. We could find some similar results that acupuncture had a treatment effect for neuropsychiatric disorders via modulating glutamate receptors and preventing neuronal excitotoxicity and hyperexcitability [52, 53]. Therefore, EA/TNS could restore the quantity of neurotransmitter receptors, but not overexpression.

Associated with these receptors, especially NMDAR, PSD-95 is a cytoskeletal component found at the synapses. PSD-95 enhances presynaptic neuron maturation, the quantity of postsynaptic glutamate receptors, and the quantity and size of dendritic spines [54]. It plays an essential role in synaptic plasticity and stabilization of synaptic alteration during LTP [55] and can be considered a biomarker for synaptic plasticity. In this study, the MCAO suppressed the expression of PSD-95, while EA increased it in both the PFC and hippocampus. Since spatial information cannot be ascertained from Western blotting, we used immunofluorescence to localize the PSD-95, and these two results were consistent.

EA on the trigeminal nerve-innervated acupoints is often used in the treatment of various psychiatric disorders, such as depression and obsessive-compulsive disorders, to name a few [56, 57]. These acupoints are innervated by the ophthalmic branch of the trigeminal nerve, from which the sensory information is sent to the trigeminal nucleus in the brainstem [19]. The nucleus is closely related to the dorsal raphe nucleus (DRN) containing serotonin- (5-HT-) producing neurons [58], and the locus coeruleus (LC) containing norepinephrine- (NE-) producing neurons [59], forming the brainstem reticular formation. It has additionally been proposed that DRN plays a crucial role in the brain's neural plasticity [60], neurogenesis [61], and synaptogenesis [62]. Previous studies have suggested that 5-HT could regulate BDNF expression in some stress animal models [63, 64].

The LC-NE system assumes an essential role in determining cognitive function, and NE can protect neurons from damage [65]. An *in vitro* study has supported that NE may be an essential modulator in BDNF expression in hippocampal neurons [66]. Our results showed that EA/TNS could enhance the BDNF/TrkB signaling pathway; this might be related to the trigeminal sensory pathway, dorsal raphe nucleus, and locus coeruleus.

In addition to neuroprotection, BDNF could both enhance spine density in hippocampal slices in long-term stimulation [67] and promote LTP induction in short-term stimulation [68]. Apart from the structural spine plasticity, the BDNF pathway has also been shown to directly increase PSD-95 at synapses, which are mediated by the phosphatidylinositol 3-kinase signaling pathway downstream of TrkB after NMDAR activation [69]. Furthermore, BDNF is considered to play a fundamental role on neurotransmitter release [70], NMDAR transmission [71], AMPAR expression alterations [72], and GABAAR transcription [73]. Our results also revealed that EA/TNS could improve the neurotransmitter receptor quantity and synaptic plasticity-related protein; this may be related to the increased BDNF secretion. Taking the above together, we suggest that EA/TNS could induce 5-HT and NE expression in the brainstem, then enhance BDNF secretion, subsequently modulate neurotransmitter receptors and PSD-95 expression, and ultimately regulate synaptic plasticity (Figure 10).

However, some limitations of this study should be noted. First, according to a study by Yang [51], the expression of NMDAR and AMPAR may change dynamically during pathological processes. However, we only investigated the long-term (2 weeks) treatment effect. Second, we were unable to analyze the infarct volumes because the ischemic areas had severe edema, or even liquefaction, after 14 days. Third, we

focused on a single protein in the postsynapses. Although this protein is related to synaptic plasticity, the evidence gathered here may be insufficient to draw definitive conclusions. Finally, the upstream of this pathway for mediation of cognitive function in the hippocampus and the PFC could be further explored and verified, especially in the brainstem.

## 5. Conclusions

To sum up, EA at *EX-HN3 (Yintang)* and *GV20 (Baihui)* could alleviate PSCI in the MCAO rat model. The mechanism of action appears to enhance neuroprotection and regulate synaptic plasticity in the hippocampus and PFC.

## Data Availability

The key data have been present in the context. The datasets used in this study can be obtained from the corresponding author upon reasonable request.

## Ethical Approval

All experimental protocols have been approved by the Committee on the Use of Live Animals in Teaching and Research of LKS Faculty of Medicine of the University of Hong Kong.

## Conflicts of Interest

The authors declare that they have no competing interest.

## Authors' Contributions

ZJZ and JGS contributed to the conception and design of the study, YZ performed the animal experiment and ZSQ the statistical analysis, YZ prepared the manuscript, and YZ, ZSQ, and BT revised the manuscript.

## Acknowledgments

We appreciate the staffs in the Faculty Core Facility, Li Ka Shing Faculty of Medicine, and lab animal unit in the University of Hong Kong, for their kind help during the experiment. This study was supported by the National Key R&D Program of China (2018YFC1705801) and General Research Fund (GRF) of Research Grant Council of HKSAR (17115017 for Z.J.Z.).

## Supplementary Materials

1 This file shows that the rat could move freely in the box during the electroacupuncture treatment. (*Supplementary Materials*)

## References

- [1] V. L. Feigin, M. H. Forouzanfar, R. Krishnamurthi et al., "Global and regional burden of stroke during 1990-2010: findings from the Global Burden of Disease Study 2010," *Lancet*, vol. 383, no. 9913, pp. 245-255, 2014.
- [2] K. Blennow, M. J. de Leon, and H. Zetterberg, "Alzheimer's disease," *Lancet*, vol. 368, no. 9533, pp. 387-403, 2006.
- [3] P. B. Gorelick, A. Scuteri, S. E. Black et al., "Vascular contributions to cognitive impairment and dementia: a statement for healthcare professionals from the American Heart Association/American Stroke Association," *Stroke*, vol. 42, no. 9, pp. 2672-2713, 2011.
- [4] N. G. M. V. Bazan and K. Cole-Edwards, "Brain response to injury and neurodegeneration: endogenous neuroprotective signaling," *Annals of the New York Academy of Sciences*, vol. 1053, no. 1, pp. 137-147, 2005.
- [5] P. W. Hickmott and I. M. Ethell, "Dendritic plasticity in the adult neocortex," *Neuroscientist. Neuroscientist*, vol. 12, no. 1, pp. 16-28, 2016.
- [6] B. Lu, G. Nagappan, X. Guan, P. J. Nathan, and P. Wren, "BDNF-based synaptic repair as a disease-modifying strategy for neurodegenerative diseases," *Nature Reviews. Neuroscience*, vol. 14, no. 6, pp. 401-416, 2013.
- [7] K. Gerrow and A. Triller, "Synaptic stability and plasticity in a floating world," *Current Opinion in Neurobiology*, vol. 20, no. 5, pp. 631-639, 2010.
- [8] G. Adelman, P. Jonas, and H. Monyer, *Ionotropic Glutamate Receptors in the CNS*, Springer Verlag, 1999.
- [9] T. C. Jacob, "Neurobiology and therapeutic potential of  $\alpha$ -5-GABA type A receptors," *Frontiers in Molecular Neuroscience*, vol. 12, p. 179, 2019.
- [10] G. K. M. Lynch, S. Halpain, and M. Baudry, "Biochemical effects of high-frequency synaptic activity studied with in vitro slices," *Federation Proceedings*, vol. 42, no. 12, pp. 2886-2890, 1983.
- [11] R. M. Sachser, J. Haubrich, P. S. Lunardi, and L. de Oliveira Alvares, "Forgetting of what was once learned: exploring the role of postsynaptic ionotropic glutamate receptors on memory formation, maintenance, and decay," *Neuropharmacology*, vol. 112, no. Part A, pp. 94-103, 2017.
- [12] S. D. Healy and C. Jozet-Alves, "Spatial memory," in *Encyclopedia of Animal Behavior*, M. D. Breed and J. Moore, Eds., pp. 304-307, Oxford: Academic Press, 2010.
- [13] I. Kahn, L. Davachi, and A. D. Wagner, "Functional-neuroanatomic correlates of recollection: implications for models of recognition memory," *Journal of Neuroscience*, vol. 24, no. 17, pp. 4172-4180, 2004.
- [14] C. Ranganath and R. T. Knight, "Prefrontal cortex and episodic memory: integrating findings from neuropsychology and functional brain imaging," *The cognitive neuroscience of memory: Encoding and retrieval*, vol. 1, p. 83, 2002.
- [15] S. Wang, H. Yang, J. Zhang et al., "Efficacy and safety assessment of acupuncture and nimodipine to treat mild cognitive impairment after cerebral infarction: a randomized controlled trial," *BMC Complementary and Alternative Medicine*, vol. 16, no. 1, 2016.
- [16] D. Min and W. Xu-Feng, "An updated meta-analysis of the efficacy and safety of acupuncture treatment for vascular cognitive impairment without dementia," *Current Neurovascular Research*, vol. 13, no. 3, pp. 230-238, 2016.
- [17] L. Chen, J. Fang, R. Ma et al., "Additional effects of acupuncture on early comprehensive rehabilitation in patients with mild to moderate acute ischemic stroke: a multicenter randomized controlled trial," *BMC Complementary and Alternative Medicine*, vol. 16, no. 1, 2016.
- [18] S. Zhang, B. Wu, M. Liu et al., "Acupuncture efficacy on ischemic stroke recovery: multicenter randomized controlled trial in China," *Stroke*, vol. 46, no. 5, pp. 1301-1306, 2015.



- [19] Z.-J. Zhang, X.-M. Wang, and G. M. McAlonan, "Neural acupuncture unit: a new concept for interpreting effects and mechanisms of acupuncture," *Evidence-based Complementary and Alternative Medicine*, vol. 2012, Article ID 429412, 23 pages, 2012.
- [20] Z.-J. Zhang, H. Zhao, G.-X. Jin et al., "Assessor-and participant-blinded, randomized controlled trial of dense cranial electroacupuncture stimulation plus body acupuncture for neuropsychiatric sequelae of stroke," *Psychiatry and Clinical Neurosciences*, vol. 74, no. 3, pp. 183–190, 2020.
- [21] X. Su, Z. Wu, F. Mai et al., "'Governor vessel-unblocking and mind-regulating' acupuncture therapy ameliorates cognitive dysfunction in a rat model of middle cerebral artery occlusion," *International Journal of Molecular Medicine*, vol. 43, no. 1, pp. 221–232, 2019.
- [22] J. Jittiwat, "Baihui point laser acupuncture ameliorates cognitive impairment, motor deficit, and neuronal loss partly via antioxidant and anti-inflammatory effects in an animal model of focal ischemic stroke," *Evidence-based Complementary and Alternative Medicine*, vol. 2019, Article ID 1204709, 9 pages, 2019.
- [23] B. Tsoi, X. Chen, C. Gao et al., "Neuroprotective effects and hepatorenal toxicity of Angong Niu Huang Wan against ischemia-reperfusion brain injury in rats," *Frontiers in Pharmacology*, vol. 10, pp. 593–593, 2019.
- [24] Z. Zhongfa, W. Junfeng, and D. Guiping, "Application of electroacupuncture at Baihui and Yintang points in Department of Mental Diseases," *Chinese Acupuncture & Moxibustion*, vol. 41, 2001.
- [25] F.-Y. Zhao, Q.-Q. Fu, Z. Zheng, L.-X. Lao, H.-L. Song, and Z. Shi, "Verum- versus Sham-Acupuncture on Alzheimer's Disease (AD) in Animal Models: A Preclinical Systematic Review and Meta-Analysis," *BioMed Research International*, vol. 2020, 21 pages, 2020.
- [26] M. Antunes and G. Biala, "The novel object recognition memory: neurobiology, test procedure, and its modifications," *Cognitive Processing*, vol. 13, no. 2, pp. 93–110, 2012.
- [27] C. Warburton and M. W. Brown, "Findings from animals concerning when interactions between perirhinal cortex, hippocampus and medial prefrontal cortex are necessary for recognition memory," *Neuropsychologia*, vol. 48, no. 8, pp. 2262–2272, 2010.
- [28] E. A. Maloney, J. R. Sattizahn, and S. L. Beilock, "Anxiety and cognition," *Wiley Interdisciplinary Reviews: Cognitive Science*, vol. 5, no. 4, pp. 403–411, 2014.
- [29] H. Kuniishi, S. Ichisaka, M. Yamamoto et al., "Early deprivation increases high-leaning behavior, a novel anxiety-like behavior, in the open field test in rats," *Neuroscience Research*, vol. 123, pp. 27–35, 2017.
- [30] L. Prut and C. Belzung, "The open field as a paradigm to measure the effects of drugs on anxiety-like behaviors: a review," *European Journal of Pharmacology*, vol. 463, no. 1-3, pp. 3–33, 2003.
- [31] Q. Tu, X. Yang, B. Ding, H. Jin, Z. Lei, and S. Bai, "Epidemiological investigation of vascular cognitive impairment post ischemic stroke," *Chinese Journal of Gerontology*, vol. 31, pp. 3576–3579, 2011.
- [32] L. Claesson, T. Lindén, I. Skoog, and C. Blomstrand, "Cognitive impairment after stroke—impact on activities of daily living and costs of care for elderly people," *Cerebrovascular Diseases*, vol. 19, no. 2, pp. 102–109, 2005.
- [33] G. H. Taylor and N. M. Broomfield, "Cognitive assessment and rehabilitation pathway for stroke (CARPS)," *Topics in Stroke Rehabilitation*, vol. 20, no. 3, pp. 270–282, 2015.
- [34] F. Liu, Z.-M. Li, Y.-J. Jiang, and L.-D. Chen, "A meta-analysis of acupuncture use in the treatment of cognitive impairment after stroke," *The Journal of Alternative and Complementary Medicine*, vol. 20, no. 7, pp. 535–544, 2014.
- [35] P. Wu, E. Mills, D. Moher, and D. Seely, "Acupuncture in post-stroke rehabilitation: a systematic review and meta-analysis of randomized trials," *Stroke*, vol. 41, no. 4, pp. e171–e179, 2010.
- [36] Z.-J. Zhang, S.-C. Man, L.-L. Yam et al., "Electroacupuncture trigeminal nerve stimulation plus body acupuncture for chemotherapy-induced cognitive impairment in breast cancer patients: an assessor-participant blinded, randomized controlled trial," *Brain, Behavior, and Immunity*, vol. 88, pp. 88–96, 2020.
- [37] B. Tsoi, S. Wang, C. Gao et al., "Realgar and cinnabar are essential components contributing to neuroprotection of Angong Niu Huang Wan with no hepatorenal toxicity in transient ischemic brain injury," *Toxicology and Applied Pharmacology*, vol. 377, p. 114613, 2019.
- [38] J. W. Yang, X. R. Wang, S. M. Ma, N. N. Yang, Q. Q. Li, and C. Z. Liu, "Acupuncture attenuates cognitive impairment, oxidative stress and NF- $\kappa$ B activation in cerebral multi-infarct rats," *Acupuncture in Medicine*, vol. 37, no. 5, pp. 283–291, 2019.
- [39] G. Wu, D. W. McBride, and J. H. Zhang, "Axl activation attenuates neuroinflammation by inhibiting the TLR/TRAF/NF- $\kappa$ B pathway after MCAO in rats," *Neurobiology of Disease*, vol. 110, pp. 59–67, 2018.
- [40] Y. S. Koo, H. Kim, J. H. Park et al., "Indoleamine 2,3-dioxygenase-dependent neurotoxic kynurenine metabolism contributes to poststroke depression induced in mice by ischemic stroke along with spatial restraint stress," *Oxidative Medicine and Cellular Longevity*, vol. 2018, Article ID 2413841, 15 pages, 2018.
- [41] W.-J. Tu, X. Dong, S.-J. Zhao, D.-G. Yang, and H. Chen, "Prognostic value of plasma neuroendocrine biomarkers in patients with acute ischaemic stroke," *Journal of Neuroendocrinology*, vol. 25, no. 9, pp. 771–778, 2013.
- [42] D. Fan, J. Li, B. Zheng, L. Hua, and Z. Zuo, "Enriched environment attenuates surgery-induced impairment of learning, memory, and neurogenesis possibly by preserving BDNF expression," *Molecular Neurobiology*, vol. 53, no. 1, pp. 344–354, 2016.
- [43] C. Cunha, R. Brambilla, and K. L. Thomas, "A simple role for BDNF in learning and memory?," *Frontiers in Molecular Neuroscience*, vol. 3, 2010.
- [44] J. Wang, L. Gao, Y.-L. Yang et al., "Low serum levels of brain-derived neurotrophic factor were associated with poor short-term functional outcome and mortality in acute ischemic stroke," *Molecular Neurobiology*, vol. 54, no. 9, pp. 7335–7342, 2017.
- [45] L. Luo, C. Li, X. Du et al., "Effect of aerobic exercise on BDNF/proBDNF expression in the ischemic hippocampus and depression recovery of rats after stroke," *Behavioural Brain Research*, vol. 362, pp. 323–331, 2019.
- [46] Y. Wang, J. Yang, H. Du, H. Zhang, H. Wan, and Y. He, "Yan-gyin Tongnao granules enhance neurogenesis in the perinfarct area and upregulate brain-derived neurotrophic factor and vascular endothelial growth factor after focal cerebral

- ischemic infarction in rats," *Molecular Biology Reports*, vol. 46, no. 4, pp. 3817–3826, 2019.
- [47] Y. Liu, C. Li, J. Wang et al., "Nafamostat Mesilate improves neurological outcome and axonal regeneration after stroke in rats," *Molecular Neurobiology*, vol. 54, no. 6, pp. 4217–4231, 2017.
- [48] X. Shi, Y. Ohta, J. Shang et al., "Neuroprotective effects of SMT-44D in mice stroke model in relation to neurovascular unit and trophic coupling," *Journal of Neuroscience Research*, vol. 96, no. 12, pp. 1887–1899, 2018.
- [49] A. Jespersen, N. Tajima, G. Fernandez-Cuervo, E. C. Garnier-Amblard, and H. Furukawa, "Structural insights into competitive antagonism in NMDA receptors," *Neuron*, vol. 81, no. 2, pp. 366–378, 2014.
- [50] M. C. Rivera-Cervantes, R. Castañeda-Arellano, R. D. Castro-Torres et al., "P38 MAPK inhibition protects against glutamate neurotoxicity and modifies NMDA and AMPA receptor subunit expression," *Journal of Molecular Neuroscience*, vol. 55, no. 3, pp. 596–608, 2015.
- [51] Z. Yang, *The research of acupuncture intervening in cerebral ischemia model rats by regulating MAPK/ERK pathway*, Guangzhou University of Chinese Medicine, Guangzhou, 2009.
- [52] C.-H. Tu, I. MacDonald, and Y.-H. Chen, "The effects of acupuncture on glutamatergic neurotransmission in depression, anxiety, schizophrenia, and Alzheimer's disease: a review of the literature," *Frontiers in Psychiatry*, vol. 10, pp. 14–14, 2019.
- [53] Q.-Y. Chang, Y.-W. Lin, and C.-L. Hsieh, "Acupuncture and neuroregeneration in ischemic stroke," *Neural Regeneration Research*, vol. 13, no. 4, pp. 573–583, 2018.
- [54] A. E. S. E. El-Husseini, D. M. Chetkovich, R. A. Nicoll, and D. S. Brecht, "PSD-95 involvement in maturation of excitatory synapses," *Science*, vol. 290, no. 5495, pp. 1364–1368, 2000.
- [55] D. Meyer, T. Bonhoeffer, and V. Scheuss, "Balance and stability of synaptic structures during synaptic plasticity," *Neuron*, vol. 82, no. 2, pp. 430–443, 2014.
- [56] Z.-J. Zhang, R. Ng, S. C. Man et al., "Dense cranial electroacupuncture stimulation for major depressive disorder—a single-blind, randomized, controlled study," *PLoS One*, vol. 7, no. 1, p. e29651, 2012.
- [57] Z.-J. Zhang, X.-Y. Wang, Q.-R. Tan, G.-X. Jin, and S.-M. Yao, "Electroacupuncture for refractory obsessive-compulsive disorder: a pilot waitlist-controlled trial," *The Journal of Nervous and Mental Disease*, vol. 197, no. 8, pp. 619–622, 2009.
- [58] K. Kubota, N. Narita, K. Ohkubo et al., "Central projection of proprioceptive afferents arising from maxillo-facial regions in some animals studied by HRP-labeling technique," *Anatomischer Anzeiger*, vol. 165, no. 2-3, pp. 229–251, 1988.
- [59] T. Takahashi, M. Shirasu, M. Shirasu et al., "The locus coeruleus projects to the mesencephalic trigeminal nucleus in rats," *Neuroscience Research*, vol. 68, no. 2, pp. 103–106, 2010.
- [60] E. C. Azmitia, "Serotonin neurons, neuroplasticity, and homeostasis of neural tissue," *Neuropsychopharmacology*, vol. 21, pp. S33–S45, 1999.
- [61] J. Brezun and A. Daszuta, "Serotonergic reinnervation reverses lesion-induced decreases in PSA-NCAM labeling and proliferation of hippocampal cells in adult rats," *Hippocampus*, vol. 10, no. 1, pp. 37–46, 2000.
- [62] E. C. Azmitia, V. J. Rubinstein, J. A. Strafacci, J. C. Rios, and P. M. Whitaker-Azmitia, "5-HT<sub>1A</sub> agonist and dexamethasone reversal of para-chloroamphetamine induced loss of MAP-2 and synaptophysin immunoreactivity in adult rat brain," *Brain Research*, vol. 677, no. 2, pp. 181–192, 1995.
- [63] D.-G. Jiang, S.-L. Jin, G.-Y. Li et al., "Serotonin regulates brain-derived neurotrophic factor expression in select brain regions during acute psychological stress," *Neural Regeneration Research*, vol. 11, no. 9, pp. 1471–1479, 2016.
- [64] R. B. Foltran and S. L. Diaz, "BDNF isoforms: a round trip ticket between neurogenesis and serotonin?," *Journal of Neurochemistry*, vol. 138, no. 2, pp. 204–221, 2016.
- [65] M. Mather and C. W. Harley, "The locus coeruleus: essential for maintaining cognitive function and the aging brain," *Trends in Cognitive Sciences*, vol. 20, no. 3, pp. 214–226, 2016.
- [66] M. J. Chen, T. V. Nguyen, C. J. Pike, and A. A. Russo-Neustadt, "Norepinephrine induces BDNF and activates the PI-3K and MAPK cascades in embryonic hippocampal neurons," *Cellular Signalling*, vol. 19, no. 1, pp. 114–128, 2007.
- [67] W. J. Tyler and L. D. Pozzo-Miller, "BDNF enhances quantal neurotransmitter release and increases the number of docked vesicles at the active zones of hippocampal excitatory synapses," *Journal of Neuroscience*, vol. 21, no. 12, pp. 4249–4258, 2001.
- [68] C. S. Rex, C.-Y. Lin, E. A. Kramár, L. Y. Chen, C. M. Gall, and G. Lynch, "Brain-derived neurotrophic factor promotes long-term potentiation-related cytoskeletal changes in adult hippocampus," *Journal of Neuroscience*, vol. 27, no. 11, pp. 3017–3029, 2007.
- [69] A. Yoshii and M. Constantine-Paton, "BDNF induces transport of PSD-95 to dendrites through PI3K-AKT signaling after NMDA receptor activation," *Nature Neuroscience*, vol. 10, no. 6, pp. 702–711, 2007.
- [70] J. N. Jovanovic, A. J. Czernik, A. A. Fienberg, P. Greengard, and T. S. Sihra, "Synapsins as mediators of BDNF-enhanced neurotransmitter release," *Nature Neuroscience*, vol. 3, no. 4, pp. 323–329, 2000.
- [71] I. Ninan, K. G. Bath, K. Dagar et al., "The BDNF Val66Met polymorphism impairs NMDA receptor-dependent synaptic plasticity in the hippocampus," *Journal of Neuroscience*, vol. 30, no. 26, pp. 8866–8870, 2010.
- [72] J. M. Reimers, J. A. Loweth, and M. E. Wolf, "BDNF contributes to both rapid and homeostatic alterations in AMPA receptor surface expression in nucleus accumbens medium spiny neurons," *European Journal of Neuroscience*, vol. 39, no. 7, pp. 1159–1169, 2014.
- [73] I. V. Lund, Y. Hu, Y. H. Raol et al., "BDNF selectively regulates GABA<sub>A</sub> receptor transcription by activation of the JAK/STAT pathway," *Science Signaling*, vol. 1, no. 41, p. ra9, 2008.

## Research Article

# Microglia TREM2: A Potential Role in the Mechanism of Action of Electroacupuncture in an Alzheimer's Disease Animal Model

Yujie Li, Jing Jiang , Qisheng Tang , Huiling Tian , Shun Wang, Zidong Wang, Hao Liu, Jiayi Yang, and Jingyu Ren

Beijing University of Chinese Medicine, Beijing, China 100029

Correspondence should be addressed to Jing Jiang; [yingxi7847@126.com](mailto:yingxi7847@126.com) and Qisheng Tang; [tangqisheng@263.com](mailto:tangqisheng@263.com)

Received 9 June 2020; Revised 29 July 2020; Accepted 18 August 2020; Published 4 September 2020

Academic Editor: Yongjun Chen

Copyright © 2020 Yujie Li et al. This is an open access article distributed under the Creative Commons Attribution License, which permits unrestricted use, distribution, and reproduction in any medium, provided the original work is properly cited.

Alzheimer's disease (AD) is one of the most serious public health concerns facing the world. Its characteristic feature is neuroinflammation due to microglial activation. Electroacupuncture is one of the therapies employed to improve the condition of patients with AD, although its mechanism of action is still to be determined. Triggering receptor expressed on myeloid cells 2 (TREM2) is a microglia-specific receptor that is involved in regulating neuroinflammation in AD. In this study, we applied senescence-accelerated mouse-prone 8 mice as the AD animal model, used the Morris water maze, and applied hematoxylin and eosin staining, immunofluorescence double staining, and Western blotting, to explore the effects and potential mechanisms of action of electroacupuncture. In summary, this study suggested that electroacupuncture treatment could improve the learning and memory abilities ( $p < 0.05$ ) and protect neurons. These effects result from acupuncture could upregulate TREM2 expression in the hippocampus ( $p < 0.01$ ), which was essential for the anti-inflammatory effects in the AD animal model. However, further studies are needed to conclusively demonstrate the mechanism of action of electroacupuncture in AD.

## 1. Introduction

As the commonest cause of dementia, Alzheimer's disease (AD) is a growing global health concern with huge implications for individuals and society [1]. This neurodegenerative disease is characterized classically by two hallmark pathologies:  $\beta$ -amyloid plaque deposition and neurofibrillary tangles of hyperphosphorylated tau [2]. In recent years, there is increasing evidence for researchers to consider brain neuroinflammation as a new feature of AD [3], which is associated with microglial activation [4]. Microglia, as the resident immune cells of the central nervous system, play an important role in maintaining tissue homeostasis and contribute towards brain development under normal conditions [5]. However, when there is neuronal injury or other insults, depending on the type and magnitude of stimuli, microglia will be activated to secrete either proinflammatory factors that enhance cytotoxicity or anti-inflammatory neuroprotective factors that assist in wound healing and tissue repair [6]. Excessive microglial activation damages the surrounding

healthy neural tissue, and the factors secreted by the dead or dying neurons in turn exacerbate the chronic activation of microglia, causing progressive loss of neurons [7]. Therefore, more researchers direct their energies into determining the mechanism of regulating microglial activation in AD.

Triggering receptor expressed on myeloid cells 2 (TREM2), as a new target in regulating microglial activation, is highly and exclusively expressed on microglia [8]. As a microglial surface receptor, TREM2 interacts with adaptor protein DAP12 (TYRO protein tyrosine kinase-binding protein (TYROBP), also known as DAP12) to initiate signal transduction pathways that promote microglial cell activation, phagocytosis, and microglial survival [9].

In order to improve the quality of life of patients with AD and delay the progression of the disease, acupuncture therapies are widely applied especially in China [10, 11]. Consequently, the mechanism of action of acupuncture in AD is to be elucidated to validate the observed therapeutic effects. Although some studies focused on the expression of TREM2 during the process of AD, there was little evidence to explain

the mechanism of acupuncture modality from regulating the expression of TREM2 [7, 12]. In addition, in our previous studies [13, 14], we had found that acupuncture therapy could inhibit the expression of proinflammatory factors in the brain of AD animal models, such as IL-1 beta and NTF-alpha. Because of TREM2 in the microglia taking part in the regulation of these proinflammatory factors, we want to focus on the upstream of this process, to investigate whether acupuncture could regulate the expression of TREM2. Overall, these aspects of studies could provide a novel angle to demonstrate the acupuncture mechanism and scientific evidence to apply this modality in AD patients.

In this study, we investigated whether acupuncture therapy improved AD by regulating the expression of TREM2 on microglia using a recognized AD animal model.

## 2. Materials and Methods

**2.1. Ethics Statement.** The experimental protocol applied in this study was approved by the Ethics Committee for Animal Experimentation of Beijing University of Chinese Medicine (ID: BUCM-4-2018111701-4045). All procedures complied with the Animal Research: Reporting of In Vivo Experiments (ARRIVE) guidelines and were performed according to the guidelines of the National Institutes for Animal Research. All researchers in this study were certified by the Animal Experimentation Center of Beijing University of Chinese Medicine.

**2.2. Animals.** Eight-month-old senescence-accelerated mouse-prone 8 (SAMP8) mice [15] and senescence-accelerated mouse-resistant 1 (SAMR1) mice weighing  $30.0 \pm 2.0$  g were purchased from the Experimental Animal Center of the First Teaching Hospital of Tianjin University of Traditional Chinese Medicine (Animal Lot: SCXK (Jing) 2014-0003). The animals were housed in the Animal Experimentation Center of Beijing University of Chinese Medicine at controlled temperature ( $24 \pm 2^\circ\text{C}$ ) and under a 12 h dark/light cycle, with sterile drinking water and a standard pellet diet available ad libitum. All mice were acclimatized to the environment for five days prior to experimentation.

**2.3. Grouping and Intervention.** Ten SAMR1 male mice were placed in the control group, and 30 SAMP8 male mice were randomly divided into three experimental groups of 10 mice each: the AD model control group (AD group), drug group, and electroacupuncture group (EA group). In the drug group, donepezil hydrochloride tablets (Eisai China Inc., H20050978) were dissolved in distilled water and delivered to the mice by oral gavage at a dose of  $0.65 \mu\text{g/g}$ . In the EA group, mice were immobilized in mouse bags. *Baihui* (GV20) and *Yintang* (GV29) were chosen for electroacupuncture for 15 min per day, with transverse puncturing at a depth of 4–5 mm using disposable sterile acupuncture needles ( $0.25 \text{ mm} \times 13 \text{ mm}$ ) (Beijing Zhongyan Taihe Medicine Company). The needles were taped and connected to the HANS-LH202 electroacupuncture device (Peking University Institute of Science Nerve and Beijing Hua Wei Industrial Development Company, Beijing, China), with the sparse

wave at 2 Hz, 2 V, and 0.1 mA. The mice in the control group, AD group, and drug group received the same 15-minute restriction as those in the EA group.

**2.4. Morris Water Maze Test.** After the 15-day intervention, mice from each group were evaluated in the Morris water maze [16]. The Morris water maze consisted of a circular tank (diameter, 120 cm; height, 50 cm) filled with opaque water, rendered with milk powder to a depth of 30 cm. A video camera (TOTA-450d, Japan) fixed to the ceiling and connected to a video recorder with an automated tracking system (China Daheng Group, China) was used to collect data. A removable platform (diameter, 9.5 cm; height, 30 cm) was placed inside the pool (at quadrant III). The pool area was conceptually divided into four quadrants (I, II, III, and IV) of equal size. Visual cues of different shapes were placed on the tank wall of each quadrant in plain sight of the mice.

**2.4.1. Hidden Platform Trial.** This trial was applied for testing the spatial learning ability of the mice. All surviving mice were trained in the standard Morris water maze with a hidden platform. Quadrants I and II were selected as entry points. Each mouse was released from the two points and had 60 s to search for the hidden platform. Two trials per day for 5 consecutive days were performed, with the visual cues kept constant.

**2.4.2. Probe Trial.** This trial was used for testing the spatial memory ability of the mice. The platform was removed the day after the hidden platform trial. Each mouse was placed in the pool once for 60 s, starting from the same initial location used in the hidden platform trial. The crossing times of the platform were recorded during the test.

**2.5. Hematoxylin and Eosin (HE) Staining.** To observe the neurons in the dentate gyrus of the hippocampus in each group, three mice were randomly chosen from each group after the Morris water maze tests, anesthetized, and had their brains removed and subjected to HE staining. Tissues were dehydrated, paraffin-embedded, and sliced (thickness, 10 mm/slice), followed by dewaxing three times in xylene for 5 min each, and then placed in anhydrous ethanol for 5 min, followed by 90% ethanol, 70% ethanol, and distilled water, each for 2 min, and then made to undergo HE staining. Thereafter, sections were dehydrated through increasing concentrations of ethanol and xylene. The dentate gyrus of the hippocampus in each specimen was viewed under a microscope (Olympus, BX53; magnification,  $\times 40$ ).

**2.6. Immunofluorescence Double Staining.** Immunofluorescence double staining was used to detect the coexpression of microglia and TREM2 expression in the dentate gyrus of the hippocampus. Sections were dewaxed and hydrated, placed in Triton X-100 (mass fraction 0.5%) for 10 min, blocked with bovine serum albumin (mass fraction 2%), and rested for 1 h at room temperature. Antibody TREM2 (Proteintech, USA; 1:150) was mixed with antibody Iba-1 (Proteintech, USA; 1:150) and incubated on sections overnight at  $4^\circ\text{C}$  and rinsed with phosphate-buffered saline



(PBS) three times. The FITC fluorescent-labeled secondary antibody (1:200) was mixed with the TRITC fluorescent-labeled secondary antibody (1:200), incubated on the slices at room temperature for 2 h, and then rinsed with PBS. The slices were scanned and imaged by the digital pathological slice scanner (NanoZoomer S210, Hamamatsu, C13239-01) after drying and then analyzed.

**2.7. Western Blotting.** To test for the expression of TREM2 protein in the hippocampus, seven mice in each group were sacrificed under anesthesia to harvest their hippocampi. After protein extraction, SDS-polyacrylamide gel electrophoresis was performed using a 10% separating gel and a 5% stacking gel. Proteins were then transferred to a 0.45  $\mu\text{m}$  polyvinylidene fluoride membrane. Membrane blocking was performed using 5% nonfat milk in Tris-buffered saline supplemented with 0.1% Tween 20. Membranes were incubated in the primary antibody (Proteintech, USA; TREM2, mouse, 1:1000) at 4°C overnight. The secondary antibody (1:2000) was added before shaking and incubating at room temperature for 1 h. The HRP-ECL luminous liquid was added, and X-ray film exposure was completed in a dark room following development and fixing. After calibrating the control markers, the scanning and analyses were performed by The Discovery Series Quantity One, version 4.6, and the relative and standardized levels of caspase-3 and tau expression were compared in each group.

**2.8. Statistical Analyses.** Statistical analyses were performed using the SPSS software, version 25.0 (SPSS, Inc., Chicago, IL, USA), and data was expressed as the mean  $\pm$  standard deviation. Multivariate analysis of variance (ANOVA) with repeated measures was used for the general linear model using the SPSS software, and pairwise comparison was used for the different groups and different measurement times. First, Mauchly's test of sphericity was used to assess whether there were relations among the repeatedly measured data. For results with  $p \leq 0.05$ , multivariate ANOVA or Greenhouse-Geisser correction was performed. The effect of treatment was evaluated by estimating the between-subject variance. Repeated measurement effect or its interactive effect with the treated group was evaluated by estimating the within-subject variance. The Bonferroni test was used to perform pairwise comparisons of the repeatedly measured data in different measurement times in each treated group. Multivariate ANOVA was used for pairwise comparison of data in different groups for each measurement time. One-way ANOVA was used after the normal distribution and homogeneity of variance were confirmed for the other dates.

### 3. Results

**3.1. EA Could Improve Learning and Memory Abilities in the AD Animal Model.** The results of the Morris water maze tests are presented in Figure 1. From Figure 1(a), we observed that the escape time of each group shortened according to the training days accumulated. Interestingly, on the fourth day of the hidden platform test, the escape

times of the EA group mice were longer than those of the third day, and on the fifth day (last day of the training), this data significantly decreased, even shorter than the third day. After the fourth day of the hidden platform trial, we reexamined the device, discovered the fault, and applied corrective measures. Thereafter, we evaluated the mice of the EA group and considered whether 3 consecutive days of training had caused excessive fatigue, preventing them from finding the platform. Therefore, on the fifth day of the hidden platform trial, we rested the EA group mice, only testing them after the mice from the three experimental groups had been tested. From the obtained results, our hypothesis proved to be correct.

From Figure 1(b), we observed that the escape times of the AD group mice were significantly longer than those of the control group mice for each day ( $p = 0.001 < 0.01$ ), which meant that the spatial learning ability of SAMP8 mice was significantly lower. However, on the third and fifth days, the escape times of the EA group mice were significantly shortened (third day,  $p = 0.029 < 0.05$ ; fifth day,  $p = 0.011 < 0.05$ ), even shorter than those of the drug group on the last day ( $p = 0.019 < 0.05$ ). These results illustrated that electroacupuncture treatment may improve the spatial ability of SAMP8 mice.

Figure 1(c) shows the platform quadrant crossing times for each group. There was a significant difference between the control group mice and the mice from the three experimental groups ( $p = 0.001 < 0.01$ ). Moreover, the EA group mice were more than the AD group mice in this data ( $p = 0.012 < 0.05$ ), which implied that spatial memory ability was also improved by electroacupuncture treatment.

**3.2. EA Could Be Neuroprotective in the Hippocampus of the AD Animal Model.** Figure 2 shows the HE staining results of the dentate gyri of the hippocampi. The control group mice demonstrated clear-dyed neurons aligned in neat rows, with round nuclei and distinct kernels in the dentate gyri. Conversely, neurons tended to be scattered and irregular, with indistinct kernels and nuclear pyknosis in the dentate gyri of the AD group mice. Subjectively, neurons of the mice in the drug and EA groups were more neatly arranged in rows and clearer in structure with less nuclear condensation, as compared to those of the AD group mice. Moreover, tissue samples from the EA group mice appeared to be most similar to those from the control group. These demonstrated that electroacupuncture may be neuroprotective to some extent.

**3.3. EA Could Upregulate the Expression of TREM2 on Microglia.** To investigate the potential neuroprotective effect of electroacupuncture in the AD animal model from the viewpoint of microglia regulating neuroinflammation and test the expression of TREM2 protein, we applied immunofluorescence double staining and Western blotting.

Red light was used to label TREM2 and green light to label microglia (Iba-1) (Figure 3). It was observed that TREM2 proteins were mainly expressed on the membranes of microglia and in the dentate gyri of the hippocampi; the

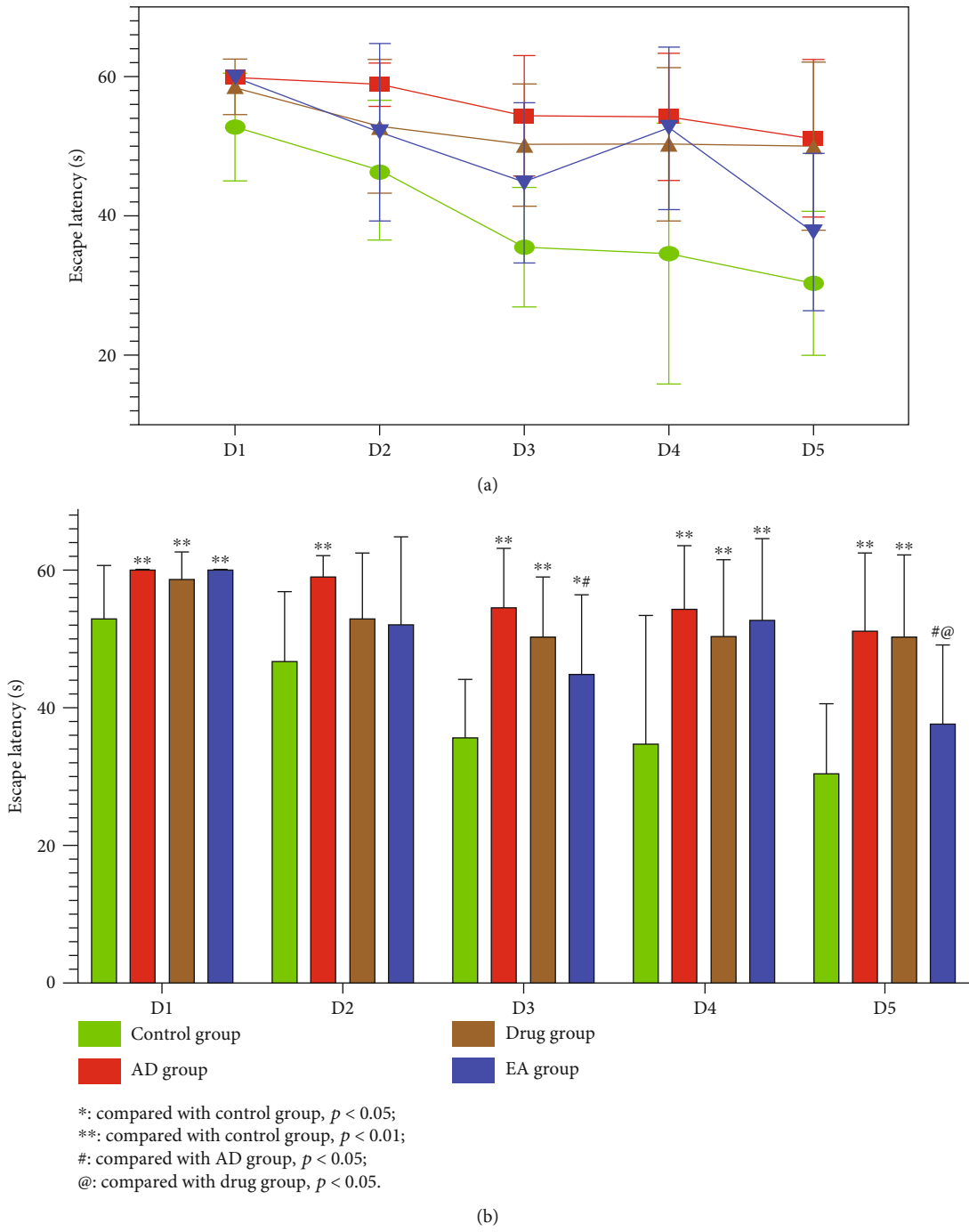


FIGURE 1: Continued.

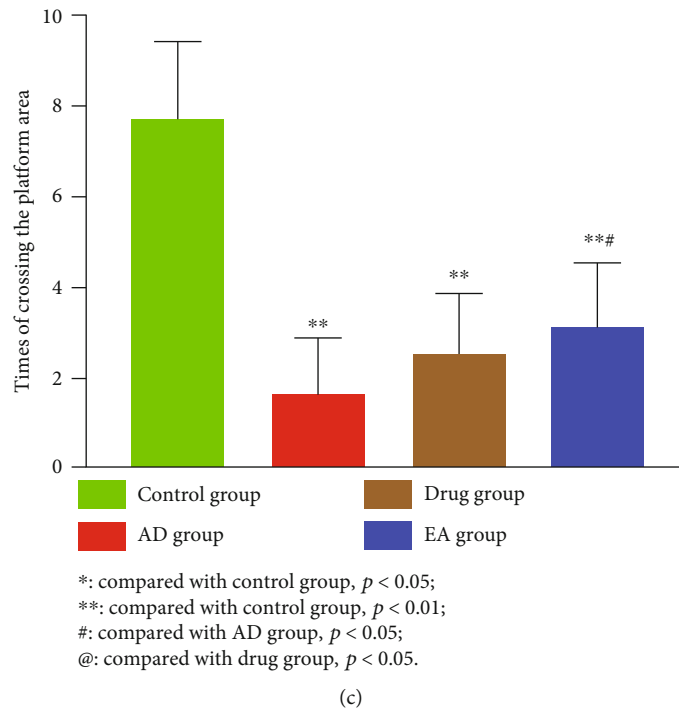


FIGURE 1: Results of the Morris water maze tests (10 mice of each group). (a, b) Results of the hidden platform trial, showing the spatial learning abilities of the mice in each group, the EA group performing better than the AD group on the third day and fifth day (third day,  $p = 0.029 < 0.05$ ; fifth day,  $p = 0.011 < 0.05$ ) and better than the drug group on the fifth day ( $p = 0.019 < 0.05$ ). (c) Results of the probe trial, showing the spatial memory abilities of the mice in each group, the EA group performing better than the AD group ( $p = 0.012 < 0.05$ ).

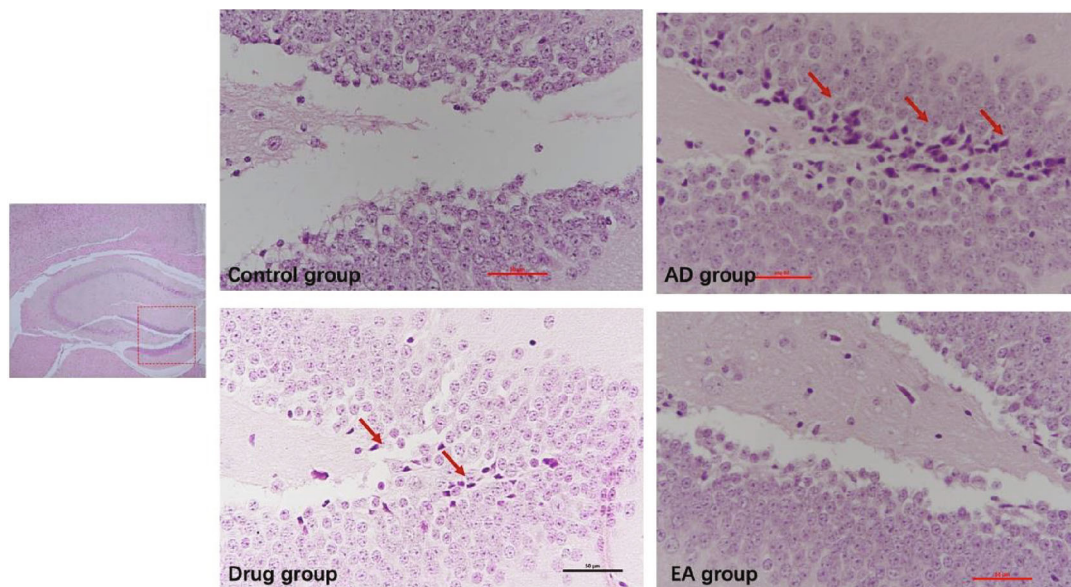


FIGURE 2: Results of HE staining in each group (3 samples of each group). In this study, we focused on the dentate gyrus zone in the hippocampus, the zone that was most related with learning and memory abilities. The red arrows point at the most neurons that lost their function in the AD group; compared with the AD group, the EA group observed less neuron apoptosis in the hippocampus.

expression of TREM2 in the control group mice was higher than that of the AD group mice.

Figure 4 shows the concentration of TREM2 proteins in the hippocampi by Western blot. The concentration of TREM2 in the hippocampi of the control group mice was found to be higher than that of the AD group mice

( $p = 0.001 < 0.01$ ). Moreover, the concentrations of TREM2 in the hippocampi of the EA group and drug group mice were also higher than that of the AD group mice ( $p = 0.001 < 0.01$ , respectively). There were only numerical advantages and no significant differences in the concentrations of TREM2 in the EA group and drug group mice.

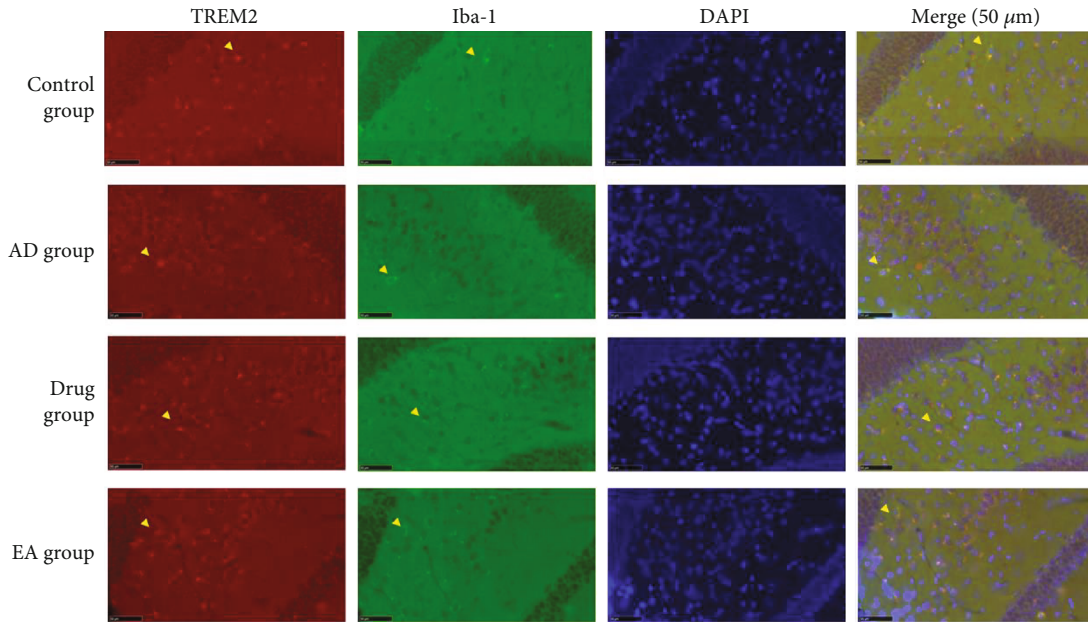


FIGURE 3: Results of immunofluorescence double staining in each group (magnification,  $\times 400$ ; 3 samples of each group). Red light revealing the expression of TREM2 on microglia, green light showing the expression of Iba-1 on microglia, and blue light showing the DNA of the nucleus in the brain. The merge showed the coexpression of TREM2 and Iba-1. The yellow arrows of each group pointed the expression of TREM2 and Iba-1 and the coexpression of TREM2 and Iba-1. We found that both TREM2 and Iba-1 were expressed on the membranes of microglia.

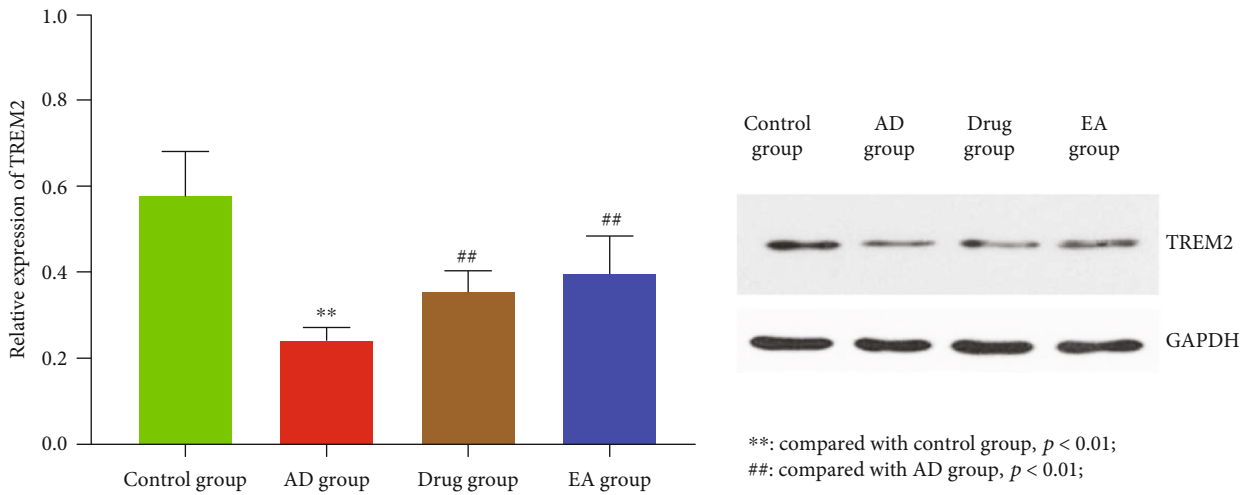


FIGURE 4: Results of the Western blotting test (in the hippocampus; 7 samples of each group). The relative expression of TREM2 for each mouse group revealing that electroacupuncture may significantly increase the expression of TREM2 in the hippocampus ( $p = 0.001 < 0.01$ ).

### 4. Discussion

Although research into the clinical and pathological features of AD spans nearly 120 years, there are still no effective treatment modalities to modify or reverse this disease [17]. Therefore, management of the risk factors associated with the disease and improving cognitive impairment or slowing the progression of the disease are the current strategies [18].

Acupuncture therapy, a treatment modality of Chinese medicine, is widely recognized and used in many countries and regions in the world. At present, acupuncture therapy is applied for improving a variety of central nervous system

diseases: dementia [19, 20], stroke [21, 22], Parkinson’s disease [23–26], spinal cord injury [27, 28], and so on [29, 30]. Clinical research in AD found this therapy to be safe, well tolerated, and effective in improving cognitive function [10].

In this study, it was demonstrated that electroacupuncture may improve spatial learning and memory abilities and be neuroprotective in the hippocampus. These results were consistent with our previous research [31, 32]. Although the escape time of the EA group mice during the hidden platform trial in the Morris water maze on the fourth day was significantly higher than that on the day before, they performed the best among the three experimental SAMP8 mouse groups on the fifth day.



The aim of this study was not only to determine the effects of electroacupuncture but also to investigate its potential mechanism of action. According to recent studies and available evidence, we considered that neuroinflammation activated by brain microglia may be “the third pathological feature” of AD [33, 34]. The magnitude of microglial activation depends on extrinsic and intrinsic conditions, for example, the type of insult, potency of the stimulus, distance from the stimulus, and immediate microenvironment [35]. Studies have implicated that the amyloid  $\beta$ -protein in the pathogenesis of AD was associated with the endogenous ligand of TREM2 [36, 37]. Moreover, current studies utilizing AD mouse models as well as human tissue have found that loss of TREM2 prevented microglia from accumulating around amyloid plaques, causing deficits in the barrier that limited neuronal injury [9]. Therefore, the expression of TREM2 on microglia could proliferate the progression of AD and be used as a target protein to demonstrate the mechanism of action of acupuncture. Another study attempting to elucidate the mechanism of action of acupuncture therapy in improving cerebral ischemia showed that TREM2 could be a potential target in EA treatment for attenuating inflammatory injury following cerebral ischemia/reperfusion [38]. However, since there were few studies evaluating the role of TREM2 expression in the mechanism of action of acupuncture therapy in AD, this study attempted to investigate the presence of any association.

In our study, immunofluorescence double staining and Western blotting were applied to illustrate the changes in the expression of TREM2 on microglia in the hippocampus of the AD animal model after electroacupuncture treatment. The results demonstrated that electroacupuncture might be neuroprotective in the hippocampus by upregulating the expression of TREM2 on microglia. In this study, we only focused on the expression of the core protein TREM2 in the hippocampus. Based on our performed studies, we found that the upregulation of TREM2 might induce the downregulation of some proinflammatory factors, such as IL-1 $\beta$  and TNF- $\alpha$ . However, as we all know, the neuroinflammation reaction activated by microglia is a complex process, which is associated with many kinds of proteins, cytokines, and proinflammatory factors [39]. Therefore, there must be some other proteins taking part in the process, which we could not examine in this study. So, in further studies, we should not only try to explore the regulation of TREM2 but also try to consider the other relative proteins, especially the downstream protein of TREM2.

## 5. Conclusion

In summary, this study suggested that electroacupuncture treatment could upregulate TREM2 expression, which is essential for the anti-inflammatory effects to protect the neurons and improvement in the learning and memory abilities in the AD animal model. However, more studies are needed to clearly elucidate the mechanism of action of electroacupuncture in AD.

## Data Availability

The data used to support the findings of this study are included within the article.

## Conflicts of Interest

There is no conflict of interest to disclose.

## Authors' Contributions

Jing Jiang designed the study. Jing Jiang and Yujie Li were the co-first authors. Jing Jiang and Qisheng Tang revised this manuscript. Jing Jiang, Yujie Li, Huiling Tian, Shun Wang, Zidong Wang, Hao Liu, Jiayi Yang, and Jingyu Ren performed the study.

## Acknowledgments

This study was supported by the National Natural Science Foundation of China Youth Fund Project (Grant No. 818041787).

## References

- [1] C. A. Lane, J. Hardy, and J. M. Schott, “Alzheimer's disease,” *European Journal of Neurology*, vol. 25, no. 1, pp. 59–70, 2018.
- [2] J. Weller and A. Budson, “Current understanding of Alzheimer's disease diagnosis and treatment,” *F1000Research*, vol. 7, 2018.
- [3] L. Guzman-Martinez, R. B. Maccioni, V. Andrade, L. P. Navarrete, M. G. Pastor, and N. Ramos-Escobar, “Neuroinflammation as a common feature of neurodegenerative disorders,” *Frontiers in Pharmacology*, vol. 10, p. 1008, 2019.
- [4] O. Mee-Inta, Z. W. Zhao, and Y. M. Kuo, “Physical Exercise Inhibits Inflammation and Microglial Activation,” *Cell*, vol. 8, no. 7, p. 691, 2019.
- [5] D. M. Angelova and D. R. Brown, “Microglia and the aging brain: are senescent microglia the key to neurodegeneration?,” *Journal of Neurochemistry*, vol. 151, no. 6, pp. 676–688, 2019.
- [6] D. Kaur, V. Sharma, and R. Deshmukh, “Activation of microglia and astrocytes: a roadway to neuroinflammation and Alzheimer's disease,” *Inflammopharmacology*, vol. 27, no. 4, pp. 663–677, 2019.
- [7] C. J. Bohlen, B. A. Friedman, B. Dejanovic, and M. Sheng, “Microglia in brain development, homeostasis, and neurodegeneration,” *Annual Review of Genetics*, vol. 53, no. 1, pp. 263–288, 2019.
- [8] K. Srinivasan, B. A. Friedman, J. L. Larson et al., “Untangling the brain's neuroinflammatory and neurodegenerative transcriptional responses,” *Nature Communications*, vol. 7, no. 1, 2016.
- [9] F. L. Yeh, D. V. Hansen, and M. Sheng, “TREM2, microglia, and neurodegenerative diseases,” *Trends in Molecular Medicine*, vol. 23, no. 6, pp. 512–533, 2017.
- [10] Y. Jia, X. Zhang, J. Yu et al., “Acupuncture for patients with mild to moderate Alzheimer's disease: a randomized controlled trial,” *BMC Complementary and Alternative Medicine*, vol. 17, no. 1, p. 556, 2017.
- [11] C. C. Yu, C. Y. Ma, H. Wang et al., “Effects of acupuncture on Alzheimer's disease: evidence from neuroimaging studies,”

- Chinese Journal of Integrative Medicine*, vol. 25, no. 8, pp. 631–640, 2019.
- [12] Y. Zhou, W. M. Song, P. S. Andhey et al., “Human and mouse single-nucleus transcriptomics reveal TREM2-dependent and TREM2-independent cellular responses in Alzheimer’s disease,” *Nature Medicine*, vol. 26, no. 1, pp. 131–142, 2020.
- [13] J. Jiang, N. Ding, K. Wang, and Z. Li, “Electroacupuncture could influence the expression of IL-1 $\beta$  and NLRP3 inflammasome in hippocampus of Alzheimer’s disease animal model,” *Evidence-based Complementary and Alternative Medicine*, vol. 2018, Article ID 8296824, 7 pages, 2018.
- [14] N. Ding, J. Jiang, M. Lu et al., “Manual acupuncture suppresses the expression of proinflammatory proteins associated with the NLRP3 inflammasome in the hippocampus of SAMP8 mice,” *Evidence-based Complementary and Alternative Medicine*, vol. 2017, Article ID 3435891, 8 pages, 2017.
- [15] B. Liu, J. Liu, and J. S. Shi, “SAMP8 mice as a model of age-related cognition decline with underlying mechanisms in Alzheimer’s disease,” *Journal of Alzheimer’s disease: JAD*, vol. 75, no. 2, pp. 385–395, 2020.
- [16] R. D’Hooge and P. P. De Deyn, “Applications of the Morris water maze in the study of learning and memory,” *Brain Research Reviews*, vol. 36, no. 1, pp. 60–90, 2001.
- [17] J. M. Long and D. M. Holtzman, “Alzheimer disease: an update on pathobiology and treatment strategies,” *Cell*, vol. 179, no. 2, pp. 312–339, 2019.
- [18] H. A. Fink, L. S. Hemmy, E. J. Linskens et al., “Diagnosis and Treatment of Clinical Alzheimer’s-Type Dementia: A Systematic Review,” in *Rockville (MD): Agency for Healthcare Research and Quality (US)*, Agency for Healthcare Research and Quality (US), Rockville (MD), USA, 2020.
- [19] G. X. Shi, Q. Q. Li, B. F. Yang et al., “Acupuncture for vascular dementia: a pragmatic randomized clinical trial,” *TheScientificWorldJOURNAL*, vol. 2015, article 161439, pp. 1–8, 2015.
- [20] J. W. Yang, G. X. Shi, S. Zhang et al., “Effectiveness of acupuncture for vascular cognitive impairment no dementia: a randomized controlled trial,” *Clinical Rehabilitation*, vol. 33, no. 4, pp. 642–652, 2018.
- [21] S. Y. Cho, M. Kim, J. J. Sun et al., “A comparison of brain activity between healthy subjects and stroke patients on fMRI by acupuncture stimulation,” *Chinese Journal of Integrative Medicine*, vol. 19, no. 4, pp. 269–276, 2013.
- [22] L. Feng, J. Zhang, C. Wei, and Y. Sun, “Clinical observation on 30 cases of transient cerebral ischemia attack treated with acupuncture and medication,” *Journal of traditional Chinese medicine = Chung i tsa chih ying wen pan*, vol. 27, no. 2, pp. 100–102, 2007.
- [23] F. K. Cheng, “The use of acupuncture in patients with Parkinson’s disease,” *Geriatric nursing (New York, NY)*, vol. 38, no. 4, pp. 302–314, 2017.
- [24] K. H. Kong, H. L. Ng, W. Li et al., “Acupuncture in the treatment of fatigue in Parkinson’s disease: a pilot, randomized, controlled, study,” *Brain and behavior*, vol. 8, no. 1, article e00897, 2018.
- [25] S. H. Lee and S. Lim, “Clinical effectiveness of acupuncture on Parkinson disease: a PRISMA-compliant systematic review and meta-analysis,” *Medicine*, vol. 96, no. 3, article e5836, 2017.
- [26] S. Yeo, M. van den Noort, P. Bosch, and S. Lim, “A study of the effects of 8-week acupuncture treatment on patients with Parkinson’s disease,” *Medicine*, vol. 97, no. 50, article e13434, 2018.
- [27] I. Estores, K. Chen, B. Jackson, L. Lao, and P. H. Gorman, “Auricular acupuncture for spinal cord injury related neuropathic pain: a pilot controlled clinical trial,” *The Journal of Spinal Cord Medicine*, vol. 40, no. 4, pp. 432–438, 2017.
- [28] Q. Fan, O. Cavus, L. Xiong, and Y. Xia, “Spinal cord injury: how could acupuncture help?,” *Journal of Acupuncture and Meridian Studies*, vol. 11, no. 4, pp. 124–132, 2018.
- [29] M. Villarreal Santiago, S. Tumilty, A. Mącznik, and R. Mani, “Does acupuncture alter pain-related functional connectivity of the central nervous system? A systematic review,” *Journal of Acupuncture and Meridian Studies*, vol. 9, no. 4, pp. 167–177, 2016.
- [30] L.-Y. Xiao, X.-R. Wang, Y. Yang et al., “Applications of acupuncture therapy in modulating plasticity of central nervous system,” *Neuromodulation: journal of the International Neuromodulation Society*, vol. 21, no. 8, pp. 762–776, 2018.
- [31] J. Jiang, K. Gao, Y. Zhou et al., “Electroacupuncture treatment improves learning-memory ability and brain glucose metabolism in a mouse model of Alzheimer’s disease: using Morris water maze and micro-PET,” *Evidence-based Complementary and Alternative Medicine*, vol. 2015, Article ID 142129, 7 pages, 2015.
- [32] J. Jiang, G. Liu, S. Shi, Y. Li, and Z. Li, “Effects of manual acupuncture combined with donepezil in a mouse model of Alzheimer’s disease,” *Acupuncture in Medicine*, vol. 37, no. 1, pp. 64–71, 2019.
- [33] C. S. Subhramanyam, C. Wang, Q. Hu, and S. T. Dheen, “Microglia-mediated neuroinflammation in neurodegenerative diseases,” *Seminars in Cell & Developmental Biology*, vol. 94, pp. 112–120, 2019.
- [34] T. M. Lancaster, M. J. Hill, R. Sims, and J. Williams, “Microglia-mediated immunity partly contributes to the genetic association between Alzheimer’s disease and hippocampal volume,” *Brain, Behavior, and Immunity*, vol. 79, pp. 267–273, 2019.
- [35] L. F. Lue, Y. M. Kuo, T. Beach, and D. G. Walker, “Microglia activation and anti-inflammatory regulation in Alzheimer’s disease,” *Molecular Neurobiology*, vol. 41, no. 2-3, pp. 115–128, 2010.
- [36] D. L. Kober and T. J. Brett, “TREM2-ligand interactions in health and disease,” *Journal of Molecular Biology*, vol. 429, no. 11, pp. 1607–1629, 2017.
- [37] C. M. Wolfe, N. F. Fitz, K. N. Nam, I. Lefterov, and R. Koldamova, “The role of APOE and TREM2 in Alzheimer’s disease-current understanding and perspectives,” *International Journal of Molecular Sciences*, vol. 20, no. 1, p. 81, 2019.
- [38] H. Xu, S. Mu, and W. Qin, “Microglia TREM2 is required for electroacupuncture to attenuate neuroinflammation in focal cerebral ischemia/reperfusion rats,” *Biochemical and Biophysical Research Communications*, vol. 503, no. 4, pp. 3225–3234, 2018.
- [39] S. Anwar and S. Rivest, “Alzheimer’s disease: microglia targets and their modulation to promote amyloid phagocytosis and mitigate neuroinflammation,” *Expert Opinion on Therapeutic Targets*, vol. 24, no. 4, pp. 331–344, 2020.

## Research Article

# Disease Stage-Associated Alterations in Learning and Memory through the Electroacupuncture Modulation of the Cortical Microglial M1/M2 Polarization in Mice with Alzheimer's Disease

Long Li,<sup>1,2</sup> Le Li,<sup>1,2</sup> Jiayong Zhang,<sup>2</sup> Sheng Huang,<sup>2</sup> Weilin Liu,<sup>3</sup> Zhifu Wang,<sup>4</sup> Shengxiang Liang,<sup>3</sup> Jing Tao,<sup>3</sup> and Lidian Chen <sup>3</sup>

<sup>1</sup>College of Rehabilitation Medicine, Fujian University of Traditional Chinese Medicine, Fuzhou, Fujian 350122, China

<sup>2</sup>Fujian Key Laboratory of Rehabilitation Technology, Fuzhou, Fujian 350122, China

<sup>3</sup>National-Local Joint Engineering Research Center of Rehabilitation Medicine Technology, Fujian University of Traditional Chinese Medicine, Fuzhou, Fujian 350122, China

<sup>4</sup>College of Integrated Traditional Chinese and Western Medicine, Fujian University of Traditional Chinese Medicine, Fuzhou, Fujian 350122, China

Correspondence should be addressed to Lidian Chen; [cld@fjtc.edu.cn](mailto:cld@fjtc.edu.cn)

Received 25 May 2020; Revised 29 July 2020; Accepted 16 August 2020; Published 28 August 2020

Academic Editor: Jing-Wen Yang

Copyright © 2020 Long Li et al. This is an open access article distributed under the Creative Commons Attribution License, which permits unrestricted use, distribution, and reproduction in any medium, provided the original work is properly cited.

Microglia are the primary cells that exert immune function in the central nervous system, and accumulating evidence suggests that microglia act as critical players in the initiation of neurodegenerative disorders, such as Alzheimer's disease (AD). Microglia seemingly demonstrate two contradictory phenotypes in response to different microenvironmental cues, the M1 phenotype and the M2 phenotype, which are detrimental and beneficial to pathogenesis, respectively. Inhibiting the M1 phenotype with simultaneous promoting the M2 phenotype has been suggested as a potential therapeutic approach for cure AD. In this study, we demonstrated that electroacupuncture at the Shenting and Baihui acupoints for 16 weeks could improve learning and memory in the Morris water maze test and reduce amyloid  $\beta$ -protein in the parietal association cortex and entorhinal cortex in mice with mild and moderate AD. Besides, electroacupuncture at the Shenting and Baihui acupoints not only suppressed M1 marker (iNOS/IL-1 $\beta$ ) expression but also increased the M2 marker (CD206/Arg1) expression in those regions. We propose that electroacupuncture at the Shenting and Baihui acupoints could regulate microglial polarization and decrease A $\beta$  plaques to improve learning and memory in mild AD mice.

## 1. Introduction

Alzheimer's disease (AD) is an age-related neurodegenerative disease that has become the fourth leading cause of death worldwide [1]. More than 50 million people are affected by dementia, and the total estimated cost of dementia is 818 billion dollars [2]. With the increasing aging population, AD has become an urgent problem to be solved for all humankind.

Over the past two decades, there has been a global cumulative investment of 600 hundred billion dollars to find a cure

for AD, and more than 95% of drugs have failed in clinical trials [3]. A progressive cognitive decline clinically characterizes AD, but pathological changes in the brain precede clinical symptoms for several years. Given the previous failures, the Food and Drug Administration drafted a guideline for the development of drugs for early-stage AD [4, 5], and current paradigms of drug design must shift from a single-target approach to developing drugs targeted at multiple disease aspects. Acupuncture is a potential therapeutic procedure that has shown evidence for clinical efficacy and safety in the treatment of chronic pain [6] and a variety of

symptoms and conditions associated with cancer [7]. Electroacupuncture (EA) has been widely used to treat neurodegenerative diseases, including dementia [8, 9]. EA could improve the Mini-Mental State Examination scores in patients with AD [10] and ameliorate cognitive deficits in animal models of AD [11, 12]. However, how EA improves cognitive function is still unknown.

Neuroinflammation has an essential impact on neurodegenerative diseases. EA is a nerve stimulation therapy that uses immunomodulation and controls inflammation to reestablish physiological homeostasis during illness. A previous study found that EA might play a neuroprotective role [13] by enhancing anti-inflammatory activity to suppress aberrant glial activation and prevent the loss of neurons in neurodegenerative disorders [14]. Microglia, the resident immune cells of the mammalian CNS, play a pivotal role in neuroinflammation. In a healthy brain, microglia are involved in modulating higher cognitive functions such as learning and memory [15, 16]. However, the function of microglia may be dynamic because of the different pathological stages of AD. Microglia are classified as ramified (quiescent/resting), activated, or amoeboid (phagocytotic). There is a model that describes the mechanism of two opposite polarization states of macrophage activation: the classically activated proinflammatory M1 macrophages and the alternatively activated anti-inflammatory M2 macrophages. The macrophage nomenclature was adopted to describe the different functional states of microglia [17]. Microglia have complex roles that are detrimental and beneficial to AD pathogenesis: M1 phenotypes are characterized by the production of inducible nitric oxide synthase (iNOS) and inflammatory cytokines (such as IL-1 $\beta$ ) and damage healthy cells, such as neurons, leading to A $\beta$  accumulation; M2 phenotypes express mannose receptor (CD206) and arginase 1 (Arg1) and downregulate neuroinflammation and remove A $\beta$  plaques.

In early-stage AD, A $\beta$  oligomers, the hydrolysis product of amyloid precursor protein by  $\beta$ - and  $\gamma$ -proteinase, lead to the M2 phenotype activation and introduce cell factors to prevent the overproduction of A $\beta$  and further pathological damage. However, the chronic A $\beta$  deposition stimulates microglia persistently [18] and causes the M1 phenotype activation to increase. In 18-month-old mice, the microglial activation is expanded into hippocampal areas free of plaques, showing that classic M1 phenotypes produce cytotoxic effects on neurons [19]. The ablation of iNOS in APP/PS1 mice can protect mice from the plaque formation and premature mortality [20]. These contradictory functions of microglia reflect their acquisition of distinct M1/M2 phenotypes in response to different microenvironmental cues [21, 22]. A study found that naringenin promotes the microglial M2 polarization and A $\beta$  degradation enzyme expression in AD [23], and the suppressor of cytokine signaling 3 suppresses the microglial polarization to the M1 phenotype by blocking the IL-6 production in vitro [24]. Therefore, with microglia, as essential members of the CNS, the conversion of phenotype and functions may lead to a novel therapeutic strategy to cure AD.

Our previous studies have demonstrated that learning and memory impairment in AD model mice could be

improved by EA [25, 26]. EA could repress the activation of microglia in various pathological models [27, 28]. Recently, research showed that the transformation of microglia into an engulfing state could reduce A $\beta$ , but overactivated microglia would accelerate the A $\beta$  deposition in AD [29]. Therefore, we wondered whether EA could regulate the microglial polarization in different pathological stages. In the present study, we chose 4- and 12-month-old APP/PS1 mice to simulate mild AD and moderate AD, respectively, aiming to investigate whether EA could regulate the microglial polarization to modulate learning and memory at different stages of Alzheimer's disease.

## 2. Methods and Materials

**2.1. Animals.** Male APPSwe/PS1B6C3-Tg [*B6C3-Tg (APP<sup>swe</sup>, PSEN1<sup>dE9</sup>) 85Dbo/MmJNju*] mice and female wild-type mice (C57/BL6) were purchased from the Model Animal Research Center of Nanjing University (SYXK2013-009) for breeding. Animals were housed 3-4 per cage in temperature (21–25°C) and light (12-h light/dark cycle) controlled rooms, with free access to food and water until the end of the experiment. All studies performed on mice were performed following the guidelines of the Fujian University of Traditional Chinese Medicine Animal Care and Use Committee, which approved all protocols used in this study.

**2.2. Experimental Design.** Data presented in this study were obtained in animals aged 4 months (mild AD) and 12 months (moderate AD). For mild AD mice, the intervention began at 4 months old and ended at 8 months old. For moderate AD mice, the intervention began at 12-month-old and ended at 16-month-old. The treatment lasted for 16 weeks. The Morris water maze (MWM) test was carried out twice before and after the intervention immediately. When trials were carried out, mice were sacrificed.

A total of 48 male APP/PS1 transgenic mice and 16 male wild-type mice were used in this study. According to age, mice were divided into mild AD and moderate AD. APP/PS1 mice were identified by polymerase chain reaction (PCR). According to the results of PCR, transgenic APP/PS1 mice were randomly divided into the AD group, the EA group, and the nonacupoint (NA) group. Wild-type (WT) littermate mice matched for age represented the WT group. There were 8 mice in each group.

**2.3. Morris Water Maze Test.** The MWM is a classical learning and memory behaviour test for rodents. The MWM device is a circular pool that is divided into four quadrants by a computer identification system to better record the performance of animals. In the place navigation test, mice were put into water to find a hidden platform within 90 seconds, which is located in the centre of the target quadrant. The mice were trained four times every day on four consecutive days. The platform was fixed for each mouse, but the swim-start position was randomized every day and alternated clockwise. The time each mouse took to find the platform within 90 seconds was recorded (escape latency). If the platform was not found within 90 seconds, the investigator



guided it to the platform and kept it on the platform for 15 seconds, and the escape latency was recorded as 90 seconds. After the place navigation test, the space exploration test was conducted on the fifth day. The platform was removed, and the mouse was placed into the water from the contralateral quadrant. The number of crossings over the original platform within 90 seconds was counted to assess the learning and memory of mice.

**2.4. Electroacupuncture Stimulation.** After the baseline measurement of the MWM test, electrical stimulation was performed. Mice in the EA group received electrical stimulation at the Shenting (DU24) and Baihui (DU20) acupuncture according to our previous study [30]. DU24 was connected with the positive pole, and DU20 was connected with the negative pole. Mice in the NA group received electrical stimulation at both side nonacupoints (the area below costal region, 2 cm superior to the posterior superior iliac spine, and ~3 cm lateral to the spine). The left side was connected with the positive pole, and the right side is connected with the negative pole. Acupuncture needles ( $\varphi$  0.3 × 13 mm, Hwato) were connected to the EA apparatus (model G6805; Suzhou Medical Appliance Factory, Shanghai, China), with a disperse-dense wave. The frequency was 1/20 Hz, and the intensity of current was 1 mA. Mice were stimulated for 16 weeks, once every other day, 3 times a week, and the treatment lasted for 30 min each time. Mice in the AD group and the WT group were fed and grasped under the same conditions without any treatment.

**2.5. Immunofluorescence.** Mice were sacrificed after anesthesia via 4% paraformaldehyde perfusion. The brain was cut into 5  $\mu$ m thick slices after paraffin embedding. After dewaxing and tissue antigen repair, sections were incubated in 5% goat serum for 1 hour at room temperature and in primary antibody overnight at 4°C. The next day, sections were incubated with fluorescein secondary antibody for 2 hours. The primary antibodies and concentrations used in this experiment included anti-Iba1 (1:500; ab5076, Abcam), anti-iNOS (1:300, ab49999, Abcam), anti-IL-1 $\beta$  (1:100, ab9722, Abcam), anti-Arg1 (1:100, 16001-1-AP, Proteintech), anti-CD206 (1:200, ab8918, Abcam), and anti-6E10 (1:1000, 803001, Biolegend). The secondary antibodies used were as follows: donkey anti-goat-Alexa 594 (1:1000; ab150132, Abcam), donkey anti-mouse-Alexa 488 (1:1000; ab150105, Abcam), donkey anti-rabbit-Alexa 488 (1:1000; ab150061, Abcam), and donkey anti-mouse-Alexa 594 (1:1000; ab150108, Abcam). After referencing *The Mouse Brain in Stereotaxic Coordinates* [31], we chose the parietal association cortex (PtA, coordinates: -1.82 mm to -2.06 mm from bregma, coronal serial sections, taking every other section for analysis) and entorhinal cortex (Ent, coordinates: -2.92 mm to -4.24 mm from bregma, coronal serial sections, taking one out of every five sections for analysis) as the regions of interest (ROIs). Four views of each piece were randomly selected for capture. An inverted laser scanning confocal microscope (LSM780, Zeiss) was used for immunofluorescence colabeling imaging, and the numbers of positive cells were manually counted. A fluorescence microscope

(DM4000 B, Leica) was used for A $\beta$  plaque imaging, and the number of plaques and plaque area fractions in the observation field were calculated by the ImageJ software. All pictures and quantifications were performed by investigators who were blinded to the experimental grouping.

**2.6. Quantitative Real-Time Polymerase Chain Reaction.** Mice were decapitated after anesthesia, and the brain tissue was separated. In detail, total RNA was isolated from tissues with RNAiso plus and reverse transcribed into cDNA using the HiScriptIIQRT SuperMix reagent kit (R223-01, Vazyme). Finally, the cDNA was quantified by qPCR using a SYBR qPCR Master Mix (Q311-02, Vazyme). The mRNA expression levels were calculated by the  $2^{-\Delta\Delta C_t}$  method after the normalization to the expression of M1 markers (iNOS/IL-1 $\beta$ ), M2 markers (CD206/Arg1), or GAPDH. All experiments were performed in triplicate and repeated at least three times. Four mice in each group were used for statistical analysis.

**2.7. Statistical Analysis.** The SPSS 21.0 software was used to perform the data analysis. The experimental data are expressed as the mean  $\pm$  SEM. Mauchly's test of sphericity was used to assess the correlation of repeated-measures data. Repeated-measures analysis of variance was performed for the place navigation test. One-way analysis of variance was applied for other data when assumptions of normality and equal variance (*F* test) were met; otherwise, the equivalent nonparametric test will be used. A value of  $P < 0.05$  was considered statistically significant.

### 3. Results

**3.1. Electroacupuncture Improved Learning and Memory in APP/PS1 Transgenic Mice.** First, we determined whether the EA stimulation could delay/reverse learning and memory impairment in APP/PS1 transgenic mice. In mild AD, the escape latency was decreased ( $P < 0.01$ , Figure 1(a)), and the number of platform crossings was increased ( $P < 0.05$ , Figure 1(b)) in the WT group compared with the AD group in the MWM test. There was no significant difference between the AD group, the EA group, and the NA group at baseline. After 16 weeks of intervention, the escape latency of the EA group was decreased comparing with the AD group ( $P < 0.01$ , Figure 1(c)), and there was a significant difference between the EA group and the NA group ( $P < 0.05$ ). In the space exploration test, mice in the EA group performed more platform crossings than mice in the AD group ( $P < 0.01$ , Figure 1(d)). There was a significant difference between the EA group and the NA group ( $P < 0.05$ ).

In moderate AD, we also found that the WT group mice had a lower escape latency ( $P < 0.01$ , Figure 2(a)) and more platform crossing times ( $P < 0.001$ , Figure 2(b)) than the AD group. There was no significant difference between the AD group, the EA group, and the NA group at baseline. After treatment, mice in the EA group spent less time finding the platform than those in the AD group ( $P < 0.01$ , Figure 2(c)), and there was a significant difference between the EA group and the NA group ( $P < 0.01$ ). Mice in the EA group showed more platform crossing times than mice in the AD group

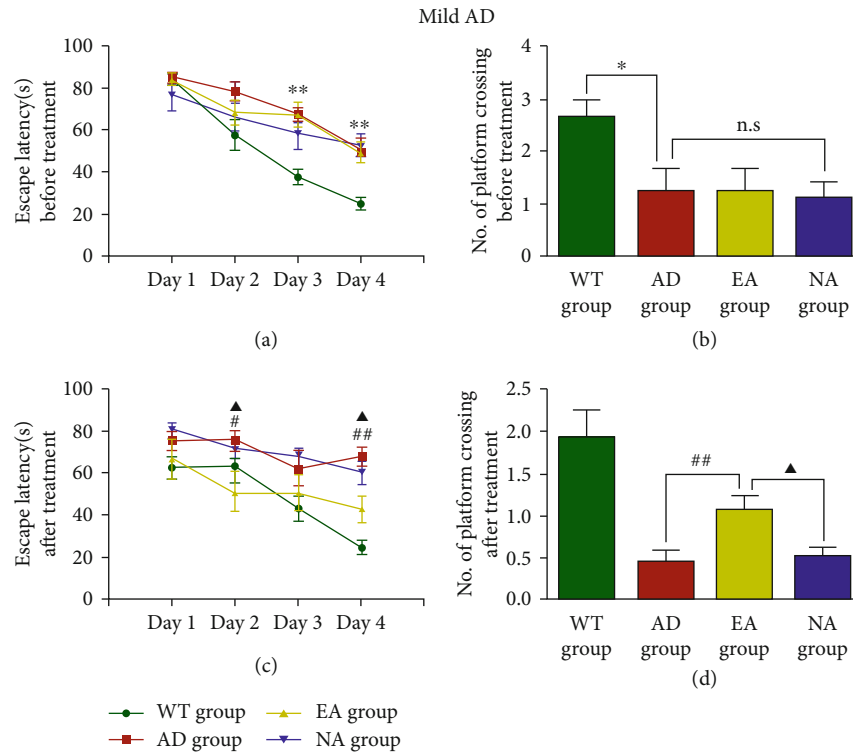


FIGURE 1: The Morris water maze test in mild AD mice. (a) Escape latency and (b) the number of platform crossings before treatment. Escape latency (c) and the number of platform crossings (d) after treatment.  $N = 8/\text{group}$ , WT group vs AD group,  $*P < 0.05$ ,  $**P < 0.01$ . AD group vs EA group,  $\#P < 0.05$ ,  $\#\#P < 0.01$ . EA group vs NA group,  $\blacktriangle P < 0.05$ , n.s. means no significant difference.

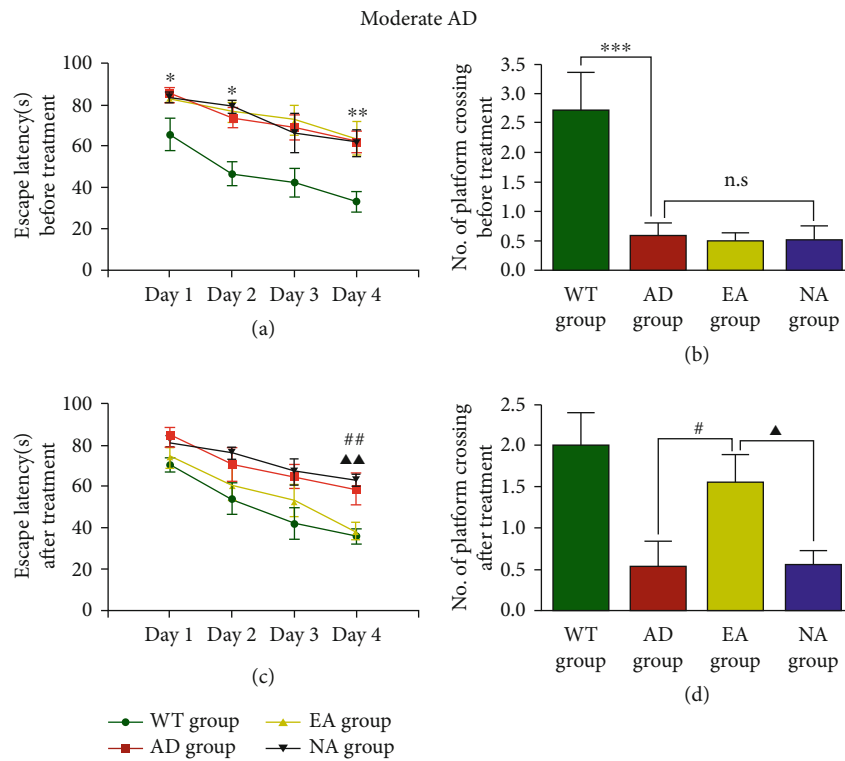


FIGURE 2: The Morris water maze test in moderate AD mice. Escape latency (a) and the number of platform crossings (b) before treatment. Escape latency (c) and the number of platform crossings (d) after treatment.  $N = 8/\text{group}$ , WT group vs AD group,  $*P < 0.05$ ,  $**P < 0.01$ ,  $***P < 0.001$ . AD group vs EA group,  $\#P < 0.05$ . EA group vs NA group,  $\blacktriangle P < 0.05$ ,  $\blacktriangle\blacktriangle P < 0.01$ , n.s. means no significant difference.

( $P < 0.05$ , Figure 2(d)). There was a significant difference between the EA group and the NA group ( $P < 0.05$ ).

These data indicated that APP/PS1 mice showed learning and memory deficits at an early age that worsened with increasing age. EA at DU24 and DU20 delayed learning and memory impairment in mice with mild and moderate AD.

**3.2. Electroacupuncture Reduced A $\beta$  Plaques in APP/PS1 Transgenic Mice.** Given that the EA stimulation could improve learning and memory in APP/PS1 mice, we next assessed its effects on A $\beta$  plaques and performed immunofluorescence with 6E10. The localization map of PtA and Ent was shown as 3a and 3b. For mild AD mice, the representative pictures of A $\beta$ -positive plaques were shown in Figure 3(c). APP/PS1 mice with EA showed a lower number and area fraction of A $\beta$ -positive plaques in the PtA than AD mice ( $P < 0.05$ , Figures 3(d) and 3(e)). There was no significant difference in A $\beta$  plaque number or area fraction in the Ent between the AD group and the EA group. For moderate AD mice, the representative pictures of A $\beta$ -positive plaques were shown in Figure 3(f). We found that the EA group showed a reduced A $\beta$ -positive plaque number in the PtA and Ent compared with the AD group ( $P < 0.01$  and  $P < 0.05$ , respectively, Figure 3(g)). However, there was no significant difference in the plaque area fraction between the AD group and EA group in the PtA and Ent (Figure 3(h)).

Collectively, these results demonstrated that EA at DU24 and DU20 could reduce the amyloid load in PtA of mild AD mice.

**3.3. Electroacupuncture Transformed the Microglial Polarization State in APP/PS1 Transgenic Mice.** Having shown that the EA stimulation reduced A $\beta$  plaques, we next aimed to investigate whether the EA stimulation could regulate the microglial polarization state and induce the expression of different phenotypes. Microglia were labeled with Iba-1, and we examined the morphological features of microglia (M1 microglia produce iNOS/IL-1 $\beta$ , and M2 microglia express CD206/Arg1) in response to the EA intervention. In mild AD, the representative pictures of the iNOS and IL-1 $\beta$  colocalization with microglia in the PtA and Ent were shown in Figures 4(a)–4(d). We observed that iNOS-Iba1 ( $P < 0.01$  in the Ent, Figure 4(f)) and IL-1 $\beta$ -Iba1 ( $P < 0.01$  in the PtA,  $P < 0.05$  in the Ent, Figures 4(g) and 4(h)) colocalizations in AD mice were significantly increased compared with those in their age-matched WT counterparts. The EA group showed a 63.96% and 64.22% decline in the iNOS-Iba1 and IL-1 $\beta$ -Iba1 colocalizations, respectively, in the Ent ( $P < 0.01$ , Figure 4(f) and  $p < 0.05$ , Figure 4(h), respectively). The representative pictures of the CD206 and Arg1 colocalization with microglia in the PtA and Ent were shown in Figures 5(a)–5(d). In the AD group mice, the CD206-Iba1 colocalization ( $P < 0.05$  in the Ent, Figure 5(f)) and Arg1-Iba1 colocalization ( $P < 0.01$  in the PtA and Ent, Figures 5(g) and 5(h)) were significantly reduced compared with those in the WT group. The CD206-Iba1 colocalization increased 55.56% in the Ent ( $P < 0.05$ , Figure 5(f)), and the Arg1-Iba1 colocalization increased 55.55% and 42.14% in the PtA and Ent, respectively ( $P < 0.01$ , Figures 5(g) and 5(h)).

In moderate AD, the representative pictures of the iNOS and IL-1 $\beta$  colocalization with microglia in the PtA and Ent were shown in Figures 6(a)–6(d). We found that the iNOS-Iba1 colocalization and IL-1 $\beta$ -Iba1 colocalization in AD mice were decreased compared with those in the WT group ( $P < 0.01$  in the PtA, Figures 6(e) and 6(g) and  $p < 0.05$  in the Ent, Figures 6(f) and 6(h)). EA at DU24 and DU20 reduced the iNOS-Iba1 colocalization in all areas (55.36% in the PtA,  $P < 0.01$ , Figure 6(e); 32.94% in the Ent,  $P < 0.05$ , Figure 6(f)) and the IL-1 $\beta$ -Iba1 colocalization in the Ent (45.62%,  $P < 0.05$ , Figure 6(h)) compared with AD mice. The representative pictures of the CD206 and Arg1 colocalization with microglia in the PtA and Ent are shown in Figures 7(a)–7(d). The CD206-Iba1 coexpression and Arg1-Iba1 coexpression were decreased in the PtA and Ent in the AD group compared with the WT group ( $P < 0.01$  or  $P < 0.05$ , Figures 7(e)–7(h)). There was no significant difference in CD206-Iba1 in the PtA and Ent between the EA group and the AD group (Figures 7(e) and 7(f)). EA at DU20 and DU24 increased the Arg1-Iba1 colocalization in the Ent compared with the AD group ( $P < 0.01$ , Figure 7(h)).

These results demonstrated that EA at DU24 and DU20 could regulate the microglial polarization state, promoting microglia to the M1 phenotype and inhibiting microglia to the M2 phenotype. Moreover, these effects were more evident in mild AD mice.

**3.4. Electroacupuncture Regulated M1/M2 mRNA Levels in APP/PS1 Transgenic Mice.** We measured the M1 (iNOS/IL-1 $\beta$ ) and M2 (CD206/Arg1) mRNA levels by qPCR. In mild AD, we found that IL-1 $\beta$  mRNA levels were increased (5, Figures 8(a) and 8(b)), and CD206 and Arg1 mRNA levels were reduced ( $P < 0.01$ , Figures 8(c) and 8(d)) in the AD group compared with the WT group. After the intervention, the mRNA levels of iNOS and IL-1 $\beta$  were reduced in the PtA and Ent ( $P < 0.01$ ), and the mRNA levels of CD206 and Arg1 were increased in the PtA and Ent ( $P < 0.05$  or  $P < 0.01$ ) of the EA group.

In moderate AD, iNOS and IL-1 $\beta$  mRNA levels were increased while CD206 and Arg1 mRNA levels were reduced in both the PtA and Ent in the AD group compared with the WT group ( $P < 0.01$ , Figures 9(a)–9(d)). There was no significant difference in iNOS, IL-1 $\beta$ , CD206, and Arg1 mRNA levels in the PtA between the AD group and the EA group. In the EA group, IL-1 $\beta$  mRNA levels were down-regulated, and CD206 mRNA levels were upregulated in the Ent ( $P < 0.01$ ) compared with the AD group.

Overall, our results showed that EA at DU24 and DU20 could regulate M1 and M2 marker mRNA levels in mild AD mice.

## 4. Discussion

In this study, we demonstrated that EA at DU24 and DU20 could improve learning and memory, drive the attenuation of A $\beta$ , and regulate the microglial M1/M2 polarization in mild AD and moderate AD.

A progressive loss of memory and cognitive impairment is principal clinical presentations of AD, and the MWM test

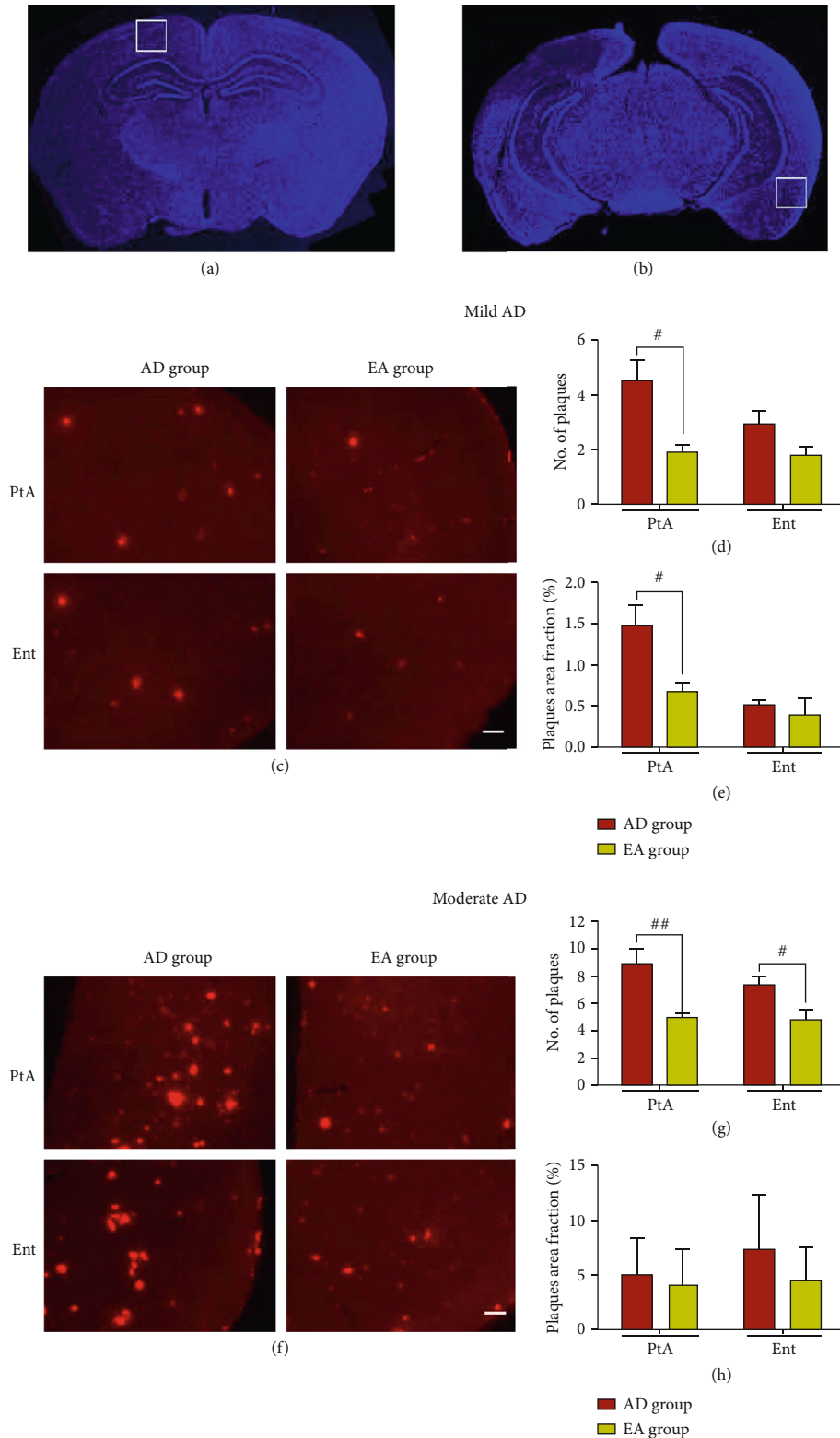


FIGURE 3: Electroacupuncture reduced A $\beta$  plaques. The localization map of PtA (a) and Ent (b). Immunofluorescence with anti-A $\beta$  (6E10) antibody in the PtA and Ent of different groups in mild AD mice (c). The average number of A $\beta$ -positive plaques (d) and average A $\beta$ -positive plaques area fraction (e) of each field of view. A $\beta$ -positive plaques in the PtA and Ent of different groups in moderate AD mice (f). The average number of A $\beta$ -positive plaques (g) and average A $\beta$ -positive plaques area fraction (h) of each field of view. Scale bar = 100  $\mu$ m,  $n = 4$ /group,  $\#P < 0.05$ ,  $\#\#P < 0.01$ .



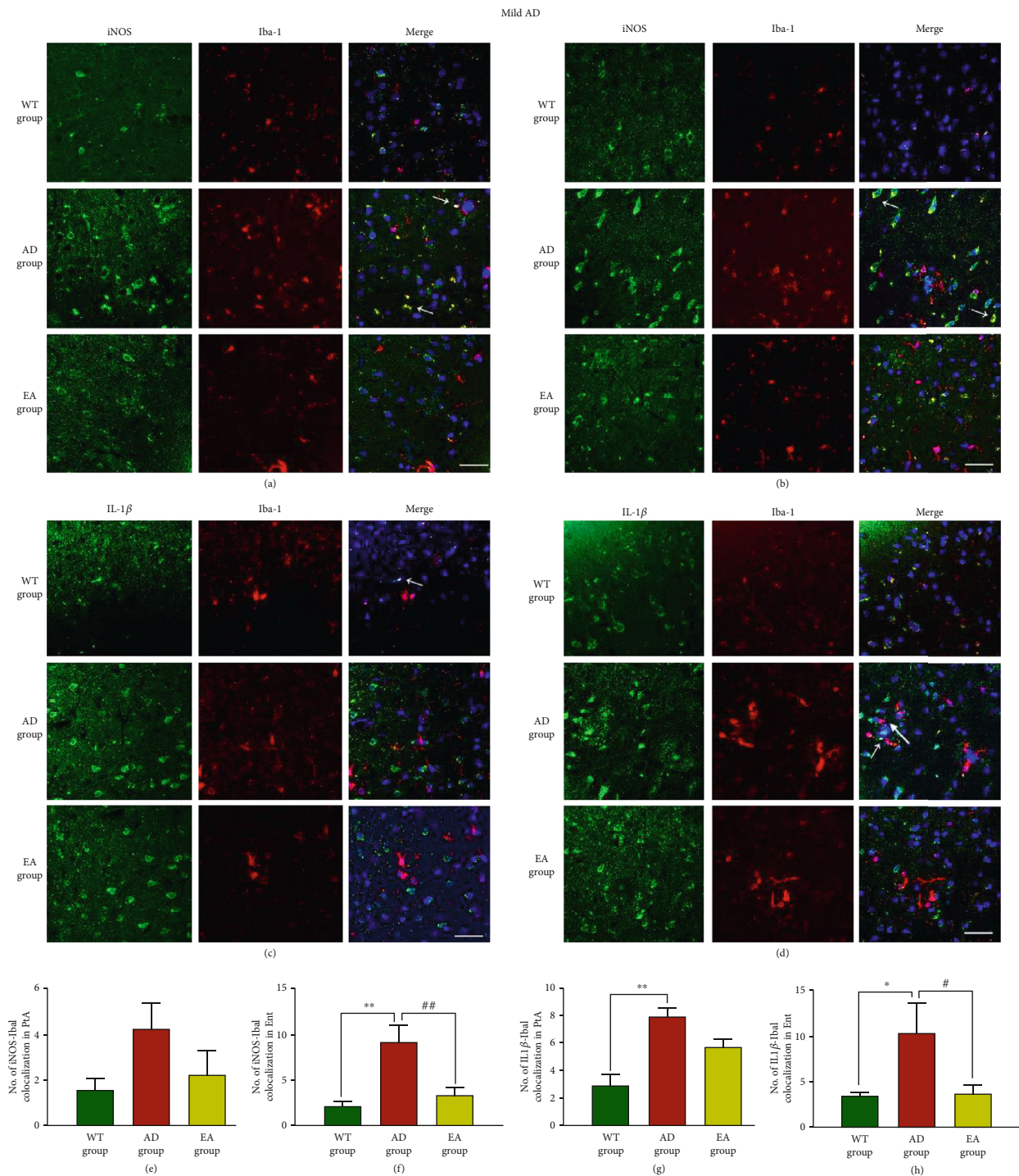


FIGURE 4: The colocalization of M1 markers and microglia in mild AD mice. Representative images of iNOS-Iba1 (a, b) and IL-1β-Iba1 (c, d) are shown in different areas. The immunofluorescence expression of the iNOS-Iba1 colocalization in the PtA (a) and Ent (b) and the number of colocalization in the PtA (e) and Ent (f). The immunofluorescence expression of the IL-1β-Iba1 colocalization in the PtA (c) and Ent (d) and the number of colocalization in the PtA (g) and Ent (h). Scale bar = 50 μm, n = 4/group, WT group vs AD group, \*P < 0.05, \*\*P < 0.01. AD group vs EA group, #P < 0.05, ##P < 0.01.

is a traditional methodology to measure learning and memory in animals. Research has suggested that a gradual decline in cognition could be detected in most 6- to 18-month-old APP/PS1 mice, and young (less than or equal to 5 months old) APP/SP1 mice showed little difference in the declining

trend of escape latency after repeated training when compared with WT mice [32]. A study indicated that there was no significant difference in escape latency between WT and APP/PS1 mice at 3 months of age, while the escape latency was significantly longer in 5-month-old APP/PS1

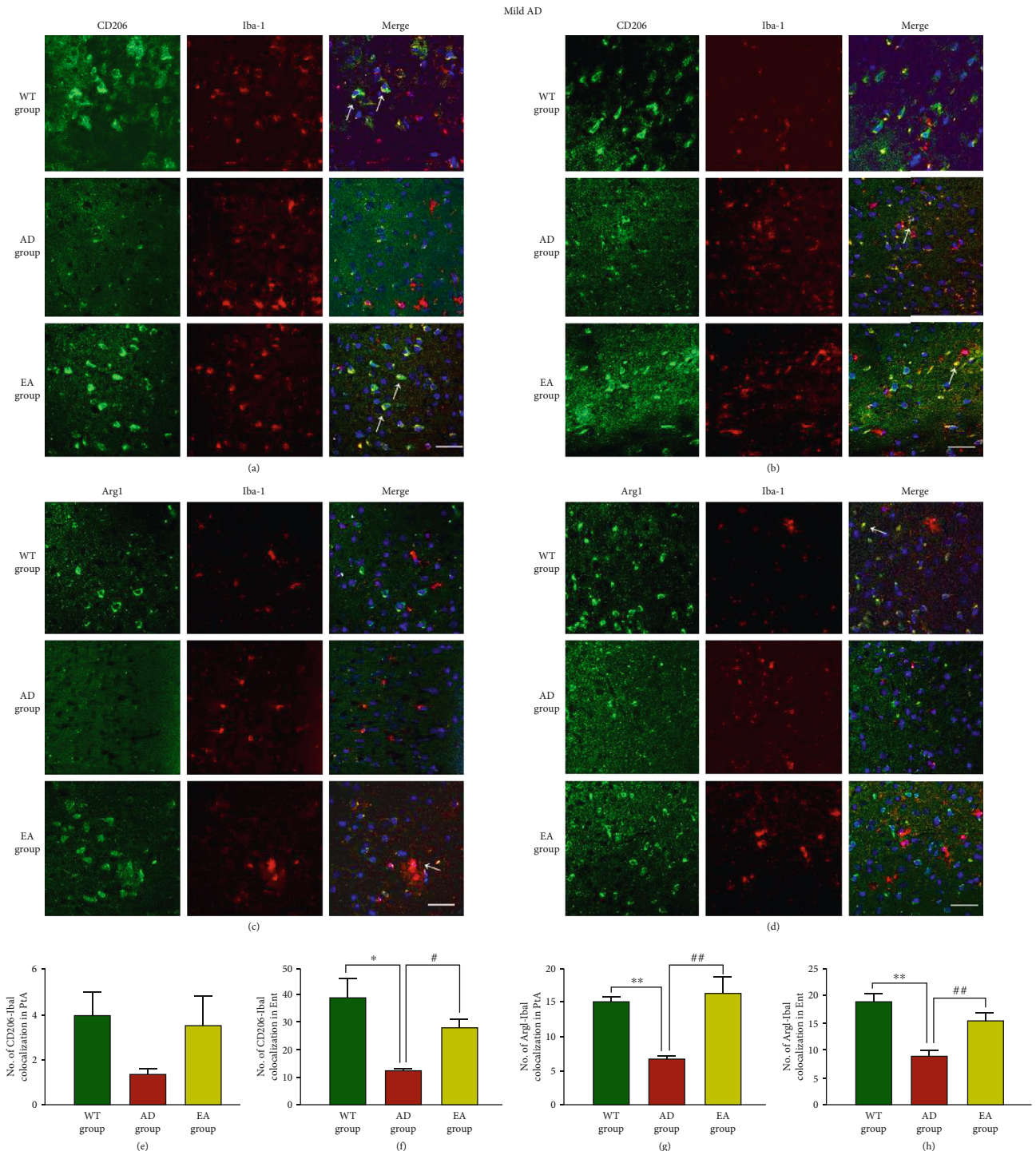


FIGURE 5: The colocalization of M2 markers and microglia in mild AD mice. Representative images of CD206-Iba1 (ab) and Arg1-Iba1 (cd) are shown in different areas. The immunofluorescence expression of the CD206-Iba1 colocalization in the PtA (a) and Ent (b) and the number of colocalization in the PtA (e) and Ent (f). The immunofluorescence expression of the Arg1-Iba1 colocalization in the PtA (c) and Ent (d) and the number of colocalization in the PtA (g) and Ent (h). Scale bar = 50  $\mu$ m,  $n = 4$ /group, WT group vs AD group, \* $P < 0.05$ , \*\* $P < 0.01$ . AD group vs EA group, # $P < 0.05$ , ## $P < 0.01$ .

mice than in their counterparts in the MWM test [33]. Therefore, we chose the 4-month-old APP/PS1 mice to simulate the mild AD stage. On the other hand,  $A\beta$  plaques were observed in APP/PS1 mice as young as 3 months of age, with linear increases with months of age, but slow growth was

observed after 12 months of age [33]. Therefore, we chose the 12-month-old APP/PS1 mice to simulate the moderate AD stage.

DU24 and DU20 are located along the governor vessel, and their stimulation is widely reported to improve cognition



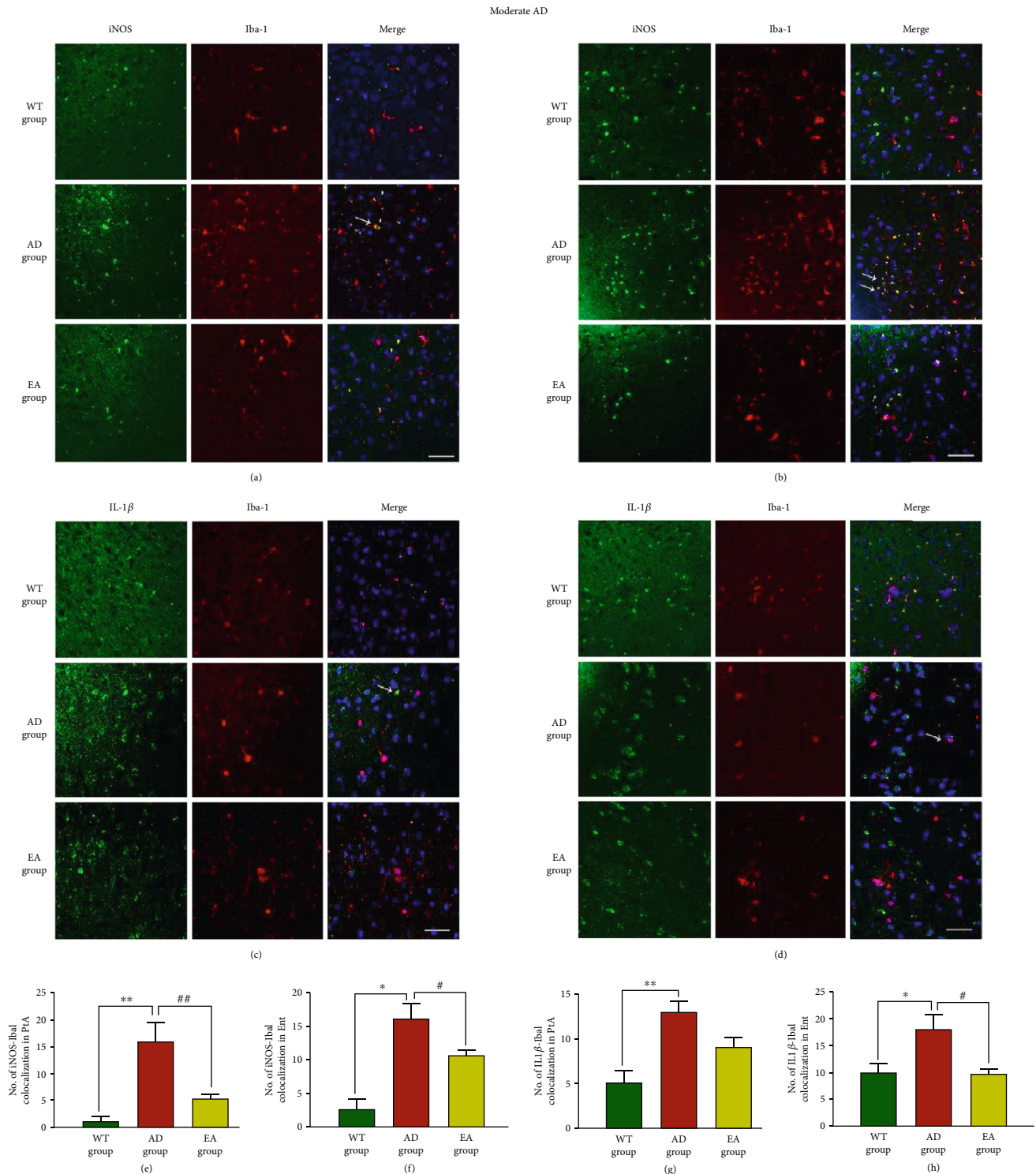


FIGURE 6: The colocalization of M1 markers and microglia in moderate AD mice. Representative images of iNOS-Iba1 (a, b) and IL-1 $\beta$ -Iba1 (c, d) are shown in different areas. The immunofluorescence expression of the iNOS-Iba1 colocalization in the PtA (a) and Ent (b) and the number of colocalization in the PtA (e) and Ent (f). The immunofluorescence expression of the IL-1 $\beta$ -Iba1 colocalization in the PtA (c) and Ent (d) and the number of colocalization in the PtA (g) and Ent (h). Scale bar = 50  $\mu$ m,  $n = 4$ /group, WT group vs AD group, \* $P < 0.05$ , \*\* $P < 0.01$ . AD group vs EA group, # $P < 0.05$ , ## $P < 0.01$ .

[34–37]. Our previous studies proved that EA at DU24 and DU20 improved cognitive deficits [34] and mediated synaptic plasticity in the periinfarct hippocampal CA1 region of

rats following ischaemic stroke [38]. Furthermore, the EA stimulation of DU24 and DU20 might reactivate cognition-related brain regions [37]. The Ent is the critical structure

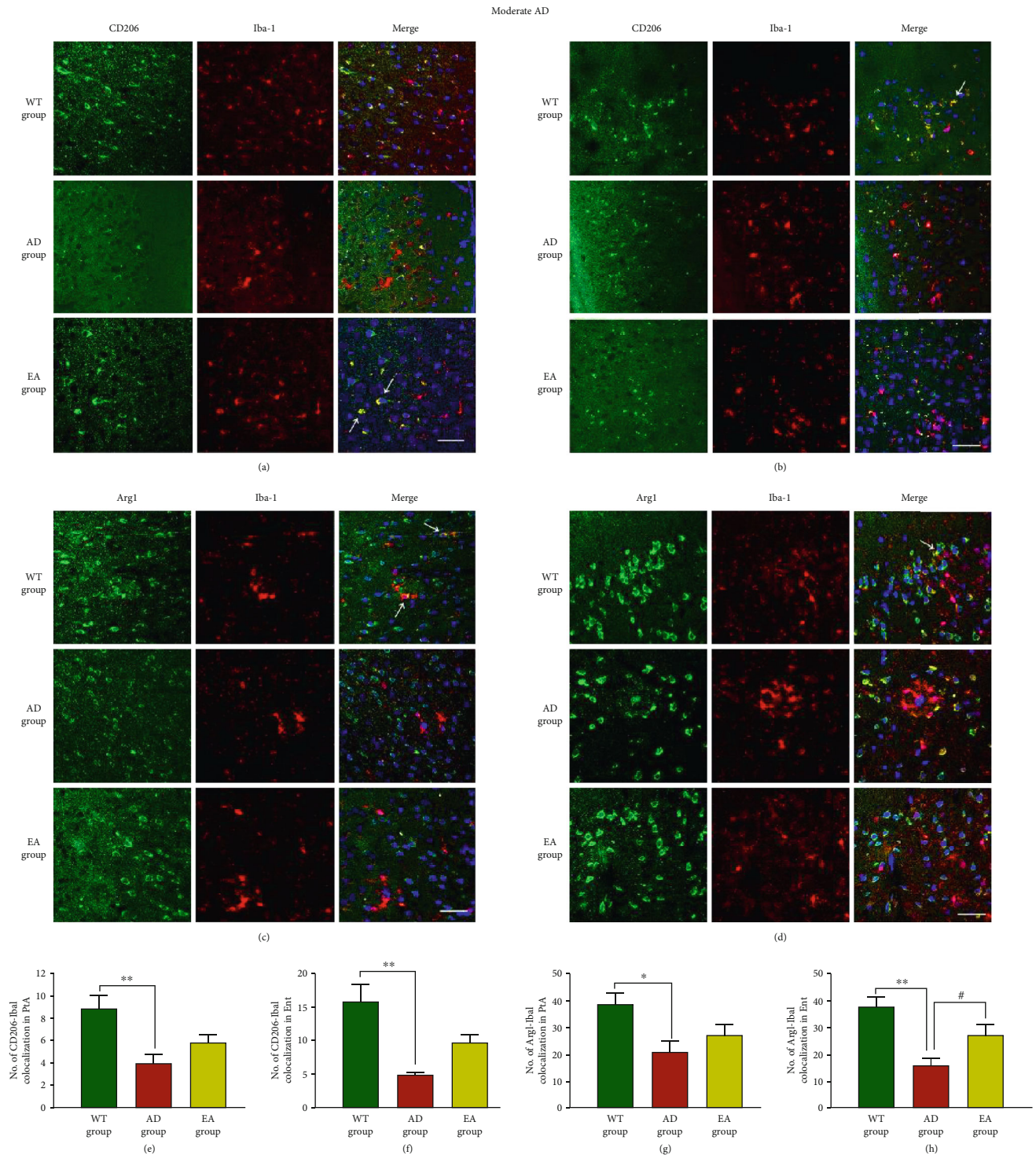


FIGURE 7: The colocalization of M2 markers and microglia in moderate AD mice. Representative images of CD206-Iba1 (a, b) and Arg1-Iba1 (c, d) are shown in different areas. The immunofluorescence expression of the CD206-Iba1 colocalization in the PtA (a) and Ent (b) and the number of colocalization in the PtA (e) and Ent (f). The immunofluorescence expression of the Arg1-Iba1 colocalization in the PtA (c) and Ent (d) and the number of colocalization in the PtA (g) and Ent (h). Scale bar = 50  $\mu$ m,  $n = 4$ /group, WT group vs AD group, \* $P < 0.05$ , \*\* $P < 0.01$ . AD group vs EA group, # $P < 0.05$ .

relaying memory-related information between the neocortex and the hippocampus, which is first affected in AD [39, 40]. The PtA is often considered to be the brain region with obvious pathological changes in neuroimaging [41]. Evidence

from [18F]flortaucipir PET and T1-weighted magnetic resonance imaging showed that the lateral and medial PtA and lateral temporal cortex were most relevant to cognitive decline in AD [42].



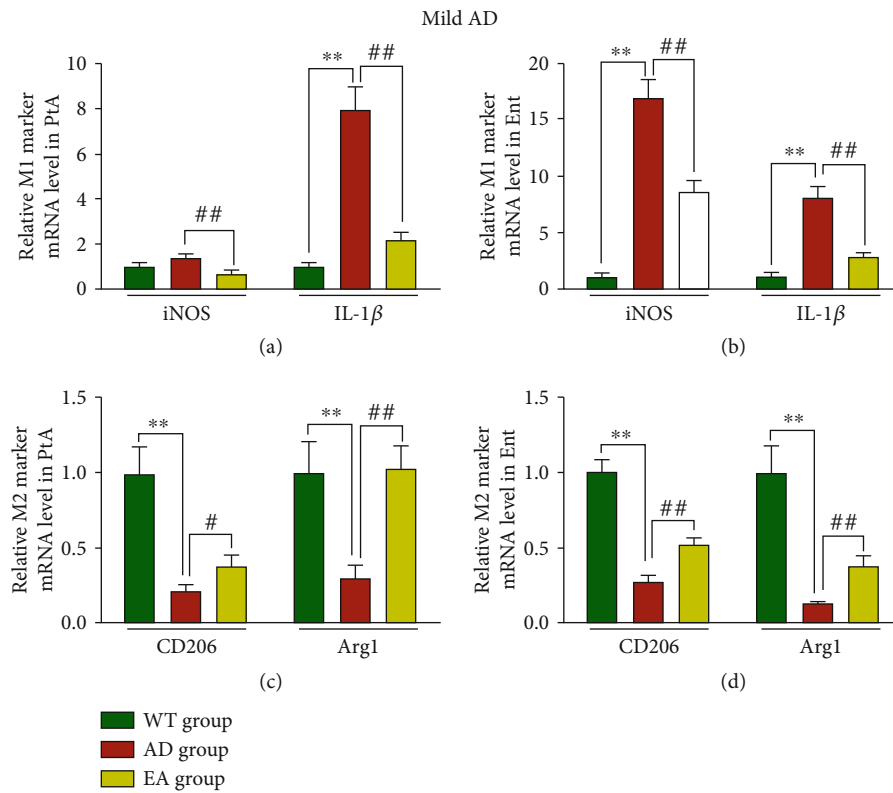


FIGURE 8: Relative M1 and M2 marker mRNA levels in mild AD mice. M1 marker mRNA levels in the PtA (a) and Ent (b). M2 marker mRNA levels in the PtA (c) and Ent (d).  $N = 4/\text{group}$ , WT group vs AD group,  $**P < 0.01$ . AD group vs EA group,  $\#P < 0.05$ ,  $\#\#P < 0.01$ .

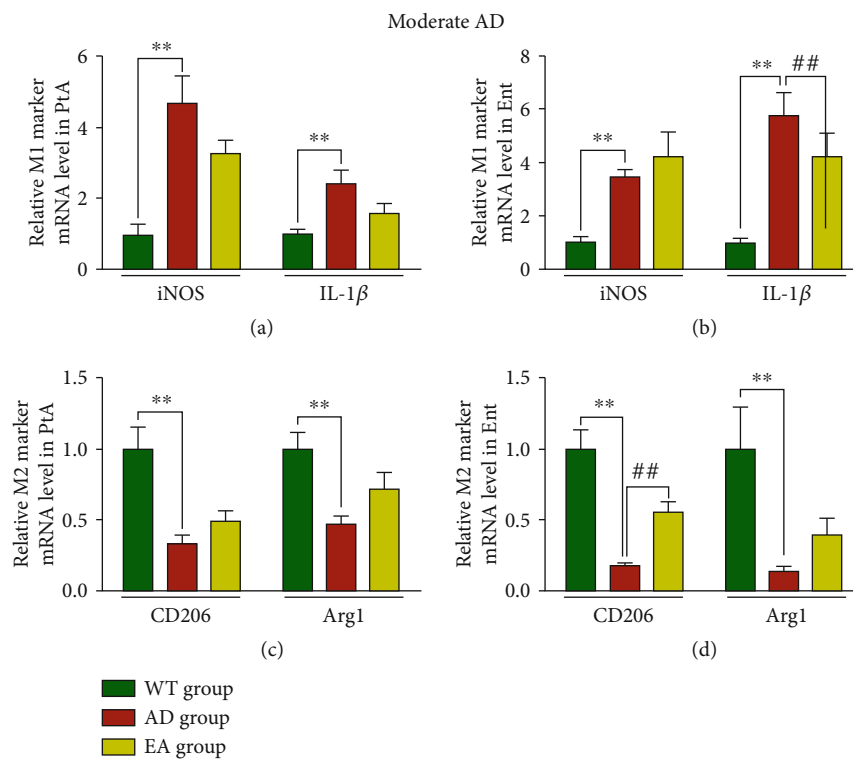


FIGURE 9: Relative M1 and M2 marker mRNA levels in moderate AD mice. M1 marker mRNA levels in the PtA (a) and Ent (b). M2 marker mRNA levels in the PtA (c) and Ent (d).  $N = 4/\text{group}$ , WT group vs AD group,  $**P < 0.01$ . AD group vs EA group,  $\#\#P < 0.01$ .

$A\beta$ , reactive gliosis, and neuroinflammation are hallmarks of AD [43]. Long considered to be secondary events to neurodegeneration, microglia-related pathways have been identified as central to AD risk and pathogenesis [44, 45]. We proved the bidirectional regulation of the DU24 and DU20 stimulation on the microglial polarization: it downregulated the M1 phenotype microglia and upregulated the M2 phenotype microglia in mild AD. EA inhibited iNOS and IL-1 $\beta$  and promoted CD206 and Arg1 in 8 months old APP/PS1 mice. However, EA could not upregulate the M2 phenotype microglia in moderate AD. We found that the iNOS and IL-1 $\beta$  colocalization decreased, but CD206 and Arg1 had no difference in immunofluorescence and mRNA level in 16 months old APP/PS1 mice. It could expound that the effect of EA on AD mice at different stages is different. Therefore, EA was more effective in mild AD mice than in moderate AD mice. EA suppressed not only the microglial polarization to the M1 phenotype but also promoted the microglial polarization to the M2 phenotype in mild AD mice.

Microglia can be neuroprotective by degrading  $A\beta$  plaques similar to action against the  $A\beta$  accumulation [46]. However, an age-dependent increase in both the number and the size of  $A\beta$  plaques in AD might reflect a diminution in the microglial phagocytic capability [47]. In the present study, we found that EA at DU24 and DU20 reduced  $A\beta$ -positive plaques in the PtA, rather than Ent in mild AD mice. It may be related to the targeting brain region under different acupoints. Research had proved that EA at DU20 and right Qubin (GB7, acupuncture) could increase glucose metabolism in the parietal lobe [48]. However, we found changes only in the number of  $A\beta$ -positive plaques, not in the area fraction in moderate AD mice. It may indicate that the effect of EA is limited, which could not eliminate the accumulation of  $A\beta$  in 16 months old APP/PS1 mice. Moreover, it needs further study.

## 5. Conclusion

EA at DU24 and DU20 reduced  $A\beta$  plaques to improve learning and memory in mild AD mice. This finding is mainly related to the microglial M1/M2 polarization inducing by EA.

## Data Availability

The data used to support the findings of this study are available from the corresponding author upon request.

## Conflicts of Interest

All authors declare no financial or commercial conflict of interest.

## Authors' Contributions

Lidian Chen and Jing Tao designed the experiment. Jiayong Zhang and Sheng Huang performed the experiment. Weilin Liu, Zhifu Wang, and Shengxiang Liang analyzed the data. Li Long and Li Le prepared the paper and contributed equally to this work.

## Acknowledgments

The present study was supported by the National Natural Science Foundation of China (NO. 81774424, 81774385, and 81704149) and Fujian Natural Science Foundation of China (2016J01391).

## References

- [1] A. Tramutola, C. Lanzillotta, M. Perluigi, and D. A. Butterfield, "Oxidative stress, protein modification and Alzheimer disease," *Brain Research Bulletin*, vol. 133, pp. 88–96, 2017.
- [2] M. Prince, *World Alzheimer Report: The Global Impact of Dementia*, Alzheimer's Disease International, London, UK, 2015.
- [3] L. S. Schneider, F. Mangialasche, N. Andreasen et al., "Clinical trials and late-stage drug development for Alzheimer's disease: an appraisal from 1984 to 2014," *Journal of Internal Medicine*, vol. 275, no. 3, pp. 251–283, 2014.
- [4] B. R. Ott, "The long and winding road toward Alzheimer prevention FDA offers new guidance on developing drugs for early-stage AD; seeks input," *R.I. Medical Journal*, vol. 96, pp. 14–15, 2013.
- [5] L. S. Schneider, "Rethinking the Food and Drug Administration's 2013 guidance on developing drugs for early-stage Alzheimer's disease," *Alzheimers Dement*, vol. 10, no. 2, pp. 247–250, 2014.
- [6] K. Kawakita and K. Okada, "Acupuncture therapy: mechanism of action, efficacy, and safety: a potential intervention for psychogenic disorders," *Biopsychosoc Med*, vol. 8, no. 1, p. 4, 2014.
- [7] W. Lu, E. Dean-Clover, A. Doherty-Gilman, and D. S. Rosenthal, "The value of acupuncture in cancer care," *Hematology/Oncology Clinics of North America*, vol. 22, no. 4, pp. 631–648, 2008.
- [8] Y. Jia, X. Zhang, J. Yu et al., "Acupuncture for patients with mild to moderate Alzheimer's disease: a randomized controlled trial," *BMC Complementary and Alternative Medicine*, vol. 17, no. 1, p. 556, 2017.
- [9] S. Shao, Y. Tang, Y. Guo, Z. Tian, D. Xiang, and J. Wu, "Effects of acupuncture on patients with Alzheimer's disease: protocol for a systematic review and meta-analysis," *Medicine (Baltimore)*, vol. 98, no. 4, article e14242, 2019.
- [10] Q. Feng, L. L. Bin, Y. B. Zhai, M. Xu, Z. S. Liu, and W. N. Peng, "Long-term efficacy and safety of electroacupuncture on improving MMSE in patients with Alzheimer's disease," *Zhongguo Zhen Jiu*, vol. 39, no. 1, pp. 3–8, 2019.
- [11] W. Dong, W. Guo, X. Zheng et al., "Electroacupuncture improves cognitive deficits associated with AMPK activation in SAMP8 mice," *Metabolic Brain Disease*, vol. 30, no. 3, pp. 777–784, 2015.
- [12] M. Zhang, G. H. Xv, W. X. Wang, D. J. Meng, and Y. Ji, "Electroacupuncture improves cognitive deficits and activates PPAR- $\gamma$  in a rat model of Alzheimer's disease," *Acupuncture in Medicine*, vol. 35, no. 1, pp. 44–51, 2017.
- [13] J. Zhao, L. Wang, and Y. Li, "Electroacupuncture alleviates the inflammatory response via effects on M1 and M2 macrophages after spinal cord injury," *Acupuncture in Medicine*, vol. 35, no. 3, pp. 224–230, 2017.
- [14] J. Deng, E. Lv, J. Yang et al., "Electroacupuncture remediates glial dysfunction and ameliorates neurodegeneration in the

- astrocytic  $\alpha$ -synuclein mutant mouse model," *Journal of Neuroinflammation*, vol. 12, no. 1, 2015.
- [15] C. N. Parkhurst, G. Yang, I. Ninan et al., "Microglia promote learning-dependent synapse formation through brain-derived neurotrophic factor," *Cell*, vol. 155, no. 7, pp. 1596–1609, 2013.
  - [16] J. C. Udeochu, J. M. Shea, and S. A. Villeda, "Microglia communication: parallels between aging and Alzheimer's disease," *Clin Exp Neuroimmunol*, vol. 7, no. 2, pp. 114–125, 2016.
  - [17] M. Czeh, P. Gressens, and A. M. Kaindl, "The yin and yang of microglia," *Developmental Neuroscience*, vol. 33, no. 3-4, pp. 199–209, 2011.
  - [18] M. Prinz, J. Priller, S. S. Sisodia, and R. M. Ransohoff, "Heterogeneity of CNS myeloid cells and their roles in neurodegeneration," *Nature Neuroence*, vol. 14, no. 10, pp. 1227–1235, 2011.
  - [19] S. Jimenez, D. Baglietto-Vargas, C. Caballero et al., "Inflammatory response in the hippocampus of PS1M146L/APP751SL mouse model of Alzheimer's disease: age-dependent switch in the microglial phenotype from alternative to classic," *The Journal of Neuroscience*, vol. 28, no. 45, pp. 11650–11661, 2008.
  - [20] C. Nathan, N. Calingasan, J. Nezezon et al., "Protection from Alzheimer's-like disease in the mouse by genetic ablation of inducible nitric oxide synthase," *The Journal of Experimental Medicine*, vol. 202, no. 9, pp. 1163–1169, 2005.
  - [21] V. Chhor, T. Le Charpentier, S. Lebon et al., "Characterization of phenotype markers and neuronotoxic potential of polarised primary microglia in vitro," *Brain Behavior & Immunity*, vol. 32, pp. 70–85, 2013.
  - [22] X. Hu, R. K. Leak, Y. Shi et al., "Microglial and macrophage polarization—new prospects for brain repair," *Nature Reviews. Neurology*, vol. 11, no. 1, pp. 56–64, 2015.
  - [23] Z. Yang, T. Kuboyama, and C. Tohda, "Naringenin promotes microglialM2polarization andA $\beta$ degradation enzyme expression," *Phytotherapy Research*, vol. 33, no. 4, pp. 1114–1121, 2019.
  - [24] N. Iwahara, S. Hisahara, J. Kawamata et al., "Role of suppressor of cytokine signaling 3 (SOCS3) in altering activated microglia phenotype in APP<sup>swe</sup>/PS1<sup>dE9</sup> mice," *Journal of Alzheimer's Disease*, vol. 55, no. 3, pp. 1235–1247, 2017.
  - [25] W. Liu, P. Zhuo, L. Li et al., "Activation of brain glucose metabolism ameliorating cognitive impairment in APP/PS1 transgenic mice by electroacupuncture," *Free Radical Biology & Medicine*, vol. 112, pp. 174–190, 2017.
  - [26] R. Lin, L. Li, Y. Zhang et al., "Electroacupuncture ameliorate learning and memory by improving N-acetylaspartate and glutamate metabolism in APP/PS1 mice," *Biological Research*, vol. 51, no. 1, p. 21, 2018.
  - [27] B. Han, Y. Lu, H. Zhao, Y. Wang, and T. Wang, "Electroacupuncture modulated the inflammatory reaction in MCAO rats via inhibiting the TLR4/NF- $\kappa$ B signaling pathway in microglia," *International Journal of Clinical & Experimental Pathology*, vol. 8, no. 9, pp. 11199–11205, 2015.
  - [28] J. Jiang, Y. Luo, W. Qin et al., "Electroacupuncture suppresses the NF- $\kappa$ B signaling pathway by upregulating cylindromatosis to alleviate inflammatory injury in cerebral ischemia/reperfusion rats," *Frontiers in Molecular Neuroscience*, vol. 10, pp. 363–363, 2017.
  - [29] C. Condello, P. Yuan, and J. Grutzendler, "Microglia-mediated neuroprotection, TREM2, and Alzheimer's disease: evidence from Optical Imaging," *Biological Psychiatry*, vol. 83, no. 4, pp. 377–387, 2018.
  - [30] S. Huang, L. Lil, Z. Wang et al., "Effect of electroacupuncture on learning-memory and expression of  $\beta$ -site amyloid precursor protein cleaving enzyme 1 in APP/PS1 mice," *Chin J Rehabil Theory Pract*, vol. 25, pp. 44–50, 2019.
  - [31] P. George and K. B.J.F, *The mouse brain in Stereotaxic Coordinates (second edition)*, Academic, San Diego, 2001.
  - [32] T. Gao, "A review on the relationship between AP level in brain and age-related changes of cognitive behavior in APP / PS1 mice," *JOURNAL OF APOPLEXY AND NERVOUS DISEASES*, vol. 32, pp. 189-190, 2015.
  - [33] S. Zhu, J. Wang, Y. Zhang et al., "The role of neuroinflammation and amyloid in cognitive impairment in an APP/PS1 transgenic mouse model of Alzheimer's disease," *CNS Neuroscience & Therapeutics*, vol. 23, no. 4, pp. 310–320, 2017.
  - [34] R. Lin, K. Yu, X. Li et al., "Electroacupuncture ameliorates post-stroke learning and memory through minimizing ultrastructural brain damage and inhibiting the expression of MMP-2 and MMP-9 in cerebral ischemia-reperfusion injured rats," *Molecular Medicine Reports*, vol. 14, no. 1, pp. 225–233, 2016.
  - [35] Y. Ye, H. Li, J. W. Yang et al., "Acupuncture attenuated vascular dementia-induced hippocampal long-term potentiation impairments via activation of D1/D5 receptors," *Stroke*, vol. 48, no. 4, pp. 1044–1051, 2017.
  - [36] Q. Zhang, Y. N. Li, Y. Y. Guo et al., "Effects of preconditioning of electro-acupuncture on postoperative cognitive dysfunction in elderly: a prospective, randomized, controlled trial," *Medicine (Baltimore)*, vol. 96, no. 26, article e7375, 2017.
  - [37] T. Wen, X. Zhang, S. Liang et al., "Electroacupuncture ameliorates cognitive impairment and spontaneous low-frequency brain activity in rats with ischemic stroke," *Journal of Stroke and Cerebrovascular Diseases*, vol. 27, no. 10, pp. 2596–2605, 2018.
  - [38] G. Xie, C. Song, X. Lin et al., "Electroacupuncture regulates hippocampal synaptic plasticity via inhibiting Janus-activated kinase 2/signal transducer and activator of transcription 3 signaling in cerebral ischemic rats," *Journal of Stroke and Cerebrovascular Diseases*, vol. 28, no. 3, pp. 792–799, 2019.
  - [39] T. Nakazono, T. N. Lam, A. Y. Patel et al., "Impaired In Vivo Gamma Oscillations in the Medial Entorhinal Cortex of Kappa-in Alzheimer Model," *Frontiers in Systems Neuroscience*, vol. 11, 2017.
  - [40] X.-Y. Li, W.-W. Men, H. Zhu et al., "Age- and Brain Region-Specific Changes of Glucose Metabolic Disorder, Learning, and Memory Dysfunction in Early Alzheimer's Disease Assessed in APP/PS1 Transgenic Mice Using 18F-FDG-PET," *International Journal of Molecular Ences*, vol. 17, no. 10, p. 1707, 2016.
  - [41] M. Mase, H. Nagai, H. Kabasawa, T. Ogawa, A. Iida, and K. Yamada, "Cerebral blood flow and metabolism in patients with cognitive impairments after minor traumatic brain injury: PET study in a chronic state," *International Congress*, vol. 1259, pp. 365–369, 2004.
  - [42] R. Ossenkoppele, R. Smith, T. Ohlsson et al., "Associations between tau, A $\beta$ , and cortical thickness with cognition in Alzheimer disease," *Neurology*, vol. 92, no. 6, pp. e601–e612, 2019.
  - [43] T. Wyss-Coray and J. Rogers, "Inflammation in Alzheimer disease—a brief review of the basic science and clinical literature," *Cold Spring Harbor Perspectives in Medicine*, vol. 2, no. 1, 2012.

- [44] T. Jonsson, H. Stefansson, S. Steinberg et al., "Variant of TREM2 associated with the risk of Alzheimer's disease," *New England Journal of Medicine*, vol. 368, no. 2, pp. 107–116, 2013.
- [45] B. Zhang, C. Gaiteri, L.-G. Bodea et al., "Integrated systems approach identifies genetic nodes and networks in late-onset Alzheimer's disease," *Cell*, vol. 153, no. 3, pp. 707–720, 2013.
- [46] K. Takata, Y. Kitamura, M. Saeki et al., "Galantamine-induced amyloid-beta clearance mediated via stimulation of microglial nicotinic acetylcholine receptors," *The Journal of Biological Chemistry*, vol. 285, no. 51, pp. 40180–40191, 2010.
- [47] K. G. Mawuenyega, W. Sigurdson, V. Ovod et al., "Decreased clearance of CNS beta-amyloid in Alzheimer's disease," *Science*, vol. 330, no. 6012, p. 1774, 2010.
- [48] Z. Fang, J. Ning, C. Xiong, and Y. Shulin, "Effects of electroacupuncture at head points on the function of cerebral motor areas in stroke patients: a PET study," *Evidence-based Complementary and Alternative Medicine*, vol. 2012, Article ID 902413, 9 pages, 2012.



## Review Article

# Machine Learning in Neuroimaging: A New Approach to Understand Acupuncture for Neuroplasticity

Tao Yin,<sup>1,2</sup> Peihong Ma,<sup>1,2</sup> Zilei Tian,<sup>1,2</sup> Kunnan Xie,<sup>1,2</sup> Zhaoxuan He,<sup>1,2</sup> Ruirui Sun,<sup>1,2</sup> and Fang Zeng<sup>1,2,3</sup> 

<sup>1</sup>Acupuncture and Tuina School/The Third Teaching Hospital, Chengdu University of Traditional Chinese Medicine, Chengdu, Sichuan, China

<sup>2</sup>Acupuncture & Brain Science Research Center, Chengdu University of Traditional Chinese Medicine, Chengdu, Sichuan, China

<sup>3</sup>Key Laboratory of Sichuan Province for Acupuncture and Chronobiology, Chengdu University of Traditional Chinese Medicine, Chengdu, Sichuan, China

Correspondence should be addressed to Fang Zeng; zeng\_fang@126.com

Received 25 June 2020; Revised 2 August 2020; Accepted 8 August 2020; Published 24 August 2020

Academic Editor: Jing-Wen Yang

Copyright © 2020 Tao Yin et al. This is an open access article distributed under the Creative Commons Attribution License, which permits unrestricted use, distribution, and reproduction in any medium, provided the original work is properly cited.

The effects of acupuncture facilitating neural plasticity for treating diseases have been identified by clinical and experimental studies. In the last two decades, the application of neuroimaging techniques in acupuncture research provided visualized evidence for acupuncture promoting neuroplasticity. Recently, the integration of machine learning (ML) and neuroimaging techniques becomes a focus in neuroscience and brings a new and promising approach to understand the facilitation of acupuncture on neuroplasticity at the individual level. This review is aimed at providing an overview of this rapidly growing field by introducing the commonly used ML algorithms in neuroimaging studies briefly and analyzing the characteristics of the acupuncture studies based on ML and neuroimaging, so as to provide references for future research.

## 1. Introduction

Neuroplasticity usually refers to brain plasticity, which means the ability of the brain to modify its organization to the altered demands and environments [1, 2]. The cumulative evidence from both animal and human studies demonstrated that the adult mammalian brain was plastic and could be remodeled by the environmental input continuously [3–5]. The long-term noxious stimulus, such as pain and depression, as well as regular exogenous interventions can reorganize the structure and function of the brain [6–9]. As the most widely used complementary therapy, acupuncture is considered to treat diseases via facilitating neural plasticity from multiple pathways, such as promoting endogenous neurogenesis, modulating synaptic plasticity, and regulating the secretion of neurotrophins and neurotransmitters, so as to affect the structural and functional plasticity of the brain [10–13].

In the past two decades, studies on acupuncture promoting brain plasticity were greatly enhanced with the development of neuroimaging techniques. Several studies focused on investigating acupuncture-induced brain structural and functional plasticity by magnetic resonance imaging (MRI), positron emission tomography (PET), and other neuroimaging methods [14, 15]. People found that acupuncture could modulate the brain functional activities, shape the gray matter structure, and remodel the white matter fiber connection [16–18] and that the modulation of acupuncture on neuroplasticity varied with the different acupuncture modalities and different acupoint stimulations [19, 20]. For instance, our previous study [21] found that acupuncture could positively modulate the functional activity of the rostral ventromedial medulla in patients with migraine and that the neural plasticity elicited by puncturing at real acupoints was more pronounced than sham acupoints.

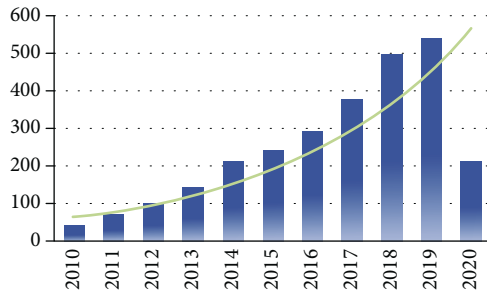


FIGURE 1: Numbers of publication on neuroimaging and machine learning in the last decade (from January 1, 2010, to June 1, 2020). The data was obtained by searching at the PubMed database with the items (Neuroimaging) AND (Machine Learning).

Currently, most neuroimaging findings of acupuncture facilitating neuroplasticity were obtained by the standard univariate analysis. It means the results were only significant at the group level, which limited their clinical translation to a certain extent. So, it is of great value to investigate how acupuncture promotes neuroplasticity and how the specific neuroplasticity affects the responses to acupuncture from the individual level. The application of multivariate pattern analysis (MVPA) and machine learning (ML) in neuroimaging studies provides an attractive method to this issue [22]. Since 2010, over 2200 studies focusing on ML in neuroimaging have been published in PubMed (pubmed.ncbi.nlm.nih.gov), and the number of these studies is increasing by 37% per year (Figure 1). With the ML algorithms and the neuroimaging features, researchers established the diagnostic and prognostic models of diseases. The interpretation of these models complemented the deficiencies of univariate analysis. They can not only assist in diagnosing diseases and in predicting individuals' responses to intervention but also provide novel insights for understanding brain plasticity. For example, Min et al. [23] found that schizophrenics who were sensitive to electroconvulsive therapy (ECT responders) had significantly higher whole-brain transfer entropy than the ECT nonresponders and that the value of whole-brain transfer entropy could be used as a reliable and plausible neuroimaging biomarker for random forest (RF) classifier to identify the ECT responders from the nonresponders. In another study, applying the baseline gray matter volume (GMV) of the subgenual cingulate cortex as a feature, Redlich and colleagues [24] successfully predicted the continued improvement of depression symptoms in patients with major depressive disorder following ECT. Simultaneously, integrating ML and neuroimaging technologies to investigate the facilitation of acupuncture on brain plasticity and using specific brain plasticity to predict acupuncture efficacy which can promote precision treatment have been a new focus in acupuncture research.

Therefore, we conducted this review by introducing the most widely used ML algorithms in neuroimaging studies briefly and analyzing these applications in the field of acupuncture promoting neural plasticity, aiming to provide an overview of this rapidly growing field and new approaches in future research.

## 2. Overview of Machine Learning in Neuroimaging

ML is a subfield of artificial intelligence which is aimed at investigating how computers can improve decisions and predictions based on data and ongoing experience [25, 26]. According to the criteria whether the training data is given a label or not, ML is divided into supervised learning, unsupervised learning, and semisupervised learning [27]. The unsupervised learning and semisupervised learning are generally applied for data reduction and feature selection [28], whereas the supervised learning is mainly used to construct the classification or regression models, which can learn the mappings between the input features and labels, to make individual-level estimations for the previously unseen data. The supervised learning includes many types, of which the most commonly used in neuroimaging research include support vector machine (SVM), decision tree (DT), RF, and artificial neural network (ANN) [29].

**2.1. Support Vector Machine.** The SVM is so far the most popular supervised learning algorithm in neuroimaging studies and is widely utilized in classification and prediction [30–33]. The principle of SVM is constructing a separating hyperplane that classifies all inputs, and the goal is searching for the optimal separating hyperplane that maximizes the margin between the hyperplane and the support vectors [34]. With different kernel functions, the distinct separating hyperplanes in different dimensions were constructed to perform the classification or prediction analysis. Among the different kinds of kernel functions in SVM models, the linear kernel and Gaussian kernel are most frequently used in neuroimaging studies [35–37]. The linear SVM is designed to solve the linear separating problems, while the RBF SVM is used primarily to seek nonlinear separating boundaries in the high-dimensional space.

**2.2. Decision Tree and Random Forest.** DT is the rooted directed tree that predicts the output based on a sequence of splits in the input feature space. The nodes split at each step by optimizing a metric, which indicates the consistency between the estimates and truth values. When the node has no subordinate to split, the traversal of this tree generates the target outcome prediction. As a typical classification algorithm with high interpretability, DT is applied predominantly for classification and disease diagnosis in neuroimaging studies [38, 39].

RF is generally the ensembles of DTs [40]. The principle of RF is consolidating multiple and diverse DTs together, and the final prediction outcome of RF is determined by the votes of each DT in the forest. As an integrated algorithm, RF can potentially yield much better prediction performance than learning with a single DT [41].

**2.3. Artificial Neural Network.** The concept of ANN is derived from the biological neural network. Similar to the synaptic connection in the brain, an ANN is composed of several layers of interconnected artificial neurons that make up the input layer, hidden layer, and output layer. As an

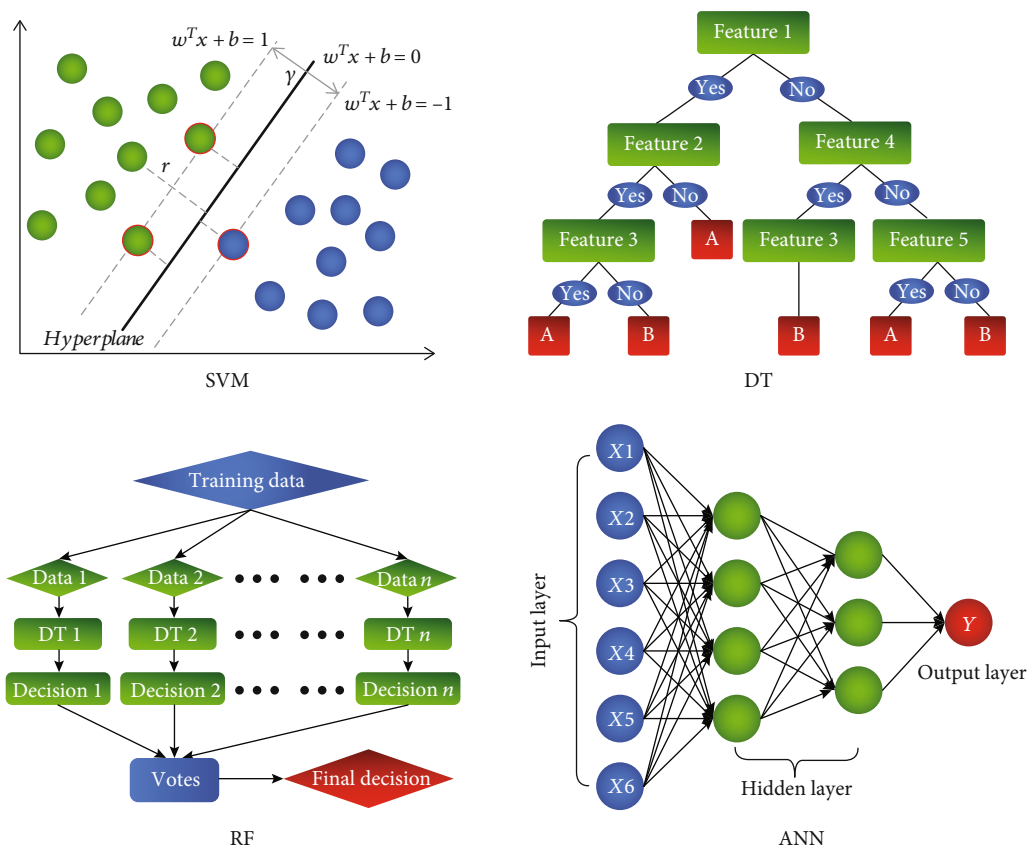


FIGURE 2: Diagrams of the commonly used machine learning algorithms in neuroimaging studies. SVM: support vector machine; DT: decision tree; RF: random forest; ANN: artificial neural network.

ultracomplex ML algorithm, ANN establishes the computational units of multiple layers by simulating signal transmission and learning the architecture of synapse [42]. Due to the flexibility of its structure, ANN has the ability to fit arbitrarily complex functions given sufficient annotated data [27]. Traditionally, the utilization of ANN is extremely limited in neuroimaging for the small training samples, while in recent years, with benefit from the open-access of the large-scale neuroimaging data repositories, the application of ANN is accelerating and has great potential to become one of the most efficient algorithms in neuroimaging studies [43, 44].

The diagrams of the above algorithms are summarized in Figure 2.

### 3. Application of Neuroimaging and Machine Learning in Acupuncture Promoting Neuroplasticity

In this review, we focused on the application of neuroimaging and ML in acupuncture promoting neuroplasticity. For a comprehensive summary of the field, we systematically searched papers in PubMed (pubmed.ncbi.nlm.nih.gov), Web of Science (<https://www.webofknowledge.com>), EBSCO (search.ebscohost.com), and CNKI (<https://www.cnki.net>) databases. According to the established inclusion and exclusion criteria, a total of ten studies were finally included

[45–54]. The details of data acquisition and literature selection process can be found in the supplementary materials (available here).

These ten studies were published from 2008 to 2020. Generally, for participant selection, these studies were performed on healthy subjects [45–47, 49, 54], patients with migraine [48, 50, 51], patients with chronic low back pain [53], and patients with functional dyspepsia [52], respectively. The sample size of these studies ranged from 12 to 94, and the average sample size of healthy subjects was 28. Except for one study that enrolled participants with a wide age span [54], these studies mainly included participants aged 20–45 years. For acupuncture intervention, nine studies [45–53] applied manual acupuncture, and one study [54] selected the electroacupuncture as the intervention method. For scan design, six studies [45–49, 54] applied the on-off block design to detect the real-time effects of acupuncture on functional brain plasticity. For imaging parameters, seven studies [45–47, 50–53] employed MRI to acquire neuroimaging data and applied the blood oxygenation level-dependent (BOLD) signal [45–47], functional connectivity [52, 53], GMV [51], and diffusion measures of white matter fibers [50] to reflect the structural and functional patterns of the brain. For machine learning parameters, eight studies [45–52] were aimed at solving the problems of pattern classification, and the other two studies [53, 54] were designed to predict pain relief following acupuncture treatment.

SVM, especially the linear SVM, was the most used ML algorithm in classification [45–52], whereas support vector regression [53] and fuzzy neural network [54] were applied in predictions. Three studies [49, 53, 54] exploited a hypothesis-based approach and selected the features of interest as inputs, and the other three studies [45, 50, 51] integrated multiple methods to find the optimal inputted features. Cross-validation, particularly the leave-one-out-cross-validation, was the popular validation strategy [45, 47–53], and only one study used independent samples as the validation set in these ten studies [54].

The detailed characteristics of these included studies were displayed in Table 1.

**3.1. Concerns of Studies on Acupuncture Promoting Neuroplasticity.** According to aims and design, these studies can be divided into three types. Among them, three studies [45–47] focused on the acupoint specificity, two studies [48, 49] were concerned with the differences and similarities of different acupuncture manipulations, and five studies [50–54] paid their attention to the prediction of acupuncture efficacy.

**3.1.1. The Acupoint Specificity.** Acupoint specificity refers that acupoints have different therapeutic effects and biophysical characteristics compared to sham acupoints and that different acupoints have relatively different therapeutic effects and biophysical characteristics [55]. In this review, three studies [45–47] focused on the acupoint specificity. One study was aimed at exploring the differences in real-time brain functional plasticity elicited by a verum acupoint and a sham acupoint. The other two studies compared the differences between different acupoints (GB40 vs. KI3 [46] and HT7 vs. PC6 [47]). These three studies had similar experimental designs, including focusing on the different points in the same nerve segments, using the multiple on-off block design, choosing the BOLD signal as features, and adopting the linear SVM algorithm to build models. For example, Li et al. [45] applied MVPA and searchlight method to decode spatial discrimination of acupuncture stimulation at GB37 and a nearby sham acupoint. The results indicated that the occipital cortex, limbic-cerebellar areas, and somatosensory cortex were the main regions with higher classification accuracy in the discrimination of the verum and sham acupoint stimulation. These studies indicated that acupuncture stimulation at different points induced distinct real-time brain functional plasticity in different regions and that MVPA could be used to investigate the real-time neuroplasticity from the individual level. Interestingly, these three studies utilized the general linear model (GLM) analysis to verify the findings obtained in MVPA, while every GLM analysis showed that the different points caused similar BOLD signal changes. It suggested that the conventional univariate analysis might not be sensitive enough to detect the neural plasticity evoked by different acupoint stimulation. This is consistent with the opinion that multivariate analysis was more sensitive than univariate analysis in neuroimaging studies [56].

Acupoint specificity is not only the core of acupuncture theory and the base of clinical practice but also the focus of acupuncture-neuroimaging research [57–59]. Our previous review [15] indicated that more than 1/3 acupuncture-neuroimaging studies focused on acupoint specificity and these studies mainly concentrated on the differences of verum acupoints and sham acupoints. From 1995 to 2016, 79 original neuroimaging articles on acupoint specificity were published in PubMed, and 53 articles focused on the difference between the verum acupoints and the sham acupoints [19]. Given the importance of acupoint specificity in acupuncture theory and clinical practice and the extensiveness in neuroimaging research, we hold that acupoint specificity is bound to become a hot spot in future ML and neuroimaging studies.

**3.1.2. Acupuncture Manipulation.** Two [48, 49] of the ten studies centered on the differences in brain functional plasticity caused by the different acupuncture manipulations. In one study [48], linear SVM was applied to classify the baseline and post acupuncture blood perfusion patterns in both verum and sham acupuncture groups. The results illustrated that the SVM classifier performed better when the training data was extracted from the verum acupuncture group. Moreover, the temporal lobe and cerebellum contributed important information for the discrimination in the verum acupuncture group. Another study [49] proposed a classification framework based on multiple ML algorithms for the two traditional acupuncture manipulations: the twirling-rotating manipulation and lifting-thrusting manipulation. The results demonstrated that with all the six graph theory properties as inputs, the SVM classifier got the highest accuracy of 92.14%. Moreover, the *post hoc* analysis also found the significant between-group differences of these six graph theory measures between two manipulations.

Acupuncture manipulation is the key in acupuncture clinical practice and significantly affects acupuncture efficacy [60]. In more than 2000 years of development, acupuncture has formed a rich variety of modalities and manipulation skills. The differences between acupuncture and moxibustion, electroacupuncture and manual acupuncture, acupuncture with *deqi* and acupuncture without *deqi*, and the reinforcing manipulation and reducing manipulation are always the key of clinical and experimental research in the acupuncture field and could be the research direction in future MVPA studies.

**3.1.3. Prediction of Acupuncture Efficacy.** The integration of ML and neuroimaging features has been extensively employed in predicting the clinical efficacy of drugs or other interventions [33, 61]. In this review, five studies focused on acupuncture efficacy prediction [50–54]. Among them, three studies [50–52] adopted the classification algorithms to predict patients' responses to acupuncture treatment. For example, Liu et al. [50] utilized the diffusion measures of the medial prefrontal cortex- (mPFC-) amygdala fiber as inputs and established a linear SVM classifier to predict the response of migraine patients to the 8-week sham acupuncture treatment. The result showed that when using each



TABLE 1: The detailed characteristics of the included studies.

Participants Sample size, gender (M/F), age (Y)	Intervention	Modality	Feature	Purpose (C/R)	ML	Feature selection	Validation	Model assessment	MVPA findings	Univariate analysis results	Conclusion
López et al., 2013	Migraine Verum ACU: 18, 3/15, 44.44 ± 9.65; sham ACU: 18, 7/11, 43.94 ± 11.98	Task-SPECT (function) Task: ACU when image data acquisition	Blood perfusion	C	Linear SVM	Filter: discarding voxels with intensity values under 25% of the maximum	LOOCV	ACC SPE SEN	The classifier performed better when the training data was extracted from the verum ACU group than from the sham ACU group.	Verum ACU yielded greater changes in the perfusion patterns than sham ACU. Verum ACU produced a more significant decrease in blood perfusion.	SVM can distinguish the SPECT images of pre- and post-ACU acquisitions. Changes in blood perfusion following verum ACU is greater than sham ACU.
Jung et al., 2019	HS 14, 14/0, 22.1 ± 1.1	Task-fMRI (function) Task: block design (16 s rest+6 s ACU +4 s stimulation location+4 s intensity report) *20	BOLD signal	C	Linear SVM	No feature selection steps	LOOCV	ACC	The classifier got an accuracy of 58.6% for classifying HT7 and PC6 with the features extracted from SI, MI, paraCL, anterior and posterior insula, SMG, ACC, vmPFC, PPC, and IPL. Using signal of ROI as feature, the classifier got higher accuracy (MI, 65%; SMA, 64%; SMG 62%; SI, 62%; and dlPFC, 62%).	No significant difference in BOLD signal alteration following HT7 and PC6 stimulation	Spatial localization of pain perceptions to ACU needle can be predicted by the neural response patterns in the somatosensory areas and the frontoparietal areas.
Yu et al., 2019	HS TR: 30, 16/14, 23-27; LT: 30, 18/12, 23-28	Task-EEG (function) Task: ACU manipulation (TR or LT) for 3 min	Graph theory	C	DT NB SVM KNN LDA BP TSK	Selecting the features of interest	6-fold CV	ACC AUC	The classifier got an accuracy of 92.14% and AUC of 0.9570 with all graph theory features as inputs. With	PLV of TR was stronger than the baseline, while PLV of LT was weaker than the baseline. The value of all the	Different ACU manipulations have different effects on functional brain networks. Classification of

TABLE 1: Continued.

Participants	Intervention	Modality	Feature	Purpose (C/R)	ML	Feature selection	Validation	Model assessment	MVPA findings	Univariate analysis results	Conclusion
Liu et al., 2018	MWOA Responder: 38, /, 22.1 ± 0.45; sham ACU at 24 sessions of NAP in 8 weeks nonresponder: 56, /, 21.5 ± 0.43	DTI (structure)	TABA	C	Linear SVM	Filter +wrapper: traversing the $p$ values of the two-sample $t$ test from 0.01 to 1 with a 0.01 interval to find the best $p$ for classifier	LOOCV	ACC SPE SEN PPV NPV	the increase of filter number, the accuracy was gradually improved. The highest accuracy was 92.37% with 6 filters in the TSK model. The single FA, MD, AD, and RD of the mPFC-amygdala fiber contributed to lackluster classification accuracy. The classifier got a higher accuracy with the combined features of FA, MD, and RD (in which ACC, SEN, SPE, PPV, and NPV were 84.0%, 90.2%, 76.7%, 82.1%, and 86.8%, respectively). The external capsule, ACG, and mPFC significantly contributed to the discrimination of responders and nonresponders.	The increased FA, decreased MD, decreased AD, and decreased RD of the mPFC-amygdala fiber were detected in MWOA patients than HS.	The variability of placebo treatment outcomes in migraineurs could be predicted from prior diffusion measures along the fiber pathways of the mPFC-amygdala.
									the increase of filter number, the accuracy was gradually improved. The highest accuracy was 92.37% with 6 filters in the TSK model. The single FA, MD, AD, and RD of the mPFC-amygdala fiber contributed to lackluster classification accuracy. The classifier got a higher accuracy with the combined features of FA, MD, and RD (in which ACC, SEN, SPE, PPV, and NPV were 84.0%, 90.2%, 76.7%, 82.1%, and 86.8%, respectively). The external capsule, ACG, and mPFC significantly contributed to the discrimination of responders and nonresponders.	the increase of filter number, the accuracy was gradually improved. The highest accuracy was 92.37% with 6 filters in the TSK model. The single FA, MD, AD, and RD of the mPFC-amygdala fiber contributed to lackluster classification accuracy. The classifier got a higher accuracy with the combined features of FA, MD, and RD (in which ACC, SEN, SPE, PPV, and NPV were 84.0%, 90.2%, 76.7%, 82.1%, and 86.8%, respectively). The external capsule, ACG, and mPFC significantly contributed to the discrimination of responders and nonresponders.	different ACU manipulations based on EEG with network features is feasible.

TABLE 1: Continued.

Participants	Intervention	Modality	Feature	Purpose (C/R)	ML	Feature selection	Validation	Model assessment	MVPA findings	Univariate analysis results	Conclusion
Yang et al., 2020	MWAO 12 sessions of ACU at GV20, GV24, bil-GB13, bil-GB8, and bil-GB20 in 4 weeks	T1 (structure)	GMV	C	Linear SVM	Filter +wrapper +embedded: traversing the $p$ values of the two-sample $t$ test from 0.0025 to 0.05 with a step of 0.0025 to select the best $p$ for classifier LASSO	10-fold CV	ACC SPE SEN AUC DSC	Using the clusters located at the frontal, temporal, parietal, precuneus, and cuneus gyri as features, the classifier got the SEN of 73%, SPE of 85%, ACC of 83%, and AUC of 0.7871.	The baseline GMV in all predictive regions significantly differed between responders and nonresponders. Alterations of migraine days were correlated with the baseline GMV of L cuneus, R cuneus, MIFG/IFG, L IPL, and SPL/IPL. The responders achieved an increase in GMV of the L cuneus after ACU.	The pretreatment brain structure could be a novel predictor for ACU treatment of MWAO.
Tu et al., 2019	6 sessions of ACU in 4 weeks, 8-12 effective acupoints were used in the real ACU group; 12 sham points were used in the sham ACU group.	Resting-fMRI (function)	ICA +rsFC	R	RBF SVR	Selecting the features of interest	5-fold CV	$R^2$ MAE	The prediction model obtained an $R^2$ of $34.3 \pm 5.5\%$ and an MAE of $1.67 \pm 0.02$ between actual and predicted treatment responses for real ACU. mPFC FC (mPFC-insula, mPFC-putamen, mPFC-caudate, and mPFC-AG) and other FC (PCC-MiFG, correlated with	Changes of pain severity correlated with baseline mPFC-SN and mPFC-AG FC in the real ACU group. Baseline mPFC-dACG FC was correlated with changes in pain severity in the sham ACU group. Changes of FC between the mPFC and insula/AG were correlated with	Pretreatment rsFC could predict symptom changes for real and sham treatment, and the rsFC characteristics that were significantly predictive for real and sham treatment differed.

TABLE 1: Continued.

Participants	Intervention	Modality	Feature	Purpose (C/R)	ML	Feature selection	Validation	Model assessment	MVPA findings	Univariate analysis results	Conclusion
Xue et al., 2011	HS 12, 9/3, 21-26 after a one-week interval	Task-fMRI (function) Task: on/off block design (1 min rest +1 min ACU) *3	BOLD signal	C	Linear SVM	Singular value decomposition	/	SDM	insula-IFG, insula-SPL, and caudate-AG) significantly contributed to prediction. The model got an $R^2$ of $29.3 \pm 5.3\%$ and an MAE of $1.52 \pm 0.04$ for sham ACU. Connections of mPFC-dACG, mPFC-SPL, mPFC-paraCL, SFG-PreCG, SFG-MiFG, and ACG-paraCL provided significant information for prediction. The performance of the classifier was not mentioned in this study. ACU stimulation at GB40 produced predominantly signal increases in the insula, red nucleus, thalamus, and amygdala. ACU at KI3 elicited more extensive decreased neural	the relief of pain severity after real treatment, while changes of FC between the mPFC and paraCL/SPL were correlated with the relief of pain severity after sham ACU treatment.	Neural response patterns between ACU stimulation at GB40 and KI3 are distinct. Conventional GLM analysis is insensitive to detect neural activities evoked by ACU stimulation.



TABLE 1: Continued.

Participants Sample size, gender (M/F), age (Y)	Intervention	Modality	Feature	Purpose (C/R)	ML	Feature selection	Validation	Model assessment	MVPA findings	Univariate analysis results	Conclusion
Yin et al., 2020	FD Responders: 21, 2/19, 21.52 ± 1.89; nonresponder: 12, 2/10, 22.83 ± 2.73	Resting-fMRI (function)	rsFC	C	Linear SVM	Wrapper: recursive feature elimination	LOOCV	ACC SPE SEN AUC	responses in the MFG, PCC, thalamus, and ACG. The classifier obtained an ACC of 84.9%, SEN of 78.6%, SPE of 89.5%, and AUC of 86.8%. The FC between R insula-L precuneus, L MIOFG-L thalamus, L insula-L ACG, R ACG-R temporal pole, R SOG-R cerebellum-3 contributed crucial information for prediction.	/	The whole- brain resting- state functional brain network has good predicting potential for ACU treatment to FD patients.
Hao et al., 2008	HS 60, /, 24-75 ACU at ST36	Task- EEG/ECG (function) Task: ACU when image data acquisition	BIS TPI LF/HF HR HRV	R	FNN	Selecting the features of interest	Validation with an independent set	AAE	With the FNN, the AAE of the estimation and true value is 10.2278.	/	The alteration of $\beta$ -endorphin following electro-ACU can be predicted by monitoring EEG and ECG signal parameters.
Li et al., 2010	HS 11/11, 21.4 ± 1.8; GB37: 11, /; NAP: 11, /, /	Task-fMRI (function) Task: on/off block design (1 min rest +two 30 s	BOLD signal	C	Linear SVM	Searchlight +singular value decomposition	LOOCV	ACC	The occipital cortex, limbic- cerebellar areas, and somatosensory cortex could	Compared with the sham group, the ACU group induced higher signal intensity at some major	Neural response patterns of brain cortex to the ACU stimulation at GB37 and a

TABLE 1: Continued.

Participants Sample size, gender (M/F), age (Y)	Intervention	Modality	Feature	Purpose (C/R)	ML	Feature selection	Validation	Model assessment	MVPA findings	Univariate analysis results	Conclusion
		ACU separated by a 50 s rest period+50 s rest)							help to differentiate the central neural response patterns induced by real or sham ACU stimulation with higher accuracy above the chance level.	regions of limbic-cerebellar system and small regions of the primary somatosensory cortex and supplementary motor area.	nearby NAP could differ from each other effectively with the application of the MVPA approach.

M/F: male/female; Y: year; C/R: classification/regression; ML: machine learning; MVPA: multivariate pattern analysis; ACU: acupuncture; SPECT: single-photon emission computed tomography; SVM: support vector machine; LOOCV: leave-one-out-cross-validation; ACC: accuracy; SPE: specificity; SEN: sensitivity; HS: healthy subjects; fMRI: functional magnetic resonance imaging; BOLD: blood oxygenation level dependent; TR: twirling-rotating manipulation; LT: lifting-thrusting manipulation; EEG: electroencephalogram; DT: decision tree; NB: naïve Bayes; KNN: K-nearest neighbor; LDA: linear discriminant analysis; BP: BP neural network; TSK: Takagi-Sugeno-Kang fuzzy system; CV: cross-validation; AUC: area under the ROC curve; PLV: phase locking value; MWOA: migraine without aura; NAP: nonacupoint; DTI: diffusion tensor image; TABA: tractography atlas-based analysis; PPV: positive predictive value; NPV: negative predictive value; FA: fractional anisotropy; MD: mean diffusion; AD: axial diffusivity; RD: radial diffusivity; GMV: gray matter volume; LASSO: least absolute shrinkage and selection operator; DSC: dice similarity coefficient; cLBP: chronic low back pain; rsFC: resting-state functional connectivity; RBF: radial basis function; SVR: support vector regression; MAE: mean absolute error; SDM: spatial discriminance map; GLM: general linear model; FD: functional dyspepsia; BIS: bispectral index; TPI: tip perfusion index; LF/HF: low/high-frequency ratio; HR: heart rate; HRV: heart rate variability; FNN: fuzzy neural network; AAE: absolute average error; L: left; R: right; SI: primary somatosensory cortex; MI: primary motor cortex; paraCL: paracentral lobe; SMG: supramarginal gyrus; ACG: anterior cingulate gyrus; vmPFC: ventromedial prefrontal cortex; PPC: posterior parietal cortex; IPL: inferior parietal lobe; dIPFC: dorsolateral prefrontal cortex; mPFC: medial prefrontal cortex; MiFG: middle frontal gyrus; IFG: inferior frontal gyrus; SPL: superior parietal lobe; AG: angular gyrus; dACG: dorsal ACG; PreCG: precentral gyrus; SFG: superior frontal gyrus; SN: subcortical network; MFG: medial frontal gyrus; ITG: inferior temporal gyrus; MiOFG: middle orbitofrontal gyrus; SOG: superior occipital gyrus.

single diffusion measure as input, the accuracy of the classifier is lackluster, whereas when multiple measures were applied the classifier could accurately discriminate responders from nonresponders with an accuracy of 84.0%. Moreover, the most discriminative white matter plasticity features that contributed to the classification were located in the external capsule, anterior cingulate gyrus, and mPFC. The other two studies [53, 54] constructed the regression models to predict the continuous improvement in symptoms after acupuncture treatment. For example, Tu et al. [53] used the features of interest as inputs to predict pain relief in patients with cLBP following 8-week verum or sham acupuncture treatment. The results showed that multiple functional connections involving mPFC could provide vital information for predicting the improvement of symptoms after both verum and sham acupuncture treatment.

These five studies on acupuncture efficacy prediction demonstrated that the specific neuroplasticity features including morphology of gray matter and white matter and cerebral functional activity patterns contained vital information for predicting the response of patients to acupuncture stimulation. The integration of ML and neuroimaging provides a new and promising approach for investigating mechanisms of acupuncture efficacy at the individual level, which has great potential for clinical translation and will be the important growth pole in acupuncture research.

In addition to the three aspects described above, there are still some other concerns that should be focused in future neuroimaging-based ML studies, for example, investigating the influences of acupuncture with different acupoint combination or different stimulation intensity on neural plasticity and predicting clinical efficacy of acupuncture with the neuroimaging features acquired under acupuncture stimulation.

*3.2. Design of Machine Learning in Studies on Acupuncture Promoting Neuroplasticity.* The application of neuroimaging techniques in acupuncture mechanism has produced remarkable advance [57, 62, 63] and developed a series of proven execution specifications [14, 19, 64]. In contrast, the integration of ML and neuroimaging in acupuncture research is still in its early stage, which inevitably brings many challenges but also the future directions.

*3.2.1. Sample Size.* Due to difficulties in data acquisition, the sample size of neuroimaging study is generally small [65, 66]. By reviewing the studies which integrated ML and neuroimaging technologies to investigate neuropsychiatric disorders, Sakai and Yamada [29] found that 45.6% of the studies from 2014 to 2018 had a sample size of fewer than 100 cases. In our review, the sample size of the included studies ranged from 12 to 94 and six studies had a sample size of fewer than 50 cases. A small sample size exacerbates the possibility of adaptive models to learn noise, which leads to the high variability of estimates and overvaluation of prediction accuracy [67]. Simulation experiments showed that even when the sample size in the neuroimaging study reached 100 cases, the error bars were still around 10% [68]. Only when the samples of the training set exceeded 200 cases did the prediction model's performance begin to plateau [69].

Therefore, when conducting an ML study to predict the efficacy of acupuncture based on the neuroimaging properties, a sample size of 200 or more cases should be guaranteed whenever possible.

*3.2.2. The Appropriateness of Feature Selection.* Considering that there are generally more features than samples in neuroimaging data, it is beneficial to take appropriate manners to eliminate the redundant features and reduce the dimension of data. The ten studies included in this review indicated that when using a single feature as input, the accuracy of the classifier is lackluster, whereas when multiple neuroimaging features applied, the accuracy of the model was significantly improved [49, 50]. This finding suggested that the properties of neuroplasticity that influenced the efficacy of acupuncture were multidimensional and complex. Moreover, another interesting finding was that both GMV and diffusion measures of white matter fiber could accurately discriminate between acupuncture-sensitive and acupuncture-insensitive migraine patients [50, 51]. Does it mean that the prediction model achieves better performance to discriminate the acupuncture responders and acupuncture nonresponders if both gray matter and white matter features are applied as inputs? In fact, the previous studies have illustrated that using multimodal rather than single-modal neuroimaging features as inputs can induce higher classification accuracy and better prediction performance [70, 71]. Therefore, future studies could attempt to use multimodal neuroimaging features as inputs to further explore the multidimensional features that predict the efficacy of acupuncture accurately.

*3.2.3. The Representativeness of Training Data.* The current ML studies generally favor seeking homogeneous subjects to establish classification and prediction models [72–74]. It reduces the underfitting of the model caused by data heterogeneity, but severely limits the generalizability of the model to the real-world data [75]. The requirements for the representativeness of training data depend on the purpose of the study. For example, when a study is aimed at investigating the effects of different acupuncture manipulations on brain plasticity, the participants should be the homogeneous individuals from the same site. However, if the study is aimed at creating a generalizable model to predict the clinical efficacy of acupuncture, the participants should be enrolled from multiple centers to represent the heterogeneous population in real life.

*3.2.4. The Validity of Labels.* The goal of ML is establishing mappings between training data and labels and then use the mappings as benchmarks for predicting the labels of the unseen data. Similar to other ML studies [76–78], the majority of current studies on acupuncture efficacy prediction use the subjective symptoms as the labels. These labels obtained with self-evaluated symptoms are subject to individual cognitive bias and have a high degree of variability. The heterogeneity yielded by subjective labels may hamper ML algorithms to discover optimal neuroimaging biomarkers and establish accurate mappings between data and labels. Therefore, applying objective biological markers as labels to establish

an objective-to-objective mapping between features and labels should be taken into consideration in future studies to reduce the influence of subjective factors on model reliability.

#### 4. Conclusion

In summary, we provided an overview of the literature on the application of ML and neuroimaging in acupuncture promoting neural plasticity. Studies published so far have preliminarily demonstrated at the individual level that different acupoint stimulation and different acupuncture manipulations had significantly different real-time modulatory effects on functional brain plasticity and that the specific structural and functional neuroplasticity features at baseline could accurately predict the improvement of symptoms following acupuncture treatment. Although this research field is currently in its early stage and faces many challenges, we still believe that integrating ML and neuroimaging techniques will be a promising approach to understand the facilitation of acupuncture on neuroplasticity in the future.

#### Data Availability

There is no original data in this review.

#### Conflicts of Interest

The authors declare that they have no competing interests.

#### Authors' Contributions

Tao Yin, Peihong Ma, and Zilei Tian contributed equally to this work.

#### Acknowledgments

This work was supported by the National Key R&D Program of China (No. 2018YFC1704600 and No. 2018YFC1704605), the National Natural Science Foundation of China (No. 81973960), and the Sichuan Science and Technology Program (No. 2020JDRC0105).

#### Supplementary Materials

The details of data acquisition and literature selection process. (*Supplementary Materials*)

#### References

- [1] K. Hötting and B. Röder, "Beneficial effects of physical exercise on neuroplasticity and cognition," *Neuroscience & Biobehavioral Reviews*, vol. 37, no. 9, pp. 2243–2257, 2013.
- [2] H. van Praag, G. Kempermann, and F. H. Gage, "Neural consequences of environmental enrichment," *Nature Reviews Neuroscience*, vol. 1, no. 3, pp. 191–198, 2000.
- [3] A. Pascual-Leone, A. Amedi, F. Fregni, and L. B. Merabet, "The plastic human brain cortex," *Annual Review of Neuroscience*, vol. 28, no. 1, pp. 377–401, 2005.
- [4] L. Mandolesi, F. Gelfo, L. Serra et al., "Environmental factors promoting neural plasticity: insights from animal and human studies," *Neural Plasticity*, vol. 2017, Article ID 7219461, 10 pages, 2017.
- [5] C. H. Zhang, Z. Z. Ma, B. B. Huo et al., "Diffusional plasticity induced by electroacupuncture intervention in rat model of peripheral nerve injury," *Journal of Clinical Neuroscience*, vol. 69, pp. 250–256, 2019.
- [6] R. Kuner and H. Flor, "Structural plasticity and reorganisation in chronic pain," *Nature Reviews Neuroscience*, vol. 18, no. 1, pp. 20–30, 2016.
- [7] E. Duzel, H. van Praag, and M. Sendtner, "Can physical exercise in old age improve memory and hippocampal function?," *Brain*, vol. 139, no. 3, pp. 662–673, 2016.
- [8] H. Johansson, M. Hagströmer, W. J. A. Grooten, and E. Franzén, "Exercise-induced neuroplasticity in Parkinson's disease: a metasynthesis of the literature," *Neural Plasticity*, vol. 2020, Article ID 8961493, 15 pages, 2020.
- [9] W. Liu, T. Ge, Y. Leng et al., "The role of neural plasticity in depression: from hippocampus to prefrontal cortex," *Neural Plasticity*, vol. 2017, Article ID 6871089, 11 pages, 2017.
- [10] L. Y. Xiao, X. R. Wang, Y. Yang et al., "Applications of acupuncture therapy in modulating plasticity of central nervous system," *Neuromodulation: Technology at the Neural Interface*, vol. 21, no. 8, pp. 762–776, 2018.
- [11] V. Protto, M. Soligo, M. E. de Stefano et al., "Electroacupuncture in rats normalizes the diabetes-induced alterations in the septo-hippocampal cholinergic system," *Hippocampus*, vol. 29, no. 10, pp. 891–904, 2019.
- [12] H. C. Lai, Q. Y. Chang, and C. L. Hsieh, "Signal transduction pathways of acupuncture for treating some nervous system diseases," *Evidence-based Complementary and Alternative Medicine*, vol. 2019, Article ID 2909632, 37 pages, 2019.
- [13] L. M. Chavez, S. S. Huang, I. MacDonald, J. G. Lin, Y. C. Lee, and Y. H. Chen, "Mechanisms of acupuncture therapy in ischemic stroke rehabilitation: a literature review of basic studies," *International Journal of Molecular Sciences*, vol. 18, no. 11, article 2270, 2017.
- [14] Z. He, L. Hou, R. Sun et al., "The status of the acupuncture mechanism study based on PET/PET-CT technique: design and quality control," *Evidence-based Complementary and Alternative Medicine*, vol. 2019, Article ID 9062924, 8 pages, 2019.
- [15] K. Qiu, M. Jing, R. Sun et al., "The status of the quality control in acupuncture-neuroimaging studies," *Evidence-based Complementary and Alternative Medicine*, vol. 2016, Article ID 3685785, 14 pages, 2016.
- [16] Y. Zou, W. Tang, X. Li, M. Xu, and J. Li, "Acupuncture reversible effects on altered default mode network of chronic migraine accompanied with clinical symptom relief," *Neural Plasticity*, vol. 2019, Article ID 5047463, 10 pages, 2019.
- [17] P. Wu, Y. M. Zhou, C. X. Liao et al., "Structural changes induced by acupuncture in the recovering brain after ischemic stroke," *Evidence-based Complementary and Alternative Medicine*, vol. 2018, Article ID 5179689, 8 pages, 2018.
- [18] H. Kim, I. Mawla, J. Lee et al., "Reduced tactile acuity in chronic low back pain is linked with structural neuroplasticity in primary somatosensory cortex and is modulated by acupuncture therapy," *NeuroImage*, vol. 217, article 116899, 2020.
- [19] K. Qiu, T. Yin, X. Hong et al., "Does the acupoint specificity exist? Evidence from functional neuroimaging studies," *Current Medical Imaging*, vol. 16, no. 6, pp. 629–638, 2020.



- [20] R. L. Cai, G. M. Shen, H. Wang, and Y. Y. Guan, "Brain functional connectivity network studies of acupuncture: a systematic review on resting-state fMRI," *Journal of Integrative Medicine*, vol. 16, no. 1, pp. 26–33, 2018.
- [21] Z. Li, F. Zeng, T. Yin et al., "Acupuncture modulates the abnormal brainstem activity in migraine without aura patients," *Neuro Image Clinical*, vol. 15, pp. 367–375, 2017.
- [22] J. V. Haxby, "Multivariate pattern analysis of fMRI: the early beginnings," *NeuroImage*, vol. 62, no. 2, pp. 852–855, 2012.
- [23] B. Min, M. Kim, J. Lee et al., "Prediction of individual responses to electroconvulsive therapy in patients with schizophrenia: machine learning analysis of resting-state electroencephalography," *Schizophrenia Research*, vol. 216, pp. 147–153, 2020.
- [24] R. Redlich, N. Opel, D. Grotegerd et al., "Prediction of individual response to electroconvulsive therapy via machine learning on structural magnetic resonance imaging data," *JAMA Psychiatry*, vol. 73, no. 6, pp. 557–564, 2016.
- [25] A. L. Samuel, "Some studies in machine learning using the game of checkers," *IBM Journal of Research and Development*, vol. 3, no. 3, pp. 210–229, 1959.
- [26] M. A. T. Vu, T. Adali, D. Ba et al., "A shared vision for machine learning in neuroscience," *The Journal of Neuroscience*, vol. 38, no. 7, pp. 1601–1607, 2018.
- [27] M. Khosla, K. Jamison, G. H. Ngo, A. Kuceyeski, and M. R. Sabuncu, "Machine learning in resting-state fMRI analysis," *Magnetic Resonance Imaging*, vol. 64, pp. 101–121, 2019.
- [28] Y. Du, Z. Fu, and V. D. Calhoun, "Classification and prediction of brain disorders using functional connectivity: promising but challenging," *Frontiers in Neuroscience*, vol. 12, p. 525, 2018.
- [29] K. Sakai and K. Yamada, "Machine learning studies on major brain diseases: 5-year trends of 2014–2018," *Japanese Journal of Radiology*, vol. 37, no. 1, pp. 34–72, 2019.
- [30] G. Orrù, W. Pettersson-Yeo, A. F. Marquand, G. Sartori, and A. Mechelli, "Using support vector machine to identify imaging biomarkers of neurological and psychiatric disease: a critical review," *Neuroscience and Biobehavioral Reviews*, vol. 36, no. 4, pp. 1140–1152, 2012.
- [31] B. Sundermann, D. Herr, W. Schwindt, and B. Pfeleiderer, "Multivariate classification of blood oxygen level-dependent fMRI data with diagnostic intention: a clinical perspective," *AJNR. American Journal of Neuroradiology*, vol. 35, no. 5, pp. 848–855, 2014.
- [32] D. Librenza-Garcia, B. J. Kotzian, J. Yang et al., "The impact of machine learning techniques in the study of bipolar disorder: a systematic review," *Neuroscience and Biobehavioral Reviews*, vol. 80, pp. 538–554, 2017.
- [33] J. M. Mateos-Pérez, M. Dadar, M. Lacalle-Aurioles, Y. Iturria-Medina, Y. Zeighami, and A. C. Evans, "Structural neuroimaging as clinical predictor: a review of machine learning applications," *NeuroImage: Clinical*, vol. 20, pp. 506–522, 2018.
- [34] F. Pereira, T. Mitchell, and M. Botvinick, "Machine learning classifiers and fMRI: a tutorial overview," *Neuro Image*, vol. 45, 1 Supplement, pp. S199–S209, 2009.
- [35] S. Song, Z. Zhan, Z. Long, J. Zhang, and L. Yao, "Comparative study of SVM methods combined with voxel selection for object category classification on fMRI data," *PLoS One*, vol. 6, no. 2, article e17191, 2011.
- [36] H. Zhuang, R. Liu, C. Wu et al., "Multimodal classification of drug-naïve first-episode schizophrenia combining anatomical, diffusion and resting state functional resonance imaging," *Neuroscience Letters*, vol. 705, pp. 87–93, 2019.
- [37] Z. Long, B. Jing, H. Yan et al., "A support vector machine-based method to identify mild cognitive impairment with multi-level characteristics of magnetic resonance imaging," *Neuroscience*, vol. 331, pp. 169–176, 2016.
- [38] J. W. Wu, S. S. Hseu, J. L. Fuh et al., "Factors predicting response to the first epidural blood patch in spontaneous intracranial hypotension," *Brain*, vol. 140, no. 2, pp. 344–352, 2017.
- [39] S. Liang, Y. Li, Z. Zhang et al., "Classification of first-episode schizophrenia using multimodal brain features: a combined structural and diffusion imaging study," *Schizophrenia Bulletin*, vol. 45, no. 3, pp. 591–599, 2019.
- [40] L. Breiman, "Random forests," *Machine Learning*, vol. 45, no. 1, pp. 5–32, 2001.
- [41] P. K. Douglas, S. Harris, A. Yuille, and M. S. Cohen, "Performance comparison of machine learning algorithms and number of independent components used in fMRI decoding of belief vs. disbelief," *Neuro Image*, vol. 56, no. 2, pp. 544–553, 2011.
- [42] J. G. Lee, S. Jun, Y. W. Cho et al., "Deep learning in medical imaging: general overview," *Korean Journal of Radiology*, vol. 18, no. 4, pp. 570–584, 2017.
- [43] H. C. Kim, P. A. Bandettini, and J. H. Lee, "Deep neural network predicts emotional responses of the human brain from functional magnetic resonance imaging," *Neuro Image*, vol. 186, pp. 607–627, 2019.
- [44] L. He, H. Li, S. K. Holland, W. Yuan, M. Altaye, and N. A. Parikh, "Early prediction of cognitive deficits in very preterm infants using functional connectome data in an artificial neural network framework," *NeuroImage: Clinical*, vol. 18, pp. 290–297, 2018.
- [45] L. Li, W. Qin, L. Bai, and J. Tian, "Exploring vision-related acupuncture point specificity with multivoxel pattern analysis," *Magnetic Resonance Imaging*, vol. 28, no. 3, pp. 380–387, 2010.
- [46] T. Xue, L. Bai, S. Chen et al., "Neural specificity of acupuncture stimulation from support vector machine classification analysis," *Magnetic Resonance Imaging*, vol. 29, no. 7, pp. 943–950, 2011.
- [47] W.-M. Jung, I.-S. Lee, Y.-S. Lee et al., "Decoding spatial location of perceived pain to acupuncture needle using multivoxel pattern analysis," *Molecular Pain*, vol. 15, p. 174480691987706, 2019.
- [48] M. M. López, J. M. Górriz, J. Ramírez, M. Gómez-Río, J. Verdejo, and J. Vas, "Component-based technique for determining the effects of acupuncture for fighting migraine using SPECT images," *Expert Systems with Applications*, vol. 40, no. 1, pp. 44–51, 2013.
- [49] H. Yu, X. Li, X. Lei, and J. Wang, "Modulation effect of acupuncture on functional brain networks and classification of its manipulation with EEG signals," *IEEE Transactions on Neural Systems and Rehabilitation Engineering*, vol. 27, no. 10, pp. 1973–1984, 2019.
- [50] J. Liu, J. Mu, T. Chen, M. Zhang, and J. Tian, "White matter tract microstructure of the mPFC-amygdala predicts interindividual differences in placebo response related to treatment in migraine patients," *Human Brain Mapping*, vol. 40, no. 1, pp. 284–292, 2018.
- [51] X.-J. Yang, L. Liu, Z.-L. Xu et al., "Baseline brain gray matter volume as a predictor of acupuncture outcome in treating migraine," *Frontiers in Neurology*, vol. 11, p. 111, 2020.

- [52] Y. Tao, S. Ruirui, H. Zhaoxuan, M. Peihong, and Z. Fang, "Resting-state functional brain network predicts responses to acupuncture treatment in functional dyspepsia," *China Journal of Traditional Chinese Medicine and Pharmacy*, vol. 35, no. 5, pp. 2581–2584, 2020.
- [53] Y. Tu, A. Ortiz, R. L. Gollub et al., "Multivariate resting-state functional connectivity predicts responses to real and sham acupuncture treatment in chronic low back pain," *NeuroImage: Clinical*, vol. 23, article 101885, 2019.
- [54] W.-s. Hao, X. Zhu, X.-r. Wang, H.-y. Yang, Z.-h. Wang, and Y.-j. Zheng, "Biochemical index variation prediction during electro-acupuncture analgesia using ANFIS method," *Journal of Shanghai Jiaotong University*, vol. 42, no. 2, pp. 177–180, 2008.
- [55] J. J. Xing, B. Y. Zeng, J. Li, Y. Zhuang, and F. R. Liang, "Acupuncture point specificity," *International Review of Neurobiology*, vol. 111, pp. 49–65, 2013.
- [56] G. Chen, N. E. Adleman, Z. S. Saad, E. Leibenluft, and R. W. Cox, "Applications of multivariate modeling to neuroimaging group analysis: a comprehensive alternative to univariate general linear model," *Neuro Image.*, vol. 99, pp. 571–588, 2014.
- [57] K. K. S. Hui, J. Liu, N. Makris et al., "Acupuncture modulates the limbic system and subcortical gray structures of the human brain: evidence from fMRI studies in normal subjects," *Human Brain Mapping*, vol. 9, no. 1, pp. 13–25, 2000.
- [58] P. J. Rong, J. J. Zhao, J. H. Gao et al., "Progress of research on specificity of meridian acupoint efficacy," *Chinese Journal of Integrative Medicine*, vol. 19, no. 12, pp. 889–893, 2013.
- [59] L. Bai, X. Niu, Z. Liu et al., "The role of insula-cerebellum connection underlying aversive regulation with acupuncture," *Molecular Pain*, vol. 14, 2018.
- [60] Z. G. Li, M. M. Wu, and C. Z. Liu, "Progress of researches on acupuncture manipulation and its quantification," *Acupuncture Research*, vol. 35, no. 1, pp. 78–81, 2010.
- [61] R. B. Rutledge, A. M. Chekroud, and Q. J. M. Huys, "Machine learning and big data in psychiatry: toward clinical applications," *Current Opinion in Neurobiology*, vol. 55, pp. 152–159, 2019.
- [62] F. Zeng, W. Qin, T. Ma et al., "Influence of acupuncture treatment on cerebral activity in functional dyspepsia patients and its relationship with efficacy," *The American Journal of Gastroenterology*, vol. 107, no. 8, pp. 1236–1247, 2012.
- [63] R. Sun, Z. He, P. Ma et al., "The participation of basolateral amygdala in the efficacy of acupuncture with *deqi* treating for functional dyspepsia," *Brain Imaging and Behavior*, 2020.
- [64] W. Huang, D. Pach, V. Napadow et al., "Characterizing acupuncture stimuli using brain imaging with FMRI—a systematic review and meta-analysis of the literature," *PLoS One*, vol. 7, no. 4, article e32960, 2012.
- [65] C. W. Woo, L. J. Chang, M. A. Lindquist, and T. D. Wager, "Building better biomarkers: brain models in translational neuroimaging," *Nature Neuroscience*, vol. 20, no. 3, pp. 365–377, 2017.
- [66] T. Wolfers, J. K. Buitelaar, C. F. Beckmann, B. Franke, and A. F. Marquand, "From estimating activation locality to predicting disorder: a review of pattern recognition for neuroimaging-based psychiatric diagnostics," *Neuroscience and Biobehavioral Reviews*, vol. 57, pp. 328–349, 2015.
- [67] R. A. Poldrack, G. Huckins, and G. Varoquaux, "Establishment of best practices for evidence for Prediction," *JAMA Psychiatry*, vol. 77, no. 5, p. 534, 2020.
- [68] G. Varoquaux, "Cross-validation failure: small sample sizes lead to large error bars," *Neuro Image*, vol. 180, Part A, pp. 68–77, 2018.
- [69] D. Scheinost, S. Noble, C. Horien et al., "Ten simple rules for predictive modeling of individual differences in neuroimaging," *Neuro Image.*, vol. 193, pp. 35–45, 2019.
- [70] J. Lee, I. Mawla, J. Kim et al., "Machine learning-based prediction of clinical pain using multimodal neuroimaging and autonomic metrics," *Pain*, vol. 160, no. 3, pp. 550–560, 2019.
- [71] A. A. Nicholson, M. Densmore, M. C. McKinnon et al., "Machine learning multivariate pattern analysis predicts classification of posttraumatic stress disorder and its dissociative subtype: a multimodal neuroimaging approach," *Psychological Medicine*, vol. 49, no. 12, pp. 2049–2059, 2019.
- [72] X. Yang, X. Hu, W. Tang et al., "Multivariate classification of drug-naive obsessive-compulsive disorder patients and healthy controls by applying an SVM to resting-state functional MRI data," *BMC Psychiatry*, vol. 19, no. 1, p. 210, 2019.
- [73] F. Mokhtari, W. J. Rejeski, Y. Zhu et al., "Dynamic fMRI networks predict success in a behavioral weight loss program among older adults," *Neuro Image.*, vol. 173, pp. 421–433, 2018.
- [74] D. Wiesen, C. Sperber, G. Yourganov, C. Rorden, and H.-O. Karnath, "Using machine learning-based lesion behavior mapping to identify anatomical networks of cognitive dysfunction: spatial neglect and attention," *Neuro Image.*, vol. 201, article 116000, 2019.
- [75] D. B. Dwyer, P. Falkai, and N. Koutsouleris, "Machine learning approaches for clinical psychology and psychiatry," *Annual Review of Clinical Psychology*, vol. 14, no. 1, pp. 91–118, 2018.
- [76] K. M. Han, D. De Berardis, M. Fornaro, and Y. K. Kim, "Differentiating between bipolar and unipolar depression in functional and structural MRI studies," *Progress in Neuro-Psychopharmacology and Biological Psychiatry*, vol. 91, pp. 20–27, 2019.
- [77] B. Cao, Q. Luo, Y. Fu et al., "Predicting individual responses to the electroconvulsive therapy with hippocampal subfield volumes in major depression disorder," *Scientific Reports*, vol. 8, no. 1, article 5434, 2018.
- [78] J. Young, M. Modat, M. J. Cardoso et al., "Accurate multimodal probabilistic prediction of conversion to Alzheimer's disease in patients with mild cognitive impairment," *NeuroImage: Clinical*, vol. 2, pp. 735–745, 2013.

## Research Article

# Acupuncture Modulates Disrupted Whole-Brain Network after Ischemic Stroke: Evidence Based on Graph Theory Analysis

Xiao Han <sup>1</sup>, He Jin,<sup>1</sup> Kuangshi Li <sup>1</sup>, Yanzhe Ning,<sup>2</sup> Lan Jiang,<sup>1</sup> Pei Chen,<sup>2</sup> Hongwei Liu,<sup>3</sup> Yong Zhang <sup>1</sup>, Hua Zhang,<sup>1</sup> Zhongjian Tan,<sup>4</sup> Fangyuan Cui,<sup>1</sup> Yi Ren,<sup>1</sup> Lijun Bai <sup>5</sup>, and Yihuai Zou <sup>1</sup>

<sup>1</sup>Department of Neurology and Stroke Center, Dongzhimen Hospital, The First Affiliated Hospital of Beijing University of Chinese Medicine, Beijing, China

<sup>2</sup>The National Clinical Research Center for Mental Disorders & Beijing Key Laboratory of Mental Disorders, Beijing Anding Hospital, Capital Medical University, Beijing, China

<sup>3</sup>Department of Neurology, Shunyi Hospital Affiliated to Beijing Hospital of Traditional Chinese Medicine, Beijing, China

<sup>4</sup>Department of Radiology, Dongzhimen Hospital, The First Affiliated Hospital of Beijing University of Chinese Medicine, Beijing, China

<sup>5</sup>The Key Laboratory of Biomedical Information Engineering, Ministry of Education, Department of Biomedical Engineering, School of Life Science and Technology, Xi'an Jiaotong University, Xi'an, China

Correspondence should be addressed to Lijun Bai; [bailijun@xjtu.edu.cn](mailto:bailijun@xjtu.edu.cn) and Yihuai Zou; [zouyihuai2004@163.com](mailto:zouyihuai2004@163.com)

Received 20 April 2020; Revised 14 June 2020; Accepted 22 July 2020; Published 19 August 2020

Academic Editor: Jing-Wen Yang

Copyright © 2020 Xiao Han et al. This is an open access article distributed under the Creative Commons Attribution License, which permits unrestricted use, distribution, and reproduction in any medium, provided the original work is properly cited.

**Background.** Stroke can lead to disruption of the whole-brain network in patients. Acupuncture can modulate the functional network on a large-scale level in healthy individuals. However, whether and how acupuncture can make a potential impact on the disrupted whole-brain network after ischemic stroke remains elusive. **Methods.** 26 stroke patients with a right hemispheric subcortical infarct were recruited. We gathered the functional magnetic resonance imaging (fMRI) from patients with stroke and healthy controls in the resting state and after acupuncture intervention, to investigate the instant alterations of the large-scale functional networks. The graph theory analysis was applied using the GRETNA and SPM12 software to construct the whole-brain network and yield the small-world parameters and network efficiency. **Results.** Compared with the healthy subjects, the stroke patients had a decreased normalized small-worldness ( $\sigma$ ), global efficiency ( $E_g$ ), and the mean local efficiency ( $E_{loc}$ ) of the whole-brain network in the resting state. There was a correlation between the duration after stroke onset and  $E_{loc}$ . Acupuncture improved the patients' clustering coefficient ( $C_p$ ) and  $E_{loc}$  but did not make a significant impact on the  $\sigma$  and  $E_g$ . The postacupuncture variables of the whole-brain network had no association with the time of onset. **Conclusion.** The poststroke whole-brain network tended to a random network with reduced network efficiency. Acupuncture was able to modulate the disrupted patterns of the whole-brain network following the subcortical ischemic stroke. Our findings shed light on the potential mechanisms of the functional reorganization on poststroke brain networks involving acupuncture intervention from a large-scale perspective.

## 1. Introduction

Following a stroke, focal ischemic lesions can result in extensive functional changes in structurally intact brain areas far beyond the infarct, which is referred to as “diaschisis” [1–3]. The cataclysmic changes in the whole-brain

network are attributable to the widespread disturbance following a focal injured site [4, 5]. These large-scale interactions between brain regions account for the behavioral deficits in patients with stroke [6]. The normalization of an abnormal connectome has been found to mirror the recovery from stroke [7, 8]. Graph theory-based network

TABLE 1: The group demographic and relevant clinical measures.

Subject	Sex	Age (yrs.)	Time of onset ( <i>d</i> )	NIHSS	FMA
Patient	19M/7F	56.42 ± 7.23	41.04 ± 29.71	3.46 ± 2.58	78.20 ± 23.46
Control	12M/9F	54.52 ± 5.11	n/a	n/a	n/a

F: female; FMA: Fugl-Meyer Assessment; M: male; NIHSS: National Institute of Health Stroke Scale.

analysis is widely used to characterize the features of the large-scale brain connectome [9–11]. The small-world model is well suited for the evaluation of complex brain networks since it reflects the integrative and segregated information processes [12, 13]. The focal lesions may disturb the spatial and temporal organization and break the optimal balance of integration and segregation [14].

Based on graph theoretical approaches, previous studies emphasized that the small-worldness was significantly lower in stroke patients than healthy controls, and it increased toward the level of controls during recovery [8]. The reductions in interhemispheric integration and intrahemispheric segregation strongly relate to the behavioral impairments of stroke [15]. In subcortical stroke patients, the reorganized network deviated away from the optimal architecture toward a more random mode during the first months after the stroke onset [16]. However, the reorganization of the entire brain pattern during stroke recovery is still disputable and elusive for now.

Acupuncture is a well-known therapeutic strategy in China for over two millennia of practice, which is also widely accepted in modern Western countries [17, 18]. Increasingly, empirical and clinical evidence suggests that acupuncture is effective and safe for subacute stroke rehabilitation [19, 20]. According to the theory of Chinese medicine, acupuncture can dynamically harmonize the inherent imbalances that result from diseases. Besides, acupuncture is more inclined to modulate the homeostasis of brain activity at a large scale [21].

The previous study identified that acupuncture altered the architecture of the functional whole-brain network in healthy subjects and the alterations displayed acupoint specificity [22–24]. Acupuncture stimulation at acupoint ST36 increased the local efficiency of healthy individuals [25]. Furthermore, another study applied the long-duration transcutaneous electric acupoint stimulation and indicated that small-world properties were modulated with lower local efficiency and nonsignificant change in global efficiency for healthy subjects [26]. But the therapeutic effects of acupuncture may depend on different conditions of clinical diseases [23, 25]. Feng et al. studied the acupuncture effects on the functional network of the whole brain in mild cognitive impairment patients [27]. They found that acupuncture had a relatively less effect on healthy controls than patients. With the help of graph theory analysis, it revealed some previously unreported features of the neural mechanism after acupuncture on patients.

The architecture of brain after subcortical infarction remains poorly understood. Moreover, little is known about the alternations in response to acupuncture on the large-scale perspective after stroke onset. The current study, there-

fore, employed the graph theoretical approaches to investigate how acupuncture affected the whole-brain functional network following a subcortical insult. We hypothesized that acupuncture was able to modulate the deviant organization of the poststroke whole-brain network.

## 2. Materials and Methods

**2.1. Subjects.** 26 ischemic stroke patients were recruited at Dongzhimen Hospital affiliated to Beijing University of Chinese Medicine. 21 healthy subjects were rolled as control with no history of neurological or psychiatric disorders. The demographic and clinical features are shown in Table 1. The inclusion criteria were as follows: aged 35–75 years; first-ever ischemic stroke; within 3 months after the onset; subcortical lesion restricted to the right hemispheric internal capsule, basal ganglia, corona radiata, and its neighboring regions; and without psychiatric disorders. The exclusion criteria were as follows: any brain abnormalities except infarction; any other physical or psychiatric conditions that may influence participation; and any MRI contraindications. All of the subjects were with right-hand dominance. The study was approved by the Ethics Committee of the Beijing University of Chinese Medicine and conducted in accordance with the Declaration of Helsinki. After being given a complete explanation of the experiment procedure, all subjects signed the informed consent.

**2.2. Clinical Assessments.** The National Institute of Health Stroke Scale (NIHSS) was performed for stroke-related neurologic deficits [28] and the Fugl-Meyer Assessment (FMA) was adopted for a quantitative measure of motor disability [29]. All patients underwent these clinical assessments (shown in Table 1).

**2.3. Experimental Paradigm.** The nonrepeated event-related fMRI design was adopted to investigate the prolonged effects of acupuncture administration [30]. Firstly, a resting-state scan was conducted for 8 min 10 sec without any stimulation as a baseline control. Then, after a DTI session, we employed an experimental functional run under acupuncture stimulation. The acupuncture stimulation was delivered using a sterile disposable silver acupuncture needle 0.3 mm in diameter and 40 mm in length. The needle was vertically inserted to a depth of 20–30 mm at the acupoint GB34 (Yanglingquan) on the right side. The GB34 situates on the fibular aspect of the leg, in the depression anterior and distal to the head of the fibula. It is commonly used in the clinical treatment for stroke [19, 31, 32]. The acupuncture administration was delivered by a balanced “tonifying and reducing” manipulation (rotating the needle clockwise and counterclockwise at



1 Hz for 60 sec) and followed by an 8 min 10 sec consecutive scan without manipulation. The procedure was performed by the same licensed and experienced acupuncturist. All subjects reported their experience (“Deqi”) of acupuncture stimulation immediately after the experiment. “Deqi” included the sensations of soreness, heaviness, fullness, pressure, and numbness [33]. The subject who experienced sharp pain would be excluded from further analysis as the sharp pain was considered an inadvertent noxious stimulation [34]. None of the subjects reported an experience of sharp pain. In this study, none of the subjects ever received thrombolytic therapy. All of the patients received conventional standard medical treatment, such as antiplatelet therapy, which complied with the *Guidelines for the diagnosis and treatment of acute ischemic stroke in China 2014* [35].

**2.4. Image Acquisitions.** The fMRI data were obtained using a 3.0 Tesla MRI scanner (Siemens, Sonata Germany) at the department of radiology of Dongzhimen Hospital, Beijing, China. During the scanning, all subjects were requested to keep their eyes closed and remain relaxed without engaging in any mental tasks. Earplugs were worn to attenuate scanner noise, and foam head holders were immobilized to minimize head movements.

Before the functional scanning, high-resolution structural information for anatomical localization was acquired using 3D MRI sequences. A single-shot, gradient-recalled echo-planar imaging sequence was used to collect the resting-state fMRI data with the following parameters: repetition time = 2000 ms, echo time = 30 ms, flip angle = 90°, matrix = 64 × 64, field of view = 225 × 225 mm<sup>2</sup>, slice thickness = 3.5 mm, gap = 1 mm, 32 interleaved axial slices, and 241 volumes. The same parameters were applied in the acupuncture-evoked fMRI with the exception that 271 volumes were acquired.

**2.5. Data Preprocessing.** The fMRI data were preprocessed with the Graph Theoretical Network Analysis (GRETNA) (<http://www.nitrc.org/projects/gretna>) and SPM12 (<http://www.fil.ion.ucl.ac.uk/spm>) toolbox based on Matlab2013b [36]. The first ten volumes were discarded to allow the adaption of the subjects and the stabilization of the magnetization. The remaining volumes were slice-timing corrected for different acquisition in slice times and realigned to the first volume for head-motion correction. Based on the head motion data, the subjects were excluded according to the criteria of maximum translation as 3 mm and rotational parameters as 3 degrees in any direction. Next, the individual functional images were normalized to the standard Montreal Neurological Institute space with 3 mm isotropic resolution by applying the transformation matrix which was derived from registering the final template file generated by DARTEL. Then, the images were smoothed with a 4 mm full-width at the half-maximum Gaussian kernel and further linearly detrended. Subsequently, several nuisance signals were regressed out, including the white matter signal, the cerebrospinal fluid signal, and 24-parameter head motion profiles [37, 38]. The global signal was not regressed out according to previous studies [39]. Then, the data were

temporally band-pass filtered (0.01-0.08 Hz) to reduce the low-frequency drift and high-frequency physiological noise.

**2.6. Network Construction.** The graph theoretical network analysis toolbox GRETNA was applied to construct the large-scale brain networks [36]. For the network nodes definition, the entire cerebral cortex was parceled into 90 (45 in each hemisphere) anatomically defined regions according to Automated Anatomical Labeling for each subject [40]. The mean time series for each of the 90 areas were extracted from the preprocessed datasets by averaging the voxel time series within each region. The edges of functional brain networks were constructed with the functional connectivity between nodes. Pearson’s correlation coefficients between the mean time series of all node pairs were calculated, resulting in a 90 × 90 correlation matrix for each subject. Fisher’s *r*-to-*z* transformation was further performed to improve the normality, and this resulted in a *z*-value matrix for each subject. The matrices were binary, and both positive and negative connections were used to achieve the whole-brain network.

**2.7. Networks Analysis.** We employed a wide range of sparsity thresholds ( $0.05 \leq \text{sparsity} \leq 0.5$ , interval = 0.01) to address a variable number of edges in different individual subjects. The sparsity is defined as the existing number of edges divided by the maximum possible number of edges in the graph [41, 42]. The global metrics contained the small-world parameters and network efficiency to depict the entire brain functional connectomes. The main small-world parameters included the clustering coefficient ( $C_p$ ), characteristic path length ( $L_p$ ), and small-worldness ( $\sigma$ ). The network efficiency included global efficiency ( $E_g$ ) and the mean local efficiency ( $E_{loc}$ ). The mean local efficiency was defined as the average efficiency of the local subgraphs. A detailed explanation of these network parameters can be found in the previous study [43]. The area under the curve (AUC) was also calculated for each network metric to provide a summarized scalar. The AUC was independent of a single threshold selection and has been proved to be highly sensitive to topological alterations in brain disorders [44, 45].

**2.8. Statistical Analysis.** The demographics and clinical profiles were analyzed by two-sample *t*-test for continuous variables and Chi-square test for categorical variables using the SPSS software version 19.0 (<http://www.spss.com>; Chicago, IL). The statistical comparisons of measures ( $C_p$ ,  $L_p$ ,  $\sigma$ ,  $E_g$ , and  $E_{loc}$ ) and their AUC were performed using independent two-sample *t*-test between stroke patients and healthy controls with age and gender as unconcerned covariates. We applied the paired *t*-test to determine the pre- and proacupuncture alterations of these large-scale network matrices. We also performed a two-tailed Spearman’s rank correlation between the AUC of parameters and the clinical measures in the stroke patients.  $p < 0.05$  was considered to be statistically significant.

### 3. Result

**3.1. Demographic and Clinical Characteristics.** In the present study, the subcortical ischemic lesions were restricted to the

motor pathways of the right hemisphere. The time of stroke onset was  $41.04 \pm 29.71$  days. There were no statistical differences in age ( $p = 0.315$ ) or sex ( $p = 0.355$ ) between the patients and healthy controls. The average score of National Institute of Health Stroke Scale (NIHSS) was  $3.46 \pm 2.58$ , and Fugl-Meyer Assessment (FMA) was  $78.20 \pm 23.46$ . Table 1 summarizes the demographic and clinical characteristics of all the subjects.

**3.2. Small-World Parameters at Resting State.** The matrices were constructed with a wide range of sparsity ( $0.05 \leq Sp \leq 0.5$ , in 0.01 increments) in all subjects. We calculated the small-world parameters and compared them between the stroke and healthy subjects. Although both groups met the criteria of the small-worldness ( $\sigma > 1$ ), the  $\sigma$  of the stroke patients had a significant reduction relative to healthy subjects ( $0.33 \leq Sp \leq 0.50$ , shown in Figure 1(a)). At the same time, the values of  $L_p$  increased at several separated sparsity in stroke 4 individuals (shown in Figure 1(c)), but the  $C_p$  did not have statistic discrepancy (shown in Figure 1(b)). To further investigate the potential causes of the decline in  $\sigma$ , we analyzed the normalized clustering coefficient ( $\gamma = C_p/C_p$  random) and the normalized characteristic path length ( $\lambda = L_p/L_p$  random), by calculating which would get the small-worldness ( $\sigma = \gamma/\lambda$ ). The stroke patients displayed a distinct decrease on the parameter  $\gamma$  in contrast with the healthy controls ( $0.33 \leq Sp \leq 0.50$ , shown in Figure 2(a)), while they did not show the difference on the  $\lambda$  (shown in Figure 2(b)). The AUC of the small-world parameters had no significant difference between stroke patients and healthy controls (shown in Figure 3).

**3.3. Acupuncture Altered Small-World Parameters.** We analyzed the alterations of matrices before and after acupuncture intervention in patients with stroke and the healthy controls. The  $\sigma$  value did not show a statistical improvement after needling. However, there was a trend of increased  $\sigma$  in postacupuncture stroke patients (shown in Figure 1(a)). The acupuncture significantly increased the  $C_p$  on the sparsity threshold of 0.16-0.21 (shown in Figure 1(b)). Also, the AUC of  $C_p$  was also conspicuously increased after acupuncture intervention relative to the resting state in the stroke patients ( $p = 0.041$ , shown in Figure 3). There were no significant changes in the parameter  $L_p$  after acupuncture intervention (shown in Figure 1(c)).

**3.4. Network Efficiency.** The between-group comparison revealed that the stroke patients exhibited notably lower  $E_g$  and  $E_{loc}$  than the healthy controls on certain sparsity thresholds (shown in Figures 4(a) and 4(b)). The AUC of network efficiency also testified a significant diminishment on the  $E_g$  ( $p = 0.045$ ) and  $E_{loc}$  ( $p = 0.008$ ) in the stroke patients (shown in Figure 5). The acupuncture intervention had no noticeable impact on the  $E_g$ , but markedly enhanced the  $E_{loc}$  at certain sparsity (shown in Figure 4) and the AUC of  $E_{loc}$  ( $p = 0.032$ , shown in Figure 5) in the patients with stroke.

**3.5. Correlations between Graph Theory Metrics and Clinical Measures.** We further analyzed the associations between the AUC of graph theory metrics and the clinical scores in the stroke patients. A significant negative correlation between the AUC of  $E_{loc}$  and the time of stroke onset was found ( $p = 0.029$ , shown in Figure 6)

## 4. Discussion

In this study, we applied the graph-based theoretical approaches to analyze the properties of the entire brain. The functional whole-brain network of the stroke patients and healthy controls before and after acupuncture intervention were constructed separately. Our results revealed that the large-scale functional patterns in both groups of subjects exhibited the small-world features; however, the patients with stroke displayed a decline on the normalized clustering coefficient ( $\gamma$ ), small-worldness ( $\sigma$ ), global efficiency ( $E_g$ ), and the mean local efficiency ( $E_{loc}$ ) at resting state in contrast with the healthy individuals. The reduced local efficiency was correlated with the duration after stroke onset. Acupuncture significantly improved the clustering coefficient and the mean local efficiency of the stroke individuals but did not make a statistic impact on the small-worldness or global efficiency. This study primarily demonstrated the modulation of acupuncture on the poststroke functional whole-brain network.

In the current study, the small-worldness was conspicuously declined in the stroke patients contrasted to the healthy subjects. To further study it, we analyzed the parameters  $\gamma$  and  $\lambda$ . In general, the usual small-world networks have relatively high  $\gamma$  and low  $\lambda$ , which combine the topological properties of both random and regular networks to maintain simultaneously high ability in segregating and integrating information. The integration and segregation are two major principles of the human brain functional organization. We found that the parameter  $\gamma$  was notably decreased in the stroke patients in the same range of sparsity, which implied that the  $\gamma$  was supposed to be responsible for the decline of the small-worldness. The  $\gamma$  was the normalized version of clustering coefficient and reflected the ability in segregating information. These changes of the large-scale patterns result from ischemic infarction which were in line with a previous study [8]. Siegel et al. showed that the small-worldness decreased after stroke onset, and they also inferred that the poststroke changes of small-worldness were a result of changes in the clustering coefficient, but not the average path length. Our findings indicated that the stroke attack altered the architecture of the functional whole-brain network. The breakdown of human brain function in stroke might be mainly involved in the segregation instead of the integration, which shifted the poststroke whole-brain network toward a random graph. Zhu et al. also reported similar results. They indicated a tendency of randomization in acute ischemic stroke patients' functional brain networks [46].

The network efficiency is an assessment of how efficiently a network exchanges information [47]. At the global level, efficiency quantifies the effectiveness of integration of distributed information across the whole-brain network where

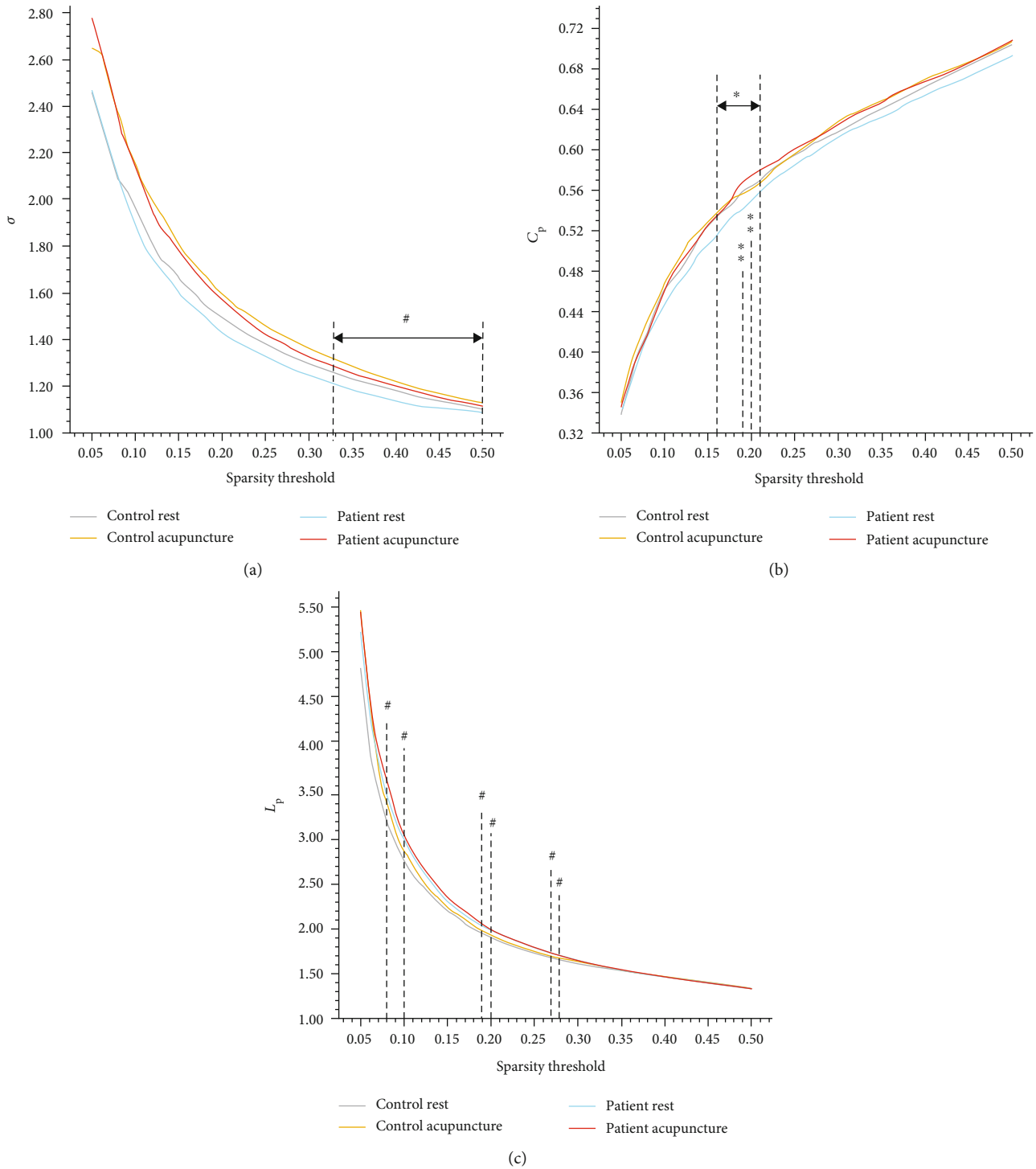


FIGURE 1: Comparison of small-world parameters ( $\sigma$ ,  $C_p$ , and  $L_p$ ) at a sparsity range of 0.05-0.50. (a) The small-worldness ( $\sigma$ ) was compared between the stroke patients and the healthy controls, as well as the resting-state and postacupuncture intervention. In the resting state, the patients with stroke exhibited significantly lower  $\sigma$  values relative to the healthy controls on a sparsity threshold from 0.33 to 0.50. However, after acupuncture intervention, the enhanced  $\sigma$  values were not statistically different from the resting state. (b) On the sparsity threshold of 0.16-0.21, the clustering coefficient of patients was notably improved by acupuncture. (c) At several separated sparsities ( $Sp = 0.08, 0.10, 0.19, 0.20, 0.27, 0.28$ ), there were statistical differences in the characteristic path length between the two groups of subjects in the resting state. # $p < 0.05$  (stroke patients vs. healthy controls, in the resting state); \* $p < 0.05$ , \*\* $p < 0.01$  (resting state vs. postacupuncture intervention, in the stroke patients).

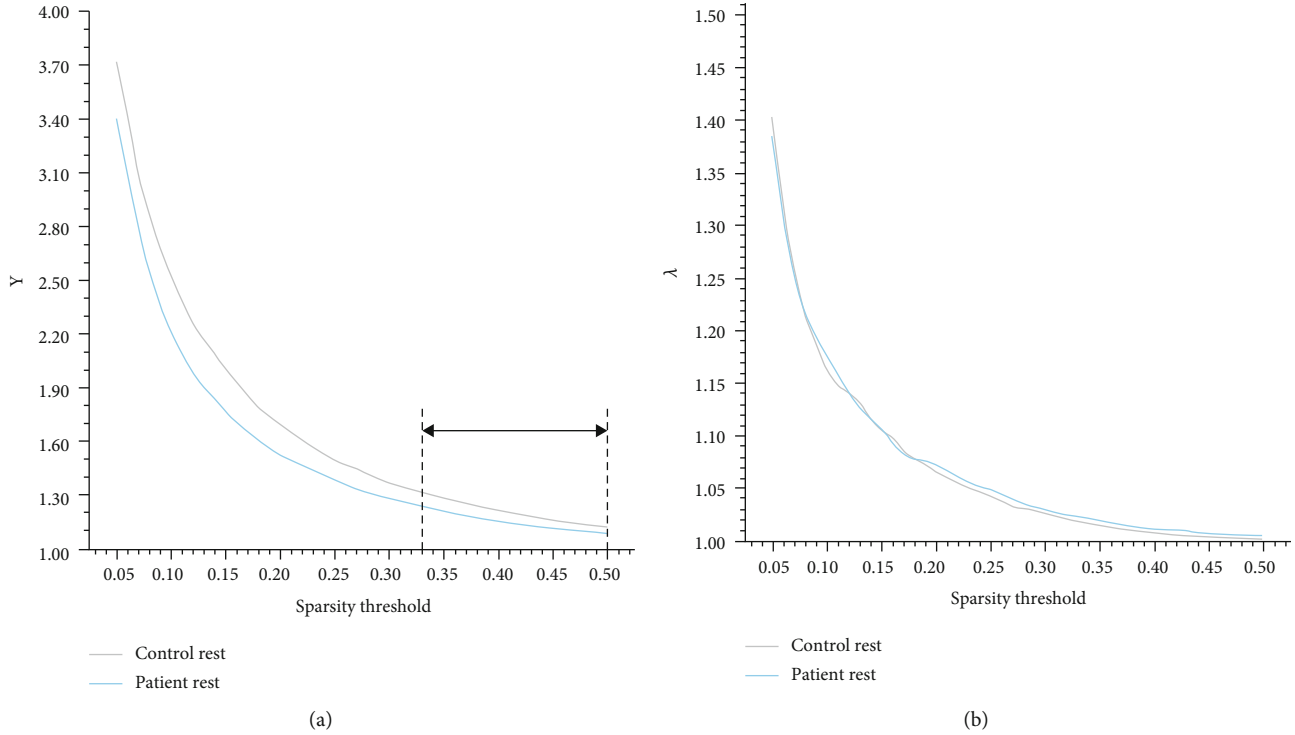


FIGURE 2: Comparison of the normalized small-world parameters ( $\gamma$ ,  $\lambda$ ). (a) The values of normalized clustering coefficient ( $\gamma$ ) decreased in the stroke patients relative to healthy controls on the sparsity threshold of 0.33-0.50. (b) There was no significant difference in the normalized characteristic path length ( $\lambda$ ) between two groups of subjects.  $^*p < 0.05$ .

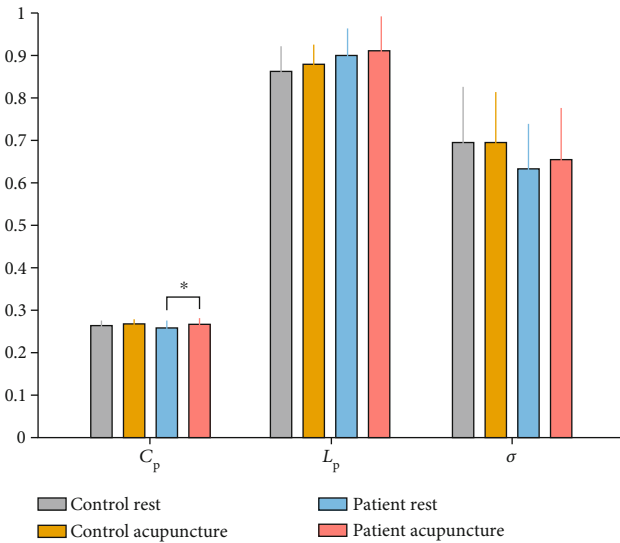


FIGURE 3: Mean area under the curve (AUC) values of the small-world parameters. The stroke patients displayed no marked discrepancy in contrast with the healthy controls on the AUC. Acupuncture intervention made a distinct improvement on the AUC of  $C_p$  values in the stroke patients.  $^*p < 0.05$ .

information is concurrently exchanged [48]. It reflects the capacity for network-wide communication [41]. The local efficiency relies on the connectivity properties in the neighborhood of a node and indicates how efficient is the communication between a region and its neighboring areas [49]. The

local efficiency is the metric that reflects the fault tolerant [47]. In the present study, not only the global efficiency but also the mean local efficiency was significantly lower in the stroke patients relative to the healthy subjects, which were in agreement with the findings of small-worldness alterations. These results revealed that the focal ischemic insult not only disrupted the ability to exchange information through the entire network but also minified the overall level of the communication within the neighborhoods. An optimal brain achieves a dynamic balance between global integration and local specialization with both relatively high global and local efficiency [50]. Some previous findings also unveiled that the brain regions of the post-stroke networks communicated less efficiently both on the global and local range [15].

Our study for the first time manifested that acupuncture was able to make an instant improvement on the poststroke clustering coefficient ( $C_p$ ), and the reduced local efficiency was also escalated. However, neither the small-worldness nor the global efficiency had significant modifications under the acupuncture intervention. It hinted that acupuncture enhanced the connection within the neighborhood regions and modulated the local information flow, which could participate in the reorganization of the poststroke brain network and the process of neural plasticity. We supposed that the acupuncture might mainly work on the recovery of the segregation function in the whole-brain network after a stroke attack. Acupuncture might be able to promote the organization of poststroke network toward a regular one. In addition,



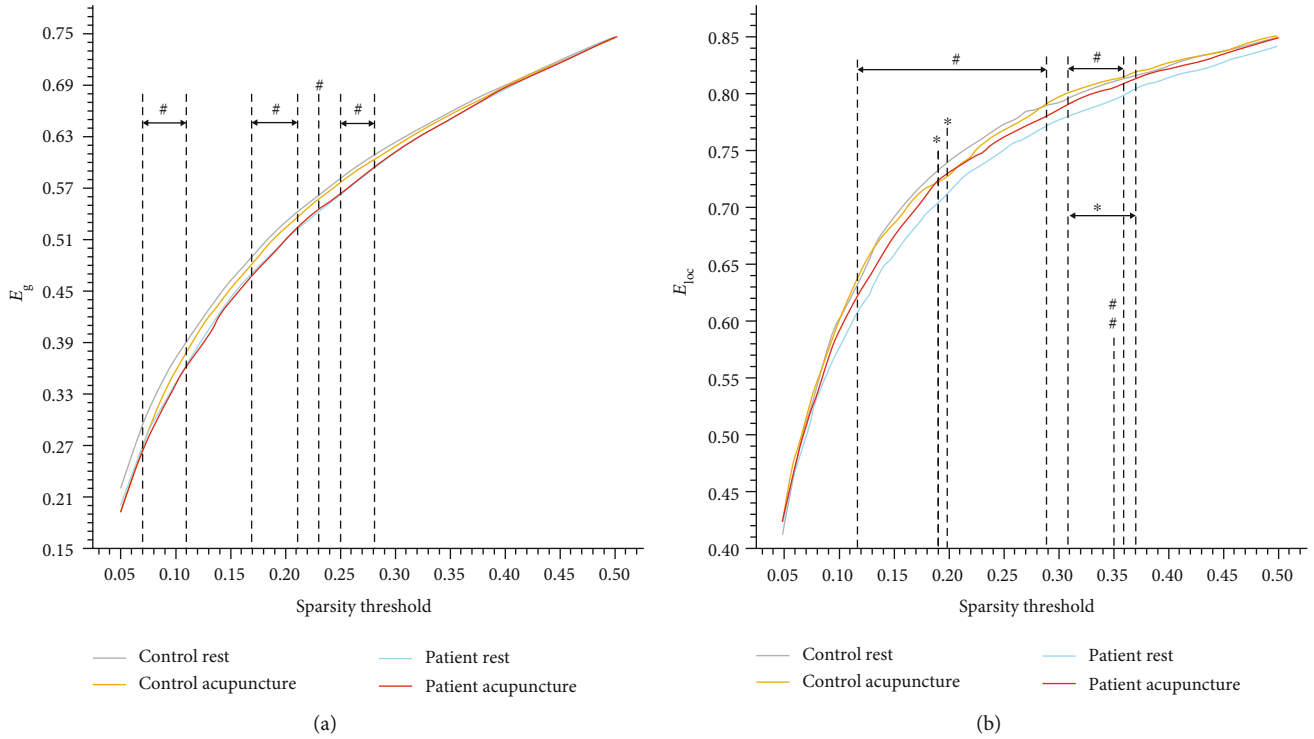


FIGURE 4: Comparison of the global ( $E_g$ ) and local ( $E_{loc}$ ) efficiency at a sparsity range of 0.05-0.50. (a) The stroke patients showed a decline in the global efficiency relative to the healthy controls at certain sparsity ( $Sp = 0.07 - 0.11, 0.17 - 0.21, 0.23, 0.25 - 0.28$ ). (b) The patients exhibited a conspicuous damage on the local efficiency than the healthy controls ( $Sp = 0.12 - 0.29, 0.31 - 0.36$ ), while acupuncture intervention showed distinct alteration on the local efficiency of the stroke patients ( $Sp = 0.19, 0.20, 0.31 - 0.37$ ).  $\#p < 0.05$ ,  $\#\#p < 0.01$  (stroke patients vs. healthy controls, in the resting state);  $*p < 0.05$  (resting state vs. postacupuncture intervention, in the stroke patients).

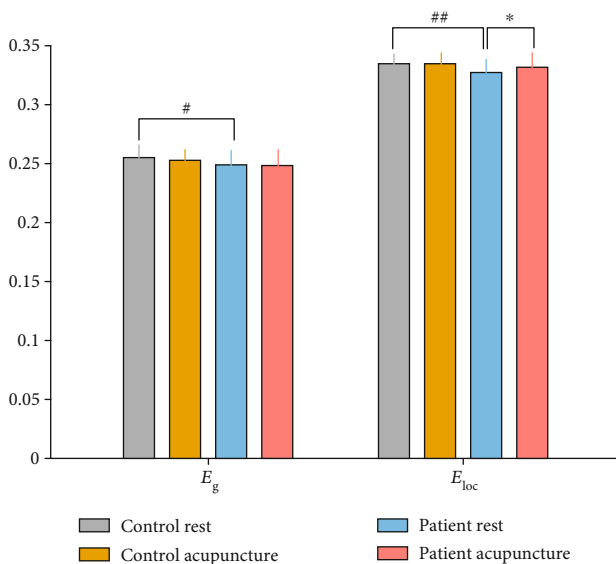


FIGURE 5: Mean area under the curve (AUC) values of the network efficiency. The patients had a significant reduction on the AUC value of both the global and local efficiency in the resting state compared with the healthy controls. Acupuncture intervention was able to make a noteworthy increase on the local efficiency, while having no distinct impact on the global efficiency.  $*p < 0.05$  (stroke patients vs. healthy controls, resting state).  $\#p < 0.05$ ,  $\#\#p < 0.01$  (stroke patients vs. healthy controls, in the resting state);  $*p < 0.05$  (resting state vs. postacupuncture intervention, in the stroke patients).

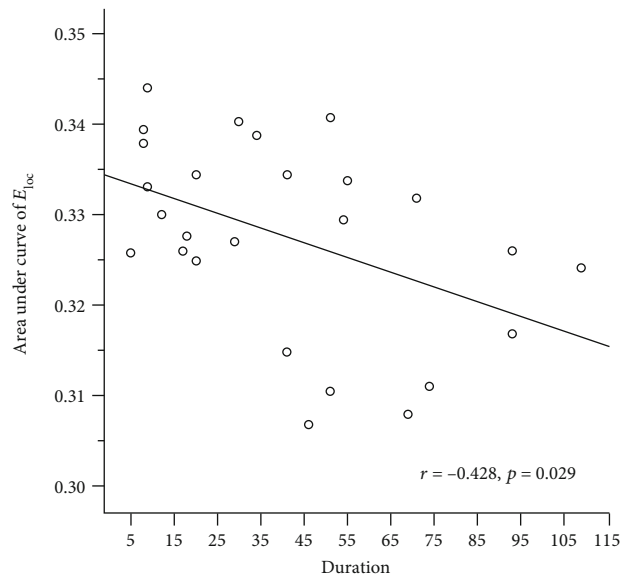


FIGURE 6: The Spearman rank correlation between the AUC of local efficiency and time of stroke onset. There was a significant negative association between the AUC of  $E_{loc}$  and the duration after stroke onset ( $p = 0.029$ ).

the above-mentioned alterations were not observed within the healthy subjects. It implied that acupuncture could mediate the poststroke whole-brain networks, and this specific

modulation arose under the condition of stroke. Nevertheless, in the present study, we focused on the instant effect of acupuncture instead of the sustained effect after a period of acupuncture treatments and just intervened on a single acupoint instead of a group of acupoints. This strategy might result in that the acupuncture intervention was not enormous enough to make statistically significant alterations on the small-worldness or the global efficiency. It is still not sure whether acupuncture can also make an influence on the small-worldness and global efficiency if we adopted a longitudinal acupuncture intervention with multiple acupoints involved. In the future, we would progress to the long-term acupuncture efficacy with various acupoints combination. It might be able to uncover more impact of acupuncture treatment on the whole-brain network. In addition, this study focused on the functional alterations on the large scale. Further investigation could combine the function and structure data of the whole-brain network to have a better understanding of the strategy of the brain responding to stroke and acupuncture.

The correlations analysis showed a significant negative association between the duration after stroke onset and the AUC of the mean local efficiency. We speculated that for the stroke patients within 3 months of onset, the local efficiency might gradually decrease over time, which might be due to the pathological dynamics after a stroke attack, such as the Wallerian degeneration. It might indicate that the application of acupuncture in the early stage of stroke can make more benefits for stroke patients, which needs to be further confirmed. The NIHSS and FMA scores showed no correlation with the AUC of the small-worldness or the network efficiency. Additionally, the parameters of the postacupuncture network matrices in the stroke patients did not associate with the clinical measures in our study. However, as this study included ischemic stroke patients within 3 months after the stroke onset, the dynamic patterns in a longer term still need further study. In future research, the stroke phase, combining the time of onset and the degree of the neurological deficits, can be taken as an important factor to uncover the different characteristics within stroke patients.

## 5. Conclusion

The present work pointed to the functional disruption of the whole-brain network in the stroke patients and the acupuncture modulation. In short, we illustrated that the stroke attack was able to reduce the small-worldness and the global and the mean local efficiency; at the same time, acupuncture can instantly increase the clustering coefficient and the mean local efficiency of the whole-brain network but not make statistically significant alterations on the small-worldness or the global efficiency. This study highlighted that acupuncture could help reorganize the disrupted poststroke whole-brain network. Our study provided an elucidation for the mechanisms of acupuncture treatment after stroke from the large-scale perspective.

## Data Availability

The datasets generated and analyzed during the current study are not publicly available due to the terms of consent

to which the participants agreed but are available from the corresponding author on reasonable request.

## Conflicts of Interest

The authors declare that there is no conflict of interests regarding the publication of this paper.

## Authors' Contributions

YZ, LB, and FC participated in the study concept and design; LJ, HL, and PC recruited the volunteers; XH, HJ, and ZT performed the experiment; KL, YN, LB, and HZ analyzed the data; XH wrote the draft of the manuscript; YZ revised the manuscript; XH is the first author; HJ and KL are the co-first authors; YZ and LB are the co-corresponding authors; all authors read and approved the final manuscripts. Xiao Han, He Jin, and Kuangshi Li contributed equally to the work.

## Acknowledgments

This research was supported by the National Natural Science Foundation of China (grant numbers 81873257, 81771914). Dr. Han was supported by a fellowship from the China Scholarship Council. The authors are grateful for the assistance of doctors at the Department of Neurology and Stroke Center in Dongzhimen Hospital affiliated to Beijing University of Chinese Medicine. In addition, the authors are thankful to all individuals who participated in this study. The authors would like to thank Qikang Zuo for providing language help.

## References

- [1] S. Finger, P. J. Koehler, and C. Jagella, "The Monakow concept of diaschisis: origins and perspectives," *Archives of Neurology*, vol. 61, no. 2, pp. 283–288, 2004.
- [2] C. Grefkes and G. R. Fink, "Connectivity-based approaches in stroke and recovery of function," *The Lancet Neurology*, vol. 13, no. 2, pp. 206–216, 2014.
- [3] C. Von Monakow, "Mood, states and mind," in *Brain and Behaviour Vol. 1*, K. H. Pribram, Ed., pp. 27–36, Penguin books, 1969.
- [4] A. Fornito, A. Zalesky, and M. Breakspear, "The connectomics of brain disorders," *Nature Reviews Neuroscience*, vol. 16, no. 3, pp. 159–172, 2015.
- [5] A. K. Rehme and C. Grefkes, "Cerebral network disorders after stroke: evidence from imaging-based connectivity analyses of active and resting brain states in humans," *The Journal of Physiology*, vol. 591, no. 1, pp. 17–31, 2013.
- [6] M. Corbetta, J. S. Siegel, and G. L. Shulman, "On the low dimensionality of behavioral deficits and alterations of brain network connectivity after focal injury," *Cortex*, vol. 107, pp. 229–237, 2018.
- [7] D. H. Lim, J. M. LeDue, M. H. Mohajerani, and T. H. Murphy, "Optogenetic mapping after stroke reveals network-wide scaling of functional connections and heterogeneous recovery of the peri-infarct," *Journal of Neuroscience*, vol. 34, no. 49, pp. 16455–16466, 2014.

- [8] J. S. Siegel, B. A. Seitzman, L. E. Ramsey et al., "Re-emergence of modular brain networks in stroke recovery," *Cortex*, vol. 101, pp. 44–59, 2018.
- [9] E. Bullmore and O. Sporns, "Complex brain networks: graph theoretical analysis of structural and functional systems," *Nature Reviews Neuroscience*, vol. 10, no. 3, pp. 186–198, 2009.
- [10] E. Bullmore and O. Sporns, "The economy of brain network organization," *Nature Reviews Neuroscience*, vol. 13, no. 5, pp. 336–349, 2012.
- [11] Y. He and A. Evans, "Graph theoretical modeling of brain connectivity," *Current Opinion in Neurology*, vol. 23, no. 4, pp. 341–350, 2010.
- [12] X. Liao, A. V. Vasilakos, and Y. He, "Small-world human brain networks: perspectives and challenges," *Neuroscience & Biobehavioral Reviews*, vol. 77, pp. 286–300, 2017.
- [13] D. J. Watts and S. H. Strogatz, "Collective dynamics of 'small-world' networks," *Nature*, vol. 393, no. 6684, pp. 440–442, 1998.
- [14] M. H. Adhikari, C. D. Hacker, J. S. Siegel et al., "Decreased integration and information capacity in stroke measured by whole brain models of resting state activity," *Brain*, vol. 140, no. 4, pp. 1068–1085, 2017.
- [15] J. S. Siegel, L. E. Ramsey, A. Z. Snyder et al., "Disruptions of network connectivity predict impairment in multiple behavioral domains after stroke," *Proceedings of the National Academy of Sciences of the United States of America*, vol. 113, no. 30, pp. E4367–E4376, 2016.
- [16] L. Wang, C. Yu, H. Chen et al., "Dynamic functional reorganization of the motor execution network after stroke," *Brain*, vol. 133, no. 4, pp. 1224–1238, 2010.
- [17] T. J. Kaptchuk, "Acupuncture: theory, efficacy, and practice," *Annals of Internal Medicine*, vol. 136, no. 5, pp. 374–383, 2002.
- [18] J.-N. Wu, "A short history of acupuncture," *The Journal of Alternative and Complementary Medicine*, vol. 2, no. 1, pp. 19–21, 1996.
- [19] J. Fang, L. Chen, R. Ma et al., "Comprehensive rehabilitation with integrative medicine for subacute stroke: a multicenter randomized controlled trial," *Scientific Reports*, vol. 6, no. 1, 2016.
- [20] X. Han, L. Bai, C. Sun et al., "Acupuncture enhances communication between cortices with damaged white matters in post-stroke motor impairment," *Evidence-Based Complementary and Alternative Medicine*, vol. 2019, Article ID 4245753, 11 pages, 2019.
- [21] D. J. Mayer, "Acupuncture: an evidence-based review of the clinical literature," *Annual Review of Medicine*, vol. 51, no. 1, pp. 49–63, 2000.
- [22] Y. Feng, L. Bai, Y. Ren et al., "Investigation of the large-scale functional brain networks modulated by acupuncture," *Magnetic Resonance Imaging*, vol. 29, no. 7, pp. 958–965, 2011.
- [23] Y. Ren, L. Bai, Y. Feng, J. Tian, and K. Li, "Investigation of acupoint specificity by functional connectivity analysis based on graph theory," *Neuroscience Letters*, vol. 482, no. 2, pp. 95–100, 2010.
- [24] H. Yu, X. Wu, L. Cai, B. Deng, and J. Wang, "Modulation of spectral power and functional connectivity in human brain by acupuncture stimulation," *IEEE Transactions on Neural Systems and Rehabilitation Engineering*, vol. 26, no. 5, pp. 977–986, 2018.
- [25] B. Liu, J. Chen, J. Wang et al., "Altered small-world efficiency of brain functional networks in acupuncture at ST36: a functional MRI study," *PLoS One*, vol. 7, no. 6, article e39342, 2012.
- [26] Y. Zhang, Y. Jiang, C. B. Glielmi et al., "Long-duration transcutaneous electric acupoint stimulation alters small-world brain functional networks," *Magnetic Resonance Imaging*, vol. 31, no. 7, pp. 1105–1111, 2013.
- [27] Y. Feng, L. Bai, Y. Ren et al., "fMRI connectivity analysis of acupuncture effects on the whole brain network in mild cognitive impairment patients," *Magnetic Resonance Imaging*, vol. 30, no. 5, pp. 672–682, 2012.
- [28] T. Brott, H. P. Adams Jr., C. P. Olinger et al., "Measurements of acute cerebral infarction: a clinical examination scale," *Stroke*, vol. 20, no. 7, pp. 864–870, 1989.
- [29] A. R. Fugl-Meyer, L. Jääskö, I. Leyman, S. Olsson, and S. Steglind, "The post-stroke hemiplegic patient. 1. A method for evaluation of physical performance," *Scandinavian Journal of Rehabilitation Medicine*, vol. 7, no. 1, pp. 13–31, 1975.
- [30] W. Qin, J. Tian, L. Bai et al., "fMRI connectivity analysis of acupuncture effects on an amygdala-associated brain network," *Molecular Pain*, vol. 4, pp. 1744–8069, 2008.
- [31] L. Chen, J. Fang, R. Ma et al., "Additional effects of acupuncture on early comprehensive rehabilitation in patients with mild to moderate acute ischemic stroke: a multicenter randomized controlled trial," *BMC Complementary and Alternative Medicine*, vol. 16, no. 1, p. 226, 2016.
- [32] M. Ratmansky, A. Levy, A. Messinger, A. Birg, L. Front, and I. Treger, "The effects of acupuncture on cerebral blood flow in post-stroke patients: a randomized controlled trial," *The Journal of Alternative and Complementary Medicine*, vol. 22, no. 1, pp. 33–37, 2016.
- [33] J. Kong, R. Gollub, T. Huang et al., "Acupuncture de qi, from qualitative history to quantitative measurement," *The Journal of Alternative and Complementary Medicine*, vol. 13, no. 10, pp. 1059–1070, 2007.
- [34] K. K. S. Hui, J. Liu, O. Marina et al., "The integrated response of the human cerebro-cerebellar and limbic systems to acupuncture stimulation at ST 36 as evidenced by fMRI," *NeuroImage*, vol. 27, no. 3, pp. 479–496, 2005.
- [35] Neurology branch of Chinese Medical Association, "Guidelines for the diagnosis and treatment of acute ischemic stroke in China 2014," *Chinese Journal of Neurology*, vol. 48, pp. 246–257, 2015.
- [36] J. Wang, X. Wang, M. Xia, X. Liao, A. Evans, and Y. He, "GRETNA: a graph theoretical network analysis toolbox for imaging connectomics," *Frontiers in Human Neuroscience*, vol. 9, 2015.
- [37] K. J. Friston, S. Williams, R. Howard, R. S. J. Frackowiak, and R. Turner, "Movement-related effects in fMRI time-series," *Magnetic Resonance in Medicine*, vol. 35, no. 3, pp. 346–355, 1996.
- [38] C.-G. Yan, B. Cheung, C. Kelly et al., "A comprehensive assessment of regional variation in the impact of head micromovements on functional connectomics," *NeuroImage*, vol. 76, pp. 183–201, 2013.
- [39] K. Murphy and M. D. Fox, "Towards a consensus regarding global signal regression for resting state functional connectivity MRI," *NeuroImage*, vol. 154, pp. 169–173, 2017.
- [40] N. Tzourio-Mazoyer, B. Landeau, D. Papathanassiou et al., "Automated anatomical labeling of activations in SPM using a macroscopic anatomical parcellation of the MNI MRI single-subject brain," *NeuroImage*, vol. 15, no. 1, pp. 273–289, 2002.

- [41] S. Achard and E. Bullmore, "Efficiency and cost of economical brain functional networks," *PLoS Computational Biology*, vol. 3, no. 2, article e17, 2007.
- [42] V. Latora and M. Marchiori, "Economic small-world behavior in weighted networks," *The European Physical Journal B - Condensed Matter and Complex Systems*, vol. 32, no. 2, pp. 249–263, 2003.
- [43] M. Rubinov and O. Sporns, "Complex network measures of brain connectivity: uses and interpretations," *NeuroImage*, vol. 52, no. 3, pp. 1059–1069, 2010.
- [44] Y. He, A. Dagher, Z. Chen et al., "Impaired small-world efficiency in structural cortical networks in multiple sclerosis associated with white matter lesion load," *Brain*, vol. 132, no. 12, pp. 3366–3379, 2009.
- [45] D. Zhang, X. Liu, J. Chen, B. Liu, and J. Wang, "Widespread increase of functional connectivity in Parkinson's disease with tremor: a resting-state FMRI study," *Frontiers in Aging Neuroscience*, vol. 7, 2015.
- [46] Y. Zhu, L. Bai, P. Liang, S. Kang, H. Gao, and H. Yang, "Disrupted brain connectivity networks in acute ischemic stroke patients," *Brain Imaging and Behavior*, vol. 11, no. 2, pp. 444–453, 2017.
- [47] V. Latora and M. Marchiori, "Efficient behavior of small-world networks," *Physical Review Letters*, vol. 87, no. 19, article 198701, 2001.
- [48] G. Deco, G. Tononi, M. Boly, and M. L. Kringelbach, "Rethinking segregation and integration: contributions of whole-brain modelling," *Nature Reviews Neuroscience*, vol. 16, no. 7, pp. 430–439, 2015.
- [49] M. Mijalkov, E. Kakaei, J. B. Pereira, E. Westman, G. Volpe, and for the Alzheimer's Disease Neuroimaging Initiative, "BRAPH: a graph theory software for the analysis of brain connectivity," *PLoS One*, vol. 12, no. 8, article e0178798, 2017.
- [50] G. Tononi, G. M. Edelman, and O. Sporns, "Complexity and coherency: integrating information in the brain," *Trends in Cognitive Sciences*, vol. 2, no. 12, pp. 474–484, 1998.



## Research Article

# Electroacupuncture-Induced Plasticity between Different Representations in Human Motor Cortex

Wei Qin Peng , Tiange Yang, Jiawei Yuan , Jianpeng Huang, and Jianhua Liu 

*Acupuncture Research Team, the Second Affiliated Hospital of Guangzhou University of Chinese Medicine, Guangzhou, China*

Correspondence should be addressed to Jianhua Liu; [jyh08@sina.com](mailto:jyh08@sina.com)

Received 24 May 2020; Revised 18 July 2020; Accepted 1 August 2020; Published 14 August 2020

Academic Editor: Jing-Wen Yang

Copyright © 2020 Wei Qin Peng et al. This is an open access article distributed under the Creative Commons Attribution License, which permits unrestricted use, distribution, and reproduction in any medium, provided the original work is properly cited.

Somatosensory stimulation can effectively induce plasticity in the motor cortex representation of the stimulated body part. Specific interactions have been reported between different representations within the primary motor cortex. However, studies evaluating somatosensory stimulation-induced plasticity between different representations within the primary motor cortex are sparse. The purpose of this study was to investigate the effect of somatosensory stimulation on the modulation of plasticity between different representations within the primary motor cortex. Twelve healthy volunteers received both electroacupuncture (EA) and sham EA at the TE5 acupoint (located on the forearm). Plasticity changes in different representations, including the map volume, map area, and centre of gravity (COG) were evaluated by transcranial magnetic stimulation (TMS) before and after the intervention. EA significantly increased the map volume of the forearm and hand representations compared to those of sham EA and significantly reduced the map volume of the face representation compared to that before EA. No significant change was found in the map volume of the upper arm and leg representations after EA, and likewise, no significant changes in map area and COG were observed. These results suggest that EA functions as a form of somatosensory stimulation to effectively induce plasticity between different representations within the primary motor cortex, which may be related to the extensive horizontal intrinsic connectivity between different representations. The cortical plasticity induced by somatosensory stimulation might be purposefully used to modulate human cortical function.

## 1. Introduction

In the mid-20th century, Penfield and colleagues described a somatotopic map of the human primary motor cortex, which revealed the rough distribution of body part representations in the human cortex [1]. The cortical representations of adjacent body parts have been shown to extensively overlap [2], and furthermore, the motor cortex reportedly contains a network of intracortical fibres that interconnect various cortical motor representations [3]. This network is dynamic and contains an anatomical substrate for topographic plasticity.

Somatosensory stimulation has been proved to modulate plasticity in the primary motor cortex [4], which is mainly defined as a change in the excitability and area of a cortical representation. In healthy subjects, short-term electrical stimulation over a peripheral nerve or a muscle motor point can increase the motor cortical excitability of the stimulated body parts [5]. Alternatively, the application of long-term

daily transcutaneous nerve electrical stimulation (TENS) to a hand muscle has been shown to result in an enlargement in the cortical representation of the stimulated muscle [6]. Acupuncture, a safe, painless, and easily performed method of somatosensory stimulation, can also modulate plasticity in the primary motor cortex [7]. This has been demonstrated, for example, by several functional magnetic resonance imaging (fMRI) studies showing that acupuncture at the GB34 acupoint of the leg activates the motor cortex in healthy subjects [8] and in patients with Parkinson's disease [9]. Moreover, a transcranial magnetic stimulation (TMS) study showed that acupuncture at LI4 of the hand significantly changes the motor evoked potentials (MEP) amplitude of hand muscle in healthy subjects [10].

However, much less is known about somatosensory stimulation-induced plasticity between different representations within the motor cortex. There is evidence that noninvasive brain stimulation of motor cortex might induce

across-representation plasticity in the primary motor cortex. Repetitive transcranial magnetic stimulation (rTMS) of the face or hand representations leads to an inhibition activity of the adjacent arm representation during transient ischemic nerve block in healthy subjects [11]. Additionally, a number of studies have shown that plasticity occurs between different representations in motor cortex in cases of peripheral nerve lesion [12, 13], brain injury [14], motor practice [15], and motor learning [16]. More importantly, modulation of the plasticity between different representations has been proposed to play a key role in functional recovery in animals with lesions [17, 18] and in patients with neurological disorders [19–21]. To date, although somatosensory stimulation treatments, including electroacupuncture (EA), have been widely used for the rehabilitation of neurological function [22–24], their mechanisms of action are still unknown.

The present study used EA to apply somatosensory stimulation to the forearm and investigated the changes in the cortical representations of the forearm, hand, upper arm, face, and leg in healthy volunteers. Changes in motor cortex representations were evaluated using a TMS protocol to test differences in the excitability and size of the cortical representation [25]. Based on previous findings that central stimulation induces plasticity within the primary motor cortex [11], we hypothesized that EA of the forearm would induce a global effect on different representations, which might provide a new approach for the treatment of neurological diseases.

## 2. Materials and Methods

**2.1. Subjects and Experimental Design.** Twelve healthy, right-handed adults (aged 26–35 years; 1 male) participated in the study. The subjects had not undergone acupuncture in the month before beginning the study and none had neurological, psychiatric, or any other medical problems or had reported any contraindications to TMS [26]. All participants were informed about the potential benefits and risks of the study and provided written consent to participate. The present study was approved by the Ethics Committee of the Guangdong Provincial Hospital of Traditional Chinese Medicine (approval no. BF2019-040-01).

The study timeline is depicted in Figure 1(c). Each subject received real and sham EA in separate sessions, with a wash-out period of at least 2 weeks. The order of interventions (real–sham or sham–real) was chosen randomly for each participant. The study is registered in the Chinese Clinical Trial Registry (no. ChiCTR-1900026290).

**2.2. Intervention.** The subjects sat comfortably on an armchair and were instructed to stay relaxed during the intervention. Acupuncture was performed by the same experienced acupuncturist under aseptic conditions using disposable acupuncture needles (diameter, 0.25 mm; length, 25 mm; Hwato, Suzhou Medical Appliance Factory, Suzhou, China).

This study used the “Waiguan” (TE5) acupoint, located on the posterior aspect of the forearm, at the midpoint of the interosseous space between the radius and the ulna, 2 B-cun proximal to the dorsal wrist crease [27] (Figure 1(a)).

In each EA session, acupuncture was performed at TE5 on the right forearm with a depth of real acupuncture insertion of about 10–15 mm. Upon the subject reporting a De Qi sensation during acupuncture, a nerve stimulator (HANS-200A, Jisheng Medical Technology Limited Company, Nanjing, China) was used to perform EA (2 Hz) at a comfortable intensity depending on the tolerance of the individual. In the sham EA sessions, a noninvasive blunt needle (diameter, 0.25 mm; length, 25 mm) supported by a sponge cushion served as the sham acupuncture setup [28]. The EA and sham EA interventions each lasted for 30 min.

**2.3. Electromyography (EMG).** EMG records were obtained from the following muscles ipsilateral to the acupuncture sites in the EA sessions: first dorsal interosseous (FDI); extensor indicis proprius (EIP); deltoid muscle (DM); orbicularis oculi (OO); and tibialis anterior (TA). However, only the EIP and FDI were recorded in the sham EA sessions.

Surface electromyography as recorded from the target muscles using 9-mm-diameter Ag/AgCl surface electrodes on a belly–tendon montage. Responses were input into an amplifier through filters with a bandpass of 20–2,000 kHz, then digitized and stored on a computer for later offline analyses. Since corticospinal excitability depends on limb posture [29], all participants maintained a specific limb position, as described below, while being seated comfortably on a chair.

For FDI and EIP recordings, the subjects maintained a static wrist extension and relaxed their fingers with the forearm resting on an armrest. For OO recordings, the subjects were asked to blink slightly to moderately activate the OO muscle. For DM recordings, to activate the middle deltoid muscle in subjects, the middle portions of the deltoids were abducted from the shoulders at a 30° angle, drawing them away from the trunk. For TA recordings, the subjects were constrained by a flexible weight placed over the dorsum of the right foot allowing for 10% of the maximum voluntary isometric contraction.

**2.4. TMS Protocol.** Based on the methods described by Nicolini et al. [25], TMS was applied to the motor cortex in the left hemisphere before and after the intervention (EA/sham EA) with a Magstim Super Rapid magnetic stimulator (Magstim Company, Dyfed, UK) equipped with a figure-of-eight coil (external wing diameter, 70 mm). The coil was orientated at 45° oblique to the sagittal plane so that the induced current flowed in a posterior–anterior direction (Figure 1(c)). All subjects wore a tight-fitting cap with a coordinate (grid, 1 × 1 cm). The resting motor threshold (RMT) was defined as the minimum stimulus intensity that elicited >50  $\mu$ V peak-to-peak amplitude in 50% of the trials with the muscles (FDI and EIP) at rest (no muscle contraction). In addition, the active motor threshold (AMT) was defined as the minimum stimulus intensity that elicited >100  $\mu$ V peak-to-peak amplitude in 50% of the trials with muscle contraction (OO, DM, and TA). The motor “hotspot” for each muscle was determined by delivering a single TMS pulse at the motor threshold to each grid point and subsequently identifying the location in the grid with the largest peak-to-peak MEPs. The TMS intensity for mapping was set at 120% of

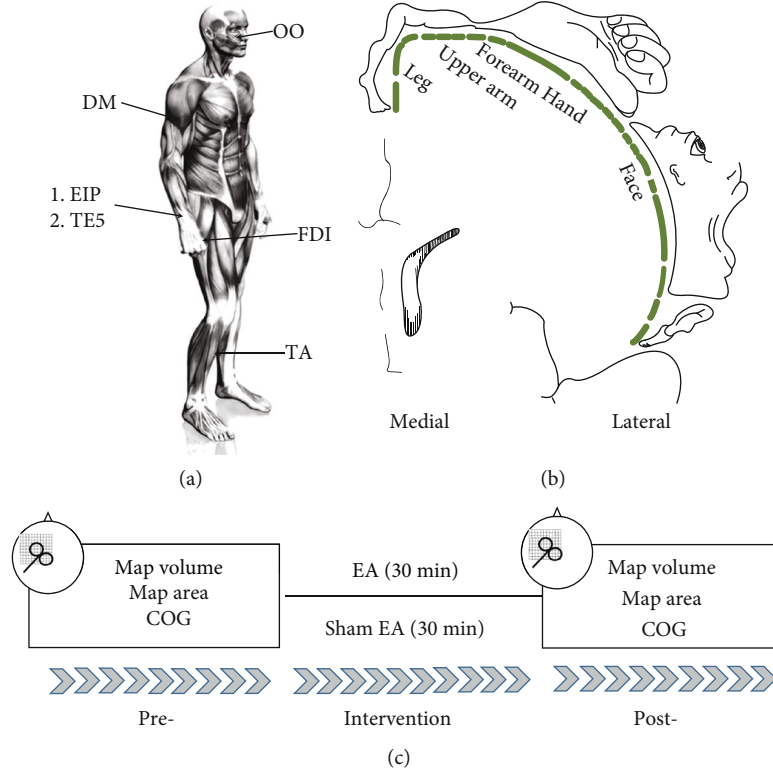


FIGURE 1: (a) Schematic drawings of a subject, showing the location of acupoint TE5 (Waiguan) and the target muscles. (b) Penfield and Rasmussen's homunculus, in which representations of the leg, upper arm, forearm, hand, and face muscles are roughly arranged in a medial-to-lateral direction. (c) Experimental paradigm. All subjects participated in EA and sham EA groups. Abbreviations: COG: centre of gravity; DM: deltoid muscle; EA: electroacupuncture; EIP: extensor indicis proprius; FDI: first dorsal interosseus; OO: orbicularis oculi; TA: tibialis anterior; TE5: Waiguan acupoint.

the motor threshold (RMT or AMT). Six successive pulses separated by intervals of 4–5 seconds were delivered to each point of the grid. A grid point was considered responsive if at least three MEPs were elicited. For each muscle, the peak-to-peak MEP amplitudes of three TMS stimuli at each grid point were averaged to determine the maximum average MEP amplitude. Only grid points that elicited an average MEP amplitude  $\geq 20\%$  of the maximum average MEP amplitude were considered active sites and included in the map. The nonactive sites delimited the mapping boundaries.

**2.5. TMS Outcomes.** The extracted TMS variables included the following: (1) map volume, (2) map area, and (3) centre of gravity (COG). The map volume was calculated as the sum of the mean amplitudes at all active sites. A standardized grid ( $1 \times 1$  cm) was used across subjects, with the number of active sites accurately representing the map area ( $\text{cm}^2$ ). The COG was computed using Equations (1) and (2), where  $MEP_i$  represents the mean amplitude of the MEPs produced at one active site [30].

$$COG_x = (\sum x_i \times MEP_i) / \sum MEP_i, \quad (1)$$

$$COG_y = (\sum y_i \times MEP_i) / \sum MEP_i. \quad (2)$$

**2.6. Statistical Analysis.** The data were analysed using IBM SPSS Statistics for Windows, version 20.0. The data were

tested for normality using Shapiro–Wilk normality tests; as some data sets did not meet the normality criteria, nonparametric statistics were used to statistically analyse them. All data are presented as the mean  $\pm$  standard deviation (SD). Wilcoxon signed-rank tests were used to compare data before (pre-) and after (post-) intervention. Mann–Whitney  $U$ -tests were used to compare data between groups.  $P < 0.05$  was considered statistically significant.

### 3. Results and Discussion

Twelve participants completed the study procedures without reporting side effects. Raw MEP data from one representative subject is shown in Figure 2.

**3.1. Effect of EA on Map Volume.** The effects of EA on map volume are shown in Figure 3. No significant differences between EA and sham EA groups were observed at baseline for the representations of the forearm (EIP; pre-EA,  $6.1 \pm 4.3$  mV vs. presham EA,  $6.8 \pm 3.6$  mV;  $P = 0.603$ ,  $Z = -0.520$ , Mann–Whitney  $U$ -tests) and hand (FDI; pre-EA,  $11.6 \pm 7.0$  mV vs. presham EA,  $12.0 \pm 6.8$  mV;  $P = 0.795$ ,  $Z = -0.260$ , Mann–Whitney  $U$ -tests). For both of these representations, significant increases were observed in the EA group following the intervention (EIP: pre-EA,  $6.1 \pm 4.3$  mV vs. post-EA,  $8.2 \pm 5.9$  mV,  $P = 0.028$ ,  $Z = -2.197$ ; FDI: pre-EA,  $11.6 \pm 7.0$  mV vs. post-EA,  $11.6 \pm 7.0$  mV,  $P = 0.008$ ,  $Z = -2.667$ ;

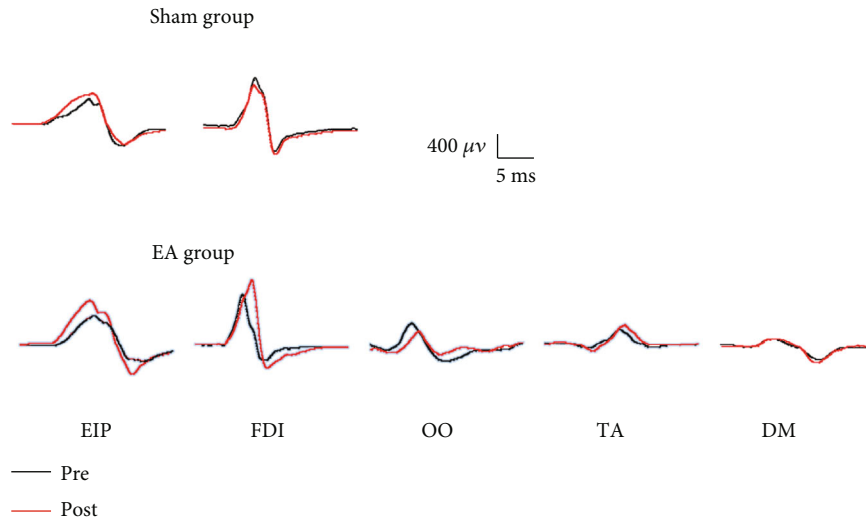


FIGURE 2: Raw MEP data (single trace) from a representative subject before (black line) and after (red line) each intervention. Abbreviations: DM: deltoid muscle; EA: electroacupuncture; EIP: extensor indicis proprius; FDI: first dorsal interosseus; MEP: motor evoked potential; OO: orbicularis oculi; TA: tibialis anterior.

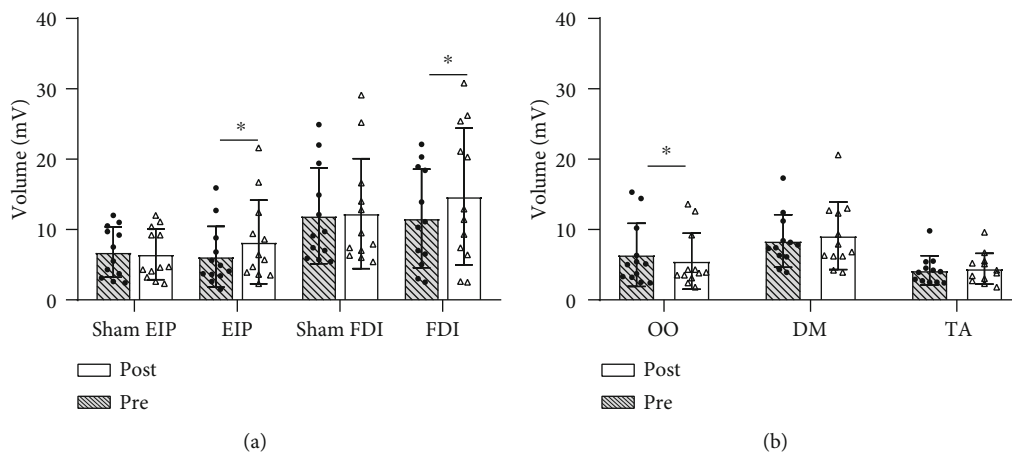


FIGURE 3: (a, b) Mean ( $\pm$ SD) changes in the map volumes of target muscles plotted with the individual data from each subject before and after the intervention. \* $P < 0.05$ , Wilcoxon signed-rank tests. Abbreviations: DM: deltoid muscle; EIP: extensor indicis proprius; FDI: first dorsal interosseus; OO: orbicularis oculi; SD: standard deviation; TA: tibialis anterior.

Wilcoxon signed-rank tests), while no significant change was observed in the sham EA group (EIP: presham EA,  $6.8 \pm 3.6$  mV vs. postsham EA,  $6.5 \pm 3.6$  mV,  $P = 1.000$ ,  $Z = 0.000$ ; FDI: presham EA,  $12.0 \pm 6.8$  mV vs. postsham EA,  $12.3 \pm 7.8$  mV,  $P = 0.937$ ,  $Z = -0.078$ ; Wilcoxon signed-rank tests). Furthermore, significant between-group effects of EA on the forearm and hand representations were observed (EIP: EA,  $2.1 \pm 2.4$  mV vs. sham EA,  $0.3 \pm 1.4$  mV,  $P = 0.010$ ,  $Z = -2.573$ ; FDI: EA,  $3.1 \pm 3.3$  mV vs. sham EA,  $0.3 \pm 2.4$  mV,  $P = 0.012$ ,  $Z = -2.513$ ; Mann-Whitney  $U$ -tests). However, a significant reduction was observed after EA in the representation of the face (OO: pre-EA,  $6.4 \pm 4.5$  mV vs. post-EA,  $5.5 \pm 4.0$  mV,  $P = 0.034$ ,  $Z = -2.119$ ). No significant changes were observed in the upper arm and leg representations (DM: pre-EA,  $8.4 \pm 3.7$  mV vs. post-EA,  $9.1 \pm 4.8$  mV,  $P = 0.330$ ,  $Z = -0.975$ ; TA: pre-EA,  $4.2 \pm 2.1$  mV vs. post-EA,  $4.4 \pm 2.2$  mV,  $P = 0.455$ ,  $Z = -0.747$ ; Wilcoxon signed-rank tests).

**3.2. Effect of EA on COG.** The COGs of the representations mapped in the present study included the medial-to-lateral leg, upper arm, forearm, hand, and face representations. The COGs of the forearm (EIP: pre-EA,  $x = 6.0 \pm 0.7$ ,  $y = 7.8 \pm 2.3$ ) and hand (FDI: pre-EA,  $x = 6.0 \pm 0.8$ ,  $y = 7.6 \pm 2.3$ ) representations were in close proximity. We observed no significant changes in the COG of any representation after the intervention (all muscles:  $P > 0.05$ , Wilcoxon signed-rank tests) (Table 1).

**3.3. Effect of EA on Map Area.** We observed no significant change in map area for any representation following the intervention (all muscles:  $P > 0.05$ , Wilcoxon signed-rank tests) (Table 1).

**3.4. Within-Representation Plasticity.** EA at TE5 on the forearm increased the map volume of the forearm muscle (EIP),



TABLE 1: Mean ( $\pm$ SD) map area and mean ( $\pm$ SD) COG pre- and postintervention for the EA and sham EA groups.

Measures	Muscle	EA		Sham EA	
		Pre	Post	Pre	Post
Area (cm <sup>2</sup> )	EIP	15.9 $\pm$ 4.2	16.2 $\pm$ 4.2	14.5 $\pm$ 2.5	13.3 $\pm$ 2.9
	FDI	13.8 $\pm$ 3.3	14.9 $\pm$ 4.7	13.5 $\pm$ 2.7	14 $\pm$ 3.3
	OO	22.2 $\pm$ 9.8	20.0 $\pm$ 8.1		
	DM	19.6 $\pm$ 4.7	18.6 $\pm$ 4.6		
	TA	14.6 $\pm$ 4.6	15.3 $\pm$ 4.5		
COG (x, y)	EIP	(6.0 $\pm$ 0.7, 7.8 $\pm$ 2.3)	(6.1 $\pm$ 0.8, 7.8 $\pm$ 2.3)	(4.7 $\pm$ 0.8, 7.4 $\pm$ 1.3)	(4.7 $\pm$ 0.7, 7.4 $\pm$ 1.2)
	FDI	(6.0 $\pm$ 0.8, 7.6 $\pm$ 2.3)	(6.2 $\pm$ 1.1, 7.7 $\pm$ 2.3)	(5.3 $\pm$ 1.0, 7.7 $\pm$ 1.5)	(5.2 $\pm$ 0.9, 7.8 $\pm$ 1.3)
	OO	(7.2 $\pm$ 1.5, 6.2 $\pm$ 1.3)	(7.1 $\pm$ 1.7, 6.1 $\pm$ 1.3)		
	DM	(4.5 $\pm$ 1.0, 8.7 $\pm$ 1.4)	(4.6 $\pm$ 1.2, 8.7 $\pm$ 1.6)		
	TA	(1.2 $\pm$ 0.6, 8.7 $\pm$ 1.5)	(1.0 $\pm$ 0.6, 8.7 $\pm$ 1.5)		

Abbreviations: COG: centre of gravity; DM: deltoid muscle; EA: electroacupuncture; EIP: extensor indicis proprius; FDI: first dorsal interosseous; OO: orbicularis oculi; SD: standard deviation; TA: tibialis anterior.

indicating increased excitability in the forearm representation (Figure 3(a)). Early studies reported that changes in MEP amplitude induced by somatosensory stimulation were supraspinal [31–33] and were affected by  $\gamma$ -aminobutyric acid (GABA)-ergic mechanisms [34]. Thus, the increase in map volume induced by EA was not the result of facilitation in the spinal circuits, but rather facilitation in the motor cortex. EA at TE5 on the forearm resulted in considerable increases in the map volume of the cortical motor representation in the absence of changes in the area and COG of the motor map. This indicates that EA led to a change in cortical excitability rather than in the distribution of the representation. Changes in map area and COG may occur as a result of long-term somatosensory stimulation or long-term deprivation of somatosensory input after amputation. In healthy subjects, long-term daily TENS of muscle in the hand [6] or daily training of a coordinated movement [15] results in an enlargement in cortical representations of the target muscles. In amputees, the representations of proximal limb have been shown to expand into the deafferented cortex (representing the hand) and cortical stimulation of the hand representation has been demonstrated to evoke contraction of the amputated stump [35, 36]. Thus, the absence of changes in the area and COG may be due to the short-term stimulation applied in the present study.

### 3.5. Plasticity between Forearm and Hand Representations.

Forearm stimulation increased the map volume of the forearm (EIP) representation and had a simultaneous analogous effect in the hand (FDI) representation (Figure 3(a)), suggesting EA-induced coactivation of the forearm and hand representations. The results obtained in this study are similar to those reported in previous studies. One study found that after the removal of the needle on LI11 and TE5 (both located on the forearm), the MEP amplitude of FDI was significantly increased compared to baseline [37]. Moreover, peripheral nerve stimulation at the wrist was shown to simultaneously induce marked changes in the cortical excitability of multiple hand muscles [5]. This plasticity may be closely related to the

extensive horizontal intrinsic connectivity between these representations in the motor cortex [3, 38]. The internal organization of these representations within the motor cortex is best described as a network having a broadly distributed overlap. Intracortical microstimulation in one position within forelimb representation was shown to simultaneously induce movement in the digits and wrist [39, 40]. Moreover, the COGs of the hand and forearm representations were found to be in close proximity in present study (Table 1), indicating high levels of overlap between these two areas. Many studies have reported overlapping activation between the forearm and hand representations in the human motor cortex. For example, one fMRI study observed that these areas exhibited shared activation following hand and forearm movement [2]. Additionally, a TMS multiple-muscle mapping study reported a >70% overlap between hand and forearm muscles [41]. However, previous studies have shown a reciprocal inhibitory effect between the forearm and hand representations in the motor cortex. An extension and lateral shift of the stump muscle representation was reported in patients with long-standing upper limb amputation [42]. Additionally, an animal study reported an expanded hand representation and a contracted forearm representation in monkey motor cortex after long-term hand training, while the reverse was observed after long-term forearm training [43].

Taken together, the above studies indicate the existence of a specific activity pattern between forearm and hand representations, with both coactivation and reciprocal inhibition due to horizontal intrinsic connectivity.

### 3.6. Plasticity between Forearm and Face Representations.

Stimulation of the forearm not only increased the map volume of the forearm (EIP) and hand (FDI) representations but also reduced the map volume of the face (OO) representation (Figure 3(b)). This indicates an inhibitory influence of EA on face representation, expressed as decreased motor cortical excitability. Both animal and human data on cortical plasticity indicate that changes in somatosensory input can

induce plasticity [44, 45]. There is an inhibitory effect between the forearm and face representations of the motor cortex; for example, patients with traumatic forearm amputation show a medial shift of their face representation toward the forearm representation [46, 47]. Following facial nerve transection in the rat, forelimb movement can be evoked from some sites where only vibrissal movement could be elicited before nerve transection, suggesting an expanded region of forelimb representation within the previous face representation in the motor cortex [48]. The hand representation of patients with facial palsy expands toward the face representation in the motor cortex contralateral to the affected side [49]. Conversely, the reduced size of the hand representation contralateral to the affected side is reversed following the application of botulinum toxin in patients with hemifacial spasm [50].

In the present study, enhanced somatosensory input following EA effectively induced an inhibitory effect between the forearm and face representations under physiological conditions. Previous research has also reported an inhibitory effect between pharynx and oesophagus representations after somatosensory stimulation of the pharynx [51]; however, the mechanisms of this inhibitory effect are unclear. Latent intracortical connections have been demonstrated to be responsible for rapid reorganization between vibrissae and forelimb representations in the motor cortex following rat facial nerve transection [48].

**3.7. Interactions between Forearm and Upper Arm Representations.** In the present study, stimulation of the forearm did not significantly affect the map volume of the upper arm representation (Table 1), which differs from the EA-induced plasticity between the forearm and hand/face representations. In human somatotopography, the forearm and upper limb representations are adjacent to one another [52]. An overlap between the forearm and upper arm representations has also been demonstrated in fMRI studies of the human motor cortex [2]. Patients with phantom limb pain after upper arm amputation have increased cortical excitability and a larger territory of upper arm representation on the amputated side compared to those of the intact side, indicating reorganization between the upper arm and forearm representations [53]. Nevertheless, a TMS multiple-muscle mapping study observed a high overlap for forearm–hand muscles and a low overlap for upper arm–forearm muscles, which may explain why the upper arm representation was not facilitated by forearm stimulation in the present study [41]. Stimulation parameters, such as the intensity, frequency, and time course, have a crucial influence on the somatosensory stimulation-induced plasticity [54]. In contrast to our findings, a previous study reported no significant changes in motor cortical excitability after 90s of manual acupuncture in healthy subjects [55]. Thus, the EA stimulation parameters used in this study may not have been sufficient to induce plasticity between the forearm and upper arm representations.

**3.8. Interactions between Forearm and Leg Representations.** The results of this study show that EA stimulation of the

forearm did not affect the map volume of the leg representation, suggesting a lack of somatosensory-induced plasticity between the forearm and leg representations. This may be due to the great anatomical distance between the forearm and the leg. Our results show that the COGs of the forearm and leg representations are poles apart. Moreover, the leg and forearm representations are separated by the arm and trunk representations, with no horizontal intrinsic connectivity between the representations of the leg and forearm.

## 4. Conclusions

The findings of the present study highlight the potential of somatosensory stimulation as a useful complementary therapy for neurological or facial diseases. We have shown that the (facilitatory or inhibitory) plasticity changes in cortical excitability induced by somatosensory stimulation were not restricted to the stimulated area but also extended to other areas. This may relate to the extensive horizontal intrinsic connectivity between different representations in the primary motor cortex.

## Data Availability

All data included in this study are available from the corresponding author upon request.

## Conflicts of Interest

The authors declare that there is no conflict of interest regarding the publication of this paper.

## Acknowledgments

The authors thank Yu Zhu and Zhiqing Zhang for help with data acquisition and analyses. Thanks to Yiling Yang for helpful discussion of the data and language advice. This study was supported by grants from the National Key Research and Development Program of China (2019YFC1709100, 2019YFC1709102), the National Natural Science Foundation of China (81873381), and the Guangdong Provincial Hospital of Traditional Chinese Medicine Science and Technology Research Projects (YN2019ML12).

## References

- [1] W. Penfield and T. Rasmussen, *The cerebral cortex of man*, MacMillan, New York, 1950.
- [2] J. D. Meier, T. N. Aflalo, S. Kastner, and M. S. A. Graziano, “Complex organization of human primary motor cortex: a high-resolution fMRI study,” *Journal of Neurophysiology*, vol. 100, no. 4, pp. 1800–1812, 2008.
- [3] G. W. Huntley and E. G. Jones, “Relationship of intrinsic connections to forelimb movement representations in monkey motor cortex: a correlative anatomic and physiological study,” *Journal of Neurophysiology*, vol. 66, no. 2, pp. 390–413, 1991.
- [4] S. M. Schabrun, M. C. Ridding, M. P. Galea, P. W. Hodges, and L. S. Chipchase, “Primary sensory and motor cortex excitability are co-modulated in response to peripheral electrical nerve stimulation,” *PLoS One*, vol. 7, no. 12, article e51298, 2012.

- [5] C. S. Charlton, M. C. Ridding, P. D. Thompson, and T. S. Miles, "Prolonged peripheral nerve stimulation induces persistent changes in excitability of human motor cortex," *Journal of the Neurological Sciences*, vol. 208, no. 1-2, pp. 79–85, 2003.
- [6] R. L. J. Meesen, K. Cuyppers, J. C. Rothwell, S. P. Swinnen, and O. Levin, "The effect of long-term TENS on persistent neuroplastic changes in the human cerebral cortex," *Human Brain Mapping*, vol. 32, no. 6, pp. 872–882, 2011.
- [7] Y. Jiang, H. Wang, Z. Liu et al., "Manipulation of and sustained effects on the human brain induced by different modalities of acupuncture: an fMRI study," *PLoS One*, vol. 8, no. 6, article e66815, 2013.
- [8] S.-S. Jeun, J.-S. Kim, B.-S. Kim et al., "Acupuncture stimulation for motor cortex activities: a 3T fMRI study," *The American Journal of Chinese Medicine*, vol. 33, no. 4, pp. 573–578, 2012.
- [9] S. Yeo, I.-H. Choe, M. van den Noort et al., "Acupuncture on GB34 activates the precentral gyrus and prefrontal cortex in Parkinson's disease," *BMC Complementary and Alternative Medicine*, vol. 14, no. 1, p. 336, 2014.
- [10] Y. L. Lo and S. L. Cui, "Acupuncture and the modulation of cortical excitability," *Neuroreport*, vol. 14, no. 9, pp. 1229–1231, 2003.
- [11] U. Ziemann, G. F. Wittenberg, and L. G. Cohen, "Stimulation-induced within-representation and across-representation plasticity in human motor cortex," *The Journal of Neuroscience*, vol. 22, no. 13, pp. 5563–5571, 2002.
- [12] E. Raffin, N. Richard, P. Giroux, and K. T. Reilly, "Primary motor cortex changes after amputation correlate with phantom limb pain and the ability to move the phantom limb," *NeuroImage*, vol. 130, pp. 134–144, 2016.
- [13] D. Yao and B. J. Sessle, "Face sensorimotor cortex undergoes neuroplastic changes in a rat model of trigeminal neuropathic pain," *Experimental Brain Research*, vol. 236, no. 5, pp. 1357–1368, 2018.
- [14] M. Caleo, "Rehabilitation and plasticity following stroke: insights from rodent models," *Neuroscience*, vol. 311, pp. 180–194, 2015.
- [15] F. Tyc and A. Boyadjian, "Plasticity of motor cortex induced by coordination and training," *Clinical Neurophysiology*, vol. 122, no. 1, pp. 153–162, 2011.
- [16] E. B. Plow and J. R. Carey, "Pilot fMRI investigation of representational plasticity associated with motor skill learning and its functional consequences," *Brain Imaging and Behavior*, vol. 6, no. 3, pp. 437–453, 2012.
- [17] M. Nishibe, E. T. R. Urban, S. Barbay, and R. J. Nudo, "Rehabilitative training promotes rapid motor recovery but delayed motor map reorganization in a rat cortical ischemic infarct model," *Neurorehabilitation and Neural Repair*, vol. 29, no. 5, pp. 472–482, 2014.
- [18] N. Dancause and R. J. Nudo, "Shaping plasticity to enhance recovery after injury," *Progress in Brain Research*, vol. 192, pp. 273–295, 2011.
- [19] J. Lee, J. Yang, C. Li et al., "Cortical reorganization in patients recovered from Bell's palsy: an orofacial and finger movements task-state fMRI study," *Neural Plasticity*, vol. 2016, Article ID 8231726, 6 pages, 2016.
- [20] G. W. Thickbroom, M. L. Byrnes, R. Stell, and F. L. Mastaglia, "Reversible reorganisation of the motor cortical representation of the hand in cervical dystonia," *Movement Disorders*, vol. 18, no. 4, pp. 395–402, 2003.
- [21] Y. Xu, Q. H. Hou, S. D. Russell et al., "Neuroplasticity in post-stroke gait recovery and noninvasive brain stimulation," *Neural Regeneration Research*, vol. 10, no. 12, pp. 2072–2080, 2015.
- [22] Y. Laufer and M. Elboim-Gabyzon, "Does sensory transcutaneous electrical stimulation enhance motor recovery following a stroke? A systematic review," *Neurorehabilitation and Neural Repair*, vol. 25, no. 9, pp. 799–809, 2011.
- [23] M. Maddocks, W. Gao, I. J. Higginson, and A. Wilcock, "Neuromuscular electrical stimulation for muscle weakness in adults with advanced disease," *Cochrane Database of Systematic Reviews*, vol. 1, article CD009419, 2013.
- [24] Y. Zhu, Y. Yang, and J. Li, "Does acupuncture help patients with spasticity? A narrative review," *Annals of Physical and Rehabilitation Medicine*, vol. 62, no. 4, pp. 297–301, 2019.
- [25] C. Nicolini, D. Harasym, C. V. Turco, and A. J. Nelson, "Human motor cortical organization is influenced by handedness," *Cortex*, vol. 115, pp. 172–183, 2019.
- [26] S. Rossi, M. Hallett, P. M. Rossini, A. Pascual-Leone, and Safety of TMS Consensus Group, "Safety, ethical considerations, and application guidelines for the use of transcranial magnetic stimulation in clinical practice and research," *Clinical Neurophysiology*, vol. 120, no. 12, pp. 2008–2039, 2009.
- [27] Pacific, WROftW, *WHO Standard Acupuncture Point Locations in the Western Pacific Region*, World Health Organization, Manila, 2008.
- [28] L.-S. Tam, P.-C. Leung, T. K. Li, L. Zhang, and E. K. Li, "Acupuncture in the treatment of rheumatoid arthritis: a double-blind controlled pilot study," *BMC Complementary and Alternative Medicine*, vol. 7, no. 1, p. 35, 2007.
- [29] D. A. Forman, J. Baarbé, J. Daligadu, B. Murphy, and M. W. R. Holmes, "The effects of upper limb posture and a sub-maximal gripping task on corticospinal excitability to muscles of the forearm," *Journal of Electromyography and Kinesiology*, vol. 27, pp. 95–101, 2016.
- [30] E. M. Wassermann, L. M. McShane, M. Hallett, and L. G. Cohen, "Noninvasive mapping of muscle representations in human motor cortex," *Electroencephalography and Clinical Neurophysiology/Evoked Potentials Section*, vol. 85, no. 1, pp. 1–8, 1992.
- [31] K. Kaneko, S. Kawai, Y. Fuchigami, G. Shiraishi, and T. Ito, "Effect of stimulus intensity and voluntary contraction on corticospinal potentials following transcranial magnetic stimulation," *Journal of the Neurological Sciences*, vol. 139, no. 1, pp. 131–136, 1996.
- [32] M. C. Ridding, B. Brouwer, T. S. Miles, J. B. Pitcher, and P. D. Thompson, "Changes in muscle responses to stimulation of the motor cortex induced by peripheral nerve stimulation in human subjects," *Experimental Brain Research*, vol. 131, no. 1, pp. 135–143, 2000.
- [33] Y. Yang, I. Eisner, S. Chen, S. Wang, F. Zhang, and L. Wang, "Neuroplasticity changes on human motor cortex induced by acupuncture therapy: a preliminary study," *Neural Plasticity*, vol. 2017, Article ID 4716792, 8 pages, 2017.
- [34] A. Kaelin-Lang, A. R. Luft, L. Sawaki, A. H. Burstein, Y. H. Sohn, and L. G. Cohen, "Modulation of human corticomotor excitability by somatosensory input," *The Journal of Physiology*, vol. 540, no. 2, pp. 623–633, 2002.
- [35] C. Mercier, "Mapping phantom movement representations in the motor cortex of amputees," *Brain*, vol. 129, no. 8, pp. 2202–2210, 2006.

- [36] S. Roricht, B. U. Meyer, L. Niehaus, and S. A. Brandt, "Long-term reorganization of motor cortex outputs after arm amputation," *Neurology*, vol. 53, no. 1, p. 106, 1999.
- [37] X.-k. He, Q.-q. Sun, H.-h. Liu, X.-y. Guo, C. Chen, and L.-d. Chen, "Timing of acupuncture during LTP-like plasticity induced by paired-associative stimulation," *Behavioural Neurology*, vol. 2019, Article ID 9278270, 10 pages, 2019.
- [38] J. N. Sanes and J. P. Donoghue, "Plasticity and primary motor cortex," *Annual Review of Neuroscience*, vol. 23, no. 1, pp. 393–415, 2000.
- [39] J. P. Donoghue, S. Leibovic, and J. N. Sanes, "Organization of the forelimb area in squirrel monkey motor cortex: representation of digit, wrist, and elbow muscles," *Experimental Brain Research*, vol. 89, no. 1, 1992.
- [40] A. Keller, "Intrinsic connections between representation zones in the cat motor cortex," *Neuroreport*, vol. 4, no. 5, pp. 515–518, 1993.
- [41] J.-M. Melgari, P. Pasqualetti, F. Pauri, and P. M. Rossini, "Muscles in "concert": study of primary motor cortex upper limb functional topography," *PLoS One*, vol. 3, no. 8, article e3069, 2008.
- [42] K. Irlbacher, B. U. Meyer, M. Voss, S. A. Brandt, and S. Rörich, "Spatial reorganization of cortical motor output maps of stump muscles in human upper-limb amputees," *Neuroscience Letters*, vol. 321, no. 3, pp. 129–132, 2002.
- [43] R. J. Nudo, G. W. Milliken, W. M. Jenkins, and M. M. Merzenich, "Use-dependent alterations of movement representations in primary motor cortex of adult squirrel monkeys," *The Journal of neuroscience : the official journal of the Society for Neuroscience*, vol. 16, no. 2, pp. 785–807, 1996.
- [44] J. N. Sanes, S. Suner, J. F. Lando, and J. P. Donoghue, "Rapid reorganization of adult rat motor cortex somatic representation patterns after motor nerve injury," *Proceedings of the National Academy of Sciences of the United States of America*, vol. 85, no. 6, pp. 2003–2007, 1988.
- [45] G. Franchi and C. Veronesi, "Long-term motor cortex reorganization after facial nerve severing in newborn rats," *The European Journal of Neuroscience*, vol. 20, no. 7, pp. 1885–1896, 2004.
- [46] A. Pascual-Leone, M. Peris, J. M. Tormos, A. P. L. Pascual, and M. D. Catalá, "Reorganization of human cortical motor output maps following traumatic forearm amputation," *Neuroreport*, vol. 7, no. 13, pp. 2068–2070, 1996.
- [47] C. Dettmers, T. Adler, R. Rzanny et al., "Increased excitability in the primary motor cortex and supplementary motor area in patients with phantom limb pain after upper limb amputation," *Neuroscience Letters*, vol. 307, no. 2, pp. 109–112, 2001.
- [48] G. Huntley, "Correlation between patterns of horizontal connectivity and the extend of short-term representational plasticity in rat motor cortex," *Cerebral cortex*, vol. 7, no. 2, pp. 143–156, 1997.
- [49] M. Rijntjes, M. Tegenthoff, J. Liepert et al., "Cortical reorganization in patients with facial palsy," *Annals of Neurology*, vol. 41, no. 5, pp. 621–630, 1997.
- [50] J. Liepert, C. Oreja-Guevara, L. G. Cohen, M. Tegenthoff, M. Hallett, and J. P. Malin, "Plasticity of cortical hand muscle representation in patients with hemifacial spasm," *Neuroscience Letters*, vol. 272, no. 1, pp. 33–36, 1999.
- [51] S. Hamdy, J. C. Rothwell, Q. Aziz, K. D. Singh, and D. G. Thompson, "Long-term reorganization of human motor cortex driven by short-term sensory stimulation," *Nature Neuroscience*, vol. 1, no. 1, pp. 64–68, 1998.
- [52] M. Lotze, M. Erb, H. Flor, E. Huelsmann, B. Godde, and W. Grodd, "fMRI evaluation of somatotopic representation in human primary motor cortex," *NeuroImage*, vol. 11, no. 5, pp. 473–481, 2000.
- [53] A. Karl, N. Birbaumer, W. Lutzenberger, L. G. Cohen, and H. Flor, "Reorganization of motor and somatosensory cortex in upper extremity amputees with phantom limb pain," *The Journal of neuroscience : the official journal of the Society for Neuroscience*, vol. 21, no. 10, pp. 3609–3618, 2001.
- [54] L. S. Chipchase, S. M. Schabrun, and P. W. Hodges, "Peripheral electrical stimulation to induce cortical plasticity: a systematic review of stimulus parameters," *Clinical Neurophysiology*, vol. 122, no. 3, pp. 456–463, 2011.
- [55] A. B. McCambridge, C. Zaslowski, and L. V. Bradnam, "Investigating the mechanisms of acupuncture on neural excitability in healthy adults," *Neuroreport*, vol. 30, no. 2, pp. 71–76, 2019.